MODERN TECHNIQUES FOR FOOD AUTHENTICATION

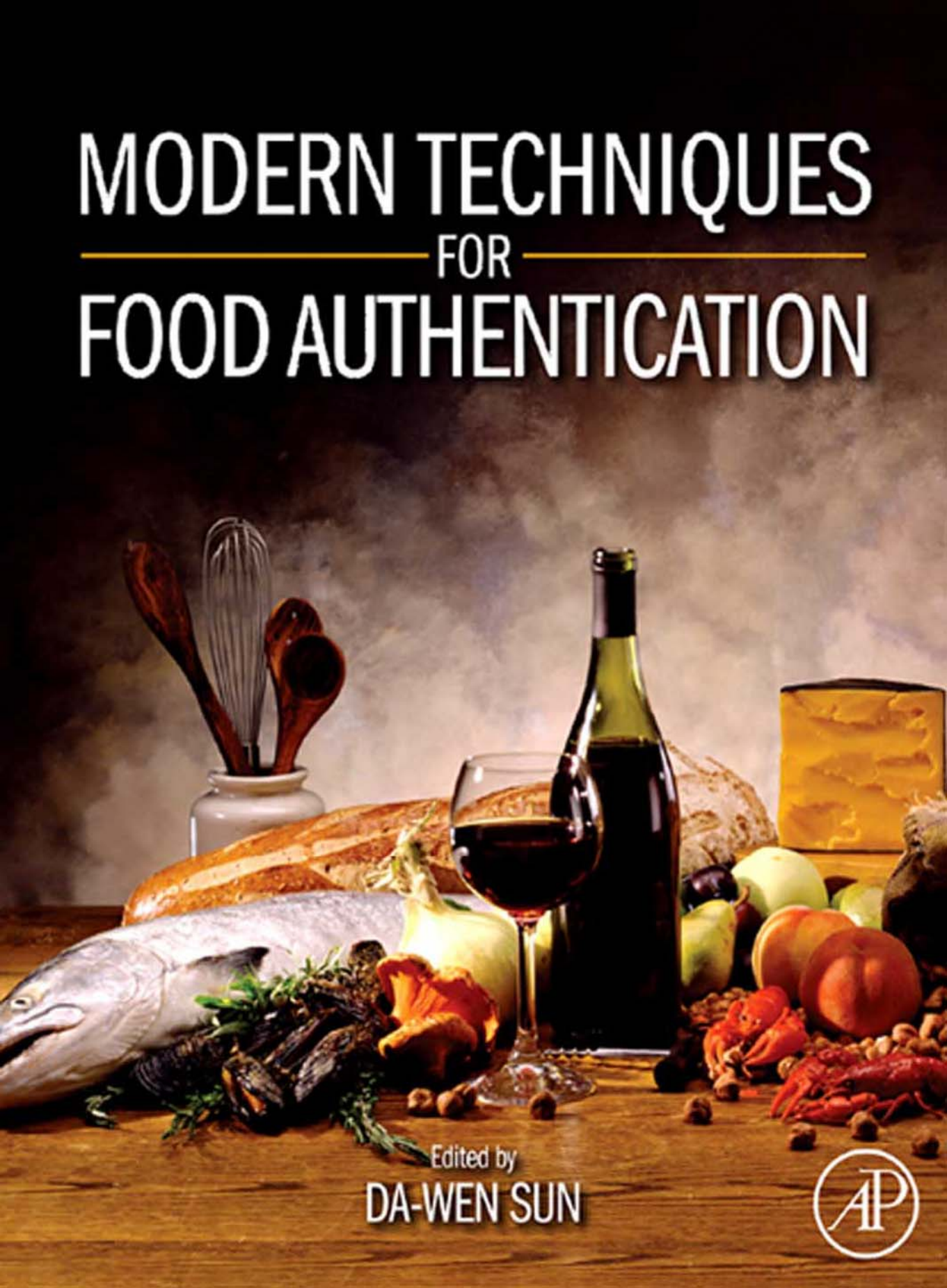

Edited by

DA-WEN SUN

This page intentionally left blank

Modern Techniques for Food Authentication

Edited by
Da-Wen Sun
Director of the Food Refrigeration and
Computerised Food Technology Research Group
National University of Ireland, Dublin
(University College Dublin)
Agriculture and Food Science Centre
Belfield
Dublin 4
Ireland

AMSTERDAM • BOSTON • HEIDELBERG • LONDON • NEW YORK • OXFORD
PARIS • SAN DIEGO • SAN FRANCISCO • SINGAPORE • SYDNEY • TOKYO
Academic Press is an imprint of Elsevier

Academic Press is an imprint of Elsevier
30 Corporate Drive, Suite 400, Burlington, MA 01803, USA
84 Theobald's Road, London WC1X 8RR, UK
525 B Street, Suite 1900, San Diego, CA 92101-4495, USA
360 Park Avenue South, New York, NY 10010-1710, USA

First edition 2008

British Library Cataloguing in Publication Data
A catalogue record for this book is available from the British Library

Library of Congress Cataloging in Publication Data
A catalog record for this book is available from the Library of Congress

ISBN: 978-0-12-374085-4

For information on all Academic Press publications
visit our web site at http://elsevierdirect.com

Typeset by Charon Tec Ltd., A Macmillan Company. (www.macmillansolutions.com)

Printed and bound in Canada

08 09 10 11 12 10 9 8 7 6 5 4 3 2 1

Contents

This page intentionally left blank

About the Editor

Born in Southern China, Professor Da-Wen Sun is an internationally recognized figure for his leadership in food engineering research and education. His main research activities include cooling, drying and refrigeration processes and systems, the quality and safety of food products, bioprocess simulation and optimization, and computer vision technology. In particular, his innovative studies on the vacuum cooling of cooked meats, pizza quality inspection by computer vision, and edible films for shelf-life extension of fruit and vegetables have been widely reported in the national and international media. Results of his work have been published in over 180 peer-reviewed journal papers and more than 200 conference papers.

He received a first-class BSc Honors and MSc in Mechanical Engineering and a PhD in Chemical Engineering in China before working in various universities in Europe. He became the first Chinese national to be permanently employed in an Irish University when he was appointed College Lecturer at the National University of Ireland, Dublin (University College Dublin) in 1995; he was then continuously promoted in the shortest possible time to Senior Lecturer, Associate Professor and full Professor. Dr Sun is now Professor of Food and Biosystems Engineering and Director of the Food Refrigeration and Computerized Food Technology Research Group in University College Dublin.

As a leading educator in food engineering, Professor Sun has significantly contributed to the field of food engineering. He has trained many PhD students, who have made their own contributions to the industry and academia. He has also given lectures on advances in food engineering on a regular basis in academic institutions internationally, and delivered keynote speeches at international conferences. As a recognized authority in food engineering, he has been conferred adjunct/visiting/consulting professorships by ten top universities in China, including Zhejiang University, Shanghai

Jiaotong University, Harbin Institute of Technology, China Agricultural University, South China University of Technology, Southern Yangtze University. In recognition of his significant contribution to food engineering worldwide, and for his outstanding leadership in the field, the International Commission of Agricultural Engineering (CIGR) awarded him the CIGR Merit Award in 2000 and again in 2006; the Institution of Mechanical Engineers (IMechE) based in the UK named him "Food Engineer of the Year 2004".

He is a Fellow of the Institution of Agricultural Engineers. He has also received numerous awards for teaching and research excellence, including the President's Research Fellowship, and has twice received the President's Research Award of University College Dublin. He is a member of CIGR Executive Board and Honorary Vice-President of CIGR, Editor-in-Chief of *Food and Bioprocess Technology – an International Journal* (Springer), Series Editor of the "Contemporary Food Engineering" book series (CRC Press/Taylor & Francis), former Editor of the *Journal of Food Engineering* (Elsevier), and editorial board member for the *Journal of Food Process Engineering* (Blackwell), *Sensing and Instrumentation for Food Quality and Safety* (Springer) and *Czech Journal of Food Sciences*. He is also a Chartered Engineer registered in the UK Engineering Council.

Contributors

Ioannis S. Arvanitoyannis (Ch. 17), Department of Agriculture, Icthyology and Aquatic Environment, School of Agricultural Sciences, University of Thessaly, Nea Ionia Magnesias, 38446 Volos, Hellas (Greece)

Vincent Baeten (Ch. 3, 4), Quality Department of Agricultural Products, Agricultural Research Centre, Chaussee de Namur 24, 5030 Gembloux, Belgium

Ángel Maquieira Catala (Ch. 13), Universidad Politécnica de Valencia, Departamento de Química, Camino de Vera s/n, 46071 Valencia, Spain

Alejandro Cifuentes (Ch. 14), Department of Food Analysis, Institute of Industrial Fermentations (CSIC), Juan de la Cierva 3, 28006 Madrid, Spain

Pierre Dardenne (Ch. 4), Quality Department of Agricultural Products, Agricultural Research Centre, Chaussee de Namur 24, 5030 Gembloux, Belgium

Gerard Downey (Ch. 3, 4), Ashtown Food Research Centre, Teagasc, Ashtown, Dublin 15, Ireland

Eric Dufour (Ch. 2, 7), Unite de Recherche Typicite des Produits Alimentaires, ENITA de Clermont-Ferrant, Site de Marmilhat, BP 35, 63370 Lempdes, France

Juan Antonio Fernández Pierna (Ch. 2, 4), Quality Department of Agricultural Products, Agricultural Research Centre, Chaussee de Namur 24, 5030 Gembloux, Belgium

Virginia García-Cañas (Ch. 14), Department of Food Analysis, Institute of Industrial Fermentations (CSIC), Juan de la Cierva 3, 28006 Madrid, Spain

Gérard Gremaud (Ch. 9), Office fédéral de la santé publique, Protection des consommateurs, Division sûreté des denrées alimentaires, Schwarzenburgstrasse 165, 3097 Liebefeld, CH-3003 Berne, Switzerland

Andreas Hilkert (Ch. 9), Termo Fisher Scientific, Hanna-Kunath Strasse 11, D-28199 Bremen, Germany

Chang-Wei Hsieh (Ch. 8), Department of Medicinal Botany and Healthcare, Da Yeh University, 112 Shan Jiau Road, Dah Tsuen, Chang Hwa 515, Taiwan

Joseph Irudayaraj (Ch. 6), Agricultrual & Biological Engineering, Purdue University, 225 S. University Street, West Lafayette, IN 47907-2093, USA

Romdhane Karoui (Ch. 2, 7), Unite de Recherche Typicite des Produits Alimentaires, ENITA de Clermont-Ferrant, Site de Marmilhat, BP 35, 63370 Lempdes, France

Ramazan Kizil (Ch. 6), ITU Campus of Ayazaga, Faculty of Chemical Engineering, Istanbul Technical University, 34469 Maslak, Istanbul, Turkey

Wen-Ching Ko (Ch. 8), Department of Bioindustrial Technology, Da Yeh University, 112 Shan Jiau Road, Dah Tsuen, Chang Hwa 515, Taiwan

Oi-Ming Lai (Ch. 15), Department of Biotechnology, Faculty of Food Science & Biotechnology, University Putra Malaysia, UPM, 43400 Serdang, Selangor, Malaysia

Riccardo Leardi (Ch. 16), Department of Pharmaceutical & Food Chemistry & Technology, University of Genoa, Via Brigata Salerno (Ponte), I-16147 Genoa, Italy

Robert E. Leven (Ch. 12), Department of Food Science, University of Massachusetts, Amherst, MA 01003, USA

Seong-Koon Lo (Ch. 15), Department of Biotechnology, Faculty of Food Science & Biotechnology, University Putra Malaysia, UPM, 43400 Serdang, Selangor, Malaysia

Marena Manley (Ch. 3, 4), Department of Food Science, Stellenbosch University, Private Bag X1, Matieland (Stellenbosch) 7602, South Africa

Isabel Martínez-Castro (Ch. 10), Departamento de Análisis Instrumental y Química Ambiental, Institute de Químíca Orgánica General (CSIC), Juan de la Cierva 3, E-28006 Madrid, Spain

Rosa Puchades (Ch. 13), Universidad Politécnica de Valencia, Departamento de Química, Camino de Vera s/n, 46071 Valencia, Spain

Ana I. Ruiz-Matute (Ch. 10), Departamento de Análisis Instrumental y Química Ambiental, Institute de Químíca Orgánica General (CSIC), Juan de la Cierva 3, E-28006 Madrid, Spain

Maria Luz Sanz (Ch. 10), Departamento de Análisis Instrumental y Química Ambiental, Institute de Químíca Orgánica General (CSIC), Juan de la Cierva 3, E-28006 Madrid, Spain

Agnes Sass-Kiss (Ch. 11), Central Food Research Institute, Unit of Analytics, Herman Otto 15, 1022 Budapest, Hungary

Andreas Schieber (Ch. 1), Department of Agricultural, Food and Nutritional Science, University of Alberta, 410 Ag/For Centre, Edmonton, Alberta T6G 2P5, Canada

Hartwig Schulz (Ch. 5), Institute of Plant Analysis, Federal Centre for Breeding Research on Cultivated Plants, Erwin-Baur Strasse 27, D-06484 Quedlinburg, Germany

Ana Cristina Soria (Ch. 10), Departamento de Análisis Instrumental y Química Ambiental, Institute de Químíca Orgánica General (CSIC), Juan de la Cierva 3, E-28006 Madrid, Spain

Preface

With the greater awareness of food safety and quality, consumers are increasingly demanding reassurance regarding the origin and content of their foods, while manufacturers need to be able to confirm the authenticity of components of their products and comply with government legislation. Therefore, protection of the rights of consumers and genuine food processors, and prevention of fraudulent or deceptive practices and the adulteration of food is an important and challenging issue facing the food industry. As a result, rapid scientific and technological advances have taken place in recent years regarding the determination of food authenticity. *Modern Techniques for Food Authentication* focuses on novel techniques developed and their recent applications in authenticating food products. The techniques covered in this book include various spectroscopic technologies, methods based on isotopic analysis and chromatography, and other techniques based on DNA, enzymatic analysis, electrophoresis and thermal methods.

Modern Techniques for Food Authentication is written by international peers who have both academic and professional credentials, highlighting the truly international nature of the work. Each chapter examines one type of technique, providing a comprehensive overview of the food authentication technology. *Modern Techniques for Food Authentication* aims to provide the engineer and technologist working in research, development and operations in the food industry with critical and readily accessible information on the art and science of food authentication technology. The book will also serve as an essential reference source to undergraduate and postgraduate students and researchers in universities and research institutions.

This page intentionally left blank

List of Abbreviations

AAA	aromatic amino acids
ADCS	automatic distillation control system
AFPL	amplified fragment polymorphism
AGE	agarose gel electrophoresis
Agm	Agmatine
AIJN	Association of the Industry of Juice and Nectars from Fruits and Vegetables of European Union
ANCA-MS	automated N/C (nitrogen/carbon) analyzer-mass spectrometry
ANN	artificial neural network
AOTF	acousto-optical tunable filter
APCI	atmospheric pressure chemical ionization
As	asymmetry factor
ATR	attenuated total reflectance
Bar	*Bar*, marker gene conferring resistance to the non-selective herbicide phosphinothricin or PPT
BHA	3-tert-butyl-4-hydroxy-anisole
BHT	2,6-di-tert-butyl-4-methylphenol
Bla	*Bla*, marker gene originating from a cloning vector that encodes a beta-lactamase not expressed in corn
BP-ANN	back-propagation artificial neural network
BSE	bovine spongiform encephalopathy
Bt	*Bacillus thuringiensis*
C16:0	palmitic acid
C18:0	stearic acid
C18:1	oleic acid
CAM	Crassulacean acid metabolism
CaMV	tobacco mosaic virus
CaMVX35S	cauliflower mosaic virus promoter
CART	classification and regression trees
CB	cocoa butter
CBE	cocoa butter equivalents

CBM	castor bean meal
CCA	canonical correlation analysis
CCD	charge-coupled device
CCSWA	common component and specific weights analysis
CDT	Canyon Diablo Troilite
CE	capillary electrophoresis
CEC	capillary electrochromatography
CGE	capillary gel electrophoresis
CI	chemical ionization
CIEF	capillary isoelectrofocusing
CLA	cluster linear analysis
CP	cloud point
Cry9C	gene encoding one of several crystalline protein delta toxins from *Bacillus thuringiensis*
CryIA(b)	gene encoding one of several crystalline protein delta toxins from *Bacillus thuringiensis*
CS	corn syrup
CTAB	hexadecyltrimethyl-ammonium bromide
CV	coefficient of variation
CVA	canonical variate analysis
Cy3	a cyanine reporter dye that fluoresces orange with a peak emission at ~550 nm
Cy5	a cyanine reporter dye that fluoresces red with a peak emission at ~670 nm
DA	discriminant analysis
DAG	diacylglycerol
DETA	dielectric thermal analysis
DFA	difructose anhydride
DGGE	denaturing gradient gel electrophoresis
DIG	digoxygenin
DMA	dynamic mechanical analysis
DNA	deoxyribonucleic acid
dNTP5′	deoxynucleotide phosphate
DOSC	direct orthogonal signal correction
DPLS	discriminant partial least squares
DSC	differential scanning calorimetry
dsPCR	double-stranded PCR
DTA	differential thermal analysis
DTGS	deuterated triglycine sulfate
EA-IRMS	elemental analyzer isotope ratio mass spectrometry
EB	ethidium bromide
EB-AGE	ethidium bromide-agarose gel electrophoresis
ECD	electron-capture detector
ECL	electrochemiluminescence
EDTA	ethylene-diamine-tetraacetic-acid

EGD	evolved gas detection
EI	electron impact
ELISA	enzyme-linked immunosorbent assay
ELS	evaporative light-scattering
ENZ	enzyme-specific sequence
EPSPS	5-enolpyruvylshikimate-3-phosphate synthase
EQCS	European Quality Control System
ESI	electrospray ionization
ESI-MS/MS	electrospray ionization-tandem mass spectrometry
EU	European Union
EVA	evolved gas analysis
EVOO	extra-virgin olive oil
EXT	extension
FA	factor analysis
FAB	fast atom bombardment
FAM	6-carboxyfluorescein
FAME	fatty acid methyl esters
FAN	free amino nitrogen
FDA	factorial discriminant analysis
FFA	free fatty acids
FFFS	front-face fluorescence spectroscopy
FG	flavanone glycosides
FID	flame ionization detector
FINS	forensically informative nucleotide sequencing
FITC	fluorescein isothiocianate
FMF	fully methoxylated flavones
FMRP	fluorescent Maillard reaction products
FSCE	free solution capillary electrophoresis
FT-IR	Fourier transform infrared
FT-MIR	Fourier transform mid-infrared
FT-NIR	Fourier transform near-infrared
FT-NIRM	Fourier transform near-infrared microscopy
FTR	Fourier transform Raman
GA	genetic algorithms
GC	gas chromatography
GC-IRMS	gas chromatography with isotope ratio mass spectrometry
GC-C-IRMS	gas chromatography combustion isotope ratio mass spectrometry
GC×GC	comprehensive bidimensional gas chromatography
GC-MS	gas chromatography coupled with mass spectrometry
GC-P-IRMS	gas chromatography pyrolysis isotope ratio mass spectrometry
GC-TC-IRMS	gas chromatography high-temperature conversion isotope ratio mass spectrometry
GDS	glucono-δ-lactone

GLC	gas-liquid chromatography
GM	genetically modified
GMO	genetically modified organism
GOX	gene encoding glucose oxidase
GPC	gel-permeation chromatography
GSC	gas-solid chromatography
h	peak height
H	height equivalent to theoretical plate
HCA	hierarchical cluster analysis
HEC	2-hydroxyethyl cellulose
HETP	height equivalent to theoretical plate
HEX	a reporter dye with peak emission at 556 nm
HFCS	high-fructose corn syrup
HLA	histocompatibility complex
Hm	high mobility
HPAEC-PAD	high-performance anion-exchange chromatography
HPDSC	high-performance differential scanning calorimetry
HPGC	high-performance gas chromatography
HPLC	high-performance liquid chromatography
HPLC-ESI-MS/MS high performance liquid chromatography coupled with electrospray	ionization-tandem mass spectrometry
HPLC-GC	high performance liquid chromatographic and gas chromatographic system
HR-MAS-NMR	high-resolution magic angle spinning nuclear magnetic resonance
HRP-SA	horse radish peroxidase-streptavidin conjugate
HS	headspace
HSM	hot-stage microscopy
IBa	i-butyl amine
ICP-MS	inductively coupled plasma mass spectrometry (ICP)-MS
ICTA	International Confederation for Thermal Analysis
ICTAC	International Confederation for Thermal Analysis and Calorimetry
i.d.	internal diameter
IEF	isoelectric focusing
IOOC	International Olive Oil Council
iPCR	inverse PCR
IR	infrared
IRMS	isotope ratio mass spectrometry
IS	internal standard
IT	ion trap
IV	iodine value

k	capacity factor
k′	average of the capacity factors
k	retention factor
k-NN	k-nearest neighbors
L	length of column
LC	liquid chromatography
LDA	linear discriminant analysis
LDR	ligation detection reaction
LED	light-emitting diode
LIF	laser-induced fluorescence
LOO	dioleoyl-linoleyl glycerol
LPH	liquid phase hybridization
LS	light-scattering
2MeBa	2-methylbutylamine
3MeBa	3-methylbutylamine
MBM	meat and bone meal
MDA	multiple discriminant analysis
MDGC	multidimensional gas chromatography
MEKC	micellar electrokinetic chromatography
MGB	minor groove binding
MIR	mid-infrared
MPCR-MHA	PCR/membrane hybridization assay
MRE	meal ready to eat
MS	mass spectrometry
MSC	multiplicative scatter correction
MS/MS	tandem mass spectrometry
mtDNA	mitochondrial DNA
MW	molecular weight
N	theoretical plate number
NA	nucleic acid
Nd:YAG	neodymium-doped yttrium aluminium garnet
NIR	near-infrared
NMR	nuclear magnetic resonance
NOS	nopaline synthase
NOS-P	promoter for nopaline synthase from *Agrobactrium tumefaciens*
NOS-T	terminator for nopaline synthase from *Agrobactrium tumefaciens*
NPN	non-protein nitrogen
nptII	neomycin phosphotransferase II, marker gene
OSC	orthogonal signal correction
OWAVEC	orthogonal wavelet correction
P&T	purge-and-trap
PAD	pulsed amperometric detector
PAGE	polyacrylamide gel electrophoresis

PC	principal component
PCA	principal component analysis
PCR	principal component regression
PCR	polymerase chain reaction
PDA	photo diode array
PDB	PeeDee belemnite
PDO	protected designation of origin
PEPC	phosphoenolpyruvate carboxylase
PGI	protected geographical indication
Phe	phenylethylamine
PLP	dipalmityl-linoleyl glycerol
PLS	palmityl-linoleyl-stearyl glycerol
PLS	partial least squares
PMF	polymethoxylated flavones
PNA	peptide nucleic acid
PNN	probalistic neural network methods
PNPP	para-nitro-phenyl phosphate
POP	2-oleopalmitin
POP	dipalmityl-oleoyl glycerol
POS	2-oleopalmitostearin
POS	oleoyl-palmitylstearylglycerol
PPP	tripalmitin
PPT	non-selective herbicide phosphinothricin
PSS	distearyl-palmityl glycerol
PTV	programmed temperature vaporizer
QC-PCR	quantitative competitive PCR
QDA	quadratic discriminant analysis
QMS	quadrupole mass spectrometry
R^2	coefficient of determination
R_s	resolution
RAPD	random amplified polymorphic DNA
RBF	radial basis Gaussian function
REs	restriction enzymes
RFLP	restriction fragment length polymorphism
RHOD	a rhodamine reporter dye with peak emission at 550 nm
RI	refractive index
RMS	root mean square
RMSECV	root mean standard error in cross-validation
RMSEP	root mean square error in prediction
RP	reversed-phase
RPD	ratio of standard deviation to root mean square error of prediction
RPD	ratio of standard deviation to standard error of prediction
rRNA	ribosomal RNA
RSD	relative standard deviation

SA	streptavidin
SCIRA	stable carbon isotope ratio analysis
SD	standard deviation
SDE	simultaneous distillation-extraction
SDS	sodium dodecyl sulphate
SECV	standard error of cross-validation
SEL	standard error of laboratory
SEP	standard error of prediction
SFC	solid fat content
SFLP	satellite fragment length polymorphism
SIMCA	soft independent modeling of class analogy
SINEs	short interspersed elements
SLAP	standard Light Arctic Precipitation
SLDA	stepwise linear discriminant analysis
SOS	distearyl-oleoyl glycerol
SOS	distearyl-oleoyl glycerol
SMP	slip melting point
S/N	signal-to-noise
SNIF	site-specific natural isotope fractionation
SNIP-IRMS	specific natural isotope profile studied by isotope ratio mass spectrometry
SNV	standard normal variate
SOS	2-oleodistearin
SPME	solid-phase microextraction
SSCP	single strand conformation polymorphism
ssDNA	single-stranded DNA
SVM	support vector machines
t_R	retention time
t_R'	corrected retention time
t_0	column dead time or hold-uptime
TA	thermal analysis
TAG	triacylglycerol
TAMRA	6-carboxy-N,N,N′,N′-tetramethylrhodamine quencher dye
TBARS	thiobarbituric acid reactive substances
TBR	tris-2,2′-bipyridy-ruthenium II
TD	thermal desorption
TET	tetrachloro-6-carboxyfluorescein
TG	thermogravimetric analysis
TIC	total ion current
TIMS	thermo-ionization mass spectrometry
TL	thermoluminescence
TLC	thin-layer chromatography
TM	thermomagnetometry
TMA	thermomechanical analysis

TMDSC	temperature-modulated differential scanning calorimetry
TMS	trimethylsilyl
TN	total nitrogen
ToF	time-of-flight
TPA	tris-propylamine
TS	target sequence
TS	thermosonimetry
TSE	transmissible spongiform encephalopathy
TSG	Traditional Specialty Guaranteed
Tyr	tyramine
UA	universal array
Unk	unknown
UPLC	ultra performance liquid chromatography
USFDA	United States Food and Drug Administration
UV	ultraviolet
UV/VIS	ultraviolet visible
V_R	retention volume
VIC	proprietary dye, Applied Biosystems
VIS	visible
VOO	virgin olive oil
V-SMOW	Vienna Standard Mean Ocean Water
w	peak width
$w_{1/2}$	peak width measured at half peak height
$w_{4,4\%}$	peak width measured at 4.4% peak height
WB	Warner-Bratzler
WILMA	wavelet interface to linear modeling analysis
WSN	water-soluble nitrogen
α	separation factor or relative retention or selectivity

1

Introduction to Food Authentication

Andreas Schieber

Introduction

Profit margins in food production are usually relatively narrow compared with other industrial sectors such as the pharmaceutical industry. Therefore, it is not surprising that attempts by some unscrupulous suppliers to maximize revenues by counterfeiting and adulterating practices are a concomitant phenomenon of the food trade, as evidenced by, for example, the use of the banned dyes Sudan I (Figure 1.1a) and Para Red (Figure 1.1b) in Worcestershire Sauce in the United Kingdom (Rayner, 2006), or the fraudulent use of slaughterhouse waste in meat products recently detected

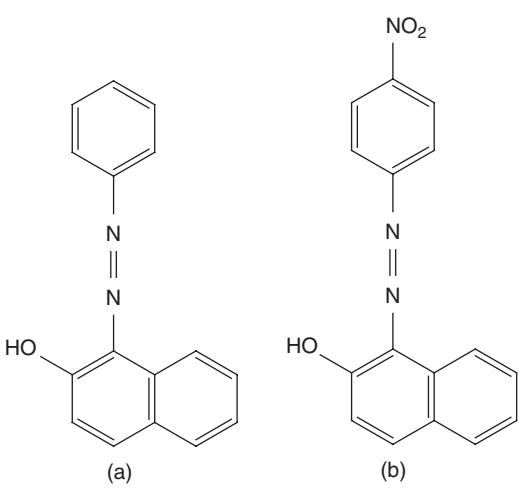

Figure 1.1 Structure of the banned azo dyes (a) Sudan I and (b) Para Red.

Modern Techniques for Food Authentication
ISBN: 978-0-12-374085-4

in Germany, which entailed extensive media coverage (see, for example, Friedrich, 2006). In his very recent treatise on adulteration of food and wine, Winterhalter (2007a) also mentions the *toxic oil syndrome* that occurred in Spain in 1981, and the addition of *ethylene glycol* to wine by some Austrian winemakers in 1985.

However, the adulteration of foods is an age-old problem rather than a feature of our time, and has a long and inglorious history. In Ancient Rome, foods as well as medicines and cosmetics were often subject to adulteration in various forms. As foods and other natural products were traded throughout the large Roman Empire, they were prone to spoilage during shipment and storage. Thus, common methods of adulteration were mixing of spoilt food with fresher food, substitution of expensive goods from abroad with inferior local products, or the fraudulent introduction of coloring or masking additives. Besides grains, which were a staple food at that time, spices and wine were affected mostly by adulterating practices. An excellent summary of the adulteration of food and other natural products in Ancient Rome has been published by Bush (2002).

In the Middle Ages the food trade was controlled by so-called *guilds* (or "gilds"), which can be considered as organizations acting for the defense of trade interests. Punishment at that time was rigorous and cruel. In Nuremberg in the fifteenth century, an adulterator of saffron was burnt over his own produce; others were buried alive or their eyes were gouged out. Other forms of punishment comprised expulsion, whipping, cutting off ears, and drowning. In some cases offenders were forced to consume their adulterated food until they died (Grüne, 2002). Later, French King Louis XIV, the "Sun King", imposed capital punishment for the adulteration of wine by the addition of pokeweed (*Phytolacca americana* L.). Today, such adulteration would be easily detected because pokeweed and grapes contain two different types of mutually exclusive pigments, betalains and anthocyanins.

While grains, bread, wine, milk and spices had been typical candidates for adulteration since antiquity, fraudulent practices were later extended to other luxurious food commodities imported from overseas, such as *tea*, *coffee* and *sugar*. For example, tea (*Camellia sinensis* L. O. Kuntze) leaves were often mixed with spent leaves or leaves from plant species other than tea. Coffee, which was an extremely expensive commodity at that time, was adulterated with chicory, roasted wheat or burnt sugar. Sugar might be blended with sand. While the adulteration of coffee and tea was fraudulent, it did not necessarily pose a risk to human health – unlike the addition of poisonous coloring substances to confectionery, which frequently contained lead, copper or mercury salts to make them more attractive to children. A review on dyes and pigments as food additives and adulterants is given by Davies (2005). Brewers often added mixtures of bitter compounds, some containing preparations of poison nut-tree (*Strychnos nux-vomica* L.) (Coley, 2005). Compared with today, food adulteration was relatively easy in former times for at least two reasons: first, knowledge of the composition of food was then barely developed, and secondly, analytical chemistry was still in its infancy even in the nineteenth century. As a consequence, customers were largely unaware of fraudulent practices. *Frederick Accum* (1769–1838), a German chemist who had come to London in 1793, was the first to make the public conscious of the extent of food adulteration. In 1820 he published his book *A Treatise on Adulterations of Food and Culinary Poisons*. Thus he can be

considered one of the pioneers of food authentication. *Arthur Hill Hassall* (1817–1894), a British physician, applied *microscopy* to detect the presence of chicory in coffee. Neglected as an analytical tool until then, the microscope became increasingly important for the identification even of traces of adulterants, living or dead insects, and foreign organic matter. Other adulterants for bulk and weight as well as for color, taste and smell that were identified by Hassall, also using chemical methods, included sawdust and vermillion in Cayenne pepper, or in wheat, potato and rice flour, as well as lead chromate and turmeric in custard powder (Coley, 2005). In view of the ample evidence of food adulteration, the first Food Adulteration Act was passed in 1860 and revised in 1872. Two years later, Hassall became the first President of the newly founded Society of Public Analysts. Further milestones in British food legislation are given by Sumar and Ismail (1995) and Coley (2005).

Both Accum's and Hassall's work had revealed the tremendous extent of food adulteration. The problem was drastically aggravated with the advent of the industrial revolution. The availability of jobs in the big towns led to a rural exodus, and people were no longer self-sufficient but increasingly reliant on the food trade and extended supply chains. Despite improved methods of food processing, the increased demand for food caused by the rapidly growing urban population entailed shortages of materials. Consequently, in an effort to keep costs as low as possible, food items were often bulked up with questionable fillers. Common types of food adulteration included the addition of flour to sausages to enhance their water-binding capacity, the addition of colorants to improve the visual appearance of foods, the extension of flour with gypsum and chalk, and the watering of milk. Counterfeiting of milk in particular posed a tremendous problem regarding public health, and contributed greatly to infant mortality at that time (Teuteberg, 1995). In Germany the first Food Act was passed in 1879; however, this was not without its problems, especially because of the lack of definitions, quality criteria and enforcement regulations. In 1881 the first food inspection office was founded in Münster, and in 1885 Bavarian chemists defined uniform methods of food analysis. In 1894 a new scientific discipline, the "food chemist", was established as a profession. For a comprehensive treatise of the beginnings of food inspection in Germany, the reader is referred to Teuteberg (1995) and Grüne (2002).

From colonial times until the mid- to late nineteenth century, food (and drug) regulation in the United States was mainly enacted at state and local levels (Law, 2004). As in the United Kingdom and Germany, the extent of food regulation by the state during the second half of the nineteenth century also increased in the United States, for a number of reasons – including the growing variety and complexity of available foods, the increased concern of consumers about the quality and safety of "new" food items, and the introduction of preservatives (which also allowed masking of food deterioration).

On one hand, significant progress in natural sciences, especially in biology, microbiology and chemistry, led to increased crop yields through the use of fertilizers and pesticides as well as to improved food quality – for example, through the fortification of feed with vitamins and other micronutrients, development of antimicrobials and vaccines, and improved methods of food preservation (Cuthbertson, 1991). On the other hand, advances in analytical chemistry provided new scientific knowledge about the composition and properties of food which could be (ab)used for fraudulent

purposes. In his treatise on food additives, Fennema (1987) discerns three phases of the history of the usage of food additives: phase I, from ancient times to about 1820, when chemicals were added to foods primarily for respectable reasons; phase II, from the early 1800s to about 1820, when intentional food adulteration in the United States as well as several other countries increased greatly in frequency and seriousness; and phase III, from 1920 to 1950, when regulatory pressures and effective methods of analysis reduced the frequency and seriousness of this problem to acceptable levels. However, it can be argued that not even the smallest level of food adulteration can be considered acceptable.

The severe devastation and serious interruption of food production in many countries as a consequence of World War II caused politicians and economists to improve agricultural trade as an indispensable prerequisite for rapid reconstruction and assured food supplies. In this context, the creation of the *Food and Agricultural Organization* (FAO) in 1945 and the *World Health Organization* (WHO) in 1948 marked important milestones. In the 1950s, the increasing and sometimes insufficiently controlled use of food additives was a major concern. Therefore, the two organizations established joint expert meetings on nutrition and related areas, such as the Joint FAO/WHO Conference on Food Additives in 1955. Further activities consisted of work on standards for food commodities such as cheese, fresh fruit and vegetables. In the early 1960s, the *Codex Alimentarius Commission* (*Codex*) was created as an intergovernmental commission to establish internationally recommended food standards; codes of hygienic practice; limits for food additives, pesticide and veterinary drug residues in foods, and for contaminants; food labeling; and others. Thus, the work of the *Codex* over the past 45 years has led to far more than 200 standards for different food products, a general standard for food labeling, and guidelines on food sampling and analysis, to mention just a few (Lupien, 2002).

In 1992, the European Union introduced the terms *Protected Designation of Origin* (PDO), *Protected Geographical Indication* (PGI) and *Traditional Specialty Guaranteed* (TSG) to encourage diverse agricultural production on one hand and to protect product names from misuse and imitation on the other (Council Regulation (EEC) No 2081/92 of 14 July 1992). This regulation was recently replaced by Council Regulation (EC) No 510/2006 of 20 March 2006 on the protection of geographical indications and designations of origin for agricultural products and foodstuffs. According to article 2 of the latter regulation, "designation of origin" means the name of a region, a specific place or, in exceptional cases, a country, used to describe an agricultural product or a foodstuff originating in that region, specific place or country, the quality or characteristics of which are essential or exclusively due to a particular geographical environment with its inherent natural and human factors, and the production, processing and preparation of which take place in the defined geographical area. The term "geographical indication" is used to describe an agricultural product or a foodstuff originating in that region, specific place or country and which possesses a specific quality, reputation or other characteristics attributable to that geographical origin, and the production and/or processing and/or preparation of which take place in the defined geographical area. In other words, a PDO covers the term used to describe foodstuffs which are produced, processed and prepared in a given geographical and using recognized know-how. In the

case of the PGI, the geographical link must occur in at least one of the stages of production, processing or preparation. Allgäuer Emmentaler cheese (Germany), Prosciutto di Parma ham (Italy), Camembert de Normandie (France) and Feta cheese (Greece) are examples of PDOs, whereas Styrian pumpkin seed oil (Austria) and Newcastle brown ale (United Kingdom) are PGIs. "Traditional Specialties Guaranteed" are subject to Council Regulation (EC) No 509/2006 of March 2006, which defines such products as traditional agricultural products or foodstuffs recognized by the Community for their specific character through their registration under this regulation. Thus a TSG does not refer to the origin, but highlights traditional character, either in the composition or means of production. Typical TSGs are Mozzarella cheese from Italy and Jamón Serrano (Serrano ham) from Spain. In view of these regulations, it becomes quite evident that not only control of the quality and authenticity with respect to the composition of a given product but also the determination of its geographical origin has become a matter of increasing attention.

The heightened interest of consumers in the provenance of the food they purchase and ingest is also a consequence of food scandals and scares. It is unlikely that the less draconic punishments compared with previous times has led to food adulteration still being a common feature today. Too often bad publicity is the most severe punishment for a producer or seller, and at the same time is that feared most by perpetrators. Fraud occurs in very diverse ways, and often the methods applied in adulteration are at least as sophisticated as those needed to detect it. Extension of fruit juices with water, blending of honey with high-fructose corn syrup, fraudulent claims about the origin, composition and treatment of products, and admixture of spoilt produce with fresh foods are only some examples. Selected cases of food adulteration and food scandals from 1981 to 2006 are listed in Table 1.1. Sophisticated analytical methods represent the most appropriate solution to food adulteration.

Table 1.1 Selected cases of food adulteration and food scandals* 1981–2006

1981	"Toxic oil syndrome": Consumption of rapeseed oil denatured with aniline caused the death of hundreds of people
1985	Ethylene glycol, a frost protection agent with a sweet taste, was added to wine to upgrade it to table-wine quality
1985	Usage of spoilt eggs in pasta products
Since 1980s	Mad cow disease
1994	Lead tetroxide in chilli powder
1996	Synthetic "apple juice" concentrate
1999	Dioxin in feed
2001	Hormones, vaccines and antibiotics in pork
2002	Antibiotics in honey from China
2003	Adulterated wine (extended with water; added alcohol, coloring, and sugar) from Eastern Europe
2004	Banned dyes used in spices
2005	Slaughterhouse waste misbranded as meat
2006	Traces of genetically modified rice detected in conventional rice in Europe

*In this context it should be noted that the presence of acrylamide in heated food, which was first detected in 2002, cannot be considered a food scandal. Acrylamide is mainly formed during the Maillard reaction or by pyrolysis of proteins (for a review, see Claus *et al.*, 2008).

Modern techniques in food authentication

Here, a brief survey of the most important analytical techniques used in food authentication is given. In the past two decades a large number of contributions, including numerous review articles dealing with quality and authenticity control, has been published, taking a technique-based (e.g. Cordella *et al*., 2002; Martinez *et al*., 2003; Reid *et al*., 2006), a compound-based (e.g. Prodolliet and Hischenhuber, 1998) or a commodity-based (e.g. Ashurst and Dennis, 1996; Dennis, 1998; Fügel *et al*., 2005a; García-González and Aparicio, 2006) approach, or combinations thereof (Lees, 2003). In view of the title and structure of this book, a technique-oriented presentation is given preference in this introductory chapter. Since each method will be discussed in much more detail in the following chapters, only selected aspects can be discussed in this treatise. Particular attention will be paid to chromatographic and spectroscopic techniques, stable isotope analysis, enzymatic and immunological as well as DNA methods. Where appropriate, recent applications will be presented to demonstrate the scientific progress that has been made – without, however, claiming full coverage of a particular area.

Chromatographic techniques

Chromatographic techniques in their various forms are amongst the most important methods used in food analysis. The term "chromatography" encompasses techniques based on adsorption and/or partition of analytes between a mobile and a stationary phase. They are usually classified according to the character of the stationary and the mobile phases, the form of the stationary phase and the driving forces of separation (Forgács and Cserháti, 2003). Thus, *gas chromatography* (GC), either performed as gas-liquid chromatography (GLC) or gas-solid chromatography (GSC), represents a method where the mobile phase is gaseous. In liquid chromatography (LC), usually referred to as *high-performance liquid chromatography* (HPLC), the solid stationary phase is applied in a column and the mobile phase is pumped through the column. *Thin-layer chromatography* (TLC) systems consist of a planar solid phase and a liquid mobile phase. Owing to the superior capability of GC and HPLC, the latter technique has only rarely been used for authentication purposes – for example, in differentiating between authentic and adulterated Noni (*Morinda citrifolia* L.) juices (Lachenmeier *et al*., 2006) and fingerprinting of flavonoids and saponins from *Passiflora* species (Birk *et al*., 2005).

Gas chromotography

For analytes to be determined by *gas chromatography*, they need to be easily vaporized without being decomposed. Therefore, volatile food constituents such as aroma compounds are particularly suitable candidates for GC analysis, mostly in combination with mass spectrometric detection. According to a review published by Cordella *et al*. (2002), GC-MS coupling is the most widely used technique (>50%), followed by GC coupled to other types of detectors. Mass spectrometers are highly useful detectors, since in many instances they provide structural information which cannot

be obtained with most other detectors. Standardization of the energy impact in electron ionization (EI) mass spectrometry has resulted in powerful databases which can be used for comparison of fragments and identification of analytes. Sample preparation for gas chromatography includes extraction and purification, which may be very tedious in some instances because of the complex food matrices. Non-volatile compounds need to be derivatized prior to separation by GC. In this context, the conversion of fatty acids to their methyl esters or transesterification of triacylglycerides using sodium methylate, the reduction and acylation of sugars, and esterification and acylation of amino acids are well-known examples.

Gas chromatography represents an analytical technique particularly suitable for the separation and characterization of food flavor and essential oil analysis, especially since the authentication of genuine flavors has become an important issue in food analysis. Owing to the pronounced complexity of natural flavors, which may exist as enantiomers, highly sophisticated techniques such as enantio-capillary GC and GC-IRMS have been demonstrated to be extremely helpful for stereospecific analysis and the determination of flavor authenticity (Mosandl, 2004). Other chiral food constituents such as hydroxy acids, amino acids and catechins may also be determined using capillary GC as quality markers of cocoa beans (Caligiani *et al*., 2007) and beer (Erbe and Brückner, 2000; Junge *et al*., 2007). Reviews of applications of enantiomeric gas chromatography have been published by Schurig (2002) and He and Beesley (2005).

The advantages of gas chromatography consist mainly of its high separation capacity, velocity, reproducibility, sensitivity and versatility, as evidenced by numerous applications – for example, in food (Lehotay and Hajšlova, 2002) and environmental analysis (Santos and Galceran, 2003), forensic science (Jaiswal *et al*., 2006) and biomedical analysis (Leis *et al*., 2004). However, in many instances derivatization of the compounds to be determined is required, which is tedious and a potential source of error (Forgács and Cserháti, 2003).

High-performance liquid chromatography

High-performance liquid chromatography (HPLC) is one of the most versatile analytical techniques and is extremely widely used in food authentication, as both polar and non-polar compounds can be analyzed. In normal-phase HPLC polar stationary phases are used and the analytes separated using non-polar mobile phases, whereas reversed-phase (RP) HPLC is characterized by hydrophobic stationary phases, e.g. C_{18} or C_8, and polar eluents. Sample constituents can be separated either isocratically (i.e. using a constant eluent composition over time) or by gradient elution. The pronounced versatility of HPLC is also due to the large number of different types of detectors available. Single- or multiple-wavelength UV-Vis detectors are widely used in routine analysis. Diode array detectors simultaneously measure absorbance across a broad spectrum of wavelengths and may provide valuable information for the tentative identification of analytes. Fluorescence detectors are particularly useful for the determination of very low analyte levels. Electrochemical detection may provide high sensitivity and selectivity, and can be applied to the analysis of redox-active compounds. Refractive-index (RI) detectors are usually employed when analytes

do not show UV absorption, for example for the determination of sugars. Mass spectrometers, especially with electrospray ionization (ESI) and atmospheric pressure chemical ionization (APCI) interfaces, are increasingly used as detectors in food authenticity studies, owing to the information that can be obtained from LC-MS analyses. Sample preparation in HPLC analysis includes virtually the same steps as in gas chromatography, although, in contrast to GC, derivatization to make analytes volatile is not required. However, derivatization as part of sample preparation may be useful to increase retention of hydrophilic compounds in RP-HPLC and improve the sensitivity, for example by introducing UV-absorbing or fluorescent groups. As a comprehensive treatise of all possible applications is beyond the scope of this chapter, the determination of selected classes of compounds by HPLC for authentication purposes is given exemplarily in the following.

Amino acids

The profile of *amino acids* has been used for the control of the authenticity of several food commodities, such as fruit juices (Hammond, 1996), honey (Molan, 1996) and wine (Arvanitoyannis, 2003). Very recent HPLC applications include the characterization of amino acids in orange juice by LC/MS-MS (Gómez-Ariza *et al*., 2005), and discrimination of the botanical origin of honey (Cotte *et al*., 2004). The HPLC determination of *amino acid enantiomers* after derivatization with *o*-phthaldialdehyde and chiral thiols (Figure 1.2) has been fully automated and applied to a large number of foodstuffs (Brückner *et al*., 1995).

Organic acids

Determination of the fingerprint, contents and stereochemistry of *organic acids* may be very helpful in authenticity control. For example, the presence of D-malic acid or an unusual ratio of citric acid and isocitric acid may be indicative of adulteration of fruit

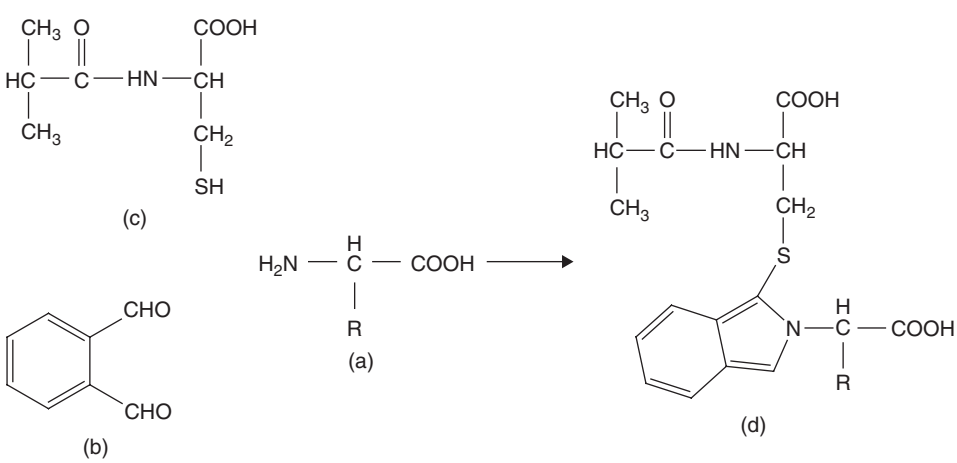

Figure 1.2 Derivatization of amino acids (a) with *o*-phthaldialdehyde (b) and chiral thiols such as *N*-isobutyryl-L-cystein (c). The diastereomeric isoindols (d) formed are analyzed by HPLC with fluorescence detection.

juices. In many instances, enzymic assays are the method of choice for their determination; however, various HPLC methods for the separation of organic acids have also been described (Pérez-Ruiz *et al*., 2004; Pundlik, 2004; Chinnici *et al*., 2005; Sáiz-Abajo *et al*., 2005). In some matrices, such as vinegar, HPLC may not be sufficient for a complete separation and needs to be complemented by another method (Cocchi *et al*., 2002). A very interesting approach to the simultaneous determination of organic acids, alcohols and metals in foods using HPLC with inductively coupled plasma atomic emission spectrometry has recently been reported (Paredes *et al*., 2006).

Polyphenolics, including anthocyanins

The term *polyphenolics* encompasses several subclasses of a group of secondary metabolites which occur virtually ubiquitously in plants. While at one time they were considered to be antinutritive compounds, polyphenolics are experiencing increased interest today, owing to their possible health benefits. From an analytical point of view, phenolic compounds have long been recognized as valuable tools in food authenticity studies (Engelhardt and Galensa, 1997). However, the limited availability of reference substances as well as the pronounced heterogeneity of this class of compounds represents a major problem in polyphenol analysis. Therefore, the preferred method used for their determination is reversed-phase HPLC, usually with diode array and mass spectrometric detection (LC-DAD-MS) (Merken and Beecher, 2000). Methods employing electrochemical detection have been summarized by Milbury (2001), and the application of RP-HPLC with Coularray® detection to the analysis of beverages and plant extracts has been reported by Jandera *et al*. (2005). Hyphenated techniques such as LC-DAD-MS provide useful structural information which is not obtained with most other methods of detection. Some recent applications in food authenticity control include the determination of polyphenolics in apple and pear fruits and products (Schieber *et al*., 2001, 2002a), strawberries (Hilt *et al*., 2003), honey (Tomás-Barberán *et al*., 2001; Dimitrova *et al*., 2007), apricot and pumpkin purées (Dragovic-Uzelac *et al*., 2005), black carrots (Kammerer *et al*., 2003) and barley and malt (Zimmermann and Galensa, 2007).

Triglycerides, carotenoids, tocopherols, and phytosterols

The predominant constituents of fatty oils are *triglycerides*, which mainly consist of *fatty acids*. While the determination of the fatty-acid profile, which is usually performed by GC in routine analysis, may be sufficient to detect comparatively simple cases of adulteration, a more comprehensive characterization of the triacylglycerides and the *unsaponifiable matter* is required in more "sophisticated" issues. Ulberth and Buchgraber (2000) as well as Kamm *et al*. (2001) extensively reviewed analytical techniques for establishing the authenticity of fats and oils. Intact triglycerides can be determined either by high-temperature gas chromatography or by RP-HPLC, which results in a fingerprint of high diagnostic value. Because of the high economic value of *olive oil* (*Olea europaea* L.) this food commodity has always been a target for adulteration, and consequently tremendous research efforts have been made in order to detect such fraudulent practices (for a recent review, see Arvanitoyannis and Vlachos, 2007). The admixture of *hazelnut oil* to olive oil represents a particular

problem, owing to the very similar profile of both the triglycerides and the unsaponifiable matter (Benitez-Sánchez *et al*., 2003). For the determination of the triglyceride composition by HPLC, the official IUPAC method 2324 has been used by the authors. For *phytosterol* analysis, HPLC is mainly used for purification of the sterol fractions, whereas individual compounds are separated and identified by GC-MS (see, for example, Zhang *et al*., 2006). The *tocopherol* profile can be determined by either normal-phase or reversed-phase liquid chromatography, the latter being advantageous with respect to column stability, reproducibility of retention times, and time required for equilibration. With respect to *carotenoid* analysis, C_{30} stationary phases are highly suitable for the separation even of geometrical isomers (Sander *et al*., 2000), and have also been used for the simultaneous determination of carotenes and tocopherols (Schieber *et al*., 2002b) and tocopherols, carotenoids and chlorophylls (Puspitasari-Nienaber *et al*., 2002). For a summary of chromatographic methods used in authenticity and traceability tests of vegetable oils and dairy products, the reader is referred to a review by Cserháti *et al*. (2005).

Spectroscopic techniques

Spectroscopic techniques, in particular infrared (IR) and nuclear magnetic resonance (NMR) spectroscopy as well as UV-Vis spectrophotometry, are widely used in food authentication. They are frequently combined with *chemometrics*, which actually is a chemical discipline that uses mathematical and statistical methods to provide maximum chemical information by analyzing chemical data (Leardi, 2003). The choice of methods depends mainly on the chemical nature and the physical state of the sample, prior knowledge, and the timescale required for results (Belton, 2000). Other issues that need to be considered are the costs of obtaining and running the analytical equipment, and the specificity of the measurements.

UV-Vis spectroscopy

In this context, *UV-Vis spectrophotometry* represents a cheap and simple technique which has found wide acceptance in analytical chemistry. Some well-known applications include the determination of the protein content (Coomassie dye-binding assay) according to Bradford, the evaluation of the progress of protein hydrolysis using ninhydrin, the photometric determination of pigments (e.g. carotenoids in margarine; Luterotti *et al*., 2006), and the detection of adulteration of virgin olive oil with refined oils. Very recently, the classification of Ligurian olive oils by multivariate analysis of data obtained from electronic nose and UV-Vis spectrophotometry measurements has been reported (Casale *et al*., 2007). A portable spectrophotometer has been used for field authenticity studies of Scotch whisky (MacKenzie and Aylott, 2004).

In instances where HPLC methods are not available, spectrophotometry has been proven to be a useful tool for the determination of phenolic compounds by the so-called *Folin-Ciocalteu assay*. However, this assay actually comes down to quantification of the antioxidant capacity of a given sample. Due to the lack of specificity, the Folin-Ciocalteu assay tends to overestimate the total phenolic content, as shown by Escarpa and González (2001). Another interesting application of UV-visible

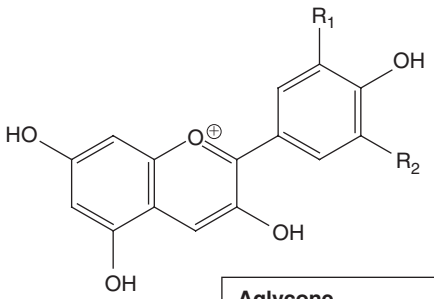

Aglycone	R_1	R_2
Pelargonidin	H	H
Cyanidin	OH	H
Delphinidin	OH	OH
Peonidin	OCH_3	H
Petunidin	OCH_3	OH
Malvidin	OCH_3	OCH_3

Figure 1.3 Structure and substitution pattern of the six major anthocyanidins usually found in nature.

spectrophotometry is the determination of the total contents of anthocyanin pigments (Figure 1.3), which show a typical absorption band in the 490–550 nm region. The shape of an anthocyanin spectrum may also provide information regarding the number and position of glycoside substitution and acylation of the sugar moiety with hydroxycinnamates (Giusti and Wrolstad, 2005). Despite the undoubted advantages of UV-Vis spectrophotometry, this technique has not experienced a great deal of innovation compared with other methods used in food authentication.

Infrared spectroscopy

Infrared (IR) spectroscopy is a rapid and non-destructive technique, thus allowing the screening of a large number of samples (Downey *et al*., 2006) that can be recovered after measurement and used later for further analyses. For this reason, IR spectroscopy is used not only for authenticity studies but also, for example, for the determination of the degree of fruit maturity, as shown for mangoes (Mahayothee *et al*., 2004). While mid-infrared spectroscopy operates between 4000 and 400 cm^{-1}, near-infrared spectroscopy utilizes the spectral range from 14 000 to 4000 cm^{-1} (Reid *et al*., 2006). According to Meurens (2003), IR is the most widely used spectrophotometric technique. A comprehensive review of NIR spectroscopy, also including instrumentation and future trends, has been provided by Benson (2003). Undoubtedly, the attractiveness of NIR for food authentication studies is given by the low running costs, the ease of use and the pronounced versatility. The latter is reflected by the countless applications, which include (but are not limited to) fruit-derived products such as jams, fruit preparations and purées (for a review see Fügel *et al*., 2005a), fruit juices (Kelly and Downey, 2005), crabmeat (Gayo and Hale, 2007), fatty oils in dietary supplements (Ozen *et al*., 2003), chocolate and chocolate products (Che Man *et al*., 2005), olive and corn oils (Vlachos *et al*., 2006; Özdemir and Öztürk, 2007), alcoholic drinks (Lachenmeier, 2007), honey (Downey *et al*., 2006), coffee (Pizarro *et al*., 2007) and muscle foods (Ellis *et al*., 2005). Gangidi *et al*. (2005) reported the determination of the spinal-cord

content in ground beef using NIR up to a limit of detection of 21 ppm. The use of chemometrics for quality and authenticity control of various food commodities such as meat and meat products (Arvanitoyannis and van Houwelingen-Koukaliaroglou, 2003), dairy products (Karoui and De Baerdemaeker, 2007; Arvanitoyannis and Tzouros, 2005) and honey (Arvanitoyannis *et al*., 2005) has been extensively reviewed.

Nuclear magnetic resonance (NMR) spectroscopy

NMR spectroscopy is well known as a powerful tool for structure elucidation, and is increasingly used also for food authenticity purposes. Like IR, it is a fast and highly versatile technique, which allows the detection of all major food components (such as amino acids, fatty acids and sugars) in a single spectrum. Hyphenation to an LC instrument may be particularly useful when analytes are present in very low quantities. Furthermore, NMR measurements are frequently combined with chemometrics, which is another commonality with IR spectroscopy. Applications in the field of food authentication include vegetable and fish oils, fruit juices, alcoholic drinks, coffee and tea, dairy products, fish and meat (Le Gall and Colquhoun, 2003). More recently, Le Gall *et al*. (2004) showed that metabolic profiling by ^{1}H NMR could be used for quality assessment and authentication of green tea.

Stable isotope analysis

The principal elements relevant for food authenticity control, i.e. hydrogen, carbon, nitrogen, oxygen and sulphur, occur as *stable isotopes* with a known mean terrestrial abundance (Kelly, 2003). However, their natural abundance is not a fixed value but shows a considerable degree of variation (or fractionation) caused by biochemical and physicochemical effects. The majority of plants use the *Calvin cycle* to fix atmospheric CO_2 (*C_3 plants*), which results in the formation of the C_3 intermediate 3-phosphoglycerate. The enzyme ribulose-1,5-bisphosphate carboxylase (rubisco) involved in this process preferentially reacts with $^{12}CO_2$ and discriminates the heavier isotope. In contrast, a number of specialized plants from warmer climates, such as sugar cane (*Saccharum officinarum* L.), maize (*Zea mays* L.), millet (*Panicum* sp.) and sorghum (*Sorghum bicolor* L. Moench), so-called *C_4 plants*, make use of the *Hatch-Slack cycle* (or C_4-dicarboxylic acid pathway), fixing CO_2 in a C_4 intermediate. Since the enzyme phosphoenolpyruvate carboxylase is less discriminating compared with rubisco, C_4 plants are less depleted in the heavy carbon isotope. A third class of plants growing in arid zones, the *Crassulacean Acid Metabolism* (CAM) plants, is capable of employing both mechanisms of CO_2 fixation. Pineapple (*Ananas comosus* L. Merr.), cactus sp. and vanilla (*Vanilla planifolia* Andr.) are well-known members of the CAM plants. Since the differences in isotope effects are very small, often occurring around the third or fourth significant figure, they are expressed using the delta (δ) notation in parts per thousand (‰) and relative to the carbon isotope ratio in a standard limestone, Pee Dee Belemnite (PDB). Thus, $\delta^{13}C$ values of C_3 plants range from −24 to −32‰, whereas C_4 plants show $\delta^{13}C$ values between −11 and −15‰. In CAM plants, values ranging from −15 to −24‰ are observed. Typical physicochemical effects causing *isotope fractionation*

include evaporation and condensation. Evaporation of water, for example, decreases the concentration of the heavy isotopomers of water. Therefore, the $\delta^{18}O$ value as well as the $^{2}H/^{1}H$ ratio ratio, relative to the Vienna Standard Mean Ocean Water (V-SMOW), can also be used for authentication purposes – for example, as a marker for the addition of groundwater to fruit juices or for the determination of the geographical origin of foods. The two analytical techniques applied to stable isotope analysis of foods, GC-IR-MS and site-specific natural isotope fractionation NMR spectroscopy, will briefly be introduced in the following, and very recent applications given. According to Reid *et al*. (2006), these techniques are perhaps the most specific and sophisticated methods for determining food authenticity. However, a more widespread application is impeded by the relatively high costs of purchase and running of the instruments.

Isotope ratio mass spectrometry (IR-MS)

For determination of the isotope ratio MS, the analytes need to be converted into a gas – typically H_2, N_2, CO, CO_2 and SO_2 – before they are ionized. For this purpose, carbon dioxide is generated from organic compounds by oxidation with copper oxide and cryogenically trapped in liquid nitrogen. Hydrogen is obtained from the reductive conversion of water using an appropriate metal such as zinc. For the determination of the ^{18}O content of water an equilibrium technique is employed using CO_2, which serves as the analyte. For a more detailed description of the principles of IRMS and practical considerations, the reader is referred to excellent reviews by Carle (1991), Meier-Augenstein (1999, 2002), Kelly (2003), and Kelly *et al*. (2005). The application of IRMS to authenticity studies of various food commodities such as honey, fruit juices and wine was described by Kelly (2003), whereas Kelly *et al*. (2005) summarized the most recent research results on meat, dairy products, beverages, cereal crops, wine, and other commodities. Pfammater *et al*. (2004) used IRMS to differentiate Swiss from foreign tomatoes. Multi-element isotope analysis was employed for authenticity studies on beef (Boner and Förstel, 2004). A report on the geographical differentiation of asparagus from Beelitz (Germany) and Poland was based on a comparatively limited set of data, and needs to be confirmed in further investigations (Meylahn *et al*., 2006). Very recently, Herbach *et al*. (2006) demonstrated that admixtures of red beet to purple pitaya-based products can be detected by the determination of the $\delta^{13}C_{V-PDB}$ value.

Site-specific natural isotope fractionation nuclear magnetic resonance spectroscopy (SNIF-NMR)

While isotope ratio mass spectrometry is a highly sensitive technique to determine the overall deuterium content of a given compound, it is not readily capable of revealing the distribution of deuterium within the compound. *SNIF-NMR* fills this analytical gap, and uses the deuterium distribution in a molecule as a chemical "tracer" to obtain information about the chemical pathway of formation and the geographical origin of a sample (Cross *et al*., 1998). A well-known application of SNIF-NMR is the detection of added sugar in fruit juices and wines. For this purpose, the sugar is usually fermented under controlled conditions and the D/H ratios are determined at the methyl and the methylene groups of the ethanol molecule. Zhang *et al*. (2002) reported that

conversion of sugars from C_3, C_4 and CAM plants into their di-isopropylidene derivatives followed by recording of the isotopic fingerprint could serve as a complementary tool without the need for fermentation. Another interesting field of application is the authenticity assessment of food flavor – in particular, the differentiation of natural and synthetic compounds such as vanillin and benzaldehyde (Schmidt *et al*., 2005). A review of the application of NMR and MS methods for the detection of adulteration of wine, fruit juices and olive oil was carried out by Ogrinc *et al*. (2003).

Enzymes in food authentication

Enzymes are essential constituents of living organisms, and are also responsible for post-harvest and *post-mortem* changes in foods. They catalyze the conversion of a plethora of compounds by increasing the reaction rates under *in vivo* conditions without being consumed themselves. Enzyme reactions are frequently associated with a deterioration of food quality – for example, by lipase-catalyzed release of free fatty acids, oxidation of fatty acids and co-oxidation of carotenoid pigments by lipoxygenases, degradation of chlorophylls by chlorophyllases, or depolymerization of cell-wall constituents by the combined action of cellulases, hemicellulases, and pectinases, resulting in tissue softening and loss of texture. Other examples are browning reactions caused by polyphenol oxidases, which lead to undesirable color changes, and the formation of bitter peptides by uncontrolled enzymatic hydrolysis of proteins.

In food analysis and authentication studies, enzymes are encountered in various respects. First, the specificity of enzymes may be utilized during sample preparation – for example, to release a particular compound which is subsequently characterized and/or quantified using other analytical techniques. A typical example is the *stereospecific analysis of triglycerides* using pancreatic lipase to determine the positional distribution of fatty acids within the triglyceride, as recently shown for the identification of cocoa-butter equivalents added to cocoa butter (Damiani *et al*., 2006). Another well-known application of enzymes used in sample preparation is the determination of the dietary fiber content of foods after enzymatic hydrolysis of starch and proteins.

Second, *enzyme activities* may be used as an indicator of the efficiency of heat treatment. For example, in the dairy industry the activities of alkaline phosphatase and peroxidase are determined to verify pasteurization and sterilization, respectively, of milk. In this context, it is interesting to note that there is an increasing demand by consumers for minimally processed fruit juices. In order to prevent consumers from fraudulent claims as to the "freshness" of such products, enzyme residual activities could also be utilized as an indicator to detect non-declared thermal treatment (Hirsch and Carle, 2005).

Third, enzymes are used as biocatalysts in the spectrophotometric determination of a large number of food constituents, such as organic acids like citrate, isocitrate, and malate (Stój and Targoński, 2006), sugars (e.g. fructose, glucose, lactose, and galactose), amino acids like glutamate and aspartate, and others. Apart from being very specific and inexpensive, these assays usually require minimum sample preparation and have been standardized and even automatized. Therefore, it is not surprising that enzymatic methods have been included in a number of national and international food regulations (Henniger, 2003). However, despite the many advantages of

this technique, enzymatic analysis does not allow the simultaneous determination of analytes, as opposed to chromatographic methods. Furthermore, due to the protein nature of enzymes, any compounds that interact with proteins (e.g. tannins) may also inhibit enzyme activities and thus impair measurements.

Finally, enzymes are involved in the determination of various analytes using *enzyme-linked immunosorbent assays* (*ELISA*). The assays are based on the measurement of the binding of the *antigen* (the analyte) with the corresponding specific *antibody*. One of the two components, i.e. either the antibody or the antigen, is immobilized onto a solid surface, such as a well plate. The action of the enzyme, which is labeled to the antibody (or, in some modifications of the assay, to the antigen) is utilized as an auxiliary reaction for quantification. The various formats of ELISA tests have been summarized by Bonwick and Smith (2004). Initially these assays were developed mainly for the detection of inferior meat species in meat bulk packages and for the detection of drug contamination – for example, antibiotics used in the treatment of mastitis. Later, they were extended to the determination of further analytes such as hormones, pesticides, mycotoxins and others. More recent reports deal with the detection of cow's milk adulteration of sheep, goat and buffalo milk (Hurley *et al*., 2004, 2006), species identification of meat products (Giovannacci *et al*., 2004; Djurdjevic *et al*., 2005) and of gum Arabic (Ireland *et al*., 2004), and authentication of grouper (*Epinephelus guaza*) (Asensio *et al*., 2003).

DNA-based methods in food authentication

DNA-based methods are of increasing importance not only in food analysis but also in medicine for the diagnosis of hereditary diseases, in forensic sciences to (for example) convict murderers and rapists, or to establish or exclude paternity. In food authentication, species identification is a predominant field of application. For example, cow's milk is avoided by some consumers for several reasons, including intolerance or allergy, religious, ethical or cultural objections, or personal preference (Hurley *et al*., 2004). Food products containing pork and lard are of great concern, especially for Islamic religions (Aida *et al*., 2007). Apart from methods based on immunoassays, the so-called *polymerase chain reaction* (*PCR*) is of greatest importance for the purpose of species authentication and has a number of advantages over immunoassays – such as the relatively high stability of DNA and its predictable behavior (Lenstra, 2003). PCR allows the million-fold amplification of a DNA fragment which is framed from two primers. In a first step, the template DNA, which serves as a master copy, is denatured by application of heat (typically 95°C), which leads to the separation of the complementary DNA bases and the formation of two single strands. Subsequently the reaction temperature is lowered to 50–65°C, which allows hybridization of the primers (annealing). The final step, the elongation of the primers, is accomplished by the action of a thermostable polymerase isolated from *Thermus aquaticus* (Taq polymerase) at 72°C. Manifold repetition of the cycle eventually leads to exponential amplification of the template DNA, which is subsequently separated by gel electrophoresis and visualized using an intercalating agent such as ethidium bromide.

PCR has recently been employed for species identification of meat samples (Rastogi *et al*., 2004) as well as seafood and fish (Bossier, 1999; Hubalkova *et al*., 2007), for halal

authentication (Aida *et al*., 2007), and for the authentication of milk and Mozzarella cheese (Bonizzi *et al*., 2006; López-Calleja *et al*., 2007). In addition, it has been used for feed authentication (Pinotti *et al*., 2005) and the identification of contaminating animals in cereals and cereal products (Eugster, 2004). The authentication of medicinal plants (Techen *et al*., 2004; Zhao *et al*., 2006) is of increasing interest in view of the rapidly growing market of dietary supplements. However, interactions of plant secondary metabolites (in particular polyphenolics) with DNA and polymerase represent a problem, and may require additional sample clean-up (Novak *et al*., 2007). Apart from species identification, the detection of *genetically modified organisms*, e.g. the *Flavr Savr tomato* (Meyer, 1995), *Roundup Ready soybean* (Boydler Andersen *et al*., 2006), and *Bt maize* (Bordoni *et al*., 2004), in food represents another important application of PCR. Furthermore, there is increased interest in the fate of transgenic DNA in livestock, which may also be investigated using DNA-based methods (Alexander *et al*., 2007).

Food authentication – still a challenging issue

Despite the advances made in food authentication so far, food adulteration will remain a serious issue in the future – not least because some problems which appear trivial have not yet been addressed in a satisfactory fashion. For example, the fruit content of fruit-derived products such as fruit preparations, jams and spreads represents an issue yet to be solved. Recent work based on the quantification of the fruit hemicellulose fraction (Fügel *et al*., 2004, 2005b, 2006; Schieber *et al*., 2005; Kurz *et al*., 2008) might contribute to a solution. The authentication of nutraceuticals and functional foods, which represent a rapidly growing sector within the overall food market, needs to be addressed, especially in view of the health claims associated with these products. The importance of establishing comprehensive compositional databases cannot be overemphasized. Our own recent work on the presence of polyphenolics has revealed that even recognized markers of food authenticity, such as phloridzin (Figure 1.4a) (Hilt *et al*., 2003) and isorhamnetin glucoside (Figure 1.4b) (Schieber *et al*., 2002), may not be valid in some instances. Therefore, not only the major components but also minor constituents need to be considered in such databases. In this context, an important aspect concerning genetically modified organisms needs to be addressed. While much is known about the effects of genetic modification on the primary metabolites

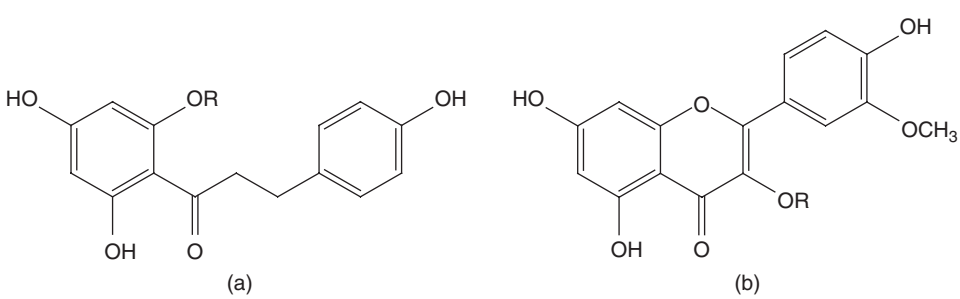

Figure 1.4 (a) Structure of phloridzin and (b) isorhamnetin-3-*O*-glucoside [R = glucose].

of plants, our knowledge regarding the changes in secondary metabolites is limited (Hostettmann and Marston, 2002). For the elucidation of their structures, hyphenated techniques such as LC-MS^n and LC-NMR are the method of choice. Irrespective of the analytical method itself, the limited availability of reference compounds still represents a problem in food authentication, especially concerning the determination of plant secondary metabolites. High-speed countercurrent chromatography is a promising technique for the recovery of target compounds in gram quantities (Ito, 2005; Winterhalter, 2007b), the potential of which should be further exploited. New approaches in food authentication will almost inevitably raise new methods of adulteration, which in turn require even more refined analytical techniques for their detection. Hopefully, this development will finally lead to the requirement of such costly measures for the perpetrators that adulteration becomes completely uneconomic.

Conclusions

It is evident that tremendous progress has been made in food authentication, and this is inextricably linked with the advances in biology and chemistry and the availability of appropriate analytical methods. Chromatography and spectroscopy in their various formats, stable isotope analysis, and immunochemical as well as DNA-based methods represent the methods currently most widely used in food authentication, the range of applications being increasingly extended. Within this introductory chapter, not nearly all techniques and all aspects of food authentication could be considered. However, it is hoped that reading this introduction to food authentication and the analytical techniques employed for the detection of food adulteration will stimulate readers' interest in the following chapters, which deal with the individual techniques in far greater detail.

References

Aida, A.A., Che Man, Y.B., Raha, A.R. and Son, R. (2007). Detection of pig derivatives in food products for halal authentication by polymerase chain reaction-restriction fragment length polymorphism. *Journal of the Science of Food and Agriculture*, **87**, 569–572.

Alexander, T.W., Reuter, T., Aulrich, K. *et al*. (2007). A review of the detection and fate of novel plant molecules derived from biotechnology in livestock production. *Animal Feed Science and Technology*, **133**, 31–62.

Arvanitoyannis, I.S. (2003). Wine authenticity. In: M. Lees (ed.), *Food Authenticity and Traceability*. Cambridge: Woodhead Publishing Ltd, pp. 426–456.

Arvanitoyannis, I.S. and van Houwelingen-Koukaliaroglou, M. (2003). Implementation of chemometrics for quality control and authentication of meat and meat products. *Critical Reviews in Food Science and Nutrition*, **43**, 173–218.

Arvanitoyannis, I.S. and Tzouros, N.E. (2005). Implementation of quality control methods in conjunction with chemometrics toward authentication of dairy products. *Critical Reviews in Food Science and Nutrition*, **45**, 231–249.

Arvanitoyannis, I.S. and Vlachos, A. (2007). Implementation of physicochemical and sensory analysis in conjunction with multivariate analysis towards assessing olive oil authentication/adulteration. *Critical Reviews in Food Science and Nutrition*, **47**, 441–498.

Arvanitoyannis, I.S., Chalhoub, C., Gotsiou, P. *et al*. (2005). Novel quality control methods in conjunction with chemometrics (multivariate analysis) for detecting honey authenticity. *Critical Reviews in Food Science and Nutrition*, **45**, 193–203.

Asensio, L., González, I., Rodríguez, M.A. *et al*. (2003). Development of a specific monoclonal antibody for grouper (*Epinephelus guaza*) identification by an indirect enzyme-linked immunosorbent assay. *Journal of Food Protection*, **66**, 886–889.

Ashurst, P.R. and Dennis, M.J. (1996). *Food Authentication*. London: Blackie Academic & Professional.

Belton, P. (2000). Spectroscopic methods for authentication – an overview. *Biotechnologie, Agronomie, Societe et Environnement*, **4**, 204–207.

Benitez-Sánchez, P.L., León-Camacho, M. and Aparicio, R. (2003). A comprehensive study of hazelnut oil composition with comparisons to other vegetable oils, particularly olive oil. *European Food Research and Technology*, **218**, 13–19.

Benson, I.B. (2003). Near infra-red absorption technology for analysing food composition. In: M. Lees (ed.), *Food Authenticity and Traceability*. Cambridge: Woodhead Publishing Ltd, pp. 101–130.

Birk, C.D., Provensi, G., Gosmann, G. *et al*. (2005). TLC fingerprint of flavonoids and saponins from *Passiflora* species. *Journal of Liquid Chromatography & Related Technologies*, **28**, 2285–2291.

Boner, M. and Förstel, H. (2004). Stable isotope variation as a tool to trace the authenticity of beef. *Analytical and Bioanalytical Chemistry*, **378**, 301–310.

Bonizzi, I., Feligini, M., Aleandri, R. and Enne, G. (2006). Genetic traceability of the geographical origin of typical Italian water buffalo Mozzarella cheese: a preliminary approach. *Journal of Applied Microbiology*, **102**, 667–673.

Bonwick, G.A. and Smith, C.J. (2004). Immunoassays: their history, development and current place in food science and technology. *International Journal of Food Science and Technology*, **39**, 817–827.

Bordoni, R., Mezzelani, A., Consolandi, C. *et al*. (2004). Detection and quantification of genetically modified maize (Bt-176 transgenic maize) by applying ligation detection reaction and universal array technology. *Journal of Agricultural and Food Chemistry*, **52**, 1049–1054.

Bossier, P. (1999). Authentication of seafood products by DNA patterns. *Journal of Food Science*, **64**, 189–193.

Boydler Andersen, C., Holst-Jensen, A., Berdal, K.G. *et al*. (2006). Equal performance of TaqMan, molecular beacon, and SYBR green-based detection assays in detection and quantification of roundup ready soybean. *Journal of Agricultural and Food Chemistry*, **54**, 9658–9663.

Brückner, H., Langer, M., Lüpke, M. *et al*. (1995). Liquid chromatographic determination of amino acid enantiomers by derivatization with *o*-phthaldialdehyde and chiral thiols. Applications with reference to food science. *Journal of Chromatography A*, **697**, 229–245.

Bush, J.F. (2002). "By Hercules! The more common the wine, the more wholesome!" Science and the adulteration of food and other natural products in Ancient Rome. *Food and Drug Law Journal*, **57**, 573–602.

Caligiani, A., Cirlini, M., Palla, G. *et al*. (2007). GC-MS detection of chiral markers in cocoa beans of different quality and geographic origins. *Chirality*, **19**, 329–334.

Carle, R. (1991). Isotopen-Massenspektrometrie. Grundlagen und Anwendungsmöglichkeiten. *Pharmazie in unserer Zeit*, **20**, 75–82.

Casale, M., Armanino, C., Casolino, C. and Forina, M. (2007). Combining information from headspace mass spectrometry and visible spectroscopy in the classification of the Ligurian olive oils. *Analytica Chimica Acta*, **589**, 89–95.

Che Man, Y.B., Syahariza, Z.A., Mirghani, M.E.S. *et al*. (2005). Analysis of potential lard adulteration in chocolate and chocolate products using Fourier transform infrared spectroscopy. *Food Chemistry*, **90**, 815–819.

Chinnici, F., Spinabelli, U., Riponi, C. and Amati, A. (2005). Optimization of the determination of organic acids and sugars in fruit juices by ion-exclusion liquid chromatography. *Journal of Food Composition and Analysis*, **18**, 121–130.

Claus, A., Carle, R. and Schieber, A. (2008). Acrylamide in cereal products: a review. *Journal of Cereal Science*, **47**, 118–133.

Cocchi, M., Lambertini, P., Manzini, D. *et al*. (2002). Determination of carboxylic acids in vinegars and in aceto balsamico tradizionale di modena by HPLC and GC methods. *Journal of Agricultural and Food Chemistry*, **50**, 5255–5261.

Coley, N. (2005). The fight against food adulteration. *Education in Chemistry*, **42**, 46–49.

Cordella, C., Moussa, I., Martel, A.-C. *et al*. (2002). Recent developments in food characterization and adulteration detection: technique-oriented perspectives. *Journal of Agricultural and Food Chemistry*, **50**, 1751–1764.

Cotte, J.F., Casabianca, H., Giroud, B. *et al*. (2004). Characterization of honey amino acid profiles using high-pressure liquid chromatography to control authenticity. *Analytical and Bioanalytical Chemistry*, **378**, 1342–1350.

Cross, J.L., Gallaher, T.N. and Leary, J.J. (1998). The application of site-specific natural isotope fractionation-nuclear magnetic resonance (SNIF-NMR) to the analysis of alcoholic beverages. *The Chemical Educator*, **3**, 1–9.

Cserháti, T., Forgács, E., Deyl, Z. and Miksik, I. (2005). Chromatography in authenticity and traceability tests of vegetable oils and dairy products: a review. *Biomedical Chromatography*, **19**, 183–190.

Cuthbertson, W.F.J. (1991). Chemistry and food: the past 150 years. *Chemistry in Britain*, **27**, 1010–1012.

Damiani, P., Cossignani, L., Simonetti, M.S. *et al*. (2006). Identification of cocoa butter equivalents added to cocoa butter. III. Stereospecific analysis of triacylglycerol fraction and some its subfraction. *European Food Research and Technology*, **223**, 645–648.

Davies, B.H. (2005). Dyes (and pigments) as food additives (and adulterants). *Dyes in History and Archaeology*, **20**, 175–181.

Dennis, M.J. (1998). Recent developments in food authentication. *Analyst*, **123**, 151R–156R.

Dimitrova, B., Gevrenova, R. and Anklam, E. (2007). Analysis of phenolic acids in honeys of different floral origin by solid-phase extraction and high-performance liquid chromatography. *Phytochemical Analysis*, **18**, 24–32.

Djurdjevic, N., Sheu, S.-C. and Hsieh, Y.-H.P. (2005). Quantitative detection of poultry in cooked meat products. *Journal of Food Science*, **70**, C586–C593.

Downey, G., Kelly, J.D. and Petisco Rodriguez, C. (2006). Food authentication – has near infrared spectroscopy a role? *Spectroscopy Europe*, **18**, 10–14.

Dragovic-Uzelac, V., Delonga, K., Levaj, B. *et al*. (2005). Phenolic profiles of raw apricots, pumpkins, and their purees in the evaluation of apricot nectar and jam authenticity. *Journal of Agricultural and Food Chemistry*, **53**, 4836–4842.

Ellis, D.I., Broadhurst, D., Clarke, S.J. and Goodacre, R. (2005). Rapid identification of closely related muscle foods by vibrational spectroscopy and machine learning. *Analyst*, **130**, 1648–1654.

Engelhardt, U. and Galensa, R. (1997). Analytik und Bedeutung von Polyphenolen in Lebensmitteln. In: H. Günzler (ed.), *Analytiker Taschenbuch 15*. Berlin: Springer, pp. 147–178.

Erbe, T. and Brückner, H. (2000). Chromatographic determination of amino acid enantiomers in beers and raw materials used for their manufacture. *Journal of Chromatography A*, **881**, 81–91.

Escarpa, A. and González, M.C. (2001). Approach to the content of total extractable phenolic compounds from different food samples by comparison of chromatographic and spectrophotometric methods. *Analytica Chimica Acta*, **427**, 119–127.

Eugster, A. (2004). Authentizitätsnachweis bei Lebensmitteln – Routine und Herausforderung. *Mitteilungen aus Lebensmitteluntersuchung und Hygiene*, **95**, 573–584.

Fennema, O.R. (1987). Food additives – an unending controversy. *American Journal of Clinical Nutrition*, **46**, 201–203.

Forgács, E. and Cserháti, T. (2003). Gas chromatography. In: M. Lees (ed.), *Food Authenticity and Traceability*. Cambridge: Woodhead Publishing Ltd, pp. 197–217.

Friedrich, S. (2006). *Lebensmittelskandale*, http://www.stern.de (accessed August 2007).

Fügel, R., Carle, R. and Schieber, A. (2004). A novel approach to quality and authenticity control of fruit products using fractionation and characterisation of cell wall polysaccharides. *Food Chemistry*, **87**, 141–150.

Fügel, R., Carle, R. and Schieber, A. (2005a). Quality and authenticity control of fruit purées, fruit preparations and jams – a review. *Trends in Food Science and Technology*, **16**, 433–441.

Fügel, R., Förch, M., Carle, R. and Schieber, A. (2005b). Determination of the fruit content of strawberry yogurt by gravimetric quantification of hemicellulose. *Journal of Applied Botany and Food Quality*, **79**, 157–159.

Fügel, R., Schieber, A. and Carle, R. (2006). Determination of the fruit content of cherry fruit preparations by gravimetric quantification of hemicellulose. *Food Chemistry*, **95**, 163–168.

Gangidi, R.R., Proctor, A., Pohlman, F.W. and Meullenet, J.-F. (2005). Rapid determination of spinal cord content in ground beef by near-infrared spectroscopy. *Journal of Food Science*, **70**, C397–C400.

García-González, D.L. and Aparicio, R. (2006). Olive oil authenticity: the current analytical challenges. *Lipid Technology*, **18**, 81–85.

Gayo, J. and Hale, S.A. (2007). Detection and quantification of species authenticity and adulteration in crabmeat using visible and near-infrared spectroscopy. *Journal of Agricultural and Food Chemistry*, **55**, 585–592.

Giovannacci, I., Guizard, C., Carlier, M. *et al*. (2004). Species identification of meat products by ELISA. *International Journal of Food Science and Technology*, **39**, 863–867.

Giusti, M.M. and Wrolstad, R.E. (2005). Characterization and measurement of anthocyanins by UV-visible spectroscopy. In: R.E. Wrolstad (ed.), *Handbook of Food Analytical Chemistry Vol. 2: Pigments, Colorants, Flavors, Texture, and Bioactive Food Components*. Hoboken, NJ: John Wiley & Sons, pp. 19–31.

Gómez-Ariza, J.L., Villegas-Portero, M.J. and Bernal-Daza, V. (2005). Characterization and analysis of amino acids in orange juice by HPLC-MS/MS for authenticity assessment. *Analytica Chimica Acta*, **540**, 221–230.

Grüne, J. (2002). Staatliche Lebensmittelüberwachung in Deutschland. *Bürger im Staat*, **52**, 188–192.

Hammond, D.A. (1996). Authenticity of fruit juices, jams and preserves. In: P.R. Ashurst and M.J. Dennis (eds), *Food Authentication*. London: Blackie Academic & Professional, pp. 15–59.

He, L. and Beesley, T.E. (2005). Applications of enantiomeric gas chromatography: a review. *Journal of Liquid Chromatography & Related Technologies*, **7–8**, 1075–1114.

Henniger, G. (2003). Enzymatic techniques for authenticating food components. In: M. Lees (ed.), *Food Authenticity and Traceability*. Cambridge: Woodhead Publishing Ltd, pp. 239–274.

Herbach, K.M., Stintzing, F.C., Elss, S. *et al*. (2006). Isotope ratio mass spectrometrical analysis of betanin and isobetanin isolates for authenticity evaluation of purple pitaya-based products. *Food Chemistry*, **99**, 204–209.

Hilt, P., Schieber, A., Yildirim, C. *et al*. (2003). Detection of phloridzin in strawberries (*Fragaria x ananassa* Duch.) by HPLC-PDA-MS/MS and NMR spectroscopy. *Journal of Agricultural and Food Chemistry*, **51**, 2896–2899.

Hirsch, A. and Carle, R. (2005). Citrussäfte – Haltbar gemacht oder frisch gepresst? *Ernährung im Fokus*, **5**, 26–30.

Hostettmann, K. and Marston, A. (2002). Twenty years of research into medicinal plants: results and perspectives. *Phytochemistry Reviews*, **1**, 275–285.

Hubalkova, Z., Kralik, P., Tremlova, B. and Rencova, E. (2007). Methods of gadoid fish species identification in food and their economic impact in the Czech Republic: a review. *Veterinarni Medicina*, **52**, 273–292.

Hurley, I.P., Ireland, H.E., Coleman, R.C. and Williams, J.H.H. (2004). Application of immunological methods for the detection of species adulteration in dairy products. *International Journal of Food Science and Technology*, **39**, 873–878.

Hurley, I.P., Coleman, R.C., Ireland, H.E. and Williams, J.H.H. (2006). Use of sandwich IgG ELISA for the detection and quantification of adulteration of milk and soft cheese. *International Dairy Journal*, **16**, 805–812.

Ireland, H.E., Clutterbuck, A., Cloquet, J.-P. *et al*. (2004). The development of immunoassays to identify and quantify species source of gum Arabic. *Journal of Agricultural and Food Chemistry*, **52**, 7804–7808.

Ito, Y. (2005). Golden rules and pitfalls in selecting optimum conditions for high-speed counter-current chromatography. *Journal of Chromatography A*, **1065**, 145–168.

Jaiswal, A.K., Millo, T. and Gupta, M. (2006). Gas chromatography and its forensic applications – a review. *International Journal of Medical Toxicology and Legal Medicine*, **8**, 30–41.

Jandera, P., Škeříková, V., Hájek, T. *et al*. (2005). RP-HPLC analysis of phenolic compounds and flavonoids in beverages and plant extracts using a CoulArray detector. *Journal of Separation Science*, **28**, 1005–1022.

Junge, M., Huegel, H. and Marriott, P.J. (2007). Enantiomeric analysis of amino acids by using comprehensive two-dimensional gas chromatography. *Chirality*, **19**, 228–234.

Kamm, W., Dionisi, F., Hischenhuber, C. and Engel, K.-H. (2001). Authenticity assessment of fats and oils. *Food Reviews International*, **17**, 249–290.

Kammerer, D., Carle, R. and Schieber, A. (2003). Detection of peonidin and pelargonidin glycosides in black carrots (*Daucus carota* ssp. *sativus* var. *atrorubens* Alef.) by high-performance liquid chromatography – electrospray ionization mass spectrometry. *Rapid Communications in Mass Spectrometry*, **17**, 2407–2412.

Karoui, R. and De Baerdemaeker, J. (2007). A review of the analytical methods coupled with chemometric tools for the determination of the quality and identity of dairy products. *Food Chemistry*, **102**, 621–640.

Kelly, J.F.D. and Downey, G. (2005). Detection of sugar adulterants in apple juice using Fourier transform infrared spectroscopy and chemometrics. *Journal of Agricultural and Food Chemistry*, **53**, 3281–3286.

Kelly, S., Heaton, K. and Hoogewerff, J. (2005). Tracing the geographical origin of food: The application of multi-element and multi-isotope analysis. *Trends in Food Science and Technology*, **16**, 555–567.

Kelly, S.D. (2003). Using stable isotope ratio mass spectrometry (IRMS). In: M. Lees (ed.), *Food Authenticity and Traceability*. Cambridge: Woodhead Publishing Ltd, pp. 156–183.

Kurz, C., Carle, R. and Schieber, A. (2008). Characterisation of cell wall polysaccharide profiles of apricots (*Prunus armeniaca* L.), peaches (*Prunus persica* L.), and pumpkins (*Cucurbita* sp.) for the evaluation of fruit product authenticity. *Food Chemistry*, **106**, 421–430.

Lachenmeier, D.W. (2007). Rapid quality control of spirit drinks and beer using multivariate data analysis of Fourier transform infrared spectra. *Food Chemistry*, **101**, 825–832.

Lachenmeier, K., Musshoff, F., Madea, B. *et al*. (2006). Authentication of noni (*Morinda citrifolia*) juice. *Deutsche Lebensmittel-Rundschau*, **102**, 58–61.

Law, M. T. (2004). History of food and drug regulation in the United States. *EH.NET Encyclopedia of Economic and Business History* (R. Whaples, ed.), http://eh.net (accessed June 2007).

Leardi, R. (2003). Chemometrics in data analysis. In: M. Lees (ed.), *Food Authenticity and Traceability*. Cambridge: Woodhead Publishing Ltd, pp. 299–320.

Lees, M. (2003). *Food Authenticity and Traceability*. Cambridge: Woodhead Publishing Ltd.

Le Gall, G. and Colquhoun, I.J. (2003). NMR spectroscopy in food authentication. In: M. Lees (ed.), *Food Authenticity and Traceability*. Cambridge: Woodhead Publishing Ltd, pp. 131–155.

Le Gall, G., Colquhoun, I.J. and Defernez, M. (2004). Metabolite profiling using ^{1}H NMR spectroscopy for quality assessment of green tea, *Camellia sinensis* (L.). *Journal of Agricultural and Food Chemistry*, **52**, 692–700.

Lehotay, S.J. and Hajšlova, J. (2002). Application of gas chromatography in food analysis. *Trends in Analytical Chemistry*, **21**, 686–697.

Leis, H.J., Fauler, G., Rechberger, G.N. and Windischhofer, W. (2004). Electron-capture mass spectrometry: a powerful tool in biomedical trace level analysis. *Current Medicinal Chemistry*, **11**, 1585–1594.

Lenstra, J.A. (2003). DNA methods for identifying plant and animal species in food. In: M. Lees (ed.), *Food Authenticity and Traceability*. Cambridge: Woodhead Publishing Ltd, pp. 34–53.

López-Calleja, I., González, I., Fajardo, V. *et al*. (2007). Quantitative detection of goats' milk in sheep's milk by real-time PCR. *Food Control*, **18**, 1466–1473.

Lupien, J.R. (2002). The precautionary principle and other non-tariff barriers to free and fair international trade. *Critical Reviews in Food Science and Nutrition*, **42**, 403–415.

Luterotti, S., Bicanic, D. and Požgaj, R. (2006). New simple spectrophotometric assay of total carotenes in margarines. *Analytica Chimica Acta*, **573–574**, 466–473.

MacKenzie, W.M. and Aylott, R.I. (2004). Analytical strategies to confirm Scotch whisky authenticity. *Analyst*, **129**, 607–612.

Mahayothee, B., Neidhart, S., Leitenberger, M. *et al*. (2004). Non-destructive determination of maturity of Thai mangoes by near-infrared spectroscopy. *Acta Horticulturae (ISHS)*, **645**, 581–588.

Martinez, I., Aursand, M., Erikson, U. *et al*. (2003). Destructive and non-destructive analytical techniques for authentication and composition analysis of foodstuffs. *Trends in Food Science and Technology*, **14**, 489–498.

Meier-Augenstein, W. (1999). Applied gas chromatography coupled to isotope ratio mass spectrometry. *Journal of Chromatography*, **842**, 351–371.

Meier-Augenstein, W. (2002). Stable isotope analysis of fatty acids by gas chromatography-isotope ratio mass spectrometry. *Analytica Chimica Acta*, **465**, 63–79.

Merken, H.M. and Beecher, G.R. (2000). Measurement of food flavonoids by high-performance liquid chromatography: a review. *Journal of Agricultural and Food Chemistry*, **48**, 577–599.

Meurens, M. (2003). Spectrophotometric techniques. In: M. Lees (ed.), *Food Authenticity and Traceability*. Cambridge: Woodhead Publishing Ltd, pp. 184–196.

Meyer, R. (1995). Nachweis gentechnologisch veränderter Pflanzen mittels der Polymerase Kettenreaktion (PCR) am Beispiel der Flavr Savr^{TM}-Tomate. *Zeitschrift für Lebensmittel-Untersuchung und -Forschung*, **201**, 583–586.

Meylahn, K., Rücker, A. and Wolf, E. (2006). Herkunftsanalyse von Spargel mittels Stabilisotopenanalyse. *Deutsche Lebensmittel-Rundschau*, **102**, 523–526.

Milbury, P.E. (2001). Analysis of complex mixtures of flavonoids and polyphenols by high-performance liquid chromatography electrochemical detection methods. *Methods in Enzymology*, **335**, 15–26.

Molan, P.C. (1996). Authenticity of honey. In: P.R. Ashurst and M.J. Dennis (eds), *Food Authentication*. London: Blackie Academic & Professional, pp. 259–303.

Mosandl, A. (2004). Authenticity assessment: a permanent challenge in food flavor and essential oil analysis. *Journal of Chromatographic Science*, **42**, 440–449.

Novak, J., Grausgruber-Gröger, S. and Lukas, B. (2007). DNA-based authentication of plant extracts. *Food Research International*, **40**, 388–392.

Ogrinc, N., Košir, I.J., Spangenberg, J.E. and Kidrič, J. (2003). The application of NMR and MS methods for detection of adulteration of wine, fruit juices, and olive oil. A review. *Analytical and Bioanalytical Chemistry*, **376**, 424–430.

Özdemir, D. and Öztürk, B. (2007). Near infrared spectroscopic determination of olive oil adulteration with sunflower and corn oil. *Journal of Food and Drug Analysis*, **15**, 40–47.

Ozen, B.F., Weiss, I. and Mauer, L.J. (2003). Dietary supplement oil classification and detection of adulteration using Fourier transform infrared spectroscopy. *Journal of Agricultural and Food Chemistry*, **51**, 5871–5876.

Paredes, E., Maestre, S.E., Prats, S. and Todolí, J. (2006). Simultaneous determination of carbohydrates, carboxylic acids, alcohols, and metals in foods by high-performance liquid chromatography inductively coupled plasma atomic emission spectrometry. *Analytical Chemistry*, **78**, 6774–6782.

Pérez-Ruiz, T., Martínez-Lozano, C., Tomás, V. and Martín, J. (2004). High-performance liquid chromatographic separation and quantification of citric, lactic, malic, oxalic and tartaric acids using a post-column photochemical reaction and chemiluminescence detection. *Journal of Chromatography A*, **1026**, 57–64.

Pfammater, E., Maury, V. and Thèthaz, C. (2004). Nachweis der Authentizität von Lebensmitteln mittels IRMS (isotope ratio mass spectrometry). und Anwendung dieser Methodik im Bereich der Lebensmittelkontrolle. *Mitteilungen aus Lebensmitteluntersuchung und Hygiene*, **95**, 585–596.

Pinotti, L., Moretti, V.M., Baldi, A. *et al*. (2005). Feed authentication as an essential component of food safety and control. *Outlook on Agriculture*, **34**, 243–248.

Pizarro, C., Esteban-Díez, I. and González-Sáiz, J.M. (2007). Mixture resolution according to the percentage of *robusta* variety in order to detect adulteration in roasted coffee by near infrared spectroscopy. *Analytica Chimica Acta*, **585**, 266–276.

Prodolliet, J. and Hischenhuber, C. (1998). Food authentication by carbohydrate chromatography. *Zeitschrift für Lebensmittel-Untersuchung und -Forschung A*, **207**, 1–12.

Pundlik, M.D. (2004). Simultaneous HPLC determination of vitamin C and carboxylic acids. *Journal of the Indian Chemical Society*, **81**, 721–723.

Puspitasari-Nienaber, N.L., Ferruzzi, M.G. and Schwartz, S.J. (2002). Simultaneous detection of tocopherols, carotenoids, and chlorophylls in vegetable oils by direct injection C_{30} RP-HPLC with coulometric electrochemical array detection. *Journal of the American Oil Chemists' Society*, **79**, 633–640.

Rastogi, G., Dharne, M., Bharde, A. *et al*. (2004). Species determination and authentication of meat samples by mitochondrial 12S rRNA gene sequence analysis and conformation-sensitive gel electrophoresis. *Current Science*, **87**, 1278–1281.

Rayner, V.J. (2006). Food color regulations: a European perspective on Sudan dyes and the future for color legislation in the EU. *Abstract of Papers, 231st ACS National Meeting, Atlanta, GA USA*. Washington, DC: American Chemical Society, p AGDF–147.

Reid, L.M., O'Donnell, C.P. and Downey, G. (2006). Recent technological advances for the determination of food authenticity. *Trends in Food Science and Technology*, **17**, 344–353.

Sáiz-Abajo, M.J., González-Sáiz, M.J. and Pizarro, C. (2005). Multi-objective optimization strategy based on desirability functions used for chromatographic separation and quantification of L-proline and organic acids in vinegar. *Analytica Chimica Acta*, **528**, 63–76.

Sander, L., Sharpless, K.E., Craft, N.E. and Wise, S.A. (2000). C_{30} stationary phases for the analysis of food by liquid chromatography. *Journal of Chromatography A*, **880**, 189–202.

Santos, F.J. and Galceran, M.T. (2003). Modern developments in gas chromatography-mass spectrometry-based environmental analysis. *Journal of Chromatography A*, **1000**, 125–151.

Schieber, A., Keller, P. and Carle, R. (2001). Determination of phenolic acids and flavonoids of apple and pear by high-performance liquid chromatography. *Journal of Chromatography A*, **910**, 265–273.

Schieber, A., Keller, P., Streker, P. *et al*. (2002a). Detection of isorhamnetin glycosides in extracts of apples (*Malus domestica* cv. 'Brettacher') by HPLC-PDA and HPLC-APCI-MS/MS. *Phytochemical Analysis*, **13**, 87–94.

Schieber, A., Marx, M. and Carle, R. (2002b). Simultaneous determination of carotenes and tocopherols in ATBC drinks by high-performance liquid chromatography. *Food Chemistry*, **76**, 377–382.

Schieber, A., Fügel, R., Henke, M. and Carle, R. (2005). Determination of the fruit content of strawberry fruit preparations by gravimetric quantification of hemicellulose. *Food Chemistry*, **91**, 365–371.

Schmidt, H.-L., Rossmann, A., Stöckigt, D. and Christoph, N. (2005). Stabilisotopenanalytik – Herkunft und Authentizität von Lebensmitteln. *Chemie in unserer Zeit*, **39**, 90–99.

Schurig, V. (2002). Chiral separations using gas chromatography. *Trends in Analytical Chemistry*, **21**, 647–661.

Stój, A. and Targoński, Z. (2006). Use of content analysis of selected organic acids for the detection of berry juice adulterations. *Polish Journal of Food and Nutrition Sciences*, **15/16**, 41–47.

Sumar, S. and Ismail, H. (1995). Adulteration of foods – past and present. *Nutrition & Food Science*, **4**, 11–15.

Techen, N., Crockett, S.L., Khan, I.A. and Scheffler, B.E. (2004). Authentication of medicinal plants using molecular biology techniques to compliment conventional methods. *Current Medicinal Chemistry*, **11**, 1391–1401.

Teuteberg, H.-J. (1995). Die Verfälschung von Nahrungs- und Genußmitteln und die Anfänge eines einheitlichen staatlichen Lebensmittelschutzes in Deutschland. *Zeitschrift für Ernährungswissenschaft*, **34**, 95–112.

Tomás-Barberán, F.A., Martos, I., Ferreres, F. *et al*. (2001). HPLC flavonoid profiles as markers for the botanical origin of European unifloral honeys. *Journal of the Science of Food and Agriculture*, **81**, 485–496.

Ulberth, F. and Buchgraber, M. (2000). Authenticity of fats and oils. *European Journal of Lipid Science and Technology*, **102**, 687–694.

Vlachos, N., Skopelitis, Y., Psaroudaki, M. *et al*. (2006). Applications of Fourier transform-infrared spectroscopy to edible oils. *Analytica Chimica Acta*, **573–574**, 459–465.

Winterhalter, P. (2007a). Authentication of food and wine. In: S.E. Ebeler, G.R. Takeoka, P. Winterhalter (eds), *Authentication of Food and Wine*. ACS Symposium Series 952, pp. 2–12.

Winterhalter, P. (2007b). Application of countercurrent chromatography to the analysis of natural pigments. *Trends in Food Science and Technology*, **18**, 507–513.

Zhang, B.-L., Billaut, I., Li, X. *et al*. (2002). Hydrogen isotopic profile in the characterization of sugars. Influence of the metabolic pathway. *Journal of Agricultural and Food Chemistry*, **50**, 1574–1580.

Zhang, X., Cambrai, A., Miesch, M. *et al*. (2006). Separation of Δ5- and Δ7-phytosterols by adsorption chromatography and semipreparative reversed phase high-performance liquid chromatography for quantitative analysis of phytosterols in foods. *Journal of Agricultural and Food Chemistry*, **54**, 1196–1202.

Zhao, Z., Hu, Y., Liang, Z. *et al*. (2006). Authentication is fundamental for standardization of Chinese medicines. *Planta Medica*, **72**, 865–874.

Zimmermann, B. and Galensa, R. (2007). One for all – all for one: proof of authenticity and tracing of foods with flavonoids. *European Food Research and Technology*, **224**, 385–393.

2

Spectroscopic Technique: Mid-infrared (MIR) and Fourier Transform Mid-infrared (FT-MIR) Spectroscopies

Romdhane Karoui, Juan Antonio Fernández Pierna and Eric Dufour

Introduction

Mid-infrared, like the other vibrational spectroscopies, represents an attractive option for quality control and screening because it is rapid, inexpensive and non-invasive. It has shown tremendous growth as an analytical tool in quality control and process monitoring. This growth is mainly due to instrumental developments and advances in chemometrics (Bertrand and Dufour, 2000).

The *chemical bonds* in the molecules have specific frequencies at which they vibrate, corresponding to *energy levels*. These vibrational frequencies are determined by the mass of the atoms, the shape (geometry) of the molecule, the stiffness of the bonds and the periods of the associated vibrational coupling. A specific vibrational mode has to be associated with changes in the permanent dipole in order to be active in the infrared area. Diatomic molecules have only one bond, which may stretch

Modern Techniques for Food Authentication
ISBN: 978-0-12-374085-4

(i.e. the distance between two atoms increases or decreases). More complex molecules may have many bonds, and vibrations can be conjugated leading to two possible modes of vibration: stretching and bending (i.e. the position of the atom changes relative to the original bond axis). In such cases the vibrations lead to infrared absorptions at characteristic frequencies that may be related to chemical groups.

In practice, to measure a sample, a beam of infrared light passes through the sample and the absorbed energy at each wavelength is recorded. This can be done in two different ways; by scanning through the spectrum with a monochromatic beam, which changes in wavelength over time, or by using a Fourier transform system to measure all the wavelengths at the same time. As a result, taking into account the effects of all the different functional groups, an *absorbance* (or *transmittance*) spectrum is obtained showing at which wavelengths the sample absorbs the infrared light, thus allowing interpretation of the chemical bonds. A unique molecular fingerprint that can be used to confirm the identity of the sample is obtained.

Three types of vibrational spectroscopy are generally distinguished: near-infrared (NIR), mid-infrared (MIR), and Raman spectroscopy.

Theory and principles

The *NIR* region lies between 12 500 and 4000 cm^{-1} (0.8–2.5 μm), and NIR spectroscopy operates with a light source from which the sample absorbs specific frequencies corresponding to overtones and combination bands of vibrational transitions of the molecule primarily of OH, CH, NH and CO groups (for more information, see Chapters 3 and 4). The *MIR* region of the electromagnetic spectrum lies between 4000 and 400 cm^{-1} (2.5–50 μm) and is associated mainly with fundamental molecular stretching and bending vibrational frequency – i.e. the frequencies of the fundamental vibration modes of the molecules (from the stable vibrational state to the first excited vibrational state in the electronic ground state). *Raman* also lies in a region similar to MIR; in contrast with the other two techniques, it involves a scattering process that arises when the incident light excites molecules in the sample, which subsequently scatter the light. Most of this scattered light is at the same wavelength as the incident light, but some is scattered at a different wavelength. The process leading to this "inelastic" scatter is called the Raman effect (for more information, see Chapters 5 and 6).

MIR spectroscopy rapidly provides information on a very large number of analytes, and the absorption bands are sensitive to the physical and chemical states of individual constituents. MIR and NIR spectroscopy have a good signal intensity compared with Raman spectroscopy, but MIR has the advantage over NIR that trace elements can be identified. It can be thought of as a molecular fingerprinting method (Hvozdara *et al*., 2002; Steiner *et al*., 2003; Mazarevica *et al*., 2004). Table 2.1 illustrated some advantages and drawbacks of MIR.

The high spectral signal-to-noise ratio obtained from modern instrumental analysis, as when using the Fourier transform infrared (FT-MIR) spectroscopy, allows the detection of constituents present in low concentrations, as well as subtle compositional and structural differences between and among multi-constituent specimens.

Table 2.1 Some advantages and drawbacks of MIR

Advantages	Drawbacks
• Relies on part of the spectrum that contains fundamental vibrations • Useful for qualitative and quantitative identification of functional groups • Characteristic and well-defined bands for organic functional groups • Unknown species can be identified	• The available energy decreases with wavelength • Expensive transmitting materials • Cells need to have short effective path lengths because most of the materials absorb in this region

MIR spectroscopic methods, and particularly FT-MIR spectroscopy, can be considered routine applications among standard laboratory techniques (Baeten *et al.*, 2000; Baeten and Dardenne, 2002). Such methods have been shown to be useful for a range of identification/authentication problems in different sectors.

Instrumentation

The first MIR instruments used a high-resolution diffraction *monochromator*, which has generally been replaced by *interferometry* technology, leading to the FT-MIR spectrometer. The main component in this spectrometer is the interferometer, the Michelson interferometer being most commonly used. An interferometer consists of two perpendicular mirrors, one moving at a constant velocity and the other being stationary (Figure 2.1). Between the mirrors there is a beam-splitter, normally made up of KBr coated with germanium (for the MIR region).

The beam-splitter splits a beam of light that enters (incident beam) into two new beams, one reflected onto the moving mirror and the other onto the fixed (stationary) mirror. The two beams are then reflected back and recombined at the beam-splitter. Owing to path differences between the mirrors, both beams undergo constructive and destructive interferences. The recombined beam is then passed on towards the sampling area, where it interacts with the sample. The transmitted, diffused or reflected light reaches the detector, where the energy is digitized, resulting in an output signal consisting of the sum of cosine waves. This is the interferogram. This interferogram consists of the intensity of energy measured versus the position of the moving mirror (function of time domain), and contains basic information about frequencies and intensities, but is not directly interpretable. The interferogram is then converted into a conventional infrared spectrum (function of frequency domain) by the mathematical function known as the Fourier transform.

Sample presentation

The development of FT-MIR instruments has been followed by the development of adequate sampling presentation techniques. Initially, the sample presentation techniques included fixed path-length transmission cells, coated or smeared films or windows, as well as hot pressed films and alkali halide pellets (KBr).

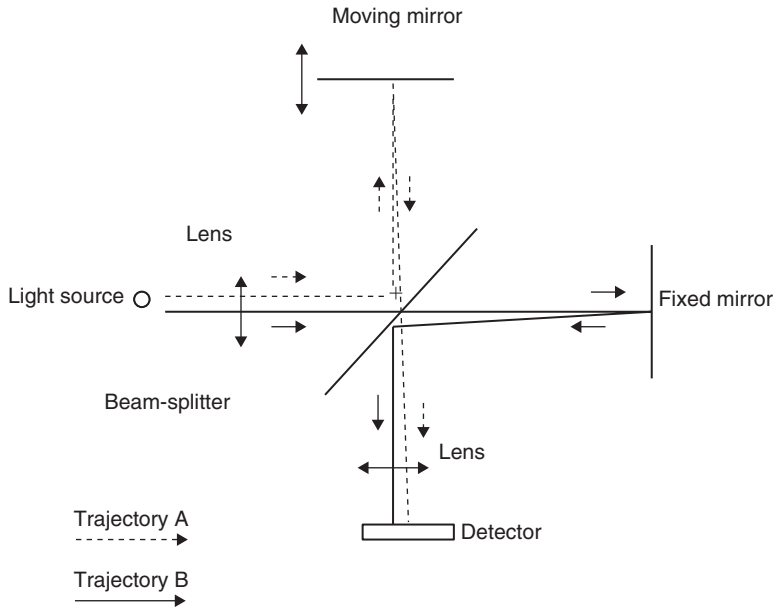

Figure 2.1 Schematic configuration of an interferometer.

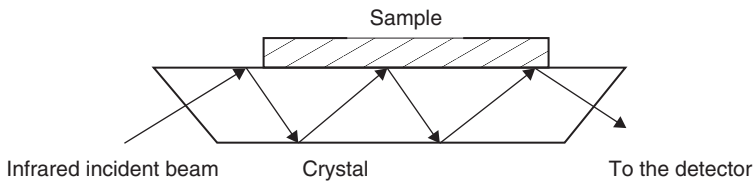

Figure 2.2 Horizontal attenuated total reflection (ATR) sampling device.

Maybe one of the most interesting developments has been the introduction of simple reflectance techniques as the *attenuated total reflectance* (*ATR*) system (Fahrenfort, 1961; Harrick, 1967) (Figure 2.2). With the ATR, the sample is in contact with a crystal of a high refraction index. This crystal is mainly made of ZnSe, Ge, ZnS, Si or diamond. The ATR system measures the changes that occur in a totally internally reflected infrared beam when the beam comes into contact with the sample. For this, the radiation coming from the *beam-splitter* reflects off the inner surface of the crystal one or more times. A standing wave, called the *evanescence wave*, is generated for each reflection. Evanescence waves are penetrating electromagnetic fields that have decreasing intensity when moving away from their source. The evanescence waves penetrate the sample and interact with it, producing a spectrum. The penetration depth depends on the incident angle, the crystal and sample refraction indexes, and the infrared ray wavenumber.

ATR is a versatile and powerful technique for infrared sampling. It is useful for sampling the surface of smooth materials that are either too thick or too opaque for transmission IR measurement. The ATR is non-destructive, little or no sample preparation is needed, and it allows fast and simple sampling. However, the ATR crystal absorbs energy at lower energy levels, and most of the used crystals have pH limitations.

There must also be good contact between the sample and the crystal to be sure that the data obtained is accurate. ATR is a good technique for measuring solids such as paper, glass, cheese, meat, soft powders and dark-colored materials, as well as liquids including non-aqueous solutions such as oils, dyes and pastes, polymers and many other organic materials.

New ATR systems are based on a diamond interface for the analysis of liquids. In most cases, this is technically realized by a diamond substrate or a sandwich layer on a common ATR-substrate (ZnSe, Ge, BaF2, …).

Other sampling accessories include thermostatized flow cells and ATR cells coupled with an appropriate pump as well as IR-cards in polyethylene that can be used successfully for the analysis of fats and oils.

New developments

More recent improvements in MIR instruments include the development of on-line spectrometers, already available for gas or exhaust monitoring. The main innovation in this area is the use of fiber-optics for the connection between the spectrometer and the sensing device. However, there are several disadvantages, including losses in coupling and transmission, moisture sensitivity and mechanical sensitivity. Current applications include the monitoring and control of cultivations of *Gluconacetobacter xylinus* and production of gluconacetan, a food-grade exopolysaccharide (Kornmann *et al*., 2004), and the evaluation of quality traits in apricot fruits (Bureau *et al*., 2006).

These developments are also used in FT-MIR spectrometers attached to microscopes (FT-MIR microscopy) in order to measure infrared spectra from a tiny part of a sample. This combination has the dual advantages of clear chemical identification of the sample components by MIR spectroscopy, and high lateral resolution as obtained by microscopy. It thus allows direct access to spatially resolved molecular and structural information regarding the analyzed area. MIR microscopy has a wide range of applications, including, among others, in pharmaceuticals, forensic trace evidence, drug contamination, catalysts, minerals, plant leaves, animal tissue, cells, and industrial products defects.

Recently MIR imaging has been of considerable interest, owing to a number of new developments – mainly in the area of astronomy, where MIR cameras enable a wide range of observations. Among these are studies of the temperature characteristics of the atmospheres of different planets, as the MIR region is where the planets emit most of their radiation. Also, owing to the dust around them, still-forming stars glow brightly in the MIR, providing information about complex molecules which then leads to investigations of how stars and planetary systems form and evolve. MIR imaging has also been applied to several problematic areas in the agricultural and food industries (Elmore *et al*., 2005).

Applications of MIR and FT-MIR in foods, drinks, cotton and wood

The application of MIR spectroscopy in combination with multidimensional statistical techniques for the evaluation of *food quality* has increased. The development of

FT-MIR in recent years affords the possibility of obtaining unique information about protein yield, protein structure and protein–protein and protein–lipid interactions without introducing perturbing probe molecules. Thus, most papers have used FT-MIR to determine the quality of food products. Analyses have focused on measurements in the 4000–900 cm^{-1} spectral region, within which three spectral regions have been used; 3000–2800 cm^{-1}; 1700–1500 cm^{-1} and 1500–900 cm^{-1}. These were selected because they are rich in information, while the inclusion of the other spectral data (i.e. 4000–3000 cm^{-1} and 2800–1700 cm^{-1}) might interfere with the extraction of useful information. Water exhibits a strong absorption band in most of the considered food products, overlapping amide I and II protein bands. Owing to the high absorbance at about 1640 cm^{-1} in the amide I and II regions, and in order to comply with the Beer-Lambert law, the path length of the cuvette has to be in the 10 μm range.

Dairy products

Monitoring the quality of cheese throughout ripening

Rapid screening techniques to determine quality characteristics of *cheeses* throughout ripening are of great interest for both industry and consumers. In common with the processed food industry at large, the dairy industry has come under increasing pressure to deliver products of high and constant quality to the marketplace.

The *ripening* process implies several complex modifications, which take place simultaneously or successively. Indeed, the biochemical transformations impart new characteristics: the paste of the cheese is modified in its composition and structure, and consequently in its appearance, consistency and color. At the same time, flavor and typical taste develop. Such processes ensure a constant excellent quality of the product, and control can be achieved by examining the phases of the production process and/or the finished products.

Proteolysis is the principal and most complex biochemical event occurring during the ripening of cheese. Indeed, during cheese ripening part of the casein is converted into water-soluble nitrogenous compounds, such as peptides and amino acids (Fox, 1989). These peptides have different solubilities in water and other solvents. Therefore, extractions with different solvents and subsequent quantification of nitrogenous compounds in the cheese extract are used to study the extent of proteolysis in cheese.

The determination of the chemical composition of cheese is a very important task which has classically been undertaken by different physicochemical methods to determine the pH-value, fat, nitrogen fractions, volatile fatty acids, organic acids contents, etc. However, such methods are cumbersome, require a great deal of time and are expensive, and in some cases the results are not very accurate. Taking this into account, the development of new methods for the determination of chemical parameters is of great importance.

Nowadays, there is a need in the cheese-processing industry for tools that can be used for real-time control of production lines to check whether in-process material, during a given processing step, meets the necessary compositional or functional specifications to reach a predetermined quality standard in the final product. In this context, spectroscopic techniques such as MIR are fast, relatively low-cost, and provide

a great deal of information with only one test. They are considered to be sensitive, non-destructive, rapid, environmentally friendly and non-invasive, making them suitable for on-line or at-line process control and appropriate for process control.

The potential of FT-MIR in monitoring the ripening time of 16 experimental semi-hard cheeses at four different times of ripening (1, 21, 51 and 81 days) has been investigated by several researchers (Dufour *et al*., 2000; Mazerolles *et al*., 2001, 2002).

In the first step, *principal component analysis* (*PCA*) was applied to the 1700–1500 cm^{-1} spectral region recorded in the investigated cheeses at different ripening times, and the pattern of each component was examined. The authors clearly demonstrated the potential of PCA to facilitate discrimination between cheeses as a function of their ripening times. In addition, the rational molecular basis for the observed discrimination of the spectral patterns and their relation to known absorptions due to amide I and II was indicated by the same researchers, who stated that one or several continuous phenomena that occurred during the ripening stage were detected at the level of amide I and II absorption bands.

In the second step, and in order to determine the link between FT-MIR and fluorescence spectra, Mazerolles *et al*. (2001) applied canonical correlation analysis (CCA); on one hand to the 1700–1500 cm^{-1} spectral region and tryptophan fluorescence spectra, and on the other hand to the 3000–2800 cm^{-1} spectral region and vitamin A spectra. A relatively high correlation was found, since the first two canonical varieties with squared canonical correlation coefficient were higher than 0.58. The researchers concluded that FT-MIR and fluorescence spectra provide a common description of cheese samples throughout ripening.

In a similar approach, Martín-del-Campo *et al*. (2007a) used FT-MIR to monitor the ripening stage of Camembert-type cheese produced at a pilot scale. Cheeses samples were analyzed at two different zones (core and under-rind) during the first 10 days of ripening, as well as after 13, 15, 17, 20 and 27 days of ripening. From the results obtained, it was reported that throughout the ripening stage the under-rind spectra showed some modification in the spectra, while only a weak difference was observed between the recorded core spectra. The authors attributed the bands observed on the FT-MIR to molecules that are present in cheeses during ripening. Indeed, carbohydrate- and organic acid-associated bands were found in the 1490–950 cm^{-1} spectral region. Other bands located around 1096 cm^{-1} (secondary alcohol ν C–O and δ O–H), 1082 cm^{-1} (δ O–H) and 1045 cm^{-1} (primary alcohol ν C–O) have been associated with lactose by the same research group, which corroborates with the findings of others (Lanher, 1991; Picque *et al*., 1993; Cadet *et al*., 2000; Coates, 2000; Grappin *et al*., 2000). For the under-rind cheese samples, an increase in the absorbance at 1160 cm^{-1} during the first 6 days followed by a decrease until the end of the ripening stage was observed. This evolution has been ascribed to the presence of monosaccharides like glucose and galactose, which come from the lactose degradation throughout the ripening stage.

Regarding the region located between 1700 and 1500 cm^{-1}, two important peaks – *amide I* at 1640 cm^{-1} (ν C=O, ν C–N) and *amide II* at 1550 cm^{-1} (δ N–H and ν C–N) – characteristic of and associated with protein response were observed, in agreement with previous findings (Dufour and Robert, 2000; Grappin *et al*., 2000; Robert and Dufour, 2000). Significant changes were recorded for amide I and II bands

for the under-rind cheese samples, but only amide II bands for the core. In addition, the ratio of absorbance amide I to absorbance amide II showed a significant change throughout the ripening stage for both cheese sections. Modifications in the intensity and position of different bands in the amide I peak have been associated with changes in casein secondary structure, protein aggregation and protein–water interaction, as reported by others (Guerzoni *et al*., 1999; Mazerolles *et al*., 2001; Vannini *et al*., 2001; Kulmyrzaev *et al*., 2005). A continuous decrease in the band located at 1652 cm^{-1} and a continuous increase in that located at 1550 cm^{-1} during the ripening of semi-hard cheeses and cheeses inoculated with different strains of *Y. lipolytica* was pointed out by Mazerolles *et al*. (2001) and Lanciotti *et al*. (2005), and Vannini *et al*. (2001), respectively. However, Guerzoni *et al*. (1999) reported a continuous increase for both amide bands in goat cheeses produced by different processes.

Considering the 3000–2800 cm^{-1} spectral region characteristic of fat, the authors noted that neither methylene (bands around 2920 and 2851 cm^{-1}) nor methyl (bands around 2954 and 2871 cm^{-1}) signal changes were significant for the core, while they were significant in the spectra recorded on the under-rind zone, confirming the findings of Dufour *et al*. (2000), and Kulmyrzaev *et al*. (2005) regarding semi-hard cheeses and soft cheeses, respectively. Regarding semi-hard cheeses, Dufour *et al*. (2000) reported an increase in the $A\nu_{as}\ CH_2/A\nu_{as}\ CH_3$ ratio throughout ripening.

Finally, and in order to extract information from the data sets, Martín-del-Campo *et al*. (2007a) applied PCA to the spectral data set and the similarity map showed good discrimination of cheese samples presenting a ripening time of 15 days or less from the others. In order to achieve interpretation at the molecular level, the researchers studied the eigenvectors corresponding to PC1 and PC2. The eigenvector 2 showed two important regions related to amide I and II, and another assigned to carbohydrates (1500–950 cm^{-1}). The former showed an opposition between a positive band located 1632 cm^{-1} (amide I) and a negative one observed around 1543 cm^{-1} (amide II) peaks. The obtained results confirmed those found previously by Mazerolles *et al*. (2001) with semi-hard cheeses and Kulmyrzaev *et al*. (2005) with soft cheeses; while the latter have pointed out that changes in the 1700–1500 cm^{-1} spectral region could classify cheeses according to their ripening times. The opposition between amide I and II was also observed. The lactate bands located at 1589 cm^{-1} and 1743 cm^{-1} have been observed in different varieties of cheeses (Guerzoni *et al*., 1999; Kulmyrzaev *et al*., 2005; Lanciotti *et al*., 2005). Martín-del-Campo *et al*. (2007a) reported that the band at 1589 cm^{-1} was found to correlate with the spectral evolution of cheese from day 1 to day 8 – the period during which the concentration of lactic acid increases from days 1–5 before decreasing after day 5 (Leclercq-Perlat *et al*., 2004).

Prediction of some chemical parameters in dairy products

FT-MIR milk analyzers are widely used in the dairy industry to determine major components such as fat, protein, lactose, solid contents, etc. Lynch and Barbano (1995) used FT-MIR to determine how well the calibration equations generated by using reconstituted *milk powders* could be used to predict the chemistry of raw milk samples. In their studies, 12 reconstituted powders and 7 raw milk samples were analyzed in 7 laboratories using FT-MIR. For each laboratory, corrected and uncorrected data were recorded.

The authors considered that corrected data reflected current calibration. The reconstituted powders were found not to provide an accurate fat calibration for testing raw milk samples, as can be obtained with raw milk calibration samples. This has been attributed primarily to differences in the characteristics of the fat in the reconstituted powders and in raw milk. Regarding protein, the analytical precision for both types of calibration were found to be comparable. In another study, the accuracy of FT-MIR to determine casein content in dairy cows' milk was investigated (Sørensen *et al*., 2003). By applying *partial least squares* (*PLS*) regression to the FT-MIR spectra and casein amount determined by reference method, *standard errors of prediction* (*SEP*) of 0.033% and 0.89% for casein concentrations in the range of 2.1–4.0% and 70.7–81.0% were found, respectively. The main conclusion of this study was that FT-MIR was found to be less sensitive to heat denaturation of whey proteins than was the reference method. The obtained results were recently confirmed by the investigations of Etzion *et al*. (2004), who succeeded in predicting protein concentrations of 26 milk standards produced at the laboratory scale for which the amount of proteins varied from 2.27 to 3.90 g $100\,g^{-1}$. However, in their study the authors observed significant interference when the water subtraction procedure was applied, which they considered to be the primary obstacle to the determination of protein level. Another problem stated by the authors has been attributed to the fact that milk spectra were influenced by other constituents, such as fat and lactose, forming a potential buffer layer between the ATR crystal and the protein cells. Using the same approach, Iñón *et al*. (2003a) utilized the same technique to predict the nutritional parameters of 83 commercially available bottles of milk covering the whole range of available brand names and types of milk in Spain – i.e. whole (25), semi-skilled (35), skimmed (23), and with (45) and without (38) additives, including nutritional modified milks for babies (5) and a milkshake with tropical fruits (1). The researchers applied PLS regression for the determination of total fat, total protein, total carbohydrates, calories and calcium, and relative precisions of 0.062 g $100\,g^{-1}$, 0.04 g $100\,g^{-1}$, 0.039 g $100\,g^{-1}$, 0.66 kcal $100\,ml^{-1}$, and 2.1 mg Ca.$100\,ml^{-1}$ were obtained, respectively. One of the main conclusions of this study is that FT-MIR-ATR could be used as a suitable technique for the classification of milk samples.

Picque and colleagues (Martín-del-Campo *et al*., 2007b) used the FT-MIR to *predict* some chemical parameters (pH, acid-soluble nitrogen, non-protein nitrogen, ammonia (NH_4^+), lactose and lactic acid) by applying PLS regression. The obtained results showed good prediction of these parameters, except for that of pH. Indeed, the accuracy obtained for dry matter and pH was in agreement with those of Karoui *et al*. (2006a) for commercial soft cheese. The authors concluded that, although the physicochemical parameters were determined at different ripening time, they were comparable to previous findings obtained on ripened cheeses.

Karoui *et al*. (2006b–2000d) have also used FT-MIR to determine chemical parameters in Emmental cheeses produced in the summer and winter seasons, and originating from different geographic origins. For Emmental cheeses produced during the summer period, Karoui *et al*. (2006c) pointed out that the best results for water-soluble nitrogen (WSN) ($R^2 = 0.91$; ratio of standard deviation to root mean square error of prediction (RPD) = 3.34) (Figure 2.3a), non-protein nitrogen (NPN) ($R^2 = 0.77$; RPD = 2.08) (Figure 2.3b), pH ($R^2 = 0.57$; RPD = 1.41), NaCl ($R^2 = 0.45$;

RPD = 1.33) and total nitrogen (TN) (R^2 = 0.43; RPD = 1.34) were obtained when the spectra were subjected to the first derivation and smoothing after being subjected to maximum normalization. The researchers concluded that FT-MIR transmission spectroscopy could be considered as an alternative technique for the determination of

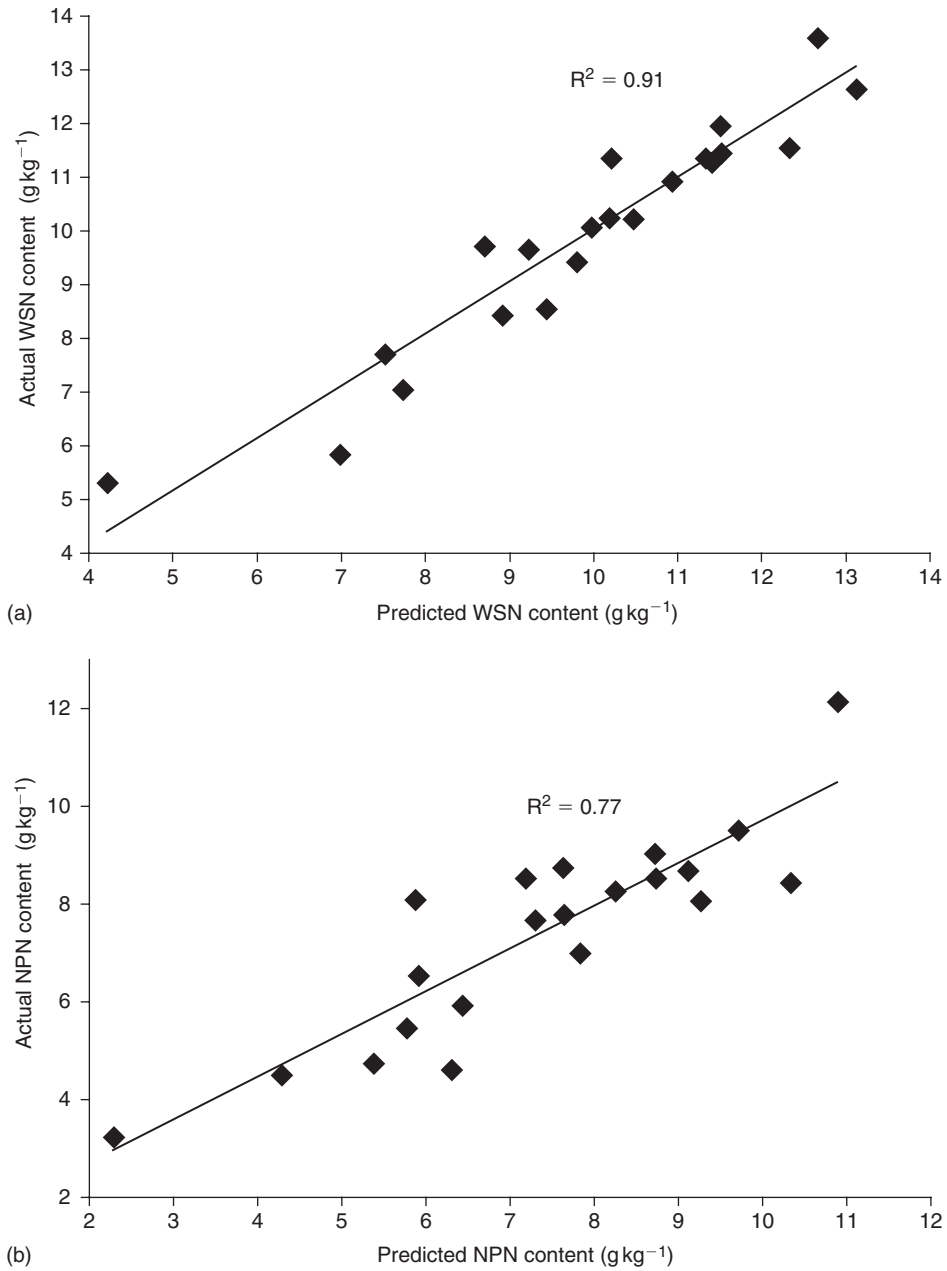

Figure 2.3 Linear regression plot of actual versus predicted (a) water soluble nitrogen (WSN) and (b) non-protein nitrogen (NPN) content of the validation data set for the Fourier transform infrared spectroscopy (FT-MIR) recorded on European Emmental cheeses produced during summer period.

NPN and WSN of Emmental cheeses produced during summer and originating from different European countries. The obtained results were in agreement with the findings of Martín-del-Campo (2007b), who found an R^2 of 0.92 and an RPD of 3.27 for NPN on soft cheese samples presenting different ripening time. In order to achieve

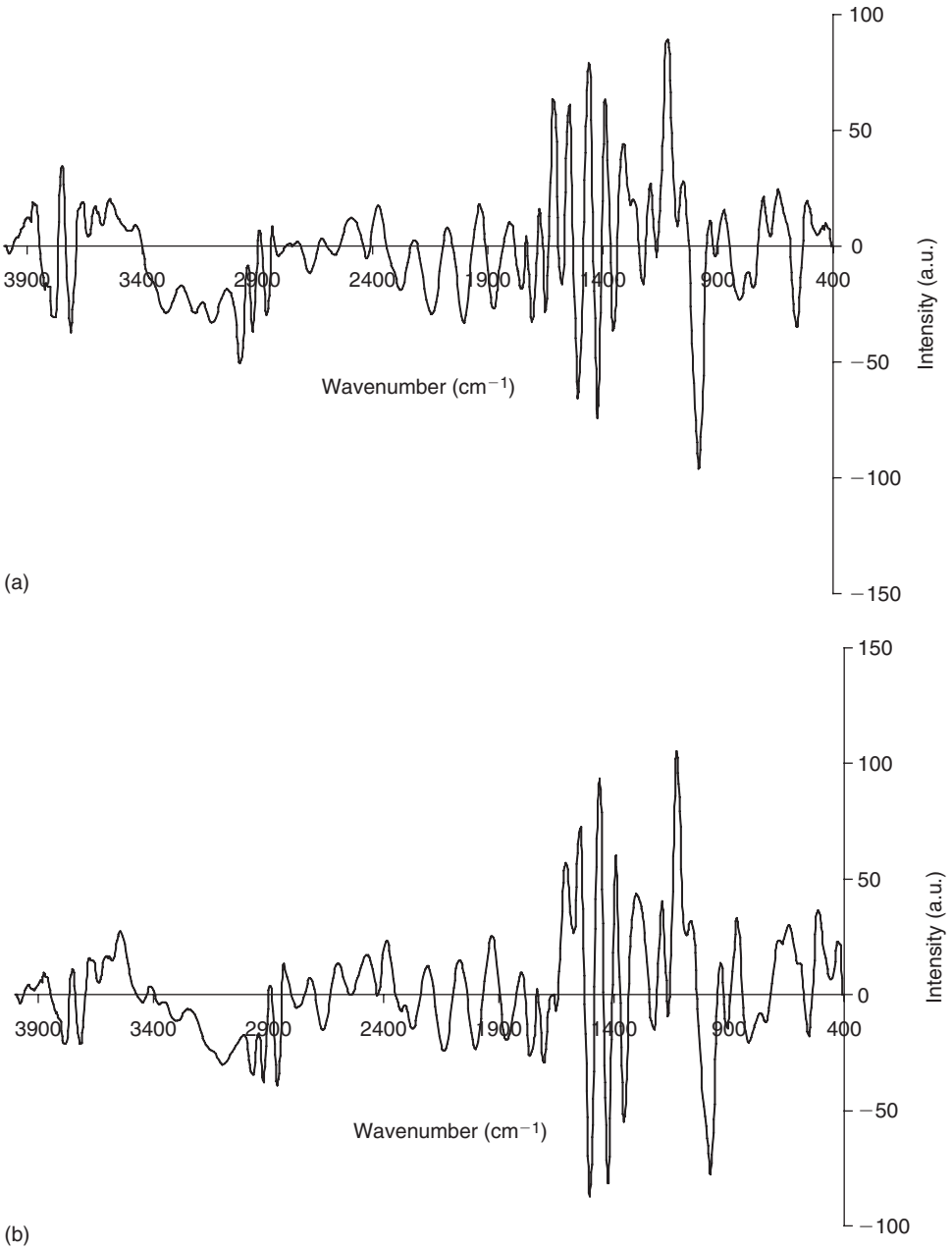

Figure 2.4 Correlation coefficient over the entire wavelength range of (a) non-protein nitrogen (NPN) and (b) water-soluble nitrogen (WSN) for the Fourier transform infrared spectroscopy (FT-MIR) recorded on European Emmental cheeses produced during the summer period.

interpretation at the molecular level, Karoui and colleagues (2006c) studied the *correlation coefficient distribution* of WSN and NPN over the entire wavelength range. They observed that the 1620–979 cm^{-1} spectral region was the most important spectral region, owing to the presence of several correlation peaks (Figures 2.4a, 2.4b). When the wavelength range of 1620–979 cm^{-1} was considered only during the PLS cross-validation stage, the resultant model for NPN and WSN provided very similar results to the model developed for the entire wavelength range.

Unsuccessful measurement of TN was achieved for Emmental cheeses produced during the summer period using the FT-MIR-PLS measurement method. The researchers reported that the obtained results confirmed their previous findings reporting that the FT-MIR cannot be used with success to predict TN in Emmental cheeses produced during winter (Karoui *et al*., 2006d). The correlation coefficients and the root mean square error of prediction (RMSEP) values reported in their study were in the same range as reported in previous investigations (Pierce and Wehling, 1994; Wittrup and Nørgaard, 1998). However, in the investigations by Karoui *et al*. (2006d) the Emmental cheeses were from variable sources – they came from different European countries, and were manufactured with raw or thermized milk, using different cheese-making procedures and ranging in age.

Karoui *et al*. (2006c) reported that quantitative measurement of pH indicates that FT-MIR can discriminate only between high and low values, while the results obtained for NaCl were not supported by the methodology since the R^2 values of the calibration and validation data sets were 0.47 and 0.45, respectively (Tables 2.2, 2.3). These values have been reported to be relatively smaller than those obtained by Karoui *et al*. (2006d) on Emmental cheeses produced during the winter. The researchers attributed these differences to the fact that a smaller range in NaCl content was considered (0.24–0.97 g 100 g^{-1}) for the summer-produced cheeses than for the winter-produced cheeses (0.19 and 1.36 g 100 g^{-1}). However, they stated that further investigation was needed to confirm this hypothesis.

In a similar approach, Karoui and colleagues (2006b) compared FT-MIR and NIR for predicting the same physicochemical parameters on Emmental cheeses produced during the winter season. The researchers suggested the use of NIR for the determination of fat and TN contents, and of FT-MIR for NaCl and NPN contents as well as for pH. Similar results were obtained for WSN using the two techniques together. The main conclusion of their study is that the combination of both NIR and FT-MIR spectra did not improve the results, since comparable results to those obtained from either the NIR or FT-MIR were obtained.

Determination of the quality and the geographic origin of dairy products at the retailed stage

Today, the European market is saturated with food products. The new challenge is not to produce a standard product which is only differentiated by price, but to produce products that have unique characteristics and meet consumer expectations. Two approaches can be used to reach these goals. On one hand, fulfilling consumer demands can be achieved through the creation of commercial brand products with unique texture, flavor or usage appeal characteristics; on the other, *Protected*

Table 2.2 Validation results of PLS cross-validation regression on calibration sample set of Emmental cheeses produced during summer period

Compositional parameter	LV	R^2	RMSECV ($g\,100\,g^{-1}$)	RPD
NaCl	11	0.47	0.127	1.37
pH*	11	0.56	0.005	1.50
NPN	12	0.71	0.085	1.85
TN	8	0.33	0.112	1.11
WSN	12	0.80	0.068	2.22

NPN, non-protein nitrogen; TN, total nitrogen; WSN, water-soluble nitrogen; LV, latent variables; R^2, determination coefficient; RMSECV, root mean square error of cross-validation; RPD, ratio of prediction deviation (Standard deviation/RMSECV)
*pH is expressed without unit.

Table 2.3 Validation of PLS cross-validation regression on validation set of Emmental cheeses produced during summer period

Compositional parameter	R^2	RMSEP ($g\,100\,g^{-1}$)	RPD
NaCl	0.45	1.54	1.32
pH*	0.57	0.07	1.41
NPN	0.77	0.99	2.08
TN	0.43	1.24	1.34
WSN	0.91	0.65	3.34

NPN, non-protein nitrogen; TN, total nitrogen; WSN, water-soluble nitrogen; LV, latent variables; R^2, determination coefficient; RMSEP, root mean square error of prediction; RPD, ratio of prediction deviation (Standard deviation/RMSEP)
*pH is expressed without unit.

Designation of Origin (*PDO*) indicates brands of a particular quality because they can be made only from raw milk possessing specific features, which also fulfills consumer demands. A PDO cheese is defined according to its geographical area of production, and also according to the description of the materials and of the technology used (Bertoni *et al*., 2001).

Several techniques for assessing the *authenticity* of PDO food products have been used, and these can be classified into two categories. *Traditional techniques*, such as gas chromatography, capillary gas chromatography of lipid fractions and electrophoretic separation of proteins, focus on the existence or absence of certain chemical compounds in the authentic product (Pillonel *et al*., 2002). Although these methods provide valuable information regarding the composition and biochemistry of cheeses, they are time-consuming and expensive processes which require highly skilled operators and are not easily adapted to online monitoring. Hence, an urgent demand exists for rapid, inexpensive and efficient techniques for quality control. A great number of non-invasive and non-destructive instrumental techniques, such as infrared and fluorescence spectroscopic techniques, have been developed for the authentication of food products. These new analytical tools require limited sample preparation and appear promising. Recently, the potential of FT-MIR for determining the *geographic*

origin of Emmental cheeses manufactured during the winter and summer seasons has also been investigated (Karoui *et al*., 2004a, 2004b, 2005a, 2005b). The application of FT-MIR to determine the shelf-life of Pasta Filata and Crescenza cheeses was investigated by Cattaneo *et al*. (2005) and Giardina *et al*. (2003), respectively. These authors reported that FT-MIR allowed the evaluation of the shelf-life period in which cheese was maintained and suggested the use of this technique for the classification of cheeses in real time on the basis of their shelf-life.

In order to obtain a more detailed description regarding the variation in the spectra recorded for cheese, Karoui *et al*. (2005b) applied the first derivative to the spectra of Emmental collected from different European regions (Figure 2.5). Contribution to the lipids can be observed in the 3000–2800 cm^{-1} spectral region, which is dominated by two strong bands at 2915 and 2846 cm^{-1} associated with methylene anti-symmetric and symmetric stretching (Dufour *et al*., 2000), respectively. Two other bands resulting from the asymmetric and symmetric stretching modes of the terminal methyl groups were also present at 2954 and 2860 cm^{-1}, respectively. Contributions to the amide I band can be observed around 1684 and 1622 cm^{-1}. This part of FT-MIR was used by other researchers (Mazerolles *et al*., 2001) to investigate the secondary structure of several proteins. The absorption bands at 1578, 1526 and 1512 cm^{-1} are generally assigned to the amide II vibrations, while that around 1578 cm^{-1} has been attributed to soluble carboxylic acids, such as lactate (which has a characteristic wavelength at 1575 cm^{-1}, as shown by Picque *et al*., 1993). The region located between 1500 and 900 cm^{-1}, called the fingerprint region, refers to C–O and C–C stretching modes (1153–900 cm^{-1}) as well as other numerous bonds (amide III) and P–O.

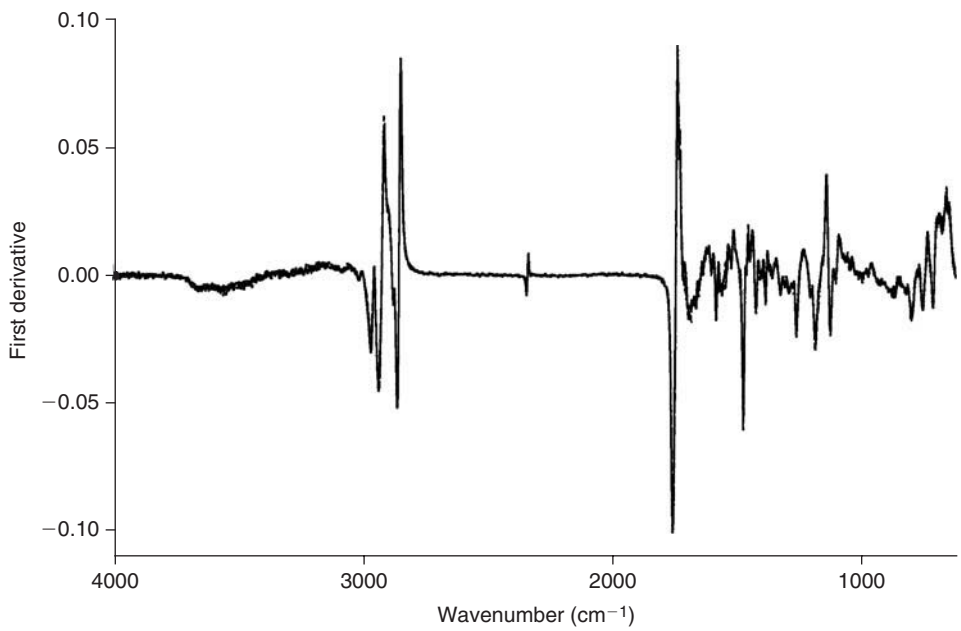

Figure 2.5 Averaged first derivative of the Fourier transform infrared spectroscopy (FT-MIR) spectra for Emmental cheeses from Austria (––), Germany (.....), Switzerland (------), France (·····) and Finland (— —).

In order to extract information from the data set and to assess the potential of FT-MIR to authenticate cheeses according to their geographic origin, Karoui and colleagues (2005b) applied PCA to the three normalized data sets corresponding to the three spectral regions (3000–2800 cm^{-1}, 1700–1500 cm^{-1} and 1500–900 cm^{-1}). For these three spectral regions, the plots of the scores for PC1 versus PC2 did not reveal any outlying samples or any obvious spatial pattern in the sample score distribution.

The authors then applied *factorial discriminant analysis* (*FDA*) to the first 20 principal components (PCs) of PCA performed on the three data sets corresponding to 3000–2800 cm^{-1}, 1700–1500 cm^{-1} and 1500–900 cm^{-1} spectral regions for the different cheeses. Before applying FDA, five groups were created, for cheeses from Austria, Finland, Germany, Switzerland and France. Regarding the 3000–2800 cm^{-1} spectral region, the authors pointed out good discrimination of Finnish cheeses from the other cheeses. In addition, correct classifications of 84.1% and 85.7% were observed for the calibration and validation data sets, respectively (Table 2.4). Analysis of this table illustrates that cheeses from Austria and Finland were well classified, while some misclassification occurred for cheeses from Switzerland, France and Germany.

Table 2.4 Classification table for Emmental cheeses produced during winter period and originating from different countries based on mid-infrared (MIR) (3000–2800 cm^{-1}, 1700–1500 cm^{-1} and 1500–900 cm^{-1}) validation data sets

Predicted[a]	**Observed**[b]				
	Austria	**Finland**	**Germany**	**France**	**Switzerland**
	MIR: 3000–2800 cm^{-1} spectral region				
Austria	**4**	—	—	1	—
Finland	—	**6**	—	—	—
Germany	—	—	**11**	1	1
France	—	—	1	**25**	5
Switzerland	—	—	1	3	**32**
% Correct classification	**100**	**100**	**84.6**	**83.3**	**84.2**
	MIR: 1700–1500 cm^{-1} spectral region				
Austria	**2**	—	—	—	—
Finland	—	**6**	—	—	—
Germany	1	—	**12**	—	—
France	1	—	1	**28**	2
Switzerland	—	—	—	2	**36**
% Correct classification	**50**	**100**	**92.3**	**93.3**	**94.7**
	MIR: 1500–900 cm^{-1} spectral region				
Austria	**2**	—	—	—	—
Finland	—	**6**	—	—	—
Germany	2	—	**13**	—	—
France	—	—	—	**30**	1
Switzerland	—	—	—	—	**37**
% Correct classification	**50**	**100**	**100**	**100**	**97.4**

[a]The number of predicted cheese samples.
[b]The number of observed cheese samples.

Considering the amide I and II regions, similar results to those obtained with the 3000–2800 cm^{-1} spectral region, i.e. 88.5 and 96.7% (Table 2.4) of correct classifications, were observed for the *calibration and validation* data sets, respectively. The researchers claimed that the best results were obtained with the 1500–900 cm^{-1} region, since the map of the FDA defined by the discriminant factors 1 and 3 allowed good discrimination between Emmental cheeses from the different countries (Figure 2.6). Indeed, cheeses from Switzerland and Finland were located on the left according to discriminant factor 1, whereas those from France, Austria and Germany were located on the right. Correct classifications amounting to 96.7% (Table 2.4) were observed for the calibration and validation sets. Table 2.4 shows that cheeses from Germany, France and Finland were totally discriminated. However, Swiss and Austrian cheeses showed less than 100% correct classification (97.4% and 50%, respectively). One of the main conclusions of this study was that the 1500–900 cm^{-1} spectral region is considered by the researchers to be a promising tool for reliable determination of the origin of Emmental cheeses. The obtained results confirmed those obtained by the same research group on Emmental cheeses produced during the summer period, since the best results were obtained by using the 1500–900 cm^{-1} spectral region (Karoui *et al*., 2004b). The obtained results were confirmed recently by Giardina *et al*. (2003) on a typical Pasta Filata cheese. These latter authors analyzed 112 cheese samples coated with biodegradable wax or paraffin at 90 and 120 days of shelf-life and found that the 1100–1035 cm^{-1} and 1720–1690 cm^{-1} spectral regions could be used to classify cheese samples according to the days of shelf-life and the type of coating.

Finally, Karoui and colleagues (2004a) assessed the potential of FT-MIR to determine the region in which Emmental cheeses were produced independently of the

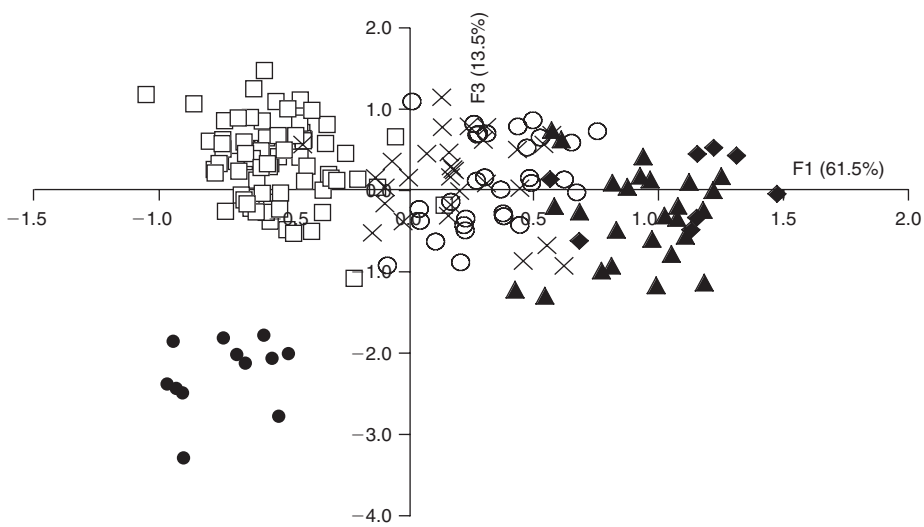

Figure 2.6 Discriminant analysis similarity map determined by discriminant factors 1 (F1) and 3 (F3) for 1500–900 cm^{-1} spectral region of Emmental cheeses produced during the winter period and originating from Austria (◆), Switzerland (□), Germany (▲), France (from thermized milk, ×; from raw milk, ○) and Finland (●).

production season by using the concatenation technique, which was analyzed by FDA. Although, the results obtained did not allow 100% correct classification of cheeses, the authors concluded that the obtained findings could be considered promising considering the significant effect of the season on the characteristics of investigated cheeses. The findings were later confirmed by the investigation of Karoui *et al*. (2005a) reporting that the FT-MIR provided relevant information on the geographical origin of both experimental Jura hard cheeses and Swiss Gruyère and l'Etivaz PDO cheeses. The researchers pointed out that the calibration stage and development of the calibration equations are the limiting steps for adopting FT-MIR as a technique for the authentication of dairy products, as these are time-consuming and costly. However, when the calibration stage is accomplished successfully, the determination of a chemical property or geographical origin can be carried out very rapidly with a single analysis for minimal cost.

Meat and meat products

The nature of some meat products (pies, sausages, burgers) offers many possibilities for adulteration. Cheaper cuts or offal may be substituted for expensive cuts, and water or vegetable matter may be added. The potential of FT-MIR to differentiate between three meats – turkey, chicken and pork – was shown by Al-Jowder *et al*. (1997). Indeed, by applying PCA to the spectral data sets, good discrimination was observed between fresh and frozen-then-thawed turkey, chicken or pork samples. The same research group also showed that FT-MIR could discriminate fresh meat from that which had previously been frozen. In another study, Al-Jowder and colleagues (1999) indicated the potential of FT-MIR to detect adulteration of raw, ground beef with certain types of offal obtained from the same species – specifically, kidney and liver. Comparing the 1000–1200 cm^{-1} spectral region, clear differentiation between the spectra of the investigated meat samples was observed. The researchers ascribed these variations to the high level of collagen in liver samples. PLS regression was then applied in order to quantify the amount of added offal. The prediction errors obtained in the calibration data sets were found to be 4.8% and 4%, respectively, for the kidney and liver samples. The same research group (Al-Jowder *et al*., 2002) has recently assessed the potential of FT-MIR to discriminate between pure beef and beef containing 20% of a range of potential adulterants, such as heart, tripe, kidney and liver. FT-MIR spectra were recorded on raw samples as well as samples cooked using two different cooking regimes. By applying chemometric tools to the collection spectra, good discrimination of pure meat samples from adulterated samples irrespective of cooking regime was found, with a correct classification of 97%. The authors pointed out the possibility of discriminating between pure beef and the other samples adulterated with heart, tripe, kidney and liver, but this became more difficult as the cooking level increased.

Some proteolytic enzymes from plants or animals have been widely used as meat tenderizers for food processing in home cooking and industrial treatment. Lizuka and Aishima (1999) assessed the potential of FT-MIR to differentiate between reference beef and beef treated with pineapple juice. The obtained results showed good

discrimination between the two meat samples. In another study, Adhikari *et al*. (2003) used FT-MIR for detecting the presence of hexanal and methyl sulfide in a meal ready-to-eat (MRE) omelet with ham, as well as to monitor changes in the levels of hexanal and methyl sulfide in selected thermally-processed MRE products held under modified-atmosphere packaging and at elevated storage temperatures. The researchers concluded that FT-MIR method could be used as a tool for routine quality analysis of stored MRE and other food products.

Cereals and cereal products

The potential of FT-MIR use in cereals and cereal products has increased over the past few years with the propagated application of chemometric tools. Cocchi *et al*. (2004) used FT-MIR to discriminate among flour samples of different cereals and pseudo-cereals, namely wheat, oats and buckwheat, subjected to different technological treatments – dehulling, toasting and puffing. The use of oats and buckwheat is currently limited to the production of low-diffusion or niche foods. When compared with major cereals, such as wheat, maize and rice, these minor cereals are interesting because of their content of natural nutrients and biologically active components. The obtained results highlighted the usefulness of FT-MIR to characterize and better understand the flour matrices. One of the main conclusions of this study was that the obtained results were considered to be encouraging in view of studying mixtures of the flours, to predict their performances in dough- and bread-making processes. In another study, Kim *et al*. (2007) used FT-MIR to determine trans fatty acids in ground cereal products without oil extraction. PLS models were developed for the prediction of trans fatty acids in ground samples using several wavelength selections on the basis of bands related to lipids. The models developed with a number of samples of 79 predicted trans fatty acids in ground samples with a *standard error of cross-validation* (*SECV*) of 1.10–1.25 (range 0–12.4%) and R^2 of 0.85–0.88, and in validation samples (n = 26) with a SEP of 0.96–1.12 (range 0–12.2%) and R^2 of 0.89–0.92, indicating sufficient accuracy for screening. Sample trans fatty acid percentages were predicted as accurately within the fingerprint region (1500–900 cm^{-1}) as within the entire range (4000–650 cm^{-1}), indicating, in concert with the regression coefficients, the importance of the isolated trans double bonds at 966 cm^{-1} in development of the model.

Lizuka and Aishima (1999) investigated the ability of FT-MIR and NIR to differentiate between 27 soy sauces produced from whole soybeans and 30 from defatted soybeans. The researchers applied factor analysis separately to MIR and NIR, and indicated the existence of some difference between the two sauces. By applying *linear discriminant analysis* (*LDA*), 94.7% and 100% correct classification were obtained for MIR and NIR spectra, respectively.

In the food industry, starch is used to modulate product characteristics such as texture, appearance and stability in a wide range of applications. In the unmodified or native form starches have limited use in the food industry, and therefore starches undergo a process of modification to modulate their properties to provide the expected thickening, water-binding, stabilizing, gelling effect or to improve the

mouth feel and shininess of the product. Fernández Pierna *et al*. (2005) evaluated the potential of FT-MIR spectroscopy to identify modified starches in a food industry environment. To do this, MIR spectra were collected with a spectral resolution of 4 cm^{-1} using a Perkin-Elmer Spectrum 2000 FTIR spectrometer (Perkin Elmer Corporation, Norwalk, CT, USA) equipped with an ATR system Specac MKII GoldenGate (Specac Inc., Smyrna, GA, USA) positioned to give an incident angle of 45°. This spectrophotometer is fitted with a wire coil operated at 1350 K as an IR light source, a potassium bromide beam-splitter and a DTGS detector. Starch samples (232) were collected from various factories located in the USA and Europe of four different classes: one unmodified and three modified. The performance of different classification methods was compared by the researchers, who applied methods such as LDA, quadratic discriminant analysis (QDA), k-nearest neighbors (k-NN), soft independent modeling of class analogies (SIMCA), PLS-DA, ANN and support vector machines (SVM). The results showed that the different discrimination methods based on FT-MIR data can be effective tools for the classification of starches according to the type of chemical modification undergone, but the best results were obtained using the SVM technique, with more than 85% of the samples correctly classified when validating the model.

Edible oils

Olive oil is classified according to purity, and can vary from *extra-virgin olive oil* (*EVOO*) to lampante, which is not fit for consumption. According to the International Olive Oil Council, *virgin olive oil* (*VOO*) is the oil obtained from the fruit of the olive tree solely by mechanical or other physical means under conditions (particularly thermal) that do not lead to adulteration in the oil, and which has not undergone any treatment other than washing, decantation, centrifugation and filtration. The high-quality EVOO may thus be mislabeled or adulterated with cheaper oil. This is not only a commercial problem but also has health implication (Kochhar and Rossell, 1984). Adulteration involves the addition of cheaper oils; the most common adulterants found in VOO are refined olive oil, residue oil, synthetic olive oil–glycerol products, seed oils (such as sunflower, soy, maize and rapeseed) and nut oils (such as hazelnut and peanut oil) (Baeten *et al*., 1996, 2005; Downey *et al*., 2002; Sayago *et al*., 2004). The low price of olive–pomace oil means that it is sometimes used for adulterating EVOO. For this reason, a rapid method to detect such a practice is important for quality control and labeling purposes.

Several techniques can be used to detect olive oil adulteration. Among them there are colorimetric reactions, and determination of iodine and saponification values, density, viscosity, refractive index, and ultraviolet absorbance (Gracian, 1968). However, these methods may be time-consuming and require sample manipulation. To overcome these handicaps, other techniques have been applied. The most noteworthy are spectroscopic techniques such as NIR, FT-MIR, nuclear magnetic resonance and fluorescence spectroscopy.

Van de Voort *et al*. (1994) used FT-MIR for the quantitative determination of peroxide values (PV) of vegetable oils in transmission mode. Calibration standards were

prepared by the addition of *t*-butyl hydroperoxide to a series of vegetable oils, along with random amounts of oleic acid and water. Additional standards were derived through the addition of mono- and diglyceride spectral contributions, as well as zero PV spectra obtained from deuterated oils. The researchers applied PLS regression to the 3750–3150 cm^{-1} region and compared the obtained values with those determined by the reference method (AOCS – American Oil Chemists Society). The reproducibility of the FT-MIR method (coefficient of variation CV = 5%) was found to be better than that of the chemical method (CV = 9%), although its accuracy was limited by the reproducibility of the chemical method. Later, the same research group (Van de Voort *et al*., 1995) used the FT-MIR to determine simultaneously the percentage *cis* and *trans* content of edible fats and oils. The system was calibrated to predict the *cis* and *trans* content of edible oils by using pure triglycerides as standards and the PLS regression method. The efficacy of the calibration was assessed by triglyceride standard addition, by mixing of oils with varying *cis/trans* contents, and by analyzing fats and oils of known iodine value. Each of the approaches verified that the FT-MIR method measured the *cis* and *trans* content in a reproducible (±0.7%) manner, with the measured accuracies being 1.5% for standard addition and 2.5% for the chemically analyzed samples. Comparisons also were made using the conventional AOCS method for the determination of *trans* isomers by FT-MIR spectroscopy, and the obtained results showed that the FT-MIR–PLS approach worked well for a wide range of *trans* contents, including those between 0 and 15%. The researchers concluded that FT-MIR could be implemented in place of a variety of AOCS wet chemical methods.

Marigheto *et al*. (1998) used FT-MIR and Raman spectroscopies to assess their ability to discriminate between oils originating from different botanical sources, and to detect added adulterants. In their studies, several oil samples were used – EVOO, refined oil, sunflower, rapeseed, soybean, sesame, hazelnut, swe*et* almond, grapeseed, safflower, peanut, walnut, mustard, corn, palm, coconut and palm kernel oils. In total, 140 spectra were collected to form a database called "pure oils", in which seven different groups were present: EVOO (n = 36), refined oil (n = 10), sunflower oil (n = 28), rapeseed oil (n = 18), soybean oil (n = 21), peanut oil (n = 9) and corn oil (n = 18). These samples were further divided into a calibration set of 84 spectra, a validation set of 27 spectra and a test set of 29 spectra. After that, 11 of the EVOO group were chosen to be adulterated with 5 seed oils and 5 EVOO were adulterated with 5 olive oils, at different levels of adulteration (5, 15, 25, 35 and 45%). The researchers then applied LDA and an *artificial neural network* (*ANN*). For FT-MIR, 100% of the samples were correctly classified by using 15 PC scores and by using an ANN with 12 PC scores. However, for Raman spectra, the best prediction was only 93.1% for 10 PC scores with LDA, which did not improve with the use of more PC. The authors concluded that FT-MIR is better than Raman for classifying oil samples and detecting adulteration. The obtained results were confirmed later by Tay *et al*. (2002), who pointed out that FT-MIR was able to discriminate EVOO from those adulterated with sunflower oil at different concentrations. This could be due to the difference in the content of free fatty acids in olive oil, as has been demonstrated by Iñón *et al*. (2003b), who indicated the ability of FT-MIR to determine the

content of free fatty acids with an R^2 of 0.996. Recently, Baeten *et al*. (2005) used FT-Raman and FT-MIR spectroscopy for the detection of the presence of hazelnut oil in olive oil at low percentages. Their study was performed on the entire oil and on its unsaponifiable matter. Different mixtures were prepared using VOO and hazelnut oils from several geographical origins in different percentages. For the univariate analysis, the Fisher coefficient was used to detect MIR spectral zones that distinguish olive from hazelnut oils. The most important differences were found in the fingerprint region characteristic of the stretching and bending vibrations of C–C and C–O groups of the molecules. Regarding multivariate analysis, stepwise LDA was applied to extract, interpret and exploit the information from the spectra. Complete discrimination between olive and hazelnut oils was observed, and it was found that adulteration can also be detected if the presence of hazelnut oil in olive oil is higher than 8%. The limit of detection is higher when the blends are of edible oils from diverse geographical origins.

Recently, Wang *et al*. (2006) examined two spectroscopic techniques, ATR-FT-MIR and fiber-optic diffuse reflectance NIR spectroscopy, for the identification of camellia oil adulteration. Camellia and soybean oil were mixed together in accurately weighed proportions to obtain calibration and validation sets of 50 adulterated samples. The amount of soybean oil as the adulterate in camellia oil ranged from 5% to 25%. By examining the 1132–885 cm^{-1} spectral region, minor differences between adulterated and pure camellia oil samples were observed, particularly at 912, 1097 and 1120 cm^{-1}, corresponding to C–H bending and C–H deformation of fatty acid. In order to extract information from the spectral data sets the authors applied PLS regression, and promising results were obtained. Indeed, the R-value of the model was around 0.99; while the values corresponding to RMSEP and the *root mean standard error of cross-validation* (*RMSECV*) were 0.67 and 0.85, respectively. The authors concluded that FT-MIR spectroscopy could be considered a powerful tool for the identification of pure camellia oil.

In another study, Guillén and Cabo (1997) reviewed the use of MIR in the study of fats and oils. Differences between dispersive and FT-MIR techniques were indicated by the researchers. The review stated the usefulness of FT-MIR for determining the degree of unsaturation or iodine value, *trans*-double bonds content, free fatty acid content, average chain length or saponification number, solid fat content, and peroxide and anisidine values.

Bellorini *et al*. (2005) assessed the abilities of various methods to differentiate the sources of fats used in feedstuff formulations. The main target was the identification of tallow (ruminant fat) and its differentiation from non-ruminant fats. Four different techniques were compared in terms of their suitability for enforcing existing and upcoming legislation on animal by-products: (1) FT-MIR applied to fat samples, (2) *gas chromatography coupled with mass spectrometry* (*GC-MS*) to determine fatty acid profiles, (3) immunoassays focusing on the protein fraction included in the fat, and (4) *polymerase chain reaction* (*PCR*) for the detection of bovine-specific DNA. Samples of the different fats and oils, as well as mixtures of these, were probed using these analytical methods. The obtained results showed that FT-MIR and GC-MS differentiated pure fat samples quite well but showed limited ability to identify the

animal species or even the animal class the fat(s) belonged to; there was no single compound or spectral signal that permitted species identification. However, immunoassays and PCR were both able to identify the species or groups of species that the fats originated from, and they were the only techniques able to identify low concentrations of tallow in a mixture of fats prepared by the rendering industry, even when the samples had been sterilized at temperatures above 133°C. The authors concluded that the combination of FT-MIR and multivariate techniques allows classification of pure samples according to their origin, but that it is not possible to use any single compound for reliable species identification.

In a similar approach, Gasperini *et al*. (2007) used FT-MIR for the classification of different food oil co- and by-products of potential use for feed preparation. Using this technique, a sure classification of fatty acid calcium soaps, fully hydrogenated fatty acids, lecithins, acid oils from chemical refining, acid oils from physical refining, and fish oils was observed. The remaining categories of animal fats, fried oils and oils recovered from exhausted bleaching earth could be differentiated by using one or two additional chemical tests.

Wine

Wine is routinely transported to bottling and packaging facilities, and between wineries for blending purposes. At present, there is no recognized method available to monitor easily the wine authenticity before and after transportation. The refractive index is commonly used as an indicator of wine dilution; however, it is not recognized as a technique to authenticate wine samples (Somers and Evans, 1974). Analytical control methods in an industrial environment, whether qualitative or quantitative, are essential in order to assess raw materials, products and by-products, as well as to optimize the manufacturing process itself. Conventional chemical methods of wine analysis involve time-consuming, laborious and costly procedures (Francis *et al*., 2005; Munck *et al*., 1998; Otto, 1999). Therefore, a robust, rapid and inexpensive method for quality assurance purposes is needed in the wine industry to ensure that wine parameters conform to specification, in order to guarantee the quality of the final product delivered to the consumer. FT-MIR could be an alternative technique to authenticate wine products. Visual examination of the infrared spectra is subjective, and often cannot discriminate between authentic and adulterated product, but the application of multivariate data analysis techniques presents the possibility of unraveling and interpreting the spectral properties of the sample and allowing classification without the use of direct chemical compositional information. One of the advantages of spectroscopic technology is that it allows the assessment of chemical structures through analysis of the molecular bonds in FT-MIR and also builds a characteristic spectrum that represents a “fingerprint” of the sample. This leads to the possibility of using spectra to determine complex attributes of organic structures in the sample, which are related to molecular chromophores, organoleptic scores and sensory characteristics.

Bevin and colleagues (2006) assessed the potential of FT-MIR to discriminate between 161 Australian wine samples originating from three grape varieties, namely

Shiraz, Cabernet Sauvignon and Merlot, and which were collected from six commercial wineries. When a wine was being dispatched for transportation to another processing site, a sample was taken and a FT-MIR spectrum obtained; when the wine arrived at its final destination, a second sample from the same wine was taken and a new spectrum acquired using an instrument of spectral similarity to the first. The two obtained spectra recorded with the same sample were then compared to confirm the authenticity of wine, or to observe changes that may have occurred during transportation.

From the FT-MIR spectra produced by the wine samples using the two instruments, the authors noticed that water and ethanol absorption peaks dominated the spectra, with the C–O stretch for primary alcohols at 1050 cm^{-1}, while the C–H stretch was observed in the 2850–2960 cm^{-1} spectral region. Regarding the 1690–1760 cm^{-1} region, it contained information relating to C=O stretching for aldehydes, carboxylic acids and esters. In order to extract information from the data sets, and to assess the variation in the wine spectra of the same wine measured using the two instruments, the authors applied chemometric tools. PCA confirmed that differences between wine samples were small. The authors concluded that discrimination between wine samples by a rapid analytical technique such as FT-MIR would be difficult (Bevin *et al*., 2006). The authors suggested the elimination of bands relating to water, since these account for approximately 85–90% of the wine sample matrix. By applying PLS regression, a good prediction of the similarity index from the FT-MIR was obtained.

In a similar approach, Edelmann *et al*. (2001) examined the potential of FT-MIR and UV-Vis for their ability to discriminate Austrian red wines of different cultivars (Cabernet Sauvignon, Merlot, Pinot Noir, Blaufränkisch (Lemberger), St Laurent and Zweiget). The authors used *cluster analysis*, a descriptive technique, to classify samples. The results obtained from the UV-VIS (250–600 nm) showed that the Pinot Noir variety was clearly separated from the other cultivars. Five of seven St Laurents were classified as belonging to the Zweiget cultivar. The Blaufränkisch, Cabernet Sauvignon and Merlot wines overlapped and could not be separated. The authors concluded that although UV-Vis spectroscopy appeared to be a promising technique, this technique was not capable of clearly separating all cultivars. Regarding the results obtained in the FT-MIR spectral region (1640–950 cm^{-1}), the best results in terms of separation of the different cultivars were achieved after applying the first derivative, since all the wine cultivars were well separated. The authors concluded that UV-Vis spectroscopy is a limited technique for the authentication of wine samples, but with FT-MIR almost complete discrimination of the investigated cultivars was achieved.

Recently, the ability of FT-MIR to discriminate between Cognac and other distilled drinks such as whiskies, rums, brandies, Armagnacs, bourbons and counterfeit products has been investigated (Picque *et al*., 2006). The spectra of raw products, dry extracts and phenolic extracts were recorded. The authors applied PCA to the 151 spectra scanned from the distilled drinks. Cognac samples were found to form a homogenous group after examining the similarity map defined by the first two PCs. Whiskies, bourbons and rums were completely separated from the Cognac group,

and displayed considerable dispersion in the factorial space. Subsequently, the authors applied PLS-DA to the three sets of spectra (dry extract spectra, phenolic dry extract spectra and concatenated spectra from the two previous sets). Whatever the spectral data, the models correctly predicted between 94 and 99% of the calibration samples. Regarding validation sets in comparison with the calibration set, the percentage of correct classification remained similar for phenolic dry extract spectra and associated spectra, but decreased by 10% for dry extract spectra. The authors concluded that FT-MIR differentiates Cognac from other distilled drinks. The infrared spectra of dry extracts and polyphenolic dry extracts provided additional information and allowed good discrimination between Cognac and non-Cognac drinks. Picque *et al*. (2006) suggested that the combination of FT-MIR with other analytical determination, such as UV-Vis spectra and/or other data analysis such as neural network, might also enhance the discrimination of counterfeit products from Cognac and other products. In a similar approach, the same research group (Picque *et al*., 2005) used FT-MIR to discriminate red wines according to their geographical origin and vintage. The dry extract of 338 wines of the same variety (Gamay), collected in three areas (Gaillac, Beaujolais and Touraine) over 4 years (1998, 1999, 2000 and 2002) were analyzed at 1800–800 cm^{-1}. The authors applied PCA to the spectral data sets, and good discrimination of wine samples according to their year of production was achieved. However, no clear separation according to the geographical origin of wines was highlighted. The authors then applied PLS regression, and 92% of the samples were correctly classified in the validation data sets (100% for the samples of 2000 and 2002, 90% for those of 1999, and 55% for the group belonging to 1998). Regarding PLS regression applied to the wine samples to determine their geographical origin, 85% of the validation samples were correctly classified. The main confusion was reported to be the classification of Gaillac and Beaujolais wines into the group of Touraine wines. The authors concluded that phenolic compounds are significant in the discrimination of red wines according to the geographic origin and year of production.

Within the framework of the TYPIC project (QLK1-CT-2002-02225; http://www.typic.org/), the Walloon Agricultural Research Centre (CRA-W) in Belgium decided to study the potential of FT-MIR to authenticate wines, the primary aim of this work being to match consumers' buying behavior and perception of typical food products with the most relevant objective attributes that define the typicality of those products. The project plans to develop suitable analytical methods to enable skilled producers of such products to characterize and guarantee taste qualities and assure the traceability of these attributes in the EU.

The samples for the study were initially selected on the basis of their main attributes related to the typicality of the wines. The study concerned a collection of 120 red wines from Germany and France. For each wine, two different vintages were studied. The French wines consisted of 20 typical Beaujolais wines (from the Beaujolais region) and 10 wines from other regions. The typical wines were divided into two groups: Beaujolais Village and Beaujolais Crus wines (Brouilly, Chénas, Chiroubles, Côte-de-Brouilly, Fleurie, Juliénas, Morgon, Moulin à Vent, Régnié and Saint-Amour). The German wine group contained 24 typical Dornfelder wines from

the Pfalz region and 6 from other regions (Dornfelder being the name of the grape variety and not a geographical designation like Beaujolais). The other wines were either Dornfelder wines cultivated in other regions (Rheinhessen, Wurtemberg) or other cultivars (Pinot Noir, Cabernet Sauvignon) harvested in the Pfalz region.

PCA was applied to the collection data sets in order to classify wines according to their origin; a certain tendency to separate them was observed. The researchers concluded that the combination of FT-MIR and chemometric methods have a great potential for the classification of wines according to typical attributes of country of origin and vintage.

Sugar and honey

In combination with multivariate statistical analyses, FT-MIR has proved to be a promising screening method with respect to predict glucose, fructose and sucrose in aqueous mixtures (Sivakesava and Irudayaraj, 2000). Spectra of different aqueous mixtures of 10, 20 and 40% total sugars with different combinations of glucose, fructose and sucrose were used for calibration and validation data sets. The best results for predicting each type of sugar content were obtained after applying the first derivative to the FT-MIR spectra. The R^2 values for the calibration models for glucose, fructose and sucrose were 0.997, 0.998 and 0.997, respectively, between the predicted values and actual values. The authors concluded that the calibration set samples were accurate in predicting sugar contents in complex mixtures and commercial beverages. One of the main conclusions of this study was that FT-MIR could be used for rapid detection of sugars in complex mixtures. These results were in agreement with previous investigations reporting that FT-MIR could be utilized to detect adulteration of maple syrup with additives such as cane and beet sugar solutions (Paradkar *et al*., 2003). The results obtained from this study showed that FT-MIR and also NIR could be used for detecting the type and level of adulterants such as pure beet and cane sugar solutions in maple syrup. However, the best results were obtained with FT-MIR rather than with NIR, since the R^2 values were more than 0.98 and 0.93 for FT-MIR and NIR, respectively. The authors suggested that the carbohydrate region (1200–800 cm^{-1}) which was assigned to C–O and C–C stretching vibration of sugars (Cocciardi *et al*., 2006), as well as the organic and amino acid (1800–1200 cm^{-1} and 3200–2800 cm^{-1}) regions, could be identified in the FT-MIR spectra and used as markers for detecting adulterants in maple syrup with a high degree of accuracy. The obtained results were in agreement with the findings of Maalouly *et al*. (2004), who used NIR and MIR to determine sugar contents in beets. In another study, Cadet and Offmann (1997) used FT-MIR combined with PCA and *principal component regression* (*PCR*) and reported that FT-MIR could be used for analysis of sugar-cane juice. Indeed, this technique was found to be more accurate than the commonly used polarimetric technique, and more convenient than HPLC. The authors claimed that FT-MIR could be easily adopted for online measurement in industry.

Recently, FT-MIR was used to determine both the geographical and botanical origin of honeys. Tewari and Irudayaraj (2005) analyzed seven floral sources of honey. The calibration data set comprised 350 samples. Classification accuracy of nearly

100% for the seven different floral honeys was obtained by using FT-MIR and z-nose methods. The main conclusion of this study was that FT-MIR technique is able to detect floral origin with 2–3 minutes based on the developed calibration. The obtained results were recently confirmed by Ruoff and colleagues (2006), who analyzed 11 unifloral and 411 polyfloral samples. The honey samples originated from Switzerland, Germany, Italy, Spain, France and Denmark. The authors applied PCA and LDA and found that the error rates ranged from 0.1% to 8.3% in both Jackknife classification and validation, depending on the honey type considered. The authors concluded that FT-MIR spectroscopy is a valuable tool for the authentication of the botanical origin and quality control of honey, and may also be useful for the determination of its geographic origin. Using a similar approach, the ability of FT-MIR to determine some chemical parameters of honey samples was investigated (Lichtenberg-Kraag *et al*., 2002). In their study more than 1600 honey samples were analyzed by FT-MIR and reference methods to develop a PLS regression-based calibration model for the major contents and properties of honey (sugars, praline, moisture, hydroxyproline, pH and electrical conductivity). For the calibration model, the R^2 was found to vary from 0.84 to 0.98, indicating acceptable calibration for most of the parameters. The authors then tested the validation spectral collection and found high correlation, since the R^2 ranged from 0.81 to 0.99; good repeatability (0.84–0.99); and no statistical difference in the reference methods. The authors concluded that not only the chemical composition but also the physical properties of honey can be determined by FT-MIR.

Fruits and vegetables

As mentioned previously, adulteration of food has occurred for a long time and has ranged from the simple addition of natural components to much more serious cases of contamination with harmful substances (Collins, 1993). As fruit is the most costly ingredient in jam, adulteration with cheaper ingredients, such as sugar or vegetable matter, may take place. In order to protect consumers from adulteration, as well as to avoid unfair competition, it is important to use analytical techniques that can assess the composition of food with a high degree of accuracy. In this context, FT-MIR has been used to differentiate between strawberry- and non-strawberry-containing jams (Defernez and Wilson, 1995). The authors used two techniques, diffuse reflectance infrared and ATR, and found that the former led to a classification success rage of almost 100%, while the latter allowed only 91% correct classification; they attributed this to the fact that ATR was strongly influenced by the spectral difference between normal and reduced total sugar content jams. Subsequently, Holland *et al*. (1998) used FT-MIR to detect adulteration of strawberry purées. In their study, 983 fruit purées (both strawberry and non-strawberry) were used for the establishment of the PLS model, and 94.3% correct classification was obtained. The long-term potential of the model was established with the years 1993 and 1994, and illustrated by analyzing fruit which were harvested in 1995, and a correct classification rate of 96.6% was observed. Finally, a blind test of the model was performed using a set of 23 fruit purée samples produced by a company and a correct classification rate of 96%

was observed, with 22 of 23 samples correctly classified. The authors concluded that the building model could be used for the analysis of fruit of subsequent years, which makes FT-MIR a potential technique for the routine screening of fruit over an extended period of time.

Recently, the ability of FT-MIR to predict nutritional parameters such as carbohydrate content and energetic value in commercially available juice fruit has been investigated by Moros *et al*. (2005). The authors analyzed 63 highly heterogeneous samples covering fruit juices and milk-added fruit juices, among others. By applying PLS regression, the authors found the RMSEP of 18.4 kJ $100\,ml^{-1}$ and 0.72 g $100\,ml^{-1}$ for the energetic value and total carbohydrates, respectively.

Coffee

Coffee is a popular food product throughout the world. A huge amount of coffee is processed, and this has been going on for a very long time. However, the processing of coffee is empirically controlled based on information provided by cup tasters and manufacturing experts, and thus process control may generally be due to the expertise accumulated in each coffee manufacturing company. Additionally, the prepared coffee is produced through many complicated operations such as roasting, grinding, blending and extraction. Furthermore, the coffee beans, as the basis of the prepared coffee, are miscellaneous, as is highly reflected by the varieties and geographical origins. An objective and stable method of evaluating prepared coffee characteristics is therefore desirable for process control, because the prepared coffee is not only the final product but also the liquid food tasted by consumers. In order to have a good grasp of the prepared coffee characteristics for process control, it is very important that not only the contents of the main components but also their molecular structures are non-destructively and simultaneously monitored in real time. Subsequently, application of spectroscopy, especially in the MIR region, to the above measurement is desirable as a high potential implement. In this context, Suchánek *et al*. (1996) pointed out that the green coffee could be quantitatively analyzed by FT-MIR. In other studies, Briandet *et al*. (1996a, 1996b) and Kemsley *et al*. (1995) investigated the potential of diffuse reflection FT-MIR to discriminate between *Arabica* and *Robusta* varieties. Briandet *et al*. (1996b) applied LDA on the principal scores, and the obtained results allowed 100% correct classification for both calibration and validation samples. The researchers concluded that FT-MIR combined with chemometric tools could be used to identify and quantify *Arabica* and *Robusta* contents of freeze-dried instant coffees, and suggested the use of this technique for off-line quality control of freeze-dried coffees. In another study, the same research group (Briandet *et al*., 1996a) examined FT-MIR as a rapid alternative to wet chemistry methods for the detection of adulteration of freeze-dried instant coffees. The spectra of pure coffees and of samples adulterated with glucose, starch or chicory in the range 20–$100\,g\,kg^{-1}$ were collected. Two different FT-MIR sampling methods were employed; diffuse reflectance and ATR. The authors tested three different statistical treatments of the spectra. First, the spectra were compressed by PCA and LDA was then performed. With this approach, a 98% successful classification rate was achieved.

Second, a simultaneous PLS regression was carried out for the content of three added carbohydrates (xylose, glucose and fructose) in order to assess the potential of FT-MIR for determining the carbohydrate profile of instant coffee, and promising results were obtained. Lastly, the discrimination of pure from adulterated coffee was performed using an ANN. A perfect rate of assignment was obtained, since the generalization ability of the ANN was tested on an independent validation data set, and again 100% correct classification was achieved. The obtained results confirmed previously investigations reporting that FT-MIR could be used to discriminate between *Arabica* and *Robusta* lyophilized coffees (Downey *et al*., 1997). The bands located in the 5700–6450 nm (1754–1550 cm^{-1}) were attributed to caffeine, while those located in the region 7700–8700 nm (1298–1149 cm^{-1}) were assigned to chlorogenic acid.

Recently, the usefulness of FT-MIR in identifying specific compounds in coffee, such as volatile and non-volatile compounds that constitute the flavor of brewed coffee, was investigated by Lyman *et al*. (2003). The 1800–1680 cm^{-1} carbonyl region for vinyl esters/lactones, esters, aldehydes, ketones, and acids was found to provide a flavor-print of the brewed coffee. The researchers stated that the heating rates of green coffee beans to the onset of the first and second cracks are important determinants of the basic taste and aroma of brewed coffee. In another study, the influences of the coffee varieties and the roasting degree on the FT-MIR spectral characteristics of brewed coffee, as well as the use of FT-MIR to determine the caffeine and chlorogenic acid contents in brewed coffee, were examined (unpublished results). Differences between the second derivatives of the FT-MIR spectra of the brewed *Arabica* and *Robusta* coffees were observed around several peaks. In addition, the brewed coffee from the Brazilian variety exhibited different spectral features from those of the other *Arabica* coffees. Moreover, the roasting conditions of the Indonesian beans were found to reflect the spectral features of the brewed coffee. Furthermore, the caffeine and chlorogenic acid contents in brewed coffee would be determined by the spectroscopic method, as well as those in the aqueous solutions. The obtained results confirmed those of Singh *et al*. (1998), who pointed out the ability of FT-MIR to predict the amount of caffeine located around 1655 cm^{-1} present in coffee, since the sensitivity of the technique was found to be less than 5 ppm.

Identification of bacteria of food interest

The identification of *microorganisms* of interest in food and food products by traditional microbiological methods is time-consuming. In addition, these methods require skilled operators and, in some cases, are unable to discriminate microorganisms at the strain level. In this context, the use of MIR to differentiate *bacteria* has been studied since the 1950s. Unfortunately, owing to the weak performance of dispersive spectrometers, these kinds of studies did not allow good discrimination. Since Naumann and coworkers (1991) published their pioneering work in the field of the identification and differentiation of microorganisms by FT-MIR, various research groups around the world have shown the validity of FT-MIR for giving sufficient information to distinguish microorganisms both at species and strain

levels. Indeed, Amiel *et al*. (2000, 2001) reported that FT-MIR provided good discrimination of bacteria between different genera, species and even strains. They first assessed the ability of FT-MIR to identify lactic acid bacteria (LAB) used in the dairy industry. Different strains were used in their study: *Lactobacillus* (12 species, 3 subspecies), *Lactococcus* (4 species, 3 subspecies), *Leuconostoc* (3 species, 3 subspecies), *Weissella* (1 species) and *Streptococcus* (2 species). The authors applied DA to the FT-MIR spectra, and 100% correct classification was obtained at the genus and species levels, while 86% was achieved at the subspecies level. Amiel *et al*. (2000) then tested 48 wild isolates which had been previously identified by biochemical testing and the RAPD method, and 100% and 69% correct classifications were obtained at the genus and species levels, respectively. The authors concluded that, although there was a relatively low number of isolates, FT-MIR could be considered as a useful technique for the discrimination and identification of LAB. Subsequently, the same research group (Amiel *et al*., 2001) used FT-MIR to point out that this technique could be used for taxonomical purposes. They illustrated this with two examples: the distinction between *Streptococcus thermophilus* and *Streptococcus salivarius*, and the taxonomic range of *Lactobacillus casei*, *paracasei*, *zeae* and *rhamnosus*. The authors reported that, concerning the taxonomic subject, their results partially confirmed those found with the reference method (Dellaglio *et al*., 1991). However, FT-MIR allowed good separation of *Lactobacillus zeae* from *Lactobacillus rhamnosus*, while API50CHL failed to differentiate between them. One of the most important conclusions of this study was that the information contained in FT-MIR spectra could be complementary to that found with genomic information, and consequently this technique could be introduced in a polyphasic taxonomic approach. The obtained results were confirmed recently by Yu and Irudayaraj (2005), who succeeded in differentiating between six microorganisms at the strain level. They reported that FT-MIR spectroscopy can provide not only molecular fingerprints of the cell envelope, but also compositional and metabolic information about the cytoplasm under different physiological conditions. This approach could be an effective alternative to traditional nutritional and biochemical methods of monitoring and assessing the effects of inhibitors and other environmental factors on microbial cell growth.

In the same field of dairy products, Lucia *et al*. (2001) investigated the suitability of FT-MIR as a rapid technique to investigate the secondary structure of proteins in aqueous solutions and its changes as a consequence of microbial proteolytic activity, as well as to identify the contribution of different strains of *Yarrowia lipolytica* used in cheese ripening. The researchers observed that significant differences in the amide I and II bands of both curds and cheeses obtained from milk inoculated with *Lactococcus lactis* subsq. *Lactis* and different strains of *Yarrowia lipolytica* occurred during the ripening stage. They concluded that FT-MIR spectroscopy could be a promising tool to monitor changes that occurred during ripening in cheeses inoculated with different strains.

The German Federal Health Office has also developed a method based on FT-MIR for the rapid identification of microorganisms. Indeed, Fehrmann *et al*. (1995) used this spectroscopic technique to classify microorganisms in the dairy industry,

especially for *clostridium* spp. The best information was found in the 1500–1000 cm^{-1} region. However, no explanation regarding the chemical compounds involved in the identification of microorganisms was given. In other studies, Fayolle *et al*. (2000) and Picque *et al*. (1993) used FT-MIR and MIR, respectively, to monitor the fermentation processes by measuring sugars, ethanol and organic acid concentrations during alcoholic and lactic fermentations. By applying PLS regression, the SEP were found to vary between 1.4 gl^{-1} and 4.5 gl^{-1} for galactose and fructose, respectively (Fayolle *et al*., 2000).

To date, several methods have been proposed to measure and to detect bacterial spoilage in meat and meat products. These include enumeration methods based on microscopy, ATP bioluminescence and the measurement of electrical phenomena, as well as detection methods based on either immunological or nucleic acid based procedures. The major drawbacks are that they are time-consuming and labor-intensive, and give retrospective information. The ideal method for on-line microbiological analysis of meat would be rapid, non-invasive, reagentless and relatively inexpensive, and these requirements can be met via the application of a spectroscopic approach. Recently, Ellis *et al*. (2004) used FT-MIR to measure biochemical changes within the meat substrate, enhancing and accelerating the detection of microbial spoilage. The authors pointed out that FT-MIR could be considered as a novel method for the quantitative detection of food spoilage. Indeed, by applying PLS regression to the FT-MIR spectra, an accurate estimation of the bacterial loads obtained by classical plating methods was observed. The authors concluded that FT-MIR is able to acquire a metabolic snapshot and quantify, non-invasively, the microbial loads of food samples accurately and rapidly in 60 seconds, directly from the sample surface. The authors also pointed out that it was evident that the FT-MIR spectra contained biochemical information that allowed correlation with the spoilage status of chicken, but they did not mention which biochemical species measured by the FT-MIR could be related to such spoilage.

Cotton and wood

Rapid identification of the nature of the extraneous matter in cotton at each stage of cleaning and processing is necessary so that action can be taken to eliminate or reduce its presence and improve efficiency and quality. To respond to this need, FT-MIR spectra of retrieved foreign matter were collected and subsequently rapidly matched to an authentic spectrum in a spectral database (Himmelsbach *et al*., 2006). The database includes contaminants typically classified as "trash", cotton plant parts, and grass plant parts. The researchers pointed out that the FT-MIR method was able to provide specific identification of extraneous materials in cotton. In another study, Nuopponen *et al*. (2006) have used FT-MIR to estimate wood density and chemical composition (lignin, cellulose and wood resin contents and densities). Using the spectral ranges 4000–2800 cm^{-1} and 1800–700 cm^{-1}, these parameters were found to present an R^2 varying from 0.6 to 0.9 after applying PLS regression. The same research group reduced the number of wavelengths to five characteristic of lignin bands located at 1600, 1510, 1273, 1220 and 1077 cm^{-1}, and similar results were

obtained. They concluded that a hand-held device based on FT-MIR could be used to determine the quality of these parameters.

Recently, the effect of temperature on wood charcoal structure and chemical composition has been investigated (Labbé *et al*., 2006). Wood charcoal carbonized at various temperatures was analyzed by FT-MIR coupled with multivariate analysis and by thermogravimetric analysis to characterize the chemical composition during the carbonization process. The multivariate models of charcoal were able to distinguish between species and between wood thermal treatments, revealing that the characteristics of the wood charcoal depend not only on the wood species, but also on the carbonization temperature. One of the main conclusions of this study was that FT-MIR was able to classify wood species for the mellowing process.

Conclusions

Over the past 20 years, researchers and users of mid-infrared spectroscopy in the field of food sciences have mainly studied the determination of the amount of the main components in food products. This knowledge is mandatory, but is not sufficient to predict the technological and organoleptic properties of processed food. As described in this chapter, infrared spectra also provide information regarding the physical states and molecular structures of the main food components, such as lipids, proteins, carbohydrates, etc. It is therefore expected that, in the coming years, infrared spectroscopy combined with chemometric tools will provide a reliable tool for the understanding of the bases of food molecular structure and, as a consequence, their qualities.

References

Adhikari, C., Balasubramaniam, V.M. and Abbott, U.R. (2003). A rapid FTIR method for screening methyl sulphide and hexanal in modified atmosphere meal, ready-to-eat entrees. *Lebensmittel-Wissenschaft und -Technologie*, **36**, 21–27.

Al-Jowder, O., Kemsley, E.K. and Wilson, R.H. (1997). Mid-infrared spectroscopy and authenticity problems in selected meats: a feasibility study. *Food Chemistry*, **59**, 195–201.

Al-Jowder, O., Defernez, M., Kemsley, E.K. and Wilson, R.H. (1999). Mid-infrared spectroscopy and chemometrics for the authentication of meat products. *Journal of Agricultural and Food Chemistry*, **47**, 3210–3218.

Al-Jowder, O., Kemsley, E.K. and Wilson, R.H. (2002). Detection of adulteration in cooked meat products by mid-infrared spectroscopy. *Journal of Agricultural and Food Chemistry*, **50**, 1325–1329.

Amiel, C., Mariey, L., Curk-Daubié, M.C. *et al*. (2000). Potentiality of Fourier transform infrared spectroscopy (FTIR) for discrimination and identification of dairy lactic acid bacteria. *Le Lait*, **80**, 445–459.

Amiel, C., Mariey, L., Denis, C. *et al*. (2001). FTIR spectroscopy and taxonomic purpose: contribution to the classification of lactic acid bacteria. *Le Lait*, **81**, 249–255.

Baeten, V. and Dardenne, P. (2002). Resumen de Espectroscopía: desarrollo en instrumentación y análisis. *Grasas y Aceites*, **53**, 45–63.

Baeten, V., Meurens, M.T., Morales, R. and Aparicio, R. (1996). Detection of virgin olive oil adulteration by Fourier transform Raman spectroscopy. *Journal of Agricultural and Food Chemistry*, **44**, 2225–2230.

Baeten, V., Aparicio, R., Marigheto, N. and Wilson, W. (2000). Olive oil analysis by infrared and Raman spectroscopy: methodologies and applications. In: J. Harwood and R. Aparicio (eds), *The Handbook of Olive Oil*. Gaithersburg, MD: Aspen, pp. 209–248.

Baeten, V., Fernández Pierna, J.A., Dardenne, P. *et al*. (2005). Detection of the presence of hazelnut oil in olive oil by FT-Raman and FT-MIR spectroscopy. *Journal of Agricultural and Food Chemistry*, **53**, 6201–6206.

Bellorini, S., Strathmann, S., Baeten, V. *et al*. (2005). Discriminating animal fats and their origins: assessing the potentials of Fourier transform infrared spectroscopy, gas chromatography, immunoassay and polymerase chain reaction techniques. *Analytical and Bioanalytical Chemistry*, **382**, 1073–1083.

Bertoni, G., Calamari, L. and Maianti, M.G. (2001). Producing specific milks for speciality cheeses. *Proceedings of the Nutrition Society*, **60**, 231–246.

Bertrand, D. and Dufour, E. (2000). *La Spectroscopie Infrarouge et ses Applications Analytiques*. Paris: Tec & Doc.

Bevin, C.J., Fergusson, A.J., Perry, W.B. *et al*. (2006). Development of a rapid "fingerprinting" system for wine authenticity by mid-infrared spectroscopy. *Journal of Agricultural and Food Chemistry*, **54**, 9713–9718.

Briandet, R., Kemsley, E.K. and Wilson, R.H. (1996a). Approaches to adulteration detection in instant coffees using infrared spectroscopy and chemometrics. *Journal of the Science of Food and Agriculture*, **71**, 359–366.

Briandet, R., Kemsley, E.K. and Wilson, R.H. (1996b). Discrimination of *Arabica* and *Robusta* in instant coffee by Fourier transform infrared spectroscopy and chemometrics. *Journal of Agricultural and Food Chemistry*, **44**, 170–174.

Bureau, S., Reich, M., Marfisi, C. *et al*. (2006). Application of Fourier-transform infrared (FT-MIR) spectroscopy for the evaluation of quality traits in Apricot fruits. *Acta Horticulturae*, **717**, 347–350.

Cadet, F. and Offmann, B. (1997). Direct spectroscopic sucrose determination of raw sugar cane juices. *Journal of Agricultural and Food Chemistry*, **45**, 166–171.

Cadet, F., Safar, M. and Dufour, E. (2000). Glucides. In: D. Bertrand and E. Dufour (eds), *La Spectroscopie Infrarouge et ses Applications Analytiques*. Paris: Tec & Doc, pp. 172–195.

Cattaneo, T.M.P., Giardina, C., Sinelli, N. *et al*. (2005). Application of FT-NIR and FT-IR spectroscopy to study the shelf-life of Crescenza cheese. *International Dairy Journal*, **15**, 693–700.

Coates, J. (2000). Interpretation of infrared spectra, a practical approach. In: R.A. Meyers (ed.), *Encyclopedia of Analytical Chemistry*. Chichester: Wiley, pp. 10815–10837.

Cocchi, M., Foca, G., Lucisano, M. *et al*. (2004). Classification of cereal flours by chemometric analysis of MIR spectra. *Journal of Agricultural and Food Chemistry*, **52**, 1062–1067.

Cocciardi, R.A., Ismail, A.A., Wang, Y. and Sedman, J. (2006). Heterospectral two-dimensional correlation spectroscopy of mid-infrared and Fourier self-deconvolved near-infrared spectra of sugar solutions. *Journal of Agricultural and Food Chemistry*, **54**, 6475–6481.

Collins, E.J.T. (1993). Food adulteration and food safety in Britain in the 19th and early 20th centuries. *Food Policy*, **18**, 95–109.

Defernez, M. and Wilson, R.H. (1995). Mid-infrared spectroscopy and chemometrics for determining the type of fruit used in jams. *Journal of the Science of Food and Agriculture*, **67**, 461–467.

Dellaglio, F., Dicks, L.M.T., Dutoit, M. and Torriani, S. (1991). Designation of ATCC 334 in place of ATCC 393 (NCDO 161) as the neotype strain of *Lactobacillus casei* subsq. Casei and rejection of the name lactobacillus paracasei. *International Journal of Systematic and Evolutionary Bacteriology*, **41**, 340–342.

Downey, G., Brinadet, R., Wilson, R.H. and Kemsley, E.K. (1997). Near- and mid-infrared spectroscopies in food authentication: coffee varietal identification. *Journal of Agricultural and Food Chemistry*, **45**, 4357–4361.

Downey, G., McIntyre, P. and Davies, A.N. (2002). Detecting and quantifying sunflower oil adulteration in extra virgin olive oils from the eastern Mediterranean by visible and near-infrared spectroscopy. *Journal of Agricultural and Food Chemistry*, **50**, 5520–5525.

Dufour, E. and Robert, P. (2000). Protéines. In: D. Bertrand and E. Dufour (eds), *La Spectroscopie Infrarouge et ses Applications Analytiques*. Paris: Tec & Doc, pp. 107–137.

Dufour, E., Mazerolles, G., Devaux, M.F. *et al*. (2000). Phase transition of triglycerides during semi-hard cheese ripening. *International Dairy Journal*, **10**, 81–93.

Edelmann, A., Diewok, J., Schuster, K.C. and Lendl, B. (2001). Rapid method for the discrimination of red wine cultivars based on mid-infrared spectroscopy of phenolic wine extracts. *Journal of Agricultural and Food Chemistry*, **49**, 1139–1145.

Ellis, D.I., Broadhurst, D. and Goodacre, R. (2004). Rapid and quantitative detection of the microbial spoilage of meat by Fourier transform infrared spectroscopy and machine learning. *Analytica Chimica Acta*, **514**, 193–201.

Elmore, D.L., Lendon, C.A. and Smith, S.A. (2005). Mid infrared imaging applications in agricultural and food sciences. In: R. Bhargava and I. Levin (eds), *Spectrochemical Analysis Using Infrared Multichannel Detectors*. Sheffield: Sheffield Analytical Chemistry Series.

Etzion, Y., Linker, R., Cogan, U. and Shmulevich, I. (2004). Determination of protein concentration in raw milk by mid-infrared Fourier transform infrared/attenuated total reflectance spectroscopy. *Journal of Dairy Science*, **87**, 2779–2788.

Fahrenfort, J. (1961). Attenuated total reflection: a new principle for the production of useful infra-red reflection spectra of organic compounds. *Spectrochimica Acta*, **17**, 698–709.

Fayolle, Ph., Picque, D. and Corrieu, G. (2000). On-line monitoring of fermentation processes by a new remote dispersive middle-infrared spectrometer. *Food Chemistry*, **11**, 291–296.

Fehrmann, A., Franz, M., Hoffmann, A. *et al*. (1995). Dairy product analysis: identification of microorganisms by mid-infrared spectroscopy and determination of constituents by Raman spectroscopy. *Journal of AOAC International*, **78**, 1537–1542.

Fernández Pierna, J.A., Volery, P., Besson, R. *et al*. (2005). Classification of modified starches by Fourier transform infrared spectroscopy using support vector machines. *Journal of Agricultural and Food Chemistry*, **53**, 6581–6585.

Fox, P.F. (1989). Proteolysis during cheese manufacture and ripening. *Journal of Dairy Science*, **72**, 1379–1400.

Francis, I.L., Høj, P.B., Dambergs, R.G. *et al*. (2005). Objective measures of grape quality are they achievable?. In *Proceedings of the 12th Australian Wine Industry Technical Conference*. Australia: Australian Wine Industry Technical Conference Inc, pp. 85–90.

Gasperini, G., Fusari, E., Della Bella, L. and Bondioli, P. (2007). Classification of feeding fats by FT-IR spectroscopy. *European Journal of Lipid Science and Technology*, **109**, 673–681.

Giardina, C., Cattaneo, T.M.P. and Giangiacomo, R. (2003). Quality control of a typical "Pasta Filata" cheese by FT-IR spectroscopy. *Italian Journal of Food Science*, **15**, 579–584.

Gracian, J. (ed.) (1968). *Analysis and Characterization of Oils, Fats and Fat Products*, Vol. 2. London: Wiley.

Grappin, R., Lefier, D. and Mazerolles, G. (2000). Analyse du lait et des produits laitiers. In: D. Bertrand and E. Dufour (eds), *La Spectroscopie Infrarouge et ses Applications Analytiques*. Paris: Tec & Doc, pp. 497–540.

Guerzoni, M.E., Vannini, L., Chaves-Lopez, C. *et al*. (1999). Effect of high pressure homogenization on microbial and chemico-physical characteristics of goat cheeses. *Journal of Dairy Science*, **82**, 851–862.

Guillén, M.D. and Cabo, N. (1997). Infrared spectroscopy in the study of edible oils and fats. *Journal of the Science of Food and Agriculture*, **75**, 1–11.

Harrick, N.J. (1967). *Internal reflectance Spectroscopy*. New York, NY: Interscience.

Himmelsbach, D.S., Hellgeth, J.W. and McAlister, D.D. (2006). Development and use of an attenuated total reflectance/Fourier transform infrared (ATR/FT-IR) spectral data base to identify foreign matter in cotton. *Journal of Agricultural and Food Chemistry*, **54**, 7405–7412.

Holland, J.K., Kemsley, E.K. and Wilson, R.H. (1998). Use of Fourier transform infrared spectroscopy and partial least squares regression for the detection of adulteration of strawberry purées. *Journal of the Science of Food and Agriculture*, **76**, 263–269.

Hvozdara, L., Pennington, N., Kraft, M. *et al*. (2002). Quantum cascade lasers for mid-infrared spectroscopy. *Vibrational Spectroscopy*, **30**, 53–58.

Iñón, F.A., Garrigues, J.M. and de la Guardia, M. (2003a). Nutritional parameters of commercially available milk samples by FTIR and chemometric techniques. *Analytica Chimica Acta*, **513**, 401–412.

Iñón, F.A., Garrigues, J.M., Garrigues, S. *et al*. (2003b). Selection of calibration set samples in determination of olive oil acidity by partial least squares-attenuated total-reflectance Fourier transform infrared spectroscopy. *Analytica Chimica Acta*, **489**, 59–75.

Karoui, R., Dufour, E., Pillonel, L. *et al*. (2004a). Determining the geographic origin of Emmental cheeses produced during winter and summer using a technique based

on the concatenation of MIR and fluorescence spectroscopic data. *European Food Research and Technology*, **219**, 184–189.

Karoui, R., Dufour, E., Pillonel, L. *et al*. (2004b). Fluorescence and infrared spectroscopies: a tool for the determination of the geographic origin of Emmental cheeses manufactured during summer. *Le Lait*, **84**, 359–374.

Karoui, R., Bosset, J.O., Mazerolles, G. *et al*. (2005a). Monitoring the geographic origin of both experimental French Jura hard cheeses and Swiss Gruyère and "Pasta Filata". *Society*, **75**, 987–992.

Karoui, R., Dufour, E., Pillonel, L. *et al*. (2005b). The potential of combined infrared and fluorescence spectroscopies as a method of determination of the geographic origin of Emmental cheeses. *International Dairy Journal*, **15**, 287–298.

Karoui, R., Mouazen, A.M., Dufour, E. *et al*. (2006a). A comparison and joint use of NIR and MIR spectroscopic methods for the determination of some chemical parameters in soft cheeses at external and central zones. *European Food Research and Technology*, **223**, 363–371.

Karoui, R., Mouazen, A.M., Dufour, E. *et al*. (2006b). A comparison and joint use of two spectroscopic methods for the determination of some parameters in European Emmental cheeses. *European Food Research and Technology*, **223**, 44–50.

Karoui, R., Mouazen, A.M., Dufour, E. *et al*. (2006c). Application of the MIR for the determination of some chemical parameters in European Emmental cheeses produced during summer. *European Food Research and Technology*, **222**, 165–170.

Karoui, R., Mouazen, A.M., Dufour, E. *et al*. (2006d). Mid infrared spectrometry: a tool for the determination of chemical parameters of Emmental cheeses produced during winter. *Le Lait*, **86**, 83–97.

Kemsley, E.K., Ruault, S. and Wilson, R.H. (1995). Discrimination between *Coffea arabica* and *Coffea canephora* variant *robusta* beans using infrared spectroscopy. *Food Chemistry*, **54**, 321–326.

Kim, Y., Himmelsbach, D.S. and Kays, S.E. (2007). ATR-Fourier transform mid-infrared spectroscopy for determination of trans fatty acids in ground cereal products without oil extraction. *Journal of Agricultural and Food Chemistry*, **55**, 4327–6333.

Kochhar, S.P. and Rossell, J.B. (1984). The Spanish toxic oil syndrome. *Nutrition of Food Science*, **90**, 14–15.

Kornmann, H., Valentinotti, S., Duboc, P. *et al*. (2004). Monitoring and control of *Gluconacetobacter xylinus* fed-batch cultures using in situ mid-IR spectroscopy. *Journal of Biotechnology*, **113**, 231–245.

Kulmyrzaev, A., Noel, Y., Hanafi, M. *et al*. (2005). Investigation at the molecular level of soft cheese quality and ripening by infrared and fluorescence spectroscopies and chemometrics – relationships with rheology properties. *International Dairy Journal*, **15**, 669–678.

Labbé, N., Harper, D. and Rials, T. (2006). Chemical structure of wood charcoal by infrared spectroscopy and multivariate analysis. *Journal of Agricultural and Food Chemistry*, **54**, 3492–3497.

Lanciotti, R., Vannini, L., Lopez, C.C. *et al*. (2005). Evaluation of the ability of *Yarrowia lipolytica* to impart strain-dependent characteristics to cheese when used as a ripening adjunct. *International Journal of Dairy Technology*, **58**, 89–99.

Lanher, B. (1991). Spectrometrie infra-rouge a transformée de Fourier et analyse multi-dimensionnelle de données spectrales. Application à la quantification et au contrôle de procédés dans le domaine des produits laitiers. PhD Thesis, Université de Bourgogne, Bourgogne, France.

Leclercq-Perlat, M.N., Buono, F., Lambert, D. *et al*. (2004). Controlled production of Camembert-type cheeses. Part I: Microbiological and physicochemical evolutions. *Journal of Dairy Research*, **71**, 346–354.

Lichtenberg-Kraag, B., Hedtke, C. and Bienefeld, K. (2002). Infrared spectroscopy in routine quality analysis of honey. *Apidologie*, **33**, 327–337.

Lizuka, K. and Aishima, T. (1999). Tenderization of beef with pineapple juice monitored by Fourier transformed infrared spectroscopy and chemometric analysis. *Journal of Food Science*, **64**, 973–977.

Lucia, V., Daniela, B. and Rosalba, L. (2001). Use of Fourier transform infrared spectroscopy to evaluate the proteolytic activity of *Yarrowia lipolytica* and its contribution to cheese ripening. *International Journal of Food Microbiology*, **69**, 113–123.

Lyman, D.J., Benck, R., Dell, S. *et al*. (2003). FTIR-ATR analysis of brewed coffee: effect of roasting conditions. *Journal of Agricultural and Food Chemistry*, **51**, 3268–3272.

Lynch, J.M. and Barbano, D.M. (1995). Evaluation of commercially available milk powder for calibration of mid-infrared analyzers. *Journal of AOAC International*, **78**, 1219–1224.

Maalouly, J., Eveleigh, L., Rutlege, D.N. and Ducauze, C.J. (2004). Application of 2D correlation spectroscopy and outer product analysis to infrared spectra of sugar beets. *Vibrational Spectroscopy*, **36**, 279–285.

Marigheto, N.A., Kemsley, E.K., Defernez, M. and Wilson, R.H. (1998). A comparison of mid-infrared and Raman spectroscopies for the authentication of edible oils. *Journal of the American Oil Chemists' Society*, **75**, 987–992.

Martín-del-Campo, S.T., Picque, D., Cosío-Ramírez, R. and Corrieu, G. (2007a). Middle infrared spectroscopy characterization of ripening stages of camembert-type cheese. *International Dairy Journal*, **17**, 835–845.

Martín-del-Campo, S.T., Picque, D., Cosío-Ramírez, R. and Corrieu, G. (2007b). Evaluation of chemical parameters in soft mold-ripened cheese during ripening by mid-infrared spectroscopy. *Journal of Dairy Science*, **90**, 3018–3027.

Mazarevica, G., Diewok, J., Baena, J.R. *et al*. (2004). On-line fermentation monitoring by mid-infrared spectroscopy. *Applied Spectroscopy*, **58**, 804–810.

Mazerolles, G., Devaux, M.F., Duboz, G. *et al*. (2001). Infrared and fluorescence spectroscopy for monitoring protein structure and interaction changes during cheese ripening. *Le Lait*, **81**, 509–527.

Mazerolles, G., Devaux, M.F., Dufour, E. *et al*. (2002). Chemometric methods for the coupling of spectroscopic techniques and for the extraction of the relevant information contained in the spectral data tables. *Chemometrics and Intelligent Laboratory Systems*, **63**, 57–68.

Moros, J., Iňón, F.A., Garrigues, S. and de la Guardia, M. (2005). Determination of the energetic value of fruit and milk-base beverages through partial-least-squares

attenuated total reflectance-Fourier transform infrared spectroscopy. *Analytica Chimica Acta*, **538**, 181–193.

Munck, L., Norgaard, L., Engelsen, S.B. *et al*. (1998). Chemometrics in food science: a demonstration of the feasibility of a highly exploratory, inductive evaluation strategy of fundamental scientific significance. *Chemometrics and Intelligent Laboratory Systems*, **44**, 31–60.

Naumann, D., Helm, D., Labischinski, H. and Giesbrecht, P. (1991). The characterization of microorganisms by Fourier transform infrared spectroscopy (FT-IR). In: W. Nelson (ed.), *Modern Techniques for Rapid Microbiological Analysis*. New York, NY: VCH Publishers, pp. 43–96.

Nuopponen, M.H., Birch, G.M., Sykes, R.J. *et al*. (2006). Estimation of wood density and chemical composition by means of diffuse reflectance mid-infrared Fourier transform (DRIFT-MIR) spectroscopy. *Journal of Agricultural and Food Chemistry*, **54**, 34–40.

Otto, M. (1999). *Chemometrics: Statistics and Computer Application in Analytical Chemistry*. Chichester: Wiley-VCH.

Paradkar, M.M., Sivakesava, S. and Irudayaraj, J. (2003). Discrimination and classification of adulterants in maple syrup with the use of infrared spectroscopic techniques. *Journal of the Science of Food and Agriculture*, **83**, 714–721.

Picque, D., Lefier, D. and Grappin, R. (1993). Monitoring of fermentation by infrared spectrometry: alcoholic and lactic fermentation. *Analytica Chimica Acta*, **279**, 67–72.

Picque, D., Cattenoz, T., Corrieu, G. and Berger, J.L. (2005). Discrimination of red wines according to their geographical origin and vintage year by the use of mid-infrared spectroscopy. *Sciences des Aliments*, **25**, 207–220.

Picque, D., Lieben, P., Corrieu, G. *et al*. (2006). Discrimination of Cognacs and other distilled drinks by mid-infrared spectroscopy. *Journal of the Science of Food and Agriculture*, **54**, 5220–5226.

Pierce, M.M. and Wehling, R.L. (1994). Comparison of sample handling and data treatment methods for determining moisture and fat in Cheddar cheese by near infrared spectroscopy. *Journal of Agricultural and Food Chemistry*, **42**, 2831–2835.

Pillonel, L., Collomb, M., Tabacchi, R. and Bosset, J.O. (2002). Analytical methods for the determination of the geographic origin of Emmental cheese. Free fatty acids, triglycerides and fatty acid composition of cheese fat. *Travaux de Chimie Alimentaire et d'hygiène*, **93**, 217–231.

Robert, P. and Dufour, E. (2000). Règles générales d'attribution des bandes spectrales. In: D. Bertrand and E. Dufour (eds), *La Spectroscopie Infrarouge et ses Applications Analytiques*. Paris: Tec & Doc, pp. 79–92.

Ruoff, K., Luginbühl, W., Künzli, R. *et al*. (2006). Authentication of the botanical and geographical origin of honey by mid-infrared spectroscopy. *Journal of Agricultural and Food Chemistry*, **54**, 6873–6880.

Sayago, A., Morales, M.T. and Aparicio, R. (2004). Detection of hazelnut oil in virgin olive oil by a spectrofluorimetric method. *European Food Research and Technology*, **218**, 480–483.

Singh, B.R., Wechter, M.A., Hu, Y. and Lafontaine, C. (1998). Determination of caffeine content in coffee using Fourier transform infra-red spectroscopy in combination with attenuated total reflectance technique: a bioanalytical chemistry experiment for biochemists. *Biochemical Education*, **26**, 243–247.

Sivakesava, S. and Irudayaraj, J. (2000). Determination of sugars in aqueous mixtures using mid-infrared spectroscopy. *Applied Engineering in Agriculture*, **16**, 543–550.

Somers, T.C. and Evans, M.E. (1974). Wine quality: correlations with colour density and anthocyanin equilibrium in a group of young red wines. *Journal of the Science of Food and Agriculture*, **25**, 1369–1379.

Sørensen, L.K., Lund, M. and Juul, B. (2003). Accuracy of Fourier transform infrared spectrometry in determination of casein in dairy cow's milk. *Journal of Dairy Research*, **70**, 445–452.

Steiner, H., Staubmann, K., Allabashi, R. *et al*. (2003). Online sensing of volatile organic compounds in groundwater using mid-infrared fibre optic evanescent wave spectroscopy: a pilot scale test. *Water Science and Technology*, **47**, 121–126.

Suchánek, M., Filipová, H., Volka, K. *et al*. (1996). Qualitative analysis of green coffee by infrared spectrometry. *Fresenius' Journal of Analytical Chemistry*, **354**, 327–332.

Tay, A., Singh, R.K., Krishnan, S.S. and Gore, J.P. (2002). Authentication of olive oil adulterated with vegetable oils using Fourier transform infrared spectroscopy. *Lebensmittel-Wissenschaft und -Technologie*, **35**, 99–103.

Tewari, J.C. and Irudayaraj, J.M.K. (2005). Floral classification of honey using mid-infrared spectroscopy and surface acoustic wave based z-nose sensor. *Journal of Agricultural and Food Chemistry*, **53**, 6955–6966.

Van de Voort, F.R., Ismail, A.A. and Sedman, J. (1994). The determination of peroxide value by fourier transform infrared spectroscopy. *Journal of the American Oil Chemists' Society*, **71**, 921–926.

Van de Voort, F.R., Ismail, A.A. and Sedman, J. (1995). A rapid, automated method for the determination of *cis* and *trans* content of fats and oils by Fourier transform infrared spectroscopy. *Journal of the American Oil Chemists' Society*, **72**, 873–878.

Vannini, L., Baldi, D. and Lanciotti, R. (2001). Use of Fourier transform infrared spectroscopy to evaluate the proteolytic activity of *Yarrowia lipolytica* and its contribution to cheese ripening. *International Journal of Food Microbiology*, **69**, 113–123.

Wang, L., Lee, F.S.C., Wang, X. and He, Y. (2006). Feasibility study of quantifying and discriminating soybean oil adulteration in camellia oils by attenuated total reflectance MIR and fiber optic diffuse reflectance NIR. *Food Chemistry*, **95**, 529–536.

Wittrup, C. and Nørgaard, L. (1998). Rapid near infrared spectroscopic screening of chemical parameters in semi-hard cheese using chemometrics. *Journal of Dairy Science*, **81**, 1803–1809.

Yu, C. and Irudayaraj, J. (2005). Spectroscopic characterization of microorganisms by Fourier transform infrared microscopy. *Biopolymers*, **77**, 368–377.

3

Spectroscopic Technique: Near-infrared (NIR) Spectroscopy

Marena Manley, Gerard Downey and Vincent Baeten

Introduction

Near-infrared (NIR) spectroscopy dates back to the early 1800s, when Fredrick William Herschel, a professional musician and astronomer (Herschel, 1800; Davies, 1991, 1998), discovered the first non-visible region in the absorption spectrum (Stark *et al*., 1986). From 1800 to the 1950s was a dormant period for NIR spectroscopy, when it took a back seat to other analytical methods that could deliver more unambiguous results, especially regarding the explanation of molecular structures (Williams and Stevenson, 1990). It was only with the work of Karl Norris and coworkers (Butler, 1983) later in the 1950s that its potential was recognized (Day and Fearn, 1982). Today, NIR spectroscopy has become the quality control method of choice in the food industry because of its advantages over other analytical techniques.

Near-infrared spectroscopy was originally limited to quantitative grain analysis, but today quantitative applications are widely used in many fields (Table 3.1).

Modern Techniques for Food Authentication
ISBN: 978-0-12-374085-4

Table 3.1 Fields of NIR spectroscopy quantitative applications

Application	References
Animal feeds	Murray and Hall, 1983; Murray *et al*., 2001
Cereals and cereal products	Osborne, 1991; Wilson *et al*., 1991; Windham *et al*., 1993; Wesley *et al*., 1999; Cozzolino *et al*., 2000; Bao *et al*., 2001; Manley *et al*., 2001a; Van Zyl and Manley, 2001; Manley *et al*., 2002
Coffee	Pizarro *et al*., 2004
Confectionary	Tarkošová and Čopíková, 2000
Cosmetics	Grunewald *et al*., 1998
Dairy	Rodriguez-Otero *et al*., 1997; Wüst and Rudzik, 2003; Blazquez *et al*., 2004
Distillation industry	Gómez-Cordovés and Bartolome, 1993; Manley *et al*., 2003
Environment	Iwamoto *et al*., 1995; Lister *et al*., 2000
Essential oils	Schulz *et al*., 1998; Schulz *et al*., 2003a
Fats and oils	Schulz *et al*., 1998; Moh *et al*., 1999
Fruit and vegetables	Kawano *et al*., 1992; Schulz *et al*., 1998; Goula and Adamopoulos, 2003; Xing *et al*., 2003; Walsh *et al*., 2004; Manley *et al*., 2007
Forage	Park *et al*., 1998; Stuth *et al*., 2003
Grapes	Cope, 2000; Esler *et al*., 2002
Herbal products	Schulz *et al*., 2002; Laasonen, 2003; Schulz *et al*., 2003b; Manley *et al*., 2004, 2006; Joubert *et al*., 2005, 2006
Honey	García-Alvarez *et al*., 2000
Manures	Reeves, 2001
Meat and fish	Downey, 1996b; Wold and Isaksson, 1997; Pink *et al*., 1999; Cozzolino and Murray, 2004; Realini *et al*., 2004
Medicine	Hock *et al*., 1997; Suto *et al*., 2004
Pharmaceuticals	Blanco *et al*., 1998
Plant species	Ren and Chen, 1997, 1999; Sato *et al*., 1998; Velasco *et al*., 1999
Spreads and condiments	Iizuka and Aishima, 1999
Tea	Grant *et al*., 1988; Hall *et al*., 1988; Osborne and Fearn, 1988; Schulz *et al*., 1999; Luypaert *et al*., 2003; Schulz, 2004; Zhang *et al*., 2004
Textiles	Cleve *et al*., 2000
Tobacco	Hana *et al*., 1997
Wine and grapes	Baumgarten, 1987; Chauchard *et al*., 2004; Cozzolino *et al*., 2004

Spectroscopic methods with specific reference to NIR spectroscopy have also been shown to have potential for discriminatory studies to determine the authenticity of several foodstuffs and food ingredients (Table 3.2).

Food authenticity issues, especially in terms of *adulteration* and incorrect labeling or description, have probably been around for as long as food has been offered for sale, with an authentic product being what it claims to be. In the recent past, however, food adulteration has become more sophisticated (Karoui and De Baerdemaeker, 2007). Foods or food ingredients that are of high value and undergo a number of processing steps are most likely to be targets for adulteration, owing to the opportunities available to, for example, replace high-quality ingredients with less expensive substitutes.

In European countries, several food products owe their reputation to traditional production techniques used in defined geographical areas. These artisan food products are therefore differentiated from other similar products (Karoui *et al*., 2005a)

Table 3.2 Fields of NIR spectroscopy qualitative applications

Application	References
Adulteration of extra virgin olive oils with sunflower oil	Downey *et al.*, 2002
Adulteration of honey	Downey *et al.*, 2003
Adulteration of maple syrup	Paradkar *et al.*, 2002
Adulteration of milk fat with foreign fat	Sato *et al.*, 1990
Adulteration of milk with other fats	Sato *et al.*, 1990; Ulbert, 1994
Adulteration of milk with non-milk fat	Sato, 1994
Adulteration of milk with substances like water, sodium chloride and skim milk powder	Pedretti *et al.*, 1993
Adulteration of orange juice	Scotter *et al.*, 1992; Shilton *et al.*, 1998
Basmati and other long-grain rice samples	Osborne *et al.*, 1997
Black teas of differing qualities	Osborne and Fearn, 1988
Bread-baking quality of different wheat varieties	Downey *et al.*, 1986; Devaux *et al.*, 1987
Classification of plant species	Lister *et al.*, 2000; Laasonen *et al.*, 2002
Classification of cultivation area	Woo *et al.*, 1999a, 1999b, 2002
Classification of processing methods	Schulz *et al.*, 2003b
Classification of herbal plants	Wang *et al.*, 2006, 2007; Mao and Xu, 2006
Classification of commercial teas	Osborne and Fearn, 1988; Budínová *et al.*, 1998
Classification of milk powders	Downey *et al.*, 1990
Classification of wines	Cozzolino *et al.*, 2003
Classification between frozen and frozen-then-thawed beef	Downey and Beauchêne, 1997a, 1997b
Classification between Robusta and Arabica coffee	Downey *et al.*, 1994, 1997; Downey and Spengler, 1996; Pizarro *et al.*, 2007
Vegetable oils	Sato, 1994
Virgin olive oils from different geographical origins	Downey and Flynn, 2002
Volatile oils	Kiskó and Seregély, 2002

and may be labeled according to the specific conditions which characterize their origin and the processing technology used (Bosset *et al.*, 1997). These are referred to as products with *Protected Designation of Origin* (*PDO*) or *Protected Geographical Indication* (*PGI*), and are often associated with high production costs; they may consequently be highly priced. This makes these products prone to adulteration with cheaper alternatives, for economic reasons.

Identifying adulterated food products has generally been done in terms of their chemical composition and/or physical properties (Downey, 1998a, 1998b). Monitoring these properties is, however, not always practical. Additionally, foods are chiefly or exclusively comprised of naturally-occurring biological material, the composition of which varies depending on the variety, species, geographical origin, year of production and manufacturing process used. This complexity of the food matrix makes the task of identifying adulterated products even more complicated.

The basic idea behind the application of NIR spectroscopy to solve authenticity problems relies on the generation of a spectroscopic fingerprint of foods (Downey, 1996a). A food product with a given chemical composition exposed to NIR radiation will have a characteristic spectrum which is essentially the result of the absorption by

various chemical constituents, although physical properties may also have an impact on the near-infrared absorbance values. Because of the variation present in any natural material, the exact composition of any given batch or sample will vary somewhat, depending on the variety, season and location; therefore, a range of typical spectra for this material will exist. For this reason, a library of representative spectra is needed to characterize any given food, and the spectrum of material under investigation may be compared to this library in order to establish its quality or authenticity. While simple in concept, this comparison is not trivial, and chemometric techniques are required for its realization.

Theory and principles

The basic principles of NIR spectroscopy involve the production, recording and interpretation of spectra arising from the interaction of electromagnetic radiation with matter (Penner, 1994). The infrared (IR) region comprises that part of the electromagnetic spectrum in the wavelength range between 780 and 100 000 nm, and is divided into near-IR, mid-IR and far-IR sub-regions (Penner, 1994; Osborne, 2000); the NIR region covers the wavelength range from 780 to 2500 nm (Osborne, 2000). When compared with spectra collected in the mid-infrared (MIR) region, a NIR spectrum normally exhibits few well-defined, sharp peaks (Williams and Stevenson, 1990). Near-infrared spectra of food constituents show broad bands which arise primarily from overtones and combinations of fundamental vibrations occurring in the MIR spectrum and, as a result, are one to three orders of magnitude weaker than the fundamental absorptions (Stark *et al*., 1986). Mid-infrared spectroscopy is typically used to determine the molecular composition of a sample.

If molecules in any given sample are illuminated by electromagnetic radiation in the NIR region, they will exhibit a large number of weak absorptions that will overlap, effectively creating broad absorption bands in the spectrum (Wetzel, 1983; Williams and Stevenson, 1990). This implies that NIR spectra are generated by chemically simple molecular groupings that have strong inter-atomic bonds; these typically are groups containing carbon (C), nitrogen (N) and oxygen (O) bonded to hydrogen (H), i.e. the most common molecules found in food (Norris, 1989; Ciurczak, 1992; Downey, 1998a). A foodstuff illuminated by electromagnetic radiation will absorb radiation at certain frequencies through bonds formed between some of the atoms present in the product (Downey, 1995). By detecting this absorption, it is possible to describe the chemical composition of an unknown mixture or food product without knowing the specific molecular structure that is responsible for the vibrational energy absorption. Therefore, despite their obvious lack of observable and discriminant details, NIR spectra are rich in chemical and physical information about organic molecules, and may therefore yield valuable information about the composition of a food product (Katsumoto *et al*., 2001). Although the differences in NIR spectra may often be too small to be noticeable by the naked eye, the true value of NIR spectroscopy as an analytical tool rests on the statistical and mathematical manipulation of the spectral data.

Instrumentation

During the last decade of the twentieth century, great advances in instrumentation and data acquisition gave NIR spectroscopy a definite place among the other established analytical methods (Wetzel, 1998, 2001). When considering NIR instrumentation, a variety of possible configurations exist. These include discrete filter, *grating monochromator* and *acousto-optical tunable filter* (AOTF) instruments, as well as *photodiode array* and *Fourier-transform interferometer* systems (Osborne *et al*., 1993; Wetzel, 1998, 2001; Barton, 2002). All NIR instruments possess the same essential building blocks (Figure 3.1): radiation source, wavelength selectors, sample presentation facility and detector (Blanco and Villarroya, 2002).

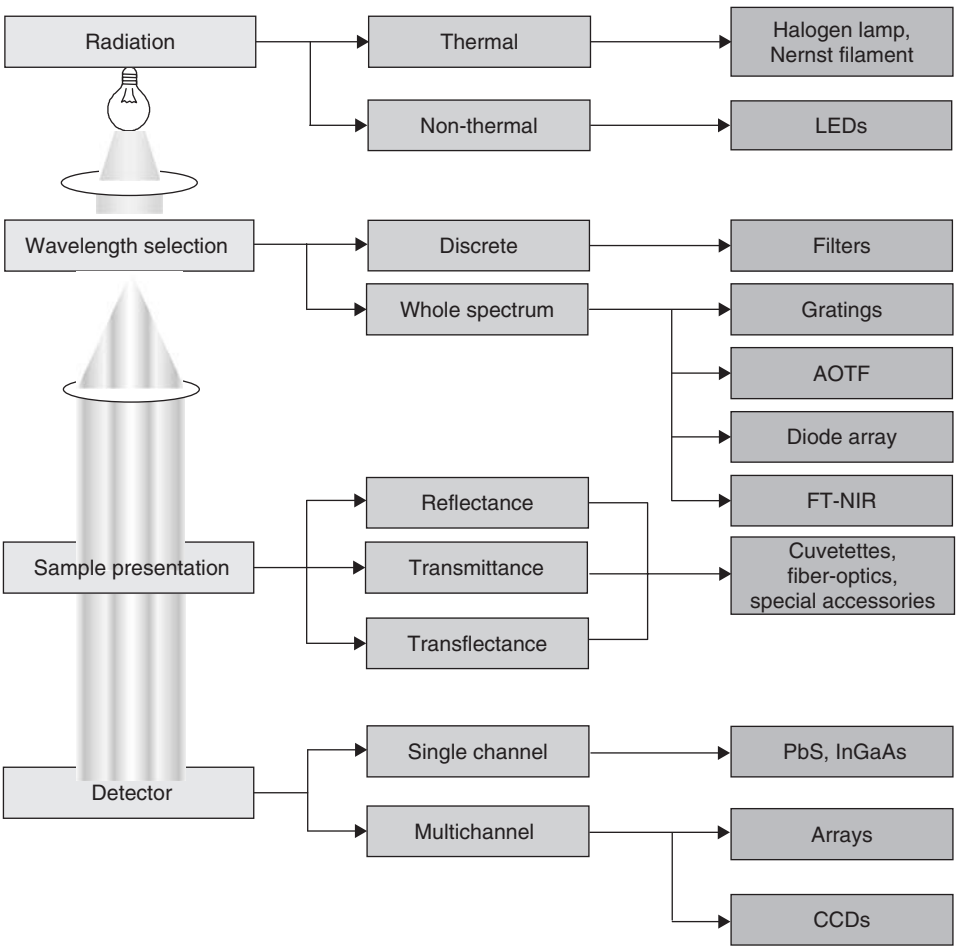

Figure 3.1 Principle features of NIR spectroscopy instrumentation (LEDs, light-emitting diode; AOTF, acousto-optical tunable filter; FT-NIR, Fourier transform near-infrared; PbS, lead sulfide; InGaAs, indium gallium arsenide; CCDs, charge-coupled devices). Reproduced with permission from Blanco and Villarroya, (2002); ©Elsevier Ltd 2002.

Radiation source

NIR radiation sources can be thermal or non-thermal. The thermal sources consist of a radiant filament producing thermal radiation – for example, the Nernst filament (a heated ceramic filament containing rare-earth oxides) or quartz-halogen lamps – and produces radiation which may span a narrow or wide range of frequencies in the NIR region (Osborne *et al*., 1993). Tungsten-halogen lamps are usually employed as thermal radiation sources, while non-thermal sources consist of discharge lamps, light-emitting diodes, laser diodes or lasers, and emit much narrower bands of radiation than the thermal sources (McClure, 2001). Non-thermal sources are the more efficient of the two types because most of the energy consumed appears as emitted radiation over a narrow range of wavelengths; they can be electronically adjusted, thus simplifying the design of the instrument and reducing its power consumption (Osborne *et al*., 1993).

Wavelength selectors

Near-infrared spectrophotometers can be distinguished on the basis of wavelength selection, i.e. discrete wavelength or continuous spectrum. A *discrete-wavelength spectrophotometer* irradiates a sample with only a few wavelengths selected using filters or light-emitting diodes (LEDs) (McClure, 2001; Blanco and Villarroya, 2002). *Filter instruments* are designed for specific applications in specific spectral regions; usually between 6 and 20 interference filters are chosen to select wavelengths that will be absorbed by certain molecular species in a specific application (Penner, 1994). These are generally the easiest to use and least expensive instruments (Osborne, 2000).

Continuous spectrum NIR instruments may include a diffraction grating or be of the diode array, AOTF or Fourier transform near-infrared (FT-NIR) type. Such instruments are much more flexible than discrete-wavelength instruments, and can be used in a wider variety of measurements (McClure, 2001; Blanco and Villarroya, 2002).

The purpose of a *grating monochromator* is to spread out radiation according to wavelength (McClure, 2001). Instruments incorporating a monochromator can be used in either transmittance or reflectance mode, depending on sample type; such equipment is normally used in a research environment when a wide range of different applications is required or when spectral information from a wide range of wavelengths is necessary for the development of an accurate and stable calibration (Osborne, 2000).

In diode array technology, all wavelengths are measured simultaneously, as each wavelength has a dedicated detector (McClure, 2001). This allows analysis of moving samples, such as a rotating sample cell or on-line applications. Diode-array NIR instruments do not use any moving optical parts, which greatly improves instrument stability.

Acousto-optical tunable filters generate discrete wavelengths across an extended range by using radio-frequency signals to change the refractive index of a crystal, usually tellurium dioxide (TeO_2) (McClure, 2001; Blanco and Villarroya, 2002). The crystal behaves as a longitudinal diffraction grating with a periodicity equal to

the wavelength of sound across the material (Osborne, 2000). The main advantage of AOTF instruments over grating instruments is their mechanical simplicity – i.e., no moving parts – thereby ensuring more reliable, reproducible wavelength scans (Osborne, 2000; Blanco and Villarroya, 2002). This makes AOTF instruments especially suitable for applications involving hazardous or harsh conditions, such as in production plants.

The *Michelson interferometer* (FT-NIR type) splits light into two beams and then recombines them after a path difference has been introduced to create the conditions for optical interference (Osborne *et al*., 1993; Wetzel, 2001). Simultaneous measurement of all wavelengths allows the light to be imaged onto one detector, making it a multiplexing instrument. The *polarization interferometer*, unlike most instruments, works with polarized light (Ciurczak, 2005). The actual interferometer consists of a moving crystalline wedge which acts as the wavelength selector and, because only a single beam passes through the instrument, the precision alignment required for the Michelson interferometer is avoided. Fourier-transform NIR instruments, with special reference to their application in authentication of agro-food products, are discussed in more detail in Chapter 4.

Sample presentation modes

One of the practical strengths of NIR spectroscopy is the wide variety of different sample presentation options which are readily available, making it possible to apply NIR spectroscopy to a wide range of sample types (liquids, slurries, powdered or solid samples, gases, etc.). These sample presentation options normally involve the use of separate, detachable accessories, and include the option of using fiber-optic probes for spectral acquisition from remote sites within a large industrial complex – such as a petrol refinery or pharmaceutical production facility (Osborne, 2000).

If the Lambert-Beer law equation (Osborne *et al*., 1993) is used to describe the contributing factors of the absorbance values of a spectrum at any wavelength, it will be a function of the path-length through which the light travels and the concentration of the constituent being measured (Wetzel, 1998). For *transmittance* measurements of liquids, the path-length is a constant determined by the thickness of the sample cuvette. This is, however, not the case for *diffuse reflectance*, with changes in both path-length due to light scatter and concentration.

The scattering of light as it passes into a granular sample is caused by interaction with a variety of angular surfaces from which the light is reflected specularly. Specularly-reflected light contains no information about the composition of a sample, and may be redirected back along the path of incidence to the detector; scattering increases the intensity of light returning to the detector but also increases the variability of the baseline due to the variable path-length of individual photons of light (Wetzel, 1998). This effect describes the detection, by diffuse reflectance, of light that is a combination of both absorbed (interaction with the sample) and scattered light (no interaction with the sample) (Wetzel, 1983). It can have a large influence on the spectrum generated, since the ratio between reflected light (absorbed and scattered) and incident light determines the absorption profile. Sample presentation

is therefore extremely important in order to minimize light scatter and, as far as possible, keep the level of scattering constant for each sample (Wetzel, 1983; Williams and Stevenson, 1990).

The influence of the particle size of granular samples on acquired spectra may be attributed to Rayleigh (elastic) scattering (Wetzel, 1983). The coarser the sample matrix, the lower the reflectance and greater the difference between the spectrum and the baseline will be. Although this effect may be of great practical value to discriminate between coarse and fine samples, it is generally a measurement complication that may be compensated for by baseline corrections which may also increase the relative size of small peaks and enlarge minor differences in large peaks (Wetzel, 1983, 1998).

Transmittance and diffuse transmittance modes

In *transmittance* measurements, reflection is generally significantly reduced so that the proportion of radiation attenuated by the sample may be measured as transmittance (Osborne, 2000). Proportionality between transmittance, the concentration of the absorbing component and the sample path-length is described by the Lambert-Beer law. Since the path-length for the specific sample may be fixed by means of a static or flow-through sample cell or a set of fiber-optic probes, the absorbance is linearly related to the concentration of absorbing component and a calibration may be developed using standard samples. The Lambert-Beer law may only be used for clear, transparent liquid samples when there is no light scattering, because scattering changes the path-length through which the radiation passes and the amount of scattering varies from sample to sample. When a sample like liquid whole milk is used, fat globules in the milk will significantly scatter incident light (which is what makes milk appear white and opaque) and thereby cause the Lambert-Beer law to be invalid. Measurements made under these conditions are described as *diffuse transmittance* (Coventry, 1988; Osborne, 2000); the wavelength region normally used for diffuse transmittance measurements is 700–1100 nm on the basis of the greater energy (and therefore penetrating power) of NIR radiation in this wavelength range. Diffuse transmittance measurements are normally used in the analysis of liquid samples, but may also be used to measure solid samples such as meat, cheese and whole grains (Penner, 1994).

Diffuse reflectance mode

Diffuse reflectance measurements are used in the analysis of solid or granular samples (Penner, 1994; Osborne, 2000). A major complication in the analysis and interpretation of diffuse reflectance measurements, which are arguably numerically the most important NIR measurements collected, is light scatter. Scattered light contains little or no information about the chemical composition of any given particulate sample (although it can facilitate the description of physical properties), and interferes, through baseline and intensity effects, with the spectral information collected. Attempts have been made to develop a mathematical basis to describe light scatter and to accommodate its effects on NIR spectra, but no completely successful strategy has been forthcoming – this has resulted in the study of spectral pre-treatment

methods such as *multiplicative scatter correction* (Geladi *et al*., 1985), derivatization (Osborne, 2000) and the *standard normal variate* transform (Barnes *et al*., 1989), among others, to address this problem.

Transflectance mode

Reflectance and transmittance modes can be combined to form a *transflectance* mode (Osborne, 2000) which can be used to analyze liquids (turbid or clear) by placing the sample between a quartz window in a sample cell and a diffusely reflecting (e.g. gold-plated) metal plate. Incident radiation is transmitted through the sample, reflected from the diffusely reflecting plate and then transmitted back through the sample. In the case of a turbid sample some radiation will be scattered as it travels through the sample, and this scattered light will then also travel back with the light reflected from the transflectance cover (Stark *et al*., 1986). Minimization of spectral interferences thus arising can be achieved through good instrument design as regards detector placement.

Interactance mode

Transmittance and reflectance can also be combined to form an *interactance* mode that will illuminate and detect radiation at laterally-separated points on the surface of a sample; fiber-optic probes are often used for such applications, which find important applications in, for example, the analysis of large samples such as whole fruit.

Detectors

Infrared detectors can be differentiated according to their spectral response, their speed of response and the minimum amount of radiant power that they can detect (McClure, 2001). There are two broad categories of IR detectors which differ in their operating principles, namely thermal detectors and photon detectors; the latter are used in NIR applications (Osborne *et al*., 1993). For photon detectors, it is necessary for the incident radiation to be strong enough to liberate charge carriers either from the crystal lattice (intrinsic detectors) or from impurities intentionally added to the host crystal during the manufacturing process (extrinsic detectors) (McClure, 2001).

The detection devices most widely-used for NIR analysis can be divided into *single-* and *multi-channel* detectors. Single-channel detectors comprise lead-salt semiconductors. Lead sulfide (PbS) is used over the range 1100–2500 nm, epitaxially grown indium gallium arsenide (InGaAs) over 800–1700 nm, and silicon detectors over 400–1100 nm (Osborne *et al*., 1993; Blanco and Villarroya, 2002). Multichannel detectors comprise diode arrays, in which several detection elements are arranged in rows, or charge-coupled devices (CCDs), in which several detection elements are arranged in planes (Stchur *et al*., 2002). Multichannel detectors can, for this reason, record many wavelengths at once, and this type of detector has given rise to NIR imaging spectroscopy – a technique in which spectra are recorded using cameras that can determine composition at different points in space and record the shape and size of the object. Making measurements at different wavelengths provides a

three-dimensional image that is a function of the spatial composition of the sample and the irradiation wavelength used (Blanco and Villarroya, 2002; Baeten and Dardenne, 2005).

Chemometrics

> Chemometrics is the chemical discipline that uses mathematics and statistics to design or select optimal experimental procedures, to provide maximum relevant chemical information by analysing chemical data, and to obtain knowledge about chemical systems.
>
> *Massart et al. (1988)*

Overlapping of the many individual absorbance bands in the NIR region results in broad bands characteristic of NIR spectra; a NIR spectrum cannot, therefore, be interpreted in a straightforward manner. Often, large amounts of spectral data are obtained from NIR instruments; these data contain considerable amounts of information about the physical and chemical properties of molecules that yield useful analytical information (Osborne *et al*., 1993; Downey, 1998a; Katsumoto *et al*., 2001; Blanco and Villarroya, 2002), but they also contain noise, uncertainties, variabilities, interactions, non-linearities and unrecognized features. One of the biggest challenges faced when analyzing spectral data is to eliminate or reduce the noise from the spectra. This not only eases visualization of the information contained in the spectra, but also maximizes the exploitation of the useful data (Wetzel, 1998; Katsumoto *et al*., 2001). Chemometrics is required to extract as much relevant information from the spectral data as possible (Wold, 1995).

Chemometrics has a fundamental role in NIR-based calibration, and method performance in deriving calibration models is an important aspect to take into account (Centner, 2000; Geladi, 2002). A variety of multivariate analysis techniques can be used to (i) extract analytical information contained in NIR spectra to develop models, and (ii) predict relevant properties of unknown samples. There are two main groups of multivariate methods which may be distinguished by the type of analysis required; qualitative and quantitative analysis.

Since the early introduction of *multivariate regression techniques* by Norris (Ben-Gera and Norris, 1968a, 1968b), the development of various mathematical procedures and the increasingly widespread availability of commercial software have contributed tremendously to the expansion and current popularity of NIR spectroscopy. Development of *calibration models* for *quantification* of constituents in samples is possible by relating physical or chemical properties of the investigated samples to the absorption of radiation in the NIR wavelength range. *Qualitative calibration models* depend on comparing spectra of the sample to be identified with spectra of known samples.

Due to the vast amount of spectral information, the large number of samples required to build classification and calibration models, and the high inter-correlation

within spectra, there is a need for variable-reduction methods that allow the dimensions of the original data to be reduced to a few uncorrelated variables containing only relevant information from the samples (Blanco and Villarroya, 2002). *Principal component analysis* (*PCA*) is such a method which searches for directions of maximum variability in spectral data sets and calculates them as new axes called principal components. The calculated principal components contain the spectral information in a reduced number of variables – for example, less than 20 – and these new variables can substitute the original data in subsequent calculations (Cowe and McNicol, 1985). The fact that these new variables are linear combinations of the original variables (absorbances at the different wavelengths) means that individual principal components may be examined graphically to reveal previously-undetectable information about the role of molecular or chemical species in any given calibration model (Cowe *et al*., 1990). By looking at the shapes of the components, it is possible to see in which parts of the spectra the contributing absorbance bands are detected (Cowe and McNicol, 1985). Principal component analysis is an *unsupervised method* (i.e. no reference to any set of analytical values is necessary to examine spectral variation), and therefore provides a simple procedure for data description and compression (Devaux *et al*., 1988).

Pre-processing of spectral data

Maximizing the significance of any spectral differences is the main aim of using pre-processing algorithms (Osborne *et al*., 1993; Hopkins, 2001). Achieving this maximization becomes very difficult if the *signal-to-noise* (*S/N*) *ratio* of a given spectrum is very small. As NIR spectroscopy utilizes light of low intensity, it will necessarily produce less sensitive responses in the excited molecules (Wetzel, 1998). To compensate for this lower sensitivity, the noise levels detected by the instrument have to be kept to a minimum to create a high S/N ratio. Noise can be caused by instrument drift during scanning, sample preparation and presentation, and by the environmental conditions within which the spectra are generated (Wetzel, 1983; Katsumoto *et al*., 2001). Environmental conditions are especially important, as they will affect the weakly absorbing bands of NIR spectroscopy much more significantly than those regions that produce strong absorptions. One way of removing noise is to collect multiple scans and average them (Katsumoto *et al*., 2001); although the achievement of significant noise-reduction levels may necessitate large numbers of repeat scans – 64 or more. If this does not reduce the noise level adequately, smoothing techniques, of which the moving average method (Savitzky and Golay, 1964) is the most common, may be used. Other common pre-processing methods include normalization (Massart *et al*., 1988; Næs *et al*., 2002), derivatives (Massart *et al*., 1988; Næs *et al*., 2002), multiplicative scatter correction (MSC) (Geladi *et al*., 1985) and standard normal variate (SNV) and de-trending (Barnes *et al*., 1989). Pre-processing techniques more recently developed include *orthogonal signal correction* (*OSC*) (Wold *et al*., 1998; Sjöblom *et al*., 1998), *direct orthogonal signal correction* (*DOSC*) (Luypaert *et al*., 2002) and *orthogonal wavelet correction* (*OWAVEC*) (Esteban-Díez *et al*., 2004a, 2005).

Smoothing

The *Savitzky-Golay moving average* (Savitzky and Golay, 1964) and other algorithms, i.e. wavelets (Katsumoto *et al*., 2001), can reduce the effect of noise on a spectrum by removing small variations in absorbance which are not expected to be meaningful.

Derivatives

One of the most common pre-processing algorithms used calculates the first or second derivatives of each spectrum (Wetzel, 1998; Næs *et al*., 2002). *Derivatives* are used to enhance slight spectral differences between samples and compensate for baseline shifts that have been caused by light scattering (Beebe *et al*., 1998). Second derivatives in particular can accentuate sharp spectral features and help resolve overlapping bands. Derivatization can minimize the effects of scattering by removing additive offsets that are independent of wavelength (first derivatives) or by removing offsets that change linearly with wavelength (second derivatives).

Normalization

Normalization is another method of removing bias from a spectrum without using derivatives (Wetzel, 1998; Næs *et al*., 2002). It is achieved by mean-centering the spectra (subtracting the average absorbance from each spectrum) and then establishing unit variances at each wavelength by dividing the absorbance at each by the relevant standard deviation. Such normalization may, however, remove valuable information from the spectral data set.

Multiplicative scatter correction

Another normalization procedure is *multiplicative scatter correction* (*MSC*) (Geladi *et al*., 1985). This approach also mean-centers the data, after which the target spectrum is curve-fitted to the average and then divided by the curve-fit value. Multiplicative scatter correction is a very useful and powerful pre-processing method for removing additive and multiplicative differences in a spectral data set; such differences are mainly caused by samples with inconsistent particle sizes (e.g. powders). Multiplicative scatter correction separates the chemical light absorption from the physical light scatter (Geladi *et al*., 1985).

Standard normal variate and de-trending

Standard normal variate (SNV) transforms spectral data by subtracting the mean of the spectra from the spectral values of each spectrum (Barnes *et al*., 1989). These centered spectra are then scaled by the standard deviation of the spectrum. Standard normal variate effectively removes the multiplicative interferences of scatter and particle size, and is applicable to individual NIR spectra. *De-trending* accounts for the variation in baseline shift and curvilinearity (Barnes *et al*., 1989).

Quantitative chemometric techniques

Quantitative NIR calibration development involves collecting a set of calibration samples with known reference values (chemical constituents, physical characteristics

or other properties) covering as much as possible the range of variation expected in future or unknown samples. Calibration development then entails the establishment of a mathematical relationship between the NIR spectrum and the reference parameters previously determined by an independent reference analytical method. The aim is therefore to fit the NIR and reference values to a straight line and compare this statistically to a theoretically perfect line through the origin at 45° to both axes. This calibration model, after being adequately validated on an independent validation set, can then be used to predict the properties or constituents in unknown samples on the basis of their NIR spectra. Regression methods commonly used are multiple linear regression (MLR), which utilizes only selected wavelengths, and principal component regression (PCR) and partial least squares (PLS) regression, both of which use the whole spectrum. More detail on these methods can be found in Næs *et al*. (2002).

Qualitative chemometric techniques

Qualitative multivariate analysis methods are being used to recognize similarities in NIR spectral data. Qualitative analyses are directed at extracting information about one or more important functional properties of a sample which can be used to screen samples on the basis of desired functional properties; these methods also find extensive application in the confirmation of authenticity or the detection of adulteration of food samples.

Qualitative multivariate data analysis techniques are known as *pattern recognition* methods (Osborne, 2000), since their application generally involves a comparison of spectra and a search for similarities or differences (Wüst and Rudzik, 2003). In terms of classification, the aim is to get as many correct classifications as possible. A decisive design parameter that has to be set prior to any classification model development is the number of classes to be considered and the particular requirements that a sample has to fulfill in order to be assigned to a certain class (Esteban-Díez *et al*., 2007). Conventionally, a spectral library of known substances is built and a model developed which describes the mean spectrum and the associated variability of each sample type in multidimensional space; the spectrum of an unknown sample is then compared to the spectral library and decision rules applied to determine the likelihood of it belonging to the library or not (Wüst and Rudzik, 2003). Qualitative applications of NIR spectroscopy may be achieved by two different broad approaches, namely unsupervised and supervised methods (Beebe *et al*., 1998; Blanco and Villarroya, 2002; Pasquini, 2003). In the former, the classes of samples used for model development are known at the outset, whereas in unsupervised methods there is no information about the class structure of the training sample set.

Unsupervised methods

Unsupervised methods, e.g. PCA and *hierarchical cluster analysis* (*HCA*), are often deployed as investigative tools in the early stages of data analysis to give indications of possible relationships between samples.

Principal component analysis

Principal component scores for similar materials tend to cluster in multidimensional space in a similar fashion to the way the data points representing individual

wavelength measurements may cluster (Mark, 1992; Downey, 1996a). Principal component analysis models are constructed using the entire data set obtained from all the measurements of the different samples to be distinguished (Mark, 1992).

Hierarchical cluster analysis

Clustering can be defined as the process of organizing objects into groups, the members of which are similar in some way. A cluster is therefore a collection of objects, which are similar to each other and dissimilar to other objects. Hierarchical cluster analysis (HCA) is a method often used for preliminary data analysis – the process is iterative, and involves assigning objects which are close to each other to a cluster, finding the closest (most similar) pair of clusters and merging them into a new, single cluster, etc., and finally computing distances (similarities) between the new cluster and each of the old clusters (Mao and Xu, 2006). The latter two steps are repeated until all items are grouped into a single cluster. An important component of a clustering procedure is the distance measure between data points; either *Mahalanobis* (Næs *et al*., 2002) or *Euclidean* (Næs *et al*., 2002) distances may be used (Mao and Xu, 2006). The most common distance measure used is the Mahalanobis distance, which describes distance in any given direction relative to the variability along the same axis.

Supervised methods

The more traditional supervised methods include *Bayes classification* or *Fisher's linear discriminant analysis* (Næs *et al*., 2002). Supervised methods commonly used to solve authenticity problems are soft independent modeling of class analogy (SIMCA), discriminant PLS (DPLS), linear discriminant analysis (LDA), multiple discriminant analysis (MDA), factorial discriminant analysis (FDA), canonical variate analysis (CVA), artificial neural networks (ANNs) and k-nearest neighbor (k-NN) analysis (Downey, 1996a; Blanco and Villarroya, 2002; Stchur *et al*., 2002). More recent classification techniques reported include support vector machine (SVM) classification (Zhao *et al*., 2006; Chen *et al*., 2007), and wavelet interface to linear modeling analysis (WILMA) (Cocchi *et al*., 2003). Some of the most commonly used supervised methods are briefly described below; more exhaustive and detailed explanations of these methods can be found in Næs *et al*. (2002).

Soft independent modeling of class analogy (SIMCA)

Apart from problems relating to simple classification, *soft independent modeling of class analogy* (*SIMCA*) is applied to a more general class of discriminatory issues, i.e. identification. It is a procedure in which raw spectra are compressed by means of principal component analysis (Downey and Beauchêne, 1997a) – data describing samples from each of the relevant number of classes or groups are collected, and separate PCA models are calculated for each of the groups for which qualitative analysis is desired (Mark, 1992). Classes are thus modeled independently of each other, and the cluster models treat new samples separately. SIMCA first centers and then compresses raw data by means of PCA (Mark, 1992; Downey and Beauchêne, 1997a); a multidimensional space is constructed containing the scores corresponding to each

group. *Mahalanobis distances* based on the principal component scores are calculated for every sample to determine the distance from the center of the cluster in the dimensional space. Each cluster model treats new samples separately, and an assessment of cluster membership is made on the basis of the distance of any given sample to the center of the cluster. An F-test is employed to measure the degree of similarity of an unknown sample spectrum to sample spectra in each modeled cluster, allowing an estimate of confidence to be attached to any identification decision (Downey, 1996a; Downey and Beauchêne, 1997a). The sum of squares of a residual spectrum can be compared to the variance within the class, providing a measure of certainty accompanying each identification (Downey, 1996a; Downey and Beauchêne, 1997a). The spectrum residual, which is an indication of how much of the spectrum of any given sample is not explained for by the PCA model, provides a reliable and sensitive measure of class membership. By combining two residual distances, the critical probability of an unknown sample belonging to a specified class may be tested. SIMCA is claimed to have advantages in the separation of very similar materials (Downey and Beauchêne, 1997a), but reported successful applications of SIMCA to food classification using NIR spectra are few in number (Downey, 1996a).

Discriminant PLS

With *discriminant PLS* (*DPLS*) it is possible to build calibration models using spectral data and knowledge of the class membership of each sample in the training (calibration) set. In *DPLS1*, used for binary classification problems, each sample is given a dummy variable equal to 0 or 1; members of the class are ascribed a value of 0, and non-members a value equal to 1. Unknown samples with a predicted value below 0.5 may be identified as belonging to the class being modeled; the converse applies to samples with predicted values equal to or greater than 0.5. Cut-off values other than 0.5 may be used, depending on the dispersion of predicted values and the confidence required for class identification decisions. *DPLS2* is used when more than two classes of material must be modeled; in this case also, the dummy variable associated with each class type is ascribed a value equal to 0 for samples belonging to the class and 1 for all other samples.

Linear discriminant analysis

Linear discriminant analysis (*LDA*) is a supervised classification technique in which the number of categories and the samples that belong to each category are previously defined (Næs *et al*., 2002). The method produces a number of linear discriminant functions, equal to the number of categories minus one, that allow samples to be classified in one or another category. The Mahalanobis distances of each object from the centroids of the categories are computed, and objects are assigned to the nearest cluster.

Factorial discriminant analysis

The aim of *factorial discriminant analysis* (*FDA*) is to predict membership of a single sample according to other defined groups; principal component analysis scores are used as the basis for FDA. During FDA, principal component scores calculated on mean-centered spectral data are normalized and the gravity center of the score

cluster for each group is determined. The Euclidean distance of each principal component score of a given sample to each of the gravity center is calculated and the individual sample assigned to the group with the nearest gravity center, subject to a maximum membership distance of two or three times the Euclidean distances. The unique feature of FDA is that principal components are incorporated into the model on the basis of decreasing classification ability, not in calculation order.

k-Nearest neighbors

k-Nearest neighbors (*k-NN*) is a reasonably simple method. To classify a new sample, its Euclidean distance from each of the samples in a training set is calculated and the *k* nearest samples are found; *k* typically has odd, integer values. The unknown is then classified to the group that has the most members amongst these neighbors (Næs *et al*., 2002).

Validation

It is critically important to assess the performance of every calibration model on an unknown set of samples, since the ultimate goal of a calibration model is to predict unknown values accurately and precisely (Geladi, 2002), and this may best be done using a test sample set which should contain a realistic representation of samples that may be encountered in the future (Osborne *et al*., 1993).

Validation or *prediction* testing refers to the calculated difference between NIR spectroscopy prediction results obtained for the constituents, properties or identification or classification, and the measurements obtained for the reference method or known identities (Næs and Isaksson, 1991). *Internal validation* involves validation of a calibration using the same sample set as that used for calibration development. An assessment based on internal validation is therefore not the same as prediction testing (Martens and Næs, 1989), which involves validation of a calibration using an independent sample set that was not involved in the calibration development. The two validation methods normally used are *independent* or *external validation* (Esbensen, 2000) and *cross-validation*, which uses the calibration data set only. External validation requires a separate, large and representative set of test objects in order to give relevant and reliable estimates of the future prediction ability of the model (Martens and Næs, 1989; Westerhaus, 1989). This is, however, not always possible, as multivariate calibration is often done because the traditional reference method for measuring the constituent or class of interest is too expensive or slow, or is otherwise undesirable. It would be most economical to use all the data available for both calibration development and for prediction testing (Martens and Næs, 1989).

Cross-validation is a very reliable validation method; it seeks to validate the calibration model on an independent test data set but, contrary to external data, it does not use samples for testing only. For cross-validation, successive samples are deleted from the calibration set. In partial cross-validation, samples are removed in groups; in full-cross validation, all samples are removed one at a time. After every deletion, a calibration is performed on the rest of the samples before being tested on

the removed samples. The first sample is then replaced into the calibration data and the next sample removed. The procedure continues until all the samples or sample groups have been deleted once (Martens and Næs, 1989; Næs and Isaksson, 1991).

The final step in NIR calibration development is statistics, which is "the art of drawing conclusions from data, and making decisions, in the presence of variability" (Wold, 1995) and is needed for interpretation of the gathered data and evaluation of the efficiency and accuracy of the calibration model.

The statistics most often used for quantitative NIR analysis are listed in Table 3.3, and include the *standard error of prediction* (*SEP*) or *standard error of cross-validation* (*SECV*); *bias*; the *coefficient of determination* (R^2); and the *ratio of standard deviation to standard error of prediction* (*RPD*) (Osborne *et al*., 1993; Williams, 2001). The SEP measures how well the calibration is going to perform in future

Table 3.3 Equations for statistical calculations

Statistic	Equation	Recommendations
SD[a]	$\sqrt{\sum y^2 - \frac{\left[\frac{\left(\sum y\right)^2}{n}\right]}{n-1}}$	
SEL[b]	$\sqrt{\frac{\sum\left(y_1 - y_2\right)^2}{2n}}$	As small as possible
SEP[c]/SECV[d]	$\sqrt{\frac{\sum_{i=1}^{n}\left(y_i - \hat{y}_i - BIAS\right)^2}{n-1}}$	As small as possible or close as possible to SEL value
V-BIAS[e]	$\frac{1}{n}\sum_{i=1}^{n}\left(y_i - \hat{y}_i\right)$	As close to zero as possible
R^2[f]	$1 - \frac{\sum_i \left(y_i - \hat{y}_i\right)^2}{\sum_i \left(y_i - \bar{y}\right)^2}$	<>0.90
RPD[g]	$\frac{SD_{\hat{y}}}{SEP}$ or $\frac{SD_{\hat{y}}}{SECV}$	5.0 or more

[a]Standard deviation; [b]standard error of laboratory; [c]standard error of prediction; [d]standard error of cross-validation; [e]bias of the validation set; [f]coefficient of determination; [g]ratio of standard deviation to standard error of prediction.

y = reference value; $\hat{y}$ = predicted value; y_i = reference value for the *ith* sample; $\hat{y}_i$ = NIR predicted values for the *ith* sample; y_1 and y_2 = duplicate reference values; n = number of samples; t = number of terms in the model.

analysis (Fearn, 2002), and should be as close as possible to the *standard error of laboratory* (*SEL*) for the constituent or property being measured. The SEP is used to evaluate the accuracy of a calibration by indicating the variability in deviations of the reference data from the NIR spectral data. The bias gives the average by which the results differ. Together, the SEP and the bias indicate and evaluate the overall accuracy of the prediction model. The SEP and bias should be as low as possible, with a slope close to 1.0 (Williams, 2001). When cross-validation is performed, the accuracy of the calibration is indicated using the SECV. The RPD enables evaluation of the SEP in terms of the SD of the reference data, and gives an indication of the efficiency of the calibration model (Williams and Sobering, 1993; Williams, 2001). The recommended RPD value for the use of NIR spectroscopy in quality control is 5.0 or more (Williams, 2001). For screening purposes, a value of more than 3.1 would be sufficient. The coefficient of determination (R^2) indicates the amount of variation in the data being explained by the calibration equation (Williams, 2001). The R^2 should be high (>0.90) to indicate a good prediction capability, while with a low value ($\leqslant 0.64$) it is not possible to obtain consistently high accuracy by NIR spectroscopy analysis.

Qualitative calibration results can be assessed on the basis of number of false positive and false negative classifications (Contal *et al*., 2002). A false positive occurs when a sample which does not belong to a given class is predicted by the model to be a member of that class. A false negative arises when a sample which does belong to a given class is not classified as such. False positives are considered the more serious of the two error types, given that they represent a failure of the model to detect non-membership or adulteration. Accuracy of classification results can also be expressed in terms of sensitivity and specificity (Esteban-Díez *et al*., 2007). Sensitivity is the proportion of samples belonging to a certain category correctly identified by the prediction model corresponding to that class – i.e. it is a measure of the ability to correctly predict true positives. Specificity is the proportion of samples not belonging to a certain class classified as foreign – i.e. it is a measure of the ability to discriminate against false positives. These parameters are valuable diagnostic tools for evaluating classification and confirmation of authenticity results, since a class-model should not only correctly classify samples as belonging to a specific class or category but also reject samples not belonging to that class.

Advantages and disadvantages

Advantages

Near-infrared spectroscopy has several advantages over other analytical techniques. It is a rapid, easily used technology that is non-destructive in nature (Day and Fearn, 1982; Osborne *et al*., 1993; Wetzel, 1998) and does not require chemical consumables (Zoecklein *et al*., 1994; Downey, 1998a, 1998b). The latter is important, as the disposal requirements for hazardous waste are becoming increasingly expensive for laboratories. Near-infrared spectroscopy requires minimal or no sample preparation or pre-treatment (Day and Fearn, 1982; Osborne, 2000). It can record complete

continuous spectra for high moisture samples, such as liquids and slurries, as well as solids (Williams and Stevenson, 1990; Blanco and Villarroya, 2002), and one of the major advantages of NIR spectroscopy is that it allows several constituents or properties to be measured at the same time (Osborne, 2000).

NIR instrumentation is often rugged, and can be used inside or outside laboratory environments (Stark *et al*., 1986). Measurements can also be carried out on-line (Osborne *et al*., 1993; Hoyer, 1997) or in-line (Singh Sahni *et al*., 2004). Portable NIR spectrophotometers such as hand-held instruments (www.polychromix.com) using micro-electromechanical systems (MEMS) (Crocombe, 2004) technology and equipment that can be carried in a backpack or mounted on a vehicle are nowadays more freely available (Blanco and Villarroya, 2002).

The most interesting advantages of NIR spectroscopy compared with other spectroscopic techniques are its ability to use longer path-lengths, and that the optical equipment is much simpler (Karoui and De Baerdemaeker, 2007). It is possible to use optical fibers and glass for windows, sample cells and lenses made from quartz glass. These are cheaper and easier than the alkali salts (such as KBr and KCl) typical of mid-infrared analyses. It is also possible to create a pseudo-homogenous spectrum from a non-homogenous sample by scanning a large area of the sample and averaging the sample's properties. The relatively deep penetration of NIR light into samples also permits better representation of the chemical properties. Once the method has been developed, the instrument can easily be used by technicians for process control purposes. The low absorptivity of absorption bands in NIR is compatible with moderately concentrated samples and longer path-lengths compared with mid-infrared analyses (Osborne *et al*., 1993). This enables spectra to be measured by transmission through intact materials, which allows rapid and non-destructive analysis as no sample preparation is needed. Intact, opaque, biological samples can also be analyzed by diffuse reflectance, which makes NIR spectroscopy a very simple technique to use and an ideal application for on-line analyses.

Disadvantages

The main disadvantage is the low sensitivity of the signal, which can limit the determination of low concentration components to be determined by the use of NIR spectroscopy (Karoui and De Baerdemaeker, 2007). This limitation of NIR absorptions, however, simplifies the spectra and restricts the information extracted to that of fundamentally strong chemical bonds between light atoms. Chemometric manipulations of the data can, though, be very revealing, if handled correctly.

The main limitation of NIR spectroscopy as an analytical technique involves its dependence on other chemical methods of analyses that are sometimes less precise and equally empirical (Osborne *et al*., 1993). A large data set incorporating large variation, which it is often difficult to obtain, is essential to build a robust calibration (Wetzel, 1998). Near-infrared spectroscopy therefore requires an extensive calibration and validation sample set to produce robust prediction models. The *reference method* often requires a lot of time for sample collection, preparation and presentation, and may involve large expense, depending upon the nature of the constituent. Effective

use and development of new calibrations requires sufficient training of the operator. Furthermore, the maintenance of a calibration set is very difficult, and this lack of sample stability over long periods of time causes problems for calibration transfer. For qualitative analysis, however, the cost of reference method analysis may not be a concern.

The initial high cost of the instrumentation is also an important factor when considering acquiring a NIR instrument for routine applications in a quality control laboratory. The purchase and running costs of NIR instruments compared with the cost of consumables used in conventional chemical methods should, however, be assessed in terms of the long-term financial implications and benefits of such an investment.

Applications in food and beverage authenticity

Increasing emphasis is being placed on non-destructive quality control methods for agricultural and biological materials necessary for composition analysis (Gunasekaran and Irudayaraj, 2001). Applications of NIR spectroscopy in the food industry were reported as early as 1938 in gelatin studies (Ellis and Bath, 1938). Nowadays, the applications of NIR in the food and beverage industries are varied, and include quantification of food ingredients and composites (Williams and Stevenson, 1990; Osborne *et al*., 1993; Iwamoto *et al*., 1995; Wetzel, 1998); food adulteration and authenticity (Downey, 1995; Downey, 1996a); the detection of external and internal defects in foods and crops (Osborne *et al*., 1993); and qualitative and sensory determinations (Osborne *et al*., 1993; Downey, 1995, 1998b; Wetzel, 1998).

In the following sections, only those applications concerning the use of NIR spectroscopy and appropriately-combined chemometric techniques to assess authenticity, identity, geographical origin, and detection and quantification of adulteration in food and food products will be discussed in more detail.

Cereals and cereal products

Wheat used for food applications consist of mainly two species – bread wheat (*Triticum aestivum*) and durum wheat (*Triticum durum*) – which are characterized by different chemical and physical properties. Based on these different properties, they will differ in functional quality, nutritional contribution and consequently commercial value. The first qualitative NIR spectroscopy analysis on wheat was performed in the 1980s, and the studies reported the possibility of discriminating between wheat varieties on the basis of their bread-baking quality (Bertrand *et al*., 1985; Downey *et al*., 1986a; Devaux *et al*., 1986, 1987). Using a wheat hardness index measured by NIR reflectance as a quality indicator, it was possible to distinguish between selected wheat samples with different bread-baking qualities on the basis of their hardness (Downey *et al*., 1986a). Near-infrared spectroscopy and FDA was used to identify a range of commercial white flours, i.e. biscuit, self-raising, household, cake, bakers' and soda bread mix (Sirieix and Downey, 1993); using this approach, it was possible to classify 97% of a set of 99 validation samples correctly. Although the identification

was largely due to particle size difference between the flours, identification was also due to the presence of inorganic additives at different levels in some flours.

More recently, separation of four commercial Italian bread wheat flours of different quality categories was attempted by means of NIR spectroscopy (Cocchi *et al*., 2005). The spectra (400–2489 nm at 2-nm intervals) were acquired in a quartz sample cell using a Foss NIRSystems 6500 spectrophotometer. The flour quality categories were defined by means of specific parameters, i.e. hectoliter weight, Hagberg Falling Number, protein content, alveograph measurements and farinograph stability. Despite the use of SIMCA and a wavelet-based feature selection/classification algorithm called WPTER, it was not possible to classify the four different categories; this was due to considerable overlap of the two intermediate quality classes. It was, however, possible to classify the two extreme classes of wheat quality with an acceptable degree of separation (Figure 3.2). Cocchi *et al*. (2005) found 2050–2350 nm to be the most informative part of the NIR spectrum for classifying the two categories of flour. This region corresponds to the combination bands of N–H bonds (2050–2070 nm), O–H bonds (2070–2100 nm), C–H bonds (2140–2200 and 2280–2335 nm) and C=O bonds (2140 and 2180–2000 nm).

In countries such as Italy (Anonymous, 1967), France and Spain, the law establishes that pasta may only be made from durum wheat semolina and water, and durum wheat adulteration with bread wheat is of particular interest. However, in northern

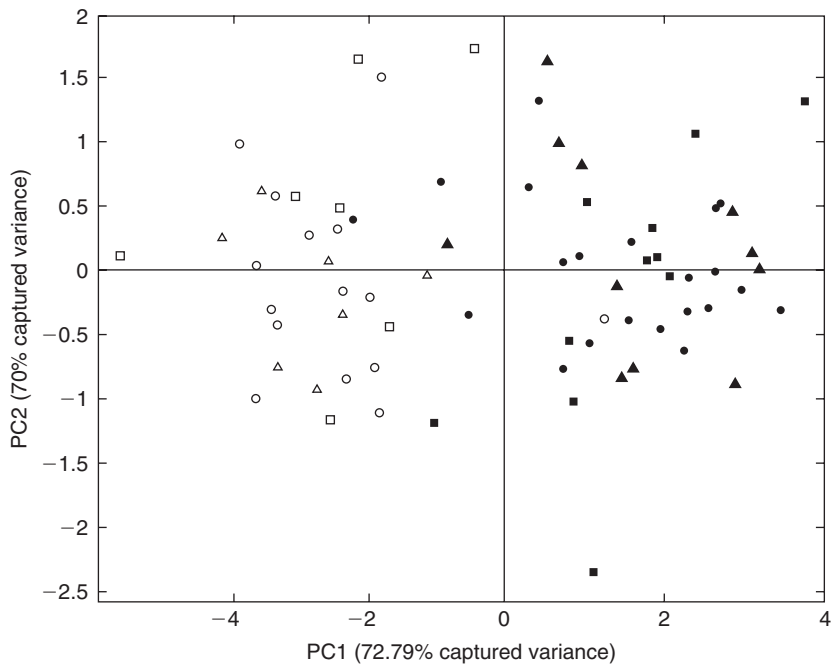

Figure 3.2 Scores plot of the first two PCs calculated by PCA on the wavelet coefficients from the WPTER selected model for the two FF (strongest) and FB (weakest) classes (circles, training set; triangles, monitoring set; squares, test set; FB, filled symbols; FF, empty symbols). Reproduced with permission from Cocchi *et al*. (2005); ©Elsevier Ltd 2005.

European and other countries, both bread and durum wheat are often allowed. The addition of bread wheat flour is treated as adulteration in Italy, as it is believed to result in a product with decreased resistance to cooking and therefore of lower quality. As accidental contamination of semolina with bread wheat is likely during harvesting or storage, the presence of bread wheat flour in percentages not higher than 3% is sometimes allowed (Anonymous, 2001). A feasibility study by Cocchi *et al*. (2006) showed that PLS and a newly developed calibration algorithm called WILMA (wavelet interface to linear modeling analysis) (Cocchi *et al*., 2003), which makes use of the advantages offered by wavelet transforms, resulted in good predictive performance when the possibility of using NIR spectroscopy to quantify the degree of adulteration of durum wheat flour with bread wheat flour was explored. Using a similar instrument set-up (Foss NIRSystems 6500 and quartz sample cell), the uncertainties associated with the developed models have been shown to be about half of the uncertainty of the current Italian official method.

Basmati, a class of rice grown in the Punjab region of India and Pakistan, can only be grown once a year, with a yield half that of other rice varieties, and its eating quality cannot be duplicated by growing the same seed in other regions; there is therefore a strong incentive for its fraudulent adulteration with other long-grain rice varieties. In a preliminary attempt, NIR transmission spectroscopy was used to classify rice as Basmati or non-Basmati (Osborne *et al*., 1997). Rice samples were analyzed using two presentation modes, i.e. bulk samples or single grains, using a Tecator Infratec 1225 grain analyzer over the wavelength range from 850 to 1050 nm. Fischer linear discriminant analysis was applied to the resulting data sets, and a perfect discrimination between Basmati and non-Basmati rice samples was achieved for the bulk samples. In the case of the single grains, the long-grain samples were, however, often misclassified as also being Basmati rice.

Coffee

Approximately 99% of commercial coffee is made from Arabica (*Coffea arabica* Linnaeus) and Robusta (*Coffea canephora* Pierre ex Froehner) varieties (Downey *et al*., 1994; Downey and Spengler, 1996). Arabica is viewed as superior in quality to Robusta, and trades at a price which is 20–25% higher than that of Robusta (Esteban-Díez *et al*., 2007; Pizarro *et al*., 2007), thereby introducing the potential for fraud. Trained personnel can generally identify between these two coffee varieties when in bean form, but this is not generally possible once the beans have been ground.

The first qualitative NIR spectroscopy work on coffee was reported by Davies and McClure (1985), who showed that it was possible to discriminate between regular and decaffeinated coffee by use of NIR spectra without calibration against caffeine content. Downey *et al*. (1994) reported on the potential of NIR and FDA to discriminate between pure (green and roasted) Arabica and Robusta coffees and blends in the form of whole and ground beans. Calibration ($n = 52$) was performed on spectra recorded in the wavelength range of 1100–2498 nm using a Foss NIRSystems 6500 instrument, and it was validated using two prediction sets ($n = 52$ and $n = 105$, respectively). For the pure whole-bean coffees, a total correct classification rate

of 96.2% was achieved. From the discriminant scores it was apparent that discriminant factor 1 separates green from roasted coffee beans while factor 2 divides Robusta coffee beans from Arabica beans. Including 50 : 50 blends (20 green and 20 roast samples), the classification rate was reduced to between 82.9 and 87.6%. Discrimination of 105 (52 samples for calibration and 53 for validation) ground-coffee blends resulted in a correct classification rate of 83%. Downey *et al*. (1994) suggested that discrimination between the two varieties was on the basis of alkaloid (e.g. caffeine) content.

Using the same instrument set-up as Downey *et al*. (1994), Downey and Spengler (1996) studied the classification of coffee blends and illustrated that PLS regression was successful in quantifying the Robusta content in Arabica bean samples blended with different levels of Robusta coffee with an accuracy that may be commercially useful. Standard errors of cross-validation of 9.21% and 3.52% respectively were obtained on second derivative spectra of whole and ground beans (Figure 3.3); the application of FDA procedures was less successful in this case. Downey and Boussion (1996) illustrated that NIR spectroscopy (NIRSystems 6500) can facilitate discrimination between beverages produced from pure Arabica, pure Robusta and Arabica/Robusta blends with a high degree of success. Laboratory prepared coffee drinks were correctly classified at rates of 87% and 95% when using lyophilized and vacuum-dried coffee respectively.

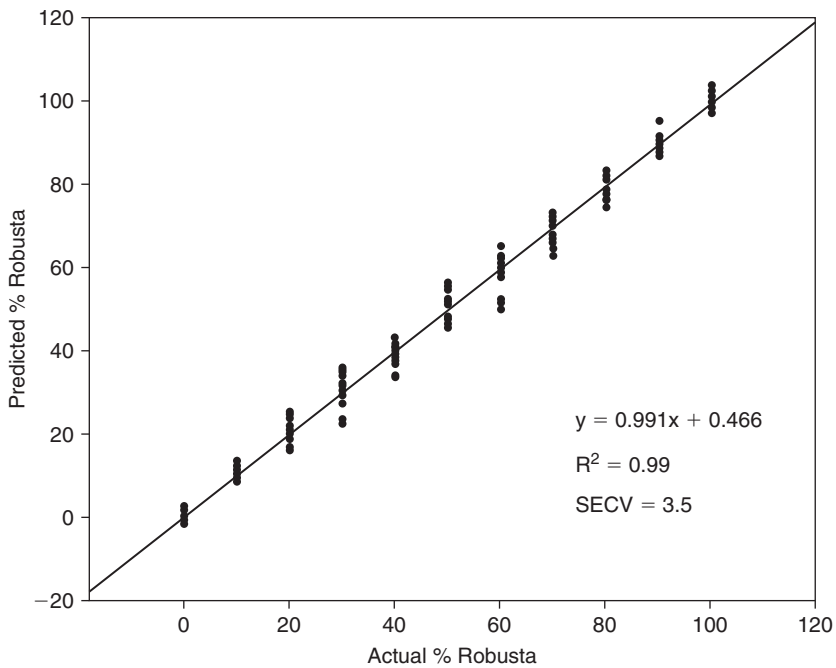

Figure 3.3 Prediction of percentage Robusta content in ground bean samples by modified partial least squares regression. Reproduced with permission from Downey and Spengler (1996); ©Irish Journal of Agricultural and Food Research 1996.

The use of combined NIR-MIR spectra for coffee varietal identification has been demonstrated (Downey *et al*., 1997). This feasibility study showed that both NIR and MIR spectroscopies have the potential to discriminate between Arabica and Robusta lyophilized coffee, while the combined spectral regions appear to offer advantages in terms of model robustness.

More recently, an improvement in NIR spectroscopy classification between Robusta and Arabica as well as between blends thereof was illustrated using a DOSC (direct orthogonal signal correction) method as a pre-processing technique (Esteban-Díez *et al*., 2007) and a potential functions method as class modeling technique (Esteban-Díez *et al*., 2004b). The spectra were recorded on an NIRSystems 5000 spectrophotometer in the wavelength range 1100–2500 nm at 2-nm intervals. Each recorded spectrum consisted of 32 co-added scans, and 5 replicates were recorded for each sample, with the samples being decompacted between each recording; an average spectrum was computed for data analysis. Five coffee categories were studied – pure Arabica, three Arabica/Robusta blends, and pure Robusta – and resulted in a 100% correct classification rate of prediction samples. Subsequently the pre-processing method OWAVEC (orthogonal wavelet correction) (Esteban-Díez *et al*., 2004a) was used by Pizarro *et al*. (2007) to improve the detection of coffee adulteration by quantifying the actual content of Robusta variety in roasted coffee samples. The regression models developed after pre-processing first derivative NIR spectra by OWAVEC were considerably better than the models obtained from raw data; results were also an improvement over other orthogonal signal correction methods tested (Table 3.4).

Fruit and fruit products

Shilton *et al*. (1998) reviewed the use of NIR spectroscopy as reported by various researchers (Scotter *et al*., 1992; Evans *et al*., 1993; Scotter and Legrand, 1994, 1995; Twomey *et al*., 1995) to demonstrate the potential of NIR spectroscopy for detecting adulteration of orange juices. Based on these studies, Shilton *et al*. (1998) argued that the use of NIR spectroscopy as a "fingerprint" technique may be more

Table 3.4 Calibration (RMSEC) and prediction (RMSEP) errors and percentages of explained variance provided by the original PLS model (constructed from mean-centered data), the PLS model developed from first derivative spectra and the PLS models built after applying OSC and DOSC methods to NIR spectra

	PLS-LVs	%RMSEC	%Expl. Var. (cal)	%RMSEP	%Expl. Var. (test)
Centering	10	2.13	99.67	2.98	99.38
First derivative	8	1.67	99.80	2.04	99.71
First derivative + OSC (2 O-LVs removed)	3	0.77	99.96	1.36	99.87
DOSC (5 O-PCs removed)	1	1.03	99.92	1.33	99.88

Reprinted with permission from Pizarro *et al*. (2007); ©Elsevier Ltd 2007.

appropriate than trying to predict specific constituent levels that may then be compared with authentic compositional databases. Subsequently, apple juice samples were also differentiated on the basis of apple variety using NIR spectroscopy combined with LDA and PLS (Reid *et al*., 2005). The results showed up to 100% correct classification of samples on the basis of apple variety.

More recently, fruit purées as well as fruit juices were effectively tested for adulteration using NIR spectroscopy (Contal *et al*., 2002; Léon *et al*., 2005). Contal *et al*. (2002) used an NIRSystems 6500 scanning monochromator equipped with a sample transport accessory and a short path-length transflectance cell (0.1-mm sample thickness) and found it to be more successful than the alternative reflectance cell (sealed with a disposable paper backing disc resulting in 0.7-mm sample thickness). Two sub-samples of each purée were scanned in duplicate, with the sample cell being rotated through approximately 120° between duplicate scans; mean spectra were used for data analysis. It was consequently possible to quantify apple adulteration in strawberry purées rapidly and non-destructively at levels down to 20% (w/w) and in raspberry purées at a level between 10 and 20% (w/w).

Honey

Honey is a high-value, completely natural product, and is defined in the Codex Alimentarius (1987) of the Food and Agriculture Organization of the United Nations as

> the natural sweet substance produced by honeybees from the nectar of plants or from secretions of living parts of plants or excretions of plant sucking insects on the living parts of plants, which the bees collect, transform by combining with specific substances of their own, deposit, dehydrate, store and leave in the honeycomb to ripen and mature.

The main components of honey are simple carbohydrates and water, leading to the possibility of honey extension by cheaper, commercially available sugar syrups. Often, preparations based on cane invert sugar, which can be tailored to mimic the natural sucrose–glucose–fructose profile of honey, are added to pure honey. This makes honey an easy target for adulteration, as the addition of these preparations is usually difficult to detect (Sivakesava and Irudayaraj, 2001). Detection of adulteration in honey is also difficult because of its large natural variability, arising from differences in species, maturity, environment, and processing and storage techniques. NIR spectroscopy has been used previously to determine the chemical composition of honey samples (Cho and Hong, 1998; Ha *et al*., 1998; Qui *et al*., 1999; García-Alvarez *et al*., 2000).

Downey *et al*. (2003) showed that DPLS can be used with a high degree of success to detect honey that has been adulterated by the addition of fructose and glucose, as 99% of the adulterated honeys in this report were correctly identified. Honey spectra were collected on a Foss NIRSystems 6500 between 400 and 2498 nm with 2-nm intervals in transflectance mode using a 0.2-mm path-length. The pure honeys were correctly identified 96% of the time. However, Downey *et al*. (2003) indicated that it might be necessary to apply temperature control during performance of the

NIR analysis. SIMCA and k-nearest neighbor models were reported not to be able to identify adulterated honey samples.

Kelly *et al*. (2006) used a similar instrument set-up, but collected spectra from 1100–2498 nm to detect adulteration of Irish artisanal honeys by adding either beet invert syrup or high-fructose corn syrup. Applying SIMCA as a classification technique, all the adulterated honeys were correctly identified as not being authentic, while 90.0% of the authentic honeys were correctly identified. When proof of authenticity is required, it is always important that no false positives occur in prediction tests (i.e. when selectivity is high) (Downey *et al*., 2006).

Meat and meat products

Regarding meat and meat products, major authenticity issues often concern the substitution or partial substitution of high-value raw materials with less costly alternatives. These can include cheaper cuts from the same or different animal species, mechanically recovered meat, offal, blood, water, eggs, gluten, or other proteins of animal or vegetable origin (Hargin, 1996; Al-Jowder *et al*., 1997, 1999, 2002; Cordella *et al*., 2002). There is also a problem with differentiating meat that has been frozen-then-thawed from fresh meat (Al-Jowder *et al*., 1997). In some countries, legislation specifically prohibits adulteration of one type of meat with that from other species, and the consumption of certain meats may be proscribed for religious reasons (Al-Jowder *et al*., 1997).

NIR spectroscopy has been reported to be useful to discriminate between kangaroo and beef meat (Ding and Xu, 1999); fresh pork, chicken and turkey (Rannou and Downey, 1997); chicken meat cuts (Ding *et al*., 1999; Fumière *et al*., 2000); lamb and beef mixtures (McElhinney *et al*., 1999); and beef, pork, and chicken (Downey *et al*., 2000); and for identification and authentication of raw meat species such as pork, chicken, lamb and beef (Cozzolino and Murray, 2004). Typical spectra of the beef, sheep, pork and chicken muscle samples in the visible and NIR regions are shown in Figure 3.4. In the latter study, based on only optical properties of the samples, an excellent differentiation of muscle species was obtained and the visible and NIR spectroscopy models correctly classified more than 85% of samples using PLS (Table 3.5). This therefore indicates that not only the pigments but also the composition of the muscle gives information which may be used for identification purposes. Intramuscular fat, fatty acids and other characteristics (such as muscle structure and type of muscle fibers) could add information to the model, and allowed discrimination between them. Cozzolino and Murray (2004) analyzed the ground meat in reflectance mode from 400–2500 nm with 2-nm intervals using an NIRSystems 6500 in a non-rotating circular cup.

Factorial discriminant analysis of combined visible-near-infrared reflectance spectra has been shown to possess the potential to discriminate between fresh and frozen-then-thawed samples of meat from one bovine species using three freeze–thaw cycles (Downey and Beauchêne, 1997a). Spectra were collected between 650 and 1100 nm on whole meat using a surface interactance fiber-optic accessory and an NIRSystems 6500. Applying FDA, a four-cluster model was found to classify all frozen samples

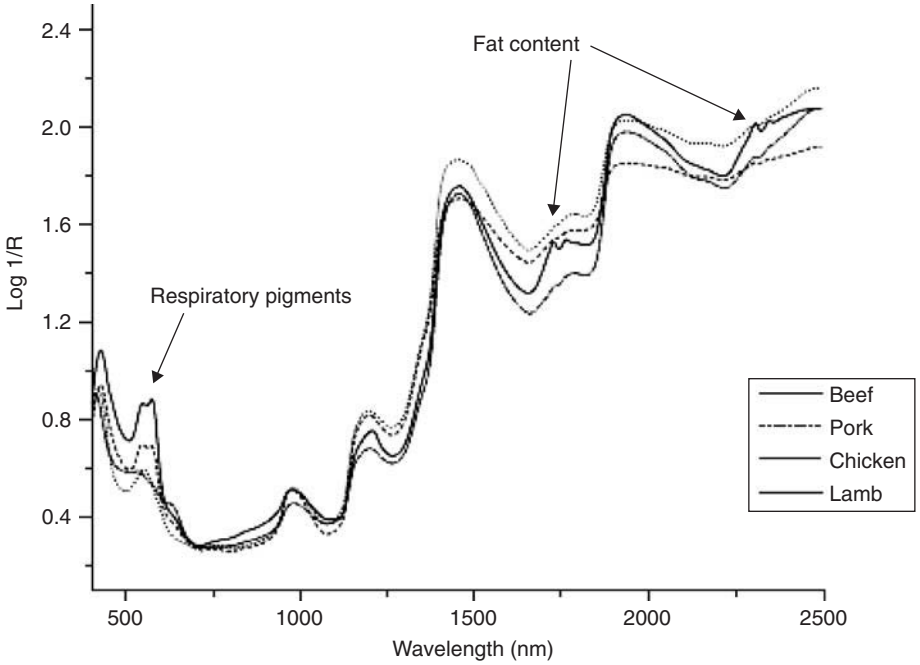

Figure 3.4 Visible and NIR mean spectra of pork, beef, lamb and chicken samples. Reproduced with permission from Cozzolino and Murray (2004); ©Elsevier Ltd 2004.

Table 3.5 Classification for meat species using PLS and PCR regression models

Spectra segment (nm)	Classification of dummy regression			
	PCR		PLS	
	CC	IC	CC	IC
400–750	90 (81%)	21 (19%)	94 (85%)	17 (15%)
1100–2500	104 (94%)	7 (6%)	104 (94%)	7 (6%)
400–2500	101 (91%)	10 (9%)	107 (96%)	4 (3%)

CC, correct classification; IC, non-classification.
Reprinted with permission from Cozzolino and Murray (2004); ©Elsevier Ltd 2004.

correctly. SIMCA did not perform as well as FDA; although it was possible to identify the fresh samples correctly, a large number of the frozen-then-thawed samples were wrongly classified as being fresh. The latter study was followed up by an alternative approach for solving this authenticity problem based on spectral measurements of dried meat drip juice (Downey and Beauchêne, 1997b). Using raw spectral data, a model with six principal components correctly classified 93.4% of the validation samples set – 3 of the 15 fresh meats were incorrectly identified but only 1 of the 46 frozen-then-thawed samples was wrongly classified as fresh. Again, SIMCA did not perform well. The fresh meat samples could be correctly identified, but there was a high degree of misclassification between the samples frozen once, twice or three times.

In an attempt to quantify the lamb content in mixtures with raw ground beef, it was reported that the accuracy of the prediction could be improved by concatenating the fingerprint region of the mid-infrared to the corresponding NIR spectra, and a SEP of 4.1% (w/w) was obtained (McElhinney *et al*., 1999).

Many of these studies are, however, preliminary or feasibility studies, often due to the difficulty of obtaining an adequate number of samples including the required level of variation. Appropriate validations should therefore be performed before commercial implementation of any such method.

Milk and dairy products

Adulteration of milk products, either by substituting a more expensive ingredient with one of lower cost or by removing a valuable component in the hope that the authorities or consumers will not detect the adulterated product, often takes place to maximize profit (Arvanitoyannis and Tzouros, 2005). Adulteration of milk and dairy products can be categorized either as not complying with legal requirements or erroneous addition of specific ingredients and material not of dairy origin, or non-compliance in terms of technological processes (Ulbert, 2003). The addition of water is one of the oldest and most obvious ways in which milk can be adulterated (Arvanitoyannis and Tzouros, 2005). Another common problem is the addition of sugar to milk.

NIR spectroscopy is widely used in the dairy industry. It was utilized for monitoring rennet coagulation in cows' milk (Laporte *et al*. 1998; O'Callaghan *et al*., 2000); reconstituted skim milk powder (Giardina *et al*., 2004); and the modifications that occurred in delactosated milk during storage (Giardina *et al*., 2003). It has also been extensively used to determine the physicochemical parameters of cheeses (Adamopoulos *et al*., 2001) and butter (Hermida *et al*., 2001). Purnomoadi *et al*. (1999) studied the effect of different feed sources on the accuracy of NIR prediction of milk fat and proteins. Filho and Volery (2005) used NIR spectroscopy to quantify solids content using a broad-based calibration that included five different fresh cheeses with low, medium and high solids contents. This was done to show that the problem of narrow concentration ranges for total solids content in fresh cheese often found in a production environment can be overcome. Blazquez *et al*. (2004) carried out a similar study for moisture, fat and inorganic salts contents in experimentally produced processed cheeses.

Cattaneo *et al*. (2005) successfully discriminated between cheeses (Italian fresh Crescenza cheese) according to their storage time using FT-NIR and PCA (refer to Chapter 4 for more detailed discussion).

The suitability of NIR spectroscopy for routine analysis of quality control to detect vegetable proteins in milk powder has been suggested by Maraboli *et al*. (2002), who developed calibrations to detect and quantify accurately the addition of non-dairy protein isolates to milk powder. After having analyzed 111 samples (11 being genuine milk powder samples and the rest prepared by mixing with soy, pea and wheat isolates) on a Bran + Luebbe InfraAnalyzer 500 from 1100–2500 nm at 4-nm intervals, the best relationship between NIR data and the quantifiable sample property was obtained by applying MLR to the first-derivative NIR absorbance values.

The five most important wavelengths included in the calibration were 1708, 2076, 2108, 2132 and 2300 nm, and it resulted in a SEP of 0.207% after analysis of 20 unknown milk powder samples.

Sato *et al*. (1990) showed that fat adulteration with as little as 3% foreign fat – for example, margarine in butter and soy milk in milk – could be detected using the limited wavelength range of 2110–2160 nm or only the two wavelengths 2124 and 2144 nm. However, if only the latter two wavelengths are to be used for screening samples for foreign fat adulteration, it will be necessary to check normal variation of the difference of the absorbance values of these two wavelengths due to feed, season and stage of lactation.

Karoui and De Baerdemaeker (2007) reviewed the use of destructive and non-destructive techniques to determine quality and/or authenticity of dairy products including NIR spectroscopy, and the principles of spectroscopic techniques coupled with chemometrics has been reviewed by Karoui *et al*. (2003).

The potential of NIR spectroscopy to predict maturity and sensory attributes of 24 Cheddar cheeses produced using 5 different renneting enzymes and stored at 4°C for up to 9 months has been investigated using a Foss NIRSystems 6500 instrument (Downey *et al*., 2005). These results still need to be validated on a larger sample set. A similar approach was followed by Blazquez *et al*. (2006), after which they recommended the use of NIR spectroscopy for routine quality assessment of processed cheese. Sensory attributes and instrumental texture measurements were predicted with sufficient accuracy to be commercially useful.

Most recently, the potential of FT-NIR spectroscopy for use in combination with chemometrics to discriminate between Emmental cheeses of various geographic origins was demonstrated (Pillonel *et al*., 2003; Karoui *et al*., 2005b; Karoui and Baerdemaeker, 2007) (refer to Chapter 4 for more detailed discussion).

Tea

Tea, made from the processed leaves of *Camellia sinensis*, is among the most popular beverages worldwide, and is of great interest due to its beneficial health properties. Green and black teas are the two most popular categories. Drying after light steaming and roasting of the leaves produces green tea, while for black tea the leaves are additionally fermented (chemically oxidized). If this fermentation is only partially carried out, Oolong tea is obtained. Due to these different processing techniques, the different tea categories will vary in their chemical structure (Chen *et al*., 2007).

One of the first discriminant studies on tea was reported by Osborne and Fearn (1988), and at the time they concluded that there is a reasonable chance of successful discrimination between black teas of differing sensory profiles on the basis of wavelengths corresponding to absorption bands in the spectra of teas. Grant *et al*. (1988) revealed that six teas differing in origins and taste could be reliably distinguished from one another using canonical variate analysis (CVA). During this investigation, Osborne and Fearn (1988) illustrated the effect of the grinding method used to prepare the samples to be much larger than the effects of sample temperature or rotation of the sample during analysis.

Using FT-NIR spectroscopy and SIMCA it was possible to identify four different tea varieties (Chen *et al*., 2006), and the potential of FT-NIR spectroscopy combined with SVM (support vector machine) methods to identify each of three tea categories (green tea, black tea and Oolong tea) was demonstrated (Zhao *et al*., 2006; Chen *et al*., 2007). These studies are discussed in more detail in Chapter 4.

Vegetable oils

In 1956, NIR chemical assignments for several chemical groups characteristic of lipids were determined by investigating the spectra of synthetic fatty acids (Holman and Edmondson, 1956). The earliest application of NIR analysis of fats and oils was published in 1991 (Sato *et al*., 1991). The fatty acid composition of fats extracted from commercially available butter and pig milk, using the Röse-Gottlieb method (IDF, 1983), as well as that of soybean oil and palm oil was determined by gas chromatography after methyl or isopropyl-esterification. NIR transflectance spectra were measured between 1600 and 2300 nm on a Bran and Luebbe InfraAnalyzer 500 and the data used to examine the fatty acid composition from a qualitative point of view. Sato *et al*. (1991) suggested that NIR spectroscopy could be used to set up a library of spectra of various fats and oils, with this then being used to detect a spectral match for an unknown sample. Other qualitative near-infrared studies applied discriminant (Bewig *et al*., 1994) and principal component (Sato, 1994) analysis to distinguish between different vegetable oils. Sato (1994) successfully classified nine varieties of vegetable oils from their PCA scores using the InfraAnalyzer 500 as before. Also using a Bran and Luebbe InfraAnalyzer 500 to collect the spectra, Bewig *et al*. (1994) derived a four-wavelength equation to separate cottonseed, peanut, soybean and canola oils successfully. The soybean oil group was, however, more dispersed than the other three groups.

Hourant *et al*. (2000), using a Foss NIRSystems 6500 instrument, have shown the potential of NIR spectroscopy for the discrimination of fats and oil. They studied 104 edible oil and fat samples from 18 different sources, either vegetable (brazil nut, coconut, corn, sunflower, walnut, virgin olive, peanut, palm, canola, soybean, sunflower) or animal (tallow and hydrogenated fish). The samples were analyzed by high-performance gas chromatography (HPGC) and NIR spectroscopy. In this work, the NIR spectral features of the most noteworthy bands were studied and discussed to design a filter-type NIR instrument. An arborescent structure, based on stepwise linear discriminant analysis (SLDA), was built to classify the samples according to their sources. Seven discriminant functions permitted a successive discrimination of saturated fats, corn, soybean, sunflower, canola, peanut, high oleic sunflower and virgin olive oils. The discriminant functions were based on the absorbance values, between three and five, from the 1700–1800 and 2100–2400 nm wavelength regions. Chemical explanations were given in support of the selected wavelengths and the arborescent structure was then validated with a test set, and 90% of the samples were correctly classified.

The increasing consumer interest in olive oil due to its nutritional and sensory properties and the economic value of olive oil compared to other vegetable oils makes this product prone to adulteration by cheaper oils. Consequently, the adulteration

of olive oil is a serious problem in the modern olive-oil industry, and is not only a crisis in major olive-producing countries but is also affecting small olive-oil suppliers and consumers in countries such as South Africa (McKenzie and Koch, 2004). Since the South African market is flooded with olive-oil imports from the Mediterranean, it has experienced local incidents of fraud (Cilliers, 2001).

Olive oil adulteration can be divided into two types; first, the blending of virgin olive oils with inferior quality olive oils such as refined olive oil or pomace oil, and secondly, the addition of other vegetable oils to olive oil (Dourtoglou *et al*., 2003). The former mainly occurs in major olive-oil producing countries such as Greece, Italy and Spain, while the addition of other vegetable oils (e.g. sunflower, canola and rapeseed) is mostly a problem in countries importing olive oil (e.g. USA and Canada) and where seed oils are locally produced and are less expensive (Li-Chan, 1994). The fatty acid composition of olive oil is the most important indicator of adulteration by other oils, and is mostly determined by gas chromatography. Since the International Olive Oil Commission (IOOC) and other official bodies have established specific limits for the percentage of distinct fatty acids in genuine olive oil, this method can be applied to distinguish pure from adulterated oils (Christopoulou *et al*., 2004). The maximum limits of fatty acids in olive oils and olive pomace oils are as follows: oleic 55.0–83.0%, stearic 0.5–5.0%, palmitic 7.5–20.0%, palmitoleic 0.3–3.5%, linoleic 3.5–21.0%, myristic $\leqslant$0.05%, linolenic $\leqslant$1.0%, arachidic $\leqslant$0.6%, eicosenoic $\leqslant$0.4%, behenic $\leqslant$0.2% and lignoceric $\leqslant$0.2% (IOC, 2006). Any fatty acid present in amounts exceeding the abovementioned limits will be indicative of adulteration with seed oil. However, assessment of the fatty acid composition is not in all cases successful in detecting fraud (Christopoulou *et al.,* 2004).

Although several studies evaluated NIR spectroscopy as an alternative quality control tool for other vegetable oils, the application of NIR spectroscopy to olive-oil quality control is a relatively new development. Principal component analysis was used to detect and quantify adulterants in virgin olive oil (Wesley *et al*., 1995). Using principal components, it was possible to predict the type of adulterant with 75% accuracy. Wesley *et al*. (1996) improved on this prediction by developing a discriminant analysis equation that could identify correctly the type of adulterant in extra-virgin oil in 90% of cases. It was also possible to measure the level of adulteration to an accuracy of $\pm$0.9% (w/w).

Downey *et al*. (2002) demonstrated the potential of NIR spectroscopy and SIMCA to discriminate between authentic extra-virgin olive oils and the same oils adulterated by the addition of a single sunflower-oil sample at levels as low as 1% (w/w). They also quantified the level of sunflower-oil adulterant present using PLS with a SECV equal to 0.8% (w/w), which is suitable for industrial use. The adulteration of olive oils with a variety of common adulterants was detected using FT-NIR spectroscopy analysis with very low error limits (Christy *et al*., 2004; Kasemsumran *et al*., 2005) (refer to Chapter 4 for more detailed discussion).

Wine and distilled alcoholic beverages

An alcoholic beverage is a complex mixture of components presenting volatile compounds, responsible for aroma and flavor, and fixed compounds consisting of a large

variety of substances with different characteristics (Arvanitoyannis *et al*., 1999). The authenticity of wine is strictly controlled by the respective national authorities (Arvanitoyannis *et al*., 1999) by methods including official sensory evaluation, chemical analysis and examination of the records kept by the wine producer. Various analytical techniques are being used to determine a wine's authenticity, as reviewed by Arvanitoyannis *et al*. (1999). These techniques are often coupled with appropriate chemometric techniques such as PCA, LDA CVA and cluster linear analysis (CLA) (Arvanitoyannis *et al*., 1999).

As is the case for other food products, the ideal is to detect adulteration or verify authenticity of an alcoholic beverage on the sample as is. In the wine industry, NIR spectroscopy has found considerable use in various applications concerning wine analysis (Kaffka and Norris, 1976; Baumgarten, 1987; Sneyd *et al*., 1989; Van de Voort, 1992; Van den Berg *et al*., 1997). Near-infrared reflectance spectroscopy proved to be very successful in the simultaneous determination of ethanol, fructose and residual sugars in botrytized-grape sweet wines (Garcia-Jares and Médina, 1997). In 1994, Burns proposed the employment of NIR spectroscopy as a future analytical technique for determinations of total phenolics in wines (Burns, 1994). Subsequently, Cozzolino *et al*. (2004) illustrated the simultaneous prediction of various phenolic compounds in fermenting must and red wine.

One of the main risks for the consumer of distilled alcoholic beverages of unknown origin is that the drinks may contain high levels of methanol, which is present in alcoholic beverages in small amounts (Pontes *et al*., 2006). The compositional quality of grape, wine and spirits determined by means of scanning NIR spectroscopy was investigated by The Australian Wine Research Institute (Gishen and Dambergs, 1998; Cope, 2000). This preliminary evaluation of the applicability of NIR spectroscopy to determine compositional quality showed considerable promise, with potential for immediate application in the wine industry.

Near-infrared spectroscopy combined with multivariate analysis (PCA, DPLS and LDA) showed promise as a rapid method to monitor the progress of red wine fermentation (Cozzolino *et al*., 2006). In this study, visible and NIR spectroscopy were used as a qualitative technique – that is, no quantification of any compositional variable was made. Cozzolino *et al*. (2006) illustrated that it was possible to detect changes that occur during fermentation and to classify the progression stage of fermentation independent of variables such as grape variety, yeast strain and temperature.

Dambergs *et al*. (2001) and Cozzolino *et al*. (2005) explored the potential of NIR spectroscopy as a tool to predict wine sensory quality. Fourier transform near-infrared spectroscopy was used to measure the percentage of sugar in grape must, and to discriminate between different must samples in terms of their free amino nitrogen (FAN) values (Manley *et al*., 2001b). It was also shown by Manley *et al*. (2001b) that FT-NIR could discriminate between Chardonnay wine samples in terms of their malolactic fermentation status using SIMCA; table wines were successfully discriminated on the basis of their ethyl carbamate content (refer to Chapter 4 for more detailed discussion).

Confirmation of wine authenticity, mainly in terms of vintage, wine age, variety and geographical origin, has received increasing attention in the recent past. Chemometric

models based on visible and NIR spectroscopy data were used to determine the origin of two different varieties of Australian white wine samples – Riesling and Chardonnay (Cozzolino *et al*., 2003). Figure 3.5 shows the visible and NIR spectra of the white wine samples analyzed. No obvious differences were detected from a visual observation of the spectra between the two white wine varieties in either the visible or NIR region (Cozzolino *et al*., 2003). Both varieties have absorption bands at 1450 nm related to the O–H second overtone of water and ethanol, at 1690 nm related to either $C–H_3$ stretch first overtone or compounds containing C–H aromatic groups, at 1790 nm related to C–H stretch first overtone, and at 1950 nm related to O–H stretch first overtone of water and ethanol. The models were constructed using PCA, PCR and DPLS on spectra collected from 400–2500 nm using a Foss NIRSystems 6500 and a 1-mm path-length cuvette. Figure 3.6 shows the PCA scores (PC1 vs PC2) derived from the second-derivative spectral data of the samples. Although there was separation of the samples by variety, some samples did overlap. The DPLS models were able accurately to classify 100% of the Riesling and 96% of the Chardonnay wines (Figure 3.7).

Manley *et al*. (2003) illustrated the potential of FT-NIR to categorize four different classes of rebate brandy, and Pontes *et al*. (2006) proposed a strategy in which FT-NIR spectroscopy and chemometric methods (PCA and SIMCA) can be used in the classification and verification of adulteration in whiskeys, brandies, rums and vodkas (refer to Chapter 4 for more detailed discussion).

Yu *et al*. (2006, 2007a) used FT-NIR to discriminate Chinese rice wine of different geographical origins and to classify Chinese rice wine with different marked age.

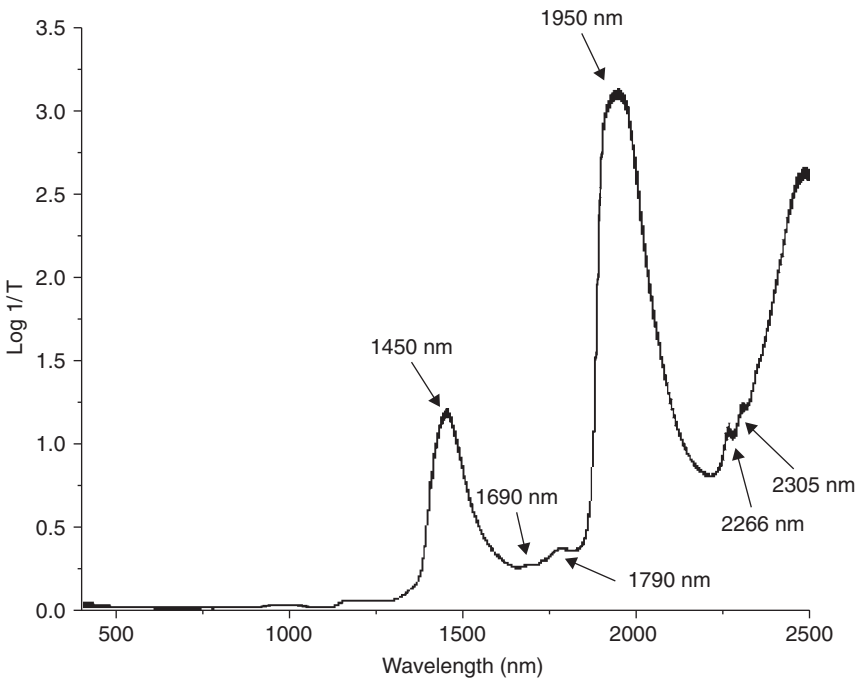

Figure 3.5 Visible and NIR spectra of white wine samples analyzed. Reproduced with permission from Cozzolino *et al*. (2003); ©American Chemical Society 2003.

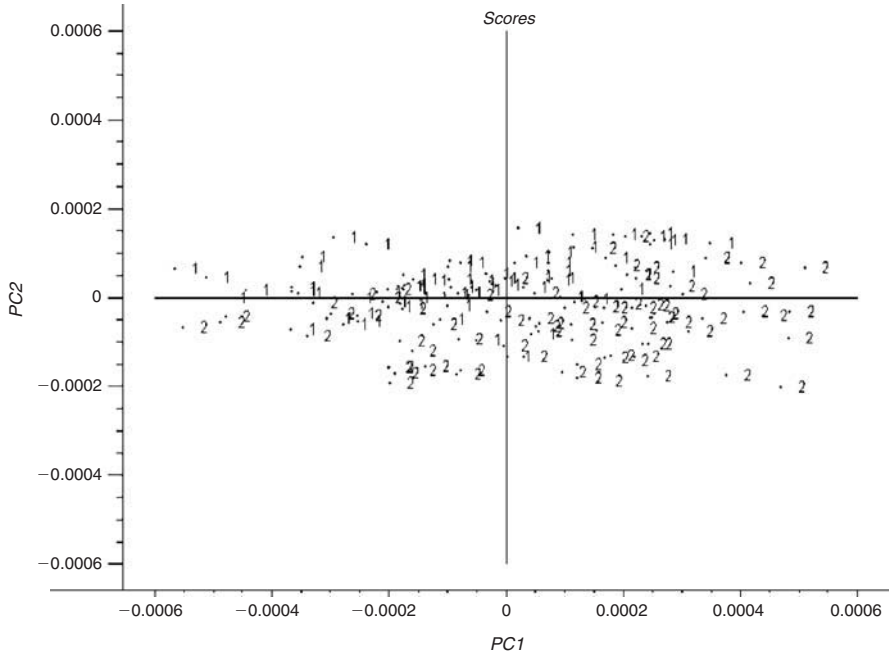

Figure 3.6 Sample score plot for PC1 and PC2 (second derivative, 400–2500 nm) for the white wines (1 = Riesling; 2 = Chardonnay). Reproduced with permission from Cozzolino *et al*. (2003); ©American Chemical Society 2003.

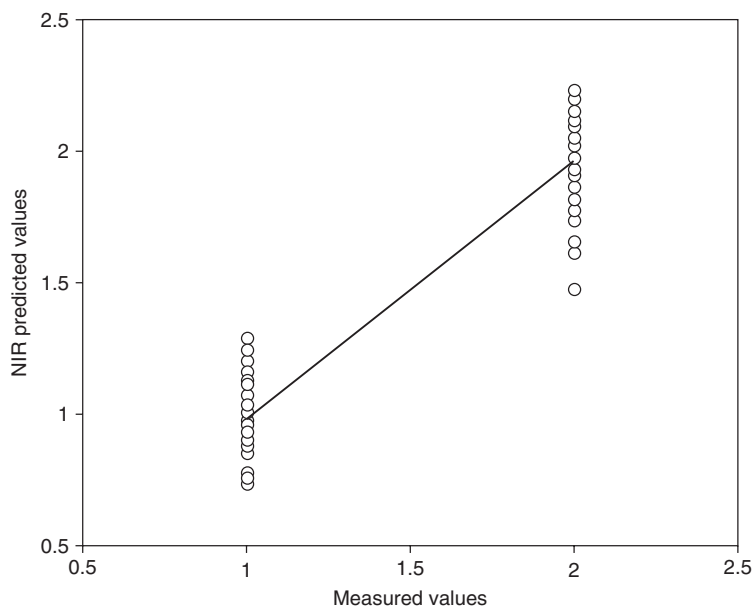

Figure 3.7 Prediction of commercial white wine varieties using DPLS regression (400–1100 nm) and second derivative (validation set). Reproduced with permission from Cozzolino *et al*. (2003); ©American Chemical Society 2003.

Yu *et al*. (2007b) evaluated the potential of visible and FT-NIR to predict the vintage year (five vintages) of Chinese rice wine in 600-ml square brown glass bottles (refer to Chapter 4 for more detailed discussion). The possibility of using NIR spectroscopy to discriminate between wine vinegar and alcohol vinegar was also illustrated using SIMCA after OSC was applied to the NIR spectral data (Saiz-Abajo *et al*., 2004). Near-infrared spectra were collected from 1100–2500 nm using a Foss NIRSystems 5000 spectrometer equipped with a liquid flow cell. Each spectrum was based on 32 co-added scans at 2-nm intervals. Three replicates of each sample were taken, and the mean value was subsequently calculated. Clear separation between the classes was observed when tartaric acid was used as a discriminating descriptor.

Conclusions

Near-infrared spectroscopy, with its unsurpassed combination of speed, accuracy and simplicity, has found its own niche in the quality control laboratories of food and beverage manufacturers worldwide. Advances in technologies such as optics, electronics, computer hardware and software, and especially chemometrics, have allowed for more powerful NIR spectroscopy instrumentation to be developed and manufactured and consequently more powerful spectral analyses. Similar to other analytical methods, it has limitations, but the capabilities of NIR spectroscopy instrumentation are continually improving to maximize the performance of this very exciting technology. There is therefore no doubt that NIR spectroscopy does have the capability and potential to solve many food authentication and adulteration problems.

Many of the reported studies investigating the use of NIR spectroscopy to confirm authentication or detect and/or quantify adulteration of food, food products and beverages until now have, however, been only preliminary or only feasibility studies, performed on a limited number of samples. This is mainly due to the cost and complexity of obtaining an adequate number of samples with sufficient variation within the sample collection. Appropriate validation should therefore always be performed before commercial implementation of any such method is considered.

An exiting new technique which will play an important role in food authentication problems in the future is *NIR chemical imaging*. This non-destructive technique combines conventional NIR spectroscopy with digital imaging. As a NIR spectrum is collected for each pixel in the image, a three-dimensional cube consisting of both spatially resolved spectra and wavelength-dependent images is created. The ability not only to quantify a chemical component but also to identify as well as locate these components within a specific sample is invaluable to understand a sample, and will surely play a huge role in future in investigating issues of adulteration.

References

Adamopoulos, K.G., Goula, A.M. and Petropakis, H.J. (2001). Quality control during processing of Feta cheese-NIR application. *Journal of Food Composition and Analysis*, **14**, 431–440.

Al-Jowder, O., Kemsley, E.K. and Wilson, R.H. (1997). Mid-infrared spectroscopy and authenticity problems in selected meats: a feasibility study. *Food Chemistry*, **59**(2), 195–201.

Al-Jowder, O., Defernez, M., Kemsley, E.K. and Wilson, R.H. (1999). Mid-infrared spectroscopy and chemometrics for the authentication of meat products. *Journal of Agricultural and Food Chemistry*, **47**, 3210–3218.

Al-Jowder, O., Kemsley, E.K. and Wilson, R.H. (2002). Detection of adulteration in cooked meat products by mid-infrared spectroscopy. *Journal of Agricultural and Food Chemistry*, **50**, 1325–1329.

Anonymous (1967). Legge 580, 4 luglio. Disciplina per la lavorazione e il commercio dei cerali, degli sfarinati, del pane e delle paste alimentary (as cited by Cocchi *et al.*, 2006).

Anonymous (2001). Decreto del President della Repubblica No 187, 9 febbraio. Regolamento per la revisione della normativa sulla produzione e commercializzazione di sfarinati e paste alimentari, a norma dell'art. 50 della L.146/94 (as cited by Cocchi *et al.*, 2006).

Arvanitoyannis, I.S. and Tzouros, N.E. (2005). Implementation of quality control methods in conjunction with chemometrics toward authentication of dairy products. *Critical Reviews in Food Science and Nutrition*, **45**, 231–249.

Arvanitoyannis, I.S., Katsota, M.N., Psarra, E.P. *et al*. (1999). Application of quality control methods for assessing wine authenticity: use of multivariate analysis (chemometrics). *Trends in Food Science and Technology*, **10**, 321–336.

Baeten, V. and Dardenne, P. (2005). Applications of near-infrared imaging for monitoring agricultural food and feed products. In: R. Bhargava and I.W. Levin (eds), *Spectrochemical Analysis Using Infrared Multichannel Detectors*. Oxford: Blackwell Publishing, pp. 283–301.

Bao, J.S., Cai, Y.Z. and Corke, H. (2001). Prediction of rice starch quality parameters by near-infrared reflectance spectroscopy. *Journal of Food Science*, **66**(7), 936–939.

Barnes, R.J., Dhanoa, M.S. and Lister, S.J. (1989). Standard normal variate transformation and de-trending of near-infrared diffuse reflectance spectra. *Applied Spectroscopy*, **43**(5), 772–777.

Barton, F.E. (2002). Theory and principles of near-infrared spectroscopy. *Spectroscopy Europe*, **14**(1), 12–18.

Baumgarten, G. (1987). The determination of alcohol in wines by means of near-infrared technology. *South African Journal of Enology and Viticulture*, **8**(2), 75–77.

Beebe, K.R., Pell, R.J. and Seasholtz, M.B. (1998). *Chemometrics: A Practical Guide*. New York, NY: John Wiley & Sons, Inc., p. 348.

Ben-Gera, I. and Norris, K.H. (1968a). Determination of moisture content in soybeans by direct spectrophotometry. *Israel Journal of Agricultural Research*, **18**, 125–132.

Ben-Gera, I. and Norris, K.H. (1968b). Direct spectrophotometric determination of fat and moisture in meat products. *Journal of Food Science*, **33**, 64–67.

Bertrand, D., Robert, P. and Loisel, W. (1985). Identification of some wheat varieties by near-infrared reflectance spectroscopy. *Journal of the Science of Food and Agriculture*, **36**, 1120–1124.

Bewig, K.M., Clarke, A.D., Roberts, C. and Unklesbay, N. (1994). Discriminant analysis of vegetable oils by near-infrared reflectance spectroscopy. *Journal of the American Oil Chemists' Society*, **71**(2), 195–200.

Blanco, M. and Villarroya, I. (2002). NIR spectroscopy: a rapid-response analytical tool. *Trends in Analytical Chemistry*, **21**(4), 240–250.

Blanco, M., Coello, J., Iturriaga, H. *et al*. (1998). Near-infrared spectroscopy in the pharmaceutical industry. *Analyst*, **124**, 135–150.

Blazquez, C., Downey, G., O'Donnell, C. *et al*. (2004). Prediction of moisture, fat and inorganic salts in processed cheese by near-infrared reflectance spectroscopy and multivariate data analysis. *Journal of Near-infrared Spectroscopy*, **12**, 149–157.

Blazquez, C., Downey, G., O'Callaghan, D. *et al*. (2006). Modelling of sensory and instrumental texture parameters in processed cheese by near-infrared reflectance spectroscopy. *Journal of Dairy Research*, **73**, 58–69.

Bosset, J.O., Berger, T., Bühler-Moor, U. *et al*. (1997). Comparison of some highland and lowland Gruyère type cheese of Switzerland: a study of their potential PDO/AOC/AOP characteristics. Authenticity and adulteration of food – the analytical approach. *Proceedings of European Food Chemistry*, **220**, 395–400.

Budínová, G., Vlácil, D., Mestek, O. and Volka, K. (1998). Application of infrared spectroscopy to the assessment of authenticity of tea. *Talanta*, **47**, 255–260.

Burns, G.H. (1994). Introduction: overview of wine analysis. In: B.W. Zoecklein, K.C. Fugelsang, B.H. Gump and F.S. Nury (eds), *Wine Analysis and Production*. New York, NY: Chapman & Hall, p. 5.

Butler, L.A. (1983). The history and background. *Cereal Foods World*, **28**, 238–240.

Cattaneo, T.M.P., Giardina, C., Sinelli, N. *et al*. (2005). Application of FT-NIR and FT-IR spectroscopy to study the shelf-life of Crescenza cheese. *International Dairy Journal*, **15**, 693–700.

Centner, V., Verdu-Andres, J., Walczak, B. *et al*. (2000). Comparison of multivariate calibration techniques applied to experimental NIR data sets. *Applied Spectroscopy*, **54**, 608–623.

Chauchard, F., Cogdill, R., Roussel, S. *et al*. (2004). Application of LS-SVM to non-linear phenomena in NIR spectroscopy: development of a robust and portable sensor for acidity prediction in grapes. *Chemometrics and Intelligent Laboratory Systems*, **71**, 141–150.

Chen, Q., Zhao, J., Zhang, G. and Wang, X. (2006). Feasibility study on qualitative and quantitative analysis in tea by near-infrared spectroscopy with multivariate calibration. *Analytica Chimica Acta*, **572**, 77–84.

Chen, Q., Zhao, J., Fang, C.H. and Wang, D. (2007). Feasibility study on identification of green, black and oolong teas using near-infrared spectroscopy based on support vector machine (SVM). *Spectrochimica Acta Part A*, **66**, 568–574.

Cho, H.J. and Hong, S.H. (1998). Acacia honey quality measurement by near-infrared spectroscopy. *Journal of Near-infrared Spectroscopy*, **6**, A329–A331.

Christopoulou, E., Lazaraki, M., Komaitis, M. and Kaselimis, K. (2004). Effectiveness of determinations of fatty acids and triglycerides for the detection of adulteration of olive oils with vegetable oils. *Food Chemistry*, **84**, 463–474.

Christy, A.A., Kasemsumran, S., Du, Y. and Ozaki, Y. (2004). The detection and quantification of adulteration in olive oil by near-infrared spectroscopy and chemometrics. *Analytical Sciences*, **20**, 935–940.

Cilliers, J. (2001). Nuus: bedrog met tafelolie oopgevlek (vervalste olyfolie). *Landbou Weekblad*, 19 Oktober.

Ciurczak, E.W. (1992). Principles of near-infrared spectroscopy. In: D.A. Burns and E.M. Ciurczak (eds), *Handbook of Near-Infrared Analysis*. New York, NY: Marcel Dekker, Inc., pp. 7–11.

Ciurczak, E.W. (2005). Revisiting the polarization interferometer. *Spectroscopy*, **20**(2), 68–73.

Cleve, E., Bach, E. and Schollmeyer, E. (2000). Using chemometric methods and NIR spectrophotometry in the textile industry. *Analytica Chimica Acta*, **420**, 163–167.

Cocchi, M., Seeber, R. and Ulrici, A. (2003). Multivariate calibration of analytical signals by WILMA (wavelet interface to linear modelling analysis). *Journal of Chemometrics*, **17**, 512–527.

Cocchi, M., Corbellini, M., Foca, G. *et al*. (2005). Classification of bread wheat flours in different quality categories by a wavelet-based feature selection/classification algorithm on NIR spectra. *Analytica Chimica Acta*, **544**, 100–107.

Cocchi, M., Durante, C., Foca, G. *et al*. (2006). Durum wheat adulteration detection by NIR spectroscopy mutivariate calibration. *Talanta*, **68**, 1505–1511.

Codex Alimentarius Commissions Standards (1987). *Codex Standards for Sugars: Standard* 12-1981, Review 1.

Contal, L., León, V. and Downey, G. (2002). Detection and quantification of apple adulteration in strawberry and raspberry pureés using visible and near-infrared spectroscopy. *Journal of Near-infrared Spectroscopy*, **10**, 289–299.

Cope, A. (2000). Industry moves closer to rapid color testing. *The Australian and New Zealand Wine Industry Journal*, **15**, 78–79.

Cordella, C., Moussa, I., Martel, A. *et al*. (2002). Recent developments in food characterization and adulteration detection: technique-oriented perspectives. *Journal of Agricultural and Food Chemistry*, **50**, 1751–1764.

Coventry, G. (1988). The development and application of NIR with particular reference to the food industry. *Food Science and Technology Today*, **2**, 130–139.

Cowe, I.A. and McNicol, J.W. (1985). The use of principal components in the analysis of near-infrared spectra. *Applied Spectroscopy*, **39**, 169–257.

Cowe, I.A., McNicol, J.W. and Cuthbertson, D.C. (1990). Principal component analysis: a chemometric approach to the analysis of near-infrared spectra. *Analytical Proceedings*, **27**, 61–63.

Cozzolino, D. and Murray, I. (2004). Identification of animal meat muscles by visible and near-infrared reflectance spectroscopy. *Lebensmittel-Wissenschaft und -Technologie*, **37**, 447–452.

Cozzolino, D., Fassio, A. and Gimenez, A. (2000). The use of near-infrared reflectance spectroscopy (NIRS) to predict the composition of whole maize plants. *Journal of the Science of Food and Agriculture*, **81**, 142–146.

Cozzolino, D., Smyth, H.E. and Gishen, M. (2003). Feasibility study on the use of visible and near-infrared spectroscopy together with chemometrics to discriminate between

commercial white wines of different varietal origins. *Journal of Agricultural and Food Chemistry*, **51**, 7703–7708.

Cozzolino, D., Kwiatkowski, M.J., Parker, M. *et al*. (2004). Prediction of phenolic compounds in red wine fermentations by visible and near-infrared spectroscopy. *Analytica Chimica Acta*, **513**, 73–80.

Cozzolino, D., Smyth, H.E., Lattey, K.A. *et al*. (2005). Relationship between sensory analysis and near-infrared spectroscopy in Australian Riesling and Chardonnay wines. *Analytica Chimica Acta*, **539**, 341–348.

Cozzolino, D., Parker, M., Damsberg, R.G. *et al*. (2006). Chemometrics and visible-near-infrared spectroscopic monitoring of red wine fermentation in a pilot scale. *Biotechnology and Bioengineering*, **95**(6), 1101–1107.

Crocombe, R.A. (2004). MEMS technology moves process spectroscopy into a new dimension. *Spectroscopy Europe*, **16**(3), 16–19.

Dambergs, R.G., Kambouris, A., Schumacher, N. *et al*. (2001). *Wine Quality Grading by Near-infrared Spectroscopy*. Glen Osmond: The Australian Wine Research Institute. Technical Publication.

Davies, A.M.C. (1991). The history of near-infrared spectroscopy. 1. The first NIR spectrum. *NIR News*, **2**, 12.

Davies, A.M.C. and McClure, F. (1985). Near-infrared analysis in the Fourier domain with special reference to process control. *Analytical Proceedings*, **22**, 321–322.

Davies, T. (1998). The history of near-infrared spectroscopic analysis: past, present and future – "From sleeping technique to the morning star of spectroscopy". *Analusis Magazine*, **26**, 17–19.

Day, M.S. and Fearn, F.R.B. (1982). Near-infra-red reflectance as an analytical technique, Part 1. History and development. *Laboratory Practice*, **31**, 328–330.

Devaux, M.F., Bertrand, D. and Martin, G. (1986). Discrimination of bread-baking quality of wheats according to their variety by near-infrared reflectance spectroscopy. *Cereal Chemistry*, **63**(2), 151–154.

Devaux, M.F., Bertrand, D., Robert, P. and Morat, J.L. (1987). Extraction of near-infrared spectral information by fast Fourier transform and principal component analysis. Application to the discrimination of baking quality of wheat flours. *Journal of Chemometrics*, **1**, 103–110.

Devaux, M.F., Bertrand, D., Robert, P. and Qannari, M. (1988). Application of multidimensional analysis to the extraction of discriminant spectral patterns from NIR spectra. *Applied Spectroscopy*, **42**, 1015–1019.

Ding, H.B. and Xu, R.-J. (1999). Differentiation of beef and kangaroo meat by visible/near-infrared reflectance spectroscopy. *Journal of Food Science*, **64**(5), 814–817.

Ding, H.B., Xu, R.-J. and Chan, D.K.O. (1999). Identification of broiler chicken meat using a visible/near-infrared spectroscopic technique. *Journal of the Science of Food and Agriculture*, **79**, 1382–1388.

Dourtoglou, V.G., Dourtoglou, T., Antonopoulos, A. *et al*. (2003). Detection of olive oil adulteration using principal component analysis applied on total and regio FA content. *Journal of the American Oil Chemists' Society*, **80**, 203–208.

Downey, G. (1995). Food quality and authenticity measurement. *Farm and Food*, **July/September**, 21–24.

Downey, G. (1996a). Authentication of food and food ingredients by near-infrared spectroscopy. *Journal of Near-infrared Spectroscopy*, **4**, 47–61.

Downey, G. (1996b). Non-invasive and non-destructive percutaneous analysis of farmed salmon flesh by near-infra-red spectroscopy. *Food Chemistry*, **55**(3), 305–311.

Downey, G. (1998a). Direct measurement of food quality and authenticity. *Analysis and Control*, **1**, 27–30.

Downey, G. (1998b). Food and food ingredient authentication by mid-infrared spectroscopy and chemometrics. *Trends in Analytical Chemistry*, **17**(7), 418–424.

Downey, G. and Beauchêne, D. (1997a). Discrimination between fresh and frozen-then-thawed beef *M. longissimus dorsi* by combined visible-near-infrared reflectance spectroscopy: a feasibility study. *Meat Science*, **45**, 353–363.

Downey, G. and Beauchêne, D. (1997b). Authentication of fresh vs. frozen-then-thawed beef by near-infrared reflectance spectroscopy of dried drip juice. *Lebensmittel-Wissenschaft und -Technologie*, **30**, 721–726.

Downey, G. and Boussion, J. (1996). Authentication of coffee bean variety by near-infrared reflectance spectroscopy of dried extract. *Journal of the Science of Food and Agriculture*, **71**, 41–49.

Downey, G. and Flynn, S.J. (2002). Discrimination between virgin olive oils from Crete, the Peloponese and other Greek Islands using near-infrared transflectance spectroscopy. In: A.M.C. Davies and R.K. Cho (eds), *Near-infrared Spectroscopy: Proceedings of the 10th International Conference*. Chichester: NIR Publications, pp. 239–241.

Downey, G. and Spengler, B. (1996). Compositional analysis of coffee blends by near-infrared spectroscopy. *Irish Journal of Agricultural and Food Research*, **35**, 179–188.

Downey, G., Bertrand, R. and Kelly, P.M. (1990). Classification of commercial skim milk powders according to heat treatment using factorial discriminant analysis of near-infrared reflectance spectroscopy. *Applied Spectroscopy*, **44**(1), 150–154.

Downey, G., Byrne, S. and Dwyer, E. (1986). Wheat trading in the Republic of Ireland: the utility of a hardness index derived by near-infrared reflectance spectroscopy. *Journal of the Science of Food and Agriculture*, **37**, 762–766.

Downey, G., Boussion, J. and Beauchêne, D. (1994). Authentication of whole and ground coffee beans by near-infrared reflectance spectroscopy. *Journal of Near-infrared Spectroscopy*, **2**, 85–92.

Downey, G., Briandet, R., Wilson, R.H. and Kemsley, E.K. (1997). Near- and mid-infrared spectroscopies in food authentication: coffee varietal identification. *Journal of Agricultural and Food Chemistry*, **45**, 4357–4361.

Downey, G., McElhinney, J. and Fearn, T. (2000). Species identification in selected raw homogenized meats by reflectance spectroscopy in the mid-infrared, near-infrared, and visible ranges. *Applied Spectroscopy*, **54**(6), 894–899.

Downey, G., McIntyre, P. and Davies, A.N. (2002). Detection and quantifying sunflower oil adulteration in extra virgin olive oils from the eastern Mediterranean by visible and near-infrared spectroscopy. *Journal of Agricultural and Food Chemistry*, **50**, 5520–5525.

Downey, G., Fouratier, V. and Kelly, J.D. (2003). Detection of honey adulteration by addition of fructose and glucose using near-infrared transflectance spectroscopy. *Journal of Near-infrared Spectroscopy*, **11**, 447–456.

Downey, G., Howard, V., Delahunty, C. *et al*. (2005). Prediction of maturity and sensory attributes of Cheddar cheese using near-infrared spectroscopy. *International Dairy Journal*, **15**(6/9), 701–709.

Downey, G., Kelly, J.D. and Petisco, C. (2006). Food authenticity – has near-infrared spectroscopy a role? *Spectroscopy Europe*, **18**(3), 10, 12–14.

Ellis, J.W. and Bath, J. (1938). Alterations in the infrared absorption spectrum of water in gelatin. *Journal of Chemical Physics*, **6**, 723–729.

Esbensen, K.H. (2000). *Multivariate Data Analysis in Practice: An Introduction to Multivariate Data Analysis and Experimental Design*, 4th edn. Oslo: Camo ASA, pp. 1–352.

Esler, M.B., Gishen, M., Francis, I.L. *et al*. (2002). Effects of variety and region on near-infrared reflectance spectroscopic analysis of quality parameters in red wine grapes. In: A.M.C. Davies and R.K. Cho (eds), *Near-infrared Spectroscopy: Proceedings of the 10th International Conference*. Chichester: NIR Publications, pp. 249–253.

Esteban-Díez, I., Gonzáles-Sáiz, J.M. and Pizarro, C. (2004a). OWAVEC: a combination of wavelet analysis and an orthogonalization algorithm as a pre-processing step in multivariate calibration. *Analytica Chimica Acta*, **515**, 31–41.

Esteban-Díez, I., Gonzáles-Sáiz, J.M. and Pizarro, C. (2004b). An evaluation of orthogonal signal correction methods for the characterisation of Arabica and Robusta coffee varieties by NIRS. *Analytica Chimica Acta*, **514**, 57–67.

Esteban-Díez, I., Gonzáles-Sáiz, J.M. and Pizarro, C. (2005). Generalization of OWAVEC method for simultaneous noise suppression, data compression and orthogonal signal correction. *Analytica Chimica Acta*, **544**, 89–99.

Esteban-Díez, I., Gonzáles-Sáiz, J.M., Sáenz-González, C. and Pizarro, C. (2007). Coffee varietal differentiation based on near-infrared spectroscopy. *Talanta*, **71**, 221–229.

Evans, D.G., Scotter, C.N.G., Day, L.Z. and Hall, M.N. (1993). Determination of the authenticity of orange juice by discriminant analysis of near-infrared spectra. *Journal of Near-infrared Spectroscopy*, **1**, 33–44.

Fearn, T. (2002). Assessing calibrations: SEP, RPD, RER and R^2. *NIR News*, **13**, 12–14.

Filho, P.A.D.A. and Volery, P. (2005). Broad-based versus specific NIRS calibration: determination of total solids in fresh cheeses. *Analytica Chimica Acta*, **544**, 82–88.

Fumière, O., Sinnaeve, G. and Dardenne, P. (2000). Attempted authentication of cut pieces of chicken meat from certified production using near-infrared spectroscopy. *Journal of Near-infrared Spectroscopy*, **8**, 27–34.

García-Alvarez, M., Huidobro, J.F., Hermida, M. and Rodriguez-Otero, J.L. (2000). Major components of honey analysis by near-infrared transflectance spectroscopy. *Journal of Agricultural and Food Chemistry*, **48**, 5154–5158.

Garcia-Jares, C.M. and Médina, B. (1997). Application of multivariate calibration to the simultaneous routine determination of ethanol, glycerol, fructose, glucose and total residual sugars in botrytized-grape sweet wines by means of near-infrared reflectance spectroscopy. *Fresenius' Journal of Analytical Chemistry*, **357**, 86–92.

Geladi, P. (2002). Some recent trends in the calibration literature. *Chemometrics and Intelligent Laboratory Systems*, **60**, 211–224.

Geladi, P., MacDougall, D. and Martens, H. (1985). Linearization and scatter-correction for near-infrared reflectance spectra of meat. *Applied Spectroscopy*, **39**(3), 491–500.

Giardina, C., Cattaneo, T.M.P. and Barzaghi, S. (2003). Study of modifications in delactosated milk during shelf-life by NIR and FT-IR spectroscopy. *Milchwissenschaft*, **58**, 363–366.

Giardina, C., Sinelli, N., Cattaneo, T.M.P. and Giangiacomo, R. (2004). 2D-IR-COSS as a tool in understanding milk rennet coagulation processes. In: A.M.C. Davies and R.K. Cho (eds), *Near-infrared Spectroscopy: Proceedings of the 11th International Conference*. Chichester: NIR Publications, pp. 187–190.

Gishen, M. and Dambergs, B. (1998). Some preliminary trails in the application of scanning near-infrared spectroscopy (NIRS) for determining the compositional quality of grape, wine and spirits, *The Australian Grapegrower and Winemaker*, **Annual Technical Issue**, 43–47.

Gómez-Cordovés, C. and Bartolome, B. (1993). Application of principal component analysis to simple determinations of brandies as a means of verifying quality. *Zeitschrift für Lebensmittel-Untersuchung und -Forschung*, **197**, 260–263.

Goula, A.M. and Adamopoulos, K.G. (2003). Estimating the composition of tomato juice products by near-infrared spectroscopy. *Journal of Near-infrared Spectroscopy*, **11**, 123–136.

Grant, A., Franklin, J.G. and Davies, A.M.C. (1988). Near-infra-red analysis: the use of multivariate statistics for investigation of variables in sample preparation and presentation of tea leaf. *Journal of the Science of Food and Agriculture*, **42**, 129–139.

Grunewald, H., Kurowski, C., Timm, D. *et al*. (1998). Rapid non-destructive raw material identification in the cosmetic industry with near-infrared spectroscopy. *Journal of Near-infrared Spectroscopy*, **6**, 215–222.

Gunasekaran, S. and Irudayaraj, J. (2001). Optical methods: visible, NIR, and FTIR spectroscopy. In: S. Gunasekaran (ed.), *Nondestructive Food Evaluation Techniques to Analyze Properties and Quality*. New York, NY: Marcel Dekker, Inc., pp. 1–37.

Ha, J., Koo, M. and Ok, H. (1998). Determination of the constituents of honey by near-infrared spectroscopy. *Journal of Near-infrared Spectroscopy*, **6**, A367–A369.

Hall, M.N., Robertson, A. and Scotter, C.N.G. (1988). Near-infrared reflectance prediction of quality, theaflavin content and moisture content in black tea. *Food Chemistry*, **27**, 61–75.

Hana, M., McClure, W.F., Whitaker, T.B. *et al*. (1997). Applying artificial neural networks: Part II. Using near-infrared data to classify tobacco types and identify native grown tobacco. *Journal of Near-infrared Spectroscopy*, **5**, 19–25.

Hargin, K.D. (1996). Authenticity issues in meat and meat products. *Meat Science*, **43**, S277–S289.

Hermida, M., Gonzalez, J.M., Sanchez, M. and Rodriguez-Otero, J.L. (2001). Moisture, solids-non-fat and fat analysis in butter by near-infrared spectroscopy. *International Dairy Journal*, **11**, 93–98.

Herschel, W. (1800). Investigation of the power to the prismatic colors to heat and illuminate objects; with remarks, that prove the different refrangibility of radiant heat.

To which is added, an inquiry into the method of viewing the sun advantageously with telescopes of large apertures and high magnifying powers. *Philosophical Transactions of the Royal Society*, **90**, 255–283 (as cited by Davies, 1991).

Hock, C., Villringer, K., MullerSpahn, F. *et al*. (1997). Decrease in parietal cerebral hemoglobin oxygenation during performance of a verbal fluency task in patients with Alzheimer's disease monitored by means of near-infrared spectroscopy (NIRS) – correlation with simultaneous rCBF–PET measurements. *Brain Research*, **755**, 293–303.

Holman, R.T. and Edmondson, P.R. (1956). Near-infrared spectra of fatty acids and some related substances. *Analytical Chemistry*, **28**(10), 1533–1538.

Hopkins, D.W. (2001). Derivatives in spectroscopy. *Near-infrared Analysis*, **2**(1), 1–13.

Hourant, P., Baeten, V., Morales, M.T. *et al*. (2000). Oils and fats classification by selected bands of near-infrared spectroscopy. *Applied Spectroscopy*, **54**(8), 1168–1174.

Hoyer, H. (1997). NIR on-line analysis in the food industry. *Process Control and Quality*, **9**, 143–152.

IDF (1983). *IDF Standard 1B*. Brussels: International Dairy Federation.

Iizuka, K. and Aishima, T. (1999). Differentiation of soy sauce by pattern recognition analysis of mid- and near-IR spectra. *Journal of Food Composition and Analysis*, **12**, 197–209.

IOC (2006). Trade standard applying to olive oils and olive-pomace oils. COI/T.15/NC no.3/Rev. 2. [www.document]. URL http://www.internationaloliveoil.org/downloads/NORMAEN1.pdf (accessed 13 August 2007).

Iwamoto, M., Kawano, S. and Ozaki, Y. (1995). An overview of research and development of near-infrared spectroscopy in Japan. *Journal of Near-infrared Spectroscopy*, **3**, 179–189.

Joubert, E., Manley, M., Gray, B.G. and Schulz, H. (2005). Rapid measurement and evaluation of the effect of drying conditions on harpagoside content in *Harpagophytum procumbens* (Devil's Claw) root. *Journal of Agricultural and Food Chemistry*, **53**(9), 3493–3502.

Joubert, E., Manley, M. and Botha, M. (2006). The use of NIRS for quantification of mangiferin and hesperidin contents of dried, green honeybush (*Cyclopia genistoides*) plant material. *Journal of Agricultural and Food Chemistry*, **54**, 5279–5283.

Kaffka, K.J. and Norris, K.H. (1976). Rapid instrumental analysis of composition of wine. *Acta Alimentaria*, **5**, 199–217.

Karoui, R. and De Baerdemaeker, J. (2007). A review of the analytical methods coupled with chemometric tools for the determination of the quality and identity of dairy products. *Food Chemistry*, **102**, 621–640.

Karoui, R., Mazerolles, G. and Dufour, E. (2003). Spectroscopic techniques coupled with chemometric tools for structure and texture determinations in dairy products: a review. *International Dairy Journal*, **13**, 607–620.

Karoui, R., Bosset, J.O., Mazerolles, G. *et al*. (2005a). Monitoring the geographic origin of both experimental French Jura hard cheeses and Swiss Gruyère and L'Etivaz PDO cheese using mid-infrared and fluorescence spectroscopies: a preliminary investigation. *International Dairy Journal*, **15**, 275–286.

Karoui, R., Dufour, E., Pillonel, L. *et al*. (2005b). The potential of combined infrared and fluorescence spectroscopies as a method of determination of the geographic origin of Emmental cheeses. *International Dairy Journal*, **15**, 287–298.

Kasemsumran, S., Kang, N., Christy, A. and Ozaki, Y. (2005). Partial least square processing of near-infrared spectra for discrimination and quantification of adulterated olive oils. *Spectroscopy Letters*, **38**, 839–851.

Katsumoto, Y., Jiang, J.-H., Berry, R.J. and Ozaki, Y. (2001). Modern pretreatment methods in NIR spectroscopy. *Near-infrared Analysis*, **2**, 29–36.

Kawano, S., Watanabe, H. and Iwamoto, M. (1992). Determination of sugar content in intact peaches by near-infrared spectroscopy with fiber optics in interactance mode. *Journal of the Japanese Society of Horticultural Science*, **61**, 445–451.

Kelly, J.D., Petisco, C. and Downey, G. (2006). Potential of near-infrared transflectance spectroscopy to detect adulteration of Irish honey by beet invert sugar and high fructose corn syrup. *Journal of Near-infrared Spectroscopy*, **14**, 139–146.

Kiskó, G. and Seregély, Z. (2002). Qualification of volatile oils using near-infrared spectroscopy and electric nose. In: A.M.C. Davies and R.K. Cho (eds), *Near-infrared Spectroscopy: Proceedings of the 10th International Conference*. Chichester: NIR Publications, pp. 57–62.

Laasonen, M. (2003). Near-infrared spectroscopy, a quality control tool for the different steps in the manufacture of herbal medicinal products. MSc Thesis, University of Helsinki, Finland.

Laasonen, M., Harmia-Pulkkinen, T., Simard, C.L. *et al*. (2002). Fast identification of *Echinacea purpurea* dried roots using near-infrared spectroscopy. *Analytical Chemistry*, **74**, 2493–2499.

Laporte, M.-F., Martel, R. and Paquin, P. (1998). The near-infrared optic probe for monitoring rennet coagulation in cow's milk. *International Dairy Journal*, **8**, 659–666.

Léon, L., Kelly, J.D. and Downey, G. (2005). Detection of apple juice adulteration using near-infrared transflectance spectroscopy. *Applied Spectroscopy*, **59**(5), 593–599.

Li-Chan, E. (1994). Developments in the detection of adulteration of olive oil. *Trends in Food Science and Technology*, **5**, 3–11.

Lister, S.J., Dhanoa, M.S., Stewart, J.L. and Gill, M. (2000). Classification and comparison of *Gliricidia provenances* using near-infrared reflectance spectroscopy. *Animal Feed Science and Technology*, **86**, 221–238.

Luypaert, J., Heuerding, S., De Jong, S. and Massart, D.L. (2002). An evaluation of direct orthogonal signal correction and other preprocessing methods for the classification of clinical study lots of a dermatological cream. *Journal of Pharmaceutical and Biomedical Analysis*, **30**(3), 453–466.

Luypaert, J., Zhang, M.H. and Massart, D.L. (2003). Feasibility study for the use of near-infrared spectroscopy in the qualitative and quantitative analysis of green tea, *Camellia sinensis* (L.). *Analytica Chimica Acta*, **478**, 303–312.

Manley, M., Van Zyl, L. and Osborne, B.G. (2001a). Deriving a grain hardness calibration for Southern and Western Cape ground wheat samples by means of the particle size index (PSI) method and Fourier transform near infrared (FTNIR) spectroscopy. *South African Journal of Plant and Soil*, **18**(2), 69–74.

Manley, M., Van Zyl, A. and Wolf, E.E.H. (2001b). The evaluation of the applicability of Fourier transform near-infrared (FT-NIR) spectroscopy in the measurement of analytical parameters in must and wine. *South African Journal of Enology and Viticulture*, **2**, 93–100.

Manley, M., Van Zyl, L. and Osborne, B.G. (2002). Using Fourier transform near infrared spectroscopy in determining kernel hardness, protein and moisture content of whole wheat flour. *Journal of Near-infrared Spectroscopy*, **10**, 71–76.

Manley, M., De Bruyn, N. and Downey, G. (2003). Classification of three-year old, unblended South African brandy with near-infrared spectroscopy. *NIR News*, **14**(5), 8–9, 11.

Manley, M., Gray, B.G., Joubert, E. and Schulz, H. (2004). NIRS: an invaluable tool for the quality control of Devil's Claw (*Harpagophytum procumbens*). In: A. Garrido-Varo and A.M.C. Davies (eds), *Near-infrared Spectroscopy: Proceedings of the 11th International Conference*. Chichester: NIR Publications, pp. 879–882.

Manley, M., Joubert, E. and Botha, M. (2006). Quantification of the major phenolic compounds, soluble solid content and total antioxidant activity of green rooibos (*Aspalathus linearis*) by means of near-infrared spectroscopy. *Journal of Near-infrared Spectroscopy*, **14**, 213–222.

Manley, M., Joubert, E., Myburgh, L. *et al*. (2007). Prediction of soluble solids content and post-storage internal quality of Bulida apricots using near-infrared spectroscopy (NIRS) with PLS, MARS and SIMCA as chemometric regression and classification techniques. *Journal of Near-infrared Spectroscopy*, **15**(3), 179–188.

Mao, J. and Xu, J. (2006). Discrimination of herbal medicines by molecular spectroscopy and chemical pattern recognition. *Spectrochimica Acta*, Part A, **65**, 497–500.

Maraboli, A., Cattaneo, T.M.P. and Giangiacomo, R. (2002). Detection of vegetable proteins from soy, pea and wheat isolates in milk powder by near-infrared spectroscopy. *Journal of Near-infrared Spectroscopy*, **10**, 63–69.

Mark, H. (1992). Qualitative discriminant analysis. In: D.A. Burns and E.M. Ciurczak (eds), *Handbook of Near-infrared Analysis*. New York, NY: Marcel Dekker Inc., pp. 360–361.

Martens, H. and Næs, T. (1989). *Multivariate Calibration*. Chichester: John Wiley & Sons, pp. 86–100, 241–254.

Massart, D.L., Vandeginste, B.G.M., Buydens, L.M.C. *et al*. (1988). *Chemometrics: A Textbook, Vol. 2*. Amsterdam: Elsevier.

McClure, W.F. (2001). Near-infrared instrumentation. In: P. Williams and K. Norris (eds), *Near-infrared Technology in the Agricultural and Food Industries*. St Paul, MN: American Association of Cereal Chemists, pp. 109–127.

McElhinney, J., Downey, G. and O'Donnell, C. (1999). Quantification of lamp content in mixtures with raw minced beef using visible near and mid-infrared spectroscopy. *Journal of Food Science*, **64**(4), 587–591.

McKenzie, J.M. and Koch, K.R. (2004). Rapid analysis of major components and potential authentication of South African extra virgin olive oils by quantitative ^{13}C nuclear magnetic resonance spectroscopy. *South African Journal of Science*, **100**, 349–354.

Moh, M.H., Che Man, Y.B., Badlishah, B.S. *et al*. (1999). Quantitative analysis of palm carotene using Fourier transform infrared and near-infrared spectroscopy. *Journal of American Oil Chemists' Society*, **76**(2), 249–254.

Murray, I. and Hall, P.A. (1983). Animal feed evaluation by use of near-infrared reflectance (NIR) spectrocomputer. *Analytical Proceedings*, **20**, 75–78.

Murray, I., Aucot, L. and Pike, I.H. (2001). Use of discriminate analysis on visible and near-infrared reflectance spectra to detect adulteration of fishmeal with meat and bone meal. *Journal of Near-infrared Spectroscopy*, **9**, 297–311.

Næs, T. and Isaksson, T. (1991). Fitting, prediction testing, cross-validation or leverage correction?. *NIR News*, **2**, 10–13.

Næs, T., Isaksson, T., Fearn, T. and Davies, T. (2002). *A user-friendly guide to multivariate calibration and classification*. Chichester, UK: NIR Publications, p. 344.

Norris, K.H. (1989). NIRS instrumentation. In: G.C. Marten, J.S. Shenk and F.E. Barton, II (eds), *Near-infrared Reflectance Spectroscopy (NIRS): Analysis of Forage Quality*. Washington, DC: United States Department of Agriculture, pp. 12–15.

O'Callaghan, D.J., O'Donnel, C.P. and Payne, F.A. (2000). A comparison of on-line techniques for determination of curd setting time using cheesemilks under different rates of coagulation. *Journal of Food Engineering*, **41**, 43–54.

Osborne, B.G. (1991). Measurement of the hardness of wheat endosperm by near-infrared spectroscopy. *Postharvest News and Information*, **2**, 331–334.

Osborne, B.G. (2000). Near-infrared spectroscopy in food analysis. In: R.A. Meyers (ed.), *Encyclopedia of Analytical Chemistry*. Chichester: John Wiley & Sons, pp. 1–13.

Osborne, B.G. and Fearn, T. (1988). Discriminant analysis of black tea by near-infrared reflectance spectroscopy. *Food Chemistry*, **29**, 233–238.

Osborne, B.G., Fearn, T. and Hindle, P.H. (1993). *Spectroscopy with Application in Food and Beverage Analysis*. Singapore: Longman Scientific and Technical, pp. 1–77, 120–141.

Osborne, B.G., Mertens, B., Thompson, M. and Fearn, T. (1997). The authentication of Basmati rice using near-infrared spectroscopy. *Journal of Near-infrared Spectroscopy*, **1**, 77–83.

Paradkar, M.M., Sakhamuri, S. and Irudayaraj, J. (2002). Comparison of FTIR, FT-Raman and NIR spectroscopy in a maple syrup adulteration study. *Journal of Food Science*, **67**, 2009–2015.

Park, R.S., Agnew, R.E., Gordon, F.J. and Steen, R.W.J. (1998). The use of near-infrared reflectance spectroscopy (NIRS) on undried samples of grass silage to predict chemical composition and digestibility parameters. *Animal Feed Science and Technology*, **72**, 155–167.

Pasquini, C. (2003). Near-infrared spectroscopy: fundamentals, practical aspects and analytical applications. *Journal of the Brazilian Chemistry Society*, **14**(2), 198–219.

Pedretti, N., Bertrand, D., Semenou, M. *et al*. (1993). Application of an experimental design to detection of foreign substances in milk. *Journal of Near-infrared Spectroscopy*, **1**, 174–184.

Penner, M.H. (1994). Basic principles of spectroscopy. In: S.S. Nielsen (ed.), *Introduction to the Chemical Analysis of Foods*. Boston, MA: Jones and Bartlett Publishers, pp. 317–324.

Pillonel, L., Luginbühl, W., Picque, D. *et al*. (2003). Analytical methods for the determination of the geographic origin of Emmental cheese: mid- and near-infrared spectroscopy. *European Food Research and Technology*, **216**(2), 174–178.

Pink, J., Naczk, M. and Pink, D. (1999). Evaluation of the quality of frozen minced red hake: use of Fourier transform near-infrared spectroscopy. *Journal of Agricultural and Food Chemistry*, **47**, 4280–4284.

Pizarro, C., Esteban-Díez, I., Nistal, A.-J. and González-Sáiz, J.-M. (2004). Influence of data pre-processing on the quantitative determination of the ash content and lipids in roasted coffee by near-infrared spectroscopy. *Analytica Chimica Acta*, **509**, 217–227.

Pizarro, C., Esteban-Díez, I. and González-Sáiz, J.M. (2007). Mixture resolution according to the percentage of robusta variety in order to detect adulteration in roasted coffee by near-infrared spectroscopy. *Analytical Chimica Acta*, **585**, 266–276.

Pontes, M.J.C., Santos, S.R.B., Araújo, M.C.U. *et al*. (2006). Classification of distilled alcoholic beverages and verification of adulteration by near-infrared spectrometry. *Food Research International*, **39**, 182–189.

Purnomoadi, A., Batajoo, K.K., Ueda, K. and Terada, F. (1999). Influence of feed source on determination of fat and protein in milk by near-infrared spectroscopy. *International Dairy Journal*, **9**, 447–452.

Qui, P.Y., Ding, H.B., Tang, Y.K. and Xu, R.J. (1999). Determination of chemical composition of commercial honey by near-infrared spectroscopy. *Journal of Agricultural and Food Chemistry*, **47**, 2760–2765.

Rannou, H. and Downey, G. (1997). Discrimination of raw pork, chicken and turkey meat by spectroscopy in the visible, near- and mid-infrared ranges. *Analytical Communications*, **34**, 401–404.

Realini, C.E., Duckett, S.K. and Windham, W.R. (2004). Effect of vitamin C addition to ground beef from grass-fed or grain-fed sources on color and lipid stability, and prediction of fatty acid composition by near-infrared reflectance analysis. *Meat Science*, **68**, 35–43.

Reeves, J.B. (2001). Near-infrared diffuse reflectance spectroscopy for the analysis of poultry manures. *Journal of Agricultural and Food Chemistry*, **49**, 2193–2197.

Reid, L.M., Woodcock, A., O'Donnell, C.P. *et al*. (2005). Differentiation of apple juice samples on the basis of heat-treatment and variety using chemometric analysis of MIR and NIR data. *Food Research International*, **38**, 1109–1115.

Ren, G. and Chen, F. (1997). Determination of moisture content of ginseng by near-infra-red reflectance spectroscopy. *Food Chemistry*, **60**, 433–436.

Ren, G. and Chen, F. (1999). Simultaneous quantification of ginsenosides in American ginseng (*Panax quinquefolium*) root powder by visible/near-infrared reflectance spectroscopy. *Journal of Agricultural and Food Chemistry*, **47**, 2771–2775.

Rodriguez-Otero, J.L., Hermida, M. and Centeno, J. (1997). Analysis of dairy products by near-infrared spectroscopy. *Journal of Agriculture and Food Chemistry*, **45**(8), 2815–2819.

Saiz-Abajo, M.J., Gonzalez-Saiz, J.M. and Pizarro, C. (2004). Classification of wine and alcohol vinegar samples based on near-infrared spectroscopy. Feasibility study on the detection of adulterated vinegar samples. *Journal of Agricultural and Food Chemistry*, **52**(25), 7711–7719.

Sato, T. (1994). Application of principal component analysis on near-infrared spectroscopic data of vegetable oils for their classification. *Journal of the American Oil Chemists' Society*, **71**(3), 293–298.

Sato, T., Kawano, S. and Iwamoto, M. (1990). Detection of foreign fat adulteration of milk fat by near-infrared spectroscopic method. *Journal of Dairy Science*, **73**, 3408–3413.

Sato, T., Kawano, S. and Iwamoto, M. (1991). Near-infrared spectral patterns of fatty acid analysis from fats and oils. *Journal of the American Oil Chemists' Society*, **68**(11), 827–833.

Sato, T., Uezono, I., Morishita, T. and Tetsuka, T. (1998). Nondestructive estimation of fatty acid composition in seeds of *Brassica napus* L. by near-infrared spectroscopy. *Journal of American Oil Chemists' Society*, **75**(12), 1877–1881.

Savitzky, A. and Golay, M.J.E. (1964). Smoothing and differentiation of data by simplified least squares procedures. *Analytical Chemistry*, **36**(8), 1627–1639.

Schulz, H. (2004). Analysis of coffee, tea, cocoa, tobacco, spices, medicinal and aromatic plants and related products. *Near-Infrared Spectroscopy in Agriculture, Agronomy Monograph no. 44*. Madison, USA: American Society of Agronomy, Crop Science, Society of America, Soil Science Society of America, pp. 345–376.

Schulz, H., Drews, H.-H., Quilitzsch, R. and Krüger, H. (1998). Application of near-infrared spectroscopy for the quantification of quality parameters in selected vegetable and essential oil plants. *Journal of Near-infrared Spectroscopy*, **6**, 125–130.

Schulz, H., Engelhardt, U.E., Wegent, A. *et al*. (1999). Application of near-infrared reflectance spectroscopy to the simultaneous prediction of alkaloids and phenolic substances in green tea leaves. *Journal of Agricultural and Food Chemistry*, **47**, 5064–5067.

Schulz, H., Pfeffer, S., Quilitzsch, R. *et al*. (2002). Rapid and non-destructive determination of the echinacoside content in Echinacea root by ATR-IR and NIR spectroscopy. *Planta Medica*, **68**, 921–925.

Schulz, H., Quilitzsch, R. and Krüger, H. (2003a). Rapid evaluation and quantitative analysis of thyme, origano and chamomile essential oils by ATR-IR and NIR spectroscopy. *Journal of Molecular Structure*, **661–662**, 299–306.

Schulz, H., Joubert, E. and Schütze, W. (2003b). Quantification of quality parameters for reliable evaluation of green rooibos (*Aspalathus linearis*). *European Food Research and Technology*, **216**, 539–543.

Scotter, C.N.G. and Legrand, A. (1994). NIR qualitative analysis – a new philosophy with special reference to raped NIR screening for fruit juice authenticity. *Food Science Technology Today*, **8**, 167–171.

Scotter, C.N.G. and Legrand, A. (1995). Near-infrared (NIR) spectroscopy as a screening technique for fruit juice verification. *Fruit Processing*, **5**, 255–260.

Scotter, C.N.G., Hall, M.N., Day, L. and Evans, D.G. (1992). The authentication of orange juice and other fruit juices. In: K.I. Hildrum, T. Isaksson, T. Næs and A. Tandberg (eds), *Near-infrared Spectroscopy. Bridging the Gap between Data Analysis and NIR Applications*. Chichester: Ellis Horwood, pp. 309–314.

Shilton, N., Downey, G. and McNulty, P.B. (1998). Detection of orange juice adulteration by near-infrared spectroscopy. *Seminars in Food Analysis*, **3**, 155–161.

Singh Sahni, N., Isaksson, T. and Næs, T. (2004). In-line near-infrared spectroscopy for use in product and process monitoring in the food industry. *Journal of Near-infrared Spectroscopy*, **12**, 77–83.

Sirieix, A. and Downey, G. (1993). Commercial wheat flour authentication by discriminant analysis of near-infrared reflectance spectra. *Journal of Near-infrared Spectroscopy*, **1**, 187–197.

Sivakesava, S. and Irudayaraj, J. (2001). Prediction of inverted cane sugar adulteration of honey by Fourier transform infrared spectroscopy. *Journal of Food Science*, **66**(7), 972–978.

Sjöblom, J., Svensson, O., Josefson, M. *et al*. (1998). An evaluation of orthogonal signal correction applied to the calibration transfer of near-infrared spectra. *Chemometrics and Intelligent Laboratory Systems*, **44**, 229–244.

Sneyd, T.N., Bruer, N.G.C. and Lee, T.H. (1989). A survey of five methods for analyzing the alcoholic strength of wine. *Proceedings of the Seventh Australian Wine Industry Technical Conference*, August 1989, Adelaide, Australia, p. 237.

Stark, E., Luchter, K. and Margoshes, M. (1986). Near-infrared analysis (NIRA): a technology for quantitative and qualitative analysis. *Applied Spectroscopy Reviews*, **22**, 335–399.

Stchur, P., Cleveland, D., Zhou, J. and Michel, R.G. (2002). A review of recent applications of near-infrared spectroscopy, and of the characteristics of a novel PbS CCD array-based near-infrared spectrometer. *Applied Spectroscopy Reviews*, **37**(4), 383–428.

Stuth, J., Jama, A. and Tolleson, D. (2003). Direct and indirect means of predicting forage quality through near-infrared reflectance spectroscopy. *Field Crops Research*, **84**, 45–56.

Suto, T., Fukuda, M., Ito, M. *et al*. (2004). Multichannel near-infrared spectroscopy in depression and schizophrenia: cognitive brain activation study. *Biological Psychiatry*, **55**, 501–511.

Tarkošová, J. and Čopíková, J. (2000). Fourier transform near-infrared spectroscopy applied to analysis of chocolate. *Journal of Near-infrared Spectroscopy*, **8**, 251–257.

Twomey, M., Downey, G. and McNulty, P.B. (1995). The potential of NIR spectroscopy for the detection of the adulteration of orange juice. *Journal of Science of Food and Agriculture*, **67**, 77–84.

Ulbert, F. (1994). Detection of milk fat adulteration by linear discriminant analysis of fatty acid data. *Journal of AOAC International*, **77**(5), 1326–1334.

Ulbert, F. (2003). Milk and dairy products. In: M. Lees (ed.), *Food Traceability and Authenticity*. Cambridge: Woodhead Publishing Ltd, pp. 357–377.

Van den Berg, F.W.J., Van Osenbruggen, W.A. and Smilde, A.K. (1997). Process analytical chemistry in the distillation industry using near-infrared spectroscopy. *Process Control and Quality*, **9**, 51–57.

Van de Voort, F.R. (1992). Fourier transform infrared spectroscopy applied to food analysis. *Food Research International*, **25**, 397–403.

Van Zyl, L. and Manley, M. (2001). Using different sample holders in determining protein and moisture content in whole flour by means of Fourier transform near infrared (FTNIR) spectroscopy. *South African Journal of Plant and Soil*, **18**(2), 50–55.

Velasco, L., Goffman, F.D. and Becker, H.C. (1999). Development of calibration equations to predict oil content and fatty acid composition in *Brassicaceae* germplasm by near-infrared reflectance spectroscopy. *Journal of American Oil Chemists' Society*, **76**(1), 25–30.

Walsh, K.B., Golic, M. and Greensill, C.V. (2004). Sorting of fruit using near-infrared spectroscopy: application to a range of fruit and vegetables for soluble solids and dry matter content. *Journal of Near-infrared Spectroscopy*, **12**, 141–148.

Wang, F., Zhang, Z., Cui, X. and Harrington, P.deB. (2006). Identification of rhubarbs by using NIR spectrometry and temperature-constrained cascade correlation networks. *Talanta*, **70**, 1170–1176.

Wang, L., Lee, F.S.C. and Wang, X. (2007). Near-infrared spectroscopy for classification of licorice (*Glycyrrhizia uralensis* Fisch) and prediction of the glycyrrhizic acid (GA) content. *Lebensmittel-Wissenschaft und -Technologie*, **40**, 83–88.

Wesley, I.J., Barnes, R.J. and McGill, A.E.J. (1995). Measurement of adulteration of olive oils by near-infrared spectroscopy. *Journal of the American Oil Chemists' Society*, **72**(3), 289–292.

Wesley, I.J., Pacheco, F. and McGill, A.E.J. (1996). Identification of adulterants in olive oils. *Journal of the American Oil Chemists' Society*, **73**(4), 515–518.

Wesley, I.J., Uthayakumaran, S., Anderssen, R.S. *et al*. (1999). Curve-fitting approach to the near-infrared reflectance measurement of wheat flour proteins which influence dough quality. *Journal of Near-infrared Spectroscopy*, **7**, 1–12.

Westerhaus, W.O. (1989). Calibration: interpretation of regression statistics. In: G.C. Marten, J.S. Shenk and J.E. Barton, II (eds), *Near-infrared Reflectance Spectroscopy (NIRS): Analysis of Forage Quality*. Washington, DC: United States Department of Agriculture, pp. 39–40.

Wetzel, D.L. (1983). Near-infrared reflectance analysis of major components in foods. In: G. Charalambous and G. Inglett (eds), *Instrumental Analysis of Foods – Recent Progress*, Vol. 1. London: Academic Press, pp. 183–202.

Wetzel, D.L. (1998). Analytical near-infrared spectroscopy. In: D.L.B. Wetzel and G. Charalambous (eds), *Instrumental Methods in Food and Beverage Analysis*. Amsterdam: Elsevier, pp. 141–194.

Wetzel, D.L. (2001). Contemporary near-infrared instrumentation. In: P. Williams and K. Norris (eds), *Near-infrared Technology in the Agricultural and Food Industries*. St Paul, MN: American Association of Cereal Chemists, pp. 129–144.

Williams, P.C. (2001). Implementation of near-infrared technology. In: P. Williams and K. Norris (eds), *Near-infrared Technology in the Agricultural and Food Industries*, 2nd edn. St Paul, MN: American Association of Cereal Chemists, pp. 145–169.

Williams, P.C. and Sobering, D.C. (1993). Comparison of commercial near-infrared transmittance and reflectance instruments for analysis of whole grains and seeds. *Journal of Near-infrared Spectroscopy*, **1**, 25–32.

Williams, P.C. and Stevenson, S.G. (1990). Near-infrared reflectance analysis: food industry applications. *Trends in Food Science and Technology*, **1**, 44–48.

Wilson, R.H., Goodfellow, B.J., Belton, P.S. *et al*. (1991). Comparison of Fourier transform mid infrared spectroscopy and near-infrared reflectance spectroscopy with differential scanning calorimetry for the study of the staling of bread. *Journal of the Science of Food and Agriculture*, **54**, 471–483.

Windham, W.R., Gaines, C.S. and Leffler, R.G. (1993). Effect of wheat moisture content on hardness scores determined by near-infrared reflectance and on hardness score standardization. *Cereal Chemistry*, **70**, 662–666.

Wold, S. (1995). Chemometrics; what do we mean with it, and what do we want from it? *Chemometrics and Intelligent Laboratory Systems*, **30**, 109–115.

Wold, J.P. and Isaksson, T. (1997). Non-destructive determination of fat and moisture in whole Atlantic salmon by near-infrared diffuse reflectance spectroscopy. *Journal of Food Science*, **62**, 734–736.

Wold, S., Antio, H., Lindgren, F. and Ohman, J. (1998). Orthogonal signal correction of near-infrared spectra. *Chemometrics Intelligent Laboratory Systems*, **44**, 175–185.

Woo, Y.-A., Kim, H.-J., Cho, J. and Chung, H. (1999a). Discrimination of herbal medicines according to geographical origin with near-infrared reflectance spectroscopy and pattern recognition techniques. *Journal of Pharmaceutical and Biomedical Analysis*, **21**, 407–413.

Woo, Y.-A., Kim, H.-J. and Chung, H. (1999b). Classification of cultivation area of ginseng radix with NIR and Raman spectroscopy. *Analyst*, **124**, 1223–1226.

Woo, Y.-A., Cho, C.-H., Kim, H.-J. *et al*. (2002). Classification of cultivation area of ginseng by near-infrared spectroscopy and ICP-AES. *Microchemical Journal*, **73**, 299–306.

Wüst, E. and Rudzik, L. (2003). The use of infrared spectroscopy in the dairy industry. *Journal of Molecular Structure*, **661–662**, 291–298.

Xing, J., Landahl, S., Lammertyn, J. *et al*. (2003). Effects of bruise type on discrimination of bruised and non-bruised "Golden Delicious" apples by VIS/NIR spectroscopy. *Postharvest Biology and Technology*, **30**, 249–258.

Yu, H., Ying, Y., Fu, X. and Lu, H. (2006). Classification of Chinese rice wine with different marked age based on near-infrared spectroscopy. *Journal of Food Quality*, **29**, 339–352.

Yu, H., Zhou, Y., Fu, X. *et al*. (2007a). Discrimination between Chinese rice wines of different geographical origins by NIRS and AAS. *European Food Research Technology*, **225**, 313–320.

Yu, H., Ying, Y., Sun, T. *et al*. (2007b). Vintage year determination of bottled Chinese rice wine by Vis-NIR spectroscopy. *Journal of Food Science*, **72**(3), E125–E129.

Zhang, M.H., Luypaert, J., Fernàndez Pierna, J.A. *et al*. (2004). Determination of total antioxidant capacity in green tea by near-infrared spectroscopy and multivariate calibration. *Talanta*, **62**, 25–35.

Zhao, J., Chen, Q., Huang, X. and Fang, C.H. (2006). Qualitative identification of tea categories by near-infrared spectroscopy and support vector machine. *Journal of Pharmaceutical and Biomedical Analysis*, **41**, 1198–1204.

Zoecklein, B.W., Fugelsang, K.C., Gump, B.H. and Nurry, F.S. (1994). *Wine Analysis and Production*. New York, NY: Chapman and Hall, pp. 89–114, 178–198, 336–340, 496–500.

This page intentionally left blank

4

Spectroscopic Technique: Fourier Transform Near-infrared (FT-NIR) Spectroscopy

Vincent Baeten, Marena Manley, Juan Antonio Fernández Pierna, Gerard Downey and Pierre Dardenne

Introduction

Correct and defensible labeling is of prime importance for the consumer and the producer of authentic food products. For the consumer, labeling and its control are essential in terms of the identification of the food product. He or she may pay more in order to get a food product with well-defined attributes, such as species or geographic origin, or more subjective features, as in products labeled home made, organic or fair trade. Food products are not only valued for their appearance, taste and nutritional value (whatever their major and minor compound composition), but also for their tremendous symbolic power. For the producer, labeling and its control are crucial in terms of economic strategy. Indeed, producers selling food with specific quality attributes invest more in the production of their food products, as they expect a substantial return. This return may be obtained by charging a higher price and/or the development of a loyal customer base.

Modern Techniques for Food Authentication
ISBN: 978-0-12-374085-4

All actors in the food chain need to have analytical tools at their disposal to verify the nature of high-value foods in particular, and to protect their brands. Ideally, these tools should permit rapid, non-destructive and inexpensive control at any point of the food chain, and should be part of the traceability strategy for the food product. For both food producers and consumers, confirmation that a food product is the one expected (i.e. the real thing) is crucial because this is the basis of mutual trust. Such confirmation requires looking beyond the mere superficial surface appearance or the composition of the products (Van der Reyden, 1996; Downey *et al*., 2006).

Among the panoply of methods for the assessment of a food product's authenticity, several vibrational spectroscopic techniques have recently been proposed. Several reports have proposed methods based on ultraviolet (UV), near-infrared (NIR), mid-infrared (MIR) and Raman spectroscopy. *Vibrational spectroscopy* techniques have been used for many years as favored tools for the study of the molecular structure of organic matter. On the other hand, for many decades several methods based on UV, NIR, MIR or Raman spectroscopy have been proposed and widely used as methods of choice for forensic studies (e.g. authentication of hair, fibers, paint, drugs and poisons) and assessment of the authenticity of art works (Brettel *et al*., 2005).

Spectroscopic methods, based mainly on NIR techniques, are often presented as new approaches for at-line, on-line and in-line control of authentication of food products. These techniques are already routinely used in the industry to control both raw materials and finished products for specific production standards as a common authenticity issue. This means that tedious reference methods only need to be used if deviations from these quality standards occur during production (Müller and Steinhart, 2007). Demonstration of the potential of vibrational spectroscopy techniques for the assessment of value-added claims like geographic origin, species discrimination, detection and quantification of adulteration and the assessment and discrimination of process type or brands have been reported since the beginning of the 1990s (Dennis, 1998).

The main limitation of the spectroscopic approach is the fact that it needs large data sets in order to calibrate any given instrument, and only few publications have dealt with the interpretation of the spectroscopic features related to specific authenticity issues. The main challenge therefore facing the spectroscopists is to extract the information in such a way that it can be used in qualitative and quantitative analysis. NIR spectra can contain up to thousands of absorbance values at defined wavelengths (i.e. variables), and the challenge is to characterize the spectral data set and isolate the variables that can be correlated with the information of interest (i.e. authenticity issue) (Baeten and Aparicio, 2000). In order to achieve this goal, a wide range of chemometric tools is at the disposal of analysts, who have to select the appropriate one according to their specific aims and the characteristics of the data set. Among the many methods proposed for authentication of food products, spectroscopic methods seem to be the preferred ones to flag suspicious samples before, during and after the production of a food product. The real future challenge for the spectroscopic techniques will be the demonstration of their daily use in the industry and the marketplace for food product authentication.

The growing interest in spectroscopic techniques for developing methods and strategies to assess the authenticity of products may be gleaned from the number

Table 4.1 Selection of EU-funded projects including research for the development and validation of spectroscopic methods

Acronym	Food product	Authenticity issue	Spectroscopic method	Web site
CO-EXTRA	GMO	Transgenic/non-transgenic	NIR imaging	http://www.coextra.eu/
FEEDFAT	Animal fats	Discrimination	MIR	http://www.ub.edu/feedfat/
TRACE	Olive oil, honey, cereal, meat	Geographic origin	NIR, MIR, Raman	www.trace.eu.org
MEDEO	Olive oil	Adulteration	MIR, Raman	http://www.cica.es/aliens/igmedeo/
SAFEED-PAP-PAP-PAP	Feed, processed animal protein	Adulteration	NIR microscopy, NIR imaging	http://safeedpap.feedsafety.org/
STRATFEED	Feed	Adulteration	NIR, NIR microscopy	http://www.stratfeed.cra.wallonie.be
TYPIC	Dry cured ham, wine	Geographic origin, brand	NIR, MIR, Raman	http://www.typic.org/

Source: www.trace.eu.org

of European projects involving these techniques and financed by the European Commission. Table 4.1 summarizes some of the European projects which include research for the development and validation of spectroscopic methods. An updated list can be found on the website of European project TRACE (Tracing the origin of food; http://www.trace.eu.org/library/links.php), which is an integrated project financed in the EU 6th Framework Programme. This particular project aims to improve the health and well-being of European citizens by delivering integrated traceability systems that will enhance consumer confidence in the authenticity of food.

This chapter is complementary to Chapter 3, which was dedicated to near-infrared spectroscopy. The focus in this chapter is specifically on Fourier transform near-infrared spectroscopy (FT-NIR) and microscopy (FT-NIRM), and their applications for the authentication of agro-food products.

Theory and instrumentation

Regarding the history of near-infrared spectroscopy, a turning point was the work of Sir Frederick William Herschel, reported in 1800. Herschel discovered that the sun's energy was not limited to what we can see. He demonstrated this by projecting a rainbow onto a bench using glass prisms which are transparent to short-wave NIR radiation. He positioned a series of blackened bulb thermometers on a bench and measured the relative heat in the different parts of the rainbow. The temperature increased by moving from the blue to the red. Herschel's scientific insight meant that he did not stop the temperature measurement when he reached the end of the visible red color region of the dispersed light, but continued to observe temperature when he placed a thermometer beyond that point. This work was a key milestone in the discovery of the electromagnetic spectrum (Davies, 1998; Pasquini, 2003).

Near-infrared spectroscopy: few elements of theory

The electromagnetic spectrum is usually divided into several regions, from high to low energy, including, among others, γ-rays, X-rays, ultraviolet (UV), visible (VIS),

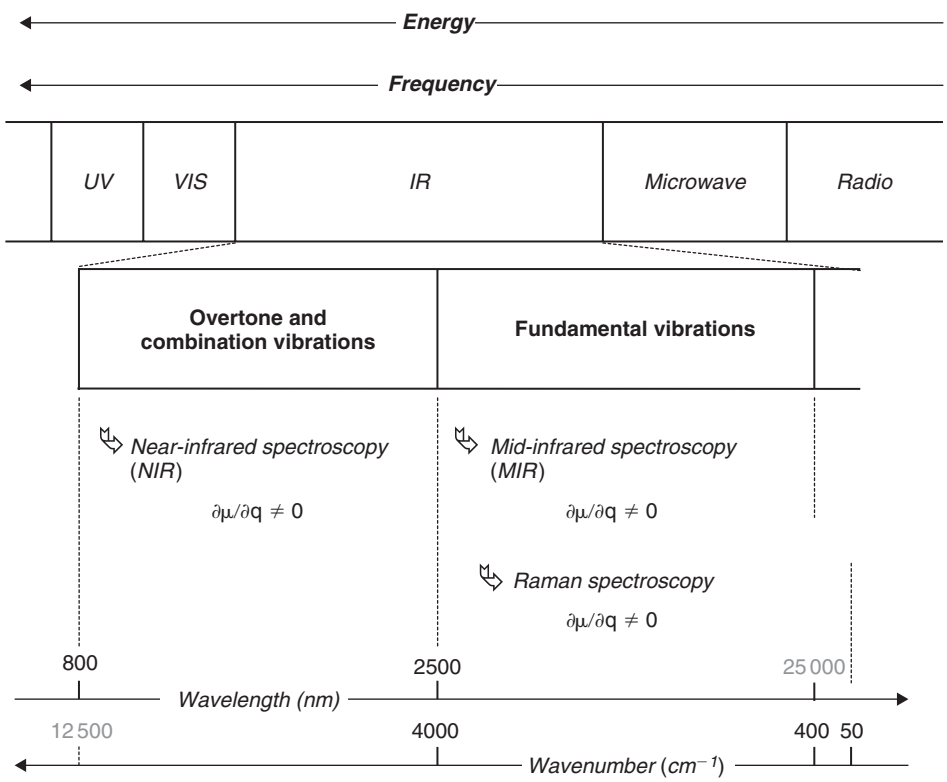

Figure 4.1 Features of the NIR and MIR regions of the electromagnetic spectrum (Source: Baeten and Dardenne, 2002).

infrared (IR), microwaves and radio waves. Specific atomic or molecular transition corresponding to different energies is characteristic of each region of the electromagnetic spectrum. Moreover, the infrared region is divided into near-infrared (NIR), mid-infrared (MIR) and far-infrared regions. Figure 4.1 shows the regions of the electromagnetic spectrum covering the spectroscopic techniques discussed in Chapters 2–6 (namely NIR, MIR and Raman spectroscopy). The figure includes the energetic transition involved as well as the corresponding wavelengths and wavenumber ranges (Baeten and Dardenne, 2002). To summarize, near-infrared spectroscopy (NIR) is a vibrational spectroscopy that concerns photon energy ($h\nu$) in the energy range of 2.65×10^{-19} J, which corresponds to the wavelength range of 750–2500 nm (and to the wavenumber range of 13 300–4000 cm^{-1}).

In order to explain the properties of electromagnetic radiation, it is necessary to refer to the classical theory describing electromagnetic radiation as a wave and the quantum theory stating that electromagnetic radiation is a stream of energetic particles. The *classical theory* says that the properties of light can be explained on the basis of an electric field associated with a perpendicular magnetic field of high frequency. This field moves in the direction of the light. The electric and magnetic fields interact with organic matter to give rise to a spectrum. The movement of the

radiation has the properties of a sine wave described by the equation $Y = A \sin \omega t$, where Y is the displacement with an amplitude A, ω is the angular velocity (rad s^{-1}) and t is the time in seconds. The frequency υ expressed as cycles per second (s^{-1} or Hz) corresponds to the number of times ($\omega/2\pi$) that the pattern is repeated in 1 second. The distance covered in one complete cycle, known as the wavelength λ, is an additional property of the wave describing the radiation. As the classical theory does not explain all the properties of the electromagnetic radiation and its interaction with matter, and fails to account for phenomena associated with the absorption of the energy, it was necessary to complement this theory.

The *quantum theory* views electromagnetic radiation as a stream of discrete particles; Planck (1925) was the first to put forward the hypothesis that the electromagnetic wave was not continuous but composed of corpuscular units called quanta. The energy of a quantum of radiation is defined (for a specific molecule all the energy levels are allowed) and characterized by its frequency (Osborne and Fearn, 1986; Lachenal, 1998a, 1998b).

As discussed before, NIR spectroscopy involves radiation in the 780–2500 nm (wavenumber range 12 800–4000 cm^{-1}) region, with energy higher than in MIR. Traditionally, NIR spectra are expressed as absorbance versus wavelength (expressed in nm). Figure 4.2 shows the NIR spectra of several agro-food products. Each spectrum was collected with a FT-NIR instrument in 40 s with a resolution of 16 cm^{-1} and is the average of 64 scans.

The advantages and drawbacks of the methods based on NIR spectroscopy are various, and can be split between analytical, spectroscopic and instrumental features. The *analytical* advantages include speed; no sample preparation; no requirement for chemical reagents; being non-destructive; the possibility to perform qualitative and quantitative analysis, and to handle almost all kind of samples irrespective of their size or shape; the relatively low cost per analysis; and the opportunity to perform direct, non-invasive and *in situ* analysis. The main analytical limitations are the need to calibrate the spectrometer, usually requiring usually hundreds or thousands of spectra with reference values and the use of chemometrics, as well as the limited number of available validated methods according to international standards.

From a *spectroscopic* point of view, NIR spectroscopy has the advantages of providing spectra with a high intensity and high resolution, and a precise spectral frequency measurement; being fluorescence-free; and ease of sample presentation. Regarding limitations, this technique is characterized by poorly-resolved spectra; the absence of information from non-polar groups; a lack of structural selectivity and of sensitivity; and spectra influenced by temperature changes.

The *instrumental* advantages of NIR spectroscopy include the marketing of push-button instrumentation; the possibility to work with aqueous samples; its suitability for at-, on- and in-line process control; its compatibility with long fiber-optics; its suitability for process monitoring; and the existence of hyphenated techniques such as NIR microscopes and imaging instruments. The main instrumental drawback is the fact that there are no officially accepted and agreed standards by all manufacturing companies for sample presentation and software to handle and exploit data treatment. A more detailed description, as well as references discussing these different

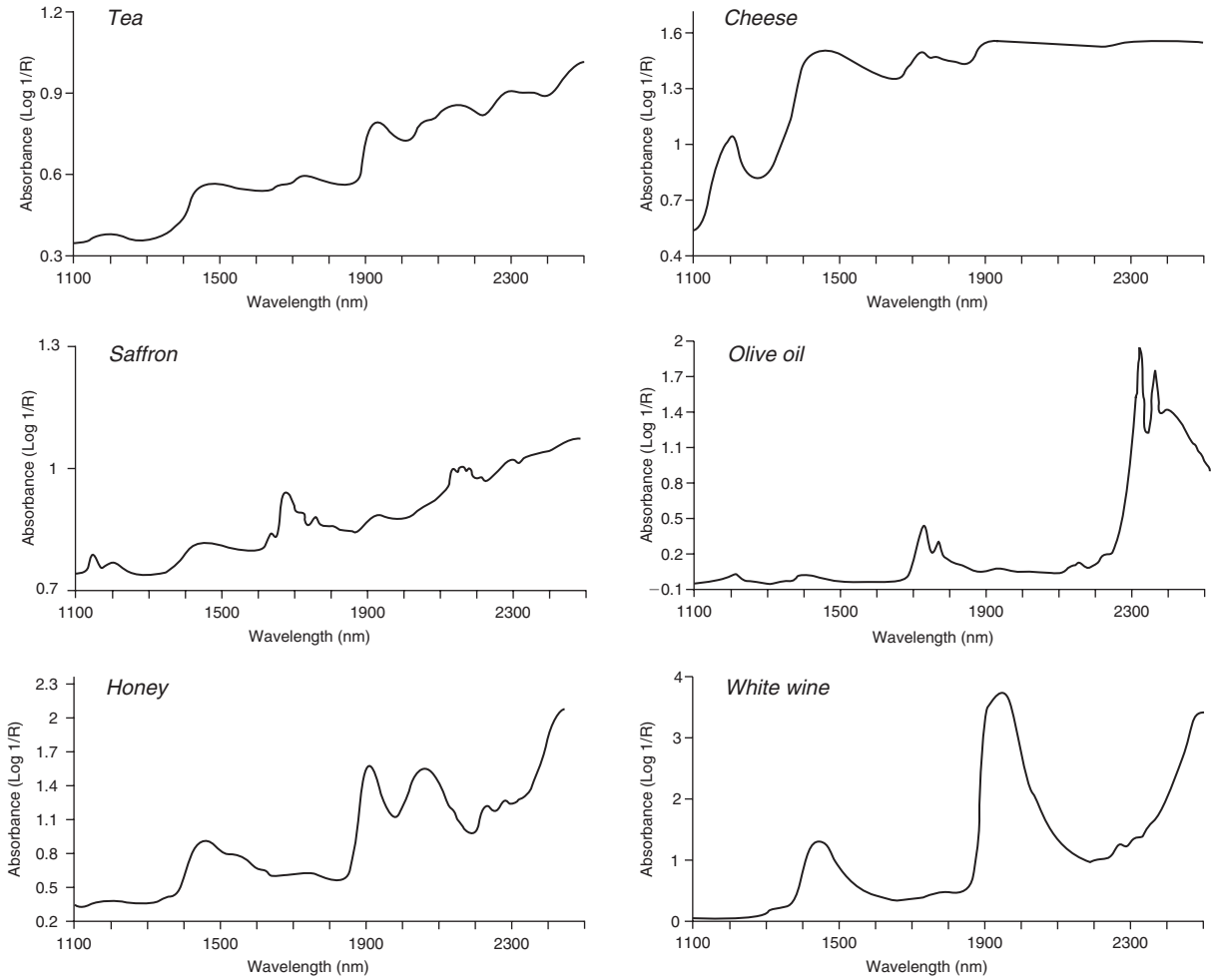

Figure 4.2 Representative NIR spectra of various agro food products (tea, saffron, honey, cheese, olive oil, white wine). Spectra have been collected with a FT-NIR spectrometer (MPA, Brüker, resolution 16 cm^{-1}, scans 60, analytical time 40 s) (Source: CRA-W).

advantages and drawbacks not only for NIR but also for MIR and Raman spectroscopy, can be found in the publication by Baeten and Dardenne (2002).

Fourier transform near-infrared spectroscopy: instrumentation features

The evolution of instrumentation in NIR spectroscopy is very rapid, particularly in process analytical chemistry, which is critical for pharmaceutical, chemical and agro-food industries. A general trend is that the analyses are moving closer to the points of sampling by means of fiber-optics allowing real-time and continuous analysis. An additional development is that of dedicated instruments combining the instrument, the interface between the instrument and the sample, as well as software integrating

data acquisition, chemometrics and data archiving for specific applications (e.g. NIR wine analysis, NIR feed or food analysis) (Ciurczak, 1991).

NIR instruments can be classified into three groups. The first group includes sequential instruments in which absorbance measurements for the respective wavelengths are collected sequentially in time. In this group we find all the instruments using monochromators, filters or other devices allowing the sequential selection of wavelengths. The second group consists of multichannel instruments having several detectors that separately record the absorbance values at several wavelengths, such as diode array instruments. The third type of spectrometer regroups the multiplex instruments in which the detector simultaneously collects information at several frequencies. Fourier transform instruments are the most common of this type of instrument (Bertrand and Baeten, 2006). Sequential and multichannel instruments are extensively described in Chapter 3 of this book. In the following paragraphs, attention is paid to multiplex instruments and more specifically to FT-NIR instruments.

Multiplex instruments based on the use of interferometers are FT-NIR spectrometers combining most of the best features in terms of wavelength precision, accuracy, high signal-to-noise ratio and high scan speed. These instruments have gained more and more importance in the last decade. They have a light source emitting in the NIR range and directing radiation to the interferometer. For example, if radiation with wavelength λ is sent to the interferometer, the radiation λ is sent to a beam-splitter that reflects approximately half of the incident radiation and transmits the other half. The reflected part of the radiation encounters a stationary mirror while the transmitted part is sent to a second mirror; both parts of the radiation are recombined at the level of the beam-splitter and directed to the sample. Because the second mirror is moving, the pathways to and from the movable mirror are variable as a function of mirror position. At different mirror positions, a difference (also referred to as retardation, δ) in path-length produces interference – both constructive and destructive interferences can occur. Constructive interference will occur when the retardation of the two mirrors is equal to $\delta = n\lambda$ (where n is an integer); the interference will be destructive when the retardation is equal to $n\lambda/2$ (where n is odd) (Williams and Norris, 2001; King *et al*., 2004). The most common interferometer is the Michelson interferometer (Williams and Norris, 2001), which includes a beam-splitter, stationary and moving mirrors, and a laser to follow the position of the moving mirror. Figure 4.3 shows the schema of the Michelson interferometer. Data accumulated during the motion of the moving mirror, information in the time domain, is transformed into information in the frequency domain through application of the fast Fourier transformation.

Advantages of Fourier transform infrared spectrometers are numerous. First, interferometers allow radiation at a range of wavelengths to be produced near-simultaneously, decreasing the time require to acquire a full spectrum. This advantage is known as the *multiplex or Fellgett advantage*. They also have a throughput advantage, as interferometers have no entrance or exit slits and all the NIR radiation passes through, is emitted or reflected from the sample and reaches the detector at once. This advantage is called the *Jacquinot advantage* (Williams and Norris, 2001). Fourier transform-based instruments also offer excellent resolution and wavelength

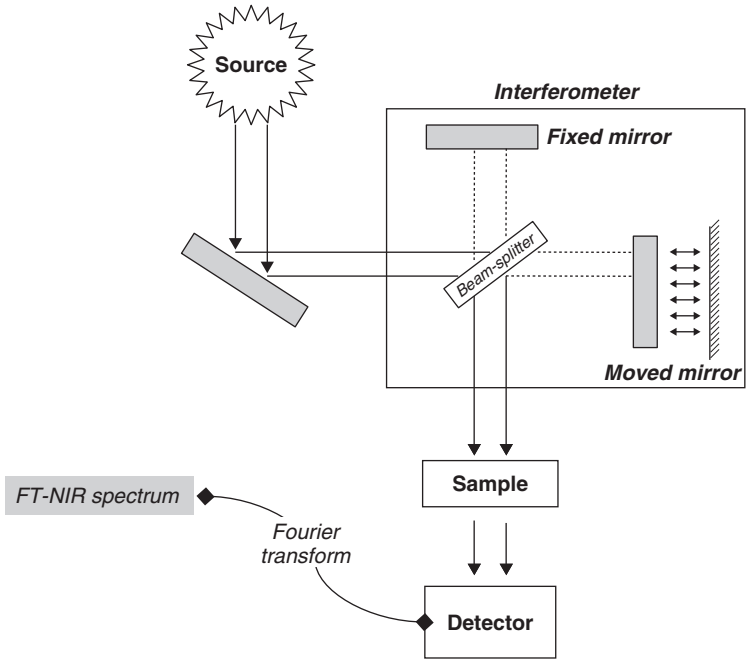

Figure 4.3 Schema of a typical Michelson interferometer including the beam-splitter, the stationary mirror and the moving mirror.

reproduction; this is possible through the use of a laser in a path parallel to the NIR path to allow verification of the moving mirror position (Williams and Norris, 2001; King *et al*., 2003).

FT-NIR allows instrument manufacturers to develop new types of instrumentation, such as the introduction of hyphenated techniques combining microscopy and FT-NIR spectroscopy. Fourier transform near-infrared microscopes allow analysts to switch from macroscopic to microscopic analysis. Infrared microscopy is routinely used as a standard laboratory procedure in forensic analysis. Actually, commercial NIR microscopes allow spectra to be collected from extremely small sample areas (5 μm × 5 μm). Such instruments include a camera and a viewing system for magnifying the visible light image of the sample to be analyzed, allowing the identification and the isolation of one point or a series of points of interest. The device allows the collection of spectra at a large number of sample points from an inhomogeneous surface (e.g. particles from food or feed meal, slices of salami) and produces a NIR map or NIR cube. Figure 4.4 presents the schema of a typical NIR microscope, while Figure 4.5 shows a picture of a NIR microscope (Perkin-Elmer photo image instrument) as well as the spectra collected from a salami sausage sliced (the spectra were collected from pieces of meat and fat). Infrared maps are obtained by the procedure of mapping that allows the automatic and sequential collection of near-infrared spectra of a series of points. The incorporation of multichannel detectors in recent NIR microscopes has made this kind of instrument more powerful because of the

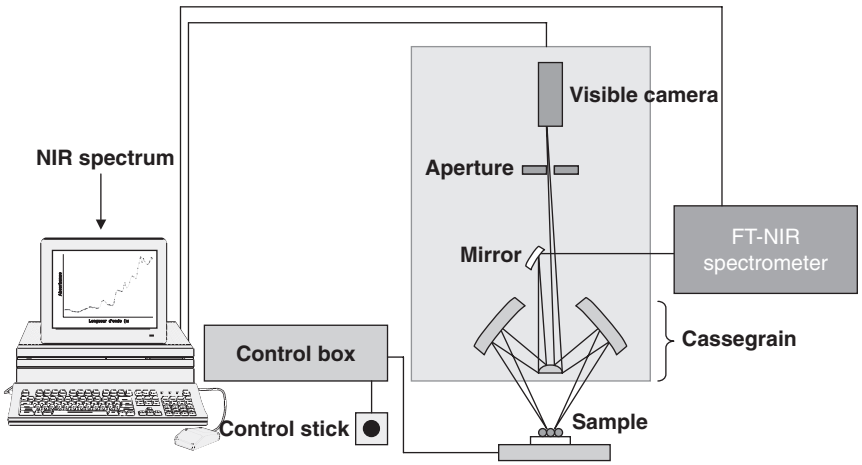

Figure 4.4 Schema of a typical near-infrared microscope.

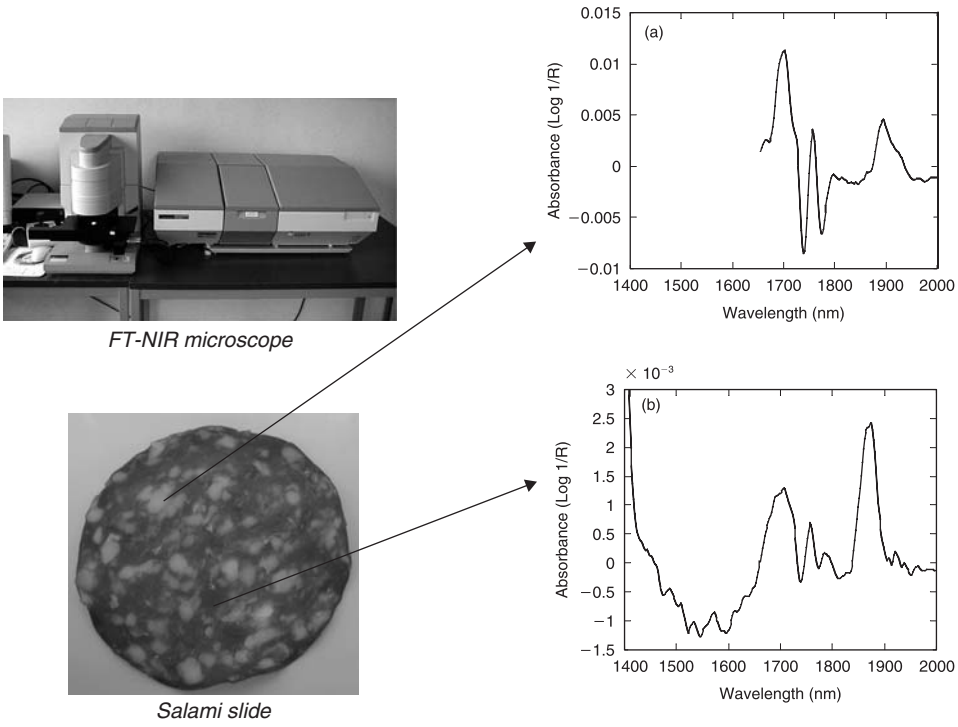

Figure 4.5 Example of a NIR microscope (Perkin-Elmer photo image instrument) and spectra collected from a salami sausage slide: (a) spectrum of meat area; (b) spectrum of fat area.

simultaneous acquisition of spectral data from several points. A multichannel detector includes several photoelectric detector elements and permits the simultaneous recording of reflected or transmitted light from a number of points. Depending on the instrument type, two kinds of camera can be distinguished; one-dimensional

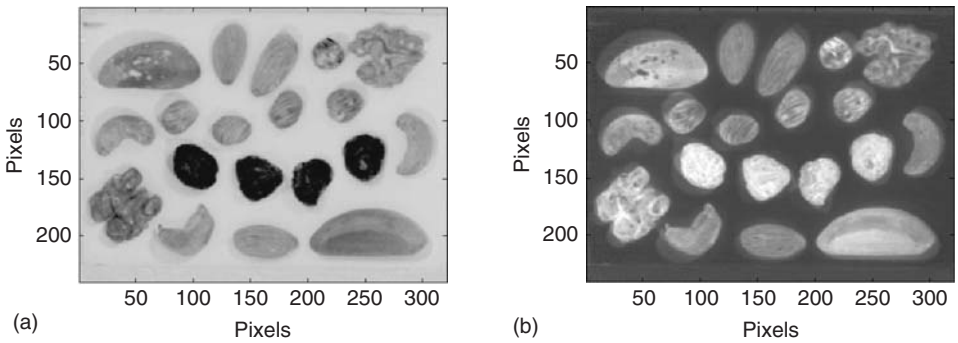

Figure 4.6 NIR images at 1420 nm and first principal component (PC1) image of a mix of dried fruits.

(i.e. a line scan camera) and two-dimensional (Baeten and Dardenne, 2002). Figure 4.6 presents the NIR images at two different wavelengths of a mixture of dried fruits.

New trends in chemometrics as applied to NIR spectroscopic data

In this section, the aim is not to give a summary of all the possible chemometric solutions for the handling, transformation and exploitation of NIR data. The focus will mainly be on two chemometric tools which, in recent years, have proved to be adequate to solve specific problems, such as co-linearity and non-linearity, associated with spectroscopic data: these are *artificial neural networks* (*ANNs*) and *support vector machines* (*SVM*). These chemometric methods are applied in order to automate the extraction of information from NIR data and to reduce the need for constant expert analysis of data. Chapters 3 and 16 give a complete overview of the mathematical techniques commonly used.

Artificial neural networks (ANNs) for authentication using spectroscopic data

An artificial neural network (ANN) is an information-processing system designed to mimic functions of the human brain, i.e. it is based on generalizations of human cognition. Among the many applications of ANNs, classification is perhaps the most interesting for data mining. In this case, the network is trained to classify certain patterns into specific groups and is then used to classify novel patterns which have never been presented to the network before. Many applications demonstrate the suitability of ANNs for classification (authentication) as well as modeling tasks. ANNs are well-known in the area of biometry for fingerprint, face or eye identification, as well as for handwritten or signature authentication. They have also been widely-used in spectroscopy, and several papers deal with the problem of authentication of various products.

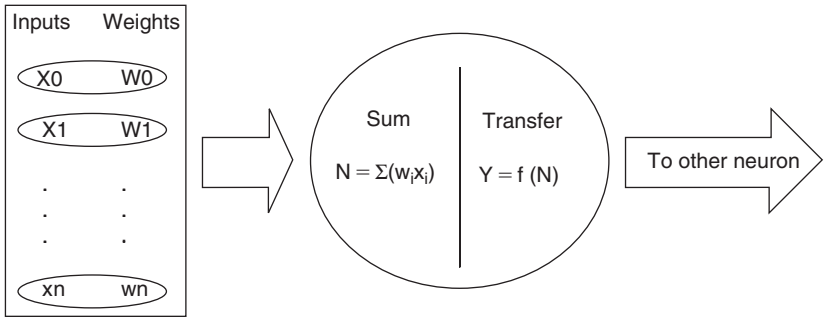

Figure 4.7 ANN – representation of a simple neuron in which all the connection weights for each input are summed, resulting in a unique complex function each time the neural network is trained with a set of inputs and outputs (w = weight).

In the *Handbook of Expert Systems in Manufacturing*, VerDuin (1991) describes how neural networks are used during the manufacture of pharmaceuticals, chemicals, rubber, plastics, metals, ceramics and foods.

The structure of an ANN consists of many simple elements called neurons. Neurons are connected via synapses (connection links) that modulate signals passing through them; each synapse has an associated weight w. The net input N is the function of all transmitted signals x_i and their corresponding weights w_i in a neuron: $N = \zeta(w_i x_i)$ (weighted sum of inputs). Each neuron applies an activation (transfer) function to its net input N in order to provide an output signal for each neuron. The output of this function is the output (activation) of another neuron connected as an input to other neurons (Figure 4.7).

A neural network is characterized by its architecture or the pattern of connections between the neurons. Neurons are arranged in several layers: an input layer that receives the inputs, a hidden layer(s) which transforms the input representation into a new "hidden" representation, and an output layer, the units of which send the predicted values out (i.e. the class label). Input data are signals x_i of the input layer, and initial weights are random values. Then an activation (transfer) function is applied, which determines the output. Normally a hyperbolic tangent function is chosen as the transfer function.

An important point is the learning algorithm or the method of determining the weights on the connections. Before using a network for prediction, it must be trained with known data. This is necessary to ensure that the network provides useful results. The most commonly-used learning algorithm is based on the "back-propagation of errors". While learning, the network compares its output with observed (known) output values of learning data. The effectiveness is usually determined in terms of the root mean square (RMS) error between the actual and the desired outputs averaged over the learning data. After comparison, the network changes weights backwards from output layer to input layer with respect to the output error.

The advantage of the ANN is its capacity for adaptation, i.e. its auto-organization and learning procedure, as well as good generalization ability. However, as explained by Despagne *et al*. (1998), this flexibility can become a pitfall because the number of

weights in an ANN is such that the training data will be rapidly overfitted when the number of samples is too low.

Support vector machines (SVM) for authentication using spectroscopic data

Support vector machines are a relatively new learning method used for binary classification. SVMs are classifiers which have demonstrated high generalization capabilities in many different tasks, including authentication. Several papers have reported on object recognition problems such as face or fingerprint authentication systems (Zhou *et al*., 2007) as well as authentication in food and feed products (Fernández Ocana *et al*., 2004; Fernández Pierna *et al*., 2005a).

The main idea of SVM is to find a decision boundary or hyperplane that separates the data perfectly into two (or more) classes. However, since the data are often not linearly separable, SVM needs to map the data from the initial (wavelength) space to a new higher-dimensional feature space in which the data can be linearly separable. Fortunately, SVM introduces the notion of the kernel trick; the advantage is that this higher-dimensional feature space does not need to be dealt with directly. As long as some necessary conditions are met, some mathematical functions are available to be considered to perform the mapping to the higher space. Linear, polynomial or radial basis Gaussian (RBF) functions are the most widely used kernels. The main difficulty when using SVM is to determine the optimal model, i.e. the optimization of the two parameters presented in SVM – the penalty C that has to be added in order to take into account those samples that cannot be separated, and the width of the Gaussian function σ in the case that a kernel is used. Figure 4.8a shows the discrimination model (or hyperplane) between olive oil and hazelnut oil when a linear kernel is applied to spectroscopic data. Figures 4.8b and 4.8c show the model with two different combinations of C and σ. The best generalization is found when using a linear kernel, or for RBF with $C = 100$ and $\sigma = 0.25$ (Figure 4.8b), i.e. when the kernel is chosen to be close to linearity and when too many objects are misclassified. It can be seen that even if some points are misclassified, the generalization for prediction is expected to be good. However, while better discrimination can be obtained using, for instance, $C = 100$ and $\sigma = 0.035$, the generalization to new samples will not be as good as for the previous model (Figure 4.8c). For this reason, the selection of the parameters for a SVM model is a very important point depending on the aim of the user; in most cases it is better to assure a good prediction for the majority of the data than to have some misclassification errors.

Capron *et al*. (2007) studied the authentication of wines from third countries using the content of 63 different chemical parameters. For this, a database containing more than 1000 samples of authentic and commercial wines from Hungary, the Czech Republic, Romania and South Africa was created. The aim of the study was to evaluate whether it is possible to determine the country of origin of a wine based on its chemical content. Multivariate tools such as partial least squares (PLS) regression, classification and regression trees (CART) and SVM were applied. One SVM model authenticated the genuine wine samples with a success rate of more than 94%.

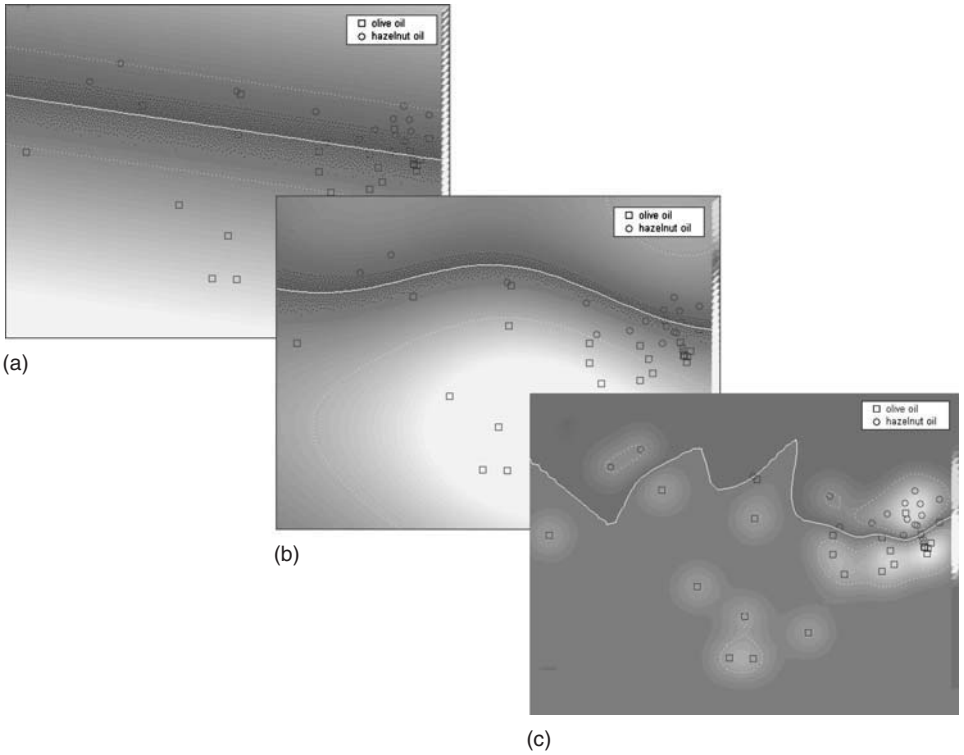

Figure 4.8 (a) SVM model using a linear kernel; (b) SVM model using a RBF kernel with C = 100 and $\sigma = 0.25$; (c) SVM model using a RBF kernel with C = 100 and $\sigma = 0.035$.

For the discrimination of commercial samples, the SVM model determined the country of origin of a wine with a correct classification rate of more than 90%.

Cogdill and Dardenne (2004) presented SVM in a familiar way for people working in chemometrics and NIR spectroscopy. Data sets of NIR spectra and reference values were compiled for apples, meat and corn, and were used for regression analysis. Each consisted of spectra from a typical NIR analyzer, and each sample type had multiple analytes. A second example consisted of animal feed spectra in order to apply discriminant analysis with the objective of detecting meat and bonemeal contamination of ruminant feed. In their study, they concluded that SVM gave a better predictive performance compared to other techniques such as discriminant PLS or ANN, and that SVM methodology has a place in NIR spectroscopy and chemometrics.

Fernández Pierna *et al*. (2005a) studied the development of a new system to detect meat and bone meal (MBM) in compound feed, which will be used to enforce legislation concerning feedstuffs enacted after the European mad cow crisis. For this, data obtained by a NIR imaging spectroscopy system have been analyzed using PLS, ANN and SVM. Although all three chemometric methods were able to model the data effectively, SVM was found to perform substantially better than PLS and ANN, exhibiting a high correct classification rate (>93%) and a much lower rate of false-positive identification (<0.4%). Subsequently, a classification of starches according

to the type of chemical modification was performed by applying different supervised discrimination methods to their associated IR data (Fernández Pierna *et al*., 2005b). Representative samples of each group were available for which the relevant characteristics (chemical modification) were known. SVM showed a correct classification rate of more than 95% when performing leave-one-out cross-validation, and more than 80% for an independent test sample set.

SVM is one of the few computationally-efficient approaches with a well-defined theory which explain its accuracy and robustness. The main advantages of SVM are its ability to minimize the generalization error and to apply non-linear classifiers by mapping the input space to a high-dimensional feature space where linear classification can be performed. Thanks to the kernel trick, SVM can be deployed by using different kernel functions, making SVM independent of the dimensionality of this feature space.

Authentication by FT-NIR

In this section, papers presenting the application of FT-NIR spectroscopic techniques for the authentication of agro-food products are reviewed. Emphasis is put on the aim of the study, the features of the spectroscopic analysis, the chemometric tools used and the results achieved.

Geographic origin assessment

Geographic origin of cheese

The research teams of Bosset and Dufour (Pillonel *et al*., 2003; Karoui *et al*., 2005; Karoui and De Baerdemaeker, 2007) studied the determination of the geographic origin of cheese using spectroscopic methods. They developed rapid, economical, non-destructive and multi-parametric methods for the geographic origin assessment of Emmental cheese and, more generally, the geographic origin of European hard cheese. Each region produces a cheese with typical features, such as the ripening time that can vary from 6 weeks to several months. The originality of the approach used by these authors lies in the fact that they simultaneously investigated several spectroscopic methods (NIR, MIR and fluorescence) and how they complement one another. NIR spectra of cheese present several absorption bands characteristic of overtones and combinations of C–H, N–H and O–H bonds (see Figure 4.2 for an example of cheese NIR spectrum). The spectra are mainly influenced by the O–H groups of water absorption bands (1470 and 1940 nm) and the $C–H_2$ groups of lipids and proteins (2173, 2350 and 2380 nm).

The FT-NIR instrument used (NIRLab N-200, Büchi Labortechnik AG, Flawil, Switzerland) was initially manufactured as an inspection tool to establish and authenticate chemical stock in factories. The NIRLab spectrometer uses a refractive wedge, which oscillates back and forth in the radiation beam to produce a difference in light path based on thickness and refractive index. It uses polarizers on either side of the dual refracting prisms. The moving prism has large amplitude of oscillation.

The consequence is that the oscillation takes place rather slowly and influences the speed of the motion. However, large amplitude allows precise repositioning (Williams and Norris, 2001).

In the first study involving FT-NIR for cheese authentication, Pillonel *et al*. (2003) investigated the potential of NIR and MIR to discriminate between the different geographic origins of Emmental cheeses. They investigated 20 cheese samples from France (Savoie and Bretagne regions), Germany (Allgaü region), Austria (Voralberg region), Finland (Middle region) and Switzerland. In this study, about 150 g of grated cheese was placed in a glass Petri dish and measured by diffuse reflection. Spectra consisted of the means of 64 co-added scans recorded from 1000 to 2500 nm with a spectral resolution of 1.25 nm (2 cm^{-1}). The authors selected spectral regions in order to eliminate zones with low signal-to-noise ratio or with no significant spectral information. To explore and exploit the information included in the spectra, principal component analysis (PCA) and linear discriminant analysis (LDA) were applied. PCA was chosen in order to reduce the number of variables, since principal component scores were used as input for the LDA technique. For LDA, the stepwise backward procedure was used. In addition, the authors used the jackknife classification test to evaluate the robustness of the discriminant functions. The goal of the application of these multivariate statistics was to asses the feasibility of NIR to address the authenticity issue. They focused initially on the discrimination between cheese samples from Switzerland and those coming from the other countries, and afterwards between samples from all the regions combined. LDA allowed a total classification of the cheese samples investigated, since 100% correct classification was obtained for the Emmental cheeses produced in the six European regions. Based on the median normalized distance calculated from the Switzerland group, they determined that the Finland samples were always the easiest group to discriminate. The study concluded the promising potential of the NIR technique. However, with only 20 samples, the models suffered from over-fitting and were consequently not very robust.

The work of Pillonel *et al*. (2003) was followed by a study including the analysis of a larger number of samples and involving NIR, MIR and front-face fluorescence spectroscopy (Karoui *et al*., 2005). In this study, 91 Emmental cheeses from different European countries (Austria, Finland, Germany, France and Switzerland) were investigated using a Büchi NIRLab N-200. The analyzed samples ranged in age from 12 to 16 weeks, and reflected the normal ageing time of commercial cheeses. Spectra were normalized by reducing the area under each spectrum to 1. PCA, factoral discriminant analysis (FDA) and common component and specific weights analysis (CCSWA) were applied. The aim of FDA was to predict membership of an individual cheese to the defined groups; CCSWA was used in order to describe the several spectroscopic data sets obtained on the analyzed samples. CCSWA deals with the total variance in data sets.

After performing FDA, the cheeses were discriminated according to their geographical origin. The first discriminant factor (63% of the total variability) allowed separation of the cheeses from Switzerland and Finland from those from Austria, France and Germany. Using all the discriminant factors, 100% of the cheeses from Austria were correctly classified, followed by 94.7%, 83.3%, 76.9% and 66.7% correct

classification for cheeses from Switzerland, France, Germany and Finland, respectively. As FDA was applied on the first 20 PCs of the PCA, it may be that the data were over-fitted, which would have increased the rate of correct classification. Therefore, the authors concluded that NIR allowed a fairly good recognition of the geographic origin of Emmental cheese. The CCSWA applied on all the spectroscopic and physicochemical data permits the conclusion that the spectral data obtained by infrared (NIR and MIR) and fluorescence spectroscopic methods were independent, and that the two first common components were related to different phenomena observed. The conclusion of the study stated that infrared spectroscopy in combination with chemometrics can be applied to characterize the geographical origin of various dairy products; front-face fluorescence spectroscopy in combination with chemometrics may be used for the identification of cheeses made from either raw or pasteurized milk.

Geographic origin of rice wines

Yu *et al*. (2007) have worked on the discrimination of Chinese rice wine of different geographical origins by NIR. Chinese wine is a sweet, golden wine made from glutinous rice and wheat. Although the Shaoxing rice wine is protected by a standard which defines it, it suffers from unfair competition by Chinese rice wine coming from other geographical origins and sold as Shaoxing rice wine. The NIR spectrum of rice wine spectrum is mainly influenced by absorption bands of O–H groups in water, ethanol absorption bands of C–H and O–H groups (2266 and 2305 nm) and sugar absorption bands (1790 nm). A NIR spectrum of sweet white wine is presented in Figure 4.2. Yu and colleagues used a Nexus FT-NIR spectrometer from the Thermo Nicolet Corporation; this instrument is equipped with a Michelson interferometer, an InGaAs detector and a quartz halogen tungsten lamp (50 W) as a broadband light source. The rice wine samples were analyzed in transmission in a 1-mm quartz cell. Air was used as a reference, and spectra were collected from 800 to 2500 nm with 32 co-added scans and a resolution of 10 nm (16 cm^{-1}). The chemometric tools used in this study were PCA and discriminant PLS using leave-one-out cross-validation, and dummy variables were used as reference values.

In their study, Yu and colleagues analyzed 38 bottles of Chinese rice wine samples of two different brands (i.e. Pagoda brand Shaoxing and Fen Lake brand Jiashan); 29 and 9 samples respectively were used for the calibration and validation sets. The NIR spectra of the samples showed some differences in the 1450-nm region, where the absorption intensities of Jiashan rice wine were slightly higher, while Shaoxing rice wine samples had higher absorption intensities in the 2266- and 2305-nm regions. PCA allowed, on the basis of the two first principal components, the discrimination of samples of the two brands from two different geographic origins in China. Analysis of the eigenvector of the two first principal components indicated that the discrimination is based on bands centered near 1410, 1450, 1884, 2064, 2336 and 2370 nm associated with O–H, C=O and C–H groups; these regions are characteristic of water, ethanol and sugar absorption bands. Using PLS regression in order to construct discriminant functions, it has been shown that the wavelength range of 1300–1650 nm gives the best calibration results in comparison to those obtained with

the full spectral range (i.e. 800–2500 nm). Of the samples in the validation set, 100% were correctly classified.

Geographic origin of saffron

The potential of NIR spectroscopy for the assessment of the geographical origin of saffron has been investigated (Zalacain *et al*., 2005). Saffron consists of the dried stigmas of *Crocus sativus* L. The price of this spice depends on its quality and its geographic origin. Zalacain and colleagues analyzed 111 samples of saffron from leading producers in Iran, Greece and Spain. Near-infrared analysis was performed using a Perkin-Elmer FT-NIR instrument equipped with a near-infrared reflectance accessory. The samples were ground and passed through a 0.5-mm sieve before NIR analysis. Approximately 2 g of each powdered saffron sample was placed onto a quartz sample plate and spectra were collected in the 1000–2500 nm range. The authors performed qualitative and quantitative multivariate analysis using principal component regression (PCR) and discriminant analysis (DA). In order to minimize the risk of overfitting, the standard error of validation was used to select the calibration equation. A spectrum of saffron (Figure 4.2) is highly influenced by the spectral profile of crocetin glycosides which constitute the major component of this material. The first stage of the work concerned the prediction of the chemical composition of the samples by NIRS; 9 and 13 principal components were used to calibrate the spectrometer for the different parameters. The authors stress the importance of the determination of the moisture content – a very important parameter, as it is fraudulent to sell water at saffron price. The second stage of the study concerned the geographical origin discrimination of the saffron samples studied. The correct identification rates were 100%, 95% and 88% for Iranian, Greek and Spanish samples respectively. The interclass distances showed that the Iranian samples were the most different from the Greek and Spanish, which were very similar.

Variety and species assessment

Discrimination of edible oil and fat sources

Discrimination of oils and fats by chemical and physical techniques has been extensively studied by various authors (Baeten *et al*., 2001a). The interest of this topic is the high price differential of oils and fats coming from different sources. The best example is the olive-oil product, which has added-value compared with other vegetable oils and thus the adulteration of it is economically worthwhile. Several researchers have studied the discrimination of oils and fats by spectroscopic methods, mainly by MIR, Raman and NIR techniques (Bewig *et al*., 1994a, 1994b; Baeten *et al*., 1998a, 1998b, 1998c, 2001a; Hourant *et al*., 2000; Yang *et al*., 2003). Considering FT-NIR spectroscopy, the research team of Van de Voort studied its potential to determine parameters such as peroxide value, *cis* and *trans* fatty acid content, iodine value and saponification number, as well as to discriminate edible oils (Dong *et al*., 1997; Li *et al*., 2000a, 2000b, 2000c). The advantage of NIR techniques in comparison with the other vibrational spectroscopy techniques lies in the ease of sample handling

(disposable vials can be used, thus reducing the time of sample preparation and avoiding the necessity for detergent to clean the cell), the possibility of producing at-line, on-line and in-line analytical solutions, and the suitability of this technique for remote use through the use of low-cost fiber-optics. An additional advantage of FT-NIR put to the fore by the team of Van de Voort is the ease of maintaining calibration stability with these instruments, in comparison to the challenge that this topic represents with dispersive NIR instruments.

In their study to discriminate edible oil products, Li *et al*. (2000a) reported on the capability of FT-NIR spectroscopy as a practical at-line process control tool for discriminating various formulated oil products. A typical spectrum of an olive oil is presented in Figure 4.2. NIR spectra of oils and fats are mainly characterized by absorption bands in the vicinities of 1720 nm (C–H vibration of –CH3, –CH2 and =C–H groups), 2140 nm (C–H vibration of =C–H groups) and the 2100–2300 nm region (C–H vibration of –CH3 and –CH2 groups). Li and colleagues used a Bomem FT-NIR analyzer equipped with a deuterated triglycine sulphate (DTGS) detector capable of scanning the spectral range between 833 and 5000 nm. The sample holder employed was a heat-controlled device which permitted the use of glass vials of different diameters. These authors used vials of 8 mm in diameter filled with about 0.5–0.7 ml of sample and temperature controlled at 75 ± 0.2°C. The spectra were collected from 833 to 2222 nm at a resolution of 10 nm; 128 scans per sample were co-added. An air background with an empty vial holder was used. Sample spectra were ratioed against the corresponding air background, and subsequently normalized to take into account inherent variation in the vial path-length. The samples used in this study corresponded to four calibration sets of fats and oils (provided by an oil processor) with different iodine value ranges (i.e. group A, 133.3–134.8; group B, 91.3–96.3; group C, 117.1–118.8; and group D, 113.7–117.0) and one validation set of 35 unknown samples. PLS regression was used as a basis for classification by the setting of discrimination criteria based on the output obtained from calibration models: NIR predicted iodine value; the spectral residual and the factor scores were used to discriminate the different groups. The NIR predicted iodine value criterion; the factor scores criterion as well as the combination of the three discrimination criteria gave the best results. The original part of the work was the definition of two sets of limits – (i) the inner region representing zones where a sample is considered to form part of the targeted population and (ii) the intermediate region where the unknown samples are likely to be part of the population – and the outside region where the unknown samples are classified as definitely not belonging to the population. The inner region was defined on the basis of PLS regression results obtained from the calibration set. The intermediate region for each criterion was included in order to be able to adjust the limits according to the deviation accepted by the manufacturer. The authors used the limits of the inner region added or subtracted by the root mean square error obtained from cross-validation of the calibration step in order to set the intermediate region limits for the targeted criterion. Li *et al*. (2000a) concluded, on the basis of the correct prediction of the validation set samples, that their approach allowed discrimination of the samples according to their group of origin. Moreover, the authors underlined the power of the approach to detect unusual samples (or, more

exactly, samples with characteristics not included in the calibration stage, i.e. a blend of samples from different categories) as not coming from one of the pre-defined groups. FT-NIR with the combined predictive and discriminant capabilities of PLS is presented as a powerful and practical analytical quality control tool.

Yang *et al*. (2007) also studied the discriminant possibilities offered by FT-NIR for the discrimination of edible oils. In their work they compared the FT-NIR results with those of FT-MIR and FT-Raman obtained on the same samples. For their near-infrared analysis they used a Nicolet 870 spectrometer including a DTGS detector and a transmission quartz cell which was cleaned with pure chloroform and dried with nitrogen gas. Each spectrum corresponded to 256 co-added scans with a resolution of 10 nm. Spectra were collected between 1250 and 5000 nm using an air spectrum as a background. Samples such as butter, cod-liver oil, lard, canola oil, coconut oil, corn oil, olive oil, peanut oil, safflower oil and soybean oil were studied. A total of 80 samples and 30 samples were used for the calibration and validation sets respectively, although the calibration and validation sets were not fully independent as the samples were issued from the same batch. The authors used linear discriminant analysis (LDA) and canonical variate analysis (CVA) in combination with principal component analysis (PCA) and partial least squares (PLS) as data compression methods. Calculated percentages of correct classification for the validation samples were between 85.6 and 92.2% for the 500–1250 nm region and 84.4–93.3 for the 1540–2500 nm region. The authors concluded that FT-MIR (95.6–98.9% correct classification of validation samples), FT-Raman (85.6–94.4% correct classification of validation samples) and FT-NIR spectroscopy (84.4–93.3% correct classification of validation samples) techniques can be used for rapid classification of edible oils and fats without the need for sample preparation. In this study, the least efficient technique seemed to be the FT-NIR spectroscopic method.

Detection and quantification of olive-oil adulteration is also an important challenge in the discrimination of vegetable oils. Several spectroscopic techniques have been tested in order to evaluate their potential in detection of this kind of olive oil fraud (Baeten *et al*., 2001a). Kasemsumran *et al*. (2005) studied the potential of FT-NIR and PLS processing to discriminate and quantify adulterated olive oils. They used a Bruker Vector 22/N FT-NIR spectrometer equipped with an InGaAs detector. Spectra were collected in the transmittance mode from the 833 to 2198 nm region with a resolution of 2.5 nm and 32 co-added scans. The sample temperature was kept at 25 ± 0.2°C. Spectra were treated by means of multiplicative scatter correction (MSC), Savitsky-Golay first derivative and Savitsky-Golay smoothing before applying multivariate analysis. PLS regression analyses were used to calibrate the spectrometer to discriminate between the adulterated and the genuine samples. Four NIR regions were tested separately to build the PLS models. Calibration and validation sets included 200 and 80 mixtures respectively, spiked with one of the four different adulterants studied (i.e. corn oil, hazelnut oil, soya oil or sunflower oil). Olive oil was mixed with the adulterants at different percentages (i.e. 2–50% w/w); a weakness of the study, however, was that the authors selected only one sample for each type of oil considered. PLS models were constructed for each adulterant type and for all considered adulterants. All the discriminant PLS models for classifying the adulterant

types in olive oils gave a correct classification rate higher than 95%, irrespective of the data pre-treatment or the spectral range used. The best prediction results of the PLS calibration models had a root mean square error of prediction (RMSEP) lower than 0.5 for corn-oil, hazelnut-oil and soya-oil adulterants, and lower than 1.1 for sunflower-oil adulterant.

Another interesting study to consider in this review of the FT-NIR methods proposed for oils discrimination is that published by Oliveira *et al*. (2007). In this study, the authors investigated the potential of FT-NIR and FT-Raman spectroscopy for the detection of diesel/biodiesel in vegetable oil. Oliveira and colleagues used a Bruker Equinox 55 FT-NIR instrument equipped with a germanium detector. Spectra were recorded using an immersion transflectance accessory with an optical path-length of 2 mm. The spectral resolution was set at 5 nm, and each spectrum was the result of 16 co-added NIR measurements. PCR, PLS and ANN calibration procedures were tested. One hundred and seventy-five blends corresponding to mixtures of diesel/biodiesel with vegetable oils (i.e. soybean oil, castor oil, palm-tree oil) in the range of 0–5% (w/w) were used in order to calibrate the spectrometer. An independent validation set was used to test the established models. For the construction of the PLS and PCR calibration models, selection of the spectral region to be used has been carried out on the basis of two experimental parameters: (i) the spectral distribution of the standard deviation in the absorbance values for the set of samples used in the calibration stage, and (ii) the spectral distribution of the relative standard deviation in the absorbance for a reduced set of representative samples. The former parameter allows the selection of the spectral region presenting the largest variation that includes most of the variability in the calibration samples, while the latter makes it possible to put to the fore the regions presenting poor signal-to-noise ratios. PCR and PLS calibration models for a quantitative detection of diesel/biodiesel blends adulterated with vegetable oils produces a RMSEP of 0.262 and 0.238 respectively. It is interesting to mention that RMSEP obtained with FT-Raman data was three to six times higher. For the ANN calibration models, the spectral regions used were selected on the basis of the spectral distribution of the standard deviation of the absorbance values of first-derivative spectra of samples used in the calibration. RMSEP of 0.371 and 0.092 for the quantitative determination of vegetable oils in diesel/biodiesel blends were obtained for the FT-NIR and FT-Raman data respectively.

Discrimination of botanical origin of honey

Ruoff and colleagues (2006) studied the botanical origin of honey using FT-NIR. The authors used a Büchi NIRLab N-200. Honey NIR spectra were collected in the 1000–2500 nm spectral range with a resolution of 2.5 nm and 64 co-added scans per sample. Honey samples were heated at 50°C for 9 hours before analysis, and poured into a clean glass Petri dish covered with the transflection plate defining a 0.6-mm path-length. Figure 4.2 presents a typical FT-NIR spectrum of honey. The most important absorption bands are observed in the 1400–2380 nm region, with a water band at 1940 nm and several bands in the 1540–2380 nm region characteristic of C–O and C–C bond vibrations of saccharides. The total of 364 honey samples from 7 years

of production originated predominantly from Switzerland. Samples were classified according to 8 honey types; 185 and 179 samples constituted the group of unifloral and multifloral samples respectively. PCA, PLS and LDA were applied to evaluate the potential of NIR data to discriminate honey samples according to their origin. Using LDA, between 29 and 100% of the unifloral honey samples from the validation set were correctly classified while only 19% of the multifloral were correctly classified. Unifloral samples coming from acacia, fir honeydew and chestnut were the easiest to discriminate by LDA.

Discrimination of pear varieties

Fourier transform near-infrared spectroscopy was also explored as a tool to discriminate samples of different pear varieties (Fu *et al*., 2007). In this study, a Nexus intelligent FT-NIR spectrometer (Thermo Electron Corporation) equipped with an InGaAs detector was used and NIR spectra were collected in the 800–2500 nm range with a resolution of 1.25 nm and a co-added scan number of 64. The authors used a fiber-optic probe to collect diffuse reflectance spectra. For each fruit sample three NIR measurements were made, each at a different location about 120° apart around the equator of the fruit. A total of 240 samples from three varieties of pear were used to study the potential of the FT-NIR technique. Spectra of fruit reveal absorption bands in the vicinity of 970, 1450 and 1940 nm, associated with the O–H vibration of water, and around 1190 and 1790 nm related to C–H vibrations of sugar and other organic matter. Fu and colleagues used discriminant analysis (DA), discriminant partial least squares (DPLS) and probalistic neural network methods (PNN) to calibrate the spectrometer. DA and DPLS models were developed using three spectral regions, i.e. 800–1500 nm, 1500–2500 nm and 800–2500 nm. The PNN method includes four layers, and is a feed-forward network with no back-propagation. The inputs used were spectral data recorded as absorbance at each wavelength. Results obtained in this study indicated the high potential of NIR to classify and discriminate fruits of different varieties. High accuracy and correct classification higher than 99% were obtained whatever the multivariate protocol used (DA, DPLS or PNN).

Detection of castor bean meal

Rodriguez-Saona and colleagues (2000) have proposed the FT-NIR technique to rapidly quantify castor bean meal (CBM) in a selection of flour-based products. CBM contains the extremely potent cytotoxic protein ricin. The authors worked with a Perkin-Elmer Spectrum Identicheck FT-NIR spectrometer, and used capped transparent vials to analyze the samples. Reflectance spectra were collected in the 1000–2500 nm NIR range with a resolution of 2.5 nm and a number of co-added scans equal to 50. Prior to calibration, spectra were centered and baseline corrected using an offset. Then, spectra were transformed using the multiplicative scatter correction pre-treatment in order to correct for the scatter effect of the particles. PCA and PLSR multivariate analyses were used to explore the NIR data. PCA analysis allowed discrimination between raw materials (i.e. CBM, soybean meal, powdered meal, tofu, egg yolk and egg white). PLSR models were able to differentiate between CBM

contamination and the addition of other protein-rich products (e.g. corn meal, egg white, defatted soybean) to the matrices. On the basis of this model, quantification of CBM contamination could be determined at level of >0.3% and 0.6% (w/w) in selected wheat flour and blueberry pancake mixes.

Discrimination of leaves from different strawberry varieties

The potential of FT-NIR for the authentication and classification of strawberry leaf varieties has been investigated by López (2002). In this study, a Paragon IdentiCheck FT-NIR system was used, recording spectra from the 1000–2500 nm range at a resolution of 2.5 nm with 32 co-added scans. Five different strawberry varieties were investigated. For each variety, spectra from both sides of the leaves and of the vascular system were recorded. The FT-NIR spectral data were analyzed using PCA and SIMCA methods. While all the varieties show very similar NIR spectra, small differences were still observed. Identification of the materials was possible using interclass distances. The authors concluded that FT-NIR enables the authentication of all strawberry varieties and their origin.

Process type assessment

Discrimination of tea categories

An interesting demonstration of the potential of NIR for the discrimination of food products has appeared in work concerning the identification of tea categories (Zhao *et al*., 2006; Chen *et al*., 2007). The most popular categories of tea are the green and the black teas. Both products involve drying and roasting of the leaves, the black tea requiring an additional step of fermentation. If the fermentation is only partially carried out, the Oolong tea category is obtained. In both studies, a Nicolet Nexus 670 FT-NIR instrument was used with standard quartz cups. Spectra were collected from 909–2632 nm at a resolution of 1.205 nm and with 64 co-added scans. Figure 4.2 presents the spectrum of a green tea sample. Water absorption bands are observed in the vicinities of 1940 and 1430 nm, bands of the carboxylic groups around 1870 nm, and bands of C–H groups around 1385, 1740 and 1720 nm. During the analysis, the authors excluded the absorption bands of water as well as the 909–1111 nm region, which exhibited a high noise level. A total of 150 samples were analyzed, comprising 50 samples of each category (i.e. green tea, black tea, Oolong tea) which were obtained from a total of 9 different geographic origins. Different data pre-processing methods were tested, including standard normal variate transformation, first and second derivatives, and smoothing. Principal component analysis (PCA), support vector machines (SVM) and back-propagation artificial neural network (BP-ANN) methods were used to exploit the variation included in the spectra, and to calibrate the spectrometer for the discrimination of tea categories. PCA analysis showed that the first three principal components were adequate to discriminate between the three categories of teas, although the samples used had considerable differences in their botanical, genetic and agronomical characteristics. For the calibration of the spectrometer with SVM and BP-ANN, the samples were split into calibration and validation sets with a proportion of 3/5 and 2/5 respectively for each category. For the green, black

and Oolong teas, 95%, 100% and 90% respectively of the validation samples were correctly classified using the SVM model developed. The results of the BP-ANN model were 75%, 100% and 80% correct classifications, respectively.

Discrimination and authentication of alcoholic beverages

Pontes and colleagues (2006) proposed a strategy in which FT-NIR and chemometric methods could be used in the classification and verification of adulteration in whiskeys, brandies, rums and vodkas. The idea was that NIR spectroscopy could be used as a screening method, and more time-consuming wet chemistry analytical techniques would then only be applied to samples showing a positive adulteration result in order to confirm the NIR result. They used a Perkin-Elmer Spectrum GX FT-NIR spectrometer, and the sample was placed in a 1-mm path-length quartz flow cell. NIR absorbance values were collected from 1100–2500 nm at a resolution of 1.25 nm and using 64 co-added scans. Analysis was performed on 69 pure and adulterated samples (some of which were adulterated with ionized water, ethanol or methanol). The sample set was divided into calibration and validation sets comprised of 40 and 29 samples respectively. Second-derivative spectra were calculated with a Savitzky-Golay filter. PCA and SIMCA methods were used for the multivariate analysis of the spectral data. PCA analysis of the calibration set allowed identification of the whiskey and vodka samples using only the two first principal components. The third and fourth PCs allowed the discrimination of brandy and rum samples. SIMCA models were constructed (n = 40) and consequently applied to classify the samples as adulterated or authentic. The prediction ability of each model was evaluated on a test set (n = 29) consisting of laboratory-prepared samples and verified adulterated alcoholic beverages supplied by a regulatory agency. The authors observed that all the samples in the test set were correctly predicted as adulterated or genuine, with a 95% confidence level.

Fourier transform near-infrared spectroscopy was also used to measure the percentage of sugar in grape must, and to discriminate between different must samples in terms of their free amino nitrogen (FAN) values (Manley *et al*., 2001). For the NIR measurements, a Perkin-Elmer Spectrum IdentiCheck spectrometer equipped with a 0.5-mm path-length quartz cell was used. Spectra of 97 samples were collected between 1000 and 2500 nm at a resolution of 2.5 nm and using 16 co-added spectra. The must samples could be classified in terms of their FAN values when SIMCA was applied as a classification method, with correct recognition rates exceeding 80% in all cases. It was also shown by these authors that FT-NIR proved to be a rapid method of discriminating between Chardonnay wine samples (n = 107) in terms of their malolactic fermentation status, using SIMCA, with recognition rates exceeding 88%. Moreover, table wines (n = 200) were also successfully discriminated in terms of their ethyl carbamate content, with recognition rates exceeding 80%. Later, Manley and her collaborators (Manley *et al*., 2003a) illustrated the potential of FT-NIR to classify four different classes of rebate brandy. The brandy samples were analyzed by collecting 16 co-added scans, from 700–2500 nm, also using a Perkin-Elmer Spectrum IdentiCheck spectrometer and presented in a 1-mm path-length quartz cell. Using SIMCA, it was possible to discriminate between the hardest and the softest brandy class of one season.

Discrimination of marked age and vintage year of alcoholic beverages

Yu and colleagues (2006) investigated the classification of rice wine with different marked ages based on FT-NIR spectroscopy. They used a Nexus FT-NIR spectrometer (Thermo Nicolet Corporation) to collect the NIR spectra from the 800–2500 nm region. The samples were scanned in a 1-mm optical path-length rectangular quartz cell at 10 nm spectral resolution and using 32 co-added scans. The 69 rice wine samples were from two different brands, of three different marked ages (1, 3 and 5 years) and two vintages (2004 and 2005). PCA and DA analysis were applied. Correct classifications of 100, 94.1 and 100% were obtained for the calibration samples with marked ages of 1, 3 and 5 years respectively. The percentage of correct classification of a validation sample set was 94.4%.

The potential to classify 3-year-old brandy from different seasons (1999, 2000 and 2001) was studied by Manley *et al*. (2003b). In this study, a Perkin-Elmer Spectrum IdentiCheck 2.0 FT-NIR system equipped with a 1-mm path-length quartz cell was used. Spectra were collected in the 700–2500 nm range, with 16 co-added scans and a spectral resolution of 5 nm. A total of 191 samples of unblended 3-year-old brandy were analyzed. PCA and SIMCA methods were applied to evaluate the discriminant power of NIR data. PCA analysis showed that samples from the 2001 season were the easiest to discriminate, while there was an overlap between samples from the 1999 and 2000 seasons.

Discrimination of the age of cheese

FT-NIR has also shown potential for the discrimination of cheese on the basis of its age. Cattaneo *et al*. (2005) worked with a MPA FT-NIR from Bruker Optics equipped with a fiber-optic probe to study the shelf-life of Crescenza cheese. This cheese represents 40% of the Italian fresh cheese market, and is only produced from pasteurized whole cow's milk. Crescenza cheese suffers from a structural and chemical modification during shelf-life. Spectra were collected from 833–2500 nm at a resolution of 10 nm and with 16 co-added scans. A total of 126 cheese samples from two types of production using different technological processes, and having been stored for 20 days, were used. The NIR spectral data were autoscaled, and second-derivative data were acquired before multivariate analysis. PCA was used for exploratory analysis of the NIR spectra. This method allowed a satisfactory sample distribution that followed the evolution of the cheeses. A clear distinction could be made between fresh (0–6 days' storage) and aged/old Crescenza cheese samples (8–20 days' storage). Applying PCA on FT-NIR spectroscopic data of a reduced range permitted the discrimination between the aged (8–10 days' storage) and older samples (14–20 days' storage). The authors concluded that the main advantage of using a spectroscopic technique was the possibility rapidly to establish a profile for the product associated with its total composition and quality.

Authentication by FT-NIR microscopy

The first study proposing the use of FT-NIR microscopy (NIRM) for authentication purpose was that published by Piraux and Dardenne for feed authentication (Piraux

and Dardenne, 1999). They proposed the use of a new method, based on NIR microscopy, for the detection and quantification of meat and bone meal (MBM) in compound feed in order to comply with the ban following the BSE crisis. Samples were measured using an AutoImage Microscope connected to a Perkin-Elmer FT-NIR, and analyzed using ANNs. With this NIRM instrument, the infrared beam is focused on each particle of a sample using a microscope in order to collect the NIR spectrum (1100–2500 nm). A collection of several hundred spectra is made, which represents the molecular NIR signature of a particle from an ingredient in the compound feed. A predictive discriminant analysis was applied to classify particles into either meat particles or particles of a different nature – i.e. not meat. An artificial neural network (multilayer perceptron network with back-propagation based on the partial least squares scores) was used to discriminate between the respective groups. Their results showed an overall error rate lower than 0.65%, giving an indication of the potential of this technique for the detection of MBM. Additionally, Baeten *et al*. (2001b) used a near-infrared microscope for the detection and quantification of ingredients of animal origin in feedingstuffs. Satisfactory results were obtained for the detection and identification of meat meal, meat and bone meal, bone meals, blood meal, fish meal (muscle chair, bone fish and scale), feather meal, poultry meal, milk powder and egg meal. Moreover, their study proved that 0.5% MBM in a compound feedingstuff can be detected by NIR microscopy.

Gizzi *et al*. (2003) published an overview of the different tests for the detection of animal tissues in feed, including PCR, immunoassay, microscopy and NIR microscopy. In their paper, they showed the main characteristics of NIRM as well as the weaknesses of the method. The main advantages of NIRM are that (i) it is directly based on NIR information; (ii) it can be confirmed by another method (e.g. PCR) that can be used as legal evidence in case of fraud; (iii) NIRM does not require expertise; (iv) it is a non-destructive method; and (v) a single analysis could enable a wide range of feed ingredients to be detected. The weaknesses involve the need to develop sample databases, the limit of detection, and the cost of the equipment. Therefore, these authors concluded that NIRM is the most suitable method for large screening applications in terms of sample output and automation, and that this method is able to achieve limits of detection (LOD) as low as 0.1%. A few years later, Baeten *et al*. (2005) have decreased this LOD by detecting the presence of MBM at concentrations as low as 0.05% mass fraction by the use of NIR microscopy applied to the sediment fraction of the feed. More recently, De la Haba *et al*. (2007) have proposed a method based on NIRM to check the presence of ruminant tissue in fish meal or in compound feeds containing fish meal in order to allow only fish meal to be used in ruminant feed. The use of pure fish material in the animal production chain poses no risk, and it is accepted that fish do not carry Transmissible Spongiform Encephalopathy (TSE). Thus, they have worked on methods permitting the detection and identification, at species level, of animal by-products included in compound feed. NIRM spectra allowed the construction of discrimination equations using support vector machines (SVM) as a chemometric tool. As a result, clear discrimination between fish meal and meal of other animal species is possible, with a high average success rate of 95%. In contrast to optical microscopy, NIRM offers one clear advantage: it is

not dependent on the subjectivity of the analyst, because particles are identified from their NIR spectral fingerprint and not by visual inspection.

NIRM has also been applied for authentication in different areas. Wilson and Moffat (2004) used a Perkin-Elmer FT-NIR IdentiCheck spectrophotometer coupled with a microscope for the authentication of Viagra tablets. A single spectrum for each tablet was taken, and some chemometric procedures (such as PCA or PLS) were used to identify the active ingredient by comparing it with the real pure compound. This study is important in the fight against counterfeit pharmaceuticals by using the spatial distribution of the active compounds. Another area of application of NIRM is in forensic laboratories to determine, among other things, the type of explosive used in terrorist attacks, or to detect the presence of illegal drugs.

An alternative to NIRM is the use of a more recent technology called NIR imaging. This technology is a powerful approach to remote sensing in precision agriculture and mineralogy, among other areas. The success of NIR imaging can be considered as due to a combination of different factors: high-performance and uncooled NIR sensitive focal plane array detectors, digitally-tunable infrared optical filters, the drastic increase in computer speed, and the increased capacity of laboratory computing platforms. The integration of these elements has already shown promising results in the determination of quality parameters for complex matrices such as pharmaceutical blends, detection of apple surface defects and contamination or the detection of animal compounds in feeding stuff (Fernández Ocana *et al*., 2004). NIR imaging allows the contemporaneous collection of spatial and spectral (and therefore chemical) information characterizing samples under test.

Conclusions

This chapter has shown applications of FT-NIR spectroscopic and microscopy techniques for the authentication of agro-food products. The potential of this technique to assess different authenticity issues is obvious, and will be used as new approaches for at-line, on-line and in-line control. The forthcoming challenge for this technique is to develop adequate strategy for the construction of large data sets in order to calibrate any given instrument. The strategy should include the extraction of the information in such a way that it can be used in qualitative and quantitative analysis as well as the implementation in routine control.

References

Baeten, V. and Aparicio, R. (2000). Edible oils and fats authentication by Fourier transform Raman spectrometry. *Biotechnology, Agronomy, Society and Environment*, **4**(4), 196–203.

Baeten, V. and Dardenne, P. (2002). Spectroscopy: developments in instrumentation and analysis. *Grasas y Aceites*, **53**(1), 45–63.

Baeten, V., Hourant, P., Morales, M.T. and Aparicio, R. (1998a). Oil and fat classification by FT-Raman spectroscopy. *Journal of Agricultural and Food Chemistry*, **46**, 2638–2646.

Baeten, V., Morales, M. T., Aparicio, R. (1998b). In: J. Sanchez, E. Cerda-Olmedo and E. Martinez-Force (eds), *Oil and Fat Analysis by FT-Raman Spectroscopy*, 13th International Symposium on Plant Lipids, 5–10 July, Seville, Spain. Seville: Université de Séville, pp. 18–21.

Baeten, V., Morales, M.T. and Aparicio, R. (1998c). Oil and fat analysis by FT-Raman spectroscopy. In: J. Sanchez, E. Cerda-Olmedo and E. Martinez-Force (eds), *Advances in Lipids Research*. Seville: University of Seville, pp. 18–21.

Baeten, V., Dardenne, P. and Aparicio, R. (2001a). Interpretation of Fourier transform Raman spectra of the unsaponifiable matter in a selection of edible oils. *Journal of Agricultural and Food Chemistry*, **49**, 5098–5107.

Baeten, V., Michotte-Renier, A., Sinnaeve, G. and Dardenne, P. (2001b). Analysis of feeding stuffs by near infrared microscopy (NIRM): detection and quantification of meat and bone meal (MBM). In: *8th International Symposium on Food Authenticity and Safety (FASIS)*, October, Eurofins Secretariat, Nantes, France. Eurofins.

Baeten, V., Von Holst, C., Garrido Varo, A. (2005). Detection of banned meat and bone meal in feedstuffs by near-infrared microscopic analysis of the dense sediment fraction. *Analytical Bioanalytical Chemistry*, **382**, 149–157.

Bertrand, D. and Baeten, V. (2006). Instrumention. In: D. Bertrand and E. Dufour (eds), *La spectroscopie infraouge*. Paris: Lavoisier, pp. 247–305.

Bewig, K., Clarke, A.D. and Roberts, C. (1994a). Discriminant analysis of vegetable oils by near infrared reflectance spectroscopy. *Journal of American Oil Chemical Society*, **71**(2), 195–200.

Bewig, K., Clarke, A.D., Roberts, C. and Unklesbay, N. (1994b). Discriminant analysis of vegetable oils using near-infrared spectroscopy. In: G.D. Batten, P.C. Flinn, L.A. Welsh and A.B. Blakeney (eds), *Leaping Ahead with Near Infrared Spectroscopy*. Melbourne: NIR Spectroscopy Group, Royal Australian Chemical Institute.

Brettel, T.A., Butler, J.M. and Saferstein, R. (2005). Forensic science. *Analytical Chemistry*, **77**(12), 3839–3860.

Capron, X., Walczak, B., de Noord, O.E. and Massart, D.L. (2005). A modification of the ICOMP criterion for estimation of optimum complexity of PCR models. *Journal of Chemometrics*, **19**, 308–316.

Capron, X., Verbeke, J. and Massart, D.L. (2007). Multivariate determination of the geographical origin of wines from four different countries. *Food Chemistry*, **101**, 1585–3597.

Cattaneo, T.M.P., Giardina, C., Sinelli, N. *et al*. (2005). Application of FT-NIR and FT-IR spectroscopy to study the shelf-life of Crescenza cheese. *International Dairy Journal*, **15**, 693–700.

Chen, Q., Zhao, J., Fang, C.H. and Wang, D. (2007). Feasibility study on identification of green, black and Oolong teas using near-infrared reflectance spectroscopy based on support vector machine (SVM). *Spectrochimica Acta Part A*, **66**, 568–574.

Ciurczak, E.W. (1991). What's new in spectroscopy instrumentation? *Spectroscopy International*, **3**(3), 18–30.

Cogdill, R.P. and Dardenne, P. (2004). Least-squares support vector machines for chemometrics; an introduction and evaluation. *Journal of Near Infrared Spectroscopy*, **12**, 93–100.

Davies, T. (1998). The history of near infrared spectroscopic analysis: past, present and future – from sleeping technique to the morning star of spectroscopy. *Analysis Magazine*, **26**, M17–M19.

De la Haba, M.J., Fernández Pierna, J.A., Fumiere, O. *et al*. (2007). Discrimination of fish bones from other animal bones in the sedimentation fraction of compound feeds by near infrared microscopy. *Journal of Near Infrared Spectroscopy*, **15**(2), 81–88.

Dennis, J. (1998). Recent developments in food authentication. *Analyst*, **123**, 151R–156R.

Despagne, F., Walczak, B. and Massart, D.L. (1998). Transfer of calibrations of near infrared spectra using neural networks. *Applied Spectroscopy*, **52**(5), 732–745.

Dong, J., Van de Voort, F.R. and Ismail, A.A. (1997). Stochiometric determination of hydroperoxides in oils by Fourier transform near-infrared spectroscopy. *Journal of American Official Analytical Chemists*, **80**(2), 345–352.

Downey, G., Daniel Kelly, J. and Petisco Rodriguez, C. (2006). Food authentication – has near infrared spectroscopy a role? *Spectroscopy Europe*, **18**(3), 10–14.

Fernández Ocana, M., Neubert, H., Przyborowska, A. *et al*. (2004). BSE control: detection of gelatine-derived peptides in animal feed by mass spectrometry. *The Analyst*, **129**, 111–115.

Fernández Pierna, J.A., Baeten, V., Michotte Renier, A. *et al*. (2005a). Combination of SVM and NIR imaging spectroscopy for the detection of MBM in compound feeds. *Journal of Chemometrics*, **18**(7–8), 341–349.

Fernández Pierna, J.A., Volery, P., Besson, R. *et al*. (2005b). Classification of modified starches by FTIR spectroscopy using support vector machines. *Journal of Agricultural and Food Chemistry*, **53**(17), 6581–6585.

Fu, X., Zhou, Y., Ying, Y. *et al*. (2007). Discrimination of pear varieties using three classification methods based on Near-Infrared spectroscopy. *American Society of Agricultural and Biological Engineers*, **50**(4), 1–7.

Gizzi, G., Van Raamsdonk, L.W.D., Baeten, V. *et al*. (2003). An overview of tests for animal tissues in feeds applied in response to public health concerns regarding bovine spongiform encephalopathy. *Scientific and Technical Review – Office International des Epizooties*, **22**(1), 311–331.

Hourant, P., Baeten, V., Morales, M.T. *et al*. (2000). Oil and fat classification by selected bands of near infrared spectroscopy. *Applied Spectroscopy*, **54**(8), 1168–1174.

Karoui, R. and De Baerdemaeker, J. (2007). A review of the analytical methods coupled with chemometric tools for the determination of the quality and identity of dairy products. *Food Chemistry*, **102**, 621–640.

Karoui, R., Dufour, E., Pillonel, L. *et al*. (2005). The potential of combined infrared and fluorescence spectroscopies as a method of determination of the geographic origin of Emmental cheeses. *International Dairy Journal*, **15**, 287–298.

Kasemsumran, S., Kang, N., Christy, A. and Ozaki, Y. (2005). Partial least squares processing of near-infrared spectra for discrimination and quantification of adulterated olive oils. *Spectroscopy Letters*, **38**, 839–851.

King, P.L., Ramsey, M.S., McMillan, P.F. and Swayze, G. (2004). Laboratory Fourier transform infrared spectroscopy methods for geologic samples. *Mineral Association of Canada*, **33**, 57–91.

Lachenal, G. (1998a). Structural investigations and monitoring of polymerisation by IR spectroscopy. *Journal of Near Infrared Spectroscopy*, **6**, 299–306.

Lachenal, G. (1998b). Analyze par spectroscopie proche infrarouge (PIR) et applications aux polymères. *Analysis Magazine*, **26**, M20–M29.

Li, H., Van De Voort, F.R., Sedman J., Ismail, A.A. (1999). Rapid determination of cis and trans content, iodine value, and specification number of edible oils by fourier transform near-infrared spectroscopy. *Journal of American Oil Chemist's Society* **76**(4), 491–497.

Li, H., Van De Voort, F.R., Ismail, A.A. *et al*. (2000a). Discrimination of edible oil products and quantitative determination of their iodine value by FT NIR spectroscopy. *Journal of the American Oil Chemist's Society*, **77**(1), 29–36.

Li, H., Van De Voort, F.R., Ismail, A.A. and Cox, R. (2000b). Determination of peroxide value by fourier transform near-infrared spectroscopy. *Journal of the American Oil Chemist's Society*, **77**(2), 137–142.

Li, H., Van De Voort, F.R., Ismail, I.A. *et al*. (2000c). Trans determination of edible oils by fourier transform near-infrared spectroscopy. *Journal of the American Oil Chemist's Society*, **77**(10), 1061–1067.

Li, Y., Brown, C.W., Sun, F.M. *et al*. (1999). Non-invasive fermentation analysis using an artificial neural network algorithm for processing near infrared spectra. *Journal of Near Infrared Spectroscopy*, **7**, 101–108.

Li, Z., Chu, X., Mouille, G. *et al*. (1999). The localization and expression of the class II starch synthases of wheat. *Plant Physiology*, **120**, 1147–1155.

López, M.G. (2002). Authentification and classification of strawberry varieties by near infrared spectral analysis of their leaves. In: A.M.C. Davies and R.K. Cho (eds), Proceeding of the 10th International Conference on Near-Infrared Spectroscopy (NIR2001), Korea, June. Wellington: NIR Publications, pp. 335–338.

Manley, M., Van Zyl, A. and Wolf, E.E.H. (2001). The evaluation of the applicability of Fourier transform near-infrared (FT-NIR) spectroscopy in the measurement of analytical parameters in must and wine. *South African Journal for Enology and Viticulture, Stellenbosch*, **22**(2), 93–100.

Manley, M., De Bruyn, N. and Downey, G. (2003a). Classification of South African brandy with near infrared spectroscopy. *NIR News*, **14**(5), 3–19.

Manley, M., De Bruyn, N. and Downey, G. (2003b). Classification of three year old, unblended South African brandy with near infrared spectroscopy. *NIR News*, **14**(5), 8–11.

Müller, A. and Steinhart, H. (2007). Recent developments in instrumental analysis for food quality. *Food Chemistry*, **102**(2), 436–444.

Oliveira, F.C., Brandao, C.R., Ramalho, H.F. *et al*. (2007). Adulteration of diesel/biodiesel blends by vegetable oil as determined by Fourier transform (FT) near infrared spectrometry and FT-Raman spectroscopy. *Anaytical Chimica Acta*, **587**, 194–199.

Osborne, B.G. and Fearn, T. (1986). Near infrared data handling and calibration by multiple linear regression. In: G.D. Batten, P.C. Flinn, L.A. Welsh and A.B.

Blakeney (eds), *Leaping Ahead with Near Infrared Spectroscopy*. Melbourne: NIR Spectroscopy Group, Royal Australian Chemical Institute.

Pasquini, C. (2003). Near infrared spectroscopy: fundamentals, practical aspects and analytical applications. *Journal of Brazilian Chemistry Society*, **14**(2), 198–219.

Pillonel, L., Luginbühl, W., Picque, D. *et al*. (2003). Determining the geographic origin of emmental cheese by mid- and near-infrared spectroscopy. *NIR News*, **15**, 14–16.

Piraux, F. and Dardenne, P. (1999). Feed authentification by near infrared microscopy. In: A.M.C. Davies and R. Giangiacomo (eds), *Proceedings of the 9th International Conference, Verona, Italy*. Wellington: NIR Publications, pp. 535–541.

Planck, M. (1925). *A Survey of Physical Theory* (transl. R. Jones and D.H. Williams). London: Methuen & Co. Ltd. (Dover editions 1960 and 1993).

Pontes, M.J.C., Santos, S.R.B., Araujo, M.C.U. *et al*. (2006). Classification of distilled alcoholic beverages and verification of adulteration by near infrared spectrometry. *Food Research International*, **39**, 182–189.

Rodriguez-Saona, L.E., Fry, F.S. and Calvey, E.M. (2000). Use of Fourier transform near-infrared reflectance spectroscopy for rapid quantification of castor bean meal in a selection of flour-based products. *Journal of Agricultural and Food Chemistry*, **48**, 5169–5177.

Ruoff, K., Luginbühl, W., Bogdanov, S. *et al*. (2006). Authentication of the botanical origin of honey by near-infrared spectroscopy. *Journal of Agricultural and Food Chemistry*, **54**(18), 6867–6872.

Van der Reyden, D. (1996). *Identifying the Real Thing*. Document prepared for School for Scanning, sponsored by the National Park Service and managed by the Northeast. New York, NY: Document Conservation Center.

VerDuin, W.H. (1991). Neural nets for custom formulation. In: R. Maus and J. Keyes (eds), *The Handbook of Expert Systems in Manufacturing*. New York, NY: McGraw-Hill, pp. 515–524.

Williams, P.C. and Norris, K. (eds) (2001). *Near-Infrared Technology in the Agricultural and Food Industries*, 2nd edn. St Paul, MN: American Association of Cereals Chemists.

Wilson, N.D. and Moffat, A.C. (2004). The use of near-infrared microscopy for the identification of counterfeit viagra tablets. *Journal of Pharmacy and Pharmacology*, **September**(Suppl.), S3.

Yang, C., Everit, J.H. and Davis, M.R. (2003). A CCD camera-based hyperspectral imaging system for stationary and airborne applications. *Geocarto International*, **18**(2), 71–80.

Yu, H., Ying, Y.B., Fu, X. and Lu, H. (2006). Classification of Chinese rice wine with different marked ages based on near infrared spectroscopy. *Journal of Food Quality*, **29**, 339–352.

Yu, H., Ying, Y.B., Sun, T. *et al*. (2007). Vintage year determination of bottled Chinese rice wine by VIS-NIR spectroscopy. *Journal of Food Science*, **72**(3), 125–129.

Yu, H., Zhou, Y., Fu, X. *et al*. (2007). Discrimination between Chinese rice wines of different geographical origins by NIRS and AAS. *European Food Research and Technology*, **225**, 313–320.

Zalacain, A., Ordoudi, S.A., Diaz-Plaza, E.M. *et al*. (2005). Near-infrared spectroscopy in saffron quality control: determination of chemical composition and geographical origin. *Journal of Agricultural and Food Chemistry*, **53**, 9337–9341.

Zhao, J., Chen, Q., Huang, X. and Fang, C.H. (2006). Qualitative identification of tea categories by near infrared spectroscopy ADN support vector machine. *Journal of Pharmaceutical and Biomedical Analysis*, **41**, 1198–1204.

Zhou, J., Gu, J. and Zhang, D. (2007). Singular points analysis in fingerprints based on topological structure and orientation field. In: *Advances in Biometrics*. Heidelberg: Springer, pp. 261–270.

This page intentionally left blank

5

Spectroscopic Technique: Raman Spectroscopy

Hartwig Schulz

Introduction

Infrared (IR) and Raman spectroscopy are complementary techniques which may provide important information regarding the composition of complex food samples. While infrared spectroscopy has been well established as a useful tool for molecular structure elucidation and various quality control purposes for more than three decades, Raman spectroscopy was restricted for a long time primarily to academic research. The development of Fourier-transform pushed the usage of Raman spectroscopy considerably, because long spectral acquisition times and photodecomposition could be significantly reduced. In contrast to IR methods, Raman spectroscopy does not require optically clear samples; even measurement through colored glass vials is possible.

The "Raman effect" was described for the first time in 1928 by the Indian scientist Sir C.V. Raman, who won the Nobel Prize for Physics in 1930 for his discovery (Raman, 1928a, 1928b). If a sample is illuminated with monochromatic light, the scattered energy consists almost entirely of the incident radiation, which is called elastic or "Rayleigh scattering". However, a small amount of the incident light ($<10^{-6}$) is scattered with a different frequency, and that is the reason why additional discrete frequencies below and above the incident Rayleigh scattering are observed. When the lines to be seen at lower frequencies (so-called Stokes lines) are presented as a spectrum of intensity versus frequency shift (the so-called Raman shift), the result is the

Modern Techniques for Food Authentication
ISBN: 978-0-12-374085-4

Raman spectrum. The radiation with higher energy is referred to as anti-Stokes-Raman scattering, which generally shows lower intensity.

The requirement for vibrational activity in Raman spectra is a change in the electronic polarizability of the analyte molecule (contrary to that, a change in the dipole moment is necessary to get an IR response). In classical terms, the interaction can be viewed as a perturbation of the molecule's electric field. In quantum mechanics, the scattering is described as an excitation to a virtual state lower in energy than a real electronic transition with nearly coincident de-excitation and a change in vibrational energy. The scattering event occurs in 10^{-14} seconds or less. In spite of the fact that Raman scattering is a weak phenomenon, in some cases traces in food materials can also be successfully studied. In particular, the *resonance Raman effect*, in which the exciting laser wavelength is adjusted to the absorption range of particular chromophores occurring in the sample, results in a significant sensitivity enhancement. A considerable increase in sensitivity can be also obtained by some special Raman techniques such as the *surface-enhanced Raman scattering* (SERS) technique, which enhances the signal by six or more orders of magnitude.

This chapter demonstrates the high potential of Raman spectroscopy, including micro-Raman techniques, for the rapid authentication of various food materials as well as the quantification of valuable or unwanted bioactive substances. Furthermore, examples of micro-measurements are presented which allow determination of the distribution of certain food components *in situ*. A more detailed theoretical overview of Raman spectroscopy, instrumentation and special sampling techniques is provided by Schrader (1995) and McCreery (2000).

Instrumentation

A Raman system typically consists of four major components: an excitation source (laser); a sample illumination system and light collection optics; a wavelength selector (filter or spectrophotometer); and a detector (photodiode array, charge-coupled devices (CCD) or photomultiplier tube (PMT)).

A sample is normally illuminated with a laser beam in the ultraviolet (UV), visible (Vis) or near-infrared (NIR) range. Scattered light is collected with a lens and is sent through an interference filter or spectrophotometer to obtain the Raman spectrum of a sample.

Since spontaneous Raman scattering is a very weak phenomenon, the main difficulty of Raman spectroscopy is in its separation from the intense Rayleigh scattering. More precisely, the major problem here is not the Rayleigh scattering itself, but the fact that the intensity of stray light from Rayleigh scattering may greatly exceed the intensity of the useful Raman signal in the close proximity to the laser wavelength. In many cases the problem is resolved by simply cutting off the spectral range close to the laser line where the stray light has the most prominent effect. Today, in most cases, interference filters (so-called notch filters) are used which cut off the spectral range of ± 80–$120\,\mathrm{cm}^{-1}$ from the laser line. This method is efficient in stray light elimination, but does not allow detection of low-frequency Raman modes in the range below $100\,\mathrm{cm}^{-1}$.

Stray light is generated in the spectrometer mainly upon light dispersion on gratings, and strongly depends on grating quality. Raman spectrometers typically use holographic gratings, which normally have much less manufacturing defects in their structure than the ruled ones. Stray light produced by holographic gratings is about one order of magnitude less intense than that from ruled gratings of the same groove density.

Using multiple dispersion stages is another way to reduce stray light. Double and triple spectrometers allow taking Raman spectra without use of notch filters. In such systems, Raman-active modes with frequencies as low as 3–5 cm^{-1} can be detected efficiently.

In earlier times, single-point detectors such as photon-counting photomultiplier tubes (PMT) were generally used. However, a single Raman spectrum obtained with a PMT detector in wavenumber scanning mode usually takes a substantial period of time, and therefore reduces the efficiency of any research or industrial activity based on this Raman analytical technique. Nowadays, more and more often researchers are using multichannel detectors like photodiode arrays (PDA) or, more commonly, charge-coupled devices (CCDs) to detect the Raman scattered light. The sensitivity and performance of modern CCD detectors are rapidly improving. In many cases, CCD is becoming the detector of choice for Raman spectroscopy.

Dispersive and Fourier transform spectrometer systems

The Raman spectrometer market is split between dispersive and non-dispersive (Fourier transform) instruments. It seems to be impossible to give a general answer as to which may be more efficient for various food materials; nevertheless, a clear trend is that more successful applications are described for FT-Raman in the field of biospectroscopy (Schrader *et al*., 1999a, 1999b).

Dispersive Raman spectrometers are the most widely used Raman systems available on the market. Today, the instruments consist of a monochromator, a CCD detector, and various laser sources ranging from 200 to 800 nm. CCDs permit fast data acquisition and present a high signal-to-noise ratio, and have replaced the formerly used photon-counting photomultiplier tube (PMT) detectors in all but a few specialized applications. In order to obtain optimal Raman spectra of food materials, the appropriate excitation wavelength of the laser must be found. Over the past two decades, argon and krypton ion lasers, emitting in the UV and visible range, were commonly applied in spectroscopy labs; however, recently the very sensitive He–Ne lasers have been used.

The main advantages of Fourier transform Raman spectroscopy over dispersive Raman techniques, which use visible laser excitation and photomultiplier detection, consist of significantly lower fluorescence and photochemical degradation of the analyzed sample. However, the Raman scattering is weaker at 1064 nm compared with visible laser excitation (e.g. argon-ion laser sources delivering 514.5 nm emission). NIR radiation from Nd:YAG lasers generally used in FT-Raman instrumentation is sufficiently lower in energy that most of the electronic transitions responsible for fluorescence are not excited. In spite of the fact that Raman scattering with an FT spectrometer is weaker and therefore detection is more difficult than in the visible region, the reduction in fluorescence allows measurement of a much wider range of various food samples. Contrary to dispersive instruments, FT-Raman provides excellent

frequency precision, which may be important in data manipulations involving spectral subtractions.

Since the NIR excitation wavelength is situated at the minimum of the water absorption spectrum, most food materials show quite weak Raman bands, and the risk of overheating the sample by the exciting radiation is minimal. Usually the depth from which Raman signals are obtained is only some millimeters for the range 700–1800 cm^{-1} (Schrader *et al*., 1999b). At wavenumbers less than 700 cm^{-1}, information regarding deeper tissue layers is also recorded.

Raman microscopy

The initial development of Raman microspectroscopy dates back to the early 1970s (Delhaye and Dhamelincourt, 1975). Today, the micro-Raman technique is a well-established method that is mainly used to measure very small samples or to obtain spatially resolved information from a sample. In order to collect the scattered light, a microscope objective is applied to focus the laser beam on the sample. The simplest application of Raman spectroscopy is acquisition of a spectrum from a single point of the sample to be analyzed. Another approach is to use an *xy* desk, allowing point-to-point mapping. The latest development of two-dimensional detectors allows monitoring of an array of several points at the same time. This so-called "global Raman imaging" can be used to select individual narrow bands of wavenumbers, preferably with a bandwidth of 10 cm^{-1} or less, to calculate images of the measured object based on these key signals. A more simple type of Raman imaging is line-profiling, consisting of a series of single-point spectra collected along a line previously selected by the user. Commercial instruments usually provide a software-controlled microscope stage that positions the sample under the laser spot according to a video image. This allows comparison of the individual Raman mapping results directly with the corresponding image of the light microscope.

SERS techniques

As already mentioned, Raman spectroscopy can suffer from problems associated with an inherent lack of sensitivity, meaning that several minor substances are often below the detection limit of this technique. Usually, most bands in the spectra are produced by substances occurring in a concentration of more than 1 g 100 g^{-1}. Only those analytes that exhibit a pre-resonance enhancement of Raman signals, such as certain carotenoids, may be observed in a somewhat lower concentration. One approach to overcome this problem is the application of the so-called *surface-enhanced Raman scattering* (*SERS*) technique. SERS spectroscopy utilizes the following effect: the Raman signal from molecules adsorbed on certain metal surfaces such as silver, gold or copper can be several orders of magnitude stronger than the Raman signal from the same molecules in bulk volume. The exact reason for such significant improvement is still under discussion. It is assumed that the first enhancement of polarizability may occur because of a charge-transfer effect or chemical bond formation between the individual metal surface and molecules under observation. This is the so-called *chemical enhancement*. A second enhancement effect may be induced by the interaction of the laser beam with irregularities on the metal surface, such as metal micro-particles or its roughness

profile. According to current opinion, laser light excites conduction electrons at the metal surface, leading to a surface plasma resonance and strong enhancement of the electric field. This effect is therefore sometimes called *electromagnetic enhancement*. Since the discovery of SERS (Fleischmann *et al*., 1974; Jeanmaire and Van Duyne, 1977), several applications in the biomedical and food sector have been published which prove that even trace components (such as pesticides, bacteria, artificial food dyes and other food additives) can be detected using this sophisticated technique (Sanchez-Cortes *et al*., 2001; Kang *et al*., 2002; Harz *et al*., 2005; Peica *et al*., 2005; Podstawka *et al*., 2007). In all cases, the choice of appropriate surface substrate is very important. The most popular and universal substrates used for SERS are electrochemically etched silver electrodes as well as silver and gold colloids with average particle size below 20 nm. One disadvantage of SERS is the difficulty of spectra interpretation. Sometimes the signal enhancement is so dramatic that Raman bands which are very weak and unnoticeable in spontaneous Raman spectra can appear in SERS. Furthermore, some trace contaminants can also contribute to additional peaks. On the other hand, because of chemical interactions with the metal surface, certain peaks which are strong in conventional Raman might not be present at all in SERS. Therefore, all the physical and chemical factors mentioned above should be considered carefully when interpreting SERS spectra – which is sometimes extremely difficult in practical usage.

Applications in the agricultural and food sectors

Agricultural crops

Vegetable oils and fats

Food materials consisting largely of lipids show characteristic Raman bands in the region of 1440–1660 cm^{-1} due to C=C stretching modes of *cis*-unsaturated fatty acids as well as CH_2-scissoring modes of saturated fatty acids. Numerous different vegetable oils (e.g. Brazil nut, coconut, corn, high oleic sunflower, olive oil, peanut, palm, palm kernel, rapeseed and soybean) as well as animal fats such as butter, hydrogenated fish oil and tallow have been analyzed by FT-Raman spectroscopy (Baeten *et al*., 1998). These authors successfully applied principal component analysis (PCA) to classify the individual samples according to their unsaturation.

Furthermore, Baeten *et al*. (1998) found that the Raman spectra show characteristic signals of oils and fats in the region between 2990 and 3020 cm^{-1} (Figure 5.1). In this context they identified Raman shifts at 3010 cm^{-1} as ν (=C–H) vibration of the methyl linoleate group (*cis*, *cis* diene) of olefinic molecules. This signal has been described as a reliable indicator of the different degrees of unsaturation (Li-Chan *et al*., 1994), and it can also be used to accurately predict the iodine value of oils and fats (Lerner *et al*., 1992). Together with other Raman shifts, this band has also been usefully applied to detect and quantify adulterations in olive oil (Aparicio *et al*., 1996; Baeten *et al*., 1996). Moreover, other scattering Raman shifts seen at 1663 and 1264 cm^{-1} were found to correlate with the fatty acid profiles analyzed by gas chromatography. The most prominent Raman signals assigned by Baeten *et al*. (1998) are presented in Table 5.1.

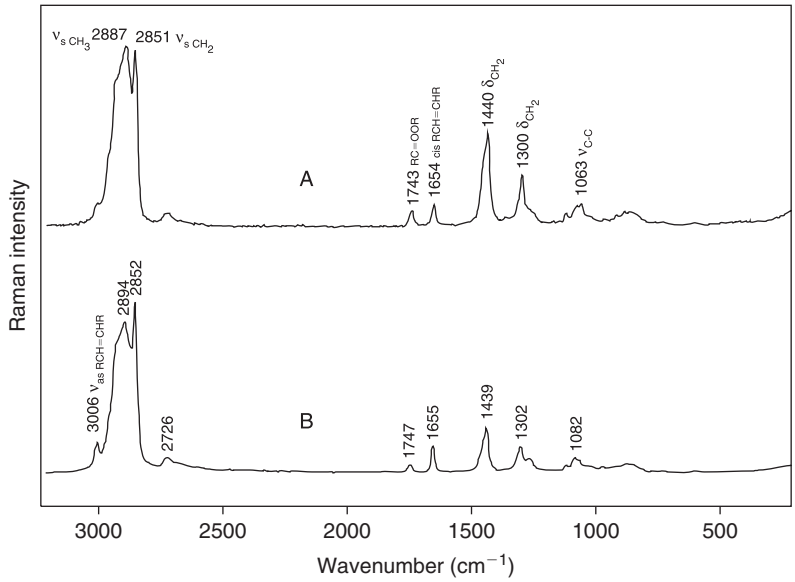

Figure 5.1 FT-Raman spectra of (a) butter and (b) olive oil.

Table 5.1 Assignment of main Raman shifts detected at spectra of edible oils (Baeten *et al.*, 1998)

Raman shift (cm^{-1})	Molecule	Functional group	Vibrational mode
3015	RCH=CHR	=C-H	ν_{as}
2970	$-CH_3$	C-H	ν_{as}
2940	$-CH_2$	C-H	ν_{as}
2900	$-CH_3$	C-H	ν_s
2860	$-CH_2$	C-H	ν_s
1750	RC=OOR	C=O	ν
1670	*trans* RCH=CHR	C=C	ν
1660	*cis* RCH=CHR	C=C	ν
1445	$-CH_2$	C-H	δ
1310	$-CH_2$	C-H	δ
1275	*cis* RCH=CHR	=C-H	δ
1100–1000	$-(CH_2)_n-$	C-C	ν
900–800	$-(CH_2)_n-$	C-C	ν

ν_s, symmetric stretching vibration; ν_{as}, asymmetric stretching vibration; δ, deformation vibration.

As indicated in Table 5.1, vegetable oils show a comparatively weak carbonyl Raman band around 1750 cm^{-1}. Beside this, additional signals can be observed in the range of 1650–1670 cm^{-1} which are due to the characteristic ν (C=C) vibrations of olefinic molecules. From Raman measurements performed on hydrogenated fish oils, it has been found that the bands near 1670 cm^{-1} are related to *trans* and the band in the area of 1660 cm^{-1} to *cis* fatty acids. In the range between 1200 and 1390 cm^{-1} two Raman bands centered near 1303 and 1270 cm^{-1} occur, which correspond to in-phase methylene twisting deformation vibration and in-plane =C–H deformation, respectively.

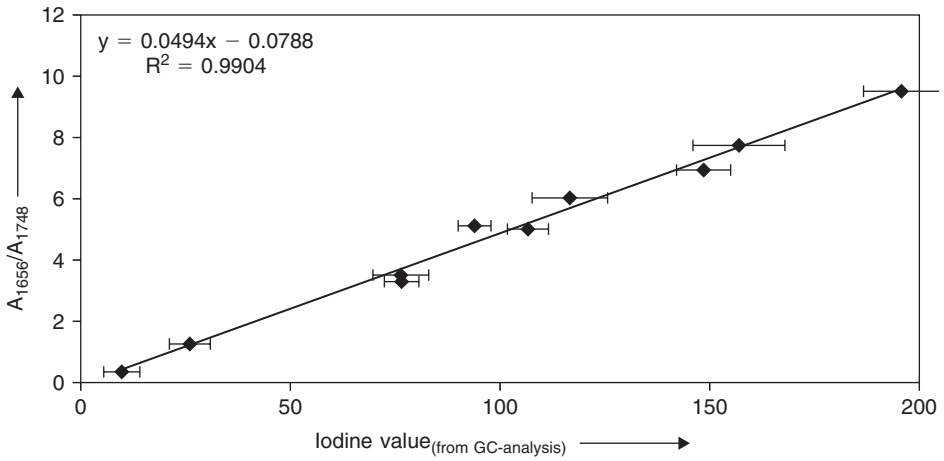

Figure 5.2 Raman area ratio ν (C=C)/ν (C=O) against the total unsaturation calculated by GC for eight oils and one fat. This calibration curve can be used to calculate the iodine value of rapeseed oil during maturation.

Sadeghi-Jorabchi *et al*. (1991) found *cis* monoene, diene and triene isomers near 1267, 1265 and 1266 cm^{-1} respectively, which indicates that these bands can be used to estimate the level of *cis* unsaturation without any interference from *trans* isomers.

The "fingerprint region" (700–1200 cm^{-1}) of the Raman spectrum contains the characteristic C–C skeletal and C–O bond vibrations. According to PCA calculations, Baeten *et al*. (1998) found that these signals mainly present information about the unsaturated fatty acids (Table 5.1).

Other authors describe Raman studies aiming to determine oil content, humidity and free fatty acid content in olives (Muik *et al*., 2003a, 2003b). Another Raman method has been proposed to quantify the amount of sunflower oil adulterant in extra-virgin olive oil from various Mediterranean sites (Heise *et al*., 2005). Recently, it has been reported that Raman spectroscopy also allows rapidly prediction of the iodine value in single rapeseeds (Reitzenstein *et al*., 2007) (Figure 5.2). Furthermore, this method can be successfully applied for breeding experiments to measure the lipid content and composition of a seedling without any destruction. Based on these studies, it was possible to distinguish seedlings of the classic rapeseed line "Drakkar" from the new genetically modified cultivar "t-mix". This successful discrimination by means of cluster analysis of the Raman data is mainly related to a lower iodine value of the genetically modified cultivar, as it contains myristic acid, which is normally not found in the fatty acid profile of rape.

Several studies have been performed applying vibrational spectroscopy to discriminate between different edible oils and fats (Marigheto *et al*., 1998; Barthus and Poppi, 2001; Yang *et al*., 2005). Beside mid- and near-infrared methods, FT-Raman spectroscopy was also found to be useful for detection of added adulterants and for identification of the individual botanical origin. In this context, linear discriminant analysis (LDA) and canonical variate analysis (CVA) provided the most efficient statistical classifications. A similar application of FT-Raman spectroscopy has been presented by Weng *et al*. (2006) to test the authenticity of *Camelia oleifera* oil used in Taiwan.

Raman spectroscopy has also been proposed as a rapid method to detect adulteration of extra-virgin olive oil with cheaper vegetable oils (Yang and Irudayaraj, 2001). Based on various extra-virgin oil samples with different amounts of olive pomace oil adulteration, a suitable calibration equation was calculated ($R^2 = 0.997$, SEP = 1.72%), allowing prediction of even low amounts of other added oils.

Today, the determination of *trans*-isomers in partially hydrogenated vegetable oils is usually performed by GC or mid-infrared spectroscopy. However, Raman spectroscopy was also evaluated in comparison with mid-IR spectroscopy to predict the content of *cis*- and *trans*-isomers in processed canola and soybean oils (Bailey and Horvat, 1972; Johnson *et al*., 2002).

Contrary to infrared-spectroscopy, FT-Raman samples typically require no preparation before spectra can be recorded. Because FT-Raman measurements are excited in the NIR region, ordinary glass is transparent to this radiation and therefore samples may be held in glass cells or capillaries during measurements.

Applying Raman spectroscopy combined with optical microscopy, the distribution of alpha-tocopherol (vitamin E) and related substances could be successfully described (Beattie *et al*., 2007). The individual Raman spectra were acquired at spatial resolutions of 0.8–2 μm.

Beattie *et al*. (2007) demonstrate that Raman microscopy is able to discriminate even between different tocopherols and oxidation products (alpha-tocopheryl quinone) in biological tissue without any sample destruction. Parker and Bisby (1993) obtained time-resolved resonance Raman spectra of the alpha-tocopheroxyl radical, which represents an intermediate in the antioxidative reaction of alpha-tocopherol in cellular membranes. The spectra reflect the extent of delocalization of the radical site due to interaction with the ion pair of the *para*-oxygen atom.

Proteins and carbohydrates

Numerous studies have been performed to obtain Raman data of plant proteins and amino acids. Some examples of Raman modes useful in the interpretation of protein structure are listed in Table 5.2. In particular, sulfur-containing amino acids such as cystine, cysteine and methionine show intensive Raman bands in the area of 500–750 cm^{-1} (S–S and S–H stretching bands) as well as in the range between 2550 and 2580 cm^{-1} (S–H stretching bands) (Figure 5.3). The peptide bonds of proteins possess several distinct vibrational modes, of which the amide I and amide III bands are mainly used for characterization of secondary structure (Susi and Byler, 1988).

Fourier transform Raman spectroscopy was also shown to be a powerful tool for the investigation of plant cell walls and their components by Séné *et al*. (1994), who observed that Raman spectra were diagnostic primarily for phenolic materials whereas IR spectra presented higher sensitivity for pectin and protein. Pectin bands were identified in the region between 900 and 200 cm^{-1}, and a sharp signal at about 854 cm^{-1} could be identified as a diagnostic band for acidic pectin. Generally, the characteristic nature of plant cell walls opens up the possibility of using Raman spectroscopy for the verification of food authenticity. Because the obtained spectral data also contain information on molecular conformation and interaction between different molecules in the

Table 5.2 Characteristic Raman vibrational modes resulting from plant proteins (Li-Chan, 1994; Peticolas, 1995)

Analyte	Wavenumber (cm^{-1})	Vibrational mode
Cystine,	510	S–S stretch
Cysteine,	525	S–S stretch
Methionine	630–670	C–S stretch
	700–745	C–S stretch
	2550–2580	S–H stretch
Tyrosine	850/830	Fermi resonance between ring fundamental and overtone
Tryptophan	760, 880, 1360	Indol ring
Phenylalanine	1006	Ring breathe
Histidine	1409	N-deuteroimidazole
Aspartic and	1400–1430	C=O stretch of carboxyl group
glutamic acid	1700–1750	C=O stretch of carboxyl or ester group
Amide I	1655–1685	Amide C=O stretch, N–H wagging
Amide III	1235–1280	N–H in-plane bend, C–N stretch

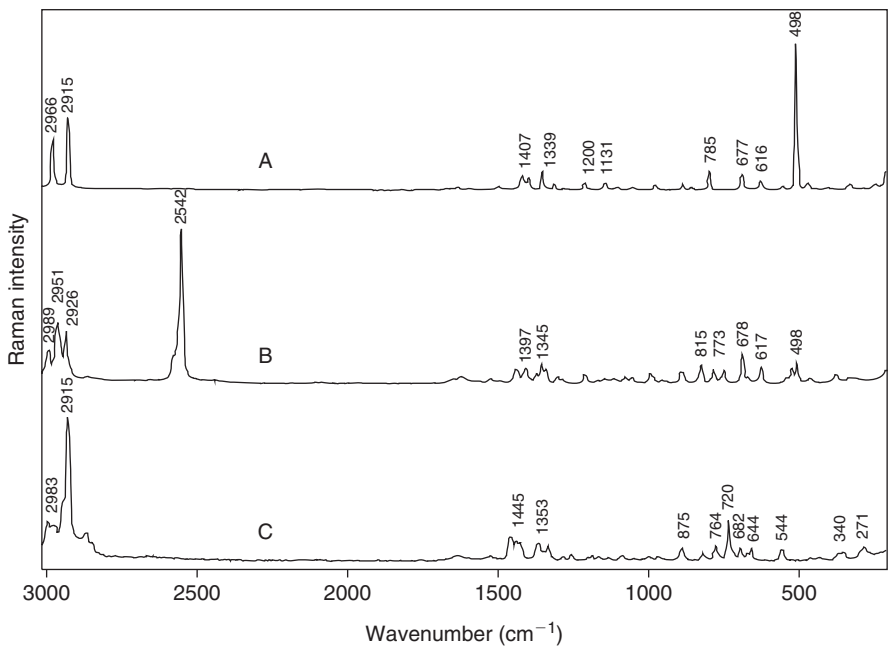

Figure 5.3 FT-Raman spectra of (a) L-cystine, (b) L-cysteine and (c) L-methionine.

sample, Raman spectroscopy in combination with chemometrical algorithms may be a new, useful alternative for rapid taxonomic classification of different plant species.

Raman spectra of non-feruloylated and feruloylated wheat arabinoxylans show specific bands at 896, 985, 1278–1462 and 1091–1123 cm^{-1} assigned to various vibrational modes of polysaccharides. The presence of β–(1→4) glycoside linkages of xylan backbone was seen at 896 cm^{-1}. Signals occurring in the range between 500 and 600 cm^{-1} were identified as vibrations arising from coupled modes of heavy atoms, C–C and C–O stretching (Barron *et al.*, 2006). Besides these signals, specific marker bands were

observed at 1598 and 1628 cm^{-1}, demonstrating the presence of ferulic acid esters. Furthermore, a quantitative determination of arabinose/xylose ratios could be successfully performed using the 855/898 and 570/494 cm^{-1} peak area ratios.

Horticultural crops

Carotenoids

In most cases, Raman measurements can be directly performed on the individual plant tissue. Usually, most intensive signals to be seen in the obtained spectra are related to various vibrational modes of different carotenoids. Although these natural colors occur in plants as minor components at the mg kg^{-1} level, very sensitive detection can be achieved by resonance Raman in the visible region, when the excitation wavelength coincides with an electronic transition of the analyzed carotenoid (Ozaki *et al*., 1992; Withnall *et al*., 2003). However, FT-Raman spectroscopy using a Nd:YAG laser (1064 nm) also provides strong carotenoid bands due to the known pre-resonance enhancement. The special advantage of NIR excitation is that the disturbing fluorescence effect of the analyzed biological material can be reduced to a minimum.

Main carotenoid bands are observed within the 1500–1550 and 1150–1170 cm^{-1} wavenumber ranges, which are related respectively to in-phase C=C and C–C stretching vibrations of the polyene chain. Furthermore, in-plane rocking modes of CH_3 groups attached to the polyene chain can be identified as peaks of medium intensity in the 1000–1020 cm^{-1} range (Rimai *et al*., 1973; Schulz *et al*., 2005a). With increasing numbers of conjugated C=C groups in the carotenoid chain, the wavenumber positions of the peaks mentioned above decreases significantly. As can be seen in Figure 5.4, a

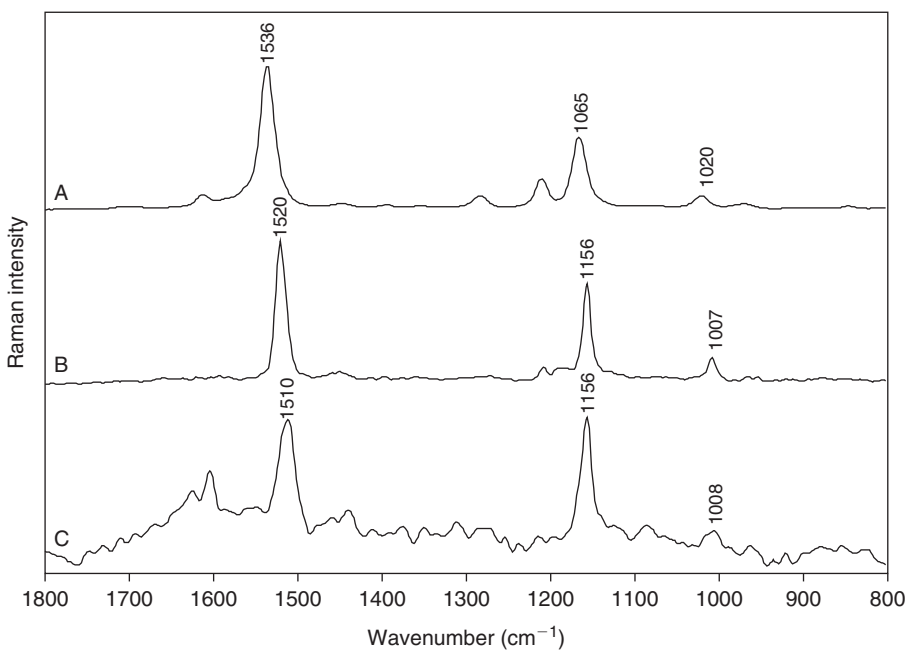

Figure 5.4 FT-Raman spectra of (a) saffron stigma, (b) orange carrot root and (c) red tomato fruit.

carotenoid band resulting from the C=C group shifts from 1536 cm^{-1} (crocetin) through 1524 cm^{-1} (lutein) to 1510 cm^{-1} (lycopene). The individual carotenoid wavenumber positions of numerous horticultural species are presented in Table 5.3. The fact that a remarkable downward shift in the polyene chain of increasing lengths can be observed allows simultaneous detection of different carotenoids (such as β-carotene and lycopene) with the same measurement. Applying Raman mapping based on the characteristic C=C stretching vibrations for 7-, 8-, 9- and 11-conjugated systems, the distribution of different carotenoids can be determined at the same time (Baranski *et al*., 2005; Schulz *et al*., 2005a; Baranska *et al*., 2006a) (Figure 5.5). Fruit ripening of various species can also be followed by Raman spectroscopy measurements. During the ripening process, carotenoids resulting from the xanthophyll pathway decline while other are accumulated.

Table 5.3 Wavenumber positions of most important carotenoid vibrational modes obtained from measurements of various fresh plant tissues (the number of double bonds in conjugated system is shown in brackets) (according to Schulz *et al*., 2005a)

Plant name	Sample	ν_1 (cm^{-1})	ν_2 (cm^{-1})	ν_3 (cm^{-1})	Carotenoids
Saffron *Crocus sativus* L.	Dry spice Stigma	1536	1165	1020	Crocetin (7)
Chamomile *Chamomilla recutita* L.	Pollen	1529	1157	1006	Carotenoid (8)
Marigold *Calendula officinalis* L.	Pollen	1524	1157	1004	Lutein (9) Antheraxanthin (9)
Nectarine *Prunus perica* L. var. *nucipersica*	Fruit	1527	1157	1005	β-cryptoxanthin (9)
Carrot *Daucus carota* L.	Yellow root	1527	1157	1006	Lutein (9)
Carrot *Daucus carota* L.	Leaf	1526	1157	1004	Lutein (9) β-carotene (9)
Basil *Ocimum basilicum* L.	Leaf	1525	1158	1005	Lutein (9) β-carotene (9)
Broccoli *Brassica oleracea* var. *italica* L.	Flower	1524	1157	1005	Lutein (9) β-carotene (9)
French bean *Phaseolus vulgaris* L.	Green pod	1524	1157	1005	Lutein (9) β-carotene (9)
Corn *Zea mays* L.	Seed	1522	1157	1005	Zeaxanthin (9)
Pumpkin *Cucurbita pepo* L.	Fruit	1524	1157	1009	β-carotene (9)
Apricot *Prunus armeniaca* L.	Fruit	1524	1156	1003	β-carotene (9)
Carrot *Daucus carota* L.	Orange root	1520	1156	1007	β-carotene (9)
Annatto *Bixa orellana* L.	Seed Seed in CCl_4	1518 1523	1154 1155	1011 1008	*cis*-bixin (9) *trans*-bixin (9)
Pepper *Capsicum annuum* L.	Red fruit	1517	1158	1004	Capsanthin (9)
Watermelon *Citrullus lanatus* Thumb.	Fruit	1510	1158	1008	Lycopene (11)
Tomato *Lycopersicon esculentum* Mill.	Fruit Purée	1510 1510	1156 1156	1004 1006	Lycopene (11) Lycopene (11)

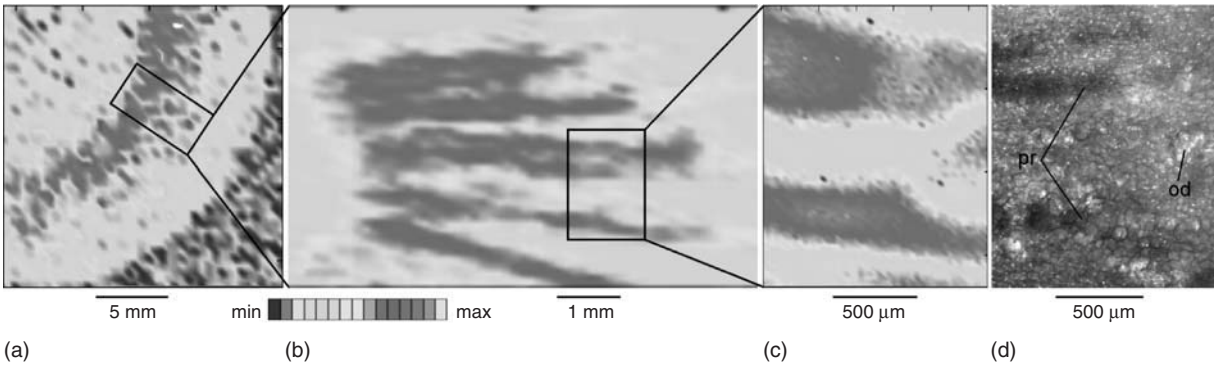

Figure 5.5 Raman maps obtained from a section of orange "Bolero" F_1 root with mapping increment of (a) 500 µm, (b) 100 µm and (c) 25 µm, respectively. The maps are colored according to the band intensity in the range of 1517–1523 cm^{-1} related to the β-carotene content in the carrot root. (d) Microscopic image of the same fragment as in map (c), stained with toluidine blue; od, oil duct; pr, phloem rays.

It has been shown that different ripening stages of bell pepper (*Capsicum annuum*), from green through pale green to red, show strong bands representing the decrease of lutein (1526 cm^{-1}) and increase of capsanthin (1517 cm^{-1}) content during fruit ripening.

Other natural pigments

In recent years, several attempts have been made to collect Raman data from different plant flavonoids. Merlin *et al*. (1985, 1994) recorded resonance Raman spectra of six common anthocyanidins and some of their glycosylated derivatives from acidic aqueous solutions. The authors observed that the spectral range between 500 and 900 cm^{-1} significantly correlates with the glycosylation pattern. It was found that anthocyanidin-3-glycoside showed a strong resonance Raman signal close to 540 cm^{-1}, while 3,5-di-glycoside exhibited the strongest feature in the range close to 630 cm^{-1}. Resonance Raman spectra were also successfully obtained from vacuoles of the wine berries (*Vitis vinifera*) (Merlin *et al*., 1985), aiming to detect the main pigment malvidin-3-glucoside. In the petals of common mallow (*Malva sylvestris*), malvidin 3,5-diglycoside could be detected in its cationic flavylium form.

Several flavones, widely distributed in the plant kingdom, have been measured as pure substances in order to study their vibrational frequencies (Vrielynck *et al*., 1994). Generally, the carbonyl stretching frequency was found at approximate 1652 cm^{-1} as a large and strong band. Furthermore, several *v* (C–C) vibrations that gather the characteristic modes of substituted benzene are located in the range between 1600 and 1400 cm^{-1}. Finally, a band detected at 1000 cm^{-1} was assigned as a "breathing" mode of the ring system.

Detailed structural studies have been performed on quercetin. A theoretical model has been validated by both vibrational and electronic spectroscopies. In this context, the positions of calculated and observed wavenumbers in the region between 600 and 1800 cm^{-1} are compared with each other and the individual vibrational modes are assigned (Cornard *et al*., 1997).

It has been demonstrated that micro-Raman spectroscopy in combination with several chemometric methods allows discrimination between the two sources of natural indigo in *Indigofera tinctoria* and *Isatis tinctoria* (Vandenabeele and Moens, 2003). The band positions corresponded with the detailed interpretation which was already provided by Tatsch and Schrader (1995).

Polyacetylenes

Beside carotenoids, –C≡C– stretching modes of polyacetylenes also show strong and polarized bands in the Raman spectrum between 2100 and 2300 cm^{-1}. Schrader *et al*. (2005) observed that the number of triple bonds as well as substituents influence the position of the –C≡C– signals. Falcarinol and falcarindiol, the most bioactive polyacetylenes in carrot roots, present intensive bands at 2258 and 2252 cm^{-1}, respectively (Baranska *et al*., 2005a; Baranska and Schulz, 2005). Applying micro-Raman mapping, it was found that the accumulation of polyacetylenes is mainly located in the outer section of the carrot root. It is assumed that polyacetylenes occur in vascular bundles in young secondary phloem as well as pericycle oil channels in the vicinity of the periderm (Baranska *et al*., 2005a). In the dried roots of American ginseng (*Panax quinquefolium*), falcarinol as well as its epoxy derivative (panaxydol) has also been found in detectable amounts, showing a characteristic Raman signal at 2260 cm^{-1} (Baranska *et al*., 2006b). However, the authors observed that this polyacetylene band shifts to 2237 cm^{-1} when fresh root samples are measured. It is assumed that polyacetylenes form a stable hydrat complex that is broken after dehydration of the fresh ginseng root. The application of Raman mapping proves that polyacetylenes are stored in special channels which are mainly located in the outer parts of the root. Other Raman studies were aimed at discriminating Korean ginseng (*Panax ginseng*) cultivated in Korea and China. In combination with pattern recognition techniques such as principal components analysis (PCA) and partial linear squares (PLS), the two geographical cultivation areas could be successfully differentiated into clearly separated groups (Woo *et al*., 1999). To build the calibration model, spectral data from 250 to 1700 cm^{-1} were used, since most structural and chemical information appeared in this region. Various plant polyacetylenes have also been detected in fool's parsley (*Aethusa cynapium*) and chamomile (*Chamomilla recutita*) (Andreev *et al*., 2001).

Essential oils

In recent years numerous studies have been performed to characterize essential oils obtained from various species by applying NIR, IR and Raman spectroscopic methods (Schulz and Baranska, 2005, 2007). Mostly, the Raman spectra obtained from essential oils demonstrate characteristic key bands that can be used as markers for chemotaxonomic discrimination of different species or chemotypes. In order to identify the individual group sequences, the interpretation is usually based on Raman spectra of the pure analytes (Daferera *et al*., 2002; Schulz *et al*., 2002, 2004a; Baranska *et al*., 2005b). Various essential oils hydro-distilled from species belonging to the genera *Origanum, Satureja, Thymbra, Coridothymus, Thymus, Lavandula, Salvia, Rosmarinus, Sideritis, Calamintha* and *Ziziphora* were analyzed by Raman

spectroscopy (Schulz *et al*., 2005b). All spectra of these plants collected in Turkey present some characteristic key bands which can be assigned to the main essential oil components, such as carvacrol, thymol, p-cymene, γ-terpinene, 1,8-cineole, camphor, β-pinene, β-caryophyllene and pulegone. It is even possible to differentiate the isomeric substances thymol and carvacrol. Whereas the ring vibration mode of thymol is seen at 740 cm^{-1}, for carvacrol this corresponding signal appears at 760 cm^{-1}. Characteristic out-of-plane CH wagging vibrations can also be seen for the other terpenoids mentioned above (for α-terpinene at 804 cm^{-1}, for γ-terpinene at 756 cm^{-1}, for 1,8-cineole at 652 cm^{-1} and for camphor at 649 cm^{-1}). Raman spectra of several commercial oils obtained from anise (*Pimpinella anisum*), fennel (*Foeniculum vulgare*), cumin (*Cuminum cyminum*), dill (*Anethum graveolens*), caraway (*Carvum carvi*), coriander (*Coriandrum sativum*), carrot (*Daucus carota*), lavender (*Lavandula angustifolia*), gentian species (*Gentiana lutea* and *Gentiana punctata*) and spike lavender (*Lavandula spika*) were also measured, and the results compared with spectra of pure standards in order to analyze their chemical composition (Andreev *et al*., 2001; Strehle *et al*., 2006). It has been found that the chemometrical interpretation of the Raman data correlate very well with analysis results measured with GC/MS methods. Application of FT-Raman spectroscopy for the evaluation of essential oils from marjoram and oregano showed remarkable variation, relating to the different genetic background of the individual plant (Baranska *et al*., 2005b).

Main components of *Eucalyptus citriodora* and *Eucalyptus globulus* have been recognized using the spectral information of the related pure terpenoids (Baranska *et al*., 2006c). A combination of Raman spectroscopy and hierarchical cluster analysis has been proved to provide a fast, easy and reliable method for chemotaxonomical discrimination of the individual eucalyptus species or proveniences. It has been found that analysis narrowed to the 1400–1750 cm^{-1} range, where characteristic signals of components other than 1,8-cineole occur, allows differentiation between *E. globulus* oil originating from Australia and from China. Furthermore, for the first time a calibration equation has been developed to predict reliably the 1,8-cineole content in essential oils of *E. globulus*.

Other Raman studies focused on the analysis of peppercorn, pepper oleoresins and pepper oil, which show broad variation according to the provenience (cultivar), climate and ripening stage of the harvested peppercorns (Schulz *et al*., 2005c). Most of the well-resolved Raman signals detected in the peppercorns and the related oleoresins have been assigned to piperine, representing the pungent principle of these products. However, the volatile fraction in various commercial pepper samples could also be successfully classified according to different types (Figure 5.6).

Chemotaxonomical studies have also been performed on various *Mentha* species (Rösch *et al*., 2002). In this context, micro-Raman spectra of five different mint species (*M. spicata spicata*, *M. spicata crispata*, *M. ×piperita citrata*, *M. ×piperita pallescens* and *M. ×piperita piperita*) have been collected. In order to obtain an optimal classification of these mint types, a hierarchical cluster analysis was performed in the spectral range between 520 and 1690 cm^{-1}.

A number of essential oils hydro-distilled from various *Lamiaceae* species have also been recognized by FT-Raman spectroscopy (Rösch *et al*., 1999; Daferera *et al*., 2002). The authors present the spectra of lavender, sage, pennyroyal, oregano, thyme, dictamus

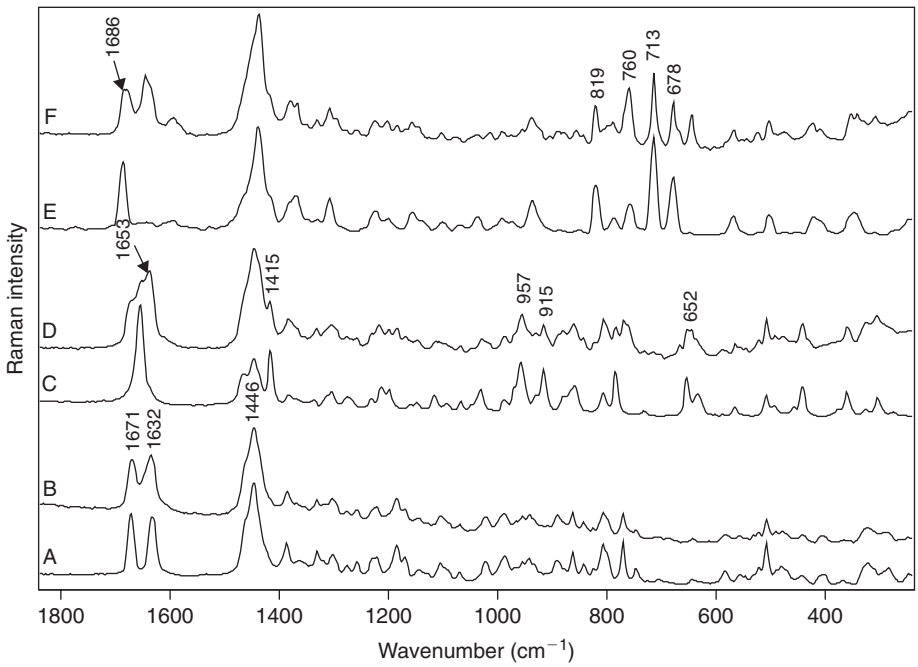

Figure 5.6 Raman spectra of different pepper oil types isolated by hydro-distillation from various commercial pepper samples: (a) pure caryophyllene standard, (b) pepper oil (caryophyllene type), (c) pure sabinene standard, (d) pepper oil (sabinene/caryophyllene type), (e) pure δ-3-carene standard, (f) pepper oil (δ-3-carene/caryophyllene/limonene type).

and marjoram, and provide assignments of the individual Raman bands which were based on spectral data of pure essential oil substances (α-terpinene, γ-terpinene, thymol, carvacrol, p-cymene, α-terpineol, β-myrcene, eucalyptol, camphor, pulegone, menthone). The Raman spectra were found to be in good agreement with the corresponding GC-MS data even in cases of isomeric substances (e.g. thymol and carvacrol), which contributes to additional information that can be used for rapid quality control purposes.

Another study demonstrated that FT-Raman spectroscopy is a very useful tool to discriminate many Apiaceaeous species, including those of similar morphology (Baranski *et al*., 2006) (Figure 5.7). Because the spectroscopically analyzed seeds germinated and developed into normal seedlings, this method seems to be of considerable importance for the evaluation of seed material stored in *ex situ* collections, even when a very limited number of seeds are available.

Besides Raman analysis of isolated essential oils, several *in situ* mapping experiments of cross-sections or surfaces have also been successfully performed. Strehle *et al*. (2006) described measurements on the endosperm region of anise fruits indicating the essential oil droplets which are detected in the wavenumber region between 1574 and 1618 cm^{-1} according to the marker band of anethole at 1604 cm^{-1}. Similar results have been obtained for measurements on fennel fruits (Strehle *et al*., 2005). Here, the essential oil was predominantly found in the outer part of the fennel fruit (pericarp). Contrary to this, the endosperm region of the analyzed fennel fruits

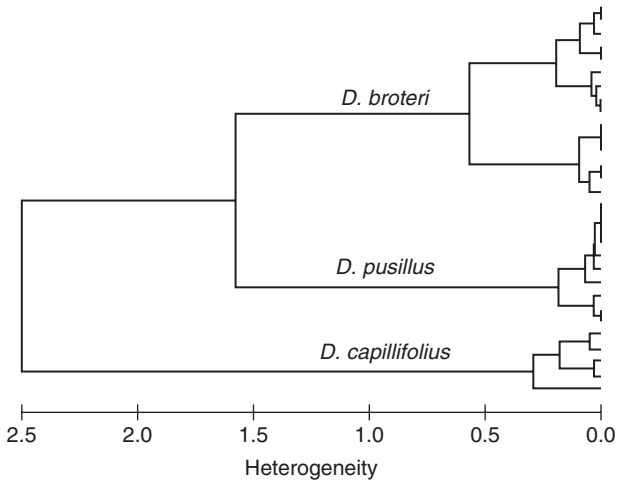

Figure 5.7 Dendrogram showing classification of *Daucus broteri*, *Daucus capillifolius* and *Daucus pusillus* individual seeds after cluster analysis of the single spectra at the wavenumber ranges of 500–900, 1500–1745 and 2800–3000 cm^{-1} using the first two factors for calculation of spectral distances and the Ward's algorithm.

present mainly Raman bands which have been assigned to fatty oil (region between 1632 and 1670 cm^{-1}).

Attempts have also been made to investigate the essential oil in *Eucalyptus globulus* and *Eucalyptus cinerea* (Baranska *et al*., 2005c). Spectra taken directly in the oil droplets of the eucalyptus leaves show a strong marker band at 652 cm^{-1} due to the ring deformation vibrational mode of 1,8-cineole. Integration of this Raman signal provides information about the essential oil distribution over a eucalyptus leaf. Furthermore, a Raman image based on the carotenoid signal at 1525 cm^{-1} has been obtained. This Raman map proves that carotenoids occur mainly outside the essential oil cavities.

Raman spectra recorded from essential oils that were hydro-distilled from different basil chemotypes show characteristic fingerprints, allowing discrimination of the individual plant species and subspecies (Schulz *et al*., 2003). As shown by Schulz *et al*. (2005c), the pungent principal as well as the main components of pepper oil give characteristic Raman signals which can be used for quality control purposes. Cluster analysis applied to Raman data sets of three different pepper oil types succeeded in discriminating these subgroups, which differ mainly in their content of sabinene, caryophyllene and δ-3-carene. Most of the well-resolved Raman signals detected in the spectra obtained from green, white and black peppercorns were assigned to piperine, which is known to be the main pungent principal in pepper. Integration of specific piperine key bands allows localization of the distribution of the alkaloid in whole pepper-berries.

Miscellaneous plant substances

Poppy (*Papaver somniferum*) seeds with very low alkaloid content are widely used, especially in Europe, in bakery products. In this context, several attempts have been made to reduce the content of morphine and other alkaloids in the seeds by breeding experiments. It has been observed that cluster analysis based on Raman spectroscopy data allows efficient discrimination between "low-alkaloid" and "high-alkaloid"

individual poppy plants (Schulz *et al*., 2004b). Raman spectra obtained by excitation at 1064 nm show no disturbing fluorescence effects, and the plant tissue can be assessed without applying any sample pre-treatments.

Several Raman studies have been performed to obtain more detailed information about plant cell walls and their constituents, such as pectins, proteins, aromatic phenolics, cellulose and hemicellulose. It has been demonstrated that the individual spectral features of the analyzed species reflect characteristic differences which principally opens the possibility of a chemo-taxonomic classification based on Raman spectra (Séné *et al*., 1994).

Micro-Raman spectroscopy has also been applied to measure the pectin in raw potato tubers, showing a unique galactoronic methyl ester peak in the area of 1745 cm^{-1} (ester carbonyl C=O stretch). Other pectin signals were observed at 858 cm^{-1} (α-anomer carbohydrate, indicating a very low degree of esterification) and at 1455 cm^{-1} (ester O–CH_3 stretch band).

Stellacyanin, a copper-containing glyco-protein occurring in cucumber (*Cucumis sativus*), has been isolated and characterized by resonance Raman spectroscopy (Nersissian *et al*., 1996). According to earlier Raman measurements performed on the Japanese lacquer tree *Rhus vernicifera* (Nestor *et al*., 1984), the most intense signals in the stellacyanin spectrum were found in the range between 340 and 430 cm^{-1}; these are due to Cu–S (cysteine) stretching modes.

At present, only limited information is available regarding the chemical composition of various fruit waxes which serve as protection against pest and disease (Prinsloo *et al*., 2004). This is the reason why attempts have been performed to study the epicuticular wax layer of mango (*Mangifera indica*) by Raman microscopy. The spectroscopic measurements prove that two morphologically distinct parts can be found in the wax layer.

Meat and animal fats

In order to distinguish different meat species, Raman spectra of chicken and turkey meat from breast and leg muscles were measured (Ellis *et al*., 2005). Generally, a strong baseline shift caused by fluorescence of the meat samples has been observed even at NIR laser excitation. Nevertheless, by applying principal component discriminant function analysis (PC-DFA) it could be clearly seen that major discrimination was between the leg and breast muscle due to the different biochemical nature of the muscle types. Smaller spectral differences were obtained for meat species; however, in spite of this fact most of the test data were assigned to the right muscle type.

Several years ago some attempts were made to obtain Raman spectra of intact single muscle fibers (Caille *et al*., 1987) and to determine myosin located in the myofibers (Asher *et al*., 1976). Furthermore, the potential of Raman spectroscopy for the objective determination of sensory quality attributes has been tested (Beattie *et al*., 2004). In this context, comparatively good prediction quality was achieved when the Raman data were used to describe the texture of the meat, the degree of tenderness and the degree of juiciness. The Raman spectra were obtained using the 785 nm excitation wavelength, and the meat tissue samples were presented on a metallic rotating spit with the long axis

of the myofibers perpendicular to the incident laser beam. The main difference between the Raman spectra of the toughest and most tender samples was seen in a change of protein bands; tougher meat was found to show increases at 1669, 1235 and 1006 cm^{-1}, correlating with a higher content of a β-sheet-containing protein in the tough meat. Another signal located around 670 cm^{-1}, which is interpreted as an S–S stretching mode, shows a positive correlation with the sensory testers' acceptability of texture. It is assumed that the disulfide groups are involved in inter- as well as intra-polypeptide bondings, resulting in a significant increase of stability of the three-dimensional protein structure.

Other studies using a laser suffered from the fact that the 1064 nm excitation wavelength was too close to the third overtone of the O–H stretches, which caused the spectral information from aqueous compartments almost to vanish (Brøndum *et al*., 2000). In spite of the fact that several Raman signals could be successfully identified, such as aliphatic and aromatic C–H stretches, amides I and II, aromatic C=C stretching vibrations as well as sharp peaks of substituted phenylic substances (e.g. phenylalanine), PCA interpretation of the Raman data presented no clear discrimination of different porcine meat samples according to pre-slaughter stress and warmed-over flavor.

Preliminary studies have also been performed to investigate whether Raman spectroscopy can be useful in measuring the water-holding capacity (WHC) of meat (Pedersen *et al*., 2003). Based on the Raman data collected from 14 different meat samples in the wavenumber range between 3200 and 500 cm^{-1}, a very good prediction quality could be achieved ($R = 0.98$, RMSECV = 0.27%). In order to describe the WHC of meat, the most important information is provided from the spectral regions 3128–3071 cm^{-1} and 951–876 cm^{-1}. It is assumed that these Raman regions contain mainly changes of NH stretching of primary amides in proteins and secondary structure information represented by the α-helical band occurring at 940 cm^{-1}.

Several years ago some studies were performed to study the conformation of selected polypeptides and proteins in the solid state and in aqueous solution (Lin and König, 1976). In this context, Raman spectra of bovine serum albumin (BSA) were recorded in the solid state, in alkaline and acidic solutions, and in the gel. Glutamic and aspartic acids were found to comprise approximate 22% of the amino acid residues in BSA. Dissolution of BSA in 0.1N NaCl solution caused a downshift in amide-I frequency from 1658 cm^{-1} to 1652 cm^{-1}. The S–S stretching mode was observed at 506 cm^{-1}.

Generally, three-dimensional structures derived from X-ray crystallography are very important to elucidate structure–function relationships for proteins. However, not all food proteins (for example, casein) can be crystallized. Therefore, some attempts have been made to predict the secondary structure of these proteins by Raman and FT-IR spectroscopic data based on sequence analysis results (Farrell *et al*., 1993). The three-dimensional structure of β-casein, representing approximate 36% of bovine casein, was successfully predicted from Raman spectroscopy data applying molecular modeling techniques (Kumosinski *et al*., 1993). The structure obtained by this approach was found to be in good agreement with biochemical cleavage results for plasmin and chymosin action on β-casein, but showed less agreement with small-angle X-ray scattering experiments. Nevertheless, the model clearly showed a loosely packed asymmetrical

structure with an axial ratio of 2:1. Hydrophobic side chains were uniformly dispersed over one end and the center surface of the structure; the N-terminal end was found to be hydrophilic. Also, Raman spectra of three other globular proteins (beef pancreas chymotrypsinogen A, beef pancreas ribonuclease, hen egg-white ovalbumin) have been recorded in the solid state and in aqueous solution (König and Frushour, 1972). The frequencies and intensities obtained for amide I and III signals were in good agreement with assignments of other polypeptides. The comparatively high intensity of the amide III band is related to a low fraction of the residues in the α-helical conformation. Furthermore, a Raman spectrum of thermally denatured chymotrypsinogen showed a decrease of the amide I frequency ($3\,cm^{-1}$). This finding is consistent with the present knowledge of the denaturation mechanism, that only slight changes in the secondary structure but an increase in solvent penetration is observed upon going from the native to the reversible denaturated state.

Milk and dairy products

It is well known that Raman spectroscopy is a valuable technique to obtain detailed information regarding the secondary structure of milk proteins. Therefore, several studies have been performed to obtain structural data of model proteins occurring in milk and various dairy products (e.g. α-lactalbumin, β-lactoglobulin, α-casein, β-casein, κ-casein, lysozyme, ovalbumin, ovomucoid and ovotransferrin) (Alizadeh-Pasdar *et al*., 2004). The main signals detected in the Raman spectra were assigned as tryptophanyl ring vibrations ($760\,cm^{-1}$) and CH stretching vibrations ($2800–3100\,cm^{-1}$) arising from amino acid side chains. Bands appearing near $2874–2897\,cm^{-1}$ are due to CH_3 symmetrical stretching and $R_3C–H$ stretching bands of aliphatic amino acids, while $=C–H$ stretching bands of aromatic acids can be found around $3061–3068\,cm^{-1}$. Furthermore, aromatic as well as aliphatic amino acids show characteristic C–H stretching bands between 2935 and $2955\,cm^{-1}$ (Howell *et al*., 1999). Basic studies for evaluating the conformation of the major milk proteins (such as casein) and of other food materials were performed (Byler *et al*., 1988; Byler and Susi, 1988). Similar experiments were used to characterize the secondary structure of casein in various cheeses obtained from ewe milk (Fontecha *et al*., 1993). The Raman bands observed at 1609 and $1616\,cm^{-1}$ were assigned to ring vibrations of side-chain aromatic amino acids, whereas one of the most prominent bands, appearing at $1655\,cm^{-1}$, was related to the α-helix segments of casein. Bands responsible for the β-sheet structures were identified at $1630\,cm^{-1}$. During ripening, an increase in β-sheet structures could be deduced from the intensity increase at $1630\,cm^{-1}$. At the same time, Raman bands due to α-helices decreased. Conformational changes of α-lactalbumin associated with lyophilization and crystallization were investigated by Raman scattering (Yu, 1974). In the amide III region, three peaks at 1272, 1258 and $1238\,cm^{-1}$ were found which correlate very well with those of pure lysozyme, indicating that α-lactalbumin may have a conformation similar to that of hen's egg-white lysozyme (Figure 5.8).

The molecular structure of whey protein, isolated from fresh raw milk, was also characterized by FT-Raman spectroscopy (Liang *et al*., 2006). For the first time, FT-Raman spectroscopic investigations of the immunoglobulin (Ig) occurring in small

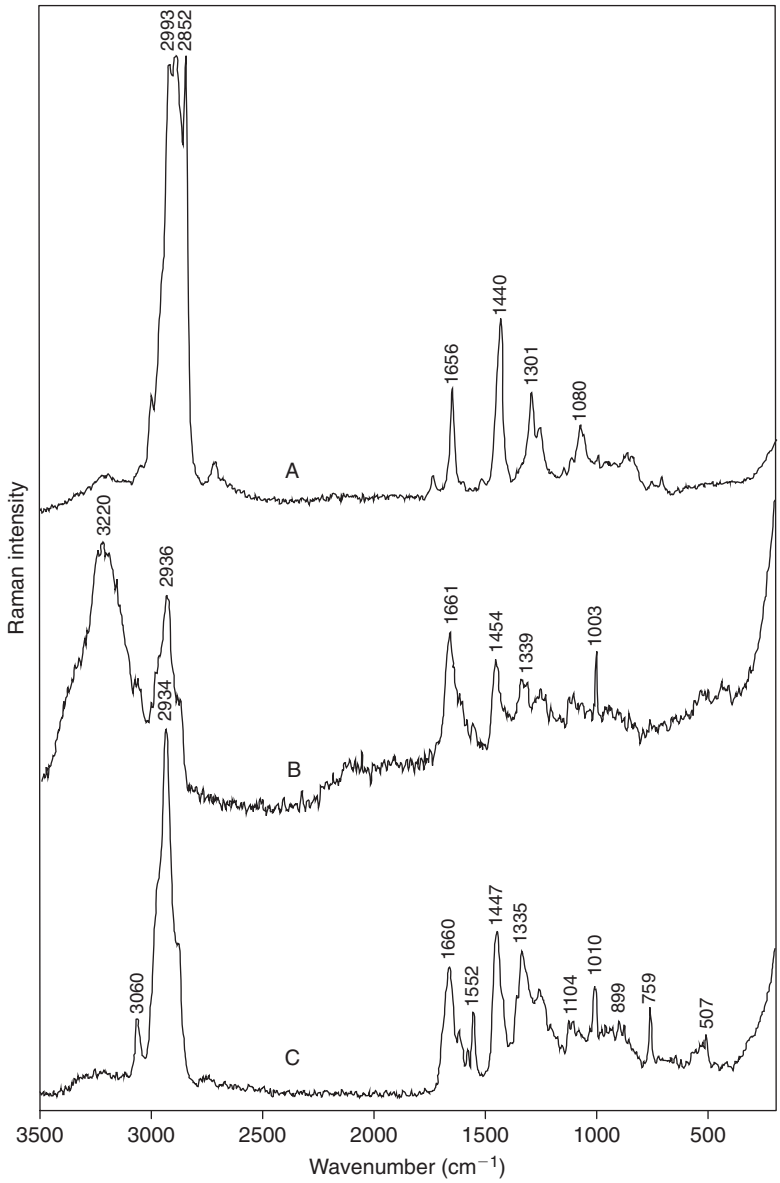

Figure 5.8 FT-Raman spectra of (a) hen's yolk, (b) hen's egg-white and (c) pure lysozyme.

amount in cow's milk were described. It was found that the secondary structure of Ig is dominated by anti-parallel β-pleated sheet. Spectra of bovine serum albumine clearly reveal that the secondary structure of this whey component is largely in α-helix form, as supported by the amide I at 1656 cm^{-1} coupling with amide III around 1260–1280 cm^{-1}. The numerous disulfide bridges which play an important role in stabilizing the individual protein structure give characteristic Raman bands diverging in the range between 510 and 540 cm^{-1}. This indicates that the conformation of disulfide groups in the analyzed whey protein substances is different.

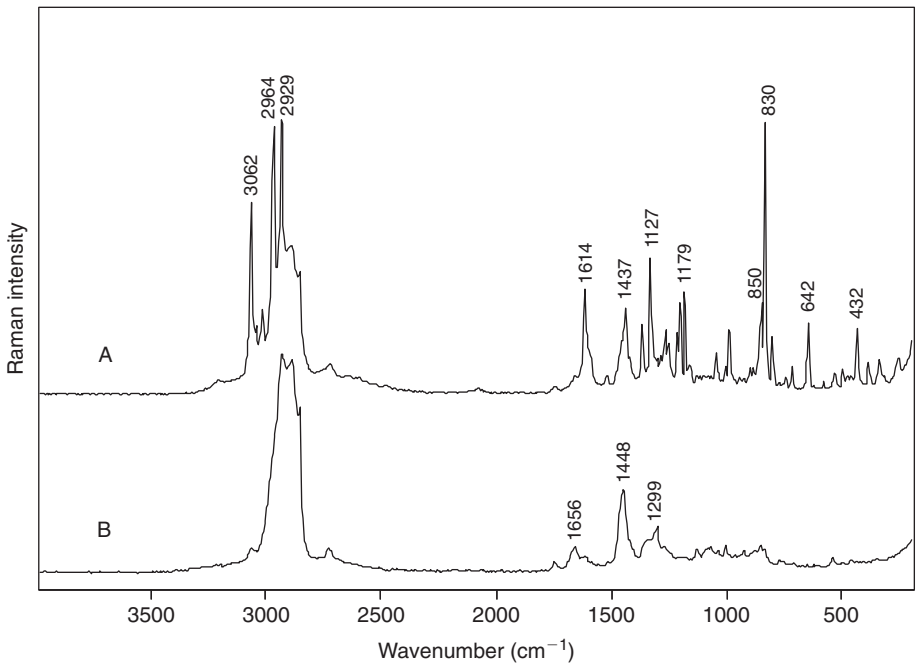

Figure 5.9 FT-Raman spectra of (a) a tyrosin standard and (b) single micro-Raman measurement obtained from a white crystal in ripe parmesan cheese.

Caseins constitute about 80% of the protein occurring in bovine milk. The two major components are α_{S1}- and β-casein, which have different secondary structures. Improved investigation to characterize the secondary structure of caseins was achieved by applying resolution-enhanced laser Raman spectroscopy (Byler *et al*., 1988). In this context, lyophilized proteins (α_{S1}-casein, β-casein, a natural mixture of bovine whole casein and micelles of the natural mixture in presence of Ca^{2+} ions) were measured in the frequency range between 1580 and 1720 cm^{-1}. In addition, the Raman spectrum of β-casein was also recorded in deuterated water. The obtained results showed that α_{S1}- and β-casein possess approximate 10% helical structure, about 20% β-structure and between 20% and 35% turns. Furthermore, it could be seen that freeze-dried micelles in the presence of Ca^{2+} ions contain an increased number of turns and higher amount of β-structure in comparison with α_{S1}- and β-caseins.

Rudzik *et al*. (2004) presented for the first time the distribution of tyrosine crystals, using micro-Raman mapping experiments. As shown in Figure 5.9, the Raman spectrum obtained from the center of the tyrosine crystal correspond exactly with the spectrum of a pure tyrosine standard, whereas the spectrum recorded from the cheese outside the crystal is dominated by lipid and amide signals. The intense Raman signals observed in the frequency range 830–850 cm^{-1} were used for integration of the mapping data.

Raman measurements of various milk-fat samples containing 2.68% conjugated linoleic acid present well-resolved bands with different scattering intensities (Meurens *et al*., 2005). Three specific signals associated with the *cis, trans* conjugated C=C in the rumenic and *trans*-10, *cis*-12-octadecadienoic acids were found

at 1652, 1438 and 3006 cm^{-1}. These Raman signals could be successfully used to accurately predict the linoleic acid concentration in milk fat.

Beverages

As already mentioned above, carotenoid molecules are strong Raman scatterers. Therefore, non-destructive resonance Raman spectroscopy is extremely valuable as a rapid screening method to continuously monitor fruit or vegetable juices during processing. Bhosale *et al*. (2004) measured juices made from carrot, tomato, orange and grape and compared the results with those obtained by extraction and subsequent HPLC, and found a high correlation between the total carotenoid content (as estimated by HPLC) and the individual Raman signals at a wide range of carotenoid levels naturally occurring in the analyzed juices. The prediction of the quality of juice by Raman measurements was improved when the samples were diluted with water to lower both scattering and optical density. Thus, the total carotenoid content measured by HPLC and Raman responses, respectively, was found to be well-correlated and statistically significant ($R = 0.98$, $P = 0.003$). Although the described method provides a potential value for the assessment of carotenoid levels in juices, the authors stress that Raman spectroscopy will never completely replace HPLC because several carotenoids cannot be distinguished by the spectroscopic method.

It was found that Raman signals due to carotenoids at around 1155 and 1525 cm^{-1}, obtained from the surface of orange peel, increase during the ripening process, reaching a maximum level at harvest time, and then decrease (Taniguchi *et al*., 1993). Interestingly, the intensity of carotenoid Raman bands correlates very well with the sugar/acid ratio of the orange juices obtained from the individual fruits. Therefore, the same authors proposed using the Raman spectra of orange peels as a method of screening the sweetness of oranges. Similar attempts have also been described for evaluating (non-destructively) the sweetness of musk-melons.

In order to study the hydrogen-bonding properties of water–ethanol of alcoholic beverages and water–ethanol mixtures of the corresponding ethanol contents, the Raman OH stretching vibrations observed at 3200 and 3400 cm^{-1} (Nose *et al*., 2004, 2005a, 2005b) were analyzed. The large OH stretching bands of H_2O were measured at different temperatures ranging from 5°C to 65°C to investigate the effect on the hydrogen-bonding strength in a 15% (v/v) ethanol–water mixture and in Japanese sake samples. The authors observed that the peak intensity of strongly hydrogen-bonded OH at *ca*. 3200 cm^{-1} decreased and at the same time the other peak of non- or weakly hydrogen-bonded OH at *ca*. 3400 cm^{-1} increased when the temperature of the sample decreased. Thus the ratio of peak intensities ($I_1 = 3200\,cm^{-1}/I_2 = 3400\,cm^{-1}$) can be principally used to evaluate the degree of the hydrogen-bonding strength of water–ethanol mixtures.

Raman spectroscopy has also been used to analyze different types of alcoholic beverages, such as whisky, vodka and sugary drinks (Nordon *et al*., 2005). Based on the comparatively strong and sharp signal observed at 880 cm^{-1}, which is attributed to the symmetric C–C–O stretch of ethanol, the alcohol content in the individual spirits can be analyzed. The authors found that a univariate calibration model is

suitable for reliable predictions. When spirit samples with ethanol concentrations in the range of 19.2–61.7% (v/v) were measured, a precision rate of 0.5% and an average accuracy of 2.9% were obtained. It was observed that the Raman signals were not limited by the diameter when the samples were measured directly in the original glass round bottles. However, the color of the glass was found to have a significant influence on the Raman spectrum, and the green bottles in particular showed comparatively high fluorescence when a 785-nm laser was used for excitation. However whisky samples also presented a large fluorescent background caused by certain components of the spirit.

Ozaki *et al*. (1992) compared the FT-Raman spectra of approximately 1-year-old Japanese tea with that obtained from fresh tea. The authors found that the relative intensities of carotenoid bands were much weaker in the spectrum of the old tea than in that of the fresh one. Based on the intensity ratio of the two bands measured at $1529\,cm^{-1}$ (carotenoid signal) and $1446\,cm^{-1}$ (protein signal), the structural changes occurring during the storage period were monitored. It is proposed that these Raman signals can be used generally as marker bands to characterize the quality of certain foodstuffs, such as fruits and vegetables.

As demonstrated by Rubayiza and Meurens (2005), Raman spectroscopy also offers the opportunity to distinguish the botanical origin of green and roasted coffees. The lipid fractions of *Coffea arabica* (Arabica) and *Coffea canephora* (Robusta) were successfully discriminated by applying PCA based on the obtained Raman data. The main spectral differences of both coffee species are due to variations in the content of kahweol, which is present at 0.1–0.3% dry matter in Arabica beans but occurs only in traces in Robusta beans. It has been found that the first principal component explains 93% of the spectral variation and corresponds directly with the kahweol level. A characteristic Raman signal of kahweol can be seen at $1478\,cm^{-1}$, which is associated with the C=C stretching in the furan cycle of the molecule.

The seeds of guarana (*Paullinia cupana*), a shrub growing in the Brazilian Amazonian rainforest, have been analyzed by Raman spectroscopy for their content of caffeine, theophylline and theobromine. Whereas the caffeine content of *Guarana* is about four times higher greater than that of the commercial *Coffea* species, the two other alkaloids occur only in traces (Edwards *et al*., 2005a).

Similar studies have been performed on cacao seeds (*Theobroma cacao*), aiming to identify main fat constituents (oleic, stearic and palmitic acids) as well as the alkaloid theobromine (Edwards *et al*., 2005b). The Raman spectrum of powdered seed kernels showed characteristic theobromine bands at $1334\,cm^{-1}$ (C–N stretching), $1225\,cm^{-1}$ (C–N stretching), $946\,cm^{-1}$ ($N–CH_3$ stretching), $776\,cm^{-1}$ (O=C–C stretching), $509\,cm^{-1}$ ($C–N–CH_3$ stretching) and $459\,cm^{-1}$ (C–N–C asymmetric deformation) (Figure 5.10). The presence of cacao butter was identified by two bands at 1744 and $1659\,cm^{-1}$, representing the C=O and C=C stretching modes of the fatty material.

For several years rooibos tea (*Aspalathus linearis*), an indigenous South African herbal tea, has been very popular in Europe and North America. It is assumed that various phenolic substances (such as aspalathin) acting as potent antioxidants may possess the main therapeutic value. Usually quality control of fermented and unfermented rooibos tea is performed by HPLC measurements, but recently non-destructive FT-Raman

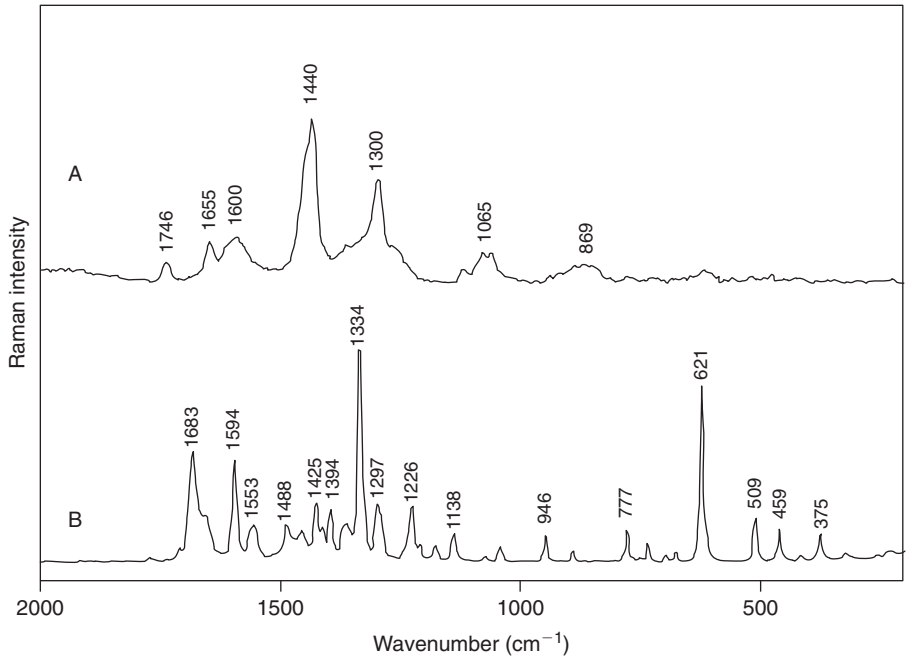

Figure 5.10 FT-Raman spectra obtained from (a) cacao bean and (b) pure theobromine.

spectroscopy was used for the first time for *in situ* identification of aspalathin and quantification of the dihydrochalcones in dried, so-called green rooibos (Baranska *et al*., 2006d). Applying two-dimensional correlation spectroscopy, characteristic key bands of aspalathin (aromatic C–H out-of-plane deformation vibration at 784 cm^{-1}) could be successfully localized and identified in the individual Raman spectra obtained from various rooibos samples. Based on this knowledge, Raman mapping revealed the spatial distribution of aspalathin within the intact dried plant material, demonstrating that this component is distributed heterogeneously in the sample, with the highest concentration in the inner part of the leaves.

Other natural remedies such as chamomile (*Chamomilla recutita*) and fennel (*Foeniculum vulgare*), which are widely used as herbal teas to cure various human disorders, have also been successfully characterized by Raman spectroscopy (Baranska *et al*., 2004). Raman mapping, obtained from transverse and longitudinal sections of fennel fruits show clearly the distribution of anethole, which is the main essential oil component to be found in the analyzed fennel chemotype. According to the literature, anethole was detected in the essential oil ducts located in the outer parts of the mericarp. Raman spectra obtained from chamomile inflorescence show strong signals in the range between 2150 and 2250 cm^{-1} due to *cis*- and *trans*-spiroethers (polyacetylenes). Mapping experiments demonstrate that these substances with antibacterial, antifungal and antimicrobial properties are accumulated in the middle part of the flower head. Simultaneously, it was found that carotenoids occur mainly in the pollen at the top of the flower heads.

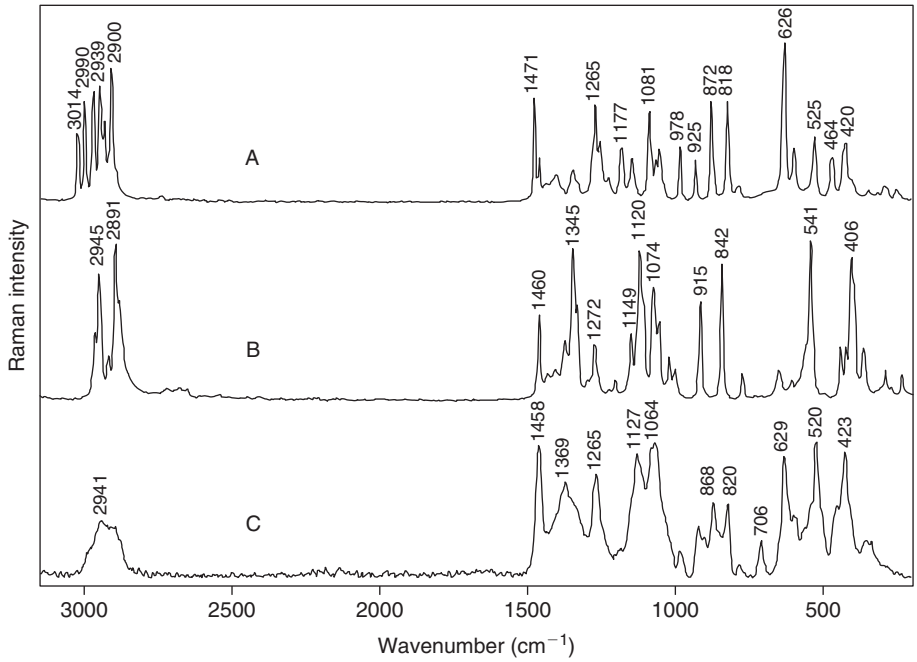

Figure 5.11 FT-Raman spectra of (a) fructose, (b) glucose and (c) orange honey.

Honey

Honey has always been a target of adulterators, for economic gain. Most adulterants are cane and beet invert syrups, which have a sucrose–glucose–fructose profile very similar to that of honey. Generally, such honey adulteration is difficult to detect due to the high variation in chemical composition according to the different floral and geographical origins.

The potential of FT Raman spectroscopy to discriminate honey from three different floral sources (clover, orange, buckwheat) and to detect the amount of possible adulterants (cane and beet invert sugar) has been described (Paradkar and Irudayaray, 2001) (Figure 5.11). The spectra obtained from different honey types showed major peaks in the area of 300–1500 cm^{-1} as well as at 2945–3384 cm^{-1}. A strong peak at 1072 cm^{-1} has been assigned as bending vibration of C(1)–H and COH in carbohydrates, with a minor contribution from the C–N of proteins and free amino acids. Another strong and sharp signal was detected at 1267 cm^{-1} resulting from the vibration of C(6)–OH and C(1)–OH of carbohydrates with a minor contribution from the amide III vibration mode. Combination vibration of CH_2 groups with a minor contribution of carboxylic groups (due to amino acids of organic acids) can be seen as a sharp peak at 1461 cm^{-1}. Stretching vibrations of CH and OH groups occur as broad peaks at 2945 and 3384 cm^{-1}, respectively. PLS and PCR analyses were successfully used for quantitative and discriminant analysis of the analyzed honey samples. For clover honey, the prediction of adulterants such as beet and cane inverts gave reliable results ($R^2 = 0.94$, SEC $< 2.52\%$, SEP $< 2.20\%$). Similar trends were found for buckwheat and orange honey.

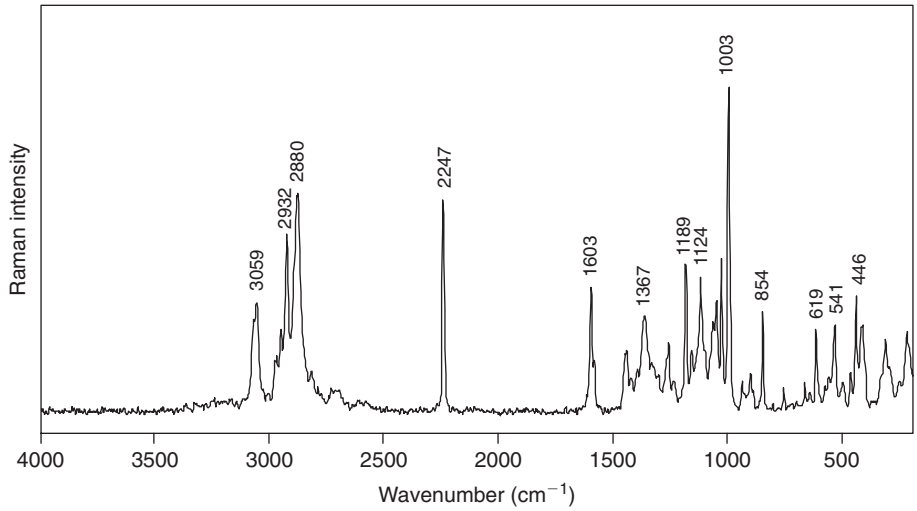

Figure 5.12 FT-Raman spectrum of pure amygdalin.

An FT-Raman spectroscopy method was also developed to predict the fructose and glucose content in various honey samples (Batsoulis *et al*., 2005). For the simultaneous determination of both sugars, the spectral range 1700–700 cm^{-1} without any baseline correction was used. Based on HPLC reference data a PLS model was established, and by applying the calibration functions both substances were correctly predicted in 10 unknown honey samples. Similar studies have also been performed by other research groups (Goodacre *et al*., 2002; Oliveira *et al*., 2002). Using the vibrational bands in the fingerprint region (500–1800 cm^{-1}), the authors succeeded in identifying the two major sugar components in honey – fructose and glucose – and at least one vibrational band was found to be characteristic for sucrose. Chemometric analyses showed that major differences between the different honey types were due to their botanical rather than their geographical origin. Arvanitoyannis *et al*. (2005) applied multivariate analysis and other statistical methods for grouping and detecting honey samples of various origins. AAS, HPLC, GC-MS, NMR, FT-Raman and NIR data were also included in these chemometric calculations.

Micro-Raman measurements

By combining Raman spectroscopy with microscopy, individual molecular information regarding various tissues can be obtained simultaneously at the cellular level. Using the point-mapping technique equipped with a *xy* stage, it may take up to several hours to map a few square millimeters. New focal plane detector systems that allow recording of an entire row or even a particular area perform mapping in a much shorter time.

Raman microspectroscopy can be successfully applied in order to characterize the distribution of amygdalin in bitter almonds (*Prunus amygdalus*) across the cotelydon (Thygesen *et al*., 2003). In this research, the nitrile group of the cyanogenic glycoside substance was observed at 2240 cm^{-1} as a strong band in the Raman spectrum (Figure 5.12). Based on this signal, a map was obtained indicating that amygdalin is

mainly present in the epidermis but occurs only in low amounts in the center of bitter almonds. This finding provides proof for the observation that amygdalin acts to prevent the attack of insects and fungi.

Besides amygdalin, five other cyanogenic glucosides were also detected in the roots and leaves of cassava (*Manihot esculenta*) and the leaves of sorghum (*Sorghum bicolor*) (Thygesen *et al*., 2004). The authors observed that the position of the nitrile triple bond frequency varies among the analyzed glycosides; those cyanogenic glycosides that contain a neighboring aromatic ring show a C≡N signal above 2240 cm^{-1} (amygdalin, sambunigrin, dhurrin), whereas for the three aliphatic cyanogenic glycosides (linamarin, linustatin, neolinustatin) this Raman signal is shifted to 2233 cm^{-1}. Applying FT-NIR Raman spectrometry, only weak CN signals were seen in the spectra; these are related to the low content of cyanogenic substances in the plant tissue (0.01% in the leaves and 0.0008% in the root). Therefore, the authors developed a SERS-based method with gold colloids to improve the sensitivity of the CN group. This very sensitive method allows measurement of weakly cyanogenic plants, but it requires a highly reproducible clean-up of the sample because the SERS signal starts to decrease immediately after mixing the analyte with the gold colloid suspension.

Micro-FT-Raman experiments have been performed in order to characterize the distribution of active principals in selected medicinal plants and spices, such as fennel (*Foeniculum vulgare*), chamomile (*Chamomilla recutita*) and curcuma (*Curcuma longa*) (Baranska *et al*., 2004). The same technique has been used to identify and quantify harpagoside in the secondary roots of devil's claw (*Harpagophytum procumbens*) (Baranska *et al*., 2005d). Some characteristic key bands due to the active principle were found in the frequency range 1600–1700 cm^{-1}. According to the Raman spectrum of pure harpagoside, these signals were assigned to –C=O, –C=C– and benzene ring stretching vibrations.

PLS models developed for harpagoside content provide sufficient reliability to classify devil's claw samples. Integration over the strongest harpagoside band (1618–1656 cm^{-1}) demonstrates that the highest concentration can be observed in the outer part of the secondary root.

Pesticides and microorganisms

Current methods of analyzing residual pesticides on the surface of vegetable and fruits are mainly based on gas chromatography and high-performance liquid chromatography combined with mass spectroscopy. Because these analytical methods are time-consuming and not easy to perform, a Raman method has been developed to detect pesticide residues on the surface of fruits (Zhang *et al*., 2006). It has been shown that even small amounts of certain pesticides (Abameclin, Petroleumoil, Chongmanjue, Cypermethrin, Zhibaoboshi) can be easily identified with 1064 nm excitation if the characteristic pesticide signals are not overlapped by strong carotene bands. Whereas at 514.5 nm excitation the fluorescence background of the Raman spectra obtained from contaminated fruits shows comparatively high fluorescence, at NIR excitation the resonance Raman effect of carotene is significantly reduced and, besides strong carotene signals, characteristic key signals of the individual pesticide compounds can also be successfully

recorded. Comparing the FT-Raman spectra of the fruits with those obtained from the pure pesticides, the contaminants left on the surfaces of pear, banana, Chinese gooseberry, orange grapes, apple and longan could be conveniently detected.

Several attempts have been made to establish micro-Raman spectroscopy methods to directly classify single microorganisms (Schuster *et al*., 2000; Grun *et al*., 2007; Kalasinsky *et al*., 2007; Krause *et al*., 2007). In this context, discrimination between different bacteria species was performed regarding variations in pattern of gene expression, protein synthesis and metabolite accumulation. It has been proved that identification of unknown bacteria species can be successfully performed if a robust Raman spectral library with numerous entries of various bacteria is collected in advance.

Latest research activities prove that FT-Raman spectroscopy can also be successfully applied for characterization and discrimination of different microorganisms, including pathogens such as *Escherichia coli*, on the surface of fruits. The spectral regions of 2800–3000 cm^{-1} and 700–1500 cm^{-1} were used to collect specific Raman data of the gram-negative types of *Legionella pneumophila*, *Aeromonades*, *Pseudomonas aeruginosa* and *Salmonella typhimurium* (Yang and Irudayaraj, 2003). Although only minor spectral effects could be related to the individual microorganisms, discriminant analysis was able to demonstrate that six different types of microorganisms could be well classified. Five different strains of *E. coli* were discriminated with an accuracy of 100%. Because the food product can be placed directly in the focused laser beam without the need for any sample pre-treatments, FT-Raman may have some potential in the near future as a fast evaluation method in specific fields of food safety analysis.

Conclusions

During the past 30 years various applications of Raman spectroscopy for an efficient measurement of food substances have been developed. It has been found that, in particular, the FT-Raman technique is extremely useful for non-destructive analysis of intact fresh biomaterials without the need to apply any sample clean-up procedures. Using excitation with the radiation of the Nd:YAG laser line at 1064 nm, fluorescence and photochemical degradation of food samples is effectively reduced to a minimum. By combining Raman spectroscopy and chemometric analysis methods, discrimination of different botanical and geographical origins or reliable classification of different vegetable oils and fats as well as meat products can be successfully achieved. Furthermore, adulterations of various food materials can be identified by chemometrics if slight spectroscopic variations are observed in the measured samples.

FT-Raman spectra of fresh plant tissues are usually dominated by bands of carotenoids. In addition, several herbs and spices show characteristic key bands of various active principals such as alkaloids, essential oil substances or sulfur substances. Specific Raman bands obtained from measurements on meat, milk, cheese and egg can be used to predict the secondary structure of various food proteins such as casein, ovalbumin, and bovine serum albumin. Based on these data, correlations with various quality parameters such as texture and degree of juiciness of meat have been successfully performed. Combining micro-Raman spectroscopy with chemometric algorithms,

a fast and easy characterization for different plant taxa can be generally achieved. Applying hierarchical cluster analysis, in most cases different species and sometimes even subspecies can be discriminated within the same genus. Microspectroscopy also allows spatially resolved investigation of heterogeneous food materials and ingredients. In this context, two different mapping techniques are available: applying line mapping changes in a specific chemical component can be regarded along a certain direction, whereas two-dimensional area mapping provides a spectroscopic image that can be directly compared to the visual image obtained by a light microscope. Dependent on the spatial resolution and the area to be analyzed, mapping experiments take several hours to days, even for FT-based instruments.

Several Raman methods presently applied for quality-control purposes have the potential to replace existing standard procedures such as GC, HPLC or other physicochemical measurements, but it must be mentioned here that this technique is usually not useful to confirm adulterations at the mg kg^{-1} or even μg kg^{-1} levels (except in substances presenting a very high Raman scattering or application of surface-enhanced Raman scattering). Raman spectroscopy equipped with the fiber-optic technique allows remote analysis and online monitoring of various quality parameters during food processing (e.g. during the wine-making process).

References

Alizadeh-Pasdar, N., Li-Chan, E.C.Y. and Nakai, S. (2004). FT-Raman spectroscopy, fluorescent probe and solvent accessibility study of egg and milk proteins. *Journal of Agricultural and Food Chemistry*, **52**, 5277–5283.

Andreev, G.N., Schrader, B., Schulz, H. *et al*. (2001). Non-destructive NIR-FT-Raman analyses in practice. Part 1. Analyses of plants and historic textiles. *Fresenius Journal of Analytical Chemistry*, **371**, 1009–1017.

Aparicio, R., Morales, M.T. and Baeten, V. (1996). Characterization of virgin olive oil adulteration by FT-Raman spectroscopy. In: R.E. MacDonald and M.M. Mossoba (eds), *87th American Oil Chemists' Society Annual Meeting, Indianapolis, USA*. Champaign, IL: American Oil Chemists' Society.

Arvanitoyannis, I.S., Chalhoub, C., Gotsiou, P. *et al*. (2005). Novel quality control methods in conjunction with chemometrics (multivariate analysis) for detecting honey authenticity. *Critical Reviews in Food Science and Nutrition*, **45**, 193–203.

Asher, I.M., Carew, E.B. and Staneley, H.E. (1976). Laser Raman spectroscopy: a new probe of the molecular conformations of intact muscle and its components. In: E. Bulbring and M.F. Shuba (eds), *Physiology of Smooth Muscle*. New York, NY: Raven, pp. 229–238.

Baeten, V., Meurens, M., Morales, M.T. and Aparicio, R. (1996). Detection of virgin olive oil by Fourier transform Raman Spectroscopy. *Journal of Agricultural and Food Chemistry*, **44**, 2225–2230.

Baeten, V., Hourant, P., Morals, M.T. and Aparicio, R. (1998). Oil and fat classification by FT-Raman spectroscopy. *Journal of Agricultural and Food Chemistry*, **46**, 2638–2646.

Bailey, G.F. and Horvat, R.J. (1972). Raman spectroscopic analysis of the cis/trans isomer composition of edible vegetable oils. *Journal of the American Oil Chemists' Society*, **49**, 494–498.

Baranska, M. and Schulz, H. (2005). Spatial tissue distribution of polyacetylenes in carrot root. *Analyst*, **130**, 855–859.

Baranska, M., Schulz, H., Rösch, P. *et al*. (2004). Identification of secondary metabolites in medicinal and spice plants by NIR-FT-Raman microspectroscopic mapping. *Analyst*, **129**, 926–930.

Baranska, M., Schulz, H., Baranski, R. *et al*. (2005a). In situ simultaneous analysis of polyacetylenes, carotenoids and polysaccharides in carrot roots. *Journal of Agricultural and Food Chemistry*, **53**, 6565–6571.

Baranska, M., Schulz, H., Krüger, H. and Quilitzsch, R. (2005b). Chemotaxonomy of aromatic plants of the genus Origanum via vibrational spectroscopy. *Analytical and Bioanalytical Chemistry*, **381**, 1241–1247.

Baranska, M., Schulz, H., Reitzenstein, S. *et al*. (2005c). Vibrational spectroscopic studies to aquire a quality control method of Eucalyptus essential oils. *Biopolymers*, **78**, 237–248.

Baranska, M., Schulz, H., Siuda, R. *et al*. (2005d). Quality control of Harpagophytum procumbens and its related phytopharmaceutical products by means of NIR-FT-Raman spectroscopy. *Biopolymers*, **77**, 1–8.

Baranska, M., Schütze, W. and Schulz, H. (2006a). Determination of lycopene and β-carotene content in tomato fruits and related products: comparison of FT-Raman, ATR-IR and NIR spectroscopy. *Analytical Chemistry*, **78**, 8456–8461.

Baranska, M., Schulz, H. and Christensen, L.P. (2006b). Structural changes of polyacetylenes in American ginseng root can be observed in situ by using Raman spectroscopy. *Journal of Agricultural and Food Chemistry*, **54**, 3629–3635.

Baranska, M., Schulz, H., Walter, A. *et al*. (2006c). Investigation of Eucalyptus essential oil by using vibrational spectroscopy methods. *Vibrational Spectroscopy*, **42**, 341–345.

Baranska, M., Schulz, H., Joubert, E. and Manley, M. (2006d). In situ flavonoid analysis by FT-Raman spectroscopy: identification, distribution, and quantification of aspalathin in green rooibos (*Aspalathus linearis*). *Analytical Chemistry*, **78**, 7716–7721.

Baranski, R., Baranska, M. and Schulz, H. (2005). Changes in carotenoid content and distribution in living plant tissue can be observed and mapped in situ using NIR-FT-Raman spectroscopy. *Planta*, **222**, 448–457.

Baranski, R., Baranska, M., Schulz, H. *et al*. (2006). Single seed Raman measurements allow taxonomical discrimination of *Apiaceae* accessions collected in gene banks. *Biopolymers*, **81**, 497–505.

Barron, C., Robert, P., Guillon, F. *et al*. (2006). Structural heterogeneity of wheat arabinoxylans revealed by Raman spectroscopy. *Carbohydrate Research*, **341**, 1186–1191.

Barthus, R.C. and Poppi, R.J. (2001). Determination of the total unsaturation in vegetable oils by Fourier transform Raman spectroscopy and multivariate calibration. *Vibrational Spectroscopy*, **26**, 99–105.

Batsoulis, A.N., Siatis, N.G., Kimbaris, A.C. *et al*. (2005). FT-Raman spectroscopic simultaneous determination of fructose and glucose in honey. *Journal of Agricultural and Food Chemistry*, **53**, 207–210.

Beattie, R.J., Bell, S.J., Farmer, L.J. *et al*. (2004). Preliminary investigation of the application of Raman spectroscopy to the prediction of the sensory quality of beef silverside. *Meat Science*, **66**, 903–913.

Beattie, J.R., Maguire, C., Gilchrist, S. *et al*. (2007). The use of Raman microscopy to determine and localize vitamin E in biological samples. *Journal of the Federation of American Societies for Experimental Biology*, **21**, 766–776.

Bhosale, P., Ermakov, I.V., Ermakova, M.R. *et al*. (2004). Resonance Raman quantification of nutritionally important carotenoids in fruits, vegetables, and their juices in comparison to high-pressure liquid chromatography analysis. *Journal of Agricultural and Food Chemistry*, **52**, 3281–3285.

Brøndum, J., Byrne, D.V., Bak, L.S. *et al*. (2000). Warmed-over flavor in porcine meat – a combined spectroscopic, sensory and chemometric study. *Meat Science*, **54**, 83–95.

Byler, D.M. and Susi, H. (1988). Application of computerized infrared and Raman spectroscopy to conformation studies of casein and other food proteins. *Journal of Industrial Microbiology and Biotechnology*, **3**, 73–88.

Byler, D.M., Farrell, H.M. and Susi, H. (1988). Raman spectroscopic study of casein structure. *Journal of Dairy Science*, **71**, 2622–2629.

Caille, J.P., Pigeon-Gosselin, M., Dousseau, F. and Pézolet, M. (1987). Orientation of the contractile proteins of muscle fibers by Raman and infrared spectroscopy. *Biophysical Journal*, **51**, 279a.

Cornard, J.P., Merlin, J.C., Boudet, A.C. and Vrielynck, L. (1997). Structural study of quercetin by vibrational and electronic spectroscopies combined with semi-empirical calculations. *Biospectroscopy*, **3**, 183–193.

Daferera, D.J., Tarantilis, P.A. and Polissiou, M.G. (2002). Characterization of essential oils from Lamiaceae by Fourier transform Raman spectroscopy. *Journal of Agricultural and Food Chemistry*, **50**, 5503–5507.

Delhaye, M. and Dhamelincourt, P. (1975). Raman microprobe and microscope with laser excitation. *Journal of Raman Spectroscopy*, **3**, 33–43.

Edwards, H.G.M., Farwell, D.W., de Oliveira, L.F.C. *et al*. (2005a). FT-Raman spectroscopic studies of guarana and some extracts. *Analytica Chimica Acta*, **532**, 177–186.

Edwards, H.G.M., Villar, S.E.J., de Oliveira, L.F.C. and Le Hyaric, M. (2005b). Analytical Raman spectroscopic study of cacao seeds and their chemical extracts. *Analytica Chimica Acta*, **538**, 175–180.

Ellis, D.I., Broadhurst, D., Clarke, S.J. and Goodacre, R. (2005). Rapid identification of closely related muscle foods by vibrational spectroscopy and machine learning. *Analyst*, **130**, 1648–1654.

Farrell, H.M., Brown, E.M. and Kumosinski, T.F. (1993). Three-dimensional molecular modelling of bovine caseins. *Food Structure*, **12**, 235–250.

Fleischmann, M., Hendra, P.J. and McQuillan, J.A. (1974). Raman spectra of pyridine adsorbed at a silver electrode. *Chemical Physics Letters*, **26**, 163–166.

Fontecha, J., Bellanato, J. and Juarez, M. (1993). Infrared and Raman spectroscopic study of casein in cheese: effect of freezing and frozen storage. *Journal of Dairy Science*, **76**, 3303–3309.

Goodacre, R., Radovic, B.S. and Anklam, E. (2002). Progress toward the rapid non-destructive assessment of the floral origin of European honey using dispersive Raman spectroscopy. *Applied Spectroscopy*, **56**, 521–527.

Grun, J., Manka, C.K., Nikitin, S. *et al*. (2007). Identification of bacteria from two-dimensional resonant-Raman spectra. *Analytic Chemistry*, ASAP Article no. 10.1021/ac070681h.

Harz, M., Rösch, P., Peschke, K.D. *et al*. (2005). Micro-Raman spectroscopic identification of bacterial cells of the genus Staphyllococcus and dependence on their cultivation conditions. *Analyst*, **130**, 1543–1550.

Heise, H.M., Damm, U., Lampen, P. *et al*. (2005). Spectral variable selection for partial least squares calibration applied to authentication and quantification of extra virgin olive oils using Fourier transform Raman spectroscopy. *Applied Spectroscopy*, **59**, 1286–1294.

Howell, N.K., Arteaga, G., Nakai, S. and Li-Chan, E.C.Y. (1999). Raman spectral analysis in the C-H stretching region of proteins and amino acids for investigation of hydrophobic interactions. *Journal of Agricultural and Food Chemistry*, **47**, 924–933.

Jeanmaire, D.J. and Van Duyne, R.P. (1977). Surface Raman spectroelectrochemistry. Part 1. Heterocyclic, aromatic, and aliphatic amines adsorbed on the anodized silver electrode. *Journal of Electroanalytical Chemistry*, **84**, 1–20.

Johnson, G.L., Machado, R.M., Freidl, K.G. *et al*. (2002). Evaluation of Raman spectroscopy for determining cis and trans isomers in partially hydrogenated soybean oil. *Organic Process Research and Development*, **6**, 637–644.

Kalasinsky, K.S., Hadfield, T., Shea, A.A. *et al*. (2007). Raman chemical imaging spectroscopy reagentless detection and identification of pathogens: signature development and evaluation. *Analytical Chemistry*, **79**, 2658–2673.

Kang, J.S., Hwang, S.Y., Lee, C.J. and Lee, M.S. (2002). SERS of dithiocarbamate pesticides adsorbed on silver surface. *Bulletin of the Korean Chemical Society*, **23**, 1604–1610.

König, J.L. and Frushour, B.G. (1972). Raman-scattering of chymotrypsinogen A, ribonuclease, and ovalbumin in aqueous solution and solid state. *Biopolymers*, **11**, 2505–2520.

Krause, M., Radt, B., Rösch, P. and Popp, J. (2007). The investigation of single bacteria by means of fluorescence staining and Raman spectroscopy. *Journal of Raman Spectroscopy*, **38**, 369–372.

Kumosinski, T.F., Brown, E.M. and Farrell, H.M. (1993). Three-dimensional molecular modelling of bovine caseins: an energy-minimized β-casein structure. *Journal of Dairy Science*, **76**, 931–945.

Lerner, B., Garry, M. and Walder, F. (1992). Characterization of polyunsaturation in cooking oils by the 910 FT-Raman. In: E.F. Vansant (ed.), *Proceedings of the 2nd International Workshop on Fourier transform infrared spectroscopy, University of Antwerp*. Antwerp: University of Antwerp, pp. 75–82.

Liang, M., Chen, V.Y.T., Chen, H.L. and Chen, W. (2006). A simple and direct isolation of whey components from raw milk by gel filtration chromatography and structural characterization by Fourier transform Raman spectroscopy. *Talanta*, **69**, 1269–1277.

Li-Chan, E.C.Y. (1994). Development in the detection of adulteration of olive oils. *Trends in Food Science and Technology*, **5**, 3–11.

Li-Chan, E., Nakai, S. and Hirotsuka, M. (1994). Raman spectroscopy as a probe of protein structure in food systems. In: R.Y. Yada, R.L. Jackman and J.L. Smith (eds), *Protein Structure–Function Relationships in Foods*. London: Chapman & Hall, pp. 163–197.

Lin, V.J.C. and König, J.L. (1976). Raman studies of bovine serum albumin. *Biopolymers*, **15**, 203–218.

Marigheto, N.A., Kemsley, E.K., Defernez, M. and Wilson, R.H. (1998). A comparison of mid-infrared and Raman spectroscopies for the authentication of edible oils. *Journal of the American Oil Chemists' Society*, **75**, 987–992.

McCreery, R.L. (2000). Raman spectroscopy for chemical analysis. In: J.D. Winefordner (ed.), *Chemical Analysis – A Series of Monographs of Analytical Chemistry and its Application*. New York, NY: Wiley-Interscience, John Wiley & Sons, Inc.

Merlin, J.C., Statoua, A. and Brouillard, R. (1985). Investigation of the in vivo organization of anthocyanins using resonance Raman microspectrometry. *Phytochemistry*, **24**, 1575–1581.

Merlin, J.C., Statoua, A., Cornard, J.P. *et al*. (1994). Resonance Raman spectroscopic studies of anthocyanins and anthocyanidins in aqueous solutions. *Phytochemistry*, **35**, 227–232.

Meurens, M., Baeten, V., Yan, S.H. *et al*. (2005). Determination of the conjugated linoleic acids in cow's milk fat by Fourier transform Raman spectroscopy. *Journal of Agricultural and Food Chemistry*, **53**, 5831–5835.

Muik, B., Lendl, B., Molina-Diaz, A. and Ayora-Canada, M.J. (2003a). Direct, reagent-free determination of free fatty acid content in olive oil and olives by Fourier transform Raman spectrometry. *Analytica Chimica Acta*, **487**, 211–220.

Muik, B., Lendl, B., Molina-Diaz, A. and Ayora-Canada, M.J. (2003b). Fourier transform Raman spectrometry for the quantitative analysis of oil content and humidity in olives. *Applied Spectroscopy*, **57**, 233–237.

Nersissian, A.M., Mehrabian, Z.A., Nalbandyan, R.M. *et al*. (1996). Cloning, expression, and spectroscopic characterization of *Cucumis sativus* stellacyanin in its nonglycosylated form. *Protein Science*, **5**, 2184–2192.

Nestor, L., Larrabee, J.A., Woolery, G. *et al*. (1984). Resonance Raman spectra of blue copper proteins: assignments from normal mode calculations and copper-63/copper-65 and H_2O/D_2O shifts for stellacyanin and lactase. *Biochemistry*, **23**, 1084–1093.

Nordon, A., Mills, A., Burn, R.T. *et al*. (2005). Comparision of non-invasive NIR and Raman spectrometrics for determination of alcohol content in spirits. *Analytica Chimica Acta*, **548**, 148–158.

Nose, A., Hojo, M., Suzuki, M. and Ueda, T. (2004). Solute effects on the interaction between water and ethanol in aged whiskey. *Journal of Agricultural and Food Chemistry*, **52**, 5359–5365.

Nose, A., Hamasaki, T., Hojo, M. *et al*. (2005a). Hydrogen bonding in alcoholic beverages (distilled spirits) and water-ethanol mixtures. *Journal of Agricultural and Food Chemistry*, **53**, 7074–7081.

Nose, A., Myojin, M., Hojo, M. *et al*. (2005b). Proton NMR and Raman spectroscopic studies of Japanese sake, an alcoholic beverage. *Journal of Bioscience and Bioengineering*, **99**, 493–501.

Oliveira, L.F.C., Colombara, R. and Edwards, H.G.M. (2002). Fourier transform Raman spectroscopy of honey. *Applied Spectroscopy*, **56**, 306–311.

Ozaki, Y., Cho, R., Ikegawa, K. *et al*. (1992). Potential of near-infrared Fourier transform Raman spectroscopy in food analysis. *Applied Spectroscopy*, **46**, 1503–1507.

Paradkar, M.M. and Irudayaray, J. (2001). Discrimination and classification of beet and cane inverts in honey by FT-Raman spectroscopy. *Food Chemistry*, **76**, 231–239.

Parker, A.W. and Bisby, R.H. (1993). Time-resolved resonance Raman spectroscopy of alpha-tocopheroxyl and related radicals in solvent, micellar and membrane systems. *Journal of the Chemical Society, Faraday Transactions*, **89**, 2873–2878.

Pedersen, D.K., Morel, S., Andersen, H.J. and Engelsen, S.B. (2003). Early prediction of water-holding capacity in meat by multivariate vibrational spectroscopy. *Meat Science*, **65**, 581–592.

Peica, N., Pavel, I., Pinzaru, S.C. *et al*. (2005). Vibrational characterization of E102 food additive by Raman and surface-enhanced Raman spectroscopy and theoretical studies. *Journal of Raman Spectroscopy*, **36**, 657–666.

Peticolas, W.L. (1995). Raman spectroscopy of DNA and proteins. *Methods Enzymology*, **246**, 389–416.

Podstawka, E., Swiatlowska, M., Borowiec, E. and Proniewicz, L.M. (2007). Food additives characterization by infrared, Raman, and surface-enhanced Raman spectroscopies. *Journal of Raman Spectroscopy*, **38**, 356–363.

Prinsloo, L.C., du Plooy, W. and van der Merwe, C. (2004). Raman spectroscopic study of the epicuticular wax layer of mature mango (*Mangifera indica*) fruit. *Journal of Raman Spectroscopy*, **35**, 561–567.

Raman, C.V. (1928a). A new radiation. *Indian Journal of Physics*, **2**, 287.

Raman, C.V. and Krishnan, K.S. (1928b). A new type of secondary radiation. *Nature*, **121**, 501–502.

Reitzenstein, S., Rösch, P., Strehle, M.A. *et al*. (2007). Nondestructive analysis of single rapeseeds by means of Raman spectroscopy. *Journal of Raman Spectroscopy*, **38**, 301–308.

Rimai, L., Heyde, M.E. and Gill, D. (1973). Vibrational spectra of some carotenoids and related linear polyenes. A Raman spectroscopic study. *Journal of the American Chemical Society*, **95**, 4493–4501.

Rösch, P., Popp, J. and Kiefer, W. (1999). Raman and surface enhanced Raman spectroscopic investigation on *Lamiaceae* plants. *Journal of Molecular Structure*, **480–481**, 121–124.

Rösch, P., Kiefer, W. and Popp, J. (2002). Chemotaxonomy of mints of genus *Mentha* by applying Raman spectroscopy. *Biopolymers*, **67**, 358–361.

Rubayiza, A.B. and Meurens, M. (2005). Chemical discrimination of Arabica and Robusta coffees by Fourier transform Raman spectroscopy. *Journal of Agricultural and Food Chemistry*, **53**, 4654–4659.

Rudzik, L., Baranska, M. and Schulz, H. (2004). Raman-Mapping an Parmesankäse. *Deutsche Milchwirtschaft*, **18**, 742–743.

Sadeghi-Jorabchi, H., Wilson, R.H., Belton, P.S. *et al*. (1991). Quantitative analysis of oils and fats by Fourier transform Raman spectroscopy. *Spectrochimica Acta*, **47A**, 1449–1458.

Sanchez-Cortes, S., Domingo, C., Garcia-Ramos, J.V. and Aznarez, J.A. (2001). Surface-enhanced vibrational study (SEIR and SERS) of dithiocarbamate pesticides on gold films. *Langmuir*, **17**, 1157–1162.

Schrader, B. (1995). *Infrared and Raman Spectroscopy, Methods and Applications*. Weinheim: VCH.

Schrader, B., Dippel, B., Erb, I. *et al*. (1999a). NIR Raman spectroscopy in medicine and biology: results and aspects. *Journal of Molecular Structure*, **480–481**, 21–32.

Schrader, B., Klump, H.H., Schenzel, K. and Schulz, H. (1999b). Non-destructive NIR-FT Raman analysis of plants. *Journal of Molecular Structure*, **509**, 201–212.

Schrader, B., Schulz, H., Baranska, M. *et al*. (2005). Non-destructive Raman analyses – polyacetylenes in plants. *Spectrochimica Acta A*, **61**, 1395–1401.

Schulz, H. and Baranska, M. (2005). Application of vibrational spectroscopy methods in essential oil analysis. *Perfumer and Flavorist*, **30**, 28–44.

Schulz, H. and Baranska, M. (2007). Identification and quantification of valuable plant substances by IR and Raman spectroscopy. *Vibrational Spectroscopy*, **43**, 13–25.

Schulz, H., Schrader, B., Quilitzsch, R. and Steuer, B. (2002). Quantitative analysis of various citrus oils by ATR/FT-IR and NIR-FT Raman spectroscopy. *Applied Spectroscopy*, **56**, 117–124.

Schulz, H., Schrader, R., Quilitzsch, R. *et al*. (2003). Rapid classification of basil chemotypes by various vibrational spectroscopy methods. *Journal of Agricultural and Food Chemistry*, **51**, 2475–2481.

Schulz, H., Baranska, M., Belz, H.H. *et al*. (2004a). Chemotaxonomic characterisation of essential oil plants by vibrational spectroscopy measurements. *Vibrational Spectroscopy*, **35**, 81–86.

Schulz, H., Baranska, M., Quilitzsch, R. and Schütze, W. (2004b). Determination of alkaloids in capsules, milk and ethanolic extracts of poppy (*Papaver somniferum* L.) by ATR-FT-IR and FT-Raman spectroscopy. *Analyst*, **129**, 917–920.

Schulz, H., Baranska, M. and Baranski, R. (2005a). Potential of NIR-FT-Raman spectroscopy in natural carotenoid analysis. *Biopolymers*, **77**, 212–221.

Schulz, H., Özkan, G., Baranska, M. *et al*. (2005b). Characterisation of essential oil plants from Turkey by IR and Raman spectroscopy. *Vibrational Spectroscopy*, **39**, 249–256.

Schulz, H., Baranska, M., Quilitzsch, R. *et al*. (2005c). Characterization of peppercorn, pepper oil and pepper oleoresin by vibrational spectroscopy methods. *Journal of Agricultural and Food Chemistry*, **53**, 3358–3363.

Schuster, K.C., Reese, I., Urlaub, E. *et al*. (2000). Multidimensional information on the chemical composition of single bacterial cells by confocal Raman microspectroscopy. *Analytical Chemistry*, **72**, 5529–5534.

Séné, C.F.B., McCann, M.C., Wilson, R.H. and Grinter, R. (1994). Fourier-transform Raman and Fourier-transform infrared spectroscopy. *Plant Physiology*, **106**, 1623–1631.

Strehle, M.A., Rösch, P., Baranska, M. *et al*. (2005). On the way to a quality control of the essential oil of fennel by means of Raman spectroscopy. *Biopolymers*, **77**, 44–52.

Strehle, K.R., Rösch, P., Berg, D. *et al*. (2006). Quality control of commercially available essential oils by means of Raman spectroscopy. *Journal of Agricultural and Food Chemistry*, **54**, 7020–7026.

Susi, H. and Byler, D.M. (1988). Fourier deconvolution of the amide I Raman band of proteins as related to conformation. *Applied Spectroscopy*, **42**, 819–826.

Taniguchi, I., Yonehara, Y., Masuda, K. *et al*. (1993). New approach for non-destructive sensing of fruit taste. *Sensors and Actuators B – Chemical*, **13**, 447–450.

Tatsch, E. and Schrader, B. (1995). Near-infrared Fourier-transform Raman-spectroscopy of indigoids. *Journal of Raman Spectroscopy*, **26**, 467–473.

Thygesen, L.G., Løkke, M.M., Micklander, E. and Engelsen, S.B. (2003). Vibrational microspectroscopy of food, Raman vs. FT-IR. *Trends in Food Science and Technology*, **14**, 50–57.

Thygesen, L.G., Jørgensen, K., Møller, B.L. and Engelsen, S.B. (2004). Raman spectroscopic analysis of cyanogenic glycosides in plants: development of a Flow Injection Surface-Enhanced Raman Scatter (FI-SERS) method for determination of cyanide. *Applied Spectroscopy*, **58**, 212–217.

Vandenabeele, P. and Moens, L. (2003). Micro Raman spectroscopy of natural and synthetic indigo samples. *Analyst*, **128**, 187–193.

Vrielynck, L., Cornard, J.P. and Merlin, J.C. (1994). Semi-empirical and vibrational studies of flavone and some deuterated analogues. *Spectrochimica Acta*, **50A**, 2177–2188.

Weng, R.H., Weng, Y.M. and Chen, W.L. (2006). Authentication of Camelia oleifera Abel oil by near infrared Fourier transform Raman spectroscopy. *Journal of the Chinese Chemical Society*, **53**, 597–603.

Withnall, R., Chowdhry, B.Z., Silver, J. *et al*. (2003). Diffuse reflection FTIR spectral database of dyes and pigments. *Spectrochimica Acta A*, **59**, 2207–2212.

Woo, Y.A., Kim, H.J. and Chung, H. (1999). Classification of cultivation area of ginseng radix with NIR and Raman spectroscopy. *Analyst*, **124**, 1223–1226.

Yang, H. and Irudayaraj, J. (2001). Comparison of near-infrared, Fourier transform-infrared and Fourier transform-Raman methods for determining olive pomace oil adulteration in extra virgin oil. *Journal of the American Oil Chemists' Society*, **78**, 889–895.

Yang, H. and Irudayaraj, J. (2003). Rapid detection of foodborne microorganisms on food surface using Fourier transform Raman spectroscopy. *Journal of Molecular Structure*, **646**, 35–43.

Yang, H., Irudayaraj, J. and Paradkar, M.M. (2005). Discriminant analysis of edible oils and fats by FTIR, FT-NIR and FT-Raman spectroscopy. *Food Chemistry*, **93**, 25–32.

Yu, N.T. (1974). Comparison of protein structure in crystals, in lyophilized state and in solution by laser Raman scattering. III. α-lactalbumin. *Journal of the American Chemical Society*, **96**, 4664–4668.

Zhang, P.X., Zhou, X., Cheng, A.Y.S. and Fang, Y. (2006). Raman spectra from pesticides on the surface of fruits. *Journal of Physics: Conference Series*, **28**, 7–11.

6

Spectroscopic Technique: Fourier Transform Raman (FT-Raman) Spectroscopy

Ramazan Kizil and Joseph Irudayaraj

Introduction

Food systems are dynamic, chemically complex and generally heterogeneous matrices of large numbers of biological molecules, so analysis requires sensitive and specific yet rapid characterization tools. Vibrational spectroscopic methods, such as Raman and infrared spectroscopy, are considered to be rapid, non-destructive analytical techniques, and provide excellent molecular specificity. A non-destructive vibrational spectroscopic technique without the need for altering the physical form of the specimens for rapid evaluation of quality of raw materials and product is a necessity for the food industry.

A non-destructive technique must not cause chemical decomposition, mechanical disturbance or photothermal damage to the sample in examination during the analysis.

Modern Techniques for Food Authentication
ISBN: 978-0-12-374085-4

An interferometry-based Raman technique with a near-IR excitation source, FT-Raman spectroscopy meets all of these requirements and is an emerging analytical technique for analyzing food products and raw materials.

Fundamentals of Raman spectroscopy

Raman spectroscopy has been gaining special interest in almost all fields of natural sciences due to its ease of use, minimal sample preparation and high sensitivity towards the molecular structure and conformation of biological substances. Raman spectroscopy is based on a special phenomenon called Raman scattering. When the incident light (a laser beam) is directed at a sample, a small portion of the light is scattered by the sample. The scattered light conveys information on the vibrational band energies of molecules. A plot of the intensities of the scattered portion of incident light versus the shifts in the frequency between the incident and scattered light is known as a Raman spectrum.

The molecular specificity of Raman spectroscopy can be best explained by the basic theory of the Raman phenomenon. When it is exposed to a material, light, as a form of electromagnetic radiation made up of electric and magnetic fields, can oscillate with the position of an electron cloud of a chemical bond of the material. Oscillations of electron clouds result in emission of photons. The emission of photons due to the light-induced oscillation in electron cloud is said to be *light scattering. Polarization* is a measure of how far an electron cloud could be driven from its equilibrium state by an external electric field. Since only molecules with distorted electron densities or polarizabilities due to energy exchange are Raman active, Raman spectroscopy is considered to be selective in detecting apolar molecules, ring structures and double- or triple-bonded structures.

Raman band intensities and basis of qualitative aspects of Raman spectroscopy

The theory of Raman scattering can be explained by both quantum-mechanical and classical mechanical approaches (Pelletier, 1999). The Raman phenomenon was discovered by Sir C.V. Raman in 1928. Placzek was the first to develop a quantum-mechanical model for Raman scattering in 1934. An empirical expression for Raman scattering intensity, I_R, can be provided as follows (Long, 2002):

$$I_R = \frac{2^4\pi^3}{45 * 3^2 * c^4} * \frac{h I_L N(\nu_o - \nu)^4}{\mu\nu(1 - e^{-h\nu/kT})}[45(\alpha'_a)^2 + 7(\gamma'_a)^2] \quad \textbf{(6.1)}$$

where c is the the speed of light ($cm^2\,s^{-1}$), h is the Planck's constant, I_L is the excitation laser intensity (photons/s), N is the number of scattering molecules, ν denotes the molecular vibrational frequency (Hz), ν_o denotes the laser excitation frequency

(Hz), μ is the reduced mass of vibrating atoms (g), k is the Boltzmann's constant, T is the absolute temperature in K, $\alpha_a' =$ mean value invariant of the polarizability tensor and $\gamma_a' =$ anisotropy invariant of the polarizability tensor.

The above equation states that Raman scattering intensity is proportional to the number of molecules being illuminated. This relationship establishes the fundamental basis for quantitative analysis using Raman spectroscopy. The Raman scattering intensity also relies on the intensity of incident light, ν, and the fourth power of the difference in frequencies of laser and associated molecular vibration, $(\nu_o - \nu)^4$. Thus, Raman scattering intensity can be increased by increasing the incident light intensity or by applying incident light of a higher frequency (shorter wavelength). Raman spectrometers can be divided into three categories based on the source of excitation. The dispersive Raman systems are equipped with a visible-range laser, UV-Raman spectrometers use UV range laser light sources, and FT-Raman set-ups include a near-IR laser, Nd:YAG (*neodymium-doped yttrium aluminum garnet*), which has the longest wavelength among all Raman spectroscopy lasers. A longer-wavelength excitation source is advantageous because it reduces the photodecomposition and fluorescence effects to a great extent, but weaker Raman signals are produced.

Raman intensity can also be expressed in a form similar to the Lambert-Beer law of absorption (Long, 2002), as

$$I_R = (I_L AK)pC \qquad \textbf{(6.2)}$$

where I_R is the measured Raman intensity (photons s^{-1}), I_L is the laser intensity (photons s^{-1}), A is the absolute Raman cross-section (cm^2 $molecule^{-1}$), K are the measurement parameters, p is the sample path-length (cm) and C is the concentration (molecule cm^{-3}).

The K value involves experimental/instrumental parameters such as optical collection efficiency and optical transmission of Raman spectrometer. The absolute Raman cross-section involves information regarding the light scattered from the molecule into a certain solid angle measured in steradians. Steradians are used to describe two-dimensional angular spans in three-dimensional space. Normal Raman scattering has a cross-section in the range of $10^{-31}-10^{-28}\,cm^2$ per molecule. This is quite low compared with that of the fluorescence of dyes, which can reach values of $10^{-16}\,cm^2$ and higher. For this reason, classical Raman spectroscopy suffers from fluorescence phenomena interference. Fortunately, the use of near-IR lasers as the excitation source can avoid the fluorescence problem. Unlike other Raman spectrometers, only FT-Raman instrumentation makes use of near-IR (1064 nm) lasers.

FT-Raman instrumentation

Fourier transform Raman spectroscopy is a specific Raman configuration designed to collect fluorescence-free and wavelength-stable measurements from a wide range of samples spanning crystals to biological tissues (Chase, 1987).

A classical FT-Raman spectrometer contains an excitation source, a Nd:YAG laser, to produce photons in the near-IR region (1064 nm), a sampling unit with proper

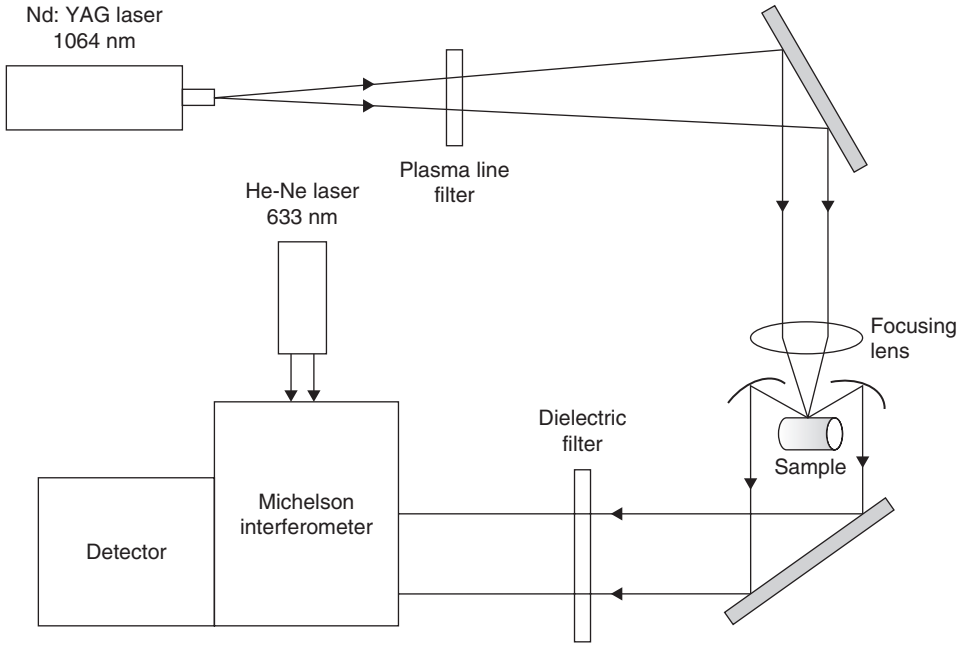

Figure 6.1 Schematic representation of an FT-Raman spectrometer.

collection optics, an interferometer comprising a fixed and moving mirrors, and a detecting unit. A schematic representation of the FT-Raman set-up is given in Figure 6.1. A He-Ne laser (633 nm "red" excitation) is made collinear to the excitation laser to aid in obtaining the most proper optical alignment. In addition to guiding the Nd: YAG laser, the He-Ne laser in FT-Raman instrumentation functions as the reference laser for the operation of the Michelson interferometer. A line filter helps to filter plasma lines, and the light is focused on a sample sitting in a sample compartment. In FT-Raman experiments, there is no need for sample preparation and the signal can be collected virtually from food samples in any physical state. The scattered light is then collected using either 180° or 90° back-scattering geometry, and passes through a dielectric filter to cut off the 1064 and 633 nm laser lines before entering the detector, which can be nitrogen cooled Ge (germanium) or room temperature InGaAs (indium gallium arsenide).

The key component of an FT-Raman spectrometer is the Michelson interferometer, composed of two perpendicular plane mirrors; one is fixed (or known as the *dynamically aligned* mirror) and the other is the moving mirror (known as the *scan mirror*). A beam-splitter is used to reflect the incident light partially (often 50%) to the fixed mirror and partially to the moving mirror. The moving (scan) mirror has a constant velocity through which an optical path difference between these two beams is introduced. The beam transmitted from the fixed mirror and the beam reflected from the moving mirror are combined into the detector, which detects an interference pattern and transfers it into an electric signal.

Applications of FT-Raman spectroscopy

Food analysis

All food systems are composed of water, proteins, lipids and carbohydrates. Analysis of these food micro-components requires determination of the nutritional value and quality assurance parameters of these food products. The chemical composition of food is often very complex, and is prone to modifications during storage or processing. The chemical specificity, ease of sampling, rapidity of measurements and non-destructive nature of FT-Raman spectroscopy make it an attractive tool for food analysis. The chemical specificity of the Raman technique stems from the fact that different molecular bonds or groups of chemical bonds are identified by characteristic frequency-shifts in the incident light. For this reason, the very first step of compositional analysis of food using FT-Raman is the attribution of characteristic frequency shifts observed in spectra to vibrational modes of molecular bonds. Tentative Raman band assignments of proteins, carbohydrates and lipids are provided in Table 6.1.

Raman analysis is mainly based on the interpretation of vibrational modes in spectra where the frequencies of vibrational peaks can be attributed to the particular chemical functional group of a sample under investigation. In other words, the position and intensity of a Raman band can be used to characterize a certain functional chemical group.

As a Raman selection rule, non-polar groups and ring structures are known to be Raman-active chemical groups that yield strong peaks and are often well resolved in the Raman spectra. Polar groups, however, produce weak Raman signals, so polar and abundant water-molecule related vibrational modes, such as the stretching and bending vibrations of O–H– do not severely cloud the spectra, unlike in NIR and IR spectroscopies. Since the Raman response can be affected by changes in both the chemical and the physical nature of molecules, Raman spectroscopy can also be used to extract useful information regarding the chemical structure and physical status of most foods (Li-Chan, 1997). The chemical composition of foods can be evaluated by inspecting the position and intensities of Raman bands, which are often well resolved and sharp if the fluorescence effect is minimized and background correction is applied.

The amide group ($–CONH_2$)-related vibrational modes of proteins are among the most useful Raman responses for studying proteins in diverse physicochemical environments. Due to the non-interference by water-related bands, Raman spectroscopy is becoming a promising tool to predict the secondary structure of proteins in food science as well as life sciences. Although the amide group-related responses can appear in seven different regions in the Raman spectrum, the amide I band, which extends from 1600 to 1700 cm^{-1}, is the most frequently investigated protein-related peak for the prediction of protein secondary structure and quantification of protein content in complex food matrices. The most important factor that makes the amide I band attractive in Raman studies is that it is generally not interfered with by fundamental vibrational modes of other molecules, such as carbohydrates, and is conformation-sensitive. Figure 6.2 shows FT-Raman spectra of wheat flour and wheat starch to illustrate that carbohydrate-related peaks do not interfere with the amide I band response of proteins. The peptide C=O group vibrations largely contribute to

Table 6.1 Raman band assignments for proteins, carbohydrates and lipids

	Vibrational modes of functional groups	Raman shift (cm^{-1})	Molecular/structural significance
Proteins	S–S stretch	510–545	*gauche* and *trans* conformation
	C–S stretch	630–670	*gauche* conformation
	C–S stretch	700–745	*trans* conformation
	S–H stretch	2550–2580	Presence of thiol of cystein residues
	Side chains: Tyrosine	640	Skeletal tyrosine side chain
		829	Buried state of OH group, Fermi doublet
		852	Exposed, state of OH group, Fermi doublet
		1614	Tyrosine and tryptophan side chain
	Tryptophan	750, 1341, 1582	Indole ring at exposed or buried states
		1000, 1609	Benzene ring, intensity calibration
	Phenylalanine	620	Skeletal vibration of the ring
	C–H stretch	2800–3000	Polarity of protein microenvironment
	C_α–H and C–H deformation	1341, 1447	
	C_α–C stretch	939	Conformation-sensitive
	Amide I, C=O stretch and N–H wag	1655, 1670, 1665	Secondary structure; α-helix (1655), β-sheet (1670), disordered structure (1665)
	Amide II, C–N stretch, N–H bend	1278, 1235, 1245	Secondary structure
Fats and oils	**Raman shift (cm^{-1})**	**Raman band assignment**	
	847	C–N stretch coupling with PO_2 stretch in phospholipids	
	1060–1090	stretch of carbonyl C—C and POC in phospholipids	
	1264	In plane =C—H deformation (*cis* transform)	
	1302	In phase CH_3 twist	
	1440	CH_2 bend	
	1650–1660	*cis* C=C stretch,	
	1670–1680	*trans* C=C stretch,	
	1746	C=O stretch in ester	
	2860	Symmetric stretch of aliphatic C—H in CH_2	
	2900	Symmetric stretch of olefinic C—H in CH_3	
	3004	Asymmetric stretch of aliphatic *cis* (=C—H) of RHC=CHR	
Carbohydrates	**Crystalline state**	**In solution**	**Raman band assignment**
	Below	Below	Skeletal modes of the ring structure
	700	700	
	763	779	C—C stretch
	860	840	C(1)—H, CH_2 deformation
	1087	1076	C—O—H bend
	1122	1124	C—O stretch, C—O—H bend
	1260–1280	1272	CH_2OH (side chain) related mode
	1339	1335	C—O—H bend, CH_2 twist
	1382	1370–1410	CH_2 scissoring, C—H and C—O—H deformation
	1460	1462	CH_2 bend
	2800–3000	2800–3000	C—H stretch
	3100–3600	3000–3600	O—H stretch

Sources: Chmielarz *et al.* (1995), Baeten *et al.* (1998), Li-Chan (1999), Naumann (2001), Tuma (2005), Kizil (2007) and Schulz and Baranska (2007).

the amide I response of proteins, as well as slight coupling of C–N stretch, C–C–N deformation and N–H wag. The amide III region (1200–1300 cm^{-1}), which includes N–H bend and C–N stretch modes, can also provide information regarding the structure of proteins.

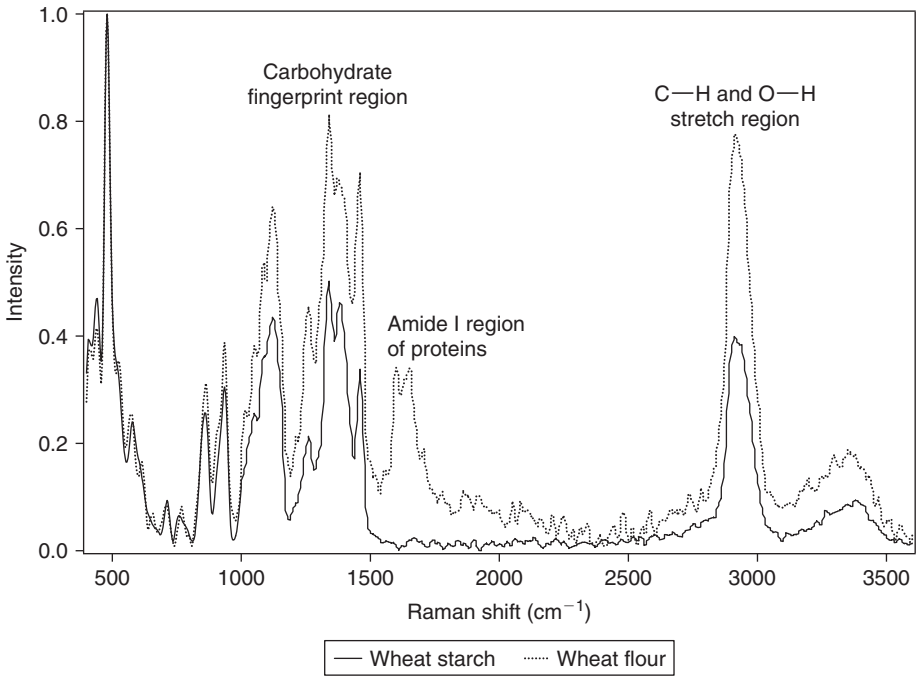

Figure 6.2 FT-Raman spectra of wheat starch and wheat flour, showing the protein content differences by the amide I response.

Proteins produce complex and overlapping Raman bands due to their huge molecular size and structural complexity. The building blocks of proteins, *amino acids*, especially those with a ring structure (such as tyrosine, tryptophan and phenylalanine), yield Raman bands that can be used to predict the chemistry of the local environment of proteins in solution. The Raman responses of the S–S bond of cystine side chains convey information regarding the *gauche* and *trans* conformers of proteins. The S–S stretching Raman response of cystine is affected by the internal rotations around the C–S and C–C bonds, so this information can be used to interpret the disulfide-bridge structure of proteins. For example, the intensities or relative areas of hen egg-white lysozyme Raman bands observed at 507 and 525 cm^{-1} have been used to predict that three of the four disulfide bonds of lysozyme are in the lowest energy, the *gauche*, state, and the other has a *gauche–trans–gauche* conformation (Li-Chan, 1999). Upon gelation of this protein, the ratio of the *gauche* state to the *gauche–trans–gauche* conformer is changed to 1:1 (Li-Chan and Nakai, 1991). Raman fingerprints of amino acids with aromatic groups provide valuable information regarding the chemical nature of the medium in which proteins are dissolved. For example, the buried and solvent-exposed tryptophan and tyrosine residues exhibit different Raman responses (Table 6.1).

Raman spectroscopy can also provide valuable information regarding the chemical structure, molecular interactions, hydrogen-bonding chemistry and quantification of carbohydrates. The skeletal vibrational modes of the carbohydrate ring structure

dominate spectra below 700 cm^{-1}. Bands due to the skeletal mode C–C stretch observed at 480 cm^{-1} have been probed to determine the level of birefringence and monitor the advance of gelatinization of starches with temperature. Raman spectroscopy has sensitivity to the anomeric carbon atom of carbohydrates, so that both α and β conformers of sugars can be used for discriminative purposes. The α-glucose of sucrose gives a Raman peak at 847 cm^{-1}, whereas β-glucose of maltose confers a Raman peak at 898 cm^{-1} in addition to the α-glucose response (Corbett *et al.*, 1991). The glycosidic linkage configurations can be characterized by monitoring the C–O–C related vibrations of the Raman spectra of high molecular weight carbohydrates. Consequently, the chemistry of polysaccharide branching and process-induced changes in the polymeric carbohydrates can be studied. Raman spectroscopy is capable of differentiating 1–4 (branching) and 1–6 (linear) type glycosidic bridge vibrational modes, which is useful for studying the chemistry of starch. As shown in Table 6.1, the Raman scattering characteristics of carbohydrates in solution are different from those of crystalline sugars.

By circumvention of the fluorescence problem of conventional Raman spectrometers using near-IR excitation sources, FT-Raman spectroscopy has become a promising tool for studying lipids in both a qualitative and a quantitative manner. The molecular structure of lipids is successfully characterized by distinct and well-resolved Raman bands, so that the spectral data can be easily converted into chemical information regarding lipids. FT-Raman spectroscopy measurement of lamb adipose tissues is provided in Figure 6.3. The C=C stretch mode of unsaturated fatty acids is characterized by a distinctive peak often observed at 1600 cm^{-1}. Due to the apolar

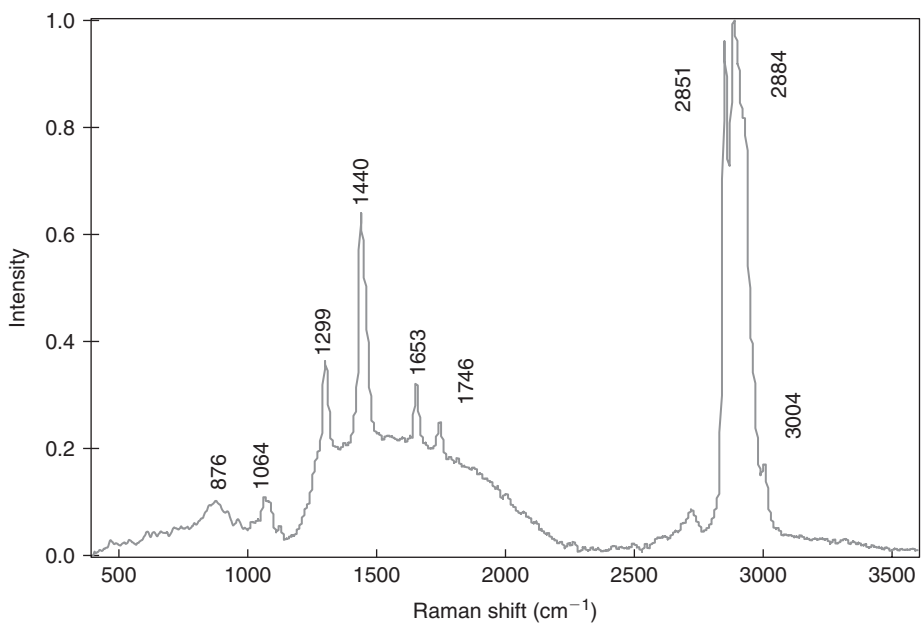

Figure 6.3 FT-Raman spectra of lamb adipose tissue.

nature of the C=C group of lipids, the vibrational modes of this group are intensely represented by Raman spectroscopy. In addition, *cis* or *trans* isomers of unsaturated fatty acids are well identified in Raman spectrum of oils and fats. As the *cis* conformation of the RCH=CHR group has a Raman scattering signal at 1660 cm^{-1}, the *trans*-double carbon bonds are characterized by the Raman mode observed at 1670 cm^{-1} (Baetan *et al.*, 1998).

The C–H group related vibrational modes are the strongest and abundant spectral responses in Raman spectra of lipids. The 2800–3000 cm^{-1} region of lipid Raman spectra is attributed to the C–H stretch, and both symmetrical and asymmetrical stretch modes contribute to this region (Table 6.1). A minor shoulder-like Raman peak at 3004 cm^{-1} is assigned to the *cis* conformer stretch of the (=C–H) group. The other bending-, twisting- and deformation-related vibrational modes of C–H groups contribute to the total Raman spectra of lipids at 1439, 1302 and 1264 cm^{-1}, respectively. The ester group (C=O) of lipids is characterized by a peak at 1746 cm^{-1}. The phospholipid content of lipids can be screened through the PO_2 and POC groups related Raman stretch bands at 847 and 1090 cm^{-1}, respectively.

As stated above, Raman spectroscopy has been found to be successful in probing the functional molecular groups of food samples, and spectral data can be converted into chemical information by means of band assignments. Raman spectroscopy provides fruitful information regarding the chemical nature of food molecules that can be used for assessment of the quality of food, including authentication or adulteration of food products, and in the determination of process-induced changes.

Authentication of fats and oils

Among the foods, oils and fats are the most attractive samples to study with FT-Raman spectroscopy due to the phase homogeneity and molecular structure. Unlike proteins and saccharides, the deliberate molecular structure of lipids makes it reasonably simple to attribute FT-Raman responses to the corresponding molecular groups. Elimination of the fluorescence background in Raman spectra of oils and fats by use of a near-IR field operating Nd:YAG laser, providing well-resolved fluorescence-free Raman bands, has led to extensive experimental studies on the authentication and quality control of edible fats and oils. In addition to qualitative structural analysis, Raman spectroscopy has also been employed to quantify the fat content in food products.

The saturation degree of fats and oils is traditionally determined by wet chemistry techniques, such as the iodine value (IV) tests conducted by the traditional titration method, which is a time-consuming and destructive technique and involves toxic chemicals in the analysis. As an alternative to the IV technique, FT-Raman spectroscopy has been employed to determine the degree of total unsaturation of pure oils and fats (Sadeghi-Jorabchi *et al*, 1990, 1991; Barthus and Poppi, 2001; Asfeth, 2005). The sensitivity of Raman spectroscopy in detecting double bond structure-related fundamental vibration modes, such as C=C and =C–H groups of fatty acids, makes it a suitable technique to correlate the level of unsaturation to spectral responses. Since iodine value is an important quality parameter of fats and oils, FT-Raman spectroscopy can be employed to determine quality indices of fats of oils.

Lipid oxidation is one of the challenging topics in food science. Oxidation of unsaturated fatty acids causes degradation of lipids and formation of off-flavors and oxidation products which are unfavorable in the food industry. This important quality criterion of lipids has been tested by a variety of techniques, including gas chromatography (GC), peroxide value, anisidine value or spectrophotometric measurements in the UV region. Employing FT-Raman spectroscopy, the oxidative deterioration in lipids can be studied at the molecular level, allowing the investigation of changes in the chemical structure during oxidation. Muik *et al.* (2005) characterized the spectral changes during oxidation of vegetable oils, using a FT-Raman set-up. Spectroscopic detection of the formation of aldehydes, isomerization of *cis* to *trans* double bonds and conjugation of double bonds due to thermal oxidation of vegetable oils were reported. The FT-Raman response was also correlated with a conventional parameter, the anisidine value, to investigate the extent of lipid oxidation.

The success and expertise in the use of FT-Raman spectroscopy in the determination of the total degree of unsaturation of fats and oils has recently been extended to the investigation of high fat containing foods such as fish and pork (Asfeth *et al.*, 2005, 2006; Olsen *et al.*, 2007). In these studies, the potential of Raman and FT-Raman spectroscopy for estimation of the fatty acid unsaturation in salmon and pork adipose tissue was investigated, and the technique was found to be a rapid and non-destructive means of predicting the level of unsaturation. The involvement of Raman spectroscopy in on-line measurement of the degree of total unsaturation in real-life samples, such as fish and animal carcasses, is of current interest in food science research.

Rapid detection of adulteration and authentication of commercial fats and oils is another application area of FT-Raman spectroscopy. For example, olive oil, with its fine flavor and aroma as well as health benefits, has a high market price and is thus prone to adulteration with cheaper seed oils for economic gain. Instead of time-consuming, expensive analytical techniques such as GC and wet chemistry, FT-Raman spectroscopy is a promising tool for detecting the authentication and adulteration of olive oil. Adulteration of virgin olive oil with olive pomace oil (Yang and Irudayaraj, 2001), and hazelnut oil (Baeten *et al.*, 2005) has been studied by FT-Raman spectroscopy. The basis of discrimination of oils using FT-Raman techniques is the differences occurring in the C=C and =C–H related vibrational modes due to the mixing of oils with different saturation level. The advances in FT-Raman instrumentation and chemometric techniques make it suitable for predicting the oil content and quality of olives.

Authentication of carbohydrate and protein-based food systems

The non-destructive nature along with the excellent molecular specificity of FT-Raman spectroscopy in characterizing proteins and carbohydrates with a high content of structural information have led to it becoming a promising protocol in the analysis of food products. The authentication and detection of adulteration of carbohydrates with a high nutritional and economic value (Paradkar and Irudayaraj, 2001, 2002), such as honey, have been investigated using FT-Raman spectroscopy.

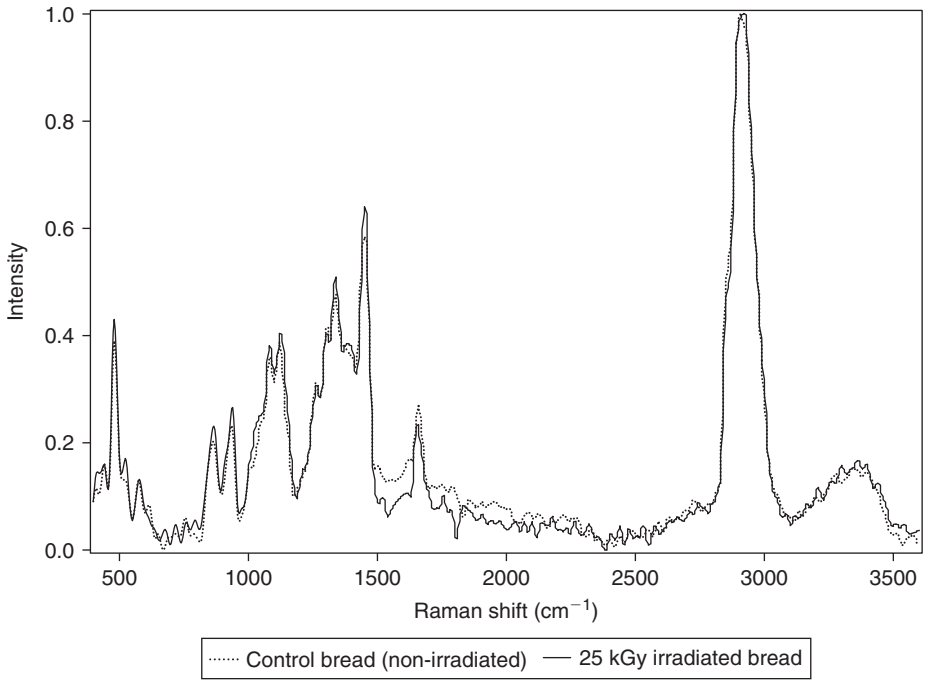

Figure 6.4 FT-Raman spectra of irradiated and control bread samples.

Since the spectral data convey chemical information regarding the structure of carbohydrates, discrimination of sugars through authentication analyses, which is conducted by chemometric methods, relies on the detection of minute changes in the molecular structure. The molecular-level fingerprint information is best treated with multivariate statistical techniques to extract the most useful interpretation regarding the sample under examination. In Figure 6.4, the spectral responses measured from both the control (non-irradiated) and the irradiated (25 kGray) bread samples are compared. The spectral change in the C–H region between 2800–300 cm^{-1} can be seen. Figure 6.5 illustrates the discrimination of 25-kGy irradiated bread samples from the control samples obtained using a pattern recognition method. Twenty control (non-irradiated) samples and twenty samples irradiated at 25 kGray were used in this analysis. Discrimination was carried out employing a multivariate method, such as canonical variate analysis, to the spectroscopic data that reflect statistically significant variations in the C–H stretch region. The clear separation of the control from the irradiated bread samples (Figure 6.5) implies the potential of FT-Raman spectroscopy along with a chemometric model in the discrimination of processed foods. Details of the discrimination model are provided elsewhere (Kemsley, 1998).

Raman signals detected at 840, 1126 and 1462 cm^{-1} can be attributed distinctively to carbohydrate molecules, and these spectral responses have been used to predict the distribution of carbohydrates in carrot roots (Ozaki *et al.*, 1992). In addition to the carbohydrate distribution in plants, *in situ* analysis of carotenoids in carrot roots has been studied non-destructively using the FT-Raman set-up (Baranska *et al.*, 2005).

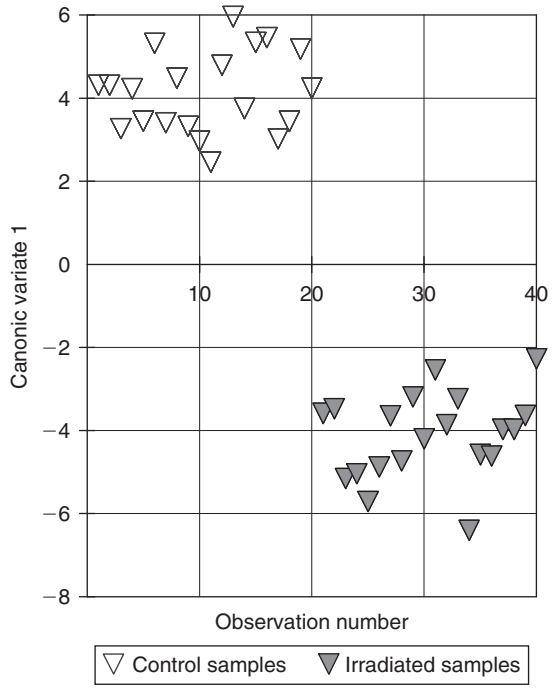

Figure 6.5 Canonical variate discrimination of control and irradiated samples.

FT-Raman spectroscopy can also be employed to monitor changes in food processing. The gelatinization and enzyme-catalyzed hydrolysis of dextranes of starch was monitored on-line by fiber-optic coupled FT-Raman spectroscopy by Schuster *et al.* (2000). Gamma irradiation induced changes in the molecular structure of starch gels, and carbohydrates (including honey and fructose) were characterized using Raman spectroscopy (Kizil and Irudayaraj, 2006, 2007). Gamma irradiation-induced changes in the C–H and skeletal vibrational modes of carbohydrates due to the attack of hydroxyl radicals were also characterized and used to classify sugars with respect to the extent of irradiation.

The structural complexity and functional properties of proteins are of primary interest to biochemists and molecular biologists. Hence, Raman spectroscopy has been widely employed to predict the structure of proteins and to determine the structure–function relations in the field of biochemistry. From the viewpoint of food science, proteins contribute to the texture of food and consequently changes in the rheological properties of food and the analysis of proteins in complex food matrices provide information about the texture and nutritional quality of food. Badii and Howell (2002) investigated the changes in fish muscle during storage, and reported that denaturation and aggregation of proteins unfavorably affected the quality of the fish.

FT-Raman spectroscopy has also found an application in the nutritional classification of cereal products (Sohn *et al.*, 2005), based on the differences in spectral responses corresponding to fat and protein contents. The protein content of milled

rice was predicted using FT-Raman spectroscopy (Liao *et al.*, 2004) to monitor the vibrational modes of the amide functional group of proteins.

Conclusions

Raman spectroscopy is emerging as a feasible analytical tool for food scientists and processors. Although not as well-established as infrared analysis in the food industry, Raman spectroscopy has already been employed for food authentication, traceability and quality control. FT-Raman spectroscopy has advantages over other types of Raman spectrometers and infrared techniques in that it is non-destructive and the sampling protocols are simplified, because an operator can collect Raman measurements through glass containers or the sample may simply be analyzed in its raw form.

Applications of FT-Raman spectroscopy to fats and oils are likely to increase, as is its use in the analysis of complex food systems. Development of chemometrics and the application of multivariate statistical tools is expected to improve the sensitivity of the measurements and the versatility of this approach.

References

Asfeth, N.K., Segtnan, V.H., Marquardt, B.J. and Wold, J.P. (2005). Raman and near-infrared spectroscopy for quantification of fat composition in a complex food model system. *Applied Spectroscopy*, **59**, 1324–1332.

Asfeth, N.K., Wold, J.P. and Segtnan, V.H. (2006). The potential of Raman spectroscopy for characterization of fatty acid unsaturation of salmon. *Analytica Chimica Acta*, **572**, 85–92.

Badii, F. and Howell, N.K. (2002). A comparison of biochemical changes in cod (*Gadus morhua*) and haddock (*Melanogammus aeglefinus*) during frozen storage. *Journal of the Science of Food and Agriculture*, **82**, 87–97.

Baeten, V., Hourant, P., Morales, M.T. and Aparicio, R. (1998). Oil and fat classification by FT-Raman spectroscopy. *Journal of Agriculture and Food Chemistry*, **46**, 2638–2646.

Baeten, V., Pierna, J.A.F., Dardenne, P. *et al*. (2005). Detection of the presence of hazelnut oil in olive oil by FT-Raman and FT-MIR spectroscopy. *Journal of the Agricultural and Food Chemistry*, **53**, 6201–6206.

Baranska, M., Schulz, H., Baranski, R. *et al*. (2005). *In situ* simultaneous analysis of polyacetylenes, carotenoids and polysaccharides in carrot roots. *Journal of Agricultural and Food Chemistry*, **53**, 6565–6571.

Barthus, R.C. and Poppi, R.J. (2001). Determination of the total unsaturation in vegetable oils by FT-Raman spectroscopy and chemometrics. *Vibrational Spectroscopy*, **21**, 99–105.

Chase, B. (1987). FT-Raman spectroscopy as an analytical tool. *Applied Spectroscopy*, **40**, 133–137.

Chmielarz, B., Bajdor, K., Labudzinska, A. and Klukowskama-Jewska, Z. (1995). Studies on the double-bond positional isomerization process in linseed oil by UV, IR and Raman spectroscopy. *Journal of Molecular Structure*, **348**, 313–316.

Corbett, E.C., Zichy, V., Goral, J. and Passingham, C. (1991). FT-Raman studies of materials and compounds of biological importance. 2. The effect of moisture on the molecular structure of the alpha-anomers and beta-anomers of D-glucose. *Spectrochimica Acta Part A – Molecular and Biomolecular Spectroscopy*, **47**, 1399–1411.

Kemsley, E.K. (1998). *Discriminant Analysis and Class Modeling of Spectroscopic Data*. Chichester: John Wiley & Sons.

Kizil, R. and Irudayaraj, J. (2006). Discrimination of irradiated starch gels using FT-Raman spectroscopy and chemometrics. *Journal of Agriculture and Food Chemistry*, **54**, 13–18.

Kizil, R. and Irudayaraj, J. (2007). Rapid evaluation and discrimination of γ-irradiated carbohydrates using FT-Raman spectroscopy and chemometrics. *Journal of the Science of Food and Agriculture*, **87**, 1244–1251.

Liao, Y.H., Wang, C.H., Tseng, C.Y. *et al*. (2004). Compositional and conformational analysis of yam proteins by near-IR FT-Raman spectroscopy. *Journal of Agricultural and Food Chemistry*, **52**, 8190–8196.

Li-Chan, E.C.Y. (1999). The applications of Raman spectroscopy in food science. *Trends in Food Science & Technology*, **7**, 361–370.

Li-Chan, E. and Nakai, S. (1991). Raman spectroscopic study of thermally and/or dithiothreitol induced gelation of lysozyme. *Journal of Agriculture and Food Chemistry*, **39**, 1238–1246.

Long, D.A. (2002). The Raman Effect: A Unified Treatment of the Theory of Raman Scattering by Molecules. New York, NY: John Wiley & Sons.

Muik, B., Lendl, B., Molina-Diaz, A. and Ayora-Canada, M.J. (2005). Direct monitoring of lipid oxidation in edible oils by Fourier transform Raman spectroscopy. *Chemistry and Physics of Lipids*, **134**, 173–182.

Naumann, D. (2001). FTIR and FT-Raman spectroscopy in biomedical research. *Applied Spectroscopy Review*, **36**, 239–298.

Olsen, E.F., Rukke, E., Flatten, A. and Isaksson, T. (2007). Quantitative determination of saturated-, monosaturated- and polyunsaturated fatty acids in pork adipose tissue with non-destructive Raman spectroscopy. *Meat Science*, **76**, 628–634.

Ozaki, Y., Cho, R., Ikegaya, K. *et al*. (1992). Potential of near Infrared FT-Raman spectroscopy in food analysis. *Applied Spectroscopy*, **46**, 1503–1507.

Paradkar, M. and Irudayaraj, J. (2001). Discrimination and classification of beet and cane sugars and their inverts in maple syrup by FT-Raman. *Applied Engineering in Agriculture*, **18**, 379–383.

Paradkar, M.M. and Irudayaraj, J. (2002). Discrimination and classification of beet and cane inverts in honey by FT-Raman spectroscopy. *Food Chemistry*, **76**, 231–239.

Pelletier, M.J. (1999). *Analytical Applications of Raman Spectroscopy*. Oxford: Blackwell Science.

Sadeghi-Jorabchi, H., Hendra, H., Wilson, P.J. and Belton, P.S. (1990). Determination of the total unsaturation in oils by FR-Raman spectroscopy. *Journal of the American Oil Chemists' Society*, **67**, 483–486.

Sadeghi-Jorabchi, H., Wilson, R.H., Belton, P.S. *et al*. (1991). Quantitative analysis of oils and fats by FT-Raman Spectroscopy. *Spectrochimica Acta*, **47A**, 1449–1458.

Schulz, H. and Branska, M. (2007). Identification and quantification of valuable plant substances by IR and Raman spectroscopy. *Vibrational Spectroscopy*, **43**, 13–25.

Schuster, K.C., Ehmoser, H., Gapes, J.R. and Lendl, B. (2000). On-line FT-Raman spectroscopic monitoring of starch gelatinization and enzyme catalyzed starch hydrolysis. *Vibrational Spectroscopy*, **22**, 181–190.

Sohn, M., Himmelsbach, D.S., Kays, S.E. *et al*. (2005). NIR-FT-Raman spectroscopy for nutritional classification of cereal foods. *Cereal Chemistry*, **82**, 660–665.

Tuma, R. (2005). Raman spectroscopy of proteins: from peptides to large assemblies. *Journal of Raman Spectroscopy*, **36**, 307–319.

Yang, H. and Irudayaraj, J. (2001). Comparision of NIR, FTIR and FT-Raman methods for determining olive pomace oil adulteration in extra virgin olive oil. *Journal of the American Oil Chemists' Society*, **78**, 889–895.

This page intentionally left blank

7

Spectroscopic Technique: Fluorescence and Ultraviolet-visible (UV-Vis) Spectroscopy

Romdhane Karoui and Eric Dufour

Introduction

Public interest in food quality and production has increased in recent decades, probably related to changes in eating habits, consumer behavior, and the development and increased industrialization of food supply chains (Christensen *et al.*, 2006). The demand for high quality and safety in food production obviously calls for high standards for quality and process control, which in turn requires appropriate analytical tools to investigate food. Fluorescence spectroscopy is an analytical technique whose theory and methodology have been extensively exploited for studies of molecular structure and function in the discipline of chemistry and biochemistry (Strasburg and Ludescher, 1995). Even though fluorescence is one of the oldest analytical methods used, it has just recently become quite popular as a tool in biological science related to food technology. An indication of that popularity is the increasing number of research publications about fluorescence, as well as the introduction of new commercially available instruments for fluorescence analysis – in particular, front-face fluorescence

Modern Techniques for Food Authentication
ISBN: 978-0-12-374085-4

spectroscopy (FFFS). Indeed, the traditional right-angle fluorescence spectroscopic technique cannot be applied to thick substances due to their large absorbance and the scattering of light, and when the absorbance of the sample exceeds 0.1 the emission and excitation spectra are both decreased and the excitation spectra are distorted. To avoid these problems, a dilution of samples is currently performed so that their total absorbance is less than 0.1. However, the results obtained on diluted solutions of food samples can not be extrapolated to native concentrated samples, since the organization of the food matrix is lost. To avoid these problems, FFFS can be used.

There are many advantages in the use of analytical fluorescence spectroscopy, as will become clear later in this chapter. Although many researchers shy away from this technique because of lack of knowledge of the fundamental principles of fluorescence, the application of fluorescence in analysis of foods has increased during the last two decades. This could be explained by the use of chemometric tools for the extraction of information contained in the spectra.

This chapter will provide the reader with a review of the basic principles of fluorescence, including the use of this technique; in particular, the most common FFFS for the assessment of the quality of several food systems will be discussed in detail.

Fluorescence spectroscopy

Definition

Fluorescence is the emission of light subsequent to absorption of ultraviolet (UV) or visible light by a fluorescent molecule or substructure called a *fluorophore*. Thus, the fluorophore absorbs energy in the form of light at a specific wavelength and liberates energy in the form of light emitted at a higher wavelength. The general principles can be illustrated by a *Jablonski diagram* (Veberg, 2006), as shown in Figure 7.1.

The first step (i) is *excitation*, where light is absorbed by the molecule, which is transferred to an electronically excited state – meaning that an electron moves from the ground singlet state, S_0, to an excited singlet state, S'_1. This is followed by a vibrational relaxation or *internal conversion* (ii), where the molecule undergoes transition from an upper electronically excited state to a lower one, S_1, without any radiation. Finally, emission occurs (iii), typically 10^{-8} seconds after excitation, when the electron returns to its more stable ground state, S_0, emitting light at a wavelength according to the difference in energy between the two electronic states.

This explanation is of course somewhat simplified. In molecules, each electronical state has several associated vibrational states. In the ground state, almost all molecules occupy the lowest vibrational level. By excitation with UV or visible light, it is possible to promote the molecule of interest to one of several vibrational levels for the given electronically excited level. This implies that fluorescence emission does not only occur at one single wavelength, but rather over a distribution of wavelengths corresponding to several vibrational transitions as components of a single electronic transition. This is why excitation and emission spectra are obtained to describe the detailed fluorescence characteristics of molecules. The fact that fluorescence is characterized

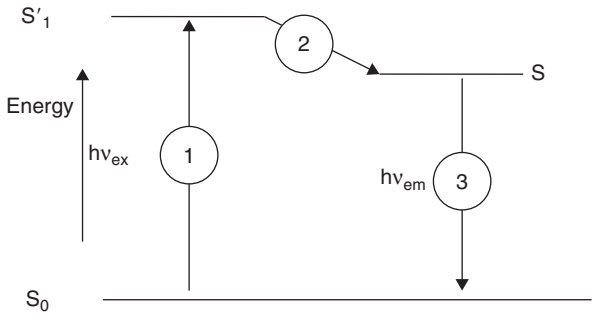

Figure 7.1 Jablonski diagram showing the basic principle of fluorescence spectroscopy.

by two wavelength parameters significantly improves the specificity of the method, compared with spectroscopic techniques based only on absorption.

Quantum yield (efficiency)

Each molecule presents a specific property, which is described by a number, named the *quantum yield* or *quantum efficiency* (ϕ).

$$\phi = \frac{\text{number of quanta emitted}}{\text{number of quanta absorbed}} = \text{quantum yield} \qquad \textbf{(7.1)}$$

As illustrated in Equation (7.1), the higher the value of ϕ, the greater the fluorescence of a compound. A non-fluorescent molecule is one whose quantum efficiency is zero or so close to zero that the fluorescence is not measurable. All energy absorbed by such a molecule is rapidly lost by collisional deactivation.

Excitation and emission spectra

Each fluorescent molecule has two characteristic spectra; the excitation and emission spectra.

Excitation spectrum

The *excitation spectrum* is defined as the relative efficiency of different wavelengths of exciting radiation in causing fluorescence. The shape of the excitation spectrum should be identical to that of the absorption spectrum of the molecule, and independent of the wavelengths at which fluorescence is measured. However, this is seldom the case, because the sensitivity and the bandwidth of the spectrophotometer (absorbance spectrum) and the spectrofluorimeter (excitation spectrum) are different. A general rule of thumb is that the longest wavelength peak in the excitation spectrum is chosen for excitation of the sample. This minimizes possible decomposition caused by the shorter-wavelength, higher-energy radiation.

Emission spectrum

The *emission spectrum* of a compound results from the re-emission of radiation absorbed by the molecule. The emission spectrum is the relative intensity of radiation emitted at various wavelengths. The quantum efficiency and the shape of the emission spectrum are independent of the wavelength of the excitation radiation. If the exciting radiation is at wavelength that differs from the wavelength of the absorption peak, less radiant energy will be absorbed and hence less will be emitted.

Stoke's shift

According to the Jablonski diagram (Figure 7.1), the energy of emission is lower than that of excitation. This implies that the fluorescence emission occurs at higher wavelengths than the absorption (excitation). The difference between the excitation and emission wavelengths is known as *Stoke's shift*, as indicated with the arrow in Figure 7.2, marking the difference between the excitation and emission spectrum of tryptophan fluorescence spectra scanned on UHT milk.

$$\text{Stoke's shift} = 10^7 \left(\frac{1}{\lambda_{ex}} - \frac{1}{\lambda_{em}} \right) \tag{7.2}$$

where λ_{ex} and λ_{em} are the maximum wavelengths for excitation and emission, respectively.

Normally, the emission spectrum for a given fluorophore is a mirror image of the excitation spectrum, as seen to some extent in Figure 7.2 for tryptophan. The general symmetric nature is a result of the same transitions being involved in both

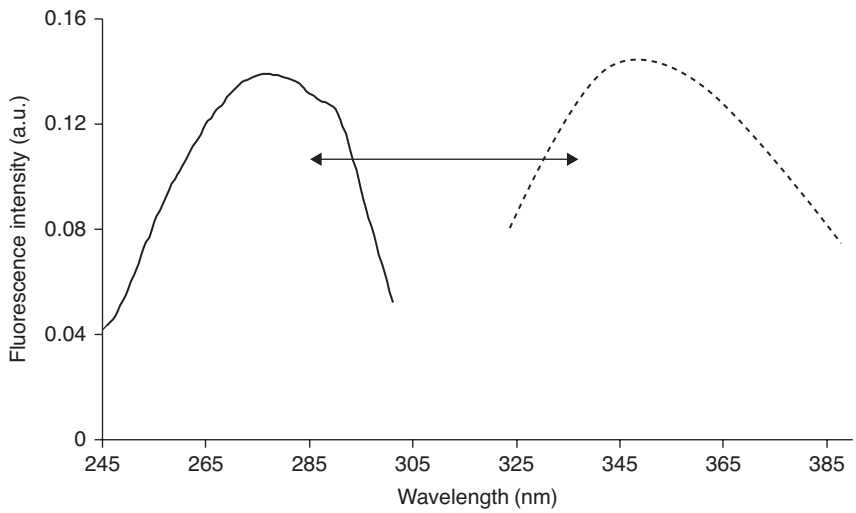

Figure 7.2 Excitation (full line) and emission (dotted line) tryptophan fluorescence spectra recorded on UHT milk.

absorption and emission, and the similarities of the vibrational levels of S_0 and S_1. However, there are several exceptions, since several absorption bands can be observed in the excitation spectrum but only the last peak is observed in the emission spectrum, representing the transition from S_1 to S_0. The fluorescence of vitamin A, as seen in Figure 7.3, is an example of this, with three absorption peaks and only one emission peak.

Normally, only emission or excitation spectra (i.e. one excitation or emission wavelength) are recorded when investigating the fluorescence of a sample. However, it can be beneficial and informative to obtain the entire fluorescence landscape (also known as 2D fluorescence spectroscopy) in order to find the exact excitation and emission maxima, as well as the correct structure of the peaks. Furthermore, it facilitates more appropriate analysis of fluorescence data from complex samples with more fluorophores present. The fluorescence decay curve of fluorophores also contains detailed information regarding their physical and chemical environment, such as the size, shape and flexibility of macromolecules (Christensen *et al.*, 2006). Instrumentation for time-resolved measurements are, however, typically complex and expensive.

Another extra dimension of fluorescence spectroscopy is *fluorescence anisotropy*. Anisotropy measurements are based on polarization of the light, and the orientation of transition moment of the fluorophores (Genot *et al.*, 1992). Knowing the fluorescence lifetime and anisotropy, the rotation time of a molecule can be determined (Dufour *et al.*, 1994). In particular, in combination with fluorescence lifetime measurements, fluorescence anisotropy is widely used to study the interactions of biological macromolecules. However, this type of fluorescence measurement is not detailed in the present chapter.

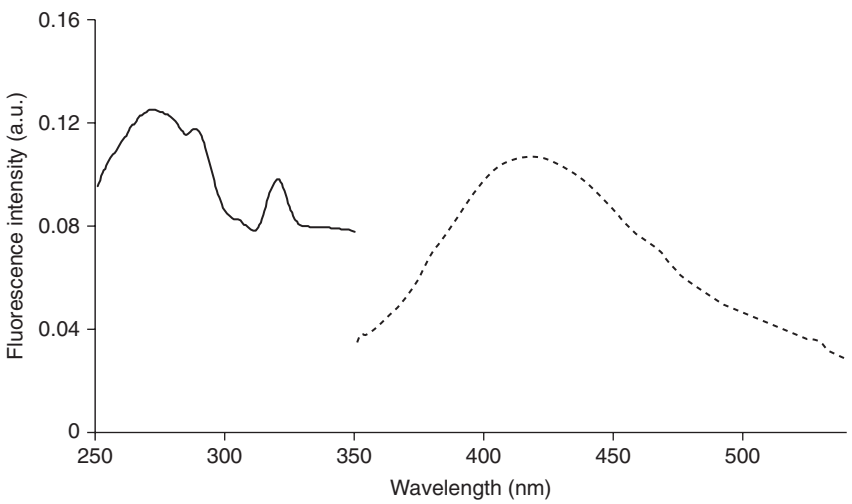

Figure 7.3 Excitation (full line) and emission (dotted line) vitamin A fluorescence spectra recorded on UHT milk.

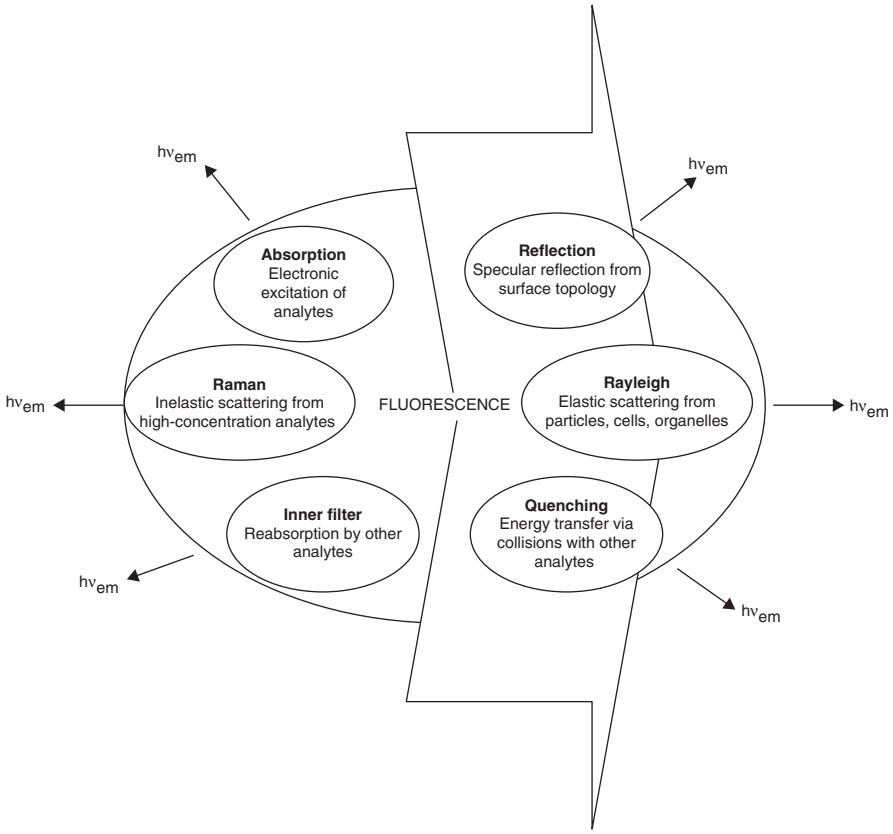

Figure 7.4 Factors affecting the fluorescence signal from complex samples.

Factors affecting fluorescence intensity

Several factors related to the nature and the concentration of fluorophores of food samples influence the fluorescence intensity, as illustrated in Figure 7.4.

Quenching

Fluorescence *quenching* represents any process leading to a decrease in fluorescence intensity of the sample (Lakowicz, 1983). It is related to the deactivation of the excited molecule by either intra- or intermolecular interactions. There are two types of quenching: *statistic* and *dynamic*. The first occurs when the formation of the excited state is inhibited due to a ground-state complex formation in which the fluorophore forms non-fluorescent complexes with a quencher molecule. Dynamic or collisional quenching refers to the process when quenchers deactivate the behavior of the excited state after its formation. The excited molecule will be deactivated by either intramolecular interaction (collision) or intermolecular activity (interaction with other molecules). One of the best-known quenchers is oxygen. A higher temperature also results in larger amount of collisional quenching due to the increased

velocities of molecules. *Resonance energy transfer* can also be considered as dynamic quenching, since an interaction between the donor and acceptor molecules could take place inducing a full or partial deactivation of the excited fluorophore (donor). The energy transfer does not involve emission of light, but a dipole–dipole interaction between the donor and acceptor molecule.

Concentration and inner filter effect

The equation defining the relationship of fluorescence intensity to concentration is:

$$I_f = \phi I_0 \left(1 - 10^{-\varepsilon l c}\right) \tag{7.3}$$

where I_f is the fluorescence intensity, ϕ the quantum yield, I_0 the intensity of the incident light, ε the molar absorptivity, l the optical depth of the sample, and c the molar concentration of the fluorophore.

According to Lakowicz (1983), for low absorbance (<0.05), the equation can be written as:

$$I_f = 2.3 \phi I_0 \varepsilon l c \tag{7.4}$$

Thus, the plot of I_f versus concentration should be linear at low concentrations and reach a maximum at higher concentrations. At higher concentrations, the observed fluorescence signal decreases in relation to the concentration of the fluorophore. The decrease is in a part caused by an attenuation of the excitation beam in the areas of the solution in front of the detection system, and by the absorption of the emitted fluorescence within the solution. This is defined as the *inner-cell* or *inner filter effect*.

The equation expressing the fluorescence intensity indicates that there are three major factors other than concentration that could affect the fluorescence intensity:

1. The quantum efficiency ϕ; the greater the ϕ, the greater the fluorescence intensity.
2. The intensity of incident light I_0; a more intense source will yield greater fluorescence. In actual practice, a very intense source can cause photodecomposition of the sample. Hence, one compromise is a source of moderate intensity (such as a mercury or xenon lamp).
3. The molar absorptivity of the compound, ε. In order to emit radiation, a molecule must first absorb radiation. Hence, the higher the molar absorptivity, the better the fluorescence intensity of the compound will be.

It should be remembered that the overall fluorescence intensity of a given sample is expressed as the sum of the fluorescence contribution from each of the inherent fluorophores present in the sample. However, due to the complex systems of food products the fluorescence intensity may not be additive, because the quenching phenomenon and interactions with the molecular environment of the fluorophores may take place.

Molecular environment

The local environment of a fluorophore has an important effect on the shape of the fluorescence spectra. In more polar environments, the fluorophore in excited state

will relax to a lower energy state of S_1. This means that the emission of polar fluorophores will be shifted towards longer wavelengths (lower energy) in more polar solvents. The structure of macromolecules and the location in macromolecules can also have a large effect on the fluorescence emission and quantum yield of a fluorophore.

The temperature, pH and color strongly affect the fluorescence signal. Increased temperature leads to increased movement of the molecules, and thereby more collisions, thus inducing a reduced fluorescence signal. It is therefore important that all samples in an experiment present the same temperature. The pH value affects the fluorescence, and most hydroxyl aromatic compounds fluoresce better at high pH (Guilbaut, 1989). The color of the sample can affect both the shape and the intensity of the spectra. Dark samples will reabsorb more of the fluorescence than bright samples.

Scatter

Scattering of the incident light affects the fluorescence signal. As mentioned in the previous section, the absorbance of the sample measured plays an important role in fluorescence measurements. Especially in turbid solutions and solid opaque samples (like most foods), the amount of scattered and reflected light affects the measurements considerably, with respect to both the sampling (i.e. the optical depth of the sampling) and the obtained (fluorescence) signal. Scattered light can be divided into Rayleigh and Raman scatter (Figure 7.5).

Rayleigh scatter refers to the scattering of light by particles and molecules smaller than the wavelength of the light. Rayleigh is so-called elastic scatter, meaning that no energy loss is involved, so the wavelength of the scattered light is the same as that of the incident light. Rayleigh scatter can be observed as a diagonal line in fluorescence landscapes for excitation wavelengths equaling the emission wavelength. The signal from fluorophores with little Stoke's shift will be situated close to the scattering line, and therefore be most affected by Rayleigh scatter. Due to the construction of grating

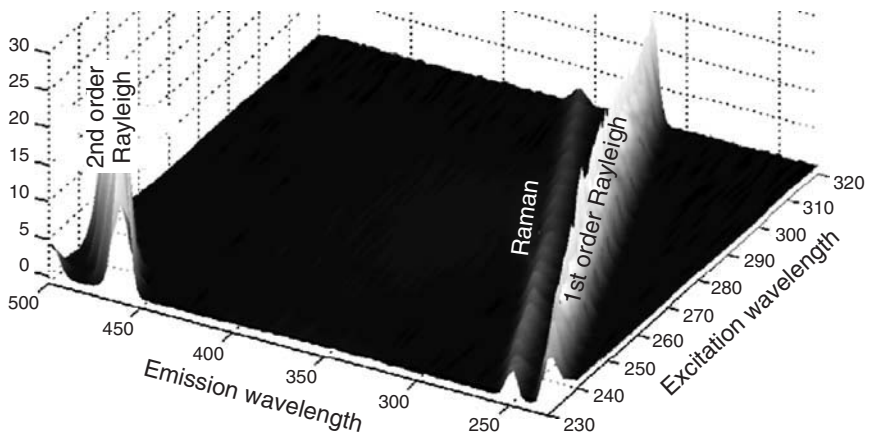

Figure 7.5 Excitation–emission matrix, highlighting Rayleigh and Raman Scatter. Fluorescence landscape of pure water (from Rinnan, 2004).

monochromators used for excitation in most spectrofluorometers, some light at the double wavelength of the chosen excitation will also pass through to the sample. For this reason an extra band of Rayleigh scatter, so-called second-order Rayleigh, will typically appear in fluorescence measurement for emission wavelengths at twice the given excitation wavelength. Rayleigh scatter can be disregarded by measuring and considering the fluorescence signal only between the first- and second-order Rayleigh scatter.

Raman scatter is inelastic scatter, due to absorption and re-emission of light coupled with vibrational states. A constant energy loss will appear for Raman scatter, meaning that the scattered light will have a higher wavelength than that of the excitation light, with a constant difference in wavenumbers. In liquid samples the solvent is decisive in the amount and nature of Raman scatter, while for solid samples it will typically be an expression of the bulk substances. Raman scatter can in most cases be neglected because of its weak contribution to the fluorescence signal.

Instrumentation

The basic set-up for an instrument for measuring steady-state fluorescence is shown in Figure 7.6. The spectrofluorometer consists of a light source (generally xenon or mercury lamp); a monochromator and/or filter(s) for selecting the excitation wavelengths; a sample compartment; a monochromator and/or filter(s) for selecting the emission wavelengths; a detector, which converts the emitted light to an electric signal; and a unit for data acquisition and analysis.

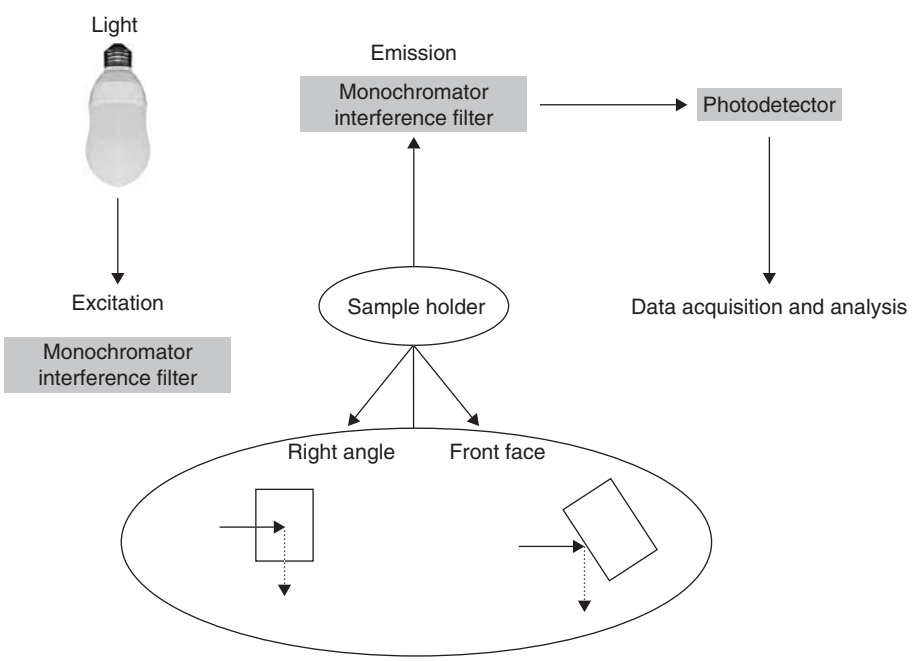

Figure 7.6 Basic set-up of a spectrofluorometer.

The sampling geometry can have substantial effect on the obtained fluorescence signal. If absorbance is less than 0.1, the intensity of the emitted light is proportional to the fluorophore concentration, and excitation and emission spectra are accurately recorded by a classical *right-angle fluorescence* device. In this case, the excitation light travels into the sample from one side, and the detector is positioned at right angles to the centre of the sample. When the absorbance of the sample exceeds 0.1, the intensity of emission and excitation spectra decreases and excitation spectra are distorted. To avoid these problems, dilution of samples is currently performed so that their total absorbance will be less than 0.1. However, the results obtained on diluted solutions of food samples cannot be extrapolated to native concentrated samples since the organization of the food matrix is lost. In addition, the dilution may change the concentration of other relevant fluorescent species below or close to the detection limit of fluorescence. To avoid these problems, FFFS can be used (Figure 7.6). In this manner it is possible to measure more turbid or opaque samples, since the signal becomes more independent of the penetration of the light through the sample. However, when front-face sampling is used, the amount of scattered light detected will increase due to the higher level of reflection from the surface topology of the sample and sample holder. To minimize these effects, it is recommended that the sample is not placed with its surface oriented at an angle of 45° to the incident beam, but rather at 30°/60° to the light source and the detector (Lakowicz, 1983).

Applications of fluorescence in foods and drinks

Recently, the application of fluorescence spectroscopy in combination with multidimensional statistical techniques for the evaluation of food quality has increased. In most of the research papers, the obtained fluorescence signal was assigned to specific fluorophores after fixing the excitation or the emission wavelength.

Dairy products

Dairy products contain several intrinsic fluorophores, which represent the most important area of fluorescence spectroscopy. They include the aromatic amino acids and nucleic acids (AAA + NA), tryptophan, tyrosine and phenylalanine in proteins; vitamins A and B_2; nicotinamide adenine dinucleotide (NADH) and chlorophyll; and numerous other compounds that can be found at a low or very low concentrations in food products.

FFFS for the authentication of milk

Dufour and Riaublanc (1997) investigated the potential of FFFS to discriminate between raw, heated (70°C for 20 minutes), homogenized, and homogenized-and-heated milks. Following principal component analysis (PCA) applied to the tryptophan and vitamin A fluorescence spectra, good discrimination between samples

as a function of homogenization and heat treatment applied to milk samples was observed. They concluded that the treatments applied to milk induced specific modifications in the shape of the fluorescence spectra. Recently, Kulmyrzaev *et al.* (2005) confirmed these earlier findings. In their research, the emission and excitation spectra of different intrinsic probes (i.e. AAA + NA, NADH and FADH) were used to evaluate changes in milk following thermal treatments in the range of 57–72°C for 0.5–30 minutes. The PCA applied on the normalized spectra allowed good discrimination of milk samples subjected to different temperatures and times. However, the above researchers only applied relatively low temperatures to milk samples, which did not allow monitoring of the development of Maillard browning reaction, which was pointed out by Schamberger and Labuza (2006); the fluorescence spectra of milks that were processed for 5, 15, 20, 25 and 30 seconds in 5°C increments from 110°C to 140°C were found to be well correlated with hydroxylmethylfurfural (HMF). Indeed, the R^2 values of >0.95 were found continuously throughout the emission wavelength range of 394 to 447 nm. In addition, the fluorescence levels increased with higher time–temperature combinations. Schamberger and Labuza (2006) concluded that FFFS could be considered a very promising method for measuring Maillard browning in milk, and could also be used as an on-line instrument for monitoring and control of the thermal processing of milk. These results were confirmed by Liu and Metzger (2007), who applied FFFS for monitoring changes in non-fat dry milk (n = 9) collected from three different manufacturers and stored at four different temperatures (4, 22, 35 and 50°C) for 8 weeks. Different intrinsic probes (fluorescent Maillard reaction products (FMRP), riboflavin, tryptophan and vitamin A) were investigated, and each of the considered spectral data sets allowed good discrimination of the milk samples stored at 50°C from the others. In addition, good discrimination of milk samples as a function of the storage time was seen. In a similar approach, Feinberg and coworkers (2006) also used fluorescence spectroscopy to identify five types of heat treatments (pasteurization, high pasteurization, direct UHT, indirect UHT and sterilization) of 200 commercial milk samples stored at 25 and 35°C for 90 days. By applying factorial discriminant analysis (FDA), Feinberg and coworkers (2006) found that tryptophan fluorescence spectra could be considered well-adapted to discriminate sterilized milks and probably pasteurized milks from the other milk samples. However, this intrinsic probe failed to discriminate the other types of milk. An explanation could be that fluorescence spectra were recorded in the pH 4.6 soluble fraction of the milk sample, inducing a loss of information. In another approach, Herbert *et al.* (1999) used FFFS to monitor milk coagulation at the molecular level. Three different coagulation processes have been studied: the *glucono-δ-lactone* (*GDL*), the *rennet-induced coagulation system*, and a mixed GDL + rennet-induced coagulation system. Emission fluorescence spectra of the protein tryptophanyl residues were recorded for each system during the milk coagulation kinetics. By applying the PCA to the collection of normalized fluorescence spectral data of the three systems, detection of structural changes in casein micelles during coagulation and discrimination of different dynamics of the three coagulation systems was achieved. Herbert *et al.* (1999) concluded that FFFS allows the investigation of network structure and molecular interactions during milk coagulation.

Most of the above-mentioned studies regarding discrimination of milks were performed at a laboratory scale on extreme and controlled samples. However, milk products from mountain areas are reputed to have specific organoleptic and nutritional qualities (Bosset *et al.*, 1999; Coulon and Priolo, 2002; Renou *et al.*, 2004), and the tracing of milk-production sites is therefore important in order to avoid fraud. Thus, it would be interesting to assess the potential of FFFS to discriminate between milks according to their geographical origin. Recently, a total of 40 milk samples – 8 produced in lowland areas (430–480 m), 16 produced in mid-level areas (720–860 m) and 16 produced in mountain areas (1070–1150 m) – from the Haute-Loire department in France at key periods of animals feeding have been analyzed (Karoui *et al.*, 2005a). Tryptophan fluorescence spectra, AAA + NA spectra and riboflavin spectra were recorded directly on these milks, with excitation wavelengths set at 290 nm, 250 nm and 380 nm, respectively. The excitation spectra of vitamin A were also recorded, with the emission wavelength set at 410 nm. By applying FDA to the spectral collection, a trend to a good separation between milks as a function of their altitudes was observed. The best results were obtained with AAA + NA fluorescence spectra, since 81.5% and 76.9% of the calibration and validation spectra, respectively, were correctly classified. However, some misclassification between milks produced in mid-level areas and the other milk samples was observed.

FFFS for monitoring the quality of cheeses during ripening

Understanding the structure of cheese, particularly protein and fat structures, and the interactions of cheese components during ripening would provide useful information in determining what constitutes a quality product. Dufour *et al.* (2000) and Mazerolles *et al.* (2001) used FFFS to monitor 16 semi-hard cheeses produced and ripened under a controlled scale. By applying PCA to the normalized tryptophan fluorescence spectra, good discrimination of cheeses presenting a ripening time of 21, 51 and 81 days was observed, while an overlap was observed between cheeses aged 1 day and those aged 21 days.

Spectral patterns associated with the PCs provide the characteristic wavelengths that may be used to discriminate between spectra. Spectral patterns are similar to spectra, and may be used to derive structural information at the molecular level. On studying the spectral pattern, a red shift of aged cheeses was observed, suggesting that the environment of old cheeses was more hydrophilic than that of young (1-day-old) cheeses. This phenomenon has been explained by a partial proteolysis of casein as well as the salting phenomenon, which may induce some changes in the tertiary and quaternary structures of casein micelles. Regarding the fluorescence spectra of vitamin A, two shoulders located at 295 and 305 nm and a maximum located at 322 nm were observed (Dufour *et al.*, 2000). In addition, the shape of the spectra changed with the ripening time (Figure 7.7). By applying PCA to the normalized vitamin A spectra, better discrimination of cheeses aged 21, 51 and 81 days from those aged 1 day was achieved.

In order to determine the link between mid-infrared (MIR) and fluorescence spectra, the authors applied canonical correlation analysis (CCA) on one hand to the

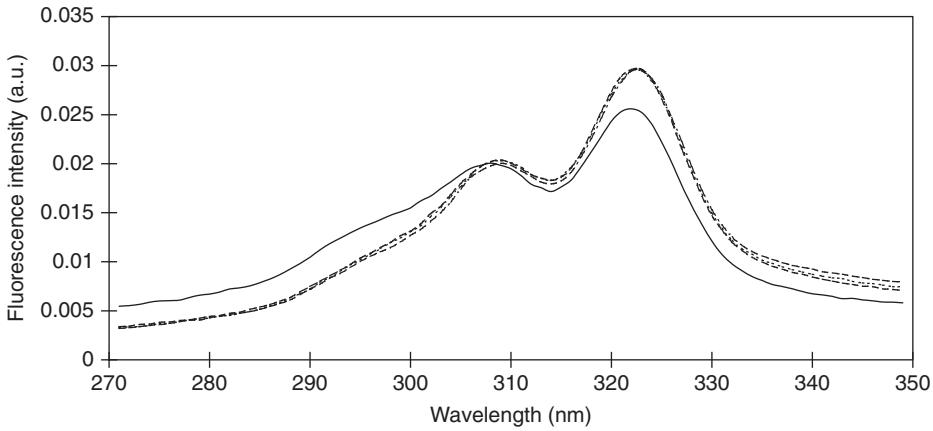

Figure 7.7 Front-face fluorescence spectra of Raclette cheeses recorded at four different times during ripening: 1 day (—), 21 days (— —), 51 days (- - - -), and 81 days (—·—·).

1700–1500 cm^{-1} spectral region and tryptophan fluorescence spectra, and on the other to the 3000–2800 cm^{-1} spectral region and vitamin A spectra. A relatively high correlation rate was found, since the first two canonical varieties had a squared canonical correlation coefficient higher than 0.58. The authors concluded that MIR and fluorescence spectra provide a common description of cheese samples.

Karoui *et al.* (2006a) continued this work by recording tryptophan, vitamin A and riboflavin spectra of 12 semi-hard cheeses (Raclette) of 4 different brands, which were produced during summer period at an industrial level. By applying common component and specific weights analysis (CCSWA) to the spectral data sets and physicochemical data, good discrimination of the four brands was observed. The same research group (Karoui and Dufour, 2006) evaluated the potential of FFFS to predict the rheological parameters of 20 semi-hard cheeses at the end of their ripening stage (60 days) from fluorescence spectra recorded at a younger stage (2 days old). By using tryptophan fluorescence spectra scanned on cheeses aged 2 days and at 20°C, the storage modulus (G′), loss modulus (G″), strain, tan (δ) and complex viscosity (η*) were predicted by using partial least squares (PLS) regression with leverage correction with R of 0.98, 0.97, 0.98, 0.98 and 0.97, respectively. Riboflavin fluorescence spectra gave slightly lower R of 0.88, 0.88, 0.92, 0.87 and 0.88, respectively. One of the main conclusions of this study was that FFFS might be useful for rapid online determination of the texture of cheeses.

FFFS for the authentication of cheese at the retail stage

To study different varieties of soft, semi-hard, and hard cheeses during ripening and at the retail stage, Dufour and coworkers used a similar approach (Herbert, 1999, 2000; Karoui and Dufour, 2003; Karoui *et al.*, 2003, 2004b, 2005b, 2005c).

The potential of FFFS to discriminate between eight groups of soft cheeses was evaluated by Herbert *et al.* (2000). In their research, tryptophan and vitamin A spectra were used as intrinsic probes to discriminate between the investigated soft cheeses

as a function of their ripening times and/or cheese-making procedures. The environment of the tryptophan residues was found to be relatively more hydrophilic for the old cheeses than for those at the young stage. This phenomenon was attributed to partial proteolysis of caseins during ripening, resulting in an increase of tryptophan exposure to the solvent. To test the accuracy of FFFS in differentiating between the eight soft cheeses, the authors applied FDA to the most relevant PCs. The results obtained showed good discrimination of cheeses, with better results obtained with vitamin A spectra (96% and 93% for the calibration and validation samples, respectively) than with tryptophan spectra (95% and 92% for the calibration and validation samples, respectively). However, in their investigations only samples taken from the center of the cheese were analyzed, which may have induced some limited interpretation in the case of the soft cheeses. Indeed, protein breakdown, lipolysis, pH, etc. differ significantly between the surface and the center of soft ripened cheeses. Thus, the matrix structure of three retailed soft cheeses (M1, M2 and M3), each with different manufacturing processes, was studied from the surface to the center of the cheese using FFFS, among other techniques (Karoui and Dufour, 2003). Cheese slices, 5-mm thick, were cut from the surface to the center of the samples. PCA applied to the tryptophan fluorescence spectra recorded for each cheese variety showed good discrimination of cheese samples as a function of their location. The environment of tryptophan residues was found to be more heterogeneous in the surface samples than in the center samples; this was attributed to the changes in the extent and type of protein–protein interactions in the protein network depending on the sampling zone. One of the limiting points of this study was the low number of cheeses. In addition, only tryptophan and vitamin A fluorescence spectra were recorded for these cheese varieties. Therefore, it would be interesting to validate the relevance of this technique to differentiate soft cheeses according to their sampling zones by using a large number of samples, and to test other intrinsic probes (such as riboflavin) which give an indication on the level of oxidation in cheeses. Karoui *et al.* (2007a) have thus recently used FFFS to investigate changes at the molecular level of both the external (E) and central (C) zones of 15 ripened soft cheeses produced according to traditional and stabilized cheese-making procedures. In order to extract all the information contained in the fluorescence spectra, CCSWA was applied to the tryptophan, vitamin A and riboflavin spectral data sets. The plane defined by the common components 1 (q_1) and 3 (q_3) showed clear discrimination between the cheese varieties and sampling zones (Figure 7.8a). Considering q_1, the C-M1 and C-M3 cheese samples had negative score values, while the other cheese samples (E-M1, E-M2, C-M2 and E-M3) exhibited mostly positive scores. In addition, good discrimination of E and C zones of M1 and M3 cheeses was observed according to the q_1. However, E-M2 and C-M2 cheese samples were not well discriminated, although they were well separated from the other cheese varieties. Figure 7.8a also shows good discrimination between stabilized cheeses (E-M3, C-M3) and traditional cheeses (E-M1, C-M1, E-M2 and C-M2) independently of the sampling zones. The spectral patterns of tryptophan, riboflavin and vitamin A fluorescence spectra associated with the q_1 are shown in Figures 7.8b, 7.8c and 7.8d, respectively. Figure 7.8b shows opposition between a negative peak located at 334 nm and a positive peak at 387 nm, indicating

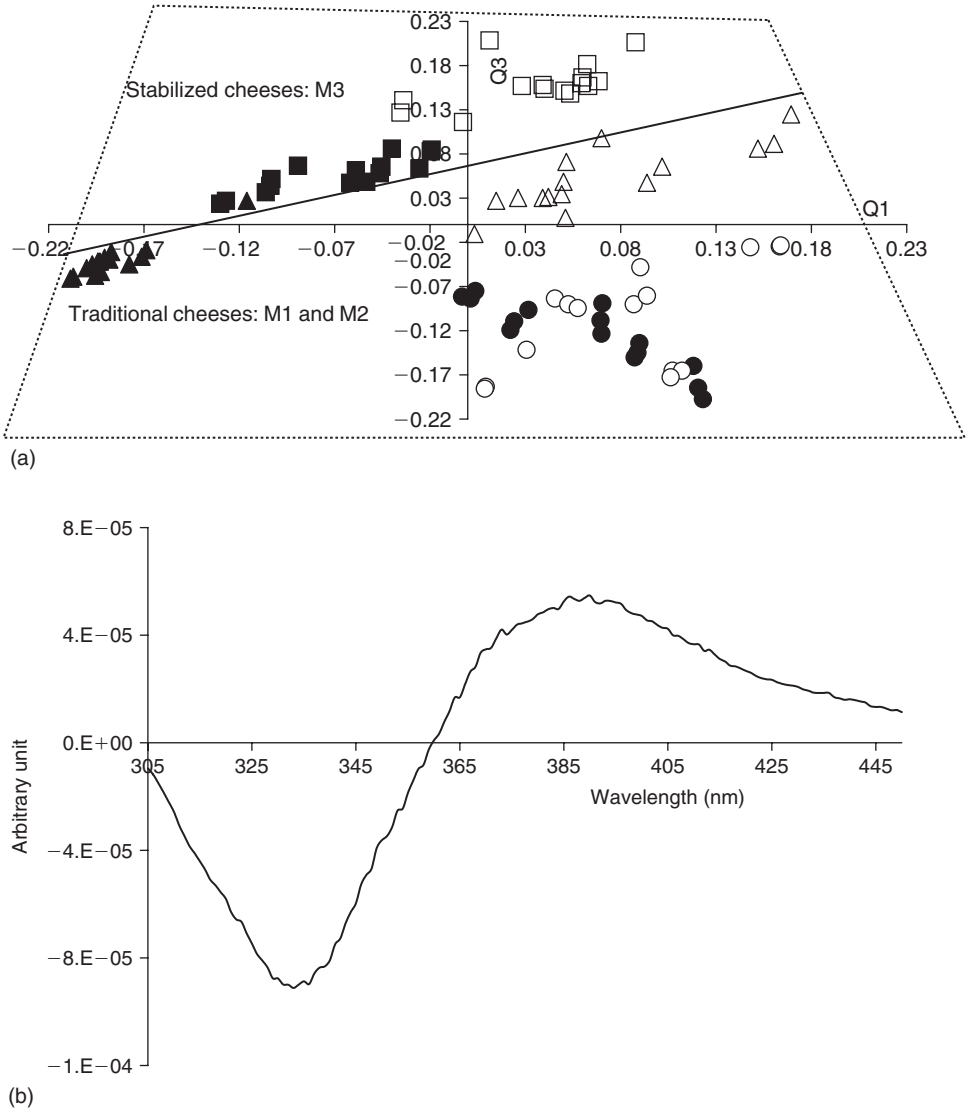

Figure 7.8 Common components and specific weights analysis (CCSWA). Similarity map defined by the common components 1 (q_1) and 3 (q_3) of external M1 zone (Δ), central M1 zone (▲), external M2 zone (o), central M2 zone (●), external M3 zone (□), and central M3 zone (■) of cheeses (a); Spectral patterns of tryptophan (b), riboflavin (c) and vitamin A (d) associated with the common component q_1.

that the E-M1, C-M2, E-M2 and E-M3 cheese samples were in a hydrophilic environment. Regarding the spectral pattern of the riboflavin, opposition between two peaks located around 460 and 495 nm and the one located at 533 nm was observed (Figure 7.8c), indicating that the C-M1 and C-M3 cheese samples were less oxidized than the other cheese samples. Finally, the spectral pattern of the vitamin A (Figure 7.8d) was characterized by two positive peaks at 313 and 330 nm and a negative peak at 285 nm. From the obtained results, it was reported that CCSWA allowed very efficient

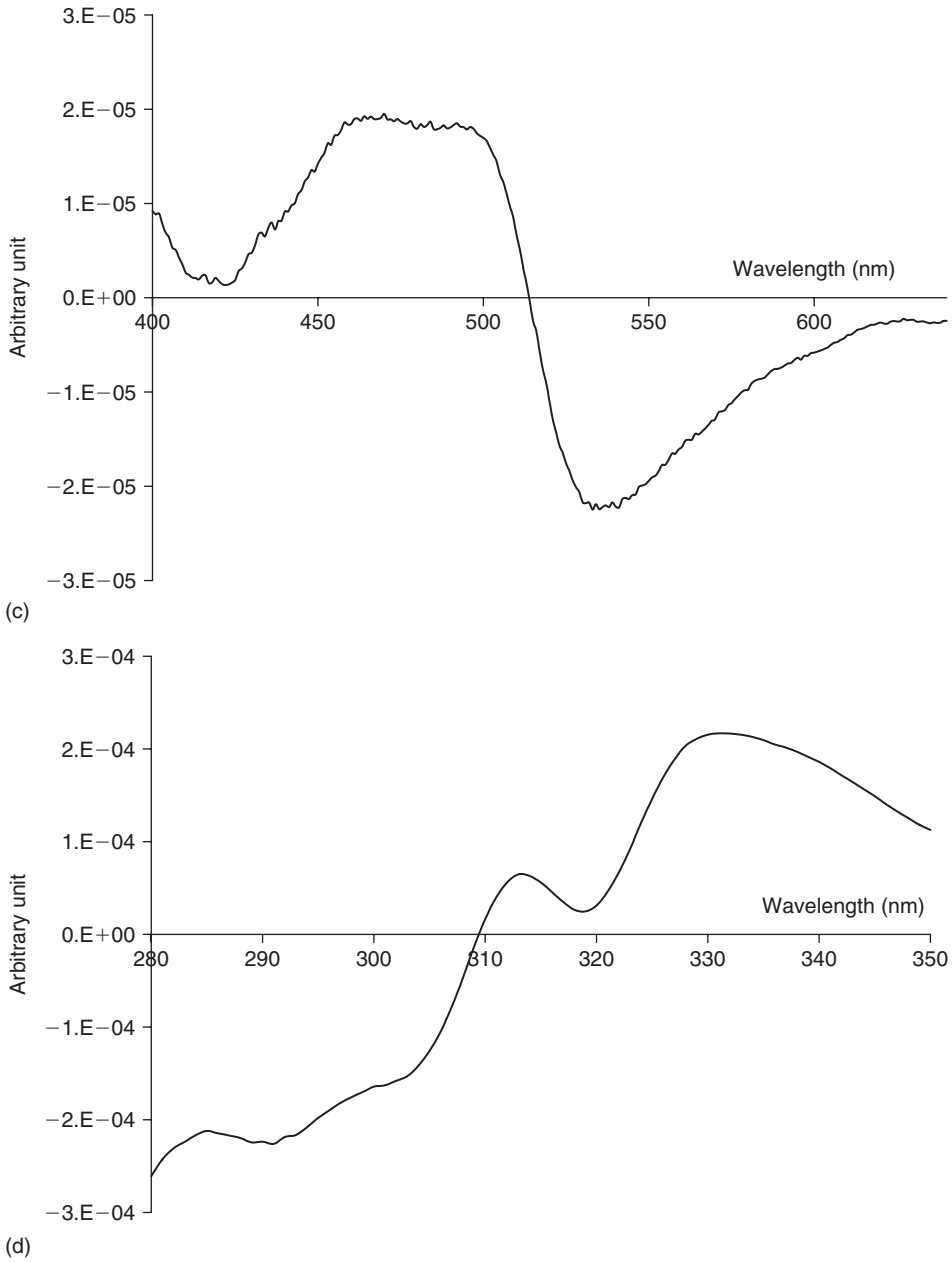

Figure 7.8 (Continued)

management of all the spectroscopic information collected for the investigated soft cheeses. Each of the investigated probes provides information which can be used for recognizing the cheese variety and sampling zone. The CCSWA method sums up this information using two common components (q_1, and q_3), taking into account the relation between the different fluorescence data sets. The results obtained from CCSWA were not observed by the PCA performed separately on each of fluorescence

spectral data set, illustrating that CCSWA methodology allowed very efficient use of all the spectroscopic information provided by the three intrinsic probes.

In a second step, the accuracy of FFFS in the determination of some selected chemical parameters collected from the E and C zones of 15 soft cheeses was assessed (Karoui *et al.*, 2006b). PLS regression applied to the normalized vitamin A fluorescence spectra provided the highest values of the determination coefficient (R^2) of 0.88, 0.86, 0.86 and 0.84 for fat, dry matter, fat in dry matter, and water-soluble nitrogen, respectively. The prediction of pH was successful only when using riboflavin spectra. The authors pointed out that FFFS could be used as a rapid technique to predict the chemical composition of soft cheeses; however, more samples are needed to confirm this assumption.

In a different approach, Karoui *et al.* (2005c) attempted to discriminate 25 Gruyère and L'Etivaz Protected Designation of Origin (PDO) cheeses. Emission spectra were scanned following excitation at 250 and 290 nm, and excitation spectra following emission at 410 nm. By applying FDA, 100% correct classification was obtained from the emission and excitation spectra. The authors concluded that FFFS could be an accurate technique for the determination of the geographic origin of cheeses. These findings were fully confirmed on Emmental cheeses originating from different European countries and manufactured during both winter and summer seasons (Karoui *et al.*, 2004a, 2004b, 2005b). One of the strong conclusions of these studies is that FFFS allows a good discrimination between Emmental cheeses produced from raw milk and those made with thermized milk.

FFFS for monitoring the oxidation of dairy products

Increasing efforts have been devoted to the development of methods that detect and quantify early lipid oxidation in food systems. Dairy products are generally susceptible to light, and they are exposed to it both during processing and in the grocery stores. This exposure causes off-flavors in milk, degrades some of its riboflavin, vitamin C and vitamin A, and induces lipid oxidation (Bosset *et al.*, 1994).

In the milk industry several methods are used to detect photo-oxidation of dairy products, including peroxide values, sensory analysis, gas chromatography, etc. However, these methods involve the use of relatively large amount of solvents, are time consuming and/or expensive. FFFS is now recognized as a sensitive method for determining the level of oxidation in dairy products; indeed, good estimation of the sensory analysis and FFFS in both sour cream (Wold *et al.*, 2002) and cheese (Wold *et al.*, 2005) has been achieved. Wold and coworkers (2005) showed that naturally occurring porphyrin and chlorophylls play an important role as photosensitizers in dairy products. The degradation of these components showed higher correlation with sensory measured lipid oxidation.

Recently, the feasibility of the use of FFFS as a non-destructive technique for monitoring oxidation at the molecular level of semi-hard cheeses made with cow's milk and collected during both the grazing period (summer) and the stabling period (autumn) was examined at the surface (20 mm from the rind) and inner (40 mm from the rind) layers throughout the ripening stage (2, 30 and 60 days old) (Karoui *et al.*, 2007b).

By applying FDA to the 400–640 nm emission fluorescence spectra recorded at the surface layer, correct classification was observed for 100% and 91.7% for the calibration and the validation spectra, respectively. With regard to the samples cut from the inner layers, the authors stated that the 400–640 nm emission fluorescence spectra failed to discriminate cheeses that were either 2 or 30 days old. The main conclusion of this study was that throughout ripening the riboflavin component was affected primarily by oxygen and light (Marsh *et al.*, 1994), while the physicochemical modification that takes place during ripening seemed to have a lesser effect than did light and oxygen. The authors concluded that the 400–640 nm emission fluorescence spectra recorded following excitation set at 380 nm at the surface layers could be considered a promising tool for monitoring the oxidation of cheeses throughout ripening.

Meat and meat products

Research regarding the application of FFFS for the evaluation of meat products has focused on the measurements of fluorescence from collagen, adipose tissues and protein (Newman, 1984; Jensen *et al.*, 1989; Frencia *et al.*, 2003).

Connective tissue and fat

The *collagen* in connective tissue is known to be an important parameter of meat quality, as it is related to the tenderness and texture of the meat. Collagen exists in several different genetic forms, four of which have been found to be present in muscle: Types I, III, IV and V. Types I, III and IV presented similar fluorescent characteristics when they were excited in the 330–380 nm spectral region (Hildrum *et al.*, 2006). *Elastin*, another important fluorophore in meat, presents quite similar fluorescence properties to those of collagen Types I, III and IV (Egelandsdal *et al.*, 2005).

Adipose tissue contains fluorescent molecules that are specific for fat. Indeed, it has been shown by several authors (see, for example, Ramanujam, 2000; Skjervold *et al.*, 2003) that the fat-soluble vitamins A, D and K exhibit fluorescence in the 387–480 nm spectral region after excitation at 308–340 nm.

Swatland (Swatland, 1987; Swatland *et al.*, 1995a, 1995b; Swatland and Findlay, 1997) could be considered the pioneer in the field of meat, with a series of papers on different aspects of the use of FFFS, starting in 1987. His work focused on measuring collagen and elastin fluorescence from the connective tissues in meat. The author reported that after excitation at 365 nm, the fluorescence emission spectra of adipose tissue exhibited a maximum at 510 nm with a secondary plateau varying from 430 to 450 nm (Swatland, 1987). The obtained fluorescence spectra of various meats were found to be correlated with biochemical and sensory analyses such as chewiness (Swatland *et al.*, 1995a), palatability (Swatland *et al.*, 1995b) and toughness (Swatland and Findlay, 1997).

Most of the studies by Swatland and coworkers (Swatland, 1987; Swatland *et al.*, 1995a, 1995b; Swatland and Findlay, 1997) were performed using a univariate data analytical approach, by the comparison of single-wavelength or extracted fluorescence-peak features. Although interesting results were achieved, the use of multivariate analysis and regression is needed for curve resolution and useful quantitative measurements

due to the complexity of fluorescence spectra. Egelandsdal and coworkers (1996) applied multivariate statistical analyses such as PCA and PLS regression to the fluorescence spectra scanned on meat products after excitation set between 300 and 400 nm. Indeed, Egelandsdal *et al.* (1996) studied isolated perimysial sheets from a type I muscle, and found a high correlation between perimysial breaking strength and fluorescence emission spectra recorded after excitation at 335 nm. Wold *et al.* (1999a, 1999b) then confirmed these previous investigations and suggested that it would be possible to measure the amount of connective tissue in ground meat by using an excitation wavelength of 380 nm. These latter authors also showed that both connective tissue and intramuscular fat content could be measured using an excitation wavelength of 332 nm. Recently, Egelandsdal *et al.* (2002) studied six different batches of beef *longissimus dorsi* samples originating from 151 animals by using FFFS and Warner-Bratzler (WB) peak values. By applying PLS regression, poor to good (R = 0.45–0.84) correlations between WB peak values and the emission spectra were obtained. In addition, minor differences in predictability were observed using excitation wavelengths of either 332 or 380 nm. The emission wavelengths containing the most relevant information about WB peak values were between 360 and 500 nm. Emission wavelengths around 375 nm, following excitation at 332 nm, were found to be related to a component in the perimysial tissue, most likely present in collagen I or III.

In another study, Møller *et al.* (2003) used FFFS to predict the age of Parma hams produced from two muscles (semimembranosus and biceps femoris) and aged for 3 months (young), 11 and 12 months (matured), and 15 and 18 months (aged). Using PLS regression, prediction of the age was considered as good, with a relative error of prediction of approximately 1 month; also, a good correlation between fluorescence and chemical, sensory and physical parameters was found.

Egelandsdal *et al.* (2005) tried to throw more light on the phenomena affecting the fluorescence signal and the ability of the FFFS technique to quantify collagen contents. Beef *masseter* and *latissimus dorsi* and pork *glutens medius* muscles, among others, were chosen for their wide differences in color and connective tissue quality and content. PLS regression was applied to their fluorescence spectra in order to predict collagen (measured as hydroxyproline), and good results were obtained (root mean square error of prediction (RMSEP) 0.55%). Similar prediction results were also obtained with complex sausage batters consisting of different kinds of muscles, and presenting a large span in myoglobin and realistic ranges in collagen and fat. One of the interesting results obtained in this study was that FFFS gave lower prediction errors for collagen content than did near-infrared (NIR) reflectance when applied to the same batters.

Tenderness and muscle types

Differences in the level of collagen within a muscle or between different muscles led to a huge difference in tenderness (Light *et al.*, 1985). Using excitation wavelengths set between 332 and 380 nm, FFFS is a promising technique for estimating tenderness in such muscles (Hildrum *et al.*, 2006). Recently, tryptophan fluorescence spectra scanned on two beef muscles (*longissimus thoracis* and *infraspinatus*) after 2 and 14 days *post mortem* showed a maximum located around 336 nm (Dufour and Frencia, 2001). In

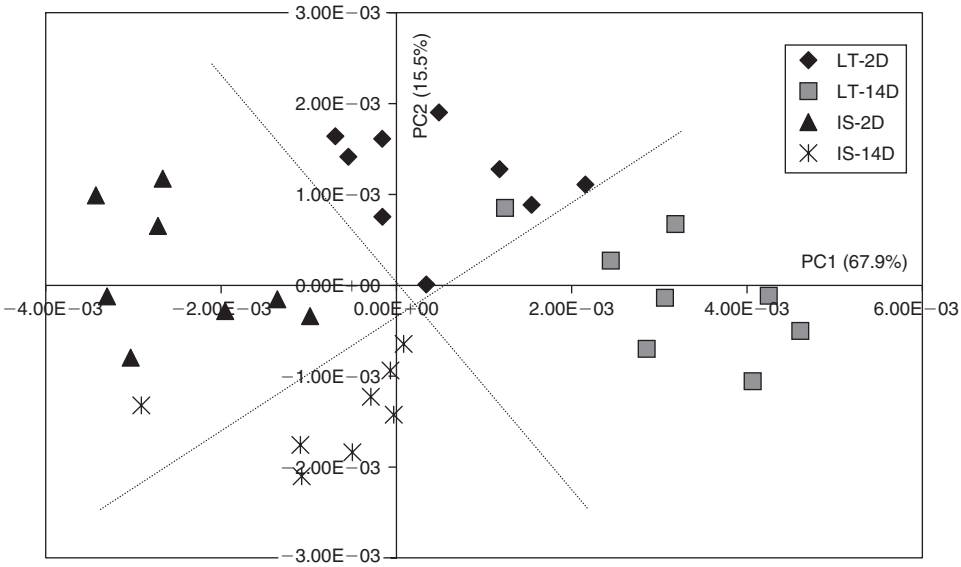

Figure 7.9 PCA similarity map defined by the principal components 1 (PC1) and 2 (PC2) for the tryptophan spectral data of *longissimus thoracis* (LT) and *infraspinatus* (IS) muscles at 2 and 14 days' *post mortem*.

addition, the maximum emission of aged muscles showed a shift to higher wavelengths (red shift). Therefore, to extract relevant information from the spectral data, the authors used multivariate statistical analysis such as PCA. The obtained results showed good discrimination of samples according to the muscle type and aging (Figure 7.9). However, with only a limited number of meat samples, the models suffered from over-fitting and consequently were not very robust against the inclusion or exclusion of samples. Further analyses with more samples are necessary to substantiate these models. This would allow more variability of the chemical properties and thus development of general mathematical models for better accuracy of the FFFS technique. Dufour and coworkers (Frencia *et al.*, 2003) therefore assessed the potential of FFFS to discriminate between five muscle types presenting different level of collagen contents and those at two points in time (2 days and 14 days post mortem). Applying FDA to the tryptophan fluorescence spectra, a correct classification rate of 82% was obtained. The authors concluded that FFFS is a powerful technique that allows a relatively good identification of muscle types according to maturation.

Preliminary results have shown that results obtained at the molecular level by FFFS are related to the macroscopic levels (sensory and rheology data sets). Indeed, Frencia *et al.* (2003) have used a descriptive technique based on CCA to investigate the correlation between fluorescence spectra (spectrofluorometer with a front-face device or coupled to a fiber-optic), mechanical properties (texturometer) and sensory attributes. The results showed strong correlation between the different methods, as depicted in Table 7.1. The authors concluded that a common description of the samples was possible from both the fluorescence and the rheology or sensory data.

In a similar approach, Lebecque *et al.* (2003) analyzed 25 *longissimus thoracis* samples from animals of different ages (between 2.5 and 8 years) and sexes. Sensory

Table 7.1 Canonical correlation coefficient (R) for the first canonical variates of canonical correlation analysis (CCA) performed on the sensory, rheology, and spectral data

	R
Sensory analysis/spectroscopy with fiber-optic	0.93
Sensory analysis/spectroscopy with front-face device	0.95
Texturometer/spectroscopy with front-face device	0.95
Spectroscopy with front-face device/with fiber-optic	0.96

analysis and tryptophan fluorescence spectra were performed on muscle samples after 7 and 12 days of aging. By applying CCA to the two methods, the first two canonical variates were correlated with squared canonical correlations that were equal to 0.57, implying that the phenomena observed at the molecular and macroscopic levels were related to the change in the texture of meat during aging. The obtained results were confirmed later by Allais *et al.* (2004) on meat emulsion and frankfurters, since good correlation was obtained from fluorescence spectra and rheology methods.

Lipid oxidation

Lipid oxidation is one of the factors limiting the quality and acceptability of meat and meat products (Veberg, 2006). As explained above, lipid oxidation can be determined by several methods, such as 2-thiobarbituric acid, sensory analysis, and dynamic headspace gas chromatography combined with mass spectrometry. Veberg *et al.* (2006) used FFFS and other destructive methods to determine the level of lipid oxidation, and explored the usefulness of this technique for detection of low levels of lipid oxidation in turkey meat. They divided 55 meat samples into two groups and stored them for 9 months at −20°C and −10°C in a vacuum or exposed to air. The emission spectra in the range of 410 nm to 750 nm measured after excitation at 382 nm showed a maximum intensity at around 468–475 nm. These fluorophores have been ascribed to the reactions that occur between aldehydes and amino acids and/or lipid radicals and amino acids (Yamaki *et al.*, 1992). The fluorescence intensities for turkey meat stored in air at −10°C were highest, followed by those meat in storage in a vacuum at −10°C, in air at −20°C, and in a vacuum at −20°C. By applying PLS regression between fluorescence spectra and the values obtained by the other traditional techniques, good correlations between fluorescence spectra and thiobarbituric acid reactive substances (TBARS), hexanal, 1-penten-3-ol, total components and sensory measured rancidity and intensity were found. One of the interesting conclusions of this study is that FFFS could be considered as a sensitive and non-destructive method for measurement of early lipid oxidation in turkey meat. The obtained results confirmed the previous findings of Olsen *et al.* (2005), in which two model matrices of pork back fat and mechanically recovered poultry meat were freeze-stored in air at −20°C for 26 weeks. They found that FFFS and gas chromatography coupled with mass spectrometry could detect oxidative changes in pork back fat earlier than the sensory panel and the electronic nose could. The authors reported that correlation of fluorescence spectra with sensory analyses is poorer than that of gas chromatography with mass spectrometry. In a similar approach,

Gatellier *et al.* (2007) monitored lipid oxidation of chicken meat by using FFFS and TBARS over 9 days. In their research study, three chicken genotypes representative of French production were compared: Standard (fast-growing line), Certified (medium-growing line) and Label (slow-growing line). These were stored in darkness at 4°C. Good correlation between emission spectra recorded after excitation at 380 nm and TBARS was found. In addition, an effect of genotype on fluorescence emission spectra was pointed out, since the fluorescence intensity of the emission spectra of Certified and Label animals after 7 days of refrigerated storage was significantly higher than that of Standard chicken meat samples.

Fish

The lipid fraction of marine fish has been shown to contain a high level of polyunsaturated fatty acids. During storage and/or processing, the degradation of polyunsaturated fatty acids can lead to the development of primary and secondary products, resulting in the formation of fluorescent compounds and the loss of essential nutriments. Indeed, Gardner (1979) has shown that relatively higher fluorescence intensity was observed at higher wavelength maxima as the quality of fish decreased. The 493/463 nm and 327/415 nm ratios have proved to be a more effective index of fish quality than other common assessment methods. Hasegawa *et al.* (1992) used FFFS for the quantitative assessment of oxidative deterioration in freeze-dried fish. Two excitation wavelengths (370 and 450 nm) exhibiting maximum emissions at 460 and 500 nm, respectively, were used, and an increase in the fluorescence intensity at 500 nm was noted, while that at 460 nm remained unchanged for fish samples stored at 25°C in the dark. The fluorophores observed at 460 nm have been related to the reaction between reducing sugars (such as glucose and ribose found in fish) and amino acid compounds which induce the activation of the Maillard reaction, while that observed at 500 nm has been attributed to the lipid oxidation products.

In a similar approach, Olsen *et al.* (2006) used an excitation wavelength of 382 nm to record spectra in the 450–750 nm region on four different batches of salmon pâté stored at 4°C for 4, 8 and 13 weeks. Citric acid or calcium disodium ethylene-diamine tetraacetate were added as metal chelators to two batches, whereas no chelator was added to the third batch. The three investigated batches contained oil, while a fourth one was made with the same amounts of ingredients but without any oil. The obtained results showed an increase in the fluorescence intensity with increased storage time for all the batches. In addition, the shape of the spectra changed largely between samples containing oil and those without oil. Indeed, samples containing oil exhibited the highest intensity in the range of 470–475 nm, while those with no added oil presented maxima between 440–450 nm. By applying PCA to the spectral data collection, a clear difference between samples according to storage time and the presence (or not) of oil was observed. The largest variation in the data sets was attributed to whether the samples contained oil or not; the storage time was the second most important factor that led to this discrimination. In a second step, the authors applied PLS regression to estimate the age of salmon pâté. The correlation coefficients for the sensory attributes, dynamic head-space data, fluorescence spectra and electronic nose sensor responses

were 0.64, 0.94, 0.93 and 0.70, respectively. The corresponding RMSEP were 3.8, 1.7, 1.8 and 3.5, respectively, illustrating that FFFS could be a suitable technique to measure lipid oxidation. This observation is confirmed by the highest level of correlation found between fluorescence spectra and sensory attributes, among the other analytical techniques.

Recently, FFFS has been used to monitor fish freshness for four different species – cod, mackerel, salmon and whiting fillets – at 1, 5, 8 and 13 days of storage (Dufour *et al.*, 2003). Emission spectra of AAA + NA, tryptophan and NADH were scanned after excitation at 250, 290 and 336 nm, respectively. The first two excitation wavelengths showed maxima located at 338 and 336 nm, respectively, while the last excitation wavelength showed two maxima located at 414 and 438 nm. For all three excitation wavelengths, the shape of the spectra illustrated some differences according to the storage time, suggesting that a fluorescence spectrum may be considered as a fingerprint. Applying FDA to the tryptophan fluorescence spectra allowed 56% correct classification of fish samples according to their storage times. Better classification was obtained from AAA + NA and NADH, since 92% and 74% correct classification was observed, respectively. The authors concluded that intrinsic fluorescence spectra could be considered as fingerprints that may allow discrimination between fresh and aged fish fillets.

Freezing is an efficient way of storing fish. It is also an excellent way to extend the storage life of fish, a fragile foodstuff. During freezing, storage and thawing, fish muscle may undergo protein denaturation and lipid oxidation due to a variety of causes (Kozima, 1983). When freezing, storage and thawing are performed properly, the sensory properties of the products are very similar to those of the fresh one. Consequently, it is not easy to differentiate between a fresh and a frozen-thawed fish. In addition, nowadays many consumers prefer fresh fish despite its higher cost. For this reason, the trading of frozen-thawed products as fresh occurs, and is a fraudulent practice. Much effort has been expended in devising methods to establish whether or not a fish has been previously frozen. A series of physical, chemical and sensory parameters have been intensively highlighted by using popular and well-known analytical methods in order to differentiate frozen from fresh fish samples. Enzymatic methods, which involve assays of mitochondrial enzymes such as β-hydroxyacyl-CoA-dehydrogenase or HADH, have been used by several authors (Gottesmann and Hamm, 1983; Garcia de Fernando *et al.*, 1992; Hoz *et al.*, 1992; Pavlov *et al.*, 1994; Fernandez *et al.*, 1999). Physical methods, which are based on the changes in dielectric properties of tissues using the fish freshness tester or torrymeter, have been used by Kim *et al.* (1987). Physiological (Yoshioka and Kitamikado, 1983), microbiological (Vyncke, 1983) and organoleptic methods (Bennett and Hamilton, 1986) have also been utilized to differentiate frozen-thawed fish from fresh fish.

All these methods are tedious and destructive, relatively expensive and time-consuming, and require highly skilled operators. Recently, attention has focused on the development of non-invasive and non-destructive instrumental techniques such as FFFS. Indeed, Aubourg *et al.* (1998) used fluorescence spectroscopy to monitor changes that occurred in sardines stored at −18°C and −10°C. Sardines stored at −18°C were sampled after 0.5, 2, 4, 8, 12 and 24 months, and those stored at −10°C

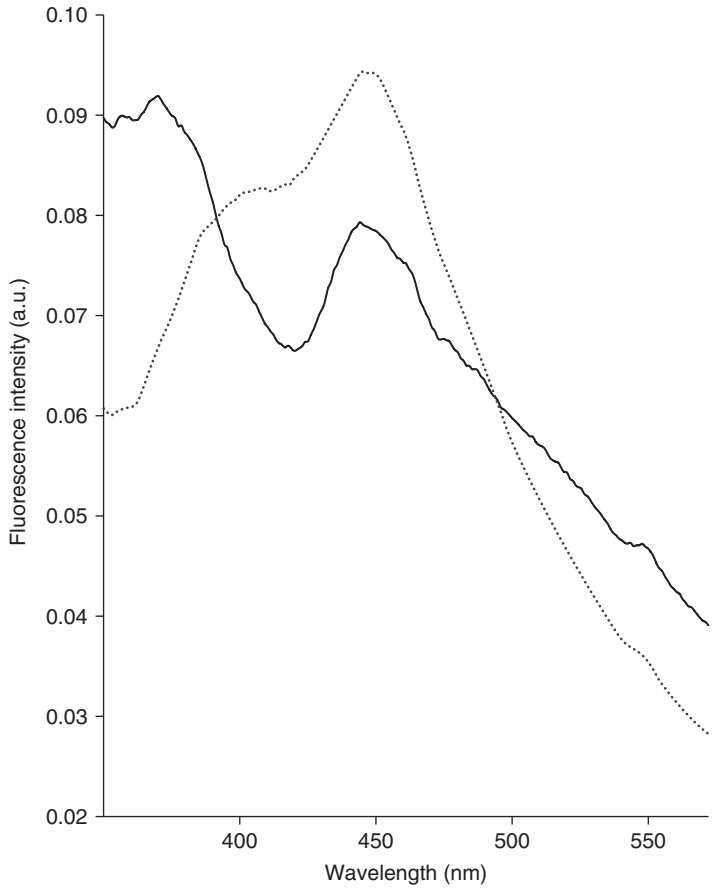

Figure 7.10 Normalized NADH fluorescence spectra (excitation 340 nm, emission 360–570 nm) of fresh (...) and frozen-thawed (—) fish fillets.

were sampled at 3, 10, 25, 60 and 120 days. Fluorescence was measured at two excitation emission maxima, 327/463 nm and 393/463 nm. The authors used the fluorescence ratio, defined as the fluorescence intensity at 327/463 nm over the fluorescence intensity at 393/463 nm, determined in aqueous and organic solutions. This ratio was found to increase throughout the whole storage time at the two temperatures when it was determined in the aqueous solution. One of the most limiting points of this study is that the authors used only maxima of emission and excitation wavelengths, which could induce some loss of information contained in the fluorescence spectra. Recently, Karoui *et al.* (2006c) demonstrated the ability of FFFS to differentiate between fresh and frozen-thawed fish. A total of 24 fish (12 fresh and 12 frozen-thawed) were analyzed by using excitation wavelengths set at 290 (tryptophan) and 340 nm (NADH). The authors tested different freezing and thawing rates. The emission spectra of NADH of fresh fish showed a maximum at 455 nm and a shoulder at 403 nm, while frozen-thawed fish was characterized by a maximum located at 379 nm and a shoulder at 455 nm (Figure 7.10).

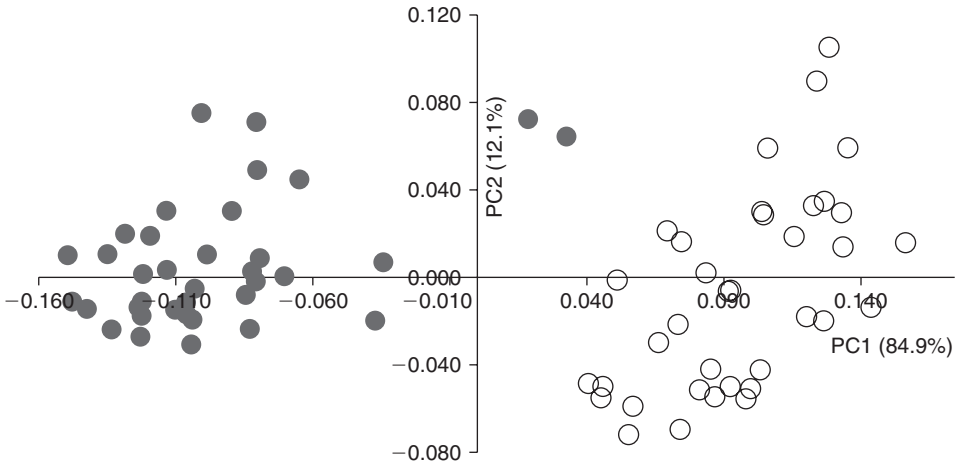

Figure 7.11 Principal component analysis similarity map determined by principal components 1 (PC1) and 2 (PC2) for the NADH fluorescence spectra of fresh (●) and frozen-thawed (○) fish fillets.

By applying PCA to NADH spectra, good discrimination between fresh and frozen fish samples was observed. Indeed, according to PC1, accounting for 84.9% of the total variance, negative scores were observed for mostly fresh samples, while positive values were observed for frozen-thawed fish samples (Figure 7.11). The authors confirmed this high level of discrimination by applying FDA to the first five PCs of the PCA performed on the NADH spectra. Indeed, 100% correct classification was obtained for the calibration and validation data sets, respectively. One of the interesting conclusions of this research was that NADH fluorescence spectra may be considered a promising tool for differentiating between fresh and frozen-thawed fish samples.

Egg and egg products

The modern poultry industry is not satisfied with the traditional system of handling and processing eggs, which is based on candling and visual inspection. Currently, the conveyer operator cannot inspect 120 000 eggs per hour and estimate the freshness, weight, bacterial infection, presence of technical spoilage and eggshell defects without elimination of subjectivity, fatigability and destruction. That is why the problem of automation of egg quality control is so difficult. In order to ensure high and consistent egg quality, an attractive and alternative strategy for determining the state of egg freshness can be achieved by sensor technologies. These techniques (such as NIR, MIR, fluorescence spectroscopies, etc.) appear to be very promising for non-destructively determining egg freshness, since they are relatively inexpensive. Such methods cannot eliminate the need for more detailed physicochemical analyses, but they may help to screen for samples that require further examination.

Freshness makes a major contribution to the quality of eggs and egg products. One of the main concerns of the egg industry is the systematic determination of egg freshness, because consumers may perceive variability in freshness as lack of quality. Egg white and egg yolk are extensively utilized as ingredients because of their

unique functional properties, such as gelling and foaming. Foams are used in the food industry in the manufacture of bread, cakes, crackers, ice creams, etc. Hen egg yolk has good emulsifying properties. The foaming and emulsifying properties of albumen and yolk, respectively, are affected by protein concentration, pH and ionic strength. The changes that occur in eggs during storage are many and complex, and affect the functional properties of egg yolk and egg albumen. These changes include thinning of albumen, increase of pH, weakening and stretching of the vitelline membrane, and increase in water content of the yolk. Freshness can be explained to some extent by objective sensory, (bio)chemical, microbial and physical parameters, and can therefore be defined as an objective attribute. Knowledge of the various descriptors of properties that are encountered in eggs immediately after laying must be known, as well as the changes in properties that take place over time. This information can be gained by performing controlled storage experiments that extend from the time after laying; loss in freshness and spoilage can thus be monitored.

Posudin (1998) assessed the potential of FFFS to determine the freshness of eggs by using ultraviolet radiation for the quality evaluation of eggs with differing levels of pigmentation. The emission spectra of different eggs showed two maxima located at 635 and 672 nm after excitation at 405, 510, 540 and 557 nm. These excitation wavelengths have been related to the pigments of porphyrin and porphyrin derivatives of florin and oxoflorin. The obtained results showed that the intensity at 672 nm depends on the egg freshness. Indeed, an eggshell emits vivid red auto-fluorescence by ultraviolet radiation, because of the presence of porphyrin. The auto-fluorescence of a fresh egg is stronger than that of an old one, since the intensity of auto-fluorescence depends on the amount of porphyrin on the shell surface. From these preliminary results, the author concluded that fluorescence spectroscopy could be a promising approach for quantitative estimation of porphyrin in eggs and thus to determine egg freshness. Recently, and for the first time, FFFS was used to monitor egg freshness during storage (Karoui *et al.*, 2006d, 2006e). The authors reported that FMRP (excitation, 360 nm; emission, 380–580 nm) recorded on thick and thin albumens and vitamin A scanned on egg yolk (emission, 410 nm; excitation, 270–350 nm) could be considered as powerful tools for the evaluation of egg freshness stored at room temperature, while tryptophan fluorescence spectra recorded on thick and thin albumens and egg yolk failed to discriminate between fresh and aged eggs.

Using excitation at 360 nm, the emission spectra recorded on fresh thick egg albumen exhibited two maxima located at 410 and 440 nm, respectively (Figure 7.12). Similar results were obtained on thin albumen of fresh eggs. The very characteristic fluorescence spectra of thick and thin albumen of eggs stored for a long time (i.e. 18 days or more) at room temperature showed a shoulder located at 414 nm and a maximum at approximately 438 nm. In addition, as the spectra showed large differences between fresh thin/thick egg albumens and those stored for a long time (29 days), the authors considered the spectra as fingerprints for freshness identification. Indeed, thick and thin albumens of fresh eggs within 2–3 days of laying had the highest intensity at 410 nm, while those of aged eggs had the lowest. The authors concluded that the shape of FMRP is correlated with the storage time: thick albumen of fresh eggs had the lowest ratio of fluorescence intensity F.I.440 nm/F.I.410 nm (e.g. 1.0),

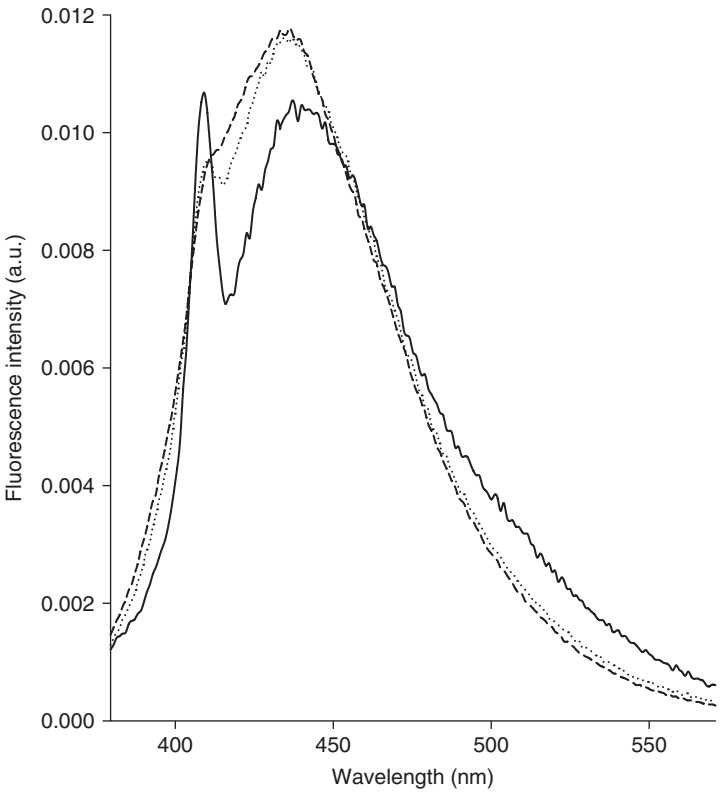

Figure 7.12 Normalized fluorescence spectra of fluorescent Maillard reaction products (FMRP) recorded following excitation at 360 nm on thick albumen of eggs stored at room temperature within 2–3 (—), 16 (...) and 29 (– – –) days after being laid.

while that of eggs stored for 29 days had the highest (i.e. 1.30). The changes in the F.I.440 nm/F.I.410 nm ratio have been ascribed to the change in the viscosity of both thick and thin egg albumens, and the formation of furosine during storage (Birlouez-Aragon *et al.*, 1998; Kulmyrzaev and Dufour, 2002). Indeed, it has been reported that during egg storage, a decrease in the viscosity of thick albumen was observed (Lucisano *et al.*, 1996). This phenomenon has been attributed to the separation of the β-fraction of ovomucin, rich in carbohydrate from the ovomucin–lysozyme complex. However, in the study by Karoui *et al.* (2006d, 2006e) eggs were stored at room temperature, and little attention has been given to the influence of temperature and relative humidity variations on fluorescence measurements, although Stadelman *et al.* (1954) observed a linear decrease of −1.15 Haugh Units per 10°C increase in testing temperature. In addition, only a relative small number of eggs (n = 79) have been investigated and a relative short time (29 days). Therefore, Karoui and coworkers have continued this work by investigating changes at the molecular level of 126 eggs stored at 12.2°C and 87% RH for 1, 6, 8, 12, 15, 20, 22, 26, 29, 33, 40, 47 and 55 days (Karoui *et al.*, 2007c). Of the intrinsic fluorophores tested, only PCA applied to the vitamin A fluorescence spectra allowed a good identification of eggs

as a function of their storage time. By applying FDA to the AAA + NA spectra, correct classification rates of 69.4% and 63.9% were observed for the calibration and validation sets, respectively. Quite similar results were obtained with AAA + NA scanned on egg yolks. The best results were obtained with vitamin A fluorescence spectra, where correct classification rates of 97.7% and 85.7% in the calibration and validation sets were obtained, respectively. The authors concluded that vitamin A fluorescence spectra provide useful fingerprints, mainly allow the identification of eggs during storage at low temperature, and could be considered as a powerful intrinsic probe for the evaluation of egg freshness.

Considering that the storage of eggs under modified atmospheric conditions is important for preserving their desirable quality, Karoui and coworkers have continued this work by testing the ability of vitamin A fluorescence spectra to monitor changes at the molecular level of 225 eggs stored at 12.2°C and 87% RH in an atmosphere containing 2% (n = 108) and 4.6% (n = 99) of CO_2 for 55 days (Karoui *et al.*, 2007d). Again, vitamin A fluorescence spectra allowed good discrimination of eggs according to both storage time and conditions, while more overlapping between egg samples was observed when the other intrinsic probes were investigated. The similarity map defined by the principal components 1 (PC1) and 3 (PC3) of eggs held in an atmosphere containing 2% of CO_2 is shown in Figure 7.13. According to PC1, accounting for 90.5% of the total variance, eggs aged 22 days or less presented

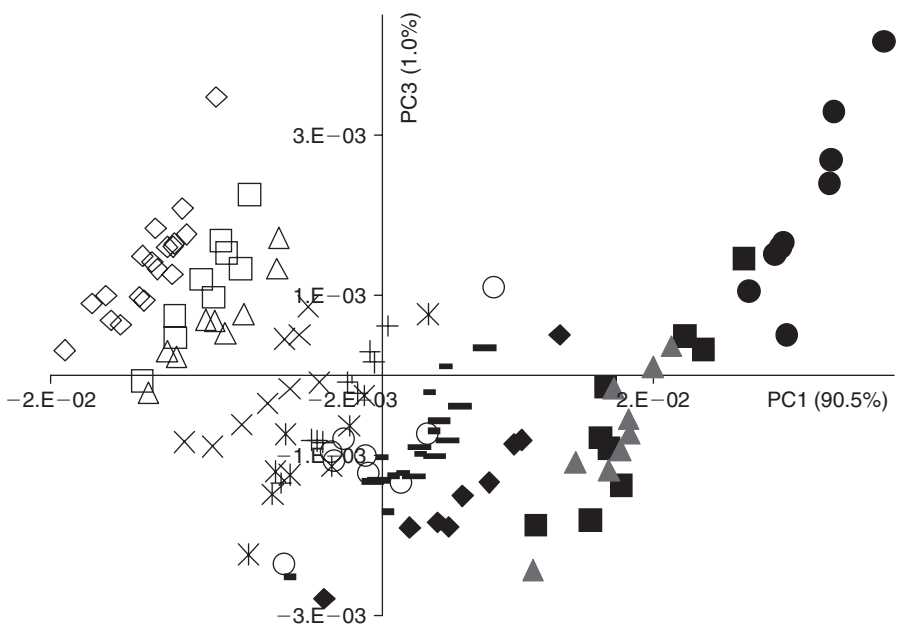

Figure 7.13 Principal component analysis similarity map determined by principal components 1 (PC1) and 3 (PC3) for vitamin A fluorescence spectra of yolk of eggs held at 12.2°C and 87% relative humidity in an atmosphere containing 2% of CO_2 for 1 (◇), 6 (□), 8 (Δ), 12 (×), 15 (✳), 20 (○), 22 (+), 26 (-), 29 (−), 33 (◆), 40 (■), 47 (▲) and 55 (●) days after being laid. Eggs aged 1 day were gathered from the farm and analyzed immediately upon arrival at the laboratory.

negative score values while those of 26 days or more had positive scores. In addition, the eggs were well separated for each storage time, except for those samples aged 20 and 22 days and those aged 26 and 29 days, where some overlapping was observed. The authors concluded that vitamin A fluorescence spectra could be considered a good indicator of egg freshness.

Edible oils

Olive oil is an economically important product of the Mediterranean countries. It has a fine aroma and pleasant taste, with excellent health benefits. The quality of olive oil ranges from the high-quality extra-virgin olive oil (EVOO) to the low-quality olive-pomace oil. EVOO is obtained from the fruit of the olive tree by mechanical pressing and without refining processes. Its acidity cannot be greater than 1%. Owing to its high quality, it is the most expensive type of olive oil. For this reason, it may be mislabeled or adulterated for economic reasons. Mislabeling often involves false information regarding the geographic origin or oil variety (Aparicio *et al.*, 1997). Adulteration involves the addition of cheaper oils; the most common adulterants found in virgin olive oil are refined olive oil, residue oil, synthetic olive oil–glycerol products, seed oils (such as sunflower, soy, maize and rapeseed) and nut oils (such as hazelnut and peanut oil) (Baeten *et al.*, 1996; Downey *et al.*, 2002; Sayago *et al.*, 2004). Owing to the low price of olive-pomace oil, it is sometimes used to adulterate EVOO. For this reason, a rapid method to detect such a practice is important for quality control and labeling purposes.

Several techniques can be used to detect olive oil adulteration, including colorimetric reactions, and determination of the iodine value, saponification value, density, viscosity, refractive index and ultraviolet absorbance (Gracian, 1968). However, these methods may be time-consuming, and require sample manipulation. To overcome these handicaps, other techniques have been applied. The most noteworthy are spectroscopic techniques such as NIR, MIR, nuclear magnetic resonance (NMR) and fluorescence spectroscopy.

Zandomeneghi *et al.* (2005) recorded the fluorescence spectra of EVOO using right angle and FFFS. The former method showed considerable artefacts and deformation, while the latter provided spectra that are much less affected by self-absorption. The authors attributed this to the self-absorption phenomena when using right-angle fluorescence, even when the spectra are corrected for inner filter effects. In another study, Sayago *et al.* (2004) applied fluorescence spectroscopy for detecting hazelnut oil adulteration in virgin olive oils. Virgin olive, virgin hazelnut and refined hazelnut oil samples and a mixture of them at 5, 10, 15, 20, 25 and 30% adulteration were analyzed after excitation at 350 nm. By performing linear discriminant analysis (LDA), 100% correct classification was achieved. In a similar approach, Kyriakidis and Skarkalis (2000) used an excitation wavelength of 360 nm to differentiate between common vegetable oils, including olive oil, olive residual oil, refined olive oil, corn oil, soybean oil, sunflower oil and cotton oil. All the oils studied showed a strong fluorescence band at 430–450 nm, except for virgin olive oil, which exhibited a low intensity at both 440 and 455 nm, a medium band around 681 nm and a strong band at 525 nm.

The latter two bands have been ascribed to chlorophyll and vitamin E compounds, respectively. The very low intensity of the peaks at 445 and 475 nm is due to the high content of phenolic antioxidants, which provide more stability against oxidation. All refined oils showed only one intense peak at 445 nm, which is due to fatty acid oxidation products formed as a result of the large percentage of polyunsaturated fatty acids present in these oils.

In recent years, instrumental improvements and the availability of software specially designed to extract the information contained in spectra have contributed to the development of fluorescence spectroscopy. Hence, it is possible to record one fluorescence excitation–emission matrix for each sample – i.e. a set of emission spectra recorded at several excitation wavelengths. Sikorska *et al.* (2004a, 2005) used synchronous fluorescence spectroscopy with excitation wavelengths from 250 to 450 nm and emission spectra in the range 290 to 700 nm. The peak located at 320 nm after excitation at 290 nm has been attributed to tocopherols, while the band located at 670 nm in emission and 405 nm in excitation belongs to pigments of the chlorophyll group. In order to compare the set of synchronous fluorescence spectra of different oils Sikorska *et al.* (2005) applied the k-nearest neighbors (k-NN) method, and good discrimination between oil samples with a very low classification error ranging between 1 and 2% and a low standard deviation value was obtained.

In a different approach, Guimet *et al.* (2004) applied PARAFAC and unfold PCA in order to assess the potential of FFFS to discriminate between virgin and pure olive oils; the ranges studied were at excitation wavelength (λ_{ex}) 300–400 nm, emission wavelength (λ_{em}) 400–695 nm, and λ_{ex} = 300–400 nm, λ_{em} 400–600 nm. The first range was found to contain chlorophylls, whereas the second range contained only the fluorescence spectra of the remaining compounds (oxidation products and vitamin E). In 2005, Guimet and coworkers applied PARAFAC to detect the adulteration of EVOO with olive-pomace oil at low levels (5%). Discrimination between the two types of oils was achieved by applying both LDA and discriminant multi-way PLS regression; the latter gave 100% correct classification.

In another study, Poulli *et al.* (2005) used synchronous fluorescence to analyze 73 samples, including 41 edible and 32 lampante virgin olive oils, collected in October and November 2002. Emission spectra in the range 350–720 nm at excitation wavelengths varying from 320 to 535 nm were recorded. By applying PCA and hierarchical cluster analysis, good classification separating the two types of oils was obtained. Recently, the same research group assessed the potential of total synchronous fluorescence spectra to detect adulteration of VOO (virgin olive oil) with other oils (Poulli *et al.*, 2007). By applying PLS regression to the excitation spectra recorded in the 250–720 nm with a wavelength interval of 20 nm, the authors found that FFFS is useful for detection of olive-pomace, corn, sunflower, soybean, rapeseed and walnut oils in VOO at levels of 2.6%, 3.8%, 4.3%, 4.2%, 3.6% and 13.8%, respectively.

The potential of fluorescence spectroscopy to monitor frying oil deterioration has also been demonstrated by using five selected excitation wavelengths varying from 395 nm to 530 nm (Engelsen, 1997). By applying PLS regression, the author showed good correlation between fluorescence spectra and quality parameters describing the deterioration (e.g. anisidine value, iodine value, oligomers and vitamin E).

Cereals and cereal products

The potential of fluorescence spectroscopy for monitoring cereals has increased over the past few years with the propagated application of chemometric tools and with technical and optical developments of the spectrofluorometer. Zandomeneghi (1999) used FFFS (excitation, 275 nm; emission, 280–575 nm) to differentiate between different cereal flours (rice, creso, maize, pandas). The same research group also utilized visible excitation set at 445 nm (emission, 460–600 nm) to differentiate between flours of five different wheat varieties, and good discrimination was observed. In another study, excitation wavelengths set at 275, 350 and 450 nm presenting fluorescence emission maxima at 335, 420 and 520 nm, respectively, were utilized to classify botanical tissue components of complex wheat flour and rye flour; the bands were attributed to AAA, ferulic acid and riboflavin components, respectively. The last fluorescent component was confirmed by Zandomeneghi and coworkers (2003), who attributed the band observed at 520 nm to riboflavin, where a standard solution at different concentration was used, while the band between 430 and 530 nm was found to be proportional to the lutein content of the flour (Zandomeneghi *et al.*, 2000).

Ferulic acid and riboflavin spectra have been reported to have good accuracy when monitoring wheat flour refinement and milling efficiency by using fluorescence imaging, and successful classification was obtained, suggesting that FFFS may be used to classify wheat cultivars (Symons and Dexter, 1991, 1992, 1993, 1996). These results have recently been confirmed by Karoui *et al.* (2006f). In our study, tryptophan fluorescence spectra of 59 samples (20 complete Kamut®, semi-complete Kamut® and soft wheat flours, 28 pasta and 11 semolinas manufactured from complete Kamut®, semi-complete Kamut® and hard wheat flours) were scanned after excitation at 290 nm. PCA performed on the flours' spectra clearly differentiated complete Kamut® and semi-complete Kamut® samples from those produced from complete and semi-complete soft wheat flours, while good discrimination of pasta samples manufactured from complete Kamut® and complete hard wheat flours from those made with semi-complete Kamut® and semi-complete hard wheat flours was achieved. The best discrimination was obtained from tryptophan spectra recorded on semolinas, since the four groups were well discriminated. Indeed, by applying FDA to the spectral collection, 86.7% and 87.9% correct classification rates were obtained for the calibration and validation samples, respectively. In a similar approach, Ram *et al.* (2004) assessed the potential of FFFS to differentiate between red and white wheat kernels. Emission spectra (370–570 nm) were recorded after excitation at 350 nm, and a clear difference was observed between the two group samples; this difference has been attributed to the morphological variation in the pericarp, and nuclear organization of the two varieties of wheat. The authors concluded that FFFS has the potential to be a rapid, low-cost and efficient method for the authentication of cereal products.

Beer and wine

Beer is a complex mixture consisting mainly of water and ethanol with about 0.5% dissolved solids. Therefore, beer analysis is important for evaluation of organoleptic

characteristics, quality, nutritional aspects and safety. Apperson *et al.* (2002) reported that fluorescence spectra of beer arise from different components such as amino acids, polyphenols and iso-α-acids. Indeed, fluorescence spectra recorded on 21 dark and light beer samples exhibited two peaks with excitation/emission maxima located at 290/340 nm and 340/430 nm (Christensen *et al.*, 2005). The first peak was attributed to protein and the latter to the complex polyphenol and iso-α-acids. By comparing spectra recorded on light beer presenting three different levels of bitterness (8.8, 16.1 and 28.5 International Bitter Units (IBU)), beer samples presenting the highest level of bitter did not differ significantly from the other two, suggesting that bitter acids are not the main contributors to the fluorescence signals. PLS regression was subsequently applied to the fluorescence spectra in order to assess the potential of this technique to determine the color and bitterness in terms of IBU. The best results were obtained by using three excitation wavelengths, set at 260, 270 and 290 nm, since a lower root mean square error of cross-validation (RMSECV) of 2.77 IBU than with the full spectrum (3.56) was observed.

In another study, Sikorska *et al.* (2004b) used fluorescence to characterize intrinsic probes of eight different Polish beers. Three-dimensional spectra were obtained by measuring the emission spectra in the range from 290 to 700 nm at excitation wavelengths ranging from 250 to 500 nm. Fluorescence spectra showed a relatively intense band with excitation at about 250 nm and emission at 350 nm, another with excitation at 350 nm and emission at 420 nm, and a final one, presenting the least intense emission band, with excitation at 450 nm and emission at 520 nm. These peaks were ascribed to aromatic amino acids, NADH, vitamins B2, B6 and B12, and this was confirmed later by the same research group (Sikorska *et al.*, 2006; Sikorska, 2007). By applying PLS regression to the spectra recorded after excitation set at 450 nm and the riboflavin content determined by reference techniques, good correlation was observed as an R of 0.97 was found. The obtained results confirmed that FFFS could be used to quantify vitamin B_2 in beer. However, owing to the low number of samples, more research is necessary before claiming the potential of this technique, and it would be interesting to correlate the spectral characteristic of beers to known beer classifications, as well as specific beer properties to the ability of FFFS to quantify AAA + NA.

Recently, the phenolic content of grape berries has been considered to be an important parameter for wine quality, as it is responsible for the color, flavor and structure of wine. Phenolic compounds, and anthocyanins in red grape varieties, are usually evaluated spectrophotometrically on solvent extracts of grape berries. The method is time-consuming, and may produce certain artefacts due to pigment instability and loss of material. Furthermore, the composition and evolution of berry phenolics with ripening depend on grape variety, viticultural practices and environmental factors. Therefore, anthocyanins have been chosen as markers of phenolic maturation because their evolution with ripening is equivalent to that of skin tannins. Agati *et al.* (2007) used FFFS to differentiate between two grape varieties at two different times. Excitation spectra were recorded in the 280–650 nm range for emission set at 685 nm, whereas emission spectra were scanned between 630 and 800 nm with excitation at 436 nm. The excitation spectra showed two maxima located at 440 and 480 nm,

corresponding to the principal absorption peaks of chlorophylls *a* and *b* and of carotenoids. A reduction of chlorophyll fluorescence intensity with increasing maturity of the berry was noted. Thus, phenolic maturity in vineyards can be determined by using a suitable portable device based on fluorescence spectroscopy. In another study, Dufour *et al.* (2006) assessed the potential of FFFS to discriminate 120 wine samples produced in France and Germany. Emission (275–450 nm) and excitation (250–350 nm) spectra were recorded directly on the wine samples. The emission spectra were characterized by a maximum at 376 nm and a shoulder at 315 nm, while the excitation spectra showed two peaks located at about 260 and 320 nm. By performing PCA on the collection of excitation spectra, good discrimination between French and German wines was observed. Correct classification of typical and non-typical Beaujolais amounting to 95% was observed for the emission fluorescence data set. The authors concluded that FFFS may provide useful fingerprints and allow the identification of wines according to variety and typicality.

Sugar

In combination with multivariate statistical analyses, fluorescence spectroscopy has proved to be a promising screening method for predicting quality parameters in beet-sugar samples (Munck *et al.*, 1998). Indeed, it has been shown that commercial sugars exhibit characteristic fluorescence, which can be used to obtain information regarding minor constituents in the sugar. Spectrofluorometry has successfully been applied to the beet-sugar manufacturing process with the use of multivariate data analysis (Munck *et al.*, 1998). The same approach with multiple excitation and emission wavelengths used by Carpenter and Wall (1972) has also been employed, but chemometric evaluation of the excitation–emission landscapes is used to extract the relevant information from the data. In a study of beet-sugar samples, it was possible to classify white-sugar samples according to factory and to predict quality parameters such as amino nitrogen, color and ash from the fluorescence data of these samples (Nørgaard, 1995). The fluorescence data of thick juice samples showed more ambiguous results owing to the more complex sample composition. Another study of beet-sugar samples utilized the three-dimensional structure of the fluorescence excitation–emission landscapes to resolve spectral excitation and emission profiles of fluorophores in sugar with a multi-way chemometric model, PARAFAC (Bro, 1999). Four fluorescent components were found to capture the variation in the fluorescence data of 268 sugar samples collected from a beet-sugar factory in a single campaign, and two of them showed spectra with a close similarity to the pure fluorescence spectra of the amino acids tyrosine and tryptophan. The concentrations of the four components estimated from the sugar samples could be correlated with several quality and process parameters, and they were characterized as potential indicator substances of the chemistry in the sugar process, which has been confirmed by the use of HPLC analysis combined with fluorescence detection on thick juice samples and evaluation by PARAFAC (Baunsgaard *et al.*, 2000a). Seven fluorophores were resolved from thick juice. Apart from tyrosine and tryptophan, four of the fluorophores were identified as high molecular weight compounds, which were related to colorants absorbing at 420 nm. Three of the high

molecular weight compounds were found to be possible Maillard reaction polymers. The last of the seven fluorophores indicated a compound with polyphenolic characteristics. In a fluorescence study of 47 raw cane sugars which were collected from many different locations and campaign years, three individual fluorophores were found; one of them, representing maximum excitation and emission at 275 and 350 nm, respectively, is characterized as an ultraviolet color precursor that participates in color development during storage. The other two (340, 420 nm and 390, 460 nm excitation /emission in the visible wavelength area), are considered to be potential colorants, which shows a link with their fluorescence behavior (Baunsgaard *et al.*, 2000b).

Recently, FFFS has been used to monitor adulteration of honey with cane-sugar syrup (Ghosh *et al.*, 2005). Five honey samples extracted from *Apis florae* hives and ten commercial cane-sugar samples were investigated. Using an excitation wavelength of 340 nm, pure honey samples were characterized by two prominent features – a shoulder located at around 440 nm and a maximum located at 510 nm, which has been ascribed to flavins – while cane-sugar syrup samples exhibited a maximum located around 430 nm. The peaks located at 440 and 430 nm in pure honey and sugar syrup samples have been attributed to NADH. Synchronous fluorescence was then applied to differentiate between pure honey and sugar syrup samples, and good discrimination between the two groups was observed. The spectra for cane-sugar syrup were characterized by a shoulder around 305 nm and a prominent band around 365 nm, while honey samples had a strong peak around 460 nm and a much weaker peak around 365 nm. The authors observed an increase in intensity at 365 and 425 nm, as well as the ratio of fluorescence intensity (FI), FI_{365}/FI_{425}, with the increase of cane-sugar syrup concentration; thus the ratio of the intensity of synchronous fluorescence of spectra at 365 nm to that of 425 nm has been suggested as a potential method to monitor the adulteration of honey with cane sugar syrup. In another study, FFFS was also used to determine the botanical origin of honeys (Ruoff *et al.*, 2005; Karoui *et al.*, 2007e). Fluorescence spectra were scanned on 62 honey samples belonging to seven floral origins after excitation at 250 nm (emission, 280–480 nm), 290 nm (emission, 305–500 nm) and 373 nm (emission, 380–600 nm), and emission set at 450 nm (excitation, 290–440 nm). By applying FDA to the four data sets (concatenation), correct classification rates of 100% and 90% were observed for the calibration and validation samples, respectively. In addition the seven honey types were well discriminated, indicating that the molecular environments, and thus the physicochemical properties, of the investigated honeys were different. One of the main findings of this study is that FFFS might be a suitable and alternative technique to classify honey samples according to their botanical origins; this was confirmed recently by Ruoff *et al.* (2006), who studied 371 honey samples originating from Switzerland, Germany, Italy, Spain, France, Slovenia and Denmark. By using chemometric tools, the error rates of the discriminant models ranged from 0.1% to 7.5%.

Fruit and vegetables

Chlorophyll fluorescence has been used as an intrinsic probe to determine the physiological status of whole plants and plant organs (Song *et al.*, 1997). This component

has been considered an efficient probe for monitoring apples during maturation, ripening and senescence (Song *et al.*, 1997). Recently, fluorescence spectroscopy has been considered to have the potential to assess the mealiness of apples (Moshou *et al*; 2005), since relatively good correlation was obtained between mealiness and fluorescence spectra. Other authors have used the chlorophyll fluorescence of apples as a potential predictor of superficial scald development during storage (DeEll *et al.*, 1996), and for the estimation of anthocyanins and total flavonoids in apples (Hagen *et al.*, 2006). In another study, Lötze *et al.* (2006) used fluorescence imaging as a non-destructive method for the pre-harvest detection of bitter pit in apples; the same technique had already been utilized to determine apple quality (Seiden *et al.*, 1996; Noh and Lu, 2007). Two excitation wavelengths, set at 265 and 315 nm, were chosen, as they yielded the richest spectra of two juice-apple varieties (Jonagold and Elstar). The spectra showed two excitation–emission maxima (315/440 and 265/350 nm) that have not been attributed to any component in apple juice (Seiden *et al.*, 1996). Applying PCA to the two juice-apple varieties, good discrimination was observed – which was not achieved with titrable acidity or soluble solids data. The authors pointed out that an increase in the ripening process of apples involves an increase in the soluble fluorescent compounds. Good correlation between soluble solids and fluorescence spectra was observed independently of the apple varieties, indicating the possibility of modeling the progression in maturity with information obtained from spectra, while fluorescence was found to correlate poorly to the amount of titrable acids in juice.

Identification of bacteria of agro-alimentary interest

The identification of microorganisms of agro-alimentary interest in food and food products by conventional phenotypic procedures based on morphology and biochemical tests involves a large quantity of reagents, and in some cases is unable to discriminate microorganisms at the strain level. In this context, Leblanc and Dufour (2002) assessed the potential of different intrinsic probes (i.e. tryptophan, AAA + NA, and NADH) to discriminate between 25 strains of bacteria in dilute suspensions. The best results were obtained by using AAA + NA spectra, where correct classification rates of 100% and 81% were observed for the calibration and validation samples, respectively. The authors noted that fluorescence spectroscopy is able to discriminate and identify bacteria at genus, species and strain levels. They concluded that the fluorescence technique could also have application in the field of monitoring bacterial growth. This assumption was later demonstrated by the same research group (Leblanc and Dufour, 2004). In their studies, the spectra of three bacteria strains (*L. lactis, S. carnosus* and *E. coli*) were recorded at different growth phases. By applying PCA to the spectra scanned on each bacteria, three groups corresponding to three main phases of growth were identified (lag phase, exponential phase and stationary phase). The authors then gathered the spectra recorded on the three bacteria into one matrix, and this new matrix was analyzed by PCA. The obtained results showed good discrimination of spectra according to bacteria and metabolic profile.

Recently, Dufour and coworkers utilized the same technique for the identification of lactic acid bacteria isolated from a small-scale facility producing traditional dry

sausages (Ammor *et al.*, 2004). Again, fluorescence spectroscopy demonstrated its ability to discriminate between *Lactobacillus sakei* subsp. *carnosus* and *Lactobacillus sakei* subsp. *sakei*. In another approach, Leriche *et al.* (2004) isolated 30 *Pseudomonas* spp. strains from milk, water, cheese center and cheese surface from two traditional workshops manufacturing raw-milk Saint Nectaire cheese. By applying FDA to the two data sets, clear linkages between groups of isolates were noted. In the first workshop, the milk was implicated being as the sole source of cheese contamination, whereas in the second workshop the milk and cheese-center isolates were found to be similar, but different from surface-cheese isolates. The authors attributed this contamination at the cheese surface to the water used during the ripening process (washing of the cheese surface). From the results obtained, it was stated that it is possible to characterize, differentiate and trace *Pseudomonas* spp. strains using the fluorescence technique. These findings were reinforced by the high correlation (using CCA) observed between the data sets obtained from the metabolic profiling and fluorescence spectroscopy.

Regarding this field, Kunnil *et al.* (2005, 2006) used different excitation wavelengths (280, 310, 340, 370 and 400 nm) for the identification of three different *Bacillus* spores mixed with one of the three different samples of domestic dust. By applying PCA, fluorescence spectroscopy showed a strong promise in correctly identifying bacterial spores. Moreover, the authors succeeded in correctly clustering together different samples of *Bacillus* spores before and after the spores had been washed and redried.

Advantages and disadvantages of fluorescence spectroscopy

Advantages

Fluorescence spectroscopy is a relevant analytical technique because of its extreme sensitivity and excellent specificity. Indeed, spectrofluorometric methods can detect concentrations of component as low as one part in 10^{10}, with a sensitivity 1000 times greater than that of most spectrophotometric methods. The main reason for this increased sensitivity could be explained by the fact that in fluorescence the emitted radiation can be increased or decreased by changing the intensity of the exciting radiant energy.

Regarding the specificity of fluorescence, it can be explained by two factors; the first is that fewer fluorescent compounds exist compared with absorbing ones, since all fluorescent compounds must absorb radiation but not all compounds that absorb radiation emit; the second is that two wavelengths are used in fluoremetry, whereas only one is used in spectrophotometry. In addition, two substances that absorb radiation at the same wavelength will probably not emit at the same wavelength. The difference between excitation and emission peaks ranges from few to several wavelengths. It is worth noting that the emission spectrum is highly dependent on the excitation wavelength; both excitation and emission spectra can be obtained. Thus,

the advantages of fluorescence spectroscopy are the absence of interference, and that higher-order data can be obtained from it.

Disadvantages

The most severe disadvantage of fluorescence spectroscopy is the strong dependence of light scatter, and there are no means for making mathematical corrections, because no information regarding the amount of scatter is contained in the spectrum. Another disadvantage is its dependence on environmental factors such as temperature, pH, ionic strength, viscosity, temperature, etc., which have to be defined and controlled during analyses in order to obtain reproducible measurements.

The ultraviolet radiation used for excitation may cause photochemical changes and/or destruction of the fluorescent compound, which will induce a decrease in the fluorescence intensity. For this reason, precautions should be taken by (i) using the longest-wavelength radiation, (ii) scanning the excitation and emission spectra immediately after fixing the emission or the excitation wavelength, (iii) not allowing the radiation to strike the sample for a long time, and (iv) protecting photochemically unstable solutions (such as quinine sulfate) from sunlight and ultraviolet laboratory light by storing them in black bottles.

Another disadvantage of the method is the quenching phenomenon, which is the reduction of fluorescence by a competing deactivating process resulting from the interaction between a fluorophore and other substances present in the system. The general mechanism of quenching can be denoted as follows:

$$
\begin{aligned}
M + h\nu &\longrightarrow M^* \text{ (Light absorption)} \\
M^* &\longrightarrow M + h\nu \text{ (Fluorescence emission)} \\
M^* + Q &\longrightarrow Q^* + M \text{ (Quenching)} \\
Q^* &\longrightarrow Q + \text{energy}
\end{aligned}
$$

Oxygen is one of the most notorious quenchers. Other common quenching is observed in luminescence processes, such as impurity quenching, temperature and concentration. Indeed, as the temperature increases, the fluorescence intensity decreases. Tryptophan, quinine and indoleacetic are among the compounds whose fluorescence varies greatly with temperature.

Conclusions

As illustrated in this chapter, intrinsic fluorophores recorded on intact food systems contain valuable information regarding the composition and nutritional values of food products. The huge potential for the application of fluorescence spectroscopy combined with multivariate statistical analyses for the evaluation of food quality has also been demonstrated. The method is suitable as an effective research tool, and can be a part of evaluation procedure for food quality. While chemical and physical

parameters may be good indicators of food quality, their assessment is less certain, and requires much more precise accumulated knowledge of the biochemistry of food products; fluorescence spectroscopy is a powerful and sensitive means of rapid food quality control. Therefore, the success of the presented method strongly suggests the application of this technique on-line in the food industry.

References

Agati, G., Meyer, S., Matteini, P. and Cerovic, Z.G. (2007). Assessment of anthocyanins in grape (*Vitis vinifera* L.) berries using a noninvasive chlorophyll fluorescence method. *Journal of Agricultural and Food Chemistry*, **55**, 1053–1061.

Allais, I., Viaud, C., Pierre, A. and Dufour, E. (2004). A rapid method based on front-face fluorescence spectroscopy for the monitoring of the texture of meat emulsions and frankfurters. *Meat Science*, **67**, 219–229.

Ammor, S., Yaakoubi, K., Chevallier, I. and Dufour, E. (2004). Identification by fluorescence spectroscopy of lactic acid bacteria isolated from a small-scale facility producing traditional dry sausages. *Journal of Microbiological Methods*, **59**, 271–281.

Aparicio, R., Morales, M.T. and Alonso, V. (1997). Authentication of European virgin olive oils by their chemical compounds, sensory attributes, and consumers' attitudes. *Journal of Agricultural and Food Chemistry*, **111**, 3–10.

Apperson, K., Leiper, K.A., McKeown, I.P. and Birch, D.J.S. (2002). Beer fluorescence and the isolation, characterisation and silia adsorption of haze-active beer protein. *Journal of the Institute of the Brewing*, **110**, 267–275.

Aubourg, S.P., Sotelo, C.G. and Pérez-Martín, R. (1998). Assessment of quality changes in frozen sardine (sardine pilchardus) by fluorescence detection. *Journal of the American Oil Chemists' Society*, **75**, 575–580.

Baeten, V., Meurens, M.T., Morales, R. and Aparicio, R. (1996). Detection of virgin olive oil adulteration by Fourier transform Raman spectroscopy. *Journal of Agricultural and Food Chemistry*, **44**, 2225–2230.

Baunsgaard, D., Andersson, C.A., Arndal, A. and Munck, L. (2000a). Multiway chemometrics for mathematical separation of fluorescent colorants and colour precursors from spectrofluorometry of beet sugar and beet sugar thick juice as validated by HPLC analysis. *Food Chemistry*, **70**, 113–121.

Baunsgaard, D., Nørgaard, L. and Godshall, M. (2000b). Fluorescence of raw cane sugars evaluated by chemometrics. *Journal of Agricultural and Food Chemistry*, **48**, 4955–4962.

Bennett, R. and Hamilton, M. (1986). Consumer acceptability of cod and whiting after chilled storage and freezing and thawing. *Journal of Food Technology*, **21**, 311–317.

Birlouez-Aragon, I., Nicolas, M., Metais, A. *et al*. (1998). A rapid fluorimetric method to estimate the heat treatment of liquid milk. *International Dairy Journal*, **8**, 771–777.

Bosset, J.O., Sieber, R. and Gallman, P.U. (1994). In: M. Mathlouthi (ed.), *Food Packaging and Preservation*. Glasgow: Blackie Academic and Professional, pp. 222–268.

Bosset, J.O., Jeangros, B., Berger, Th. *et al*. (1999). Comparison de fromages à pâte dure de type Gruyère produits en région de montagne et de plaine. *Revue Suisse d'Agriculture*, **31**, 17–22.

Bro, R. (1999). Exploratory study of sugar production using fluorescence spectroscopy and multi-way analysis. *Chemometrics and Intelligent Laboratory Systems*, **46**, 133–147.

Carpenter, F.G. and Wall, J.H. (1972). Fluorescence in commercial sugar. In: F.G. Carpenter and J.H. Wall (eds), *Proceedings of the 1972 Technical Session on Cane Sugar Refining Research*. New Orleans, LA: USDA-ARS, pp. 47–61.

Christensen, J., Ladefoged, A.M. and Nøgaard, L. (2005). Rapid determination of bitterness in beer using fluorescence spectroscopy and chemometrics. *Journal of the Institute of Brewing*, **111**, 3–10.

Christensen, J., Nøgaard, L., Bro, R. and Engelsen, S.B. (2006). Multivariate autofluorescence of intact food systems. *Chemical Reviews*, **106**, 1979–1994.

Coulon, J.B. and Priolo, A. (2002). La qualité sensorielle des produits laitiers et de la viande dépend des fourrages consommés par les animaux. *INRA Production Animales*, **15**, 333–342.

DeEll, J.R., Prange, R.K. and Murr, D.P. (1996). Chlorophyll fluorescence of Delicious apples at harvest as a potential predictor of superficial scald development during storage. *Postharvest Biology and Technology*, **9**, 1–6.

Downey, G., McIntyre, P. and Davies, A.N. (2002). Detecting and quantifying sunflower oil adulteration in extra virgin olive oils from the eastern Mediterranean by visible and near-infrared spectroscopy. *Journal of Agricultural and Food Chemistry*, **50**, 5520–5525.

Dufour, E. and Frencia, J.P. (2001). Les spectres de fluorescence frontale : une empreinte digitale de la viande. *Viandes et Produits Carnés*, **22**, 9–14.

Dufour, E. and Riaublanc, A. (1997). Potentiality of spectroscopic methods for the characterisation of dairy products, I – Front-face fluorescence study of raw, heated and homogenised milks. *Le Lait*, **77**, 657–670.

Dufour, E., Genot, C. and Haertlé, T. (1994). β-Lactoglobulin binding properties during its folding changes studied by fluorescence spectroscopy. *Biochemical and Biophysical Acta*, **1205**, 105–112.

Dufour, E., Mazerolles, G., Devaux, M.F. *et al*. (2000). Phase transition of triglycerides during semi-hard cheese ripening. *International Dairy Journal*, **10**, 87–99.

Dufour, E., Frencia, J.P. and Kane, E. (2003). Development of a rapid method based on front-face fluorescence spectroscopy for the monitoring of fish freshness. *Food Research International*, **36**, 415–423.

Dufour, E., Letort, A., Laguet, A. *et al*. (2006). Investigation of variety, typicality and vintage of French and German wines using front-face fluorescence spectroscopy. *Analytica Chimica Acta*, **563**, 292–299.

Egelandsdal, B., Kvaal, K. and Isaksson, T. (1996). Autofluorescence spectra as related to tensile properties for perimysium from bovine masseter. *Journal of Food Science*, **61**, 342–347.

Egelandsdal, B., Wold, J.P., Sponnich, A. *et al*. (2002). On attempts to measure the tenderness of *longissimus dorsi* muscles using fluorescence emission spectra. *Meat Science*, **60**, 187–202.

Egelandsdal, B., Dingstad, G., Tøgersen, G. *et al*. (2005). Autofluorescence quantifies collagen in sausage batters with a large variation in myoglobin content. *Meat Science*, **69**, 35–46.

Engelsen, S.A. (1997). Explorative spectrometric evaluations of frying oil deterioration. *Journal of the American Oil Chemistry Society*, **74**, 1495–1508.

Feinberg, M., Dupont, D., Efstathiou, T. *et al*. (2006). Evaluation of tracers for the authentification of thermal treatments of milks. *Food Chemistry*, **98**, 188–194.

Fernandez, M., Mano, S., Garcia de Fernando, G.D. *et al*. (1999). Use of β-hydroxyacyl-CoA-dehydrogenase (HADH) activity to differentiate frozen from unfrozen fish and shellfish. *European Food Research and Technology*, **209**, 205–208.

Frencia, J.P., Thomas, E. and Dufour, E. (2003). Measure of meat tenderness using front-face fluorescence spectroscopy. *Science des Aliments*, **23**, 142–145.

Garcia de Fernando, G.D., Fernandez, M., Diaz, O. *et al*. (1992). An objective method to differentiate between fresh and thawed trout meat (*Salmo gairdneri*). *Archiv fur Lebensmittelhygiene*, **43**, 13–14.

Gardner, H.W. (1979). Lipid hydroperoxide reactivity with proteins and amino acids: a review. *Journal of Agricultural and Food Chemistry*, **27**, 220–229.

Gatellier, P., Gomez, S., Gigaud, V. *et al*. (2007). Use of fluorescence front face technique for measurement of lipid oxidation during refrigerated storage of chicken meat. *Meat Science*, **76**, 543–547.

Genot, C., Tonetti, F., Montenay-Garestier, T. *et al*. (1992). Front-face fluorescence applied to structural studies of proteins and lipid-protein interactions of visco-elastic food products. 1 – Designation of front-face adaptor and validity of front-face fluorescence measurements. *Sciences des Aliments*, **12**, 199–212.

Ghosh, N., Verma, Y., Majudmer, S.K. and Gupta, P.K. (2005). A fluorescence spectroscopic study of honey and cane sugar syrup. *Food Science and Technology Research*, **11**, 59–62.

Gottesmann, P. and Hamm, R. (1983). New biochemical methods of differentiating between fresh meat and thawed, frozen meat. *Fleischwirtschaft*, **63**, 219–220.

Gracian, J. (ed.) (1968). *Analysis and Characterization of Oils, Fats and Fat Products*, Vol. 2. London: Wiley.

Guilbaut, G.G. (1989). Principles of fluorescence spectroscopy in the assay of food products. In: L. Munck and A. Francisco (eds), *Fluorescence Analysis in Foods*. Copenhagen: Longman Group, pp. 33–58.

Guimet, F., Ferré, J., Boqué, R. and Rius, F.X. (2004). Application of unfold principal component analysis and parallel factor analysis to the exploratory analysis of olive oils by means of excitation–emission matrix fluorescence spectroscopy. *Analytica Chimica Acta*, **515**, 75–85.

Guimet, F., Ferré, J. and Boqué, R. (2005). Rapid detection of olive-pomace oil adulteration in extra virgin olive oils from the protected denomination of origin "Siurana" using excitation–emission fluorescence spectroscopy and three-way methods for analysis. *Analytica Chimica Acta*, **544**, 143–152.

Hagen, S.F., Solhaug, K.A., Bengtsson, G.B. *et al*. (2006). Chlorophyll fluorescence as a tool for non-destructive estimation of anthocyanins and total flavonoids in apples. *Postharvest Biology and Technology*, **41**, 156–163.

Hasegawa, K., Endo, Y. and Fujimoto, K. (1992). Oxidative deterioration in dried fish model systems assessed by solid sample fluorescence spectrophotometry. *Journal of Food Science*, **57**, 1123–1126.

Herbert, S. (1999). Caractérisation de la structure moléculaire et microscopique de fromages à pâte molle. Analyse multivariée des données structurales en relation avec la texture. PhD Thesis, École Doctorale Chimie Biologie de l'Université de Nantes, Nantes, France.

Herbert, S., Riaublanc, A., Bouchet, B. *et al*. (1999). Fluorescence spectroscopy investigations of acid- and rennet-induced milk coagulation of milk. *Journal of Dairy Science*, **82**, 2056–2062.

Herbert, S., Mouhous Riou, N., Devaux, M.F. *et al*. (2000). Monitoring the identity and the structure of soft cheeses by fluorescence spectroscopy. *Le Lait*, **80**, 621–634.

Hildrum, K.I., Wold, J.P., Segtnan, V.H. *et al*. (2006). New spectroscopic techniques for online monitoring of meat quality. In: L.M.L. Nollet and F. Toldra (eds), *Advanced Technologies for Meat Processing*. London: Taylor & Francis, pp. 88–129.

Hoz, L., Yustes, C., Camara, J.M. *et al*. (1992). β-Hydroxyacyl-CoA-dehydrogenase (HADH) differentiates unfrozen from frozen-thawed crawfish (*Procambarus clarkii*) and trout (*Salmo gairdneri*) meat. *International Journal of Food Science and Technology*, **27**, 133–136.

Jensen, S.A., Reenberg, S. and Munck, L. (1989). Fluorescence analysis in fish and meat technology. In: A.D. Francisco (ed.), *Fluorescence Analysis in Foods*. London: Longman Group, pp. 181–192.

Karoui, R. and Dufour, E. (2003). Dynamic testing rheology and fluorescence spectroscopy investigations of surface to centre differences in ripened soft cheeses. *International Dairy Journal*, **13**, 973–985.

Karoui, R. and Dufour, E. (2006). Prediction of the rheology parameters of ripened semi-hard cheeses using fluorescence spectra in the UV and visible ranges recorded at a young stage. *International Dairy Journal*, **16**, 1490–1497.

Karoui, R., Mazerolles, G. and Dufour, E. (2003). Spectroscopic techniques coupled with chemometric tools for structure and texture determinations in dairy products: a review. *International Dairy Journal*, **13**, 607–620.

Karoui, R., Dufour, E., Pillonel, L. *et al*. (2004a). Fluorescence and infrared spectroscopies: a tool for the determination of the geographic origin of Emmental cheeses manufactured during summer. *Le Lait*, **84**, 359–374.

Karoui, R., Dufour, E., Pillonel, L. *et al*. (2004b). Determining the geographic origin of Emmental cheeses produced during winter and summer using a technique based on the concatenation of MIR and fluorescence spectroscopic data. *European Food Research and Technology*, **219**, 184–189.

Karoui, R., Martin, B. and Dufour, E. (2005a). Potentiality of front-face fluorescence spectroscopy to determine the geographic origin of milks from the Haute-Loire Department (France). *Le Lait*, **85**, 223–236.

Karoui, R., Dufour, E., Pillonel, L. *et al*. (2005b). Determination of the geographic origin of Emmental cheeses by combining infrared and fluorescence spectroscopies. *International Dairy Journal*, **15**, 287–298.

Karoui, R., Bosset, J.O., Mazerolles, G. *et al*. (2005c). Monitoring the geographic origin of both experimental French Jura hard cheeses and Swiss Gruyère and L'Etivaz PDO cheeses using mid-infrared and fluorescence spectroscopies. *International Dairy Journal*, **15**, 275–286.

Karoui, R., Dufour, E. and De Baerdemaeker, J. (2006a). Common components and specific weights analysis: a tool for monitoring the molecular structure of semi-hard cheese throughout ripening. *Analytica Chimica Acta*, **572**, 125–133.

Karoui, R., Mouazen, A.M., Dufour, E. and De Baerdemaeker, J. (2006b). Utilisation of front-face fluorescence spectroscopy for the determination of some chemical parameters in soft cheeses at external and central zones. *Le Lait*, **86**, 155–169.

Karoui, R., Thomas, E. and Dufour, E. (2006c). Utilisation of rapid technique based on front-face fluorescence spectroscopy for differentiating between fresh and frozen-thawed fish fillets. *Food Research International*, **39**, 349–355.

Karoui, R., Kemps, B., Bamelis, F. *et al*. (2006d). Development of a rapid method based on front face fluorescence spectroscopy for the monitoring of egg freshness: 1 – Evolution of thick and thin albumens. *European Food Research and Technology*, **223**, 303–312.

Karoui, R., Kemps, B., Bamelis, F. *et al*. (2006e). Development of a rapid method based on front face fluorescence spectroscopy for the monitoring of egg freshness: 2 – Evolution of yolk. *European Food Research and Technology*, **223**, 180–188.

Karoui, R., Cartaud, G. and Dufour, E. (2006f). Front-face fluorescence spectroscopy as a rapid and non-destructive tool for differentiating various cereal products: a preliminary investigation. *Journal of Agricultural and Food Chemistry*, **54**, 2027–2034.

Karoui, R., Dufour, E., Schoonheydt, R. and De Baerdemaeker, J. (2007a). Characterisation of soft cheese by front face fluorescence spectroscopy coupled with chemometric tools: effect of the manufacturing process and sampling zone. *Food Chemistry*, **100**, 632–642.

Karoui, R., Dufour, E. and De Baerdemaeker, J. (2007b). Front face fluorescence spectroscopy coupled with chemometric tools for monitoring the oxidation of semi-hard cheeses throughout ripening. *Food Chemistry*, **101**, 1305–1314.

Karoui, R., Schoonheydt, R., Decuypere, E. *et al*. (2007c). Front face fluorescence spectroscopy as a tool for the assessment of egg freshness during storage at a temperature of 12.2°C and relative humidity of 87%. *Analytical Chimica Acta*, **582**, 83–91.

Karoui, R., Schoonheydt, R., Decuypere, E. *et al*. (2007d). Front-face fluorescence spectroscopy as a tool for the assessment of egg freshness during storage under modified atmosphere. *Food Chemistry*, **582**, 83–91.

Karoui, R., Dufour, E., Bosset, J.O. and De Baerdemaeker, J. (2007e). The use of front face fluorescence spectroscopy to classify the botanical origin of honey samples produced in Switzerland. *Food Chemistry*, **101**, 314–323.

Kim, J.B., Murata, M. and Sagakuchi, M. (1987). A method for the differentiation of frozen-thawed from unfrozen fish fillets by a combination of torrymeter readings and K values. *Nippon Suisan Gakkaishi*, **53**, 159–164.

Kozima, T.T. (1983). Effect of temperature fluctuations on quality of frozen fish. *Refrigeration*, **58**, 23.

Kulmyrzaev, A. and Dufour, E. (2002). Determination of lactulose and furosine in milk using front-face fluorescence spectroscopy. *Le Lait*, **82**, 725–735.

Kulmyrzaev, A., Levieux, D. and Dufour, E. (2005). Front-face fluorescence spectroscopy allows the characterization of mild heat treatment applied to milk. Relations with the denaturation of milk proteins. *Journal of Agricultural and Food Chemistry*, **53**, 502–507.

Kunnil, J., Sarasanandarajah, S., Chacko, E. *et al*. (2005). Identification of Bacillus spores using clustering and principal components of fluorescence data. *Aerosol Science and Technology*, **39**, 1–7.

Kunnil, J., Sarasanandarajah, S., Chacko, E. and Reinisch, L. (2006). Effect of washing on identification of *Bacillus* spores by principal component analysis of fluorescence data. *Applied Optics*, **45**, 3659–3664.

Kyriakidis, N.B. and Skarkalis, P. (2000). Fluorescence spectra measurement of olive oil and other vegetable oils. *Journal of AOAC International*, **83**, 1435–1439.

Lakowicz, J.R. (1983). Fluorophores. In: J.R. Lakowicz (ed.), *Principles of Fluorescence Spectroscopy*. New York, NY: Plenum Press, pp. 63–93.

Lebecque, A., Laguet, A., Chanonat, M. *et al*. (2003). Joint analysis of sensory and instrumental data applied to the investigation of the texture of Charolais meat. *Science des Aliments*, **23**, 172–175.

Leblanc, L. and Dufour, E. (2002). Monitoring the identity of bacteria using their intrinsic fluorescence. *FEMS Microbiology Letters*, **211**, 147–151.

Leblanc, L. and Dufour, E. (2004). Monitoring bacteria growth using their intrinsic fluorescence. *Sciences des Aliments*, **24**, 207–220.

Leriche, F., Bordessoules, A., Fayolle, K. *et al*. (2004). Alteration of raw-milk cheese by *Pseudomonas* spp.: monitoring the sources of contamination using fluorescence spectroscopy and metabolic profiling. *Journal of Microbiological Methods*, **59**, 33–41.

Light, N., Champion, A.E., Voyle, C. and Bailey, A.J. (1985). The role of epimysial, perimysial and endomysial collagen in determining texture in 6 bovine muscles. *Meat Science*, **13**, 137–149.

Liu, X. and Metzger, L.E. (2007). Application of fluorescence spectroscopy for monitoring changes in nonfat dry milk during storage. *Journal of Dairy Science*, **90**, 24–37.

Lötze, E., Huybrechts, C., Sadie, A. *et al*. (2006). Fluorescence imaging as a non-destructive method for pre-harvest detection of bitter pit in apple fruit (*Malus domestica* Borkh). *Postharvest Biology and Technology*, **40**, 287–294.

Lucisano, M., Hidalgo, A., Comelli, E.M. and Rossi, M. (1996). Evolution of chemical and physical albumen characteristics during the storage of shell eggs. *Journal of Agricultural and Food Chemistry*, **44**, 1235–1240.

Marsh, R., Kajda, P. and Ryley, J. (1994). The effect of light on the vitamin B_2 and the vitamin A content of cheese. *Nahrung*, **38**, 527–532.

Mazerolles, G., Devaux, M.F., Duboz, G. *et al*. (2001). Infrared and fluorescence spectroscopy for monitoring protein structure and interaction changes during cheese ripening. *Le Lait*, **81**, 509–527.

Møller, J.K.S., Parolari, G., Gabba, L. *et al*. (2003). Monitoring chemical changes of dry-cured Parma ham during processing by surface autofluorescence spectroscopy. *Journal of Agricultural and Food Chemistry*, **51**, 1224–1230.

Moshou, D., Wahlen, S., Strasser, R. *et al*. (2005). Chlorophyll fluorescence as a tool for online quality sorting of apples. *Biosystems Engineering*, **91**, 163–172.

Munck, L., Nørgaard, L., Engelsen, S.B. *et al*. (1998). Chemometrics in food science – a demonstration of the feasibility of a highly exploratory, inductive evaluation strategy of fundamental scientific significance. *Chemometric and Intelligent Laboratory Systems*, **44**, 31–60.

Newman, P.B. (1984). The use of video image-analysis for quantitative measurements of fatness in meat: 2. Comparison of via, visual assessment and total chemical fat estimation in a commercial environment. *Meat Science*, **10**, 161–166.

Noh, H.K. and Lu, R. (2007). Hyperspectral laser-induced fluorescence imaging for assessing apple fruit quality. *Postharvest Biology and Technology*, **43**, 193–201.

Nørgaard, L. (1995). Classification and prediction of quality and process parameters of thick juice and beet sugar by fluorescence spectroscopy and chemometrics. *Zuckerindustrie*, **120**, 970–981.

Olsen, E., Vgot, G., Ekeberg, D. *et al*. (2005). Analysis of the early stages of lipid oxidation in freeze-stored pork back fat and mechanically recovered poultry meat. *Journal of Agricultural and Food Chemistry*, **53**, 338–348.

Olsen, E., Veberg, A., Vogt, G. *et al*. (2006). Analysis of early lipid oxidation in salmon pâté with cod liver oil and antioxidants. *Journal of Food Science*, **71**, S284–S292.

Pavlov, A., Garcia de Fernando, G.D., Diaz, O. *et al*. (1994). Effect of freezing on the β-hydroxyl-CoA-dehydrogenase (HADH) activity of fish meat. *Zeitschrift für Lebensmittel-Untersuchung und -Forschung*, **198**, 465–468.

Posudin, Y.I. (1998). *Lasers in Agriculture*. New York, NY: Science Publishers.

Poulli, K.I., Mousdis, G.A. and Georgiou, C.A. (2005). Classification of edible and lampante virgin olive oil based on synchronous fluorescence and total luminescence spectroscopy. *Analytica Chimica Acta*, **542**, 151–156.

Poulli, K.I., Mousdis, G.A. and Georgiou, C.A. (2007). Rapid synchronous fluorescence method for virgin olive oil adulteration assessment. *Analytica Chimica Acta*, **105**, 369–375.

Ram, M.S., Seitz, L.M. and Dowell, F.E. (2004). Natural fluorescence of red and white wheat kernels. *Cereal Chemistry*, **81**, 244–248.

Ramanujam, N. (2000). Fluorescence spectroscopy *in vivo*. In: R.A. Meyers (ed.), *Encyclopedia of Analytical Chemistry*. London: Wiley, pp. 20–56.

Renou, J.P., Deponge, C., Gachon, P. *et al*. (2004). Characterization of animal products according to geographic origin and feeding diet using nuclear magnetic resonance and isotope ratio mass spectrometry: cow milk. *Food Chemistry*, **85**, 63–66.

Rinnan, A. (2004). Application of PARAFAC on spectral data. PhD Thesis, The Royal Veterinary and Agricultural University, Copenhagen, Denmark.

Ruoff, K., Karoui, R., Dufour, E. *et al*. (2005). Authentication of the botanical origin of honey by front-face fluorescence spectroscopy, a preliminary study. *Journal of Agricultural and Food Chemistry*, **53**, 1343–1347.

Ruoff, R., Luginbühl, W., Künzli, R. *et al*. (2006). Authentication of the botanical and geographical origin of honey by front face fluorescence spectroscopy. *Journal of Agricultural and Food Chemistry*, **54**, 6858–6866.

Sayago, A., Morales, M.T. and Aparicio, R. (2004). Detection of hazelnut oil in virgin olive oil by a spectrofluorimetric method. *European Food Research and Technology*, **218**, 480–483.

Schamberger, G.P. and Labuza, T.P. (2006). Evaluation of front-face fluorescence for assessing thermal processing of milk. *Journal of Food Science*, **71**, 69–74.

Seiden, P., Bro, R., Poll, L. and Munck, L. (1996). Exploring fluorescence spectra of apple juice and their connection to quality parameters by chemometrics. *Journal of Agricultural and Food Chemistry*, **44**, 3202–3205.

Sikorska, E. (2007). Analysis of vitamin B2 using front-face intrinsic beer fluorescence. *European Food Research and Technology*, **225**, 43–48.

Sikorska, E., Romaniuk, A., Khmelinskii, V. *et al*. (2004a). Characterization of edible oils using total luminescence spectroscopy. *Journal of Fluorescence*, **14**, 25–35.

Sikorska, E., Górecki, T., Khmelinskii, I.V. *et al*. (2004b). Fluorescence spectroscopy for characterization and differentiation of beers. *Journal of the Institute of Brewing*, **110**, 267–275.

Sikorska, E., Górecki, T., Khmelinskii, I.V. *et al*. (2005). Classification of edible oils using synchronous scanning fluorescence spectroscopy. *Food Chemistry*, **89**, 217–225.

Sikorska, E., Górecki, T., Khmelinskii, I.V. *et al*. (2006). Monitoring beer during storage by fluorescence spectroscopy. *Food Chemistry*, **96**, 632–639.

Skjervold, P.O., Taylor, R.G., Wold, J.P. *et al*. (2003). Development of intrinsic fluorescent multispectral imagery specific for fat, connective tissue, and myofibers in meat. *Journal of Food Science*, **68**, 1161–1168.

Song, J., Deng, W. and Beaudy, R.M. (1997). Changes in chlorophyll fluorescence of apple fruit during maturation, ripening, and senescence. *Horticultural Science*, **32**, 891–896.

Stadelman, W.J., Ziegler, F. and Darroch, J.G. (1954). The effect of egg temperature on its broken-out albumen quality evaluation. *Poultry Science*, **33**, 1082–1083.

Strasburg, G.M. and Ludescher, R.D. (1995). Theory and applications of fluorescence spectroscopy in food research. *Trends in Food Science & Technology*, **6**, 69–75.

Swatland, H.J. (1987). Autofluorescence of adipose tissue measured with fiber optics. *Meat Science*, **19**, 277–284.

Swatland, H.J. and Findlay, C.J. (1997). On-line probe prediction of beef toughness, correlating sensory evaluation with fluorescence detection of connective tissue and dynamic analysis of overall toughness. *Food Quality and Preference*, **8**, 233–239.

Swatland, H.J., Gullet, E., Hore, T. and Buttenham, S. (1995a). UV fiber-optic probe measurements of connective tissue in beef correlated with taste panel scores for chewiness. *Food Research International*, **28**, 23–30.

Swatland, H.J., Nielsen, T. and Andersen, J.R. (1995b). Correlations of mature beef palatability with optical probing of raw meat. *Food Research International*, **28**, 403–416.

Symons, S.J. and Dexter, J.E. (1991). Computer analysis of fluorescence for the measurement of flour refinement as determined by flour ash content, flour grade color, and tristimulus color measurements. *Cereal Chemistry*, **68**, 454–460.

Symons, S.J. and Dexter, J.E. (1992). Estimation of milling efficiency: prediction of flour refinement by the measurement of pericarp fluorescence. *Cereal Chemistry*, **69**, 137–141.

Symons, S.J. and Dexter, J.E. (1993). Relationship of flour aleurone fluorescence to flour refinement for some Canadian hard common wheat classes. *Cereal Chemistry*, **70**, 90–95.

Symons, S.J. and Dexter, J.E. (1996). Aleurone and pericarp fluorescence estimators of mill stream refinement for various Canadian wheat classes. *Journal of Cereal Science*, **23**, 73–83.

Veberg, A. (2006). Fluorescence spectroscopy of food lipid oxidation. PhD Thesis, Department of Chemistry, Biotechnology and Food Science, Norwegian University of Life Science, Norway.

Veberg, A., Olsen, E., Vogt, G. *et al*. (2006). Front face fluorescence spectroscopy – a rapid method to detect early lipid oxidation in freeze stored minced turkey meat. *Food Science*, **71**, 364–370.

Vyncke, W. (1983). Shelf life of thawed cod fillet kept in ice. *Zeitschrift für Lebensmittel-Untersuchung und -Forschung*, **177**, 19–21.

Wold, J.P., Kvaal, K. and Egelandsdal, B. (1999a). Quantification of intramuscular fat content in beef by combining autofluorescence spectra and autofluorescence images. *Applied Spectroscopy*, **53**, 448–456.

Wold, J.P., Lundby, F. and Egelandsdal, B. (1999b). Quantification of connective tissue (hydroxyproline). In round beef by autofluorescence spectroscopy. *Journal of Food Science*, **64**, 377–383.

Wold, J.P., Jørgensen, K. and Lundby, F. (2002). Nondestructive measurement of light-induced oxidation in dairy products by fluorescence spectroscopy and imaging. *Journal of Dairy Science*, **85**, 1693–1704.

Wold, J.P., Veberg, A., Nilsen, A. *et al*. (2005). The role of naturally occurring chlorophyll and porphyrins in light-induced oxidation of dairy products. A study based on fluorescence spectroscopy and sensory analysis. *International Dairy Journal*, **15**, 343–353.

Yamaki, S., Kato, T. and Kikugawa, K. (1992). Characteristics of fluorescence formed by the reaction of proteins with unsaturated aldehydes, possible degradation products of lipid radicals. *Chemical and Pharmaceutical Bulletin*, **40**, 2138–2142.

Yoshioka, K. and Kitamikado, M. (1983). Differentiation of freeze-thawed fish from fresh fish by the examination of medulla of crystalline lens. *Bulletin of the Japanese Society of Scientific Fisheries*, **49**, 151–154.

Zandomeneghi, M. (1999). Fluorescence of cereal flours. *Journal of Agricultural and Food Chemistry*, **47**, 878–882.

Zandomeneghi, M., Festa, C. and Carbonaro, L. (2000). Front-surface absorbance spectra of wheat flour: determination of Carotenoids. *Journal of Agricultural and Food Chemistry*, **48**, 2216–2221.

Zandomeneghi, M., Carbonaro, L., Calucci, L. *et al*. (2003). Direct fluorometric determination of fluorescent substances in powders: the case of riboflavin in cereal flours. *Journal of Agricultural and Food Chemistry*, **51**, 2888–2895.

Zandomeneghi, M., Carbonaro, L. and Caffarata, C. (2005). Fluorescence of vegetable oils: olive oils. *Journal of Agricultural and Food Chemistry*, **53**, 759–766.

8

Isotopic-spectroscopic Technique: Site-specific Nuclear Isotopic Fractionation Studied by Nuclear Magnetic Resonance (SNIF-NMR)

Wen-Ching Ko and Chang-Wei Hsieh

Introduction

The isotopic content and distribution in molecules from plants and animals are influenced by environmental factors and synthetic routes, and thus can be used to trace the origin of a given compound by comparison with a chemically identical molecule coming from another source. Methods for detecting the "synthetic" or "natural" origin of a chemical species are based on isotopic analysis. Isotope ratio mass spectrometry provides the overall molecular isotope content, but cannot directly measure the isotopic ratios at several positions in a given molecule. One of the most notable contributions of high-resolution nuclear magnetic resonance (NMR) to food authentication

Modern Techniques for Food Authentication
ISBN: 978-0-12-374085-4

is its use in measuring the isotopic content, at the natural abundance level, of specific molecular sites in a given species. The technique, known as SNIF-NMR® for site-specific natural isotope fractionation studied by NMR, was developed in the early 1980s by Professors Gerard and Maryvonne Martin at the University of Nantes (Martin and Martin, 1990). This improves the performance of isotopic methods and supplies genuine proof of the "natural" or "synthetic" origin of a molecule (Martin and Martin, 1995).

The earliest use of SNIF-NMR was to detect the "chaptalization" or enrichment of wines. The addition of beet sugar, cane sugar or concentrated rectified must to the grape must or wine before or during fermentation is often used in order to increase the natural ethanol content in wine and thereby increase its market value. This leads to consumer deception, since sugar addition is not declared on the product. A common type of economic fraud, when successful, is the misrepresentation of cheap wine or the mixing of excellent and expensive wines with low-quality wines, often originating from other geographical regions or even countries (Brescia *et al.*, 2003). For this reason, the SNIF-NMR method was officially adopted in 1987 by the International Office of Vin and Wine, and by the Commission of the European Community (Regulation EC 2676/90, 1990).

Nowadays, it is used in a number of other areas – for authentication, identification, detection of adulteration, compliance with standards of international trade, and deduction of the chemical transformation matrix (especially valuable in the absence of experimental data for the reaction pathway, which is often far too complex to be measured anyway). The methods are particularly well developed for alcohol in fermented and distilled beverages, for carbohydrates in fruit juice, for triacylglycerol lipids and their derivatives (fatty acids and glycerol) from marine, animal and plant oils, and for essential oils used in flavors and fragrances. Qualification for "appellation d'origine controllée" for products may be based in the future on SNIF-NMR analysis. In general, the information associated with the site-specific isotope ratios of chemical species extracted from a food product or ingredient can provide insight into the botanical and/or geographical origin of the species, making SNIF-NMR a powerful tool for food and beverage authentication.

Natural isotope fractionation

Stable isotopes occur naturally, and most elements are found in a composition of one overwhelmingly abundant isotope and one or more isotopes of low abundance. The isotopes most commonly measured in assessments of origin are ratios of the light element isotopes $^{2}H/^{1}H$, $^{13}C/^{12}C$, $^{15}N/^{14}N$, $^{18}O/^{16}O$ and $^{34}S/^{32}S$, and the heavy element isotopes $^{87}Sr/^{86}Sr$ (Rossmann, 2001).

The isotopic content and distribution in molecules from plants and animals are influenced by the climate, the isotopic distribution in the nutrients absorbed, and the metabolic pathways involving the molecules. It is therefore well recognized that, regarding products synthesized in natural conditions, stable isotopes present in natural abundance are an important source of information regarding the history of each chemical species.

Stable carbon isotope ratio analysis (*SCIRA*) has been used successfully for many years in monitoring processed fruit and vegetable products (Rau *et al.*, 2005). SCIRA compares carbon isotope ratio values in samples for different photosynthesis cycles of the plants, with different ratios indicating that samples were produced by different photosynthesis cycles. Plants such as rice, with a Calvin-Benson photosynthetic cycle (C_3), are reported to have $^{13}C/^{12}C$ values ranging from −21‰ to −32‰. Plants such as sugar cane, having a Hatch-Slack photosynthetic cycle (C_4), are reported to have values ranging from −12‰ to −19‰ (Calvin and Bassham, 1962; Smith and Epstein, 1971). In addition to the dual-inlet *isotope ratio mass spectrometer* (*IRMS*), AOAC (1995) specifies that automated ^{15}N and ^{13}C is permitted for use in fast detection of stable carbon isotope ratios (Brookes *et al.*, 1991). As *automated N/C analyzer-mass spectrometry* (*ANCA-MS*) is fast and easy to perform, it is recognized as an effective tool to measure the $^{13}C/^{12}C$ values of any liquid or solid. Since the success of SCIRA in distinguishing between cane- and corn-based alcohol in sake samples (Martin G.E. *et al.*, 1983), stable carbon isotope ratios have been employed to detect adjunct ingredients in other alcoholic beverages such as wine (Weber *et al.*, 1997), brandy (Hogben and Mular, 1976; Simpkins and Rigby, 1982; Pissinato *et al.*, 1999), whiskey (Parker *et al.*, 1998) and beer (Brooks *et al.*, 2002). It was also concluded by Brooks and colleagues (2002) that the stable carbon isotope ratio of an alcoholic beverage is an indicator of the quantity of C_3 and C_4 ingredients used in its production.

However, variations in isotope content also exist between different molecular sites within the same species, and in a number of cases SNIF-NMR can provide direct access to this information. In theory, most elements are potential targets for site-specific isotope content determination. From the point of view of NMR spectroscopy, the nucleus studied must fulfill a number of requirements – for instance, ^{18}O has a nuclear spin quantum number, I, of zero, and is therefore NMR inactive and thus cannot be used to measure $^{18}O/^{16}O$ ratios by this technique. Other elements such as deuterium (I = 1), ^{13}C and ^{15}N (I = 1/2) are accessible to NMR spectroscopy. In general, the major applications of the SNIF-NMR technique have so far been developed for deuterium, for which there is a wide range of interesting examples of food authentication.

Determining site-specific ratios by nuclear magnetic resonance (NMR)

Isotopic distribution in products is defined in terms of their isotopic abundances, A, or isotopic ratios, R, as in the following equation:

$$A = \frac{\text{heavy}}{\text{heavy} + \text{light}} \cdots R = \frac{\text{heavy}}{\text{light}} \qquad \textbf{(8.1)}$$

A and R are expressed as percentages (%) or parts per million (ppm), depending on the nature of the atomic constituent being considered. Similarly, a site-specific

isotopic ratio, R_i, can be defined as the ratio of heavy to light atoms of the same element in a specific site i. For example, in natural organic compounds there are on average 150 deuterium atoms (^{2}H or D) among 1 million hydrogen atoms. The deuterium content and its distribution in organic materials is not random, and nor is it always the same (Martin G.J. *et al.*, 1983a; Fauhl and Wittkowski, 2000). Therefore, deuterium/hydrogen (D/H) ratios measured at the methyl site $(D/H)_I$ and methylene site $(D/H)_{II}$ of ethanol in wine differ significantly according to the origin of the sugar from which the alcohol is produced (Martin G.J. *et al.*, 1983a; Masud *et al.*, 1999). Besides ethanol, this has been shown to be the case for other molecules, such as glucose or glycerol (Hermann, 1999; Zhang *et al.*, 2000; Pionnier *et al.*, 2003). The characteristic site-specific distribution of deuterium within a molecule can be visualized by means of high-resolution ^{2}H nuclear magnetic spectroscopy.

For deuterium, a site-specific ratio would represent the ratio of the number of deuterium atoms to the number of protons (^{1}H) in a specific site i, given as:

$$R_i = \left(\frac{D}{H}\right)_i \tag{8.2}$$

In this case, the number of D atoms in site i can be considered equivalent to the number of monodeuterated isotopomers of type i – an isotopomer being defined as equivalent chemical species of different isotopic content. The overall isotope ratio $\bar{R}$ is then the weighted average of the isotope ratios R_i of its n monodeuterated isotopomers i.

Site-specific ratios R_i can be determined directly from Equation (8.2) (Regulation EC 2676/90, 1990; Regulation EC 2347/91, 1991), provided that the overall isotope ratio is available from SIRMS measurements. This is an external referencing method. Mass spectrometry measurements are not required for an internal standard, but are used in the NMR determination. In this internal referencing procedure, a precisely known quantity of a working standard, WS, is added to a weighted amount of sample X. The isotope ratios of each site i can then be calculated from the following equation (Colquhoun and Lees, 1997):

$$R_i^x = \frac{P^{WS}}{P_i^x} \times \frac{M^X}{M^{WS}} \times \frac{m^{ws}}{m^x} \times \frac{T_i}{t^x} R^{WS} \tag{8.3}$$

where P^{WS} and P_1^X are the stoichiometric numbers of protons in WS and site i of X, M^{WS} and M^X; m^{ws} and m^x are the molecular weights and masses of WS and X, respectively; t^x is the purity (w/w) of the sample X; and T_i, is the ratio of the areas of the ^{2}H-NMR signal of site i of X and of the working standard WS.

For example, ethanol (CH_3CH_2OH) has three monodeuterated isotopomers at a natural abundance level. The deuterium can be located on the methyl site (I), on the methylene site (II) or on the hydroxyl site (III) of the ethanol molecule. Figure 8.1 shows the typical ^{2}H-NMR spectra of ethanol with tetramethylurea (TMU) certified

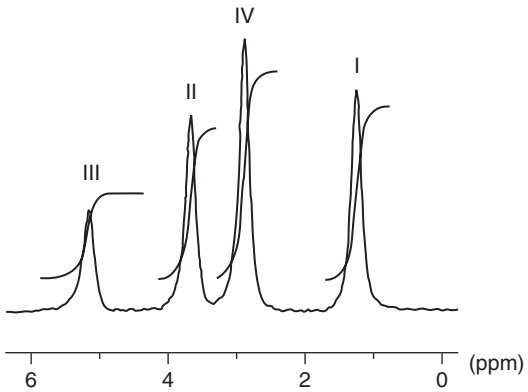

Figure 8.1 The typical ^{2}H-NMR spectra of natural ethanol; the signals I, II, III and IV refer to the working standards CH_2DCH_2OH, CH_3CHDOH, CH_3CH_2OD, and TMU, respectively (Hsieh *et al.*, 2005).

as a reference standard. As shown, the signals I, II, III and IV refer to the working standard CH_2DCH_2OH, CH_3CHDOH, CH_3CH_2OD and TMU, respectively. According to the EU and AOAC protocol (Regulation EC 2676/90, 1990; Martin *et al.*, 1996), the parameters $(D/H)_I$, $(D/H)_{II}$, and R can be calculated by:

$$D/H_I = 1.5866 \times T_I \times \frac{m_{st}}{m_A} \times \frac{(D/H)st}{t_m^D} \quad \textbf{(8.4)}$$

$$D/H_{II} = 2.3799 \times T_{II} \times \frac{m_{st}}{m_A} \times \frac{(D/H)st}{t_m^D} \quad \textbf{(8.5)}$$

$$R = 2(D/H)_{II} / (D/H)_I \quad \textbf{(8.6)}$$

where $(D/H)_I$ is the isotope ratio associated with molecule I, $(D/H)_{II}$ is the isotope ratio associated with molecule II, m_{st} is the weight of TMU, m_A is the weight of the ethyl alcohol sample, t_m^D is the alcoholic strength of the ethyl alcohol sample and $(D/H)_{st}$ is the isotope ratio of internal standard (TMU) supplied by the Community Bureau of References.

A relative parameter, R, can be obtained directly from the NMR spectrum using the intensities I_I, and I_{II} of the CH_2D and CHD signals. The symbol r describes the internal distribution of deuterium and represents the deuterium content of the methylene site, with the methyl site chosen as a reference and given the statistical value of 3 (Hsieh *et al.*, 2005). If ^{2}H were randomly distributed in the ethanol molecule, r would be equal to 2 (Table 8.1). Experimental values of r are generally greater than 2 and differ according to the source of the alcohol, reinforcing the premise of a non-statistical distribution of deuterium depending on origin.

Table 8.1 The ^2H fingerprints of fermentative ethanol in Taiwanese rice-spirits using different varieties of rice (Hsieh *et al.*, 2005)

Rice-spirits	Isotopic variable		
	$(D/H)_I$ (ppm)	$(D/H)_{II}$ (ppm)	r*
TK-8	98.9 ± 0.3[c]	122.1 ± 0.2[b]	2.5[a]
TCS-10	99.7 ± 0.3[b]	119.0 ± 0.3[c]	2.4[b]
MS	108.7 ± 0.3[a]	126.8 ± 0.3[a]	2.3[c]

*relative intramolecular deuterium distribution
TK-8, rice-spirit made from Taikeng 8; TCS-10, rice-spirit made from Taichung sen 10; MS, a molasses spirit.

^2H-NMR for quantitative determinations of site-specific ratios

Owing to the very low natural abundance of ^2H, it is very unlikely, in nature, that isotopomers of small molecules containing more than one deuterium atom will be found. It is even more unlikely that two deuterium atoms will be located in such close proximity as to be subject to spin–spin coupling. Therefore, all signals in ^1H-decoupled ^2H-NMR spectra appear as singlets, which is helpful for carrying out the quantification needed to calculate the site-specific hydrogen isotope ratios $(D/H)_I$ of each position in the molecule (Schneider, 2007). Deliberate deuterium labeling has been used to study chemical or biochemical reaction mechanisms, and since deuterium chemical shifts are almost identical to the corresponding proton chemical shift, the investigation of specifically labeled sites in the ^2H spectrum can provide valuable information to help elucidate a complex ^1H spectrum of the same compound. An advantage of SNIF-NMR, however, is that it measures D/H ratios at the natural abundance level without recourse to lengthy labeling experiments. For a given natural substance, SNIF-NMR gives information about the chemical pathway of biosynthesis and in some cases also about the geographical origin of the sample (Martin and Martin, 1999).

Choice of isotopic probe for SNIF-NMR analysis

^2H-NMR investigation of site-specific natural isotope fractionation (SNIF-NMR) is presently the only way to access directly and simultaneously the hydrogen isotope ratios $(D/H)_I$ associated with different positions, I, in a given molecule. During the various exchange phenomena that are likely to intervene in the course of photosynthetic pathways, the first stored molecule formed is far from being homogeneous (Zhang *et al.*, 1994). Unfortunately, some compounds, such as polymeric and even simple carbohydrates, are not suitable for direct observation by ^2H-NMR. A further source of systematic variations in results can be traced back to sample preparation (extraction, purification, derivation) of the isotopic probe to be used. In this context, ethanol, obtained by fermenting the sugars in strictly standardized conditions, offers a very attractive probe that enables carbohydrates with different

molecular structures to be compared (Martin and Martin, 1981). Since the natural abundance isotopic ratios of the non-exchangeable hydrogens of sugars depend on their physiological and environmental conditions of photosynthesis (Martin and Martin, 1990), the isotopic distribution in the alcoholic fermentation products may reflect the origin of the carbohydrate precursors. It was found that the site-specific isotopic ratio of the methyl group of ethanol $(D/H)_{CH_3}$ mainly depends on those of the non-exchangeable hydrogens of sugars, while that of the methylene group is strongly related to that of the fermentation medium (Martin G.J. *et al.*, 1983b; Martin *et al.*, 1986). Thus, ethanol is a good isotopic probe for the recognition of the origin of its precursor, based on the $(D/H)_{CH_3}$ value. The ethanol probe is used in official analytical methods for the control of commodity authenticity (Martin *et al.*, 1996).

By resorting to this common probe, it could be shown that plant physiological properties and environmental factors exert significant influence on the kinetic and thermodynamic isotope effects associated with hydrogen transfers, intervening in different photosynthetic pathways (Martin and Martin, 1990). In addition, the isotopic probe must be suitable for ^{2}H-NMR spectroscopy in terms of sensitivity, integration of NMR signals, and availability of an internal reference. Besides ethanol, acetic acid, lactic acid and vanillin could also be used as isotopic probes applied with SNIF-NMR.

Preparation of sample for NMR measurement

Tetramethylurea (TMU), with known isotopic content, is used as an internal standard. A 1.3-ml TMU solution is placed into a previously weighed bottle and weighed to the nearest 0.1 mg. Then 3.2 ml of the ethanol sample is poured into the bottle and again weighed to the nearest 0.1 mg (mA). Finally, 150 µl C_6F_6 is added and homogenized by shaking (Martin *et al.*, 1996).

NMR instrumentation

An NMR spectrometer fitted with specific "deuterium" probe tuned to characteristic frequency V_0 of field B_0 is particularly desirable for a deuterium frequency of 61.4 MHz or higher, which corresponds to a nominal ^{1}H frequency of 500 MHz (9.4 T). A field-frequency locking device, usually a fluorine lock, is required to avoid field drift and subsequent broadening of the signals occurring; also an automatic sample changer (optional); appropriate data-processing software; and 10-mm or 15-mm diameter high-precision NMR sample tubes are also required.

Determination of isotope parameters

In order to determine the isotope parameters, the sample (i.e. ethanol) is first transferred into a 10-mm or 15-mm tube, which is then placed into the probe. For obtaining NMR spectra, the following conditions should be maintained:

- a constant probe temperature of 28–29°C
- an acquisition time of at least 6.8 s for 1200 Hz spectral width (16 K memory) (i.e. *ca*. 20 ppm at 61.4 MHz or 27 ppm at 46.1 MHz)
- a 90° pulse.

The following must also be carried out:

- adjustment of the acquisition time (the delay time before acquisition must be the same as the dwell time)
- quadrature detection by setting offset O1 between the OD and CHD signals of ethanol
- determination of the value of decoupling offset O2 from the proton spectrum obtained through the decoupling coil on the same tube (good decoupling is achieved when O2 is set to the middle of the frequency interval existing between the CH_3 and CH_2 groups; note that O1 and O2 represent the frequency positions for observation and decoupling channels, respectively, on Bruker spectrometers)
- application of broadband decoupling to remove line splitting due to $^2H \sim {}^1H$ interactions (the probability of bideuterated species at the natural abundance level is extremely low, therefore $^2H,^2H$ coupling can be ignored)
- assessment of the number of scans – for each spectrum, the number of scans per spectrum (N_S) must be sufficient to obtain signal-to-noise ratio as specified in B_0 (e.g. for $B_0 = 7.05\,T$, $V_0 = 46.05\,MHz$ and for $B_0 = 9.4\,T$, $V_0 = 61.4\,MHz$); the set of NS accumulations was repeated 10 times (NE = 10 times) (N_S values depend on types of spectrometer and probe used; Table 8.2 lists some typical N_S used for various spectrometers).

Most NMR users are very familiar with the need for good magnetic homogeneity in order to obtain sharp, well-resolved peaks. To obtain this, shimming is usually performed by optimizing the deuterium lock signal from the deuterated solvent in which the sample is dissolved (Cross *et al.*, 1998). The application of the SNIF-NMR method to deuterium is limited by the fact that normal NMR instruments use deuterium as a lock, so there are two choices when observing ^2H-NMR signals – i.e. running the instrument unlocked or using the ^{19}F lock. Running it unlocked requires shimming by using the free induction decay (FID) of any nucleus present in the sample that yields a reasonable signal-to-noise ratio in one pulse. In the deuterium SNIF-NMR experiment, the obvious choice is to shim on the proton FID. This is accomplished by setting the acquisition parameters of the instrument to observe the single-pulse FID in a continuous mode. In this mode the spectrometer displays the FID and the integrated area from a single pulse, then erases those data and displays the result from the next pulse. As these pulses are acquired, the shims are adjusted by

Table 8.2 Typical number of scans per spectrum used for various spectrometers

Spectrometer	N_S for 10-mm probe
7.05 Tesla	304
9.40 Tesla	200
11.70 Tesla	104

N_S, number of scans.

the operator to obtain the best FID shape and the greatest integrated area. The NMR analysis, without lock, presents the problem of instrument drift, which is particularly significant when analysis must cover a long period of time (more than 2 hours, as is the case with natural abundance deuterium determination). The ^{19}F lock configuration has some evident drawbacks, as a special channel (receiver, transmitter, and probe), usually very expensive, must be installed and tuned to ^{19}F, and an appropriate fluorine-containing solution must be added in the probe coil, in some cases physically separated from the sample under study (i.e. in a capillary inside the sample tube). Vignali *et al.* (2007) described an inexpensive external unit that allows the use of the commercial high-resolution NMR spectrometer for ^{2}H observation with a ^{1}H lock system. The external unit does not require any tuning, is extremely easy to use, and could be a cheaper and more straightforward alternative to the more expensive ^{19}F lock configuration. Vignali *et al.* (2007) obtained the ^{1}H lock, which was used with a Bruker AMX-400 NMR spectrometer to successfully determine the site-specific ^{2}H contents of ethanol and acetic acid.

In a comparative exercise designed to assess the influence of spectrometer performance on the precision of the quantitative data obtained (Guillou *et al.*, 1988), 3 ethanol samples of different origins were distributed to 15 laboratories operating very different spectrometer systems, with basic magnetic fields varying from 4.7 to 9.4T. The study gave a repeatability of 0.8% and a confidence interval (95%) of 0.25%. It also showed that the reproducibility of 2–3% obtained on the different NMR systems could be reduced to 1% when dedicated and highly automated procedures were used (Martin and Trierweiler, 1994).

Such considerations of precision and accuracy are important, particularly for a technique in which the results have official implications. Certified reference materials (a set of three ethanol samples of different origins in sealed NMR tubes, CRM 123) are available from the Community Bureau of Reference of the European Commission for instrument calibration (Martin *et al.*, 1994), and since the early studies the use of dedicated analytical systems for SNIF-NMR, as discussed below, have become more widespread.

Examples for detection of adulteration

The following discussion will highlight some of the more commonly performed tests by SNIF-NMR.

Adulteration of fruit juice

The use of SNIF-NMR has been extended to fruit juices (Martin and Martin, 1995) to detect the undeclared addition of sugar, either as beet sucrose or modified sugar syrups, to the juice or concentrate. For example, because certain sweeteners such as cane, corn and beet sugars cost less than freshly squeezed orange juice, they could be added to the juice illegally to extend it in conjunction with the addition of groundwater. Selling juice that has been adulterated with these sweeteners and sold as 100% pure, without the declared addition of these compounds on the label, may result in prosecution by regulatory agencies.

At the beginning of the 1980s, Martin *et al.* (1982, 1983b) proposed a new method to distinguish between certain types of sugars. The measurements are performed by ^{2}H-NMR. The analysis measures ethanol obtained from the fermentation of sugars and starches. The method is based on the measurement of the ratio of deuterium/hydrogen (D/H) at the methyl position (defined as $(D/H)_I$) and methylene position (defined as $(D/H)_{II}$) of the ethanol. It has been established that the $(D/H)_I$ ratios of ethanol are related to the sugars used for fermentation and the water in which this occurs. For example, ethanol from apples has a typical $(D/H)_I$ of 100.9 ppm, and ethanol from sugar beets has a $(D/H)_I$ of 94.1 ppm (Martin *et al.*, 1982). Therefore, if sugar beets have been added to apple juice, ^{2}H-NMR analysis will detect this adulteration. This method is called SNIF-NMR, and has been adopted by the AOAC as the standard method for detecting beet-sugar addition to fruit juice (Martin *et al.*, 1996; Pupin *et al.*, 1998).

Sample treatment: the SNIF-NMR concept

The SNIF-NMR concept has been developed (Figure 8.2) as a completely integrated push-button system that covers each step of the analytical chain. Fermentation is a necessary step in the SNIF-NMR analysis of fruit juices because ethanol is the probe molecule for authenticity testing of fruit juice.

A fruit juice concentrate, for example, is first diluted to a standard °Brix value using water of known isotopic content. Fermentation of the resulting solution is then carried out with a standard yeast strain (Martin *et al.*, 1983a), and takes between 3 and 5 days, depending on the type of fruit being analyzed. A commercial enzyme kit is used at the end of this step to ensure complete transformation of all the sugar. The ethanol is then distilled off using a computer-controlled Cadiot column fitted with a Teflon spinning band (the *automatic distillation control system*, *ADCS*). The ADCS was developed specifically for laboratories using ^{2}H-NMR to analyze wines, spirits and fruit juices. The recovery yield of ethanol is calculated from the alcohol content determined before and after distillation. This must be greater than 95% by mass to avoid any occurrence of isotopic fractionation. The software includes automated calculation of the distillation yield and isotopic effect, and enables a fractionation and efficiency check. Finally, a data-processing module provides on-line calculations of isotopic parameters and interpretation of the results using a reference knowledge base (Colquhoun and Lees, 1997).

Calculations

An interpretation strategy to assess orange, grapefruit and apple authenticity has been proposed by Martin *et al.* (1996). Each fruit type, from an authentic database and beet-sugar adulteration, can be quantified by:

$$\text{Adulteration } (\%) = \frac{(D/H)_I \text{min} - (D/H)_I x}{(D/H)_I \text{min} - 92} \times 100\% \qquad \textbf{(8.7)}$$

where $(D/H)_I x$ is the value measured on the product to be analyzed after normalization for the deuterium content of juice water, and $[(D/H)_I \text{min}]$ is the minimum quantity of added sugar (percent total sugars) using the lowest D/H_I ratio for authentic juices of the same origin.

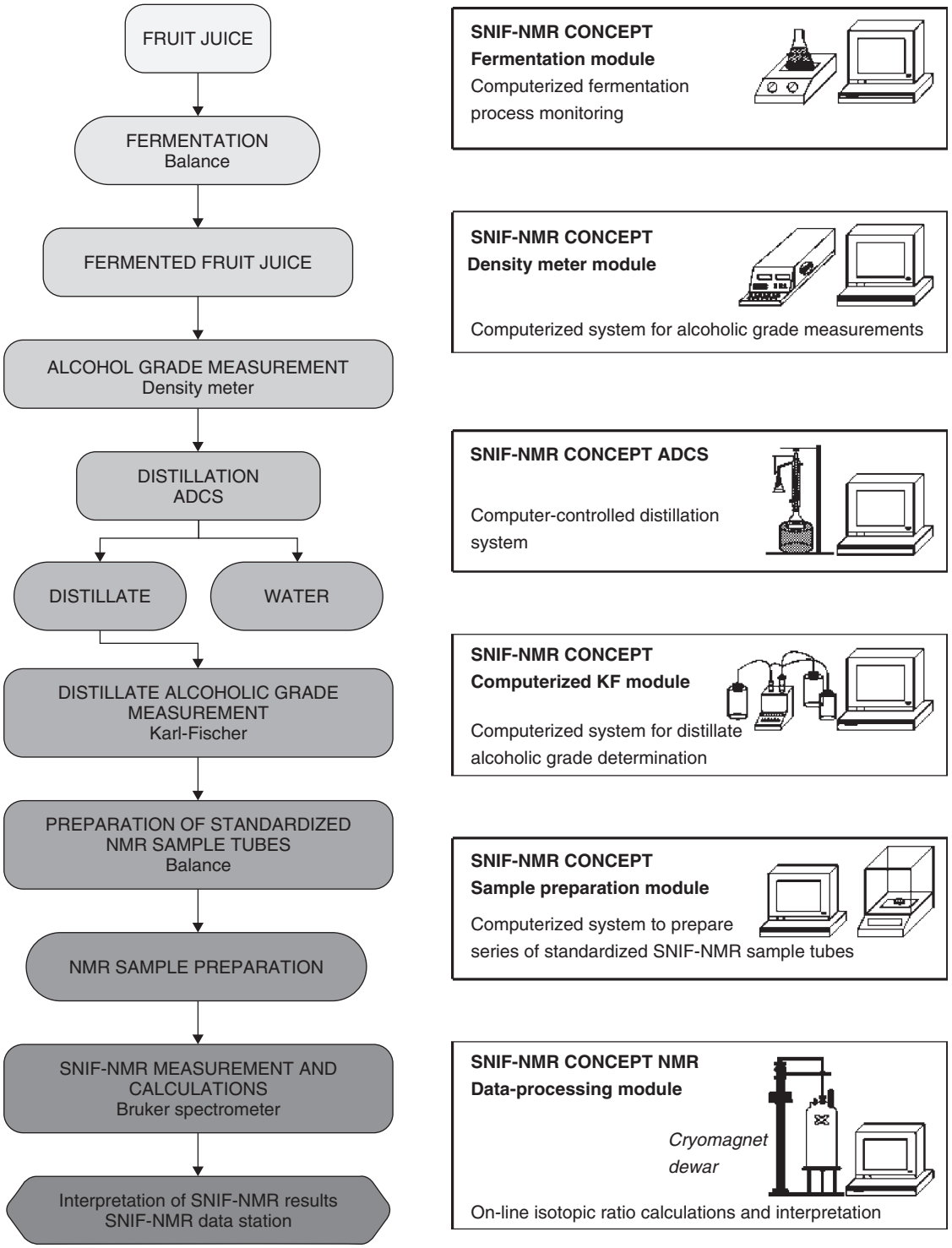

Figure 8.2 Steps in the automated SNIF-NMR® analysis for adulteration of fruit juices (Colquhoun and Lees, 1997).

If $(D/H)_I x > (D/H)_I min$, then no significant addition of beet sugar is detected. If $(D/H)_I x < (D/H)_I min$, then calculate the amount of added beet sugar (%).

If added cane or corn sugar (% C) is also detected with ^{13}C analysis, $(D/H)_I x$ must be corrected for the influence of cane or corn sugar (% C_4) as given by:

$$\text{Corrected}\left(D/H\right)_I x = \left(D/H\right)_I x - \left(\%C_4/100\right) \times \left[110 - \left(D/H\right)_I min\right] \qquad \textbf{(8.8)}$$

Minimum $(D/H)_I$ (ethanol) values proposed are 103–107 ppm for orange juice, 102–106 ppm for grapefruit juice, 99–106 ppm for grape juice and 107–111 ppm for pineapple juice (AOAC, 1998).

Adulteration of wine

Adulteration of wine and brandy can happen in many different ways – for example, by addition of non-grape ethanol (the main fraud in brandy production); addition of non-grape sugar, water, or other unauthorized substances; undeclared mixing of wines from different wards, geographical areas or countries; and mislabeling of variety and/or age of the wine or brandy. Authentication of wines and brandies is an important problem to which SNIF-NMR method analysis has made a significant contribution. It has been shown that very different internal natural distributions of the deuterium isotope exist in ethanol samples of various origins. Quantitative ^2H-NMR, at the natural abundance level, provides a new and efficient tool for investigating these distributions, and original selective parameters are introduced. Comparison of D/H ratios and the ratio R between the intensities of methyl and methylene signals in deuterium spectra enables discrimination between natural and enriched wines, and also makes it possible to differentiate wines based on the geographical origin. SNIF-NMR analysis of ethanol has proved that the isotopic ratio of the $(D/H)_{CH_3}$ is strongly representative of the source of the fermented sugar (e.g. grape, beet, maize, wheat). Therefore, detection of sugar adulteration presents few problems. Besides, the R parameter varies from about 2.2 for gins and rums, which are obtained from corn and sugar cane, respectively, to 2.7 for ethanols extracted from sugar beet, and bourbon whiskies are unambiguously differentiated from malt scotch whiskies (Martin *et al.*, 1983a). Ogrinc *et al.* (2001) investigated the authenticity and geographical origin of wines produced in Slovenia by a combination of IRMS and SNIF-NMR methods. A total of 102 grape samples of selected wines were carefully collected in three different wine-growing regions of Slovenia in 1996, 1997 and 1998. The stable isotope data were evaluated using principal component analysis (PCA) and linear discriminant analysis (LDA). The isotopic ratios to discriminate between coastal and continental regions, namely the deuterium/hydrogen isotopic ratio of the methylene site in the ethanol molecule $(D/H)_{II}$ and $\delta^{13}C$ values (delta (δ) means the difference between observed and calculated values), including $\delta^{18}O$ values in the PCA and LDA, made it possible to distinguish between the two continental regions Drava and Sava. It was found that $\delta^{18}O$ values are modified by meteorological events during grape ripening and harvest. The usefulness of isotopic parameters for detecting adulteration or watering and to assess the geographical origin of wines is improved only when they are used concurrently.

In addition, good results concerning the characterization of wine authenticity and the classification of wines according to the geographical origin were also obtained by means of stable isotope ratios determined by SNIF-NMR (Brescia *et al.*, 2003). The European Union adopted this method for controlling chaptalization (Regulation EC 2676/90, 1990). Subsequently, a reasonable and representative database of authentic wines from the wine-growing countries of the European Union was established, and is constantly growing (Regulation EC 2347/91, 1991).

Adulteration of acetic acid

The denominations of vinegars, such as wine vinegar, cider vinegar, alcohol vinegar, cereal vinegar, malt vinegar, honey vinegar and whey vinegar, are obtained by bacterial or chemical oxidation of ethanol resulting from the fermentation of various sugars. All of them must be genuine products. Products derived from blends of final products or from the fermentation of mixtures of raw materials are illegal in many countries, especially Spain (Royal Decree, 1993).

The most common fraudulent practice in the elaboration and commercialization of vinegar is the mixture of different proportions of wine vinegar and alcohol vinegar. These blends are sold under the denomination of wine vinegar, as if they were a pure product. Another common type of fraud is the addition of acetic acid of a non-biological origin to different types of vinegar in order to comply with vinegar industry regulations. These adulterated products do not represent any safety risk for human health, but they constitute a fraud for consumers and are unfair practices for other vinegar producers (Sáiz-Abajo *et al.*, 2004).

The first of the adulterations mentioned above can currently be eliminated thanks to the research initiated by Remaud *et al.* (1992) and completed by Belton *et al.* (1996), Vallet *et al.* (1998), Hermann (2001), Boffo and Ferreira (2006) and Vignali *et al.* (2007) based on SNIF-NMR. For the analysis, the vinegar is extracted with ethyl ether in a Soxhlet apparatus and the acetic acid is distilled off using a spinning band Cadiot column similar to that used for the distillation of alcohol for the isotopic analysis of fruit juice. The $(D/H)_I$ content of the methyl site of the acetic acid is measured from the ^{2}H-NMR spectrum using *N*,*N*-tetramethylurea (TMU) as the working standard (Remaud *et al.*, 1992).

This method is based on the deuterium-to-hydrogen ratio at a specific position (methyl group) of acetic acid obtained by fermentation, through different biosynthetic mechanisms which result in different isotopic ratios. The SNIF-NMR technique enables detection of the addition of 5% of synthetic acetic acid to any vinegar sample, which makes such addition unprofitable.

Adulteration of honey

Honey is a valued sweet and viscous substance produced by bees from flower nectar or from honeydew. Floral honey is composed mainly of the carbohydrates fructose and glucose. While demand for honey is increasing, production is in decline for a variety of socioeconomic reasons. Extension of honey by the addition of other sweet

substances such as sucrose solution and high-fructose corn syrup (HFCS) at some stage during production or processing could be an attractive means of economic adulteration. Identifying this type of adulteration is important for financial reasons.

Many different analytical techniques are employed in authenticity testing of honey. Among them are NMR spectroscopy (Lindner *et al.*, 1996), HPLC (Swallow and Low, 1990; Nozal *et al.*, 2001), GC (Low and South, 1995) and carbon isotope ratio analysis (White *et al.*, 1998; Garcia-Wass, 2002). The most widely used is high-performance liquid chromatography (HPLC), but this methodology does not detect low levels of adulteration and nor is it adequate for the more sophisticated falsifications. This stable carbon isotope ratio analysis (SCIRA) has been used to detect adulteration in honey. Some researches report that SNIF-NMR involved only honey from acacia, chestnuts and lavender. As was shown in previous work (Cotte *et al.*, 2007), the $(D/H)_I$ ratio is specific to a given floral origin.

However, by comparing the carbon isotope ratios in the protein and the sugars of honey, both should be the same if they come from the same source. Some laboratories can determine whether the honey was adulterated, and can estimate the percentage of adulteration by the difference in the $^{13}C/^{12}C$ ratios between the sugar in the honey and its protein. Nevertheless, these techniques, except for NMR spectroscopy, are time-consuming and will destroy samples; NMR spectroscopy can produce more precise results for authenticity confirmation of honey quality, even though the method most commonly chosen these days is isotope ratio analysis (Padovan *et al.*, 2003).

Adulteration of organic acid

Owing to the common adulteration of food with substances such as organic acid, a methodology for measuring the natural deuterium distribution in citric acid by the SNIF-NMR method is presented. Although citric acid is not a favorable probe for the SNIF-NMR method, dioxine exhibits a unique signal, well separated from those of triethyl citrate (TEC). TEC is commercially available, offers the advantage of being very stable and relatively well adapted, and is the usual and official reference for SNIF-NMR analysis. Besides, TEC is retained as a molecular probe for ^{2}H-NMR. The method provides efficient criteria for characterizing the authenticity of lemon juices (Gonzalez *et al.*, 1998). The combination of C_{13} and deuterium measurements of extracted citric acid is proposed as a routine method for optimum detection of exogenous citric acid in all kinds of fruit juices. The correlation between $\delta^{13}C$ values of sugars and of both acids is very specific, and reinforces the discriminating power of the SNIF-NMR method. The deuterium content of TEC was calibrated with respect to TMU by means of ^{2}H-NMR, and the sample lemon juice showed a D/H ratio of 148 ppm (Gonzalez *et al.*, 1998). Moreover, it has been shown that the simultaneous use of the $^{13}C/^{12}C$ ratios of citric acid and other fruit-juice components (such as sugars or other organic acids) also determined by IRMS leads to a lower detection limit. It can be found that the citric acid isolated from authentic fruit juices systematically shows higher D/H values than its non-fruit counterpart, which reached 149 ppm produced by fermentation of various sugar sources (Jamin *et al.*, 2005). Although different kinds of microorganisms are used in lactic acid and

ethanol fermentation, the same intermediate, pyruvate and the same enzymatic reduction with NADH are involved. Isotopic characterization of lactic acid in C_4 sugars had higher (D/H) values for the non-exchangeable sites of the carbohydrates that reached 148 ppm (Zhang *et al.*, 2003). The typical mean values and dispersion ranges of the isotopic parameters computed for lactic acid and for ethanol obtained by fermentation pyruvate of C_3 and C_4 materials or synthesized from fossil sources illustrated the analytical potential of the isotopic methods.

Adulteration of nicotine

The geographical limits of tobacco plant growth are from approximately latitudes 60°N to 40°S. Most countries within these limits have some tobacco production. Because the tobacco is distinct in different countries, it is possible to establish the isotopic fingerprint of the nicotine molecule extracted from tobacco leaves which have been harvested in different countries and undergone different curing processes, by using the SNIF-NMR method (site-specific deuterium content). Besides, with its three stable isotope pairs (^{2}H/^{1}H, ^{13}C/^{12}C, ^{15}N/^{14}N) and 12 distinguishable deuterium isotopomers, nicotine is potentially an attractive probe for a multi-element and multi-site approach to tobacco characterization (Figure 8.3). The biosynthesis and metabolism of tobacco alkaloids have been extensively investigated, leading to a clear understanding of the biosynthesis of 3-pyridyl derivatives and especially nicotine, the most characteristic product of tobacco (Leete, 1983). Therefore, nicotine must be chemically degraded into nicotinic acid so that the intramolecular distribution of carbon and nitrogen isotopes can be studied (Figure 8.4). Regarding carbon and nitrogen ratios of nicotine, these showed European nicotine to be more depleted in nitrogen 15 ($\delta^{15}N = -8.0‰$, $\sigma = 1.3$) than the others ($\delta^{15}N = -4.5‰$, $\sigma = 1.2$). Interestingly, the African and commercially available nicotine had nearly the same $\delta^{15}N$ values ($\delta^{15}N = -4.3‰$, $\sigma = 0.6$) (Jamin *et al.*, 1997). From a general point of view, it has been shown that the deuterium distribution in plant metabolites provides information regarding the environment of the plant (Cotte *et al.*, 2007). The results showed that the isotope ratios of sites 1, 3 and 12 were negatively correlated. The deuterium content

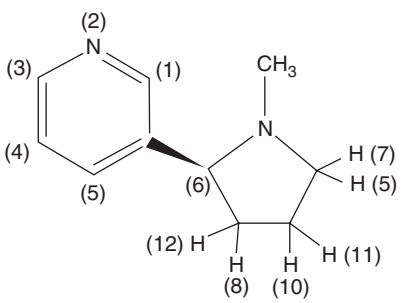

Figure 8.3 Nicotiana tabacum nicotine molecule contains 23 non-equivalent sites associated with 12 monodeuterated isotopomers. Ratios of the protons at each site to those at other sites throughout the molecule lead to site-specific natural isotope fractionation (SNIF-NMR®), which results in the ability to differentiate the natural *Nicotiana tabacum* nicotine (Jamin, 1997).

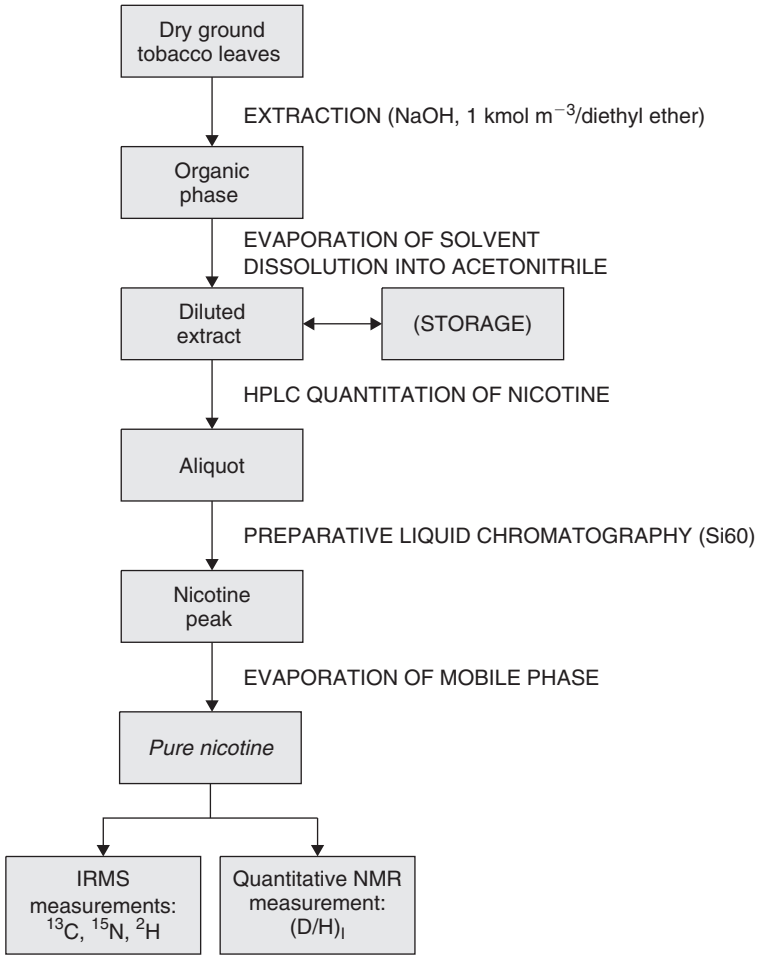

Figure 8.4 Chemical degradation of nicotine to nicotinic acid that computed the site-specific isotope ratios by NMR and IRMS (Jamin, 1997).

of sites 1, 3 and 12, which were related to the water in the biosynthetic medium, decreased (Jamin *et al.*, 1997). A non-statistical distribution of the stable isotopes of carbon and hydrogen in the nicotine molecule was observed and interpreted in terms of biosynthetic origin. A combination of compositional and isotopic analytical variables is expected to improve the performance of tobacco authentication, since botanical, technological and geographical factors can be considered simultaneously. Therefore, such a strategy will provide complementary information on the isotopic fractionation effects associated with the biosynthetic pathway in the field environment.

Conclusions

The outlook for food authentication indicates that research into relatively novel techniques such as SNIF-NMR®, which is perhaps the most sophisticated and specific

technique for determining food authenticity, is required. In principle, any compound that can be extracted from a food matrix without incurring isotopic fractionation and in sufficient quantity that a sufficiently well-resolved spectrum can be obtained is a potential target for SNIF-NMR. However, the financial cost of purchasing and operating such a high-specification NMR instrument is significant, and time-consuming sample preparation is required before analysis can take place. These techniques are not likely to find widespread application in the food industry unless the instrument and running costs are lowered.

References

AOAC (1995). Corn and Cane Sugar Products in Honey. In: *Official Methods of Analysis of AOAC International*. Arlington, VA: AOAC 978.17.

AOAC (1998). Beet Sugar in Fruit Juices (SNIF-NMR) Method. In: *Official Methods of Analysis of AOAC International*. Gaithersburg, MD: AOAC 995.17.

Belton, P.S., Delgadillo, I., Colmes, E. *et al*. (1996). Use of high-field ^{1}H-NMR spectroscopy for the analysis of liquid foods. *Journal of Agricultural and Food Chemistry*, **44**, 1483–1487.

Boffo, E.F. and Ferreira, A.G. (2006). Biosynthetic origin of acetic acid using SNIF-NMR. *Química Nova*, **29**, 456–458.

Brescia, M.A., Koĕir, I.J., Caldarola, V. *et al*. (2003). Chemometric classification of Apulian and Slovenian wines using ^{1}H-NMR and ICP-OES together with HPICE data. *Journal of Agricultural and Food Chemistry*, **51**, 21–26.

Brooks, J.R., Buchmann, N., Phillips, S. *et al*. (2002). Heavy and light beer: a carbon isotope approach to detect C_4 carbon in beers of different origins, styles, and prices. *Journal of Agricultural and Food Chemistry*, **50**, 6413–6418.

Brookes, S.T., Barrie, A. and Davies, J.E. (1991). A rapid $^{13}C/^{12}C$ test for determination of corn syrups in honey. *Journal of AOAC International*, **74**, 627–629.

Calvin, M. and Bassham, J.A. (1962). *The Photosynthesis of Carbon Compounds*. New York, NY: W.A. Benjamin.

Colquhoun, I.J. and Lees, M. (1997). Nuclear magnetic resonance spectroscopy. In: P.R. Ashurst and M.J. Dennis (eds), *Analytical Methods of Food Authentication*. London: Blackie Academic & Professional, pp. 36–74.

Cotte, J.F., Casabianca, H., Lhéritier, J. *et al*. (2007). Study and validity of ^{13}C stable carbon isotopic ratio analysis by mass spectrometry and ^{2}H site-specific natural isotopic fractionation by nuclear magnetic resonance isotopic measurements to characterize and control the authenticity of honey. *Analytica Chimica Acta*, **582**, 125–136.

Cross, J.L., Gallaher, T.N., Leary, J.J. and Schreiner, S. (1998). The application of site-specific natural isotope fractionation-nuclear magnetic resonance (SNIF-NMR) to the analysis of alcoholic beverages. *The Chemical Educator*, **3**, 1430–1471.

Fauhl, C. and Wittkowski, R. (2000). Oenological influences on the D/H ratios of wine ethanol. *Journal of Agricultural and Food Chemistry*, **48**, 3979–3984.

Garcia-Wass, F. (2002). The use of pyrolysis mass spectrometry in orange juice authentication. *Fruit Process*, **12**, 389–392.

Gonzalez, J., Eric, J., Remaud, G. *et al*. (1998). Authentication of lemon juices and concentrates by a combined multi-isotope approach using SNIF-NMR and IRMS. *Journal of Agricultural and Food Chemistry*, **46**, 2200–2205.

Guillou, C., Trierweiler, M. and Martin, G.J. (1988). Repeatability and reproducibility of site-specific isotope ratios in quantitative ^{2}H-NMR. *Magnetic Resonance in Chemistry*, **26**, 491–496.

Hermann, A. (1999). Determination of site-specific D/H isotope ratios of glycerol from different sources by ^{2}H-NMR spectroscopy. *Zeitschrift für Lebensmittel-Untersuchung und -Forschung A*, **208**, 194–197.

Hermann, A. (2001). Determination of D/H isotope ratio in acetic acid from vinegars and pickled products by ^{2}H-NMR-spectroscopy. *European Food Research Technology*, **212**, 683–686.

Hogben, R. and Mular, M. (1976). Major congeners of Australian and imported brandies and other spirits as indicators of authenticity. *Journal of the Science of Food and Agriculture*, **27**, 1108–1114.

Hsieh, C.W., Wang, H.J., Chang, C.M. and Ko, W.C. (2005). Detection of molasses-spirit in rice-spirits from TK-8 and TCS-10 by SNIF-NMR method. *Journal of Food and Drug Analysis*, **13**, 251–255.

Jamin, E., Naulet, N. and Martin, G.J. (1997). Multi-element and multi-site isotopic analysis of nicotine from tobacco leaves. *Plant, Cell and Environment*, **20**, 589–599.

Jamin, E., Martin, F., Santamaria-Fernandez, R. and Lees, M. (2005). Detection of exogenous citric acid in fruit juices by stable isotope ratio analysis. *Journal of Agricultural and Food Chemistry*, **53**, 5130–5133.

Leete, E. (1983). Biosynthesis and metabolism of the tobacco alkaloids. In: S.W. Pelletier (ed.), *Alkaloids Chemical and Biological Perspectives*, Vol. 1. New York, NY: John Wiley & Sons, pp. 85–153.

Lindner, P., Bermann, E. and Gamarnik, B. (1996). Characterization of citrus honey by deuterium NMR. *Journal of Agricultural and Food Chemistry*, **44**, 139–140.

Low, N.H. and South, W. (1995). Determination of honey authenticity by capillary gas chromatography. *Journal of AOAC International*, **78**, 1210–1218.

Martin, G.E., Burggraff, J.M., Alfonso, F.C. and Figert, D.M. (1983). Determination of authenticity of sake by carbon isotope ratio analysis. *Journal of AOAC International*, **66**, 1405–1408.

Martin, G.G., Wood, R. and Martin, G.J. (1996). Detection of added beet sugar in concentrated and single strength fruit juices by deuterium nuclear magnetic resonance (SNIF-NMR method): Collaborative study. *Journal of AOAC International*, **79**, 917–928.

Martin, G.J. and Martin, M.L. (1981). Deuterium labeling at the natural abundance level as studied by high field quantitative deuterium NMR. *Tetrahedron Letters*, **22**, 3525–3528.

Martin, G.J. and Martin, G.G. (1995). In: S. Nagy and R.L. Wade (eds), *Methods to Detect Adulteration of Fruit Juice Beverages*, Vol. 1. Auburndale, FL: AgScience International, pp. 1–27.

Martin, G.J. and Trierweiler, M. (1994). Ethanol reference materials for ^{2}H-NMR determinations (SNIF-NMR). *BCR Information*, EUR 14395 EN.

Martin, G.J., Martin, M.L., Mabon, F. and Michon, F.J. (1982). Identification of the origin of natural alcohols by natural abundance hydrogen-2 nuclear magnetic resonance. *Analytical Chemistry*, **54**, 2380–2382.

Martin, G.J., Martin, M.L., Mabon, K. and Michon, M.J. (1983a). A new method for the identification of the origin of ethanols in grain and fruit spirit: high-field quantitative deuterium nuclear magnetic resonance at the natural abundance level. *Journal of Agricultural and Food Chemistry*, **31**, 311–315.

Martin, G.J., Zhang, B.L., Martin, M.L. and Dupuy, P. (1983b). Application of quantitative deuterium NMR to the study of isotope fractionation in the conversion of saccharides to ethanols. *Biochemical and Biophysical Research Communications*, **111**, 890–896.

Martin, G.J., Zhang, B.L., Naulet, N. and Martin, M.L. (1986). Deuterium transfer in the bioconversion of glucose to ethanol studied by specific isotope labeling at the natural abundance level. *Journal of American Chemical Society*, **108**, 5116–5122.

Martin, G.G., Wood, R. and Martin, G.J. (1996). Detection of added beet sugar in concentrated and single strength fruit juices by deuterium nuclear magnetic resonance (SNIF-NMR1 method): Collaborative study. *Journal of AOAC International*, **79**, 917–928.

Martin, G.J., Trierweiler, M., Ristow, R. *et al*. (1994). The certification of the three reference ethanols by SNIF-NMR: BCR Certified Reference Material CRM 123. *BCR Information*, EUR 15347 EN.

Martin, M.L. and Martin, G.J. (1990). Deuterium NMR in the study of site-specific natural isotope fractionation. In: H. Günther (ed.), *NMR Basic Principles and Progress*, Vol. 23. Heidelberg: Springer-Verlag, pp. 1–60.

Martin, M.L. and Martin, G.J. (1999). Site-specific isotope effects and origin inference. *Isotopic Analysis*, **27**, 209–213.

Masud, Z., Vallet, C. and Martin, G.L. (1999). Stable isotope characterization of milk components and whey ethanol. *Journal of Agricultural and Food Chemistry*, **47**, 4693–4699.

Nozal, M.J., Bernal, J.L., Toribio, L. *et al*. (2001). High-performance liquid chromatographic determination of methyl anthranilate, hydroxylmethylfurfural and related compounds in honey. *Journal Chromatography*, **917**, 95–103.

Ogrinc, N., Košir, I.J., Kocjančič, M. and Kidrič, J. (2001). Determination of authenticy, regional origin, and vintage of Slovenian wines using a combination of IRMS and SNIF-NMR analyses. *Journal of Agricultural and Food Chemistry*, **49**, 1432–1440.

Padovan, G.J., Jong, D.D., Rodrigues, L.P. and Marchini, J.S. (2003). Detection of adulteration of commercial honey samples by the $^{13}C/^{12}C$ isotopic ratio. *Food and Chemical Toxicology*, **82**, 633–636.

Parker, I.G., Kelly, S.D., Sharman, M. *et al*. (1998). Investigation into the use of carbon isotope ratios ($^{13}C/^{12}C$) of Scotch whisky congeners to establish brand authenticity using gas chromatography-combustion-isotope ratio mass spectrometry. *Journal of Agricultural and Food Chemistry*, **63**, 423–428.

Pionnier, S., Robins, R.J. and Zhang, B.L. (2003). Natural abundance hydrogen isotope affiliation between the reactants and the products in glucose fermentation with yeast. *Journal of Agricultural and Food Chemistry*, **51**, 2076–2082.

Pissinato, L., Martinelli, L.A., Victoria, R.L. and Camargo, P.B. (1999). Using stable carbon isotopic analyses to access the botanical origin of ethanol in Brazilian brandies. *Food Research International*, **32**, 665–668.

Pupin, A.M., Dennis, M.J., Parker, I. *et al*. (1998). Use of isotopic analyses to determine the authenticity of brazilian orange juice (Citrus sinensis). *Journal of Agricultural and Food Chemistry*, **46**, 1369–1373.

Rau, Y.H., Lin, G.P., Chang, W.S. *et al*. (2005). Using $^{13}C/^{12}C$ isotopic ratio analysis to differentiate between rice spirits made from rice and cane molasses. *Journal of Food and Drug Analysis*, **13**, 159–162.

Regulation EC 2676/90 (1990). Detecting enrichment of grape musts, concentrated grape musts, rectified concentrated grape musts and wines by application of nuclear magnetic resonance of deuterium (SNIF-NMR/RMN-FINS). *Official Journal of the European Communities*, **L272**, 1–192.

Regulation EC 2347/91 (1991). On the collection of samples of wine products for the purposes of cooperation between member states and for analysis by nuclear magnetic resonance, including analysis for the purposes of the community databank. *Official Journal of the European Communities*, **L214**, 32–36.

Remaud, G., Guillou, C., Vallet, C. and Martin, G.J. (1992). A coupled NMR and MS isotopic method for the authentication of natural vinegars. *Fresenius' Journal of Analytical Chemistry*, **342**, 457–461.

Rossmann, A. (2001). Determination of stable isotope ratio in food analysis. *Food Reviews International*, **17**, 347–381.

Royal Decree (1993). Royal Decree NO. 2070/1993 of November 26th. *Official State Gazette*, **293**, 8 December.

Sáiz-Abajo, M., González-Sáiz, J. and Pizarro, C. (2004). Classification of wine and alcohol vinegar samples based on near-infrared spectroscopy. Feasibilily study on the detection of adulterated vinegar samples. *Journal of Agricultural and Food Chemistry*, **52**, 7711–7719.

Schneider, B. (2007). Nuclear magnetic resonance spectroscopy in biosynthetic studies. *Progress in Nuclear Magnetic Resonance Spectroscopy*, **51**, 155–198.

Simpkins, W.A. and Rigby, D. (1982). Detection of the illicit extension of potable spirituous liquors using ^{13}C:^{12}C ratios. *Journal of the Science of Food and Agriculture*, **33**, 898–903.

Smith, B.N. and Epstein, S. (1971). Two categories of $^{13}C/^{12}C$ ratios for higher plants. *Plant Physiology*, **47**, 380–384.

Swallow, K.W. and Low, N.H. (1990). Analysis and quantitation of the carbohydrates in honey using high-performance liquid chromatography. *Journal of Agricultural and Food Chemistry*, **38**, 1828–1832.

Vallet, C., Arendt, M. and Martin, G.J. (1998). Site specific isotope fractionation of hydrogen in the oxydation of ethanol into acetic acid. Application to vinegars. *Biotechnology Techniques*, **2**, 83–88.

Vignali, C., Caligiani, A. and Palla, G. (2007). Quantitative ^{2}H-NMR spectroscopy with ^{1}H lock extender. *Journal of Magnetic Resonance*, **187**, 120–125.

Weber, D., Rossmann, A., Schwarz, S. and Schmidt, L. (1997). Correlations of carbon isotope ratios of wine ingredients for the improved detection of adulterations I. Organic acids and ethanol. *Zeitschrift für Lebensmittel-Untersuchung und -Forschung A*, **205**, 158–164.

White, J.W., Winters, K., Martin, P. and Rossmann, A. (1998). Stable carbon isotope ratio analysis of honey: validation of internal standard procedure. *Journal of AOAC International*, **81**, 610–619.

Zhang, B.L., Buddrus, S. and Martin, M.L. (2000). Site-specific hydrogen isotope fractionation in the biosynthesis of glycerol. *Bioorganic Chemistry*, **28**, 1–15.

Zhang, B.L., Fallourd, V., Role, C. and Martin, G.J. (2003). Comparsion of isotopic fractionation in lactic acid and ethanol fermentations. *Bioorganic Chemistry*, **31**, 227.

Zhang, B.L., Quemerais, B., Martin, M.L. and Williams, J.M. (1994). Determination of the natural deuterium distribution in glucose from plants having different photosynthetic pathways. *Phytochemical Analysis*, **5**, 105–110.

This page intentionally left blank

9

Isotopic-spectroscopic Technique: Stable Isotope Ratio Mass Spectrometry (IRMS)

Gérard Gremaud and Andreas Hilkert

Introduction

Authenticity has been defined by the Codex Alimentarius as the retention of all physical, chemical, organoleptical and essential nutritional characteristics of original food products (Anonymous, 2004). Conversely, non-authentic products have by definition been subjected to alterations of their properties. These alterations frequently induce slight but often measurable changes of their isotopic distribution. Consequently, analytical techniques such as *isotope ratio mass spectrometry* (*IRMS*), which allows the accurate determination of the *stable isotopes ratios* ($^{2}H/^{1}H$, $^{13}C/^{12}C$, $^{15}N/^{14}N$, $^{18}O/^{16}O$, $^{34}S/^{32}S$), have become increasingly popular and are among the most favored tools for assessing the authenticity of food products. As described in a recent review of techniques to assess authenticity (Cordella *et al*., 2002), stable isotope determinations, used either alone or in combination with other chemical or physical variables, were

Modern Techniques for Food Authentication
ISBN: 978-0-12-374085-4

cited in almost half of all studies related to this theme. The aim of this chapter is to present an introduction to the basic principles underlying the application of IRMS to food authenticity and to review the literature recently published on this subject.

Theory and principles

The distribution of light stable isotopes observed in processed foodstuffs is the result of changes introduced in the isotopic composition of raw materials by the many *isotopic fractionations* occurring at almost every step of the food elaboration process – such as chemical or biochemical reactions, distillation and evaporation. The distribution of stable isotopes in raw products reflects the enrichment of the nutrients given to the plant or animal organisms which synthesized them, and the fractionations introduced by the metabolism. Furthermore, global geochemical phenomena govern the enrichment of organic and inorganic matter in the environment. The major factors affecting the specific isotopes in processed food, raw materials and in the environment are further presented in following paragraphs.

The isotopic enrichments measured by IRMS are expressed in per mil units (‰) against international standards in the delta (δ) notation, as given in the following equation, taking carbon as an example:

$$\delta^{13}C[‰] = \left(\frac{^{13}C/^{12}C_{sample}}{^{13}C/^{12}C_{std}} - 1 \right) \times 1000‰ \qquad \textbf{(9.1)}$$

Primary international standards are *Vienna Standard Mean Ocean Water*, *V-SMOW* ($^{18}O/^{16}O$, D/H), *Pee Dee Belemnite*, *PDB* ($^{13}C/^{12}C$), atmospheric air ($^{15}N/^{14}N$), and *Canyon Diablo Troilite*, *CDT* ($^{34}S/^{32}S$). Their δ values are zero according to definition. As some of these primary standards are no longer commercially available, secondary standards with precisely known delta values are proposed for the same isotopes.

Oxygen and hydrogen

Temperature is the major factor governing the enrichment of oxygen ($\delta^{18}O$) and hydrogen ($\delta^{2}H$) in precipitations globally. Temperature gradients induce corresponding $\delta^{18}O$ and $\delta^{2}H$ gradients, and models can be developed to reflect these gradients. As shown by Sturm *et al*. (2005), the equation $\delta^{18}O‰ = 0.695T_{annual} - 13.6$, which is based on previous work by (Dangaard, 1964), was able to predict its enrichment relatively well in precipitations at mid- and high latitudes. However, at lower latitudes the isotopic content of precipitation was found to be more closely related to the amount of rainfall, with the rainy season demonstrating depleted values. In addition to this global trend, local effects of continentality and altitude also alter the isotope distribution of precipitation significantly. *Continentality* describes the progressive isotopic depletion of clouds moving inland from the coast. This effect is stronger in winter than in summer. The second significant local effect is the elevation or altitude

effect, which is due to cooling of the vapor masses as they rise over the landscape. The depletion of $\delta^{18}O$ and for $\delta^{2}H$ varies between about −0.15 and −0.5‰, between about −1 to −4‰ per 100-m rise in elevation. Data regarding the isotopes in precipitations as well as further explanations of the underlying mechanisms are available at http://isohis.iaea.org. The isotopic enrichment of exchangeable oxygen and hydrogen in plants and animals is usually shifted in relation to that which is found in the local precipitations, because the enrichment of all sources of absorbed water is altered by plant or animal metabolism. The abundances of hydrogen and oxygen isotopes in the environment are correlated and obey the same rules. Similarly, in food products the exchangeable oxygen and hydrogen enrichments in the same sample are correlated parameters. Therefore, only one of them is usually measured.

Carbon

Plants can be classified into three categories according to their metabolism. Most plants, including all trees, have Calvin cycle metabolism, and are often referred to as *C3 plants* after the number of carbon atoms of the first organic acid synthesized during photosynthesis. A typical food plant representative of C3 metabolism, such as sugar beet, demonstrates $\delta^{13}C$ enrichments ranging from −26 to −30‰. Plants growing in tropical regions rely on the Hatch-Slack metabolism, and are called *C4 plants*. Maize, sugar cane and sorghum are typical representatives of C4 food plants, and their $\delta^{13}C$ enrichments range from −12 to −14‰. Finally, plants growing in arid climates and relying on the Crassulacean acid metabolism are called *CAM plants*. As CAM metabolism is similar to C4 metabolism, CAM plants (e.g. pineapple, cactus and vanilla) have $\delta^{13}C$ enrichments in a range between those of C3 and C4 plants. Because of isotope effects, the biosynthetic pathways of C3, C4 or CAM plants produce metabolites with typical enrichments. This fact is used in several authentication methods. When differentiation based on the overall enrichments of typical C3, C4 or CAM plants metabolites is not sufficient, one further level of complexity can be reached by examining the site-specific enrichment of a given target molecule. Indeed, each carbon atom has a specific enrichment reflecting the isotopic fractionation occurring at every step of the biosynthetic process, and the differences in enrichment between different sites of a molecule are only governed by the plant's metabolism and not by the environment.

In terrestrial animals, the enrichments are mostly linked to the type of feed ingested and are further altered by the animal's metabolism. Moreover, the enrichment within the same animal is not evenly distributed in space and between metabolites. For example, the $\delta^{13}C$ enrichment of animal proteins is about 3‰ higher than that of their lipids because of fractionation occurring during the lipid biosynthesis. In eggs, for example, the average $\delta^{13}C$ value of the egg membrane was found to be 1 to 4‰ lower than that of egg white, which in turn was about 2‰ lower than that of egg yolk (Sakamoto *et al*., 2002).

In marine organisms, the predominant metabolic process affecting the $\delta^{13}C$ of organic carbon is the fixation of inorganic carbon dissolved in seawater. The enrichments of marine foods lie between $\delta^{13}C$ −22‰ and −15‰.

Nitrogen

The fixation of atmospheric nitrogen ($\delta^{15}N$ of 0.0‰ per def.) is accomplished by symbiotic bacteria which thrive on the roots of some plants. These bacteria convert nitrogen into ammonium. The fixation process itself does not induce a large fractionation (about 0–2‰ shift); however, further assimilation of ammonium into the nitrogen metabolism can have a considerable effect, with a range from 0 to a 27‰ shift. The bacterial nitrification/denitrification processes of the biomass also yield depleted nitrogen with −10 to −40 $\delta^{15}N$‰ vs air. Conversely, fractionation during mineralization is close to zero. Synthetic fertilizers, which exhibit enrichments close to 0‰ vs air, induce correspondingly depleted nitrogen values in the agricultural products on which they have been used. The $\delta^{15}N$ enrichments in plants is also influenced by the plant species (e.g., clover is known to be depleted in ^{15}N), the type of soil in which the plant is grown (which can influence all of the mineralization, nitrification and denitrification processes that occur), and the type of fertilizer that has been applied (mineral or organic N). In animals, the $\delta^{15}N$ enrichments are known to increase with increasing feeding position in the food chain (trophic level). In marine systems, predatory fish have higher values (+8.5‰) than omnivorous fish (+7‰), and omnivorous fish themselves have higher values than marine particulate organic matter (+5‰) (Fry, 1988).

Sulfur

The rules underlying sulfur $\delta^{34}S$ enrichment in plant and animal products are less clearly understood than for the other isotopes. It is known that natural fractionation occurs at several steps during the metabolism of sulfur. Fractionation occurs first during exchange reactions between sulfates and sulfides, followed by kinetic isotopic effects due to the bacterial reduction of sulfate, and finally by precipitation of sulfates in seawater. The isotopic composition of sulfur from plants is influenced by the geological structure, the atmospheric deposition of sulfur, and the use of sulfur-containing fertilizers and sulfate-rich sea sprays in coastal locations (Wagner, 2005). No changes of sulfur isotopic enrichments have been recorded in animals along the trophic chains.

Equipment and instruments

Isotope ratio mass spectrometer

Mass spectrometers for isotope ratio measurements uses dedicated static magnetic sector fields and multi-collection with discrete *Faraday cups* for the simultaneous quantification of all ion beams with precision in the determination of isotopes in the sub ppm range (Figure 9.1). The ion source is optimized for the ionization of simple gases like CO_2, N_2, CO, H_2 and SO_2. Consequently, all samples have to be converted into simple gases prior to transfer into the isotope ratio MS (IRMS). This concentrates the isotope information into a few ion beams, which is one of the fundamental steps in reaching the very high precisions required to detect natural isotope variations.

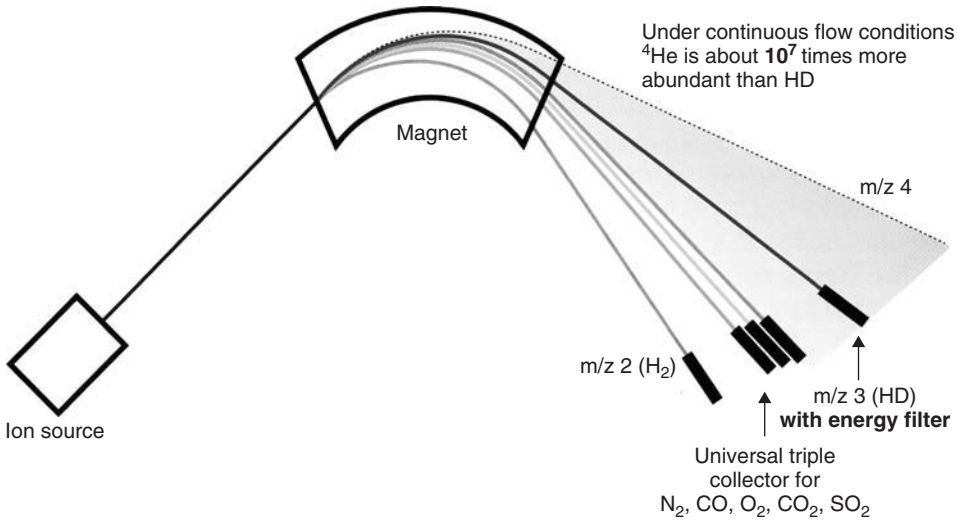

Figure 9.1 Isotope ratio mass spectrometer with ion source, magnet and the array of Faraday cups for simultaneous isotope detection.

The variety of isotope ratio MS applications originates from the different strategies of converting organic and inorganic matter into gases. Technologies such as gas chromatography (GC), liquid chromatography (LC) and elemental analyzer (EA) can be coupled in parallel with a single isotope ratio MS, as they all use the same open split interface for the final transfer to the mass spectrometer.

Ionization

Ion sources applied in IRMS use a "closed source design", which ensures a high yield of ions. The only major exit for gas molecules and ions is the entrance slit into the analyzer. Ion production efficiencies of modern isotope ratio MS range from 500 to 2000 molecules per ion, i.e. the number of molecules required to yield one ion. On the other hand, molecules which are not ionized must leave the ion source fast enough to maintain the performance of transient signals applied from chromatographic preparation devices.

Molecules are ionized by bombardment with electrons (electron impact ionization, EI) forming positively charged ions such as CO_2^+ ($M + e^- \rightarrow M^+\bullet + 2e^-$). Electrons are released from a hot filament made from tungsten, rhenium or thoriated iridium. The electrons are accelerated by electrostatic potentials to strike the gas molecules with a collision energy of between 50 and 150 eV, and a homogeneous magnetic field of 100 to 500 Gauss is used to keep the electrons on a spiral path to increase the ionization probability. Ions are extracted vertical to the direction of the electron beam by a field generated by a repeller potential, an outside extraction lens, or a combination of both.

Two basic modes for the extraction of ions from the ion source are available. In the *dual inlet* mode, a low extraction potential minimizes the translational energy spread of ions entering the ion optics, resulting in the highest stability of the isotope ratios measured. In contrast, longer residence times of ions in the source result in ion molecule

Table 9.1 Most common masses for isotope ratio determination

Isotope	Corresponding pure gas	Ions (m/z)
δ^2H	H_2	2, 3
$\delta^{15}N$	N_2	28, 29, 30
$\delta^{18}O$	CO	28, 29, 30
$\delta^{13}C$, $\delta^{18}O$	CO_2	44, 45, 46
$\delta^{34}S$	SO_2	64, 66

reactions which reduce the isotope ratio linearity, i.e. the constancy of an isotope ratio in relation to changing signal intensities. This requires static signals with matching signal heights of sample and reference gases, as used in dual inlet applications. In the *continuous flow* mode, high extraction potentials result in very low residence times of the formed ions and deliver the required isotope ratio linearity for all chromatography-based applications, which submit transient signals in a helium carrier stream into the IRMS.

After extraction from the source region, the ions are typically accelerated by 2.5–10 kV to form an ion beam which enters the magnetic sector analyzer through the entrance slit.

Mass separation

Electromagnets are generally used in commercial isotope ratio mass spectrometers to allow a fast switch of the magnetic field from the masses of H_2 to CO, and N_2 to CO_2 (see Table 9.1), but also to monitor background ions like m/z 18 (H_2O) and m/z 15 (CH_4), which are indicators for the quality of different continuous flow conversion techniques. The magnetic field deflects the accelerated ions vertical to their flight direction and vertical to the magnetic field. Ions with the same kinetic energy and charge are deflected in relation to their masses, such that an ion with a small mass describes a smaller radius than an ion with a higher mass. Small instruments serve a mass range of up to m/z 70 with separation of adjacent masses. Larger instruments expand this range to m/z 130 and higher. They apply a higher accelerating voltage, giving higher sensitivity, higher resolution and better peak shapes than instruments with a lower accelerating voltage.

Multiple ion collection

The measurement of isotope ion currents is performed simultaneously for each isotope, using dedicated Faraday cups with individual amplifier electronics. This is done in order to cancel out ion beam fluctuations due to temperature drifts or electron beam variations. It is the only way that the required high precision can be achieved. Standard collector set-ups to individual arrays of multiple discrete Faraday cups along the focal plane allow a great variety of simultaneous isotope and molecular ratio measurements.

Universal triple collector

The most commonly used collector array is a combination of two wide Faraday cups with a narrow Faraday cup in the middle, as shown in Figure 9.2. This combination

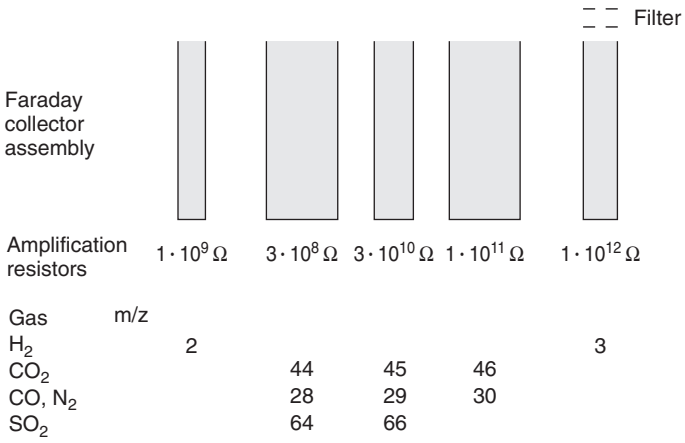

Figure 9.2 Typical Faraday cup arrangement for measurement of the isotope ratios of the most common gas species.

allows the universal measurement of all isotope ratios in C, N, O and S required in life sciences. The amplification of the different ion currents is defined by high-ohm resistors that amplify all the signals into the dynamic range of the integration and conversion electronics. For example, the amplifications of the three masses of CO_2 (44, 45, 46) are respectively 1, 100 and 333, according to the natural abundance of the major isotopes ^{12}C ,^{13}C, ^{16}O, ^{17}O, ^{18}O.

Hydrogen collector

For the measurement of HD/H_2, two additional cups are used either on a separate focal plane on a small radius at a magnet field strength similar to that used for C, N, O isotopes, or on the same focal plane as the universal triple collector. In this case, a lower magnetic field strength should be applied. The latter allows the positioning of an energy discrimination filter in front of the m/z 3 cup. In continuous flow applications measuring HD/H_2 in helium as a carrier gas, the contribution of low-energy m/z 4 (He^{+}•) ions would interfere with the very small signal of HD ions on m/z 3. Therefore, an energy discrimination filter rejects all ions with kinetic energies lower than the used acceleration voltage. This way, a clean m/z 3 ion beam is channeled to the collector (Brand, 2007).

Data acquisition and processing

Continuous and simultaneous data acquisition from all relevant ion beams without any loss of information from any collector is one of the basic features of isotope ratio mass spectrometers. In classical applications with static signals, the ion currents can be accumulated over several seconds, then digitalized and stored. In continuous flow applications, transient chromatographic signals require a time resolution $\geqslant$5 Hz. Fast switching buffer systems ensure the continuous integration of each chromatographic trace.

Table 9.2 Isobaric interferences when measuring $\delta^{13}C$ and $\delta^{18}O$ from CO_2

Ion (m/z)	Isotope composition
44	$^{12}C^{16}O^{16}O$
45	$^{13}C^{16}O^{16}O$, $^{12}C^{16}O^{17}O$
46	$^{12}C^{16}O^{18}O$, $^{12}C^{17}O^{17}O$, $^{13}C^{16}O^{17}O$

Several mathematical corrections on the acquired data are conducted by the isotope software and data system. Electronic and chemical backgrounds are determined and subtracted according to applications with static or transient signals. Interferences from other isotope species of the same mass require the determination of additional masses to allow the quantification of the interfering species and its correction. Algorithms for a fully automated correction of isobaric ion contributions are implemented in modern IRMS data systems. For example, three collectors for masses 44, 45 and 46 are necessary for the determination of $d^{13}C$ (see Table 9.2). To determine and cancel the isobaric interference of $^{12}C^{16}O^{17}O$ on m/z 45, the m/z 46 signal has to be measured. This information is used, together with the knowledge of the theoretical relationships between ^{17}O and ^{18}O in CO_2, in order to correct the m/z 45 signal (Santrock *et al.*, 1985).

When molecules like H_2O and H_2 are ionized in a mass spectrometer they have the ability to protonate other molecules, forming MH^+ ions. This leads to a higher signal in the M + 1 ion beam, and would result in an artificially higher isotope ratio if no correction was applied. Consequently, water backgrounds have to be low and stable in IRMS in order to be cancelled out by the sample-to-reference comparison. When H_2 is ionized in the IRMS, some H_3^+ ions are formed which cause isobaric interference to the HD ion. Since H_3^+ formation is related to the amount of H_2 applied, the H_3^+ factor can be determined and corrected for. The H_3^+ factor is required to be low and very stable over long periods of time.

When chromatography is used as part of the continuous flow IRMS application, separation of the isotope species of a given compound (isotopomers) can take place in the GC column. Because of the lower molar volume of the heavier components and the resulting differences in mobile/stationary phase interactions, heavier components can elute slightly earlier from a chromatographic column (Matucha *et al.*, 1991). Figure 9.3 shows the chromatographic elution profiles of CO_2 derived from an organic compound by combustion isotope ratio MS. The difference in elution time is usually less then 0.1 s. The software measures the separation and corrects it during calculation of the isotope ratios. Continuous flow applications make special use of the chromatographic isotope separation effect by displaying the typical S-shaped ratio traces during analysis. This information is used to check the integrity of a GC peak.

Sample preparation devices and interfaces

In isotope ratio MS, all organic and inorganic compounds have to be converted into simple gases such as CO_2, N_2, CO, H_2 and SO_2. The technology of a preparation

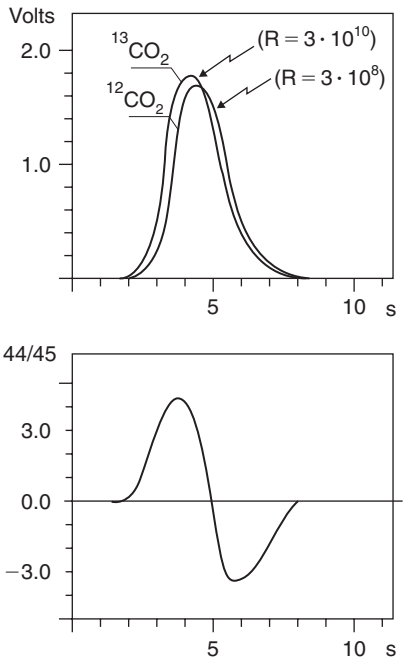

Figure 9.3 Chromatographic elution profiles of CO_2 derived from an organic compound by combustion isotope ratio MS (top) resulting in the typical S-shaped isotope ratio trace of masses 45/44 (bottom).

device is closely related to the interface and its transfer mode. The latter is either a dual inlet system with a change-over interface for the viscous flow transfer of off-line prepared sample gas, or open split interfaces with continuous flow transfer submitting transient sample peaks transported in a helium gas stream.

Viscous flow isotope ratio MS

The classical way of analyzing samples in an IRMS is by the expansion of a clean gas from a container into the sample volume of a dual inlet system. The reference volume of the dual inlet system is filled with a reference gas of known isotope ratio. Both gases are transferred under viscous conditions through stainless-steel capillaries to a change-over valve. Sample and reference are admitted alternatively to the ion source or a waste-line pump by the change-over valve. By compression or expansion of the sample and reference volumes, the transferred amount of gas is adjusted to achieve matching signal intensities to rule out any signal size dependent effects.

HDO water equilibration

In a water equilibration system which is linked to a dual inlet mass spectrometer system, samples are filled in glass containers, which are either linked via individual valves to a manifold system or closed by septa for later transfer using an autosampler. The sample containers are then carefully evacuated and the headspace is filled with CO_2 for $d^{18}O$ determination or H_2 for d^2H determination. The samples are kept

at a stable temperature for a defined period of time so that isotopes in the water can equilibrate with the gas in the headspace. For H_2 gas analysis, a platinum catalyst is required. Equilibration takes about 8 hours for ^{18}O and less than 1 hour for ^{2}H. Temperature stability, gas tightness and efficient removal of water during the gas transfer into the dual inlet system are mandatory. Equilibration systems can be used for samples with high contamination of organic materials, as only the water exchanges its isotope information with the gas. Samples applied are usually in the range of a few milliliters. Other preparation devices such as carbonate preparation devices, which can also be linked to a dual inlet system, are not usually used for food authenticity control and will not be described here.

Continuous flow isotope ratio MS

Continuous flow isotope ratio MS is defined by the use of a helium carrier gas stream coupled with an open split interface for the transfer of sample into the IRMS. Chromatographic separation is usually involved in continuous flow applications either before or after the conversion process. In compound-specific isotope analysis, complex mixtures of organic compounds are separated by gas chromatography (GC) or by liquid chromatography (LC) prior to the on-line conversion of each compound into a simple gas like CO_2. The design of the interface makes it possible to preserve the chromatographic resolution of the complete sample. In bulk stable isotope analysis, the entire sample is converted into simple gases using conventional elemental analyzers (EA) or special high-temperature elemental analyzers (TC/EA). The simple gases produced (CO_2, N_2, H_2, CO and SO_2) are thereafter subjected to chromatographic separation. This allows the analysis of more than one gas, and accordingly a multiple isotope ratio analysis, by applying just one single sample to flash combustion or high-temperature conversion. A comparison of the experimental set-ups for bulk stable isotope analysis (BSIA) and compound specific isotope analysis (CSIA) is shown in Figure 9.4.

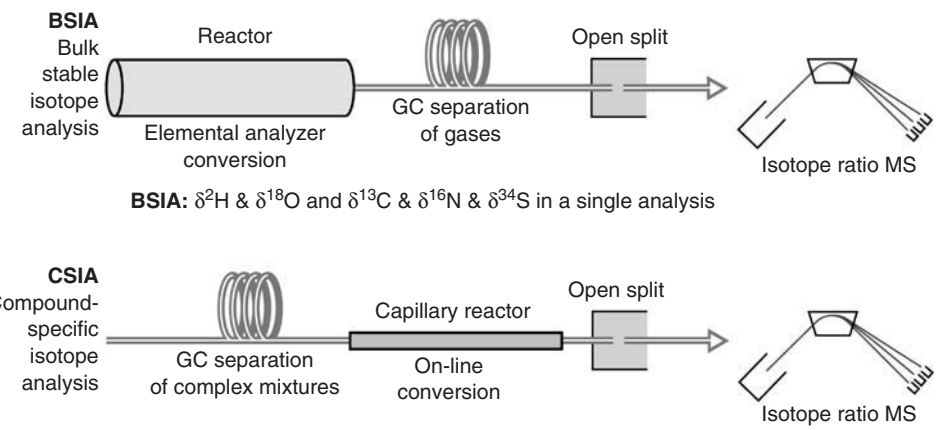

Figure 9.4 Comparison of bulk stable isotope analysis (BSIA) and compound-specific isotope analysis (CSIA).

In all continuous flow applications coupled to isotope ratio MS, an open split interface is mandatory to provide the required long-term pressure stability in the gas ion source of the isotope ratio MS. Reference gases of known isotope ratio are applied through a separate open split, thus eliminating all effects on both the sample and the reference. The precision of the measurement is greatly improved by relating the isotope ratios of the sample directly to those of the reference at each run. Additional functions, such as combustion, reduction, high-temperature conversion, chromatography, removal of water and helium dilution, can be part of such interfaces. From the open split, the analyte gases transported in the helium carrier are transferred through fused silica capillaries into the isotope ratio MS. Hence, more than one interface can remain coupled in parallel to the isotope ratio MS.

Basic interface technology

Open split

For high-precision isotope ratio determination, the ion source pressure must be kept absolutely constant. For this reason, each continuous flow system has to be interfaced to the IRMS via an open split. The basic principle of an open split is to pick up a minor part of the helium/sample stream by a transfer capillary at ambient pressure – i.e. an open tube or a wide capillary – and transfer it into the IRMS. A helium stream added separately ensures protection from ambient air. Retracting the transfer capillary into a zone of pure helium allows either cutting out parts of the chromatogram or carrying out maintenance of the interface, such as release of CO_2 trapped in $d^{15}N$ mode. In all modes a constant flow of helium into the IRMS and consequently constant ion source conditions are maintained.

Dilution

Because there is considerable variability in nature in the relative amounts of C, N, H, O and S, and because the ionization efficiencies of the analyte species (CO_2, N_2, H_2, CO and SO_2) differ significantly, applications in EA-IRMS have to be managed in a large and variable dynamic range. Helium can be used to dilute large sample peaks. The dilution happens in the open split, at the very last point before transfer into the ion source, in order to eliminate any possible effects on the integrity of the sample gas (Figure 9.5). Because the carrier gas flow rates of EA are of the order of 90 ml min^{-1}, a dilution of 1 : 100 of the direct output of the EA would require 9000 ml min^{-1} of dilution gas. To miniaturize the open split design and to reduce helium consumption a pre-split removes most of the EA effluent, and therefore dilutions up to 1 : 100 can be served with low amounts of helium. In combination with the dynamic range of the IRMS, a wide total sample size range can be covered, as similar but even more automated dilution techniques are available when using devices with the multiple loop injection technique.

Referencing

In IRMS, measurement of isotope ratios requires that sample gases be measured relative to a reference gas of known isotope ratio. This is the only way to achieve the required

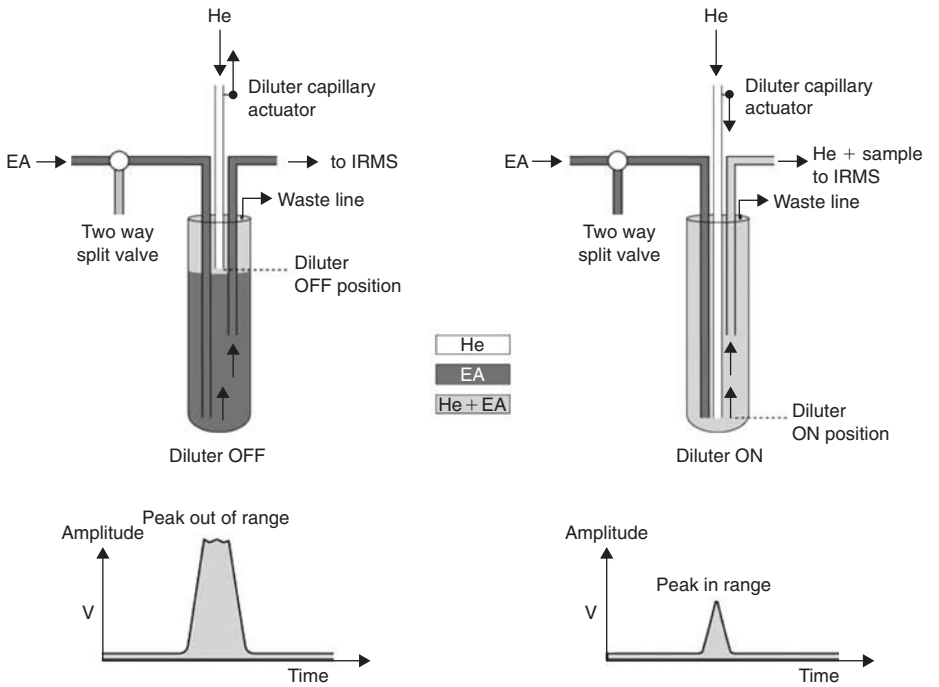

Figure 9.5 Use of the open split to obtain an adequate dilution.

precision of <1.5 ppm for, for example, ^{13}C (0.15‰ in the δ-notation). For the purpose of sample-standard referencing, a cylinder of calibrated reference gas can be used for extended periods of time. An inert fused silica capillary supplies the reference gas in the µl min^{-1} range into the miniaturized mixing chamber. Under software control, this capillary is lowered into the mixing chamber for, for example, 20 s, thus creating a helium–reference gas mixture which flows into the IRMS via a second gas line. This generates a rectangular, flat-topped gas peak without changing any pressures or gas flows (Figure 9.6). The use of reference gases instead of reference bulk material for standardization reduces the operational costs by almost 50% while increasing the sample throughput by almost 50%. The reference gas consumption is negligible, and thus gases can be kept trickling continuously, ensuring constant conditions in the supply lines and pressure regulators. The reference gases used are pure nitrogen (N_2), carbon dioxide (CO_2), hydrogen (H_2), carbon monoxide (CO) and sulfur dioxide (SO_2) (Werner and Brand, 2001).

Elemental analyzer – isotope ratio MS (EA-IRMS)

The most widely used continuous flow application is the coupling of an elemental analyzer (EA) to an isotope ratio MS (IRMS). It is estimated that almost half of all IRMS systems currently in use are coupled to an EA. Most importantly, the complete sample is first converted into gases, followed by their chromatographic separation. This allows isotope ratio analysis of more than one element in the sample, resulting in multiple element isotope ratio analysis.

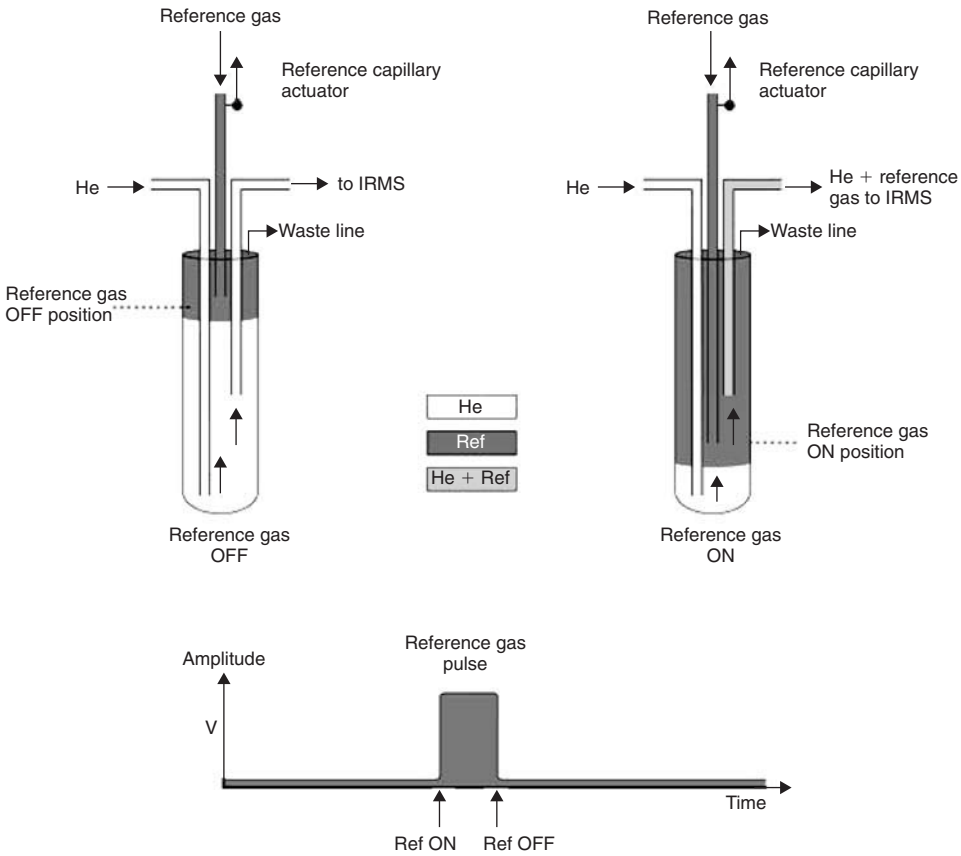

Figure 9.6 Production of the reference gas peak.

Two basic conversion techniques are applied: *Dumas combustion*, using a conventional EA, and quantitative high-temperature conversion, using a specific EA (i.e. the TC/EA). This technique is also known as high-temperature carbon reduction or quantitative high-temperature pyrolysis (Werner *et al*., 1999).

Combustion for ^{13}C, ^{15}N and ^{34}S determinations

The first fully automated elemental analyzer was introduced in 1968. Almost 20 years later, the first direct coupling of the EA to an IRMS was reported. It needed another 10 years for the breakthrough of this technique to provide C and N isotope ratios from a single sample as well as providing S isotope ratios from inorganic and organic bulk samples.

The complete sample conversion is achieved by an additional pulse of oxygen for optimum combustion delivered into the reactor before admitting the sample, which is wrapped inside a tin capsule. The exothermic character of the reaction of the tin leads to a temperature of up to 1800°C for a few seconds, providing a flash combustion. NO_x formed during combustion is subsequently reduced on copper to N_2. H_2O produced by the combustion is removed in a chemical trap, followed by the

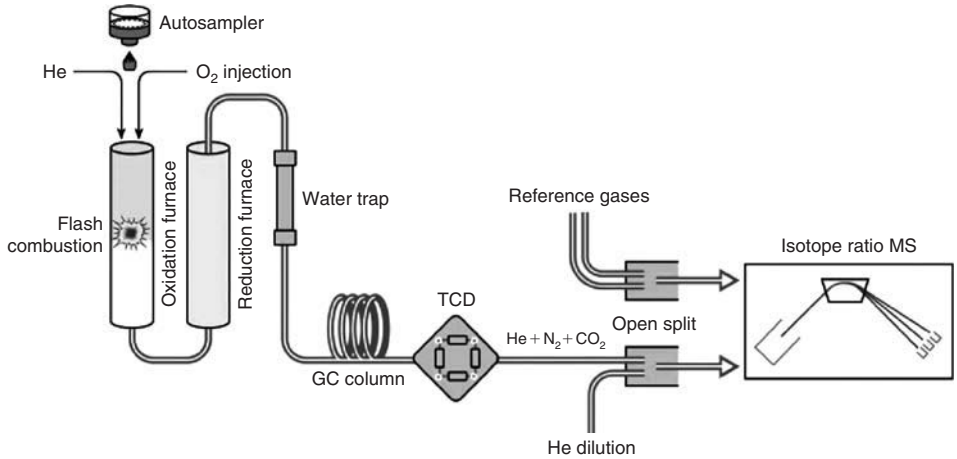

Figure 9.7 Configuration of the elemental-analyzer IRMS system. The sample first undergoes flash combustion followed by a reduction. After drying, the gases are separated in a chromatographic column. The effluent gases are diluted to the adequate concentration before their introduction into the IRMS system.

separation of the gases in a packed isothermal GC column. The isotope ratios $^{13}C/^{12}C$, $^{15}N/^{14}N$ and $^{32}S/^{34}S$ can be measured simultaneously on the produced N_2, CO_2 and SO_2. The typical configuration of an EA-IRMS is shown in Figure 9.7.

Although EA-IRMS is slightly less precise than the dual inlet viscous flow technique, its greater ease of use and simplicity are significant advantages when compared with the time-consuming and frequently operator-biased off-line preparation of clean gas samples required by the dual inlet techniques. The low-cost and high-throughput analysis with a quite high overall precision has revolutionized the isotope ratio analysis of bulk samples.

A standard sample size for bulk carbon and nitrogen isotope ratio analysis is in the range of 20 to 100 µg. Below 20 µg, the carbon blank from the tin capsules starts to get into the same range as the sample itself. Hence, samples smaller than 20 µg can be admitted using silver capsules, which have a considerably lower carbon blank.

For small nitrogen contents, the gas tightness of the autosampler providing the solid samples as well as the purity of the oxygen applied play the most important role. Specific autosamplers and sample introduction techniques with almost no nitrogen blank allow achievement of the low µg level, and even levels of less than 1 µg of nitrogen in samples like specific soil and sediment samples.

Quantitative high-temperature conversion for ^{2}H and ^{18}O

Quantitative high-temperature conversion, also referred to as high-temperature pyrolysis, is a new technique in which oxygen present in a compound is converted to CO, and hydrogen contained in a compound is converted to H_2 (Figure 9.8). The process is rapid and quantitative in a reducing environment at high temperatures, typically exceeding 1400°C. In combination with an open split interface for referencing, and

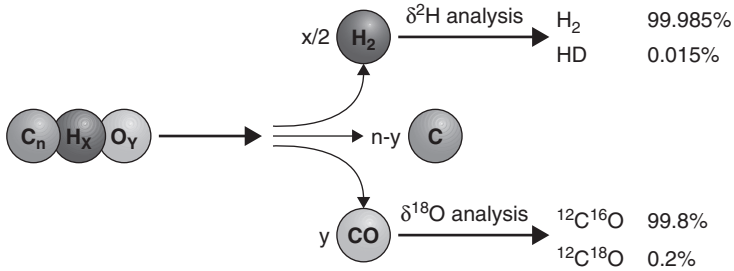

Figure 9.8 High-temperature conversion: The oxygen present in a compound is converted to CO, and hydrogen is converted to H_2. Excess carbon is deposited as glassy carbon.

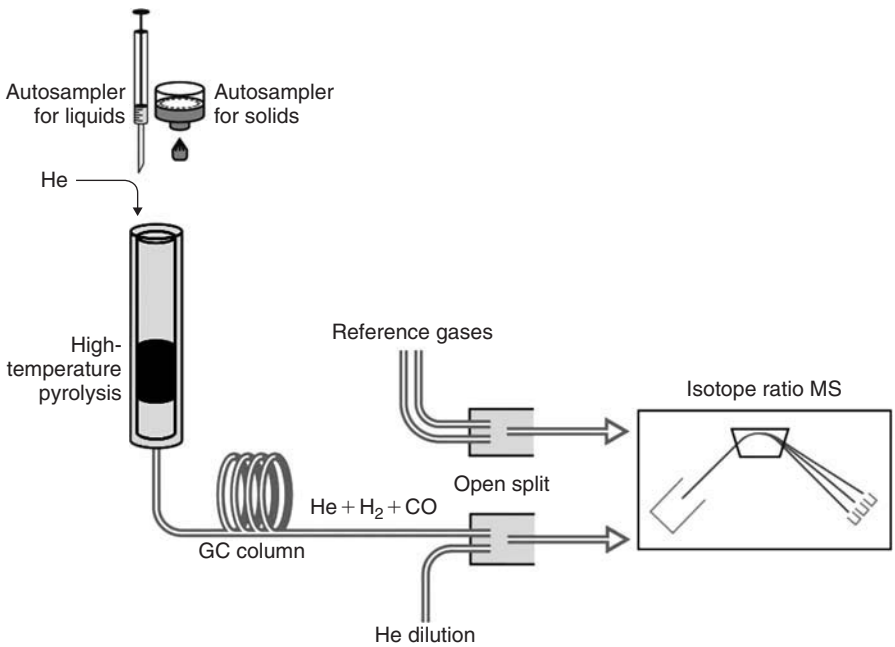

Figure 9.9 High-temperature conversion elemental analyzer.

automated dilution, this set-up facilitates the conversion reaction, isothermal separation of reaction gases, transfer into the IRMS and referencing against standard gases (Figure 9.9). The high-temperature conversion reactor consists of a glassy carbon tube with a glassy carbon filling, ensuring that neither sample nor reaction gases come into contact with oxygen-containing surfaces (e.g. Al_2O_3) while at high temperatures. This is the only technology that enables memory-free conversion reactions with no restrictions on compound type.

The chromatographic separation of H_2 and CO, in combination with a modern isotope ratio MS capable of HD on-line operation and fast magnet jump, gives way to simultaneous hydrogen and oxygen isotope ratio determination of all organic compounds. Due to its high operation temperature, restrictions of individual sample

classes do not exist. Selected inorganic compounds can also be analyzed, such as nitrates, phosphates, sulfates and even biotites. The most prominent high-temperature application is the isotope ratio analysis of hydrogen and oxygen in water samples. For this application, an autosampler for liquid samples and a septum-equipped injector is used on top of the EA. Typical sample amounts for water are $<0.5\,\mu l$. The analysis of smaller water samples depends on the quality of the syringe transfer and injection technique. Both isotope ratios can be determined within the same injection, making this set-up perfectly suitable for high-throughput doubly-labeled water analysis or screening of water resources. The typical measurement time is about 5 minutes per sample for oxygen and less than 3 minutes for hydrogen isotope ratio determination. A determination of both isotope ratios in one run takes about 6 minutes (Werner, 2003).

Gas chromatography–isotope ratio MS (GC-IRMS)

Beside the bulk analysis of samples for isotope ratio MS investigation, the *compound-specific isotope analysis* (*CSIA*) carries unique additional isotope information regarding natural and also synthetic processes. Such a GC combustion interface consists of a state-of-the-art gas chromatograph for capillary fused silica columns, which can separate highly complex compound mixtures (Figure 9.10). Samples are submitted by a variety of available injector types, such as the split/splitless injector for flash evaporation in an inert chamber with split or total sample transfer onto the capillary column. The design of the vaporization chamber ensures wide linearity even with relatively large sample sizes. Cold on-column and programmable temperature vaporizing injectors give access to a discrimination-free and thermal degradation-free sample introduction into the capillary column with the highest GC performance. Detectors such as the *flame ionization detector* (*FID*) can be run in parallel for additional sample information in modes like ^{15}N and ^{18}O application.

Today, all injection modes can be automated by using autosamplers for liquid and gas head-space injections. In addition, more specific automated GC injection

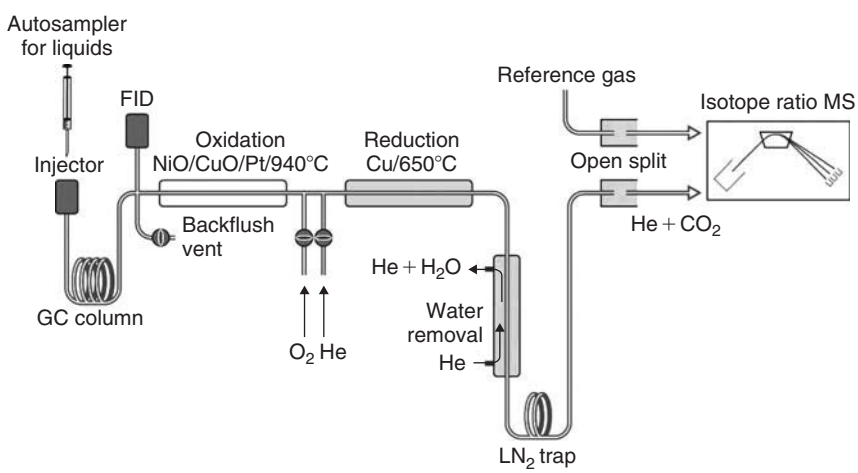

Figure 9.10 GC combustion interface.

techniques, such as heated head-space, solid-phase microextraction (SPME), thermal desorption, and purge and trap, can be applied to cover the full range of GC samples. More specific loop injection systems also coupled with cryogenic pre-concentration techniques give access to low ppm- and even ppb-level trace gases (e.g. CO_2, CH_4, N_2O and CO).

The conversion of compounds into the simple gases H_2, CO_2, N_2 or CO, which is mandatory for high-precision compound-specific isotope ratio analysis, subsequently erases any direct structural information. The integration of a quadrupole mass specific detector together with a GC combustion interface allows the parallel acquisition of structural information and high-precision isotope ratio determination within a single GC analysis.

Combustion for ^{13}C and ^{15}N determination

GC-combustion IRMS for the determination of $^{13}C/^{12}C$ was first proposed in 1984, and the capability of analyzing $^{15}N/^{14}N$ was added in 1992. All compounds eluting from a GC column are oxidized in a capillary reactor to CO_2, N_2, and H_2O at 940 to 1000°C. NO_x produced in the oxidation reactor is reduced to N_2 in a capillary reduction reactor at 650°C. The H_2O formed in the oxidation process is usually removed by an on-line water-removal system using a water permeable polymeric capillary. For the analysis of $^{15}N/^{14}N$, all CO_2 is retained in a liquid nitrogen trap before transfer into the isotope ratio MS through an open split interface (Brand *et al*., 1994; Merritt *et al*., 1995).

Due to the capillary design of the reactor, which ensures maintenance of the GC resolution, all solvents have to be removed before the oxidation furnace. Ideally, a backflush system reverses the flow through the oxidation reactor towards an exit directly after the GC column to cut off all eluting solvent. After elution of the predominant solvent peak, the backflush is set off for a direct transfer of each compound eluting from the GC column straight through the reactors into the isotope ratio MS.

High-temperature conversion for ^{2}H and ^{18}O determination

Quantitative pyrolysis or high-temperature conversion (GC-TC) was introduced in 1996 for the determination of $^{18}O/^{16}O$ ratios, and was followed by D/H ratio determination in 1998. This occurred simultaneously with the development of an isotope ratio MS using an energy filter for the m/z 3 collector suppressing the low energy $^{4}He^{+}$ ions, which would otherwise corrupt the HD^{+} signal.

Quantitative pyrolysis by high-temperature conversion of organic matter for the conversion of organic O and H to CO and H_2 requires an inert and reductive environment at very high temperatures, to prevent any H- or O-containing materials from reacting or exchanging with the analyte. Because quantitative conversion is achieved in the reactor, no additional clean-up is required.

For the determination of $^{18}O/^{16}O$, the analyte must not come in contact with the ceramic tube which is used to protect against air, and for stability. The pyrolysis takes place in an inert platinum inlay. Due to the catalytic properties of the platinum, the reaction can be performed at 1280°C. Depending on the number of C, O and H

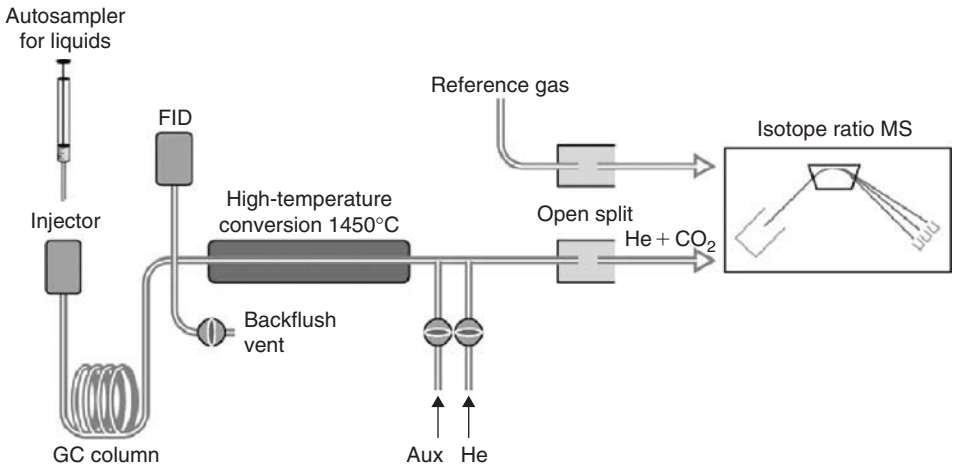

Figure 9.11 GC high-temperature conversion interface.

atoms in the molecule, CO and H_2 plus a carbon deposit are formed. Although all organic structures can be converted with good GC performance and precision for $d^{18}O$ analysis, some compounds show an offset, which requires internal referencing by compounds with a known isotope ratio.

For the determination of D from organic compounds, the reaction is performed in an empty ceramic tube at 1450°C. Tests have shown that such high temperatures are required to ensure quantitative conversion. The use of a catalyst must be avoided to eliminate the risk of adsorption of H_2, which would lead to temperature-dependent fractionation. The GC-TC reactor is catalyst-free, and therefore eliminates fractionation during high-temperature conversion. Even CH_4 can be converted with completely reproducible and linear results (Burgoyne and Hayes, 1998). The configuration of the GC-TC-IRMS system is shown in Figure 9.11.

Liquid chromatography–isotope ratio MS (LC-IRMS)

With the introduction of compound-specific isotope analysis by GC coupled to isotope ratio MS, the immediate demand for similar applications using HPLC was created. In GC combustion the carrier is helium, which does not interfere with the essential combustion step prior to isotope ratio MS. On the other hand, the liquid mobile phase has prevented a similar direct conversion. Earlier LC isotope ratio MS approaches were based on the removal of the liquid phase prior to combustion, thus risking fractionation of the isotope ratios of the eluted compounds. The new concept for coupling HPLC with IRMS leaves the compounds in the effluent and oxidizes them in the liquid phase. The resulting CO_2 compound peaks are then separated from the effluent and analyzed with the IRMS (Krummen *et al.*, 2004). The configuration of the LC-IRMS system is shown in Figure 9.12.

Such a preparation device using the aqueous phase as a carrier can be used in either of two operational modes, for compound-specific isotope analysis (HPLC

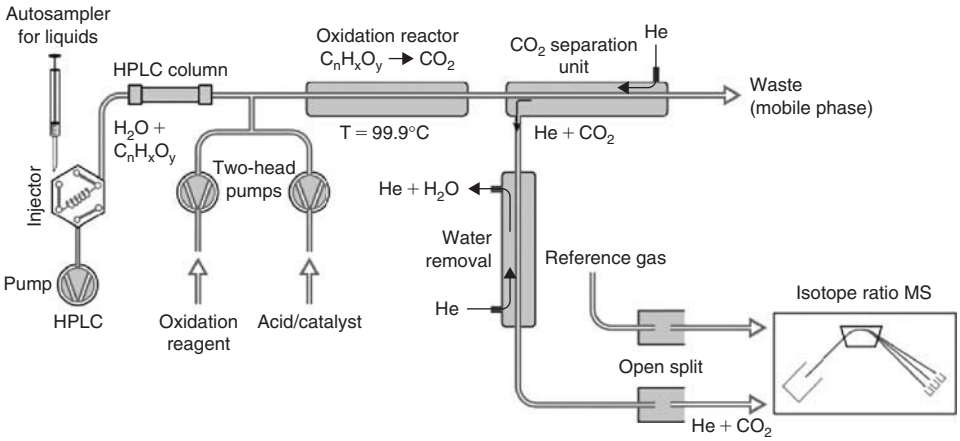

Figure 9.12 HPLC with chemical conversion device and interface.

mode) and for bulk stable isotope analysis (μ-EA mode). In the HPLC mode, samples are injected by a loop injection valve in front of the HPLC column. The mixture of organic compounds in the sample is separated at the HPLC column, and the constant flow of the mobile phase is maintained through the oxidation system. The direct injection mode (μ-EA mode) provides a fast analysis of all water-soluble materials which are injected after the HPLC column, and is thus a bulk measurement.

A constant aqueous mixture of oxidation reagent (peroxodisulfate) and phosphoric acid is added to the mobile phase prior to the capillary oxidation reactor, which operates at 100°C. All organic compounds are converted individually and quantitatively into CO_2 without isotope fractionation. When leaving the oxidation reactor, the mobile phase is cooled and individual CO_2 peaks are separated from the liquid phase by a membrane exchanger. The CO_2 is transferred into a counterflow of helium with close to 100% degassing efficiency. The individual CO_2 peaks transported in the He stream are subsequently dried in an on-line gas-drying unit (Nafion™) and then admitted to the isotope ratio mass spectrometer via an open split, as illustrated in Figure 9.12. LC-IRMS give direct access to compound-specific $d^{13}C$ information of all water-soluble molecules, such as sugars, amino acids, short-chain organic acids and alcohols.

Multiple loop injection–isotope ratio MS

Continuous flow (CF) preparation devices and interfaces with multiple loop injection apply strategies of the "classical" dual inlet systems to achieve high analytical precision and accuracy. Multiple analyses of sample gas pulses without interruption of the sample transfer increases the statistical significance of the final mean value. Internal reproducibility of the individual measurements, which is a commonly used measure of analytical quality, is added to CF-IRMS. Drawbacks of the dual inlet system, like off-line sample preparation and purification, ineffective use of the sample gas, contamination with other gases, lengthy data acquisitions, and cost, are overcome. All sorts of head-space samples, including water equilibration, carbonates and atmospheric gases (e.g. CO_2, O_2, N_2) can be handled.

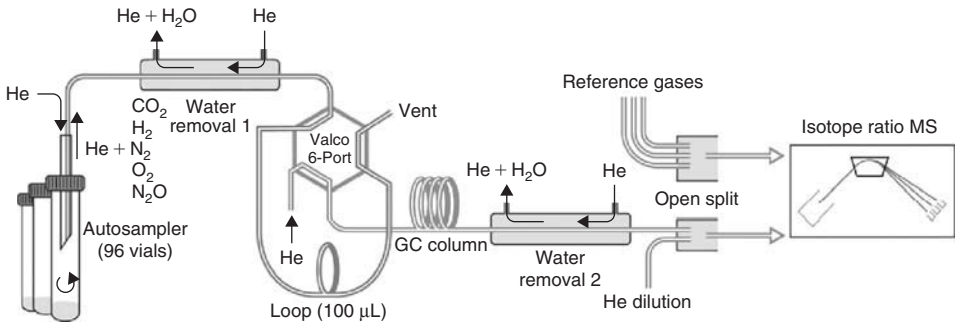

Figure 9.13 Multiple loop injection interface.

The gas sampling system includes a two port needle which adds a gentle flow of helium into the sample vial, thus diluting and displacing sample gas. Water is removed from the sample gas through diffusion traps. The loop injector aliquots the sample gas onto a GC column, which separates the molecular species. The dual inlet principle of repetitive measurements of sample and standard gas is not only retained but also generalized. The sample volume is the sample vial (instead of a metal bellows), and the reference gas volume is a pressurized gas tank. The sample gas is transported in helium, which allows GC separation and facilitates fractionation-free transport of the sample aliquots (Figure 9.13). In a typical experiment, 10 aliquots of the sample will be taken from the sample vial, dried and cleaned online, and measured against reference gas pulses. The sample consumption is much lower than for the dual inlet system, while comparable precisions are achieved, including an analysis of internal reproducibility.

Multiple loop injection adds the unique property in continuous flow to evaluate and adjust the response of an unknown sample gas. If the signal height of the first sample peak exceeds a pre-defined threshold, the diluter is activated, resulting in a three-fold reduction in signal height for the subsequent sample peaks. This allows the analysis of samples that would otherwise be too large to be measured. The dilution is performed in the open split, just before transfer into the ion source, eliminating any possible effects on the integrity of the sample gas (Figure 9.14).

An application of the multiple loop injection technique is the measurement of the D/H and $^{18}O/^{16}O$ ratios of water. There is a very diverse range of applications, ranging from studies of variations in natural isotope abundance in the hydrologic cycle to authenticity control of beverages, to metabolic studies using D- or ^{18}O-enriched tracers in humans and animals. This extreme range of sample types demands a flexible, general-purpose analytical solution, which can provide high precision, high accuracy and high throughput analysis of $^{18}O/^{16}O$ and D/H. Aqueous samples of <0.5 ml are placed in 10-ml screw top vials using disposable pipettes. For D/H, a platinum catalyst is added. The vials are sealed with septa, and all air is removed from the sample vials by an automated, autosampler-assisted flushing procedure which uses a mixture of either H_2 or CO_2 in helium. The H_2 or CO_2 in the flushing helium stream is used as equilibration gas. After the required equilibration time (D, 40 min; ^{18}O, 20 h) the

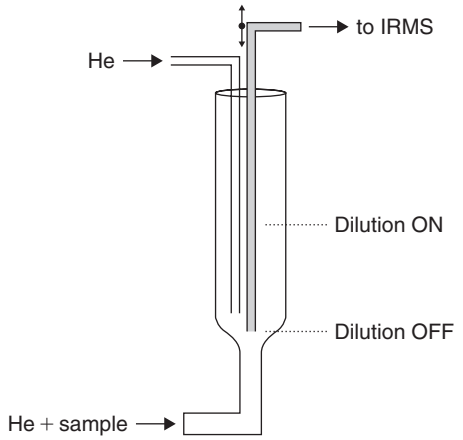

Figure 9.14 Open split with automatic dilution capability.

whole batch of samples is analyzed. The use of repetitive loop injection (1–2 min per replicate) achieves analytical precision comparable to that of a dual inlet system.

Recent applications in food authenticity

The following sections are written based on a literature search on the application of light stable isotopes to authenticity by considering publication dates starting from 1999 to the present day. Literature in this field published before this date has been comprehensively reviewed by Rossmann (2001) and Kelly (2003), and is not covered here.

Tracing the geographical origin of foods

As mentioned in a previous review (De la Fuente and Juarez, 2005), natural isotope fractionation might be the best answer regarding the question of assessing the geographical origin of food. This technique has been used recently for matrices such as milk and milk products, fruits, vegetables, juices, meat, cereals, wine and pistachios, as reported here.

Meat

In a preliminary study of lamb meat, the variables $\delta^{15}N_{protein}$, $\delta^{13}C_{protein}$ and $\delta^{13}C_{fat}$ were proposed by Piasentier *et al*. (2003). Samples were collected from six EU or EFTA countries spanning from Italy to Iceland from animals kept on several typical diets (milk, pasture, cereals). Carbon data were found to be correlated with the feeding regime. By nitrogen data, lower values of $\delta^{15}N_{protein}$ were found for Iceland (1.9–3.2‰) than for the other countries (3.7‰ to 8.0‰) for animals receiving a similar diet. The rate of correct attribution of a country of production was between 50% and 100%. Carbon and nitrogen data alone could indeed be insufficient to

determine the origin of food, but were useful when taken together with other variables, as shown in a study by Sacco *et al*. (2005) in which a combination of $\delta^{15}N_{bulk}$, $\delta^{13}C_{bulk}$ and high-resolution magic angle spinning nuclear magnetic resonance (HR-MAS-NMR) on lamb meat from five different production sites of southern Italy was found to reach a 96% correct prediction ability by using discriminant analysis (DA).

In the case of beef meat, measurements of $\delta^{15}N$, $\delta^{13}C$ and $\delta^{34}S$ were conducted on defatted muscle samples to identify both the geographical origin and the feeding history (Schmidt *et al*., 2005a). Results from samples from six European countries plus the USA and Brazil showed much lower $\delta^{13}C$ average values for European countries (−21‰) than for the USA or Brazil (−12.3 and −10.0‰ respectively). Nitrogen values gave few clues to differentiate European meat from meat produced elsewhere, but some significant regional differences were observed at the European level. The study, which also compared Irish meat samples from organic and conventional production, concluded that the carbon, nitrogen and sulfur variables were useful to distinguish the group "organic" from the group "conventional", even if both groups were not fully separated and the mechanisms leading to different values were not fully understood.

The best results regarding the testing of the geographical were achieved using oxygen data. In a study of beef meat samples from four production sites in Germany and one in Argentina, Hegerding *et al*. (2002) showed that, for Argentina's samples, their $\delta^{18}O_{meat\ water}$ values ranged from −1.60 to 3.94‰ and their $\delta^{18}O_{meat\ water}$ values could be easily separated from those of Germany's samples, which ranged −2.3 to −5.8‰ $\delta^{18}O_{meat\ water}$. However, the $\delta^{18}O$ data were not sufficient to distinguish between German regions. In a study of meat from Charolais steers raised in three different sites in France differing in altitude and in distance from the sea Renou *et al*. (2004) showed that the meat samples from these sites could not be distinguished on the base of $\delta^{18}O$. The reason was the impact of diet (maize silage or pasture). This impact on $\delta^{18}O$ was significant at two sites, and the animals kept on pasture had higher average $\delta^{18}O$ than those kept on maize silage. A dependence of $\delta^{18}O$ on the time of slaughtering was also recorded, which could be explained by seasonality. In a comprehensive study, Boner and Forstel (2004) and Boner (2005) further investigated the differentiation of the geographical origin of beef, with samples from northern and southern Germany as well as from Argentina. All the German samples came from organic farms, which means that the cattle were mostly fed with feed produced on site. The effect of age of the animal at the time of slaughter was found to be negligible on all the isotopic variables ($\delta^{2}H_{meat\ water}$, $\delta^{18}O_{meat\ water}$, $\delta^{34}S_{protein}$, $\delta^{15}N_{protein}$) investigated. Conversely, results showed that changes in $\delta^{2}H_{meat\ water}$ and $\delta^{18}O_{meat\ water}$ during the year were of relatively large amplitude, owing to changes in groundwater intakes. The values were close to those of groundwater only in the winter season. This seasonal variation might overlap the variations due to close geographical origins. Thus, when the date of slaughtering was known, a much better separation could be achieved. Groundwater enrichment was a major factor affecting the enrichments in muscle tissue, and Boner (2005) postulated that a 5‰ difference of $\delta^{18}O$ values of groundwater from two geographical locations should be sufficient to achieve a clear discrimination based on $\delta^{18}O_{meat\ water}$. Separation of the ^{18}O-depleted

German meat from the ^{18}O-enriched meat from Argentina was possible in this way. Boner (2005) further demonstrated that animals transferred to another region for slaughtering and given water with a different enrichment changed their body-water enrichment slightly, although not significantly. By examining the $\delta^{34}S_{protein}$ data, the German samples showed significantly lower values than the Chilean samples, but not lower than the Argentinean samples, which were slightly more enriched although not significantly. Finally, at the local level, a fair separation of the German regions could be achieved by combining the $\delta^{15}N_{protein}$ data with sulfur data.

The oxygen isotopes also provided useful information for other types of meat. As shown by Franke *et al*. (2007) on poultry meat and dried beef meat samples, poultry samples produced in Switzerland could be easily distinguished from samples produced in countries with a very different climate, such as Brazil, on the basis of the $\delta^{18}O_{water}$ data. Compared with other species, poultry's isotopic distribution might be less influenced by seasonal variations, as the animals mostly eat dry feeds and receive the majority of their water by drinking (local) water. Another finding from the same study was that, even in the case of dried beef meat, the oxygen isotopic information was mostly retained, giving indications of the country of origin of the raw meat.

Milk

In a study of two sites, one at low elevation in Rennes (200 m above sea level), and the other on a mountain range in Marcenat (1100 m above sea level), milk samples were collected and analyzed by IRMS for their $\delta^{18}O$ and $\delta^{2}H$ enrichments of the milk water and by nuclear magnetic resonance (NMR) spectroscopy to determine the ^{13}C enrichment of the triglycerides fraction (Deponge *et al*., 2001). As frequently reported elsewhere, the $\delta^{18}O$ and $\delta^{2}H$ enrichments were correlated and gave equivalent information, with a tendency for oxygen to yield more precise values. The season (winter or summer) and the type of feed (grazing, hay, grass silage and maize silage) given to the cows influenced the $\delta^{18}O$ of milk significantly. Using $\delta^{18}O$ values, both origins could be well separated with the exception of milk from Rennes produced with maize silage, which could not be separated from that from Marcenat produced with grass. By adding the ^{13}C NMR variables, separation was achieved over all groups. More recently, Renou *et al*. (2004) performed a study using the milk from cows receiving pasture, maize silage, grass silage or hay. The same production sites and the same variables as above were used, but samples included water fraction from milk and cows' drinking water. It was shown that the $\delta^{18}O$ and $\delta^{2}H$ of drinking water were both highly significantly different between the plain and mountain sites, and so were the enrichments of milk's water. The impact of the different feed produced highly significant differences in isotope ratios, and on the Marcenat site the milk from cows receiving the driest food (hay) showed much lower enrichments (−9.4‰) than that from those at pasture (−4.9‰). This was explained by the simple fact that the animals receiving drier feed compensated by drinking more (depleted) water. The breed apparently plays no role, as was shown in a study of the possible impact of a cow's breed on the $\delta^{18}O_{milk\ water}$ performed by Ritz *et al*. (2005). Representatives of all five breeds examined (Tarentaise, Limousine, Salers,

Montbéliarde and Holstein) were kept in the same conditions, and milk samples were taken every week for 4 weeks. It was found that the Limousine and Salers breeds produced milk that was significantly more enriched than those of the other breeds. Ritz *et al*. (2005) explained this finding by the fact that these two breeds still had their calves at the time of the study, whereas the others were already milked twice a day. These different physiological conditions might lead to metabolic changes which would be reflected by alterations of isotopic values.

Butter

In a large study, Rossmann *et al*. (2000) investigated possible methods to check the geographical origin of butter samples from European regions, the USA, New Zealand and Australia. The variables $\delta^{18}O_{bulk}$, $\delta^{13}C_{bulk}$, $\delta^{18}O_{water}$, $\delta^{13}C_{protein}$, $\delta^{15}N_{protein}$ and $\delta^{34}S_{protein}$ were determined by IRMS, and additionally $^{87}Sr/^{86}Sr$ was determined by inductively coupled plasma mass spectrometry (ICP)-MS. Results showed that no link with a geographical region could be established on the basis of $\delta^{15}N_{protein}$, as mean values ranged from 4.9 to 6.5‰ and drastically different locations, such as Florida and the alpine regions of Europe, showed the same values. Seasonality was further investigated on one site, and $\delta^{15}N$ data were higher in September and October when fodder plants were fed to the cows. These plants were found to be enriched in ^{15}N when they were fertilized with organic manure. Carbon data $\delta^{13}C_{bulk}$ showed a wide range (−33.3 to −18.2‰), and this variable was mostly influenced by the percentage of maize in the feed. The fact that extreme values cited were found in the same group (Western Europe) confirmed the use of high-maize diets in some places in Europe. The $\delta^{18}O_{water}$ data also showed a wide range (−0.6 to −10.5‰), but were clearly linked with the local climate. However, a clear separation of geographical origin was not possible on this basis alone. Finally, the $\delta^{34}S_{protein}$ data were also partly linked with the geographical origin, and samples from maritime regions showed significantly higher values than more continental ones. This was explained by the sea spray containing sulfate of marine origin, which is known to have higher enrichment than that from soil.

Cheese

In order to assess the authenticity of the geographical origin in the case of Pecorino Sardo, a ewes' milk cheese produced in Sardinia, Manca *et al*. (2001) measured the $\delta^{15}N_{casein}$, $\delta^{13}C_{casein}$ as well as the distribution of some free amino acids in samples from the Sardinia, Apuglia and Sicilia producing regions of Italy. It was found that carbon isotopic data overlapped, whereas $\delta^{15}N_{casein}$ from Sicily tended to be slightly lower than the others. By combining the isotopic data with the high-performance liquid chromatography (HPLC) measurements of amino acids using principal component analysis (PCA), cluster analysis and linear discriminant analysis (LDA), it was possible to achieve differentiation of all three regions.

In a preliminary study of a limited amount of Emmental cheese samples from several regions in Europe (Switzerland, Allgäu in Germany, Finland, Vorarlberg in Austria,

and Brittany and Savoie in France), the $\delta^{18}O_{water}$ of water gained by freeze-drying, $\delta^{18}O_{glycerol}$ and $\delta^{13}C_{glycerol}$ of glycerol from fat hydrolysis, as well as $\delta^{15}N$, $\delta^{13}C$, $\delta^{2}H$ and $^{87}Sr/^{86}Sr$ from the pH 4.3-insoluble fraction, were used to assess the geographical origin (Pillonel *et al*., 2003; Pillonel, 2005). It was found that most of these variables, with the exception of $\delta^{18}O_{glycerol}$, were highly discriminating. Using the four variables from the pH 4.3-insoluble fraction in a principal component analysis allowed differentiation of the regions of Finland, Bretagne and Savoie from the other regions. Nevertheless, it was shown in a later study, focusing on Swiss vs non-Swiss origin of Emmental and encompassing more samples, that the isotopic variables from the pH 4.3-insoluble fraction alone ($\delta^{15}N$, $\delta^{13}C$, $\delta^{2}H$ and $\delta^{34}S$) were no longer sufficient to achieve 100% correct identification. This goal was, however, achieved by adding 11 further chemical, physical and microbiological variables and applying DA to these variables (Pillonel *et al*., 2005). Applying a similar approach for Raclette cheese, Pillonel *et al*. (2004) proved that the isotopic variables from the pH 4.3-insoluble fraction $\delta^{15}N$, $\delta^{13}C$, $\delta^{2}H$ and $\delta^{34}S$ were sufficient to differentiate between two French production regions, the northwest and eastern/central France. By adding one further parameter (calcium concentrations), it was shown that 100% correct classification was achieved regarding the Swiss, northwest France and eastern/central France regions.

In the case of cheeses with a Protected Designation of Origin (PDO), the milk has to be produced within a precisely defined geographical area. Thus, the authentication might be easier, as a better link with this geographical origin might be expected. This was confirmed in a study by Brescia *et al*. (2005) of a PDO mozzarella made from buffalo milk and produced in the two geographically close regions of Apulia and Campania. Milk and cheese samples were subjected to IRMS ($\delta^{15}N_{bulk}$, $\delta^{13}C_{bulk}$) and high-resolution $^{1}H\text{-}NMR_{aqueous\ extracts}$. For cheese samples, the isotopic and NRM data treated together by chemometric methods allowed 100% classification for both production regions. In the case of milk samples, IRMS data alone were sufficient to achieve a separation.

A similar approach was used for cow and sheep cheeses from Sardinia and other Italian production regions (Chiacchierini *et al*., 2002) in a study where the $\delta^{15}N$, $\delta^{13}C$ enrichments of casein were determined by IRMS. Data reduction using LDA allowed significant separation of all origins, and it was found that seasonality did not influence the data significantly. In a study by Giaccio *et al*. (2003), $\delta^{15}N_{casein}$, $\delta^{13}C_{casein}$ and $^{18}O_{glycerol}$ were used to assess the geographical origin of cows; and sheep's cheeses from the Italian regions of Friul and Abruzzi. A discriminatory power of 100% between groups was reported. In the case of Sardinia's Peretta cows' milk cheese, Manca *et al*. (2006) used $\delta^{15}N_{casein}$, $\delta^{13}C_{casein}$, $\delta^{2}H_{casein}$, $\delta^{34}S_{casein}$ and $^{18}O_{glycerol}$ and $\delta^{13}C_{glycerol}$ to distinguish authentic Sardinian cheese made with local milk from cheese produced with milk from northern Europe. Data evaluation using PCA and hierarchical clusters allowed differentiation between cheeses produced with local milk and cheeses produced using imported milk. It was found that $\delta^{13}C_{casein}$ as well as $^{18}O_{glycerol}$ and $\delta^{13}C_{glycerol}$ contributed mostly to the principal components. Interestingly, $^{18}O_{glycerol}$ belonged to the variables which were not significant in the case of Emmental cheeses (Pillonel *et al*., 2003).

Asparagus

To distinguish the geographical origin of asparagus grown in Germany from that grown in Poland, in regions about 300 km apart, a database was created by measuring $\delta^{18}O$ and $\delta^{2}H$ values in water, protein and cellulose fractions and $\delta^{13}C$-values in protein and cellulose fractions from authentic samples (Meylahn, 2007). Using these results and discriminant analysis, Meylahn (2007) defined a model that permitted separation of the two proveniences.

Wine

In a study of 96 authentic samples of red grape collected in the Valencia, Alicante and Utiel-Requena producing regions of Spain over three different years, Gimenez *et al*. (1999) used a combination of $\delta^{13}C_{ethanol}$ measured by IRMS and $D/H_{ethanol}$ measured on both sites of the molecule by *site-specific natural isotopic fractionation studied by nuclear magnetic resonance* (*SNIF-NMR*) to retrace the geographical origins of the wines. It was concluded that this approach might produce some useful results, although 100% correct attribution was not achieved in all cases. Based on same measurements, a study by Kosir *et al*. (2001) of Slovenian wines from a coastal (wet, warm) and two continental (drier, cooler) regions targeted the issues of geographical origin and sugaring (chaptalization). Kosir *et al*. (2001) confirmed that these combined techniques allowed correct identification of very different geographical origins of Slovenia (coastal and continental), but not of the two continental regions, which were closer in space and climate, and allowed the detection of chaptalization with C4 sugars. After adding $\delta^{18}O_{water}$ as a further parameter, the separation of both continental regions was better (Ogrinc *et al*., 2001). The use of internal standardization with the wines' organic substances, such as organic acids, was suggested for further studies. As concluded by Martin *et al*. (1999) in the case of Bordeaux wines, the site-specific $D/H_{ethanol}$, $\delta^{13}C_{ethanol}$ and $\delta^{18}O_{water}$ variables could be useful, but are often not sufficient to permit geographical identification at a local level.

The same conclusions were reached by Gremaud *et al*. (2002) in a study of authentic Swiss wine samples, where the D/H ratios of ethanol were measured on both sites by NMR and $\delta^{18}O_{water}$ was measured by IRMS. It was found that these variables were not sufficient to clearly identify a geographical area at the Swiss level. Moreover, climatic events occurring in the last weeks before grapes were harvested were found to influence the final $\delta^{18}O_{water}$ enrichments, and samples collected from the same spot at 1-week intervals exhibited significant differences. To improve the separation, Gremaud *et al*. (2004) added to the model more variables, such as the concentration of trace elements and some classical variables for wine analysis such as ethanol, glycerol, organic acids, pH, dry matter and density. Using LDA, a good separation of geographically close Swiss regions was achieved.

Pistachios

Pistachio samples collected over two consecutive years from the USA, Turkey and Iran were subjected to bulk $\delta^{13}C$, $\delta^{15}N$ and C/N analysis by IRMS. Results showed that year-to-year variability but not pistachio varieties produced significant

differences on the measured variables for some production areas. A simple plot of $\delta^{15}N$ vs C/N proved useful to achieve a separation of all three countries, with <5% misclassification (Anderson & Smith, 2006). Recently, Heier (2007) proposed the use of $\delta^{15}N$, $\delta^{13}C$ and $\delta^{18}O$ on pistachio bulk, pistachio oil, and defatted pistachio residue. A good but not complete separation of the three countries could be achieved by using different combinations of two variables. A classification model including the measured variables was developed which allowed 100% correct reattribution of all the samples by origin.

Wheat

Wheat samples from Canada, Europe and the USA were subjected to ICP-MS (Cd, Pb, Se, Sr) and bulk isotopic $\delta^{13}C$ and $\delta^{15}N$ IRMS analysis in order to trace their geographical origins (Branch *et al*., 2003). Results showed that $\delta^{13}C$ but not $\delta^{15}N$ was a good indicator of origin. Discriminant analysis using both IRMS and ICP-MS data yielded 100% correct attribution. The carbon isotope data alone were sufficient to achieve a separation in some cases. Other conclusions were reached in a study of wheat cultivars grown in three different regions of Denmark, in which $\delta^{15}N$ and not $\delta^{13}C$ showed significant difference between group averages (Husted *et al*., 2004). The type of soil fertilizers used locally could be the major influence on nitrogen isotopes. Wheat originating from the northern and western regions of Denmark, where soils had been fertilized with cattle and pig manure for more than 10 years, had higher enrichments than that from the eastern region, where the area selected had never received organic manure.

In a study encompassing wheat samples from Canada, Australia, Turkey, and southern, central and northern Italy, Brescia *et al*. (2002a) measured bulk $\delta^{18}O$, $\delta^{13}C$ and $\delta^{15}N$ enrichments. Although the average values for all variables measured at the six origins were significantly different, the isotopic data alone were not sufficient to separate the origins. Brescia *et al*. (2002b) performed a similar study with the same variables, plus ^{1}H spectroscopy obtained by HR-MAS-NMR, on samples from two cultivars of durum wheat harvested in northern, central and southern Italy. They observed that treatment of IRMS data by linear discriminant analysis allowed differentiation of the geographical origins, and that NMR data were applicable to confirm the varietal origin.

Rice

Dennis (1999) and Kelly *et al*. (2002) showed that bulk stable isotopes $\delta^{18}O$ and $\delta^{13}C$ measured by IRMS plus selected chemical variables directly related to the local soil composition, such as rare earths and alkaline-earth elements measured by ICP-MS, were adequate to distinguish Indo-Pakistani basmati rice from rice grown in Europe or the USA. The impact of depleted meteoric waters from the Himalaya was reflected in lower $\delta^{18}O$ in carbohydrate of the Indo-Pakistani rice, which also exhibited lower $\delta^{13}C$ values than those of other origins.

Pears

In the framework of a study by Perez *et al*. (2006) to identify the geographical origin of fruits, trace elements as well as isotopic ($\delta^{13}C_{bulk}$ and $15N_{bulk}$) variables were

measured in pears from Oregon and Argentina. In the pears from Oregon, some sublocations were significantly separated on the base of nitrogen data. However, no clear separation was found between those from Oregon (ranging from −2 to +4‰) and those from Argentina (ranging from 0 to +2‰). Inversely, carbon data from Argentina were clearly depleted compared with those from Oregon, and might be useful for testing the geographical origin.

Green coffee

In a study to retrace the geographical origin of green coffee beans, Serra *et al*. (2005a) proposed the use of $\delta^{13}C_{bulk}$, $\delta^{15}N_{bulk}$, both measured by IRMS, and $\delta^{10}B_{bulk}$, measured by TIMS. Boron might be a potential marker of the geographical origin, as already reported by Wieser *et al*. (2001), although it was included into some fertilizers. Samples were collected from the three producing continents, i.e. Asia, Africa (n = 12) and South and Central America (n = 29). Results showed an overlap of carbon data, but with some differentiation between the ranges in Africa (−26.6 to −23.9‰) and in Asia (−28.1 to −25.9‰ Nitrogen data showed the same pattern, with data from Africa being close to those from America, and both tending to be more enriched than Asia. Boron values were depleted for America and enriched for Africa. Unfortunately, Asia had a large range of values covering the ranges of both other origins. Finally, an overall correct classification rate of 88% was reported.

Distinguishing natural from synthetic molecules

Natural and synthetic pure aroma molecules

In a study of benzaldehyde from bitter almond oil, Ruff *et al*. (2000) showed that the natural molecule could easily be distinguished from its synthetic counterpart by using gas chromatography pyrolysis IRMS (GC-P-IRMS). The δ^2H values of benzaldehyde from natural sources (cassia, bitter almond oil, kernels, fruits or leaves) ranged from −83‰ to −189‰, whereas in the benzaldehyde synthesized from toluene they ranged from +420 to +668‰. More problematic was benzaldehyde synthesized from benzal chloride, which showed values ranging −78‰ to −85‰. Semi-synthetic sources produced from cinnamic aldehyde (from cassia oil) also fell in the range of natural benzaldehyde ($\delta^2H = -136$‰).

As the production of natural vanilla beans does not cover the global demand of food manufacturers for vanilla, there is a widespread use of synthetic vanilla aroma. Fully synthetic vanilla shows isotope ratios that fall relatively far from those of the natural molecule, which makes their identification easy. However, new sources have been developed by semi-synthesis from natural precursors – e.g. lignin from the paper industry, eugenol from cloves, and ferulic acid from rice bran. In order to distinguish the natural vanillin from its semi-synthetic equivalents, vanilla was isolated and converted into guaiacol from which $\delta^{13}C$ and $\delta^{18}O$ enrichments were determined and compared with guaiacol from semi-synthetic and synthetic sources (Bensaid *et al*., 2002). Results showed that carbon data in particular could be useful to draw conclusions about the synthetic or semi-synthetic nature of vanilla. As shown by

Fronza *et al*. (2003), specific sites' $\delta^{18}O$ measurements of degradation products 4-hydroxy-3-methoxy-benzaldehyde and 3-methylanisole were useful, and about $3\Delta\delta$ between natural (from vanilla beans) and synthetic (from guaiacol) molecules was found. By degradation of the vanillin molecule to 2-methoxy-4-methyl phenol, the $\delta^{18}O$ enrichment at the carbonyl site was obtained. The lower (19.7 $\delta^{18}O$‰) enrichment of the extracted vanilla clearly distinguished synthetic vanilla (26.9–28.8 $\delta^{18}O$‰) from semi-synthetic vanilla from lignin (25.5‰–26.2 ‰).

Synthetic and natural *trans*-anethole were subjected to $\delta^{13}C$ and $\delta^{2}H$ determinations by GC-C-IRMS and GC-P-IRMS, respectively. The observed $\delta^{2}H_{V\text{-}SMOW}$ ranges of −20 to −79‰ for synthetic sources slightly overlapped with the values from natural source (−71 to −99‰). The ranges for $\delta^{13}C$ were confounded (Bilke and Mosandl, 2002).

Site-specific measurements of D/H (by NMR) and $\delta^{18}O$ (by IRMS) were performed on coumarin and several derivatives, such as methyl cinnamate and dihydrocoumarin (melilotol). The D/H values showed large differences in enrichments between natural and synthetic forms (Brenna *et al*., 2005). The $\delta^{18}O$ measurements of degradation products were found to be useful in distinguishing between sources.

Natural apple-juice aromas are produced by physical processes from fresh juice. In a preliminary study, Elss *et al*. (2006) concentrated on the impact of technology on the $\delta^{13}C$ and $\delta^{2}H$ values of three aroma compounds, E-2-hexenal, 1-hexanol, and E-2-hexenol measured by GC-C-IRMS and GC-P-IRMS, respectively. It was shown that the enrichments were slightly more depleted in aromas than in corresponding apple juices. However, these differences were clearly smaller than the differences between natural and synthetic aroma components.

Pear aroma contains hundreds of products, of which around 150 have been identified. However, to be amenable to GC-C-IMRS and GC-P-IMRS, a minimal amount (0.5–1.5 µg) on the column are required. Therefore, seven aroma components were chosen in the chromatogram of aroma components from pear fruits, pear juice, pear-based baby food and pear brandy for $^{13}C/^{12}C$ and $^{2}H/^{1}H$ ratio measurements. The measured enrichments were compared, in two-dimensional plots, with pure reference molecules of natural or synthetic origins. The ranges of authentic aromas differed from synthetic references in most cases, with 1-hexanol showing the clearest differentiation (Kahle *et al*., 2005).

Because high-acidity fruit juices are preferred and sell at a higher price, a method aimed at the detection of undeclared addition of malic acid was developed. It is a known principle that the overall enrichment of organic matter is governed by the environmental influences and the plant metabolic pathways, whereas the distribution of the enrichment at each site of a specific molecule depends only on the plant metabolic pathways. The enrichment of the carboxyl site of malic acid was assessed by site-specific ^{13}C-IRMS measurements. This carboxyl group was released in the form of CO_2 by using a specific enzymatic decarboxylation. Because of a strong isotopic effect by the biosynthesis, this site was enriched in the natural product. Conversely, the malic acid of synthetic origin showed depleted values of the carboxylic group. Using this method, Jamin *et al*. (2000) could detect malic acid additions down to a level of 10–15% of the total malic acid.

Fink *et al*. (2004) studied methyl cinnamate extracted from a natural source (*ocimum basilicum*) as well as its synthetic counterpart for their ^{2}H and ^{13}C enrichments by high-resolution gas chromatography coupled with combustion or pyrolysis interface to an IRMS (HRGC-C/P-IRMS). Natural and synthetic molecules showed significant differences in both carbon and hydrogen data. In particular, hydrogen data allowed easy discrimination, with $\delta^{2}H$ enrichments ranging between −123 and −176‰, and +328 and 360‰, for natural and synthetic products respectively.

As shown in a study by Hoer and colleagues to distinguish aromas of natural and synthetic origins, the $\delta^{2}H$ ranges of natural and synthetic decanal, linalool and linalyl acetate were partly overlapping whereas, using E-2-hexenal (leaf aldehyde) and E-2-hexenol, a separation of more than 100 Δδ was observed (Hoer *et al*., 2001a). Citral, measured as the mix of neral and geranial isomers, exhibited values of +38‰ to −177‰ $\delta^{2}H$ for synthetic geranial and +29‰ to −197‰ $\delta^{2}H$ for synthetic neral, and showed no overlap with natural counterparts (−264 to −303‰ and −266 to −300‰ respectively) (Hoer *et al*., 2001b). The values for natural sources, constituted from different plants such as lemon, orange and lemongrass, all lay in a very narrow range, whereas those for synthetic sources ranged over more than 200 Δδ.

Jung *et al*. (2005) used $\delta^{13}C$ (GC-C-IRMS), $\delta^{18}O$ and $\delta^{2}H$ (GC-P-IRMS) to check the authenticity of the botanical origin of linalool and linaly acetate. The ranges for $\delta^{2}H$ values of synthetic linalool (n = 7) and synthetic linalyl acetate (n = 3) lay 56 and 100 Δδ respectively, lower than natural counterparts. In the case of $\delta^{18}O$, the synthetic and natural linalool ranges were 30 Δδ apart, but much closer for linalyl acetate, at 7 Δδ. The carbon isotopes showed a clear difference between synthetic and natural sources in the case of linalyl acetate but not linalool.

Estragol and methyl eugenol from basil, estragon and pimento were studied by HRGC-C/P-IRMS (Ruff *et al*., 2002). Their $\delta^{2}H$, $\delta^{18}O$ and $\delta^{13}C$ values were compared with those of estragol and methyl eugenol from commercial chemicals, and from a man-made synthesis of eugenol and turpentine oil. For both target substances, the ranges of nature-identical and natural isotopic data were confounded.

To check the authenticity of alpha- and beta-ionone (raspberry aroma) by combustion- or pyrolysis-IRMS, these substances required preliminary separation by multidimensional GC (MDGC). This required the use of a GC system that had the property of maintaining a constant flow rate. This was important, as pyrolysis reactors are sensitive to flow rates and hydrogen values will be unstable otherwise. The accuracy of the MDGC-C/P-IRMS technique for $\delta^{2}H$ measurement was proved by comparison with a reference method (EA-IRMS) on a pure standard. Differences between both methods were less than 1 delta (Sewenig *et al*., 2005).

Decalactones are important components of prunus aroma, which is present in peach, apricot and nectarines. Using GC-C-IRMS and GC-P-IRMS, Tamura *et al*. (2005) investigated the synthetic, biotechnological and authentic (extracted from fruits) sources of these compounds. Results of $\delta^{13}C$ and $\delta^{2}H$ measurements of γ- and d-decalactones indicated that different botanical origins of fruit had no significant influence on results. Using these isotopic data, differentiation of natural molecules from synthetic and biotechnological counterparts was easy.

Differentiation between betanins from pitaya and from red beet

The δ^2H and $\delta^{13}C$ of betanins from violet-fleshed pitaya were measured by HRGC-C/P-IRMS (Herbach *et al*., 2006). While $\delta^{13}C$ betanins from pitaya, a CAM plant, ranged from −17.0‰ to −17.7‰ those from red beet were lay between −26.9 and −27.7‰ which was typical of C3 plants.

Identification of natural vs synthetic caffeine

To detect the undeclared use of synthetic caffeine in solid food and beverages, natural caffeine isolated from coffee (*cofea arabica*), tea (*camellia sinensis*), guarana (*paullinia cupana*) and maté (*Ilex paraguariensis*) was compared with synthetic caffeine. The $\delta^{13}C$ and $\delta^{18}O$ values of both origins were compared using EA-C/P-IRMS (Richling *et al*., 2003). The isolation, which was performed by liquid–liquid extraction and purified by recrystallization, was shown to produce no significant isotopic fractionation. Two-dimensional plots of $\delta^{13}C$ vs $\delta^{18}O$ allowed clear differentiation between synthetic and natural caffeine. The ranges for $\delta^{13}C$ and $\delta^{18}O$ values of synthetic references were from −37.9 to −40.0‰ and from +13.5 to +17.1‰, respectively, and the ranges for those of natural caffeine were from −32.3 to −25.9‰ $\delta^{13}C$ and from +4.1 to −7.9‰ $\delta^{18}O$.

According to the international wine code (OIV), only natural tartaric acid extracted from grapes can be used as an acidifying agent in wine and musts, which is commercially produced by washing the grape's residual seeds and skins or by extraction from dregs, followed by crystallization. Inversely, synthesis starts from fossil oil, which is converted into butanol and then tartaric acid through multiple steps. In order to check the origin of this substance, the $\delta^{13}C$ and $\delta^{18}O$ values of pure samples were compared using EA-C/P-IRMS. Results for oxygen showed that average values (and ranges) of natural and synthetic sources were +26.7‰ (+30.3‰ to +25.2‰) and +16.7‰ (+20.9‰ to +13.0‰) respectively, indicating easy identification of both sources. However, results were less clear for carbon, with −21.8‰ (−21.1‰ to −22.6‰) for the natural and −23.6‰ (−20.5‰ to −28.7‰) for the synthetic molecule (Serra *et al*., 2005b).

Characterization of the sources of CO_2 in carbonated beverages

A simple method was developed by Calderone *et al*. (2005) in order to measure the $\delta^{13}C$ of CO_2 added to sparkling beverages. Results showed a range of values spanning from −54 to +5‰ $\delta^{13}C$. The use of these data to assess the authenticity of CO_2 source was suggested. The measurements showed massive differences between average values for natural sparkling water (+1.05‰) and artificially carbonated water (−54.15‰).

Distinguishing agricultural and farming practices

Distinguish organic from conventional products

Based on the knowledge that little or no maize feed was used in the production of German organic meat, Boner (2005) performed a comparison between the

$\delta^{13}C_{protein}$ values of organic and conventional beef meat from Germany. Organic and conventional samples ranged from −20.3 to −28.2‰ and from −12 to −26‰ respectively. A cut-off value of −20‰ was proposed as a higher level for animals receiving no maize-based feed.

The avoidance of synthetic fertilizers in organic agriculture is another relevant trait that can be exploited for authentication. Indeed, farm-produced fertilizers such as hog manure ($\delta^{15}N$ of total N = +5.1‰), cattle manure (+7.9‰) or compost (+17.9 ± 1.2‰) (Choi *et al*., 2003) are more enriched than synthetic fertilizers, which show depleted values (−2 to +1‰). Accordingly, plants receiving farm-produced fertilizers were also found to be more enriched (+14.6 ± 3.3‰) than those receiving synthetic ones (+4.1 ± 1.7‰).

Truchot *et al*. (2003) proposed using a database of $\delta^{13}C$, $\delta^{15}N$ and $\delta^{18}O$ values from organic and conventional agricultural products to classify these products using discriminating analysis. The method focused on the detection of fraudulent use of synthetic vs natural fertilizers. More recently, Rapisarda (2005) used $\delta^{15}N_{pulp}$ and $\delta^{15}N_{amino\ acids}$ to evaluate the feasibility of differentiation between bio and conventional orange juices. Juices from organic fruits showed significantly higher mean values than those from conventional production. These data, taken together with other variables (vitamin C and synephrine), gave a correct attribution rate of 91% using linear discriminating analysis. In a study of tomatoes, paprika, lettuce, cabbage, onion, Chinese cabbage and wheat, Schmidt *et al*. (2005b) targeted the $\delta^{15}N_{bulk}$, $\delta^{13}C_{bulk}$, $\delta^{2}H_{water}$ as well as $\delta^{18}O_{water}$. Results showed that $\delta^{15}N_{bulk}$ values in particular were useful to differentiate organic and conventional tomatoes and paprika. However, for other commodities no significant differences could be evidenced. Schmidt *et al*. (2005b) suggested that the reason for the high enrichments found also in conventional products might be due to ^{15}N enrichment in soil following NH_3 evaporation and denitrification. The other variables brought no significant improvement.

Distinguishing "farmed" from "wild"

Wild and farmed salmon were compared on the basis of a multivariable approach using $\delta^{13}C_{fish\ oil}$, and $\delta^{2}H_{fish\ oil}$ measured by IRMS, and using SNIF-NMR measurements and classical GC-FID analysis (Aursand *et al*., 2000). Several peaks on the high ^{2}H-NMR spectrum of the fish oil were selected, and their deuterium enrichments were used as separated variables. In the first step, the less discriminating variables were filtered out and the remaining eight variables ($\delta^{2}H_{fish\ oil}$, D/H of three peaks of the NMR spectrum, and the amounts of 16:0, 16.1n-9, 18.1n-9 and 22.1n-9) were combined. A correct classification rate of 100% of wild and farmed origins was achieved.

Iberian pork meat is produced from typical Iberian swine that are free-ranging and feed mostly on acorns foraged in the forests. To distinguish the meat produced in this way from that from Iberian swine or white swine receiving conventional food, the $\delta^{13}C$ and $\delta^{34}S$ values of adipose tissue and liver (Gonzalez *et al*., 2001) were measured. A two-dimensional plot of both variables allowed differentiation of the samples according to the diet of the animal.

Detecting adulteration

Fraudulent addition of water

Because of its high popularity and limited seasonal availability, fresh orange juice is at risk of being adulterated with reconstituted concentrates or simply diluted with water. In an attempt to tackle the issue, a database of $\delta^{18}O_{water}$ of 400 authentic fresh orange-juice samples from six major Australian citrus-producing areas was developed over five production years (Simpkins *et al*., 1999). The data showed year-to-year and seasonal variations of up to 8‰. The geographical location of the production site also had an effect on the enrichments, whereas storage conditions of oranges had no or little impact. The overall span of values for Australian fresh orange juices ranged from +10‰ to +15‰. As fully reconstituted juice exhibited clearly lower values, it was concluded that admixture up to 50% would be detectable using these data. This relatively high detection level is due to the fact that cut-off values should take into account the natural variability of $\delta^{18}O_{water}$ in the products. To overcome this problem, some researchers proposed measuring correlations of oxygen-containing metabolites. Houerou (1999) used the correlation of $\delta^{18}O$ enrichments of fruit metabolites such as sugar and citric acids. Great care had to be taken in order to standardize all isolation and preparation steps of these metabolites that might otherwise introduce more variability because of unreproducible fractionations. Jamin *et al*. (2003) proposed a method based on the fact that a correlation does exist between $\delta^{18}O_{sugars}$ (measured as $\delta^{18}O_{fermentative\ ethanol}$) and $\delta^{18}O_{water}$. The sugars were first fermented into ethanol, which was isolated by high-yield distillation and purified from the remaining water using a molecular sieve. In this method, ethanol was generated directly in fruit juice by yeasts. Its enrichment was measured by pyrolysis-IRMS. The mentioned correlation could be verified, and addition of extraneous water produced significant deviation from the correlation. This method, which was patented (Jamin *et al*., 2003), can be applied for every liquid containing a fermentescible sugar. A detailed study was conducted to investigate the fractionation occurring at the fermentation and distillation steps (Monsallier-Bitea *et al*., 2006), and it was found that as distillation involved a normal fractionation of about 0.997, high yields (>95%) and standardized conditions were required to obtain reproducible results. A plot of authentic direct orange juice $\delta^{18}O_{fermentative\ ethanol}$ vs $\delta^{18}O_{water}$ produced a straight correlation line. Blends with juice from concentrate produced a deviation from this line, indicating adulteration.

Fraudulent addition of sugar

Addition of sugar to juices and concentrates

To detect the addition of C4 sugars, for example in the form of high-fructose corn syrup, $\delta^{13}C_{sugars}$ was determined in authentic Australian orange juices. Results from 35 samples collected over a whole year and of two varieties (Navel and Valencia) yielded a cut-off of −23.5‰ for juices without C4 sugars added (Antolovich *et al*., 2001). Although the method based on cut-off values determined on single variables

might work well, it had the drawback of having to take into account the whole range of natural variation occurring because of, for example, year-to-year climatic changes or slight changes in agricultural practices. Therefore, methods using internal standardization are increasingly employed. These methods are based on the fact that the differences in enrichment between some components of a food product remain the same, even when these enrichments change due to environmental factors. Using this principle, Gonzalez *et al*. (1999) proposed the so-called specific natural isotope profile-IRMS (SNIP™-IRMS) method, which was based upon correlations of the $\delta^{13}C$-values between several metabolites isolated from fruit juices. This method was tested successfully on pineapple juice, where fructose, glucose and sucrose fractions were separated by ion exchange columns clean-up followed by preparative HPLC. In the case of adulterated juices, this correlation was no longer observed. Using this method, C3 sugar additions as low as 3% could be detected.

In the case of Australian orange juices, Simpkins *et al*. (2000) used the differences between sugars and the calcium-precipitated acids in juices. Indeed these differences were found to be consistently in the range of 0.7 to 1.5‰ ($n = 23$). The same principle was applied to individual sugars, pectin, and citric acid from orange, grapefruit and apple juices by Day *et al*. (2001). Where good correlations were observed, a linear model with a defined slope and interception could be defined. Juices adulterated by the addition of extraneous C4 sugars could be detected by the fact that they were out of the confidence range of the correlation curves. Day *et al*. (2001) reported that correlations between sugars and pectin or acids respectively were poor, whereas they were quite good between $\delta^{13}C_{sucrose}$ vs $\delta^{13}C_{glucose}$. Using this technique, named ^{13}C-isotope relations of individual sugars (IRIS), a lower detection limit down to the level of 4% added C4 sugars was reported.

As simple bulk ^{13}C measurements were not appropriate to detect adulteration with sugar syrup from the same plant metabolic group (e.g. a C3 crop adulterated with another C3 sugar syrup), measurement of D/H ratios were proposed, as they were more sensitive to the small differences in metabolism produced by environmental factors. In order to obtain sugars in the form that was amenable to on-line GC-pyrolysis-IRMS, Kelly *et al*. (2003) first converted these sugars into hexamethylenetetramine derivatives which retained the D/H and $^{13}C/^{12}C$ ratios of the parent sugars. By applying this method to 100 apple-juice samples from all over the world, using high-fructose corn syrup (HFCS) and beet medium inverted syrup (BMIS) as potential adulterants, a two-dimensional plot of both isotopes yielded perfect separation. This GC-pyrolysis-IRMS method showed a sensitivity of −0.66‰ on D/H ratios for each addition of 1% w/w of BMIS.

More recently, a method for solving the weaknesses of the existing NMR methods in detecting the addition of a mixture of C3 and C4 extraneous sugars was proposed by Jamin *et al*. (2004), who collaboratively validated the method based on the measurement of $\delta^{13}C_{\text{fermentative ethanol}}$ by IRMS. As the result, it offered the advantage of comparing the samples with two cut-off values, one $D/H_{\text{fermentative ethanol}}$ by SNIF-NMR and one $^{13}C_{\text{fermentative ethanol}}$ by IRMS, thus allowing better identification of fraudulent samples.

Addition of sugar to wines and musts

As C4 sugars from corn or cane are used in the second fermentation of sparkling wines from Brazil, the variable $\delta^{13}C_{CO2}$ was proposed by Martinelli *et al*. (2003) to control the authenticity of these sparkling wines against similar wines produced in more temperate regions, where C3 sugars were mostly used. The results showed a clear correlation of $\delta^{13}C$ values with the amount of C4 sugar. "Doux" sparkling wines averaged −20.1‰, whereas "sec" wines were around −15.8‰. In contrast, sparkling wines from Europe and Chile/Argentina showed depleted values of −25.5‰ and −26.1‰, respectively.

In a study by Versini *et al*. (2006), $\delta^{13}C$ data from wine and must fractions were investigated for correlations that could be used for internal standardization. In musts, a correlation between $\delta^{13}C_{\text{total free sugars}}$ and $\delta^{13}C_{\text{heterosides sugars}}$ was found, with the latter being consistently about 1.7‰ lower than the former. In wines, some correlations existed between $\delta^{13}C_{\text{amino acids}}$ and $\delta^{13}C_{\text{ethanol}}$. Using the correlation lines obtained, and taking into consideration uncertainty on slope and intercept, it was possible to detect an addition of C4 sugar at a level of 10%, although the bulk enrichments for total sugars remained within the natural variation range and the adulteration would thus have otherwise remained undetected. It was found that wines produced in the same conditions had an enriched amino acid fraction compared with the alcohol fraction. The same observation was made for commercial wines, except in the case of wines with known addition of C4 sugars. Using the correlation between $\delta^{13}C_{\text{amino acids}}$ and $\delta^{13}C_{\text{ethanol}}$, C4 sugar additions down to 10% of the final alcohol concentration could be detected.

Addition of sugar to honey

The direct comparison of bulk isotopic $\delta^{13}C$ data with a cut-off value (−21.5‰) proved to work well in the case of C4 sugar addition, such as HFCS, to honeys produced from C3 flowers. As this simple method had to cope with natural variations introduced by the various botanical origins, Antinelli *et al*. (2001) proposed using the abovementioned method combined with pollen analysis by microscopy, by which the evidence about the botanical origin of honey could be found and the measured $\delta^{13}C$ values could be compared with published values for this botanical source.

An elegant method of getting rid of some variability due to environmental factors is to use a correlation between $\delta^{13}C_{\text{bulk}}$ (ranging from −21.8 to $-30.4 \pm 0.3\delta$‰) and $\delta^{13}C_{\text{protein}}$ (Moguel-Ordonez *et al*., 2005). The study, performed on honeys produced on the Yucatan peninsula, showed that the addition of extraneous C4 sugars would shift $\delta^{13}C_{\text{bulk}}$ toward more positive values whereas $\delta^{13}C_{\text{protein}}$ would remain the same. A difference between both variables exceeding 0.9 $\Delta\delta$ was considered as a proof of adulteration. The percentage of C4 sugars added can be calculated based on this principle:

$$\text{C4 Sugar } [\%] = \frac{\delta^{13}C_{\text{honey protein}} - \delta^{13}C_{\text{honeybulk}}}{\delta^{13}C_{\text{honey protein}} - (-9.7)} \times 100\% \qquad \textbf{(9.2)}$$

Equation (9.2) was used on Brazilian honey samples, and it proved to be appropriate, as most of the 40 samples tested showed enrichment differences <1 $\Delta\delta$ (Padovan *et al*., 2003). Padovan *et al*. (2003) determined experimentally that this cut-off corresponded to an addition of 7% pure sugar or 10% sucrose syrup. This standardization could be applied to honey from various geographical origins. However, there are some special cases where this standardization cannot be applied, as shown by a large study conducted in China with over more than 300 monofloral honeys from 26 botanical origins (Guo *et al*., 2006). This study found that the $\Delta\delta$ (protein-bulk) was negative in about half of the monoflorals examined, ranging from -0.80 to -0.02 $\Delta\delta$, and positive in other cases (ranging from 0.02 to 2.38), with three honeys (namely upland cotton, common buckwheat and lychee) exceeding the $\Delta\delta$ of 0.9, being 2.38, 1.14 and 0.94 respectively (Guo *et al*., 2006).

Detection of adulterated royal jelly

Natural royal jelly is produced from honeybees by incomplete digestion of honey and pollen. To achieve mass production at cheaper prices, these natural starting materials are replaced by high-fructose corn syrup and yeast extracts that are fed to the honeybees. In order to detect this fraud, a study was performed in which royal jelly samples from several production areas in Europe, Thailand, Indonesia and China were examined for their $^{13}\delta C_{bulk}$ and $^{15}\delta N_{bulk}$ enrichments (Stocker *et al*., 2006). Additionally, the botanical source was determined by microscopy using the pollen distribution in the samples. The isotopic data, combined into a two-dimensional plot, yielded an area corresponding to authentic honey products. Using this method, the authenticity of royal jelly could be successfully assessed (Bengsch *et al*., 2006).

Detection of the addition of glycerol to wine

The fraudulent addition of glycerol to low-quality wines could be detected in the past by the GC detection of synthetic glycerol by-products. Nowadays, the use of better-quality synthetic glycerol or even glycerol from natural sources has urged the development of more specific methods. The correlation of $\delta^{13}C_{glycerol}$ and $\delta^{13}C_{ethanol}$ was therefore studied (Calderone *et al*., 2004) in wines produced from various geographical regions and vine varieties. A good correlation could be established between these variables for most wines, except in cases where grapes were colonized with the "noble rot" fungus *botrytis cinerea*. In such cases, significant amounts of glycerol with a different enrichment were produced by the "noble rot" fungus. Calderone *et al*. (2004) concluded that the proposed method did not fit for these cases. Later, Jung *et al*. (2006) proposed the use of $\delta^{13}C_{glycerol}$ and $\delta^{18}O_{glycerol}$ by GC-C-IRMS and GC-P-IRMS respectively. Results showed that extraction procedures for glycerol did not produce significant isotopic fractionation, but the method was useful in some cases to detect the addition of extraneous glycerol. In the case of glycerol from beet sugar, the ranges for both isotopes overlapped with the range of authentic wines.

Detection of adulteration of fats and oils

Owing to their similar fatty acid compositions, some blends of oils and fats cannot be easily detected by gas chromatography, and the $\delta^{13}C_{bulk}$ of oil was generally not sufficient for unambiguous identification (Kelly and Rhodes, 2002), with the exception of C4 oils such as maize oil. Therefore, in the case of adulteration of C3 oils with other C3 oils, multi-isotopic methods or compound- as well as position-specific IRMS is preferred. For this purpose, a combination of ^{1}H (NMR), bulk $\delta^{18}O$, $\delta^{13}C$ (IRMS) and site-specific ^{2}H-NMR was proposed (Fauhl, 1999). Results from pure hazelnut, pure olive and mixed oils samples examined by discriminant analysis were satisfactory for blends containing more than 20% hazelnut oils. The compound-specific approach was further investigated in a study into the applicability of $\delta^{13}C_{bulk}$ (EA-RMS) and $\delta^{13}C$ of individual fatty acid such as palmitic and oleic acid (Spangenberg and Ogrinc, 2001). Covariation was found between the $\delta^{13}C$ values of palmitic and oleic acid, and this was proposed as a possible criterion to detect admixtures or impurities. These isotopic data combined with fatty acid concentrations determined by GC were found useful to distinguish pure olive oil from seed oils. As older oils were slightly less enriched than younger ones, it was suspected that aging of the oils might influence the isotopic data.

Using the variables $\delta^{13}C_{bulk}$, $\delta^{13}C_{16:0}$, $\delta^{13}C_{18:0}$, $\delta^{13}C_{18:1}$, and chromatographic data combined by PCA, the feasibility of the quantification of cocoa butter equivalents (CBEs) in chocolate was investigated. Spangenberg and Dionisi (2001) concluded that these variables allowed pure CBE and cocoa butter (CB) to be distinguished. A detection level of 15% CBE in CB was suggested. CB of southern American origin could be easily distinguished from that produced in Asia.

In order to test the plant or animal origin of free or esterified *glycerol*, $\delta^{18}O_{glycerol}$ and $\delta^{13}C_{glycerol}$ measurements were performed by IRMS. Results ranged from -33 to -29.5‰ and from -13.9 to -15.3‰ $\delta^{13}C$ for C3 and C4 plants, respectively. The oxygen data ranged from $+16$ to $+27.6$‰ $\delta^{18}O$ for all plants. Animal fats ranged somewhere between, as they were mostly influenced by the type of fat included in feed. Fronza *et al*. (2001) therefore suggested the application of these results to test the plant or animal origin of glycerol.

Testing of plant or animal origin of protein in food

Because *L-tyrosine* molecules from animal and plant sources are synthesized by different biochemical pathways, their $\delta^{18}O$ values are different. Based on consideration of these pathways, it was postulated that tyrosine from plant sources should have an enrichment of about $+30$‰, while tyrosine of animal origin should be between $+6$‰ and $+30$‰, depending on the ratio of tyrosine from food to tyrosine from endogenous production. To test this hypothesis, tyrosine samples from various origins were first converted to 3-(4-methoxyphenyl)-1-chloropropane, using a five-step reaction scheme, in order to permit specific measurements of the oxygen enrichment at the p-OH site. Experimental data confirmed the above hypothesis, and it was suggested that this finding could be used to test the plant or animal origin of protein in food and in animal feed (Fronza *et al*., 2002).

Detection of added citric acid in fruit juices

Citric acid is both a natural component of fruit juices and a widely used food additive. To distinguish between native citric acid from fruits and citric acid produced from fermentation of C3 or C4 carbohydrates, citric acid was subjected to δ^2H and $\delta^{13}C$ measurement using IRMS (Jamin *et al*., 2005). A method was presented that used the conversion of citric acid to calcium citrate to measure the non-exchangeable hydrogen by IRMS. Results showed that the δ^2H data were useful for the purpose of authentication. Indeed, calcium citrate from authentic fruit juices had higher δ^2H values (153.6 to 159.0‰) than those from citrate produced from commercial carbohydrate fermentation sources (147.7‰ for C3 starting material and 148.6‰ for C4 and C3 + C4 starting materials).

Detection of reconstituted vs raw milk

Based on the assumption that raw milk and reconstituted milk of same origin should have slightly different $\delta^{18}O$ and δ^2H due to the cattle metabolism during milk production, a method was proposed by Lin *et al*. (2003) based on the IRMS measurement of an aqueous solution produced from milk after treatment with activated charcoal. As expected, there was a significant difference between the enrichments of raw milk and those of milk reconstituted using the local water. Moreover, it was confirmed that raw milk from a defined origin should only be compared with reconstituted milk from the same origin.

Tracing the botanical origin

Botanical origin of fermentative ethanol in spirits

According to Mexican law, all 100% agave tequila should be bottled in Mexico. In order to distinguish between 100% tequila and mixed (misto) tequila, which is produced from agave and sugar cane, their $\delta^{18}O_{ethanol}$ and $\delta^{13}C_{ethanol}$ were determined. It was shown that these combined data were not sufficient to distinguish authentic tequila from mixed tequila (Aguilar-Cisneros *et al*., 2002). Bauer-Christoph *et al*. (2003) went further on this theme with measurements on spirits of $\delta^{13}C_{ethanol}$ combined with site-specific δ^2H enrichments of ethanol by NMR and gas chromatography, and found that not the isotopic data but the gas chromatographic analysis of the volatiles produced the most discriminant data.

Authentic rice spirits made from rice molasses as starting materials face concurrence with spirits produced by fermentation of cane molasses and aromatized with rice flavorings. To distinguish both qualities, Rau *et al*. (2005) measured $\delta^{13}C_{ethanol}$ using IRMS. Ethanol fermented from rice, which is a C3 plant, was easily separated from ethanol from cane (a C4 plant).

Botanical origin of beer ingredients

Traditional beer ingredients include water, yeast, malted barley and hops (both C3 plants). However, additional sugars and starches from C4 plants (corn or cane) are frequently added to increase the alcohol content in the final product. As this addition

is against the law in some countries, a study was performed on 160 samples, where the $\delta^{13}C$ values were determined on the dry residue of 25 ml of beer. An equation for calculation of the percentage of C4 carbon in each beer sample was developed (Brooks *et al*., 2002).

Botanical origin of monofloral honeys

In a study encompassing both adulteration with added sugar and the question of botanic origin of monofloral honeys, the isotopic data $\delta^{13}C_{bulk}$, $\delta^{13}C_{protein}$, $^{13}C_{fermentative\ ethanol}$, (IRMS) and $D/H_{fermentative\ ethanol}$ (NMR) were measured from commercial acacia honeys and from authentic acacia, heather, fir, citrus, lavender, lime and sunflower honeys (Giraudon *et al*., 2000). Using a plot of $\delta^{13}C_{fermentative\ ethanol}$, (IRMS) vs $D/H_{fermentative\ ethanol}$ (NMR), it was shown that some groups (such as citrus and sunflower) were easily separated from another. However, the overall rate of correct attribution was below 70%.

Botanical origin of cinnamaldehyde

Cinnamaldehyde, which is an important flavor component of cinnamon, can be obtained from several plant sources. *C. ceylanicum* (Ceylon) is the most valuable source, whereas *C. cassia* (cassia) and *C. burmanii* (cassia vera) are frequently used as cheaper alternatives. A study was launched in order to identify both sources. Cinnamaldehyde was extracted from these sources and $\delta^{13}C_{cinnamaldehyde}$ and $\delta^{2}H_{cinnamaldehyde}$ measurements were performed on bulk ground bark and distillates. Results showed that identification of Ceylon cinnamon was feasible based on $\delta^{2}H_{cinnamaldehyde}$, as its range was from −112 to −101‰ (n = 9) for Ceylon, whereas the range for other sources (*cassia*, *cassia vera*) was from −128 to −142‰ (n = 8) (Sewenig *et al*., 2003).

Strengths and limitations

Practicability

As described above, sample preparation for IRMS measurements can be very straightforward (e.g. direct equilibration with CO_2). This aspect, combined with small sample size and unrivaled precision, is one of the most important advantages of IRMS techniques. In addition, often other analytical techniques cannot provide the required information. However, drawbacks are more obvious when sample preparations involve multiple off-line steps that include several physical treatments (e.g. extraction, cryodistillation, azeotropic distillation, preparative chromatography) or chemical and biochemical reactions. For example, when non-quantitative distillations are used, fractionation occurs when the compounds of interest undergo vapor pressure isotope effects. As shown by Baudler (2006), for the same molecules, carbon and hydrogen isotopologues can have different comportments. Even extraction procedures can lead to fractionation, and Schlechtriem *et al*. (2003) demonstrated that different lipid extraction procedures led to significantly different $\delta^{13}C$ values among

the lipid fractions. When chemical or biochemical reactions are involved (e.g. derivatization to increase volatility, fermentation of sugar into ethanol), fractionations may occur due to isotopic effects caused by the reaction itself or by equilibration of the products with the reaction medium. Therefore, it is advisable to test the isotopic effects at all steps of the method and to use strictly standardized experimental conditions (Jamin *et al*., 2003). The availability of further easy and reliable sample preparation procedures may be a limiting factor for the development of isotopic techniques.

Use of chemometric methods

The procedure generally used in authenticity studies consists of establishing a range of values for authentic samples, and comparing it with the range of values of non-authentic samples. Ideally, a single-variable approach would be sufficient. However, with the increasing complexity of the question being asked, the number of measured variables tends to increase. Accordingly, data reduction methods should be applied in order to handle these variables simultaneously. Therefore, chemometric methods such as principal component analysis (PCA) and linear discriminant analysis (LDA) are often used. Briefly, PCA examines the spatial distribution of samples in a multi-dimensional space (each dimension is a variable) and describes which variables are most responsible for the separation. These variables are then subjected to linear combination in order to fit into two or three new dimensions (principal components, PC) in such a way that the distances between individuals are maximized. The coefficients used to multiply the original variables to obtain the PCs are called the loadings. This method is blind, as the model does not know which sample belongs to which group. Conversely, in LDA the groups are predefined by the operator and the axes are calculated in such a way that distances between groups are maximized. Both PCA and LDA are powerful methods with which it is possible to detect even relatively minor differences between groups. However, it was found that deceptively high separation rates might occur in preliminary studies, which are not always confirmed by follow-up studies with more samples. The most plausible explanation for this might be that, for economical and practical reasons, the sample sets for "authentic" and "non-authentic" samples are too restricted and do not adequately cover the whole range of possible values. Thus, false positives or false negatives cannot always be avoided.

Applicability of different isotopic variables to authenticity

Table 9.3 summarizes the isotopic variables reported in the literature as successful parameters. It can be seen that $\delta^{18}O_{water}$ is the most appropriate for the purpose of determining the geographical origin of agricultural products. The isotopic ratio of oxygen in local meteoric water and groundwater is indeed mostly influenced by local geographic and climatic conditions, and not by human activity. Thus, it bears the characteristics of a *primary indicator* of the geographic origin. When this water enters

Table 9.3 Successful variables for food authentication

Isotopic variable (technique)	Application (number of studies reviewed)
Testing of the geographical origin of food products	
$\delta^{34}S_{protein}$ (EA-IRMS)	Meat (2), cheese (2), butter (1)
$\delta^{18}O_{water}$ (equilibration IRMS)	Meat (4), milk (2), butter (1), asparagus (1), wine (4), cheese (1)
$\delta^{18}O_{glycerol}$ (EA-IRMS)	Cheese (2)
$\delta^{18}O_{bulk}$ (EA-IRMS)	Pistachios (1), wheat (1), rice (2), butter (1)
$\delta^{15}N_{protein}$ (EA-IRMS)	Meat (2), cheese (3)
$\delta^{15}N_{bulk}$ (EA-IRMS)	Cheese (1), pistachios (2), wheat (2), pears (1), coffee (1), meat (1)
$\delta^{13}C_{protein}$ (EA-IRMS)	Meat (1), butter (1), cheese (4), asparagus (1)
$\delta^{13}C_{defatted\ muscle}$ (EA-IRMS)	Meat (1)
$\delta^{13}C_{fat}$ (EA-IRMS)	Meat (1)
$\delta^{13}C_{bulk}$ (EA-IRMS)	Butter (1), cheese (1), pistachios (1), wheat (2), pears (1), coffee (1), rice (2)
$\delta^{13}C_{glycerol}$ (EA-IRMS)	Cheese (2)
$\delta^{13}C_{cellulose}$ (EA-IRMS)	Asparagus (1)
$\delta^{2}H_{protein}$ (EA-IRMS)	Cheese (4)
Organic agriculture	
$\delta^{34}S_{defatted\ muscle}$ (EA-IRMS)	Meat (1)
$\delta^{15}N_{defatted\ muscle}$ (EA-IRMS)	Meat (1)
$\delta^{15}N_{protein}$ (EA-IRMS)	Meat (1)
$\delta^{15}N_{casein}$ (EA-IRMS)	Cheese (2)
$\delta^{15}N_{bulk}$ (EA-IRMS)	Wheat (2), vegetables (3)
$\delta^{15}N_{pulp}$, $\delta^{15}N_{amino\ acids}$ (EA-IRMS)	Orange juice (1)
$\delta^{13}C_{protein}$ (EA-IRMS)	Meat (1)
$\delta^{13}C_{defatted\ muscle}$ (EA-IRMS)	Meat (1)
Wild/farmed	
$\delta^{34}S_{liver}$ (EA-IRMS)	Pork meat (1)
$\delta^{13}C_{fat}$ (EA-IRMS)	Pork meat (1)
$\delta^{2}H_{oil}$ (EA-IRMS)	Salmon (1)
Natural/synthetic	
$\delta^{18}O_{site\text{-}specific}$ (GC-P-IRMS)	Vanilla (1), coumarin (1)
$\delta^{18}O_{compound\ specific}$ (EA-IRMS)	Tartaric acid (1)
$\delta^{18}C_{compound\ specific}$ (GC-C-IRMS)	Aromas (2)
$\delta^{13}C_{compound\ specific}$ (GC-C-IRMS)	Aromas (7), betanins (1)
$\delta^{13}C_{caffeine}$ (EA-IRMS)	Caffeinated food or beverage (1)
$\delta^{13}C_{site\text{-}specific}$ (GC-C-IRMS)	Vanilla (1), malic acid (1)
$\delta^{2}H_{compound\ specific}$ (GC-P-IRMS)	Aromas (10), betanins (1)
$\delta^{2}H_{caffeine}$ (EA-IRMS)	Caffeinated food or beverage (1)
Adulteration of food	
$\delta^{18}O_{water}$ (IRMS, equilibration)	Water addition in orange juice (2), reconstituted milk (1)
$\delta^{18}O_{citric\ acid}$, $\delta^{18}O_{sugar}$ (EA-IRMS)	Water addition in orange juice (1)
$\delta^{18}O_{ferment.\ ethanol}$, $\delta^{18}O_{sugar}$ (EA-IRMS)	Water addition in fruits juice (2)
$\delta^{18}O_{tyrosine\ (site\text{-}spec.)}$ (EA-IRMS)	Plant or animal origin of protein (1)
$\delta^{18}O_{glycerol}$ (EA-IRMS)	Plant or animal origin of glycerol (1), glycerol addition to wines (1)
$\delta^{18}O_{bulk}$ (EA-IRMS)	Blending of oils (1)

(*Continued*)

Table 9.3 (Continued)

Isotopic variable (technique)	Application (number of studies reviewed)
$\delta^{18}O_{ethanol}$ (EA-IRMS)	Botanical origin of ethanol (1)
$\delta^{15}N_{bulk}$ (EA-IRMS)	Royal jelly, sugar feeding of honeybees (1)
$\delta^{13}C_{sugars}$ (EA-IRMS)	Sugar addition to orange juice (2)
$\delta^{13}C_{sucrose}$, $\delta^{13}C_{glucose}$ (EA-IRMS)	Sugar additions to fruit juices (2)
$\delta^{13}C_{glycerol}$ (EA-IRMS)	Plant or animal origin of glycerol (1), glycerol addition to wines (1)
$\delta^{13}C_{sugar}$, $\delta^{13}C_{org.\ acids}$ (EA-IRMS)	Sugar additions to fruit juices (2)
$\delta^{13}C_{glycerol}$, $\delta^{13}C_{ethanol}$ (GC-C-IRMS)	Glycerol addition to wines (1)
$\delta^{13}C_{fermentative\ ethanol}$ (GC-C-IRMS)	Sugar additions to fruit juices (1), botanical origin of honey (1)
$\delta^{13}C_{ethanol}$ (EA-IRMS)	Botanical origin of ethanol (2)
$\delta^{13}C_{CO2}$ (IRMS)	C4 sugar addition to wines (1)
$\delta^{13}C_{total\ free\ sugars}$, $\delta^{13}C_{\ heterosides\ sugar}$ (EA-IRMS)	C4 sugar addition to wines (1)
$\delta^{13}C_{bulk}$ (EA-IRMS)	C4 sugar addition to honey (1), royal jelly, sugar feeding of honeybees (1), blending of oils (2), botanical origin of beer's components (1)
$\delta^{13}C_{bulk}$, $\delta^{13}C_{protein}$ (EA-IRMS)	C4 sugar addition to honey (3)
$\delta^{13}C_{fatty\ acids}$ (GC-C-IRMS)	Blending of oils (1), CBE in cocoa butter (1)
$\delta^{2}H_{fructose}$ (GC-C-IRMS)	Sugar additions to fruit juices (1)
$\delta^{2}H_{citric\ acid}$ (EA-IRMS)	Added citric acid in juices (1)

When two variables are given, the correlation of both was used.

the food chain, it influences the oxygen enrichment of the food products. For these reasons, $\delta^{18}O_{water}$ was found to be the most cited variable in the reviewed literature.

The isotopic variables of nitrogen, sulfur and carbon mostly have the characteristics of a *secondary indicator* for the geographic origin, as they are usually mostly determined by the type of feed given and the agricultural practices used. Nevertheless, sulfur and nitrogen can sometimes also be used as primary indicators of the geographic origin. Indeed, sulfur isotopes ($\delta^{34}S_{protein}$) can be influenced in coastal areas by ^{34}S-rich sea sprays. Nitrogen, although mostly influenced by agricultural practices, especially the type of fertilizer used, can also be influenced by local soil and climatic conditions, such as the humidity of the soil, and some authors have suggested that nitrogen can provide useful indications regarding the geographical origin. Compared with other isotopes, nitrogen is often the least appropriate for the purpose of identifying the geographical origin of a sample.

The development of on-line pyrolysis techniques has provided a very powerful tool to investigate and test natural vs synthetic products. Of 18 publications reviewed, 13 used this technique, mostly successfully. A limitation, however, is that a sufficient number of representative references for natural and synthetic samples should be included. This may be difficult when several different natural and synthetic sources exist. Moreover, the borderline between natural and synthetic products is becoming increasingly difficult to define owing to the use of semi-synthesized products (chemical synthesis from natural precursors) and products obtained from bio-fermentation of natural substrates. When the enrichments measured in the whole molecule are not sufficient to discriminate natural from synthetic products, site-specific isotopic

measurements are used. This is very powerful, as the precision of IRMS systems can be combined with the valuable information on site-specific enrichments. Unfortunately, the main drawback is that some methods still require lengthy off-line sample preparation procedures that include several steps of purification using chemical and/or biochemical reactions, all which are likely to introduce fractionation. Thus, the development of further robust and easy on-line methods to produce the required fragments may be a prerequisite for more widespread use of site-specific IRMS.

Applications for organic agriculture

By law, organic agriculture has to respect a set of practices defined in the specific regulations for this type of agriculture. Among these are the mandatory use of minimal amounts of organically produced roughage, and the avoidance of synthetic fertilizers. Both practices have consequences for the isotopic distribution of carbon and nitrogen in agricultural products. Indeed, the analysis of ^{15}N (synthetic vs farm-produced fertilizers) and ^{13}C (maize vs no maize) isotopes has given useful indications in many cases. Nevertheless, it is important to be aware that the regulations regarding organic agriculture do not explicitly exclude maize or other C4 plants from animal feed. Moreover, it is not mandatory that these feeds are produced on-site. They can legally be imported from elsewhere, provided that they were produced according to the rules of organic agriculture. Furthermore, nothing forbids conventional agriculture from using mostly farm-produced fertilizers and no maize. Therefore it might be difficult to differentiate organic agriculture using the isotopic variables mentioned above, and false-negative results could occur.

Application for the detection of food adulteration

Although the measurement of single isotope bulk enrichments might be successful where large differences in ranges between authentic and non-authentic samples exist, they have the drawback of having to cope with large variability introduced by environmental factors. To deal with this variability, either costly databases of authentic samples or conservative cut-off values have been proposed. One interesting new development in this field has been the use of the internal standardization principle, which uses the covariation of the enrichment of some components (pure molecules or extract fractions) of the same food product (e.g. $^{13}C_{protein}$ vs $^{13}C_{bulk}$).

Conclusions

Stable isotope methods have brought insight of unprecedented amplitude into the field of food product authentication. The methods themselves are becoming increasingly accurate, specific and collaboratively validated. Frequently, there are no analytical techniques other than IRMS that can provide the required information.

This chapter emphasizes the importance of being aware that isotopic fractionation can occur at every step during food production, as well as during the analytical processes necessary for sample preparation, and that this should be taken into consideration when

choosing the analytical techniques to be used and also for interpreting the results correctly. When statistical tools are used, their limitations should be fully understood and taken into account. To achieve these goals, multidisciplinary teams should be involved.

Definitions

EIE	Equilibrium isotope effect. Uneven distribution of heavy and light isotopomers in the products and substrates of a chemical system at the thermodynamic equilibrium
Fractionation	For a chemical or biochemical reaction, the fractionation is defined as $\alpha = \frac{r_{substrate}}{r_{product}}$, where r is an isotope ratio. The fractionation is the expression of an isotope effect.
Isotopes	Atoms having the same number of protons (atomic number) in the nucleus, but a different a number of neutrons
Isotopomers	Molecules having the same structure but a different isotopic composition (e.g. $^{1}H_2{}^{16}O$, $^{1}H_2{}^{18}O$, $^{2}H_2{}^{16}O$ = (D_2O), $HD^{16}O$ and $D_2{}^{18}O$ are isotopomers).
Isotope ratio	The isotope ratio r is defined as $r = \frac{\text{isotope 1}}{\text{isotope 2}}$
Kinetic isotopic effect (KIE)	The reaction rate constants of light (k_{light}) and heavy (k_{heavy}) isotopomers are different when the molecule-isotope bond becomes affected by the reaction step which is determinant for the kinetic. The KIE is expressed as $KIE = \frac{k_{light}}{k_{heavy}}$. This effect is especially strong when replacing one hydrogen with a deuterium.
Primary indicator	Variables whose value is directly linked with the characteristic investigated. Primary indicators aren't related to human activities.
Secondary indicator	Variable which is indirectly linked with the characteristic investigated (e.g. which is determined by the food technological process, or agricultural practices).

Acknowledgement

The contribution of Martin Gränicher (Swiss Federal Office of Public Health) to the literature search is gratefully acknowledged.

References

Aguilar-Cisneros, B.O., Lopez, M.G., Richling, E. *et al*. (2002). Tequila authenticity assessment by headspace SPME-HRGC-IRMS analysis of C-13/C-12 and O-18/O-16 ratios of ethanol. *Journal of Agricultural and Food Chemistry*, **50**, 7520–7523.

Anderson, K. and Smith, B. (2006). Effect of season and variety on the differentiation of geographic growing origin of pistachios by stable isotope profiling. *Journal of Agricultural and Food Chemistry*, **54**, 1747–1752.

Anonymous (2004). Report of the Fourth Session of the *ad hoc* Codex Intergovernmental Task Force on Fruit and Vegetable Juices, Fortaleza (Ceará), Brazil, 11–15.

Antinelli, J., Clement, M.C., Moussa, I. *et al*. (2001). Detection of cane sugar in honeys by isotopic and microscopic analysis: comparative study. *Annales des Falsifications de l'Expertise Chimique et Toxicologique*, **94**, 13–22.

Antolovich, M., Li, X. and Robards, K. (2001). Detection of adulteration in Australian orange juices by stable carbon isotope ratio analysis (SCIRA). *Journal of Agricultural and Food Chemistry*, **49**, 2623–2626.

Aursand, M., Mabon, F. and Martin, G.J. (2000). Characterization of farmed and wild salmon (*Salmo salar*) by a combined use of compositional and isotopic analyses. *Journal of the American Oil Chemists' Society*, **77**, 659–666.

Baudler, R., Adam, L., Rossmann, A. *et al*. (2006). Influence of the distillation step on the ratios of stable isotopes of ethanol in cherry brandies. *Journal of Agricultural and Food Chemistry*, **54**, 864–869.

Bauer-Christoph, C., Christoph, N., Aguilar-Cisneros, B.O. *et al*. (2003). Authentication of tequila by gas chromatography and stable isotope ratio analyses. *European Food Research and Technology*, **217**, 438–443.

Bengsch, E., Kettrup, A., Stocker, A. and Rossmann, A. (2006). Authenticity confirmation of royal jelly and/or its components through (multi) isotope analysis. Patent No. 14.2006.

Bensaid, F.F., Wietzerbin, K. and Martin, G.J. (2002). Authentication of natural vanilla flavorings: isotopic characterization using degradation of vanillin into guaiacol. *Journal of Agricultural and Food Chemistry*, **50**, 6271–6275.

Bilke, S. and Mosandl, A. (2002). $^{2}H/^{1}H$ and $^{13}C/^{12}C$ isotope ratios of trans-anethole using gas chromatography-isotope ratio mass spectrometry. *Journal of Agricultural and Food Chemistry*, **50**, 3935–3937.

Boner, M. (2005). Stable isotope variation as a tool to trace the authenticity of beef. PhD Thesis, Rheinischen Friedrich-Wilhelm Universität, Bonn.

Boner, M. and Forstel, H. (2004). Stable isotope variation as a tool to trace the authenticity of beef. *Analytical and Bioanalytical Chemistry*, **378**, 301–310.

Branch, S., Burke, S., Evans, P. *et al*. (2003). A preliminary study in determining the geographical origin of wheat using isotope ratio inductively coupled plasma mass spectrometry with ^{13}C, ^{15}N mass spectrometry. *Journal of Analytical Atomic Spectrometry*, **18**, 17–22.

Brand, W.A. (2007). Mass spectrometer hardware for analyzing stable isotopes ratios. In: P.A. De Groot (ed.), *Handbook of Stable Isotope Analytical Techniques*. Amsterdam: Elsevier, pp. 835–856.

Brand, W.A., Tegtmeyer, A.R. and Hilkert, A.W. (1994). Compound-specific isotope analysis – extending toward $^{15}N/^{14}N$ and $^{18}O/^{16}O$. *Organic Geochemistry*, **21**, 585–594.

Brenna, E., Fronza, G., Fuganti, C. *et al*. (2005). Stable isotope characterization of the ortho-oxygenated phenylpropanoids: Coumarin and melilotol. *Journal of Agricultural and Food Chemistry*, **53**, 9383–9388.

Brescia, M.A., Di Martino, G., Guillou, C. *et al*. (2002a). Differentiation of the geographical origin of durum wheat semolina samples on the basis of isotopic composition. *Rapid Communications in Mass Spectrometry*, **16**, 2286–2290.

Brescia, M.A., Di, M., Fares, C. *et al*. (2002b). Characterization of Italian durum wheat semolina by means of chemical analytical and spectroscopic determinations. *Cereal Chemistry*, **79**, 238–242.

Brescia, M.A., Monfreda, M., Buccolieri, A. and Carrino, C. (2005). Characterisation of the geographical origin of buffalo milk and mozzarella cheese by means of analytical and spectroscopic determinations. *Food Chemistry*, **89**, 139–147.

Brooks, J., Buchmann, N., Phillips, S. *et al*. (2002). Heavy and light beer: a carbon isotope approach to detect C4 carbon in beers of different origins, styles, and prices. *Journal of Agricultural and Food Chemistry*, **50**, 6413–6418.

Burgoyne, T.W. and Hayes, J.M. (1998). Quantitative production of H_2 by pyrolysis of gas chromatographic effluents. *Analytical Chemistry*, **70**, 5136–5141.

Calderone, G., Naulet, N., Guillou, C. and Reniero, F. (2004). Characterization of European wine glycerol: stable carbon isotope approach. *Journal of Agricultural and Food Chemistry*, **52**, 5902–5906.

Calderone, G., Naulet, N., Guillou, C. *et al*. (2005). Analysis of the ^{13}C natural abundance of CO_2 gas from sparkling drinks by gas chromatography/combustion/isotope ratio mass spectrometry. *Rapid Communications in Mass Spectrometry*, **19**, 701–705.

Chiacchierini, E., Bogoni, P., Franco, M. *et al*. (2002). Characterization of the regional origin of sheep and cow cheeses by casein stable isotope ($^{13}C/^{12}C$ and $^{15}N/^{14}N$) ratios. *Journal of Commodity Science*, **41**, 303–315.

Choi, W.-J., Ro, H.-M. and Hobbie, E.A. (2003). Patterns of natural ^{15}N in soils and plants from chemically and organically fertilized uplands. *Soil Biology and Biochemistry*, **35**, 1493–1500.

Cordella, C., Moussa, I., Martel, A.C. *et al*. (2002). Recent developments in food characterization and adulteration detection: technique-oriented perspectives. *Journal of Agricultural and Food Chemistry*, **50**, 1751–1764.

Dangaard, W. (1964). Stable isotopes in precipitation. *Tellus*, **XVI**, 436–468.

Day, M., Correia, P. and Hammond, D. (2001). ^{13}C-IRIS: an improved method to detect the addition of low levels of C4-derived sugars to juices. *Journal of AOAC International*, **84**, 957–963.

De la Fuente, M.A. and Juarez, M. (2005). Authenticity assessment of dairy products. *Critical Reviews in Food Science and Nutrition*, **45**, 563–585.

Dennis, M.J. (1999). Multidimensional methods for determining the authenticity of basmati rice. In: *Proceeding of the 5th Conference on Food Authenticity, La Baule*. Nantes: Eurofins Scientific, pp. 365–370.

Deponge, C., Coulon, J.B., Bonnefoy, J.C., *et al*. (2001). Caractérisation du lait en fonction de son origine géographique et du mode d'alimentation par RMN ^{13}C et SMRI. [13C NMR and IRMS methods to characterize the milk according to diet and geographical origin]. In: Proceedings of the 8th rencontres autour des recherches sur les ruminants, Paris, 5–6 décembre. Paris: INRA.

Elss, S., Preston, C., Appel, M. *et al*. (2006). Influence of technological processing on apple aroma analyzed by high resolution gas chromatography-mass spectrometry and on-line gas chromatography-combustion/pyrolysis-isotope ratio mass spectrometry. *Food Chemistry*, **98**, 269–276.

Fauhl, C. (1999). Detection of adulteration of olive oil with hazelnut oil by discriminant analysis based on analytical data obtained by NMR, IRMS and high resolution-high temperature GC. In: *Proceeding of the 5th European Symposium on Food Authenticity, La Baule, France*. Nantes: Eurofins, pp. 305–338.

Fink, K., Richling, E., Heckel, F. and Schreier, P. (2004). Determination of $^{2}H/^{1}H$ and $^{13}C/^{12}C$ isotope ratios of (E)-methyl cinnamate from different sources using isotope ratio mass spectrometry. *Journal of Agricultural and Food Chemistry*, **52**, 3065–3068.

Franke, B. M., Koslitz, S., Micaux, F. *et al*. (2007). Tracing the geographic origin of poultry meat and dried beef with oxygen and strontium isotope ratios. *European Food Research and Technology*, in press (published on-line, January 2007).

Fronza, G., Fuganti, C., Grasselli, P. *et al*. (2001). Delta(13)C- and delta(18)O-values of glycerol of food fats. *Rapid Communications in Mass Spectrometry*, **15**, 763–766.

Fronza, G., Fuganti, C., Schmidt, H.L. and Werner, R.A. (2002). The delta18O-value of p-OH group of L-Tyrosine permits the assignement of its origin to animal or plant sources. *European Food Research and Technology*, **215**, 55–58.

Fronza, G., Fuganti, C., Serra, S. *et al*. (2003). Stable isotope characterisation of food phenylpropanoids: raspberry ketone, vanillin, resveratrol, phenylacetic acid and tyrosol. In: *Proceedings of the Weurman Flavor Research Symposium, 10th, Beaune, France*. Paris: Editions Tec&Doc, pp. 429–432.

Fry, B. (1988). Food web structure on Georges Bank from stable C, N and S isotopic composition. *Limnology and Oceanography*, **33**, 1182–1190.

Giaccio, M., Del Signore, A., Di Giacomo, F. *et al*. (2003). Characterization of cow and sheep cheeses in a regional scale by stable isotope ratios of casein ($^{13}C/^{12}C$, $^{15}N/^{14}N$) and glycerol ($^{18}O/^{16}O$). *Journal of Commodity Science*, **42**, 193–204.

Gimenez, M., Salazar, D. and Solana, I. (1999). Regional origin assignment of red wines from Valencia (Spain) by ^{2}H NMR and ^{13}C IRMS stable isotope analysis of fermentative ethanol. *Journal of Agricultural and Food Chemistry*, **47**, 2645–2652.

Giraudon, S., Danzart, M. and Merle, M.H. (2000). Deuterium nuclear magnetic resonance spectroscopy and stable carbon isotope ratio analysis/mass spectrometry of certain monofloral honeys. *Journal of AOAC International*, **83**, 1401–1409.

Gonzalez, J., Remaud, G., Jamin, E. *et al*. (1999). Specific natural isotope profile studied by isotope ratio mass spectrometry (SNIP-IRMS): $^{13}C/^{12}C$ ratios of fructose, glucose, and sucrose for improved detection of sugar addition to pineapple juices and concentrates. *Journal of Agricultural and Food Chemistry*, **47**, 2316–2321.

Gonzalez, M., Gonzalez, P., Hernandez, M. and Sanchez, G. (2001). Stable isotope analysis as an analytical technique for the characterization of products from Iberian swine. *Eurocarne*, **11**, 125–137.

Gremaud, G., Pfammatter, E., Piantini, U. and Quaile, S. (2002). Classification of Swiss wines on a regional scale by means of a multi-isotopic analysis combined with

chemometric methods. *Mitteilungen aus Lebensmitteluntersuchung und Hygiene*, **93**, 44–56.

Gremaud, G., Quaile, S., Piantini, U. *et al*. (2004). Characterization of Swiss vineyards using isotopic data in combination with trace elements and classical parameters. *European Food Research and Technology*, **219**, 97–104.

Guo, F., Chun, L., Yan, Z. *et al*. (2006). Study on distribution pattern of stable carbon isotope ratio of Chinese honeys by isotope ratio mass spectrometry. *Journal of the Science of Food and Agriculture*, **86**, 315–319.

Hegerding, L., Seidler, D., Danneel, H.J. *et al*. (2002). Oxygen isotope ratio analysis for the determination of the origin of beef. *Fleischwirtschaft*, **82**, 95–100.

Heier, A. (2007). *Nachweis der geographischen Herkunft von Pistazien*. Dissertation, Bundesinstitut für Risikobewertung, Berlin.

Herbach, K.M., Stintzing, F.C., Elss, S. *et al*. (2006). Isotope ratio mass spectrometrical analysis of betanin and isobetanin isolates for authenticity evaluation of purple pitaya-based products. *Food Chemistry*, **99**, 204–209.

Hoer, K., Ruff, C., Weckerle, B. *et al*. (2001a). Flavor authenticity studies by $^{2}H/^{1}H$ ratio determination using on-line gas chromatography pyrolysis isotope ratio mass spectrometry. *Journal of Agricultural and Food Chemistry*, **49**, 21–25.

Hoer, K., Ruff, C., Weckerle, B. *et al*. (2001b). $^{2}H/^{1}H$ ratio analysis of flavor compounds by on-line gas chromatography-pyrolysis-isotope ratio mass spectrometry (HRGC-P-IRMS): citral. *Flavour and Fragrance Journal*, **16**, 344–348.

Houerou, G. (1999). Determination of $^{18}O/^{16}O$ isotopic ratio of sugar, citric acid and water from single strength orange juice. *Rapid Communications in Mass Spectrometry*, **13**, 1257–1262.

Husted, S., Mikkelsen, B.F., Jensen, J. and Nielsen, N.E. (2004). Elemental fingerprint analysis of barley (*Hordeum vulgare*) using inductively coupled plasma mass spectrometry, isotope-ratio mass spectrometry, and multivariate statistics. *Analytical and Bioanalytical Chemistry*, **378**, 171–182.

Jamin, E., Lees, M., Fuchs, G. and Martin, G.G. (2000). Detection of added L-malic acid in apple and cherry juices – site-specific ^{13}C-IRMS method. *Fruit Processing*, **10**, 434–436.

Jamin, E., Guerin, R., Gonthier, L. *et al*. (2003). *Detection of water added to food liquids by isotope ratio mass spectrometry*. Ed Eurofins: Patent.

Jamin, E., Martin, F. and Martin, G.G. (2004). Determination of the 13C/12C ratio of ethanol derived from fruit juices and maple syrup by isotope ratio mass spectrometry: collaborative study. *Journal of AOAC International*, **87**, 621–631.

Jamin, E., Martin, F., Santamaria-Fernandez, R. and Lees, M. (2005). Detection of exogenous citric acid in fruit juices by stable isotope ratio analysis. *Journal of Agricultural and Food Chemistry*, **53**, 5130–5133.

Jung, J., Sewenig, S., Hener, U. and Mosandl, A. (2005). Comprehensive authenticity assessment of lavender oils using multielement/multicomponent isotope ratio mass spectrometry analysis and enantioselective multidimensional gas chromatography-mass spectrometry. *European Food Research and Technology*, **220**, 232–237.

Jung, J.C., Jaufmann, T., Hener, U. *et al*. (2006). Progress in wine authentication: GC-C/P-IRMS measurements of glycerol and GC analysis of 2,3-butanediol stereoisomers. *European Food Research and Technology*, **223**, 811–820.

Kahle, K., Preston, C., Richling, E. *et al*. (2005). On-line gas chromatography combustion/pyrolysis isotope ratio mass spectrometry (HRGC-C/P-IRMS). of major volatiles from pear fruit (*Pyrus communis*) and pear products. *Food Chemistry*, **91**, 449–455.

Kelly, S.D. (2003). Using stable isotope ratio mass spectrometry (IRMS) in food authentification and traceability. In: M. Lees (ed.), *Food Authenticity and Traceability*. Abington: Woodhead Publishing Ltd, pp. 156–183.

Kelly, S.D. and Rhodes, C. (2002). Emerging techniques in vegetable oil analysis using stable isotope ratio mass spectrometry. *Grasas y Aceites (Sevilla), Special issue: Emerging Techniques*, **53**, 34–44.

Kelly, S.D., Baxter, M., Chapman, S. *et al*. (2002). The application of isotopic and elemental analysis to determine the geographical origin of premium long grain rice. *European Food Research and Technology*, **214**, 72–78.

Kelly, S.D., Rhodes, C., Lofthouse, J.H. *et al*. (2003). Detection of sugar syrups in apple juice by δ^2H and $\delta^{13}C$ analysis of hexamethylenetetramine prepared from fructose. *Journal of Agricultural and Food Chemistry*, **51**, 1801–1806.

Kosir, I.J., Kocjancic, M., Ogrinc, N. and Kidric, J. (2001). Use of SNIF-NMR and IRMS in combination with chemometric methods for the determination of chaptalisation and geographical origin of wines (the example of Slovenian wines). *Analytica Chimica Acta*, **429**, 195–206.

Krummen, M.A., Hilkert, A.W., Juchelka, D. *et al*. (2004). A new concept for isotope ratio monitoring liquid chromatography/mass spectrometry. *Rapid Communications in Mass Spectrometry*, **18**, 2260–2266.

Lin, G.P., Rau, Y.H., Chen, Y.F. *et al*. (2003). Measurements of δD and $\delta^{18}O$ stable isotope ratios in milk. *Journal of Food Science*, **68**, 2192–2195.

Manca, G., Camin, F., Coloru, G.C. *et al*. (2001). Characterization of the geographical origin of Pecorino Sardo cheese by casein stable isotope $^{13}C/^{12}C$ and $^{15}N/^{14}N$ ratios and free amino acid ratios. *Journal of Agricultural and Food Chemistry*, **49**, 1404–1409.

Manca, G., Franco, M.A., Versini, G. *et al*. (2006). Correlation between multielement stable isotope ratio and geographical origin in Peretta cows' milk cheese. *Journal of Dairy Science*, **89**, 831–839.

Martin, G.J., Mazure, M., Jouitteau, C. *et al*. (1999). Characterization of the geographic origin of Bordeaux wines by a combined use of isotopic and trace element measurements. *American Journal of Enology and Viticulture*, **50**, 409–417.

Martinelli, L., Moreira, M., Ometto, J. *et al*. (2003). Stable carbon isotopic composition of the wine and CO_2 bubbles of sparkling wines: detecting C4 sugar additions. *Journal of Agricultural and Food Chemistry*, **51**, 2625–2631.

Matucha, M., Jockisch, W., Verner, P. and Anders, G. (1991). Isotope effect in gas-liquid chromatography of labeled compounds. *Journal of Chromatography*, **588**, 251–258.

Merritt, D.A., Freeman, K.H., Ricci, M.P. *et al*. (1995). Performance and optimization of a combustion interface for isotope ratio monitoring gas-chromatography mass-spectrometry. *Analytical Chemistry*, **67**, 2461–2473.

Meylahn, K. (2007). Herkunftsanalyse von Spargel mittels Stabilisotopenanalyse. *Deutsche Lebensmittel-Rundschau*, **102**, 523–526.

Moguel-Ordonez, Y., Echazarreta, C.M. and Mora-Escobedo, R. (2005). $\delta^{13}C$ isotopic index of honeys produced in the Yucatan peninsula, Mexico. *Journal of Apicultural Research*, **44**, 49–53.

Monsallier-Bitea, C., Jamin, E., Lees, M. *et al*. (2006). Study of the influence of alcoholic fermentation and distillation on the oxygen-18/oxygen-16 isotope ratio of ethanol. *Journal of Agricultural and Food Chemistry*, **54**, 279–284.

Ogrinc, N., Kosir, I., Kocjancic, M. and Kidric, J. (2001). Determination of authenticity, regional origin, and vintage of Slovenian wines using a combination of IRMS and SNIF-NMR analyses. *Journal of Agricultural and Food Chemistry*, **49**, 1432–1440.

Padovan, G.J., de, J., Rodrigues, L.P. and Marchini, J.S. (2003). Detection of adulteration of commercial honey samples by the 13C/12C isotopic ratio. *Food Chemistry*, **82**, 633–636.

Perez, A.L., Smith, B.W. and Anderson, K.A. (2006). Stable isotope and trace element profiling combined with classification models to differentiate geographic growing origin for three fruits: effects of subregion and variety. *Journal of Agricultural and Food Chemistry*, **54**, 4506–4516.

Piasentier, E., Valusso, R., Camin, F. and Versini, G. (2003). Stable isotope ratio analysis for authentication of lamb meat. *Meat Science*, **64**, 239–247.

Pillonel, L. (2005). Geographic origin of European Emmental. Use of discriminant analysis and artificial neural network for classification purposes. *International Dairy Journal*, **15**, 557–562.

Pillonel, L., Badertscher, R., Froidevaux, P. *et al*. (2003). Stable isotope ratios, major, trace and radioactive elements in Emmental cheeses of different origins. *Lebensmittel-Wissenschaft und -Technologie*, **36**, 615–623.

Pillonel, L., Buetikofer, U., Rossmann, A. *et al*. (2004). Analytical methods for the detection of adulteration and mislabelling of Raclette Suisse and Fontina PDO cheese. *Mitteilungen aus Lebensmitteluntersuchung und Hygiene*, **95**, 489–502.

Pillonel, L., Badertscher, R., Casey, M. *et al*. (2005). Geographic origin of European Emmental cheese: characterisation and descriptive statistics. *International Dairy Journal*, **15**, 547–556.

Rapisarda, P. (2005). Nitrogen metabolism components as a tool to discriminate between organic and conventional citrus fruits. *Journal of Agricultural and Food Chemistry*, **53**, 2664–2669.

Rau, Y., Lin, G., Chang, W. *et al*. (2005). Using C-13/C-12 isotopic ratio analysis to differentiate between rice spirits made from rice and cane molasses. *Journal of Food and Drug Analysis*, **13**, 159–162.

Renou, J., Bielicki, G., Deponge, C. *et al*. (2004). Characterization of animal products according to geographic origin and feeding diet using nuclear magnetic resonance and isotope ratio mass spectrometry. Part II: Beef meat. *Food Chemistry*, **86**, 251–256.

Richling, E., Hoehn, C., Weckerle, B. *et al*. (2003). Authentication analysis of caffeine-containing foods via elemental analysis combustion/pyrolysis isotope ratio mass spectrometry (EA-C/P-IRMS). *European Food Research and Technology*, **216**, 544–548.

Ritz, P., Gachon, P., Garel, J. *et al*. (2005). Milk characterization: effect of the breed. *Food Chemistry*, **91**, 521–523.

Rossmann, A. (2001). Determination of stable isotope ratios in food analysis. *Food Reviews International*, **17**, 347–381.

Rossmann, A., Haberhauer, G., Hoelzl, S. *et al*. (2000). The potential of multielement stable isotope analysis for regional origin assignment of butter. *European Food Research and Technology*, **211**, 32–40.

Ruff, C., Hoer, K., Weckerle, B. *et al*. (2000). 2H/1H ratio analysis of flavor compounds by on-line gas chromatography pyrolysis isotope ratio mass spectrometry (HRGC-P-IRMS): benzaldehyde. *Journal of High Resolution Chromatography*, **23**, 357–359.

Ruff, C., Hoer, K., Weckerle, B. *et al*. (2002). Authenticity assessment of estragole and methyl eugenol by on-line gas chromatography-isotope ratio mass spectrometry. *Journal of Agricultural and Food Chemistry*, **50**, 1028–1031.

Sacco, D., Brescia, M.A., Buccolieri, A. and Jambrenghi, A.C. (2005). Geographical origin and breed discrimination of Apulian lamb meat samples by means of analytical and spectroscopic determinations. *Meat Science*, **71**, 542–548.

Sakamoto, N., Ishida, T., Arima, T. *et al*. (2002). Concentrations of radiocarbon and isotope compositions of stable carbon in food. In: K. Morita (ed.), *International Symposium on Isotope Effects in Physics, Chemistry and Engineering, Nagoya, Japan, August 22–24*. Published in the *Journal of Nuclear Science and Technology*, **39**(4), 323–328.

Santrock, J., Studley, S.A. and Hayes, J.M. (1985). Isotopic analyses based on the mass spectrum of carbon dioxide. *Analytical Chemistry*, **57**, 1444–1448.

Schlechtriem, C., Focken, U. and Becker, K. (2003). Effect of different lipid extraction methods on delta13C of lipid and lipid-free fractions of fish and different fish feeds. *Isotopes in Environmental and Health Studies*, **39**, 135–140.

Schmidt, O., Quilter, J.M., Bahar, B. *et al*. (2005a). Inferring the origin and dietary history of beef from C, N and S stable isotope ratio analysis. *Food Chemistry*, **91**, 545–549.

Schmidt, H., Rossmann, A., Voerkelius, S. *et al*. (2005b). Isotope characteristics of vegetables and wheat from conventional and organic production. *Isotopes in Environmental and Health Studies*, **41**, 223–228.

Serra, F., Guillou, C.G., Reniero, F. *et al*. (2005a). Determination of the geographical origin of green coffee by principal component analysis of carbon, nitrogen and boron stable isotope ratios. *Rapid Communications in Mass Spectrometry*, **19**, 2111–2115.

Serra, F., Reniero, F., Guillou, C.G. *et al*. (2005b). 13C and 18O isotopic analysis to determine the origin of L-tartaric acid. *Rapid Communications in Mass Spectrometry*, **19**, 1227–1230.

Sewenig, S., Hener, U. and Mosandl, A. (2003). Online determination of 2H/1H and 13C/12C isotope ratios of cinnamaldehyde from different sources using gas chromatography isotope ratio mass spectrometry. *European Food Research and Technology*, **217**, 444–448.

Sewenig, S., Bullinger, D., Hener, U. and Mosandl, A. (2005). Comprehensive authentication of (E)-alpha(beta)-ionone from raspberries, using constant flow

MDGC-C/P-IRMS and enantio-MDGC-MS. *Journal of Agricultural and Food Chemistry*, **53**, 838–844.

Simpkins, W.A., Patel, G., Collins, P. *et al*. (1999). Oxygen isotope ratios of juice water in Australian oranges and concentrates. *Journal of Agricultural and Food Chemistry*, **47**, 2606–2612.

Simpkins, W.A., Gordhan, P., Harrison, M. and Goldberg, D. (2000). Stable carbon isotope ratio analysis of Australian orange juices. *Food Chemistry*, **70**, 385–390.

Spangenberg, J.E. and Dionisi, F. (2001). Characterization of cocoa butter and cocoa butter equivalents by bulk and molecular carbon isotope analyses: implications for vegetable fat quantification in chocolate. *Journal of Agricultural and Food Chemistry*, **49**, 4271–4277.

Spangenberg, J.E. and Ogrinc, N. (2001). Authentication of vegetable oils by bulk and molecular carbon isotope analyses with emphasis on olive oil and pumpkin seed oil. *Journal of Agricultural and Food Chemistry*, **49**, 1534–1540.

Stocker, A., Rossmann, A., Kettrup, A. and Bengsch, E. (2006). Detection of royal jelly adulteration using carbon and nitrogen stable isotope ratio analysis. *Rapid Communications in Mass Spectrometry*, **20**, 181–184.

Sturm, K., Hoffmann, G., Langmann, B. and Stichler, W. (2005). Simulation of δ18O in precipitation by the regional circulation model REMOiso. *Hydrological Processes*, **19**, 3425–3444.

Tamura, H., Appel, M., Richling, E. and Schreier, P. (2005). Authenticity assessment of gamma- and delta-decalactone from prunus fruits by gas chromatography combustion/pyrolysis isotope ratio mass spectrometry (GC-C/P-IRMS). *Journal of Agricultural and Food Chemistry*, **53**, 5397–5401.

Truchot, E., Berthou, L. and Gavard, P. (2003). Isotopic analysis for detection of chemical fertilizers in the production of organic food crops and for product certification. Ed. L Laboratoire, Patent No. 15.2003.

Versini, G., Camin, F., Ramponi, M. and Dellacassa, E. (2006). Stable isotope analysis in grape products: C-13-based internal standardisation methods to improve the detection of some types of adulterations. *Analytica Chimica Acta*, **563**, 325–330.

Wagner, H. (2005). Stable isotope signatures – a method for the determination of the geographic origin? *Mitteilungsblatt der Fleischforschung Kulmbach*, **44**, 217–222.

Werner, R.A. (2003). The online $^{18}O/^{16}O$ analysis: development and application. *Isotopes in Environmental and Health Studies*, **39**, 85–104.

Werner, R.A. and Brand, W.A. (2001). Referencing strategies and techniques in stable isotope ratio analysis. *Rapid Communications in Mass Spectrometry*, **15**, 501–519.

Werner, R.A., Bruch, B.A. and Brand, W.A. (1999). ConFlo III – an interface for high precision d13C and d15N analysis with an extended dynamic range. *Rapid Communications in Mass Spectrometry*, **13**, 1237–1241.

Wieser, M.E., Iyer, S.S., Krouse, H.R. and Cantagallo, M.I. (2001). Variations in the boron isotope composition of Coffea arabica beans. *Applied Geochemistry*, **16**, 317–322.

10

Chromatographic Technique: Gas Chromatography (GC)

A.C. Soria, A.I. Ruiz-Matute, M.L. Sanz and I. Martínez-Castro

Introduction

The term *chromatography* describes a broad range of analytical techniques for the separation of mixtures. A chromatographic system comprises two phases: a *mobile phase* (gas, liquid or supercritical fluid) and an immiscible *stationary phase* (solid or liquid). Analytes are distributed between the mobile and the stationary phases during the process depending on their relative affinity for both. Therefore, compounds with higher affinity for the stationary phase are retained more and elute later than those with higher affinity for the mobile phase. Stationary phases are usually set in a column (column chromatography), although paper or thin-layer chromatography (planar chromatography) are also used.

The main varieties of column chromatography are gas chromatography (GC), where the mobile phase is a gas, and liquid chromatography (HPLC), where the mobile phase is a liquid.

Gas chromatography was introduced in 1952 by James and Martin, who attempted to separate 17 fatty acids; they designed and constructed the first equipment and described the theory. In this technique the mobile phase is always an inert gas which transports the analytes through the stationary phase placed in a column. The separation process is mainly governed by the interaction of solutes with the stationary phase.

Modern Techniques for Food Authentication
ISBN: 978-0-12-374085-4

Theory and fundamentals

Chromatographic flow

Due to the compressibility of gases, the density, pressure and velocity (u) of the carrier gas vary in a non-linear way through the column, and it is therefore necessary to specify at which column point they are measured or calculated. A compression correction factor (j), which takes into account the mobile phase compressibility in the column, is defined as:

$$j = \frac{3}{2}\frac{\left(p_i/p_o\right)^2 - 1}{\left(p_i/p_o\right)^3 - 1} \tag{10.1}$$

where p_i and p_o are the inlet and outlet pressures, respectively. p_i can be adjusted in the range of 5–700 kPa, whereas p_o is usually ambient pressure.

The average linear velocity of the carrier gas ($\bar{u}$) is proportional to the linear velocity at the column outlet (u_o):

$$\bar{u} = ju_o \tag{10.2}$$

In practice, $\bar{u}$ is obtained by dividing the column length (L) by the retention time of an unretained compound (the *hold-up time*, t_M):

$$\bar{u} = L/t_M \tag{10.3}$$

The flow rate at the column outlet (F_c) can be easily measured and related to the average flow rate through $\bar{F} = jF_c$. It is also related to linear velocity:

$$\bar{F} = ku_o = k\frac{\bar{u}}{j} \tag{10.4}$$

Retention parameters

The retention volume (V_R) for a given compound is the volume of the mobile phase passed through the column from the injection point to the peak maximum, or during its *retention time* (t_R). The relationship between these parameters is described by:

$$t_R = V_R/F_c \tag{10.5}$$

The net retention volume (V_N) takes into account the compression correction factor and the hold-up time:

$$V_N = jF_c\left(t_R - t_M\right) \tag{10.6}$$

Migration of the solutes through the column

When a compound is introduced into a chromatographic column, it occupies a defined zone which starts moving through the column. The function that describes the distribution of the concentration in the zone is similar to a Gauss function. If a mixture of compounds is introduced, the compounds are distributed between the mobile and stationary phases according to their distribution coefficients. Each compound is eluted at a different t_R, and therefore they are separated.

The relationship between the time that the sample component resides in the stationary phase and the time that it resides in the mobile phase is measured through the *retention factor* (k).

$$k = t_R / t_M \tag{10.7}$$

The relative retention value calculated for two adjacent peaks is also called the *separation factor* (α), and by definition is always ≥ 1:

$$\alpha = V_{N2}/V_{N1} = (t_{R2} - t_M)/(t_{R1} - t_M) \tag{10.8}$$

Efficiency and resolution

The variation of *efficiency* (H) with the carrier gas velocity is described by the van Deemter equation (van Deemter *et al*., 1956):

$$H = A + \frac{B}{u} + (C_S + C_M)u \tag{10.9}$$

where A is the eddy-diffusion and B is the longitudinal diffusion. C_S and C_M represent, respectively, the contributions of the stationary and the mobile phases to the zone spreading caused by the resistance to mass transfer and other diffusion phenomena. When an open capillary column is used, the Golay's equation (Golay, 1968) can be used instead:

$$H = \frac{B}{u} + (C_S + C_M)u \tag{10.10}$$

In most cases, C_S is negligible when compared with C_M.

The *Resolution* (R_S) between two adjacent peaks is defined as:

$$R_S = \frac{(t_{R2} - t_{R1})}{(w_{b1} + w_{b2})/2} = \frac{2(t_{R2} - t_{R1})}{w_{b1} + w_{b2}} \tag{10.11}$$

and is easily calculated by measurement of retention times and peak widths at base (w_b) in the chromatogram. Since the main objective of chromatography is resolving mixtures, this parameter is quite important. Resolution is related both to column

efficiency (which depends on the column design) and to the separation factor (which depends on the solutes and the stationary phase) through the expression:

$$R_S = \frac{\sqrt{N}}{4}\frac{k}{1+k}\frac{\alpha-1}{\alpha} \quad \text{and also} \quad R = 1/4\sqrt{L/H}\,\frac{k}{1+k}\frac{\alpha-1}{\alpha} \qquad \textbf{(10.12)}$$

where N, the number of theoretical plates, is:

$$N = L/H \qquad \textbf{(10.13)}$$

Equation (10.12) indicates that substances with similar values of α need high values of N (namely, long and efficient capillary columns) to be resolved. This separation may also be achieved by choosing another stationary phase which provides a different value of the separation factor.

The mobile phase

Nitrogen, helium, hydrogen or argon is usually employed in the mobile phase, and is usually known as the *carrier gas*. High-purity gases are necessary, because traces of impurities such as oxygen or water can react with the solutes, spoil the stationary phase or disturb the detector response.

Helium is recommended to achieve faster separation, but nitrogen is a less expensive alternative. Hydrogen also gives very fast separation, but is harmful and requires special care. The choice of carrier gas is often dependent upon the type of detector to be used.

The stationary phase

The stationary phase may be solid or liquid, giving rise to two main chromatographic modes: gas-solid chromatography (GSC) and gas-liquid chromatography (GLC). The first mode is especially useful for measuring physical parameters and for the analysis of certain compounds such as permanent gases or very polar small molecules. The analytical separations of organic substances are mainly carried out by GLC, thus only this mode will be described here.

Liquid phases are usually polymeric molecules with enough stability and viscosity to stand on the column at the temperature of analysis, and capable of dissolving the solutes fast. These polymers are often cross-linked to improve the phase stability and to extend the column life.

The separation mechanism is mainly partition, although other mechanisms, like chirality, mesomerism and complex formation, may also contribute to the separation. For the study of food adulteration, the most interesting are:

- *Partition*. Compounds dissolved in the liquid phase are in equilibrium with its vapor (Henry's law); the elution order may be proportional to the boiling points when the phase is non-polar, or very different depending on the activity coefficients when the phase is polar.

- *Chirality*. Enantiomer pairs always co-elute when chromatographied on achiral phases. However, liquid phases possessing chiral groups can show a greater interaction with one of the pair members, which is then relatively more retained. As chiral interaction energies are small, α values are usually close to 1 and high efficiency is required, as is provided by capillary columns. Chiral phases are based on peptides, on amide-substituted polysiloxanes or on substituted cyclodextrins.

The liquid stationary phases have to be thermally stable over a wide temperature range. Other properties to be noted are polarity and selectivity. *Polarity* depends on the functional groups present in the molecule of liquid phase, and is usually defined by various empirical scales. That described by McReynolds (1970) is based on an additive model which describes 10 different molecular interactions represented by 10 solutes-probes and a series of saturated hydrocarbons. These interactions are described by several parameters (McReynolds constants) deduced from the retention observed in the studied phase and in squalane, which is set as the zero of this polarity scale. The first five McReynolds constants appear in most commercial catalogs as indicators of the polarity.

Table 10.1 shows some characteristics of the most-used liquid phases. Hydrocarbons (like squalane or Apolane) are used to obtain reference data. Polysiloxanes showing a wide polarity range (with methyl, phenyl, trifluoropropyl, or cyanoalkyl substituents) are commonly called "silicones" and are the most widely used phases, since they possess good thermal stability and high permeability towards solutes. Polyethyleneglycols with different chain lengths (from MW 150 until near 4.10E6) are another family of highly used liquid phases. Phases based on the carborane skeleton are specially recommended for high-temperature separations.

Selectivity represents the discrimination power of a phase towards very similar molecules due to its ability to interact in a specific way with every solute. It can be estimated by the separation factor α, calculated by Equation (10.8).

Table 10.1 Some common liquid phases used in GC

Composition	Commercial name	Polarity*	T range (°C)
Squalane	Squalane	0	20–120
Branched hydrocarbon	Apolane	71	35–260
100% methyl silicone	OV-1, SE-30, OV-101, SP-2100, CP-Sil 5CB, DB-1, SPB-1, BP-1	222	30–330
94% methyl, 5% phenyl, 1% vinyl silicone	SE-54, DB-5, CP-Sil 8CB, SPB-5, BP-5, AT-5	336	50–300
50% methyl, 50% phenyl silicone	OV-17, DB-17, SP-2250, HP-50, SPB-50	884	20–350
50% methyl, 50% trifluoropropyl silicone	OV-210, SP-2401, DB-210	1520	20–275
50% methyl, 25% phenyl, 25% cyanopropyl silicone	OV-225, XE-60, DB-225, CP-Sil 43CB, BP-15	1813	20–250
Poly(ethyleneglycol)	Carbowax, Superox, DB-Wax, CP-Wax 52CB, BP-20	2308	60–225
Poly(ethyleneglycol) modified	FFAP, SP-1000, AT-1000, OV-351, Nukol, CP-Wax 58CB, BP-21	2746	50–250
100% cyanopropyl silicone	OV-275, CP-Sil 88, SP-2340, Silar 10C	4219	30–250

*Polarity is expressed as the sum of the five first constants of McReynolds.

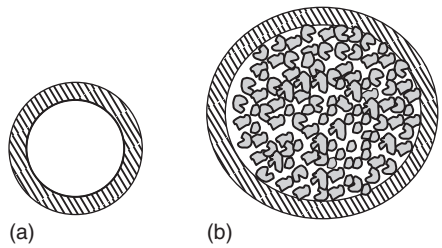

Figure 10.1 Cross-section of a wall-coated capillary column (a) and a packed column (b).

Table 10.2 Dimensions of GC columns

Type	Diameter (mm)	Length (m)	df (μm)	dp (μm)
Capillary	0.1–0.5	1–100	0.1–5	—
Micropacked	0.8–1	2–7	—	80–200
Packed	2–6	2–7	—	80–500

df: film thickness;
dp: particle diameter

Columns

There are two general types of columns: open-tubular (also called capillary) and packed (Figure 10.1).

Packed columns consist of a glass or metal tube packed with inert solid particles (100–250 μm). Analytes are either adsorbed onto the surface of these particles (GSC) or dissolved in the film of liquid stationary phase coating them (GLC). The mobile phase circulates through the interstitial channels among particles. At present these columns are mainly used for permanent gas analysis, and they are cheap, robust and easy to handle.

For capillary columns, the most frequently used GLC columns are open-tubular: the stationary phase is distributed on the inner wall, and the mobile phase circulates through a central channel. The capillary tubing is usually made of fused silica; this is a fragile material which is generally externally covered with a thin layer of polyimide in order to reinforce it. Table 10.2 presents the typical dimensions of the analytical columns used in GC.

Effect of column dimensions on the separation

Since system efficiency depends on the dimensions of the analytical column, the columns should be chosen in order to achieve the desired resolution in the minimum time. Efficiency depends on all column dimensions: length, inner diameter and particle size. It is directly related to column length, as shown in Equation (10.13), and inversely related to inner diameter as its square appears in the C_M term of Golay's Equation (10.10). The efficiency of a packed column is strongly related to the particle diameter, which appears in two terms (A and C_M) of the van Deemter Equation (10.9). The efficiency of open columns is very high, since it is possible to use very long columns with a moderate pressure drop of between 0.1 and 7 kg cm^{-2}.

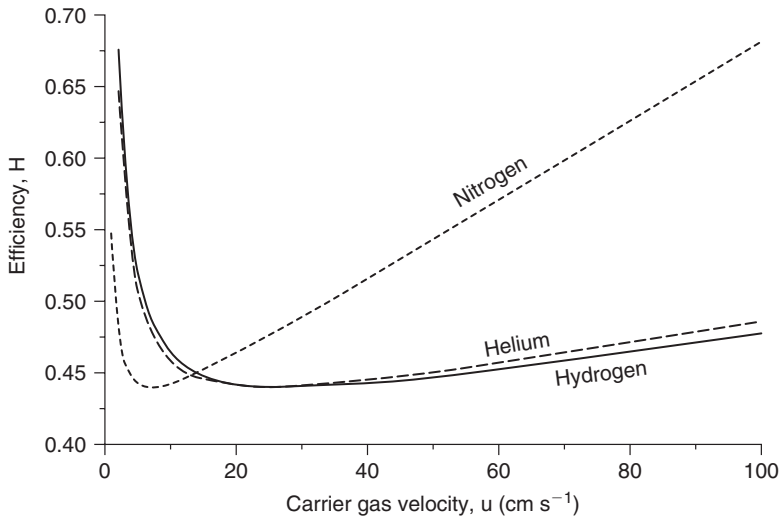

Figure 10.2 Variation of H (efficiency) with u (carrier gas velocity) for the most used carrier gases.

Capillary columns with the inner wall covered by a porous layer (PLOT) or by a solid particle layer (SCOT) where the stationary phase is coated have high sample load capacity and also high efficiency.

Operating conditions

The optimization of separations is usually carried out by changing the flow rate of the carrier gas and the column temperature; other parameters are related to both injector and detector operation modes.

The flow rate is usually controlled through either a pressure regulator or a flow controller. For a given compound, Equation (10.5) predicts that t_R is inversely proportional to the flow rate. This should be adjusted in order to achieve a linear velocity close to the van Deemter optimum (Equation (10.9)); higher flow rates will reduce the analysis time (Figure 10.2).

The influence of temperature on retention time is very high. When the temperature is raised, both V_R and t_R decrease. In practice, temperature operation should be adjusted to obtain a retention factor (k) between 1 and 15. When a mixture contains compounds with a high span of volatility, it is not possible to find an optimum temperature to elute all components in a reasonable time. Since oven temperature is easily changed, it can be programmed during the chromatographic run and thus each compound will be analyzed under adequate conditions.

Instrumentation

As shown in Figure 10.3, a gas chromatograph is constituted by three main parts: (i) the injector to introduce and volatilize the sample; (ii) the oven where the chromatographic column is placed; and (iii) the detector, which provides a signal for each of

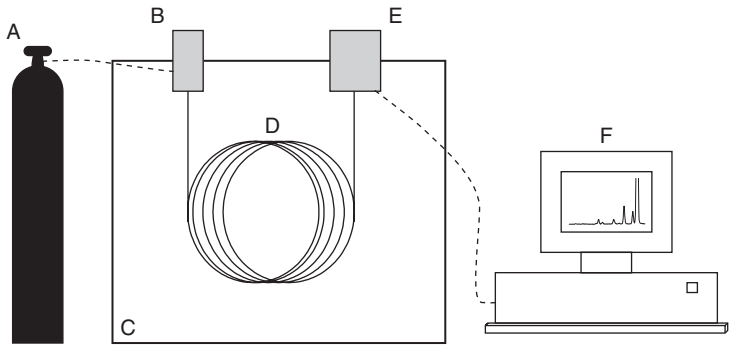

Figure 10.3 Schematic of a GC system: A, gas container; B, injector; C, oven; D, column; E, detector; F, acquisition system.

the compounds previously separated in the column. This part of the chapter is dedicated to summarizing the main characteristics of the most commonly used injection systems and detectors. Instrumentation of multidimensional GC is also described as being one of the greatest advances of this technique in the last few years (Marriott and Shellie, 2002; Adahchour *et al*., 2006).

Injection systems

The *injector port* is a hot chamber containing a glass liner where the compounds are volatilized and swept by a stream of inert carrier gas into the column. This chamber is closed by a rubber or microseal septum which is perforated by the needle of a syringe to introduce the sample. There are three main types of injectors: on-column, split/splitless and programmed temperature vaporizer (PTV).

In *on-column* or direct injection, the whole sample is volatilized in the chamber and introduced into the column. The linear speed of the carrier gas has to be higher than or similar to that in the column to avoid band broadening. On-column injectors require the use of capillary columns with internal diameter within the range of 0.2–0.5 mm.

The most common injectors are *split/splitless*. In the split mode, there is an opened valve which allows the carrier gas to be split into two ways: to the column and to the split vent. The purpose of this system is to avoid band broadening due to differences in the column and glass liner diameters. In the splitless mode, the valve is closed during the splitless time to introduce a higher amount of sample and is opened again after this time. To avoid band broadening, the temperature of the oven is decreased to concentrate the compounds at the head of the column. When the valve is opened, the oven temperature is rapidly raised according to the chromatographic program.

In the PTV, the sample is introduced into a cold chamber, the temperature of which is progressively raised. The solvent is partially evaporated and vented through the split line, and the sample thus becomes more concentrated before being introduced into the column. It is very useful for large-volume injections (LVI) of very diluted samples.

It is also worth mentioning the evolution that has taken place over the past few years in the development of external systems coupled on-line to the gas chromatograph for automated sample injection (Ridgway *et al*., 2007). Autosamplers provided with a microsyringe are commonly employed nowadays for the analysis of gas or liquid samples with high reproducibility and throughput. However, the coupling of several volatile fractionation techniques such as *thermal desorption* (*TD*), *solid phase microextraction* (*SPME*), *purge-and-trap* (*P&T*), etc., has also become of great importance for the automated and solvent-free analysis of liquid or solid food samples.

TD involves sample heating without solvent in a flow of carrier gas to isolate volatile compounds from the matrix and their subsequent cryogenic trapping in an adsorbent (e.g. Tenax) trap, which is in turn heated to release the volatiles into the transfer line (connection between the TD unit and the column).

SPME is a sample-preparation technique developed in the early 1990s by Arthur and Pawliszyn (1990), in which a fiber coated with an extracting phase is used to isolate volatiles from the liquid or gas phases. After extraction, SPME fiber is transferred to the injection port of a gas chromatograph, where desorption of the analytes takes place.

In P&T, an inert gas is bubbled through a sample to isolate the volatile compounds from the matrix. These volatiles are trapped on an adsorbent (or concentrator), usually at ambient temperature, which is then heated to release the isolated compounds into the carrier gas stream. Samples requiring volatile fractionation and preconcentration prior to GC separation can be introduced via such a system.

Detectors

A large number of detectors are used in GC. Universal detectors are those sensitive to a wide range of components present in a wide range of concentrations; the most common among them are the flame ionization detector (FID) and the thermal conductivity detector (TCD). However, there are other selective detectors widely used in analytical laboratories for the analysis of specific substances. These include the electron capture detector (ECD), nitrogen phosphorus detector (NPD), flame photometric detector (FPD), photoionization detector (PID), pulsed discharge ionization detector (PDD), etc.

The greatest advances in GC detectors arise from the coupling of different techniques (*mass spectrometry* (MS), infrared spectroscopy (IR) and nuclear magnetic resonance (NMR)) which provide additional structural information. That is the case in *mass spectrometry* (MS), infrared (IR) and nuclear magnetic resonance (NMR)-based detectors.

The FID and MS are by far the most commonly utilized detectors in food analysis, and specifically in the determination of food authenticity. In FID, the flame is produced by the combustion of hydrogen in air. A voltage of 100–300 V is applied between the flame and an electrode located away from it, which produces a low intensity current. When the organic compounds moving with the carrier gas reach the flame they are ionized, and an increase in the current is then measured. This detector is very sensitive and has a wide linear range.

The MS detector gives a measurement of the mass to charge (m/z) ratio of the produced ions, with a characteristic plot (mass spectrum) being obtained for each

compound. A MS system is composed of three main parts: the ion-source, which produces the ions from each compound; the mass analyzer to separate the ions of different m/z ratios; and the detector which collects the ions. Electronic impact and chemical ionization are the operation modes of the ion sources used for GC analysis. At present, there are a large number of MS analyzers that can be coupled to GC, although the more utilized ones are the quadrupole (Q-MS) and the ion trap (IT-MS). However, others, such as time-of-flight (ToF), magnetic sector, IT-ToF, Q-ToF, triple quadrupole (QqQ) or ToF-ToF, are also used.

Multidimensional GC

Multidimensional GC (MDGC) appeared due to the necessity of separating complex mixtures of volatile compounds which cannot be resolved by only one column (dimension). There are two kinds of MDGC: the so-called *multidimensional gas chromatography or heart-cut GC* (*GC-GC*) and *comprehensive two-dimensional gas chromatography* (*GC × GC*).

In GC-GC, two columns with different stationary phases are connected by a valve which allows the introduction of a selected fraction (heart-cut) of the eluate from the first column (first dimension) into the second one (second dimension) for its further separation.

In GC × GC, the whole sample is separated on the two columns and this separation should be as independent (orthogonal) as possible. The separation of the analytes is usually carried out using a non-polar GC column (typically 15–30 m × 0.25–0.32 mm × 0.1–1 μm) in the first dimension (1D) and a short polar column (typically 0.5–2 m × 0.1 mm × 0.1 μm) in the second dimension (2D); analytes are therefore separated according to their volatility in 1D and their polarity in 2D. However, the reverse combination can also provide good results, depending on the compounds to be separated. In GC×GC, the two columns are coupled by an interface or *modulator* which focuses the effluent of the first column in four to six narrow peaks and injects them periodically onto the second capillary column for a very rapid separation (Figure 10.4). There are different types of modulators: thermal desorption, cryogenic

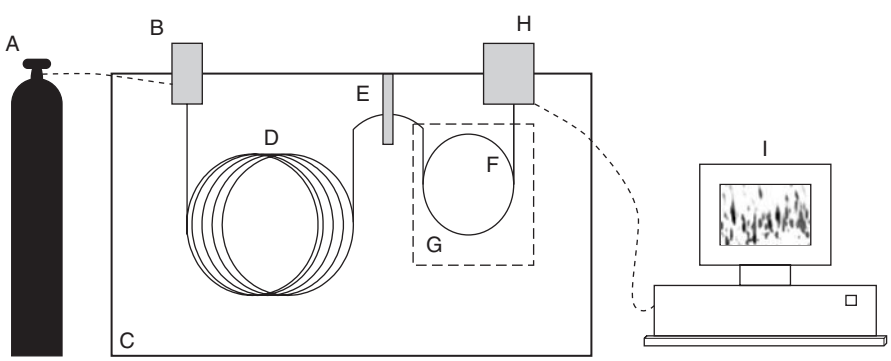

Figure 10.4 Schematic of a GC×GC system: A, gas container; B, injector; C, oven; D, first dimension; E, modulator; F, second dimension; G, second oven (optional); H, detector; I, acquisition system.

and valve-based modulators (Adahchour *et al*., 2006). The most widely used are the cryogenic jet systems, which retain the analytes using liquid CO_2, expanding gaseous CO_2 or nitrogen cooled to −180°C (Dallüge *et al*., 2003). The re-injection into the second dimension is carried out by applying a pulse of hot air or by switching the modulator off; compounds are then eluted with the oven temperature.

Detectors to be used in GC×GC are conditioned by the rapid separation in the second dimension. It means that the internal volume has to be small and the data acquisition rate high. The FID, ECD and ToF are the most common. Advantages of GC×GC over 1D GC are higher sensitivity and resolution power.

Applications

Oils and fats

The authentication of oils and fats is one of the fields where GC first started to achieve excellent results. Edible oils and fats are mainly constituted by saturated and unsaturated fatty acids (from C12 to C22) esterified with glycerol forming triacylglycerols (triglycerides, TAG), and small amounts of sterols (free and esterified with fatty acids), terpenic alcohols, hydrocarbons, vitamins, etc. Since biosynthetic pathways in every animal or vegetal species are different, distinction of their fats and oils is possible by means of qualitative and quantitative differences in these compounds. Expensive products such as cocoa fat, olive and almond oils are occasionally adulterated with cheaper fats with analogous physical properties. Similarly, the addition of pork fat to tallow is forbidden in certain countries, whereas addition of tallow to lard is considered to be adulteration in others. Moreover, untreated oils or fats might be mixed with refined oils, and products with Protected Denomination of Origin (PDO) replaced with alternatives. The analysis of the composition of fatty acids, triglicerides, sterols and other minor compounds is currently carried out by GC and covers almost all the lipidic components.

Fatty acids

Fatty acid (FA) composition is very easily determined by GC; usually a previous conversion of glycerides into more volatile compounds is necessary. Fatty acid methyl esters (FAME) are the most popular derivatives used for FA analysis, since they are volatile enough to be separated on most GC columns. The subject has been extensively reviewed (Knapp, 1979; Aldai *et al*., 2005). Free fatty acids (FFA) can be methylated by acid catalysis in a methanol solution, using reagents such as boron trifluoride or diazomethane. Triacylglycerols can be previously hydrolyzed in an acid medium to give FFA, which in turn will be methylated as above. However, the easiest method for the analysis of triacylglycerols is that of direct transesterification in methanol with a basic catalyst, such as sodium methoxide, potassium hydroxide or tetramethylammonium hydroxide.

FAME analysis using packed columns coated with polar phases has afforded (among others) the detection of vegetable fats such as palm kernel and coconut

(Iverson, 1972) and also sal and shea fats (Padley and Timms, 1980) added to cocoa fat; of 5% of vegetable oils (Kapoulas and Passaloglou-Emmanouilidou, 1981) added to olive oil based on the proportion of C18:3 content; and the addition of safflower oil to sunflower oil (Mariani and Bellan, 1997). Although these methods can still be used, nowadays FAMEs are better separated on capillary columns coated with polar phases; those based on cyanoalkyl silicones in particular are preferred when unsaturated isomeric FAs are present. The use of more efficient columns has allowed new parameters for detecting more sophisticated frauds. Thus, the presence of low-quality deodorized olive oil in virgin olive oil was detected by the presence of 9(*E*),11(*E*)-18:2 acid; its methyl ester was investigated by GC coupled to acetonitrile CI-MS and CI-MS/MS (Saba *et al*., 2005). The use of multivariate statistical analysis has improved detection limits, since the information is provided not for a single indicator but for the overall FA composition; difficulties owing to the natural variability of fats and oils can also be obviated (Ulberth, 1995; Giacomelli *et al*., 2006).

At present these methods can be improved by the use of capillary columns with an internal diameter close to 0.1 mm, which give similar resolution in a few minutes, saving time and carrier gas. Fast GC has been used by Mondello *et al*. (2004a) as a convenient methodology to detect adulterations of nine different fats; GC×GC was also considered as a convenient technique for the analysis of the most complex mixtures.

Triacylglycerols

The number of triacylglycerols (TG) in natural fats is very high. An oil sample consisting of only 5 different fatty acids may give 5^3 different triacylglycerols. However, this distribution is not random; FAs are esterified in the three positions of glycerol in a stereospecific way which is characteristic of every species. Thus the information obtained from TAG composition is much more complex and specific than that supplied by the FA composition. This fact has been used to detect the presence of transesterified fats in natural fats, using a stereospecific lipase to cleave the FA esterified in a specific position and analyzing FAME in this fraction. Dourtoglou *et al*. (2003) analyzed different vegetable oils: total fatty acids and their regiospecific distribution in positions 1 and 3 were determined using a specific lipase from *Mucor miehei*, and resulting data were subjected to PCA. It was possible to distinguish pure oils from mixtures and to discriminate between different types of seed oil used for adulteration.

At present, the analysis of intact triacylglycerols affords valuable information to characterize the purity of fats. This analysis was at first developed by HPLC, but the use of short GC capillary columns (less than 5 m) coated with thin films of thermally stable phases allows very good results. Fused silica capillary columns were introduced early on (Geeraert and Sandra, 1987).

Besides special columns, triacylglycerol analysis requires very careful sample introduction, since their boiling points are very high and it is necessary to completely vaporize the mixture, thus avoiding both thermal decomposition and discrimination by molecular weight. The most used injection modes are on-column (Molkentin and Precht, 2000) and PTV (Banfi *et al*., 1999).

TAG analysis has been successful in the detection of 5% seed oils in olive oil (Antoniosi *et al*., 1993) and for detection of 5% cocoa butter equivalents (vegetable fats similar to cocoa butter) in chocolate (Simoneau *et al*., 1999; Buchgraber *et al*., 2004).

Sterols

The analysis of sterol fraction by GC was started in the 1960s as a method to detect animal fats in vegetable oils or *vice versa* (Mordret, 1968). The method required a long sample preparation time, with saponification, solvent extraction and thin-layer chromatography (TLC) fractionation. Several approaches have been attempted to find a faster and easier method. Direct GC analysis of the unsaponifiable omitting TLC (Giacometti, 2001) or the use of gel-permeation chromatography instead of TLC fractionation prior GC (Carstensen and Schwack, 2002) have been proposed among others.

Cholesterol is the main sterol in animal fats, but phytosterols are characteristic of every vegetable oil. The new vegetal varieties with different fatty acid composition (such as canola oil or high-oleic sunflower oil) make it difficult for detection using classical markers such as erucic or linoleic acids, but the analysis of sterols shows the typical composition of the vegetal species – canola oil sterols are similar to those of rapeseed oil, with a clear peak of brassicasterol, characteristic of the *Brassicaceae*, whereas sunflower oils display their typical Δ7-sterols independent of their oleic content. The classical methods for GC analysis of sterols required the use of packed columns lightly coated with non-polar stationary phases working at a high temperature (about 270°C). Packed columns have been replaced by capillary columns which afford better separation of isomeric sterols; the coupling with MS has allowed the identification of new compounds, which in turn improves the identification of any adulterant oil. Separation of the Δ5-sterols from the Δ7-sterols permitted detection of the adulteration of pumpkin seed oil with other vegetable oils (Mandl *et al*., 1999).

The use of coupled LC-GC is an interesting way to simplify the analysis of minor components, since this technique saves pre-treatments before chromatographic analysis. Adulteration of olive oil may be carried out using desterolized sunflower oil, where the indicator compound (a Δ7-sterol) used for detection has been removed, but it has been proved that Δ7-sterols are isomerized to Δ8(14)- and Δ14-sterols during the process. Results of LC-GC analysis of olive oil containing desterolized sunflower oil have shown that measurement of Δ8(14)-sterols in the oil was a suitable method for detecting the adulteration (Biedermann *et al*., 1996).

The analysis of sterols is also useful for detecting admixtures of processed fats in natural fats. Bleaching oils during refination results in dehydration of sterols to give hydrocarbons which are not present in the original fats, and are hence indicators for industrially refined oils. They have been useful for detecting refined fats added to chocolate (Crews *et al*., 1997) and for refined oils added to virgin oils (Cert *et al*., 1994). The analysis consists of several steps: extraction, fractionation on silica gel and GC on a fused silica capillary column (0.25 mm × 25 m × 0.25 μm) coated with 5% phenyl methyl silicone, working at a programmed temperature.

Other minor compounds

Triterpenic alcohols and tocopherols are characteristic compounds of the different vegetable species. Their analysis is carried out in a similar way to that of sterols: they are components of the unsaponifiable, and should be fractionated by TLC or on silica columns prior to GC analysis. Triterpene alcohols allowed detection of sal fat, shea fat and illipe butter in cocoa butter (Soulier *et al*., 1990). Determination of the concentration of triterpene alcohols permitted detection of the adulteration of virgin olive oil with 5% olive-pomace oil (Ntsourankoua *et al*., 1994).

Lupeol and an unknown compound containing a lupane skeleton were detected (after saponification, extraction, TLC and silylation) in the 4,4′-dimethylsterol fraction of hazelnut oils; both compounds proved to be good markers for detecting less than 4% hazelnut oil in olive oil (Damirchi *et al*., 2005) (Figure 10.5).

Detection of 10% solvent extracted oil in cold-pressed olive oil was achieved by RPLC-GC using a PTV as an interface for direct analysis of triterpenic alcohols erythrodiol and uvaol. The proposed method was used to determine extra-virgin olive oil adulteration (Blanch *et al*., 1998). Tocopherol analysis was used for authentication of sesame seed oils (Aued-Pimentol *et al*., 2006).

Volatiles

Volatile analysis has scarcely been used for the purpose of detecting adulteration in oils, but in those cases where the composition of fatty acids and sterols is very similar these methodologies represent a useful alternative. SPME prior to GC-MS allowed the detection of an admixture of sunflower oil with poppy seed oil in relevant amounts (5–40%) by using α-pinene as a marker (Krist *et al*., 2006).

Filbertone (*E*-5-methylhept-2-en-4-one), a chiral compound which is found in hazelnuts, has been proposed as a marker to detect the addition of this oil to olive oil. It can be determined by SDE followed by GC or directly by LC-GC; in both cases a chiral column is necessary (Blanch *et al*., 1999).

Dairy products

This field has been recently revised (de la Fuente and Juarez, 2005). Adulteration of dairy products may be carried out by substituting part of the fat or protein; adding low-cost dairy products (mainly whey derivatives); mixing milk of different species; and mislabeling products protected by PDO. GC is especially well suited for detecting foreign fat in milk fat and for distinguishing mixtures of species through fat analysis; it has also been used for authentication of cheeses.

Foreign fat in milk fat

FAME

The methodologies used are those described above for fats and oils; nevertheless, it is necessary to take into account the special composition of ruminant milk fats, which contain relevant quantities of short-chain fatty acids, as well as a very complex mixture of *cis*- and *trans*- unsaturated acids with 18 carbons. Thus, FAME

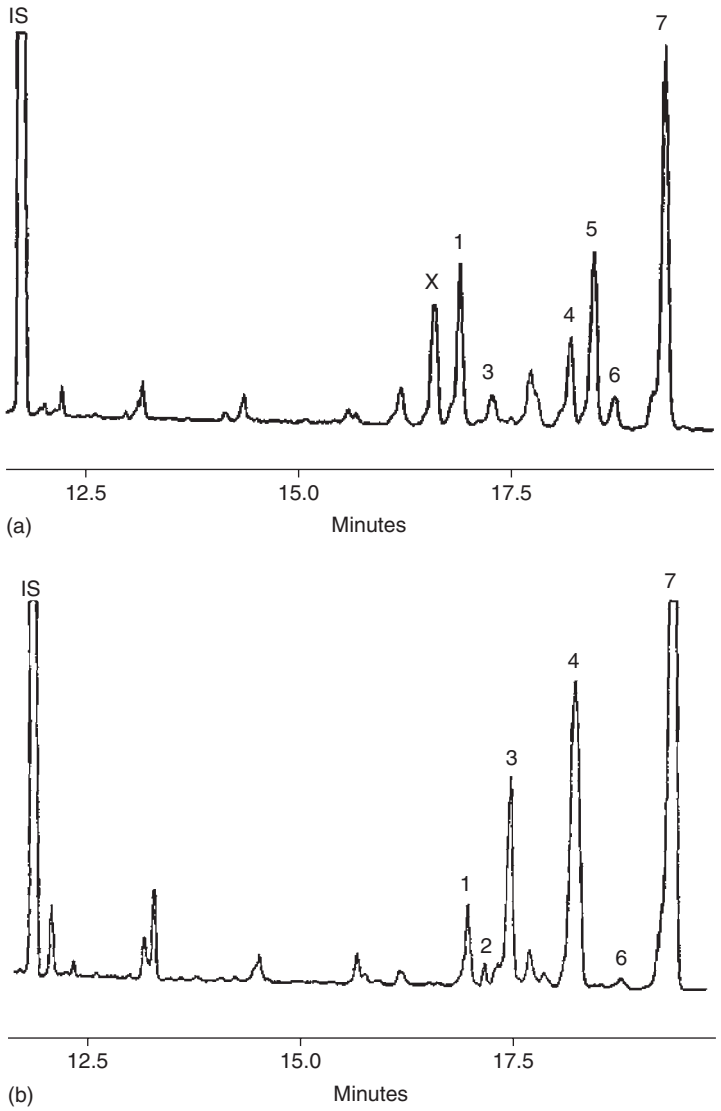

Figure 10.5 Trimethylsilyl ethers from 4,4′-dimethylsterols of (a) hazelnut oil and (b) olive oil. Peaks: IS, internal standard; 1, δ-amyrin; 2, taraxerol (detected only in virgin olive oil samples); 3, β-amyrin; 4, cycloartanol; 5, lupeol (detected only in hazelnut oil); 6, Δ7-sterol; 7, 24-methylenecycloartanol. Reprinted with permission from Damirchi *et al*. (2005); ©AOCS Press.

analysis requires the use of long, very polar columns: formerly polyester-based stationary phases were used, but nowadays cyanoalkyl silicones 50–60 m in length are recommended. A programmed temperature is always necessary, starting at a low temperature (about 70°C) to separate methyl butyrate from methanol and other solvents; separation of all the isomers of oleic and linoleic acid (which have nutritional relevance, and can also help to characterize the origin of dairy products) is very difficult to accomplish. Fortunately, detection of foreign fats usually does not require a complete separation of these isomers.

Concentration ranges of the major fatty acids and of certain fatty acid ratios to identify foreign fats in mixtures with milk fat were tested (Ulberth, 1994); linear discriminant analysis was successful in distinguishing pure from adulterated milk fats; detection limits were between 3% and 10%. Nevertheless, the natural variability of milk fat makes this approach useless when the level of adulteration is low. Thus, addition of vegetable fats mainly relies on sterol analysis, whereas addition of animal fats is better detected by TG analysis.

TAG

TAG analysis of milk fat displays a really complex profile, which has not been entirely resolved either by GC or by HPLC. At present the resolution achieved is enough to resolve most adulteration cases (Precht, 1991), including mixtures with other milk-fat species (Goudjil *et al*., 2003). Mixtures of pure ewe milk fat and different amounts of lard, palm oil and cow milk fat could be detected using multiple regression equations.

Different calculation methods, including neural networks, have been assayed (Lipp, 1996). Techniques and advances in TAG analysis of milk fat are similar to those indicated for other fats, with the drawback that the number of triacylglycerols in milk fat is higher than in other fats (Povolo *et al*., 1999; Molkentin and Precht, 2000; Naviglio and Raia, 2003).

Sterols

Detection of vegetable oils in milk fat is easy using sterol analysis (Mariani, 1995), since the main compound in the latter is cholesterol, and only small quantities of minor precursors (desmosterol, lathosterol and lanosterol) have been reported.

Detection of vegetable fats is indeed standardized (IDF, 1992). As indicated above, the preparation method requires saponification of fat, extraction of unsaponifiable and TLC fractionation to obtain a pure sterol fraction, which is then injected in GC; this is a long and tedious procedure. Several methods have been proposed to simplify this; some of them propose suppressing TLC fractionation and analyzing free sterols (Precht, 2001) or their TMS derivatives (EU, 1992). Another procedure, useful for testing the purity of milk fat, is to convert triacylglycerols into their methyl esters (one-pot reaction) and analyze the reaction mixture, since sterols elute after FAME (Alonso *et al*., 1997). A faster but more expensive method is the use of LC-GC coupling (Kamm *et al*., 2002).

Refined animal fats can also be detected by sterol analysis: 3,5-cholestadiene, a hydrocarbon derived by reduction from cholesterol during refining, was used as an index for addition of refined beef tallow to butter (Mariani *et al*., 1994).

Others

Long-chain ketones were detected by GC as indicators of the addition of transesterified fats to natural fats, including milk fat (Martín-Lomas *et al*., 1975).

Volatiles

Volatile compounds analyzed by GC have been proposed for authentication of cheeses: as an example, high mountain cheeses have a higher level of terpenes than those

manufactured with milk from animals grazing on the plain or at the farm (Mariaca *et al*., 1997). Volatiles have also been useful to distinguish the thermal treatment undergone by milk (Contarini *et al*., 1997).

Spices and flavors

Spices and flavors, traditionally used to impart an appealing aroma and to mask off-flavors in food, are expensive additives, and therefore have been frequently targeted for adulteration. Main fraudulent practices involve mixing spices with other less valuable natural substances (e.g. other plant parts, inexpensive varieties, etc.), whereas essential oils are usually adulterated with synthetic components. Two different approaches are generally followed for authenticity assessment: (i) the search for specific markers of the adulterant, and (ii) the study of differences in the analytical fingerprints gathered for authentic and adulterated samples.

Solvent extraction, steam distillation, micro-simultaneous steam distillation-solvent extraction (MSDE), etc., have been traditionally employed for characterization of the aroma of spices (Tarantilis and Polissiou, 1997); their main handicaps are the fractionation of thermolabile components and the over-enrichment of the extracts obtained in high boiling-point constituents. Headspace techniques (HS), although biased towards the fractionation of high-volatility components, do not require the use of organic solvents and minimize artefacts, with advantages in reproducibility being obtained if they are automated (García and Sanz, 2001). On-line coupling of thermal desorption to gas chromatography-mass spectrometry (TD-GC-MS) has been applied to determine the authenticity of Spanish saffron (*Crocus sativus* L.) (Alonso *et al*., 1998). TD-GC-MS analysis of 252 authentic saffron samples showed a consistent TIC fingerprint around the elution time of safranal, the major volatile in saffron and responsible for its aroma (Figure 10.6a). This chromatographic interval showed a different profile for "false saffron" (*Carthamus tinctorious* L.) (Figure 10.6b) and synthetic safranal (Figure 10.6c), and therefore could be used as an indicator of saffron authenticity.

GC-MS in combination with other techniques has also been employed for identification of adulteration of black pepper (*Piper nigrum* L.) powder with ground papaya (*Carica papaya* L.) seeds at levels as low as 2%. TLC of the extracts obtained by supercritical carbon dioxide extraction allowed the isolation of a fluorescent band which could be marker of the presence of papaya powder in black pepper powder. Compounds present in this band were tentatively identified by GC-MS as *n*-nonanal, *n*-decanal and *n*-dodecanal (Bhattacharjee *et al*., 2003).

GC has been extensively used for identification and detection of adulteration of essential oils (Prager and Miskiewicz, 1982; Dugo *et al*., 1992; Loesing, 1999). Spencer *et al*. (1997) tried to detect the presence of cornmint oil (from *Mentha arvensis*) in the more highly priced peppermint (*Mentha piperita*) oil. GC analysis of peppermint vs cornmint oil using a Supelcowax-10 polar capillary column showed high concentrations of isopulegol and another compound, tentatively identified as neoisopulegol, as characteristic of cornmint samples. Levels for these compounds in mint oils were therefore suggested as indicators of the adulteration of peppermint oil

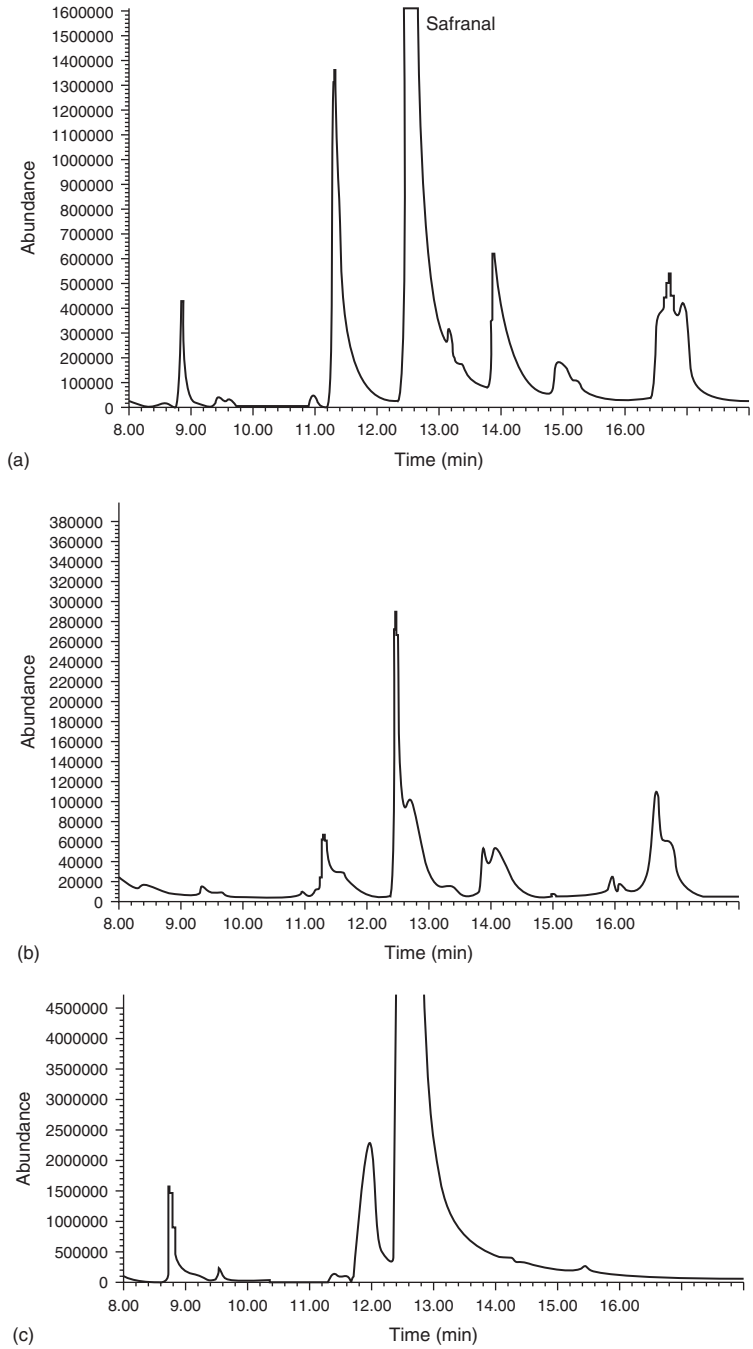

Figure 10.6 "Fingerprint" region for authentication of saffron: (a) authentic saffron, (b) "false saffron" (*Carthamus tinctorious* L.) and (c) synthetic safranal. Reprinted with permission from Alonso *et al*. (1998); ©International Association for Food Protection.

with cornmint oil. GC-olfactometry (GC-O) and aroma-extract dilution analysis (AEDA) has also been applied to analyze differences in composition and odor potency of unrectified Yakima peppermint oil and a dementholized Chinese cornmint oil (Benn, 1998).

However, essential oils are usually complex samples, and often monodimensional GC (1D GC) proves to be insufficient for their complete separation. Dimandja *et al*. (2000) showed the advantages in terms of resolution and sensitivity of GC×GC-FID for the separation of peppermint and spearmint (*Mentha spicata*) essential oils. The set of columns employed for comprehensive GC separation included a DB-1 column (10 m × 100 µm i.d. × 3.5 µm) connected through a thermal modulation unit to an OV-1701 column (2 m × 100 µm i.d. × 0.5 µm d_f). A two- to three-fold increase in the number of compounds separated for both mint essential oils and the possibility of qualitatively assigning unidentified compounds to chemical classes (e.g. monoterpene hydrocarbons) by means of the use of structured chromatograms were the main advantages of GC×GC-FID over 1D GC. Differences in peppermint and spearmint GC×GC fingerprints are suggested to be of utility for detection of products of essential oil adulteration.

A different approach for assessment of authenticity involves GC analysis of the enantiomeric distribution of chiral compounds in both authentic and adulterated samples, with modified cyclodextrins being the stationary phases of choice for most applications (König *et al*., 1997). Coleman and Lawrence (2000) analyzed by automated SPME-GC-MS the enantiomeric excess of chiral monoterpene hydrocarbons in peppermint, spearmint and rosemary (*Rosmarinus officinalis*) essential oils from different origin, with excellent reproducibility (relative standard deviation (RSD) <5%). Short exposure times (6 s) of a 7-µm polydimethylsiloxane SPME fiber to the headspace above submicroliter samples provided the required sensitivity for analysis. Changes in enantiomeric patterns were used to ascertain the origin and authenticity of these oils. The combination of normal and chiral phases in comprehensive gas chromatography has also been reported for authenticity assessment of citrus essential oils (Dugo *et al*., 2005).

On-line coupling of GC with isotope ratio mass spectrometry (GC/IRMS) has also gained importance in authenticity control of flavors. Combination of isotopic data (stable isotope ratios for carbon ($\delta^{13}C$), nitrogen ($\delta^{15}N$) and hydrogen ($\delta\chi^{2}H$)) with gas chromatographic data for characteristic aroma compounds has been reported to assess the genuineness of natural vanilla (Kaunzinger *et al*., 1997) and for origin-specific analysis and authenticity control of mandarin (Faulhaber *et al*., 1997), lemon (*Citrus limon*) and lemongrass (*Cymbopogon winterianus*) (Nhu-Trang *et al*., 2006) essential oils.

Honey

Honey is a natural substance produced by honey bees from the nectar of plants or from the secretions that are found over them. Its composition is variable and depends on numerous factors – floral type, climate, processing and storage conditions, etc. (White, 1978).

As honey is a product of limited supply and relative high price, its quality assurance becomes extremely important. Honey fraud can involve the addition of industrial

sugar syrups, or its sale under a false name (Cotte *et al*., 2004). Corn syrups (CS), invert syrups (IS) obtained by acidic or enzymatic hydrolysis from refined beet or cane sucrose, and high-fructose corn syrups (HFCS), mainly produced by enzymatic hydrolysis and isomerization of corn starch, are the most common sweeteners that can be added directly to honey after harvest or fed to bees during the harvest to improve yield (Swallow and Low, 1994).

Taste and flavor, the two most significant attributes of honey, are mainly dependent on its botanical origin. Both organoleptic properties contribute to honey quality and may also help to determine its authenticity. The high sensitivity and resolving power of GC combined with the qualitative and quantitative information provided by MS make this technique an appropriate tool for the characterization of the complex mixtures of volatile compounds and carbohydrates in honey, being widely used to detect its adulterations and establish its authenticity.

Volatiles

The GC profile of volatile compounds of honey represents a "fingerprint" of the product which can be used to determine its floral origin (Radovic *et al*., 2001). GC analysis of honey requires a prior fractionation stage to isolate the volatiles from the sugar matrix. Several studies have been reported on different techniques for the fractionation of honey volatiles, such as solvent extraction (Rowland *et al*., 1995), simultaneous steam distillation-extraction (SDE) (Bouseta and Collin, 1995) and P&T (Overton and Manura, 1994). SPME followed by GC-MS has recently proved to be useful for analysis of the volatile fraction from different honeys (Guidotti and Vitali, 1998; Soria *et al*., 2003).

The botanical origin of honey has been extensively characterized by GC analysis of its volatile composition. Although some authors suggest certain specific compounds as being characteristic of honeys from a specific floral source (e.g. acyloins for eucalyptus honeys by de la Fuente *et al*. (2007)), most of the studies consider groups of compounds as indicators of floral origin (Guyot *et al*., 1998; Castro-Vázquez *et al*., 2007). Honeys from nine different botanical sources and eight geographical origins were studied by Radovic *et al*. (2001). P&T analysis was performed by adsorption of volatiles on a Tenax trap, followed by desorption at 280°C and cryofocus at −120°C in a glass-lined tube before GC-MS separation on a DB-WAX capillary column. Although appropriate markers were found for distinguishing among botanical origins, the classification of the samples according to geographical origin was more difficult to establish. Although the establishment of marker compounds for assessing the origin of honeys would be very advantageous, present knowledge on this subject is rather limited.

Mannas and Altuğ (2007) used SPME-GC-MS for the estimation of thyme-honey authenticity and for detection of its adulteration. They found that an excessive amount of volatiles such as thymol and carvacrol indicated honey adulteration with thyme essential oil. It was noted that 3,4,5-trimethoxybenzaldehyde may be a possible marker for determining thyme-honey authenticity.

Owing to the complexity of honey aroma, co-elution of some compounds can occur, making their identification difficult. Recently, MDGC has been applied to the

study of honey aroma in order to characterize its botanical origin as well as to detect fraud. The use of SPME-GC×GC-ToF MS by Čajka *et al*. (2007) allowed a rapid and comprehensive examination of the honey volatile profile, identifying a total of 164 volatile compounds. In this study, the best sorption capacity was obtained by a divinylbenzene/carboxen/polydimethylsiloxane 50/30-μm fiber, and the best resolution for the studied compounds by the combination of DB-5 × Supelcowax-10 columns. However, the examination of a large set of honey volatile profiles of different botanical and geographical origins is needed to assess the feasibility of this strategy for traceability purposes.

Carbohydrates

Regarding carbohydrate fraction, honey is probably the most complex mixture of oligosaccharides in nature, and the study of these compounds has been used to identify fraud. Carbohydrates must be transformed into appropriate volatile compounds for GC analysis, and several methods of derivatization have been developed. Trimethylsilyl ethers (Sweeley *et al*., 1963), trifluoroacetates (Sullivan and Schewe, 1977) and alditol acetates (Björndal *et al*., 1967) have been the most popular derivatives, giving a different compound for each anomeric form of the sugar (up to six). Converting sugars to oximes prior to trimethylsilylation reduces the peaks formed for each sugar to two: *E*- and *Z*-oxime isomers (Laine and Sweeley, 1971; Low and Sporns, 1988).

Many authors have developed GC methods to characterize sugars in monofloral and honeydew honeys and to establish honey authenticity; combination of sugar and physicochemical data was, however, necessary in most of the studies to obtain reliable results (Mateo and Bosch-Reig, 1997; Astwood *et al*., 1998; Sanz *et al*., 2004). Maltose and isomaltose contents and their ratios have been used to detect adulteration with syrups using GC, allowing the detection of 30% of adulteration (Doner *et al*., 1979). More recently, Low and South (1995) described the presence of specific marker peaks for IS that were either absent or present in low amounts in authentic honey. The detection limit for invert sugar addition was 5%.

Cotte *et al*. (2003) combined the use of HPAEC-PAD and GC-FID data with statistical processing by principal component analysis (PCA) to demonstrate the addition of IS and CS to honey samples. Application to acacia, chestnut and lavender honeys allowed the detection of adulteration resulting from addition of 5–10% of sugar syrups.

Recently, the use of difructose anhydrides (DFAs) as possible markers of IS and HFCS adulteration has been proposed (Ruiz-Matute *et al*., 2007a). Their presence in these kinds of syrups was described for the first time in this work, their proportions being dependent on the syrup type considered. As these compounds were not detected in any of the 20 honey samples analyzed, their presence in honey was proposed as a marker of adulteration. The detection of DFAs in the adulterated honeys required a previous enrichment step based on incubation with yeast (*S. cerevisiae*) to remove major sugars and to preconcentrate these compounds. This methodology allowed the detection of adulteration with 5% syrup (Figure 10.7).

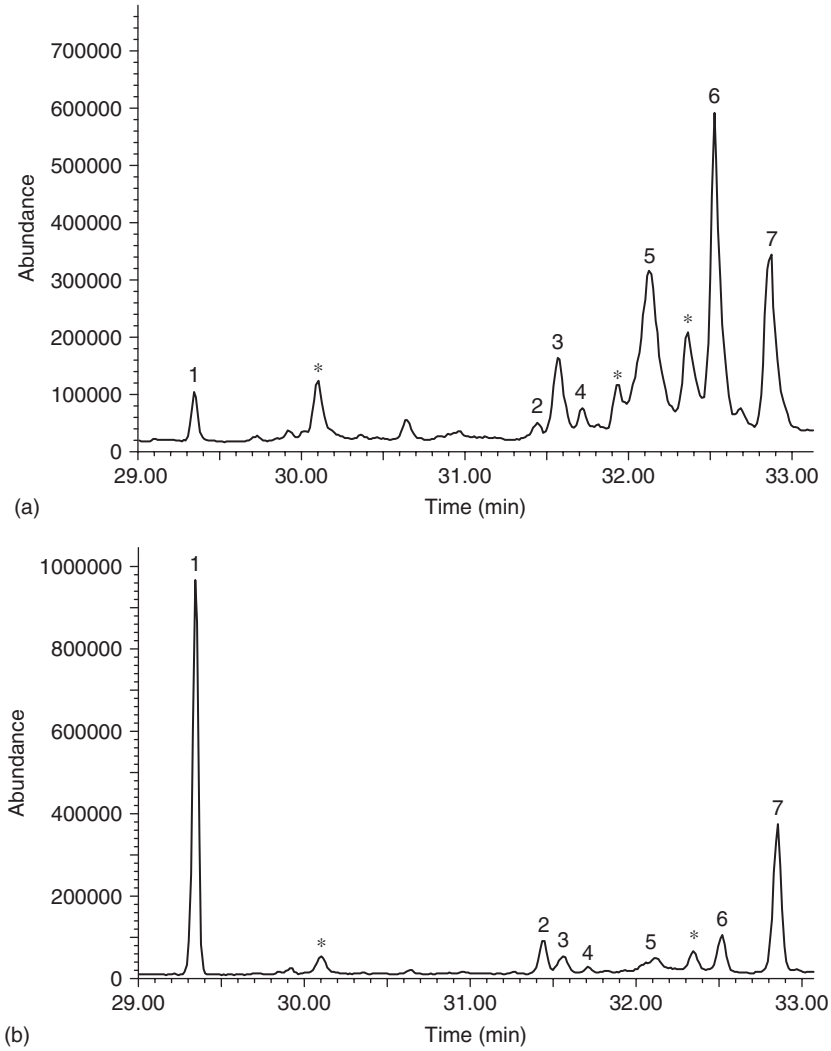

Figure 10.7 Gas chromatographic profile of DFAs region in a nectar honey adulterated with (a) 20% of IS and (b) 20% of HFCS after yeast treatment. 1, DFA1; 2, DFA3; 3, DFA5; 4, DFA6; 5, DFA7; 6, DFA9; 7, DFA10; *unknown.

Fruit juices

Fruit juices are complex mixtures of sugars, organic acids, volatile flavors, fatty acids, sterols, amino acids, flavonoids, pigments, etc., in water. Adulteration of industrially processed juices usually consists of substitution of the authentic material with cheaper alternatives. Partial replacement of fruit juice with water, sugar, fruit-derived products (pulpwash, peel, etc.) or with less expensive fruit varieties (e.g. addition of grapefruit to orange juice) are common adulteration practices. It is permitted to bulk fruit juices with these substances for different purposes (e.g. to correct the acidity or for sweetening), but such additions are only allowed if they are properly labeled.

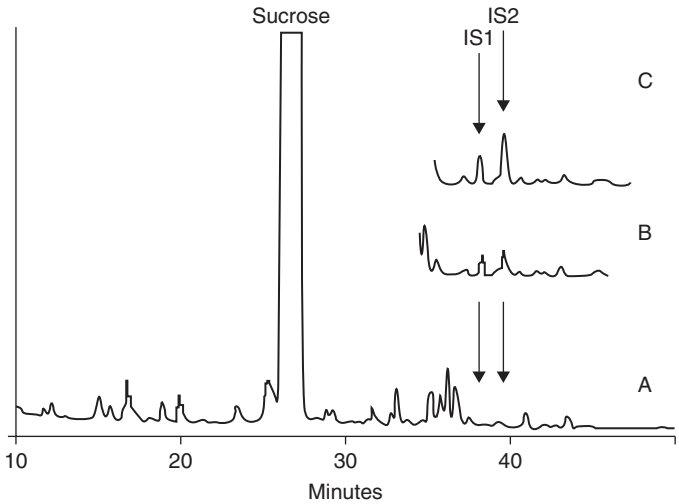

Figure 10.8 Capillary GC chromatograms of apple juice concentrates: A, authentic, untreated; B, authentic, heat-treated; C, sample B spiked with 10% invert sugar (IS); IS1 and IS2, marker peaks for the presence of IS. Peak height ratios IS2/IS1: sample B 1.31, sample C 1.70. Reprinted with permission from Prodolliet and Hischenhuber (1998). ©Springer-Verlag.

Although juices from a single fruit are the most extensively consumed, compounded juices from different fruits have started being commercialized to expand the market. In order to guarantee the authenticity of compounded beverages and to avoid adulteration, the declared presence of every single juice needs to be confirmed.

Addition of sweeteners

Carbohydrates account for more than 98% of the total soluble solids in fruit juices. Therefore, the replacement of natural sugars by inexpensive sweeteners with a composition resembling that of the authentic sugars is the most common and profitable adulteration practice. Similarly to honey, adulteration of juices mainly involves the undeclared addition of IS and HFCS.

Oligosaccharide fingerprints gathered by GC-FID have been employed to detect adulteration of orange and apple juices with both IS and HFCS at percentages as low as 5% (Low, 1995, 1996). Sample preparation included dilution with water to 5.5° Brix, freeze-drying and trimethylsilylation of the carbohydrates prior to their gas chromatographic analysis using a DB-5 column. The addition of IS to juice was detected by the presence of two unidentified marker peaks (IS1 and IS2) thought to be formed during sucrose inversion (Prodolliet and Hischenhuber, 1998; Figure 10.8). IS1 and IS2 have been recently identified as turanose and *O*-β-D-fructofuranosyl-(2→6)-D-glucose, respectively (Thavarajah and Low, 2006). Although IS1 and IS2 may also be present in thermally-processed authentic juices, the ratio IS1/IS2 in heated juices is significantly different from that observed for apple and orange juices adulterated with IS, with the critical IS1/IS2 value not being generally agreed at the present time. Additionally, the areas for both marker peaks in juices submitted to excessive heating are considerably lower than those corresponding to 5% invert

sugar adulteration. Stöber *et al*. (1998) tried to overcome the lack of reproducibility between laboratories in the estimation of the IS1/IS2 ratio by standardization of the methodology proposed by Low. Comparison of the results from a test juice with those from an external reference apple juice showing a peak ratio at the IS1/IS2 cut-off limit allowed different laboratories to reach similar conclusions (authentic/adulterated), independent of the chromatographic set-up employed.

Gansser and Busmann (1998) observed the interference of a natural constituent of apples (catechine) with the IS2 marker peak when applying the method suggested by Low (Low, 1995, 1996) to detect the addition of IS to apple-juice concentrates. Inclusion of solid-phase extraction on RP-18 cartridge as part of the sample preparation allowed the removal of catechine prior to the GC analysis of juice without interfering with the IS1/IS2 ratio.

The detection of the two tautomeric forms of isomaltose has also been proposed to trace the adulteration of apple and orange juices with high fructose syrup from corn and palm (Low, 1995, 1996). Oligosaccharide fingerprinting by GC of white grape juices from Argentine showed that maltose and isomaltose are not natural constituents of grape juice, but they can be originated from extended storage of lees juice in SO_2. Therefore, the presence of isomaltose may not necessarily indicate the adulteration of white grape juice with HFCS (Low, 1998). Two other oligosaccharides have also been proposed to detect adulterations with high fructose syrup from inulin (HFSI) (Low and Hammond, 1996).

Myo-inositol and the *myo*-inositol/fructose ratio have also been proposed as indices to assess the quality and genuineness of orange juices (Villamiel *et al*., 1998). GC-FID analysis of carbohydrates after derivatization with trimethylsilylimidazole and trimethylchlorosilane showed that both indices were lower in samples made from concentrates than in freshly squeezed or straight-processed orange juices.

Authentication of a declared fruit juice

Sterols have been proposed as useful markers for detecting juices of pineapple, passionfruit, orange and grapefruit in compounded beverages (Ng and Hupé, 1998). One-step liquid–liquid extraction into hexane, with ethanol being added to precipitate pectins and other emulsifying agents, followed by GC-MS was carried out to analyze sterols in juices. Overlapped peaks corresponding to structurally similar compounds were common in sterol GC-MS profiles, with extracted-ion chromatograms being a valuable tool for improving their separation. Ergostanol and stigmastanol were found to be markers for pineapple juice, whereas passionfruit was characterized by the presence of an unidentified compound with mass spectra m/z 424, 165, 205, 69 and 41. Higher stigmasterol/campesterol ratios were found for both orange and grapefruit juices, and the differentiation of both citrus juices required the additional estimation of the ratio of two semivolatile flavors (valencene/nootkatone).

Addition of pulpwash

Pulpwash is the residue exhaustively extracted by repeated water washing from the previously pressed pulp used to manufacture fruit juice. Its addition to pure juice

concentrates is not allowed in the US and in the EU (Prodolliet and Hischenhuber, 1998). Kauschus and Thier (1985) developed a capillary GC method for the detection of orange pulpwash in juice, based on the determination of galacturonic acid. Methanolysis and subsequent silylation of polysaccharides (pectine) led to a uniform GC pattern for orange juices independent of their origin, from which it was possible to determine the juice content of citrus beverages.

Addition of synthetic aromas

Stereochemistry has been demonstrated to be a useful tool for food authentication. The study of the enantiomeric composition of 10 chiral terpenes was proposed by Ruiz del Castillo *et al*. (2003a) to detect the addition of synthetic aromas to commercial fruit beverages. SPME using a 100-μm poly(dimethylsiloxane) fiber coating was employed for volatile isolation under non-racemization conditions. GC-FID separations were performed on a 25 m × 0.25 mm chiral capillary column coated with 0.25-μm Chirasil-β-Dex. The enantiomeric excess of limonene, linalool and α-terpineol in natural products was found to be 100, 100 and 80% for the (+)-enantiomer, respectively. Any deviation from these values was attributed to the addition of synthetic aromas or inappropriate thermal processing of fruit beverages under analysis.

With a similar purpose, on-line coupling of reverse phase liquid chromatography with gas chromatography (RPLC-GC) has been employed to determine the enantiomeric composition of chiral terpenes in fruit drinks, orange aroma and orange essential oils without previous sample pre-treatment (Ruiz del Castillo *et al*., 2003b).

Coffee

Coffee is an expensive product that can be a target for fraud by means of adulterations with cheaper commodities or false designations in relation to its variety or geographical origin, which affects its final price.

Fraud in coffee varieties

Coffea arabica and *Coffea robusta*, the two main coffee species, have different values for consumers due to their sensorial properties, and therefore different prices in the market. Coffee blends of these two varieties are preferred, as they combine both characteristic flavors. However, it is necessary to define the composition of these blends, because the higher value of *C. arabica* beans makes this coffee a target for fraud. Unroasted coffee can easily be differentiated by its sugar and amino acid contents (Singhal *et al*., 1997); however, these compounds are modified during processing. Therefore, it is important to establish analytical methodologies to discriminate between coffee species after roasting to detect potential adulteration of high-quality coffee brews with cheaper products. Different authors have used GC methods for this purpose (Sanz *et al*., 2002; Rocha *et al*., 2003). Although there are some studies based on fatty acid composition of Arabica and Robusta coffees (Alves *et al*., 2003), most GC analyses focus on the determination of the volatile compounds characteristic of coffee aroma. Different approaches, such as static headspace (Kallio *et al*., 1988),

on-column injections (Shimoda and Shibamoto, 1990) or P&T systems (Liu *et al*., 2004), have been applied to the extraction of these compounds, which are commonly later analyzed by GC-MS using mainly polyethylene glycol capillary columns. Nevertheless, HS-SPME is the most widely used technique for the extraction of volatile compounds in coffee brews, since it is simple, rapid, solvent-free and inexpensive (Yang and Peppard, 1994). Several studies have compared the effectiveness of SPME fibers with different coatings (Freitas *et al*., 2001; Rocha *et al*., 2003), with polydimethylsiloxane being the one commonly chosen for the characterization of the volatile composition of coffee varieties (Zambonin *et al*., 2005). However, Mondello *et al*. (2004b) demonstrated the suitability of a triple phase coating (DVB/CAR/PDMS) for the isolation of compounds within a wide range of volatility.

Around 150 compounds have been identified and quantified from different chemical families (aldehydes, alcohols, pyrazines, pyrroles, etc.) in blends of roasted *C. arabica* and *C. robusta*, and significant differences in most of their contents have been observed (Sanz *et al*., 2002). It is worth noting that blends containing high proportions of *C. robusta* showed greater concentrations of guaiacol (Mondello *et al*., 2005) and sulfur compounds, mainly methanethiol (Holscher and Steinhart, 1992), than those with high percentages of *C. arabica*. In general, these last blends showed more elevated concentrations of other volatile compounds such as ketones, alcohols, pyrroles, furans, etc. (Sanz *et al*., 2002). However, some discrepancies in discriminating between coffee varieties have been found by different authors, regarding the contents of aldehydes or pyrazines (Sanz *et al*., 2002; Leino *et al*., 1991; Zambonin *et al*., 2005).

Recently, HS-SPME coupled to GC×GC-FID (Mondello *et al*., 2004b) has been used to evaluate the differences in the volatile composition of these two coffee varieties. The use of two columns (Supelcowax-10 as first dimension and 5% BPX-5 as second dimension) and a longitudinally modulated cryogenic system permitted the separation of nearly a thousand analytes, allowing discrimination of both coffee varieties based on quantitative data. Ryan *et al*. (2004) continued these studies by analyzing the same coffee bean samples by GC×GC-ToF MS. Two sets of columns, polar/non-polar (SolGel-WAX × BPX-5) and non-polar/polar (BPX-5 × BP-20) were tested. As it can be seen in Figure 10.9, the first combination was more effective in the separation of coffee volatiles. This technique was shown to be the most suitable tool for accurate peak identification and quantification, although some assays using GC×GC-qMS at a reduced mass scanning range (40–400) demonstrated that it can be an alternative to GC×GC-TOF MS for the analysis of the target analytes.

Coffee beans can be roasted either adding sugar during the process (torrefacto coffees) or without sugar addition (conventional or natural coffees). Previous studies have observed that torrefacto roasting masks the poor sensorial properties of Robusta coffee (Maeztu *et al*., 2001), and could be used fraudulently to hide the low-quality beans. GC-MS studies of volatile compounds have detected a higher content of pyrazines, furans and pyridines in torrefacto coffees compared with natural roasted coffees (Sanz *et al*., 2002; López-Galilea *et al*., 2006). Recently, the presence of difructose anhydrides (DFAs) has been described in torrefacto coffees. These compounds are formed by caramelization, and can provide useful information related to the

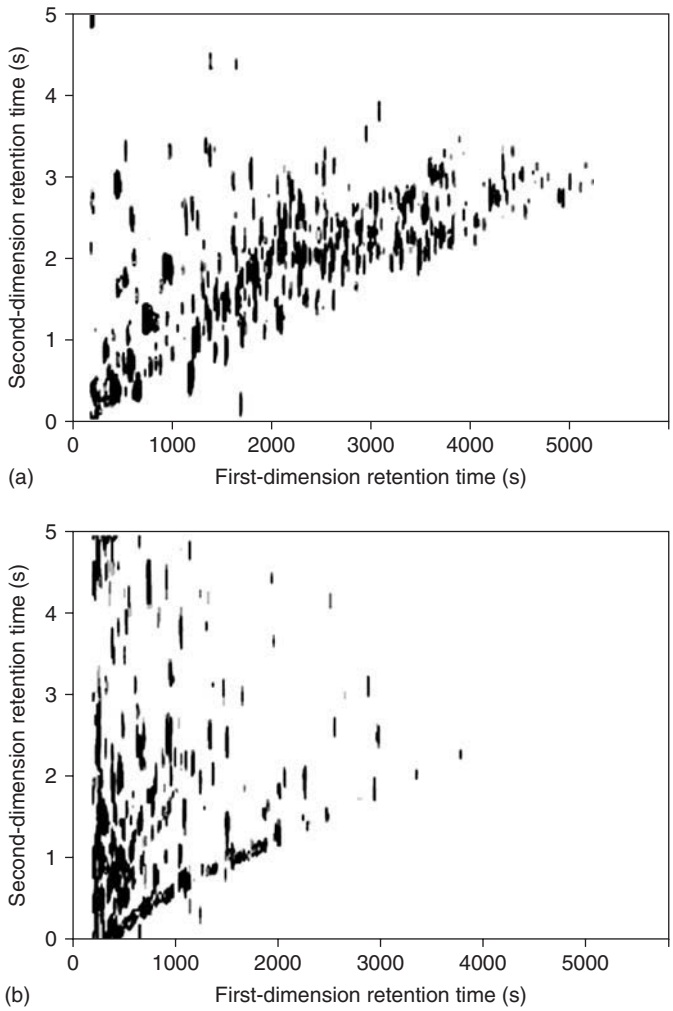

Figure 10.9 Bidimensional GC contour plots for volatile composition of Arabica coffee using (a) the polar/non-polar column set and (b) the non-polar/polar column set. Reprinted with permission from Ryan *et al*. (2004); ©Elsevier.

degree of torrefacto roasting and be used as quality markers to detect fraud (Montilla *et al*., 2006). GC analysis of these compounds required a previous derivatization process to obtain their trimethylsilyl derivatives.

Authentication of geographical origin

Prices of coffee are also dependent on its geographical origin. The volatile compositions of these products can be different, and both producers and consumers select them in terms of their aroma. Freitas and Mosca (1999) used a P&T device connected to GC to analyze the aroma fraction of coffees of different geographical origins (samples from Africa, Asia and America). Data were treated using multivariate analysis.

Arabica roasted coffees were better grouped according to their geographical origin than those from Robusta, whereas green coffees could not be discriminated among them. Zambonin *et al*. (2005) combined HS-SPME-GC-MS with multivariate analysis to discriminate among coffees from Africa and Central and South America.

Adulteration with cheaper products

It has also been reported that commercial coffees have been adulterated with coffee husks, cereals, malt, maltodextrins, soy and caramel (Prodolliet and Hischenhuber, 1998; Stöber *et al*., 2004). Free fructose, free glucose, sucrose, mannitol, total glucose and total xylose have been proposed as markers of these adulterations (Davis *et al*., 1990; Prodolliet and Hischenhuber, 1998). More recently, a GC method has been optimized to determine the sugar and polyalcohol content (mainly bornesitol) of coffee and its substitutes based on cereals, carob or chicory. Trimethylsilyl derivatives of sugars were analyzed by GC. Differences in their chromatographic profiles were found, and this information is useful to detect adulteration of coffee with these products (Ruiz-Matute *et al*., 2007b).

Alcoholic beverages

Wines and vinegars

Adulteration of wines is mainly based on the use of grapes from vineyards of different varieties or geographical origins, although dilution of wine with inferior products, falsification of the race of wine and/or of the manufacture method, and preparation of artificial wines are other practices that affect the quality of wine (Savchuk *et al*., 2001).

The authenticity of wine is regulated by authorities, and many authors have focused their efforts on finding new methodologies to detect fraud. GC is not the most common technique selected for these purposes, although some studies concerning the analysis of volatile compounds in wine should be highlighted (Arvanitoyannis *et al*., 1999). The analysis of volatile compounds by P&T coupled to GC allowed the discrimination of white wines produced in different regions of Spain; identification of these compounds was carried out by using an IT detector, and data were treated by multivariate analysis (cluster analysis, principal component analysis, k-nearest neighbors) (García-Jares *et al*., 1995). Other works have focused on the distinction of grape varieties: SPME-GC-FID was used to study the minor and major volatile compounds of 16 wines from 4 different varieties (Pozo-Bayón *et al*., 2001). The use of stepwise discriminant analysis allowed 100% correct classification of these wines using four variables: 1-propanol, ethyl octanoate, *cis*-3-hexen-1-ol and octanoic acid. Different substances have been proposed as markers of the contact of wine with oak, the oak lactones being the most important (Singleton, 1995).

The proportions of *myo*- and *scyllo*-inositol have been proposed, in a multiparametrical approach along with isotopic methods, for the control of adulteration with sugar of concentrated rectified musts (Monetti *et al*., 1996).

GC-MS methods have been developed to detect the addition of industrial glycerol to wines (Lampe *et al*., 1997). 3-Methoxy-1,2-propandiol and cyclic diglycerols are present in synthetic glycerol, but not in grapes or authentic wines. Therefore, their

presence can be considered as an indication of such adulteration. Modifications of the method (extraction of compounds with chloroform, silylation before analysis or use of a silicone oil stationary phase) have been carried out by Otteneder *et al*. (1999) and Bononi *et al*. (2001) to improve the separation of the compounds and reduce the detection limits.

It is also necessary to mention some works published regarding vinegar authenticity. The most common adulteration of this product is the addition of alcohols of different origins to the base wine used to produce wine vinegars, thus reducing manufacturing costs (Saiz-Abajo *et al*., 2005). Antonelli *et al*. (1997) have suggested the analysis of polyalcohols to differentiate between different kinds of vinegars. Apple vinegar was easily distinguishable from wine vinegars due to the high content of sorbitol, whereas alcohol vinegars showed a very low content of polyalcohols.

Other alcoholic beverages

GC and GC-MS have been used to determine the authenticity of alcoholic beverages such as vodka, gin, cognac and whiskey (Savchuk *et al*., 2001). Acetone, 2-butanol, crotonaldehyde and other impurities typical of synthetic alcohols have been chosen as markers for the authenticity of vodkas, whereas fatty acids, glycols or other typical low-volatility components of juniper-berry extracts can be used to differentiate cheap gins (prepared by infusing plant raw material) from higher-priced (distilled gins). Different methods based on the analysis of volatile compounds of cognacs and brandies on polar, medium and low-polarity stationary phases have been developed to determine aging of cognac spirits, replacement of cognac spirits by alcohol produced from non-grape materials or the contact of cognac spirit with oakwood (Savchuk *et al*., 2001). Bauer-Christoph *et al*. (2003) also proposed a GC method to asses the authenticity of tequilas by means of determining methanol and 2-/3-methyl-1-butanol concentrations. It was possible to differentiate between tequila derived from 100% agave and tequila produced from other sugar sources (mixed tequilas).

Conclusions

GC is an affordable technique which provides great versatility and really high resolution for the analysis of adulterants in food. Complex mixtures of volatile compounds can be directly analyzed by GC, but there is also a number of interesting derivatives for the study of non-volatile polar molecules. When coupled to spectroscopic techniques, especially to mass spectrometry, it affords additional structural information for compound identification.

It is at present the most widely used technique for authentication of oils and fats, by means of the analysis of fatty acids and triglycerides, as well as sterols and other minor components.

GC analysis of volatile compounds can be carried out in different ways, and the results are dependent on the used fractionation technique. GC has proved to be useful for authentication of cheeses, wines, honeys, flavors, species, coffee, etc.

The presence of inexpensive sweeteners in products such as honeys and juices can be detected by GC analysis of carbohydrates. Although in many aspects LC gives equivalent results, there are GC methods capable of better detecting minor components which can be relevant for authentication.

References

Adahchour, M., Beens, J., Vreuls, R.J.J. and Brinkman, U.A.Th. (2006). Recent developments in comprehensive two-dimensional gas chromatography (GC×GC). II. Modulation and detection. *Trends in Analytical Chemistry*, **25**, 540–553.

Aldai, N., Murray, B.E., Najera, A.I. *et al*. (2005). Derivatization of FA and its application for conjugated linoleic acid studies in ruminant meat lipids. *Journal of the Science of Food and Agriculture*, **85**, 1073–1083.

Alonso, G.L., Salinas, M.R. and Garijo, J. (1998). Method to determine the authenticity of aroma of saffron (*Crocus sativus* L.). *Journal of Food Protection*, **61**, 1525–1528.

Alonso, L., Fontecha, J., Lozada, L. and Juárez, M. (1997). Determination of mixtures in vegetable oils and milk fat by analysis of sterol fraction by gas chromatography. *Journal of the American Oil Chemists' Society*, **74**, 131–135.

Alves, M.R., Casal, S., Oliveira, M.B.P.P. and Ferreira, M.A. (2003). Contribution of FA profile obtained by high-resolution GC/chemometric techniques to the authenticity of green and roasted coffee varieties. *Journal of the American Oil Chemists' Society*, **80**, 511–517.

Antonelli, A., Zeppa, G., Gerbi, V. and Carnacini, A. (1997). Polyalcohols in vinegar as an origin discriminator. *Food Chemistry*, **60**, 403–407.

Antoniosi Filho, N.R., Carrilho, E. and Lancas, F.M. (1993). Fast quantitative analysis of soybean oil in olive oil by high-temperature capillary gas chromatography. *Journal of the American Oil Chemists' Society*, **70**, 1051–1053.

Arthur, C.L. and Pawliszyn, J. (1990). Solid phase microextraction with thermal desorption using fused silica optical fibers. *Analytical Chemistry*, **62**, 2145–2148.

Arvanitoyannis, I.S., Katsota, M.N., Psarra, E.P. *et al*. (1999). Application of quality control methods for assessing wine authenticity: Use of multivariate analysis (chemometrics). *Trends in Food Science & Technology*, **10**, 321–336.

Astwood, K., Lee, B. and Manley-Harris, M. (1998). Oligosaccharides in New Zealand honeydew honey. *Journal of Agricultural and Food Chemistry*, **46**, 4958–4962.

Aued-Pimentol, S., Takemoto, E., Antoniassi, R. and Badolato, E.S.G. (2006). Composition of tocopherols in sesame seed oil: an indicative of adulteration. *Grasas y Aceites*, **57**, 205–210.

Banfi, S., Bergna, M., Povolo, M. and Contarini, G. (1999). Programmable temperature vaporizer (PTV) applied to the triglyceride analysis of milk fat. *Journal of High Resolution Chromatography*, **22**, 93–96.

Bauer-Christoph, C., Christoph, N., Aguilar-Cisneros, B.O. *et al*. (2003). Authentication of tequila by gas chromatography and stable isotope ratio analyses. *European Food Research and Technology*, **217**, 438–443.

Benn, S. (1998). Potent odorants in peppermint and cornmint oils characterized by GC-O and AEDA. *Perfumer & Flavorist*, **23**, 5–6.

Bhattacharjee, P., Singhal, R.S. and Gholap, A.S. (2003). Supercritical carbon dioxide extraction for identification of adulteration of black pepper with papaya seeds. *Journal of the Science of Food and Agriculture*, **83**, 783–786.

Biedermann, M., Grob, K., Mariani, C. and Schmidt, J.P. (1996). Detection of desterolized sunflower oil in olive oil through isomerized Δ7-sterols. *Zeitschrift für Lebensmittel-Untersuchung und -Forschung*, **202**, 199–204.

Björndal, H., Lindberg, B. and Svensson, S. (1967). Gas-liquid chromatography of partially methylated alditols as their acetates. *Acta Chemica Scandinavica*, **21**, 1801–1804.

Blanch, G.P., Villen, J. and Herraiz, M. (1998). Rapid analysis of free erythrodiol and uvaol in olive oils by coupled reversed phase liquid chromatography-gas chromatography. *Journal of Agricultural and Food Chemistry*, **46**, 1027–1030.

Blanch, G.P., Caja, M.M., Ruiz del Castillo, M.L. and Herraiz, M. (1999). A contribution to the study of the enantiomeric composition of a chiral constituent in hazelnut oil used in the detection of adulterated olive oil. *European Food Research and Technology*, **210**, 139–143.

Bononi, M., Favale, C., Lubian, E. and Tateo, F. (2001). A new method for the identification of cyclic diglycerols in wine. *Journal International des Sciences de la Vigne et du Vin*, **35**, 225–229.

Bouseta, A. and Collin, S. (1995). Optimized Likens-Nickerson methodology for quantifying honey flavours. *Journal of Agricultural and Food Chemistry*, **43**, 1890–1897.

Buchgraber, M., Senaldi, C., Ulberth, F. and Anklam, E. (2004). Detection and quantification of cocoa butter equivalents in cocoa butter and plain chocolate by gas liquid chromatography of triacylglycerols. *Journal of the AOAC International*, **87**, 1153–1163.

Čajka, T., Hajslova, J., Cochran, J. *et al*. (2007). Solid phase microextraction-comprehensive two-dimensional gas chromatography-time-of-flight mass spectrometry for the analysis of honey volatiles. *Journal of Separation Science*, **30**, 534–546.

Carstensen, B. and Schwack, W. (2002). GPC isolation and gas chromatographic determination of minor compounds in vegetable oils. *Lipid Technology*, **14**, 135–138.

Castro-Vázquez, L., Díaz-Maroto, M.C. and Pérez-Coello, M.S. (2007). Aroma composition and new chemical markers of Spanish citrus honeys. *Food Chemistry*, **103**, 601–606.

Cert, A., Lanzon, A., Carelli, A.A. *et al*. (1994). Formation of stigmasta-3,5-diene in vegetable oils. *Food Chemistry*, **49**, 278–283.

Coleman, W.M. and Lawrence, B.M. (2000). Examination of the enantiomeric distribution of certain monoterpene hydrocarbons in selected essential oils by automated solid-phase microextraction-chiral gas chromatography-mass selective detection. *Journal of Chromatographic Science*, **38**, 95–99.

Contarini, G., Povolo, M., Leardi, R. and Toppino, P.M. (1997). Influence of heat treatment on the volatile compounds of milk. *Journal of Agricultural and Food Chemistry*, **45**, 3171–3177.

Cotte, J.F., Casabianca, H., Chardon, S. *et al*. (2003). Application of carbohydrate analysis to verify honey authenticity. *Journal of Chromatography A*, **1021**, 145–155.

Cotte, J.F., Casabianca, H., Chardon, S. and Lheritier, J.L. (2004). Chromatographic analysis of sugars applied to the characterisation of monofloral honey. *Analytical and Bioanalytical Chemistry*, **380**, 698–705.

Crews, C., CalvetSarrett, R. and Brereton, P. (1997). The analysis of sterol degradation products to detect vegetable fats in chocolate. *Journal of the American Oil Chemists' Society*, **74**, 1273–1280.

Dallüge, J., Beens, J. and Brinkman, U.A.Th. (2003). Comprehensive two-dimensional gas chromatography: a powerful and versatile analytical tool. *Journal of Chromatography A*, **1000**, 69–108.

Damirchi, S.A., Savage, G.P. and Dutta, P.C. (2005). Sterol fractions in hazelnut and virgin olive oils and 4,4′-dimethylsterols as possible markers for detection of adulteration of virgin olive oil. *Journal of the American Oil Chemists' Society*, **82**, 717–725.

Davis, G.E., Garwood, V.W., Barfuss, D.L. *et al*. (1990). Chromatographic profile of carbohydrates in commercial coffees. 2. Identification of mannitol. *Journal of Agricultural and Food Chemistry*, **38**, 1347–1350.

De la Fuente, E., Valencia-Barrera, R.M., Martínez-Castro, I. and Sanz, J. (2007). Occurrence of 2-hydroxy-5-methyl-3-hexanone and 3-hydroxy-5-methyl-2-hexanone as indicators of botanic origin in eucalyptus honeys. *Food Chemistry*, **103**, 1176–1180.

De la Fuente, M.A. and Juarez, M. (2005). Authenticity assessment of dairy products. *Critical Reviews in Food Science and Nutrition*, **45**, 563–585.

Dimandja, J.M.D., Stanfill, S.B., Grainger, J. and Patterson, D.G., Jr. (2000). Application of comprehensive two-dimensional gas chromatography (GC×GC) to the qualitative analysis of essential oils. *Journal of High Resolution Chromatography*, **23**, 208–214.

Doner, L.W., White, J.W. and Phillips, J.G. (1979). Gas-liquid chromatographic test for honey adulteration by high fructose corn syrup. *Journal of the Association of Official Analytical Chemists*, **69**, 186–189.

Dourtoglou, V.G., Dourtoglou, T., Antonopoulos, A. *et al*. (2003). Detection of olive oil adulteration using principal component analysis applied on total and regio FA content. *Journal of the American Oil Chemists' Society*, **80**, 203–208.

Dugo, G., Lamonica, G., Cotroneo, A. *et al*. (1992). High resolution gas chromatography for detection of adulterations of citrus cold-pressed essential oils. *Perfumer & Flavorist*, **17**, 57–58.

Dugo, G., Tranchida, P.Q., Cotroneo, A. *et al*. (2005). Advanced and innovative chromatographic techniques for the study of citrus essential oils. *Flavour and Fragrance Journal*, **20**, 249–264.

European Union (EU) (1992). Reference method for the determination of sitosterol and stigmasterol in butteroil. Commission Regulation EEC No 3942/92 of 22 of December. *Official Journal of the European Communities*, **L399**, 29–38.

Faulhaber, S., Hener, U. and Mosandl, A. (1997). GC/IRMS analysis of mandarin essential oils. 1. $\delta^{13}C_{PDB}$ and $\delta^{15}N_{AIR}$ values of methyl N-methylanthranilate. *Journal of Agricultural and Food Chemistry*, **45**, 2579–2583.

Freitas, A.M.C. and Mosca, A.I. (1999). Coffee geographic origin – an aid to coffee differentiation. *Food Research International*, **32**, 565–573.

Freitas, A.M.C., Parreira, C. and Vilas-Boas, L. (2001). Comparison of two SPME fibers for the differentiation of coffee by analysis of volatile compounds. *Chromatographia*, **54**, 647–652.

Gansser, D. and Busmann, D. (1998). Application of Low's fingerprint method for the investigation of apple juice concentrates. *Fruit Processing*, **8**, 91–96.

García, M.A. and Sanz, J. (2001). Analysis of *Origanum vulgare* volatiles by direct thermal desorption coupled to gas chromatography–mass spectrometry. *Journal of Chromatography A*, **918**, 189–194.

García-Jares, C., García-Martín, S. and Cela-Torrijos, R. (1995). Analysis of some highly volatile compounds of wine by means of purge and cold trapping injector capillary gas chromatography. Application to the differentiation of Rias Baixas Spanish white wines. *Journal of Agricultural and Food Chemistry*, **43**, 764–768.

Geeraert, E. and Sandra, P. (1987). Capillary GC of triglycerides in fats and oils using a high temperature phenylmethylsilicone stationary phase. II. The analysis of chocolate fats. *Journal of the American Oil Chemists' Society*, **64**, 100–105.

Giacomelli, L.M., Mattea, M. and Ceballos, C.D. (2006). Analysis and characterization of edible oils by chemometric methods. *Journal of the American Oil Chemists' Society*, **83**, 303–308.

Giacometti, J. (2001). Determination of aliphatic alcohols, squalene, alpha-tocopherol and sterols in olive oils: direct method involving gas chromatography of the unsaponifiable fraction following silylation. *Analyst*, **126**, 472–475.

Golay, M.J.E. (1968). Height equivalent to a theoretical plate of an open tubular column lined with a porous layer. *Analytical Chemistry*, **40**, 382–384.

Goudjil, H., Fontecha, J., Fraga, M.J. and Juarez, M. (2003). TAG composition of ewe's milk fat. Detection of foreign fats. *Journal of the American Oil Chemists' Society*, **80**, 219–222.

Guidotti, M. and Vitali, M. (1998). Identification of volatile organic compounds present in different honeys through SPME and GC/MS. *Industrie. Alimentari*, **37**, 351–353, 356.

Guyot, G., Scheirman, V. and Collin, S. (1998). Floral origin markers of chestnut and lime tree honeys. *Journal of Agricultural and Food Chemistry*, **46**, 625–633.

Holscher, W. and Steinhart, H. (1992). Investigation of roasted coffee freshness with an improved headspace technique. *Zeitschrift für Lebensmittel-Untersuchung und -Forschung*, **195**, 188–192.

International Dairy Federation (IDF) (1992). Official methods for analysis of sterols in dairy products. Milk and milk products determination of cholesterol content. International Standard 159/1992, Brussels, Belgium.

Iverson, J.L. (1972). Gas-liquid chromatographic detection of palm kernel and coconut oils in cacao butter. *Journal of the Association of Official Analytical Chemists*, **55**, 1319–1322.

James, A.T. and Martin, A.J.P. (1952). Gas-liquid partition chromatography – the separation and micro-estimaton of volatile fatty acids from formic acid to dodecanoic acid. *Biochemical Journal*, **50**, 679–690.

Kallio, H., Leino, M. and Solarinne, L. (1988). Analysis of the headspace of foodstuffs near room temperature. *Proceedings of the 9th International Symposium on Capillary Chromatography*. Heidelberg: Huethig Verlag Publisher, pp. 191–200.

Kamm, W., Dionisi, F., Hischenhuber, C. *et al*. (2002). Rapid detection of vegetable oils in milk fat by on-line LC-GC analysis of beta-sitosterol as marker. *European Journal of Lipid Science and Technology*, **104**, 756–761.

Kapoulas, V.M. and Passaloglou-Emmanouilidou, S. (1981). Detection of adulteration of olive oil with seed oils by a combination of column and gas liquid chromatography. *Journal of American Oil Chemists' Society*, **58**, 694–697.

Kaunzinger, A., Juchelka, D. and Mosandl, A. (1997). Progress in the authenticity assessment of vanilla. 1. Initiation of authenticity profiles. *Journal of Agricultural and Food Chemistry*, **45**, 1752–1757.

Kauschus, U. and Thier, H.P. (1985). The composition of soluble polysaccharides in fruit juices. *Zeitschrift für Lebensmittel-Untersuchung und -Forschung*, **181**, 395–399.

Knapp, D.R. (1979). *Handbook of Analytical Derivatization Reactions*, 1st edn. New York, NY: Wiley-Interscience.

König, W.A., Fricke, C., Saritas, Y. *et al*. (1997). Adulteration or natural variability? Enantioselective gas chromatography in purity control of essential oils. *Journal of High Resolution Chromatography*, **20**, 55–61.

Krist, S., Stuebiger, G., Bail, S. and Unterweger, H. (2006). Detection of adulteration of poppy seed oil with sunflower oil based on volatiles and triacylglycerol composition. *Journal of Agricultural and Food Chemistry*, **54**, 6385–6389.

Laine, R.A. and Sweeley, C.C. (1971). Analysis of trimethylsilyl O-methyloximes of carbohydrates by combined gas-liquid chromatographic-mass spectrometry. *Analytical Biochemistry*, **43**, 533–538.

Lampe, U., Kreisel, A., Burkhard, A. *et al*. (1997). Method for detection of added industrial glycerol in wine. *Deutsche Lebensmittel-Rundschau*, **93**, 103–110.

Leino, M., Lapvetelainen, A., Menchero, P. *et al*. (1991). Characterization of stored Arabica and Robusta coffees by headspace-GC and sensory analysis. *Food Quality and Preference*, **3**, 115–125.

Lipp, M. (1996). Determination of the adulteration of butter fat by its triglyceride composition obtained by GC. A comparison of the suitability of PLS and neural networks. *Food Chemistry*, **55**, 389–395.

Liu, J.M., Li, N., Wen, M.J. and Jiang, G.B. (2004). Determination of volatile sulfur compounds in beverage and coffee samples by purge-and-trap on-line coupling with a gas chromatography-flame photometric detector. *Microchimica Acta*, **148**, 43–47.

Loesing, G. (1999). A simple authenticity test for onion oil. *Deutsche Lebensmittel-Rundschau*, **95**, 234–236.

López-Galilea, I., Fournier, N., Cid, C. and Guichard, E. (2006). Changes in headspace volatile concentrations of coffee brews caused by the roasting process and the brewing procedure. *Journal of Agricultural and Food Chemistry*, **54**, 8560–8566.

Low, N.H. (1995). Apple and orange juice authenticity analysis by capillary gas chromatography with flame ionization detection. *Fruit Processing*, **11**, 362–367.

Low, N.H. (1996). Determination of fruit juice authenticity by capillary gas chromatography with flame ionization detection. *Journal of the AOAC International*, **79**, 724–737.

Low, N.H. (1998). Oligosaccharide fingerprinting and chemical composition of white grape juice from Argentina. *Fruit Processing*, **8**, 97–101.

Low, N.H. and Hammond, D.A. (1996). Detection of high fructose syrup from inulin in apple juice by capillary gas chromatography with flame ionization detection. *Fruit Processing*, **4**, 135–139.

Low, N.H. and South, W. (1995). Determination of honey authenticity by capillary gas chromatography. *Journal of the AOAC International*, **78**, 1210–1218.

Low, N.H. and Sporns, P. (1988). Analysis and quantitation of minor disaccharides and trisaccharides in honey, using capillary gas-chromatography. *Journal of Food Science*, **53**, 558–561.

Maeztu, L., Andueza, S., Ibáñez, C. *et al*. (2001). Multivariate methods for characterization and classification of espresso coffees from different botanical varieties and types of roast by foam, taste, and mouthfeel. *Journal of Agricultural and Food Chemistry*, **49**, 4743–4747.

Mandl, A., Reich, G. and Lindner, W. (1999). Detection of adulteration of pumpkin seed oil by analysis of content and composition of specific Delta7-phytosterols. *European Food Research and Technology*, **209**, 400–406.

Mannas, D. and Altuğ, T. (2007). SPME/GC/MS and sensory flavour profile analysis for estimation of authenticity of thyme honey. *International Journal of Food Science and Technology*, **42**, 133–138.

Mariaca, R.G., Berger, T.F.H., Gauch, R. *et al*. (1997). Occurrence of volatile mono- and sesquiterpenoids in highland and lowland plant species as possible precursors for flavor compounds in milk and dairy products. *Journal of Agricultural and Food Chemistry*, **45**, 4423–4434.

Mariani, C. and Bellan, G. (1997). Detection of sunflower oil in safflower oil. *Rivista Italiana Sostanze Grasse*, **74**, 225–230.

Mariani, C., Venturini, S., Fedeli, E. and Contarini, G. (1994). Detection of refined animal and vegetable fats in adulteration of pure milkfat. *Journal of the American Oil Chemists' Society*, **71**, 1381–1384.

Mariani, C., Venturini, S. and Grob, K. (1995). Identification of desterolized high oleic sunflower oil in olive oil. *Rivista Italiana Sostanze Grasse*, **72**, 473–482.

Marriott, P. and Shellie, R. (2002). Principles and applications of comprehensive two-dimensional gas chromatography. *Trends in Analytical Chemistry*, **21**, 573–583.

Martín-Lomas, M., Martínez-Utrilla, R., Martínez-Castro, I. and Juárez, M. (1975). Identification of carbonyl compounds in transesterified fats detection in milk fat. *Fette Seifen Anstrichmittel*, **83**, 7–10.

Mateo, R. and Bosch-Reig, F. (1997). Sugar profiles of Spanish unifloral honeys. *Food Chemistry*, **60**, 33–41.

McReynolds, W.O. (1970). Characterization of some liquid phases. *Journal of Chromatographic Science*, **8**, 685–691.

Molkentin, J. and Precht, D. (2000). Equivalence of packed and capillary GC columns for detection of foreign fat in butter by use of the triglyceride formula method. *Chromatographia*, **52**, 791–797.

Mondello, L., Casilli, A., Tranchida, P.Q. *et al*. (2004a). Evaluation of fast gas chromatography and gas chromatography-mass spectrometry in the analysis of lipids. *Journal of Chromatography A*, **1035**, 237–247.

Mondello, L., Casilli, A., Tranchida, P.Q. *et al*. (2004b). Comprehensive multidimensional GC for the characterization of roasted coffee beans. *Journal of Separation Science*, **27**, 442–450.

Mondello, L., Costa, R., Tranchida, P.Q. *et al*. (2005). Reliable characterization of coffee bean aroma profiles by automated headspace solid phase microextraction-gas chromatography-mass spectrometry with the support of a dual-filter mass spectra library. *Journal of Separation Science*, **28**, 1101–1109.

Monetti, A., Versini, G., Dalpiaz, G. and Reniero, F. (1996). Sugar adulterations control in concentrated rectified grape musts by finite mixture distribution analysis of the myo- and scyllo-inositol content and the D/H methyl ratio of fermentative ethanol. *Journal of Agricultural and Food Chemistry*, **44**, 2194–2201.

Montilla, A., Ruiz-Matute, A.I., Sanz, M.L. *et al*. (2006). Difructose anhydrides as quality markers of honey and coffee. *Food Research International*, **39**, 801–806.

Mordret, F. (1968). Direct gas chromatographic analysis of rapeseed oil sterols. *Revue Française des Corps Gras*, **15**, 675–681.

Naviglio, D. and Raia, C. (2003). Application of a HRGC method on capillary column Rtx(R). 65-TAG for triglyceride analysis to monitor butter purity. *Analytical Letters*, **36**, 3063–3094.

Ng, L.K. and Hupé, M. (1998). Analysis of sterols: a novel approach for detecting juices of pineapple, passionfruit, orange and grapefruit in compounded beverages. *Journal of the Science of Food and Agriculture*, **76**, 617–627.

Nhu-Trang, T.T., Casabianca, H. and Grenier-Loustalot, M.F. (2006). Authenticity control of essential oils containing citronellal and citral by chiral and stable-isotope gas-chromatographic analysis. *Analytical and Bioanalytical Chemistry*, **386**, 2141–2152.

Ntsourankoua, H., Artaud, J. and Guerere, M. (1994). Triterpene alcohols in virgin olive oil and refined olive pomace oil. *Annales des falsifications, de l'expertise chimique et toxicologique*, **87**, 91–107.

Otteneder, H., Zimmer, M. and Schaab, J. (1999). Determination of the addition of glycerine to wine. *Deutsche Lebensmittel-Rundschau*, **95**, 172–175.

Overton, S.V. and Manura, J.J. (1994). Flavor and aroma in commercial bee honey – a purge-and-trap thermal-desorption technique for the identification and quantification of volatiles and semivolatiles in honey. *American Laboratory*, **26**, 45–53.

Padley, F.B. and Timms, R.E. (1980). The determination of cocoa butter equivalents in chocolate. *Journal of the American Oil Chemists' Society*, **57**, 286–293.

Povolo, M., Bonfitto, E., Contarini, G. and Toppino, P.M. (1999). Study on the performance of three different capillary gas chromatographic analyses in the evaluation of milk fat purity. *High Resolution Chromatography*, **22**, 97–112.

Pozo-Bayón, M.A., Pueyo, E., Martín-Álvarez, P.J. and Polo, M.C. (2001). Polydimethylsiloxane solid-phase microextraction–gas chromatography method for the analysis of volatile compounds in wines. Its application to the characterization of varietal wines. *Journal of Chromatography A*, **922**, 267–275.

Prager, M.J. and Miskiewicz, M.A. (1982). Gas chromatographic-mass spectrometric analysis, identification and detection of adulteration of natural and concentrated lemon oils. *Journal of the AOAC*, **65**, 166–171.

Precht, D. (1991). Detection of adulterated milkfat by fatty acid and triglyceride analysis. *Fett: Wissenschaft Technologie*, **93**, 538–544.

Precht, D. (2001). Cholesterol content in European bovine milk fats. *Nahrung*, **45**, 2–8.

Prodolliet, J. and Hischenhuber, C. (1998). Food authentication by carbohydrate chromatography. *Zeitschrift für Lebensmittel-Untersuchung und -Forschung*, **207**, 1–12.

Radovic, B.S., Careri, M., Mangia, A. *et al*. (2001). Contribution of dynamic headspace GC-MS analysis of aroma compounds to authenticity testing of honey. *Food Chemistry*, **72**, 511–520.

Ridgway, K., Lalljie, S.P.D. and Smith, R.M. (2007). Sample preparation techniques for the determination of trace residues and contaminants in foods. *Journal of Chromatography A*, **1153**, 36–53.

Rocha, S., Maeztu, L., Barros, A. *et al*. (2003). Screening and distinction of coffee brews based on headspace solid phase microextraction/gas chromatography/principal component analysis. *Journal of the Science of Food and Agriculture*, **84**, 43–51.

Rowland, C.Y., Blackman, A.J., Darcy, B.R. and Rintoul, G.B. (1995). Comparison of organic extractives found in leatherwood (eucryphia lucida). Honey and leatherwood flowers and leaves. *Journal of Agricultural and Food Chemistry*, **43**, 753–763.

Ruiz del Castillo, M.L., Caja, M.M. and Herraiz, M. (2003a). Use of the enantiomeric composition for the assessment of the authenticity of fruit beverages. *Journal of Agricultural and Food Chemistry*, **51**, 1284–1288.

Ruiz del Castillo, M.L., Caja, M.M., Blanch, G.P. and Herraiz, M. (2003b). Chiral evaluation of aroma-active compounds in real complex samples. *Journal of Food Science*, **68**, 770–774.

Ruiz-Matute, A.I., Soria, A.C., Martínez-Castro, I. and Sanz, M.L. (2007a). A new methodology based on GC-MS to detect honey adulteration with commercial syrups. *Journal of Agricultural and Food Chemistry*, **55**, 7264–7269.

Ruiz-Matute, A.I., Montilla, A., del Castillo, M.D. *et al*. (2007b). A GC method for simultaneous analysis of bornesitol, other polyalcohols and sugars in coffee and its substitutes. *Journal of Separation Science*, **30**, 557–562.

Ryan, D., Shellie, R., Tranchida, P. *et al*. (2004). Analysis of roasted coffee bean volatiles by using comprehensive two-dimensional gas chromatography–time-of-flight mass spectrometry. *Journal of Chromatography A*, **1054**, 57–65.

Saba, A., Mazzini, F., Raffaelli, A. *et al*. (2005). Identification of 9(*E*),11(*E*)-18:2 fatty acid methyl ester at trace level in thermal stressed olive oils by GC coupled to acetonitrile CI-MS and CI-MS/MS, a possible marker for adulteration by addition of deodorized olive oil. *Journal of Agricultural and Food Chemistry*, **53**, 4867–4872.

Saiz-Abajo, M.J., González-Saiz, J.M. and Pizarro, C. (2005). Orthogonal signal correction applied to the classification of wine and molasses vinegar samples by near-infrared spectroscopy. Feasibility study for the detection and quantification of adulterated vinegar samples. *Analytical Bioanalytical Chemistry*, **382**, 412–420.

Sanz, C., Maeztu, L., Zapalena, M.J. *et al*. (2002). Profiles of volatile compounds and sensory analysis of three blends of coffee: influence of different proportions of Arabica and Robusta and influence of roasting coffee with sugar. *Journal of the Science of Food and Agriculture*, **82**, 840–847.

Sanz, M.L., González, M., de Lorenzo, C. *et al*. (2004). Carbohydrate composition and physico chemical properties of artisanal honeys from Madrid (Spain): occurrence of *Echium* sp honey. *Journal of the Science of Food and Agriculture*, **84**, 1577–1584.

Savchuk, S.A., Vlasov, V.N., Appolonova, S.A. *et al*. (2001). Application of chromatography and spectrometry to the authentication of alcoholic beverages. *Journal of Analytical Chemistry*, **56**, 214–231.

Shimoda, M. and Shibamoto, T. (1990). Isolation and identification of headspace volatiles from brewed coffee with an on-column GC/MS method. *Journal of Agricultural and Food Chemistry*, **38**, 802–804.

Simoneau, C., Hannaert, P. and Anklam, E. (1999). Detection and quantification of cocoa butter equivalents in chocolate model systems: analysis of triglyceride profiles by high resolution GC. *Food Chemistry*, **65**, 111–119.

Singhal, R.S., Kulkarni, P.R. and Dinanath, V.R. (1997). Tea, coffee and cocoa. *Handbook of Indices of Food Quality and Authenticity*. Cambridge: Woodhead Publishing Ltd, pp. 458–488.

Singleton, V.L. (1995). Maturation of wines and spirits: comparisons, facts and hypotheses. *American Journal of Viticulture and Enology*, **46**, 98–115.

Soria, A.C., Martínez-Castro, I. and Sanz, J. (2003). Analysis of volatile composition of honey by solid phase microextraction and gas chromatography-mass spectrometry. *Journal of Separation Science*, **26**, 793–801.

Soulier, P., Farines, M. and Soulier, J. (1990). Triterpene alcohols, 4-methylsterols and 4-desmethylsterols of sal and illipe butters. *Journal of the American Oil Chemists' Society*, **67**, 388–393.

Spencer, J.S., Dowd, E. and Faas, W. (1997). The genuineness of two mint essential oils. *Perfumer & Flavorist*, **22**, 37–38, 41–45.

Stöber, P., Lamoureux, T., Martin, G.G. *et al*. (1998). Standardisation of the detection of invert sugar addition to apple juice by capillary gas chromatography. *Zeitschrift für Lebensmittel-Untersuchung und -Forschung*, **207**, 332–339.

Stöber, P., Giller, V., Spack, L. and Prodolliet, J. (2004). Estimation of the measurement uncertainty of the high-performance anion-exchange chromatographic determination of carbohydrates in soluble (instant) coffee. *Journal of the AOAC International*, **87**, 647–656.

Sullivan, J.E. and Schewe, L.R. (1977). Preparation and gas-chromatography of highly volatile trifluoroacetylated carbohydrates using N-methyl bis (trifluoroacetamide). *Journal of Chromatographic Science*, **15**, 196–197.

Swallow, K.W. and Low, N.H. (1994). Determination of honey authenticity by anion-exchange liquid chromatography. *Journal of the Association of Official Analytical Chemists*, **77**, 695–702.

Sweeley, C.C., Bentley, R., Makita, M. and Wells, W.W. (1963). Gas-liquid chromatography of trimethylsilyl derivatives of sugars and related substances. *Journal of the American Chemical Society*, **16**, 2497–2507.

Tarantilis, P.A. and Polissiou, M.G. (1997). Isolation and identification of the aroma components from saffron (*Crocus sativus*). *Journal of Agricultural and Food Chemistry*, **45**, 459–462.

Thavarajah, P. and Low, N.H. (2006). Isolation and identification of select oligosaccharides from commercially produced total invert sugar with a proposed mechanism for their formation. *Journal of Agricultural and Food Chemistry*, **54**, 2754–2760.

Ulberth, F. (1994). Detection of milk-fat adulteration by linear discriminant-analysis of fatty-acid data. *Journal of the AOAC International*, **77**, 1326–1334.

Ulberth, F. (1995). Quantification of foreign fat in foreign fat/mixtures by multivariate regression analysis of fatty acid data. *Journal of Agricultural and Food Chemistry*, **43**, 1556–1660.

Van Deemter, J.J., Zuiderweg, F.J. and Klinkenberg, A. (1956). Longitudinal diffusion and resistance to mass transfer as causes of nonideality in chromatography. *Chemical Engineering Science*, **5**, 271–280.

Villamiel, M., Martínez-Castro, I., Olano, A. and Corzo, N. (1998). Quantitative determination of carbohydrates in orange juice by gas chromatography. *Zeitschrift für Lebensmittel-Untersuchung und -Forschung A*, **206**, 48–51.

White, J.W. (1978). Honey. *Advances in Food Research*. New York, NY: Academic Press Inc, pp. 287–374.

Yang, X. and Peppard, T. (1994). Solid-phase microextraction for flavor analysis. *Journal of Agricultural and Food Chemistry*, **42**, 1925–1930.

Zambonin, C.G., Balest, L., De Benedetto, G.E. and Palmisano, F. (2005). Solid-phase microextraction-gas chromatography mass spectrometry and multivariate analysis for the characterization of roasted coffees. *Talanta*, **66**, 261–265.

This page intentionally left blank

11

Chromatographic Technique: High-performance Liquid Chromatography (HPLC)

Agnes Sass-Kiss

Introduction

High-performance liquid chromatography (HPLC) is a separation method that can be applied to analyze compounds of different properties, from the low up to very high molecular mass substances. Highly volatile compounds do not fit the HPLC method. Recently, HPLC techniques have been coupled with spectrometric or spectroscopic techniques, such as mass spectrometry (MS), nuclear magnetic resonance (NMR) spectroscopy and Fourier transform Raman (FTR) spectroscopy, in order to analyze complex mixtures of compounds through separation, identification and quantification in a single step and in one place. HPLC has several major advantages, and is therefore a widely used technique for research, and is applied in many different fields including pharmaceuticals, food, cosmetics, energy industries and environmental conservation.

The application of huge numbers of HPLC methods proves their essential role in authenticity tests for the food industry, where efficient, reliable and sensitive analytical

Modern Techniques for Food Authentication
ISBN: 978-0-12-374085-4

methods are needed. Most recently, the rapid development of HPLC technology has resulted in the detection and discovery of minor and specific compounds or groups thereof. The knowledge of these kinds of components provides the basis for detecting adulteration and fraud for profit, and preventing evasion of the laws passed in the interest of food authenticity. *Authenticity* of a food means that it contains solely the materials that are labeled on the packaging. Authentic food is natural, pure, undiluted, and does not contain undeclared ingredients. The rule and regulations presented help to assure the quality of food products.

The history of chromatography dates back to the early nineteenth century. Prior to the 1970s, open-column chromatography was used commercially in laboratories. The term *HPLC* originated because of the high-pressure technique used for reducing analysis time. After numerous development steps, instruments became able to function at pressures of up to 6000 psi (400 bar). With improvement of the columns and detectors, essential development was achieved in performance, so the technique was renamed *high-performance liquid chromatography* (HPLC) in the mid- to late 1970s. During this period, new methods, including reverse phase liquid chromatography, allowed for improved separation between very similar compounds. By the 1980s, computers and automation added convenience to HPLC analysis. At the beginning of the twenty-first century, a new level in performance was achieved by further improvement in the column technology leading to the use of adsorbent of smaller particle size (1.7 µm), and development of instrumentation that allow the application of high pressure up to 1000 bar for delivering the solvent. Resolution, speed and sensitivity increased. This new technology is called *ultra-performance liquid chromatography* (*UPLC*) (de Villiers *et al*., 2006; Cooper *et al*., 2007).

Principle of liquid chromatography

Theory of separation in liquid chromatography (Macrae, 1982; Snyder and Kirkland, 1974; Newton, 1982; Schoenmakers, 1986; Pool and Poole, 1991)

Liquid chromatography is a separation method that uses a column filled with solid support (adsorbent) and a liquid moving through the support bed. The compounds move from the top of the column with the mobile phase, through the adsorbent, during which time the individual compounds separate. The solid support, over which the mobile phase continuously flows, is called the stationary phase. Migration of compounds with different speed through the stationary phase is due to the difference in their distribution between the mobile and the stationary phase. The retention of a compound is determined by the magnitude of its partition coefficient between the two phases, i.e. the retention depends on the level of interaction of the compound with the stationary phase.

Information obtained from a chromatographic process is revealed by a chromatogram, which is a record of the concentration profile of the sample compounds. The chromatogram (Figure 11.1) is series of patterns (normal Gaussian peak) of compounds generated by a detector, which senses the change in concentration of the individual

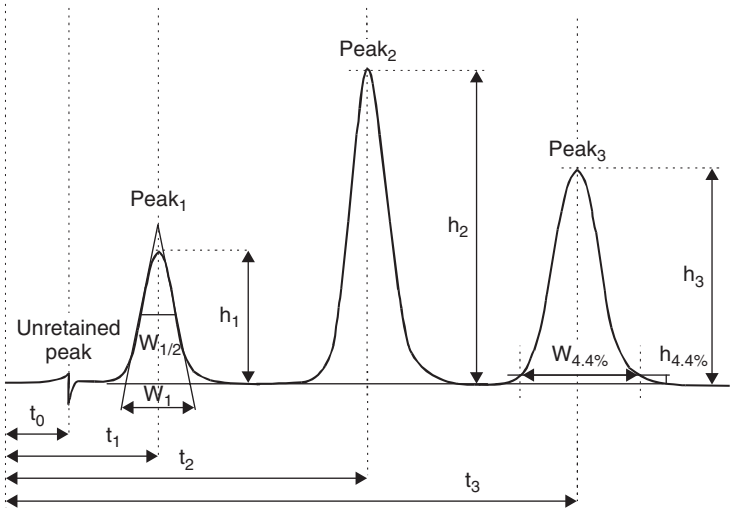

Figure 11.1 Chromatographic peaks and their attributes. t_0, hold-up time or column dead time; t_{1-3}, retention time; h_{1-3} peak height, w peak width, $w_{1/2}$, peak width measured at half peak height, $w_{4,4\%}$ peak width measured at 4.4% peak height ($h_{4.4\%}$).

compound at the end of the column as a function of the time (or volume of the mobile phase). The chromatogram provides complex information about a sample, such as the number of separated compounds, and the quantity (peak height or peak area) and identity (retention parameters) of individual compounds.

The length of time required for a compound to pass through a chromatographic column is called the *retention time* (t_R). Moving through the column, different molecules spend different lengths of time in the stationary phase, but the same amount of time in the mobile phase. This latter time is called the *column dead time* or *hold-up time* (t_0). The time the molecules spend in the stationary phase is called the corrected retention time (t_R'), which is calculated as the difference between the retention time and the dead time:

$$t_R' = t_R - t_0 \tag{11.1}$$

As liquids can be considered to be incompressible, in liquid chromatography the retention is usually measured in units of time for convenience.

The ratio of corrected retention time to dead time is the capacity factor of the compound, which characterizes the separation. The capacity factor (k) is calculated as follows:

$$k = t_R'/t_0 = (t_R - t_0)/t_0 \tag{11.2}$$

The relative retention of two neighboring components is described by:

$$\alpha = t_R'_{(peak1)}/t_R'_{(peak2)} = k_{(peak1)}/k_{(peak2)} \tag{11.3}$$

where α is the *separation factor*. The separation factor is also known as the *relative retention* or *selectivity*.

As the molecules migrate through the column, the zone of compounds broadens continually during their passage. The extent of zone broadening determines the chromatographic efficiency, which can be expressed by the theoretical plate number (N) or by the height equivalent to the theoretical plate (*H* or *HETP*). The theoretical plate is proportional to the length of column (L):

$$N = L/H \tag{11.4}$$

A smaller value of H indicates a more efficient column with a higher N value. *Column efficiency* refers to the performance of the stationary phase, providing information about its kinetic performance and how well the column is packed.

The mathematical description of chromatographic column efficiency is obtained from the van Deemter equation:

$$H = A + B/u + Cu \tag{11.5}$$

where u is the linear velocity of the mobile phase. A is the term for eddy diffusion, representing several pathways for a component to find its way through the column. The mobile phase velocity also affects the eddy diffusion. A higher flow rate results in a greater zone-broadening effect. B is the term for longitudinal diffusion, describing a band-broadening process that is inversely related to the mobile phase velocity. In HPLC this term is negligible, since diffusion coefficients of liquids are very small compared with those of gases (as in gas chromatography). C is the coefficient of the mass transfer. In order to obtain a small value of H and allow efficient separation to be achieved, support of small particles, eluent of low viscosity, a longer column and a higher temperature should be used.

The theoretical plate number can be measured by several methods, applying the following formula:

$$N = a\,(t_r/w)^2 \tag{11.6}$$

where a is a constant depending on the height of the peak (where it is measured), t_r is the relative retention time of peak and *w* is the peak width (Figure 11.1). The value of a depends on the calculation method; it can be 5.57, 25, 16 when the peak width is measured at half peak height ($w_{1/2}$), at 4.4% peak height, and at the baseline respectively. The peak width (w) is the distance between the intersection of baseline and tangent line to both sides of peak.

Many chromatographic peaks do not show the pattern of normal Gaussian distribution. The theoretical plate is not affected by chromatographic anomalies (Figure 11.2) such as peak "tailing" and "fronting".

The formula for the asymmetry of a peak, i.e. the *asymmetry factor*, can be calculated from the shape of the peak:

$$As = b/a \tag{11.7}$$

where a is the distance between the peak maximum and peak front measured at 10% of the peak height, and b is the distance between the peak maximum and peak tail measured at 10% of the peak height.

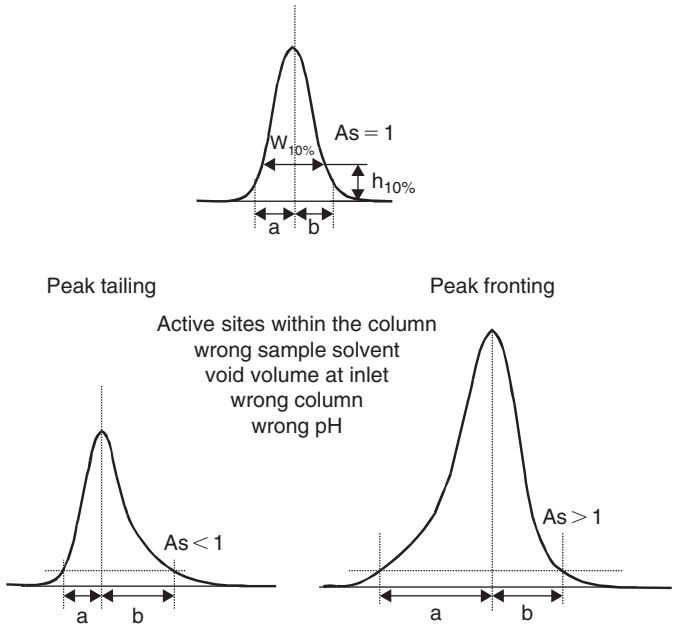

Figure 11.2 Anomalies of chromatographic peaks. As, asymmetry factor; w10%, peak width measured at 10% peak height ($h_{10\%}$).

The degree of separation of two peaks is characterized by the relative separation, namely *resolution*. The resolution of two peaks can be calculated from adjustable chromatographic variables such as the selectivity, efficiency and capacity factor of separated compounds by the following formula:

$$R_s = N^{1/2}/4(\alpha - 1)/\alpha k'/1 + k' \qquad \textbf{(11.8)}$$

where k′ is the average of the capacity factor of the two peaks of interest. If R_s is 1.25, the separation of two peaks is considered satisfactory.

Instrumentation (Fekete, 2000; Newton, 1982; Pool and Poole, 1991; Simpson, 1982; Snyder and Kirkland, 1974)

Figure 11.3 shows a schematic diagram of a HPLC instrument. It consists of a delivery system, columns, detectors, and an operation and control system.

Delivery system

The delivery system in liquid chromatography consists of a high-pressure pump, check valves, flow controllers, a mixing chamber, a pulse dampener and pressure transducers. The system should be able to deliver the solvents from the reservoirs through the whole chromatograph at high pressure (up to 500 bar) at a broad range of flow rate (0.1–10 ml min^{-1}), with minimal flow fluctuation, ensuring reproducibility of retention time and baseline stability of detectors. By blending the solvents in

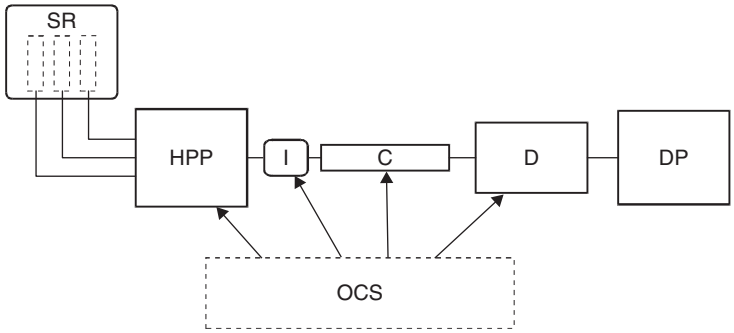

SR, solvent reservoir; HPP, high-pressure pump; I, injector; C, column; D, detector; OCS, operation and control system; DP, data processing.

Figure 11.3 Block diagram of HPLC instrument.

the mixing chamber, the high-pressure pump insures the constant composition of the eluent during isocratic separation, while increasing eluent strength with time should be achieved during gradient elution. Sophisticated instruments are equipped with a solvent degasser by applying a helium purge or vacuum.

Some factors affecting the performance of the delivery system can be controlled by preparation of the eluent. Degassing of eluent is used to prevent gas-bubble formation in the mobile phase. Bubbles, formed mainly from oxygen, can cause degradation of samples and phases, and furthermore affect the sensitivity and baseline stability of detectors. Degassing can be carried out by applying a vacuum, ultrasonic treatment or a purge with helium. Refluxing solvent was found to be the most efficient method for reducing oxygen concentration. Solid particles in eluent can cause disorders during separation, thus affecting the pressure and efficiency of solvent delivery and leading to the fluctuation of the flow rate. Therefore, filtration of solid particles from the solvents or sample solution is an important step before analysis.

Column

The column is an open stainless-steel capillary tube filled with the solid support. The column is the heart of the chromatograph; however, high efficiency in separation and quantification can be achieved only if the column is placed in a well-designed chromatographic instrument. The diameter of a column in analytical separation is about 2–5 mm; its length is about 10–30 cm. Application of a pre-column is essential for saturation of the moving phase with the stationary phase before reaching the column, thereby increasing the life of the column. Pre-columns need to be replaced quite frequently. Injection of samples into the column can be carried out manually or by an autoinjection procedure. Keeping the column at constant temperature, using a thermostat, is important in liquid–liquid or ion exchange chromatography.

Packing materials in the columns in HPLC can be grouped based on different characteristics – rigid solids, firm or soft gels, ball- or irregularly-shaped particles, porous internally or porous on the surface. The attributes of packing materials in the column

Table 11.1 Classification of high-performance liquid chromatographic methods

Stationary phase	Mobile phase	Name of chromatographic method
Polar	Apolar	*Normal phase HPLC*: the stationary phase is more polar in relation to mobile phase
Apolar	Polar	*Reversed phase HPLC*: the stationary phase is more apolar in relation to mobile phase
Apolar	Polar	*Reversed phase ion-pair HPLC*: mobile phase consists of hydrophobic ions (1–100 mmol l^{-1}), which have opposite charge to compounds of interest for ion-pair formation
Charged groups on the surface	Buffer	*Ion exchange chromatography*: ionic and/or easily ionized compounds are separated on immobilized charged groups on stationary phase
High-diameter porous particles	Water or organic solvent	*Size-exclusion chromatography*: separation can be reached for polymers by differences in molecular size on non-sorptive stationary phase of controlled pore size (if organic gels are used for protein separation this is named gel filtration)
Enantiomeric compound is immobilized on the surface	Water or organic solvent	*Chiral HPLC* is based on various stereochemical interactions between enantiomeric compounds and the stationary phase
Low hydrophobic attributes	High salt content of eluent, decreasing the salt content during separation	*Hydrophobic interaction chromatography* uses hydrophobic properties of proteins.

vary depending on the chromatographic method. The chromatographic techniques can be divided into classes based on the type and quality of the stationary and mobile phases. The various liquid chromatographic methods are summarized in Table 11.1.

Silica gel is the most frequently used adsorbent in liquid chromatography, as it has several attributes that are significant in high-performance liquid chromatography. The mechanical stability is a crucial criterion for particles packed in the column. During separation under high pressure, the particles must not be allowed to fragment because this will decrease the kinetic efficiency of the column. Silica gel is a porous material; the size (6–20 nm) of the pores determines the area per unit of the particles (50–500 $m^2 g^{-1}$). The average particle size used in HPLC is 3–10 µm. The silanol groups have acidic pH. The number and the activity of silanol groups on the surface of silica gel particles affect the polarity of the silica gel (Figure 11.4).

Almost all chemically bonded and polymer-encapsulated packaging material in use today is prepared from a macroporous silica substrate. Polymer-encapsulated phases are prepared by coating the silica surface with an immobilized thin layer of polymer. The bonded phases are prepared by the reaction of free silanol groups on the surface with reactive organosilane. The disadvantage of silica-based bonded phases is the limited range of pH 2–8 in their application. At low pH, hydrolysis of alkyl syloxane exists, while at high pH, the solubility of silica gel limits its use. Several factors (activity of organosilane, solvent, catalytic reaction time, temperature, etc.) influence the quality of the bonded phases. Table 11.2 shows the structure of some siloxane-bonded phases applied in HPLC.

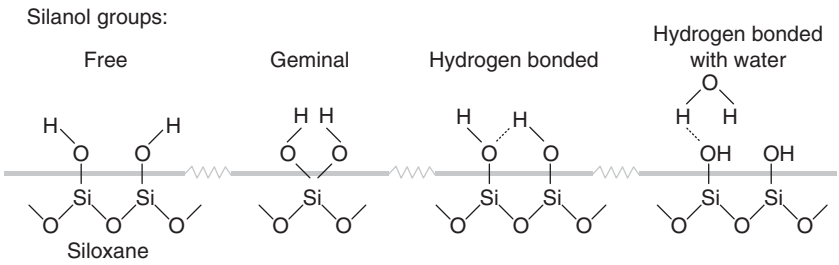

Figure 11.4 Silanol groups of different activity on the surface of silica gel.

Table 11.2 Structure and utilization of siloxan bonded phases

Phases	Application	Structure
C1 C2 C3 C4 C6 C8	Reversed phase materials with less retention than C18, useful for ion-pair chromatography, hydrophobic interaction chromatography, separation for proteins and peptides	–Si–CH_3 –Si–C_2H_5 –Si–C_3H_7 –Si–C_4H_9 –Si–C_6H_{13} –Si–C_8H_{17}
C18	Classic reversed phase material for separation of huge number of compounds from small molecular weight up to proteins	–Si–$C_{18}H_{37}$
C30	Reversed phase material, useful for separation of carotenoids	–Si–$C_{30}H_{61}$
Phenyl	Reversed phase material, useful for separation of aromatic compounds, useful for separation of proteins and peptides	–Si–C_3H_6
CN	Both reversed phase and normal phase material, weak anion-exchanger	–Si–C_3H_6–CN
NH2	Both reversed phase and normal phase material, weak anion-exchanger	–Si–C_3H_6–NH_2
NO2	Normal phase material, useful for separation of aromatic and compounds containing double bonds	–Si–NO_2
OH	Both reversed phase and normal phase material, useful for separation of proteins, peptides (gel filtration chromatography)	–Si–C_3H_6–O–CH_2–CH–CH OH OH
SAX	Strong anion-exchange material for separation of bases (nucleotides, nucleosides) or organic acids	–Si–C_3H_6–N^+–$(CH_3)_3$
SCX	Strong cation-exchange material for separation of organic acids	–Si–C_3H_6–SO_2–OH
WCX	Weak cation-exchange material for separation of organic acids, useful for basic proteins and peptides	–Si–CH_2–COOH
WAX	Weak anion-exchange material for acidic proteins and peptides	–Si–C_3H_6–N–$(CH_2CH_3)_2$

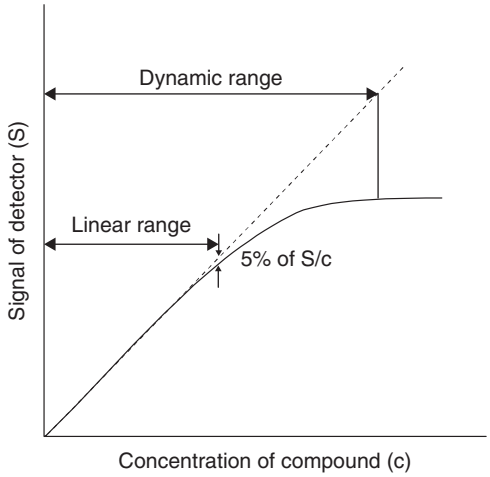

Figure 11.5 Dynamic and linear range of detectors.

Detectors

Another essential element of a high-performance liquid chromatographic instrument is the detector, which generates a record of the presence and the amount of components after elution from the column. There are several criteria for an efficient detector, such as sensitivity to a low concentration of analyte, a small detector volume to avoid additional band broadening, and a fast response to changes in sample concentration. The performance of detectors is characterized by the detector cell volume, the dynamic and linear range of the detector (Figure 11.5), a low limit of detection, limited detector noise and a constant time.

Depending on the physical and chemical characteristics of the components, suitable detectors can be chosen for use in HPLC. A sensitive universal detector, which can be used to detect almost all compounds, does not exist in liquid chromatography. However, Table 11.3 lists the most commonly used detectors in HPLC. Normally, the nature of the analytes determines the type of a detector to be applied in a study.

Nowadays, HPLC systems coupled with mass spectrometer (MS) or MS/MS are available at several laboratories. An interface is needed for vaporizing the molecules from the liquid phase in the abovementioned detectors, which are useful tools for identifying compounds by generating their spectra.

Sample preparation (Imai and Toyo'oka, 1988; Pool and Poole, 1991)

Before the separation of studied components, samples need to be prepared so they are in a suitable form for separation and detection. Sometimes, simple dilution and/or filtration is sufficient. Many methods using different physical properties can be applied to isolate compounds of interest. One of the most frequent used techniques for isolation of non-volatile components is *extraction*. Depending on the phase of sample matrix containing the compounds of interest, liquid–liquid or solid–liquid extraction can be used.

Table 11.3 Detectors used in high-performance liquid chromatography

Detectors	Detection limit
Refractive index (*RI*) *detector* – uses the ability of compounds to bend or refract light	~10–100 ng
Light-scattering (*LS*) *detector* or *evaporative light-scattering* (*ELS*) *detector* – measures the scattered light by particles in a solution or after nebulizing in a heated tube before detection cell	
Ultra violet (UV)-visible detector – uses the ability of compounds to absorb light Fixed wavelength detector – measures at one wavelength, usually 254 nm Variable wavelength detector – measures at one wavelength at a time, using broad range of wavelengths Photo diode array detector (PDA) – creates UV and/or visible spectrum in optional ranges of wavelengths simultaneously, suitable for identification of some compounds (primarily for carotenoids)	~0.1 ng
Electrochemical detector – measures compounds which undergo oxidation or reduction reactions passing through between electrodes of different electrical potential	~0.01–0.001 ng
Conductivity detector – measures the conductivity of compounds in a solution	~1–10 ng
Fluorescent detector – measures compounds, which absorb light then re-emit at given wavelengths	~0.01–0.001 ng
Mass spectrometry (*MS*) *detector* – measures ionized compounds, passing through a mass analyzer and detects the ion current; creates MS spectrum of the analyzed compounds; it is one of the most proper methods for identification of compounds Methods for ionization: electron impact (EI) – uses electron current or beam created under high electric potential Chemical ionization (CI) – uses ionized gas to remove electrons from the compounds, less aggressive method Fast atom bombardment (FAB) – uses Xenon atoms accelerated at high speed	~0.1–0.001 ng

To fractionate a sample after solvent extraction, liquid chromatography or solid-phase extraction can be utilized. In the latter technique, small cartridges filled with sorbents of small particle size are used by applying proper solvents for matrix simplification or for isolation of component(s) of interest. A large number of adsorbents can be found in the market, such as silica-based bonded-phase sorbents or macroreticular porous polymers, polyurethane foam adsorbents or ion-exchange resins. The advantages of solid-phase extraction are the opportunity for enrichment of a highly diluted analyte, and its time-saving automatization.

Derivatization of compounds is necessary in HPLC primarily to improve the response of detectors. Derivatization can be carried out before (pre-column) or after (post-column) separation.

Reagents used for UV-visible detection should contain a chromophore group with a large molar absorption coefficient. The reagents should be small and non-polar in order not to change the separation characteristics of the molecules of interest. The chromophore group in the chemical structure of the reagent molecule is primarily a derivative of a benzene ring. Reagents applied in fluorescent detection should have a significant fluorescent response. Fluorescent derivatives are primarily used in the determination of amines and amino acids, and in labeling proteins and enzymes or peptides. Some fluorescent compounds are also used for derivatization of acids and alcohols. Reagents used for electrochemical detection can be found among those

used in UV-visible and fluorescent detection. Oxidative reagents are favored over reductive ones because of difficulties in excluding oxygen from both the samples and the mobile phase.

Quantitative analysis (Macrae, 1982; Snyder and Kirkland, 1974)

One of the more essential purposes of chromatographic methods is to determine the quantity of components in a sample solution. Quantitative analysis is based on the determination of the magnitude of the detector signal for the component of interest. The signal should change linearly with the quantity of compounds, and the signal can be measured as the height or area of a chromatographic peak. Most HPLC instruments purchased in the market include integrators or computers that can perform acquisition and management.

Precision of quantitative analysis in HPLC is affected by several factors, such as the accuracy of injection, and the processes of separation and detection. Furthermore, errors may also originate from methods of sample preparation and calibration. Detectors generate signals for various compounds with different sensitivity, and therefore calibration curves should be drawn for each peak of interest separately. In this case, quantitation is based on a comparison of the peak area/height of the sample with the calibration curve of a standard of the analyte concerned. Use of internal standards is especially important for quantitation of low concentration analytes, and/or if a wide range of concentrations of compounds is expected in the sample. The errors due to sample preparation (extraction, derivatization) or injection can be decreased by applying an inner standard. To achieve valuable results using the inner standard method, completely separated peaks are needed. The primary requirement for an inner standard is that the peak be completely separated from the other peaks of interest. Secondly, the inner standard should fall in a blank area of the chromatogram of the sample, and should be as near as possible to the compounds analyzed.

The validation of an analytical method is an assurance of precise analysis. It means that a validated method is accurate, specific, reproducible and rugged over the specified range where the sample will be analyzed.

Applications

Authenticity of fruit juices

Authentication of processed fruit juices is commonly used now in Europe in order to detect adulteration, as required by the Code of Practice for Fruit and Vegetable Juices (Association of the Industry of Juice and Nectars from Fruits and Vegetables of European Union (AIJN), 2003). It represents a collection of minimum and maximum values and/or ranges specifying criteria for authenticity in multicomponent analysis.

Within Europe, the AIJN and several self-control systems form the European Quality Control System (EQCS) for the fruit-juice industry. The principal goals of

the control system are to ensure fair and free competition in the juice industry; to harmonize the work with constant interpretation of analytical results, and to improve the system for warning of falsification.

However, in spite of all the rules and current regulations, the possibility of adulteration cannot be removed from the food industry. Dilution with water, which is the simplest method of fruit-juices adulteration, has been used for many years. Owing to increasing information regarding the chemical composition of fruits, more refined methods are now used for adulteration. Supplementation with cheaper juices or with pulp wash and peel extract is a sophisticated practice (Petrus and Attaway, 1980; Petrus *et al*., 1984). One of the differences in adulteration of various juices is in the juice material used for fraud. Because of the lesser cost of apple concentrate, it may be used as an adulterant; in other situations, apple-juice products may fall prey to adulteration with a cheaper juice (Andrade *et al*., 1998).

The fight against fraud requires accurate and extensive knowledge regarding the minor and specific chemical composition of fruits or fruit juice. Therefore, one of the targets of research is to study individual minor components or groups of components specific to the variety and/or species of raw material. One of the best analytical tools for this purpose is high-performance liquid chromatography. To date, numerous compounds have been investigated for their suitability in assessing the authenticity of juices.

Organic acids (especially isocitric acid), sugar components and free amino acids have been investigated by several workers (Elkins *et al*, 1988; Wallrauch and Faethe, 1988; White and Cancalon, 1992). The potential of flavonoids and carotenoids compounds for the detection of fraud in juices has been particularly studied. Chemometric methods in the evaluation of the composition of these specific compounds can provide an effective tool for determination of authenticity of fruit products with differentiation of samples according to species, geographical origin, etc.

Detection of sugars

One method of adulteration in the juice industry is the addition of beet medium- and high-invert sugar or high-fructose corn syrup. The use of these natural substances for fraud means sophisticated methods of detection are required. Application of the stable carbon isotope ratio is now the most accepted and effective method for the detection of such adulteration with natural syrups. However, several applications of HPLC are used to identify sugar supplements in fruit juices.

The major carbohydrates present in juices are glucose, fructose and sucrose. Some fruits, such as apple, pear, quince, cherry, sour cherry, apricot and prune, contain carbohydrate alcohol, namely sorbitol. Several columns are available for HPLC analysis of reducing sugar compounds. A carbohydrate analysis column (Hong and Wrolstad, 1986) or ion-exchange column cross-linked with calcium allows complete analysis of the reducing sugars mentioned above (Mattick, 1988). Investigation of the ratio of reducing sugar does not always provide accurate results, as reducing sugar ratios can change in fruit species depending on their variety, maturity, growing condition, geographic origin, etc.

Determination of the ratio of sugar components or the proportion of sugar and sorbitol may lead to success in determining supplementation with sweeteners (Sharkasi *et al*., 1982; Pilando and Wrolstad, 1992; Thavarajah and Low, 2006). Determination of sorbitol in juice products which naturally do not contain sorbitol indicates the addition of other fruits. For example, in blackcurrant juice, the addition of 10% sour cherry juice can be detected on the basis of the sorbitol level (Hofsommer and Koswig, 2005). Measured deviations in the sorbitol/sucrose and sorbitol/total sugar ratios can be used to detect the addition of pear juice to apple juice (Sharkasi *et al*., 1982). Adulteration of blackberry juice concentrates and wines with the juice of sorbitol-containing fruits can be also detected by the determination of carbohydrate and sorbitol contents (Wrolstad *et al*., 1982).

The other approach to this problem is the investigation and determination of oligosaccharides in fruit juices by HPLC. This seems to be an effective method for indicating adulteration with undeclared sweeteners. Orange juice is an example of a juice that is rich in sucrose, and therefore orange juices are susceptible to the addition of medium-invert syrups, including sucrose. Investigation of the oligosaccharide patterns of adulterated orange juice can lead to identification of fraud (Brause, 1992).

Trace oligosaccharides, which are present in much higher concentrations in beet invert sugar than in juices, can be analyzed on anion-exchange column filled with a quaternary amine type resin, as shown by several workers (Hughes and Johnson, 1982; Rocklin and Phol, 1983; Low and Swallow, 1991; Swallow *et al*., 1991; White and Cancalon, 1992; Low and Wudrich, 1993; Wudrich *et al*., 1993; Hammond, 2001). Carbohydrates absorb weakly in UV and visible light. However, the sensitivity of the refractive index detector is normally too low to detect minor compounds such as oligosaccharides. Conversely, a pulsed amperometric detector coupled with liquid chromatography provides one of the best methods for detection of carbohydrates added to juices for the purpose of adulteration. Some HPLC methods for sugar analysis with sample preparation are summarized in Table 11.4.

As indicated in Table 11.4, the oligosaccharide profile is useful in screening citrus and pineapple juices for potential adulteration. The methods described in Table 11.4 provide a good estimation of beet-sugar addition to citrus juices. A limitation of these methods is that endogenous saccharides can interfere with those of low beet medium-invert sugar (White and Cancalon, 1992). The high sensitivity of the pulsed amperometric detector can be also used to detect the addition of enzyme-treated pulp washes to juice. The oligogalacturonide fragment produced from the degradation of pectin during enzyme treatment can be detected even when a low level of pulpwash (10%) is added to a juice (Hammond, 2001).

Detection of acids

Depending on the fruit species, the main organic acids in fruits are tartaric acid (grapes), citric acid (citrus fruits, apricot) and malic acid (apple, pear, quince, grapes, apricot). For oranges, depending on the variety, degree of maturity, climatic conditions, origin, etc., citric acid levels can vary between 7.6 and 11.5 $g\,l^{-1}$. In some cases, the maximum values of citric acid may be considerably exceeded (Elkins *et al*.,

Table 11.4 High-performance liquid chromatographic methods for separation of mono-, di- and oligosaccharides

Sugars	Sample preparation*	Condition of HPLC separation	Detection	Refs
Raffinose	Orange: no sample preparation	Column: Supelcosil LC18, isocratic elution, mobile phase: 0.2 mol l^{-1} phosphate puffer (pH 6.3)	H_2O_2 sensitive electrochemical detector, coupling with enzyme-reactor where H_2O_2 produced from raffinose by galactosidase	1
Reducing sugars	Grapefruit: no sample preparation	CarboPac PA1 (Dionex) anion-exchange column, isocratic elution, mobile phase: 0.14 mol l^{-1} NaOH, ambient temperature	Pulsed amperometric detector	2
	Apple, pear: no sample preparation	[a]Du Pont Zorbax amine column with amine guard column, isocratic elution, mobile phase: acetonitrile/water (76/24), [b]Capcell-Pak-NH2 column, isocratic elution, mobile phase: acetonitrile/water (80/20), [c]CarboPac PA1 column, isocratic elution, mobile phase: 60 mmol l^{-1} NaOH	Refractive index detector	2[a],3[b],4[c]
	Apple passing through activated C18 Sep-Pak cartridge	Aminex HPX-87C monosaccharide analysis column with Carbo-C micro-guard column, isocratic elution, mobile phase: 200 mg L^{-1} $Ca(NO_3)_2$	UV-visible detector	5
	Blackberry and plum: using cation- and anion-exchange columns after extraction with alcohol	Aminex HPX-87 cation-exchange column in Ca form, isocratic elution, mobile phase: deionized water, column temperature: 86.9°C	Refractive index detector	6
Oligosaccharides	Grapefruit[4], orange[7,8]: using cation and anion-exchange resin and additionally C18 Sep-Pak cartridge	Two CarboPac PA1 anion-exchange columns with guard[7,4], CarboPac PA1 connected in series[8], gradient elution, mobile phase: A: 100 mmol l^{-1} NaOH, B: 100 mmol l^{-1} NaOH containing 100 or 200 mmol NaOAc, C: 300 mmol l^{-1} NaOH[4,7,8], post-column reagent: 300 mmol l^{-1} NaOH, delivery system is used to minimize baseline drift[4,7], introducing a switching valve to divert simple sugars to waste[8]	Pulsed amperometric detector	4, 7, 8
	Orange: juice is mixed with Celite resin, centrifugation, supernatant is eluted through a C18 SPE cartridge, eluent is passed through cation- and anion-exchange cartridges connected in series	Two CarboPac PA1 anion-exchange columns with guard CarboPac PA1 connected in series (switching valve was incorporated between the two analytical columns), isocratic elution mobile phase: 300 mmol l^{-1} NaOH, temperature: 30°C	Pulsed amperometric detector	9
	Citrus juices: passing through On-guard H cartridge	CarboPac PA-100 column with guard column, gradient elution, mobile phase: A: 2 mmol sodium acetate in 100 mmol l^{-1} NaOH, B: 400 mmol sodium acetate in 100 mmol l^{-1} NaOH	Pulsed amperometric detector	10
Oligo-galact-uronides	Citrus juices: passing through On-guard H cartridge	CarboPac PA-100 column with guard column, gradient elution, mobile phase: A: 2 mmol sodium acetate in 100 mmol l^{-1} NaOH, B: 800 mmol sodium acetate in 100 mmol l^{-1} NaOH	Pulsed amperometric detector	10

*Each sample preparation method contains filtration before HPLC analysis.

1, Mögle *et al*., 1993; 2, Richard and Widmer, 1990; 3, Thavarajah and Low, 2006; 4, Low and Wudrich, 1993; 5, Pilando and Wrolstad, 1992; 6, Wrolstad *et al*., 1982; 7, Swallow *et al*., 1991; 8, White and Cancalon, 1992; 9, Iuliano, 1996; 10, Hammond, 2001.

1988; AIJN, 2003). D-isocitric acid can be found in small concentrations in most fruit juices, such as orange (65–200 $mg\,l^{-1}$), grapefruit (140–350 $mg\,l^{-1}$), lemon (230–500 $mg\,l^{-1}$), pineapple (80–250 $mg\,l^{-1}$), apricot (75–200 $mg\,l^{-1}$), tomato (65–150 $mg\,l^{-1}$), blackcurrant (160–150 $mg\,l^{-1}$) and peach (30–160 $mg\,l^{-1}$) (AIJN, 2003). Since D-isocitric acid is not used as an adulterant because of its high production cost, these compounds could be applied to estimate the fruit content of juice products. The ratios of citric acid and isocitric acid characterize the fruit species listed above, even though the values change with variety, origin, etc.

In apple, the principal organic acid is L-malic acid. Synthetically produced malic acid consists of the raceme D/L mixture. The much higher cost of L-malic acid compared with that of the D/L mixture discourages the use of L-malic acid as adulterant. Therefore, the measurement of D-malic acid alone is sufficient to detect the illegal addition of synthetic malic acid. A ratio of L-malic acid/total malic acid below the value of 0.9 indicates non-authentic apple juice (Elkins *et al*., 1988; AIJN, 2003). In a collaborative study by 14 laboratories using 10 apple-juice samples, the use of the ratio was recommended for testing authenticity (Elkins and Heuser, 1994). In pineapple, the citric acid/L-malic acid ratio is close to 2, and this value can therefore be used as an index of authenticity of pineapple products (Cámara *et al*., 1994).

Several types of HPLC column are available for the separation of acids. The most often used column is ion suppression reversed phase. The mobile phase used for separation is 0.2-M phosphate buffer (pH 2.2–2.4) (Coppola and Starr, 1986; Elkins and Heuser, 1994; Kiss and Sass-Kiss, 2005). The other common column types are those filled with polymer-based ion-exchange resin. The applied mobile phase for this type of columns is usually inorganic acids (H_2SO_4, H_3PO_4) of 0.005 $mol\,l^{-1}$ concentration (Cámara *et al*., 1994). For these columns, sample preparation does not involve complicated extraction procedures. Shui and Leong (2002) devised an HPLC method for the separation of acids and phenolic compounds in fruit juices in a single separation step (in apple samples), and indicated that the method could be used to evaluate the authenticity of juices.

However, for determination of isocitric acid (Eckert *et al*., 1987; Saccani *et al*., 1994; Kvasnička *et al*., 2002), several HPLC methods are described in the literature. Among them, the simple enzymatic method is preferred in analytical laboratories, since sample preparation before chromatographic analysis is highly complicated for other methods.

Detection of phenolic compounds

Phenolic constituents are secondary plant metabolites. They have an important role in the flavor and color of plants, and are significant chemical and nutritional components. The specific composition and levels of phenolic compounds can be used as an indicator of fruit-juice adulteration. They can be divided into two major groups – phenolic acids and related compounds, and flavonoids. Phenolic acids include derivatives of cinnamic acid (such as p-cumaric, caffeic, ferulic, chlorogenic, p-cumaroylquinic and neochlorogenic acid) and derivatives of benzoic acid (such as p-hydroxi benzoic, protocatechuic, vanillic and gallic acid). The "cinnamics" occur in nature in ester form

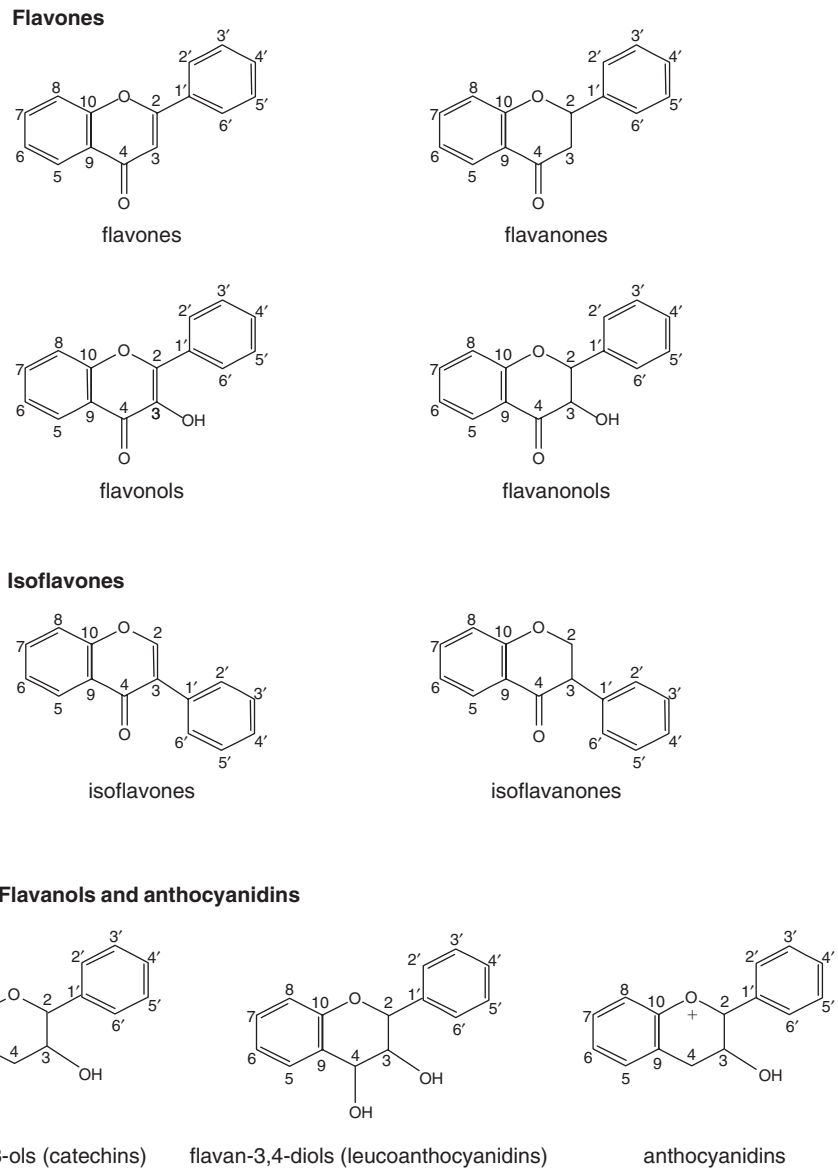

Figure 11.6 Structure of flavonoids.

with other compounds (e.g. the ester of caffeic acid with chlorogenic acid or with quinic acid), while "bensoics" usually occur in the free form (Spanos and Wrolstad, 1992). Flavonoids (Bruckner, 1964), which are mostly biological pigments, belong to the phenyl derivatives of the benzopyrane structure (Figure 11.6).

As shown in Figure 11.6, the benzopyrane structure consists of two benzene rings joined to each other by a heterocyclic six-member ring containing one oxygen atom. The main flavonoid groups differ in the heterocyclic ring. Phenolic hydroxyl groups may belong to the ring at the 3, 5, 6, 7, 3′, 4′, and 5′ positions, which may be free,

methylated or bound to sugar. Flavonoids are synthesized in plants, and their composition varies according to the plant species. Flavanones, flavonols and anthocyanidines are the flavonoid groups that occur mostly in the glycosilated form in fruits. The flavonol glycosides are found mainly in the skin of the fruits. Other flavonoid groups widely occurring in fruits are the flavan-3-ols (catechins), procyanidins (condensed tannins) formed by the polymerization of flavan-3-ols or/and flavan-3,4-diols (Ooghe *et al*., 1994a; Spanos and Wrolstad, 1992).

Plant species (even cultivars) each have a characteristic flavonoid composition, which is as specific as a fingerprint and is therefore suitable for chemotaxonomic studies. These component groups can be used in authenticity tests in spite of several compounds not yet being identified (Ooghe *et al*., 1994a; Bronner and Beecher, 1995; Hofsommer and Koswig, 2005).

Citrus fruits

Flavanone glycosides are most abundant in citrus flavonoids. Their sugar components are mono- or di-saccharides of ramnose and/or glucose (Bohm, 1975; Park *et al*., 1983; Peterson *et al*., 2006a). Polymethoxylated flavones can be found with specific distribution in citrus, mainly in the flavedo part of the fruit (Mouly *et al*., 1998). Flavanone glycosides and polymethoxylated flavones that have been identified in citrus fruits are listed in Table 11.5.

Flavanone glycosides can be determined by different analytical methods, of which HPLC is one of the most effective for their separation and quantitative determination. The original procedure was developed by Fisher and Wheaton (1976), who employed C18 reverse phase column with water and acetonitrile isocratic elution. Recently, this mobile phase has been modified with other solvents of small volumes to allow the separation of flavanone glycosides in a reasonable time. Table 11.6 summarizes some chromatographic methods with sample preparation. The detection of compounds performed with the HPLC method is almost always by UV detection at 260–283 nm.

In sweet orange, the major flavanone glycosides are hesperidin and narirutin. Hesperidin can be found in the largest quantity. Since hesperidin is insoluble, it can be found in juices in the form of a fine suspension. The flavanone glycoside patterns in orange and mandarin are similar. Grapefruit contains hesperidin, narirutin, naringin and neohesperidin; however, the amount of hesperidin and neohesperidin is very small. Naringin and neohesperidin scarcely occur or cannot be detected in orange juice (Rouseff, 1988a). Differences in the composition of flavanone glycosides between orange and grapefruit provide a tool for detection of addition of grapefruit juice to orange juice. In another collaborative study, by 15 laboratories, it was established that determination of naringin and neohesperidin in orange juice by HPLC is a reliable method for detecting the presence of grapefruit juice in orange juice (Widmer, 2000).

Since there are several cultivars that contain naringin and can legally be present in commercial orange juice, the use of naringin alone to detect the presence of grapefruit juice is clearly impossible (Rouseff *et al*., 1997; Rouseff, 1988a). However, the naringin/neohesperidin ratio can be used to differentiate orange juices that may include added grapefruit juice or other naringin-containing citrus cultivars. Addition

Table 11.5 Flavonoids of some citrus species and hybrids

(Poly)methoxylated flavones, flavones	Flavanone glycoside	Citrus fruits (Refs)
	Didymin	Clementine (7), grapefruit (2,9), lemon (9), mandarin (4), orange (2,4,7), ortanique (7), satsuma (7), sour orange (4), tangelo (4), tangor (2,4)
	Eriocitrin	Grapefruit (9), lemon (9), mandarin (4), orange (4), sour orange (4), tangelo (4), tangor (4)
	Hesperidin	Clementine (7), grapefruit (3,2,9), lemon (6,9), mandarin (3,4,6), orange (3,2,4,6,7), ortanique (7), pummelo (6), satsuma (7), tangelo (3,4), tangor (3,2,4)
	Naringin	Grapefruit (1,3,2,9), lemon (6,9), mandarin (6), orange (3,4,6), pummelo (6), sour orange (3,4), tangelo (3,4)
	Narirutin	Clementine (7), grapefruit (1,3,2,9), lemon (9), mandarin (4), orange (3,2,4,7), ortanique (7), pummelo (3), satsuma (7), sour orange (4), tangelo (3,4), tangor (3,2,4)
	Neoeriocitrin	Grapefruit (9), orange (4), sour oranges (4), tangelo (4)
	Neohesperidin	Grapefruit (2), lemon (6), mandarin (6), pummelo (6), orange (6), sour orange (4), tangelo (4)
	Poncirin	Grapefruit (2,9)
Apigenin*-7-O glucoside		Orange (8)
Diosmetin-7-O rutinoside (diosmin)		Lemon (6), mandarin (6), orange (6), ortanique (6), pummelo (6)
Heptamethoxyflavone		Clementine (7), orange (5,7), ortanique (7), satsuma (7), tangelo (5)
Hexamethoxyflavone		Orange (2), tangor (2)
Hexamethyl-O-gossypetin		Clementine (7), orange (7), ortanique (7), satsuma (7)
Hexamethyl-O-quercetagetin		Clementine (7), orange (7), ortanique (7), satsuma (7)
Isosinensetin		Clementine (7), orange (7), ortanique (7), satsuma (7)
Luteolin*		Lemon (6), mandarin (6), orange (6), ortanique (6)
Luteolin*-7-O-glucoside		Orange (8)
Nobiletin		Clementine (7), orange (2,5,7), ortanique (7), tangelo (5), tangor (2)
Scutellarein* and heptamethoxyflavone		Orange (2), tangor (2)
Sinensetin		Clementine (7), lemon (6), orange (2,5,6,7), ortanique (7,6), pummelo (6), tangelo (5), tangor (2)
Tangeretin		Clementine (7), orange (2,5,7), ortanique (7), tangor (2), tangelo (5)
Tetramethyl-O-isoscutellearin		Clementine (7), ortanique (7)
Tetramethyl-O-scutellarein		Clementine (7), orange (5,7), ortanique (7), tangelo (epi-), mesocarp (5)

*Non-methoxylated flavone.
Clementine, mandarin (*Citrus reticulata*), grapefruit (*Citrus paradisi*), orange (*Citrus sinensis*), ortanique (*Citrus reticulata* × *Citrus sinensis*), pummelo (*Citrus maxima* or *Citrus grandis*), satsuma (*Citrus unsihu*), sour orange (*Citrus aurantium*), tangelo (*Citrus paradisi* × *Citrus reticulata or Citrus paradisi* × *Citrus grandis*), tangor (*Citrus reticulata* × *citrus sinensi*).
1, Fisher and Wheaton, 1976; 2, Mouly *et al*., 1998; 3, Rouseff *et al*., 1987; 4, Peterson *et al*., 2006a; 5, Pan *et al*., 2002; 6, Wang *et al*., 2007; 7, Sentandreu *et al*., 2007; 8, de Simóne *et al*., 1992; 9, Peterson *et al*., 2006b.

of citrus aurantium and/or *C. bergamia* to orange (*C. sinensis*) may be detected by the presence of naringin and lack of presence of some other specific flavonoids. Addition of tangerin (mandarin) or a hybrid of orange and tangerin may be established by a strongly decreased hesperidin/narirutin ratio (Ooghe *et al*., 1994a).

The composition of polymethoxilated flavones in citrus juices differs greatly. The specific variation of the polymethoxilated flavone pattern provides another tool for differentiation of citrus juices (Mouly *et al*., 1998). Ooghe *et al*. (1994b) established

Table 11.6 HPLC separation of flavanone glycosides and polymethoxylated flavones

Compounds	Sample preparation	HPLC separation	Refs
PMFs	Extraction of juice three times with benzene, centrifugation, separation of benzene layer, drying under N_2 at 40°C, dissolving	Column: Novapak RP C18, gradient elution, mobile phase: A: water/tetrahydrofuran (84/16), B: water/acetonitrile/tetrahydrofuran (42/42/16), A/B from 100/0 to 0/100, temperature: 35°C, PDA detector: 340 nm	1, 2, 3, 4
FMFs and FGs	Extraction of juice with benzene, elution of FGs and FMFs with water/acetonitrile (4/6) on a C-18 Sep-Pack cartridge activated + inner standards	Column: Luna II C18, gradient elution, mobile phase: A: water/tetrahydrofuran (98.75/1.25), pH:3,5 with H_3PO_4, B: acetonitrile/tetrahydrofuran (98.75/1.25), A/B from 100/0 to 30/70, ambient temperature, PDA detector: 280 nm (FGs), 330 nm (FMFs)	5
PMFs and FGs	Dilution of juice samples with dimethyl formamide, placing in water bath at 90°C, centrifugation	Column: Alltima C18 with pre-column of the same resin, gradient elution, mobile phase: A: acetonitrile, B: water/acetic acid (96/4), A/B from 0/100 to 70/30, PDA detector: 280 nm (FGs), 330 nm (PMFs)	6
Flavanone glycosides		Column: LiChrospher^R 100RP 18, gradient elution, mobile phase: A: 0.5% acetic acid in water, B: 0.5% acetic acid in aqueous-acetonitrile (50/50), A/B from 95/5 to 0/100, ambient temperature, PDA detector: 280 nm, 330 nm	7
		Column: Nucleosil C18, isocratic elution, mobile phase: water/acetonitrile/tetrahydrofuran/acetic acid (80/16/3/1), PDA detector: 280 nm	8
Flavanone glycosides	No sample preparation filtration	Column: µBondapack C18, isocratic elution, mobile phase: water/acetonitrile (80/20), PDA detector: 280 nm	9
	Centrifugation	Column: Supelco C18 with Speroi-5 C-18 pre-column, isocratic elution, mobile phase: water/acetonitrile/glacial acetic acid (79.5/20/0.5), PDA detector: 280 nm	10
	Sample + inner standard (rhoifolin) centrifugation, extraction of solids with methanol two times, centrifugation, collection of supernatants, dilution	Column: Alltima C18, isocratic elution, mobile phase: water/acetonitrile/2-propanol/formic acid 158/23/19/0.2, PDA detector: 283 nm, 335 nm	11
	Sample + inner standard (rhoifolin) + methanol, warming at 55°C in water bath, centrifugation, extraction of solids with methanol in water bath, centrifugation, combination of supernatants, dilution, filtration		
	Freeze-dried sample + 62.5% methanol containing BHA (tert-butyl-4-hydroxy anisole), sedimentation, dilution with water	Column: Purospher RP C18, gradient elution, mobile phase: A: water with 1% formic acid, B: 100% acetonitrile, A/B from 95/5 to 40/60, detectors: PDA at UV maxima of compounds, mass spectrometer	12
	Putting fruit juices in boiling water bath, centrifugation	Column: Novapak RP C18, gradient elution, mobile phase: A: 80 ml 0.25 mol l^{-1} K_2HPO_4, +400 µl 85% H_3PO_4 diluted to 2 l with water; B: 40 ml 0.25 mol l^{-1} K_2HPO_4, +200 µl 85% H_3PO_4, +507.65 g acetonitrile diluted to 1 l in water, A/B from 100/0 to 0/100, PDA detector: 280 nm	4, 13, 14, 15
	Taking juice onto Sep-Pak C-18 cartridge, washing the cartridge with 10% methanol, elution of flavanone glycosides with methanol	Column: Zorbax ODS C18, isocratic elution, mobile phase: water/acetonitrile/glacial acetic acid (79.5/20/0.5), detector: fixed wavelength UV-visible, 280 nm	16

FMFs, fully methoxylated flavones; PMFs, polymethoxylated flavones; FGs, flavanone glycosides; PDA, photodiode array.
1, Ooghe *et al.*, 1994b; 2, Sendra *et al.*, 1988; 3, Rouseff and Ting, 1979; 4, Ooghe and Detavernier, 1997; 5, Sentandreu *et al.*, 2007; 6, Mouly *et al.*, 1998; 7, Wang *et al.*, 2007; 8, Pupin *et al.*, 1998; 9, Fisher and Wheaton, 1976; 10, Rouseff, 1988b; 11, Bronner and Beecher, 1995; 12, Justesen *et al.*, 1998; 13, Schnüll, 1990; 14, Wade, 1992; 15, Ooghe *et al.*, 1994a; 16, Rouseff *et al.*, 1987.

in their study that determinations of flavanone glycosides and polymethoxylated flavones are complementary techniques. Using these two groups of compounds together with various patterns gives a good chance of detecting adulteration of orange juices.

Other fruits

Besides citrus fruits, other fruits being studied include apple, pear, quince, plum, apricot, peach and berries. Table 11.7 lists the phenolic compounds in these fruits. These phenolic compounds are also specific "fingerprints" to detect the adulteration of juices of these fruits (McRae *et al*., 1990; Spanos and Wrolstad, 1990a, 1992; Tomás-Lorente *et al*., 1992; Tanriöven and Ekşi, 2005).

There are one or two key compounds among phenolics which are specific to just one type of fruit. Phloridzin (phloretin 2′-glucoside), for example, occurs only in apple, while isorhamnetin glycoside and arbutin (hydroquinone-glucoside) are specific to pear. Determination of these compounds is a useful tool to detect adulteration. Many HPLC methods can be used for the separation and determination of phenolic compounds, as reported in the literature. Some of them are summarized in Table 11.8.

The most common use of the methods listed in Table 11.8 is to study the chemical composition of apple, because of its popularity and low price, and because apple purée or juice is the most favored natural adulterant of other fruit juices. Using colometric electrode array detectors, Sontag and Bernwieser (1994) concluded that the phenolic compositions of apple and pear are very simple but different, and therefore it is possible to detect adulteration of pear nectar with apple juice down to a level of 1%. Dragovic-Uzelac *et al*. (2005) proved in their study that the addition of apple purée to apricot purée during the processing of commercial apricot nectars and jams could be easily detected by the presence of phloretin 2′-glucoside and phloretin 2′-xylosilglucoside. Phloretin 2′-xylosilglucoside in particular could be used as a marker in detecting the adulteration of apricot nectars containing $\geqslant$10% apple purée. In apricot jams, it could detect a minimum of 20% apple purée.

In certain situations apple juice may be adulterated with pear juice. Since arbutin and isorhamnetin glycosides are characteristic of pear juice, they may be used as an indicator of the adulteration of apple juice with pear juice (Spanos and Wrolstad, 1990a). Silva *et al*. (2000) have studied several samples of processed quince jams that also contained arbutin, and suggested that these jam samples had been adulterated with pear purée.

Detection of anthocyanins

Anthocyanins are the flavonoid-type pigments responsible for the red to dark-blue color of fruits, flowers and vegetables. They are glycoside(s) of anthocyanidins. Anthocyanins are present in high content in berries such as strawberry, raspberry, blackberry, red- and blackcurrant. Figure 11.7 shows the structure of anthocyanidins, with the most frequent combination of side groups and their names.

There is a special interest in natural anthocyanins in the food industry because they may potentially be used as alternatives to synthetic colorants. There are some analytical methods available in the literature based on the structure (Goiffon *et al*., 1999)

Table 11.7 Phenolic compounds of fruits and/or fruit products

	Fruit species	Apple								Pear						Quince		White grape		Apricot			Peach		Pineapple	Orange		Strawberry		Raspberry	
	References	1	2	3	4	5	10	6	12	1	2	5	8	6	12	1	9	6	5	5	4	4	5	12	5	5	12	11	12	11	12
Phenolic acids and derivatives, aldehydes	caffeic acid		+		+	+		+	+		+	+	+	+	+			+	+	+	+		+	+	+		+		+		+
	chlorogenic acid isomers						+																								
	4-O-caffeoylquinic acid															+	+														
	5-O-caffeoylquinic acid	+								+							+														
	caffeoyl ester																		+	+	+		+								
	caftaric acid																	+													
	cinnamic acid																												+		+
	chlorogenic acid		+	+	+	+	+	+		+	+	+	+	+		+	+			+	+		+			+					
	p-coumaric acid	+			+	+		+	+			+	+	+	+			+	+	+	+		+	+	+	+	+		+		+
	coumaroyl ester (of tartaric acid)																		+												
	coumaroylquinic acid					+		+				+		+											+						
	coutaric acid																	+													
	3,4-dihydroxybenzoic aldehyde					+						+							+	+			+		t						
	ellagic acid																											+		+	
	ellagic acid derivative																											+		+	
	ferulic acid					t		+	+			t		+	+			+	+	+	+		+	+	+	+	+		+		+
	feruloyl ester (of tartaric acid)																		+												
	feruloylglucose					+						+													+	+					
	gallic acid								+									+	+										+		+
	2-S-glutathionylcaftaric acid																	+													
	p-hydroxybenzoic acid					+				+	b								+	+	+	+	+	+	+		+		+		
	p-hydroxybenzoic aldehyde					+					d												+		+	t					
	sinapic acid								n						+									+	+	+	+		+		+
	syringic aldehyde					t						+								+	+		+		+	+					
	vanillic acid														+									+			+				
	vanillic aldehyde					t			n			+								+	+		+		t	t					

(*Continued*)

Table 11.7 (Continued)

	Fruit species	Apple								Pear						Quince		White grape		Apricot			Peach		Pineapple	Orange		Strawberry		Raspberry	
	References	1	2	3	4	5	10	6	12	1	2	5	8	6	12	1	9	6	5	5	4	4	5	12	5	5	12	11	12	11	12
Coumarins	aesculetin					+														+	+		*t*								
	scopoletin																			+	+					t					
Catechins/procyanidins	(+)-catechin		+		+	+		+		+	+			+				+	+				+								
	catechin-catechin-gallate isomers																	+													
	catechin-gallate																	+													
	(−)-epicatechin		+	+	+	+		+		+	+	+	+	+				+	+		+		+								
	(−)-epigallocatechin			+																											
	(−)-epigallocatechin gallate			+																											
	procyanidin B1		+															+													
	procianidin B2		+		+			+										+													
	procyanidin B3																	+													
	procianidin B4																	+													
Dihydrochalcones	phloretin 2′-glucoside (*phloridzin*)	+	+		+	+	+	+																							
	phloretin 2′-xylosilgalactoside							+																							
	phloretin 2′-xylosilglucoside	+	+		+			+																							
Hydroquinones	hydroquinone-glucoside (*arbutin*)										+			+																	
Flavonol glycosides	2,3-dihydroquercetin-rhamnoside																	+													
	2,3-dihydrokaempferol-rhamnoside																	+													
	isorhamnetin-glucoside													+																	
	isorhamnetin-glycoside										+	+		+																	

Flavonol glycosides	kaempferol 3-O-rutinoside																	+													
	kaempferol 3-O-glucosid												+						+												
	kaempferol glycoside															+				+											
	myricetin 3-O-rhamnoside																	+													
	quercetin 3-O-galactoside				+	+	+		+		+			+	+			+				+									
	quercetin 3-O-glucoside				+	+	+				+		+					+	+	+		+					+		+		
	quercetin 3-O-glucuronide																										+		+		
	quercetin 3-O-rhamnoside	+			+	+	+		+					+	+			+													
	quercetin 3-O-xyloside	+				+								+	+																
	quercetin 3-O-arabinoside				+	+	+															+									
	quercetin glycoside		+							+						+															
	quercetin 3-O-rutinoside (rutin)		+	+	+	+	+			+	+			+	+			+	+	+		+		+							
Flavonols	kaempferol				+								+					+				+									
	myricetin																					+									
	quercetin				+						+		+					+	+	+		+									

t, trace; bd, hydroxyl benzoic acid derivative; n, not detected in all varieties.

1, Andrade *et al*., 1998; 2, Escarpa and González, 1999; 3, Shui and Leong, 2002; 4, Dragovic-Uzelac *et al*., 2005; 5, de Simóne *et al*., 1992; 6, McRae *et al*., 1990; 7, Thavarajah and Low, 2006; 8, Tanriöven and Ekşi, 2005; 9, Silva *et al*., 2000; 10, Spanos and Wrolstad, 1992; 11, Versari *et al*., 1997; 12, Mattila *et al*., 2006.

Table 11.8 HPLC separation of phenolic compounds of fruit samples

Fruits	Sample preparation	HPLC separation	Detection	Refs
Apple[a], quince[a], pear[a], plum[b], peach[b], sour orange[b], apricot[b] strawberry[b]	Evaporation to dryness of butanol extract of samples, dilution with acidic water (pH 2, HCl), filtration, passing through Amberlie XAD-2, after washing column with water (pH 2 with HCl) eluting phenolic fraction with methanol, evaporation, re-dissolving	Column: Spherisorb ODS2, gradient elution, mobile phase: A: water/formic acid (19/1), B: methanol, A/B from 95/5 to 20/80 *column: Lichrochart 100 RP-18, gradient elution, mobile phase A: water/formic acid (95/5), B: methanol, A/B (95/5) from A/B 95/5 to 20/80	PDA detector 280, 350 nm	1[a], 2[a], 3[b]*
Apple, pear	Isolation of flavonoids: extraction of samples with methanol (containing 1% BHT) in dark, hydrolysis of glycosides: extraction of samples with ethyl acetate, hydrolysis with 2 mol l^{-1} HCl, clean-up with Sep-Pak C18, isolation of procyanidins: elution of diluted samples on Sephadex LH-20 with 20% methanol	Column: Nucleosil 120, C18, gradient elution, mobile phase: A: 0.01 mol l^{-1} phosphoric acid, B: methanol or acetonitrile, A/B from 95/5 to 0/100 or from 98/2 to 65/35	PDA detector, 280 nm	4
Apple[a], pear[b], quince[c]	Centrifugation of juice + inner standard (ethyl syringate)*, or extraction of juice with methanol**, elution of phenolic compounds through polyamide column with methanol, evaporation, re-dissolving	*Column: Lichrospher 100 C18, isocratic elution, mobile phase: methanol/glacial acetic acid/water (35/2/63) column temperature: 32°C, **column: Hypersil ODS, C18, isocratic or gradient elution, mobile phase: A: 1% acetic acid, B: acetonitrile, A/B (81/19) or A/B from 85/15 to 75/25	*Colorimetric electrode array detector, **PDA detector, 284 nm	6[a*], 5[b**], 8[c**]
Apple, pear, orange, peach, apricot, grape, pineapple	Concentration of juice, extraction with diethyl ether, then with ethyl acetate, evaporation after pooling the fractions	Column: Nova-Pak C18, gradient elution for low molecular weight phenolics, and flavan-3-ols, mobile phase: A: 2% acetic acid, B: methanol/ acetic acid/water (30/2/68), A/B from 100/0 to 15/85, isocratic elution for flavonol glycosides, mobile phase: A: 2.5% acetic acid, B: tetrahydrofuran/water/acetic acid (50/47.5/2.5), A/B (65/35), isocratic elution for flavonol aglycons, mobile phase: water/methanol/ acetic acid (57.5/37. 5/5)	PDA detector, 280 nm, 340 nm 254 nm, 365 nm	7
Pear[a], grape[b]	[a]Pear: isolation of *phenolics* using C18 Sep-Pak, evaporation, re-dissolving, [b]grape: filtration for phenolic acids and flavonol glycosides, isolation of procyanidins using Sephadex LH-20, evaporation, re-dissolving	Column: Supelcosil LC-18 with ODS guard column, gradient elution, mobile phase: A: 0.07 mol l^{-1} KH_2PO_4 (pH: 2.5 with phosphoric acid), B: methanol, A/B from 98/2 to 60/40	PDA detector, 280 nm, 320 nm	9[a] 10[b]

BHT, 2,6-di-tert-butyl-4-methylphenol.
1, Andrade *et al*., 1998; 2, Silva *et al*., 2000; 3, Tomás-Lorente *et al*., 1992; 4, Escarpa and González, 1999; 5, Hollborn *et al*., 1990; 6, Sontag and Bernwieser, 1994; 7, de Simóne *et al*., 1992; 8, Wald and Galensa, 1989; 9, Spanos and Wrolstad, 1990b; 10, Spanos and Wrolstad, 1990a.

and concentration of anthocyanins in fruits (Gonçalves *et al*., 2004; Pantelidis *et al*., 2007; Versari *et al*., 1997), but information on such methods is incomplete, partly due to limitations in analytical methods.

Wu and Prior (2005) carried out a systematic study to identify and characterize anthocyanins in various berries (blueberry, cranberry, strawberry, blackberry and raspberry), plum, peach, sweet cherry, apple and nectarine. The Code of Practice (AIJN, 2003) defines protocols for HPLC determination of anthocyanin patterns using callistephine as the inner standard. The composition of these acid-like compounds gives a specific fingerprint on HPLC chromatograms, in the same way as the phenolic compounds discussed above. As processing and storage conditions affect the composition of anthocyanins, they can be used as markers to determine the authenticity of fruit products (Versari *et al*., 1997).

Detection of carotenoids

The other group of pigments distributed widely among living organisms are carotenoids. Carotenoids are synthesized only in plants, and it is thought that animals are not capable of synthesizing carotenoids (Brush, 1981; Simpson *et al*., 1981), apart from some bacterial species (Mallorqui *et al*., 2005; Hohmann-Marriott and Blankenship, 2007). The color of citrus fruits is mostly due to carotenoids, which are yellow to red. Carotenoids may be destroyed during processing, and therefore colorant may be added to juice products to improve their final color or to mask deficiencies (Nagy, 1997). The most common adulterants are β-carotene and β-apo-8′-carotenal, lycopene, or natural carotenoid extracts such as marigold flower (Gregory *et al*., 1986), paprika (Minguez-Mosquera and Hornero-Méndez, 1993; Gnayfeed *et al*., 2001; Daood *et al*., 2006), citrus-peel extract or mandarin and tangerine juice (Philip *et al*., 1989). Addition of mandarin and tangerin extracts is allowed at levels up to 10% in orange juice in some countries, but is forbidden in Europe. Paprika extracts are used for coloring orange juice drinks in Europe (Mouly *et al*., 1999a).

Many researchers have studied citrus carotenoid profiles using HPLC. Table 11.9 summarizes the conditions of sample preparation and HPLC separation in these studies. Of all the carotenoids present in orange juice, β-cryptoxanthin has the highest concentrations (Fisher and Rouseff, 1986; Gregory *et al*., 1986; Rouseff *et al*., 1996). The major carotenoids in orange juice containing OH groups can form fatty acid esters such as lauric, myristic and palmitic acids. The concentration of individual carotenoids depends significantly on the fruit's variety (Pupin *et al*., 1999) and geographical origin (Mouly *et al*., 1999a, 1999b).

In a study conducted by Philip *et al*. (1989), it was established that the calculated ratio of cryptoxantin esters to lutein diesters could be used to detect addition of tangerine juices to orange juices at levels above 25%. Using this method, the addition of synthetic carotenoids, β-carotene and β-apo-8′-carotenal could be detected at levels above $5\,mg\,kg^{-1}$ in orange juice concentrate. In addition, Pan *et al*. (2002) could detect addition of $100\,g\,kg^{-1}$ tangelo to orange juice on the basis of the ratio of polymethoxylated flavones to carotenoids, using canonical discrimination analysis.

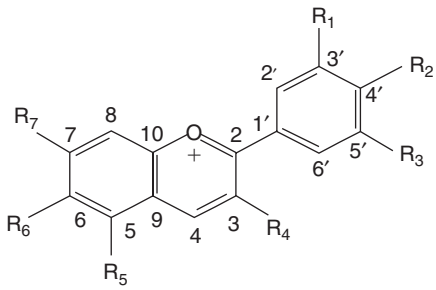

Anthocyanidins	R_1	R_2	R_3	R_4	R_5	R_6	R_7
Cyanidin	—OH	—OH	—H	—OH	—OH	—H	—OH
Delphinidin	—OH	—OH	—OH	—OH	—OH	—H	—OH
Pelargonidin	—H	—OH	—H	—OH	—OH	—H	—OH
Malvidin	$—OCH_3$	—OH	$—OCH_3$	—OH	—OH	—H	—OH
Peonidin	$—OCH_3$	—OH	—H	—OH	—OH	—H	—OH
Petunidin	—OH	—OH	$—OCH_3$	—OH	—OH	—H	—OH

Figure 11.7 Structure of anthocyanidins.

Table 11.9 HPLC separation of carotenoids of citrus fruit juices

Sample preparation	HPLC separation	Refs
Homogenization of samples with methanol, filtration, extraction of residue with acetone, addition of 10% methanolic HCl to combined filtrate, extraction with petroleum ether, evaporation, dissolving of residue in acetone	Column: Waters Resolve C18 with guard column of the same resin, gradient elution, mobile phase: A: methanol, B: ethyl acetate, A/B from 100/0 to (0/100), detection: variable-wavelength UV detector, 465 nm	1
Precipitation of juice with aqueous solution of $ZnSO_4H_2O + K_4[Fe(CN_6)]3H_2O$, centrifugation, extraction of precipitate with acetone, extraction of supernatant with light petroleum, evaporation of petroleum, hydrolysis of residue with 10% methanolic KOH, extraction of carotenoids with diethyl ether, evaporation, dissolving of residue	Column: YMC C30 not end capped, gradient elution, mobile phase: A: methyl tert-butyl ether, B: methanol, C: water, A/B/C from 5/90/5 to 50/50/0, detection: PDA detector, 290, 350, 430, 486 nm	2, 3
Extraction of juice with ethyl acetate containing BHT, evaporation, dissolving	Column: Vydac 201TP54 C18 with guard column Alltima C18, isocratic elution, mobile phase: acetonitrile/methanol/1,2-dichloromethane (30/35/5) with 0,1% BHT, 0,1% triethyl amine, and 0,05 mol ammonium acetate, detection: spectra focus scanning detector, 450 nm	4
Centrifugation of juice, two times extraction of residue with methanol, hydrolysis with 10% methanolic KOH, extraction of carotenoids with ethylene chloride, evaporation, dissolving, sample clean-up on C18 column with methanol/water 95/5 followed methylene chloride	Column: Du Pont Zorbax ODS, gradient elution,mobile phase: acetonitrile, methylene chloride, tetrahydrofuran, and ethyl acetate, detection: PDA detector, 465 nm	5

BHT, 2,6-di-tert-butyl-4-methylphenol; PDA, photodiode array.
1, Philip *et al.*, 1989; 2, Rouseff *et al.*, 1996; 3, Mouly *et al.*, 1999b; 4, Pupin *et al.*, 1999; 5, Fisher and Rouseff, 1986.

Authenticity of wines

Wine is defined as a drink made from the fermented juice of fruit or plants and containing 10–15% alcohol by volume. If a drink is not produced in this way, it is not wine. The authenticity of wines represents conformity with established regulations and standards; wines are also considered to be adulterated if the label on the bottle is not accurate. Wines illegally brought to the market may be adulterated (Tattay, 2001), and such adulteration may occur both before or after fermentation. Adulterated wines may include unauthorized additives, or have been produced by unauthorized processes. The methods of adulteration are often similar to those used in fruit juices, such as dilution with water, or the addition of sugar, acids, and forbidden colorants (Midkiff and Buscemi, 1988; Botos, 1999). The wine is also adulterated if the level of authorized substances exceeds specified limits.

The losses and changes in characteristic compounds during the wine-making process (fermentation, filtration, clarification) and during ageing affect the species-specific chemical composition so that it becomes simpler than and/or different from that in juices (Somers, 1971; Midkiff and Buscemi, 1988; Liao *et al*., 1992). An important characteristic of wines is the geographic origin, which greatly affects flavor, aroma and the full-bodied taste. For this reason, the geographic origin is considered to be an important factor in the market. Protection of origin is attributed only to a high-quality product, and details its geographical region and/or subjective factors. Protection of the quality and the origin of wines are closely related.

Several HPLC methods described for the detection of sugars and sorbitol in fruits (Table 11.4) can be adapted to wine analysis. For example, HPLC is a suitable tool for determination of artificial colorants in wines (Virtanen and Lehtonen, 1999). Several compounds have been studied as key compounds in differentiating quality and/or variety. Ellagic acid can be regarded as a characteristic compound of barrique wine ageing, and could become a marker of maturity. Fural aldehydes, absent in natural wine, can be considered typical components of barrique wine (Matějíček *et al*., 2005). Shikimic acid can be useful for differentiation of red wine varieties (Etiévant *et al*., 1989; Holbach *et al*., 2001; Mardones *et al*., 2005).

In recent years, coupled with computer-based pattern recognition analysis (principal component analysis, discriminant analysis), the chromatographic separation techniques have become effective tools in authenticity testing. Several workers have studied polyphenolic compounds such as phenolic acids and derivatives, and flavonoids, anthocyanins (Kallithraka *et al*., 2001; deVilliers *et al*., 2004; Gambelli and Santaroni, 2004; Makris *et al*., 2006), amino acids (Vasconcelos and das Neves, 1989; Soufleros *et al*., 2003) and acids (Mardones *et al*., 2005) using HPLC methods to study their suitability for authenticity testing. It is thought that these compound classes can be used for the classification and differentiation of wines according to grape variety and/or geographic origin, by means of statistical methods.

One category of wines is sweet or dessert wines, which are highly priced, smooth- and full-bodied with a pleasant bouquet. These wines are produced from grapes infected by *Botrytis cinerea* (noble rot). In suitable weather conditions, the infected grapes take on a raisin-like form, known in Hungary as aszú grapes. Aszú grapes contain

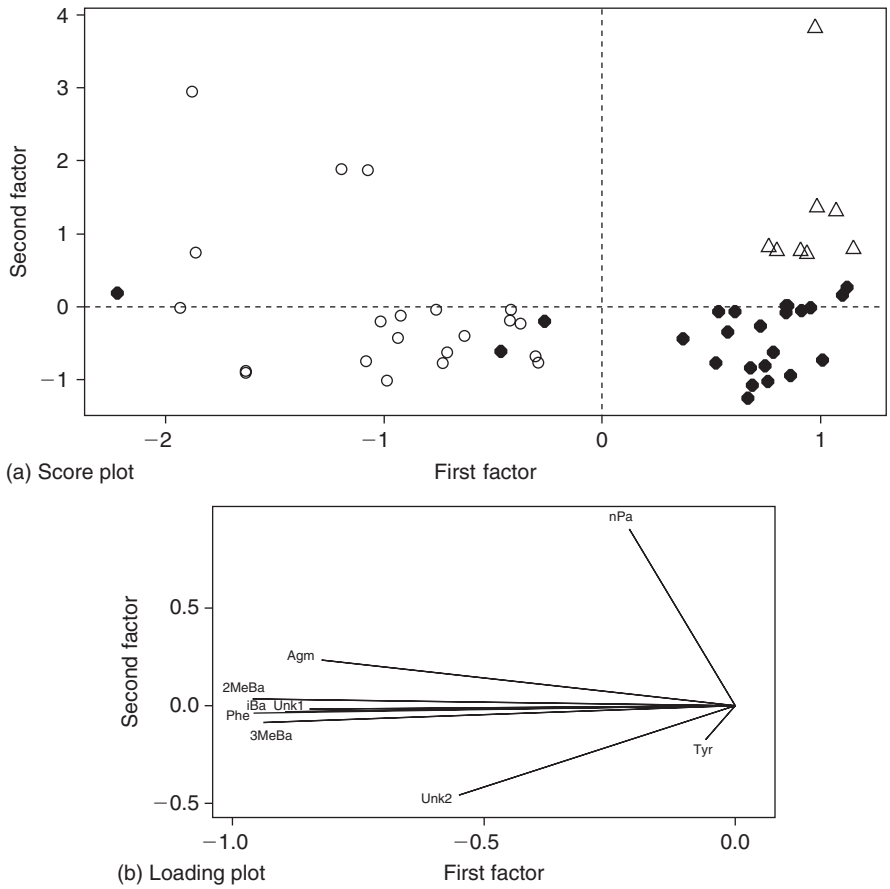

Figure 11.8 Score plot and loading plot of variables (biogenic amines) of normal and botrytized wine specialities originating from Hungary (Tokaji Aszú) and abroad. ○, Tokaji Aszú and Tokaji Aszú essence; ●, foreign botrytized wines; Δ, Hungarian non-botrytized (white) wines; variance, 71%. Variables: i-butyl amine (iBa), unknown1 (Unk1), tyramine (Tyr), unknown2 (Unk2), 2-methylbutylamine (2MeBa), agmatine (Agm), unknown3 (Unk3), 3-methylbutylamine (3MeBa), n-pentylamine (nPa), phenylethylamine (Phe).

biogenic amines, which appear in particular during infection with *Botrytis cinerea*. The composition of biogenic amines consists primarily of primer aliphatic amines specific for botrytized wines (Sass-Kiss *et al*., 2000; Sass-Kiss and Hajós, 2005; Kiss *et al*., 2006). Using multivariate factor analysis (FA) and linear discriminant analysis (Figure 11.8), Tokaji aszú wines could be classified and differentiated from normal wines and botrytized wines of other geographic origin (Kiss and Sass-Kiss, 2005). The specificity of amine composition, which depends on infection with *Botrytis cinerea* and the wine-making technology, provides the basis for discrimination.

A simple and alternative graphical method for differentiation is shown in Figure 11.9, which gives similar results for the differentiation of Tokaji wines from others. Plotting the logarithm of the concentration of amines of Tokaji aszú wines in a web diagram (Kiss and Sass-Kiss, 2005; Sass-Kiss *et al*., 2005), their shapes should be

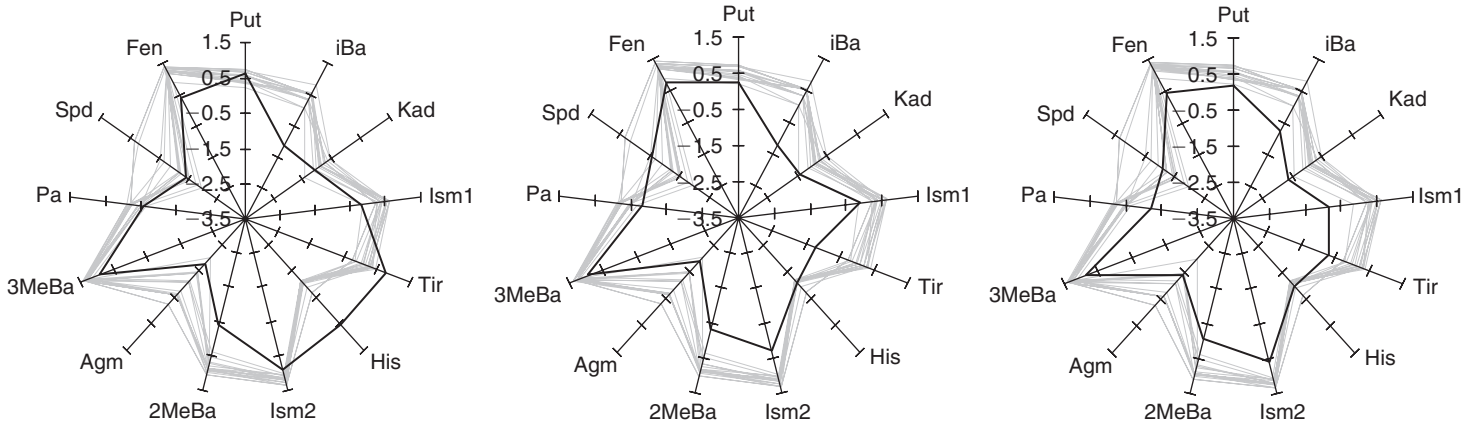

(a) Tokaji aszú wines and foreign botrytized wines

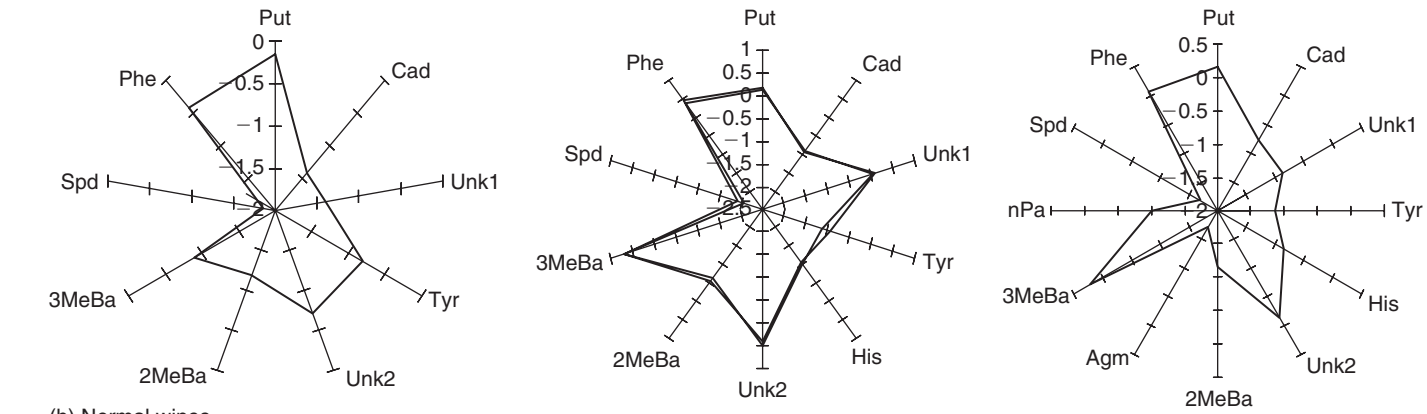

(b) Normal wines

Figure 11.9 Spider-web diagram of logarithm of amine concentration of normal and aszú wines.

similar to each other; the shapes of the diagrams for wines of other origin and normal wines are different.

Authenticity of honey

Honey is a naturally sweet material that is collected from the nectar of living plant organs by *Apis mellifera* bee species or insects. The sweet substance is delivered to the workers in the hive, which alter it enzymatically, before storing, ripening and dehydrating it. The European Directive relating to honey (Council Directive 2001/110/EC) lays down rules regarding the composition and manufacture of honey. For specific quality criteria, the botanical origin, or regional, territorial and topographical origin of honey products should be indicated. In honey, one group of compounds derives from plants and the others from bees. Some of these compounds appear or change during the maturation of honey.

As with other food products, honey is prone to adulteration. A common type of fraud is dilution of honey with water or by the addition of syrups (for example, high-fructose corn syrup, (HFCS)). One sophisticated form of manipulation is based on feeding bees with sugars and syrups. Another method is mislabeling regarding the floral and geographical origin of the honey (Anklam, 1998). The major carbohydrates in honey are glucose (26.3–39.8%) and fructose (35.9–42.1%). Saccharose (sucrose) is present at 1.7–2.9% in honey (Souci *et al*., 2000), and the average ratio of fructose to glucose is 1.2/1. Besides these two main monosaccharides, honey also contains a relatively high number of carbohydrates, such as di-, tri- and tetra-saccharides (Anklam, 1998).

As in other foods, the sugar compounds in honey can be determined by various methods. One of the more effective techniques is HPLC. Anion-exchange liquid chromatography coupled with pulsed amperometric detection (PAD) is the best way to ascertain honey authenticity, in a similar way to the methods discussed above regarding fruits. Analysis of the fingerprint of oligosaccharides is extremely good for detecting the addition of invert syrups or HFCS to honeys, at levels as low as 5–10% (Lipp *et al*., 1988; Swallow and Low, 1990; Swallow and Low, 1994; Cordella *et al*., 2003; Cotte *et al*., 2003). Goodall *et al*. (1995) studied the oligosaccharide profiles of 91 British authentic honey samples, using canonical discriminant analysis. They established that oligosaccharide profiles may have a potential role in identifying the floral origin of honey; however, they stated that this procedure alone would not allow definite determination of all floral types.

Phenolics make up a class of compounds, similar to those in fruits, that give information about the floral and geographic origin of honey owing to its floral-specific composition. High numbers of phenolic compounds have been identified in honey, as in fruits. The sample preparation and HPLC separation for phenolic compounds of honey and for fruit are similar, and in certain cases the same as those used in juices (Ferreres *et al*., 1991; Yao *et al*., 2003, 2005; Kenjerić *et al*., 2007). Phenolic compounds again provide a fingerprint for the botanical (Gil *et al*., 1995) or geographical (Anklam, 1998; Tomás-Barberán *et al*., 1993) origin of honeys, and some marker compounds have been found among flavonoids, such as hesperetin in citrus honey

(Ferreres *et al*., 1993, 1994a), tricetin, myiricetin and two derivatives in heather honey (Ferreres *et al*., 1994b), and pinobankin, pinocembrin and chrisin in eucalyptus honey (Martos *et al*., 2000). By studying phenolic acids from several different monofloral honey types, Dimitrova *et al*. (2007) found several compounds that can be served as markers in the quality control of honey.

Authenticity of oils, butter and coffee

Vegetable oils

Oils of plant origin can be divided into seed oils and fruit oils. The chemical composition of oils is considered to be less complex regarding constituents than for other foods. However, this does not mean that fraud practices are any less diverse in this area, or that these methods of fraud do not cause serious problems in the assessment of authenticity. In vegetable oil, the most often used adulteration process is dilution with cheaper oil.

The main useful compounds of vegetable oils for detecting the authenticity of oils and fats are triacylglycerols and fatty acids. Minor components such as (phyto)sterols or tocopherols, carotenoids and sterens can be also used to detect adulteration. The triglyceride fraction of oils and fats can be analyzed by HPLC techniques on a reversed phase column. The mobile phase usually used for the separation of triglycerides consists primarily of acetonitrile with a less polar solvent such as acetone or dichloromethane. The proportion of solvent may vary depending on the samples studied. For the separation of positional isomers, argentation high-performance liquid chromatography (Ag-HPLC) appears promising. The use of a UV detector is difficult owing to the low absorbance of triacylglycerols. The most used detector types are refractive index detectors or light-scattering detectors. The refractive index detector is suitable only for isocratic separation, whereas the light-scattering detector offers the opportunity of using gradient elution. Mass spectrometric detectors have begun to be used in laboratories recently (Neff and Byrdwell, 1995; Kamm *et al*., 2001; Andrikopoulos, 2002a, 2002b; Andrikopoulos *et al*., 2004; Buchgraber *et al*., 2004). Some HPLC methods used in the analysis of triacylglycerols in oils and fats are shown in Table 11.10.

The fatty acids in triacylglycerols are specific to the plant species. The species-specific distribution of the fatty acid in triacylglycerols allows detection of the addition of oils of foreign origin, and of the degree of adulteration. The trilinolein content of virgin olive oil is usually less than 0.3%, while other oils (peanut, corn, oat, soybean, sunflower, sesame, grape and canola) contain trilinolein at higher levels. Soybean oil is detectable at levels above 4% in olive oil on the basis of the trilinolein content (Kamm *et al*., 2001; Lee *et al*., 2001; Marikkar *et al*., 2005). Salivaras and McCurdy (1992) have detected adulteration of olive oil with canola oil at levels above 7.5% using recognition pattern analysis of triacylglycerols. Based on the HPLC analysis of wax esters using statistical tests, adulteration of olive oils with solvent extracted oils can be identified (Amelio *et al*., 1993).

In order to study tocopherols, carotenoids and chlorophylls, several researchers (Tan, 1989; Psomiadou and Tsimidou, 1998; Bonvehi *et al*., 2000) have provided some alternative sensitive tools for detecting adulteration of vegetable oils (Dionisi *et al*., 1995).

Table 11.10 HPLC separation of triacylglycerols

Samples: oils or fats	HPLC separation	Detection	Refs
Sesame, perilla	Column: μBondapak C18, isocratic elution, mobile phase: acetone/acetonitrile (50/50), temperature: 30°C	Refractive index detector	1
Palm*, lard, beef chicken, mutton	Column: LiChroCART 100-RP-18 or Novena C18*, isocratic elution, mobile phase: acetone/acetonitrile (63.5/36.5), temperature: 30°C	Refractive index detector	2, 3*
Lymph	Column: Supelcosil LC-C18, gradient elution, mobile phase: A: acetonitrile, B: 2-propanol/hexane (2/1), A/B from 75/25 to 55/45 or * from 90/10 to 40/60	Evaporative light-scattering detector, * atmospheric pressure chemical ionization-MS	4
Olive, canola	Column: Supelcosil LC-18 with ODS-5S pre-column, isocratic elution, mobile phase: acetone/acetonitrile (93/7)	Refractive index detector	5
Soybean, rapeseed, palm, linseed	Column: Superspher RP-100 C18, gradient elution, mobile phase: 1) from acetonitrile/isooctane 90/10 to acetonitrile/ethanol/isooctane (40/35/25), 2) from acetonitrile to acetonitrile/ethanol (59/41), temperature: 50°C	Light-scattering detector	6
Rapeseed, sunflower, soybean, linseed, palm, macadamia, almond, poppy-seed, hazel nut, Brazil-nut, pistachio	Columns: two Nova-Pak C18 connected in series, gradient elution, mobile phase: A: water B: acetonitrile, C: 2-propanol, A/B/C from 30/70/0 trough 0/100/0 to 0/40/60, temperature: 40°C	UV detector, 205 nm Atmospheric pressure chemical ionization-MS	7
Dracocephalum moldavica, *Silybum arianum*, evening primrose, corn, amaranth	Column: Nova-Pak C18, gradient elution, mobile phase: A: acetonitrile, B: ethanol A/B from 100/0 to 30/70, temperature: 40°C		
Palm, trans hardened fat (cis-, trans-triacylglycerols)	Column: ChromSpher Lipids™ cation-exchange silver ion mode, gradient elution, mobile phase A: acetonitrile, B: dichloromethane/1,2-dichloroethane (1/1) C: acetone, A/B/C from 0/98/2 trough 0/40/60 to 20/80/0	Laser light-scattering detector	8

MS, mass spectrometry.
1, Lee *et al*., 2001; 2, Marikkar *et al*., 2005; 3, Haryati *et al*., 1998; 4, Mu and Høy, 2000; 5, Salivaras and McCurdy, 1992; 6, Bergqvist and Kaufmann, 1993; 7, Holčapek *et al*., 2003; 8, Smith *et al*., 1994.

Puspitasari-Nienaber *et al*. (2002) found that the carotenoid/carotene profile analyzed by HPLC coupled with a thermal lens spectrometric (TLS) detector is characteristic and can be used to assess the authenticity of linseed, olive, sesame and wheat-germ vegetable oils. The concentrations of total β-carotene and α-carotene together with the ratio of trans to cis-isomers of β-carotene are reliable indices for the rapid screening of oils (Luterotti *et al*., 2002).

The other highly studied fraction of oils and fats is the sterols, which may be used to detect authenticity. Recently, one of the most favorable analytical tools for analysis of these compounds has been liquid chromatography coupled with gas chromatography on-line (LC-GC). The addition of solvent-extracted oils to cold-pressed extra-virgin olive oil can be detected through investigation of free erythrodiol and uvaol in olive oils. No sample preparation is needed prior to LC-GC analysis, apart

from filtration (Blanch *et al*., 1998). By determining filberton enantiomers on-line coupled with HPLC-GC, the adulteration of olive oils with levels of around 5–10% of virgin and refined hazelnut oils (del Castillo *et al*., 1998; Flores *et al*., 2006) can be detected. According to the international ring test using tyrosol and an unknown component as key compounds, HPLC analysis was found to be suitable for detecting the addition of pressed hazelnut oil to virgin olive oil in 80% of the studied samples (Zabaras and Gordon, 2004).

Cocoa butter and coffee

Cocoa butter is a highly valued substance used not only in the food but also in the confectionery industry. Directive 2000/36/EC of the European Parliament allows utilization of vegetable fats in cocoa products at levels of up to 5%, besides cocoa butter. In this case, the fatty acid composition of vegetable fats permitted for supplementation should be similar to that of cocoa butter. These vegetable fats are termed as cocoa butter equivalent (CBE). Detection and quantification of CBE fats is one of the main targets of authenticity tests of cocoa butter (Lipp and Anklam, 1998a, 1998b; Ulberth and Buchgraber, 2003). Determination of the triacylglycerols profile is a useful tool for authenticity assessment of cocoa butter and for the estimation of CBE content in chocolate (Buchgraber *et al*., 2000; Dionisi *et al*., 2004). Addition of foreign fats (except illipé) to cocoa butter can be estimated on the basis of determining triglycerides such as dipalmityl-oleoyl glycerol (POP), oleoyl-palmityl-stearyl glycerol (POS) and distearyl-oleoyl glycerol (SOS) (Eiberger and Matissek, 1994a, 1994b). Dionisi *et al*. (2004) has devised a mathematical model to assess the amount of CBE added to cocoa butter. The ratio of triacylglycerols in both POS/PLP (dipalmityl-linoleyl glycerol) and POP/PLS (palmityl-linoleyl-stearyl glycerol) perfectly discriminates cocoa butter and CBEs at up to 5% in chocolate (Hernández *et al*., 1991). The main triacylglycerols, POP, SOS, LOO (dioleoyl-linoleyl glycerol) and PSS (distearyl-palmityl glycerol), were used in discriminant analysis to separate 20 samples according to their geographical origin.

Some minor fat components, such as individual tocopherol or tocotrienol isomers, can be also used as indicators of the addition of CBE oils to cocoa butter. However, quantitative determination of CBE in mixtures in genuine cocoa butter seems to be limited (Lipp *et al*., 2001). The distribution and content of amino acids in raw cacao vary with different origin, and in some cases, country- and even region-specific differences could be found (Rohsius *et al*., 2006).

Coffee is also valuable, and a highly popular drink throughout the world. There are two commercially important species, *Coffea canephora* var. *robusta* and *Coffea arabica*. Arabica is considered to be of better quality, with a fine flavor, and is marketed at a relatively higher price than robusta. After roasting, visual differences between the two species disappear; therefore one of the main targets of authenticity tests is to indicate whether Robusta has been added to Arabica coffee. HPLC is a good tool for analysis of triacylglycerols and tocopherol (Gonzáles *et al*., 2001; Segall *et al*., 2005b) or phenolic acids (Andrade *et al*., 1997), which are present in coffee. Some HPLC methods for analysis of these compounds are listed in Table 11.11.

Table 11.11 HPLC separation of cocoa butter and coffee

Components	Samples	HPLC separation	Detection	Refs
Triacylglycerols	Cocoa butter	Column: Microsorb RP C18 and Supelcosil RP C18 connected in series, isocratic elution, mobile phase: acetonitrile/2-propanol/hexane (57/38/5), ambient temperature	PDA detector, ESI-MS/MS	1
		Column: Lichrospher 100-5-RP18, isocratic elution,mobile phase: acetonitrile/chloroform (40/60)	Evaporative light-scattering detector	2
		Column: Spherisorbe ODS2 or one or two Hypersil ODS connected in series, isocratic or gradient elution, mobile phase: acetonitrile/ dichloromethane (70/30) or from 80/20 to 45/54 respectively, temperature: 30°C	Evaporative light-scattering detector	3
	Coffee bean	Column: Microsorb RP-C18 and Supercosil RP C-18 connected in series, isocratic elution, mobile phase: acetonitrile/2-propanol/hexane (57/38/5)	PDA detector, ESI-MS/MS	4
	Soxhlet extract of coffee	Column: Superspher 100 RP-18, isocratic elution, mobile phase: acetonitrile/acetone (50/50), temperature: 40–35°C	Refractive index detector	5
Tocopherols	Soxhlet extract of coffee	Column: Lichrospher Si60, isocratic elution, mobile phase: hexane/2-propanol (99/1), temperature: 40–35°C	Fluorescence detector, 330 nm (excitation 290 nm)	5
Tocopherols tocotrienols	Cocoa butter, CBE	Column: Lichrosorb Si60, gradient elution, mobile phase A: methyl *tert*-butyl ether/hexane (3/100), B: methyl *tert*-butyl ether/hexane (10/100) A to B	Fluorescence detector, 330 nm (excitation 290 nm)	6

CBE, cocoa butter equivalent; ESI-MS/MS, electrospray ionization-tandem mass spectrometry; PDA, photodiode array.
1, Segall *et al*., 2005a; 2, Dionisi *et al*., 2004; 3, Buchgraber *et al*., 2000; 4, Segall *et al*., 2005b; 5, Gonzáles *et al*., 2001; 6, Lipp *et al*., 2001.

Authenticity of cheese and milk

Dairy products have been consumed since early times. The high volume of cheese production and consumption in the world makes the regulation of authenticity of cheese products an important issue. False labeling of milk regarding the animal origin, and the use of reconstituted milk powder have been the subjects of study for authenticity. The originality of the cheese depends on several factors, such as the cheese-making process and the milk as the raw material. Both of them depend on the geographical origin. The confirmation of geographic origin is therefore necessary in order to ensure a dairy product's authenticity (Simpkins and Harrison, 1995; De la Fuente and Juárez, 2005; Karoui and Baerdemaeker, 2007).

Reverse phase HPLC separation can be utilized for the analysis of several fractions of milk proteins, such as casein (Mayer *et al*., 1997; Veloso *et al*., 2002, 2004; Mayer 2005) and/or β-lactoglobulins (Ferreira and Caçote, 2003; Enne *et al*., 2005) or furosine, which comes from the fructolysine complex at the beginning of the Maillard reaction during heat treatment of milk. These substances are useful for determining

Table 11.12 HPLC separation of milk and cheese

Samples	Compounds	HPLC method	Detection	Refs
Bovine, ovine, caprine milk, their mixture in milk and cheese	β-lactoglobulins	Column: Chrompack P 300 RP with pre-column Chrompack P RP, gradient elution, mobile phase: A: 0.1% trifluoroacetic acid, B: 0.1% trifluoroacetic acid in acetonitrile/water (80/50), A/B from 64/36 to 40/60, temperature: 45°C	PDA detector, 215 nm	1
Mixtures: cow, and/or sheep and/or goat milk	β-lactoglobulins, α-lactalbumin, albumin	Column: perfusion reversed phase POROS 1 10R/glycerol prepared in laboratory, gradient elution, mobile phases: A: acetonitrile/water/formic acid (5/75/20); B: acetonitrile/water (93/7), A/B from 75/25 to 65/35, temperature: 50°C	PDA detector, 280 nm	2
Bovine milk in buffalo cheese	β-lactoglobulins, α-lactalbumin	Column: C4 Phenomenex, gradient elution, mobile phase: A: 0.1% trifluoroacetic acid, B: 0.1% trifluoroacetic acid in acetonitrile, A/B from 65/35 to 10/90 ambient temperature	UV detector, 205 nm	3
Caprine, ovine, bovine milk in cheese *cow, ewe, goat milk in cheese	para-κ-casein, *γ-casein and para-κ-casein	Column: Shodex IEC CM-825 (cation-exchange), wide-pore (1000 Å), gradient elution, mobile phase: A: 10 mmol malonic acid, 5 mol urea in water (pH 6.0 with NaOH), B: the same as A containing 0.5 mol l^{-1} NaCl, A/B from 100/0 to 0/100, temperature: 30°C	UV/VIS detector, 280 nm	4, 5*
Ovine, bovine in caprine milk	α-, β-, κ-casein	Column: Chrompack P 300 RP with pre-column Chrompack P RP, gradient elution, mobile phase A: 0.1% trifluoroacetic acid, B: acetonitrile/water/trifluoroacetic acid (95/5/0.1), A/B from 71/29 to 0/100, temperature: 46°C	Variable-wavelength UV detector, 280 nm	6, 7

PDA, photodiode array.
1, Ferreira and Caçote, 2003; 2, Torre *et al*., 1996; 3, Enne *et al*., 2005; 4, Mayer, 2005; 5, Mayer *et al*., 1997; 6, Veloso *et al*., 2002; 7, Veloso *et al*., 2004.

milk origin and the possible adulteration of cheese products (De la Fuente and Juárez, 2005; Karoui and Baerdemaeker, 2007). The methods of determination of these compounds are generally based on ion-exchange chromatography using an acidic mobile phase modified with acetonitrile. Gradient elution is usually applied in time-consuming analysis. Several of those HPLC methods are summarized in Table 11.12. Precipitation at pH 4 (Veloso *et al*., 2002, 2004; Ferreira and Caçote, 2003; Enne *et al*., 2005) or hydrolyzation by plasmine are usually used for the isolation of proteins from cheese or milk (Mayer *et al*., 1997; Volitaki and Kaminarides, 2001).

Analysis of casein by HPLC is a well-standardized method for the detection of rennet whey addition to milk powder (EU, 1990). Separation and quantification of major casein fractions (γ-, α-, β- and para κ-casein) may be a useful tool for recognition of the addition of foreign milk to milk or cheese (Mayer *et al*., 1997; Veloso *et al*., 2002; Mayer, 2005). By analyzing α-casein using HPLC, 20% bovine milk could be detected in ovine milk cheese (Veloso *et al*., 2004).

Torre *et al*. (1996) developed a HPLC method based on the analysis of β-lactoglobulins. The method seemed to be useful in the detection of homologous whey proteins from admixture of milks of different species (cow, sheep and goat). High levels of denatured β-lactoglobulins, furosine and lactulose may indicate addition of heated milk at high temperature. High levels of furosine indicate the presence of reconstituted milk powder (Villamiel *et al*., 1999). Quantification of β-lactoglobulins by HPLC can be used for determining the origin of milk from different animal species – for example, bovine, ovine and caprine milk in cheese (Ferreira and Caçote, 2003) and bovine-milk addition to water buffalo mozzarella (Enne *et al*., 2005) could be detected.

Conclusions

Applications of HPLC for the determination of authenticity of food products have been discussed here. The success of the HPLC technique in the analysis of complex matrices such as foods has been demonstrated.

One of the objectives in the fight against adulteration is to develop sensitive analytical methods to detect the presence or determine the lack of specific compound(s) which characterize the raw material of foods of plant or animal origin. The main advantage of HPLC regarding authenticity is its ability to separate and detect compound(s) or compound groups that are at low levels in food products of interest. Relatively low molecular mass compounds or those of higher molecular mass, such as proteins, are chosen as targets of analysis, and by using these compounds good results can be obtained in the determination of authenticity. HPLC is an excellent tool for studying and discovering the minor and specific compounds mentioned above. The application of chemometric methods provides further advantages in the evaluation of HPLC data.

References

Amelio, M., Rizzo, R. and Varazini, F. (1993). Separation of wax esters from olive oils by high performance liquid chromatography. *Journal of the American Oil Chemists' Society*, **70**(8), 793–796.

Andrade, P.B., Leitão, R., Seabra, R.M. *et al*. (1997). 3,4-Dimethoxycinnamic acid levels as a tool for differentiation of *Coffea canephora* var. *robusta* and *Coffea arabica*. *Food Chemistry*, **61**(4), 511–514.

Andrade, P.B., Carvalho, A.R.F., Seabra, R.M. and Ferreira, M.A. (1998). A previous study of phenolic profiles of quince, pear, and apple purees by HPLC diode array detection for detection for evaluation of quince puree genuineness. *Journal of Agricultural and Food Chemistry*, **46**(3), 968–972.

Andrikopoulos, N.K. (2002a). Triglyceride species compositions of common edible vegetable oils and methods used for their identification and quantification. *Food Reviews International*, **18**(1), 71–102.

Andrikopoulos, N.K. (2002b). Chromatographic and spectroscopic methods in the analysis of triacylglycerol species and regiospecific isomers of oils and fats. *Critical Reviews in Food Science and Nutrition*, **42**(5), 473–505.

Andrikopoulos, N.K., Chiou, A. and Mylona, A. (2004). Triacylglycerol species of less common edible vegetable oils. *Food Reviews International*, **20**(4), 389–403.

Anklam, E. (1998). A review of analytical methods to determine the geographical and botanical origin of honey. *Food Chemistry*, **63**(4), 549–562.

Association of the Industry of Juices and Nectars from Fruits and Vegetables of the European Union (AIJN) (2003). Reference guide. In: *Code of Practice for Evaluation of Fruit and Vegetable Juices*. Brussels: AIJN, pp. 6.1–6.19.

Bergqvist, M.H.J. and Kaufmann, P. (1993). A multivariate optimization of triacylglycerol analysis by high-performance liquid-chromatography. *Lipids*, **28**(7), 667–675.

Blanch, G.P., Villén, J. and Herraiz, M. (1998). Rapid analysis of free erythrodiol and uvaol in olive oils by coupled reversed-phase liquid chromatography–gas chromatography. *Journal of Agricultural and Food Chemistry*, **46**(3), 1027–1030.

Bohm, B.A. (1975). Flavanones and dihydroflavonols. In: J.B. Harborne, T.J. Mabry and H. Harborne (eds), *The Flavonoids*. London: Chapman and Hall, pp. 560–631.

Bonvehi, J.S., Coll, F.V. and Rius, I.A. (2000). Liquid chromatographic determination of tocopherols and tocotrienols in vegetable oils, formulated preparations, and biscuits. *Journal of the AOAC International*, **83**(3), 627–634.

Botos, E.P. (1999). Ha más van a palackban. (If there is anything else in the bottle.). *Élet és Tudomány*, **45**, 16–20.

Brause, A. (1992). Verfahren zum Nachweis von Fruchtsaftverfälschung – Perspectiven 1991. *Flüssiges Obst*, **59**(4), 178–182.

Bronner, W.E. and Beecher, G.R. (1995). Extraction and measurement of prominent flavonoids in orange and grapefruit juice concentrates. *Journal of Chromatography A*, **705**(2), 247–256.

Bruckner, Gy. (1964). Heterocyclic compounds. In: G. Bruckner (ed.), *Szerves Kémia* (*Organic Chemistry*), Vol. 3(1). Budapest: Tankönyvkiadó, pp. 369–392.

Brush, A.H. (1981). Carotenoids in wild and captive birds. In: J.C. Bauernfeind (ed.), *Carotenoids as Colorant and Vitamin A Precursors. Technological and Nutritional Applications*. Food Science and Technology A Series of Monographs (G.F. Stewart, B.S. Schweigert and J. Hawthorn, eds). New York, NY: Academic Press, pp. 463–538.

Buchgraber, M., Ulberth, F. and Anklam, E. (2000). Comparison of HPLC and GLC techniques for the determination of the triglyceride profile of cocoa butter. *Journal of Agricultural and Food Chemistry*, **48**(8), 3358–3363.

Buchgraber, M., Ulberth, F., Emons, H. and Anklam, E. (2004). Triacylglycerol profiling by using chromatographic techniques. *European Journal of Lipid Science and Technology*, **106**(9), 621–648.

Cámara, M.M., Díez, C., Torija, M.E. and Cano, M.P. (1994). HPLC determination of organic acids in pineapple juices and nectar. *Zeitschrift für Lebensmittel-Untersuchnung und -Forschung*, **198**(1), 52–56.

Cooper, K.A., Campos-Gimenez, E., Alvarez, D.J. *et al*. (2007). Rapid reversed phase ultra-performance liquid chromatography analysis of the major cocoa polyphenols

and inter-relationships of their concentrations in chocolate. *Journal of Agricultural and Food Chemistry*, **55**(8), 2841–2847.

Coppola, E.D. and Starr, M.S. (1986). Liquid-chromatographic determination of major organic acids in apple juice and cranberry juice cocktail-collaborative study. *Journal of the AOAC*, **69**(4), 594–597.

Cordella, C.B.Y., Militão, J.S.L.T. and Cabrol-Bass, D. (2003). A simple method for automated pretreatment of usable chromatographic profiles in pattern-recognition procedures: application to HPAEC-PAD chromatograms of honey. *Analytical and Bioanalytical Chemistry*, **377**(1), 214–219.

Cotte, J.F., Casabianca, H., Chardon, S. *et al*. (2003). Application of carbohydrate analysis to verify honey authenticity. *Journal of Chromatography A*, **1021**(1–2), 145–155.

Council Directive (2001). Council Directive 2001/110/EC of the Council of the European Union of 20 December 2001 relating to honey. *Official Journal of the European Communities*, **L10/47**. 12.1.2002.

Daood, H.G., Kapitany, J., Biacs, P. and Albrecht, K. (2006). Drying temperature, endogenous antioxidants and capsaicinoids affect carotenoid stability in paprika (red pepper spice). *Journal of the Science of Food and Agriculture*, **86**(14), 2450–2457.

De la Fuente, M.A. and Juárez, M. (2005). Authenticity assessment of dairy products. *Critical Reviews in Food Science and Nutrition*, **45**(7–8), 563–585.

del Castillo, M.L.R., Caja, M.D., Herraiz, M. and Blanch, G.P. (1998). Rapid recognition of olive oil adulterated with hazelnut oil by direct analysis of enantiomeric composition of filbertone. *Journal of Agricultural and Food Chemistry*, **46**(12), 5128–5131.

de Simóne, B.F., Pérez-Ilzarbe, J., Hernández, T. *et al*. (1992). Importance of phenolic compounds for characterization of fruit juices. *Journal of Agricultural and Food Chemistry*, **40**(9), 1531–1535.

de Villiers, A., Vanhoenacker, G., Majek, P. and Sandra, P. (2004). Determination of anthocyanins in wine by direct injection liquid chromatography-diode array detection-mass spectrometry and classification of wines using discriminant analysis. *Journal of Chromatography A*, **1054**(1–2), 195–204.

de Villiers, A., Lestremau, F., Szucs, R. *et al*. (2006). Evaluation of ultra performance liquid chromatography Part I. Possibilities and limitations. *Journal of Chromatography A*, **1127**(1–2), 60–69.

Dimitrova, B., Gevrenova, R. and Anklam, E. (2007). Analysis of phenolic acids in honeys of different floral origin by solid-phase extraction and high-performance liquid chromatography. *Phytochemical Analysis*, **18**(1), 24–32.

Dionisi, F., Prodolliet, J. and Tagliaferri, E. (1995). Assessment of olive oil adulteration by reversed-phase high-performance liquid chromatography/amperometric detection of tocopherols and tocotrienols. *Journal of the American Oil Chemists' Society*, **72**(12), 1505–1511.

Dionisi, F., Golay, P.A., Hug, B. *et al*. (2004). Triacylglycerol analysis for the quantification of cocoa butter equivalents (CBE) in chocolate: feasibility study and validation. *Journal of Agricultural and Food Chemistry*, **52**(7), 1835–1841.

Directive 2000/36/EC of the European Parliament and the Council of 23 June 2000 relating to cocoa and chocolate products intended for human consumption. *Official Journal of the European Communities*, **L197**, 19–25.

Dragovic-Uzelac, V., Pospišil, J., Levaj, B. and Delonga, K. (2005). The study of phenolic profiles of raw apricots and apples and their puree by HPLC for the evaluation of apricot nectars and jams authenticity. *Food Chemistry*, **91**(2), 373–383.

Eckert, M., Baumann, G. and Gierschner, K. (1987). Vergleiche hochdruckflüssigkeitschromatographische und enzymatische Analyze der Fruchsäuren in Fruchsäften. *Flüssiges Obst*, **54**(3), 134–138.

Eiberger, T. and Matissek, R. (1994a). Zum Nachweise von Kakaobutteräquivalent mittels HPLC. *Lebensmittelchemie*, **48**, 49–55.

Eiberger, T. and Matissek, R. (1994b). Ansätze und Daten zum Nachweis von Kakaobutteräquivalent CBE. *Lebensmittelchemie*, **48**, 133–134.

Elkins, E.R. and Heuser, J.R. (1994). Detection of adulteration in apple juice by L-malic/total malic acid ratio – collaborative study. *Journal of the AOAC International*, **77**(2), 411–415.

Elkins, E.R., Heuser, J.R. and Chin, H. (1988). Detection of adulteration in selected fruit juices. In: S. Nagy, J.A. Attaway and M.E. Rhodes (eds), *Adulteration of Fruit Juice Beverages*. New York, NY: Marcel Dekker Inc, pp. 317–402.

Enne, G., Elez, D., Fondrini, F. *et al*. (2005). High-performance liquid chromatography of governing liquid to detect illegal bovine milk's addition in water buffalo mozzarella: Comparison with results from raw milk and cheese matrix. *Journal of Chromatography A*, **1094**(1–2), 169–174.

Escarpa, A. and González, M.C. (1999). Fast separation of (poly)phenolic compounds from apples and pears by high-performance liquid chromatography with diode-array detection. *Journal of Chromatography A*, **830**(2), 301–309.

Etiévant, P., Schlich, P., Cantagrel, R. *et al*. (1989). Varietal and geographic classification of French red wines in terms of major acids. *Journal of the Science of Food and Agriculture*, **46**(4), 421–438.

EU (1990). Rules for granting aid to skimmed milk processed into compound feeding stuffs and skimmed-milk powder intended in particular for feed for calves, Commission Regulation 2426/90 of 21 of August. *Official Journal of the European Communities*, **L228**, 9–14.

Fekete, J. (2000). Nagyhatékonyságú folyadékkromatográfia. (High pressure liquid chromatography). In: J. Kőmives (ed.), *Környezeti Analitka (Environmental Analytic)*. Budapest: Műegyetemi Kiadó, pp. 194–293.

Ferreira, I.M.P.L.V.O. and Caçote, H. (2003). Detection and quantification of bovine, ovine and caprine milk percentages in protected denomination of origin cheeses by reversed-phase high-performance liquid chromatography of beta-lactoglobulins. *Journal of Chromatography A*, **1015**(1–2), 111–118.

Ferreres, F., Tomás-Barberán, F.A., Gil, M.I. and Tomás-Lorente, F. (1991). An HPLC technique for flavonoid analysis in honey. *Journal of the Science of Food and Agriculture*, **56**(1), 49–56.

Ferreres, F., García-Viguera, C., Tomás-Lorente, F. and Tomás-Barberán, F.A. (1993). Hesperetin: a marker of the floral origin of citrus honey. *Journal of the Science of Food and Agriculture*, **61**(1), 121–123.

Ferreres, F., Giner, J.M. and Tomás-Barberán, F.A. (1994a). A comparative-study of hesperetin and methyl anthranilate as markers of the floral origin of citrus honey. *Journal of the Science of Food and Agriculture*, **65**(3), 371–372.

Ferreres, F., Andreda, P. and Tomás-Barberán, F.A. (1994b). Flavonoids from Portuguese heather honey. *Zeitschrift für Lebensmittel-Untersuchnung und -Forschung*, **199**(1), 32–37.

Fisher, J.F. and Rouseff, R.L. (1986). Solid-phase extraction and HPLC determination of β-cryptoxanthin and α- and β-carotene in orange juice. *Journal of Agricultural and Food Chemistry*, **34**(6), 985–989.

Fisher, J.F. and Wheaton, T.A. (1976). High-pressure liquid-chromatographic method for resolution and quantitation of naringin and naringenin rutinoside in grapefruit juice. *Journal of Agricultural and Food Chemistry*, **24**(4), 898–899.

Flores, G., del Castillo, M.L.R., Herraiz, M. and Blanch, G.P. (2006). Study of the adulteration of olive oil with hazelnut oil by on-line coupled high performance liquid chromatography and gas chromatographic analysis of filbertone. *Food Chemistry*, **97**(4), 742–749.

Gambelli, L. and Santaroni, G.P. (2004). Polyphenols content in some Italian red wines of different geographical origins. *Journal of Food Composition and Analysis*, **17**(5), 613–618.

Gil, M.I., Ferreres, F., Ortiz, A. *et al*. (1995). Plant phenolic metabolites and floral origin of rosemary honey. *Journal of Agricultural and Food Chemistry*, **43**(11), 2833–2838.

Gnayfeed, M.H., Daood, H.G., Biacs, P.A. and Alcaraz, C.F. (2001). Content of bioactive compounds in pungent spice red pepper (paprika) as affected by ripening and genotype. *Journal of the Science of Food and Agriculture*, **81**(15), 1580–1585.

Goiffon, J.P., Mouly, P.P. and Gaydou, E.M. (1999). Anthocyanin pigment determination in red fruit juices, concentrated juices and syrups using liquid chromatography. *Analytica Chimica Acta*, **382**(1–2), 39–50.

Gonçalves, B., Landbo, A.K., Knudsen, D. *et al*. (2004). Effect of ripeness and postharvest storage on the phenolic profiles of cherries (*Prunum avium* L.). *Journal of Agricultural and Food Chemistry*, **52**(3), 523–530.

Gonzáles, A.G., Pablos, F., Martín, M.J. *et al*. (2001). HPLC analysis of tocopherols and triglycerides in coffee and their use as authentication parameters. *Food Chemistry*, **73**(1), 93–101.

Goodall, I., Dennis, M.J., Parker, I. and Sharman, M. (1995). Contribution of high-performance liquid chromatographic analysis of carbohydrates to authenticity testing of honey. *Journal of Chromatography A*, **706**(1–2), 353–359.

Gregory, G.K., Chen, T.S. and Philip, T. (1986). Quantitative analysis of lutein esters in marigold flowers (Tagetes erecta) by high performance liquid chromatography. *Journal of Food Science*, **51**(4), 1093–1094.

Hammond, D.A. (2001). Synergy between liquid chromatographic-pulsed amperometric detection and capillary-gas chromatographic methods for detection of juice adulteration. *Journal of the Association of Official Analytical Chemists International*, **84**(3), 964–975.

Haryati, T., Man, Y.B.C., Ghazali, H.M. *et al*. (1998). Determination of iodine value of palm oil based on triglyceride composition. *Journal of the American Oil Chemists' Society*, **75**(7), 789–792.

Hernández, B., Castellote, A.I. and Permanyer, J.J. (1991). Triglyceride analysis of cocoa beans from different geographical origin. *Food Chemistry*, **41**(3), 269–276.

Hofsommer, H.J. and Koswig, S. (2005). Zum Nachweis von Aronia in schwarzer Johannisbeere. *Flüssiges Obst*, **6**, 289–293.

Hohmann-Marriott, M.F. and Blankenship, R.E. (2007). Hypothesis on chlorosome biogenesis in green photosynthetic bacteria. *FEBS Letters*, **581**(5), 800–803.

Holbach, B., Marx, R. and Zimmer, M. (2001). Bedeutung der Shikimisäure und des Anthocyanspektrums für die Charakterisierung von Rebsorten. *Lebensmittelchemie*, **55**, 32–34.

Holčapek, M., Jandera, P., Zderadička, P. and Hrubá, L. (2003). Characterization of triacylglycerol and diacylglycerol composition of plant oils using high-performance liquid chromatography-atmospheric pressure chemical ionization mass spectrometry. *Journal of Chromatography A*, **1010**(2), 195–215.

Hollborn, E., Wald, B., Galensa, R. and Herrmann, K. (1990). Nachweis von Apfelbestandteilen in Lebensmitteln mittels HPLC nach Festphasenextraktion. *Deutsche Lebensmittel-Rundschau*, **86**(1), 1–3.

Hong, V. and Wrolstad, R.E. (1986). Cranberry juice composition. *Journal of the AOAC*, **69**(2), 199–207.

Hughes, S. and Johnson, D.C. (1982). High-performance liquid chromatographic separation with triple-pulse amperometric detection of carbohydrates in beverages. *Journal of Agricultural and Food Chemistry*, **30**(4), 712–714.

Imai, K., Toyo'oka, T. (1988). Design and choice of suitable labelling reagents for liquid chromatography. In: R.W. Frei, K. Zeich (eds), *Selective Sample Handling and Detection in High-Performance Liquid Chromatography*, Journal of Chromatography Library, Vol. 39. Amsterdam: Elsevier Science Publishers B.V., pp. 209–288.

Iuliano, T.A. (1996). A simplified method for determining undeclared sweeteners added to pure orange juice. *Journal of the AOAC International*, **79**(6), 1381–1387.

Justesen, U., Knuthsen, P. and Leth, T. (1998). Quantitative analysis of flavonols, flavones, and flavanones in fruits, vegetables and beverages by high-performance liquid chromatography with photo-diode array and mass spectrometric detection. *Journal of Chromatography A*, **799**(1–2), 101–110.

Kallithraka, S., Arvanitoyannis, I., El-Zajouli, A. and Kefalas, P. (2001). The application of an improved method for trans-resveratrol to determine the origin of Greek red wines. *Food Chemistry*, **75**(3), 355–363.

Kamm, W., Dionisi, F., Hischenhuber, C. and Engel, K.H. (2001). Authenticity assessment of fats and oils. *Food Reviews International*, **17**(3), 249–290.

Karoui, R. and De Baerdemaeker, J. (2007). A review of the analytical methods coupled with chemometric tools for the determination of quality and identity of dairy products. *Food Chemistry*, **102**(3), 621–640.

Kenjerić, D., Mandić, M.L., Primorac, L. *et al*. (2007). Flavonoid profile of Robinia honeys produced in Croatia. *Food Chemistry*, **102**(3), 683–690.

Kiss, J. and Sass-Kiss, A. (2005). Protection of originality of Tokaji Aszú: amines and organic acids in botrytized wines by high-performance liquid chromatography. *Journal of Agricultural and Food Chemistry*, **53**(26), 10 042–10 050.

Kiss, J., Korbász, M. and Sass-Kiss, A. (2006). Study of amine composition of botrytized grape berries. *Journal of Agricultural and Food Chemistry*, **54**(23), 8909–8918.

Kvasnička, F., Voldřich, M., Pyš, P. and Vinš, I. (2002). Determination of isocitric acid in citrus juice – a comparison of HPLC, enzyme set and capillary isotachophoresis methods. *Journal of Food Composition and Analysis*, **15**(6), 685–691.

Lee, D.S., Lee, E.S., Kim, H.J. *et al*. (2001). Reversed phase liquid chromatographic determination of triacylglycerol composition in sesame oils and the chemometric detection of adulteration. *Analytica Chimica Acta*, **429**(2), 321–330.

Liao, H., Cai, Y. and Haslam, E. (1992). Polyphenol interactions. Anthocyanins: copigmentation and colour changes in red wines. *Journal of the Science of Food and Agriculture*, **59**(3), 299–305.

Lipp, M. and Anklam, E. (1998a). Review of cocoa butter and alternative fats for use in chocolate – part A. *Compositional data. Food Chemistry*, **62**(1), 73–97.

Lipp, M. and Anklam, E. (1998b). Review of cocoa butter and alternative fats for use in chocolate – part B. Analytical approaches for identification and determination. *Food Chemistry*, **62**(1), 99–108.

Lipp, J., Ziegler, H. and Conrady, E. (1988). Detection of high fructose- and other syrups in honey using high-pressure liquid chromatography. *Zeitschrift für Lebensmittel-Untersuchnung und -Forschung*, **187**(4), 334–338.

Lipp, M., Simoneau, C., Ulberth, F. *et al*. (2001). Composition of genuine cocoa butter and cocoa butter equivalents. *Journal of Food Composition and Analysis*, **14**(4), 399–408.

Low, N.H. and Swallow, K.W. (1991). Detection of beet medium invert sugar addition to orange juice by high performance liquid chromatography. *Fluessiges Obst*, **58**(1), 2–5.

Low, N.H. and Wudrich, G.G. (1993). Detection of inexpensive sweetener addition to grapefruit juice by HPLC-PAD. *Journal of Agricultural and Food Chemistry*, **41**(6), 902–909.

Luterotti, S., Franko, M. and Bicanic, D. (2002). Fast quality screening of vegetable oils by HPLC-thermal lens spectrometric detection. *Journal of the American Oil Chemists' Society*, **79**(10), 1027–1031.

Macrae, R. (1982). Theory of liquid column chromatography. In: R. Macrae (ed.), *HPLC in Food Analysis*. New York, NY: Academic Press Inc, pp. 1–26.

Makris, D.P., Kallithraka, S. and Mamalos, A. (2006). Differentiation of young red wines based on cultivar and geographical origin with application of chemometrics of principal polyphenolic constituents. *Talanta*, **70**(5), 1143–1152.

Mallorqui, N., Arellano, J.B., Borrego, C.M. and Garcia-Gil, L.J. (2005). Signature pigments of green sulfur bacteria in lower Pleistocene deposits from the Banyoles lacustrine area (Spain). *Journal of Paleolimnology*, **34**(2), 271–280.

Mardones, C., Hitschfeld, A., Contreras, A. *et al*. (2005). Comparison of shikimic acid determination by capillary zone electrophoresis with direct and indirect detection with liquid chromatography for varietal differentiation of red wines. *Journal of Chromatography A*, **1085**(2), 285–292.

Marikkar, J.M.N., Ghazali, H.M., Man, Y.B.C. *et al*. (2005). Distinguishing lard from other animal fats in admixtures of some vegetable oils using liquid chromatographic data coupled with multivariate data analysis. *Food Chemistry*, **91**(1), 5–14.

Martos, I., Ferreres, F., Yao, L.H. *et al*. (2000). Flavonoids in monospecific eucalyptus honeys from Australia. *Journal of Agricultural and Food Chemistry*, **48**(10), 4744–4748.

Matějíček, D., Mikeš, O., Klejdus, B. *et al*. (2005). Changes in contents of phenolic compounds during maturing of barrique red wines. *Food Chemistry*, **90**(4), 791–800.

Mattick, L.R. (1988). An evaluation of the methodology for determining the authenticity of apple juice concentrate. In: S. Nagy, J.A. Attaway and M.E. Rhodes (eds), *Adulteration of Fruit Juice Beverages*. New York, NY: Marcel Dekker Inc, pp. 175–193.

Mattila, P., Hellström, J. and Törrönen, R. (2006). Phenolic acids in berries, fruits, and beverages. *Journal of Agricultural and Food Chemistry*, **54**(19), 7193–7199.

Mayer, H.K. (2005). Milk species identification in cheese varieties using electrophoretic, chromatographic and PCR techniques. *International Dairy Journal*, **15**(6–9), 595–604.

Mayer, H.K., Heidler, D. and Rockenbauer, C. (1997). Determination of the percentage of cows', ewes' and goats' milk in cheese by isoelectric focusing and cation-exchange HPLC of γ- and para-κ-caseins. *International Dairy Journal*, **7**(10), 619–628.

McRae, K.B., Lidster, P.D., DeMarco, A.C. and Dick, A.J. (1990). Comparison of the polyphenol profiles of apple fruit cultivars by correspondence-analysis. *Journal of the Science of Food and Agriculture*, **50**(3), 329–342.

Midkiff, C.R., Jr. and Buscemi, B.C. (1988). Detection of adulteration in fruit wines. In: S. Nagy, J.A. Attaway and M.E. Rhodes (eds), *Adulteration of Fruit Juice Beverages*. New York, NY: Marcel Dekker Inc, pp. 175–211.

Minguez-Mosquera, M.I. and Hornero-Méndez, D. (1993). Separation and quantification of the carotenoid pigments in red peppers (*Capsicum annuum* L.), paprika and oleoresin by reversed-phase HPLC. *Journal of Agricultural and Food Chemistry*, **41**(10), 1616–1620.

Mögle, R., Schulte, E. and Galensa, R. (1993). Nachweis von raffinose in orangensaft mittels HPLC-enzymreaktor-kopplung and electrochemischer detection. *Deutsche Lebensmittel-Rundschau*, **89**(8), 251–253.

Mouly, P.P., Gaydou, E.M. and Auffay, A. (1998). Simultaneous separation of flavanone glycosides and polymethoxylated flavones in citrus juices using liquid chromatography. *Journal of Chromatography A*, **800**(2), 171–179.

Mouly, P.P., Gaydou, E.M. and Corsetti, J. (1999a). Characterization of paprika (*Capsicum annuum*) extract in orange juices by liquid chromatography of carotenoid profiles. *Journal of Agricultural and Food Chemistry*, **47**(3), 968–976.

Mouly, P.P., Gaydou, E.M., Lapierre, L. and Corsetti, J. (1999b). Differentiation of several geographical origins in single-strength Valencia orange juices using quantitative comparison of carotenoid profiles. *Journal of Agricultural and Food Chemistry*, **47**(10), 4038–4045.

Mu, H.L. and Høy, C.E. (2000). Application of atmospheric pressure chemical ionization liquid chromatography-mass spectrometry in identification of lymph triacylglycerols. *Journal of Chromatography B*, **748**(2), 425–437.

Nagy, S. (1997). Economic adulteration of fruit beverages. *Fruit Processing*, **4**, 124–131.

Neff, W.E. and Byrdwell, W.C. (1995). Soybean oil triacylglycerol analysis by reversed-phase high-performance liquid-chromatography coupled with atmospheric-pressure

chemical-ionization mass-spectrometry. *Journal of the American Oil Chemists' Society*, **72**(10), 1185–1191.

Newton, R. (1982). Instrumentation for HPLC. In: R. Macrae (ed.), *HPLC in Food Analysis*. New York, NY: Academic Press Inc, pp. 28–76.

Ooghe, W.C. and Detavernier, C.M. (1997). Detection of the addition of *Citrus reticulata* and hybrids to *Citrus sinensis* by flavonoids. *Journal of Agricultural and Food Chemistry*, **45**(5), 1633–1637.

Ooghe, W.C., Ooghe, S.J., Detavernier, C.M. and Huyghebaert, A. (1994a). Characterization of orange juice (*Citrus sinensis*) by flavanone glycosides. *Journal of Agricultural and Food Chemistry*, **42**(10), 2183–2190.

Ooghe, W.C., Ooghe, S.J., Detavernier, C.M. and Huyghebaert, A. (1994b). Characterization of orange juice (*Citrus sinensis*) by polymethoxylated flavones. *Journal of Agricultural and Food Chemistry*, **42**(10), 2191–2195.

Pan, G.G., Kilmartin, P.A., Smith, B.G. and Melton, L.D. (2002). Detection of orange juice adulteration by tangelo juice using multivariate analysis of polymethoxylated flavones and carotenoids. *Journal of the Science of Food and Agriculture*, **82**(4), 421–427.

Pantelidis, G.E., Vasilakakis, M., Manganaris, G.A. and Diamantidis, G. (2007). Antioxidant capacity, phenol, anthocyanin and ascorbic acid contents in raspberries, blackberries, red currants, gooseberries and cornelian cherries. *Food Chemistry*, **102**(3), 777–783.

Park, G.L., Avary, S.M., Byers, J.L. and Nelson, D.B. (1983). Identification of bioflavonoids from citrus. *Food Technology*, **37**(12), 98–105.

Peterson, J.J., Dwyer, J.T., Beecher, G.R. *et al*. (2006a). Flavanones in oranges, tangerines (mandarins), tangors, and tangelos: a compilation and review of the data from the analytical literature. *Journal of Food Composition and Analysis*, **19**, S66–S73.

Peterson, J.J., Beecher, G.R., Bhagwat, S.A. *et al*. (2006b). Flavanones in grapefruit, lemons, and limes: A compilation and review of the data from the analytical literature. *Journal of Food Composition and Analysis*, **19**, S74–S80.

Petrus, D.R. and Attaway, J.A. (1980). Visible and ultraviolet absorption and fluorescence excitation and emission characteristics of Florida orange juice and orange pulpwash: detection of adulteration. *Journal of the AOAC*, **63**(6), 1317–1331.

Petrus, D.R., Fellers, P.J. and Anderson, H.E. (1984). Orange juice adulteration: detection and quality effects of dilution, added orange pulpwash, turmeric and sorbate. *Journal of Food Science*, **49**(6), 1438–1443.

Philip, T., Chen, T.S. and Nelson, D.B. (1989). Detection of adulteration of California orange juice concentrates with externally added carotenoids by liquid chromatography. *Journal of Agricultural and Food Chemistry*, **37**(1), 90–95.

Pilando, L.S. and Wrolstad, R.E. (1992). Compositional profiles of fruit juice concentrates and sweeteners. *Food Chemistry*, **44**(1), 19–27.

Pool, C.F. and Poole, S.K. (1991). *Chromatography Today*. Amsterdam: Elsevier Science Publishers B.V., pp. 1–103, 545–599, 736–946.

Psomiadou, E. and Tsimidou, M. (1998). Simultaneous HPLC determination of tocopherols, carotenoids, and chlorophylls for monitoring their effect on virgin olive oil oxidation. *Journal of Agricultural and Food Chemistry*, **46**(12), 5132–5138.

Pupin, A.M., Dennis, M.J. and Toledo, M.C.F. (1998). Flavonone glycosides in Brazilian orange juice. *Food Chemistry*, **61**(3), 275–280.

Pupin, A.M., Dennis, M.J. and Toledo, M.C.F. (1999). HPLC analysis of carotenoids in orange juice. *Food Chemistry*, **64**(2), 269–275.

Puspitasari-Nienaber, N.L., Ferruzzi, M.G. and Schwartz, S.J. (2002). Simultaneous detection of tocopherols, carotenoids, and chlorophylls in vegetable oils by direct injection C-30 RP-HPLC with coulometric electrochemical array detection. *Journal of the American Oil Chemists' Society*, **79**(7), 633–640.

Richard, W., Jr. and Widmer, W.W. (1990). Application of high-performance anion-exchange chromatography with pulsed amperometric detection to sugar analysis in citrus juices. *Journal of Agricultural and Food Chemistry*, **38**(10), 1918–1921.

Rocklin, R.D. and Phol, C.A. (1983). Determination of carbohydrates by anion-exchange chromatography with pulsed amperometric detection. *Journal of Liquid Chromatography*, **6**(9), 1577–1590.

Rohsius, C., Matissek, R. and Lieberei, R. (2006). Free amino acid amounts in raw cocoas from different origins. *European Food Research and Technology*, **222**(3–4), 432–438.

Rouseff, R.L. (1988a). Differentiating citrus juice using flavanone glycoside concentration profiles. In: S. Nagy, J.A. Attaway and M.E. Rhodes (eds), *Adulteration of Fruit Juice Beverages*. New York, NY: Marcel Dekker Inc, pp. 49–65.

Rouseff, R.L. (1988b). Liquid chromatographic determination of naringin and neohesperidin as a detector of grapefruit juice in orange juice. *Journal of the AOAC*, **71**(4), 798–802.

Rouseff, R.L. and Ting, S.V. (1979). Quantitation of polymetoxilated flavones in orange juice by high-performance liquid chromatography. *Journal of Chromatography*, **176**, 75–87.

Rouseff, R.L., Martin, S.F. and Youtsey, C.O. (1987). A quantitative survey of narirutin, naringin, hesperidin, and neohesperidin in citrus. *Journal of Agricultural and Food Chemistry*, **35**(6), 1027–1030.

Rouseff, R.L., Raley, L. and Hofsommer, H.J. (1996). Application of diode array detection with a C-30 reversed phase column for the separation and identification of saponified orange juice carotenoids. *Journal of Agricultural and Food Chemistry*, **44**(8), 2176–2181.

Saccani, G., Gherardi, S., Trifiro, A. *et al*. (1994). Determination of organic acid in fruit juices by ion chromatography. *Industrie delle Bevande*, **23**, 423–429.

Salivaras, E. and McCurdy, A.R. (1992). Detection of olive oil adulteration with canola oil from triacylglycerol analysis by reversed-phased high-performance liquid chromatography. *Journal of the American Oil Chemists' Society*, **69**(9), 935–938.

Sass-Kiss, A. and Hajós, G. (2005). Characteristic biogenic amine composition of Tokaji aszú-wines. *Acta Alimentaria*, **34**(3), 227–235.

Sass-Kiss, A., Szerdahelyi, E. and Hajós, G. (2000). Study of biologically active amines in grapes and wines by HPLC. *Chromatographia*, **51**, S316–S320.

Sass-Kiss, A., Szerdahelyi, E. and Hajós, G. (2005). The effect of *Botrytis cinerea* on the biogenic amine composition of grapes and aszu-wines. In: D.M.L. Morgan, F. Bauer and A. White (eds), COST Action 917 Biogenically Active Amines in Food, Vol. VII. Brussels: COST Action 917, pp. 204–209.

Schnüll, H. (1990). New analytical methods for determining the authenticity of fruit juice. *Flüssiges Obst*, **57**(1), 28–42.

Schoenmakers, P.J. (1986). *Optimization of Chromatographic Selectivity: A Guide to Method Development. Journal of Chromatography Library,* Vol. 35. Amsterdam: Elsevier Science Publishers B.V., pp. 1–113.

Segall, S.D., Artz, W.E., Raslan, D.S. *et al*. (2005a). Analysis of triacylglycerol isomers in Malaysian cocoa butter using HPLC-mass spectrometry. *Food Research International*, **38**(2), 167–174.

Segall, S.D., Artz, W.E., Raslan, D.S. *et al*. (2005b). Triacylglycerol composition of coffee beans (*Coffea canephora* P.) by reversed phase high-performance liquid chromatography and positive electrospray tandem mass spectroscopy. *Journal of Agricultural and Food Chemistry*, **53**(25), 9650–9655.

Sendra, J.M., Navarro, J.L. and Izquierdo, L. (1988). C18 solid phase isolation and high performance liquid chromatography/ultraviolet diode array determination of fully methoxylated flavones in citrus juices. *Journal of Chromatographic Science*, **26**(9), 443–448.

Sentandreu, E., Izquierdo, L. and Sendra, J.M. (2007). Differentiation of juices from clementine (*Citrus clementina*), clementine hybrids and satsuma (*Citrus unshiu*) cultivars by statistical multivariate discriminant analysis of their flavanone-7-O-glycosides and fully methoxylated flavones content as determined by liquid chromatography. *European Food Research and Technology*, **224**(4), 421–429.

Sharkasi, T.Y., Bendel, R.B. and Swanson, B.G. (1982). Dilution and solids adulteration of apple juice. *Journal of Food Quality*, **5**(1), 59–72.

Shui, G. and Leong, L.P. (2002). Separation and determination of organic acids and phenolic compounds in fruit juices and drinks by high-performance liquid chromatography. *Journal of Chromatography A*, **977**(1), 89–96.

Silva, B.M., Andrade, P.B., Mendes, G.C. *et al*. (2000). Analysis of phenolic compounds in the evaluation of commercial quince jam authenticity. *Journal of Agricultural and Food Chemistry*, **48**(7), 2853–2857.

Simpkins, W. and Harrison, M. (1995). The state of art in authenticity testing. *Trends in Food & Technology*, **6**(10), 321–328.

Simpson, C.F. (1982). Separation modes in HPLC. In: R. Macrae (ed.), *HPLC in Food Analysis*. New York, NY: Academic Press Inc, pp. 80–120.

Simpson, K.L., Katayama, T. and Chichester, C.O. (1981). Carotenoids in fish feeds. In: J.C. Bauernfeind (ed.), *Carotenoids as Colorant and Vitamin A Precursors. Technological and Nutritional Applications*. New York: Academic Press, pp. 463–538.

Smith, K.W., Perkins, J.M., Jeffrey, B.S.J. and Phillips, D.L. (1994). Separation of molecular species of cis- and trans-triacylglycerols in trans-hardened confectionary fats by silver-ion high-performance liquid chromatography. *Journal of the American Oil Chemists' Society*, **71**(11), 1219–1222.

Snyder, L.R. and Kirkland, J.J. (1974). *Introduction to Modern Liquid Chromatography*. New York, NY: John Wiley & Sons, Inc. Hungarian issue, Budapest: Műszaki Könyvkiadó, pp. 21–124.

Somers, T.C. (1971). The polymeric nature of wine pigments. *Phytochemistry*, **10**(9), 2175–2186.

Sontag, G. and Bernwieser, I. (1994). HPLC coupled with a coulometric electrode array detector. *Deutsche Lebensmittel-Rundschau*, **90**(3), 72–74.

Souci, S.W., Fachman, W. and Kraut, H. (2000). *Food Composition and Nutrition Tables*, 6th edn. Stuttgart: Medpharm ScientificPublishers, pp. 1075–1076.

Soufleros, E.H., Bouloumpasi, E., Tsarchopoulos, C. and Biliaderis, C.G. (2003). Primary amino acid profiles of Greek white wines and their use in classification according to variety, origin and vintage. *Food Chemistry*, **80**(2), 261–273.

Spanos, G.A. and Wrolstad, R.E. (1990a). Influence of variety, maturity, processing, and storage on phenolic composition of pear juice. *Journal of Agricultural and Food Chemistry*, **38**(3), 817–824.

Spanos, G.A. and Wrolstad, R.E. (1990b). Influence of processing and storage on the phenolic composition of Thompson seedless grape juice. *Journal of Agricultural and Food Chemistry*, **38**(7), 1565–1571.

Spanos, G.A. and Wrolstad, R.E. (1992). Phenolics of apples, pear, and white grapes juices and their changes with processing and storage. A-review. *Journal of Agricultural and Food Chemistry*, **40**(9), 1478–1487.

Swallow, K.W. and Low, N.H. (1990). Analysis and quantitation of the carbohydrates in honey using high-performance liquid chromatography. *Journal of Agricultural and Food Chemistry*, **38**(9), 1828–1832.

Swallow, K.W. and Low, N.H. (1994). Determination of honey authenticity by anion-exchange liquid chromatography. *Journal of the AOAC International*, **77**(3), 695–702.

Swallow, K.W., Low, N.H. and Petrus, D.R. (1991). Detection of orange juice adulteration with beet medium invert sugar using anion-exchange liquid chromatography with pulsed amperometric detection. *Journal of the Association of Official Analytical Chemists*, **74**(2), 314–345.

Tan, B. (1989). Palm carotenoids, tocopherols and tocotrienols. *Journal of the American Oil Chemists' Society*, **66**(6), 770–776.

Tanriöven, D. and Ekşi, A. (2005). Phenolic compounds in pear juice from different cultivars. *Food Chemistry*, **93**(1), 89–93.

Tattay, L. (2001). *A bor és az agrártermékek eredetvédelme* (Protection of Origin of Wines and Agricultural Products). Budapest: Mezőgazda Kiadó, p. 225.

Thavarajah, P. and Low, N.H. (2006). Adulteration of apple with pear juice: emphasis on major carbohydrates, proline, and arbutin. *Journal of Agricultural and Food Chemistry*, **54**(13), 4861–4867.

Tomás-Barberán, F.A., Ferreres, F., Garćia-Viguera, C. and Tomás-Lorente, F. (1993). Flavonoids in honey of different geographical origin. *Zeitschrift für Lebensmittel-Untersuchnung und -Forschung*, **196**, 38–44.

Tomás-Lorente, F., García-Viguera, C., Ferreres, F. and Tomás-Barberán, F.A. (1992). Phenolic compounds analysis in the determination of fruit jam genuineness. *Journal of Agricultural and Food Chemistry*, **40**(10), 1800–1804.

Torre, M., Cohen, M.E., Corzo, N. *et al*. (1996). Perfusion liquid chromatography of whey proteins. *Journal of Chromatography A*, **729**(1–2), 99–111.

Ulberth, F. and Buchgraber, M. (2003). Analytical platform to assess the authenticity of coca butter. *European Journal of Lipid Science and Technology*, **105**(1), 32–42.

Vasconcelos, A.M.P. and das Neves, H.J.C. (1989). Characterization of elementary wines of Vitis vinifera varieties by pattern recognition of free amino acid profiles. *Journal of Agricultural and Food Chemistry*, **37**(4), 931–937.

Veloso, A.C.A., Teixeira, N. and Ferreira, A.C.A. (2002). Separation and quantification of the major casein fractions by reversed-phase high-performance liquid chromatography and urea–polyacrylamide gel electrophoresis. Detection of milk adulterations. *Journal of Chromatography A*, **967**(2), 209–218.

Veloso, A.C.A., Teixeira, N., Peres, A.M. *et al*. (2004). Evaluation of cheese authenticity and proteolysis by HPLC and urea–polyacrylamide gel electrophoresis. *Food Chemistry*, **87**(2), 289–295.

Versari, A., Biesenbruch, S., Barbanti, D. *et al*. (1997). Effects of pectolytic enzymes on selected phenolic compounds in strawberry and raspberry juices. *Food Research International*, **30**(10), 811–817.

Villamiel, M., Arias, M., Corzo, N. and Olano, A. (1999). Use of different thermal indices to assess the quality of pasteurized milks. *Zeitschrift für Lebensmittel-Untersuchung und -Forschung*, **208**(3), 169–171.

Virtanen, S.A.M. and Lehtonen, P. (1999). Determination of synthetic colorants and natural carmine in wines. *Journal International des Sciences de la Vigne et du Vin*, **33**(3), 145–147.

Volitaki, A.J. and Kaminarides, S.E. (2001). Detection of bovine milk in bovine Halloumi cheese by HPLC analysis cheese caseins hydrolysed by plasmin. *Milchwissenschaft International*, **56**(4), 207–210.

Wade, R.L. (1992). New analytical methods in the USA for detecting fruit juice adulteration. *Flüssiges Obst*, **59**(2), 62–72.

Wald, B. and Galensa, R. (1989). Nachweis von Fruchtsaftmanipulation bei Apfel- und Birnensaft. *Zeitschrift für Lebensmittel-Untersuchnung und -Forschung*, **188**(2), 107–114.

Wallrauch, S. and Faethe, W. (1988). Amino acids: criteria for the evaluation of fruit juices. In: S. Nagy, J.A. Attaway and M.E. Rhodes (eds), *Adulteration of Fruit Juice Beverages*. New York, NY: Marcel Dekker Inc, pp. 21–48.

Wang, Y.C., Chuang, Y.C. and Ku, Y.H. (2007). Quantitation of bioactive compounds in citrus fruits cultivated in Taiwan. *Food Chemistry*, **102**(4), 1163–1171.

White, D.R., Jr. and Cancalon, P.E. (1992). Detection of beet sugar adulteration of orange juice by liquis chromatography/pulsed amperometric detection with column switching. *Journal of the AOAC International*, **75**(3), 584–587.

Widmer, W. (2000). Determination of naringin and neohesperidin in orange juice by liquid chromatography with UV detection to detect the presence of grapefruit juice: collaborative study. *Journal of the AOAC International*, **83**(5), 1155–1164.

Wrolstad, R.E., Culberston, J.D., Cronwell, C.J. and Mattick, L.R. (1982). Detection of adulteration in blackberry juice concentrates and wines. *Journal of the AOAC*, **65**(6), 1417–1423.

Wu, X. and Prior, R.L. (2005). Systematic identification and characterization of anthocyanins by HPLC-ESI-MS/MS in common foods in the United States: fruits and berries. *Journal of Agricultural and Food Chemistry*, **53**(7), 2589–2599.

Wudrich, G.G., McSheffrey, S. and Low, N.H. (1993). Liquid-chromatographic detection of a variety of inexpensive sweeteners added to pure orange juice. *Journal of the AOAC International*, **76**(2), 342–354.

Yao, L., Datta, N., Tomás-Barberán, F.A. *et al*. (2003). Flavonoids, phenolic acids and abscisic acid in Australian and New Zealand Leptospermum honeys. *Food Chemistry*, **81**(2), 159–168.

Yao, L., Jiang, Y., Singanusong, R. *et al*. (2005). Phenolic acids in Australian Melaleuca Guioca, Lhophostemon, Banksia and Helianthus honeys and their potential for floral authentication. *Food Research International*, **38**(6), 651–658.

Zabaras, D. and Gordon, M.H. (2004). Detection of pressed hazelnut oil in virgin olive oil by analysis of polar components: improvement and validation of the method. *Food Chemistry*, **84**(3), 475–483.

This page intentionally left blank

12

DNA-based Technique: Polymerase Chain Reaction (PCR)

Robert E. Levin

Introduction

Due to its sensitivity, specificity, simplicity, robust nature and speed compared with protein-based methods, the PCR appears to be the ideal assay for confirming the identity of and quantifying the species present in meat, dairy and marine food products, in addition to detecting and quantifying gene lines derived from genetically modified organisms (GMOs). Early methods for discrimination of species were based on DNA–DNA hybridization with specific probes. However, more recently, amplification of species-specific target DNA sequences via the PCR has proven to be a more sensitive and rapid technique. In addition, restriction analysis of resulting amplicons has allowed even greater discrimination. For those interested in DNA probes for meat species identification, the reader is referred to the review by Meyer and Candrian (1996), where this subject is presented in detail.

Gene sequences in mitochondrial DNA (mtDNA), particularly the mtCytochrome b gene (*Cytb*), are now commonly targeted for species identification. There are several advantages to the use of mt genes. Mammalian cells normally harbor 800–1000 mitochondria per cell, resulting in enhanced sensitivity of the PCR assays due to the inherent multicopy presence of mt genes. Also, mtDNA is considered to have evolved more rapidly than nuclear DNA and therefore represents greater sequence diversity, so as to facilitate the identification of closely related species (Brown

Modern Techniques for Food Authentication
ISBN: 978-0-12-374085-4

et al., 1993). In addition, the nucleotide sequences of the mt*Cytb* gene from a large number of animal species are available from GenBank. However, it is important to keep in mind that mitochondrial DNA is derived solely from the maternal progenitor of a given animal. For this reason, hybrids and hybrid species will be undetected as hybrids if only the mtDNA gene sequences are amplified. For detection of hybrid animal species, the use of *satellite fragment length polymorphism* (*SFLP*) on centromeric satellite DNA (usually satellite IV, satellite 1.711b or satellite 1.709) is used. Satellite DNA has the advantage in that it consists of tandem repeated sequences which become species-specific via the process of concerted evolution so as to reflect the progenitor history of the animal (Elder and Turner, 1995).

Species detection in final food products has become increasingly important with respect to food adulterated with less costly and less desirable or even objectionable species for health, economic, religious, esthetic or legal reasons. Allergic reactions to the presence of small amounts of specific species can result in intense and life-threatening anaphylactic symptoms. Individuals suffering from celiac disease are unable to tolerate even small quantities of gluten derived from wheat, barley or rye (Davidson and Bridges, 1987). The presence of GMO grain, with specific labeling indicating such, in the European Union (EU) is presently restricted to no more than 0.9%. All of these factors have contributed to the development of molecular techniques, in particular the PCR, for detecting small quantities of tissue derived from specific species or from specific varieties, strains or lines of a given species.

Universal primer systems for mt*Cytb* PCR can allow identification of several species within a single analysis. The PCR systems involving only short amplicons can be successful in identifying several species with the use of multiplex assays involving the simultaneous amplification of different amplicons with different pairs of primers for each species (Matsunaga *et al*., 1999). However, for restriction fragment length polymorphism analysis (RFLP), amplicons have to be larger so as to encompass one or more restriction sites. In processed food products, degradation of DNA to a few hundred base pairs, allowing only a short amplicon, may preclude restriction analysis.

Stability of DNA in foods

Most food products contain sufficient levels of DNA from the tissue of origin to allow detection and quantification as a result of the extreme sensitivity of the PCR if significant DNA degradation has not occurred and if PCR inhibitors have been removed. High molecular weight DNA (20–50 kbp) has been found to be readily isolated from fresh meat (Ebbehoj and Thompson, 1991). Refrigerated storage of raw meat resulted in degradation of the DNA to average lengths of 15–20 kbp. Heating meat to 121°C for 10 minutes before DNA extraction reduced the average length to 300 bp. DNA extracted from blood sausage has been found to be larger than 20 kbp (Candrian, 1994). However, DNA from salami was degraded to an average length of 100 bp to 15 kbp (Candrian, 1994). Interestingly, DNA isolated from bread was found to have an average length of 300 bp. Highly degraded DNA may still be amplified, as long as the average DNA strand is not less than the desired DNA sequence to be amplified (Meyer

and Candrian, 1996). This means that the smaller the amplicon, the larger will be the number of intact target sequences to be amplified. Conversely, the larger the amplicon, the fewer will be the number of intact target sequences, resulting in a much lower efficiency of detection. An amplicon of 60–80 bp is therefore ideal for detection of low levels of species-related DNA in foods that have undergone a significant level of degradation. This precludes the use of conventional PCR with resolution and visualization of the resulting amplicons using an agarose gel slab and ethidium bromide (EB) respectively. This limitation results from the fact that such small amplicons will electrophoretically migrate at or near the leading edge of migration along with transfer RNA, making molecular weight confirmation of the band difficult or impossible. However, real-time PCR is ideally suited to the amplification of target sequences of 60–80 bp in length and their quantification based on a standard curve.

Methods of DNA extraction from foods

Foods can be expected to contain a wide variety of PCR inhibitors, including complex polysaccharides (Lantz *et al*., 1997), hemoglobin (Ruano *et al*., 1992), urea (Khan *et al*., 1991), DNases in oysters (author's unpublished observation) and proteases in milk (Powell *et al*., 1994) and oysters (Blackstone *et al*., 2003). Presently, two methods are most frequently used for the extraction and purification of high-quality DNA from a wide variety of raw materials and food products. The CTAB method is based on a "classical" protocol for plant tissue. Food samples are incubated in the presence of the detergent *hexadecyltrimethyl-ammonium bromide* (*CTAB*), then extracted with chloroform, and the DNA is precipitated with isopropanol. The second involves the treatment of the food sample (usually meat) with proteinase K and SDS followed by the use of a DNA-binding silica resin (Wizard™, Promega Inc.) to purify the released DNA. Meyer (1999) has reviewed a variety of modifications of these two methods in addition to a number of alternative DNA extraction methods applied to foods.

Molecular techniques used to discriminate between similar species and strains

Random amplified polymorphic DNA (RAPD)

In conventional PCR, a known DNA sequence is amplified by using two primers. The first anneals to the 5′ end of the sequence on the A strand and is extended inward with *Taq* polymerase from the 3′ end of the primer, whereas the second anneals to the 3′ of the B strand and is also extended inward from the 3′ end (Figure 12.1). After the first cycle and denaturation, four target sequences are then available for duplication. The sequence is usually highly specific for the target gene.

With RAPD, a single random primer of about 10 nucleotides is used with no known target sequence being required, and the first round of amplification results in single

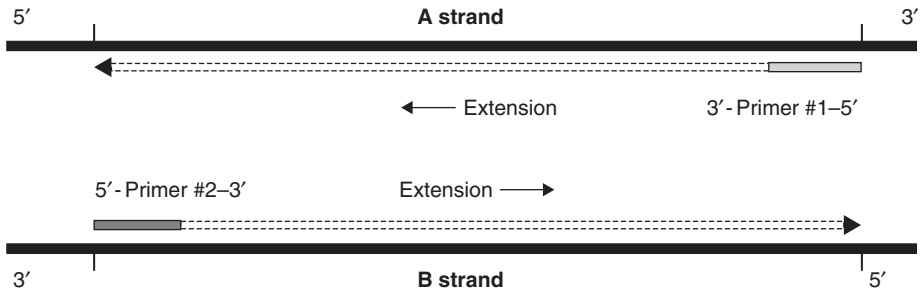

Figure 12.1 Amplification of a known target sequence with a pair of two different primers.

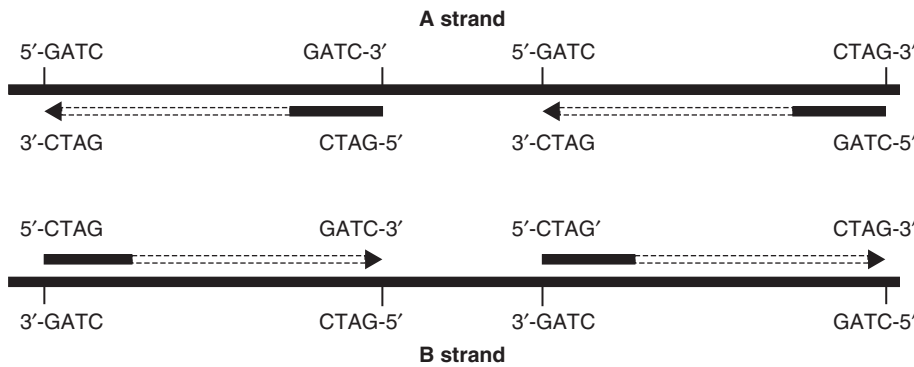

Figure 12.2 Random amplification of polymorphic DNA sequences with a single random primer.

strands having palindromatic termini (Figure 12.2) (Levin, 2003). The single randomly chosen primer targets specific but unknown sites in the genomic DNA, which are polymorphic (repeating) with respect to the terminal sequences that the single primer anneals to. During subsequent cycles a number of different target sequences are amplified, many of which will be of differing base-pair length so as to generate a variety of DNA bands, resulting in a specific DNA banding pattern for each species (Figure 12.3). The RAPD method is most frequently used for identifying identical clonal isolates of pathogenic bacteria involved in outbreaks or in sanitation studies (Soto *et al*., 1999; Tu *et al*., 2005). It has also been used successfully for distinguishing mammalian species (Koh *et al.*, 1998).

The ratio of primer to template in the RAPD reaction is critical. A hazy smear obscuring the amplified bands on the agarose gel is usually caused by failure to saturate the DNA template with primer. This is easily corrected by adjusting the ratio of primer to template.

Real-time PCR

Real-time PCR refers to the detection of PCR-amplified target DNA (amplicons) usually after each PCR cycle. The signal is readily followed on a computer screen, where each point is automatically plotted and the extent of amplification is followed as an

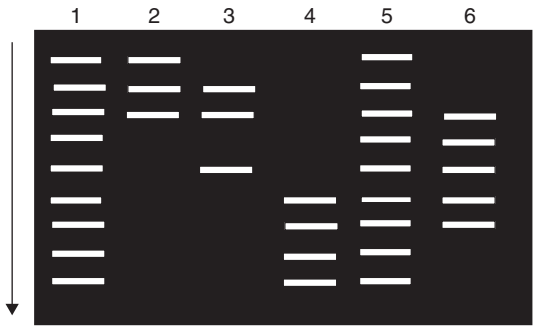

Figure 12.3 RAPD DNA banding patterns of distinguishable strains of the same species. Strains corresponding to lanes 1 and 5 have identical banding patterns and are therefore considered of identical clonal origin. Strains corresponding to lanes 2, 3, 4 and 6 are distinguishable from each of the other five strains on the basis of DNA banding patterns.

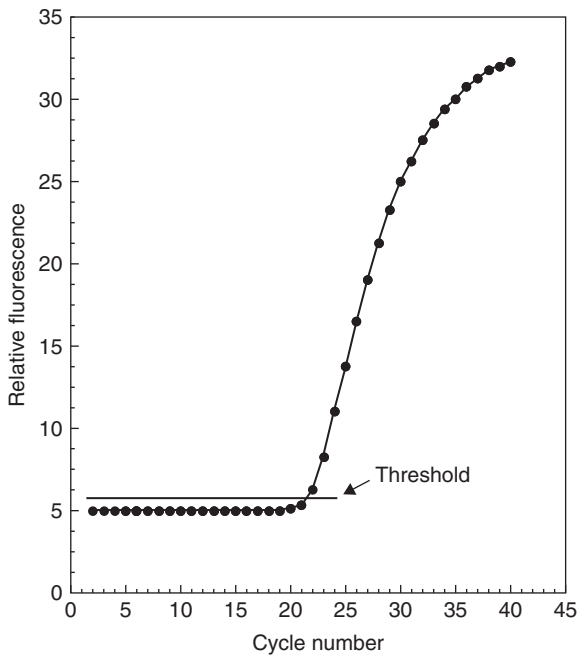

Figure 12.4 Real-time PCR amplification profile derived from a single PCR reaction.

ongoing continual direct graphical plot (Figure 12.4). Computer software handles all of the preprogrammed calculations and plotting of data. Conventional thermocyclers often require 2 to 3 hours to complete 35–40 "thermal" cycles. Much of this time is consumed by the "ramp" time required to traverse from one temperature to another. Real-time PCR units offer a number of advantages compared to conventional PCR. The incorporation of air heating and cooling, capillary sample systems and thermoelectrically controlled blocks have greatly reduced ramp times. The use of shortened target DNA sequences (60–70 bp) in real-time PCR results in more efficient

amplification than standard PCR, where amplicons are required to be at least 200 bp in length to allow detection in agarose gels, and also allows reduced extension times. In addition, conventional PCR requires visualization of amplified products after agarose gel electrophoresis, which usually involves an additional 30 to 60 minutes. Real-time PCR completely eliminates this step through the use of a fluorometer built into the real-time PCR thermal cycler that measures the intensity of fluorescence after each amplification cycle. Real-time PCR systems also allow the option of programmed generation of a thermal denaturation curve of the amplified product after the PCR that allows automatic calculation of the thermal denaturation temperature (Tm) value of the amplicon when SYBR Green is the fluorescent reporter molecule. This is most useful in confirming the identity of an amplicon.

The quantitative range with conventional PCR is no more than 1.5 to 2.0 log cycles, whereas with real-time PCR an operational range of at least 5 to 6 log cycles is usually achieved. Because of the significantly increased cost of reagents, particularly the fluorescent probes and dyes, compared with reagents used with conventional PCR, the reaction volume is usually reduced to 10–20 µl.

In addition to detection of amplicons, real-time PCR units can quantify amplified target DNA and differentiate amplicons with point mutation or sequence variation. Sequence variation can be assessed on the basis of Tm variations derived from the analysis of melting curves of duplexes formed by fluorescent probes and amplicons. An additional advantage of real-time PCR is that two or more different PCR reactions (multiplex real-time PCR) amplifying different target sequences can be followed and quantified in the same PCR tube.

Real-time PCR depends on the emission of an ultraviolet (UV)-induced fluorescent signal that is proportional to the quantity of DNA that has been synthesized. Several fluorescent systems have been developed for this purpose. The simplest, least expensive and most direct fluorescent system for real-time PCR involves the incorporation of the dye *SYBR Green*, whose fluorescence under UV greatly increases when bound to the minor groove of double-helical DNA. SYBR Green lacks the specificity of fluorescent DNA probes, but has the advantage of allowing a DNA melting curve to be generated and software calculation of the Tm of the amplicon after the PCR. This allows identification of the amplified product and its differentiation from primer dimers which also result in a fluorescent signal with SYBR Green but usually have a lower Tm value. The fluorescent signal is measured immediately after the extension step of each cycle, since thermal denaturation yielding single-stranded DNA eliminates fluorescence with SYBR green. A software plot of the negative first derivative of the thermal denaturation plot yields a bell-shaped symmetrical curve, the mid-point of which yields the Tm value for the amplified product (Figure 12.5). Interference of the amplicons signal by the signal resulting from primer-dimer formation can be eliminated by raising the temperature to a critical point that is above the Tm of the primer-dimer formed (resulting in thermal denaturation of the primer-dimers) but below the Tm of the amplicons prior to measuring the intensity of florescence emission.

The use of custom-synthesized dual-labeled probes allows multiplex real-time PCR assays. Such dual-labeled probes harbor a *fluorophore* (fluorescent emitter dye)

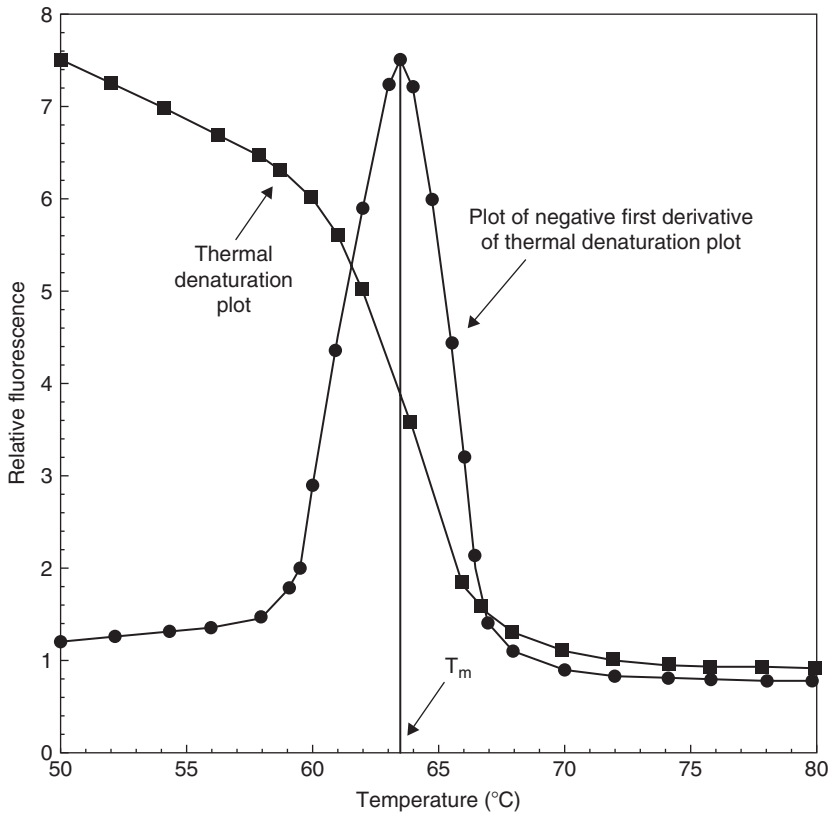

Figure 12.5 Determination of Tm value from thermal denaturation plot of an amplicon involving SYBR Green and real-time PCR.

at the 5′-end and a quencher dye at the 3′-end, which are close enough to prevent emitted fluorescence of the emitter. During primer extension, *Taq* polymerase cleaves the probe from the 5′ to the 3′ direction, releasing the reporter dye, which then emits fluorescence as a result of its increased distance from the quencher. Fluorescence is then measured following each extension stage of every cycle. Increasing amounts of the single-stranded amplicons will bind increasing amounts of the probe. The various types of probes that are available for real-time PCR have been previously described in detail (Levin, 2004).

With quantitative real-time PCR, the software calculates a value termed ΔRn or ΔRQ from the following: $\Delta Rn = (Rn^+)P - (Rn^-)$, where Rn^+ = emission intensity of reporter/emission intensity of the quencher at any given time in a reaction tube, and Rn^- = emission intensity of reporter/emission intensity of quencher measured prior to PCR amplification in the same reaction tube (Heid *et al*., 1996). The ΔRn mean values are plotted on the Y-axis and the number of cycles is plotted on the X-axis. During the early cycles, the ΔRn remains at base line. When a sufficient amount of hybridization probe has been cleaved by the 5-nuclease activity of *Taq* polymerase, the intensity of reporter fluorescence emission increases to a detectable level. A threshold level of

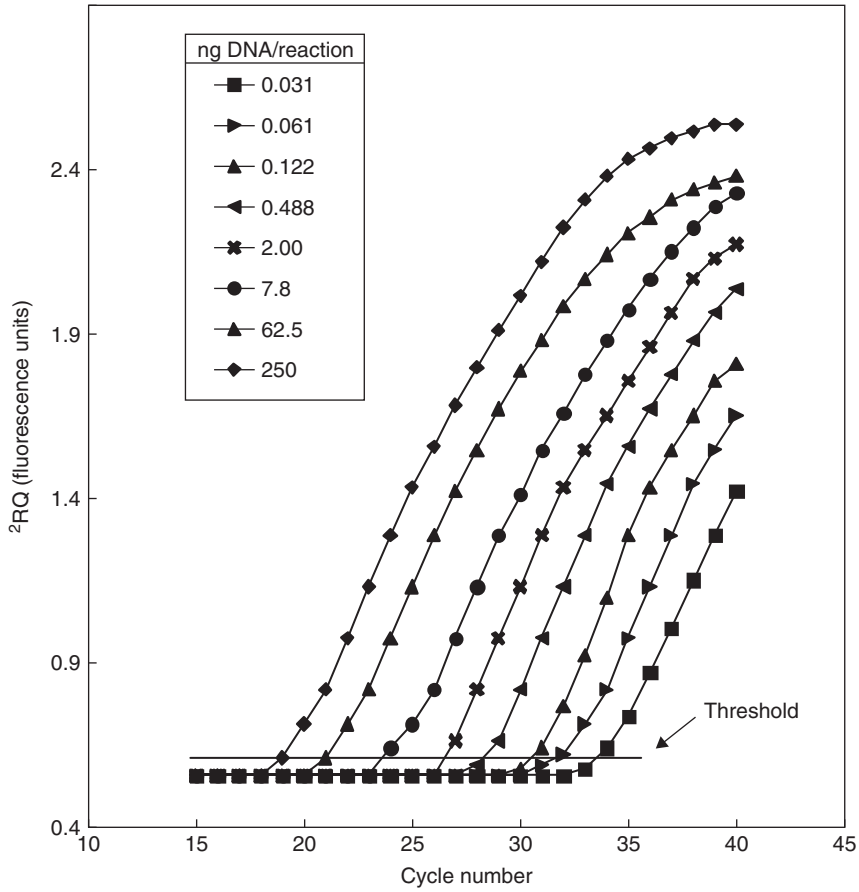

Figure 12.6 Real-time PCR profiles of amplification of different starting quantities of target DNA.

emission above the base line is selected, and the point at which the amplification plot crosses the threshold is defined as the Ct value and represents the number of cycles at which the log phase of product accumulation is initiated or first detected (Figure 12.4). The threshold is usually set at 10 times the standard deviation (SD) of the base line. By setting up a series of wells containing a 4 to 5 log span of genomic DNA concentrations, a series of amplification plots is generated by the software in real-time (Figure 12.6). The amplification plots shift to the right as the quantity of input target DNA is reduced. Note that the flattened slopes and early plateaus do not influence the calculated Ct values. The Ct values decrease linearly with increasing target quantity. A plot of the resulting Ct values on the Y axis versus the log of the ng of input genomic DNA yields a straight line (Figure 12.7), which is then used as a standard curve for quantitation of samples with unknown levels of genomic DNA. This approach and the original nomenclature of Heid *et al*. (1996) have been universally adapted for quantitative PCR.

Real-time PCR assays utilizing SYBR Green are usually not suitable for multiplex amplification because the emission spectrum of SYBR Green is identical for all

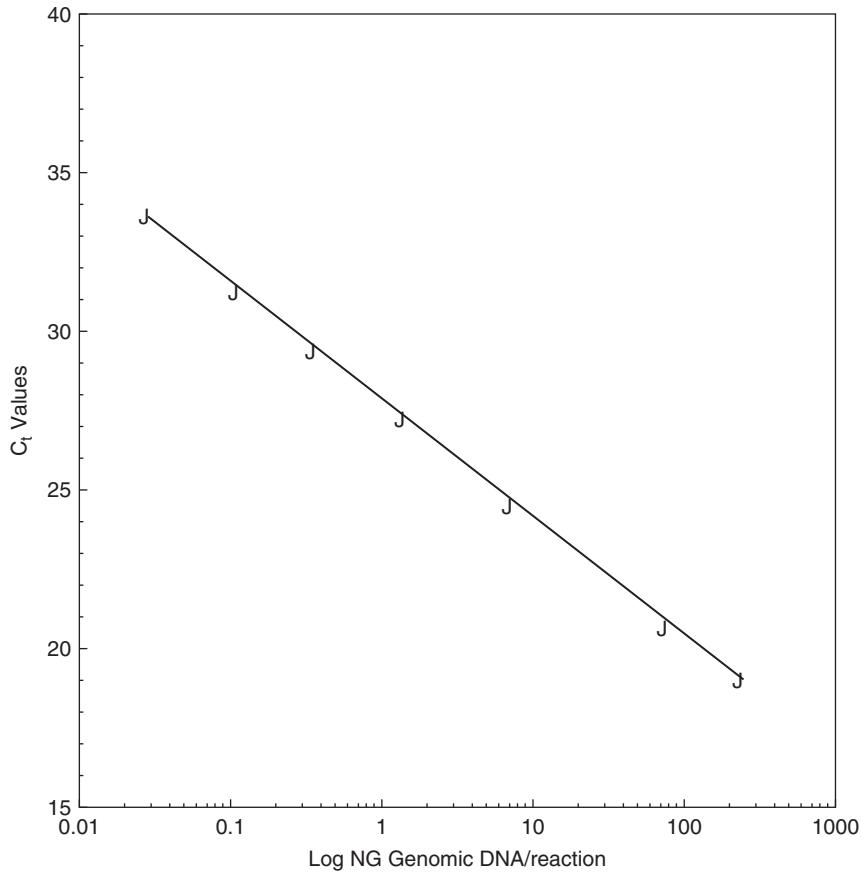

Figure 12.7 Standard curve for real-time PCR relating C_T values to log ng of genomic targets.

amplicons. However, the software program accompanying real-time PCR analytical systems is able to generate peak Tm values by plotting the negative first derivative of each amplicon's distinct melting curve. Hernández *et al*. (2003) exploited this feature of SYBR Green for distinguishing the multiplex derived amplicons from several GM strains of maize.

Nested PCR assays

There are two forms of nested PCR assays; fully nested and semi-nested. *Fully-nested PCR* assays involve the initial use of a pair of external primers that amplify the entirety of the target sequence to yield a primary amplicon. In a second PCR amplification, an internal pair of primers is utilized that amplifies a target sequence internal to both ends of the initial amplicon (Figure 12.8). The internal or nested PCR, in being applied to the product of the external primers, greatly increases both sensitivity of detection and specificity. With the *semi-nested PCR* assay, an initial pair of external primers is utilized to again yield a primary amplicon. The secondary

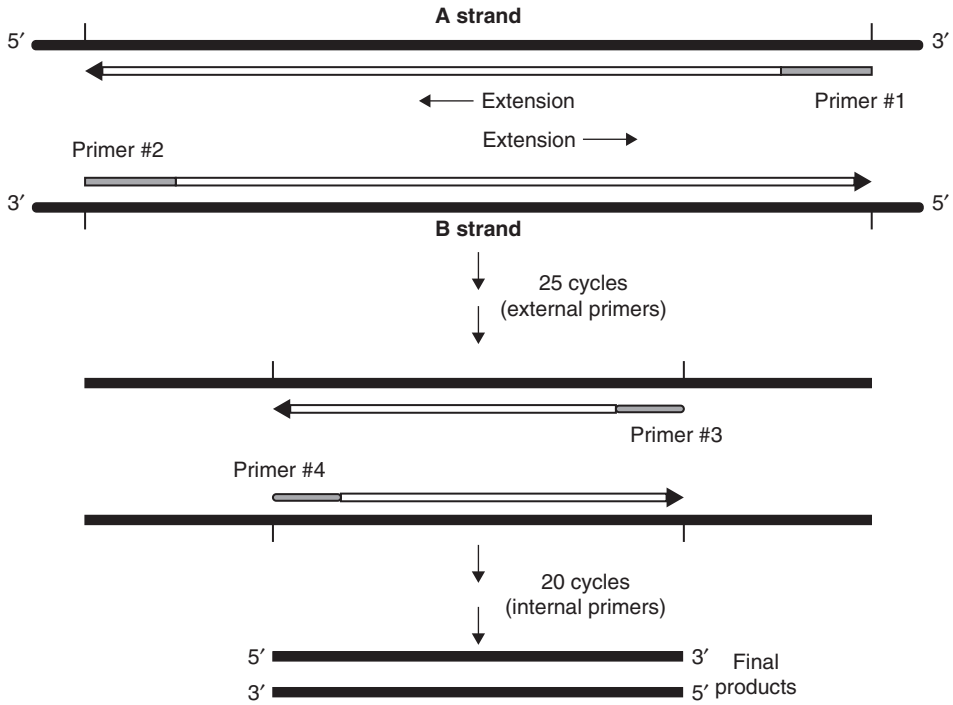

Figure 12.8 Two-tube nested PCR. Amplification with external primers for 25 cycles followed by amplification of an aliquot for 20 cycles using internal nested primers.

pair of primers consists of either the initial forward or initial reverse primer used in conjunction with an opposing internal primer so that the resulting secondary amplicon has only one end internal to the initial amplicon. The use of two pairs of primers spanning the boundary of two or three genetic elements is regarded as sufficiently specific for detection and identification of a specific GMO strain or line.

Quantitative competitive PCR (QC-PCR) for determining the percent of a species present in a mixture

In using the PCR for quantification of a specific species in a mixture, an important consideration is the partial inhibition of the PCR derived from trace tissue components which will result in an erroneously low estimate of the level of the target species. One approach to overcome this problem is to use an internal standard for competitive PCR. The advantage of competitive PCR is that it automatically corrects for partial PCR inhibition. *Quantitative competitive PCR* (*QC-PCR*) was first described by Gilliland *et al*. (1990). Wolf and Lüthy (2001) were the first to apply it to the quantitative detection of animal species in food products. A competitive DNA sequence is synthesized by the PCR that is either 30–50 bp larger or shorter than the target sequence to be co-amplified, so as to allow both amplicon bands to be distinguished on an agarose gel. The internal standard (IS) is constructed so that its 5′ and

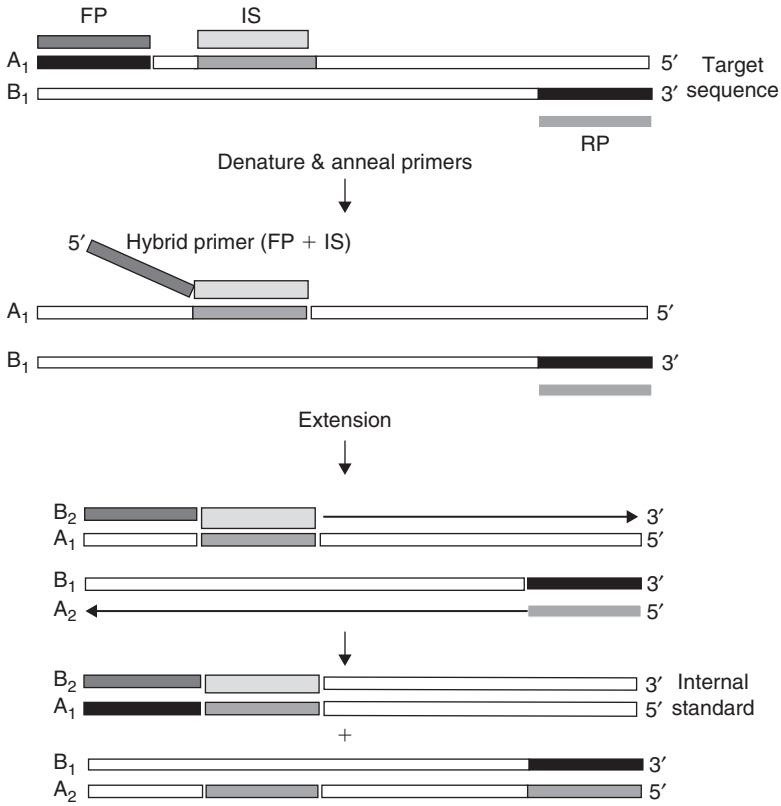

Figure 12.9 Protocol for PCR synthesis of internal competitive PCR standard.

3′ terminal sequences are homologous to the primer pair to be used to simultaneously amplify the target sequence (TS) (Figure 12.9). A uniform standard amount of the IS is added to each PCR assay tube in a series containing varying amounts of the TS. During the co-amplification with the single pair of primers, partial inhibition of the PCR during annealing of the primers and their extension will occur to the same extent with respect to amplification of both the TS and IS. This results in the ratio of the intensity of both bands in an ethidium bromide agarose gel remaining constant for a given percent of the species in the sample with partial PCR inhibition. A standard curve is then derived by plotting the log of the ratio of fluorescent intensity (TS/IS) against the log of the amount of the target species added to a mixed sample. The precise numerical level of fluorescent intensity of each band is determined by photographing the gel and using the public domain NIH Image 1.61 software program. The resulting fluorescent agarose bands from an unknown sample are similarly photoanalyzed and the quantity of the species in the mixed sample determined from the ratio of numerical fluorescence of TS/IS from the standard curve (Wang and Levin, 2005). Alternatively, if an approximate percent content of the target species is satisfactory, visual inspection of the relative band intensities to identify the equivalence point (Figure 12.10) can be used as described by Wolf and Lüthy (2001).

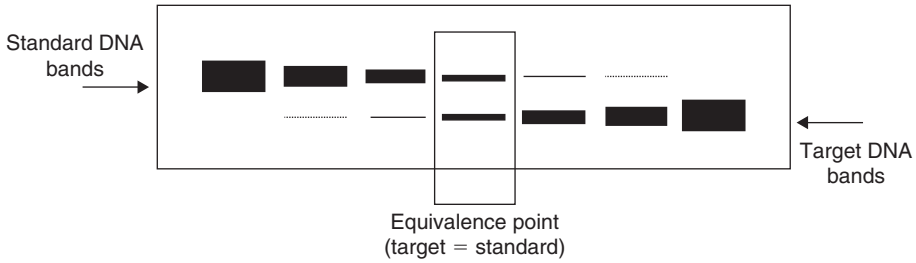

Figure 12.10 Agarose gel resolution of constant amount of internal competitive PCR standard and variable amounts of target DNA illustrating equivalence point.

Restriction fragment length polymorphism (RFLP)

Restriction fragment length polymorphism (*RFLP*) is a technique in which species may be differentiated by analysis of patterns derived from cleavage of their DNA by restriction nucleases. If two species differ in the distance between sites of cleavage by a particular restriction endonuclease, the length of the fragments produced will differ when the DNA is digested with such a restriction enzyme. The differences of the patterns generated can be used to differentiate species (and even strains) from one another. DNA is first extracted from tissue and purified. The PCR amplification of a sequence from a gene, such as that of mitochondrial 12S ribosomal RNA (mt12S rRNA), is then undertaken. The resulting amplicon is then cleaved with one or more restriction endonucleases and the resulting segments resolved by agarose electrophoresis with visualization of the DNA bands with EB.

PCR-single strand conformation polymorphism (PCR-SSCP)

PCR-single strand conformation polymorphism (*SSCP*) involves PCR amplification of a sequence from a suitable gene (usually the mt*Cytb* gene) followed by denaturation and electrophoresis of the resulting single-stranded DNA (ssDNA) through a non-denaturing polyacrylamide gel, and visualization of a limiting number of DNA bands. Under appropriate conditions, especially low temperature and non-denaturing conditions, single DNA strands fold into structures that migrate according to their shape. DNA strands of different sequence usually do not assume the same shape, and therefore have distinct gel mobilities. These mobility differences are based primarily on tertiary rather than secondary DNA structure (Liu *et al*., 1999). It should be noted that interaction between residual PCR primers and ssDNAs may occur, resulting in the formation of mixed bands (Cai and Touitou 1993; Kasuga *et al*., 1995). The sensitivity of the technique is inversely proportional to the size of the fragment. Single base-pair differences are generally resolved 99% of the time for 100- to 300-bp fragments, while with 400-bp fragments the resolution of single base-pair differences occurs at least 80% of the time (Sunnucks *et al*., 2000). Conformational changes and migration of ssDNA are influenced by the size of PCR fragments, the electrophoresis temperature, the percentage of polyacrylamide, the ratio of acrylamide to bis-acrylamide, and the

ionic strength of the electrophoresis buffer (Miterski *et al*., 2000). The technique is sensitive enough to detect one base exchange or a few differences in short (100- to 140-bp) DNA fragments (Hayashi, 1996). In addition, PCR-SSCP can also be used to identify fish species in mixed products, with very distinct patterns usually consisting of fewer bands than RAPD (Rehbein *et al*., 1999). Since EB does not stain ssDNA well, staining with silver or gold stains is commonly used in addition to autoradiography involving the labeling of the amplified DNA with a ^{32}P-labeled dNTP.

Amplified fragment length polymorphism (AFLP)

Amplified fragment length polymorphism (*AFLP*) is PCR-based, and results in the development of DNA banding profiles. However, it differs from RAPD and RFLP in that it involves initial restriction of genomic DNA, followed by ligation of adaptors complementary to the restriction sites and selective PCR amplification of a subset of the adapted restriction fragments. These fragments are then visualized on denaturing polyacrylamide gels by labeling one of the primers. Its greatest advantage is in its sensitivity to detect genomic polymorphism. Vos *et al*. (1995) have presented the mechanism in detail. Target DNA is prepared by first digesting to completion 50–200 ng of purified genomic DNA, with two restriction enzymes, one such as *Eco*RI (6-bp recognition sequence) that results in few restriction cuts and one such as *Mse*I (4-bp recognition sequences) that results in a large number of restriction cuts. The frequent cutter will generate small DNA fragments, while the rare cutter reduces the number of fragments to be amplified, since only the rare cutter/frequent cutter fragments are amplified. This in turn limits the number of selective nucleotides needed for selective amplification. In addition, the use of two restriction enzymes makes it possible to label one strand of the double-stranded PCR (dsPCR) products, which prevents "doublets" on the gel due to unequal mobility of the two amplified strands.

Restriction of genomic DNA with *Eco*RI and *Mse*I will result in three classes of restriction fragments, *Mse*I−*Mse*I fragments (>90%), *Eco*RI−*Mse*I fragments and *Eco*RI−*Eco*RI fragments. The *Eco*RI−*Mse*I fragments (several thousand) will be about twice the number of *Eco*RI restriction sites, and a small number will be *Eco*RI−*Eco*RI fragments. Following restriction, an *Eco*RI adapter and an *Mse*I adapter are added with T4 DNA ligase (Figure 12.11). AFLP adapters are comprised of a core sequence and a restriction enzyme-specific sequence. The structure of the *Eco*RI-adapter is:

5′-CTCGTAGACTGCGTACC
CATCTGACGCATGGTTAA-5′

The structure of the *Mse*I-adapter is:

5′-GACGATGAGTCCYGAG
TACTCAGGACTCAT-5′

For PCR amplification of only the *Eco*RI − *Mse*I fragments, *Eco*RI and *Mse*I primers are used simultaneously in a PCR (Figure 12.11). The AFLP primers consist of three parts; a core sequence, a restriction enzyme specific sequence (ENZ), and

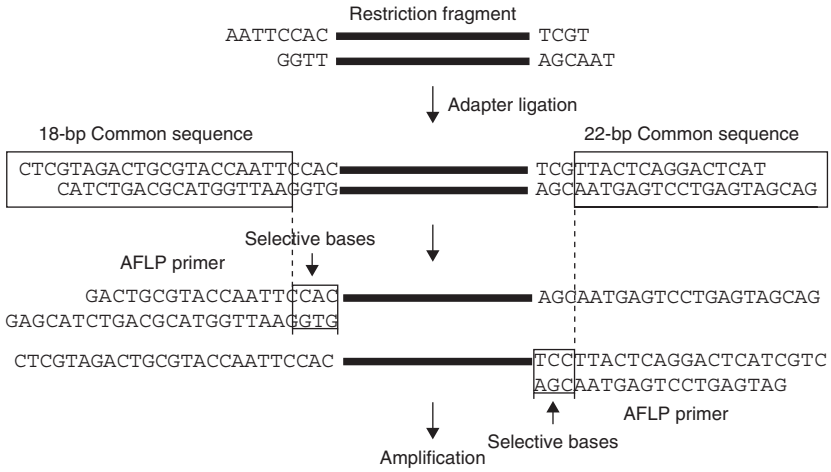

Figure 12.11 Diagrammatic representation of the AFLP technique. Redrawn from Vos *et al.* (1995), with permission.

a selective extension (EXT) of usually one to three nucleotides chosen by the investigator which extend into the unknown portion of the fragment, thereby reducing the number of fragments amplified. This is illustrated below for *Eco*RI and *Mse*I primers with three selective nucleotides (NNN):

	CORE	ENZ	EXT
*Eco*RI	5′-GACTGCGTACC	AATTC	NNN-3′
*Mse*I	5′-GATGAGTCCTGAG	TAA	NNN-3

With the first PCR only one selective extension nucleotide is used, which results in amplification of ~1/16 of all *Eco*RI−*Mse*I fragments. The PCR products are then diluted 10-fold and the PCR repeated with the same primers containing three selective nucleotides (Figure 12.11), which results in amplification of ~1/4000 of the *Eco*RI−*Mse*I fragments. If the *Eco*RI primer is labeled in the second PCR, then only the restriction fragments with an *Eco*RI site will be detected.

The two-step PCR results in reduction of background smears and large amounts of template DNA, allowing many gel banding profile comparisons. The final amplicons are thermally denatured and subjected to electrophoresis in 10% polyacrylamide denaturing gel electrophoresis. The AFLP procedure typically detects more polymorphism per reaction than RFLP or RAPD analysis. Any combination of infrequent/frequent cutting restriction nucleases can be used for generating large numbers of banding profiles among disparate samples.

An important aspect of the AFLP procedure is that adding selective nucleotides to the primers reduces the number of bands about four-fold with each selective nucleotide. Another important feature of the technique is that all primers start with

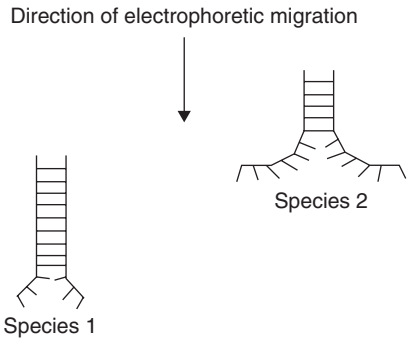

Figure 12.12 DGGE example. DNA denaturation of 16S rDNA segments of equal length but differing in nucleotide sequence from two distinct species. Direction of electrophoretic migration is parallel to an increasing denaturant polyacrylamide gel.

a 5′-guanine (G) residue so as to prevent double bands. The AFLP procedure has been found to be insensitive to the amount of template DNA, with the exception of extremely low or extremely high DNA concentrations (Vos *et al*., (1995).

Denaturing gradient gel electrophoresis (DGGE)

Denaturing gradient gel electrophoresis (*DGGE*) separates DNA fragments of the same length on the basis of differences in base-pair sequences, and is capable of distinguishing single base changes in a segment of DNA. It is usually applied to a mixture of 16S RNA gene fragments amplified by the PCR using a common pair of primers from samples containing more than one species. With the use of a denaturing gradient acrylamide gel, double-stranded DNA is subjected to electrophoretic migration in an increasing denaturant environment. This results in discrete segments undergoing "melting" or denaturation, referred to as "melting domains". When the Tm of the lowest melting domain is reached, the DNA will become partially denatured, creating branched or Y-shaped molecules at the leading end (Figure 12.12). Partial denaturation of the DNA reduces its mobility in the gel. Since the Tm of a particular melting domain is sequence-specific, the presence of one or more base-pair differences will alter the melting profile of that DNA when compared to the same DNA fragment from another species. Variations in DNA sequence of two species will therefore result in variable mobility shifts at different positions in the gel. If a fragment completely denatures, its migration becomes a function of size. In a typical DGGE system, the temperature is held constant and the denaturing environment is created by a linear denaturing gradient formed with urea and formamide. A solution of 100% denaturant consists of 7 M urea and 40% formamide. Usually a gradient of 0 to 100% denaturant is prepared in a 6 to 10% polyacrylamide. The concentration of the polyacrylamide is dependent on the size of the fragment. With the gradient parallel to the electric field, different species will form distinguishable bands. Each band in a DGGE gel is believed to represent a single species.

Species-specific PCR assays

Genetically modified organisms (GMOs)

Genetic and biological characteristics of GMOs

A *genetically modified organism* (*GMO*) is usually defined as a living organism whose genetic composition has been altered by the insertion of a new gene encoding a desired protein that is expressed. A typical insert (gene construct or *cassette*) in a GMO is composed of at least three elements: (i) the *promoter*, which functions as an on/off switch for reading of the inserted gene; (ii) the gene that has been inserted and that encodes the desired protein, and (iii) the *terminator*, which functions as a stop signal for reading of the inserted cassette. A gene construct or cassette must be integrated into the genome of the organism to become stably inherited.

At present, the PCR is the most commonly used DNA-based method for detection of GMOs and involves amplification of specific DNA sequences that are unique to GMOs. Subsequent agarose gel electrophoresis (AGE) allows the detection, quantification and size of the resulting amplified target sequence (amplicon) to be estimated. The identity of the amplicon may be further verified by DNA sequencing or digestion of the PCR product with restriction endonucleases (RFLP) followed by fragment analysis with AGE. Real-time PCR is presently considered the most reliable method for quantification of GMOs (Miraglia *et al*., 2004).

Molecular methods for detection of GMOs

A variety of methods, such as PCR, PCR-RFLP, Southern hybridization, DNA sequencing, real-time quantitative PCR, PCR biosensor technology, microarray technology and peptide nucleic acid (PNA) clamping, have all been utilized to increase the specificity of GMO analysis. Detection of GMOs is limited to foods and food products in which sufficient intact DNA is present for detection. In general, no DNA is detectable in highly heat-treated food products, hydrolyzed plant protein (e.g. soya sauce), purified lecithin, starch derivatives (e.g. maltodextrin, glucose syrup) and refined chemical substances such as refined soya oil (Meyer, 1999). All of the above techniques involve PCR to amplify specific DNA target sequences from GMOs, which are discussed in detail below with specific examples.

The transgenic cassette

GMOs are biological species whose genomes have been modified by the introduction of an exogenous gene able to express an additional protein that confers new characteristics. The foreign gene is usually inserted into a gene "cassette" consisting of an expression promoter (P), a structural gene encoding the new protein, and an expression terminator sequence (T). Two of the frequently utilized sequences for genetically modified (GM) grains and fruits commonly inserted into most of the available transgenic products are the promoter of the 35S subunit of rRNA cauliflower mosaic virus (CaMVX35S) and the nopaline synthase (NOS) terminator (NOS-T) from the plant pathogenic bacterium *Agrobacterium tumefaciens*. The two proteins most

frequently encoded by genetic inserts in GMOs are the Cry protein and the enzyme 5-enolpyruvylshikimate-3-phosphate synthase (EPSPS), discussed below.

Bt GMOs

Transgenic Bt corn contains genetic material from the soil-borne bacterium *Bacillus thuringiensis* (Bt). During spore formation, Bt produces a crystal-like or "Cry" protein which, when ingested by susceptible larvae, particularly of the order Lepidoptera such as the European corn borer, disrupts the intestinal wall, resulting in death. The Cry protein is known as the *delta toxin*, is completely harmless to all mammals and is encoded by the *CryIA(b) (Cry)* gene. The insecticidal effects of sprayed application of Bt cultures to field crops is of short duration, usually dissipating within about 2 weeks due to UV, heat, dryness or oxidation. Transgenic corn plants producing their own Cry protein circumvent these problems with no need for field application.

EPSPS GMOs

Glyphosate is a general herbicide applied to food and non-food field crops such as soybeans, field corn and hay for the destruction of weeds. Glyphosate controls weeds by inhibiting the enzyme EPSP synthase necessary for plant growth. EPSP synthase-resistant GMOs contain the gene encoding CP4 EPSP synthase derived from a soil bacterium (*Agrobacterium* sp., strain CP4). This gene produces an enzyme (EPSPS) that is functionally identical to plant EPSP synthase but which is not inhibited by glyphosate, allowing GMO field crops containing the gene insert to be sprayed with glyphosate for weed control.

Specificity of PCR-based GMO detection methods

PCR-based GMO assays can be divided into four levels of specificity (Miraglia *et al*., 2004). "Screening" methods are the least specific, and usually relate to target DNA sequences such as promoters and terminators that are commonly present in most GMOs. The second level of sensitivity normally targets a sequence of the protein-encoding gene. Examples are the EPSPS gene coding for tolerance to the general herbicide glyphosate and the Bt gene coding for the delta toxin of *Bacillus thuringiensis*, imparting resistance to certain insects. The third level of specificity involves the junctions between two DNA elements in a cassette, such as the promoter and the protein-encoding gene. These methods target DNA sequence junctions not present in natural genomes. Different GMOs, however, may share the same promoter and protein-encoding gene. The fourth and highest level of specificity occurs when the target sequence is derived from the junction between the inserted cassette and the recipient genome, and is referred to as an *event-specific method*.

It is important to recognize that the high level of sensitivity of molecular techniques such as PCR can result in the detection of low levels of inadvertent GMO contamination. Such contamination may result from cross-fertilization with maize pollen in fields, or cross-contamination of crops with dust during harvesting, transportation, milling and food processing. In addition, false-positive results from PCR

assays targeting the P-35S, nos 3′, and *npt*II sequences may be due to infection of food plants by tobacco mosaic virus (CaMV) or contamination by microorganisms such as the soil bacterium *Agrobacterium tumefaciens* containing the *nos* or *npt*II target sequences. An additional limitation of the PCR in identifying specific GMO strains occurs when cross-breeding between two GMO strains occurs, which results in "stacked genes" when, for example, an insect-resistant GMO strain is combined with a herbicide-tolerant GMO. Both cassettes may reside on different chromosomes. Quantitative PCR cannot distinguish between the gene-stacked GMO and a mixture of the two parental GMOs (Miraglia *et al*., 2004).

Applications of PCR methodology for detection of GMOs

The GM corn Bt11 expresses a 6.3-kbp DNA sequence containing the *Bacillus thuringiensis (Bt)* transgene coding for the cryIA(b) delta-endotoxin which imparts resistance of the Br11-corn strain against lepidopteron insects, especially the European corn borer. In addition, the strain also harbors a pat transgene for tolerance to the non-selective herbicide *phosphinothricin* (*PPT*). Zimmerman *et al*. (2000) reported on the development of a competitive quantitative PCR assay for Bt11 involving the genomic sequence at the 5′-site of the integrated transgenic sequence. The inverse PCR (iPCR) used employed a pair of primers that amplified a 207-bp sequence comprised mostly of the transgenic vector but extended by 11 nucleotides into the genomic integration site so as to avoid amplification of the repeated GM DNA in the corn genome. The assay was capable of detecting 1% Bt11-DNA. The assay system overcomes two problems involved in the application of conventional PCR for quantification of GMOs; the first encompasses different copy numbers of integrated constructs in different GMOs, and the second involves different GMOs containing identical transgenic constructs. In addition, the amplification of only one integrated target results in highly accurate quantification, independent of how many constructs being integrated into the genome. The utilization of iPCR allowed amplification of unknown sequences without cloning. The competitive PCR was calibrated to a 1% GMO content by performing the competitive PCR with a constant level of a 1% mixture of Bt11 with varying levels of competitor DNA to obtain a visual equivalence point whereby a 1% level results in equivalent band intensity from a known quantity of competitive DNA. The resulting inverted PCR system amplified DNA only from Bt11 corn yielding the 207-bp amplicon, whereas conventional corn as well as BT176, MaiseGard™, and LibertyLinkTM T25 failed to yield amplicons. The assay is therefore highly specific for the quantitative detection of only the Bt11 corn strain.

Rapid quantitative real-time PCR methodology was developed by Vaïtilingom *et al*. (1999) for detection of *Maximizer maize event 176* and *Rounded Ready*™ soy and soybeans in foods. For each GMO, two PCR primer systems were used, one for the total detection of maize or soybean (endogenous PCR systems) and the other for specific detection of the GMO. For maize, the endogenous PCR system amplified a 69-bp sequence of the 10-kdalt *zein* gene and the transgenic PCR system amplified a 105-bp sequence of the *cryIA(b)* gene. For soybean, the endogenous PCR system amplified an 81-bp sequence of the *Le1* lectin gene and the transgenic system amplified

a 146-bp sequence of the CP4 *EPSPS* gene. Endogenous probes were labeled with the fluorescent reporter dye tetrachloro-6-carboxyfluorescein (TET) at the 5′-end and the transgenic probes with 6-carboxyfluorescein (FAM) at the 5′-end. The fluorescent quencher dye 6-carboxy-N,N,N′,N′-tetramethylrhodamine (TAMRA) was used to label the 3′-ends of the probes. The PCR reactions utilized multiplex systems comprised of the maize endogenous and transgenic primer pairs in the same PCR tube. A similar strategy was used for soybean; 0.01% transgenic DNA could be detected, and 2 pg of total or transgenic DNA per gram of starting material could be detected, which is at least 10-fold more sensitive in GMO detection than the quantitative competitive PCR reported by Stüder *et al*. (1998). The real-time PCR assays required only 3 hours after DNA extraction.

Wurz *et al*. (1999) developed two different PCR assays for determining (i) the threshold levels of GMO content in foods via competitive PCR and (ii) the ratio of transgenic to non-transgenic components present using real-time PCR. The two methods use the soybean lectin *le1* gene as a general soybean gene. The first method uses a competitive conventional PCR approach in which the *Roundup Ready*™ soy (RRS) DNA and the general soy DNA content are measured by two independent competitive PCRs. The second is a quantitative approach using real-time PCR and Taqman probes to generate a standard curve for the RRS DNA and for the general soy *le1* gene DNA, allowing the ratio of the two to be determined. A RRS content of 0.5% was clearly distinguished from a RRS content of 0.5% using the double competitive PCR method. Wurz *et al*. (1999) indicated that the copy number of both the target and competitor DNA should be identical or similar and that, for reliable quantitation at the 1% level, at least 10 000 copies of amplifiable DNA of the soy genome should be present in the PCR (~50 ng of DNA).

A number of studies have been conducted in which GM DNA derived from feed ingredients has not been detected in milk, meat or eggs (Flachowsky and Aulrich, 2001; Phipps *et al*., 2002). A possible explanation is that the diet-derived DNA is degraded in the digestive tract to small fragments detectable in fecal material but not taken up by the circulatory system (Chowdbury *et al*., 2004). Agodi *et al*. (2006) found from PCR screening of 60 milk samples involving 12 different milk brands that 15 (25%) contained GM maize sequences and 7 (11.7%) contained GM soybean sequences; and concluded that the detection of GM DNA in milk reflects either fecal contamination or airborne contamination with feed DNA or feed particles respectively, with other environmental sources also being possible. The primers were those described by Vaïtilingom *et al*. (1999). One set of primers ZETM1/ZETM3 was used for the total detection of maize (EM endogenous maize) targeting the *Zein* gene, which encodes a methionine-rich Zein protein from maize, and another primer set Sltm1/Sltm2 was used for the total detection of soy (ES endogenous soy), targeting the Le 1 lectin gene *le1*. For detection of *Maximizer* maize (TM transgenic maize), a set of primers Crytm1/Crytm2 targeting the *CryIA(b)* gene, encoding the CRYIA(b) protein (Bt-delta-endotoxin) from *Bacillus thuringiensis* was used. For detection of *Roundup Ready*™ soybean (TS transgenic soybean), the primer set Sttmf3a/Sttmf2a was used to target the CP4 *EPSPS* gene, encoding the enzyme 5-enolpyruvoylshikimate-3-phosphate synthase derived from *Agrobacterium* sp. strain CP4. Vaïtilingom *et al*.

(1999) used four sets of primers in a multiplex PCR format, and labeled each primer pair at the 5′-end with FAM, RHOD, TET or HEX respectively for automated generation of an electropherogram distinguishing amplicon intensities and bp size. Spiking experiments indicated that 10 pg of GM DNA in 200 µl of milk could be detected.

James *et al*. (2003) developed three independent multiplex PCR procedures for detecting multiple target sequences in genetically modified (GM) soybeans (*Roundup Ready*), maize (event 176, Bt11, Mon810 and T14/25) and canola (Gt73, HCN92/28, MS8/RF3 and Oxy235). Internal control targets were included to eliminate false negatives. Since each set of primers generated a single band from the corresponding GM target sequence, a given strain or line harboring multiple transgenic modifications could be readily detected from the two or three resulting agarose bands with differing bp lengths. These systems can also be used to detect the presence of unspecified GMOs, including unapproved lines, since many GM crops contain at least one of the targets detected by the primers.

Hernández *et al*. (2003) cleverly exploited the ability of real-time PCR software to generate the Tm values of resulting amplicons by developing a multiplex SYBR Green I mediated real-time PCR detection assay for three different GM maize lines and one GM soybean line. Differentiation was based on the differences in Tm values of the amplicons. In so doing, they found that amplicon pairs differing by at least 1.5ºC in Tm could still be identified in a duplex format, whereas amplicons differing by only 1.2ºC produced only single peak melting curves. A triplex real-time PCR assay was therefore developed for *Maximizer* maize 176, Bt11 maize and MON810 maize, with resulting Tm values of 76.9, 85.2 and 88.9 respectively. The sensitivity of detection for the duplex GM maize system was 0.1%, and for the soybean duplex system it was 1%. The method, however, is unsuitable for precise quantification.

Yamaguchi *et al*. (2003) compared a multiplex PCR assay with an ELISA assay for detecting GM maize. Primer pairs were designed to amplify a 437-bp sequence of the Bt11 *cry1A(b)* gene, a 522-bp sequence of the Btm *pat* gene, a 619-bp sequence of the Event176 *cry1A(b)* gene, a 199-bp sequence of the MON810 *cry1A(b)* gene, and a 231-bp sequence of the LIBERTY *pat* gene. One pair of primers amplified a 329-bp sequence of the zein protein gene (Kirihara *et al*., 1988) as a control to ensure against false negatives. The PCR method had the advantage of distinguishing between the various GM lines of maize from one another, which the ELISA was unable to do. Yamaguchi *et al*. (2003) presented schematic diagrams of genetic maps illustrating the origin of the primers which encompassed gene junctions for specific recognition of the individual maize lines.

The maize line GA21 was developed to exhibit tolerance to the Roundup glyphosate herbicide. Hernández *et al*. (2004) were able to amplify a nucleotide sequence corresponding to the polylinker plasmid vector flanked by the *r-act* promoter and *nopaline synthase* 3′-terminator in transgenic maize line GA21, constituting a unique junction region between the transgenic and plasmid vector by real-time PCR. Duplex real-time PCR assays were performed with SYBR Green, Amplifluor™ and Taqman systems targeting the same 72-bp junction region, together with a primer pair that amplified a sequence of the *maize invertase* (*ivr*) gene as an external control. Taqman™ and SYBR Green systems yielded similar sensitivities, while the

Amplifluor system was slightly less sensitive. The Amplifluor system is based on a universal hairpin primer. The Taqman system exhibited a detection level of 0.01% for GA21 DNA, which is notably less than the threshold of 1% for the accidental presence of GMOs due to field contamination during cultivation. Three real-time PCR systems involving SYBR Green, Amplifluor and Taqman were found to be specific, highly sensitive and reliable for both identification and quantification of GA21 DNA.

Currently, many GMOs can be detected because they share the same DNA promoter and terminator sequences. A molecular screening method based on multiplex-PCR was developed by Forte *et al*. (2005) for the detection of GM soybeans and maize. The multiplex assay consisted of a primer pair that amplified a 414-bp sequence of the soybean lectin gene *le1* as a negative soy control and a pair of primers that amplified a 277-bp sequence of the *zein* gene of maize as a negative maize control. A pair of primers was also used that amplified a 180-bp sequence of the NOS terminator, in addition to a pair of primers that amplified an 83-bp sequence of the 35S promoter, both of which are common to GM Bt176 maize and GM *Roundup Ready* soybean. Since the GMO sequences amplified are external to the specific transgenes they do not allow GM strains to be identified, but are capable of distinguishing approved from certain non-approved GM strains. Both GM primer pairs detected 0.1% *Roundup Ready*™ soy, Bt176 maize and Bt11 maize.

Greiner *et al*. (2005) made use of primers from the Official Collection of Test Methods (OCTM) (1998, 2002) for the qualitative and quantitative detection of GM soy (*Roundup Ready* soy) and maize (Bt176 *Maximizer* maise, Bt11 maize, MON810 *Yield Gard* corn, and T25 *Liberty*^{R} link maize) in commercial processed foods in Brazil. A total of 100 foods containing maize and soy were analyzed in 2000 and again in 2001. In 2000, 13 of the 100 soy samples contained *Roundup Ready*, whereas in 2001, 21 of the 100 samples contained *Roundup Ready* soy. In Brazil, the majority of food products that tested positive for transgenic soy or maize contained more than 1% as determined by real-time PCRs. In 2000, 15% of the soy- and 25% of the maize-containing products contained less than 1% GMOs, while in 2001 only 14% of the soy- and 13% of the maize-containing products contained less than 1% GMOs. Some of these products were above the 4% limit allowed in Brazil, and were not appropriately labeled. These results emphasize the importance of having convenient and reliable techniques available for quantitative assessment of GMOs in food products.

Liu *et al*. (2005) employed a double monoplex PCR system with unique dual-labeled electrochemiluminescence (ECL) probes for detection of GM capsicum, tomatoes and *Arabidopsis thalianicus*. The methodology utilized tris-propylamine (TPA) and tris (2,2′-bipyridyl) ruthenium II (TBR) for quantifying amplified DNA. TPA and TBR are oxidized at approximately the same voltage on an anodic surface. After deprotonation, TPA chemically reacts with TBR, resulting in electron transfer. The resulting TBR molecule relaxes to its ground state by emitting a photon at 614 nm. TPA decomposes to dipropyl amine in this reaction. The TBR is recycled. The PCR products were mixed with two pairs of probes. One pair of primers (35S sense/35S antisense) was utilized to amplify a 195-bp sequence of the 35S promoter, and the other pair of primers (NOS sense/NOS antisense) amplified a 180-bp

sequence of the NOS terminator. Both of the PCR products (20 µl) were then mixed independently with an equal volume of one of the two probes. One set of probes (35S 1/35S 2) was designed to hybridize to different locals along the 35S amplicon. Probe 35S 1 was labeled at the 3′-end with biotin and probe 35S 2 was labeled at the 5′-end with TBR. A second set of probes (NOS 1/NOS 2) was designed to hybridize to different locals along the NOS amplicon. After hybridization of the probes, streptavidin (SA)-coated magnetic beads were added to capture the amplicons. The samples were then added to a flow ECL detection cell with TPA added. A magnet interfaced with the anodic electrode captured the magnetic beads, resulting in a chemical reaction between TPA- and TBR-labeled amplicons yielding luminescence only from the amplified GMO sequences. The ECL system has the advantage of high sensitivity of detection, with the limit of detection being 100 fmol of PCR products and the dynamic range extending over six orders of magnitude. This methodology has also been applied for the detection of GM soy and papaya (Liu *et al*., 2004a).

The GMO corn *MaisGard*™ is resistant to the European corn borer due to the insertion and expression of the *cryIA(b)* gene that encodes the delta-toxin from *Bacillus thuringiensis* ssp. *kurtaki*. This gene controlled by a 35S promoter from the cauliflower mosaic virus is flanked at its 5′-site by the corn-specific intron 1 of heat shock protein 70 (hsp 70). Zimmerman *et al*. (1998) made use of a nested PCR system for the specific detection and quantification of *MaisGard*. The system utilized a primer pair mgd1/mg2 that amplified an outer 401-bp fragment spanning a region of the 35S-promoter through the hsp70 exon and into the hsp70 intron, and a primer pair mg3/mgd4 that amplified a 149-bp fragment also spanning the interface of the 35S promoter and the hsp exon 1 (Figure 12.13). A nested high mobility (hm)-system was also used for amplifying sequences of the high-mobility protein present in all corn as a positive control for all corn strains assayed. This system involved the outer primers hm1/hm2 and the inner primers hm3/hm4. No other transgenic corn could be detected other than *MaisGard*, since no other GM corn contains this specific gene interface involving the 35S promoter, the hsp70 exon and the hsp70 intron 1.

Liu *et al*. (2004a, 2004b) described a liquid-phase hybridization (LPH) method for developing a LPH-PCR-ELISA assay for detecting and quantifying *Roundup Ready*™ soybean and BT1 maize in food products. A 185-bp fragment of the 35S CaMVX35S

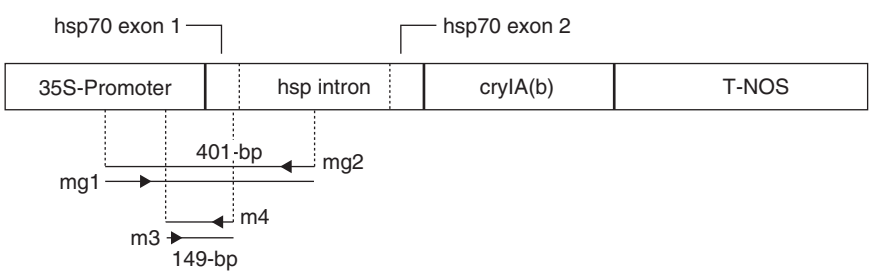

Figure 12.13 Map of the MaisGard™ transgene illustrating the location of the 35S promoter, the hsp70 exon1, the hsp70 intron 1, the delta-endotoxin cryIA(b), the NOS terminator, and the location of the primers. Redrawn from Zimmerman *et al*. (1998), with permission.

promoter was amplified with primers 35S-F/35S-R. The 35S-F primer was labeled at the 5′-end with biotin and the resulting amplicon was hybridized with the digoxygenin (DIG)-labeled probe 35-S-P. In addition, primers nos-F/nos-R were used to amplify a 180-bp fragment of the NOS terminator and hybridized with a DIG-labeled probe nos-P. A control DNA fragment from the soybean lectin locus was amplified with the primers lec-F/lec-R. The lec-F primer was labeled with biotin. The resulting amplicon was hybridized with a DIG-labeled probe lec-P. A control DNA fragment from the maize invertase locus was co-amplified with primers inv-F/inv-R. The inv-F primer was labeled with biotin. The resulting amplicon was hybridized with a DIG-labeled probe inv-P. Hybridization products were transferred to SA-coated microplate wells and processed with alkaline phosphatase conjugated to DIG-IgG with para-nitro-phenyl phosphate (PNPP) as a colorimetric substrate. The limit of detection was 0.3% for *Roundup Ready*™ soy and 0.15% for Bt1 maize. The major advantage of this LPH-PCR-ELISA is that it has a more accurate digital readout than conventional agarose gel-electrophoresis, and is therefore ideally suited for quantification of GMOs in foods.

Abdullah *et al*. (2006) made use of conventional PCR to determine the percent distribution of GMO soy in raw soybeans and soybean products (soy flour, tofu, fucuk, tempe and soy sauce) in Malaysia. The primers p35S1-5/p35S1-3 amplified a 101-bp sequence of the CaMVX promoter. The primers HA-nos118-r/HA-nos118-f amplified a 118-bp sequence of the nos-terminator. The primers RRO1/RRO4 amplified a 356-bp sequence of the *Roundup Ready*™ soy-specific gene. The primers Lectin 1/Lectin 6 were used to amplify a 318-bp sequence of the *lectin* gene, present in all strains of soy as a positive control. Results from assaying a total of 85 soy-based food products involving 6 soy food types yielded 18 samples positive for the 35 s promoter, the NOS terminator and the EPSPS/RR gene. No targeted DNA sequences from five samples of soy sauce were amplified, due presumably to DNA degradation during the soy-sauce fermentation process.

Moriuchi *et al*. (2007) applied quantitative real-time PCR for the detection of *Roundup Ready* soy in a variety of processed soy products, including tofu and soymilk. A pair of primers Le1n02-5′/Le1n0-3′ was used for detection of the *lectin* gene and a pair of primers RRS01-5′/RRs01-3′ amplified a sequence derived from the CTP4-CP4 EPSPS junction with the RRS (*RRS* gene). Respective dual-labeled probes were labeled at the 5′-end with FAM and with TAMRA at the 3′-end. The assay system was capable of detecting 0.16% *Roundup Ready* soy in the soy content of various soybean processed foods. Precise quantification was based on the preliminary determination of copy numbers of both the *lectin* and *RRS* genes in the various soy products.

Membrane based detection systems for GMOs

Su *et al*. (2003) described the development of a multiplex PCR/membrane hybridization assay (MPCR-MHA) for the detection of foreign genes present in GMOs. Primers were labeled with biotin at the 5′-end. Biotinylated MPCR products were detected by hybridization to oligonucleotide probes immobilized on a nylon membrane with subsequent colorimetric detection using SA conjugated alkaline phosphatase. GMO soy

samples yielded colored dots derived from 18S rRNA, CaMV 35S, Tnos amplicons and one from CP4EPSPE for specific identification of glyphosate herbicide tolerance. GMO maize samples yielded colored dots derived from 18S rRNA, CaMV 35S, Tnos, nPtII amlicons, and one from *CryIA(b)* for specific identification of the presence of the gene encoding the delta toxin of *B. thuringiensis* for insect resistance. Potato samples yielded colored dots derived from 18S rRNA, CaMV 35S, Tnos, npII amplicons, and one from CryIIA for identifying the presence of the gene for insect resistance. Rice samples yielded colored dots derived from 18S rRNA, CaMV 35S, Tnos, npII amplicons and one from CP4EPSPS for identification of herbicide tolerance. A pair of primers designed to amplify a sequence derived from the 18S rRNA gene which is present in all plants and highly conserved was used as a general positive control for all samples. The identifying primers were designed to detect the presence of GMOs and the foreign protein expressed. However, they were not designed to identify the specific strain of GMO, which normally requires amplification of the junction sequence of two adjacent genes. The assay can be completed within 5 hours.

Yoke-Kqueen *et al*. (2006) reported on the development of a membrane-based detection system for GMO soy in various foods. The PCR was used to develop a set of two double-stranded probes labeled with biotin-N4-dCTP. The primer pairs EPSPS-F/EPSPS-R and P35S-F/P35S-R used amplified 134 and 101-bp sequences of the *EPSPS* and *P35S* promoter genes, respectively, which were applied to a nitrocellulose or nylon membrane. The dots were allowed to dry and were then exposed to UV to crosslink the DNA to the membrane. The membrane was then incubated in blocking solution and washed, and labeled probes were applied. The membrane was then washed and conjugate solution containing HRP-SA added and washed. A chemiluminescent substrate was then added for 1 minute, blotted dry, and the membrane placed into an X-ray film cassette with X-ray film for 10 minutes. The film was subsequently developed and fixed. Standards were utilized for semi-quantitative assessment of the GMO in foods. Both probes were found to be capable of detecting 2% or more of GM in food samples.

Microarrays

The major advantage of *microarrays* is that they allow the employment of large numbers of amplicons to be used to screen many samples simultaneously. An oligonucleotide microarray usually consists of a glass chip to the surface of which is applied an array of a number of sequence-specific nucleotide probes. Microarray technology offers the advantage of rapid automated detection of PCR amplicons and circumvents the problem associated with the generation of non-specific products in multiplex reactions. Peano *et al*. (2005a) developed a multiplex PCR system for the simultaneous detection of target sequences derived from *Roundup Ready*™ soy, maize MO11810, Bt176, Bt11 and GA21, utilizing slide microarray technology. Primer pairs were designed to amplify the junction regions of the transgenic cassettes. The endogenous lectin gene of soy and that of the *zein* gene of maize were included as internal controls to assess the efficiency of all amplifications. A universal array (UA) was used to detect unique junction sequences of the GMOs. A UA consists of a set of synthetic oligonucleotides called Zip Codes or tags with similar thermodynamic characteristics

but different sequences; with the sequences unrelated to those targeted. A ligation detection reaction (LDR) was involved which required the design of two adjacent oligonucleotide probes, specific for each sequence to be analyzed. A *discriminating probe* is 5′-fluorescently labeled and a *common probe* carries at its 3′-end a unique artificial sequence called a Zip Code, complementary to a *Zip Code* sequence in the UA (Figure 12.14).

These probes hybridize at adjacent sites on the purified amplicons and a thermostable ligase joins the ends, linking the fluorescent label with a complementary or cZip Code (Figure 12.14). The PCR thermal cycling between 94°C and 58°C is then undertaken in the presence of the thermostable DNA ligase to maximize the amount of ligated product. The resulting products are hybridized onto the UA, where the cZip Code directs the ligated oligonucleotide to the corresponding Zip Code. To prepare the UA, Zip Codes carrying an additional polyd$(dA)_{10}$ tail at the 5′-end were spotted onto CodeLink slides. The fluorescent signals from nucleotides bound to the Code Link slides were detected using a laser scanner with a green laser for the Cy3 dye at the 5′-end of the discriminating probes. The limit of detection for each GMO was 1% or 0.2 ng of DNA, which corresponds to about 50 copies for Bt11, Bt176, GA21 and MON811 maize and about 100 copies for *Roundup Ready*™ soy. The multiplex PCR used was found not to generate amplicons quantitatively related to the amount of initial target DNA present, so that the LDR-PCR analysis system is limited to qualitative analysis. A 210-bp fragment encompassing the junction CP4EDSPS and terminator NOS gene sequences was amplified with primers RR2075-F/NOSterN-R for detection

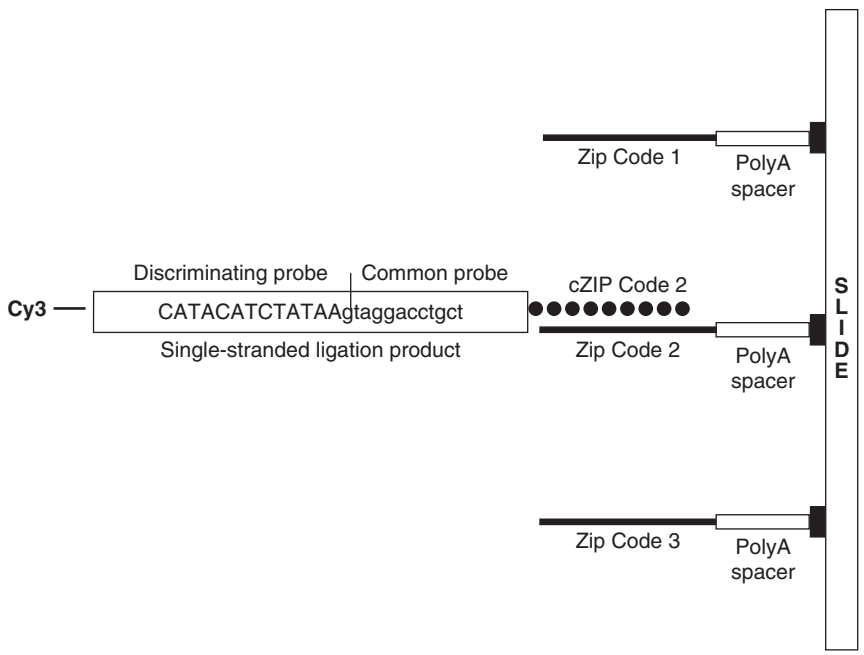

Figure 12.14 Multiplex PCR product ligation and hybridization to a universal array. Redrawn from Peano *et al.* (2005a).

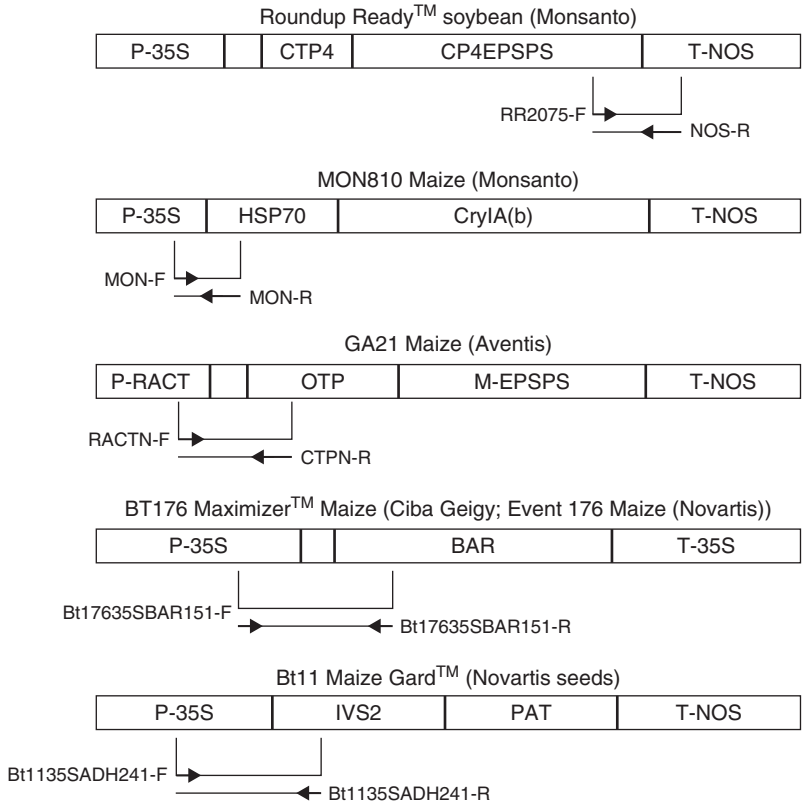

Figure 12.15 Linear maps of recombinant DNA junction regions of GMOs showing position of primers. Redrawn from Peano *et al*. (2005a) with permission.

of *Roundup Ready* soy (Figure 12.15). A 241-bp fragment encompassing the junction of the 35S promoter and IVS2 gene sequences was amplified with the primers Bt1135SADH241-F/Bt1135SADH241-R for detection of Bt11 *MaizeGuard*™ (Figure 12.15). A 151-bp fragment encompassing the junction of the 35S promoter and BAR gene sequences was amplified with primers Bt17635SBAR151-F/Bt17635SBAR151-R for detection of Bt176 maize (Figure 12.15). A 193-bp fragment encompassing the junction of the RACT promoter and the OTP gene sequences was amplified with primers RACTN-F/RACTN-R for detection of GA21 maize (Figure 12.14). A 101-bp fragment encompassing the junction of the 35S promoter and HSP70 gene sequences was amplified with primers MON-F/MON-R for detection of MON810 maize (Figure 12.14). In addition, an 81-bp sequence of the soybean *lectin* gene was amplified with the primers Lectin-F/Lectin-R and a 133-bp sequence of the maize *zein* gene was amplified with primers Zeindeg-F/Zein133-R as positive controls.

Xu *et al*. (2006) reported on the development of a multiplex-PCR coupled with a DNA array system simultaneously targeting 18 specific DNA sequences associated with GMOs in addition to the soy *lectin* gene, the maize *protein* gene, and the *18S rRNA* highly conserved plant gene as controls. A total of 21 primer pairs and

corresponding probes were designed. Each probe contained a 5′-amine group and a 10-nucleotide poly-dT spacer. The amine group enabled the probe to be covalently attached to the aldehyde-activated glass slides. The poly-dT_{10} oligonucleotide arm is used as a link to facilitate the hybridization between amplicons and homologous probes. Amplicons were labeled by incorporation of Cy5-dCTP during the PCR. Three types of GMO microarrays were designed. The first is the screen chip that contains screen and control probes. It includes category probes such as the 35S promoter, nos terminator, PPtII terminator, 35S terminator, nos promoter and the FMV promoter, which encompasses more than 95% of GM plants. The second is the species-specific chip. For soy, the microarray consisted of category probes such as lectin, 35S promoter, nos terminator and EPSPS. For maize, the microarray consists of category probes such as zein, 35S promoter, nos terminator, 35S terminator, Bar, PAT, CryIA(b) and Cry9C. For canola, the microarray consisted of category probes such as Fbp, 35S promoter, FMV35S promoter, nos terminator, Bar, PAT, *GOX* gene, Barstar and Barnase. For cotton, the microarray consisted of category probes such as Rbc1, 35S promoter, nos terminator, Npt terminator and CryIA(c). The third type is the integrated chip. It is the integration of the various species-specific chips and is suitable for multiple detections. A sequence of the *18S rRNA* gene was included in all chips as a positive control for evaluating DNA quality and PCR efficiency, since it is highly conserved and present in all plant tissue. After the PCR, 8 µl of product was mixed with an equal volume of hybridization solution, denatured at 95°C for 5 min, and applied onto a chip under a cover slip. Chips were then incubated at 55°C for 1 h for hybridization, and then washed and dried. The chips were subsequently scanned with a confocal scanner, and fluorescence quantified with computer software. A negative control probe from human HLA that is unrelated to all the target sequences was used to assess the background of the microarrays. The 35S promoter commonly used in GMO detection is derived from the CaMV, and therefore a false-positive result can occur when the virus has infected non-GM plants. A control probe was therefore designed, based on the CaMV-CP sequence. When the CaMV-CP is positive, it can be concluded that the sample is contaminated by the infecting virus. When the 35S promoter is positive while the CaMV-CP is negative, the sample is transgenic.

Peptide nucleic acid (PNA) clamping inhibition of the PCR

A PNA is a DNA mimic, with a polyamide instead of a phosphodiester backbone, that forms very stable duplexes with complementary DNA or RNA oligomers (Peano *et al*., 2005b). A PNA pseudo-peptide backbone is composed of N-2 aminoethylglycine repeating units, and is not degraded by proteases or peptidases. PNA clamping is a method to discreetly modulate the PCR. It is capable of specific inhibition of amplification of target sequences differing by only a single base-pair, and can therefore be used to assess DNA band identity. Peano *et al*. (2005b) developed PNA methodology for identification of *Roundup Ready* soy, MON811, Bt176, Bt11, and GA21 maize. The minimum concentration of each PNA resulting in PNA clamp inhibition of the PCR targeting a specific transgenic sequence was determined. A correlation between this minimum concentration and the percent of the GMO target sequence in the sample was established. Primer pairs were designed for amplifying specific DNA

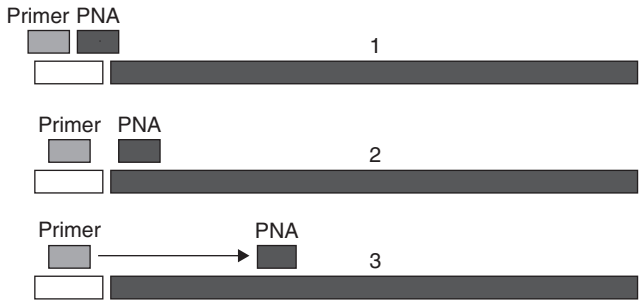

Figure 12.16 Schematic illustrations of the possible mechanisms of PCR inhibition by PNA clamping. When the PNA and PCR primer target binding sites overlap, PNA clamping results in primer exclusion (1). When the PNA binding site is adjacent to the PCR primer binding site, the PNA prevents polymerase access to the PCR primer (2). When the PNA target site is located at a distance from the PCR primer site, PNA clamping results in extension arrest (3) (Orum *et al*. 1993). Redrawn from Peano *et al*. (2005b), with permission.

sequences corresponding to the junction regions of the five corresponding transgenic cassettes (Figure 12.15). PNAs were designed to match a specific region of each transgene suitable for PCR clamping and adhered to the generally accepted criteria for the design of PNAs in which the length was between 11 and 15 nucleotides, allowing for sufficient specificity and solubility, low self-complementarity, and low purine (in particular guanine) content, to avoid self-aggregation, and sufficiently high melting temperature (63–77°C). The best strategy to obtain efficient PNA clamping inhibition of the PCR was found to involve a PNA of 15 nucleotides sharing a maximum of 2 nucleotides with the adjacent primer. The cost of PNA synthesis is high; however, a low amount of PNA is utilized in each PCR reaction, ensuring that at least 20 000 reactions are possible with a single batch of PNA. The technique is presently limited to semiquantification of GMOs. The mechanism of PNA clamping inhibition of the PCR is presented in Figure 12.16.

Dip stick biosensor

Kalogianni *et al*. (2006) reported on the development of the first DNA biosensor in a dry dipstick configuration for visual detection and confirmation of GMO-related 35S rRNA and NOS sequences by rapid (7-min) hybridization following the PCR. The primers P-35S-F amplified a 207-bp fragment from the *35S rRNA* gene sequence; the primers T-NOS-F/TNOS-R amplified a 123-bp fragment from the NOS terminator sequence; and the primers *Lectin*-F/Lectin-R amplified a 181-bp sequence of the lectin gene sequence. In addition, probes with oligo (dA) tails at the 3′-ends specific for the NOS, 35S and Lectin amplicons were utilized. For GMO screening, oligo dT-conjugated gold particles are placed on the conjugation pad and allowed to dry (Figure 12.17). Each amplicon product (10 µl) is mixed with 1 µl of a dA-tailed specific probe. The preparations are then heated at 95°C for 2 min for denaturation and then hybridized at 37°C for 5 min. A 5-µl aliquot of each is then applied to the conjugation pad of the dipstick next to the gold nanoparticles (area S, Figure 12.17). The bottom portion (wick) of the sensor is then immersed in the developing solution.

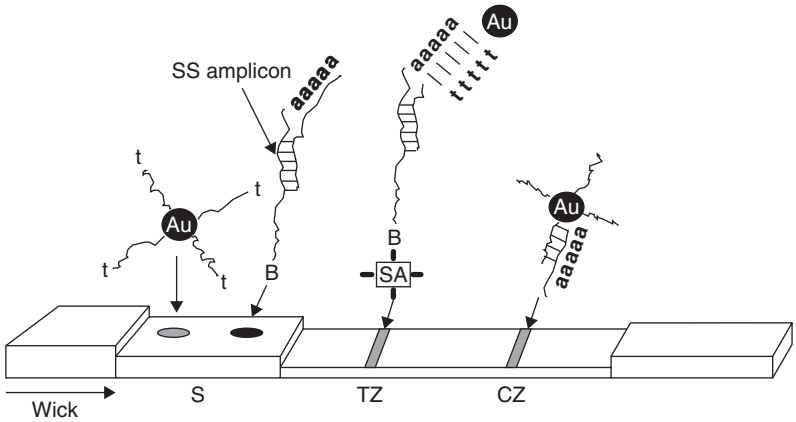

Figure 12.17 Schematic illustration of the operational principles of the nanoparticle-based biosensor for visual detection of GMOs. Biotinylated PCR amplicon is hybridized to a specific oligo(dA)-tailed probe and loaded onto sample application area (S). As the developing solution migrates upward (direction of arrow) it rehydrates the oligo(dT)-conjugated gold nanoparticles, which are then coupled with the amplicon through poly(dA/dT) of the probe by hybridization. The first red line is formed in the test zone (TZ) as the immobilized streptavidin binds the complex through the biotinylated amplicon. The second red line develops in the control zone (CZ), when the excess conjugated gold nanoparticles hybridize with the immobilized oligo(dA) probe. B, biotin; SA, streptavidin. Redrawn from Kalogianni *et al.* (2006), with permission.

As the developing solution migrates along the strip it rehydrates the aligned (dT)-gold nanoparticle conjugate, which hybridizes with the free oligo (dA) tail of the probe hybridized to the amplicon. The hybrids are then captured through the 5′-end of the biotin-labeled target DNA by immobilized SA, forming a characteristic red line derived from the 40-nm diameter gold nanoparticles that have a red color. If target DNA is not present, then the oligonucleotide nanoparticle conjugates are not captured at the test zone by the immobilized streptavidin. The excess of nanoparticle conjugates form hybrids with immobilized oligo (dA) fragments at the control zone of the sensor, resulting in a second red line. A red line at the control zone confirms the proper functioning of the sensor. A positive result therefore yields two red lines with a continuous increase of the intensity of the red line in the test zone as the amount of target DNA increases up to a plateau region which can be made use of for semiquantitative analysis. The major advantages of this system are visual detection in a few minutes without the need for AGE, and its simplicity.

Non-GMO grains and seeds

Plant storage proteins are known to be highly species-specific. Hernández *et al.* (2005) developed a series of real-time PCR assays for quantitative detection of barley, rice, sunflower and wheat based in part on species-specific storage proteins. The primers hor1/hor2 amplified a 73-bp sequence of the barley *γhordein* gene which encodes a storage protein, the primers orgi/org2 amplified a 68-bp sequence of the rice *gos9* gene, the primers tri1/tri2 amplified a 93-bp sequence of the wheat acetyl-CoA carboxylase gene (*acc1*), and the primers hel1/hel2 amplified a 60-bp sequence

of the sunflower *hel* gene encoding the HELIANTHIN or 11S storage protein. The probes were labeled at the 5′-end with FAM and with TAMRA at the 3′-end.

Wild and cultivated wheats (*Triticium* spp.) exist as diploid (AA), tetraploid (AABB and AAGG) and hexaploid (AABBDD and AAAAGG) forms. Morphological features can be used to assign an intact plant to the correct ploidy level. However, problems frequently occur with identification of incomplete ears and dehucked grain. This is particularly relevant in archeobotany, where agriculturally important varieties are often impossible to distinguish in the archeological record. Interestingly, hexaploids (AABBDD) do not exist in the wild, and the origins and subsequent spread of prehistoric wheat are questions that cannot be answered without the determination of the ploidy levels of archeobiological remains. DNA has been found to be present in ancient mummified maize (Rollo *et al*., 1988, 1991). Allaby *et al*. (1994) extended this work to wheat, and successfully used the PCR to amplify ancient DNA from 2000- and 3000-year-old charred grains. Sallares *et al*. (1995) described a PCR system that distinguishes the A, B and D genomes in wheat DNA. PCRs were directed at the "non-transcribed spacer" regions of the rDNA loci. The spacers within the D genome locus have a 71-bp insertion that is absent from the corresponding A and B loci. The PCR amplicon sizes therefore enabled D− and D+ genomes to be distinguished by PCR with an internal primer that does not anneal to A genome sequences. The primers 1B/2D distinguished the A, B and D genomes, while the internal primer 3A used in conjunction with the 1B primer distinguished the A and B genomes (Table 12.1).

Spelt is the traditional hard-grained wheat of the Alamanns of central Europe, and has over the past century been somewhat displaced by high-yielding cultivars of common bread wheat. The advent of organically grown foods has created a niche market for spelt. However, the smaller yields and the required dehulling after threshing make spelt more costly than wheat. Spelt flour is available in specialty outlets at a cost of up to 50% above that of conventional wheat flour. There is therefore an incentive for fraudulent partial or complete replacement of spelt flour with conventional flour. Von Büren *et al*. (2001) developed a QC-PCR for the quantitative determination of the presence of wheat flour in spelt flour. The wheat-specific primers GAG31/GAG28 amplified a 236-bp sequence of the γ-gliadin *GAG56P* gene which is present in spelt and conventional wheat. An internal competitive PCR standard was constructed for quantification which was based on an equivalence point. Applying the two PCR primers, a wheat-specific amplicon of 236-bp was generated from each of five different wheat cultivars. Spelt cultivars in addition to other cereals and soy failed to yield an amplicon. The assay was able to detect the presence of 0.01% to 0.1% wheat in spelt. The spelt-specific *ok* allele differs from the conventional wheat specific *fo* allele of the *GAG56P* gene by a 9-bp deletion/duplication and a linked *Bst*4CI restriction site. The primers GAG15/GAG16 and the restriction nuclease *Bst*4CI were therefore used for PCR-RFLP. The primers GAG15/GAG16 yield an amplicon of 350-bp with spelt and 359-bp with wheat, respectively. The two amplicons compete in the PCR, functioning as natural internal competitive PCR standards for each other. Since the spelt specific *ok* allele contains a *Bst*4CI restriction site, it yields additional fragments of 272 and 296 bp. The resulting 359 PCR band of wheat

Table 12.1 PCR primers and DNA probes[a]

Species	Primer or probe	Sequence (5′–3′)	Size of amplified sequence (bps)	Gene or DNA target sequence	References
Bovine	L8129	GCC-ATA-TAC-TCT-CCT-TGG-TGA-A	270	mt $tRNase^{Lys}$-ATPase8-ATPase6	Tartaglia *et al*. (1998)
	H8357	GTA-GGC-TTG-GGA-ATA-GTA-CGA			Tartaglia *et al*. (1998)
Bovine	LBOF	GCC-ATA-TAC-TCT-CCT-TGG	~200	8^+ region of mt *ATPase* 6/8	Tartaglia *et al*. (1998)
	LBOR	GTA-GGC-TTG-GGA-ATA-GTA			Tartaglia *et al*. (1998)
Poultry	LCHF	GGG-ACA-CCC-TCC-CCC-TTA	~200	8^+ region of mt *ATPase* 6/8	Tartaglia *et al*. (1998)
	LCHR	GGA-GGG-CTG-GAA-GAA-GGA			Colgan *et al*. (2001)
Porcine	LPOF	GCC-TAA-ATC-TCC-CCT-CAA	~200	8^+ region of mt *ATPase* 6/	Tartaglia *et al*. (1998)
		GAA-AGA-GGC-AAA-TAG-ATT-TTC			Colgan *et al*. (2001)
Ovine	FOV	TTA-AAG-ACT-GAG-AGC-ATG-ATA	~200	8^+ region of mt *ATPase* 6/	Colgan *et al*. (2001)
	RPO	GAA-AGA-GGC-AAA-TAG-ATT-TTC			Colgan *et al*. (2001)
Ruminant		GAA-AGG-ACA-AGA-GAA-ATA-AGG	104	16S RNA	Dalmasso *et al*. (2004)
		TAG-GCC-CTT-TTC-TAG-GGC-A			Dalmasso *et al*. (2004)
Pork		CTA-CAT-AAG-AAT-ATC-CAC-CAC	290	12S rRNA–tRNA Val	Dalmasso *et al*. (2004)
		ACA-TTG-GAT-CTT-CTA-GGT			Dalmasso *et al*. (2004)
Fish		TAA-GAG-GC-CGG-TA-AAC-TC	224	12S rRNA	Dalmasso *et al*. (2004)
		GTG-GGG-TAT-CTA-ATC-CCA-G			Dalmasso *et al*. (2004)
Poultry		TGA-GAA-CTA-CGA-GCA-CAA-AC	183	12S rRNA	Dalmasso *et al*. (2004)
		GGG-CTA-TTG-AGC-TCA-CTG-YY			Dalmasso *et al*. (2004)
Bovine	mtDNA	ACA-AAT-CCT-CAC-AGG-CCT-ATT-C	271	mt*Cytb*	Verkaar *et al*. (2002)
		TAG-GAC-GTA-TCC-TAT-GAA-TGC-T			
Bovine	mtDNA	ATG-GCA-TAT-CCC-ATA-CAA-CTA-G	651	mt*Cyt ox II*	Verkaar *et al*. (2002)
		ACT-TTA-GTG-GGA-CTA-ACT-CAA-G			Verkaar *et al*. (2002)
Bovine satellite	DNA	AAG-CTT-GTG-ACA-GAT-AGA-ACG-AT	604	satellite IV	Verkaar *et al*. (2002)
		CAA-GCT-GTC-TAG-AAT-TCA-GGG-A			Verkaar *et al*. (2002)
Bovine satellite	DNA	CTG-GGT-GTG-ACA-GTG-TTT-AAC	822	satellite 1.711B	Verkaar *et al*. (2002)
		TGA-TCC-AGG-GTA-TTC-GAA-GGA			Verkaar *et al*. (2002)
Goose	mtCytb1	CCA-TCT-GCT-TAG-CCA-CAC-AAA-TCC-TA	~300	mt*Cytb*	Colombo *et al*. (2002a)
	mtCytb2	TAT-GTT-TCT-TTG-GAC-TTT-GTG-TCC-TC			Colombo *et al*. (2002a)
Chicken	CF	TCA-CAA-ACC-TAT-TCT-CAG-CAA-TT	120	mt*Cytb*	Hird *et al*.(2003)
	CR	GGG-GAG-GAG-GAA-GTG-TAA-A			Hird *et al*.(2003)
Turkey	TF	CCT-TCC-TAA-TCG-CAG-GA	101	mt*Cytb*	Hird *et al*.(2003)
	TR	TGG-AAT-GGG-ATT-TTG-TCA-GC			Hird *et al*.(2003)
Deer	RD-1	TCA-TCG-CAG-CAC-TCG-CTA-TAG-TAC-ACT	194	mt*Cytb*	Matsunaga *et al*. (1998)
	RD-2	ATC-TCC-AAG-TAG-GTC-TGG-TGC-GAA-TAA			Matsunaga *et al*. (1998)

(*Continued*)

Table 12.1 (Continued)

Species	Primer or probe	Sequence (5′–3′)	Size of amplified sequence (bps)	Gene or DNA target sequence	References
Swine	GHP1	CAT-CCT-TGG-GGG-TCT-C	225	Growth hormone gene	Wolf and Lüthy (2001)
	GHP2	TTT-CAT-CTC-TTT-CCA-TTC-TTG			Wolf and Lüthy (2001)
22 spp.	CYT b1	CCA-TCC-AAC-ATC-TCA-GCA-TGA-TGA-AA	359	mt*Cytb*	Partis *et al*. (2000) from Carr and Marshall (2000)
	CYT b2	GCC-CCT-CAG-AAT-GAT-ATT-TGT-CCT-CA			Partis *et al*. (2000) from Carr and Marshall (2000)
Bovine	12SpVACADIR	TTA-GTT-GAA-TTA-GGC-CAT-GAA-GCA	84	Mt*12S rDNA*	Martín *et al*. (2006)
	12SpVACAINN	GTT-TAA-ATA-GGG-TTA-AGA-TGC-ACT-CAA-TC			Martín *et al*. (2006)
Sheep	12SpOVJDIR	CTA-AGA-ATA-GAG-TGC-TTA-GTT-GAA-CCA-GG	121	Mt*12S rDNA*	Martín *et al*. (2006)
	12SpOVJINN	GTC-TCC-TCT-CGT-GTG-GTT-CAG-ATA			Martín *et al*. (2006)
Goat	12SpCABRADIR	AAA-CGT-GTT-AAA-GCA-CTA-CAT-C	122	Mt*12S rDNA*	Martín *et al*. (2006)
	12SpCABRAINV	GTC-TTA-GCT-ATA-GTG-TAT-CAG-CTG-CA			Martín *et al*. (2006)
Beef	Satellite DNA	TGT-ACG-AAG-AAA-TGT-GCG-G	218	1.109 satellite	Guoli *et al*. (1999)
		TCA-ATG-CAA-AGG-ACA-AGC-CTG-C			Guoli *et al*. (1999)
Chicken	Exon	TTT-GCG-GAT-CCA-CAT-CTG-CTG-GAG	391	α-cardiac actin	Hopwood *et al*. (1999)
	Intron	GAT-ACA-GGT-ACC-ACT-CAT-AAA-TGA-GAC-CAT-CAG-G			Hopwood *et al*. (1999)
Meat	Forward	CAA-CTG-GGA-TTA-GAT-ACC-CCA-CTA	456	Mt*12S rRNA*	Girish *et al*. (2004)
	Reverse	GAG-GGT-GAC-GGG-CGG-TGT-GT			Girish *et al*. (2004)
C. Allig.	Alli-M	GCA-CTT-CTC-ATC-GGG-TGA-C	180	mt*Cytb*	Yan *et al*. (2005)
	Alli-R	ACG-TGC-TCT-CGT-GAA-GGT-AG			Yan *et al*. (2005)
Univ.	L1091	AAA-CTG-GGA-TTA-GAT-ACC-CCA-CTA-T	~400	mt*12S rRNA*	Yan *et al*. (2005) from Kocher *et al*. (1989)
	H1478	GAG-GGT-GAC-GGG-CGG-TGT-GT			Yan *et al*. (2005) from Kocher *et al*. (1989)
Bovine		GCC-ATA-TAC-TCT-CCT-TGG-TGA-CA	271		Lahiff *et al*. (2001) from Tartaglia *et al*. (1998)
		GTA-GGC-TTG-GGA-ATA-GTA-CGA			Lahiff *et al*. (2001) from Tartaglia *et al*. (1998)
Chicken		GGG-ACA-CCC-TCC-CCC-TTA-ATG-ACA	266		Lahiff *et al*. (2001)
		GGA-GGG-CTG-GAA-GAA-GGA-GTG			Lahiff *et al*. (2001)
Swine		GCC-TAA-TCT-CCC-CTC-AAT-GGT-A	212		Lahiff *et al*. (2001)
		ATG-AAA-GAG-GCA-AAT-AGA-TTT-TCG			Lahiff *et al*. (2001)
Sheep		TTA-AAG-ACT-GAG-AGC-ATG-ATA	225		Lahiff *et al*. (2001)
		ATG-AAA-GAG-GCA-AAT-AGA-TTT-TCG			Lahiff *et al*. (2001)
Chicken	Forward	GAC-CAT-CAG-CTG-ATG-AGC-CAA-G	327	α-cardiac actin	Lockley and Bardsley (2002)
Turkey	Forward	GAT-GTG-GAT-TAG-TTG-TGC-AGG-AAT-AC	159	α-cardiac actin	Lockley and Bardsley (2002)

	Reverse	TTT-GCG-GAT-CCA-CAT-CTG-CTG-GAA-G		α-cardiac actin	Lockley and Bardsley (2002)
Bovine	Forward	TTT-CTT-GTT-ATA-GCC-CAC-CAC-AC	98	1.711B	Walker *et al*. (2003)
	Reverse	TTT-CTC-TAA-AGG-TGG-TTG-GTA-AG			Walker *et al*. (2003)
Porcine	Forward	GAC-TAG-GAA-CCA-TGA-GGT-TGC-G	134	PRE-1SINE	Walker *et al*. (2003)
	Reverse	AGC-CTA-CAC-CAC-AGC-CAC-AG			Walker *et al*. (2003)
Chicken	Forward	CTG-GGT-TGA-AAA-GGA-CCA-CAG-T	169	CR1 SINE	Walker *et al*. (2003)
	Reverse	GTG-ACG-CAC-TGA-ACA-GGT-TG			Walker *et al*. (2003)
Ruminants	Forward	CAG-TCG-TGT-CCG-ACT-CTT-TGT	100	Bov-tA2 SINE	Walker *et al*. (2003)
	Reverse	AAT-GGC-AAC-ACG-CTT-CAG-TAT-T			Walker *et al*. (2003)
Universal	Forward	CAA-ACT-GGG-ATT-AGA-TAC-CCC-ACT-AT	456	*12S* mt*rRNA*	Girish *et al*. (2005) from Kocher *et al*. (1989)
Universal	Reverse	GAG-GGT-GAC-GGG-CGG-TGT-GT			Girish *et al*. (2005) from Kocher *et al*. (1989)
Random	50–06	AGG-TTC-TAG-C			Koh *et al*. (1998)
Random	80–04	CGC-CCG-ATC-C			Koh *et al*. (1998)
Maize EM	Zetm1	FAM-TGT-TAG-GCG-TCA-TCA-TCT-GTG-G	69	*zein*	Agodi *et al*. (2006) from Vaïtilingom (1999)
	Zetm3	FAM-TGC-AGC-AAC-TGT-TGG-CCT-TAC			Agodi *et al*. (2006) from Vaïtilingom (1999)
Maize TG	Crytm1	RHOD-GTG-GAC-AGC-CTG-GAC-GAG-AT	105	*CRYIA(B)*	Agodi *et al*. (2006) from Vaïtilingom (1999)
	Crytm2	RHOD-TGC-TGA-AGC-CAC-TGC-CGA-AC			Agodi *et al*. (2006) from Vaïtilingom (1999)
Soy EM	Sltm1	TET-AAC-CGG-TAG-CGT-TGC-CAG	81	*le1*	Agodi *et al*. (2006) from Vaïtilingom (1999)
	Sltm2	TET-AGC-CCA-TCT-GCA-AGC-CTT-T			Agodi *et al*. (2006) from Vaïtilingom (1999)
Soy TG	Sttmf3a	HEX-GCA-AAT-CCT-CTG-GCC-TTT-CC	146	CP4 *EPSPS*	Agodi *et al*. (2006) from Vaïtilingom (1999)
	Sttmr2a	HEX-CTT-GCC-CGT-ATT-GAT-GAC-GTC			Agodi *et al*. (2006) from Vaïtilingom (1999)
Soy	bac1	GAT-CCT-CCA-ATC-CAG-ACA-CTG	319	B-actin	James *et al*. (2003) from Promega Inc.
	bac2	GAA-CTA-TGA-ATT-ACC-TGA-TGG			James *et al*. (2003) from Promega Inc.
Soy	LecMP1	GGG-TGA-GGA-TAG-GGT-TCT-CTG	210	soy lectin	James *et al*. (2003) from Promega Inc.
	LecMP2	GCG-ATC-GAG-TAG-TGA-GAG-TCG			James *et al*. (2003) from Promega Inc.
Soy	sttmf3a	GCA-AAT-CCT-CTG-GCC-TTT-CC	145	cp4-epsps	James *et al*. (2003) from Vaïtilingom *et al*. (1999)
	sttmr2a	CTT-GCC-CGT-ATT-GAT-GAC-GTC			James *et al*. (2003) from Vaïtilingom *et al*. (1999)

(*Continued*)

Table 12.1 (Continued)

Species	Primer or probe	Sequence (5′–3′)	Size of amplified sequence (bps)	Gene or DNA target sequence	References
Soy	35SFZMP1	CCG-ACAQ-GTG-GTC-CCA-AAG-ATG	158	P35S promoter	James *et al*. (2003) from Vaïtilingom *et al*. (1999)
	35SFZMP2	AGA-GGA-AGG-GTC-TTG-CGA-AGG			James *et al*. (2003) from Vaïtilingom *et al*. (1999)
Soy	nosFZMP1	GAA-TCC-TGT-TGC-CGG-TCT-TG	125	*NOS ter*	James *et al*. (2003) from Vaïtilingom *et al*. (1999)
	nosFZMP2	GCG-GGA-CTC-TAA-TCA-TAA-AAA-CC			James *et al*. (2003) from Vaïtilingom *et al*. (1999)
Canola	NPTII-3	GAG-GCT-ATT-CGG-CTA-TGA-CT	271	NPTII	James *et al*. (2003) from Beck *et al*. (1982)
	NPTII-4R	AAG-GTG-AGA-TGA-CAG-GAG-AT			James *et al*. (2003) from Beck *et al*. (1982)
Maize	Ivr-F	CCG-CTG-TAT-CAC-AAG-GGC-TGG-TAC-C	226	maize inertase	James *et al*. (2003) from Ehlers *et al*. (1997)
	Ivr-R	GGA-GCC-CGT-GTA-GAG-CAT-GAC-GAT-C			James *et al*. (2003) from Ehlers *et al*. (1997)
Maize	crylA 4-5′	GGA-CAA-CAA-CCC-MAA-CAT-CAA-C[a]	152	*crylA(b)*	James *et al*. (2003) from Matsuoka *et al*. (2000)
	crylA 4-3′	GCA-CGA-ACT-CGC-TSA-GCA-G[a]			James *et al*. (2003) from Matsuoka *et al*. (2000)
Maize	patF2	GAA-GGC-TAG-GAA-CGC-TTA-CG	262	*pat*	James *et al*. (2003) from Permingeat *et al*. (2002)
	patR2	GCC-AAA-AAC-CAA-CAT-CAT-GC			James *et al*. (2003) from Permingeat *et al*. (2002)
Maize	barF2	GCA-CAG-GGC-TTC-AAG-AGC-GTG-GTC	177	bar	James *et al*. (2003) from Permingeat *et al*. (2002)
	barR2	GGG-CGG-TAC-CGG-CAG-GCT-GAA			James *et al*. (2003) from Permingeat *et al*. (2002)
Canola	PL-1C	CGA-AAT-CGG-TAG-ACG-CTA-CG	387	*tml*	James *et al*. (2003) from Taberlet *et al*. (1991)
		GGG-GAT-AGA-GGG-ACT-TGA-AC			James *et al*. (2003) from Taberlet *et al*. (1991)
Canola	cruMPF1	TGG-CTA-AAG-GTA-CGT-GAA-TCT-G	258	cruciferin gene	James *et al*. (2003) from Taberlet *et al*. (1991)
	cruMPR1	CTC-TCC-CCA-TAA-GAC-CTT-CTC-C			James *et al*. (2003) from Taberlet *et al*. (1991)
Canola	goxF3	TAA-GGC-ACT-CCG-TAA-CCT-CAT-C	509	*gox* 247	James *et al*. (2003) from Taberlet *et al*. (1991)

	goxR2	TGT-GGT-ATC-CAC-GTT-CGG-TAT-C			James *et al*. (2003) from Taberlet *et al*. (1991)
Canola	bx3	ACT-TTC-AAA-GCA-GCC-GCT-CTT	459	*oxy*	James *et al*. (2003) from Demeke *et al*. (2002)
	bx4	CAC-CCG-AAC-CAA-CGC-TAA-GTT-T			James *et al*. (2003) from Demeke *et al*. (2002)
Canola	bnaseMPF1	ATC-AAA-AGG-GAA-CCT-TGC-AGA-C	202	*bamase*	James *et al*. (2003) from Demeke *et al*. (2002)
	bnaseMPR1	CTG-ATA-ATG-GTC-CGT-TGT-TTT-G			James *et al*. (2003) from Demeke *et al*. (2002)
Canola	patF1	GAT-ATG-GCC-GCG-GTT-TGT-GAT	186	pat	James *et al*. (2003) from Demeke *et al*. (2002)
	patR1	TTC-CAG-GGC-CCA-GCG-TAA-G			James *et al*. (2003) from Demeke *et al*. (2002)
Maize	IVR1-F	CCG-CTG-TAT-CAC-AAG-GGC-YGG-TAC-C[a]	226	Maize *inv*	Greiner *et al*. (2005) from OCTM (2002)
	IVR1-R	GGA-GCC-CGT-GTA-GAG-CAT-GAC-GAT			Greiner *et al*. (2005) from OCTM (2002)
Soy	GMO3	GCC-CTC-TAC-TCC-ACC-CCC-ATC-C	118	Soy *lec*	Greiner *et al*. (2005) from OCTM (1998)
	GMO4	GCC-CAT-CTG-CAA-GCC-TTT-TTG-TG			Greiner *et al*. (2005) from OCTM (1998)
Bt176 maize	Cry03	CTC-TCG-CCG-TTC-ATG-TCC-GT	211	Bt11	Greiner *et al*. (2005) from OCTM (2002)
	Cry04	GGT-CAG-GCT-CAG-GCT-GAT-GT			Greiner *et al*. (2005) from OCTM (2002)
Bt11 maize	IVS2-2	CTG-GGA-GGC-CAA-GGT-ATC-TAA-T	189	Bt11	Greiner *et al*. (2005) from OCTM (2002)
	PAT-B	GCT-GCT-CTA-GCT-GGC-CTA-ATC-T			Greiner *et al*. (2005) from OCTM (2002)
MON810 maize	VWO1	TCG-AAG-GAC-GAA-GGA-CTC-TAA-CG	178	MON810	Greiner *et al*. (2005) from OCTM (2002)
	VW03	TCC-ATC-TTT-GGG-ACC-ACT-GTC-G			Greiner *et al*. (2005) from OCTM (2002)
T25 maize	T25-F7	ATG-GTG-GAT-GGC-ATG-ATG-TTG	209	T25	Greiner *et al*. (2005) from OCTM (2002)
	T25-R3	TGA-GCG-AAA-CCC-TAT-AAG-AAC-CC			Greiner *et al*. (2005) from OCTM (2002)
Roundup-Ready™ soy	p35s-f2	TGA-TGT-GAT-ATC-TCC-ACT-GAC-G	172	$P^{35}s$	Greiner *et al*. (2005) from OCTM (2002)
	petu-r1	TGT-ATC-CCT-TGA-GCC-ATG-TTG-T			Greiner *et al*. (2005) from OCTM (2002)

(*Continued*)

Table 12.1 (Continued)

Species	Primer or probe	Sequence (5′–3′)	Size of amplified sequence (bps)	Gene or DNA target sequence	References
Endog.maize	Zetm1	TGT-TAG-GCG-TCA-TCA-TCT-GTG-G	69	*Zein*	Vaïtilingom *et al*. (1999)
	Zetm3	TGC-AGC-AAC-TGT-TGG-CCT-TAC			Vaïtilingom *et al*. (1999)
	Zetmp	ATC-ATC-ACT-GGC-ATC-GTC-TGA-AGC-GG			Vaïtilingom *et al*. (1999)
Trans. maize	Crytm1	GTG-GAC-AGC-CTG-GAC-GAG-AT	105	*CryIA(b)*	Vaïtilingom *et al*. (1999)
	Crytm2	TGC-TGA-AGC-CAC-TGC-GGA-AC			Vaïtilingom *et al*. (1999)
	Crytmp	AAC-AAC-AAC-GTG-CCA-CCT-CGA-CAG-G			Vaïtilingom *et al*. (1999)
Endog. soy	Sltm1	AAC-CGG-TAG-CGT-TGC-CAG	81	*le1*	Vaïtilingom *et al*. (1999)
	Sltm2	AGC-CCA-TCT-GCA-AGC-CTT-T			Vaïtilingom *et al*. (1999)
	Sltmp	TTC-GCC-GCT-TCC-TTC-AAC-TTC-ACC-T			Vaïtilingom *et al*. (1999)
Trans. soy	Sttmf3a	GCA-AAT-CCT-CTCG-CCC-TTT-CC	145	CP4 *EPSP*	Vaïtilingom *et al*. (1999)
	Sttmr2a	CTT-GCC-CGT-ATT-GAT-GAC-GTC			Vaïtilingom *et al*. (1999)
	Sttmpa	TTC-ATG-TTC-GGC-GGT-CTC-GCG			Vaïtilingom *et al*. (1999)
Endog. soy	le1-F	GAC-GCT-ATT-GTG-ACC-TCC-TC		*le1*	Wurz *et al*. (1999)
	le1-R	CAG-GGG-CAT-AGA-ACG-TG			Wurz *et al*. (1999)
	le1-F	GAC-GCT-ATT-GTG-ACC-TCC-TC		*le1*	Wurz *et al*. (1999)
	le1-R	TGT-CAG-GGG-CAT-AGA-AGG-TG			Wurz *et al*. (1999)
GA21 maize	GA141F	GGA-TCC-CCC-AGC-TTG-CAT	72		Hernández *et al*. (2004)
	GA212R	TTT-GGA-CTA-TCC-CGA-CTC-TCT-TCT			Hernández *et al*. (2004)
	GA160P	FAM-CCT-GCA-GGT-CGA-GGT-CAT-TCA-TAT-GCT-T-TAMRA			Hernández *et al*. (2004)
GA21 maize	GA141ZF	act-gaa-cct-gac-cgt-aca-GGA-TCC-CCC-AGC-TTG-CAT[b]	72		Hernández *et al*. (2004)
	GA212R	TTT-GGA-CTA-TCC-CGA-CTC-TCT-TCT			Hernández *et al*. (2004)
Endog. maize	IVR7F	GCG-CTC-TGT-ACA-AGC-GTG-C		*ivr1*	Hernández *et al*. (2004)
	IVR8R	GCA-AAG-TGT-TGT-GCT-TGG-ACC			Hernández *et al*. (2004)
	IVR78P	VIC-CAC-GTG-AGA-ATT-TCC-GTC-TAC-TCG-AGC-C-TAMRA			Hernández *et al*. (2004)
Endog. soy	F	TGC-CGA-AGC-AAC-CAA-ACA-TGA-TCC-T	414	*le1*	Forte *et al*. (2005) from Brodmann *et al*. (1997)
	R	TGA-TGG-ATC-TGA-TAG-AAT-TGA-CGT-T			Forte *et al*. (2005) from Brodmann *et al*. (1997)
Endog. maize	F	AGT-GCG-ACC-CAT-ATT-CCA-G	277	*zein*	Forte *et al*. (2005) from Stüder et al. (1997)
	R	GAC-ATT-GTG-GCA-TCA-TCA-TTT			Forte *et al*. (2005) from Stüder *et al*. (1997)
GMO NOS	F	GAA-TCC-TGT-TGC-CGG-TCT-TG	180	*nos*	Forte *et al*. (2005) from Lipp *et al*. (1999)
	R	TTA-TCC-TAG-TTT-GCG-CGC-TA			Forte *et al*. (2005) from Lipp *et al*. (1999)

GMO 35S	F	TGC-CTC-TGC-CGA-CAG-TGG-TC	83	*35S*	Forte *et al*. (2005) from Trapman *et al*. (2002)
	R	AAG-ACG-TGG-TTG-GAA-CGT-CTT-C			Forte *et al*. (2005) from Trapman *et al*. (2002)
Bt11 maize	Bt11-1	TAT-CAT-CGA-CTT-CCA-TGA-CCA	207	*cry1A(b)*	Zimmerman *et al*. (2000)
	Bt11-2	AGC-CAG-TTA-CCT-TCG-GAA-AA			Zimmerman *et al*. (2000)
Bt11 maize	ir^{c}-F	GGT-ACA-GTA-CAC-ACA-CAT-GTA-T	437	IVS6-*cry1A(b)*	Yamaguchi *et al*. (2003)
	ir^{c}-R	GAT-GTT-TGG-GTT-GTT-GTC-CAT			Yamaguchi *et al*. (2003)
Bt11 maize	ht^{d}-F	CCT-TCG-CAA-GAC-CCT-TCC-TCT-ATA	522	35S-*pat*	Yamaguchi *et al*. (2003)
	ht^{d}-R	AGA-TCA-TCA-ATC-CAC-TCT-TGT-GGT-G			Yamaguchi *et al*. (2003)
Maize 176	ir^{c}-F	AGA-TTC-TTC-ACT-CCG-ATG-CAG-CCT-A	619	PEPC prom-*cry1A(b)*	Yamaguchi *et al*. (2003)
Event maize	ir^{c}-R	GAT-GTT-TGG-GTT-GTT-GTC-CAT			Yamaguchi *et al*. (2003)
	ir^{c}-F	AGT-TTC-CTT-TTT-GTT-GCT-CTC-CT	194	hsp70 int.1-*cry1A(b)*	Yamaguchi *et al*. (2003)
MON810	ir^{c}-R	GAT-GTT-TGG-GTT-GTT-GTC-CAT			Yamaguchi *et al*. (2003)
LIBERTY maize	ht^{d}-F	CCT-TCG-CAA-GAC-CCT-TCC-TCT-ATA	231	35S-*pat*	Yamaguchi *et al*. (2003)
	ht^{d}-R	AGA-TCA-TCA-ATC-CAC-TCT-TGT-GGT-G			Yamaguchi *et al*. (2003)
zein	F	TGC-TTG-CAT-TGT-TCG-CTC-TCC-TAG	329	*zein*	Yamaguchi *et al*. (2003)
	R	GTC-GCA-GTG-ACA-TTG-TGG-CAT			Yamaguchi *et al*. (2003)
Barley	hor1	AGA-CAA-GGC-GTG-CAG-ATC-G	73	γ-hordein	Hernández *et al*. (2005)
Barley	hor2	GAC-CCT-GGA-CGA-GCA-CAC-AT			Hernández *et al*. (2005)
Barley	hor-probe	CCT-CAG-CCG-CAA-CAG-GTG-GGT-C			Hernández *et al*. (2005)
Rice	org1	TTA-GCC-TCC-CGC-TGC-AGA	68	*gos9*	Hernández *et al*. (2005)
Rice	org2	AGA-GTC-CAC-AAG-TGC-TCC-CG			Hernández *et al*. (2005)
Rice	orb-probe	FAM-CGG-CAG-T6T-GGT-TGG-TTT-CTT-CGG			Hernández *et al*. (2005)
Wheat	tri1	TGC-CCA-TTG-TCG-GCC-TTA	93	*acc1*	Hernández *et al*. (2005)
Wheat	tri2	GCA-TTC-CAA-CCA-TCT-GCC-C			Hernández *et al*. (2005)
Wheat	tri-probe	TGC-CTC-GAC-AAC-ACC-ATC-GCT-ATC0-C			Hernández *et al*. (2005)
Wheat	UnivF	CAA-GTA-TGT-CAT-AGA-GAT-TTG-AA		PKABA1	Ronning *et al*. (2006)
Wheat	UnivR	GTA-ACC-GAA-GTC-ACA-AAT-CT			Ronning *et al*. (2006)
Wheat probe	Taest	FAM-TCG-CAC-CTC-GGC-T-MGBNFQ			Ronning *et al*. (2006)
Barley probe	Hvulg	VIC-TCG-CTC-CTC-GAC-TC-MGBNFQ			Ronning *et al*. (2006)
Sunflower	hel1	CTC-GAG-CAC-CTC-CGG-CT	60	*hel*	Ronning *et al*. (2006)
Sunflower	hel2	AGC-GTG-GAA-AGA-GGC-GAA-CTC-CG			Ronning *et al*. (2006)
Sunflower	hel-probe	GGA-TTG-GAT-GGC-ATT-CGG			Ronning *et al*. (2006)
WBR11	Sense	GGT-AAC-TTC-CAA-ATT-CAG-AGA-AAC	196 & 201	*trnL*	Dahinden *et al*. (2001)
WBR13	Antisense	TCT-CTA-ATT—TAG-AAT-TAG-AAG-GAA			Dahinden *et al*. (2001)
Mussel	MusRFLP-F	CGA-GGC-CCC-GTA-ATT-GGA-ATG-A	230–237	18S rDNA	Santaclara *et al*. (2006)
	MusRFLP-R	TCA-GTC-AAG-AGC-ACC-AAG-GGC			Santaclara *et al*. (2006)
Mussel	MusRFLP-F	CGA-GGC-CCC-GTA-ATT-GGA-ATG-A	167–169	18S rDNA	Santaclara *et al*. (2006)
	MusFINS-R	AAA-CCG-GGA-GGT-AGG-TCA-GG			
Mussel	Pspp-F	AYA-AAC-GGA-GGT-TAC-GGT-TTC[a]	171–207	–	Santaclara *et al*. (2006)
	Pspp-R	GTG-CGA-GGC-MRA-WRW-GGA-AAA[a]			Santaclara *et al*. (2006)

(*Continued*)

Table 12.1 (Continued)

Species	Primer or probe	Sequence (5′–3′)	Size of amplified sequence (bps)	Gene or DNA target sequence	References
Mussel	CHORO-F	AGG-ATC-ATT-ACC-GCA-ATA-CGA-T	100	–	Santaclara *et al*. (2006)
	CHORO-R	AAA-CGA-CGK-AGG-ACT-TTG-CRTa			Santaclara *et al*. (2006)
Mussel	Me 15	CCA-GTA-TAC-AAA-CCT-GTG-AAG-A	126–180	adhes. prot. Gene	Santaclara *et al*. (2006) from Inoue *et al*. (1995)
	Me 16	TGT-TGT-CTT-AAT-AGG-TTT-GTA-AGA			Santaclara *et al*. (2006) from Inoue *et al*. (1995)
Crustaceans	F-primer	TAA-AGT-CTG-GCC-TGC-CCA	205	16S rDNA	Brzezinski (2005)
	R-primer	GCT-TTA-TAC-GGT-CTT-ATC-GT			Brzezinski (2005)
Tuna	59–3	AAA-CTG-CAG-CCC-CTC-AGA-ATG-ATA-TTT-GTC-CTC-A	123	mt*Cytb*	Rehbein *et al*. (1999)
	59–5	GCT-GGT-ACC-TCT-ACA-AAG-AAA-CAT-GAA-ACA			Rehbein *et al*. (1999)
Red snapper	L232	GAT-AGT-CTC-GTT-AGC-ACA-AAA-GCT-TGG-T	~850	mt12S rDNA	Zhang *et al*. (2006)
	H231	TGA-CTG-CAG-AGG-GTG-ACG-GGC-GGT-GTG-T			Zhang *et al*. (2006)
Red snapper	L231	TCA-AAC-TGG-GGA-TTA-GAT-ACC-CCA-CTA-T	~450	mt12S rDNA	Zhang *et al*. (2006)
	H231	TGA-CTG-CAG-AGG-GTG-ACG-GGC-GGT-GTG-T			Zhang *et al*. (2006)
Soy	Le1n02-5′	GGC-CTC-TAC-TCC-ACC-CCC-A		*lel*	Moriuchi *et al*. (2007)
Lectin	Le1n02-3′	GCC-CAT-CTG-CAA-GCC-TTT-TT			Moriuchi *et al*. (2007)
	Le1-probe	FAM-AGC-TTC-GCC-GCT = YCC-TTC-AAC-TTC-ACTAMRA			Moriuchi *et al*. (2007)
RRS	RRS01-5′	CCT-TTA-GGA-TTT-CAG-CAT-CAG-TGG		RRS gene	Moriuchi *et al*. (2007)
	RRS01-3′	GAC-TTG-TCG-CCG-GGA-ATG			Moriuchi *et al*. (2007)
RRS-probe		FAM-CGC-AAC-CGC-CCG-CAA-ATC-C-TAMRA			Moriuchi *et al*. (2007)
Pectinid	ISA1	AGG-TCC-TGT-GAA-TGG-TTT-GAC-GAG	~470	16S mtrRNA	Colombo *et al*. (2004) from Palumbi *et al*. (1991)
Scallops	OSA2	CAA-GCC-TTA-GGA-TAT-CCA-GAG-CCA-AC			Colombo *et al*. (2004) from Palumbi *et al*. (1991)
Messolongi	16SARL	CGC-CTG-TTT-ATL-AAA-AAC-AT	600–630	16S mtrRNA	Klossa-Kilia *et al*. (2002) from Palumbi *et al*. (1991)
Roe	16SARH	CCG-GTG-TGA-ACT-CAG-ATC-ACG-T			Klossa-Kilia *et al*. (2002) from Palumbi *et al*. (1991)
Molluscs	16SAR	CGC-CTG-TTT-ATC-AAA-AAC-AT	600–700	16S mtrRNA	Colombo *et al*. (2002b) from Bonnaud *et al*. (1998)
	16SBR	CCG-GTC-TGA-ACT-CTG-ATC-AT			Colombo *et al*. (2002b) from Bonnaud *et al*. (1998)

Billfish	L-CYTBF	GCT-ATI-CAC-TAY-ACM-TCR-GAC[a]	348	mt*cytb*	Hsieh *et al*. (2005)
	H-CYTBF	GCC-TCC-TCA-0RAT-TCA-TTG-GAC[a]			Hsieh *et al*. (2005)
Pisces	5SA	TAC-GCC-CGA-TCT-CGT-CCG-ATC	210–430	16S mtRNA	Karaiskou *et al*. (2005) from Pendas *et al*. (1995)
	5SB	CAG-GCT-GGT-ATG-GCC-GTA-AGC			Karaiskou *et al*. (2005) from Pendas *et al*. (1995)
Cod	cytB1	CCA-TCC-AAC-ATC-TCA-GCA-TGA-TGA-AA	307	mt*cytb*	Comi *et al*. (2005) from Barlet and Davidson (1991)
	cytB2	CCC-CTC-AGA-ATG-ATA-TTT-GTC-CTC			Comi *et al*. (2005) from Barlet and Davidson (1991)
	GC clamp	GCC-AGC-GGC-CCG-GCG-CCG-GCC-GGG-CGG-CGG-GGG-CCG-CGG-C			
Puffer fish	L14841	AAA-AAG-CTT-CCA-TCC-AAC-ATC-TCA-GCA-TGA-TGA-AA	376	mt*cytb*	Chen *et al*. (2002)
Puffer fish	L15149	TGA-GGA-CAA-ATA-TCC-ATT-CTG-AGG-GGC-TGC-AGT-TT			Chen *et al*. (2002)
Wreck fish	12S1	AAA-CTA-GGA-TTA-GAT-ACC-CTA-TTA-T	436	12 rDNA	Asensio *et al*. (2000)
Wreck fish	12S2	AAG-AGC-GAC-GGG-CGA-TGT-GT			Asensio *et al*. (2000)
35S sense		GCT-CCT-ACA-AAT-GCC-ATC-A	195	35S rRNA	Liu *et al*. (2005)
35S antisense		GAT-AGT-GGG-ATT-GTG-CGT-CA			Liu *et al*. (2005)
35S probe 1		CGG-CAG-AGG-CAT-CTT-CAA-CGA-TGG-CC-biotin			Liu *et al*. (2005)
35S probe 2		Ru-TTT-CCA-CGA-TGC-TCC-TCG-TGG-GTG-GG			Liu *et al*. (2005)
NOS sense		GAA-TCC-TGT-TGC-CGG-TCT-TG	180	NOS terminator	Liu *et al*. (2005)
NOS antisense		TTA-TCC-TAG-TTT-GCG-CGC-TA			Liu *et al*. (2005)
NOS probe 1		CCA-TCT-AAA-TAA-CGT-CAT-GCA-T-biotin			Liu *et al*. (2005)
NOS probe 2		Ru-CGC-GTA-TTA-AAT-GTA-TAA-TTG-CG			Liu *et al*. (2005)
Mg1	P-35S	TAT-CTC-CAC-TGA-CGT-AAG-GGA-TGA-C	401	35S rRNA	Zimmerman *et al*. (1998)
Mg2	hsp70	TGC-CCT-ATA-ACA-CCA-ACA-TGT-GCT-T		hsp70	Zimmerman *et al*. (1998)
Mg3	P-35S	ACT-ATC-CTT-CGC-AAG-ACC-CTT-CCT-C	149	35S-rRNA	Zimmerman *et al*. (1998)
Mg4	hsp70	GCA-TTC-AGA-GAA-ACG-TGG-CAG-TAA-C		hsp70	Zimmerman *et al*. (1998)
hm1		CTA-CTT-TGA-CTT-TCC-CTT-AAT-GAC			Zimmerman *et al*. (1998)
hm2		AGC-AGG-AGC-AGT-GTA-TAT-ACA-CAT			Zimmerman *et al*. (1998)
hm3		GAA-ATC-CCT-GAG-CGA-GTC-GGT-A			Zimmerman *et al*. (1998)
hm4		GCG-ATG-GCC-TTG-TTG-TAC-TCG-A			Zimmerman *et al*. (1998)
35S-F		biotin-GCT-CCT-ACA-AAT-GCC-ATC-A	195	35S rRNA	Liu *et al*. (2005)
35S-R		GAT-AGT-GGG-ATT-GTG-CGT-CA			Liu *et al*. (2005)
35S-P		DIG-CAA-CCA-CGT-CTT-CAA-AGC-AA			Liu *et al*. (2005)
nos-F		biotin-GAA-TCC-TGT-TGC-CGG-TCT-TG	180	*NOS* terminator	Liu *et al*. (2005)
nos-R		TTA-TCC-TAG-TTT-GCG-CGC-TA			Liu *et al*. (2005)
nos-P		DIG-TGC-CGG-TCT-TGC-GAT-GAT-TAT-CAT-A			Liu *et al*. (2005)
lec-F		biotin-CCA-GCT-TCG-CCG-CTT-CCT-TC		*NOS* terminator	Liu *et al*. (2005)

(*Continued*)

Table 12.1 (Continued)

Species	Primer or probe	Sequence (5′–3′)	Size of amplified sequence (bps)	Gene or DNA target sequence	References
lec-R		GAA-GCC-AAG-CCC-ATC-TGC-AAG-CC			Liu *et al*. (2005)
lec-P		DIG-CTT-CAC-CTT-CTA-TGC-CCC-TGA-CAC			Liu *et al*. (2005)
inv-F		biotin-TGG-CGG-ACG-ACG-ACT-TGT		*inv*	Liu *et al*. (2005)
inv-R		AAA-GTT-TGG-AGG-CTG-CCG			Liu *et al*. (2005)
inv-P		DIG-CGA-GCA-GAC-CGC-CGT-GTA-CTT-CTA-CC			Liu *et al*. (2005)
P35S1-5		ATT-GAT-GTG-ATA-TCT-CCA-CTG-ACG	101	35S rRNA	Abdullah *et al*. (2006) from Tengel *et al*. (2001)
P35S1-3		CCT-CTC-CAA-ATG-AAA-TGA-ACT-TCC-T			Abdullah *et al*. (2006) from Tengel *et al*. (2001)
HA-nos118-R		GAC-ACC-GCG-CGC-GAT-AAT-TTA-TCC	118	NOS terminator	Abdullah *et al*. (2006) from Lipp *et al*. (1999)
HA-nos118-f		GCA-TGA-CGT-TAT-TTA-TGA-GAT-GGG			Abdullah *et al*. (2006) from Lipp *et al*. (1999)
RR soy	RR01	TGG-CGC-CCA-AAG-CTT-GCA-TGG-C	356	EPSPS enzyme	Abdullah *et al*. (2006) from Tengel *et al*. (2001)
	RR04	CCC-CAA-GTT-CCT-AAA-TCT-TCA-AGT			Abdullah *et al*. (2006) from Tengel *et al*. (2001)
Lectin 1		GAC-GCT-ATT-GTG-ACC-TCC-TC	318	*le1*	Abdullah *et al*. (2006) from Tengel *et al*. (2001)
Lectin 6		GAA-AGT-GTC-AAG-CTT-AAC-AGC-GAC-G			Abdullah *et al*. (2006) from Tengel *et al*. (2001)
Soy	Lectin-F	TCC-ACC-CCC-ATC-CAC-ATT-T	81	*le1*	Peano *et al*. (2005a)
	Lectin-R	GGC-ATA-GAA-GGT-GAA-GTT-GAA-GGA			Peano *et al*. (2005a)
Maize	Zeindeg-F	TAC-AAG-GAT-GCG-ATA-CAC-ACA	133	*Zein*	Peano *et al*. (2005a)
	Zein133-R	TAC-AAG-GAT-GCG-ATA-CAC-ACA			Peano *et al*. (2005a)
RR soy	RR2075-F	CTG-CCT-GAT-GAG-CTC-GAA-TTC	210	*CP4EPSPS-TNOS*	Peano *et al*. (2005a)
	MOSterN-R	GCG-GGA-CTC-TAA-TCA-TAA-AAA-CCC			Peano *et al*. (2005a)
Maize	Bt1135SADH241-F	CAA-TCC-CAC-TAT-CCT-TCG-CAA	241	*35S rRNA-IV 2*	Peano *et al*. (2005a)
	Bt1135SADH241-F	GTA-GAC-GTC-GGT-GTG-GCA-GA			Peano *et al*. (2005a)
Maize	Bt17635SBAR151-F	TTC-TTA-TAG-GGT-TTC-GCT-CAG-CTG	151	*35S rRNA-BAR*	Peano *et al*. (2005a)
	Bt17635SBAR151-R	GGT-TGA-CGA-TGG-TGC-AGA-CC			Peano *et al*. (2005a)
Maize	RACTN-F	TCC-CTC-AGC-ATT-GTT-CAT-CGG-TA	193	*RACT-OTP*	Peano *et al*. (2005a)
	CTPN-R	ACC-ATG-TTG-GCC-TGA-GCA-GG			Peano *et al*. (2005a)
Maize	MON-F	TGG-AGA-GGA-GAC-GCT-GAC-AA	101	*35S rRNA-HSP79*	Peano *et al*. (2005a)
	MON-R	GCA-TTC-AGA-GAA-ACG-TGG-CAG-TA			Peano *et al*. (2005a)
Soy	lectin Disc-P	Cy3-GTA-GCG-TTG-CCA-GCT-TCG-CCG			Peano *et al*. (2005a)
	lectin Comm-P	CTT-CCT-TCA-ACT-TCA-CCT-TCT-ATG-cca-tct-tgc-gcg-gca-gct-cgt-cga-ccg[e]			Peano *et al*. (2005a)
Maize	Zein Disc-P	Cy3-ATG-CGA-TAC-ACA-CAT-CAG-CTA-GTC-CTA-A			Peano *et al*. (2005a)

	Zein Comm-P	TGA-TGC-CAC-CGA-CTT-TAC-TTAGG-AAA-Acc-gta-ccc-ttc-cgc-tgg-aga-ttt-ac[e]			Peano *et al*. (2005a)
Soy	RRsoy Disc-P	Cy3-GCC-TGA-TGA-GCT-CGA-ATT-CGA-GC			Peano *et al*. (2005a)
	RRsoy Comm-P	TCG-GTA-CCG-GAT-CCA-TTC-CGC-Gct-tga-gcg-atg-acg-gac-ggg-aaa-ag[e]			Peano *et al*. (2005a)
Maize	Bt11maize Disc-P	Cy3-CTC-TAG-CGA-AGA-TCC-TCT-TCA-CCT-C			Peano *et al*. (2005a)
	BT11maize Comm-P	GCT-CTG-CCA-CAC-CGA-CGT-CTA-caa-agc-ggg-cgg-cga-tcg-cga-atg-tc[e]			Peano *et al*. (2005a)
Maize	Bt176maize Disc-P	Cy3-ATC-TGT-TGG-GGA-TCT-ACC-ATG-AGC-C			Peano *et al*. (2005a)
	BT176maize Comm-P	CAG-AAC-GAC-GCC-CGG-CCG-agg-att-gca-ccg-tca-gca-cca-ccg-ag[e]			Peano *et al*. (2005a)
Maize	GA21 maize Disc-P	Cy3-CGA-TAA-GCT-GGG-CTG-CAG-GAA-TTC			Peano *et al*. (2005a)
	GA21 maize Comm-P	CGA-AAG-ACA-AAG-ATT-ATC-GCC-ATG-GCg-tgg-tcc-atc-aca-aac-ag[e]			Peano *et al*. (2005a)
Maize	MON810 maize Disc-P	Cy3-GCA-GAT-CTA-CCG-TCT-TCG = GTA-CG			Peano *et al*. (2005a)
	MON810 maize Comm-P	CGC-TCA-CTC-CGC-CCT-CTG-Ctg-tgc-gcc-cga-gat-cgg-tat-ccc-cg[e]			Peano *et al*. (2005a)
Wheat	1B F-primer	GGC-CAT-GGA-AAA-CTG-GGC-AA		rDNA	Sallares *et al*. (1995)
Wheat	2D R-primer	GCG-TTT-CAA-AAC-AGT-GTA-CCC			Sallares *et al*. (1995)
Wheat	3A I-primer	AGC-GAA-AAC-ATG-TCT-CAT-GGC			Sallares *et al*. (1995)
Salmon/trout	L14735	AAA-AAC-CAC-CGT-TGT-TAT-TCA-ACT-A		mt*Cytb*	Dooley *et al*. (2005) from Russell *et al*. (2000)
	H15149	GCI-CCT-CAR-AAT-GAY-ATT-TGT-CCT[a]			Dooley *et al*. (2005) from Russell *et al*. (2000)
GMOs	T-NOS-F	GAG-TCC-TGT-TGC-CGG-TCT-TG	207	NOS terminator	Kalogianni *et al*. (2006)
	T-NOS-R	GGG-ACT-CTA-ATC-ATA-AAA-ACC-CAT			Dooley *et al*. (2005) from Russell *et al*. (2000)
NOS-P		ACA-TGC-TTA-ACG-TAA-TTC-AAC-AGA			Dooley *et al*. (2005) from Russell *et al*. (2000)
Wheat/spelt	GAG31	GCA-GCA-AGA-ACA-ACA-AGA-ACA-AA	236	*GAG56P*	von Büren *et al*. (2001)
Wheat/spelt	GAG28	CGG-CGA-CTA-CGT-TGG-A			von Büren *et al*. (2001)
Wheat/spelt	GAG15	GCA-ACC-ACA-ACA-ACA-ATT-TTC-T	350 & 359	*GAG56D*	von Büren *et al*. (2001)
Wheat/spelt	GAG16	GAT-ATA-GTG-GCA-GCA-GGA-TAT-G			von Büren *et al*. (2001)
GMOs	P35S-F	CGA-AGG-ATA-GTG-GGA-TTG-TGC-GTC		35S rRNA	von Büren *et al*. (2001)
	P35S-R	AAG-GTG-GCT-CCT-ACA-AAT-GCC-ATC			von Büren *et al*. (2001)
	35S-P	GCA-AGT-GGA-TTG-ATG-TGA-TAT-CTC			von Büren *et al*. (2001)
Soy	Lectin-F	GAC-GCT-ATT-GTG-ACC-TCC-TC		*le1*	von Büren *et al*. (2001)
	Lectin-R	TGT-CAG-GGG-CAT-AGA-AGG-TG			von Büren *et al*. (2001)
	Lectin-P	AAT-GTG-GAT-GGG-GGT-GGA-GTA-GAG			von Büren *et al*. (2001)

(*Continued*)

Table 12.1 (Continued)

Species	Primer or probe	Sequence (5′–3′)	Size of amplified sequence (bps)	Gene or DNA target sequence	References
Fish	L14735	AAA-AAC-CAC-CGT-TGT-TAT-TCA-ACT-A	464	mt*Cytb*	Wolf *et al.* (2000)
	H15149ad	GDCN-CCT-CAR-AAT-GDAY-ATT-TGT-CCT-CA[a]			Wolf *et al.* (2000)
RR soy	RRS-F	CCA-TTC-TTG-AAA-GAT-CTG-CT	102	CP4EPSPS/NOS-T	Peano *et al.* (2005b)
	RRS-R	ATC-CCA-CTA-TCC-TTC-GCA-A			Peano *et al.* (2005b)
Maize	Bt176Cle-F	CGA-ACT-CGA-TGC-CGT-CGA-TGT	96	35SCAMV/bar	Peano *et al.* (2005b)
	Bt176Cle-R	CCC-TTC0AAC-TTC-AGC-AAC-GCC			Peano *et al.* (2005b)
Maize	BT11Cle-F	AAC-CGC-GAG-TTG-TTG-TAT	131	35SCaMV/adh intron	Peano *et al.* (2005b)
	BT11Cle-R	CCT-TAC-TCT-AGC-GAA-GAT-CCT			Peano *et al.* (2005b)
Maize	MONCle-F	GCA-GAT-CTA-CCG-TCT-TCG-GTA-CG	98	35SCaMV/hsp70 intron	Peano *et al.* (2005b)
	MONCle-R	CTC-GCA-ATC-ACC-ACA-CAA-GAG-AG			Peano *et al.* (2005b)
Maize	GA21-F	TCC-CTC-AGC-ATT-GTT-CAT-CGG-TA	120	Actin promoter/CTP	Peano *et al.* (2005b)
	GA21-R	ACC-ATG-TTG-GCC-TGA-GCA-GG			Peano *et al.* (2005b)
RR soy	PNA	PNA H-CTA-GAG-TCA-GCT-TGT-NH_2			Peano *et al.* (2005b)
Maize	BT176	PNA H-ACA-CCT-CGT-TGC-CGC-NH_2			Peano *et al.* (2005b)
Maize	Bt11	PNA H-ATA-TCT-ACT-GAC-AAA-NH_2			Peano *et al.* (2005b)
Maize	MON810	PNA H-H-AGC-CCA-GCT-TAT-CGT-NH_2			Peano *et al.* (2005b)
Maize	GA12	PNA H-AGE-CCA-GCT-TAT-CGT-NH_2			Peano *et al.* (2005b)
Soy	EPSPS-F	GTC-TTC-CCG-TTA-CCT-TGC-GC	134	*ESPSP*	Peano *et al.* (2005b)
	EPSP-R	CTC-GAT-GAC-CGT-CGT-GAT-GC			Peano *et al.* (2005b)
Soy	P35S-F	ATT-GAT-GTC-ATA-TCT-CCA-CTG-ACG-T	101	*35S rRNA*	Peano *et al.* (2005b)
	P35S-R	CCT-CTC-CAA-ATG-AAA-TGA-ACT-TCC-T			Peano *et al.* (2005b)
Sesame	F-primer	TTA-CCA-GAG-GGC-TAG-GGA-CCT-T	66	2S albumin	Brzezinski (2007)
Sesame	R-primer	AAC-TCG-GAA-TTG-GCA-TTG-CT			Brzezinski (2007)
Sesame	probe	FAM-CTCGCA-GGT-GCA-ACA-TGC-GAC-C			Brzezinski (2007)
Bovine	12SM-FW	CTA-GAG-GAG-CCT-GTT-CTA-TAA-TCG-ATA-A	233	mt12S rRNA	Inéz *et al.* (2005)
	12SBT-RV	TGG-TTT-CAT-AAT-AAC-TTT-CGC-GCT			Inéz *et al.* (2005)
Bovine	12SM-FW	CTA-GAG-GAG-CCT-GTT-CTA-TAA-TCG-ATA	346	mt12S rRNA	López-Calleja *et al.* (2005)
	12SBT-REV2	AAA-TAG-GGT-TAG-ATG-GAC-TGA-ATC-CAT			López-Calleja *et al.* (2005)
Buffalo	12SBUF-REV	TTC-ATA-ATA-ACT-TTC-GTG-TTG-GGT-GT		mt12S rRNA	López-Calleja *et al.* (2005)
Bovine	CytOx IIa	AYG-GCA-TAT-CCC-ATA-CAA-CTA-G	651	mt*Cyt ox* II	Mayer (2005) from Verkaar *et al.* (2002)
	CytOx IIb	ACT-TTA-GTG-GGA-CTA-ACT-CAA-G			Mayer (2005) from Verkaar *et al.* (2002)

Bovine	BosL-15794	TTC-TAT-TTA-AAC-TAT-TCC-CTG-AAC	413	mtDNA	Mayer (2005) from Maudet and Taberlat (2001)
	BosH-16102	GAT-ATA-CTA-TCA-AGA-ATG-AAT-TTG-AC			Mayer (2005) from Verkaar *et al*. (2002)
Bovine	Cow-14814	GGC-TTA-TAT-TAC-GGG-TCT-TAC-ACT	279	Mt*Cytb*	Bottero *et al*. (2002)
	Cow-15092	GGC-AAT-TGC-TAT-GAT-GAT-AAA-TGG-A			Bottero *et al*. (2002)
Bovine	Bos taurus1	GTA-CTA-CTA-GCA-ACA-GCT-TA	256	mt12S rRNA	Bottero *et al*. (2003)
	Bos taurus2	GCT-TGA-TTC-TCT-TGG-TGT-AGA-G			Bottero *et al*. (2002)
Sheep	Sense 959	ATA-TCA-ACC-ACA-CGA-GAG-GAG-AC	172	mt12S rRNA	Bottero *et al*. (2003)
	Antisense 1130	TAA-ACT-GGA-GAG-TGG-GAG-AT			Bottero *et al*. (2002)
Goat	Sense 144	GGC-CCT-CCA-AAT-CAA-TAA-G	326	mt12S rRNA	Bottero *et al*. (2003)
		AGT-GTA-TCA-GCT-GCA-GTA-GGG-TT			Bottero *et al*. (2002)
Bovine	Sense 916	GTA-CTA-CTA-GCA-ACA-GCT-TA	256	mt2S rRNA	Bottero *et al*. (2003)
		GCT-TGA-TTC-TCT-TGG-TGT = AGA-G			Bottero *et al*. (2002)

[a] Y = C or T, R = A or G, N = A or G or C or T, M = A or C, W = A or T, I = inosine.
[b] Lower case: Z sequence of the Amplifluor™ primer
[c] Insect resistance gene
[d] Herbicide tolerance gene
[e] Lower case indicates cZip Codes, complementary to the Zip code sequences of the universal array

versus the final spelt bands (350, 272 and 296 bp) were used for unique analysis of the band ratios for competitive quantification of wheat in spelt flour samples. PCR-RFLP analysis revealed that among seven commercial spelt samples, one contained no spelt, one contained 11% wheat, and a third contained 28% wheat.

Ronning *et al*. (2006) developed a duplex real-time PCR assay for simultaneous detection and quantification of wheat and barley in foods. Universal primers UnivF/UnivR were used that amplify a sequence of the serine/threonine protein kinase *PKABA1* gene present in both wheat and barley as single copies. The minor-groove-binding (MGB) probe Taest, specific for wheat, was labeled with the fluorescent reporter FAM at the 5′-end and with the non-fluorescent quencher MGBNFQ at the 3′-end. The MGB probe Hvulg, specific for barley, was labeled with VIC at the 5′-end and with MGBNFQ at the 3′-end. The limits of detection were 5 and 10 PCR-forming units for wheat and barley, respectively. Positive amplification was achieved with 10 different wheat cultivars and nine different barley cultivars. Amplification did not occur with oat, rye, maize, rice, timothy, durra, cabbage, cauliflower, soybean, pea, bean, lens, peanut, tomato, rape seed, potato, eggplant, and pepper.

Sesame seeds have recently become recognized as the source of major allergens resulting in either a delayed-type hypersensivity reaction, characterized by atopic dermatitis, or an immediate-type response resulting in anaphylactic shock in severe cases (Brzezinski, 2007). Sesame seeds may contain as many as 100 allergens, including oleosins, seed storage proteins, and the β-globulin or 2S albumin proteins. The 2S albumin proteins are small, water-soluble proteins which are notably resistant to proteolytic digestion, in addition to thermal and chemical denaturation, and have been determined to be allergenic in Brazil nuts, cashews, hazelnuts, walnuts and mustard seeds. Brzezinski (2007) developed a real-time PCR assay for the specific detection of sesame-seed DNA in food products. The forward and reverse primers amplified a 66-bp sequence of the sesame seed 2S albumin gene. A dual-labeled probe with FAM at the 5′-end and TAMRA at the 3′-end was used for detection of amplification. The assay did not cross-react with DNA from edible seeds such as pumpkin, poppy and sunflower seeds, nor from tree nuts such as almonds, Brazil nuts, cashews, hazelnuts and walnuts, in addition to four varieties of peanuts. The assay was found capable of detecting 5 pg of purified sesame-seed DNA as well as 0.01% of ground sesame seeds added to ground-wheat crackers.

Individuals allergic to gluten, which induces celiac disease, must avoid ingestion of wheat, barley and rye (WBR). The maximum level of gliadin (a gluten protein) in foods labeled “gluten-free” is recommended to be 100 ppm by the *Codex Alimentarius*. Dahinden *et al*. (2001) developed a quantitative competitive PCR assay for the detection of gluten-free foods contaminated with celiac-toxic cereals. The assay simultaneously detects WBR-DNA on the basis of a non-coding region of the chloroplast *trnL* (intergeneric spacer region) gene. The primer pair WBU/WBR13 yielded amplicons of 201-bp with rye and wheat, and 196-bp with barley. The assay was calibrated using a 221-pb internal competitive standard and equivalence point method, to 0.02% and 0.2% wheat DNA, corresponding to 10 ppm and 100 ppm gliadin. The QC-PCR assay was correlated with an ELISA assay based on a monoclonal antibody to a portion of the ω from wheat, barley, and rye. A positive WBR-PCR

signal and a negative ELISA assay for gliadin indicates a possible gliadin-free wheat, barley or rye starch addition. Both types of assays therefore complement one another. A negative WBR-PCR result and a positive ELISA suggest a WBR-free gliadin additive. Interestingly, 10 of 15 foods samples supposedly free of gluten were found free of gliadin, while one sample contained more than 100 ppm gliadin.

Meat products

Mammals and amphibians

In the United Kingdom, Europe and the USA there is currently a ban on feeding ruminants with ruminant-derived proteins in order to prevent the transmission of bovine spongiform encephalopathy (BSE). The failure of immunoassays to detect bovine proteins due to protein denaturation during the rendering process has resulted in PCR being the method of choice for detecting bovine tissue in feed. mtDNA sequences are preferred for distinguishing species by PCR amplification because they are known to be less conserved than is nuclear DNA (Kocher *et al*., 1989) and have the additional advantage of being multicopy, with up to 1000 copies per cell (Partis *et al*., 2000) resulting in enhanced detection sensitivity. Tartaglia *et al*. (1998) developed a dedicated PCR assay for bovine meat and bone meals (MBM) in feeds. The primers L8129/H8357 amplified a 271-bp bovine mtDNA fragment encoding the 3′-portion of $tRNA^{Lys}$, the ATPase subunit 8 (ATPase8) and the amino-terminal portion of the ATPase subunit 6 (ATPase6). This mtDNA region was chosen because both ATPase8 and ATPase6 exhibit a relatively high degree of variation among vertebrates. In addition, the $tRNA^{Lys}$-ATPase8-ATPase6 gene configuration is not found in the mtDNA of higher plants. Tissue from sheep, swine, horse, rabbit, chicken and turkey failed to yield an amplicon. Less than 0.125% of bovine-derived MBM (MBM) could be detected. The use of two restriction nucleases further confirmed the identity of the 271-bp bovine amplicon. *Dpn*II yielded two fragments of 57 and 214-bp, while *Ssp*I yielded three fragments of 66, 84 and 118-bp. The assay, however, was not designed to discriminate between the various other bovine species, including taurine cattle, water buffalo, African buffalo, zebu, banting, gaur, bison and yak, that are also consumed. Interestingly, hybridization of different bovine species is not uncommon, and invalidates any assay based on the maternally transmitted mtDNA. The American buffalo is bred for its beef quality and is derived from crossings of bison with cattle (Verkaar *et al*., 2002). Verkaar *et al*. (2002) described two complementary methods for bovine species identification. The first involves the PCR and restriction fragment length polymorphism (PCR-RFLP) of resulting amplicons, and is based on species-specific mutations on mtDNA of cytochrome b and cytochrome oxidase II. This method has the drawback in that only the maternal linage is identified. The second involves the application of the PCR to amplification of centromeric satellite DNA (satellite IV and satellite 1.711b) followed by restriction of the resulting amplicons yielding satellite fragment length polymorphism (PCR-SFLP). Since this assay is based on nuclear DNA, it offers the advantage of detecting interspecies hybridization. For PCR-RFLP with the mt*Cytb* amplicons, the following restriction endonucleases were used: *Alu*I, *Xba*I, *Stu*I, *Bam*HI, *Hin*fI and *Taq*I. For PCR-RFLP with the satellite IV amplicons,

*Ban*II and *Mse*I were used, and with satellite 1.711b amplicons, *Hind*III, *Taq*I and *Sau* 3A1 were used for restriction. From the combined restriction sites and resulting agarose bands derived from the two mitochondrial genes, the mtPCR-RFLP assay resulted in detection of all nine species. However, while discrimination of all nine bovine species was achieved, taurine cattle and zebra were not differentiated. African zebu have emerged by introgression (species hybridization) and have retained mtDNA of the taurine type, making it necessary to use satellite DNA sequences to detect such hybrids. Via the process of concerted evolution, the tandem repeated sequences in satellite DNA of hybrids become species-specific (Elder and Turner, 1995), reflecting both progenitors. A comparison of restriction banding patterns of such a suspected hybrid breed of cattle with those from the progenitor breeds yielded hybrid patterns using both mt*Cytb* and satellite IV amplicon restriction analysis. Elder and Turner (1995) concluded that (i) all relevant reference animals should be tested in parallel, (ii) PCR-RFLP differentiation should be based on at least two different restriction enzyme sites in order to exclude intraspecies polymorphism, and (iii) at least one RT-SFLP assay should be used if hybrid species are to be excluded. Because of the large size of several of the amplicons (651, 604 and 822 bp), the assay system is not suitable for processed or cooked meats, where significant DNA degradation may occur. In addition, the assay system is not suitable for meat samples comprised of more than one bovine species. The system is, however, ideally suited for unprocessed samples that originate from a single animal or from a homogeneous species.

RAPD was used by Koh *et al*. (1998) to generate banding patterns for raw meat samples from 10 species: wild boar, pig, horse, buffalo, beef, deer, dog, cat, rabbit and kangaroo. A total of 29 commercially available random primers, each 10 nucleotides in length, with GC contents ranging from 50 to 80%, were evaluated for their specificity and efficiency. With the use of an 80% GC primer (80-04) unique banding patterns were generated for 9 of the 10 species, with the pig and the horse failing to be distinguished. The use of the 50% GC primer (50-06) clearly distinguished pig from horse.

Guoli *et al*. (1999) selected a pair of primers to specifically amplify a 218-bp sequence of beef 1.709 satellite DNA that was shorter than the 3009-bp fragments that result from DNA degradation by heat processing meat. The assay was ideally suited for mixed meat samples and was positive for DNA derived from bovine, buffalo and yak meat, but negative for 10 additional mammals, and for fish, chicken and goose. A minimum of 33.6 fg of DNA from raw beef samples and 0.32 pg of DNA from cooked beef samples (120°C for 30 min) were detected by conventional PCR.

Partis *et al*. (2000) developed a PCR-RFLP technique for the identification of 22 animal species, including 5 fish species. The primer pair CYT b1/CYT b2 amplified a 359-bp sequence of the mt*Cyt b* gene. Resulting amplicons were digested with *Hae*II and *Hinf*I. All 22 species were distinguished, using the two restriction nucleases, except for kangaroo and buffalo. Each of the two nucleases generated from one to four DNA bands. The PCR amplicons and PCR-RFLP products were separated on 9% polyacrylamide gels and visualized by staining with ethidium bromide. Cooking (0.5 g in a microwave oven set on high for 30 s) did not affect the DNA banding profiles. The method, however, was found to be unsuitable for analyzing mixtures.

Colgan *et al*. (2001) developed a series of PCR assays specific for identification of bovine, poultry, porcine and sheep material in meat and bone meal (MBM). Two methods of DNA extraction were compared. One consisted of a simple lysis procedure involving overnight digestion in a lysis buffer containing EDTA, Triton X100 and Proteinase K. A 50- to 100-µl aliquot of the supernatant was diluted from 1:50 to 1:100, and 10 µl of these dilutions were incorporated directly into a 100-µL PCR. The second method consisted of using the QIA amp blood kit (QIAGEN). The bovine primer pair (LBOF/LBOR) from Tartaglia *et al*. (1998) amplified a sequence from the 8+ region of the *ATPase 6* gene. Additional primer pairs specific for the 8+ region of the *mtATPase 6* gene of poultry, pigs and sheep were also utilized. DNA extracted by the simple lysis procedure had an accuracy of 72.5% with regard to correctly generating amplicons for the predicted species in MBM. The QIA amp tissue kit yielded an accuracy of 60%. These values are thought to reflect extensive DNA degradation in the negative MBM samples, since inhibition of the PCR was shown not to take place when erroneously negative samples were seeded with fresh tissue from species known to be present. The limit of sensitivity of detection was found to be 0.3% for bovine and sheep primers, and 1% for the porcine primers.

Dalmasso *et al*. (2004) developed a multiplex PCR assay for the identification of poultry, ruminant, fish and pork materials in feedstuffs. Primers were designed from different regions of mitochondrial DNA (12S rRNA, tRNA Vae and 16s rRNA), yielding amplicons from 104 to 183 bp that were species-specific. DNA was extracted with the Dneasy Tissue kit (Qiagen). The detection limit for fish was 0.004%; that for ruminants, poultry and pork 0.002%, and that for bovine blood meal 0.1%.

Girish *et al*. (2004) developed a PCR assay for distinguishing meat from cattle, buffalo, sheep, goat, swine, yak and mitune (wild Asian ox). A single pair of universal primers was used to amplify a 456-bp sequence of the mt12S rRNA gene from each mammalian species. Sequencing of the resulting amplicons allowed a 407-bp region to be aligned, from which the seven species were distinguished. Heating the meat for 30 min at 120°C reduced the level of amplification but still yielded visible amplicons. The method, however, is not applicable to mixtures of meat species.

Girish *et al*. (2005) applied PCR-RFLP to a segment of the mt12S rRNA gene for distinguishing between meat from beef, buffalo, sheep and goat. The single pair of universal primers used yielded a 456-bp amplicon with meat from each species. The banding patterns resulting from restriction of the amplicons with the restriction endonucleases *ALU*I, *Hha*I, *Apo*I and *Bsp*TI allowed each of the four species to be identified. The technique was not suitable for meat mixtures, although consistent results were obtained with both fresh and processed meat samples.

Martin *et al*. (2006) developed individual PCR assays for the specific identification of bovine, sheep and goat DNAs in feedstuffs. The three pairs of primers designed generated amplicons of 84, 121 and 122 bp for cattle, sheep and goat tissue, respectively, from the 12S rRNA mt gene. Each amplicon was found to be highly species-specific with no cross-species amplification from 30 animal species (13 mammals, 12 fish and 5 birds) in addition to 8 plant species. The detection limit using the bovine specific primer pair was 0.1% in an oats-bovine mixture, which was not modified by heating at 133°C for 20 min.

Among the DNA target sequences available for distinguishing between species are *short interspersed elements* (*SINEs*), which reside within almost every genome studied to date (Deininger and Batzer, 1995). Most SINEs are thought to have been spread throughout each genome through an RNA-mediated duplication process. Because each of the SINE families within the different genomes has been derived independently, they can serve as novel markers for identification of a species. Primers can therefore be designed within the core sequence of the SINE so as to generate a homogeneous product composed entirely of the repeated core sequence that is amplified. Walker *et al*. (2003) designed four SINE-based real-time PCR assays using SYBR Green for species-specific detection and quantification of bovine, porcine, chicken and ruminant DNA. The primers yielded amplicons of 98, 134, 169 and 100 bp, respectively. Bovine DNA was detected at 0.005%, porcine at 0.0005% and chicken at 0.05% in meat mixtures.

Sika deer meat is highly valued in Japan because it is lean and has a sweet taste and little off-flavor. The replacement by imported red deer meat prompted Matsunaga *et al*. (1998) to develop a PCR-RFLP assay for distinguishing deer meat from other species, and for differentiating sika from red deer meat. Tissue was macerated and placed in a cell lysis solution containing EDTA and 1% SDS for 30 min. DNA was then extracted with phenol/chloroform/isoamyl alcohol (25:24:1) and then with chloroform. RNA was degraded with RNase, and the DNA was again solvent-extracted and finally precipitated with ethanol. The primer pair RD-1/RD-2 were designed to amplify a 194-bp fragment of the mt*Cytb* gene from red and sika deer, but not from cattle, pig, chicken, sheep, goat, horse and rabbit DNA. Although cooking the meat reduced the PCR product, deer meat could still be detected in meat heated at 120°C for 30 min. To discriminate between red and sika deer, amplicons were restricted with endonucleases (*Eco*RI, *Bam*HI and *Sca*I). The red deer amplicon was digested by *Eco*RI to yield two fragments (67 bp and 127 bp) but was not digested by *Bam*HI or *Sca*I. The sika deer amplicon was not digested by *Eco*RI, but was digested by *Bam*HI to two fragments (48 bp and 146 bp) and by *Sca*I to two fragments (49 bp and 145 bp). The red deer meat was therefore readily differentiated from the sika deer meat using *Eco*RI, *Bam*HI or *Sca*I.

Wolf and Lüthy (2001) developed a quantitative competitive PCR for the determination of the percent porcine tissue in a tissue mixture with meat from other species. The primer pair used (GHP1/GHP2) amplified a 225-bp sequence of the swine growth hormone gene and also a 255-bp sequence derived from a 30-bp insertion into the mid-portion of the 225-bp target sequence. The primer pair was specific for the swine species, and did not yield an amplicon with DNA derived from cattle, sheep, chicken and turkey. The sensitivity was 100 pg of swine DNA corresponding to 0.1% of a mixture.

The method of DNA extraction can significantly influence the amplification efficiency. Lahiff *et al*. (2001) developed species-specific PCR assays for identification of sheep, swine, chicken and bovine species in meat and bone meal (MBM). Two methods of DNA extraction were used. The first was that of Boom *et al*. (1999), involving a silica particle guanidiniumisocyanate procedure. The second involved the use of the Q1Amp Blood Kit (Qiagen). The kit yielded higher quality and a higher

yield of DNA, with greater amplification sensitivity. The identity of the resulting amplicons was confirmed from restriction endonuclease digestion products yielding two specific fragments from each amplicon. Restriction was not required for species identification. The limits of detection in meat mixtures were: cattle (1%), sheep (5%), swine (1%) and poultry (5%).

The commercial farming and exploitation in China of the endangered Chinese alligator has resulted in illegal and inappropriately labeled Chinese alligator meat. This prompted Yan *et al*. (2005) to develop multiplex PCR assay for the identification of meat from the Chinese alligator. One pair of primers, Alli-M and Alli-R, was highly specific for the Chinese alligator and was designed using sequence variations of the mtCyt*b* gene between the Chinese alligator and other crocodilians so as to amplify a 180-bp sequence. A universal pair of primers L1091/H1478 was used to amplify an approximately 400-bp sequence derived from the 12S rRNA gene from three crocodilian species in addition to chicken, duck, cattle and swine, and presumably from all or most other animals, including fish (Kocher *et al*., 1989). This pair of primers served as a positive control to prevent false-negative results in case of PCR inhibition. Amplicons were detected with both fresh and cooked meat samples. Both sets of primers could also conceivably be used for determining the percent of Chinese alligator meat in a mixed meat product, based on the ratio of the two amplicons and a suitable standard curve.

The time and temperature used for cooking meat can greatly influence the extent of DNA degradation. Arslan *et al*. (2006) studied the effects of various cooking methods on the PCR detection of beef. The meat was cooked by boiling at 97.5°C for 140, 200 or 230 min, by roasting at 200°C for 80, 120 or 150 min, by autoclaving at 120°C for 30, 60 or 90 min, and by pan-frying for 45 min, to achieve acceptable sensory attributes or longer until unacceptable at a meat temperature of 115°C with a fat temperature of 173°C. A primer pair developed by Tartaglia *et al*. (1998) was used that amplified a 271-bp fragment of mtDNA. Results indicated that, with the exception of pan-frying for 80 min, beef was identified in all samples including the broth and roasted meat. The method of Koh *et al*. (1998) was used, with slight modification, for DNA extraction.

Avian species

Hopwood *et al*. (1999) developed a conventional PCR assay for identification of chicken in meat mixtures. The PCR utilized a pair of primers derived from the conserved sequence of all actin genes, and also utilized the variability in intron sequence rather than size. The assay comprised the use of a conserved PCR primer that annealed to a known coding sequence within the exon 7 segment of a chicken α-*cardiac* gene, and the second primer annealed to the immediately preceding 5′ non-coding intronic sequence. These primers generated a DNA band of 391 bp from both chicken and turkey DNA, but none with duck, pheasant, pig, sheep or horse DNA. Restriction of the resulting amplicons with *Hae*III or *Rsa*I allowed discrimination between chicken and turkey DNA. The chicken band was clearly detectable with DNA from mixtures containing 1% chicken and 99% lamb, and from meat heated at 120°C for 30 min.

Lockley and Bardsley (2002) developed a PCR assay with a set of two forward primers (one for chicken and one for turkey) and a single common reverse primer for distinguishing between meat from the two species. The primers encompassed the 5′ terminus of exon 7 of the α-*cardiac* actin gene and part of the preceding intron, and exploited the intron sequence variability between chicken and turkey. The resulting amplicon from chicken was 327 bp and that from turkey was 159 bp. The primers did not show cross-amplification with pig, sheep or cattle DNA. When the three primers were used together in the same PCR reaction, it was possible to detect 10% chicken in 90% turkey, and 25% turkey in 75% chicken. Interestingly, when the species-specific forward primers were used individually with the common reverse primer in separate PCR tubes, 1% of one meat was detected in the presence of 99% of the other, although this required increasing the number of thermal cycles from 35 to 40 to overcome a faint band with 1% turkey.

Mortara goose salami is a typical product of the Lomellina area of Italy. Duck and turkey, which are considered of lower quality, are often substituted. Colombo *et al*. (2002a) developed a PCR for specific detection of goose tissue in this product. Alignment of goose, turkey and chicken mt*Cytb* gene sequences allowed selection of a primer pair (goose 1/goose 2) for amplification of a sequence from the mt*Cytb* gene from only the goose of about 300 bp. Swine and duck tissue were used as controls and failed to yield amplicons. Chicken was not used as a control species because it is not often used as a substitute for goose, and its homology with goose is much lower than that of duck. To assure that all five goose strains examined yielded just one amplicon and the other species yielded no amplicons, amplification was optimized by increasing the annealing temperature of 5°C to enhance stringency, and lowering the primer concentration from 20 to 5 pmol/reaction.

Hird *et al*. (2003) developed PCR assays for detection of turkey and chicken in processed meat products. The species-specific primers used were designed with turkey- or chicken-specific 3′ bases derived from point mutations on the mt*Cytb* gene between highly conserved regions of DNA. Amplicons of 120 and 101 bp were produced with turkey and chicken, respectively. DNA was extracted with the GeElute™ Mammalian genomic DNA extraction kit (Sigma). A two-step PCR cycling protocol was used to reduce the cycling time by 30 min. Amplicons were detected by adding 100 µl of 1000-fold diluted Vistra Green dye (Amersham Pharmacia Biotech) to 10 µl of PCR reactions in white opaque microplate wells. Fluorescence was determined with a fluorescent microplate reader. Vistra Green is non-fluorescent until it binds to double-stranded DNA. Amplicons were detected with raw, boiled and autoclaved chicken and turkey meat. The primer pairs were highly specific, with no cross-reactions with pork, lamb, rabbit, venison or duck.

Seafood

Shellfish

Mussels are a heterogeneous group of shellfish with a large number of genera and species. The genus *Mytilus* comprises the most commonly marketed mussels for human consumption. The absence of shells in canned and other edible mussel products

prevents morphological identification. An additional confounding factor is the ability of mussels to generate hybrid individuals when two species are in contact.

Colombo *et al*. (2004) designed a pair of PCR primers, designated ISA1 and ISA2, that amplified a ~470-bp fragment of 16S mtDNA specific for pectinoid scallops. The resulting amplicon readily distinguished these scallop species from several samples of vertebrate fish meal, tunafish, and bovine DNA.

Santaclara *et al*. (2006) made use of the PCR, PCR-RFLP and forensically informative nucleotide sequencing (FINS) for the identification of 11 mussel species. A two-tiered approach was used to enable identification of all 11 species examined. The first tier employed PCR-RFLP using primers MusRFLP-F/MusRFLP-R for generating amplicons of 230 to 237 bp derived from a nuclear small-subunit 18S rDNA sequence. The resulting amplicons were restricted with *Bsa*HI, *Cac*81, *Afa*I, *Msp*I and *Nla*III for identification of *Mytilus* sp. (group I) in addition to groups 3 and 4 consisting of 6 species. An alternate first-tier approach consisted of the FINS methodology that involved the use of the primer pair MusRFLP-F/MusFINS-R that yielded amplicons of 167 to 169 bp, also from the 18S rDNA sequence. These amplicons were then sequenced, leading to detection of groups 1, 2, 3 and 4, comprising 4 genera and 6 species. The second tier of assays consisted in part of PCR-RFLP designed to identify species of *Mytilus* (group 1), which involved the use of the primer pair Me 15/Me 16 that yielded amplicons of 126, 168 and 180 bp depending on the species, and was derived from the adhesive protein gene. These amplicons were then restricted with *Aci*I for final *Mytilus* species differentiation. For discrimination of species in groups 2 and 3, a multiplex PCR was utilized in the second tier employing primer pairs CHORO-F/CHORO-R and Pspp-F/Pspp-R that yielded amplicons (from an internal transcribed space 1 region located between the 18S rDNA, i.e. the nuclear small-subunit rRNA gene and the 5.8 S rDNA gene) of 100 and 171 to 207 bp, depending on the species. These amplicons were then restricted with *Btg*I and *Afa*I to achieve final differentiation of the three species in the group 2 genus and the two species in the group 3 genus.

Cephalopods

Colombo *et al*. (2002b) applied PCR-RFLP for differentiation of two cephalopod mollusk (squid) families to assist in avoiding illegal substitutions. A primer pair 16SAR/16SABr was utilized to amplify 16S mtrDNA sequences. Resulting amplicons were restricted with *Asn*I. Members of the family *Loliginidae* yielded a characteristic 200-bp band, while members of the family *Omnastrephidae* yielded 200- and 600- to 700-bp bands.

Crustaceans

Anaphylactic shock caused by shrimp in a sensitized individual can be brought about by an extraordinary low dose (Stensma, 2003). Brzezinski (2005) developed PCR-RFLP methodology for the detection and species identification of crustacean DNA (shrimp, American lobsters, spiny lobsters, crawfish, blue crabs, snow crabs, Dungeness crabs and king crabs) in raw and uncooked foods. The forward and reverse primers

amplified a 205-bp sequence of the 16S rRNA gene. Digestion of PCR products was undertaken with seven restriction nucleases: *Ase*I, *Bce*AI, *Bsm*AI, *Dra*I, *Hind*III, *Rsa*I, and *Ssp*I. The assay was able to detect 0.1% shrimp added to pork before and after cooking.

Fish species

Wolf *et al*. (2000) applied PCR-RFLP for the differentiation of 23 fish species. Universal primers for fish species L14735/H15149ad were used to amplify a 464-bp sequence of the *Cytb* gene. The primer L14735 hybridizes to the strongly conserved t-RNA *glu* gene, whereas, the primer H15149ad is derived from a universal primer, previously described (Kocher *et al*., 1989), by introducing fish-specific nucleotide variations within the priming site. Restriction of amplicons was performed with *Alu*I, *Dde*I, *Hae*II, *Hine*II, *Hinf*I, *Mbo*II, *Nla*III and *Taq*I. All eight restriction enzymes (REs) yielded reasonable restriction patterns. The four REs – *Nla*II, *Dde*I, *Hae*III and *MB*oII – collectively allowed differentiation of all 23 fish species.

Nile perch fillets are frequently labeled and marketed either as grouper or wreck fish in Spain. Although fillets from these three fish species are similar in texture, the quality attributes and price are higher for the later two (Asensio *et al*., 2000). In addition, grouper and wreck fish are closely related species that may be misidentified in the marketplace, resulting in wreck fish being sold as grouper, which is more in demand. Asensio *et al*. (2000) reported on the development of a PCR-RFLP assay for distinguishing these three species. The primers used 12S1/12s2 and amplified a 436-bp sequence of a conserved region of the mt 12S rRNA gene from all three species. Restriction of the 436-bp amplicon derived from the wreck fish by *Rsa*I yielded fragments of 346 and 90 bp, grouper yielded fragments of 189, 173 and 74 bp, and Nile perch yielded fragments of 234 and 202 bp. Restriction by *Sau*96I with the amplicon from wreck fish yielded fragments of 402 and 34 bp, grouper yielded fragments of 224, 178 and 34 bp, and Nile perch yielded fragments of 224 and 212 bp.

Klossa-Kilia *et al*. (2002) developed a PCR-RFLP assay based on a mt 16S rRNA gene segment for authentication of Messolongi fish roe from Greece. The universal primers of Palumbi *et al*. (1991), 16sERL/16SBRH, were used. Digestion of amplicons with *Bst*NI, *Taq*I and *Hindf*I, and resulting agarose electrophoresis and staining with EB readily distinguished the ovarian roe of *Mugil cephalus* from that of other related fish species in the Messolongi lagoon having different market values. *M. cephalus* yielded an amplicon of 630 bp; while that of the other species yielded amplicons of about 600 bp. No difference in RFLP pattern was obtained using DNA from fresh fish tissue or fish roe, as would be expected.

The hake genus (*Merluccius*) is comprised of 12 species distributed throughout the Atlantic and Pacific oceans. Castillo *et al*. (2003) developed PCR-methodology for distinguishing three hake species (*M. merlucius*, *M. bilinearis* and *M. hubbsi*) utilizing the amplification of two microsattelite loci (Mmer UEA W01 and Mmer HK3b). All of the individual samples (139 total, derived from 60, 41 and 38 of each of the respective species) yielded one or two allele bands per locus, corresponding to diploid inheritance. The total number of alleles (based on bp-length and sequencing) for each species varied from 5 to 31 for both loci.

Dooley *et al*. (2005) reported on the improvement of a PCR-RFLP approach for distinguishing between salmon and trout tissue by replacing agarose-gel electrophoresis (AGE) for fragment separation and analysis by employing a chip-based capillary electrophoresis (CE) system. Fragment resolution with the CE system was superior to AGE with detection of small fragments (~25 bp) not resolved by AGE. The LabChips used are 3-cm^2 disposable single-use units containing etched capillaries attached directly to the sample loading wells. DNA fragments are separated using capillary electrophoresis, and detected using laser-induced fluorescence. The PCR primers used (L14735/H15149) amplified a 464-bp region of the mt *Cytb* gene present in all fish species. However, mean PCR product sizes obtained from salmon and trout were 461 bp (SD = 8.6) and 455 bp (SD = 9.6), respectively. Sequenced fragments from both species were found to be 464 bp in length. Dooley *et al*. (2005) suggested that the apparent fragment size difference may be the result of DNA folding, due to sequence variation, which may have affected the migration rates of the amplicons from both species. Digestion of salmon and trout amplicons with *Hae*III produced three bands from each species of about 34, 100 and 315 bp. Interestingly, only two fragments of 130 and 350 bp from both species were reported by Russell *et al*. (2000), using the same pair of primers and AGE, with the 34-bp band not reported. Digestion of the amplicons from salmon and trout with *Dde*I yielded a band of about 100 bp from both species, along with two larger bands of about 315 and 324 bp (salmon) and 340 and 348 bp (trout). In contrast Russell *et al*. (2000) reported restriction fragments with *Dde*I of 350 and 130 bp with salmon and 360 and 130 bp with trout. The absence of the second larger band from each species reported by Russell *et al*. (2000) was presumably due to the inability of AGE to distinguish between the 315- and 324-bp fragments from salmon and the 340- and 348-bp fragments from trout. Detection sensitivity was determined using DNA of admixtures from salmon and trout. Amplification of DNA admixtures yielded a single PCR product. Restriction digests were produced using *Dde*I and *Sau*3AI. The *Sau*3AI did not cleave the trout amplicon, so that banding profiles of admixtures were not as complex with *Sau*3AI as with *Dde*I. Results from PCR-RFLP with *Dde*I readily distinguished the presence of both species containing as little as 5% salmon. It was not possible to detect trout DNA when present at less than 25% of admixtures. Digests of amplicons with *Sau*3AI also failed to detect trout DNA when present at a level of less than 25% in admixtures. These results indicated preferential amplification of the salmon DNA relative to the amplification of the trout DNA. Alteration of the Mg_2 concentration and/or the annealing temperature may eliminate such preferential amplification.

Raw (sashimi) and fried fish derived from five species of billfish are highly favored and costly in Taiwan, resulting in cheaper fish occasionally being substituted, with fraudulent mislabeling. Hsieh *et al*. (2005) developed PCR-RFLP methodology for detection of all five species of raw, frozen and heat-treated tissue. The primer pair L-CYTBF/H-CYTBF amplified a 348-bp sequence from the *Cytb* gene. The restriction endonucleases *Bsa*JI, Cac8I and *Hpa*III were used independently to generate distinct banding patterns for each species. Each restriction nuclease generated one or two DNA bands from each species.

Maldini *et al*. (2006) made use of AFLP for the identification and discrimination of 32 seafood species. A series of 10 primer pairs were utilized for generation of over 40 DNA bands per species. Genomic DNA was first digested with *Eco*RI and *Taq*I endonucleases. *Eco*RI and *Taq*I adapters were then ligated to the digestion products. Pre-amplification with primers containing one selective nucleotide was then performed. Resulting amplicons were diluted 30-fold and subjected to a second PCR with the *Eco*RI primer labeled with Cy5 and the unlabeled *TaqI* primer having three or four selective nucleotides. AFLP banding profiles were able to differentiate various inbred populations of a given species due to land-locked isolation in different geographic areas, in addition to differentiating all of the 32 species examined.

Zhang *et al*. (2006) made use of a semi-nested PCR-RFLP procedure for discriminating four species of salted red snapper and two morphologically similar species of different genera. An ~850-bp sequence of the mt12S rRNA gene was first amplified with primers L232/H231 (Table 12.1). The resulting amplicon of 850 bp was then subjected to a semi-nested PCR with primers L231/H231 generating an amplicon of ~450 bp, which was then subjected to restriction. A single combined restriction digestion reaction utilizing *Hae*II, *Sca*I and *SnaB*I allowed discrimination of the four red snapper species; however, for discrimination of the two non-red-snapper species, restriction with the endonuclease *Mae*II was required.

In estimating the size of fish stocks, the egg-production method is frequently used, and is based on identification of eggs collected during plankton surveys. This procedure is critically dependent on the correct identification of eggs. *Macrorhamphosus scolopax* (a snipe fish) is widespread in the Western Atlantic, Western Indian and Pacific Oceans, in addition to the Mediterranean Sea. Although the species is not commercially important, its geographic distribution overlaps significantly with three species of horse mackeral (*Trachurus tracurus*, *T. mediterraneus* and *T. Picuratus*) which are of commercial significance. The spawning seasons of these three species overlap with that of *M. scolopax*, and they all have morphologically similar eggs. Karaiskou *et al*. (2005) therefore made use of PCR-RFLP analysis of a ~590-bp sequence of the 16S mtrRNA gene to distinguish eggs of *M. scolopax* from those of the European *Trachurus* species. The universal primers H3080/L2510 of Palumbi *et al*. (1991) were utilized to amplify a 590-bp sequence of the 16S rRNA mtDNA gene followed by restriction with *Eco*RV and *Pml*I. With *Eco*RV digestion, *M. scolopax* yielded two fragments of ~340 bp and ~250 bp from the 590-bp 16S mtrDNA segment with no recognition site present in any of the *Trachurus* species. With *pml*I digestion, *M. scolopax* yielded two fragments of ~360 bp and 230 bp from the 590-bp 16S mtrDNA segment, while the 590-bp amplicon from the three *Trachurus* species remained uncut. In addition, a pair of primers 53A/5SB was used to amplify 210- to 430-bp segments of the 5S rDNA gene. The organization of 5S rDNA encompasses little intraspecies-specific polymorphism, but does offer a high level of interspecies variability, and is therefore ideal for species identification. Amplification of the 5S rRNA gene from *M. scolopax* yielded bands of 350 bp and 370 bp; while the 5S rRNA patterns from the three *Trachurus* species yielded notably different sized bands. *T. tracurus* yielded bands of 210 bp and 230 bp, *T. mediterraneus* yielded bands of 410 bp and 430 bp, and *T. Picuratus* yielded bands of ~210 bp and

~35 bp. These results all yielded visually distinct banding patterns and allowed ease of distinction.

Comi *et al*. (2005) made use of RFLP, SSCP and DGGE in attempting to distinguish between cod-fish tissue and tissue from similar species. Amplification of a 307-bp sequence of the *mt cytochrome* (*B Cytb*) gene was used for SSCP and RFLP with the primers cytB1/cytB2 of Barlet and Davidson (1991). RFLP studies utilized the restriction nucleases *Nla*III and *Rsa*I. With DGGE analysis, a GC-clamped *Cytb*1 primer was used in the amplification reaction to increase the sensitivity of the method for the detection of point mutations. DGGE was found to have greater discriminatory power than SSCP or RFLP, and was able to distinguish all eight species.

Rehbein *et al*. (1999), in a multi-laboratory collaborative study, assessed the ability of PCR-SSCP to discriminate eight species of fish sold as tuna fish. A pair of primers (9-3/59-5) was used to amplify a 123-bp amplicon derived from the mt*Cytb* gene. The methodology took into consideration that in canned tuna, only DNA residues of ~100 bp are found (Mackie, 1997). Variations of SSCP patterns were found to occur between certain of the eight laboratories for some of the identical samples. However, each species gave a characteristic banding pattern in each collaborating laboratory, with the exception of bluefin and yellowfin tuna, where the amplicons had the same DNA sequence. However, as long as samples and references were amplified and denatured under identical conditions, and run side-by-side on the same gel, inter-laboratory differences did not interfere with the reliability of PCR-SSCP for species identification.

Colombo *et al*. (2005) used the primers of Rehbein *et al*. (1999) to discriminate between four species of tunafish using PCR-SSCP and computer-assisted gel analysis. However, inter-gel identification failed with all four species because the intra-species electrophoretic mobility varied between gels. This observation emphasizes the necessity for comparing banding patterns from different species or samples in the same gel when using SSCP.

Tetrodotoxin (TTX) is a powerful paralytic toxin derived from the toxic puffer fish (*Lagocephalus lunaris*), and is categorized as a classic sodium-channel blocking agent. The non-toxic puffer fish, *L. gloveri* is the most abundant puffer fish, and the only puffer fish species that can be legally sold as food in Taiwan. For purposes of food safety, the ability to rapidly identify the species from which fillets are derived is of considerable importance. Chen *et al*. (2002) amplified a 376-bp fragment of the cytochrome *b* gene from toxic and non-toxic species, with primers L14841/H15149. The resulting amplicons were restricted with *Hin*fI. The toxic puffer fish (*L. lunaris*) yielded DNA fragments of 206 and 170 bp, while no restriction fragments occurred from the amplicons of three non toxic puffer fish species.

Milk and dairy products

Fraudulent incorporation of cheaper bovine milk in the manufacture of high grade sheep and goat cheeses is considered common practice (Inéz *et al*., 2007). A variety of protein-based methods are available for the identification of the species of origin for milk and cheese products. These include isoelectric focusing (IEF) of γ and para-k-caseins,

urea-polyacrylamide gel electrophoresis (urea-PAGE) of αS1-caseins, and cation exchange high-pressure liquid chromatography (HPLC) of para-k-caseins. However, pasteurized milk or casein used for cheese production can be expected to yield erroneous results with these techniques, due to protein denaturation (Mayer, 2005). In addition, Mayer (2005) found that in a comparative study involving these protein-based techniques and the PCR, αS1-caseins undergo degradation during cheese ripening. Raw and pasteurized milk from healthy mammary glands has been found to contain large numbers of somatic cells ($1.6 \times 10^5 l^{-1}$ of raw milk; $8.5 \times 10^5\ l^{-1}$ of pasteurized milk) (López-Calleja *et al*., 2005), which are predominantly leukocytes but also epithelial cells, both of which contain genomic and mitochondrial DNA suitable for PCR amplification. The persistence of these somatic cells present in milk during cheese manufacture and maturation has allowed the use of PCR to distinguish the species of origin and the presence of unlabeled sources of milk curd in cheeses.

Mayer (2005) utilized four pairs of cattle-specific primers for PCR for identification of the species of origin with milk and cheese varieties. Primer pairs BosL-15794/BosH-16102 and Cytox IIa/Cytox IIb were able to detect 0.5% and 2.5% bovine milk, respectively, in over-ripe Camembert cheese made with mixtures of bovine and sheep's milk. Primer pairs Cytox IIa/Cytox IIb, Cow-14814/Cow-15092, and Bos taurus 1/Bos taurus 2 were able to detect the presence of bovine milk in several commercial Feta cheese samples labeled as being derived entirely from sheep's milk.

López-Calleja *et al*. (2005) developed a specific PCR method for detecting the presence of bovine milk in both buffalo milk and buffalo mozzarella cheese. The assay is based on the amplification of species-specific fragments derived from the mtDNA 12S rRNA gene using the bovine-specific primers 12SM-FW/12SBT-REV2. The forward primer is specific for bovine, buffalo, sheep's and goat's milk, while the reverse primer is specific for bovine milk and yields a 346-bp amplicon. In addition, a buffalo-specific amplicon was generated using the forward primer and a buffalo-specific reverse primer 12SBUF-REV2 I that yielded a 222-bp amplicon for use as a positive control. The detection threshold for milk and cheese of bovine origin was 0.1%. The pasteurization of milk had no effect on the threshold level of sensitivity.

Inéz *et al*. (2007) reported on the development of a PCR and indirect ELISA assay for detecting the presence of bovine milk in sheep and goat milk cheeses. The PCR assay was bovine specific and relied on the mtDNA 12S rRNA gene; while the indirect ELISA assay involved the use of a monoclonal antibody against bovine β-casein which is the fraction displaying the highest level of antigenicity. The specific bovine primers used (12SM-FW/12SBT-RV) amplified a 223-bp sequence of the mtDNA 12S rRNA gene. EB-AGE was used for detection of amplicons. The 223-bp amplicon was visually detected even when samples contained as little as 1% bovine milk. When commercial bovine rennet was diluted 1:5000 and 1:8000, the 223-pb amplicon was slightly visible; whereas at 1:10 000 dilution the amplicon was barely visible. This observation was considered to reflect a potential cause for false-positive results. Normally 1 ml of rennet is added to 5 to 10 l of milk constituting 1:5000 and 1:10 000 dilutions (Inéz *et al*., 2007). However, authentic sheep and goat cheeses produced by bovine calf rennet failed to yield a detectable amplicon. This observation was attributable to the removal of most of the rennet with the whey after the curd is

formed. Several commercial sheep and goat cheeses, including 1% and 2% positive controls, found to be PCR positive were also found to be positive with the ELISA assay. The ELISA assay has the advantage over the PCR of being less expensive and more practical for routine use in the field, allowing faster processing of large numbers of samples without the need for sample digestion or DNA purification.

A multiplex PCR able to identify cows', goats' and sheep's milk in dairy products was developed by Bottero *et al*. (2003). Specific primers for each species were designed, targeting 12S and 16S rRNA genes, so as to result in amplicons of different length (goat, 172 bp; sheep, 326 bp; and bovine, 256 bp). When goat and bovine milk were mixed, the detection threshold for bovine milk was 0.1%. When curds from goat and bovine milk were mixed, the detection threshold for bovine curd was 0.5%.

Conclusions

The PCR is an extremely powerful biochemical tool that has allowed the genetic discrimination of related food species in addition to allowing the quantitative determination of the presence of a single species at low levels in a given food. With the advent of real-time PCR the quantitative range is now extended from no more than 2.0 log cycles with agarose gels to, frequently, 6 log cycles with real-time PCR.

GMOs presently involve the insertion of genes imparting resistance to certain herbicides and/or resistance to insects. The PCR has made possible the determination of the presence or absence of genetically modified strains (GMOs) in food products, particularly through the amplification of DNA segments derived from unique junction sequences between genes in inserted gene cassettes.

Gene sequences in mtDNA, notably the *Cytb* gene, are now frequently targeted for species identification. Such mtDNA sequences have the advantage of being present in large copy numbers (800 to 1000) per cell, imparting enhanced detection sensitivity to the PCR. In addition, mtNA is thought to have evolved more rapidly than nuclear DNA, resulting in greater sequence diversity for distinguishing closely related species. For the detection of hybrid animal species, specific sequences derived from centromeric satellite DNA are used. Satellite DNA has the advantage in that it consists of tandem repeated sequences which are species-specific and reflect the progenitor history of the animal.

A variety of complementary molecular techniques have been developed for use in conjunction with the PCR for species and strain identification and detection. These include RAPD, nested-PCR, multiplex PCR, quantitative competitive PCR, PCR-RFLP, PCR-SSCP, and AFLP. In addition, a number of unique matrix-based assay systems have been developed in conjunction with the PCR for enhanced utility of detection of GMOs. These include membrane-based hybridization assay systems, microarrays, and dipstick biosensors.

Application of the PCR for the detection of closely related and unrelated species and genetically modified strains of a given species is well established, and can be expected to continue to evolve as new and creative applications of the PCR are developed.

References

Abdullah, T., Radu, S., Hassan, Z. and Hashim, J. (2006). Detection of genetically modified soy in processed foods sold commercially in Malaysia by PCR-based method. *Food Chemistry*, **98**, 575–579.

Agodi, A., Barchitta, M., Grillo, A. and Sciacco, S. (2006). Detection of genetically modified DNA sequences in milk from the Italian market. *International Journal of Hygiene and Environmental Health*, **209**, 81–88.

Allaby, R., Jones, M. and Brown, T. (1994). DNA in charred wheat grains from the iron age hillfort at Danebury, England. *Antiquity*, **68**, 126–132.

Arslan, A., Ilhak, O. and Calicioglu, M. (2006). Effect of method of cooking on identification of heat processed beef using polymerase chain reaction (PCR) technique. *Meat Science*, **72**, 326–330.

Asensio, L., González, I., Fernández, A. *et al*. (2000). Identification of Nile perch (*Lates niloticus*), grouper (*Epinephelus guaza*), and wreck fish (*Polyprion americanus*) by polymerase chain reaction-restriction fragment length polymorphism of a 12S rRNA gene fragment. *Journal of Food Protection*, **63**, 1248–1252.

Barlet, S. and Davidson, W. (1991). Identification of *Thunnus tuna* species by the polymerase chain reaction and direct sequence analysis of their mitochondrial cytochrome b gene. *Canadian Journal of Aquatic Science*, **48**, 309–317.

Beck, E., Ludwig, G., Auerswald, E. *et al*. (1982). Nucleotide sequence and exact localization of the neomycin phosphotransferase gene from transposon Tn5. *Gene*, **19**, 327–336.

Blackstone, G., Nordstrom, J., Vickery, M. *et al*. (2003). Detection of pathogenic *Vibrio parahaemolyticus* in oyster enrichments by real-time PCR. *Journal of Microbiological Methods*, **53**, 149–155.

Bonnaud, L., Rodhuse, P. and Bouher-Rodoni, R. (1998). A phylogenetic study of the squid family Onychoteuthidae (Cephalopoda: Oegopsida). *Proceedings of the Royal Society of London B*, **265**, 1761–1770.

Boom, R., Sol, C., Salimans, M. *et al*. (1999). Rapid and simple method for the purification of nucleic acid. *Journal of Clinical Microbiology*, **28**, 495–503.

Bottero, M., Civera, T., Anastasio, A. *et al*. (2002). Identification of cow's milk in "buffalo" cheese by duplex poymerase chain reaction. *Journal of Food Protection*, **65**, 362–366.

Bottero, M., Civera, T., Nucera, D. *et al*. (2003). A multiplex polymerase chain reaction for the identification of cows', goats', and sheep's milk in dairy products. *International Dairy Journal*, **13**, 277–282.

Brodmann, P., Eugster, A., Hübner, P. *et al*. (1997). *Mitteilungen aus dem Gebiteder Lebensmittelun Tersuchung und Hygiene*, **88**, 722–731. (available at http://biotech.jrc.it/documents/GMOPPC report 02.pdf).

Brown, J., Beckenbach, K., Beckenbach, A. and Smith, M. (1993). Intraspecific DNA sequence variation of the mitochondrial control region of white sturgeon (*Acipenser transmontanus*). *Molecular Biology and Evolution*, **10**, 326–341.

Brzezinski, J. (2005). Detection of crustacean DNA and species identification using a PCR-restriction fragment length polymorphism method. *Journal of Food Protection*, **68**, 1866–1873.

Brzezinski, J. (2007). Detection of sesame seed DNA in foods using real-time PCR. *Journal of Food Protection*, **70**, 1033–1036.

Cai, Q. and Touitou, I. (1993). Excess PCR primers may dramatically affect SSCP efficiency. *Nucleic Acids Research*, **21**, 3909–3910.

Candrian, U. (1994). Die Polymerasen-Kettenreaktion in der Lebensmittelanalytik. *Mitteilungen aus dem Gebiete der Lebensmitteluntersuchung und Hygien*, **85**, 704–718.

Carr, S. and Marshall, H. (1991). Detection of intraspecific DNA sequence variation in the mitochondrial cytochrome b gene of Atlantic cod (*Gadus morhua*) by the polymerase chain reaction. *Canadian Journal of Fisheries and Aquatic Science*, **48**, 48–52.

Castillo, A., Martinez, J. and Garcia-Vaquez, E. (2003). Identification of Atlantic hake species by a simple PCR-based methodology employing microsattelite loci. *Journal of Food Protection*, **66**, 2130–2134.

Chen, T., Hsieh, Y., Tsai, Y. *et al*. (2002). Identificiton of species and measurement of tetrodotoxin in dressed fillets of the puffer fish, *Lagocephalus lunaris*. *Journal of Food Protection*, **65**, 1670–1673.

Chowdbury, E., Mikamik, O., Murata, H. *et al*. (2004). Fate of maize intrinsic and recombinant genes in calves fed genetically modified maize Bt11. *Journal of Food Protection*, **67**, 365–370.

Colgan, S., O'Brien, L., Maher, M. *et al*. (2001). Development of a DNA-based assay for species identification in meat and bone meal. *Food Research International*, **34**, 409–414.

Colombo, F., Marchisio, E., Pizzini, A. and Contoni, C. (2002a). Identification of the goose species (*Anser anser*) in Italian "mortara" salami by DNA sequencing and a polymerase chain reaction with an original primer pair. *Meat Science*, **61**, 291–294.

Colombo, F., Cerioli, M., Colombo, M. *et al*. (2002b). A simple polymerase chain reaction fragment length polymorphism (PCR-RFLP) method for the differentiation of cephalopod mollusk families *Loliginidae* from *Omnastrephidae*, to avoid substitutions in fishery field. *Food Control*, **13**, 185–190.

Colombo, F., Trezzi, I., Bernardi, C. *et al*. (2004). A case of identification of pectinid scallop (*Pecten jacobaeus*, *Pecten maximus*) in a frozen and seasoned food product with PCR technique. *Food Control*, **15**, 527–529.

Colombo, F., Mangiagalli, G. and Renon, P. (2005). Identification of tuna species by computer-assisted and cluster analysis of PCR-SSCP electrophoretic patterns. *Food Control*, **16**, 51–53.

Comi, G., Iacumin, L., Rantsiou, K. *et al*. (2005). Molecular methods for the differentiation of species used in production of cod-fish can detect commercial frauds. *Food Control*, **16**, 37–42.

Dahinden, I., von Büren, M. and Lüthy, J. (2001). A quantitative competitive PCR system to detect contamination of wheat, barley or rye in gluten-free food for coeliac patients. *European Food Research Technology*, **212**, 228–233.

Dalmasso, A., Fontanella, E., Piatti, P. *et al*. (2004). A multiplex PCR assay for the identification of animal species in feedstuffs. *Molecular and Cellular Probes*, **18**, 81–87.

Davidson, A. and Bridges, M. (1987). Coeliac disease: a critical review of aetiology and pathogenesis. *Clinica et Chimica Acta*, **163**, 1–40.

Deininger, P. and Batzer, M. (1995). SINE-maser genes and population biology. *The Impact of Short Interspersed Elements (SINEs) on the Host Genome*. Georgetown, TX: R.G. Landes.

Demeke, T., Giroux, R., Reitmeier, S. and Simon, S. (2002). Development of a polymerase chain reaction assay for the detection of three canola transgenes. *Journal of the American Oil Chemists' Society*, **79**, 1015–1019.

Dooley, J., Sage, H., Brown, H. and Garrett, S. (2005). Improved fish species identification by use of lab-on-a-chip technology. *Food Control*, **16**, 601–607.

Ebbehoj, K. and Thompson, P. (1991). Species differentiation of treated meat products by DNA hybridization. *Meat Science*, **30**, 221–234.

Ehlers, B., Strauch, E., Goltz, M. *et al*. (1997). Nachweiss gentechnisher Veränderungen in Mais mittels PCR. *Bundesgsundheitsbl*, **40**, 118–121.

Elder, J. and Turner, B. (1995). Concerted evolution of repetitive DNA sequences in eukaryotes. *Quarterly Review of Biology*, **70**, 297–320.

Flachowsky, G. and Aulrich, K. (2001). Nutritional assessment of feeds from genetically modified organism. *Journal of Animal Feed Science*, **10**, 181–194.

Forte, V., Di Pinto, A., Martino, C. *et al*. (2005). A general multiplex-PCR assay for the general detection of genetically modified soya and maize. *Food Control*, **16**, 535–539.

Gilliland, G., Perrin, S., Blanchard, K. and Bunn, H. (1990). Analysis of cytokine mRNA and DNA: detection and quantitation by competitive polymerase chain reaction. *Proceedings of the National Academy of Science USA*, **87**, 2725–2729.

Girish, P., Anjaneyula, A., Viswas, K. *et al*. (2004). Sequence analysis of mitochondrial 12 rRNA gene can identify meat species. *Meat Science*, **66**, 551–556.

Girish, P., Anjaneyula, A., Viswas, K. *et al*. (2005). Meat species identification by polymerase chain reaction-restriction fragment length polymorphism (PCR-RFLP) of mitochondrial 12S rRNA gene. *Meat Science,* **70**, 107–112.

Greiner, R., Konietzny, U. and Villavicencio, A. (2005). Qualitative and quantitative detection of genetically modified maize and soy in processed foods sold commercially in Brazil by PCR-based methods. *Food Control*, **16**, 753–759.

Guoli, Z., Mingguang, Z., Zhijiang, Z. *et al*. (1999). Establishment and application of a polymerase chain reaction for identification of beef. *Meat Science*, **51**, 233–236.

Hayashi, K. (1996). PCR SSCP. Single strand conformation polymorphism analysis of PCR products. In: U. Landegren (ed.), *Laboratory Protocols for Mutation Detection*. Oxford: Oxford University Press, pp. 14–22.

Heid, C.A., Stevens, J., Livak, K.J. and Williams, P.M. (1996). Real time quantitative PCR. *Genome Research*, **6**, 986–994.

Hernández, M., Rodríquez-Lázaro, D., Esteve, T. *et al*. (2003). Development of melting temperature-based SYBR Green I polymerase chain reaction methods for multiplex genetically modified organism detection. *Analytical Biochemistry*, **323**, 164–170.

Hernández, M., Esteve, T., Prat, S. and Pla, M. (2004). Development of real-time PCR systems based on SYBR® Green I, Amplifor™ and Taqman® technologies for specific quantitative detection of the transgenic maize event GA21. *Journal of Cereal Science*, **39**, 99–107.

Hernández, M., Esteve, T. and Pla, M. (2005). Real-time polymerase chain reaction based assays for quantitative detection of barley, rice, sunflower, and wheat. *Journal of Agricultural and Food Chemistry*, **53**, 7003–7009.

Hird, H., Goodier, R. and Hill, M. (2003). Rapid detection of chicken and turkey in heated meat products using the polymerase chain reaction followed by amplicon visualization with vista green. *Meat Science*, **65**, 1117–1123.

Hopwood, A., Fairbrother, K., Lockley, A. and Bardsley, R. (1999). An actin gene-related polymerase chain reaction (PCR) test for identification of chicken in meat mixtures. *Meat Science*, **53**, 227–231.

Hsieh, H., Chai, T. and Hwang, D. (2005). Using the PCR-RFLP method to identify the species of different processed products of billfish meats. *Food Control*, **18**, 369–374.

Inéz, M., López-Calleja, I., González, I. *et al*. (2007). Application of an indirect ELISA and a PCR technique for detection of cows' milk in sheeps' and goats' milk cheeses. *International Dairy Journal*, **17**, 87–93.

Inoue, K., Waite, J., Matsuoka, M. *et al*. (1995). Interspecific variations in adhesive protein sequence of *Mytilus edulis*, *M. galloprovinvialis*, and *M. trossulus*. *Biological Bulletin*, **189**, 370–375.

James, D., Schmidt, A., Wall, E. *et al*. (2003). Reliable detection and identification of genetically modified maize, soybean, and canola by multiplex PCR analysis. *Journal of Agricultural Food Chemistry*, **51**, 5829–5834.

Kalogianni, D., Koraki, T., Christopoulos, T. and Ioannou, P. (2006). Nanoparticle-based DNA biosensor for visual detection of genetically modified organisms. *Biosensors and Bioelectronics*, **21**, 1069–1079.

Karaiskou, N., Triantafyllidis, A., Margaroni, M. *et al*. (2005). A double DNA approach for identifying *Macrorhamhosus scolopax* (Pisces, Centriscidae). *ICES Journal of Marine Science*, **62**, 1683–1690.

Kasuga, T., Cheng, J. and Mitchelson, K. (1995). Metastable single-strand DNA conformational polymorphism analysis results in enhanced polymorphism detection. *PCR Methods and Applications*, **4**, 223–227.

Khan, G., Kangro, H., Coates, P. and Heath, R. (1991). Inhibitory effects of urine on the polymerase chain reaction for cytomegalovirus DNA. *Journal of Clinical Pathology*, **44**, 360–365.

Kirihara, J., Petri, J. and Messing, J. (1988). Isolation and sequence of a gene encoding a methionine rich 10-kDa zein protein from maize. *Gene*, **71**, 359–370.

Klossa-Kilia, E., Papasotiropoulos, V., Kilias, G. and Alahiotis, S. (2002). Authentication of Messolongi (Greece) fish roe using PCR-RFLP analysis of 16S rRNA mtDNA segment. *Food Control*, **13**, 169–172.

Kocher, T., Thomas, W., Meyer, A. *et al*. (1989). Dynamics of mitochondrial DNA evolution in animals: amplification and sequencing with conserved primers. *Proceedings of the National Academy of Sciences USA*, **86**, 6196–6200.

Koh, M., Lim, C., Chua, S. *et al*. (1998). Random amplified polymorphic DNA (RAPD) fingerprints for identification of red meat animal species. *Meat Science,* **48**, 275–285.

Lahiff, S., Glennon, M., O'Brien, L. *et al*. (2001). Species-specific PCR for the identification of ovine, porcine, and chicken species in meat and bone meal (MBM). *Molecular and Cellular Probes*, **15**, 27–35.

Lantz, P., Matsson, M., Wadström, T. and Rådström, P. (1997). Removal of PCR inhibitors from human faecal samples through the use of an aqueous two-phase system for sample preparation prior to PCR. *Journal of Microbiological Methods*, **28**, 159–167.

Levin, R.E. (2003). Application of random amplified polymorphic DNA (RAPD) and pulsed-field gel electrophoresis (PGFE) analysis to *Listeria monocytogenes*: a review of methodology and results. *Food Biotechnology*, **17**, 217–236.

Levin, R.E. (2004). The application of real-time PCR to food and agricultural systems. A review. *Food Biotechnology*, **18**, 97–133.

Lipp, M., Brodmann, P., Pietsch, K. *et al*. (1999). IUPAC collaborative trial study of a method to detect genetically modified soybeans and maize on dried powder. *Journal of AOAC International*, **82**, 923–928.

Liu, Q., Feng, J., Buzin, C. *et al*. (1999). Detection of virtually all mutations-SSCP (DOVAM-S): a rapid method for mutation scanning with virtual 100% sensitivity. *Biotechniques*, **26**, 932–942.

Liu, J., Xing, D., Shen, X. and Zhu, D. (2004a). Detection of genetically modified organisms by electrochemiluminescence PCR method. *Biosensors and Bioelectronics*, **20**, 436–441.

Liu, G., Su, W., Xu, Q. *et al*. (2004b). Liquid-phase hybridization based PCR-ELISA for detection of genetically modified organisms in food. *Food Control*, **15**, 303–306.

Liu, J., Xing, D., Shen, X. and Zhu, D. (2005). Electrochemiluminescence polymerase chain reaction detection of genetically modified organisms. *Analytica Chimica Acta*, **537**, 119–123.

Lockley, A. and Bardsley, R. (2002). Intron variability in an actin gene can be used to discriminate between chicken and turkey DNA. *Meat Science*, **61**, 163–168.

López-Calleja, I., Alonso, G., Fajardo, V. *et al*. (2005). PCR detection of cow's milk in water buffalo milk and mozzarella cheese. *International Dairy Journal*, **125**, 1122–1129.

Mackie, J. (1997). Methods of identifying species of raw and processed fish. In: G.M. Hall (ed.), *Fish Processing Technology*, 2nd edn. London: Blackie Academic and Professional, pp. 160–199.

Maldini, M., Marzano, F., Fortes, G. *et al*. (2006). Fish and seafood traceability based on AFLP markers: elaboration of a species database. *Aquaculture*, **261**, 487–494.

Martín, I., García, T., Fajardo, V. *et al*. (2006). Species-specific PCR for the identification of ruminant species in feedstuffs. *Meat Science*, **75**, 120–127.

Matsunaga, T., Chikuni, K., Tanabe, R. *et al*. (1998). Determination of mitochondrial cytochrome B gene sequence for red deer (*Cervus elaphus*) and differentiation of closely related deer meats. *Meat Science*, **49**, 379–385.

Matsunaga, T., Chikuni, K., Tanabe, R. *et al*. (1999). A quick and simple method for the identification of meat species and meat products by PCR assay. *Meat Science*, **51**, 143–148.

Matsuoka, T., Kawashima, Y., Kuribara, K. *et al*. (2000). A method of detecting recombinant DNAs from four lines of genetically modified maize. *Journal of The Food Hygiene Society of Japan*, **41**, 137–143.

Maudet, C. and Taberlat, P. (2001). Detection of cows' milk in goats, cheeses inferred from mitochondrial DNA poymorphism. *Journal of Dairy Research*, **68**, 229–235.

Mayer, H. (2005). Milk species identification in cheese varieties using electrophoretic chromatographic and PCR techniques. *International Dairy Journal*, **15**, 595–604.

Meyer, R. (1999). Development and application of DNA analytical methods for the detection of GMOs in food. *Food Control*, **10**, 391–399.

Meyer, R. and Candrian, U. (1996). PCR-based DNA analysis for the identification and characterization of food components. *Lebensmittel-Wissenschaft und -Technologie*, **29**, 1–9.

Miraglia, M., Berdal, K., Brera, C. *et al*. (2004). Detection and traceability of genetically modified organisms in the food production chain. *Food and Chemical Toxicology*, **42**, 1157–1180.

Miterski, B., Krüger, R., Wintermeyer, P. and Epplen, J. (2000). PCR/SSCP detects reliably and efficiently DNA sequence variations in large scale screening projects. *Combinatorial Chemistry & High Throughput Screening*, **3**, 211–218.

Moriuchi, R., Monma, K., Sagi, N. *et al*. (2007). Applicability of quantitative PCR to soy processed foods containing Roundup ready Soy. *Food Control*, **18**, 191–195.

Official Collection of Test Methods (1998). OCTM in accordance with Article 35 LMBG, classification no L 23.01.22–1, March 1998 (loose leaf edition): Detection of a genetic modification of soybeans by amplification of the modified DNA sequence by means of the polymerase chain reaction (PCR) and hybridization of the PCR product with a DNA probe or restriction analysis. German Federal Food Act – Food Analysis, Article 35, Beuth, Berlin, Köln.

Official Collection of Test Methods (2002). OCTM in accordance with Article 35 LMBG, classification no L 15.05.01, June 2002 (loose leaf edition): Detection of a genetic modification of maize (Bt176, Bt11, MON810, T25) by amplification of the modified DNA sequence by means of the polymerase chain reaction (PCR) and hybridization of the PCR product with a DNA probe or restriction analysis. German Federal Food Act – Food Analysis, Article 35, Beuth, Berlin, Köln.

Orum, H., Nielsen, P., Egholm, M. *et al*. (1993). Single base pair mutation analysis by PNA direct PCR clamping. *Nucleic Acids Research*, **21**, 5332–5336.

Palumbi, S., Martin, A., Romano, S. *et al*. (1991). *The Simple Fools Guide To PCR, version II*. Honolulu: University of Hawaii.

Partis, L., Coan, D., Guo, Z. *et al*. (2000). Evaluation of a DNA fingerprinting method for determining the species origin of meats. *Meat Science*, **54**, 369–376.

Peano, C., Bordoni, R., Gulli, M. *et al*. (2005a). Multiplex polymerase chain reaction and ligation detection reaction/universal array technology for the traceability of genetically modified organisms in foods. *Analytical Chemistry*, **346**, 90–100.

Peano, C., Lesignoli, F., Gulli, M. *et al*. (2005b). Development of a peptide nucleic acid polymerase chain reaction clamping assay for semiquantitative evaluation of genetically modified organism content in food. *Analytical Biochemistry*, **344**, 174–182.

Pendas, A., Moran, P., Martinez, J. and Garcia-Vazquez, E. (1995). Application of 5S rDNA in brown trout and in Atlantic salmon by brown trout hybrid identification. *Molecular Ecology*, **4**, 275–276.

Permingeat, H., Reggiardo, M. and Vallejos, R. (2002). Detection and quantification of transgenes in grains by multiplex an real-time PCR. *Journal of Agriculture and Food Chemistry*, **50**, 4431–4436.

Phipps, R., Beever, D. and Humphris, D. (2002). Detection of transgenic DNA in milk from cows receiving herbicide tolerant CP4EPSPS soyabean meal. *Livestock Production Science*, **74**, 269–273.

Powell, H., Gooding, C., Garrett, S. *et al*. (1994). Proteinase inhibition of the detection of *Listeria monocytogenes* in milk using the polymerase chain reaction. *Letters in Applied Microbiology*, **18**, 59–61.

Rehbein, H., Mackie, I., Pryde, S. *et al*. (1999). Fish species identification in canned tuna by PCR-SSCP: validation by a collaborative study and investigation of intra-species variability of the DNA patterns. *Food Chemistry*, **64**, 263–268.

Rollo, F., Amici, A., Salvi, R. and Garbuglia, A. (1988). Short but faithful pieces of ancient DNA. *Nature*, **335**, 774.

Rollo, F., Venanzi, F. and Amici, A. (1991). Nucleic acids in mummified plant seeds: biochemistry and molecular genetics of pre-columbian maize. *Genetical Research*, **58**, 193–201.

Ronning, S., Knut, G., Berdal, C. *et al*. (2006). Novel reference gene, PKABA1, used in a duplex real-time polymerase chain reaction for detection and Quantification of wheat- and barley-derived DNA. *Journal of Agricultural and Food Chemistry*, **54**, 682–687.

Ruano, G., Pagliaro, E., Schwartz, T. *et al*. (1992). Heat-soaked PCR: an efficient method for DNA amplification with applications in forensic analysis. *Biotechniques*, **13**, 266–274.

Russell, V., Hold, G., Pryde, S. *et al*. (2000). Use of restriction fragment length polymorphism to distinguish between salmon species. *Journal of Agriculuture and Food Chemistry*, **48**, 2184–2188.

Sallares, R., Allaby, R. and Brown, T. (1995). PCR-based identification of wheat genomes. *Molecular Ecology*, **4**, 509–514.

Santaclara, F., Espiñeira, M., Cabado, A. *et al*. (2006). Development of a method for the genetic identification of mussel species belonging to *Mytilus*, *Perna*, *Aulacomya*, and other genera. *Journal of Agricultural Food Chemistry*, **54**, 8461–8470.

Soto, S., Guerra, B., González-Hevia, M. and Mendoza, M. (1999). Potential of three-way randomly amplified polymorphic DNA analysis as a typing method for twelve *Salmonella* serotypes. *Applied and Environmental Microbiology*, **65**, 4830–4836.

Stensma, D. (2003). The kiss of death: a severe allergic reaction to shellfish induced by a good-night kiss. *Mayo Clinic Proceedings*, **78**, 221–222.

Stüder, E., Dahinden, I., Luthy, J. and Hubner, P. (1997). Nachweis des gentechnisch veranderten Maximizer Mais mittels der Polymerase-Kettenreaktion (PCR). *Mitteilungen aus dem Gebieteder Lebensmittelun Tersuchung und Hygiene*, **88**, 515–524.

Stüder, E., Rhyner, C., Luthy, J. and Hübner, P. (1998). Quantitative competitive PCR for the detection of genetically modified soybean and maize. *Zeitschrift für Lebensmittel-Untersuchung und -Forschung*, **207**, 207–213.

Su, W., Song, S., Long, M. and Liu, G. (2003). Multiplex polymerase chain reaction/membrane hybridization assay for detection of genetically modified organisms. *Journal of Biotechnology*, **105**, 227–233.

Sunnucks, P., Wilson, A., Beheregaray, L. *et al*. (2000). SSCP is not difficult: the application and utility of single-stranded conformation polymorphism in evolutionary biology and molecular ecology. *Molecular Ecology*, **9**, 1699–1710.

Taberlet, M., Olm Gielly, L., Pautou, G. and Bouvet, J. (1991). Universal primers for amplification of three non-coding regions of chloroplast DNA. *Plant and Molecular Biology*, **17**, 1105–1109.

Tartaglia, M., Saulle, E., Pestalozza, S. *et al*. (1998). Detection of bovine mitochondrial DNA in ruminant feeds; a molecular approach to test for the presence of bovine derived materials. *Journal of Food Protection*, **61**, 513–518.

Tengel, C., Schvssler, P., Setke, E. *et al*. (2001). PCR-based detectin of genetically modified soyabean and maize in raw and highly processed foodstuffs. *BioTechniques*, **31**, 426–429.

Trapman, S., Catalani, P., Conneely, P. *et al*. (2002). The certification of reference materials of dry mixed soya powder with different mass fraction of Roundup Ready™ soya. *Certified Reference Materials IRMM-410S*. Geel: European Commission, Joint Research Centre, Institute for Reference Materials and Measurement (IRMM).

Tu, Z., Eisner, W., Kreiswirth, B. and Blaser, M. (2005). Genetic divergence of *Campylobacter fetus* strains of mammal and reptile origins. *Journal of Clinical Microbiology*, **43**, 3334–3340.

Vaïtilingom, M., Pijnenburg, H., Gendre, F. and Brignon, P. (1999). Real-time quantitative PCR detection of genetically modified Maximizer maize and Roundup Ready Soybean in some representative foods. *Journal of Agricultural Food Chemistry*, **47**, 5261–5266.

Verkaar, E., Nijman, I., Boutaga, K. and Lenstra, J. (2002). Differentiation of cattle species in beef by PCR-RFLP of mitochondrial and satellite DNA. *Meat Science*, **60**, 365–369.

Von Büren, M., Stadler, M. and Lüthy, J. (2001). Detection of wheat adulteration of spelt flour and products by PCR. *European Food Research Technology*, **121**, 234–239.

Vos, P., Hogers, R., Bleeker, M. *et al*. (1995). AFLP: a new technique for DNA fingerprinting. *Nucleic Acids Research*, **23**, 4407–4414.

Walker, J., Hughes, D., Aners, B. *et al*. (2003). Quantitative intra-sort interspersed element PCR for species-specific DNA identification. *Analytical Biochemistry*, **316**, 259–269.

Wang, S. and Levin, R.E. (2005). Quantitative detection of *Vibrio vulnificus* by competitive polymerase chain reaction. *Food Biotechnology*, **19**, 193–204.

Wolf, C. and Lüthy, J. (2001). Quantitative competitive (QC). PCR for quantification of porcine DNA. *Meat Science*, **57**, 161–168.

Wolf, C., Bergener, M., Hübner, P. and Lüty, J. (2000). PCR-RFLP analysis of mitochondrial DNA: differentiation of fish species. *Lebensmittel-Wissenschaft und -Technologie*, **33**, 144–150.

Wurz, A., Bluth, A., Zeltz, P. *et al*. (1999). Quantitative analysis of genetically modified organisms (GMO) in processed food by PCR-based methods. *Food Control*, **10**, 385–389.

Xu, J., Miao, H., Wu, H. *et al*. (2006). Screening genetically modified organisms using multiplex-PCR coupled with oligonucleotide microarray. *Biosensors and Bioelectronics*, **22**, 71–77.

Yamaguchi, H., Sasaki, K., Yumtsu, H. and Kamada, H. (2003). Two detection methods for genetically modified maize and the state of its import into Japan. *Food Control*, **14**, 201–206.

Yan, P., Wu, X., Shi, Y. *et al*. (2005). Identification of Chinese alligators (*alligator sinensis*) meat by diagnostic PCR of the mitochondrial cytochrome *b* gene. *Biological Conservation*, **121**, 45–51.

Yoke-Kqueen, C., Radu, S. and Ling, M. (2006). Membrane based detection of genetically modified organisms in some representative foods. *Food Control*, **17**, 631–636.

Zhang, J., Huang, H., Cai, Z. and Huang, L. (2006). Species identification in salted products of red snappers by semi-nested PCR-RFLP based on the mitochondrial 12S rRNA gene sequence. *Food Control*, **17**, 557–563.

Zimmerman, A., Hemmer, W., Liniger, M. *et al*. (1998). A sensitive detection method for genetically modified MaisGard™ corn using a nested PCR-system. *Lebensmittel-Wissenschaft und -Technologie*, **31**, 664–667.

Zimmerman, A., Lüthy, J. and Pauli, U. (2000). Event-specific transgene detection in Bt11 corn by quantitative PCR at the integration site. *Lebensmittel-Wissenschaft und -Technologie*, **33**, 210–216.

13

Enzymic Technique: Enzyme-linked Immunosorbent Assay (ELISA)

Ángel Maquieira Catala and Rosa Puchades

Introduction

Immunochemical techniques are simple and powerful analytical methods applicable to all types of analytes, from low molecular weight substances (e.g. antibiotics) to highly complex entities such as enzymes, viruses or microorganisms.

The first immunoassay was developed by Yalow and Berson in 1960, for the determination of insulin in blood. Since then immunoassays have extended to a large number of fields, ranging from basic research to routine control (e.g. pregnancy test). Due to its sensitivity, selectivity and versatility, immunoassay has become a very popular tool, including in authentication work, where (for instance) discriminating between different animal species in meat, or detecting cow's milk adulteration in sheep's milk, is routine.

The introduction of enzyme immunoassays deserves special mention, because their properties and performances make them a very useful methodology.

Immune function, antibody structure and properties

The immune defense is the mechanism developed by many animal species against pathogen germs and other agents unknown by the invaded organism. The acquired

Modern Techniques for Food Authentication
ISBN: 978-0-12-374085-4

Table 13.1 Comparison of the different isotypes of human immunoglobulins

Isotype	IgG	IgA	IgM	IgD	IgE
Heavy chain	γ	α	μ	δ	e
Structure	Monomer	Monomer Dimer	Pentamer	Monomer	Monomer
Molecular mass (Da)	150 000	160 000 400 000	900 000	180 000	190 000
Carbohydrate (%)	2.9	7.5	10.9	9-18 (myeloma)	Variable (till 20%)
Serum concentration (mg ml^{-1})	10–13	0.5–3	0.5–2.5	0.003	10^{-4}
Properties	Principal seric IgG. Ratio >85%	Principal in secretions; polymerize	Increases in initial immune response	Main on the surface of B cells	Allergy antibodies

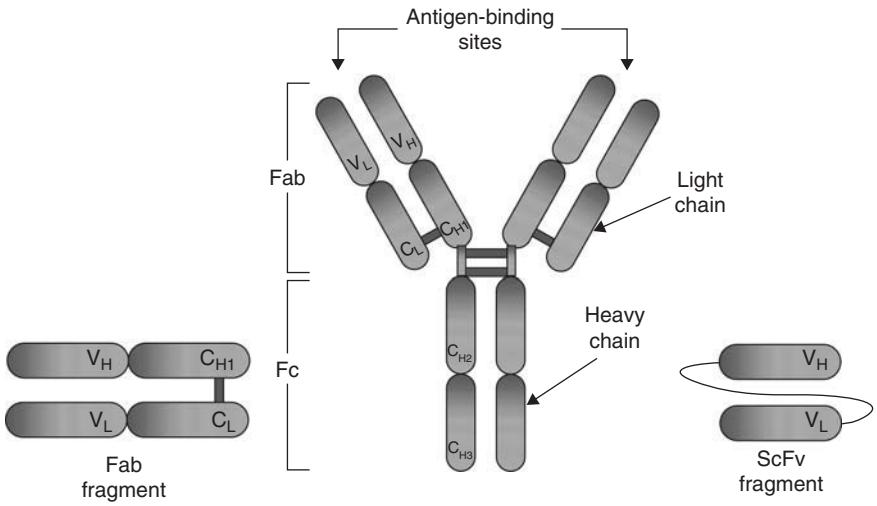

Figure 13.1 Structure of an IgG1 and its fragments Fab and ScFv.

immune system is involved in the response against the invader agent (microorganisms, viruses or macromolecular substances). It is characterized by its high selectivity, since it generates specific proteins, named antibodies, which recognize the foreign system.

Antibodies are expressed in different media and concentrations, depending on the species. In mammals they are present mainly in blood, but also in other body fluids, such as tears, saliva and milk. In oviparous animals and bird they are also expressed in eggs. Antibodies are glycoproteins, produced by plasmatic cells, from the γ-globulin group, named immunoglobulins (Igs).

Immunoglobulins are composed of several polypeptide chains, and their molecular weight ranges from 150 to 900 kDa, with a carbohydrate content of between 2 and 15% and an isoelectric point in the range 4.4–9.5. They are classified into five isotypes (Table 13.1), depending on the structure of their peptide chains (α, μ, γ, δ, ε), their functional activity and tissue distribution as immunoglobulins G (IgG), A (IgA), M (IgM), D (IgD) and E (IgE). In mammals, immunoglobulins G are in the highest ratio, also being the most employed as immunoanalytical reagents, while the other Igs do not play an important role in these applications.

Depending on their origin, IgGs can be found as monomers or in larger associations. Monomers have a basic structure (Figure 13.1) of four polypeptide chains in

a Y-shape, which are really two repeated chains – two light (L) and two heavy (H). The two heavy chains are bound to each other by two disulfide bridges, and each one is bound to a light chain by another disulfide bridge. Heavy chains have a carbohydrate molecule in the tail region as a prosthetic group. Antibody fragments (e.g. Fab, ScFv) with lower size but maintaining the binding functions of the whole molecule are obtained by enzymatic IgG treatment or cloning technologies. These reagents are useful as diagnostic and also therapeutic agents (Hudson and Kortt, 1999).

In an antibody, two regions are clearly distinguished in both the heavy and the light chains. The *variable region* (V) in the amine terminal extreme of the molecule (Fab, fragment antigen binding) is the zone of the antibody that interacts with the antigen, therefore being responsible for its selectivity. These active sites of specific recognition of the antibody (paratopes) interact with a region of the antigen that is also able to bind the antibody (epitope), and their amino acid sequence is different depending on the type of IgG. Antibodies are bifunctional molecules, i.e. they possess two recognition sites for the antigen.

The *constant regions* (C) in L and H chains show minimum variation of amino acid sequences among the immunoglobulins. The constant region of the two H chains, the carboxy-terminal end of each peptide chain, forms the tail of the antibody (C_H, C_L). It acts as an anchorage zone for the receptors of some determined cells. Furthermore, this region gives to the antibody the different characteristics of each type of immunoglobulin (such as the ability to pass through the placenta, appear in secretions, activate the complement, etc.).

Antigen–antibody interaction

The binding between an antigen and an antibody is mostly due to non-covalent weak interactions: hydrogen bonds, electrostatic, hydrophobic and van der Waals. This binding is reversible, and obeys the Mass Action Law (Goldsby *et al*., 2003):

$$\mathrm{Ab} + \mathrm{Ag} \rightarrow \mathrm{Ab{-}Ag\ complex} \qquad \textbf{(13.1)}$$

where the affinity constants is $Ka = [Ab{-}Ag]/[Ab] \cdot [Ag]$, $[Ab{-}Ag]$ is the molar concentration of the antibody–antigen complex, [Ab] is the molar concentration of the free epitope, and [Ag] is the molar concentration of binding points on the antigen.

Affinity constant values are very high, in the range $10^8 - 10^{10}$ M. The specific binding between IgG and antigen occurs at the combining sites, both having complementary structures, and forms a complex between them. The intensity of this binding is called the *affinity*. The binding strength depends not only on the chemical forces but also on the best stereospatial accommodation between the epitope and the paratope. This is termed the *goodness of fit*.

On the other hand, antibodies of low affinity can still bind strongly if they do so with more than one epitope at the same time. This is related to the valence, or avidity, of the immunointeraction. The effect of the multivalence property of an interaction antibody–antigen is equivalent to combining the respective affinities.

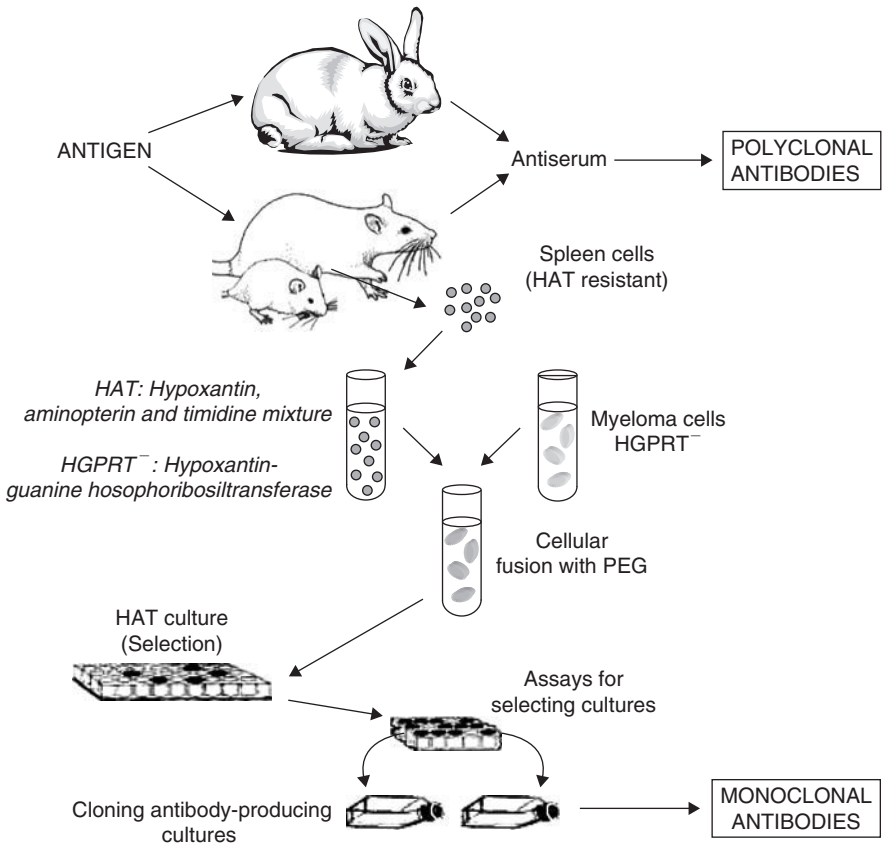

Figure 13.2 Obtention of polyclonal and monoclonal antibodies.

For *in vitro* assays, the most important properties are *affinity* and *selectivity*. Antibodies in competitive assays are assumed to be univalent reagents, which give a second-order reaction, because they are employed at high dilutions. Also, in solid-phase formats, molecular flexibility plays an important role related to the assay design. Both antigen–antibody interaction characteristics are reflected in the sensitivity and the specificity of the final assay.

Type of antibodies

Antibodies for use in analytical methods can be harvested directly from an animal immunized with the antigen of interest. Antibodies and proteins with similar properties can also be developed by other techniques (Harlow and Lane, 2007).

Classical antibodies can be categorized as polyclonal (P_{Abs}) or monoclonal (M_{Abs}), depending on their heterogeneity. The former are obtained (Figure 13.2) in high amounts directly from the blood serum of mammals and from avian eggs, and constitute a heterogeneous mixture of IgGs of different affinity and selectivity for the antigen that they have raised. Monoclonal antibodies, obtained by means of

Table 13.2 Comparison of the characteristics between antibody types

Polyclonal	Monoclonal	Recombinant
Heterogeneous mixture of IgGs; variable properties	IgGs – an only type; identical properties	Proteins with performances similar to those of monoclonal antibodies
Requires animal immunization	Requires animal immunization	Does not require animal immunization
Supply limited to the production of each immunized animal	Theoretically unlimited supply	Unlimited supply; requires specialized materials and staff
High IgGs concentration	Low IgGs concentration	Low recombinant protein concentration
Variable properties depending on the species and individual	Homogeneous properties related with the selected clone	Homogeneous properties
Rapid production (*ca*. 3 months)	Slow production (*ca*. 1 year)	Rapid production (1–2 months) but unsure, depending on target
Low production cost	High production cost	Medium–low production cost
Used directly as blood serum or purified solution to any format	Used directly or as enriched solution to any format	Phage expression with drawbacks for some developments

the hybridoma technology developed by Kohler and Milstein (1975), are IgGs generated by a group of genetically identical cells (clone); they also have exactly the same properties but, unlike polyclonal antibodies, they can in theory be produced in unlimited amounts, which can vary from animal to animal.

In practice, both types of antibodies have performances that make them ideal depending on their use. Table 13.2 lists the characteristic features of the different types of antibodies as immunoreagents.

On the other hand, recombinant antibodies are proteins, developed by means of genetic engineering technology, from libraries that produce a good number of proteins with different affinities for the targeted substance. They are obtained by expressing the functional regions of the antibodies in relatively simple and cheap host systems (Hall *et al*., 1997), as well as by genetic modification at DNA level. Genetic engineering techniques allow reproduction of several amino acid sequences of antibodies on the surface of a bacteriophage and, later, the selection of sequences of interest. This technology allows the acquisition of high-affinity and -selectivity antibodies and also contributes to improving their stability, being a well-established technology for macromolecular and superior aggregates. Its versatility and advantages will undoubtedly cause it to overcome traditional methods of antibody-raising.

Immunoassays

Immunoassays form a group of methodologies to detect the nature of a target or determine the amount of a substance or more complex structure (proteins, virus, cell, tissue component) using an immunological reaction.

Representative applications of IAs are to follow the proliferation of microorganisms in culture, to study the response of an allergic substance, to determine the

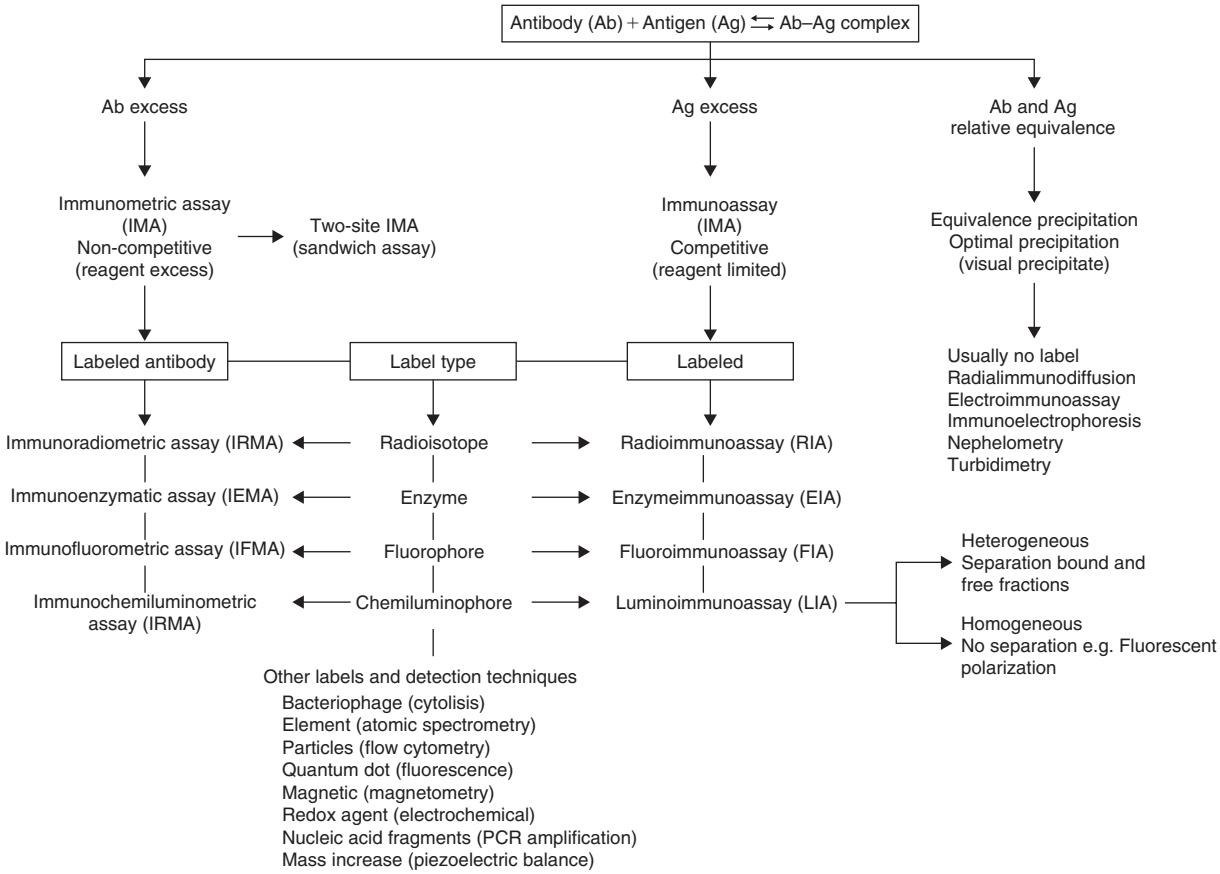

Figure 13.3 Classification of the immunoassays and working formats.

presence of fish meat in pork sausages, and to quantify the level of antibiotic residues in bottled milk.

The immunoassay concept includes simple precipitation of antibody–antigen complexes, agglutination of cells or particles, electrophoresis, homogeneous and heterogeneous assays (luminescent, enzymatic, etc.) and, finally, immunochromatographic and immunosensing methods.

Based on the type of marker employed in tracing reagents, immunoassays can be divided into enzyme immunoassays (EIAs), radio immunoassays (RIAs) and fluoroimmunoassays (FIAs), which match the specificity of antibodies with the sensitivity of enzymatic reactions, radiochemical measurements or luminescence (fluorescence, chemiluminescence), respectively. These potentialities can be combined, leading to diverse immunoassays and working formats (Figure 13.3).

Different features must be considered when selecting the immunotechnique to be used. Among them, reagent characteristics, marker type, format, sample nature and analyte concentration, sensitivity, selectivity, accuracy and precision, ease of use and availability are the more important.

Enzyme immunoassays

Although fluorescent and chemiluminescent labels have become more popular in the last few years, enzyme markers such as horseradish peroxidase (HRP), alkaline phosphatase (AP), β-galactosidase or glucose-oxidase are still the most used and the best fitting to the different approaches.

Enzyme immunoassays are based on antigen–antibody recognition that can be visualized directly (with the naked eye) or with the help of an instrument (photometer, fluorometer, etc.). Unlike other applications, the interaction does not mean a detectable phenomenon (precipitation), and it is necessary to use a reagent (tracer) that contains a substance (marker) whose activity can be related to the extent of the antibody–antigen reaction. This allows the acquisition of qualitative and quantitative information. Regarding sensitivity, ELISAs are around 1000 times more sensitive than other immunoassay techniques, apart from radioimmunoassays, which have a similar performance.

From a practical point of view, enzyme immunoassays are widely used immunochemical methods, with the enzyme-linked immunosorbent assay being the most applied, representing 90% of all immunoassays performed.

Enzymes were introduced as alternative to radioisotopes in immunoassays. They have important advantages as markers when compared with small molecules (chromophors and fluorophors) and with particles (gold, etc.), the main ones being the amplification of the analytical signal due to the catalytic transformation of the substrate, always in excess, and control of the reaction time.

As the enzyme immunoassay concept is broad, the number of possible configurations is enormous. Based on general concepts, they can be classified in two main groups: *homogeneous* and *heterogeneous*. Enzyme immunoassays are homogeneous when the analyte–antibody interaction takes place in solution with no physical separation of the analyte, immunoreaction and sample matrix products. This format exploits a change in enzyme activity that can occur when antibody binds to an antigen labeled with an enzyme. As the antibody–antigen binding provides the signal, separation between bound and free tracer is not necessary (Henderson *et al*., 1986; Wu, 2006). It shows important advantages, such as simplicity and rapidity, but it is difficult to apply to food analysis because of the interference of sample matrix components. Among the heterogeneous immunoassay formats, the ELISA are the most relevant.

ELISA

This group of immunoassays is based on the immobilization of one of the immunoreagents (antigen or antibody) and the use of enzyme markers. Different supports can be employed, with the most popular being 96-well polystyrene plates, plastic tubes and magnetic particles.

Regarding the format design, an ELISA is developed by means of the following steps. First, the reagent, antigen or antibody is immobilized on a support (rigid polymer, membrane, particle, etc.), then the immobilized reagent is incubated with a mixture of its complementary, antibody or antigen and sample, for the required time – frequently until equilibrium. Finally, the extent of the reaction is displayed, directly or in a second step, by means of the enzyme tracer and its substrate.

ELISA types

All ELISA formats are classified as heterogeneous immunoassay because the interaction takes place on the support/solution interface, which allows the analyte to be separated from the matrix.

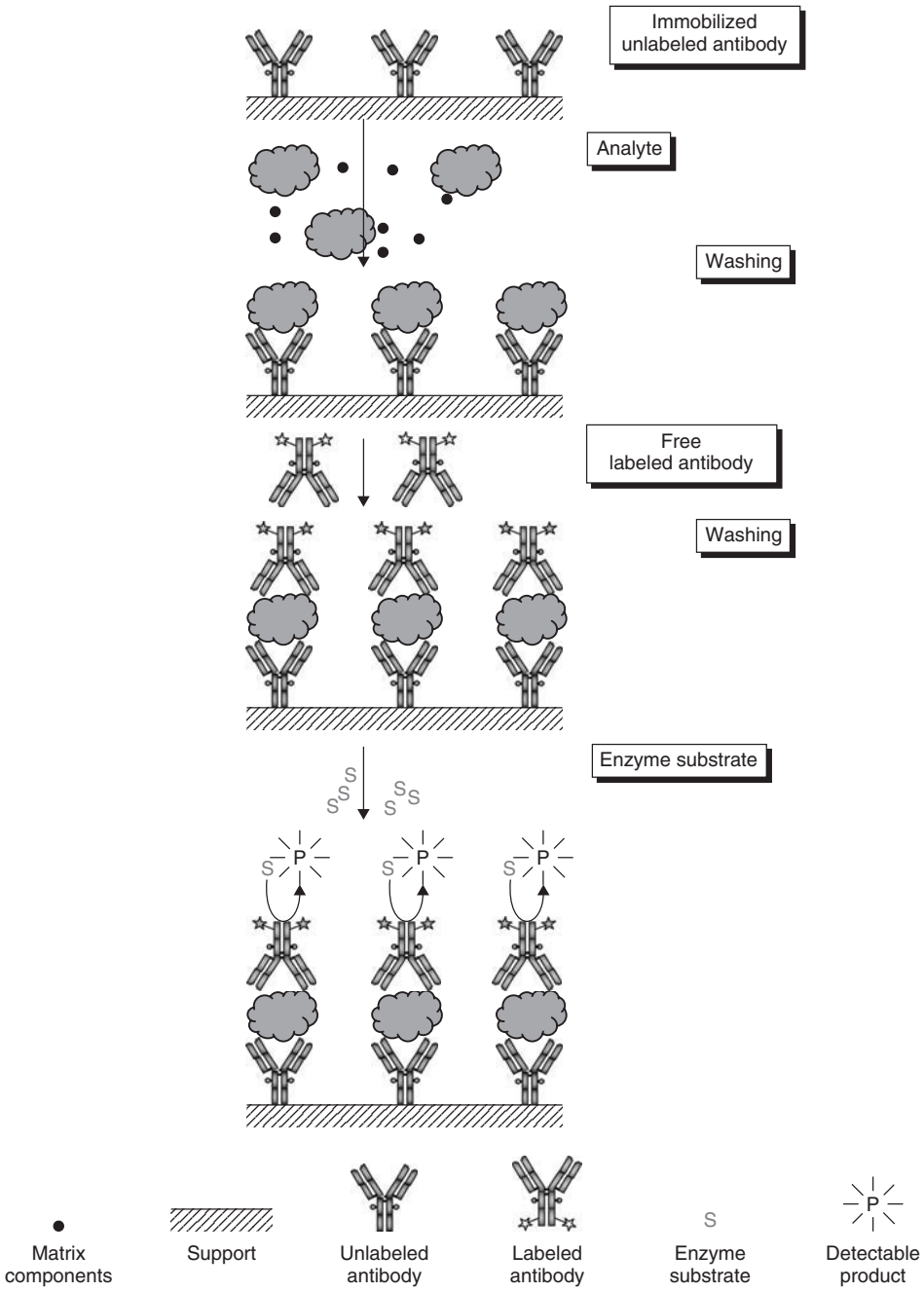

Figure 13.4 Scheme of a non-competitive sandwich ELISA.

Depending on the auxiliary system employed for measuring the extent of the analyte–antibody binding, ELISAs may be *competitive* or *non-competitive*. The former employs competition between the analyte and an analogous molecule for the binding sites of the antibody, which is added in a limited amount. The latter are all those that are not based on this general principle. Non-competitive formats are based on the measurement of the bound sites when using the antibody in excess. Unlabeled antibodies are immobilized, while labeled antibodies are added in solution. This configuration can be carried out only when the target analyte has two or more different binding sites and, furthermore, antibodies that recognize specifically each binding site are available. This format is named the two-site (sandwich type) immunoassay (Figure 13.4).

Regarding the working sequence of the competitive format, ELISAs can be (i) direct (Figure 13.5), where the analyte and a labeled structurally similar hapten or antigen are both in solution and compete for binding to the antibody, which is immobilized on a solid support, or (ii) indirect (Figure 13.6), where the antigen or hapten is immobilized, and the analyte (sample) and the antibody are added in solution. In this format, a secondary enzyme-marked antibody is used as a tracer.

Direct and indirect formats display different results. Normally, the direct format has the advantage of being a simpler assay because it needs one step less than the indirect format. However, the indirect format frequently results in greater sensitivity, especially if polyclonal serum is used, and this is why this protocol is often preferred.

As it can be seen in Figures 13.5 and 13.6, in both the direct and indirect formats, hapten conjugates and analyte compete for the antibody-binding sites. The extent of this reaction is later displayed by means of an enzyme substrate, which produces a colored or luminescent product, or even a precipitate. After a suitable reaction period, the product is quantified visually or instrumentally and related to the analyte concentration in the sample.

ELISA characteristics

The immobilization of an antigen or an antibody on the surface of the working support, generally a 96-well polystyrene microplate, is frequently carried out by direct adsorption (coating). Nevertheless, other methods, such as covalent binding, capture anti-antibody, protein A or avidin-biotin interaction, are also employed. On most occasions, these procedures show a better performance (sensitivity, selectivity, lower unspecific adsorption) than those based on adsorption. However, the simplicity and good results achieved with direct coating mean that there is not necessarily justification, *a priori*, for the choice of these other immobilization methods.

From a qualitative point of view, ELISA is an interesting tool due to the high selectivity of the antibodies. Thus, if specific immunoreagents for a target are available, the positive recognition of this substance is conclusive regarding their presence or nature. As immunoassays can be directly developed on tissue, it is possible to detect both *in vivo* and *in vitro* the nature of many substances, from molecules to organized structures such as tumors. Immunohistological methods are a good example of the possibilities of the immunoassay qualitative applications (Dabbs, 2006). Another example is the direct recognition of cells in blood, and of microorganisms,

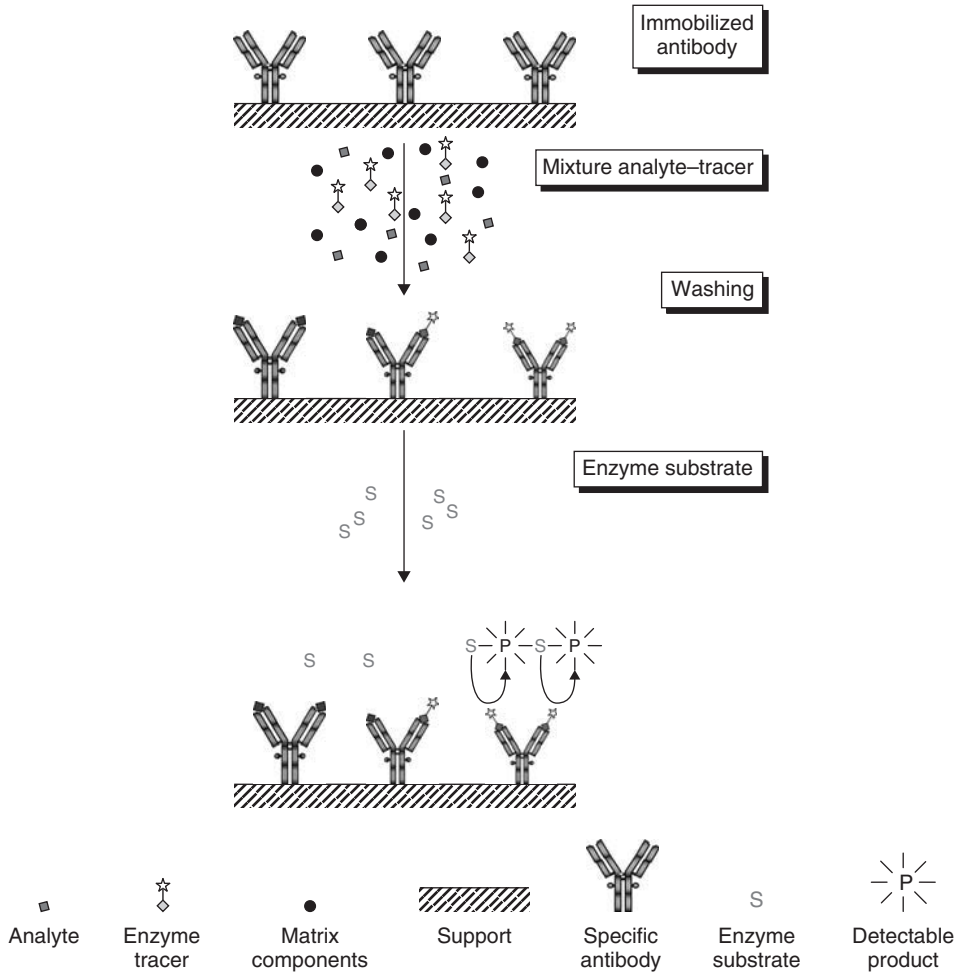

Figure 13.5 Scheme of a direct competitive ELISA.

viruses, celiac proteins, etc. In addition, it must be remembered that few methodologies reach this level of performances with such high sensitivity and simplicity.

For quantification, there are several well-established theoretical and empirical models (mass-action law, linear, logistic, non-uniformity of variance, spline functions, etc.). Among them, the logistic model (Baud, 1993) is the most frequently used, being mathematically provided by the following four-term equation:

$$Y = (AD)/\left[1 + (x/C)B\right] + D \qquad \textbf{(13.2)}$$

where A and D are the maximum and minimum signals corresponding to zero and infinite concentrations respectively, B is the slope of the sigmoid calibration curve, and C is the analyte concentration resulting in 50% inhibition of tracer binding (IC_{50}).

Quantification is carried out in parallel to the sample analysis by employing a standard curve for the analyte. Dose–response calibration curves are plotted with

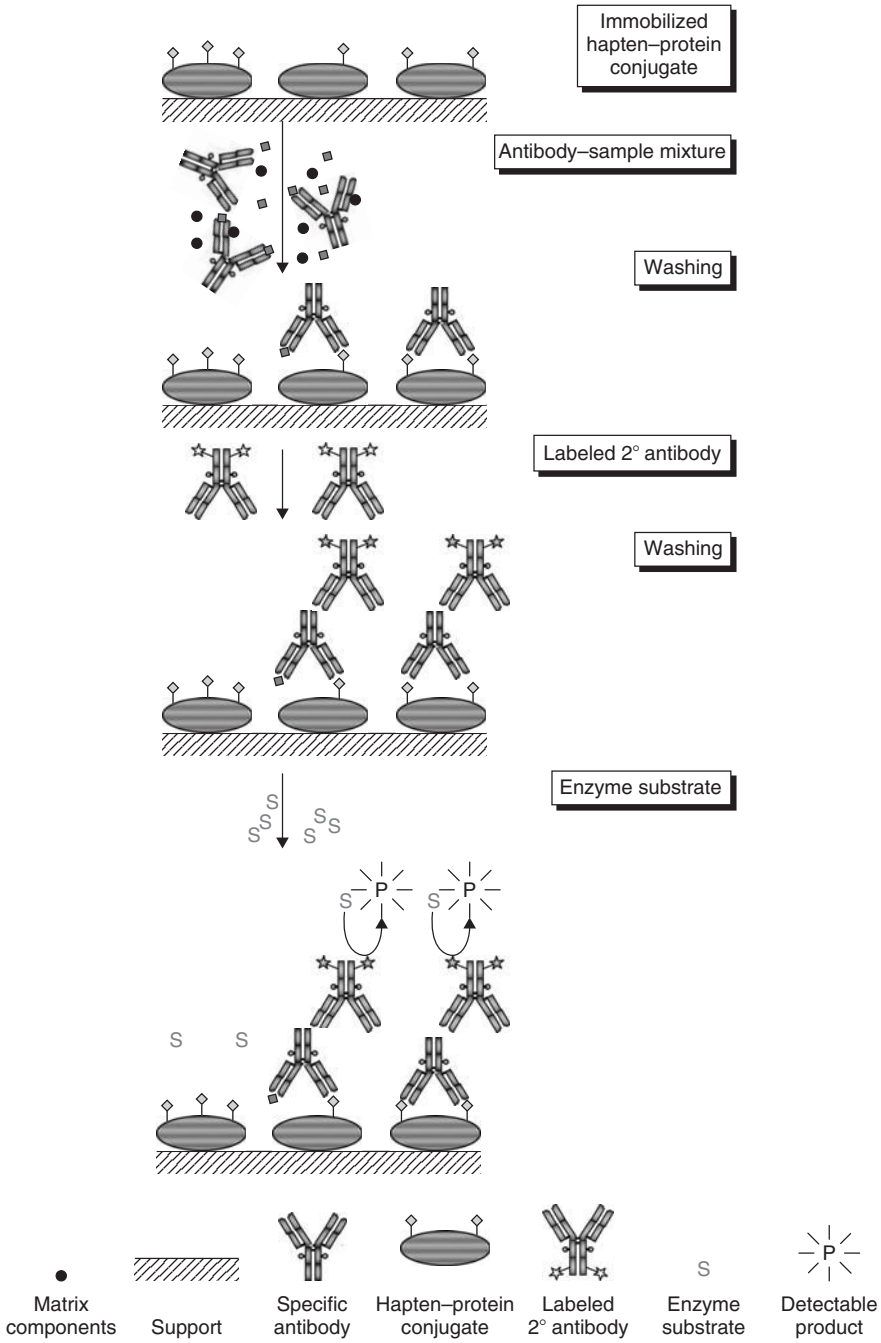

Figure 13.6 Scheme of an indirect competitive ELISA format.

the measured signal intensity (optical: absorbance, fluorescence, etc.; electrochemical: current, difference of potential, etc.; mass, or another property) vs the logarithm of the standard concentrations. Curves are generally sigmoid, showing a linear zone around the IC_{50}. Other important parameters of the curve are the limit of detection

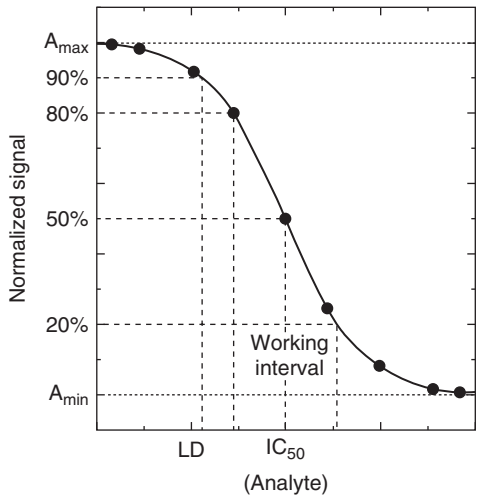

Figure 13.7 Calibration curve of the logistic model for a competitive immunoassay.

(LOD, the analyte concentration that originates from a signal diminution of 10% with respect to the blank) and the limit of quantification (signal diminution 20%). In the most sensitive assays the limits of detection and quantification are in the ng l^{-1} range, while the highest limits are in the mg l^{-1} range. In this type of curve, the working dynamic range is defined as the analyte concentration interval producing a signal between 80% and 20% of the range defined by the maximal and minimal asymptotes (A_{max} and A_{min} in Figure 13.7).

For the non-competitive sandwich format, the calibration curve is a mirror shape of that from competitive assays. In this case, the measured signal increases with the analyte concentration, and the slope is positive. The limit of detection and quantification, the IC_{50} and the dynamic range are defined in the same way as for competitive formats.

When considering the use of the immunoassay as a tool to discriminate between different analytes with similar chemical and structural characteristics, it is important to know its selectivity (frequently known as its cross-reactivity), because the higher the selectivity the easier the full analytical process is, thus reducing the sample treatment and assay time, and increasing the accuracy and throughput. In addition, the quality of the information obtained is improved.

The presence of interfering substances decreases the selectivity. Cross-reactivity (CR) is the capacity of an assay to discriminate between similar substances. It is measured from the sensitivity data (IC_{50}) obtained for the compared substances, and is calculated as the percentage cross-reactivity using the following equation:

$$CR(\%) = \left(IC_{50}\ \text{analyte}/IC_{50}\ \text{interferent}\right) \times 100\% \qquad \textbf{(13.3)}$$

An assay with cross-reactivity to different compounds as low as 10% is considered to be specific. This condition is reached by many immunoassays.

In general, immunoassays are designed to reach maximum selectivity, being very specific to the target compound. However, it is also possible to set up generic immunoassays to determine a whole family of compounds (Pastor-Navarro *et al.*, 2007).

Reduction of the cross-reactant interference effects is achieved by minimizing or eliminating the disturbing substances. Differences in the design or development of the assays make a contribution. First, using monoclonal antibodies increases the selectivity, and works with a sandwich format, thus eliminating the previous interferences by the sample treatment or blocking the disturbing compound while the assay is performed. Secondly, optimizing the assay by adjusting the incubation times, temperature and buffer composition contributes to improving the selectivity.

Selectivity is also influenced by unspecific interactions. This problem is due to the fact that reagents or sample components behave as specific reagents (antigen or antibody); the result is a high background signal with a small slope, and thus a loss of sensitivity and accuracy and, in extreme cases, masking of the immunoreaction and illogical results. To minimize this, it is necessary to change the format or the support (nature or properties), employ a carrier protein different from that used in the immunogen preparation (Butler, 1996), and add surfactants or non-specific proteins to the reagents.

Assay presentations

ELISAs can be developed on different supports, and they are designed for concrete applications that include, for instance, determining a given compound, performing multiple assays in parallel, or screening a high number of samples. The most employed supports include the following:

1. *Polystyrene plates*. They are normally used in the laboratory for quantitative analysis. Each plate contains 96 wells (8 columns and 12 rows), which can be used independently. Immunoreagents (antibodies or antigens) are immobilized on the well surface. For instance, in the direct competitive ELISA, the assay begins with the competition between the analyte and the competitor (an analog marked with an enzyme) until equilibrium is reached (15–60 min). After incubation with a substrate (15 min or longer), the extent of the reaction is measured by means of a plate reader (UV-vis or luminescent detector). An LD of 0.1 μg l^{-1} or lower is reached in many cases. This format allows the performance of hundreds of determinations daily, and has been adapted for routine analysis.
2. *Tubes*. In this case, and also for the direct competitive format, antibodies are immobilized on the bottom surface of polystyrene tubes (7.5 cm high × 1.2 cm inner diameter, 5-ml capacity). The competition between the analyte and the enzyme tracer is stopped after reaching equilibrium (normally 5–10 min), since in field assays a short incubation period is required. Analyte concentration can be estimated visually after 2 min of enzyme substrate reaction, thereby obtaining qualitative yes/no results. A portable photometer can be used in order to improve accuracy and sensitivity. This support is adequate for field analysis, but does not have the working capacity of polystyrene plates.
3. *Magnetic particles*. These are formed from a ferrous nucleus coated with a functionalized material (silica, plastic) where antibodies are immobilized by adsorption or covalently; their size is in the 100-nm region, and their active surface is large. The assay format is similar to that described for the other supports.

In this case, optimized volumes of sample, tracer and antibody are mixed and incubated for 15 min, and the unbound components are then separated by means of a magnetic field. After washing, the substrate is added and finally the enzyme reaction is stopped. Results are obtained in less than 60 min visually, or by employing an appropriate detector (plate or tube reader). The precision and sensitivity achieved are in general equal to or better than those obtained with plates or tubes.

As described below, it is possible to purchase commercial kits for the qualitative and quantitative determination of many substances. Frequently, assays applicable to authentication work are purposely developed for the particular analyte and matrix of interest. Kits can thus be used for screening when they are applied to extracts obtained by validated methods, or when they are combined with rapid extraction processes that have been especially developed for them.

Advantages and disadvantages of ELISA

One of the benefits of immunoassays is their high sample throughput, giving a large data volume. In addition, the use of immunoassays can help to generate the information required to validate new sampling plans in a cost-effective manner. The major advantage of this approach is that immunoreagents can be developed to respond specifically to the target of interest (i.e. proteins), thereby enabling recognition and quantitation of that analyte exclusively. Moreover, ELISA is sensitive and specific, fast and cheap, easy to perform, and the investment in equipment is much less than in other techniques.

Several limitations are envisaged for quantitative determination with protein-based methods. An accurate measurement is only possible if (i) sample matrices are identical to the reference material, or (ii) matched standard materials or standards that have been validated for the matrix are available.

The disadvantages of the ELISA approach include the initial difficulty in producing an antibody specific to a particular target. However, this is a minor problem to overcome when the selectivity of the technique is taken into account.

Heat lability of proteins is the main obstacle to the general application of these methods although the use of antibodies directed against heat-denaturated meat proteins is an interesting alternative. A comparison of the advantages and drawbacks of the immunochemical techniques is given in Table 13.3.

The ELISA technique has much potential for the authentication of food products, but to date limited advances have been made in extending its authentication capabilities. The authenticity of food and the methodology for testing have been well-known topics in food science for many years (Woolfe *et al*., 2004). Problems of authentication exist in all areas of the food industry, and, depending on the type of food and the possible adulteration, different analytical approaches for its detection may be applied. A concise overview of the principal food authentication techniques that have been successfully applied since 2001 has been reported by Reid *et al*. (2006).

The immunoassay provides an invaluable tool for the food scientist concerned with quality control and safety assurance, and a number of books regarding the use

Table 13.3 Advantages and drawbacks of the immunochemical techniques

Advantages	Drawbacks
High sensitivity and selectivity	Availability of adequate immunoreagents
High working capacity	Immunoreagent stability
Simplicity of working protocols	Single-analyte determination
Low instrumental requirements	Matrix interferences
Little sample treatment	Difficulty in non-aqueous media
Minimum sample size (μL volumes)	Qualitative information difficult to interpret, sometimes
Reduced wasting chemicals	Need of confirmation of screening results
Employment as screening method	Methodology still not well accepted in food area
In-situ application	Occasionally, need of working protocols validation
Low cost per sample analysis	High cost of commercial kits
Work from batch to full automation	Standardization between protocols
Application from chemicals to proteins and other macromolecules, including direct detection in sample (e.g. tissues)	Need of Reference Materials

of immunoassays in foods (see, for example, Lees, 2005; Ebeler *et al*., 2007) have been published.

Food authentication testing – recent applications

The aim of this section is to provide an updated review of the antibody-based methodologies that have shown potential for addressing the issues related to the authenticity of foods and food products, and also to collate information on ongoing research into this matter, focusing on ELISA configurations.

Adulteration issues in animal products are described for meat, fish and dairy products, and the origin of feedstuffs, fruit-juice fraud and detection of irradiated food are also considered. Finally, identification of genetically modified organisms is considered.

Meat and meat-based products

The adulteration of meat with that of other species not only constitutes economic fraud, thereby betraying consumers' trust in the meat industry, but is also a concern for those with a religious or moral aversion to particular meat species, and those who suffer from meat allergies.

DNA-based methods and ELISA techniques have been the most widely used for meat authentication. Although DNA-based methods are the most specific and sensitive for meat species identification, they require expensive laboratory equipment and a certain degree of knowledge. For these reasons, ELISA techniques are applied for the routine analysis of large sample series (Goldsby *et al*., 2003).

Different ELISA methods have been used in the past few years for identifying meats of different animal species using antibodies against muscular and serum animal proteins or thermostable proteins. Qualitative and quantitative studies have also been reported to identify the origin of heat-processed meat products (Chen and Hsieh, 2000; Ayaz *et al*., 2006; Liu *et al*., 2006).

Recent research using ELISA-based techniques includes detection of the presence of meat from different species in food products (Hsieh, 2005). Adulteration of hamburgers with meat of different animal species was identified at concentrations as low as 0.6% by a dot-ELISA using P_{Abs} produced against bovine, chicken, swine and horse albumin with high specificity (Macedo-Silva *et al*., 2000). Also, an indirect competitive ELISA (IC-ELISA) using P_{Abs} for specific identification of heat-processed poultry, horse, kangaroo and rat muscular tissue, with a sensitivity of 1–5%, has been reported by Rencova *et al*. (2000).

Several attempts have been made to develop M_{Abs} for the identification of different meats. For this, the selected species marker needs to possess a unique antigenic region for a given species that is not present in the counterpart molecules of other species. In addition, thermal stability of the species marker antigen is indispensable in developing IAs for the detection of the species origin of heat-processed meats.

An indirect ELISA was standardized to identify the cooked and raw (native) muscle antigens of pig and their differentiation from muscle antigens of cattle, buffalo, sheep, goat and chicken. Based on cut-off indirect ELISA values (0.14 for cooked, 0.10 for raw), differentiation of pig meat from the cooked and raw muscle samples of cattle, buffalo, sheep, goat and chicken, at a minimum level of 1%, is possible (Jha *et al*., 2003).

The Hsieh' research group (Chen and Hsieh, 2000, 2001a, 2001b) is very active in this area, and several studies have been reported in the past few years. First, the production of a porcine-specific M_{Abs} raised against crude porcine protein extract that recognized a 24-kDa thermostable skeletal muscle protein (TSMP) was reported. The ELISA developed was demonstrated to be a valuable tool for the detection of pork in a variety of heat-processed meat products (Chen and Hsieh, 2000), with a LOD of 0.5% (w/w) pork in heterologous meat mixtures. Furthermore, the presence of TSMP in the troponin (Tn) fraction was supposed and tentatively identified as TnI (Chen and Hsieh, 2001a). In other studies, individual subunits of porcine troponin were separated and compared, confirming that the TSMP is skeletal troponin I (sTnI). Heat treatment of sTnI up to 126°C for 120 min did not diminish its solubility and antigenicity. The antigenic specificity and thermal stability of sTnI indicate its potential as a thermostable species marker for the identification of the origin of meats in severely heated products (Chen and Hsieh, 2001b).

The feasibility of using M_{Abs} in an indirect ELISA system for the assessment of the EPT (endpoint heating temperature) in precooked ground beef and pork was also investigated by Hsieh *et al*. (2002). A 12-kD antigenic component was identified as a thermo-stable protein that could be used as an EPT indicator for heat-processed pork and beef.

Recently, a sandwich ELISA was developed for the sensitive detection of porcine skeletal muscle in raw and heat-processed meat and feed products. Heat treatment of meat samples (132°C, 2 h) did not affect the assay performance. The sandwich ELISA is able to detect 0.05% (w/w) of laboratory-adulterated pork in chicken, 0.1% (w/w) pork in beef mixtures, 0.05% (w/w) pork meal in soy-based feed, and 1% commercial meat and bone meal (MBM), containing an unknown amount of pork, in soy-based feed. The specificity of the assay was 100%, and no false-positive results were found (Liu *et al*., 2006).

Color intensity	Negative	Positive		
	–	+	++	+++
Adulteration levels of raw lamb-in-pork (%, w/w)	0	0.05	0.50	1.00

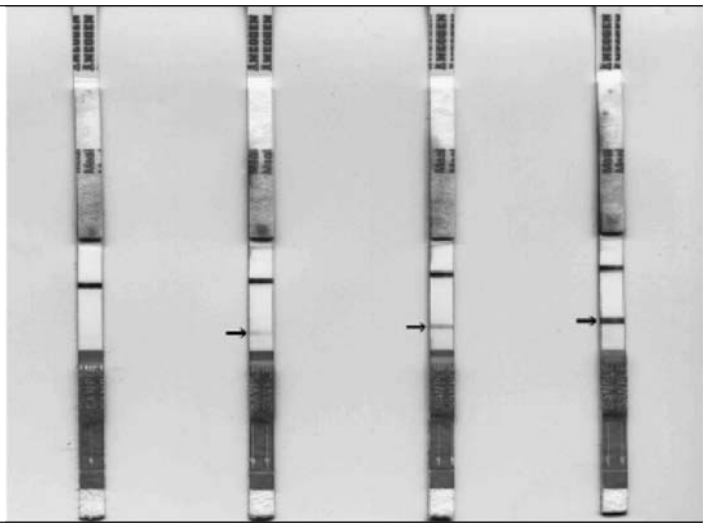

Figure 13.8 Illustration of color intensity of the positive line in the Result Zone of the test strips. The samples shown include raw meat containing various levels (0%, 0.05%, 0.50% and 1%, w/w) of ground lamb in ground pork, which were extracted in five-fold volumes (v/w, ml g^{-1}) of the kit-provided extraction solvent. The extracts were heated at 100°C for 10 min before assay. Reproduced from Quinchum and Hsieh, 2007.

An ELISA was developed by Chen *et al*. (2006) to study the thermal denaturation of tropomyosin (Tm) using cooked beef. The ELISA employed a M_{Ab} raised against bovine Tm for quantifying residual Tm in muscle extracts.

Because of the advantages of M_{Abs}, commercial kits for raw and cooked meat species have been developed. The detection of the presence of beef and/or sheep's meat in raw and heat-processed meat products for human consumption is possible using the Reveal for Ruminant in MBM assay test. Quinchum and Hsieh (2007) demonstrated that the LOD of the assay for lamb-in-pork could be as low as 0.05% (w/w) in only 20 min (Figure 13.8). Although this ruminant assay cannot distinguish between bovine and ovine species, this can be accomplished if necessary by the 96-well ELISA plate format.

Furthermore, some companies (such as Strategic Diagnostics Inc., Tepnel, Neogen Co., Eurofins, and ELISA Technologies Inc., among others) have developed a variety of meat species test kits (Table 13.4) that identify the species content in cooked, raw and thermally processed meat, meat products and animal feed. Both types of tests provide rapid, reliable and cost-effective screening regarding the meat species identification (Bonwick and Smith, 2004; Giovannacci *et al*., 2004). In fact, some of these test kits are being used by regulatory agencies to detect the adulteration of meat species and in enforcing national and international laws and regulations.

An evaluation of the performances of different commercial ELISA kits for identification of animal species in processed meat products has been made by Giovannacci

Table 13.4 Characteristics of some commercially available ELISA formats for species discrimination in foods

Analyte	Company	Kit name	Primary matrices	Format	Detection limit
Cows' milk	R-Biopharm Rhone Ltd	RIDASCREEN® CIS	Sheep's and goats' milk and cheese	Microtiterplate	*0.1% cows' milk in sheep's/goats' milk and cheese*
Cow's milk	R-Biopharm Rhone Ltd	RIDASCREEN Quick CIS	Sheep's and goats' milk and cheese	Reaction strips	*0.5% cows' milk in sheep's and goats' milk and cheese*
Goats' milk	R-Biopharm Rhone Ltd	RIDASCREEN GIS	Sheep's milk or cheese	Microtiterplate	*1% goats' milk in sheep's milk*
Bovine casein	R-Biopharm Rhone Ltd	RIDASCREEN Casein	Sheep's and goats' milk and cheese	Microtiterplate	*0.5% bovine casein in cheese*
Cows' milk	ZEU Inmunotec	RC Bovino	Sheep's and goats' milk and cheese	Microtiterplate	*0.01% cows' milk in sheep's/goats' milk* *0.51% cows' milk in sheep's/goats' cheese*
Cows' milk	ZEU Inmunotec	IC Bovino	Sheep's and goats' milk and cheese	Strips	*0.5–1% cows' milk in sheep's/goats' milk* *1–2% cows' milk in sheep's/goats' cheese*
Goats' milk	ZEU Inmunotec	RC Caprino	Sheep's milk or cheese	Microtiterplate	*0.01% goats' milk in sheep's milk* *0.5% goats' milk in sheep's cheese*
Goats' milk	ZEU Inmunotec	IC Caprino	Sheep's milk or cheese	Strips	*0.5–1% goats' milk in sheep's milk* *1–2% goats' milk in sheep's cheese*
Non-durum wheat	R-Biopharm Rhone Ltd	PASTASCAN	Pasta	Membrane strips	*3% non-durum wheat in pasta*
Non-durum wheat	R-Biopharm Rhone Ltd	DUROTEST® S	Durum wheat (semolina)	Membrane strips	*3% non-durum wheat in semolina*
Pork/beef/poultry/horse	Tepnel BioSystems Ltd	Biokits (Cooked) Species Identification Kit	Cooked/canned meats/meat products, blood and rendered material of animal origin in animal feeds	Microtiterplate	*<1% pork/beef/poultry/horse even in highly-treated/autoclaved samples*
Sheep	Tepnel BioSystems Ltd	Biokits (Cooked) Species Identification Kit	Cooked/canned meats/meat products, blood and rendered material of animal origin in animal feeds	Microtiterplate	*<2% sheep even in highly-treated/autoclaved samples*
Cow/pig/poultry/sheep	Tepnel BioSystems Ltd	Biokits (Raw) Species Identification Kit	Raw meats/meat products, milk and animal plasma	Microtiterplate	*<1% cow/pig/poultry/sheep*
Cow/pig/poultry/sheep/horse	Tepnel BioSystems Ltd	Biokits FAST Kit	Raw meats/meat products, milk and animal plasma	Immunostick	*<2% cow/pig/poultry/sheep/horse*

et al. (2004). The assays were performed using cooked species identification ELISA kits from Tepnel according to the manufacturer's instructions (Tepnel Biosystems Limited, 2001).

Recently, the Cooked Meat Species Identification Kit (ELISA-TEK, Gainesville, FL) was used by Ayaz *et al*. (2006) to detect meat species in processed meat and meat products by the M_{Ab} sandwich ELISA technique according to the manufacturer's instructions. The assays were completed in 5 h, and a simple aqueous extraction of samples was performed.

The main infectivity in transmissible spongiform encephalopathies (TSEs) is found in tissues of the central nervous system (CNS). The removal and destruction of specified risk material (e.g. brain and spinal cord) is mandatory to protect human and animal health from the risk of BSE (bovine spongiform encephalopathy). Some potential markers to detect CNS in processed food products have been identified, including proteins such as neuron-specific enolase (NSE) and glial fibrillary acidic protein (GFAP).

Bülte *et al*. (2001) reported that the LOD of the GFAP–ELISA is $<0.2\%$ CNS tissue in meat products. This ELISA was practiced as a quick and easy method, but could not define the origin of CNS as bovine, ovine or porcine.

The development and validation of a fluorescent ELISA for GFAP, which can be used as a rapid and sensitive method (0.2-ng GFAP) to detect CNS tissue in meat products, are reported by Schmidt *et al*. (2001).

Other highly specific immunochemical methods developed for the detection of CNS in heat-treated meat products using NSE and GFAP as markers have been published (Lücker *et al*., 2000). These methods have recently become available in the form of test kits, and have been used in a monitoring study of several meat products, including heat-treated meat products such as cooked sausage (Weyandt, 2001).

In order to evaluate the performance characteristics of the kits, an international intercomparison study on both CNS test kits has been conducted (Hagáis *et al*., 2002). The methods differ in the type of marker and methodology applied. One uses Western blotting, i.e. BrainosticTM test (Schebo Biotech, 2001), to detect NSE, while the other is based on ELISA, i.e. the RIDASCREEN Risk Material test (R-Biopharm, 2001), for the detection of GFAP. The sensitivity of both test kits is 100% at 0.5% CNS in non-heated and moderately processed materials, while for strongly heated materials the ELISA test kit is superior to the Western blot method. The specificity is 100% for the ELISA test kit for all samples, irrespective of the heat treatment, while the Western blot test kit varies in the 95%–100% range depending on the thermal treatment. Both test kits can be applied to gain information regarding the composition of meat products such as sausages (Agazzi *et al*., 2002).

Recently, a study to detect risk material in processed meat products was conducted by Yesilbag and Kalkan (2005) by means of the commercially available RIDASCREEN® risk material test (R-biofarm GmbH, Germany); the authors concluded that mixing of CNS tissue with the meat products still occurs.

On the other hand, non-meat proteins are used as additives in meat products because of their nutritional and functional properties, soybean proteins being the most widely employed due to their emulsifying and stabilizing properties, and their capacity to increase the water-holding capacity and improve the texture of the final

product. Different ELISAs for identifying and quantifying soy protein in meat products have been developed (Macedo-Silva *et al*., 2001; Brandon and Frieman, 2002).

Recently, Koppelman *et al*. (2004) have set-up a P_{Ab}-based sandwich ELISA test applicable for the quantification of soy ingredients and soy-containing foods, reaching a sensitivity of $1\,mg^{-1}$.

Immunochemical diagnostic kits for the rapid detection and quantification of soy proteins in foods are also commercially available (Neogen Co., ZEU Inmunotec, ELISA Systems, and Tepnel, among others). The kits contain all the necessary reagents, controls and accessories for rapid on-site testing.

Milk and dairy products

Adulteration is a common problem in the dairy industry because it can be easily applied to milk and derivates. Differences in price and seasonal availability might make adulteration of expensive sheep's milk with cheaper goats' milk attractive. In many European countries, laws require producers to state the type of milk used for manufacturing cheese or other dairy products (Mayer, 2005). Apart from the possible economic loss, accurate species identification is important for consumers who may have specific food allergies, or for religious, ethical or cultural reasons (Recio *et al*., 2004). As a result of this fraudulent practice, adequate control methods are required to evaluate the authenticity of milk and dairy products (Moatsou and Anifantakis, 2003; Hurley *et al*., 2004a).

A range of analytical methods to detect fraud have been developed, and are constantly being modified and reassessed in order to be one step ahead of manufacturers who pursue these illegal activities (Hurley *et al*. 2004a; López-Calleja *et al*., 2007). The work by de la Fuente and Juárez (2005) provides an updated and extensive overview from 1991 to 2003 of the main applications of analytical techniques, together with their advantages and disadvantages for detecting the authenticity of dairy products. The scope and limits of different tools are also discussed.

Several alternative methods based on ELISA using both P_{Abs} and M_{Abs} have been developed to authenticate the species of origin of milk products, and these might be applicable to routine analysis (López-Calleja *et al*., 2006a, 2006b). Target antigens include caseins, lactoglobulins, immunoglobulins and other whey proteins (Hu *et al*., 2000; Wu *et al*., 2000). While whey proteins may be denatured by thermal treatment modifying their immunoreactivity, caseins are not affected by heat treatment and are thus more suitable for use in immunological methods for detecting milk mixtures in heat-treated dairy products (Fukal *et al*., 2002; Vítková *et al*., 2002). On the other hand, for species identification in milk and mixed cheese varieties, ELISA techniques based on antibodies against bovine immunoglobulins (P_{Abs}) are not appropriate, because the addition of heated milk or of bovine caseinate cannot be detected, whereas the use of M_{Abs} to detect bovine γ-caseins is well suited even in these cases (Mayer, 2005).

In cheese, preservation of their epitopes depends on protein hydrolysis during cheese ripening. This problem could be overcome by the use of antigenic casein fractions (Senocq *et al*., 2001) that are not affected by proteolytic reactions.

Antibody-based analytical methods using both M_{Abs} and P_{Abs} against caseins, whey proteins and synthetic peptides for the detection of milk from different species have been reviewed by Moatsou and Anifantakis (2003). Recently, López-Calleja *et al*. (2006c) applied an indirect ELISA using a M_{Ab} against bovine β-casein that proved to detect adulteration in non-declared cows' cheeses.

Another protein found in milk, bovine immunoglobulin G (IgG), has been successfully used as a target antigen in a simple ELISA based on an immunoblotting, or commercial kits (r-Biopharm or Tepnel Biokits Bovine Casein Kit). However, these methods are unable to distinguish between cows' milk and buffalo milk.

Sensitive IC-ELISA using antibodies raised against bovine IgG has been developed by Hurley *et al*. (2004b). The ELISA was effective for the detection and quantification of adulteration of sheep's, goats' or buffalo milk with cows' milk, and had a LOD of 0.1% (v/v) cows' milk adulteration. With goats'- and sheep's-milk cheeses, a LOD of only 5% adulteration with cows' milk cheese was found, whereas with buffalo-milk cheese the LOD was 2.5% adulteration.

Using the same M_{Abs}, a highly specific sandwich ELISA has been developed which enables the detection of cows' milk adulteration of sheep, goat or buffalo milk (sensitivity of 0.001%, 0.01% and 0.001%, respectively). Detection limits in cheese were 0.001% in goats' cheese and 0.01% in sheep or buffalo cheese (Hurley *et al*., 2006). The assay was highly reproducible with both intra- and inter-assay coefficient of variation $<10\%$. However, the assay is unable to detect bovine IgG in UHT milk, as the heat treatment required to produce such products seems to denature the target epitope. The detection limits reported in this paper are by far more sensitive than those previously reported for IC-ELISA (Hurley *et al*., 2004b), and are competitive when compared with previous immunological and DNA-based methods (de la Fuente and Juárez, 2005).

On the other hand, vegetable proteins can be added to milk in order to increase fiber content and hydration properties, but their use as supplements and substitutes for bovine milk protein is forbidden. Although wheat gluten, pea, rice, potato, bean and soluble cereal hydrolyzed proteins can also be used as vegetable substitutes, soy protein, owing to its low price and high availability in the market, is likely to be the major adulterant. Rozenfeld *et al*. (2002) developed a P_{Ab} against cows' milk proteins, and specific M_{Abs} against bovine α-casein, β-casein and γ-casein. With the P_{Ab}, a low CR (about 0.02%) was observed with a soy protein extract. M_{Ab} did not show any activity against soy proteins from the undiluted soy milk (containing 7.2% soy beans) tested (CR $<0.01\%$), and the detection of cows' milk in expensive soy milk seems to be a possible future application.

A collaborative study (Manso *et al*., 2002) involving eight international laboratories was conducted to evaluate two electrophoretic procedures and an indirect competitive ELISA method using P_{Abs} for the determination of the fraudulent addition of vegetable proteins (soy, pea and wheat proteins) in different dairy products subjected to low and high heat treatments. SDS-CE provided slightly better accuracy, but ELISA presented the advantage of being suitable for samples containing wheat proteins, which could not be detected by SDS-CE. ELISA results from high-heat treated samples were lower than the real values; this fact was attributed to protein denaturation.

Several ELISAs based on the detection of bovine caseins, native or heat-denatured bovine whey proteins or IgG have been published (Sanchez *et al*., 2002). Although these assays can detect cows' milk in the milk of other species at levels below 0.1%, the analysis takes several hours. For this reason, immunoassay kits (Table 13.4) for species authentication in milk and cheese have been developed and are commercially available from different companies (e.g. ZEU Inmunotec (http://www.zeu-inmunotec.com), Euro-Diagnostica), which require minimal training and equipment, and are used for the rapid identification and quantification of the milk species in dairy products. ELISA kits to detect the adulteration of milk and dairy products with vegetal proteins are also commercially available, with quantification limits of 0.69% chickpea protein in milk, 0.08% soy protein in milk and 0.26% whey protein in milk (ZEU Inmunotec).

Fish and fishery products

In an effort to overcome fraudulent practices, new regulations concerning the labeling of seafood products have been recently introduced in Europe (Berrini *et al*., 2006). Accordingly, since January 2002 it has been obligatory in the European Union to include the name of the fish species, the geographical capture zone and the production method (wild or cultivated) when labeling fishery products (Council Regulation (EC) No. 104/2000 of the European Parliament).

There is a clear trend in the international market towards labeling products with information about their origin, composition and quality, which brings about the need to develop and standardize analytical methods either to confirm the information given by the label or to uncover fraud (Martinez *et al*., 2003). In November 2004, fish authenticity was discussed at the Local Authority Update Seminar organized by Eurofins Scientific (www.eurofins.co.uk/laupdate/seminars).

Traceability is or will soon be obligatory as well. However, the fact is that at present only the species can be reliably documented by analyzing the protein component (Etienne *et al*., 2000; Mackie *et al*., 2000) and, more easily, by using DNA-based techniques (Martinez *et al*., 2001; Chapela *et al*., 2002). However, correct identification often depends on how the product has been treated, and for heavily treated products it seems that only techniques that target small fragments may be appropriate (Piñeiro *et al*., 2001; López *et al*., 2002).

Several biochemical methods have been applied to identify fish species of commercial interest, and proteomics has recently been shown to be suitable (Martinez and Friis, 2004). Piñeiro *et al*. (2003) gave a recent review of a wider range of applications of proteomics to marine products.

Fish species identification has mostly been performed by genetic (Weder *et al*., 2001) and immunological techniques (Céspedes *et al*., 1999) that are suitable for routine analysis of a large number of samples. In terms of simplicity and speed, antibody-based methods are most appropriate.

Applications of immunological assays for the detection and quantification of proteins in meat and milk products have been well documented, as described above. In contrast, work related to fish species identification is scarce, partly because of the variety of fish species that are commercialized (Mackie *et al*., 1999). On the other

hand, the discrimination of fish species becomes a problem when the usual identifying characteristics are removed on processing and only a portion of flesh is available (Tepedino *et al*., 2001). IA systems are not generally of value for cooked flesh products, as the antibodies are normally raised against undenatured proteins. For all these reasons, only a limited number of immunoassays have been developed and none is available for wide-scale commercial use (Dooley *et al*., 2005). The use of ELISA assays is therefore an interesting approach to the development of rapid methods for assessing the authenticity of fish products. In this area, a very active research group has been working for years on the development of different strategies (Asensio *et al*., 2002) using both P_{Abs} and M_{Abs}.

An indirect ELISA has been developed by Fernández *et al*. (2002) for the identification of fishery products such as red snapper, salmon, trout and various clam species. The assay was performed using P_{Abs} against clam solution proteins in two different formats: microtiter plates and immunostick tubes. Using this format, an indirect ELISA for the specific identification of grouper (*Epinephelus guaza*), wreck fish (*Polyprion americanus*) and Nile perch (*Lates niloticus*) fillets using P_{Abs} has been developed by Asensio *et al*. (2003a). The simplicity of the immunostick colorimetric ELISA and the short time required for analysis (less than 1 hour) make it suitable for screening purposes without the need for auxiliary equipment.

In other work (Asensio *et al*., 2003b), a M_{Ab} that is specific to grouper (*Epinephelus marginatus*) and thus enables the discrimination of this species from wreck fish (*Polyprion americanus*) and other less valuable fish sold in the marketplace has been developed. As a complementary approach, this antibody has been used in two indirect ELISA formats (microtiter plates and immunostick tubes) for the rapid authentication of grouper and wreck fish (*Polyprion americanus*). The M_{Ab} was tested against native and thermally-treated (cooked and sterilized) soluble muscle protein extracts from several commonly marketed fish, and only reacted with the grouper and wreckfish species (Asensio *et al*., 2003c).

More recently, a PCR-ELISA technique was developed for the semiquantitative detection of Nile perch (*Lates niloticus*) in experimentally sterilized fish muscle mixtures (Asensio *et al*., 2004).

Feedstuffs

Bovine spongiform encephalopathy (BSE), commonly referred to as "mad cow disease", has had a significant impact on the livestock industry. Because BSE is spread through animal feed, the main strategy for preventing the establishment and spread of the disease is to prohibit the use of proteins derived from mammalian tissue in feed for ruminant animals. Enforcement of these regulations relies on the ability to identify the presence of forbidden proteins in the feed. Accurate analytical methods for detecting prohibited material in feedstuffs are needed to ensure compliance with the new regulations. PCR-based methods are specific and sensitive, but generally are not able to distinguish between different tissues of the same species. As reported above, immunological methods have played a central role in the species identification of raw and heat-processed meats. However, most immunoassays for meat speciation are

not applicable to feed detection because of the denaturation of protein antigens by the high-temperature rendering process. The official enzyme immunoassay method for analyzing mammalian proteins of rendered animal material in the UK utilizes antisera raised against heat-stable proteins (Ansfield *et al*., 2000). This method, which detects most mammalian proteins without discriminating between prohibited and allowed proteins, requires the complement of microscopic analysis to confirm the presence of mammalian meat and bone meal. Issues relating to current methodology as well as other potentially useful analytical methods of testing for animal material in food have been reviewed (Momcilovic and Rasooly, 2000; von Holst *et al*., 2006).

Chen *et al*. (2002) developed several MAbs against TnI for the detection and differentiation of rendered muscle tissue in animal feed. The indirect ELISAs developed employing these M_{Abs} specifically detect muscle TnI without cross-reaction to gelatin, blood/serum proteins and milk proteins, and the entire analysis, including sample extraction, can be performed in less than 6 hours. The sensitivity (LOD between 0.3 and 2%) and specificity of these assays make it possible to detect low amounts of muscle tissue in feed samples without any concentration procedure. The M_{Abs} has been used by two companies (Neogen Co. and ELISA Technologies Inc.) to design rapid test kits.

Subsequently, the same researchers (Chen *et al*., 2004) developed a new sensitive ELISA to detect prohibited bovine and ovine muscles in feedstuffs. The ELISA was applied for quantitative determination of heat-treated bovine and ovine meat meals in different feeds, in the presence of non-prohibited species (porcine, chicken or turkey meat). Extractable bovine and ovine TnI was determined with detection limits of 5.0 and 4.0 ng ml^{-1}, respectively, when the matching feed matrices were used in the calibration curves.

The immunoassay developed by Kim *et al*. (2005) could differentiate bovine MBM from other species of MBM and ingredients used for commercial animal feeds, and detect down to a level of 0.05% MBM mixed in animal feed.

Recently, rapid feed-testing methods that could be used by regulators to verify compliance during routine inspections have become available. The development of a sensitive test for ruminant (e.g. cow, sheep, goat, deer and elk) materials is complicated by the lack of a suitable ruminant-specific marker that is present in the sample in a high enough concentration.

Given the apparent need for rapid screening tests, Muldoon *et al*. (2004) described the development of a rapid, immunochromatographic strip test that can detect 0.1% MBM in animal feed. The test takes 15 min to perform, and large numbers of samples can be screened for PAPs (processed animal proteins) in animal feeds simultaneously. The strip contains a second test that can detect 1% mammalian-specific MBM in feed. The assay was validated using 150 negative control feed samples in a spike-recovery study.

In a separate intercomparison study, the rapid test strip was evaluated in conjunction with microscopy (Gizzi *et al*., 2003), PCR and other immunoassay methods for the determination of PAPs and mammalian MBM and their differentiation from other PAPs in feed (DG SANCO, 2003). The test was sensitive, specific and accurate for the analysis of total PAPs and mammalian-specific MBM at detection limits of 0.1%

(w/w) and 0.5% (w/w), respectively. It was also shown that poultry meal and fish meal did not interfere with the mammalian-specific test.

Finally, a single-step lateral flow immunochromatographic ruminant assay (Reveal for Ruminant in MBM) has become commercially available (Quinchum and Hsieh, 2007). This test kit is specifically designed for the surveillance of bovine spongiform encephalopathy (BSE) epidemics, and is based on the detection of ruminant skeletal muscle protein, troponin (Tn), which is recognized by specific monoclonal antibodies (Klein *et al*., 2003). In a validation study (Klein *et al*., 2005), this test was found to be specific to ruminant muscle protein without any cross-reactivity with many feed ingredients, and capable of detecting as little as 1% ruminant tissue in animal feed products. In another evaluation study (Myers *et al*., 2005), this test demonstrated 100% selectivity (0% false-positive results) with a detection limit of 2% bovine MBM in dairy feed.

Miscellaneous

Unlike for speciation in meat or milk, where the number of ELISA developments for authenticity testing is very high, in other foods (such as fruit juices, honey, oils, etc.) these developments are scarce, and so far other analytical techniques are generally used (Ebeler *et al*., 2007).

Fruit juices

Fruit juices and nectars are an important and fast-growing sector of the food industry. Primary objectives in beverage and juice quality control are to ensure the authenticity of the juice products and to be able to detect adulteration.

Basic adulteration can be based on simple dilution with water, but the main authenticity issues are those that arise from substitution of the authentic named material with cheaper substitutes (Jezek and Suhaj, 2001). Furthermore, due to increasing information on the composition of fruits, more refined methods of adulteration are being used. Most of these are based on supplementation of juice with pulp and peel extracts, or with some cheaper fruit juice (Tzouros and Arvanitoyannis, 2001).

In this field, some immunochemical techniques are applied to recognize these adulterations and thus ensure appropriate labeling. Sass-Kiss and Sass (2000) identified tissue- and species-specific peptides 24 and 27 kDa in citrus fruits, to develop antibodies against these particular peptides from orange juice and peel and to test their suitability for quality control of commercial orange juice products using the Western blot technique (Gosling, 2000). The antibodies developed seem to be useful for determining the juice content in commercial citrus beverages, and for evaluating the peel contamination in them.

Tissue- and species-specific peptides of the grapefruit have been investigated by SDS-PAGE and Western blot (Sass-Kiss and Sass, 2002). P_{Abs} were developed against isolated peptides from the juice and one peptide from the peel. Two of the P_{Abs} were used for testing commercial grapefruit juice products. One of the commercial juice products declared as 100% grapefruit juice did not give a positive reaction with this antibody, whereas a pale but clearly visible band appeared in the peptide

sample of the 40% red-grapefruit juice nectar. The data confirm that addition of grapefruit by-products to grapefruit juice can be detected. Finally, the authenticity of orange fruit-based drinks has been discussed by Soukupová *et al*. (2003).

Honey

Authenticity immunochemical tests are mainly based on the detection of pollen proteins (Baroni *et al*., 2002). The development of a rapid, specific and sensitive ELISA is proposed by Baroni *et al*. (2004). Two proteins identified as characteristic of sunflower pollen were isolated and used as coating antigens in a competitive ELISA that allows both identification and quantification of sunflower pollen in honey when it is present at levels over 10%, with an adequate linear response between 10 and 90% of pollen (CV% ranged from 4 to 14%). Although the method is less sensitive than the standard technique (melissopalynology), it shows the advantage of simultaneously analyzing several samples in a short time.

Gum source

Gum arabic from *Acacia Senegal* is commonly used in foods and beverages as a stabilizer, emulsifier and thickener. Adulteration of gum arabic with other *Acacia* and non-*Acacia* gums is a potential problem.

Immunoassays have the potential to be used for speciation and adulteration of gums. Several M_{Abs} have been raised against *Acacia* gums with varying degrees of specificity (Pickles *et al*., 2004), and different ELISAs have been developed that are able to quantify gums in samples of gum arabic or food (Ireland *et al*., 2004a). An IC-ELISA method using M_{Abs} was developed (Ireland *et al*., 2004b) to detect adulteration of *A. senegal* gum with *A. seyal* (0.6% w/w) or *C. erythrophyllum* (0.2% w/w). The limit of detection was around $5\,\mu g\,ml^{-1}$, and intra- and inter-assay CV (%) values for each ELISA were typically $<10\%$.

Irradiated foods

Irradiation technology has mainly been used in foods for enhancing its hygienic quality, reducing spoilage and extending shelf-life. Food irradiation has been recognized and regulated as an effective technology in many countries (Molins, 2001). The framework Directive 1999/2/CE, concerning irradiated food, states that the words "irradiated" or "treated with ionizing radiation" must appear on the label or packaging. Additionally, Directive 1999/3/CE contains an initial European Community list of foods and food ingredients authorized for irradiation treatment, and sets a maximum overall average absorbed radiation dose of 10 kGy for this purpose – for example, for grains and nuts doses <1 kGy can be used for disinfestations. On the basis on this information, the development of reliable and rapid methods for detection of irradiated food is desirable.

During the past decade a number of analytical methods have been investigated for the detection of radiation treatment of foods, including DNA comet assay and ELISA (Khan *et al*., 2005). The DNA comet assay offers great potential as a rapid tool to detect whether a wide variety of foodstuffs have been irradiated. Nevertheless,

ELISA methods have been demonstrated to be as rapid and simpler, and can be carried out using low-cost instrumentation. When food is treated, DNA thymidines are transformed into dihydrothymidines (DiHT); Deeble *et al*. (1994) obtained antibodies against these modified bases and successfully quantified these changes by ELISA in the range of 40 Gy. More recently, Tyreman *et al*. (2004) developed a fast, competitive ELISA test to identify DiHT, and detected treated prawn species with a working range of 0.5–2 kGy (CV $<$10%).

Fats and oils

Food authenticity has become a focal point attracting the attention of producers, consumers and policy-makers. Although in most cases adulteration of fats and oils does not suppose a threat to public health, the fundamental rights of consumers can be violated by fraudulent malpractice.

A range of analytical methods to detect fraud in these matrices has been developed, especially RMN, Raman or isotopic techniques. The technical merits of different analytical platforms, including immunoassay, to establish the authenticity of oils and fats was reviewed by Ulberth and Buchgraber (2000). Furthermore, the FSA (2003) has encouraged the development of molecular markers for the detection of olive-oil adulteration.

On the other hand, the last European chocolate Directive 2000/36/EC allows the addition of up to 5% of a number of vegetable fats other than cocoa butter (CB) – the so-called "cocoa butter equivalents" (CBEs) – to chocolate. Unfortunately, the Directive does not cover aspects regarding methods of analysis for law enforcement. The first step accomplished by the Joint Research Center (JRC) was a critical reappraisal of potentially promising analytical methods aimed at the identification and quantification of the addition of CBEs to chocolate. Different approaches to quantify this adulteration have been outlined by Buchgraber *et al*. (2003).

Genetically modified foods

The traceability and labeling (T&L) proposal (European Council, 2003) provides the definition of traceability for genetically modified (GM) foods, and methods for its implementation. Both T&L genetically modified organisms are current issues that are considered in trade and regulation, and are gaining worldwide interest due to the ever-increasing global diffusion and the related socio-economical implications (Jensen and Sandoe, 2002).

An important aspect in GM food analysis is quantitation, since the maximum limits of GMO (genetically modified organisms) in food are the basis for labeling in the EU. Although efforts have been taken to harmonize the analytical methodology at national, regional and international levels, no normative international standards have been established yet. Lack of coherence between analytical methodologies and their applicability, and legislation, is a major problem.

A discussion including the definition of units of measurements, expression of GM material quantities, terminology and inconsistent legal status of products derived from related but slightly different transformation routes is provided by Holst-Jensen *et al*.

(2006). Current methodologies for the analysis of GMOs are focused on one of two targets – the transgenic DNA inserted, or the novel protein(s) expressed – in a GM product. A review of current state-of-the-art techniques, current needs and limitations in the area of GMO detection is given by Miraglia *et al*. (2004) and Hernandez *et al*. (2005).

For most protein-based methods, ELISAs are widely employed, and a large number of articles have been published describing the detection, identification and quantification of transgenic materials in bulk grain samples (Lipton *et al*., 2000; Lih-Ching *et al*., 2001; Anklam *et al*., 2002; Stave, 2002). However, the heat lability of proteins is the main obstacle to general application of these methods, although the use of antibodies directed against heat-denaturized meat proteins was an interesting development.

A combination of sensitivity, specificity and cost-effectiveness in terms of analytical performance is allied to a diverse array of assay formats suitable for laboratory and field use. The efficiency of screening formats should be examined with respect to false-positive rates, disappearance of marker genes, increased use of specific regulator sequences and the increasing number of GM foods. Recently, the European Commission included two significant changes in its political agreement: a 0.9% threshold for the labeling of GM food and feed; and a 0.5% threshold instead of 1% for the presence of GM material in food or feed, or for processing (European Commission, 2004).

The following aspects should be considered before we review alternative applications of ELISA in detecting GM in foods:

- *Sampling*. The reliability and costs of the two steps of the control methodologies (sampling and testing) play a crucial role in the traceability of GMOs. Kay and Paoletti (2002) published an overview of the sampling strategies for the screening of large grain shipments, of primary ingredients, and of specific (GM) ingredients in final food products. One of the priorities of the recently installed ENGL (European Network of GMO Laboratories) is to identify and develop appropriate sampling strategies to support EU legislation (ENGL, 2003; EC-JRC, 2003a, 2003b).
- *Reference materials*. Emphasis is placed (Frewer *et al*., 2004) on the quality assurance of the analytical data represented by the adequate availability of suitable Certified Reference Materials (CRM) for different applications, and the need for harmonized guidelines for validation studies. Standard reference materials are required for method development, to translate test results in terms of % GMO, and to ensure uniform test performance throughout the EU. The evaluation of a *Roundup Ready* Soy Bean Certified Reference Material and the strategies for successful implementation of testing are discussed by Stave (1999).
- *Immunoassay validation.* Optimization and validation assays for ELISA are important aspects for standardizing this technology for GMO detection. Assay validation for food analysis is complex, considering the large diversity of food matrices. Factors regarding optimization and validation are given by Lipp *et al*. (2000).

The validation of the first international method according to ISO 5725 (for a specific protein-targeting immunological method) for the detection of a genetically modified plant variety was carried out by the Joint Research Centre (SDI, 2003).

The validated method had been designed as a sandwich ELISA with M_{Abs} against the protein CP4 EPSPS (Lipp *et al*., 2000).

Today's marketed GM-crop plants frequently possess novel genes that are transcriptionally regulated by different promoters. For instance, Event 176 (GM-maize) has been transformed with two synthetic *Cry1Ab* genes. *Cry1Ab* production was quantified by ELISA in leaves, pollen, roots and kernels among three genotypes. It was found that gene expression in kernels was below levels of quantification (Agbios, 2003). Consequently, an immunoassay directed against *Cry1Ab* of Event 176 for commodity testing of kernels might be of limited use (Miraglia *et al*., 2004).

Recently, a commercial ELISA kit (EnviroLogix Inc., 2003) recommended for detecting and quantifying the CryIAb/CryIAc proteins in corn- and cotton-leaf tissue, single-seed and bulk grain samples was applied by Margarit *et al*. (2006) to detect CryIA(b) protein present in the transgenic Bt maize in different foods obtained from the market. No CryIA(b) protein was detected in highly-processed food. The highest amount of CryIA(b) protein found was less than 0.1 mg l^{-1}. The integrity of CryIA(b) protein determined by Western blot using a polyclonal immuno-purified antibody suggests that this protein is highly degraded under the harsh conditions during food processing, as indicated by Terry *et al*. (2002).

In addition, some companies (Neogen Co., Strategic Diagnostics Inc. and Eurofins, for example) have developed rapid immunochemical screening tests for the detection of GMO in foods (see Table 13.5). These test kits are best used for raw agricultural or slightly processed products, as they have limitations when used in highly processed foods.

Semi-quantitative immunoassays come in a wide variety of formats. Particularly popular are dipstick procedures, often based on lateral flow devices that are economical, amenable to point-of-sale application and suitable as an initial screening method, giving results in 5–10 minutes. Different test kits based on this format have been developed commercially to detect CryI(Ab) in corn plants, seeds and grain, in addition to CP4 EPSPS protein in soybean, canola, cotton and sugar beet (Lipton *et al*., 2000). A study of the field performance of a kit that employs lateral flow immunotechnology to detect soybeans GM resistant to the herbicide glyphosate is made by Fagan *et al*. (2001). The kit is useful in screening large quantities of soybeans that contain high levels of GM material, but is not effective in monitoring for GM material at levels of 1.0% or lower. Statistical analyses performed in order to assess the error indicated that the primary contributors were limitations in operator performance, rather than defects in test kit materials, while sample size may play a secondary role.

On the other hand, since existing immunological methods for GMO quantification measure only one analyte, taxon-related quantitations cannot be carried out. These methods can therefore only be applied to food samples consisting entirely of one taxon. However, although commercially available lateral flow strips are currently limited to a few biotechnology-derived protein-producing GM products, strips that can simultaneously detect multiple proteins are being developed.

Besides lateral flow devices, other immunoassay formats using magnetic particles as the solid support surface (Brett *et al*., 1999) or antibody-coated ELISA format tube (Ahmed, 2002) are also available for GMO detection.

Table 13.5 Characteristics of some commercially available ELISA formats for the detection of genetically modified organisms (GMOs) in foods

Matrix	Application	Analyte class	Trade name	Format	Detection limit	Company
Rice	Bulk grain	PAT/bar protein expressed in LibertyLink rice (Evet LL601 and/or Event LL62)	QuickStix™ Kit for LibertyLink® rice	Lateral flow membrane strips	1.33% Event LL601 rice or 0.02% Event rice	*Envirologix*
Soybean	Bulk grain	CP4 EPSPS protein at levels typically expressed in genetically modified bulk soybean	QuickStix™ Kit for *Roundup Ready*® soybeans	Lateral flow membrane strips	1 soybean in 1000, 0.1%	*Envirologix*
Soybean	Ground grain and flour	CP4 EPSPS enzyme coded for by the *Roundup Ready* gene in soybeans and soy flour	QuantiPlate™ Kit for *Roundup Ready* soybeans and soy flour	Microwell plate	0.02% *Roundup Ready* Soy	*Envirologix*
Soybean and soy products	Toasted meals, tofu, concentrates, DF & FF flour, soy milk	CP4 EPSPS protein (*Roundup Ready*) in genetically enhanced soybeans and soy products	GMO Soya RUR TM ELISA Test Kit	Microtiter plate	0.1% GMO	*Strategic Diagnostics Inc.*
Soybeans	Various food fractions	CP4 EPSPS protein expressed by *Roundup Ready*	GMO RUR Soya Test Kit	Sandwich ELISA microtiter plate	0.1% GMO	*Strategic Diagnostics Inc.*
Corn	Ground corn, corn flour, corn meal	Cry1Ab protein	GMO Bt Maize Test Kit	Microtiter well	0.15% Cry1Ab	*Strategic Diagnostics Inc.*
Corn	Ground corn, corn flour, corn meal	Cry9C protein	GMO Bt9 Maize Test Kit	Microtiter well	0.0075% Cry9C	*Strategic Diagnostics Inc.*
Corn	Bulk grain	Cry1Ab/Bt11, Cry9C, Event 603, Cry3Bb, Cry1F, T25-PAT/pat, and/or Cry34 proteins at levels typically expressed in GM corn grain	QuantiComb™ Kit for Bulk Grain	Lateral flow membrane strips	Varies by analyte, from 0.01% (1 kernel in a pool of 1000) to 1% (1 kernel in a pool of 100)	*Envirologix*
Corn	Bulk corn, grain, meal, flour	Crystalline Cry1Ab protein expressed by genetically modified plants and derived from *Bacillus thuringiensis*	QuickStix™ Kit for Cry1 Ab Bulk Grain	Lateral flow membrane strips	1% (1 positive kernel in 100)	*Envirologix*

Corn	Corn-leaf and -seed tissue, soy-leaf tissue	CP4 EPSPS protein at the levels typically expressed in GM soy leaf, corn leaf or corn single-seed tissue	QuantiStix™ Kit for *Roundup Ready* Plant Tissue	Lateral flow membrane strips	Presence or absence of CP4 EPSPS protein	*Envirologix*
Corn	Corn-leaf tissue	Cry1Ab and Cry3Bb, proteins at levels typically expressed in genetically modified corn leaf	QuickStix Combo Kit YieldGard®	Lateral flow membrane strips	Presence or absence in leaf tissue	*Envirologix*
Corn	Plant tissue, seeds, bulk grain	Crystalline Cry1Ab and Cry1Ac proteins expressed by genetically modified plants and derived from *Bacillus thuringiensis*	QualiPlate™ Kit for Cry1Ab/Cry1Ac	Antibody-coated microwell plate (solid plate)	Presence or absence	*Envirologix*
Corn	Corn-leaf tissue, seeds, ground grain-cotton leaf and seed	CP4 EPSPS enzyme coded for the Roundup Ready gene in Corn Event 603 and Cotton	QuantiPlate™ Kit for Roundup Ready Corn Event 603 and cotton	Antibody-coated microwell plate (solid plate)	0.1% Event 603 corn-leaf and -seed: 100% positive or 100% negative	*Envirologix*
Canola	Canola leaf and seed tissue	CP4 EPSPS protein at the levels typically expressed in GM canola leaf or seed	QuickiStix™ Kit for *Roundup Ready* Canola Leaf & Seed	Lateral flow membrane strips	Presence or absence of CP4 EPSPS protein	*Envirologix*
Sugar beets	Sugarbeet seeds	CP4 EPSPS protein at the levels typically expressed in GM sugar beet seed	QuickiStix™ Kit for *Roundup Ready* Bulk Sugar Beet Seed	Lateral flow membrane strips	0.1% (1 *Roundup Ready* seed in 999 conventional seeds)	*Envirologix*
Alfalfa	Alfalfa bulk seed, leaf tissue, and alfalfa hay (cored & ground samples)	CP4 EPSPS protein at the levels typically expressed in *Roundup Ready* alfalfa	QuickiStix™ Kit for *Roundup Ready* Alfalfa	Lateral flow membrane strips	1 alfalfa seed in a total of 600 for bulk seed, approximately 5% in hay (depends level of the plant), presence or absence in leaf testing	*Envirologix*

Advances are also being made in combining antibody methods with instrumental techniques. For example, in addition to the hyphenated methods, such as immunoassay-mass spectrometry, considerable advances are now being made in real-time observations of antibody binding to target molecules. The developed new methodologies include the use of microarrays and biosensors (López *et al*., 2003).

Since the frequency of events is continuously increasing, this will greatly increase difficulties in testing and, in turn, traceability. In this respect, it is foreseen that the testing methods will have to evolve towards a multi-event system in order to control any GMO-related traceability system. The work of Miraglia *et al*. (2004) deals with new diagnostic methodologies, such as the microarray-based methods that allow for the simultaneous identification of the increasing number of GMOs on the global market in a single sample (some of these techniques have also been discussed for the detection of unintended effects of genetic modification by Cellini *et al*., 2004).

Alternative ELISA developments

In this section, some uses of alternative immuno-based methods to tackle the authentication detection problem are summarized.

Currently, enzyme-linked immunosorbent assay (ELISA) performed in a microtiter plate is the most common technique used for immunoassay. However, with the demand for multiplexing capability, shorter analysis time, smaller sample volume and higher sensitivity, other techniques are being explored to perform immunoassays.

Some approaches pursued in miniaturized high-throughput screening systems are the development of microplates with a larger number of wells (from 96 to 384, 1536 and finally to 3456) and the design of microfabricated devices capable of performing continuous flow assays. This trend is associated with the development of robotics and high-performance liquid-handling devices that can rapidly add volumes down to several microliters or nanoliters per well, taking into account the low total-assay volumes.

For immunoassays, many researchers have pointed out several advantages of microfluidics over other techniques performed on a microtiter plate. The fabrication materials and techniques available for microfluidics, the advantages of these devices for immunoassays and the incorporation of microbeads to improve their function have been reviewed by Lim and Zhang (2007).

Dip-sticks and biosensors are alternative techniques that are also based on antigen–antibody interaction. These rapid tests, and the better-known lateral flow devices, are the subject of much academic research (Krska *et al*., 2004) and as reported above, commercial products are also available.

In the dipstick format, either antigen (indirect competitive format) or antibody (sandwich format) are immobilized on membranes. One to three successive working steps require an overall time of 30 minutes to 3 hours, and give semi-quantitative results. The one-step test strips used in the lateral flow device enable yes/no results within 5–10 minutes. The availability of rapid validated tests for determination of specific proteins would considerably improve food labeling and consumer safety.

Regarding these screening methods, there is very little available in terms of recommended validation procedures. AOAC International has a method-validation program designed specifically for test-kit methods. Performance-tested certified kits are evaluated for accuracy, precision, limits of detection, false-positive or false-negative rates, ruggedness, cross-reactivity, stability, lot-to-lot consistency and matrix effects, and are compared with an existing method. As indicated by Eurofins Scientific Group (Eurofins Scientific, http://www.eurofins.com), although the limits of detection (LODs) for the ELISA tests have been validated with a precision that has never been reached before on a large variety of matrices, the performance of a method, and especially its sensitivity, can vary according to the product. It is therefore recommended that the limit of detection is first established for the matrix concerned. Recently, a validation procedure for screening methods has been published by González *et al*. (2007).

In addition, immunoanalysis can be incorporated into sensor systems that can be automated for on-line, high-throughput analysis. Immunosensor systems based on the use of enzymes as labels could follow the same basic principles as enzyme immunoassays. The sensor systems differ from "conventional" immunoassays in the degree of automation, the detection principle, the solid phase to which the Ab is bound, and the reusability of the bio-recognition layer.

Horseradish peroxidase (HRP), alkaline phosphatase (AP) and urease have been used as labels with absorciometric, luminometric and electrochemical detection. The sensor system protocol is similar to the corresponding microtiter plate assay-antibody immobilization, the addition of sample, the addition of enzyme tracer (both solutions may be premixed and applied simultaneously), the washing of the sensor, the addition and incubation of the enzyme substrates, and detection. Adding labels to immunosensors often leads to improved sensitivity and a lower detection limit. However, the application of these enzyme-tracer based immunosensors for determining high-molecular weight proteins in foods has been scarce.

Immunosensor systems show some distinct advantages over conventional immunoassays because they offer reduced analysis times for single samples, which is particularly important for on-site or on-line analysis, and they can be automated, which reduces experimental error and speeds analysis. However, automated devices appear to be rather bulky as long as conventional tubing, pumps and valves are used. Thus, microtechnology could significantly contribute to simpler devices.

The transfer of immunoassays onto microchips has already been described, and they prove valuable for food analysis, and especially for contaminants. However, there are areas of food chemistry (i.e. authenticity) that have not as yet benefited from these sensors. The application of affinity sensors to food analysis is not fully exploited, and more collaboration between analytical chemists and food chemists is needed. A review of different types of immunosensors, their applications, and examples of commercially available biosensor instruments are addressed by Patel (2002).

Multianalyte dipstick tests were a first step for miniaturization and cost savings, but most of them lack automation. A recent strategy for miniaturization is the use of microarrays produced with spotting devices, enabling the immobilization of proteins in the lower nanoliters range at defined positions on a surface. The potential of protein-sensing assay formats (including enzyme tracer-based assay), their automation,

and the development of microarray formats are reviewed by Bilitewski (2006). Finally, the main advantages and disadvantages of ELISA test kits and biochip array biosensors have been compiled by Toldrá and Reig (2006).

To summarize, the new and future trends in the development of protein immunoassays as tools for food authentication include, among others: immunosensors (Sankaran *et al*., 2007), optical-fiber sensors and neural-networks microfluidic immunoassays (Lim and Zhang, 2007), microarrays (Bilitewski, 2006; Harwanegg and Hiller, 2006), and nano-material-based devices and nanobiosensors (Chau *et al*., 2007).

Conclusions

In the new immunoanalytical developments for food authentication, consideration should be given to the selection of the antigen bound by the antibody, the accuracy, validation and matrix effects. Good practice guides, recognized or normalized methods, collaborative studies, reference materials and accreditation of analysis by independent organizations are very useful tools to give more reliable results.

As an analytical tool, immunochemical technology is robust, rapid, inexpensive, reliable and easy to use. However, the rate-limiting steps in immunoassay development and application are the need for widespread availability of appropriate antibodies and standards, the difficulties of producing antibodies to particular sequences from a protein, and the inability to generate on demand antibodies capable of reacting normally at extreme pH or with high concentrations of salt or solvent. These are areas where the application of recombinant antibody technology should bring considerable benefits as it becomes possible to more easily select antibodies with rare properties and to manipulate the properties of antibodies already available.

The use of immunological methods for the detection of adulteration in foods has resulted in the development of sensitive, reliable assays capable of detecting low levels of significant variations in these matrices. The use of monoclonal antibodies, careful selection of target antigen, and suitable ELISA format has greatly increased the food analyst's ability to distinguish between species in foods.

The main developments in the future can be expected to focus not only on enhancement of existing analytical methods, but also on sample preparation steps. Finally, more effort is still needed for the validation of new analytical methods. The validation process, as well as the development and assessment of new reference materials via collaborative trials, will continue to be an important issue in the authenticity of food products.

Assessment of authenticity of food and food products will be a difficult task, and in most cases will require the measurement of several markers. Furthermore, fraudulent practices tend to be quite innovative, and manufacturers are well aware of the weaknesses in food inspection systems. Therefore, within the food quality framework, the development of new methods will be needed with the involvement of immunosensors, chips-microarrays and other novel bioanalytical tools.

References

Agazzi, M.E., Barrero-Moreno, J., Lücker, E. *et al*. (2002). Performance comparison of two analytical methods for the detection of tissues of the central nervous system in sausages: results of an interlaboratory study. *European Food Research and Technology*, **215**, 334–339.

Agbios (2003). *GM Database*. Merrickville: Agbios. Available from http://www.agbios.com/dbase.php?

Ahmed, F.E. (2002). Detection of genetically modified organisms in foods. *Trends in Biotechnology*, **20**(5), 215–223.

Anklam, E., Gadani, F., Heinze, P. *et al*. (2002). Analytical methods for detection and determination of genetically modified organism in agricultural crops and plant derived food products. *European Food Research and Technology*, **214**, 3–26.

Ansfield, M., Reaney, S.D. and Jackman, R. (2000). Production of a sensitive immunoassay for detection of ruminant and porcine proteins, heated to >130°C at 2.7 bar, in compound animal feedstuffs. *Food and Agricultural Immunology*, **12**, 273–284.

Asensio, L., Gonzalez, I., Fernández, A. *et al*. (2002). Application of random amplified polymorphic DNA (RAPD) analysis for identification of grouper (*Epinephelus guaza*), wreck fish (*Polyprion americanus*) and Nile perch (*Lates niloticus*) fillets. *Journal of Food Protection*, **65**(2), 432–435.

Asensio, L., Gonzalez, I., Rodriguez, M.A. *et al*. (2003a). Identification of grouper (Epinephelus guaza), wreck fish (Polyprion americanus), and Nile perch (Lates niloticus) fillets by polyclonal antibody-based enzyme-linked immunosorbent assay. *Journal of Agricultural Food Chemistry*, **51**(5), 1169–1172.

Asensio, L., Gonzalez, I., Rodriguez, M.A. *et al*. (2003b). Development of a monoclonal antibody for grouper (*Epinephelus marginatus*) and wreck fish (*Polyprion americanus*) identification using an indirect enzyme-linked immunosorbent assay. *Journal of Food Science*, **66**, 886–889.

Asensio, L., Gonzalez, I., Rodriguez, M.A. *et al*. (2003c). Development of a monoclonal antibody for grouper (*Epinephelus marginatus*) and wreck fish (*Polyprion americanus*). Authentication using an indirect ELISA. *Journal of Food Science*, **68**(6), 1900–1903.

Asensio, L., Gonzalez, I. and Rodriguez, M.A. *et al*. (2004). PCR-ELISA for the semiquantitative detection of Nile perch (*Lates niloticus*) in sterilized fish muscle mixtures. *Journal of Agricultural Food Chemistry*, **52**(14), 4419–4422.

Ayaz, Y., Ayaz, N.D. and Erol, I. (2006). Detection of species in meat and meat products using enzyme-linked immunosorbent assay. *Journal of Muscle Foods*, **17**, 214–220.

Baroni, M.V., Chiabrando, G.A., Costa, C. and Wunderlin, D.A. (2002). Assessment of the floral origin of honey by SDS-page immunoblot techniques. *Journal of Agricultural Food Chemistry*, **50**, 1362–1367.

Baroni, M.V., Chiabrabdo, G.A., Costa, C. *et al*. (2004). Development of a competitive ELISA for the evaluation of sunflower pollen in honey samples. *Journal of Agricultural and Food Chemistry*, **52**, 7222–7226.

Baud, M. (1993). Data analysis, mathematical modelling. In: R.F. Masseyeff, W.H. Albert and N.A. Staines (eds), *Methods of Immunological Analysis*, Vol. 1: *Fundamentals*. New York, NY: VCH Publishers, Inc, pp. 656–671.

Berrini, A., Tepedino, V., Borromeo, V. and Secchi, C. (2006). Identification of freshwater fish commercially labeled "perch" by isoelectric focusing and two-dimensional electrophoresis. *Food Chemistry*, **96**, 163–168.

Bilitewski, U. (2006). Protein-sensing assay formats and devices. *Analytica Chimica Acta*, **68**, 232–247.

Bonwick, G.A. and Smith, C.J. (2004). Immunoassays: their history, development and current place in food science and technology. *International Journal of Food Science and Technology*, **39**, 817–827.

Brandon, D.L. and Frieman, M. (2002). Immunoassays to soy proteins. *Journal of Agriculture and Food Chemistry*, **50**, 6635–6642.

Brett, G.M., Chambers, S.J., Huang, L. and Morgan, M.R.A. (1999). Design and development of immunoassays for detection of proteins. *Food Control*, **10**, 401–406.

Buchgraber, M., Ulberth, F., Anklam, E. and Geel, B. (2003). The new EU chocolate directive – a cascaded approach to provide methods for the detection of fraud and to quantify adulteration. In: J. Lojza, T. Cajka, V. Kocourek and J. Hajslovà (eds), *1st International Symposium on Recent Advances in Food Analysis*. Prague: Institute of Chemical Technology, p. 36.

Bülte, M., Horlacher, S. and Simon, P. (2001). *Validation of "RIDASCREEN risk material" test as detection method for central nervous tissue in raw and heated meat products compared to the integrated detection method on the basis of Western blot (INV)*. Giessen, Germany: Institute of Veterinary Food Science, Justus Liebig University.

Butler, J.E. (1996). Solid phases in immunoassay. In: E.O. Diamandis and T.K. Christopoulos (eds), *Immunoassay*. San Diego, CA: Academic Press, pp. 205–225.

Cellini, F., Chesson, A., Colquhoun, I. *et al*. (2004). Unintended effects and their detection in genetically modified crops. *Food and Chemical Toxixology*, **42**, 1089–1125.

Céspedes, A., García, T., Carrera, E. *et al*. (1999). Indirect enzyme-linked immunosorbent assay for the identification of sole (*Solea solea*), European plaice (*Pleuronectes platessa*), flounder (*Platichthys flesus*), and Greenland halibut (*Reinhardtius hippoglossoides*). *Journal of Food Protection*, **62**, 1178–1182.

Chapela, M.J., Sotelo, C.G., Calo-Mata, P. *et al*. (2002). Identification of cephalopod species (Ommastrephidae and Loliginidae) in seafood products by forensically informative nucleotide sequencing (FINS). *Journal of Food Science*, **67**(5), 1672–1676.

Chau, C.-F., Wu, S.-H. and Yen, G.-C. (2007). The development of regulations for food nanotechnology. *Trends in Food Science and Technology*, **18**, 269–280.

Chen, F.-C. and Hsieh, Y.-H.P. (2000). Detection of pork in heat-processed meat products by monoclonal antibody-based ELISA. *Journal of AOAC International*, **83**(1), 79–85.

Chen, F.-C. and Hsieh, Y.-H.P. (2001a). Separation and characterization of a porcine-specific thermostable muscle protein from cooked pork. *Journal of Food Science*, **66**(6), 799–803.

Chen, F.-C. and Hsieh, Y.-H.P. (2001b). Porcine troponin I: a thermostable species marker protein. *Meat Science*, **61**(1), 55–60.

Chen, F.-C., Hsieh, Y.-H.P. and Bridgman, R.C. (2002). Monoclonal antibodies against troponin I for the detection of rendered muscle tissues in animal feedstuffs. *Meat Science*, **62**, 405–412.

Chen, F.-C., Hsieh, Y.-H.P. and Bridgman, R.C. (2004). Monoclonal antibody-based enzyme-linked immunosorbent assay for sensitive detection of prohibited ruminant proteins in feedstuffs. *Journal of Food Protection*, **67**(3), 544–549.

Chen, F.-C., Hsieh, Y.-H.P., Bridgman, R.C. and Kilonzo-Nthenge, A. (2006). Kinetics of tropomyosin as a predictive model for verifying thermal processing of beef products. *Journal of Food Protection*, **69**(10), 2447–2453.

Commission Regulation (EC) (2005). Commission Regulation (EC) No. 260/2005 of 16 February 2005 amending Regulation (EC) No 999/2001 of the European Parliament and of the Council as regards rapid tests. *Official Journal*, **L46**. 17.02.2005.

Dabbs, D.J. (2006). *Diagnostic Immunohistochemistry*, 2nd edn. Amsterdam: Elsevier.

Deeble, D.J., Christiansen, J.F., Jones, M. *et al*. (1994). Detection of irradiated food based on DNA base changes. *Food Science and Technology Today*, **8**, 96–98.

de la Fuente, M.A. and Juárez, M. (2005). Authenticity assessment of dairy products. *Critical Reviews in Food Science and Nutrition*, **45**, 563–585.

DG SANCO (2003). Intercomparison study for the determination of processed animal proteins including meat and bone meal in animal feed [WWW document] (URL http://europa.eu.int/comm/food/food/biosafety/bse/bse50_en.pdf).

Dooley, J.J., Sage, H.D., Brown, H.M. and Garrett, S.D. (2005). Improved fish species identification by use of lab-on-a-chip technology. *Food Control*, **16**, 601–607.

Ebeler, S.E., Takeoka, G.R. and Winterhalter, P. (2007). *Authentication of Food and Wine*. New York, NY: American Chemical Society Publication Series No 952.

EC-JRC (2003a). *Sampling*. Joint Research Centre, European Commission, Ispra. Available from http://biotech.jrc.it/sampling.htm.

EC-JRC (2003b). *Database on Methods for Detection*, *Identification and Quantification of GMOs*. Food Products and Consumer Goods Unit. Institute for Health and Consumer Protection. Joint Research Centre, European Commission, Ispra. Available from http://139.191.1.19/GMO methods.htm.

ENGL (2003). *European Network of GMO Laboratories*. Institute for Health and Consumer Protection. Joint Research Centre, European Commission, Ispra. Available from http://engl.jrc.it/

EnviroLogix Inc. (2003). *CryIAb/c Plate Kit. EnviroLogix Inc. 500*. Riverside Industrial Parkway, Portland, Maine 0410301418, USA. Available from http://www.envirologix.com/library/

Etienne, M., Jérôme, M., Fleurence, J. *et al*. (2000). Identification of fish species after cooking by SDS-PAGE and urea-IEF: a collaborative study. *Journal of Agricultural Food Chemistry*, **48**(7), 2653–2658.

European Commission (2004). Commission Regulation (EC) No. 641/2004 of 6 April 2004 on detailed rules for the implementation of Regulation (EC). No. 1829/2003 of the European Parliament and of the Council as regards the application for the authorisation of new genetically modified food and feed, the notification of existing products and adventitious or technically unavoidable presence of genetically modified material which has benefited from a favourable risk evaluation. *Official Journal*, **L102**, 14–25.

European Council (2003). Common Position Adopted by the Council on 17 March 2003 with a View to the Adoption of a Regulation of the European Parliament and of the Council Concerning the Traceability and Labelling of Genetically Modified Organisms and the Traceability of Food and Feed Products Produced from Genetically Modified Organisms and Amending Directive 2001/18/EC. 15798/1/02 REV1. Brussels: European Council. Available from http://europa.eu.int/comm/food/fs/gmo/

Fagan, J., Schoel, B., Haegert, A. *et al*. (2001). Performance assessment under field conditions of a rapid immunological test for transgenic soybeans. *International Journal of Food Science and Technology*, **36**, 1–11.

Fernández, A., García, T., Asensio, L. *et al*. (2002). Identification of the clam species *Ruditapes decussates* (grooved carpet shell), *Venerupis romboides* (yellow carpet shell) and *Venerupis pullastra* (pullet carpet shell) by ELISA. *Food and Agricultural Immunology*, **14**(1), 65–71.

Frewer, L., Lassen, J., Kettlitz, B. *et al*. (2004). Societal aspects of genetically modified foods. *Food and Chemical Toxicology*, **42**, 1181–1193.

Fukal, L., Karamonova, L., Vítková, M. *et al*. (2002). Distinguishing raw, pasteurized, UHT-treated and bath-sterilized commercial milks by their interaction with immunoprobes against caseins and whey proteins. *Italian Journal of Food Science*, **14**(3), 207–215.

Giovannacci, I., Guizard, C., Carlier, M. *et al*. (2004). Species identification of meat products by ELISA. *International Journal of Food Science and Technology*, **39**, 863–867.

Gizzi, G., van Raamsdonk, L.W.D. and Baeten, V. (2003). An overview of tests for animal tissues in feeds applied in response to public health concerns regarding bovine spongiform encephalopathy. *Revue Scientifique et Technique*, **22**, 311–331.

Goldsby, R.A., Kindt, T.J., Osborne, B.A. and Kuby, J. (2003). Enzyme-linked immunosorbent assay. In: *Immunology*. New York, NY: Freeman and Company, pp. 148–150.

González, C., Prichard, E., Spinelli, S. *et al*. (2007). Validation procedure for existing and emerging screening methods. *Trends in Analytical Chemistry*, **26**(4), 315–322.

Gosling, J.P. (ed.) (2000). *Immunoassays: A Practical Approach*. Oxford: Oxford University Press.

Hagáis, M.-E., Barrero-Moreno, J., Lücker, E. *et al*. (2002). Performance comparison of two analytical methods for the detection of tissues of the central nervous system in sausages: results of an interlaboratory study. *European Food Research Technology*, **215**, 334–339.

Hall, J.C., O'Brien, G.M. and Webb, S.R. (1997). Phage-display technology for environmental analysis. In: D.S. Aga and E.M. Thurman (eds), *Immunochemical Technology for Environmental Applications*. Washington, DC: ACS Symposium series No. 657, p. 22.

Harlow, W. and Lane, D. (2007). *Using Antibodies. A Laboratory Manual*. Cold Spring Harbor, NY: CHS Press, pp. 495.

Harwanegg, Ch. and Hiller, R. (2006). Protein microarrays for the diagnosis of allergic diseases: state-of-the-art and future development. *Allergen Immunology*, **38**(7), 232–236.

Henderson, D.R., Friedman, S.B., Harris, J.B. *et al*. (1986). CEDIA, a new homogeneous immunoassay system. *Clinical Chemistry*, **32**, 1637–1641.

Hernandez, M., Rodríguez-Lázaro, D. and Ferrando, A. (2005). Current methodology for detection, identification and quantification of genetically modified organisms. *Current Analytical Chemistry*, **1**, 203–221.

Holst-Jensen, A., De Loose, M. and Van Den Eede, G. (2006). Coherence between legal requirements and approaches for detection of genetically modified organisms (GMOs) and their derived products. *Journal of Agriculture and Food Chemistry*, **54**, 2799–2809.

Hsieh, Y.-H.P. (2005). Meat species identification. In: Y.H. Yu (ed.), *Handbook of Food Science, Technology, and Engineering*, Vol. 1. Boca Raton, FL: CRC Press, pp. 1–19.

Hsieh, Y.-H.P., Zhang, S., Chen, F.-C. and Shen, S.C. (2002). Monoclonal antibody-based ELISA for assessment of the endpoint heating temperature of ground pork and beef. *Journal of Food Science*, **67**(3), 1149–1154.

Hu, C.B., Ding, H.C. and Chen, S. (2000). Rapid detection of bovine milk adulteration in caprine milk. *Taiwanese Journal of Agricultural Chemistry and Food Science*, **39**, 405–414.

Hudson, P.J. and Kortt, A.A. (1999). High avidity scFv multimers; diabodies and triabodies. *Journal of Immunological Methods*, **231**(1–2), 177–189.

Hurley, I.P., Ireland, H.E., Coleman, R.C. and Williams John, H.H. (2004a). Application of immunological methods for the detection of species adulteration in dairy products. *International Journal of Food Science and Technology*, **39**, 873–878.

Hurley, I.P., Coleman, R.C., Ireland, H.E. and Williams John, H.H. (2004b). Measurement of bovine IgG by indirect competitive ELISA as a means of detecting milk adulteration. *Journal of Dairy Science*, **87**(3), 543–549.

Hurley, I.P., Coleman, R.C., Ireland, H.E. and Williams John, H.H. (2006). Use of sandwich IgG ELISA for the detection and quantification of adulteration of milk and soft cheese. *International Dairy Journal*, **16**, 805–812.

Ireland, H.E., Haines, J., Bonwick, G.A. *et al*. (2004a). *Validation of ELISAs for the Detection and Quantification of Gums in Foodstuffs*. London: Food Standards Agency (FSA).

Ireland, H.E., Clutterbuck, A., Cloquet, J.-P. *et al*. (2004b). The development of immunoassays to identify and quantify species source of gum Arabic. *Journal of Agricultural Food Chemistry*, **52**, 7804–7808.

Jensen, K.K. and Sandoe, P. (2002). Food safety and ethics. The interplay between science and values. *Journal of Agricultural and Environmental Ethics*, **15**, 245–253.

Jezek, J. and Suhaj, M. (2001). Application of capillary isotachophoresis for fruit juice authentication. *Journal of Chromatography A*, **916**, 185–189.

Jha, V.K., Ashwani, K. and Usha, V.M. (2003). Indirect enzyme-linked immunosorbent assay in detection and differentiation of cooked and raw pork from meats and other species. *Journal of Food Science and Technology*, **40**(3), 254–256.

Kay, S. and Paoletti, C. (2002). *Sampling Strategies for GMO Detection and/or Quantification*. EUR 20239 EN. Joint Research Centre, European Commission, Ispra. Available from http://biotech.jrc.it/doc/

Khan, A.A., Khan, H.M. and Delincée, H. (2005). DNA Comet Assay – a rapid screening method for detection of irradiated cereals and tree nuts. *Food Control*, **16**, 141–146.

Kim, S.H., Huang, T.S., Seymour, T.A. *et al*. (2005). Development of immunoassay for detection of meat and bone meal in animal feed. *Journal Food Protection*, **68**, 1860–1865.

Klein, F.E., Pielack, D.W., Lupo, A.J. and Hsieh, Y.-H.P. (2003). The BSE firewall: an easy-to-use immunochromatographic device for the detection of ruminant proteins. Presentation for the 117th AOAC International Annual Meeting, September, Atlanta. Available from http://www.neogen.com/BSE_Presentation0903.htm (accessed 28 May 2006).

Klein, F., Lupo, T., Pielack, D. and Mozola, M. (2005). Validation study of a lateral-flow immunoassay for detection of ruminant by-product material in animal feeds and feed ingredients – performance-tested method (SM) 010405. *Journal of AOAC International*, **88**, 1583–1592.

Kohler, G. and Milstein, C. (1975). Continuous cultures of fused cells secreting antibody of predefined specificity. *Nature*, **256**, 495–497.

Koppelman, S.J., Lakemond, C.M.M., Vlooswijk, R. and Hefle, S.L. (2004). Detection of soy proteins in processed foods: Literature overview and new experimental work. *J. AOAC International*, **87**(6), 1398–1407.

Krska, R., Welzig, E. and Baumgartner, S. (2004). Immunoanalytical detection of allergenic proteins in food. *Analytical and Bioanalytical Chemistry*, **378**, 63–65.

Lees, M. (ed.) (2005). *Food Authenticity and Traceability*. Cambridge: Woodhead Publishing Ltd.

Lih-Ching, C., Yen-Ling, C., Jei-Hwa, Y. *et al*. (2001). Detection of four types of genetically modified maize by polymerase chain reaction and immuno-kit methods. *Journal of Food and Drug Analysis*, **9**, 50–57.

Lim, C.T. and Zhang, Y. (2007). Bead-based microfluidic immunoassays. *Biosensors and Bioelectronics*, **22**, 1197–1204.

Lipp, M., Anklam, E. and Stave, J. (2000). Validation of an immunoassay for detection and quantitation of a genetically modified soybean in feed and food fractions using reference materials: interlaboratory study. *Journal of AOAC International*, **83**, 919–927.

Lipton, C.R., Dautlick, J.X., Grothaus, G.D. *et al*. (2000). Guidelines for the validation and use of immunoassays for determining of introduced proteins in biotechnology enhanced crops and derived food ingredients. *Food Agricultural Immunology*, **12**, 153–164.

Liu, L., Chen, F.-C., Dorsey, J. and Hsieh, Y.-H.P. (2006). Sensitive monoclonal antibody-based sandwich ELISA for the detection of porcine skeletal muscle in meat and feed products. *Journal of Food Science*, **71**(1), M1–M6.

López, J.L., Marina, A., Alvarez, G. and Vazquez, J. (2002). Application of proteomics for fast identification of species-specific peptides from marine species. *Proteomics*, **2**, 1658–1665.

López, M., Mallorquín, P. and Vega, M. (2003). Tecnologías Moleculares de Trazabilidad Alimentaria. Informe de Vigilancia Tecnológica. Genoma España. Sector agroalimentario. Fundación española para el desarrollo de la investigación genómica y proteómica/Fundación general de la Universidad Autónoma de Madrid, pp. 78.

López-Calleja, I., González, E., Fajardo, V. *et al*. (2006a). Autentificación de especies animales en leche y productos lácteos I. (Técnicas basadas en el análisis de proteínas). *CTC Alimentación*, **28**, 55–67.

López-Calleja, I., González, E., Fajardo, V. *et al*. (2006b). Autentificación de especies animales en leche y productos lácteos II. (Técnicas basadas en el análisis de proteínas). *CTC Alimentación*, **28**, 73–79.

López-Calleja, I.M., González, I., Fajardo, V. *et al*. (2006c). Application of an indirect ELISA and a PCR technique for detection of cows' milk in sheep's and goats' milk cheeses. *International Dairy Journal*, **17**, 87–93.

López-Calleja, I.M., González, I., Fajardo, V. *et al*. (2007). Quantitative detection of goats' milk in sheep's milk by real-time PCR. *Food Control*, **18**, 1466–1473.

Lücker, E., Eigenbrodt, E., Wenisch, S. *et al*. (2000). Identification of central nervous system tissue in retail meat products. *Journal of Food Protection*, **63**, 258–263.

Macedo-Silva, A., Barbosa, S.F.C., Alkmin, M.G.A. *et al*. (2000). Hamburger meat identification by dot-ELISA. *Meat Science*, **56**, 189–192.

Macedo-Silva, A., Shimokomaki, M., Vaz, A.J. *et al*. (2001). Textured soy protein quantification in commercial hamburger. *Journal of Food Composition and Analysis*, **14**, 469–478.

Mackie, I.M., Pryde, S.E., Gonzales-Sotelo, C. *et al*. (1999). Challenges in the identification of species of canned fish. *Trends in Food Science and Technology*, **10**, 9–14.

Mackie, I., Craig, A., Etienne, M. *et al*. (2000). Species identification of smoked and gravad fish products by sodium dodecylsulphate polyacrylamide gel electrophoresis, urea isoelectric focusing and native isoelectric focusing: a collaborative study. *Food Chemistry*, **71**, 1–7.

Manso, M.A., Cattaneo, T.M., Barzaghi, S. *et al*. (2002). Detection of vegetable proteins in milk products by electrophoretic and immunochemical methods: in-house prevalidation tests and collaborative trials. *Bulletin of International Dairy Federation*, **371**, 25–34.

Margarit, E., Reggiardo, M.I., Vallejos, R.H. and Permingeat, H.R. (2006). Detection of BT transgenic maize in foodstuffs. *Food Research International*, **39**, 250–255.

Martinez, I. and Friis, T.J. (2004). Application of proteome analysis to seafood authentication. *Proteomics*, **4**, 347–354.

Martinez, I., Friis, T.J. and Seppola, M. (2001). Requirements for the application of protein sodium dodecyl sulfate–polyacrylamide gel electrophoresis and randomly amplified polymorphic DNA analyses to product speciation. *Electrophoresis*, **22**, 1526–1533.

Martinez, I., Aursand, M., Erikson, U. *et al*. (2003). Destructive and non-destructive analytical techniques for authentication and composition analyses of foodstuffs. *Trends in Food Science and Technology*, **14**, 489–498.

Mayer, H.K. (2005). Milk species identification in cheese varieties using electrophoretic, chromatographic and PCR techniques. *International Dairy Journal*, **15**, 595–604.

Miraglia, M., Berdal, K.G., Brera, C. *et al*. (2004). Detection and traceability of genetically modified organisms in the food production chain. *Food and Chemical Toxicology*, **42**, 1157–1180.

Moatsou, G. and Anifantakis, E. (2003). Recent developments in antibody-based analytical methods for the differentiation of milk from different species. *International Journal of Dairy Technology*, **56**, 133–138.

Molins, R.A. (ed.) (2001). *Food Irradiation: Principles and Applications*. New York, NY: Wiley.

Momcilovic, D. and Rasooly, A. (2000). Detection and analysis of animal materials in food and feed. *Journal of Food Protection*, **63**(11), 1602–1609.

Muldoon, M.T., Onisk, D.V., Brown, M.C. and Stave, J.W. (2004). Targets and methods for the detection of processed animal proteins in animal feedstuffs. *International Journal of Food Science and Technology*, **39**, 851–861.

Myers, M.J., Yancy, H.F., Farrell, D.E. *et al*. (2005). Evaluation of two commercial lateral-flow test kits for detection of animal proteins in animal feed. *Journal of Food Protection*, **68**, 2656–2664.

Pastor-Navarro, N., Gallego-Iglesias, E., Maquieira, A. and Puchades, R. (2007). Development of a group-specific immunoassay for sulfonamides. Application to bee honey analysis. *Talanta*, **71**, 923–933.

Patel, P.D. (2002). (Bio)sensor for measurement of analytes implicated in food safety: a review. *Trends in Analytical Chemistry*, **21**(2), 96–115.

Pickles, N.A., Ireland, H.E., Al-Assaf, S. and Williams, J.H.H. (2004). Applications of immunoassays in hydrocolloid research. In: P.A. Williams, D. Wedlock and G.O. Phillips (eds), *Gums and Stabilisers for the Food Industry: Designing Structure into Foods*. London: Royal Society of Chemistry, pp. 317–327.

Piñeiro, C., Vazquez, J., Marina, A.I. *et al*. (2001). Characterization and partial sequencing of species-specific sarcoplasmic polypeptides from commercial hake species by mass spectrometry following two-dimensional electrophoresis. *Electrophoresis*, **22**, 1545–1552.

Piñeiro, C., Barros-Velazquez, J., Vazquez, J. *et al*. (2003). Proteomics as a tool for the investigation of seafood and other marine products. *Journal of Proteome Research*, **2**, 127–135.

Quinchum, R. and Hsieh, Y.-H.P. (2007). Evaluation of a commercial lateral flow test for rapid detection of beef and sheep content in raw and cooked meats. *Meat Science*, **76**(3), 489–494.

R-Biopharm (2001). *Instruction Manual for RIDASCREEN® Risk Material Test*. Darmstadt: R-Biopharm.

Recio, I., García-Risco, M.R., Amigo, L. *et al*. (2004). Detection of milk mixtures in Halloumi Cheese. *Journal of Dairy Science*, **87**, 1595–1600.

Reid, L.M., O'Donnell, C.P. and Downey, G. (2006). Recent technological advances for the determination of food authenticity. *Trends in Food Science and Technology*, **12**, 344–353.

Rencova, E., Necidova, L. and Svoboda, L. (2000). Identification by ELISA of poultry, horse, kangaroo, and rat muscle specific proteins in heat processed products. *Veterinarni Medicina*, **45**(12), 353–356.

Rozenfeld, P., Docena, G.H., Añón, M.C. and Fossati, C.A. (2002). Detection and identification of a soy protein component that cross-reacts with caseins from cow's milk. *Clinical & Experimental Immunology*, **130**, 49–58.

Sanchez, L., Perez, M.D., Puyol, P. *et al*. (2002). Determination of vegetal proteins in milk powder by enzyme-linked immunosorbent assay: interlaboratory study. *Journal of AOAC International*, **85**(6), 1390–1397.

Sankaran, D.R., Gobi, K.V. and Miura, N. (2007). Recent advancements in surface plasmon resonance immunosensor for detection of small molecules of biomedical, food and environmental interest. *Sensors and Actuators B*, **121**, 158–177.

Sass-Kiss, A. and Sass, M. (2000). Immunoanalytical method for quality control of orange juice products. *Journal of Agricultural Food Chemistry*, **48**, 4027–4031.

Sass-Kiss, A. and Sass, M. (2002). Distribution of various peptides in citrus fruits (grapefruit, lemon, and orange). *Journal of Agricultural Food Chemistry*, **50**, 2117–2120.

Schebo Biotech AG (2001). *Instruction Manual for the Brainostic™ Test*. Giessen: Schebo Biotech.

Schmidt, G.R., Yemm, R.S., Childs, K.D. *et al*. (2001). The detection of central nervous system on beef carcasses and in comminuted beef. *Journal of Food Protection*, **64**(12), 2047–2052.

SDI (2003). *GMO Food Ingredient Testing, Soya Kit User's Guide*, Rev. 031703, Ver. 2.1. Newark, NJ: Strategic Diagnostics. Available from http://www.sdix.com/PDF/Products/7100000.User%20Guide%20for%20Soya%20Grain%20Kit%20v2.1.pdf.

Senocq, D., Dupont, D., Rolet-Répécaud, O. and Levieux, D. (2001). Monoclonal antibodies against bovine β-casein: production and epitope characterization. *Food and Agricultural Immunology*, **13**, 213–224.

Soukupová, V., Krátká, J., Cizková, H. *et al*. (2003). Authenticity of orange fruit drinks in the Czech market. In: J. Lojza, T. Cajka, V. Kocourek and J. Hajslovà (eds), *1st International Symposium on Recent Advances in Food Analysis*. Prague: Institute of Chemical Technology, p. 93.

Stave, J.W. (1999). Detection of new or modified proteins in novel foods derived from GMO-future needs. *Food Control*, **10**, 367–374.

Stave, J.W. (2002). Protein immunoassay methods for detection of biotech crops: applications, limitations, and practical considerations. *Journal of AOAC International*, **85**(3), 780–791.

Tepedino, V., Berrini, A., Borromeo, V. *et al*. (2001). Identification of commercial fish species belonging to the orders pleuronectiformes and gadiformes: library of isoelectric focusing patterns. *Journal of AOAC International*, **84**(5), 1600–1607.

Tepnel Biosystems Limited (2001). *(Cooked) Species Identification Test Kit for the Qualitative Determination of Species Content in Meats/Meat Products by Enzyme Immunoassay, Technical Instructions*. Deeside: Tepnel Biosystems Ltd.

Terry, C.F., Harris, N. and Parkes, H.C. (2002). Detection of genetically modified crops and their derivatives: critical steps in sample preparation and extraction. *Journal of AOAC International*, **85**(3), 768–774.

Toldrá, F. and Reig, M. (2006). Methods for rapid detection of chemical and veterinary drug residues in animal foods. *Trends in Food Science and Technology*, **17**, 482–489.

Tyreman, A.L., Bonwick, G.A., Smith, C.J. *et al*. (2004). Detection of irradiated food by immunoassay – development and optimization of an ELISA for dihydrothymidine in irradiated prawns. *International Journal of Food Science and Technology*, **39**, 533–540.

Tzouros, N.E. and Arvanitoyannis, I.S. (2001). Agricultural products: synopsis of employed quality control methods for the authentication of foods and application of chemometrics for the classification of foods according to their variety or geographical origin. *Critical Reviews in Food Science and Nutrition*, **41**, 287–319.

Ulberth, F. and Buchgraber, M. (2000). Authenticity of fats and oils. *European Journal of Lipid Science and Technology*, **102**, 687–694.

Vítková, M., Rauch, P. and Fukal, L. (2002). Optimisation of indirect competitive ELISA of α-, β-, and .vkappa.-caseins for the recognition of thermal and proteolytic treatment of milk and milk products. *Czech Journal of Food Science*, **20**(2), 53–62.

von Holst, C., Boix, A., Baeten, V. *et al*. (2006). Determination of processed animal proteins in feed: the performance characteristics of classical microscopy and immunoassay methods. *Food Additives and Contaminants*, **23**, 252–264.

Weder, J.K.P., Rehbein, H. and Kaiser, K.P. (2001). On the specificity of tuna-directed primers in PCR-SSCP analysis of fish and meat. *European Food Research Technology*, **213**, 139–144.

Weyandt, R.G. (2001). Detection of BSE-risk materials. *Fresenius Journal of Analytical Chemistry*, **371**, 574–575.

Woolfe, M., McQuillan, M. and Burns, J. (2004). *Review of The Food Standards Agency's Research Programme on Food Authenticity and Labelling (Q01 And Q02). Final Report (July)*. London: Food Standards Agency.

Wu, A.H.B. (2006). A selected history and future of immunoassay development and applications in clinical chemistry. *Clinical Chimica Acta*, **369**, 119–124.

Wu, F.Y., Tsao, P.H., Lin, S. *et al*. (2000). Production of monoclonal antibody against cows' milk protein. *Journal of Chinese Society of Animal Science*, **29**, 337–343.

Yalow, R.S. and Berson, S.A. (1959). Assay of plasma insulin in human subjects by immunological methods. *Nature*, **184**, 1648–1649. Reference is supplied. Please change the year in the text for 1959.

Yesilbag, K. and Kalkan, A. (2005). Detection of central nervous system tissues as BSE specified risk material in meat products in Turkey. *Food Control*, **16**, 11–13.

14

Electrophoretic Technique: Capillary Zone Electrophoresis

Alejandro Cifuentes and Virginia García-Cañas

Introduction

During the last decade, regulatory agencies from several countries have been issuing food regulations that are every day becoming more and more demanding regarding the authenticity of foods. Apart from the evident reasons related to food safety and quality (including health concerns caused by, for example, allergies to proteins not declared on the label), other motivations are behind the need of these new regulations, including economic and religious issues.

Common adulteration practices include the fraudulent substitution of more expensive animal and plant species with cheaper ones, the addition of non-animal proteins to meat products, and the presence of protected or non-authorized organisms (species, genetically modified varieties) in foods, etc. A good example of the multiple food authenticity issues that can nowadays be addressed is provided in Table 14.1.

Although these are issues relevant to both the food industry and regulatory agencies, food authenticity (including identification of animals or plants species, geographical origin, processing, etc.) is a difficult task. For this reason, the verification of food authenticity has to be faced by developing selective and sensitive methods

Modern Techniques for Food Authentication
ISBN: 978-0-12-374085-4

Table 14.1 Examples of food authenticity issues (modified from Kvasnicka, 2005)

Commodity	Issue
Beverages	Single malt whisky replaced with blended one Inappropriate sugar addition to increase alcohol content in wine Incorrect declaration of vintage or geographical origin of wine
Cereals	Foods labeled as "gluten-free" containing gluten Undeclared replacement of durum wheat with common wheat (pasta) Basmati rice replaced with non-Basmati rice Incorrect declaration of geographical and cultivar origin of premium long-grain rice
Fruit and vegetable	Undeclared water and/or sugar addition to fruit juice Undeclared acid addition to fruit juice Undeclared pulpwash or peel-extract addition into fruit juice Incorrect declaration of fruit type
Herbs and spices	Adulteration with water to increase weights of spices or herbs Incorrect botanical declaration of herbs or spices Intentional addition of low-value materials to spices or herbs
Meat and fish	Incorrect declaration of species Undeclared addition of offal Undeclared use of mechanically recovered meat Labeling previously frozen meat (or fish) as fresh Undeclared use of plant additives to meat products
Milk and dairy products	Distinction between cheese made of cows', sheep's, buffalo and/or goats' milk Undeclared addition of water to milk Substitution of cheese analog Distinction between cheese made from raw and heat-treated milk
Oils and fats	Undeclared addition of other vegetable oils to single-seed oils Undeclared addition of poorer quality oils to extra-virgin olive oil Hazelnut oil addition to olive oil Butter adulterated with hydrogenated oil and animal fats Addition of non-cocoa fats to chocolate
Others	Incorrect declaration of floral or geographical origin of honey Undeclared sugar addition to honey Undeclared addition of substitutes such as maltodextrins in coffee Arabica × Robusta Addition of meat species in processed vegetarian foods Undeclared use of genetically modified organisms in food

able to find a compound (or group of compounds) that can be used as marker of a given species, geographical origin, method of food processing, etc. (Sotelo and Pérez-Martín, 2003). Therefore, faster, more powerful, cleaner and cheaper analytical procedures are required by food chemists, regulatory agencies and quality control laboratories to meet these demands. As a consequence, there is a growing interest in the development of innovative analytical procedures, which meet all the aforementioned requirements, for ensuring the authenticity of the food supply.

Among the different analytical techniques that can be employed to analyze foods and food compounds, the use of *capillary electrophoresis* (CE) has emerged as a good alternative due to the multiple analytical advantages that this technique

Table 14.2 Reviews on capillary electromigration methods in food analysis and related areas published in the period 2003–2006

Subject	Reference
General review of CE in food analysis	Cifuentes (2006)
Organic contaminants in food by CE	Juan-García *et al*. (2005)
CE in food authenticity	Kvasnicka (2005)
CE for the analysis of meat authenticity	Vallejo-Cordoba *et al*. (2005)
CE in routine food analysis	Castañeda *et al*. (2005)
Analysis of natural antioxidants by capillary electromigration methods	Herrero *et al*. (2005)
Capillary electrophoresis-mass spectrometry in food analysis	Simó *et al*. (2005a)
Analysis of low molecular weight carbohydrates in foods and beverages	Martínez-Montero *et al*. (2004)
Analysis of pesticides in foods by CE	Hernández-Borges *et al*. (2004)
Detection of genetically modified organisms in foods	García-Cañas *et al*. (2004a)
Combined use of molecular techniques and CE in food analysis	García-Cañas *et al*. (2004b)
Chiral electromigration methods in food analysis	Simó *et al*. (2003)
Analysis of beer components by CE methods	Cortacero-Ramírez *et al*. (2003)
Determination of urea pesticide residues in vegetable and water samples	Berrada *et al*. (2003)
CE for short-chain organic acids and inorganic anions	Galli *et al*. (2003)
Analysis of antibiotics by CE	Flurer (2003)
Amino acid analysis by CE	Poinsot *et al*. (2003)
Food additives and micronutrients	Blake (2004)
General review on CE in food analysis	Frazier and Papadopoulou (2003)

provides. Thus, CE offers high analysis speed, high separation efficiencies, great variety of applications, reduced sample and solvents consumption, and automatization. These characteristics have contributed to the increasingly growing number of applications of CE in food science and technology (Cifuentes, 2006) since its development in the 1980s (Jorgenson and Lukacs, 1983).

A wide array of molecules, including small ions, amino acids, carbohydrates, organic acids, vitamins, lipids, flavonoids, additives, contaminants, peptides, proteins and DNA fragments, have been analyzed using CE in different food matrices (Cifuentes, 2006). As an example of the great interest that the use of CE in food analysis has brought about, Table 14.2 shows some useful reviews published in the period 2003–2006 on this topic; interested readers are directed to these reviews.

In the following sections, a description of the basic instrumentation, operating principles and modes of CE is provided. Next, a revision of the main applications of this analytical technique in food science and technology is given, with special focus on its relevance for food authentication. This chapter concludes with a critical discussion about the main advantages and disadvantages of CE and some future outlooks of this relatively new technique in the food analysis domain.

Equipment and instrumentation used in CE

A scheme of the basic instrumentation required in CE equipment is shown in Figure 14.1. The separation of the analytes is performed inside the capillary, which is usually made of fused silica. The capillary dimensions range from 25 to 100 μm inner

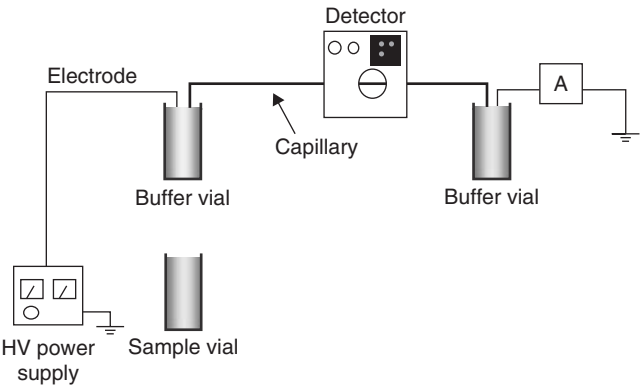

Figure 14.1 Basic capillary electrophoresis instrumentation.

diameter and from 25 to 100 cm in length. These silica capillaries are fragile, so they are coated externally with polyimide to add flexibility and resistance.

The buffer-filled capillary is placed between two vials usually filled with the same buffer. During the injection, the inlet buffer is substituted by a vial containing the sample. A small volume of sample (nanoliters) is introduced into the capillary by pressure, vacuum, or applying a difference of voltage (electromigration). Once the injection is complete, the vial containing the sample is changed for the vial with the separation buffer. After that, an electric field is applied to start the separation. In CE equipment, the high-voltage power supplies employed usually provide voltages ranging from 0 to 30 kV. The analytes are separated based on their different electrophoretic mobility under the influence of the electrical field, moving to the detection point as pure bands. The capillary needs to be thermostatized, to dissipate the heat generated by the Joule effect and to maintain a constant temperature from one analysis to another, assuring reproducibility.

A small section of the outer polyimide coating is removed near the outlet end of the capillary to form the detection window; thus the detection is done on-column (i.e. in the same capillary). This type of continuous detection has permitted the automation of this technique, and has eliminated dead volumes by avoiding any connection that increases separation efficiency. Besides, the technique allows quantitative analysis. On the other hand, the narrow optical path-length of these detection windows (25–100 μm) and the low injection volumes (nanoliters) provide poor detection limits, making it difficult for the application of CE for the analysis of traces.

Fused silica presents physicochemical characteristics compatible with UV-Vis detection, as it is almost transparent to the radiation in this part of the spectrum. Therefore, the detector most frequently used is the UV-Vis, followed by *laser induced fluorescence* (LIF) detectors and mass spectrometers. However, other detection systems such as those based on amperometry, conductivity and light-emitting diodes are growing in popularity.

Theory and principles of CE

The capillary inner wall contains silanol groups that become ionized, gaining negative charge in contact with the separation buffer (as shown in Figure 14.2). The degree of

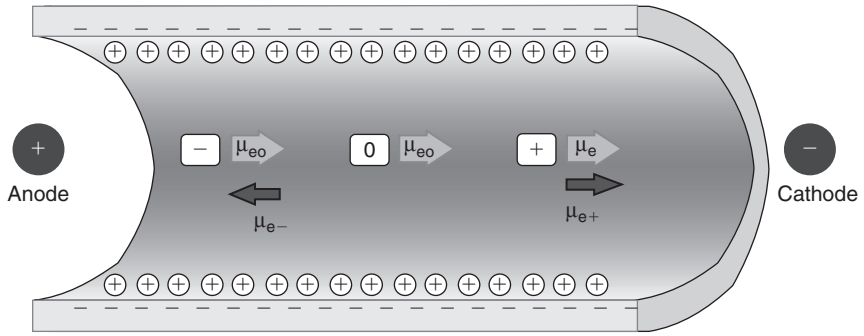

Figure 14.2 Electrophoretic separation by FSCE of three types of substances: with positive electric charge (+), negative electric charge (−) and neutral substances (0).

ionization is basically controlled by the separation buffer pH (negative charges appear in aqueous solutions with pH over 3–4). The wall, negatively charged, attracts the cations from the buffer, creating an electrical double layer. This double layer has two zones; a *fixed* zone next to the capillary wall, where the interactions between the negatively charged silanol groups and the positive ions of the buffer are so strong that they compensate for the thermal agitation, and a *diffuse* zone, further away from the wall.

Under the influence of the electric field, the positive charges of the diffuse zone move to the cathode and drag with them the associated solvation water. The result is a global movement of the buffer inside the capillary towards the cathode; this is defined by the *electro-osmotic mobility*, μ_{eo}:

$$\mu_{eo} = \frac{\varepsilon\zeta}{\eta}$$

where ε is the buffer dielectric constant, η is the buffer viscosity, and ζ (zeta potential) can be approximately defined as the potential generated between the negative charge excess at the capillary surface and the positive charge excess at the double layer. This last factor will determine, among other parameters, the electro-osmotic flow magnitude. This electro-osmotic flow will move all the substances in the interior of the capillary at the same speed because this is a system property – that is to say, it will not introduce selectivity, and therefore it will not permit the separation of the substances. One of the most important characteristics of this electro-osmotic flow is that the flow profile is nearly flat inside the capillary and it provides high separation efficiency compared to the typical parabolic profile of a fluid moving under hydrodynamic forces, as in HPLC.

Moreover, under an electric field, the charged substances undergo an additional *electromigration* process inside the capillary, in which each charged analyte tends to move to its opposite pole. Thus, ions experience two opposite forces; one due to the electric field (electro-osmosis plus/minus electromigration) and the other due to the friction. Using Stokes approximation, where the particle is considered as a rigid sphere, the friction force (F_r) for a substance in any media is given by the equation $F_r = 6\pi\eta r_p v_e$, where r_p is the particle radii, η the media viscosity and v_e the particle velocity.

On the other hand, the charged particle in an electric field undergoes an electric force, $F_e = qE$, where q is the charge of the particle under the electric field E. The electric field is the result of dividing the applied voltage by the total capillary length.

Both forces become equal, $F_r = F_e$, thus the particle takes a linear uniform movement where the velocity has the following expression:

$$v_e = \frac{q}{6\pi\eta r_p} E$$

The *electrophoretic mobility*, μ_e, is defined as being equal to:

$$\mu_e = \frac{q}{6\pi\eta r_p}$$

The electrophoretic mobility is the parameter that controls the selectivity of the separation system through the relation q/r_p in the form of *free solution capillary electrophoresis* (FSCE), which is the most common mode of CE. As will be seen below, there can be other parameters that, depending on the mode of CE used, can control this selectivity – for example, the hydrophobicity, the isoelectric point, etc. The relation q/r_p is directly related to the ratio charge/volume of the substances. That is to say, for a group of substances with the same amount of electrical charge, the substances with a greater molecular size will have a lower q/r_p relation and their electrophoretic mobility μ_e will be minor, so it will be possible to separate them from those substances of a smaller size and therefore higher electrophoretic mobility.

In a fused silica capillary, generally both electrophoretic and electro-osmotic migration are simultaneous and can be added or substracted, depending on the electric charge of the substances, as shown in Figure 14.2. Frequently the electro-osmotic mobility due to the capillary wall is higher than the electrophoretic mobility of the analytes. Thus, the final velocity that the substances are going to adopt inside the capillary will be decided by the addition or subtraction (according to whether they go in the same or in the opposite direction) of these factors:

$$v = (\mu_{eo} \pm \mu_e)E$$

The specific *migration time* of a charged substance will then be given by the expression

$$t_m = \frac{l}{(\mu_{eo} \pm \mu_e)E}$$

where l is the capillary length from the injection to the detection point.

Modes of CE

There are different modes of CE, mainly based on both the nature of the separation media introduced in the capillary, and the characteristics of the analytes to be separated. Interestingly, the instrumentation is practically the same for all of them. Although some other modes, including *capillary isotachophoresis* (Pospichal *et al*., 1989), have been

described for CE (Venema *et al*., 1998; Erny and Cifuentes, 2006), they are currently rarely used in the authentication of food. In the following sections, a short description of the main existing and more frequently used CE modes in this area is provided.

Free solution capillary electrophoresis (FSCE)

Free solution capillary electrophoresis (*FCSE*) is the most frequently used CE mode today (Jorgenson and Lukacs, 1983). The capillary is filled with a plain buffer solution, allowing the simultaneous separation of positively and negatively charged substances when the magnitudes of the electrophoretic and electro-osmotic mobilities are suitable. Following these criteria, compounds with higher positive charge density and smaller radius will migrate first.

FSCE presents several limitations (although frequently some of them can be overcome by using other different CE modes) that can be summarized as follows: (i) generally, separation of uncharged species or analytes with the same charge to mass ratio (like, for example, DNA fragments or protein-sodium dodecylsulfate complexes) cannot be accomplished by using FSCE; (ii) compounds bearing a high positive electrical charge density can be adsorbed onto the capillary wall (this adsorption will influence negatively the separation process); (iii) coefficients of variation for peak areas are in the range from 2 to 5% in real sample analysis; and (iv) the sensitivity of the technique does not permit trace analysis. It is interesting to note that points (iii) and (iv) are common to all the CE modes.

Micellar electrokinetic chromatography (MEKC)

This CE mode was initially developed to solve the limitation related to the separation of non-charged compounds (Terabe *et al*., 1984), although it can also be applied to the separation of charged substances.

Micellar electrokinetic chromatography involves the addition to the separation buffer of a surfactant at a concentration level at which micelles are formed. These micelles constitute a stable second phase, which in chromatographic terms acts as a pseudo-stationary phase that moves into the capillary. Usually sodium dodecyl sulfate micelles are used in MEKC, bearing negative charge, and therefore they migrate to the anode. Neutral analytes will interact with the micelles depending on their specific partition coefficient. Figure 14.3 shows the separation of three neutral substances with different affinity for the micelles, namely a compound T that irreversibly interacts with the micelles, a compound P with a medium interaction, and a compound N that does not interact with the micelles. Thus, the migration time of compound T (t_m) that interacts irreversibly with the micelles will be the same as that of the micelles. It will depend upon the electro-osmotic flow and the electrophoretic mobility of the micelles (μ_{eo} and μ_{em}). The compound P partially interacts with the micelles, and its migration time (t_p) will depend as much upon the electrophoretic and electro-osmotic mobilities as upon the compound partition coefficient between the aqueous buffer and the micelles. Compound N does not interact with the micelles. As it has no charge, the only driving force to the detector will be the electro-osmotic flow. Therefore, it

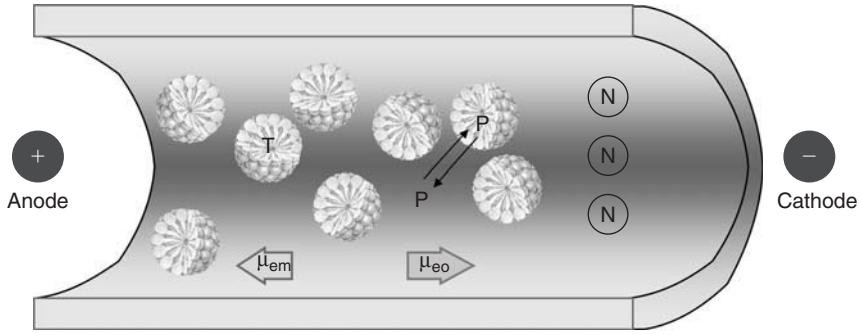

Figure 14.3 Electrophoretic separation by MEKC of three neutral compounds (T, P and N) with different hydrophobicities.

has a migration time (t_o) corresponding to the electro-osmotic mobility (which can be considered similar to the dead volume in HPLC). The difference between t_m and t_o is the so-called *separation window*. The compounds to be separated will have migration times within this window, and this fact limits the separation power of MEKC. In summary, the mechanism of separation depends on differences in distribution coefficients of the analytes between the aqueous and the micellar pseudo-stationary phases.

Capillary gel electrophoresis (CGE)

In *capillary gel electrophoresis*, the capillary is filled with a buffer solution containing a gel that will act as a molecular sieve. The most important application of this technique is the separation of compounds with the same charge/mass ratio, but with different molecular mass (Cohen and Karger, 1987) – for example, DNA fragments, polysaccharides, SDS-protein complexes or ionic polymers. In CGE, the molecules with smaller molecular size are able to pass through the pores of the molecular sieve formed inside the capillary and migrate first, whereas larger molecules are delayed by the gel and migrate later.

The first gels to be used in the latter 1980s were made from cross-linked polyacrylamide covalently linked to the capillary wall. However, they had many problems related to low reproducibility, resistance and stability. Nowadays, they have been substituted by the polymeric networks. These are hydrophilic non-cross-linked polymers that are dissolved in the buffer solution in a concentration usually higher than the so-called *entanglement concentration*, over which a net is formed that acts as a molecular sieve (although, according to Barron *et al*. (1993), it is not necessary to reach that concentration to obtain the effect of a molecular sieve). Some of the more frequently used polymers are linear polyacrylamide, polyethyleneglycol, polyethylenoxide, polyvinylalcohol, hydroxiethylcellulose, methylcellulose, etc.

Capillary isoelectrofocusing (CIEF)

Capillary isoelectrofocusing (*CIEF*) has mostly been applied to the separation of peptides and proteins, as shown in the pioneer work published by Hjertén and Zhu

(1985). Usually, a mixture of *ampholytes* with different pH values is introduced into the capillary together with the sample (the peptides and proteins to be separated). When an electric field is applied, a pH gradient inside the capillary is first established due to the ampholytes, which are distributed from the anode (with low pHs) to the cathode (with high pH values). Peptides or proteins with positive or negative charge, under the influence of the electric field, move through the capillary to the anode or cathode until they reach the zone of the capillary in which the pH of the buffer is the same as their *isoelectric point* – that is to say, they achieve a pH value in which the number of their positive and negative charges is the same. At this pH value analyte migration stops, as its global electrical charge will be zero. When all the compounds have achieved their isoelectric point within the capillary, elution is generally performed by applying a low-pressure (keeping the run-voltage on) in the anodic end, moving the focused bands towards the detection point. The capillaries used in this mode usually have an internal coating that decreases or eliminates the electro-osmotic flow, because that flow would in most cases prevent the formation of the pH gradient.

Capillary electrochromatography (CEC)

Capillary electrochromatography (*CEC*) has great similarity to liquid chromatography. In CEC, the capillary is filled with silica particles (3–10 μm in diameter and either derivatized or not) that act as a stationary phase. The buffer acts as a mobile phase that moves when an electric field is applied. Its velocity is proportional to the electro-osmotic flow (i.e., $\nu_{eo} = \mu_{eo}E$). Neutral compounds are carried by the electro-osmotic flow and they interact specifically with the stationary phase (in the same way as in HPLC) that originates their separation.

As with MEKC, the CEC mode was mainly developed to separate non-charged compounds in CE (Knox and Grant, 1987). This technique is currently under development, with the short life of the packed capillaries being one of its main limitations. These capillaries, apart from being time consuming to prepare and/or expensive, frequently cause the formation of bubbles in the interior as a result of the application of the electric field. This makes the capillaries useless for further applications. Moreover, the potential CEC in real-life samples has still to be proved.

Application of CE to food authentication

Analytical strategies such as the use of biomarkers or the use of profiling fingerprints are known to offer the potential for rapid food characterization and identification purposes. In this regard, CE can be a helpful analytical tool based on its mentioned properties of high speed, elevated efficiency and wide number of applications, making CE a technique capable of delineating subtle compositional differences among different species, geographical origins, food processes, etc. A variety of CE methods has been developed for ensuring the authenticity of foods (Kvasnicka, 2005). Below, relevant and representative CE approaches applied to the analysis of DNA, proteins and other food constituents in order to solve different food authenticity problems are discussed.

DNA analysis

Food authenticity testing by means of DNA analysis relies on the detection of one or more relatively rare features of the organism's genome at a certain taxonomic level, which depends on the degree of specificity required for identification. Hence, techniques that allow the rapid amplification of specific DNA sequences, particularly in polymerase chain reaction (PCR), have been fundamental in this field. A shortcoming of DNA amplification-based methods accounts for the necessity for sensitively detecting the presence of the target sequence (amplicon) after amplification. This final step has traditionally been performed *by agarose gel electrophoresis* (*AGE*). Apart from the insufficient resolution and sensitivity of AGE, the use of carcinogenic substances and the need to visualize the amplicons have made it not too user-unfriendly for adequate diagnostic testing. To overcome such limitations, a good solution is the combination of CGE methods with PCR-based methods to successfully amplify and detect DNA sequences with high sensitivity and specificity in an automatic mode (García-Cañas *et al*., 2004b). Examples of the application of PCR-based plus CGE techniques in authenticity analysis of raw materials and food products are discussed below.

The benefits of using PCR in combination with CGE to detect *genetically modified organisms* (*GMOs*) in foods were first reported by García-Cañas *et al*. (2002a). The developed CGE method allowed reproducible separations of DNA fragments ranging from 80 to 500 bp in 20 minutes, using commercially available polymers together with bare fused silica capillaries. The method combined a routine of washing the capillary with 0.1-M hydrochloride acid followed by a rinsing step with a dissolution containing 1% polyvinyl alcohol; after that, the capillary was filled with a running buffer containing 2-hydroxyethyl cellulose (HEC). Two amplification reactions were performed separately in parallel to obtain an amplicon of the transgene present in transgenic maize Bt 176, and an amplicon of a gene naturally present in maize. The analysis of the PCR products demonstrated that the sensitivity of the procedure was enough to detect 1% of transgenic maize in maize flour; however, the peak obtained for the amplified DNA was too close to the detection limit. In this regard, the sensitivity of the method could be greatly enhanced with further modifications which included the use of a LIF detector together with the addition of intercalating dyes to the running buffer (García-Cañas *et al*., 2002b). From the comparison of four fluorescent intercalating dyes, it was shown that the use of YOPRO-1 provided optimum conditions in terms of sensitivity (i.e. LOD was 1000 zmol, calculated for a 200-bp DNA fragment), efficiency (up to 2.4×10^6 plates·m^{-1}), speed of analysis, reproducibility and cost per run. The CGE-LIF procedure using YOPRO-1 as the intercalating dye provided ultrasensitive detection of genetically-modified maize DNA and allowed the detection of 0.01% of transgenic maize in flour by direct injection of the PCR amplified sample (García-Cañas *et al*., 2002c).

In addition to the aforementioned methods, CGE has also demonstrated great potential when combined with other PCR amplification-based techniques, such as quantitative competitive PCR (QC-PCR) and multiplex PCR, for quantitation of Bt 176 transgenic maize in food (García-Cañas *et al*., 2004c) and simultaneous detection of five transgenic maize lines (Bt11, Bt176, MON810, GA21 and T25) in a single

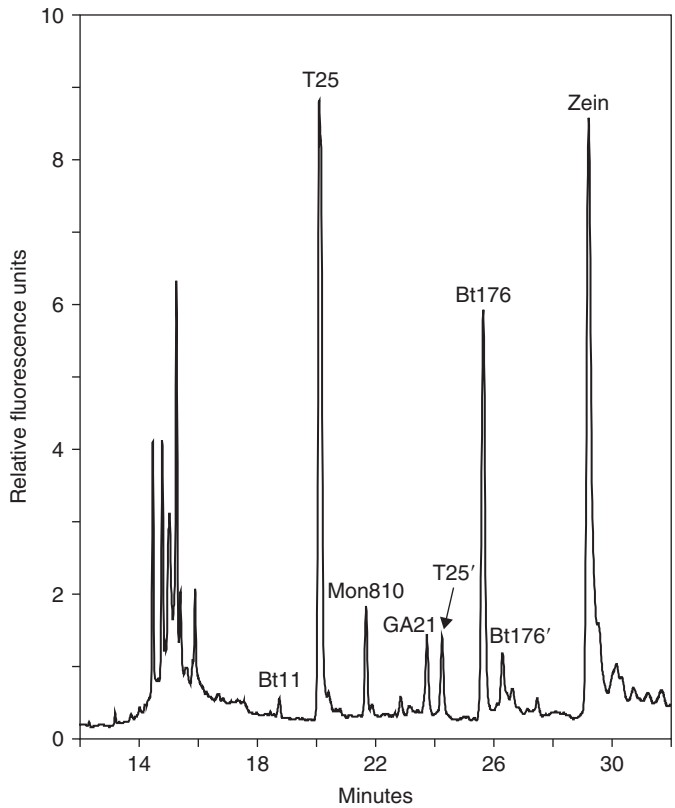

Figure 14.4 GCE-LIF electrophoregram of a multiplex PCR amplification of maize DNA containing 0.67% Bt11, 1.94% T25, 0.94% MON810, 0.91% GA21 and 0.24% Bt176 maize DNA. Peak identification: Bt11, 110-bp Bt11 maize DNA; T25, 149-bp T25 maize DNA; Mon810, 199-bp MON810 maize DNA; GA21, 270-bp GA21 maize DNA; Bt176, 343-bp Bt176 maize DNA; zein, 508-bp zein maize DNA fragments. Redrawn from García-Cañas *et al*. (2004d).

analysis (Figure 14.4; García-Cañas *et al*., 2004d), respectively. These studies demonstrated that CGE-LIF provided better resolution and a signal/noise ratio improvement of *ca*. 700-fold compared with AGE, and that CGE-LIF can be a useful tool for the optimization of the multiplex PCR conditions.

DNA-profiling techniques aimed at the analysis of polymorphisms are also used in food authentication. The most popular of these techniques is the *restriction fragment length polymorphism* (*RFLP*) analysis, which is based on the examination of polymorphic DNA loci characterized by variable-length restriction fragments. RFLP analysis has seen huge application in DNA identification analysis in many research fields. In food science, a study concerning meat identification, based on RFLP analysis, has made evident the significance of the choice of the method used to analyze restriction fragments, demonstrating sensitivity lower than 1% beef contamination in heat-treated pork meat when CGE-LIF was applied instead of AGE (Sun and Lin, 2003). A variant of this technique, referred to as *terminal-RFLPs*, which employs fluorescently

labeled primers, has been used successfully for the differentiation of goats', sheep's, buffalo and cows' milk in dairy products (Lanzilao *et al*., 2003).

Apart from RFLP analysis, other DNA-profiling methods have been used in combination with CGE for ensuring authenticity of the food supply. This is the case for both *random amplified polymorphic DNA* (*RAPD*) and *microsatellite marker analysis*, which have been applied to differentiate grape (*Vitis vinifera*) varieties of interest in wine production. The benefit of using CGE-LIF in detecting the amplified DNA products (fingerprint) is that it ensures the detection of low-concentration products and thereby the integrity of the genomic fingerprint. The simplicity and highly discriminatory power of this technique combined with the high resolution and sensitivity of CGE-LIF demonstrated good potential for the characterization and differentiation of grape varieties and clones (Siles *et al*., 2000). Alternatively, Rodríguez-Plaza *et al*. (2006) has recently proposed a novel method that provides reproducible and efficient DNA separations with adequate size assignments by CGE-LIF. The method, applied to the analysis of microsatellite markers, provides characteristic DNA profiles and allows differentiation of two varieties of grape employed in wine production.

Analysis of proteins

Proteins may be good biomarkers for the differentiation and identification of species and variety in raw materials. Traditionally, the protein composition of raw materials has been examined by polyacrylamide gel electrophoresis slabs. However, improved sensitivity and accuracy can be achieved by adopting alternative analytical techniques based on CE. The separation of proteins has nowadays become one of the main applications of CE; nevertheless, the separation of these biopolymers using fused-silica capillaries is strongly hampered by solute adsorption onto the capillary wall. This phenomenon is one of the main reasons for observed efficiency loss, poor reproducibility in migration times and low protein recovery rates. Adsorption is generally due to electrostatic interactions between positively charged residues of the proteins and negatively charged silanol groups, which are intrinsic to the fused-silica capillary surface. However, undesired interactions between proteins and the capillary wall can be reduced by different means, including (i) the use of highly alkaline or acidic buffers, (ii) the addition of substances to the separation buffer able to shield the negative charges of the capillary wall (polymers, high salt concentrations), (iii) the use of physically adsorbed coatings of the capillary wall, and (iv) chemical modification of the silica surface. Some of these approaches have been used for protein profiling by CE in authenticity testing of a variety of food commodities, including cereals, grain legumes, meats, fish, milk, smoked paprika, etc. (Frazier and Papadopoulou, 2003; Cifuentes, 2006).

The protein composition of cereals can be examined, in terms of its profile of prolamines and/or glutenins, by CE. Several FSCE-UV methods have been proposed for protein profiling of cereals. However, rapid, reproducible and high-resolution separation of cereals has been achieved by the use of isoelectric buffers containing low-viscosity polymers to differentiate wheat (Capelli *et al*., 1998) and barley (Lookhart *et al*., 1999) cultivars. Alternatively, CGE methods for the separation of SDS-protein complexes have also been used to obtain high-resolution profiles of wheat

high molecular weight glutenin subunits, in order to characterize wheat cultivars (Werner *et al*., 1994).

Recently, the protein profiles of high-quality seed lentils (*Lens culinaris* Medik) obtained by FSCE-UV using uncoated fused-silica capillaries and a separation buffer containing imino diacetic acid, hydroxypropylmethylcellulose and 20% ACN, were compared and differentiated from those obtained from seeds of vetch (*Vicia* spp.) (Piergiovanni and Taranto, 2005). A similar FSCE-UV method was developed for the separation and detection of methanol-soluble protein extracts from paprika samples in uncoated silica capillaries (Hernández *et al*., 2006). Qualitative and quantitative differences were detected among the CE profiles of paprika adulterated with different varieties of pepper. With this method, it was possible to detect levels of adulterant paprika as low as 5% in high-quality smoked paprika "pimenton de La Vera".

Casein and whey proteins (lactoglobulins) can be analyzed and their CE patterns used for milk authentication purposes (Herrero-Martínez *et al*., 2000). Identification and quantitation of cows', sheep's and goats' milk in binary and ternary mixtures can be achieved by assessing the differences between casein patterns obtained by FSCE-UV and multivariate regression analysis, with a prediction error lower than 3% (Molina *et al*., 2000).

The detection of species-specific proteins can be used for identification of fish and *meat* species. Gallardo *et al*. (1995) proposed the analysis of sarcoplasmic fish proteins by FSCE to differentiate eight fish species. CGE separation of SDS-protein complexes in combination with linear discriminant analysis to investigate the protein composition of water and saline extracts of turkey, beef and pork meat has been carried out by Vallejo-Cordoba *et al*. (2005). Despite the good results obtained with these methods, species distinction becomes difficult in complex matrices or heat-treated samples. For this reason, PCR-based methods are usually preferred for species identification in processed food, due to their better reliability and sensitivity and to the higher stability of DNA over proteins.

In addition to species identification analysis, detection of *meat extenders* is an important issue in meat authenticity analysis. Accordingly, Simó *et al*. (2004a) detected adulteration of ground meat with 5% of egg-white by CE-MS using a physically adsorbed capillary coating. Using this CE-MS method, the electrostatic adsorption of basic proteins onto the capillary wall is significantly reduced by rinsing the capillary with a polymer aqueous solution for 2 minutes. The coating protocol is compatible with *electrospray ionization* (*ESI*)-MS, providing reproducible separations (%RSD values ($n = 5$) $<1\%$ for analysis time and $<5\%$ for peak heights).

Analysis of chiral compounds

Enantioselective separations can be used for identifying adulterated foods and beverages (Armstrong *et al*., 1990). The use of CE for enantiomer separations provides fast and efficient separations in this type of analysis. Moreover, the availability of many *chiral selectors* and the minimal consumption of such compounds during a CE run have to be considered as an additional advantage of capillary electromigration methods.

Different methods based on MEKC-LIF have been developed to analyze derivatized D- and L-amino acids in food. *Cyclodextrins* and their derivatives are the main

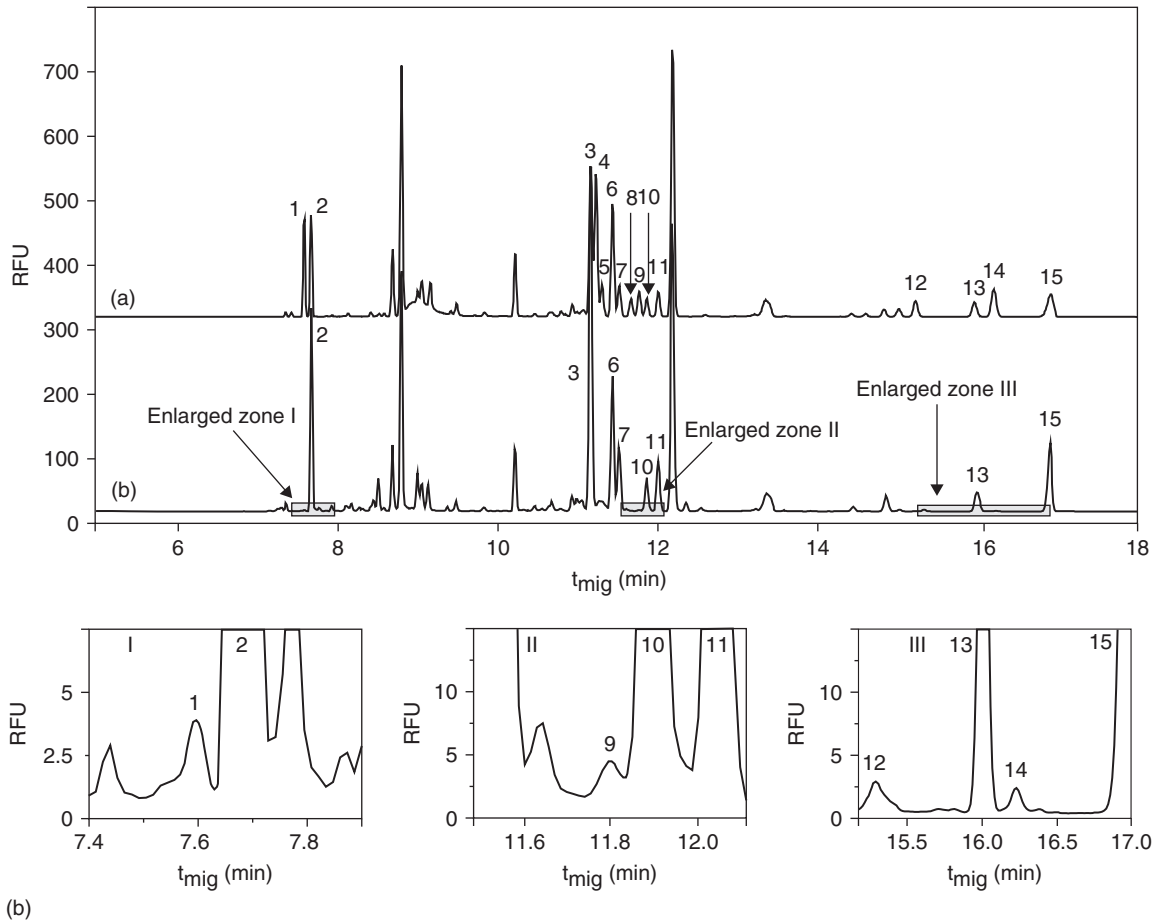

Figure 14.5 Chiral MEKC-LIF separation of (a) standard FITC amino acids, (b) orange juice from concentrate. Peak identification: 1, D-Arg; 2, L-Arg; 3, L-Pro; 4, D-Pro; 5, D-Asn; 6, GABA; 7, L-Asn; 8, D-Ser; 9, D-Ala; 10, L-Ser; 11, L-Ala; 12, D-Glu; 13, L-Glu; 14, D-Asp; 15, L-Asp. Redrawn from Simó *et al*. (2004a).

chiral selectors included in the separation buffer for this type of separations. In addition, representative groups of D- and L-amino acids in foods and beverages can be derivatized with fluorescein isothiocianate (FITC) to enhance the sensitivity when fluorescence detection is employed. An added benefit of derivatization is facilitation of the chiral separation of amino acids, since inclusion and interaction with the chiral selector becomes more discriminating. Using this procedure, a mixture of 14 D- and L-amino acids (i.e., D/L-Asp, Glu, Ser, Asn, Ala, Pro, Arg) plus the non-chiral γ-aminobutyric acid (GABA) were analyzed in orange juices by MEKC-LIF (Simó *et al*., 2002). This method in combination with discriminant analysis was successfully used to classify processed orange juices, including nectars, products reconstituted from concentrates, and pasteurized orange juices not from concentrates (Figure 14.5) (Simó *et al*., 2004b). Following a similar MEKC-LIF strategy, FITC derivatized amino acids (D/L- Pro, Ala, Arg, Glu and Asp) were separated in less than

20 minutes (Carlavilla *et al*., 2006). This simple and fast method was applied to the quantitative analysis of chiral amino acids to differentiate several types of vinegars.

In addition to the MEKC-LIF methods, a CE-MS method was developed to analyze the chiral amino acids D/L-Asp, -Glu, -Ser, -Asn, -Ala, -Pro and -Arg, plus γ-aminobutyric acid in orange juices (Simó *et al*., 2005b). Some of the typical limitations observed when combining ESI-MS and non-volatile chiral selectors as cyclodextrins were solved by using a physical coating of the capillary. Using this method, adulterations as low as 0.8% (with respect to the total amino acid content) of D/L-Asp in orange juices, in which only the L-forms of the amino acids are expected to occur, can be detected.

Herrero *et al*. (2007) have also demonstrated the great possibilities of chiral-MEKC-LIF in investigating the different D/L-amino acid profiling provided by conventional and transgenic maize, which could allow their differentiation.

Analysis of other compounds

Besides the aforementioned target compounds, there are other analytes of considerable significance in food authenticity testing. A number of CE methods that allow the determination of these compounds in food have been developed to assist in food authenticity issues (Kvasnicka, 2005). Some representative examples are discussed below.

FSCE with indirect UV detection has been applied to the analysis of α-galactosides (raffinose, stachyose, verbascose and ajugose) in various plant species belonging to the genera *Lupinus*, *Pissum*, *Brassica* and *Hordeum* (Andersen *et al*., 2005). The CE method in combination with chemometrics demonstrated that the profile of α-galactosides in seeds depended on both genera and plant species to a certain extent. However, Andersen *et al*. (2005) indicated that it would be necessary to analyze a larger data set to make a prediction of plant origin when unknown α-galactosides-containing materials are analyzed.

CE can also be used to analyze both the organic acids and mineral contents in order to evaluate, for example, the authenticity of fruit juices. To illustrate this point, Weston *et al*. (1992) achieved fast separations of four cations (sodium, potassium, calcium and magnesium) in orange juices by FSCE using indirect UV detection together with the addition of a complexing agent (α-hydroxyisobutyric acid) to the running buffer. Saavedra *et al*. (2000) have developed a novel FSCE-UV method for the detection and quantitation of four organic acids, namely isocitric, malic, tartaric and citric acid, in orange juices. The CE method, which features minimal sample treatment (dilution and filtration), showed detection limits below the mean values that are normally found in orange juices. Different orange juices were analyzed by this method, and clear differences could be found between commercial juices and freshly-pressed orange juices. Moreover, the addition of grapefruit to orange juice could be detected by the presence of tartaric acid.

The characterization of the polyphenolic fraction in wine by FSCE-UV has demonstrated the usefulness of this technique to differentiate various types of wine (Pazourek *et al*., 2000). Using FSCE in combination with a fast-scanning detector,

with no need for sample pre-concentration, characteristic profiles of the polyphenolic fraction were obtained from different wine samples.

Future outlook

Despite the multiple applications of CE in food authenticity, there are still some problems that have to be addressed before it can be considered as a mature and routine technique in this area. Thus, although the volumes of sample usually consumed per analysis in CE are a few nanoliters, the sensitivity in terms of concentration is not very high, which precludes the use of CE for determination of trace compounds. To enhance the sensitivity, different strategies have been applied – for example, using sample preconcentration, stacking procedures, more sensitive detection systems (such as laser-induced fluorescence, amperometric detector), etc. Also, in order to improve both sensitivity and mainly selectivity, CE can be interfaced with other techniques such as *electrospray mass spectrometry* (MS) to bring about a very powerful hyphenated technique (Simó *et al*., 2005a). On-line coupling of CE with electrospray-MS may solve the identification problems associated with unknown compounds detected in the complex food matrices usually analyzed. Moreover, the application of CE-MS to food analysis, including food authentication, is an important and practically unexplored working field. Some other new and interesting developments that are currently being worked on in the CE domain will probably be applied for food analysis in the near future. These developments include multi-capillary arrays (Trotha *et al*., 2002), CE interfaced with biosensors (Bossi *et al*., 2003), and chip-based separations (Reyes *et al*., 2002). As an example, authentication of coffee by combining PCR analysis and chip-CE has already been demonstrated (Spaniolas *et al*., 2006). The development of these systems will be important in helping to overcome throughput limitations and sensitivity problems in CE.

Conclusions

Since the development of CE in the 1980s, the features of this separation technique, including its high analysis speed, high separation efficiency, great variety of applications and reduced sample and solvents consumption, have contributed to an increasingly growing number of applications of CE in food science and technology, including its use for solving many analytical problems related to food authenticity. As an example, some representative applications of CE have been shown and discussed in this chapter, including the CE separation of DNA fragments, proteins, chiral compounds, galactosides, cations, organic acids or polyphenols for addressing different food authenticity issues. These examples clearly show that CE can be used in food and regulatory laboratories as a powerful analytical technique complementary to other more established or new analytical procedures. Despite these remarkable applications of CE, the ongoing instrumental and methodological developments of CE aimed to improve its sensitivity, reproducibility and applications range are also expected to continue in the future.

Acknowledgements

V.G-C. would like to thank CSIC for an I3P postdoctoral grant. This study has been supported by an AGL2005-05320-C02-01 and AGL2005-06726-C04-02 Projects (Ministerio de Educacion y Ciencia) and the S-505/AGR-0153 ALIBIRD-Project (Comunidad Autonoma de Madrid).

References

Andersen, K.E., Bjergegaard, C., Moller, P. *et al*. (2005). Compositional variations for alpha-galactosides in different species of Leguminosae, Brassicaceae, and barley: A chemotaxonomic study based on chemometrics and high-performance capillary electrophoresis. *Journal of Agricultural and Food Chemistry*, **53**, 5809–5817.

Armstrong, D.W., Chang, C.D. and Li, W.Y. (1990). Relevance of enantiomeric separations in food and beverage analyses. *Journal of Agricultural and Food Chemistry*, **38**, 1674–1677.

Barron, A.E., Soane, D.S. and Blanch, H.W. (1993). Capillary electrophoresis of DNA in uncross-linked polymer solutions. *Journal of Chromatography A*, **652**, 3–16.

Berrada, H., Font, G. and Molto, J.C. (2003). Determination of urea pesticide residues in vegetable, soil, and water samples. *Critical Reviews in Analytical Chemistry*, **33**, 19–41.

Blake, C. (2004). New techniques for analysing food additives and micronutrients. *Food Science and Technology*, **18**, 25–27.

Bossi, A., Castelletti, L., Piletsky, S.A. *et al*. (2003). Towards the development of an integrated capillary electrophoresis optical biosensor. *Electrophoresis*, **24**, 3356–3363.

Capelli, L., Forlani, F., Perini, F. *et al*. (1998). Wheat cultivar discrimination by capillary electrophoresis of gliadins in isoelectric buffers. *Electrophoresis*, **19**, 311–318.

Carlavilla, D., Moreno-Arribas, M.V., Fanali, S. and Cifuentes, A. (2006). Chiral MEKC-LIF of amino acids in foods: analysis of vinegars. *Electrophoresis*, **27**, 2551–2557.

Castañeda, G., Rodríguez-Flores, J. and Ríos, A. (2005). Analytical approaches to expanding the use of capillary electrophoresis in routine food analysis. *Journal of Separation Science*, **28**, 915–924.

Cifuentes, A. (2006). Recent advances in the application of capillary electromigration methods for food analysis. *Electrophoresis*, **27**, 283–303.

Cohen, A.S. and Karger, B.L. (1987). High-performance sodium dodecyl sulfate polyacrylamide gel capillary electrophoresis of peptides and proteins. *Journal of Chromatography A*, **397**, 409–417.

Cortacero-Ramírez, S., Hernainz-Bermudez de Castro, M., Segura-Carretero, A. *et al*. (2003). Analysis of beer components by capillary electrophoretic methods. *Trends in Analytical Chemistry*, **22**, 440–445.

Erny, G.L. and Cifuentes, A. (2006). Field amplified separation in capillary electrophoresis (FAsCE): a capillary electrophoresis mode. *Analytical Chemistry*, **78**, 7557–7562.

Flurer, C.L. (2003). Analysis of antibiotics by capillary electrophoresis. *Electrophoresis*, **24**, 4116–4127.

Frazier, R.L. and Papadopoulou, A. (2003). Recent advances in the application of capillary electrophoresis for food analysis. *Electrophoresis*, **24**, 4095–4105.

Gallardo, J.M., Sotelo, C.G., Piñeiro, C. and Pérez-Martín, R.I. (1995). Use of capillary zone electrophoresis for fish species identification. Differentiation of flatfish species. *Journal of Agricultural and Food Chemistry*, **43**, 1238–1244.

Galli, V., Garcia, A., Saavedra, L. and Barbas, C. (2003). Capillary electrophoresis for short-chain organic acids and inorganic anions in different samples. *Electrophoresis*, **24**, 1951–1981.

García-Cañas, V., González, R. and Cifuentes, A. (2002a). Highly reproducible capillary gel electrophoresis (CGE) of DNA fragments using uncoated columns. Detection of genetically modified maize by PCR-CGE. *Journal of Separation Science*, **25**, 577–583.

García-Cañas, V., González, R. and Cifuentes, A. (2002b). Detection of genetically modified maize by the polymerase chain reaction and capillary gel electrophoresis with UV detection and laser-induced fluorescence. *Journal of Agricultural and Food Chemistry*, **50**, 1016–1021.

García-Cañas, V., González, R. and Cifuentes, A. (2002c). Ultrasensitive detection of genetically modified maize DNA by capillary gel electrophoresis with laser-induced fluorescence using different fluorescent intercalating dyes. *Journal of Agricultural and Food Chemistry*, **50**, 4497–4502.

García-Cañas, V., Cifuentes, A. and González, R. (2004a). Detection of genetically modified organisms in foods by DNA amplification techniques. *Critical Reviews in Food Science and Nutrition*, **44**, 425–436.

García-Cañas, V., González, R. and Cifuentes, A. (2004b). The combined use of molecular techniques and capillary electrophoresis in food analysis. *Trends in Analytical Chemistry*, **23**, 637–643.

García-Cañas, V., Cifuentes, A. and González, R. (2004c). Quantitation of transgenic Bt Event-176 maize using double quantitative competitive polymerase chain reaction and capillary gel electrophoresis laser-induced fluorescence. *Analytical Chemistry*, **76**, 2306–2313.

García-Cañas, V., González, R. and Cifuentes, A. (2004d). Sensitive and simultaneous analysis of five transgenic maizes using multiplex polymerase chain reaction capillary gel electrophoresis, and laser-induced fluorescence. *Electrophoresis*, **25**, 2219–2226.

Hernández, A., Martín, A., Aranda, E. *et al*. (2006). Detection of smoked paprika "Pimentón de la Vera" adulteration by free zone capillary electrophoresis (FZCE). *Journal of Agricultural and Food Chemistry*, **54**, 4141–4147.

Hernández-Borges, J., Frías-García, S., Cifuentes, A. and Rodríguez-Delgado, M.A. (2004). Pesticide analysis by capillary electrophoresis. *Journal of Separation Science*, **27**, 947–963.

Herrero, M., Ibáñez, E. and Cifuentes, A. (2005). Analysis of natural antioxidants by capillary electromigration methods. *Journal of Separation Science*, **28**, 883–897.

Herrero, M., Ibáñez, E., Martin-Alvarez, P.J. and Cifuentes, A. (2007). Analysis of chiral amino acids in conventional and transgenic maize. *Analytical Chemistry*, **79**, 5071–5077.

Herrero-Martínez, J.M., Simó-Alfonso, E.F., Ramis-Ramos, G. *et al*. (2000). Determination of cow's milk in non-bovine and mixed cheeses by capillary electrophoresis of whey proteins in acidic isoelectric buffers. *Journal of Chromatography A*, **878**, 261–271.

Hjertén, S. and Zhu, M. (1985). Adaptation of the equipment for high-performance electrophoresis to isoelectric focusing. *Journal of Chromatography A*, **346**, 265–270.

Jorgenson, J.W. and Lukacs, K.D. (1983). Capillary zone electrophoresis. *Science*, **222**, 266–272.

Juan-García, A., Font, G. and Picó, Y. (2005). Determination of organic contaminants in food by capillary electrophoresis. *Journal of Separation Science*, **28**, 793–812.

Knox, J.H. and Grant, I.H. (1987). Miniaturisation in pressure and electroendosmotically driven liquid chromatography: some theoretical considerations. *Chromatographia*, **24**, 135–143.

Kvasnicka, F. (2005). Capillary electrophoresis in food authenticity. *Journal of Separation Science*, **28**, 813–825.

Lanzilao, I., Burgalassi, F., Ebranati, E. *et al*. (2003). Species identification in dairy products by innovative molecular techniques. Part I: Terminal-RFLP. *Industrie alimentari*, **42**, 595–601.

Lookhart, G.L., Bean, S.R. and Jones, B.L. (1999). Separation and characterization of barley (Hordeum vulgare L.) hordeins by free zone capillary electrophoresis. *Electrophoresis*, **20**, 1605–1612.

Martínez-Montero, C., Rodriguez-Dodero, M.C., Guillen-Sanchez, D.A. and Barroso, C.G. (2004). Analysis of low molecular weight carbohydrates in food and beverages: a review. *Chromatographia*, **59**, 15–30.

Molina, E., de Frutos, M. and Ramos, M. (2000). Capillary electrophoresis characterization of the casein fraction of cheeses made from cows', ewes' and goats' milks. *Journal of Dairy Research*, **67**, 209–216.

Pazourek, J., González, G., Revilla, A.L. and Havel, H. (2000). Separations of polyphenols in Canary Islands wine by capillary zone electrophoresis without preconcentration. *Journal of Chromatography A*, **874**, 111–119.

Piergiovanni, A.R. and Taranto, G. (2005). Simple and rapid method for the differentiation of *Lens culinaris* Medik. from false lentil species. *Journal of Agricultural and Food Chemistry*, **53**, 6593–6597.

Poinsot, V., Bayle, C. and Couderc, F. (2003). Recent advances in amino acid analysis by capillary electrophoresis. *Electrophoresis*, **24**, 4047–4062.

Pospichal, J., Gebauer, P. and Bocek, P. (1989). Measurement of mobilities and dissociation constants by capillary isotachophoresis. *Chemical Reviews*, **89**, 419–430.

Reyes, D.R., Iossifidis, D., Auroux, P.A. and Manz, A. (2002). Micro total analysis systems. 1. Introduction, theory, and technology. *Analytical Chemistry*, **74**, 2623–2636.

Rodríguez-Plaza, P., González, R., Moreno-Arribas, M.V. *et al*. (2006). Combining microstellite markers and capillary gel electrophoresis with laser-induced fluorescence to identify the grape (*Vitis vinifera*) variety of musts. *European Food Research and Technology*, **223**, 625–631.

Saavedra, L., García, A. and Barbas, C. (2000). Development and validation of a capillary electrophoresis method for direct measurement of isocitric, citric, tartaric and malic acids as adulteration markers in orange juice. *Journal of Chromatography A*, **881**, 395–401.

Siles, B.A., O'Neil, K.A., Fox, M.A. *et al*. (2000). Genetic fingerprinting of grape plant (*Vitis vinifera*) using random aplified polymorphic DNA (RAPD) analysis and dynamic size-sieving capillary electrophoresis. *Journal of Agricultural and Food Chemistry*, **38**, 5903–5912.

Simó, C., Barbas, C. and Cifuentes, A. (2002). Sensitive micellar electrokinetic chromatography-laser-induced fluorescence method to analyze chiral amino acids in orange juices. *Journal of Agricultural and Food Chemistry*, **50**, 5288–5293.

Simó, C., Barbas, C. and Cifuentes, A. (2003). Chiral electromigration methods in food analysis. *Electrophoresis*, **24**, 2431–2441.

Simó, C., Elvira, C., González, N. *et al*. (2004a). Capillary electrophoresis-mass spectrometry of basic proteins using a new physically adsorbed polymer coating. Some applications in food analysis. *Electrophoresis*, **25**, 2056–2064.

Simó, C., Martín-Álvarez, P.J., Barbas, C. and Cifuentes, A. (2004b). Application of stepwise discriminant analysis to classify commercial orange juices using chiral micellar electrokinetic chromatography-laser induced fluorescence data of amino acids. *Electrophoresis*, **25**, 2885–2891.

Simó, C., Barbas, C. and Cifuentes, A. (2005a). Capillary electrophoresis-mass spectrometry in food analysis. *Electrophoresis*, **26**, 1306–1318.

Simó, C., Rizzi, A., Barbas, C. and Cifuentes, A. (2005b). Chiral capillary electrophoresis-mass spectrometry of amino acids in foods. *Electrophoresis*, **26**, 2885–2891.

Sotelo, C.G. and Pérez-Martín, R.I. (2003). Species identification in processed seafoods. In: M. Lees (ed.), *Food Authenticity and Traceability*. Cambridge: Woodhead Publishing Ltd, pp. 323–346.

Spaniolas, S., May, S.T., Bennett, M.J. and Tucker, G.A. (2006). Authentication of coffee by means of PCR-RFLP analysis and lab-on-a-chip capillary electrophoresis. *Journal of Agricultural and Food Chemistry*, **54**, 7466–7470.

Sun, Y.L. and Lin, C.S. (2003). Establishment and application of a fluorescent polymerase chain reaction-restriction fragment length polymorphism (PCR-RFLP) method for identifying porcine, caprine, and bovine meats. *Journal of Agricultural and Food Chemistry*, **51**, 1771–1776.

Terabe, S., Otsuka, K., Ichikawa, K. *et al*. (1984). Electrokinetic separations with micellar solutions and open-tubular capillaries. *Analytical Chemistry*, **56**, 111–113.

Trotha, S., Reichl, U., Thies, F.L. *et al*. (2002). Adaption of a fragment analysis technique to an automated high-throughput multicapillary electrophoresis device for the precise qualitative and quantitative characterization of microbial communities. *Electrophoresis*, **23**, 1070–1079.

Vallejo-Cordoba, B., González-Córdova, A., Mazorra-Manzano, M.A. and Rodríguez-Ramírez, R. (2005). Capillary electrophoresis for the analysis of meat authenticity. *Journal of Separation Science*, **28**, 826–836.

Venema, E., Kraak, J.C., Tijssen, T. and Poppe, H. (1998). Electrically driven capillary size exclusion chromatography. *Chromatographia*, **48**, 347–354.

Werner, W.E., Wiktorowicz, J.E. and Kasarda, D.D. (1994). Wheat varietal identification by capillary electrophoresis of gliadins and high molecular weight glutenin subunits. *Cereal Chemistry*, **71**, 397–402.

Weston, A., Brown, P.R., Heckenberg, A.L. *et al*. (1992). Effect of electrolyte composition on the separation of inorganic metal cations by capillary ion electrophoresis. *Journal of Chromatography*, **602**, 249–256.

This page intentionally left blank

15

Thermal Technique: Differential Scanning Calorimetry (DSC)

Oi-Ming Lai and Seong-Koon Lo

Introduction

Thermal analysis is defined as a group of techniques in which the physical property of a substance is measured as a function of temperature whilst the substance is subjected to a controlled temperature program (Wendlandt, 1986a). Some of the techniques used to carry out thermal analysis include differential thermal analysis (DTA), *differential scanning calorimetry* (*DSC*), thermogravimetric analysis (TG), hot-stage microscopy (HSM), thermomechanical analysis (TMA), dynamic mechanical analysis (DMA), dielectric thermal analysis (DETA) and thermoptometry. Some of the lesser-known techniques include evolved gas analysis (EVA), evolved gas detection (EGD), thermosonimetry (TS), thermoluminescence (TL), thermomagnetometry (TM), a combination of techniques such as thermogravimetry-mass spectroscopy, and many more. It should be noted that, despite the vast literature published on the application of thermal analysis (TA) methods in numerous research areas, it is often used in combination with other TA/analytical techniques to supplement, complement or confirm the results or information obtained. The use of a single TA method is often insufficient to provide all the required information regarding a system. In this chapter, we will review fully the application of one thermal technique, notably DSC, in

Modern Techniques for Food Authentication
ISBN: 978-0-12-374085-4

the area of food authentication. The basic theory and principles of operation, as well as the advantages and limitations of this analytical technique, will be discussed. A compilation of all the books written on DTA/DSC and other thermal techniques from 1937–1980 can be found in Lombardi (1980). Readers who are interested in the principles, design, development and operation of other thermal techniques are directed to the excellent publications of Wendlandt (1986a), and those cited in this chapter.

Differential scanning calorimetry

The Nomenclature Committee of the International Confederation for Thermal Analysis (ICTA), later known as the International Confederation for Thermal Analysis and Calorimetry (ICTAC), has defined DSC as "A technique in which the difference in energy inputs into a substance and a reference material is measured as function of temperature whilst the substance and reference materials are subjected to a controlled temperature program" (Mackenzie, 1980). Of all the TA techniques, DSC is the most versatile, with a wide range of applications in numerous areas (Griffin and Laye, 1992). There are two major classes of DSC instruments commercially available: *power-compensation DSC* and *heat-flux DSC*.

Basic principles

DSC is useful in the study of endothermic and exothermic phenomena of matter. In DSC, the difference in temperature (ΔT) between the sample and the reference material is measured under the same temperature program. The heat capacity of the sample can also be obtained by determining the input of energy into the sample and reference. When the sample is heated at a constant rate (dT_P/dt = constant), the temperatures of the furnace (T_P), reference (T_R) and sample (T_S) change with time (t). The relationship between T and t, and ΔT and t for furnace, reference and sample is indicated in Figures 15.1(a) and 15.1(b), respectively. At steady state, ΔT_R and ΔT_S are constants of dT_P/dt. According to Newton's law of cooling, the transfer of heat from the furnace to the sample, i.e. the heat flow rate, dq_S/dt, can be represented by this equation:

$$dq_S/dt = 1/R(T_P - T_S) \qquad \textbf{(15.1)}$$

where R is the heat resistance between the furnace and the sample. From Equation (15.1), we can clearly see that the heat resistance, R, is the reciprocal of the heat transfer constant, dq_S/dt. Since the heat transferred to the sample is used for heating the sample and the sample cell, the heat flow rate is represented by the following equation:

$$dq_S/dt = \left[C_S(T) + C_{CS}(T)\right] dT_P/dt \qquad \textbf{(15.2)}$$

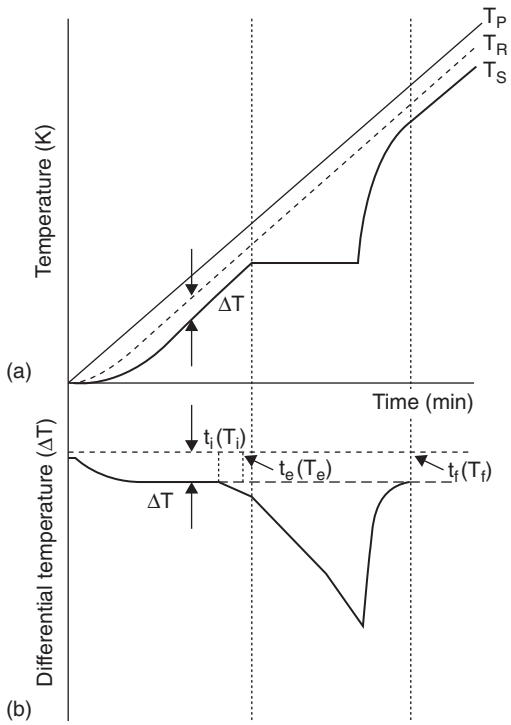

Figure 15.1 (a) Change in temperature of reference, T_R, and sample, T_S, with increasing furnace temperature, T_P; (b) typical signal output converted to differential temperature, ΔT, with time, t. Source: Ozao (2004).

where $C_S(T)$ and $C_{CS}(T)$ are the heat capacities of the sample and the sample cell, respectively. Equations (15.1) and (15.2) can also be applied to the reference cell as follows:

$$\begin{aligned} dq_R/dt &= 1/R(T_P - T_R) \\ &= \left[C_R(T) + C_{CR}(T)\right] dT_P/dt \end{aligned} \qquad \textbf{(15.3)}$$

where $C_R(T)$ and $C_{CR}(T)$ are the heat capacities of the reference and the reference cell, respectively. From Equations (15.1), (15.2) and (15.3), the following equation can be derived:

$$\begin{aligned} dq_S/dt - dq_R/dt &= -1/R(T_S - T_R) \\ &= \left\{\left[C_{CS}(T) - C_{CR}(T)\right] + \left[C_S(T) - C_R(T)\right]\right\} dT_P/dt \end{aligned} \qquad \textbf{(15.4)}$$

Since the same material is used for the sample cell and reference cell, the heat capacity and the mass of the sample cell will be the same as those of the reference cell. Therefore,

$$C_{CS}(T) = C_{CR}(T) \qquad \textbf{(15.5)}$$

Upon substitution of Equation (15.5) into Equation (15.4), the following equation can be derived:

$$1/R(\Delta T) = \left[C_S(T) - C_R(T)\right] dT_P/dt \quad \textbf{(15.6)}$$

where $\Delta T \equiv T_R - T_S$ or

$$d\Delta q/dt \equiv dq_S/dt - dq_R/dt = \left[C_S(T) - C_R(T)\right] dT_P/dt \quad \textbf{(15.7)}$$

The heat transfer of the heat-flux type DSC is a well-defined path of heat resistance R. Therefore, the difference in heat capacity of the sample and the reference can be derived by measuring the differential temperature, $\Delta T = T_R - T_S$. In power-compensation type DSC, the difference in the energy supplied per unit time of the sample and reference is measured to give Equation (15.7).

However, the reader should be aware that the technique of DSC is based on relative measurements that are not made in thermal equilibrium. In addition, the outputs of the DSC instrument are represented by voltages as a function of time that are further transformed to temperature (K or °C) and heat flow rate (W or Js^{-1})

$$d\Delta q/dt = K(T) d\Delta q_m/dt = \left[C_S(T) - C_R(T)\right] dT_P/dt \quad \textbf{(15.8)}$$

where K(T) is a temperature-dependent factor and $d\Delta q_m/dt$ is the measured signal.

Power-compensation differential scanning calorimetry

In power-compensated DSC, heat is added to the sample or to the reference material as needed so that the two substances remain at the similar temperature (Meisel and Seyboldare, 1981). Both the sample and reference materials are supplied with separate heaters or micro-ovens, and their temperatures are identically maintained by platinum resistance thermometers. This results in different amounts of heat being supplied to each of the specimens as appropriate. In 1963, when the first power-compensation DSC was introduced, their holders were made from stainless-steel cup and support and a platinum wire sensor which allowed the sample holders to operate at temperature ranges between −125 and 500°C. These were then replaced with platinum-iridium alloy for the sample holder, platinum wire for both the sensor and heater, and α-alumina for insulation in the holders. Such design allowed the sample holders to operate at higher temperature ranges of up to 725°C.

Figure 15.2 illustrates the basic circuitry principle of a power-compensated DSC. There are two separate heating circuits; the *average-heating controller*, and the *differential heating circuit*. In the average-heating controller, the temperatures of the sample and reference are measured and averaged, and the heat output of the average temperature of the sample and reference increases at a predetermined rate (McNaughton and Mortimer, 1975). The average temperature then serves as the abscissa for the thermal curve (Wendlandt, 1986b). The differential-temperature controller monitors the difference in temperature between the sample and reference (because of the exothermic or endothermic reaction in the sample) and automatically adjusts the power to either the

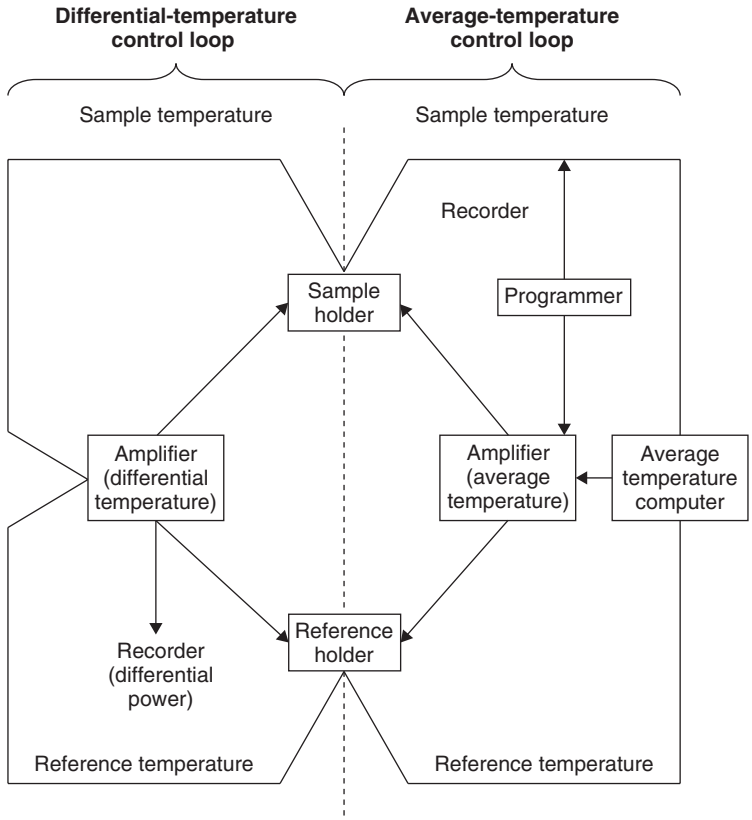

Figure 15.2 Schematic diagram of a Perkin-Elmer DSC instrument. Source: Wendlandt (1986d).

reference or sample holders in such a way that their temperatures are identical. This is the null-balance principle. Thus, the temperature of the sample holder is always the same as that of the reference holder by continuous and automatic adjustment of the heater power (Griffin and Laye, 1992). A signal, proportional to the difference between the power input to the sample and that to the reference, is fed into a recorder. This difference in power, usually in milliwatts, is the information most frequently plotted as a function of sample temperature (Haines and Wilburn, 1995). The area under the peak is then proportional to the heat energy absorbed or liberated during the transition. The recorder can also be used to register the average temperature of the sample and reference (McNaughton and Mortimer, 1975).

Heat-flux differential scanning calorimetry

The principle of the heat-flux system developed by Tian and Calvet during the 1920s is that the sample and reference materials are simultaneously heated on a fixed thermal conduction path and the temperature difference between them is proportionate to the difference in heat flow between the two materials (Wendlandt, 1986b). The signal (temperature difference) is then converted to a power difference using the calorimetric sensitivity (Haines and Wilburn, 1995).

The construction of a heat-flux system was fully described by DuPont systems. Figure 15.3 shows the schematic diagram of a commercially available heat-flux DSC cell in cross-section. A constantan disc transfers heat to sample and reference positions. It also serves as one element of the temperature-measuring thermoelectric junctions. The sample and reference are contained in pans positioned on raised platforms on the constantan disc. Heat is transferred through the disc and through the pan sample into the contained sample and reference during a scan. The differential heat flow is monitored by chromel-constantan area thermocouples formed by the junction of the constantan disc and the chromel wafer attached to the underside of the disc. Sample temperature is monitored directly via chromel–alumel thermocouples formed from chromel and alumel wires connected to the underside of the chromel wafers. This shows that the differential heat flow into the pans is directly proportionate to the difference in output of the two-thermocouple junctions. Software linearization of the cell calibration is utilized to maintain calorimetric sensitivity (Ford and Timmins, 1989).

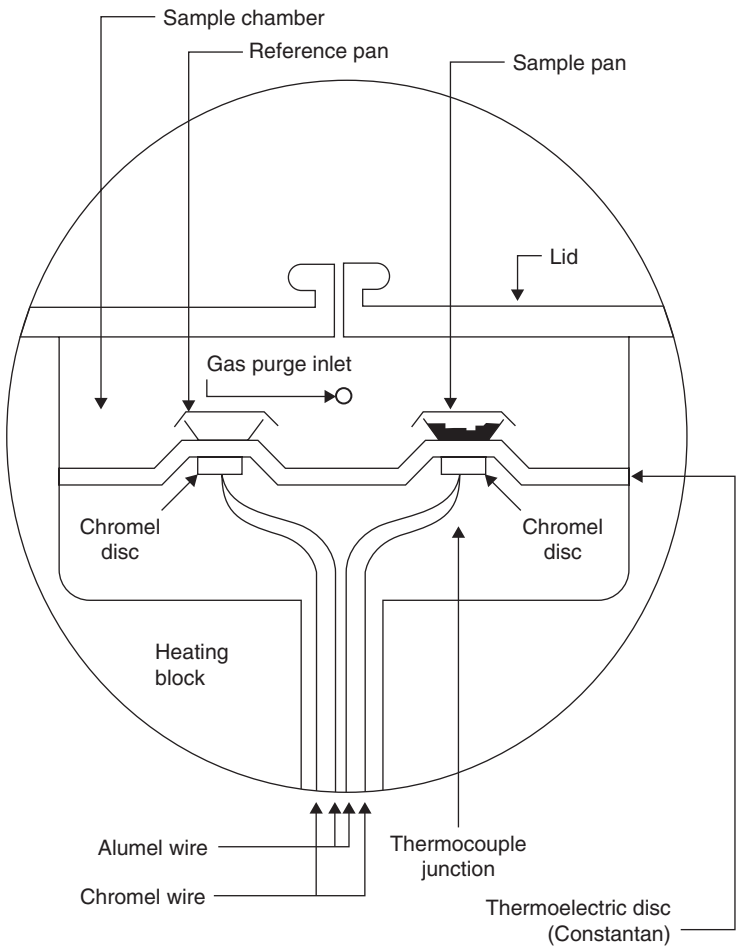

Figure 15.3 Cross-section of a heat-flux DSC cell. Source: TA Instruments.

Temperature-modulated differential scanning calorimetry

Temperature-modulated differential scanning calorimetry (TMDSC) was first introduced by Reading (1993). TMDSC is different from conventional DSC in that a low-frequency sinusoidal or non-sinusoidal (e.g. sawtooth) perturbation ranging from approximately 0.001 to 0.1 Hz (1000- to 10-s period) is applied on the temperature control program. TMDSC data analysis involves separating the total heat flow or apparent heat capacity into reversing and non-reversing components. The reversing component of the heat flow is obtained from the amplitude of the first harmonic of the heat flow using a Fourier transform of the data. The amplitude of the heat flow can be measured directly in a power-compensated DSC, and can be calculated from the temperature difference between the sample and reference in a heat-flux DSC. The non-reversing heat flow is defined as the difference between the average heat flow and the reversing heat flow. The non-reversing heat capacity is the difference between the normalized average heat flow divided by the underlying heating rate and the reversing heat capacity. In the absence of thermal events, the reversing heat capacity is the frequency-independent heat capacity and the non-reversing heat capacity is zero. However, in the presence of a thermal event, the reversing heat flow is considered to reflect reversible sensible heat effects (i.e. those due to changes in the heat capacity), and the non-reversing heat flow to reflect irreversible kinetic effects. This assumption is valid only if the kinetics related to the process being measured is linear and if the kinetic response does not make contributions to the first harmonic (Simon, 2001). The application of such a complex temperature modulation allows the simultaneous measurement of response at multiple frequencies (Wunderlich *et al*., 2000). The advantages of TMDSC include improved resolution and sensitivity, as well as the ability to separate overlapping peaks (Gill *et al*., 1993; Reading, 1993; Reading *et al*., 1993).

Triple-cell differential scanning calorimetry

The triple-cell DSC concept was proposed by Wunderlich (1987). The sample section consists of three cells, in which one cell contains the sample to be measured, one contains the reference material, and the last is empty. Figure 15.4 shows a block diagram of the triple-cell DSC. The differences in temperature between the sample and the empty cell, and between the reference and the empty cell, are detected by thermocouples under a constant heating rate. The heat capacity of the sample is determined by comparison of these two signals, after subtracting the heat capacity of the empty cell.

High-performance differential scanning calorimetry

High-performance DSC (HPDSC), being a current development of DSC technology, is capable of fast scanning rates of up to 500°C min^{-1} as compared to 40°C min^{-1} by conventional DSC. This high scanning rate allows for a higher throughput as well as sensitivity enhanced by a factor of ten. Other advantages of HPDSC include negligible instrument drift, small sample mass (down to 400 ng) and the prevention of thermal degradation of the sample.

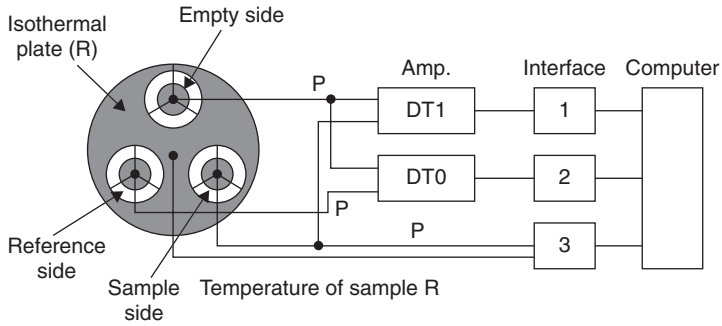

Figure 15.4 Schematic diagram of a triple-cell DSC. Source: Takahashi (2004).

Factors affecting DSC curves

The effects of various factors that influence the results of DSC were reviewed in detail by Wendlandt (1986c), who identified 16 factors that the practitioner should be aware of before using DSC. Some of these factors are attributed to the design of the DSC instrument, and the properties of the sample are beyond the control of the practitioner. However, other "controllable" factors should be carefully considered by the practitioner in order to obtain good quality results. Some of these factors and their effects are summarized below.

Scanning rate

The heating rate of a DSC is directly proportional to the procedural initial deviation temperature (T_I) that the instrument can detect, the procedural peak minimum temperature (ΔT_{min}) and the procedural final temperature (T_F) of the peak. The effect of the heating rate on the peak area depends on the temperature axis, i.e. T_R, T_S or, external to the furnace, (T_E). If $T_S - T_R$ is plotted against T_S, then the peak area will be proportional to the heating rate if the latter remains constant during the analysis. However, if the peak area is derived from $T_S - T_R$ versus time, then it is not dependent on the heating rate. Higher heating rates will cause a decline in the resolution of two adjacent peaks, thereby concealing one of the peaks. On the other hand, too low a heating rate will cause the peak areas to be very small or entirely disappear. Wendlandt (1986c) noted that this only happens on certain types of instruments, depending on the type of sample holder. A higher heating rate will also cause the rate of heat absorption to increase, therefore resulting in a greater peak height or differential temperature, ΔT_{min}. The reason for this is that since the return to the baseline is a function of time and temperature difference, the return will be at a higher actual temperature at higher heating rates. Therefore, for the detection of small transitions, it is suggested that a higher heating rate be used so that the peak amplitude of the peaks can be increased.

Furnace atmosphere

In general, two types of gaseous atmosphere can be used. The first type is a static gaseous atmosphere, which is usually in an enclosed system. It is very difficult to

obtain good reproducibility using the static gaseous atmosphere, as the atmosphere surrounding the sample is continually changing in concentration due to gas evolution by the sample and by the furnace convection currents. The second type is the dynamic gaseous atmosphere, which involves the maintenance of the gas flow either through the furnace or through the sample and reference materials. Under controlled conditions, this type of gaseous atmosphere is simple to maintain and reproduce.

If the sample is reactive towards certain gaseous components around its vicinity, the gas pressure of the system will influence the peak temperature and peak shape. This change will be more thermodynamically distinct when the gaseous environment is identical to the evolved or absorbed gas. The correlation between the transition temperature and gas pressure can be expressed by the Clapeyron equation:

$$dp/dT = \Delta H/T\Delta V \qquad (15.9)$$

where p is the vapor pressure, ΔH is the heat of phase transition, and ΔV is the change in volume of the system due to the phase transition.

In general, when the purge gas is inert and different from the effluent gas, increasing the gas flow rate reduces the peak temperature at which volatilization occurs. Under certain operating conditions, when the purge gas is the same as the effluent gas, the volatilization peak either shifts to a higher temperature or is left unchanged in relation to zero flow rate. This phenomenon is related to the partial pressure changes of the effluent gas in the vicinity of the sample surface. When the purge gas dilutes the effluent gas, the partial pressure of the effluent gas decreases with increasing flow rate, thereby causing the peak to shift towards lower temperatures.

When the evolved gas has a fixed partial pressure, the sample will not start to dissociate to a significant extent until the dissociation pressure of the reaction equals or exceeds the partial pressure of the gaseous component in the surrounding atmosphere. Therefore, a higher partial pressure of the surrounding gas will increase the dissociation temperature of the sample.

Gas-pressure changes can also affect the DSC curve. Wendlandt (1986c) reported that an increase in the gas pressure of the system would cause an increase in the transition temperatures, T_I, ΔT_{min} and T_F. At low gas pressures ($<$1 Torr) the product gases are rapidly taken away, thus shifting the transition temperatures towards the lower temperature region. At the same time, the peak resolution diminishes.

Calibration of the instrument

The temperature and energy scales of the DSC instrument must be properly calibrated in order for it to achieve high accuracy. Calibration standards of well-established transition temperatures, which cover much of the temperature range of the DSC, are widely available. These calibration standards are in their pure form ($\geqslant$99.99% purity based on vapor analysis) and stable, and, if possible, have a negligible vapor pressure. Most of these calibration standards are metal, and some have melting temperatures that are fixed points on the International Practical Temperature Scale. Calibration standards of organic origin should always be used in sealed vessels to prevent sample losses through vaporization. Laboratory-grade chemicals should not be used as calibration standards even if the melting temperature is clearly

described. The presence of trace amounts of impurities will have a significant effect on the observed transition temperature.

A standard temperature calibration procedure for DSC instruments has been published by ASTM E 967 (1999). At least two standard reference materials are chosen to bracket the temperature range of interest. A small piece (1–2 mg) of the reference material is cut from the center of the metal block for use in the calibration procedure. The practitioner has to be sure not to use any standard materials that have been exposed to air, as oxidation of the metal surface changes the melting temperature of the material. It is also important to note the physical form of the standard material used for the calibration. Standard materials in the form of fine powder will show a different transition temperature and enthalpy from those in block form. This is due to the difference in surface area of the standard materials. The calibration of temperature should be conducted on the heating cycle rather than the cooling cycle, as significant supercooling of the metal can occur in the cooling cycle, resulting in difficult temperature calibration. In addition, temperature calibration should be performed under the same experimental conditions as for the proposed experiment. An identical heating rate should be used, as the observed melting temperature is strongly influenced by the temperature gradient between the sample and the sample holder. During the transfer of the standard material into the sample vessel, care must be taken to ensure that only one droplet is formed in the sample vessel. If more than one droplet is present, multiple transition peaks may be observed.

Sample mass

The area of the DSC curve peak corresponds to the heat of reaction or phase transition and, therefore, the mass of the sample. The peak area is also inversely proportional to the thermal conductivity (k); directly proportional to the density (ϕ) and the heat of reaction or phase transition (ΔH), but is independent of the specific heat. This relationship can be written as the following equation:

$$A \propto \phi r^2 \Delta H l / k \tag{15.10}$$

where A is the peak area ($\Delta T \times$ time), r is the sample radius and l is the length of the sample. Equation (15.10) can be rewritten as

$$A = \phi V \Delta H / k \tag{15.11}$$

where V is the volume of the sample, and therefore

$$A = G m \Delta H / k \tag{15.12}$$

where G is the calibration factor and m is the sample mass. An increase in sample mass has been known to increase the peak minimum temperature (Wendlandt, 1986c).

Particle size and packing

There are several findings regarding the effects of sample particle size and distribution on the peak areas and ΔT_{min} values. The first relates to the influence of grinding

of the sample, which reduces the particle size of the sample, as compared with using a larger particle size sample. Samples of larger particle size often show narrow and reproducible DSC curves, while the transition temperatures of powdered samples often shift to higher temperatures and show a "smear-over" effect, appearing over a much larger temperature range than in the case of the larger particle size sample (Wendlandt, 1986c). The degree and type of crystallinity of the sample is also said to have an influence on the shape of the DSC curve. Samples with a higher degree of crystallinity will result in a sharper peak, and *vice versa*. If the sample is irregularly shaped, sample deformation may occur during heating, thereby increasing the noise level of the sample baseline. Occasionally, the noise level may be large enough to be mistaken for a transition peak.

In general, the sample must be in good thermal contact with the sample vessel to facilitate proper heat flow between the heat source and the sample, thus reducing thermal lag. In other words, proper packing of the sample in the sample vessel is necessary to ensure minimum void formation between the sample particles. This is because the thermal conductivity of air is very low compared with that of the sample.

For hydrophilic samples, proper storage and handling conditions must be maintained to minimize moisture absorption from the air, which can result in mass variations. When exposed to humid air, the mass increase is most pronounced during the first 5 minutes of exposure before gradually leveling off. Therefore, the use of a dry box under dry inert gas is necessary.

Diluent

A diluent in a sample on the DSC curve can reduce the heat effect, and in turn reduce the peak area. However, if the samples are sufficiently diluted with an inert diluent, the physical properties will be nearly the same, resulting in a peak area being directly proportional to the heat of the reaction or transition (Wendlandt, 1986c). The variation in thermal conductivity of the diluent is the main reason for the change in peak area. High conductivity allows for more efficient transfer of the thermal effect to the thermojunction in the center of the sample. However, high thermal conductivity of the diluent can cause a decrease in the peak area when the diluted sample is in direct contact with a metal sample block. It is also important to know that the diluent should not react with the sample during the heating process. "Masking" effects, where shifts in the transition temperature of the peak are caused by the product of a reaction between the diluent and the sample, have been observed in certain cases (Wendlandt, 1986c).

Sample vessel

Various types of sample vessel material are commercially available for DSC. The common materials used aluminum, carbon, gold, platinum, silver and stainless steel. The choice of sample vessel material is dependent on the maximum operating temperature used for the experiment – the maximum operating temperature of the experiment should not be higher than the melting temperature of the vessel material. If the

sample vessel should melt on the sample holder, alloying can occur and the sample holder will then have to be replaced. When analyzing a large amount of sample at a slow scanning rate, it is recommended that a sample vessel made of a high thermal conductivity material such as silver be used.

It is also important to consider the shape of the sample vessel to be used for a particular type of sample. Open-type sample vessels that do not seal hermetically are normally used for samples that are in a form of a film, powder, block or fiber. Samples that can be easily volatilized, sublimed or decomposed under experimental conditions should be placed in a hermetically sealed-type sample vessel.

Purge gas

The type and purity of the purge gas has a significant influence on the shape of the DSC curve. Nitrogen gas is the most commonly used purge gas when operating at temperatures above ambient temperature. The nitrogen gas should be dry, and free of impurities such as oxygen. There are a number of commercially available grades of nitrogen gas, with purities ranging from 99.99 to 99.9999%. Air is not used as a purge gas because of its complex composition and high water-vapor content.

For sub-ambient temperatures, a number of inert gases (such as argon, helium and nitrogen) may be applied. The selection of the purge gas is mainly dependent on the experimental conditions used. It should be noted that if the purge gas is changed, recalibration of the DSC instrument, based on the new purge gas, must be performed.

Application in foods

It is very common to come across fraudulent activities in various consumer sectors, including the food industry. This has led to the development of many new techniques for the authentication of food products, as more consumers are becoming aware of food safety issues. The authentication of food products is also of primary concern for food manufacturers, as they do not wish to be subject to unfair competition from unscrupulous manufacturers who gain an economic advantage from misrepresentation of the food being sold. From a legislative point of view, high standards have been set requiring food manufacturers to provide quality labels that specify the chemical composition of each food product; from an economic point of view, the authentication of a food product is essential to avoid unfair competition that can lead to destabilization of the market and disrupt the national and regional economies.

Regarding food, the DSC technique is widely used in the characterization of food components and the study of physicochemical changes of these components as the food is subjected to various temperature effects. However, the use of DSC for the detection of adulteration in food is currently limited to the few examples described below.

Edible oils and fats

In the oils and fats industry, the physical property of an oil or fat is mostly used as a measurement for quality control and authentication. Certain specifications are set

down for individual products in terms of the slip melting point (SMP), cloud point (CP) or solid fat content (SFC) at a particular temperature. For this application, DSC would seem ideally suited to the task of characterization. In fact, DSC has been used in the characterization of oils and fats for many years (Cebula and Smith, 1992), but few researchers have dedicated their work to utilizing the DSC technique for the authentication of oils and fats. Some of their works are reviewed below.

Confectionery fats

Confectionery fats make up approximately one-third of the overall ingredients in chocolate. It is the unique melting characteristics of these specialty fats that give chocolate its desirable organoleptic traits. The quality of confectionery fat can affect certain parameters of the chocolate manufacturing process, especially at the tempering and cooling stages. This is the main reason why it is of utmost importance to monitor the quality and authenticity of these fats.

Genuine high-quality cocoa butter (CB), being one of the most expensive edible fats, is mostly used in premium chocolate. It is composed of specific triacylglycerols having three predominant fatty acids, namely palmitic acid (C16:0), stearic acid (C18:0) and oleic acid (C18:1). Combinations of these fatty acids make up three main triacylglycerol (TAG) types – 2-oleopalmitin (POP), 2-oleopalmitostearin (POS) and 2-oleodistearin (SOS) – constituting approximately 80% of triacylglycerols in cocoa butter (Timms, 2003). Upon proper tempering, these triacylglycerols can form β′ polymorph crystals with a melting point just below human body temperature. It is this unique blend of triacylglycerols that gives cocoa butter its desirable masticatory melting behavior and consistency. Owing to the high cost of cocoa butter and an increasing demand for confectionery products, confectioners may blend other natural edible fats with one or more triacylglycerols that are similar to cocoa butter with the cocoa butter itself. These are termed *cocoa butter equivalents* (CBE), and include sal butter, mango butter, kokum butter, illippe butter, shea butter and palm mid fraction. The quality of these CBE fats is of great concern to most confectioners, as the composition of certain minor components in these fats greatly interferes with the crystal formation of these triacylglycerols.

Cebula and Smith (1992) reported on the possible use of DSC for the detection of two minor components, diacylglycerol (DAG) and tripalmitin (PPP), which, if present in CB-CBE blends, can cause changes in the crystallization properties of the overall fat. They found that even the presence of about 4.4% of DAG and 3.9% of PPP in the CBE led to a distinct increase in peak sharpness and area in the cooling curve (Figure 15.5). The heating curves (Figure 15.6) revealed changes in peak formation. The small trailing shoulder increased as the concentration of PPP increased while that of DAG decreased. This is because the presence of elevated levels of trisaturated TAGs (such as PPP and DAG) had increased the rate of crystallization at the early stages. In addition, the crystallization of DAG causes retardation in polymorphic transitions of TAG on heating. The data collected from this work are useful in further applying this thermal technique for the detection of adulterated oils and fats.

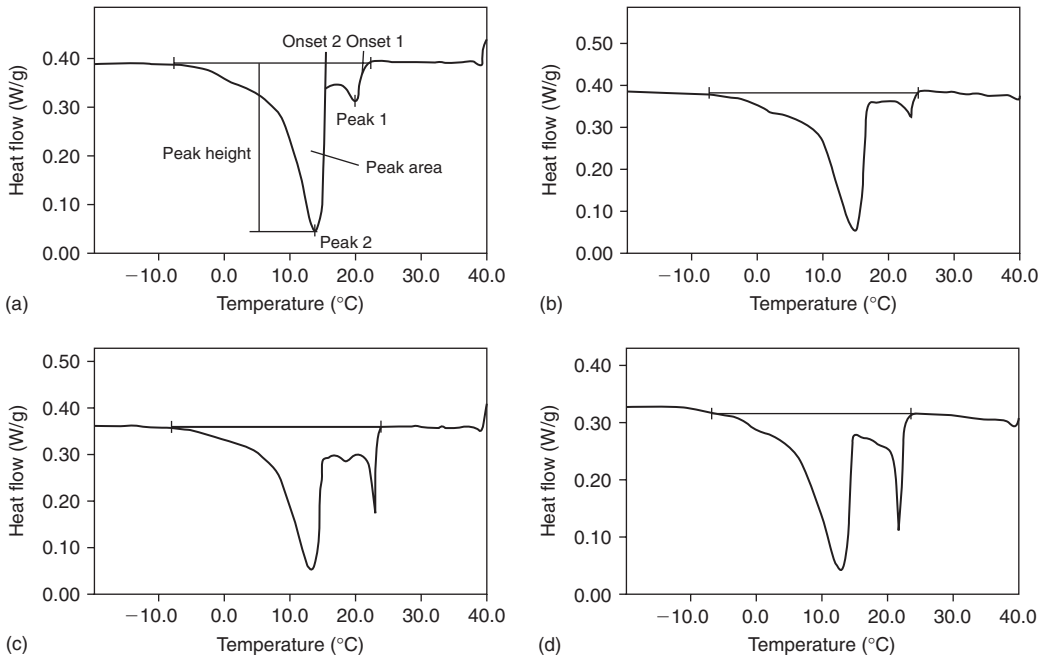

Figure 15.5 DSC cooling curves of (a) coberine, (b) coberine + 4.4% diacylglycerol (DAG), (c) coberine + 3.9% enriched tripalmitin (PPP), and (d) coberine + 4.4% DAG + 3.9% PPP. Source: Cebula and Smith (1992).

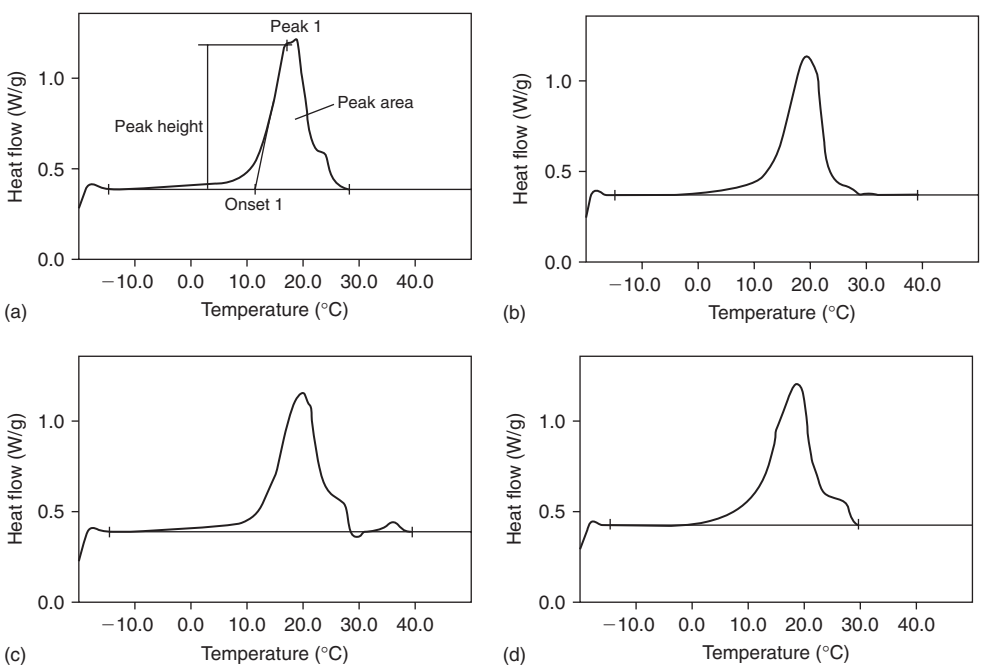

Figure 15.6 DSC heating curves of (a) coberine, (b) coberine + 4.4% diacylglycerol (DAG), (c) coberine + 3.9% enriched tripalmitin (PPP), and (d) coberine + 4.4% DAG + 3.9% PPP. Source: Cebula and Smith (1992).

Vegetable oils

The vegetable oil market is the largest part of the world edible-oils market pie, with over 121 million metric tonnes produced globally in 2006, with the expectation of expansion beyond the 126 million tonnes mark by the end of 2007 (USDA, 2007). In 2006, the major vegetable oils included palm oil (36.8 million tonnes), soybean oil (35.9 million tonnes), rapeseed oil (17.8 million tonnes), sunflower seed oil (10.8 million tonnes), peanut oil (4.9 million tonnes), cottonseed (4.7 million tonnes), palm kernel oil (4.6 million tonnes), coconut oil (3.3 million tonnes) and olive oil (3 million tonnes). Based on these figures, it is clear that huge quantities of vegetable oils are being traded on the market daily throughout the world. This makes it difficult to monitor deceitful traders who blend these vegetable oils with other cheaper fats. As with other consumer products, certain quality control measures have to be in place to provide a continual check for any discrepancies and to verify the genuineness of claims made by traders for these vegetable oils.

In a multi-religious and multicultural world, it is essential that vegetable oils are authenticated as being free of any animal fats, particularly lard and beef tallow. Therefore, reliable methods for the detection of such adulterants are necessary for the vegetable oil industry to be able to verify the true composition of oils. Several studies have been published that describe the use of DSC for the detection of animal fats, such as lard, beef tallow and chicken fat, in palm oil and canola oil (Marikkar *et al*., 2001, 2002a, 2002b, 2003a).

Marikkar *et al*. (2002a) described the use of heating and cooling curves to monitor the presence of lard, beef tallow and chicken fat as adulterants in canola oil. Canola oil samples were separately spiked with lard, beef tallow and chicken fat in a concentration range of 1–20%. Gradual changes could be observed in the cooling curves as the concentration of the adulterants increased (Figure 15.7). The cooling curve of pure canola oil was shown to have a major exothermic peak at −60.8°C and two

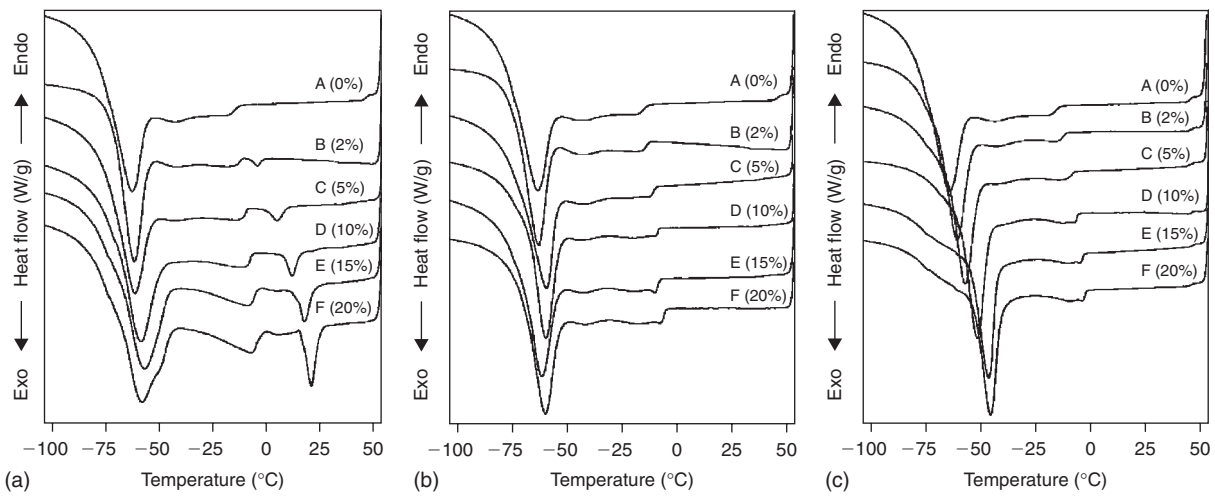

Figure 15.7 Comparison of DSC cooling curves of canola oil blended with (a) beef tallow, (b) chicken fat and (c) lard at various concentrations. Source: Marikkar *et al*. (2002a).

minor peaks at −40.5 and −17.0°C, and no peaks were found in the temperature region beyond −10.7°C (Figure 15.7). As the canola oil was blended with even a small amount of beef tallow, peaks corresponding to higher melting-point triacylglycerols started to appear in the higher-temperature region of the cooling curve. However, Marikkar *et al*. (2002a) noted that the visibility of this higher temperature peak was not detectable at an adulterant concentration of below 2%. As the adulterant concentration increased to 20%, the peak was found gradually to increase in size, and shifted slightly towards a higher temperature. This peak was only applicable to beef tallow, as no similar observations were found for the samples adulterated with chicken fat and lard. In the samples adulterated with chicken fat and lard, peaks at −17, −40.5 and −60.8°C were significantly influenced by the adulterants. The peak at −40.5°C was found to have gradually disappeared, while the peak at −17°C had increased in size, resulting in a broader peak shifting towards a higher temperature. The peak at −60.8°C was the most influenced by the increasing presence of chicken fat and lard. As the percentage of chicken fat and lard increased in the sample, this peak was noted to increase in peak width and shift towards a higher temperature. Unfortunately, the cooling curves of chicken-fat-adulterated canola oil and lard-adulterated canola oil were not significantly different from each other, making it almost impossible to distinguish between adulteration with chicken fat and that with lard. Marikkar *et al*. (2002a) also reported that no discrimination was found with these data, even after subtractive procedures carried out by using the DSC software, and it was necessary to look into the possibility of using the heating curves for differentiation.

The heating curves of canola oil adulterated with 2–20% of beef tallow, chicken fat and lard are shown in Figure 15.8. In the absence of any adulterants, the melting profile of canola oil is characterized by two overlapping peaks; a larger and higher temperature transition at −17.8°C, and a smaller and lower temperature transition

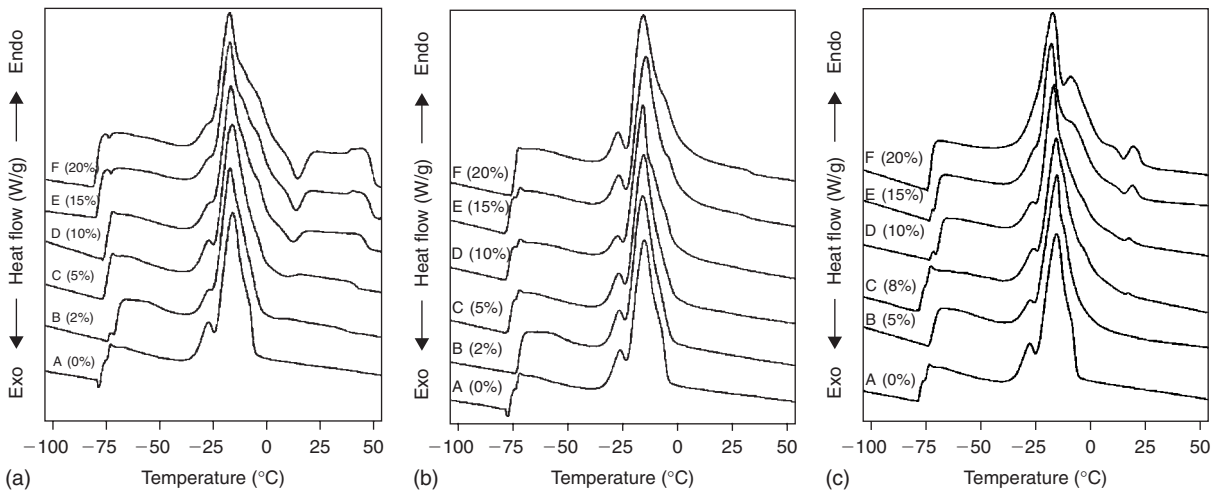

Figure 15.8 Comparison of DSC heating curves of canola oil blended with (a) beef tallow, (b) chicken fat and (c) lard at various concentrations. Source: Marikkar *et al*. (2002a).

at −28°C. Complete thermal transition of canola oil was observed at −5.5°C; beyond this point, no further thermal transition was found. In the canola oil samples adulterated with chicken fat and lard, significant differences in heating profiles were reported. Marikkar *et al*. (2002a) noted that the minor peak at −28°C of canola oil was affected by the addition of beef tallow and lard. As the concentration of these adulterants increased to 20%, this peak gradually overlapped with the neighboring major peak. However, this trend was not significant for the chicken fat adulterant, and thus cannot be used to detect the presence of chicken fat in canola oil. At the higher temperature region, from −5.5 to 50°C, interesting and distinct features that reflect the nature of adulterants of beef tallow and lard were seen, but not of chicken fat. This work has made it possible to use DSC to detect the presence of beef tallow and lard as adulterants in canola oil, but failed to establish the presence of chicken fat under the specific conditions of the study.

In a similar development, Marikkar *et al*. (2003a) published DSC data on the detection of beef tallow, chicken fat and lard in palm olein. The animal fats used in this study were at concentrations ranging from 1 to 20%. The detection of the adulterants in palm olein was solely established using cooling profiles. Based on the results of the previous study, it can be expected that the cooling curve of palm olein will be altered in a systematic way by increasing the concentration of the adulterant fat. Indeed, these changes were clearly evident in the cooling curves of palm olein and its mixtures with beef tallow, chicken fat and lard (Figure 15.9). Marikkar *et al*. (2003a) reported that a shoulder peak at −54.8°C was shown to be very sensitive to animal fat adulteration of palm olein. This peak was found to disappear when the adulteration level of the sample exceeded 3%. Pure palm olein does not show any peak beyond its major exothermic peak at 1.5°C. Upon adulteration with beef tallow, a new peak at the region between 8.5 and 19°C was observed (Figure 15.9). Marikkar *et al*. (2003a) hypothesized that this feature could be an indication of beef tallow adulteration in palm olein, since such a peak did not appear in all of the chicken fat and lard adulterated samples that were tested. As for the samples containing chicken fat and lard, a shoulder peak started to appear at the lower temperature region of the cooling curve (Figure 15.9) as the level of adulterant increased. At the same time, the disappearance of another shoulder peak at −54.8°C was reported. Upon comparison of the peak temperatures, Marikkar *et al*. (2003a) noted that the maximum peak temperatures of the shoulder peaks corresponding to the adulteration of chicken fat and lard were close. Another important observation regarding the effect of chicken fat and lard on the cooling curves is the shift of the peak corresponding to the lard adulterant towards the higher temperature region, and the shift of the peak corresponding to chicken fat towards the lower temperature region, as the concentration of the corresponding adulterant increases. This feature may be attributed to the different physical and chemical properties of chicken fat and lard. To further confirm the accuracy of the detection method, Marikkar *et al*. (2003a) applied subtractive procedures using the DSC software to the data, and the resulting curves are shown in Figure 15.10. The data clearly show that the adulteration of lard on palm olein caused a slight augmentation of its principal peak while showing an additional shoulder peak at the lower temperature region. On the contrary, the presence of chicken fat in palm olein

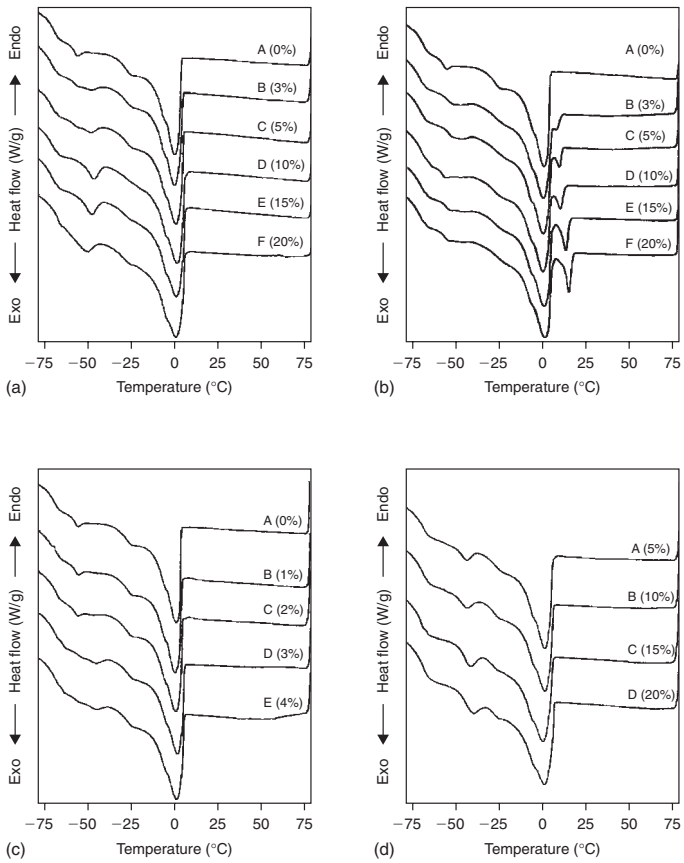

Figure 15.9 Comparison of DSC cooling curves of palm olein blended with (a) beef tallow, (b) chicken fat and (ci & ii) lard at various concentrations. Source: Marikkar *et al*. (2003).

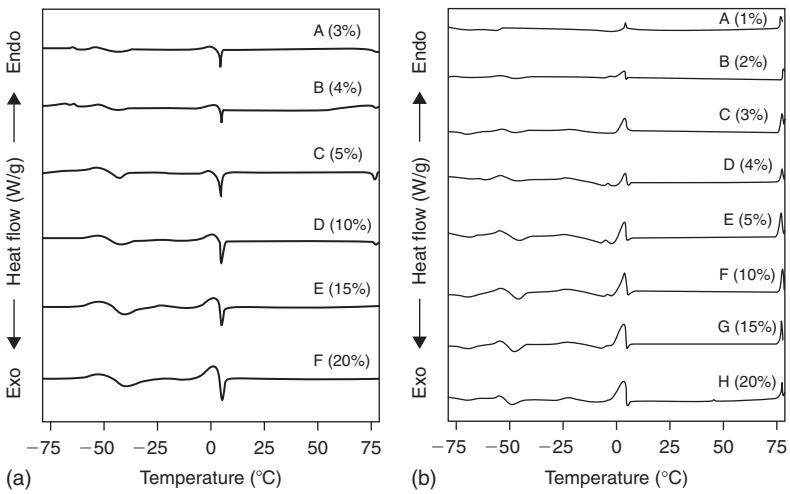

Figure 15.10 DSC subtracted curves of palm olein blended with (a) lard and (b) chicken fat at various concentrations. Source: Marikkar *et al*. (2003).

caused a slight reduction in the principal peak while creating an additional shoulder peak at the lower temperature region. This distinction in subtractive curves could be used as a means of differentiating lard adulteration from chicken fat adulteration in palm olein.

Marikkar *et al*. (2001) carried on further studies to determine whether the alteration of the fatty acid positions of lard triacylglycerols by chemical randomization would have an effect in the detection of lard adulteration in palm oil. It is known that blending of lard into vegetable oils can also be performed using randomized lard in place of genuine lard, as randomization has been shown to improve the physical properties of lard (Sreenivasan, 1978). Lard extracted from the adipose tissues of pig was chemically interesterified in the presence of sodium methoxide as a catalyst. In this work, Marikkar *et al*. (2001) also focused their attention on the cooling characteristics of the adulterated samples. A comparison of cooling profiles of genuine lard, chemically randomized lard, beef tallow, mutton tallow and chicken fat revealed significant differences between lard and the other animal fats (Figure 15.11). The cooling curves of both genuine and chemically randomized lard indicated two major exothermic peaks at 4.9 and −16.9°C, and 10.4 and −16.1°C, respectively. As for

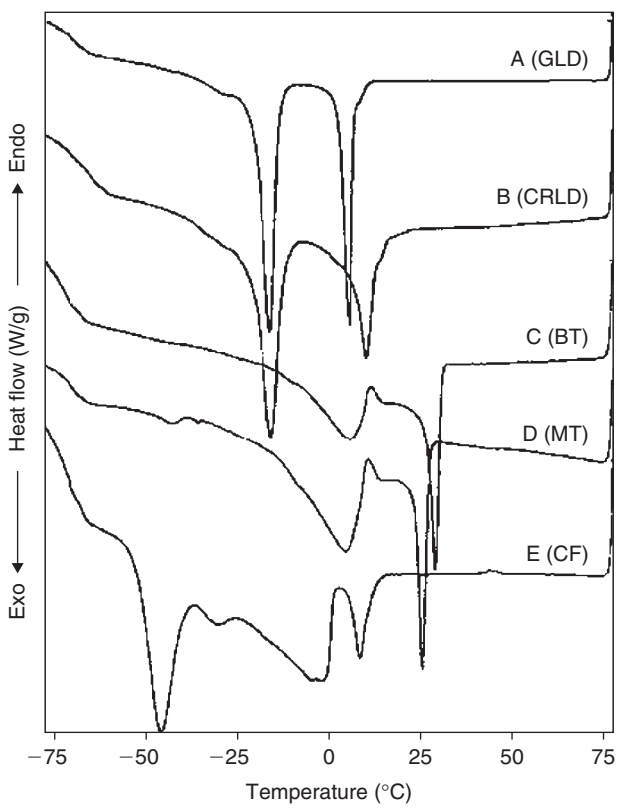

Figure 15.11 DSC cooling curves of lard (A), chemically randomized lard (B), beef tallow (C), mutton tallow (D) and chicken fat (E). Source: Marikkar *et al*. (2001).

the cooling curve of palm oil, two major exothermic peaks at 17.8 and 1.3°C and two smaller shoulder peaks at −6.8 and −43.9°C were exhibited (Figure 15.12). From the data obtained, it is apparent that the chemical randomization of lard resulted in a slight peak broadening and changes in peak height and position. In the palm oil samples adulterated with 1–20% of genuine and chemically randomized lard, certain peak variations were noted (Figure 15.12). Marikkar *et al*. (2001) noted that the shoulder peak at −43.9°C is of particular interest, as it was observed to be sensitive towards lard or randomized lard adulteration in palm oil. As the level of adulteration increased from 1 to 20%, the peak area was found to increase and a shift in maximum peak temperature towards a higher temperature region was detected. Marikkar *et al*. (2001) believed that a particular group of lower melting-point triacylglycerols common to palm oil and lard or randomized lard was the cause of the shoulder peak

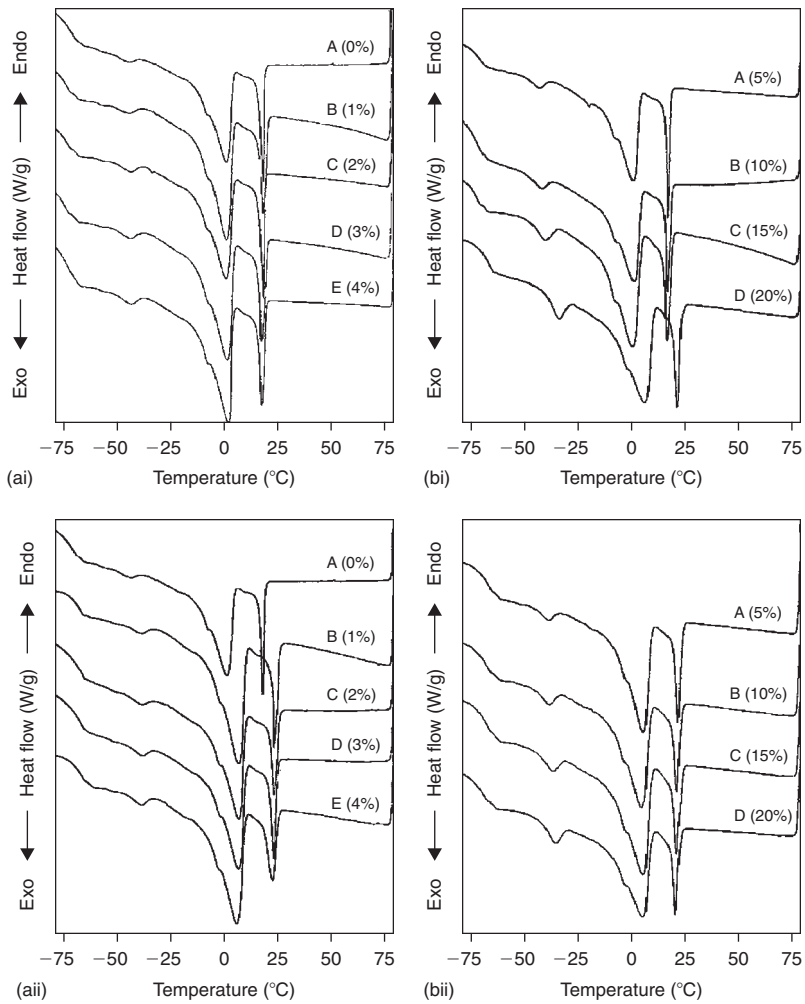

Figure 15.12 Comparison of DSC cooling curves of palm oil blended with (ai & ii) lard and (bi & ii) chemically randomized lard at various concentrations. Source: Marikkar *et al*. (2001).

augmentation, while the shift of the peak temperature was due to the fact that the oil samples behaved as a binary mixture after being adulterated with genuine or chemically randomized lard. A stepwise multiple linear regression analysis showed good correlation between the concentrations of genuine or chemically randomized lard adulterants from 1 to 20% and the peak parameters. Apart from using lard as an adulterant, Marikkar *et al*. (2001) also investigated the effects of other animal fats, such as beef tallow, mutton tallow and chicken fat, as adulterants on palm oil (Figure 15.13). When blended at concentrations from 2 to 20%, the cooling curves of both beef and mutton tallow did not reveal any peaks that were caused by their adulteration like those found in the lard-adulterated palm oil samples. In the case of the palm oil sample adulterated with chicken fat, the peak caused by the adulteration was reported to be at a position closer to the lard adulteration peak. However, a simple statistical test was conducted and confirmed that these two peaks were significantly distinguishable.

In another related work, Marikkar *et al*. (2002b) conducted a study to look into the effect of enzymatically interesterified lard as an adulterant on the cooling curves of adulterated palm oil. Results from the fatty acid and triacylglycerol composition analyses revealed that the palmitic acid at the *sn*-2 fatty acid position of genuine lard was partially replaced with oleic acid, thereby decreasing the ratio of saturated to unsaturated fatty acids in the *sn*-2 position of the triacylglycerol of enzymatically interesterified lard. A comparison of cooling curves between both genuine and enzymatically interesterified lard indicated that there are clear differences between the two fats, which could be attributed to the changes in their triacylglycerol profiles (Figure 15.14). The cooling curves of the lard-palm oil blends containing from 0.2 to 20% of enzymatically interesterified lard showed variations in transition temperatures (Figure 15.15). A typical cooling curve of an unadulterated palm oil has

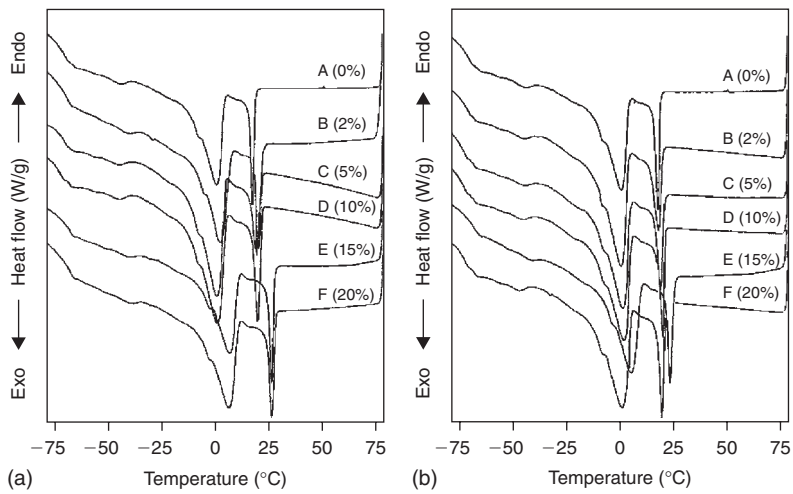

Figure 15.13 Comparison of DSC cooling curves of palm oil blended with (a) beef tallow and (b) mutton tallow at various concentrations. Source: Marikkar *et al*. (2001).

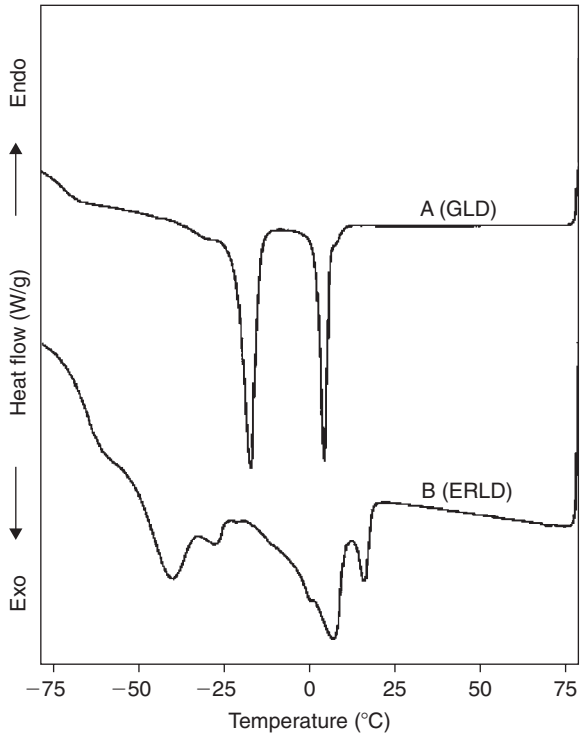

Figure 15.14 DSC cooling curves of lard (A) and enzymatically randomized lard (B). Source: Marikkar *et al*. (2002b).

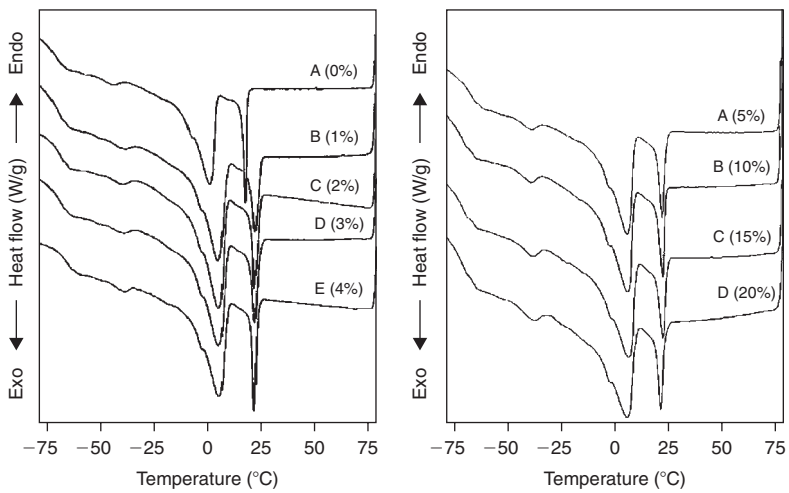

Figure 15.15 Comparison of DSC cooling curves of palm oil blended with enzymatically randomized lard at various concentrations. Source: Marikkar *et al*. (2002b).

two major peaks at 17.75 and 1.25°C and two minor peaks at −6.82 and −43.86°C. Marikkar *et al*. (2002b) added that the shoulder peak appearing at −43.86°C is sensitive towards the effects of adulteration caused by either genuine or chemically randomized lard. This observation was clearly indicated in the cooling curves of

the adulterated samples, as the peak gradually and proportionally increases in size with the concentration of adulterant. As a result, Marikkar *et al*. (2002b) were able to obtain a good correlation between the concentration of lard in the adulterated palm oil sample and the corresponding peak parameters. In an attempt to develop a quantitative relationship between the cooling curve and the concentration of adulterant, Marikkar *et al*. (2002b) investigated three independent variables (namely peak area, peak height and peak onset) on the dependent variable, i.e. the concentration of adulterant, by subjecting the data to a stepwise multiple linear regression analysis. The results revealed that changes in peak area for samples containing less than 1% of enzymatically interesterified lard were insignificant, thereby negating the possibility of applying this method for lard detection in samples containing less than 1% of the adulterant. Marikkar *et al*. (2002b) also commented on the fact that this DSC method was able to distinguish between adulteration of palm oil with lard from that with other animal fats, such as beef tallow, mutton tallow and chicken fat.

Butterfat

Butter is another fat that is widely consumed throughout the world. The production of butter involves the churning of fresh or fermented cream or milk. Butterfat is a highly saturated oil with significant amounts of C4–C14 fatty acids. Owing to the high cost of butter, margarine has often been used as a cheaper alternative fat. For the same reason, certain unscrupulous and unethical manufacturers market butter that has been adulterated with less expensive vegetable or animal fats. In the past, various analytical methods for the detection of non-dairy fats in butter were successful in detecting the presence of vegetable fats (International Dairy Federation, 1965, 1966); however, very few methods were able to recognize animal fats as adulterants in butterfat and most of these were either difficult to perform or time-consuming (Timms, 1980; Geeraert and Sandra, 1985). Furthermore, the natural variability of butterfat composition, due to the difference in the diet of the animals, compounds the existing problems of data interpretation. Many trials have been conducted in an attempt to establish the relationship between fatty acid profiles and the integrity of butter, but the validity of these analytical methods are controversial (Muuse *et al*., 1986; Precht, 1990). It is also reported that an animal fat adulterant of up to 10–15% in butter cannot be proven by fatty acid analysis because of their natural variations (Gray, 1973; Biliaderis, 1983). Moreover, the fact that most of the animal fat adulterants present in butter are usually at levels below 10% makes it almost impossible to use fatty acid analysis to determine whether or not the butter has been adulterated.

The disadvantages of such methods prompted Coni *et al*. (1994) to work on the application of DSC to detect fraudulent practices in butter production and monitor the authentication of butter. Coni *et al*. (1994) investigated the detection of chicken fat in butter at concentrations of 2, 5, 10, 15 and 20% using DSC. Heating curves of the samples were complex and not easily interpretable. Furthermore, the tempering procedures and storage temperature of butter have been reported to affect heating curves significantly (Sato *et al*., 1989). Therefore, Coni *et al*. (1994) decided to use the cooling curve, which is influenced only by the chemical composition of the sample and not by the initial crystalline state, for their work. The results revealed that

the DSC is an efficient method for characterizing pure animal fats as well as their mixtures (Figure 15.16). Figures 15.16(a) and 15.16(b) show the cooling curves of pure butterfat and chicken fat, respectively, while Figure 15.16(c) indicates the cooling curve of a mixture of butterfat and 20% chicken fat. Based on these data, distinct differences between pure butterfat and pure chicken fat can be observed, but not in the case of the fat mixture. A further data processing step, subtracting the normalized butterfat curve from the normalized butterfat/chicken fat mixture, is required to show statistically acceptable differentiation. The resulting curves show a small peak at approximately −12°C (Figure 15.17), and the area of this peak was found to be directly proportional to the amount of chicken fat added to butterfat. Figure 15.18 indicates that good linear correlation can be obtained between the exothermic peak and the range of compositions that are of practical interest (2–20%).

Several years later, Aktaş and Kaya (2001) reported on the detection of beef tallow and margarine in butterfat by DSC. Aktaş and Kaya (2001) investigated the effects

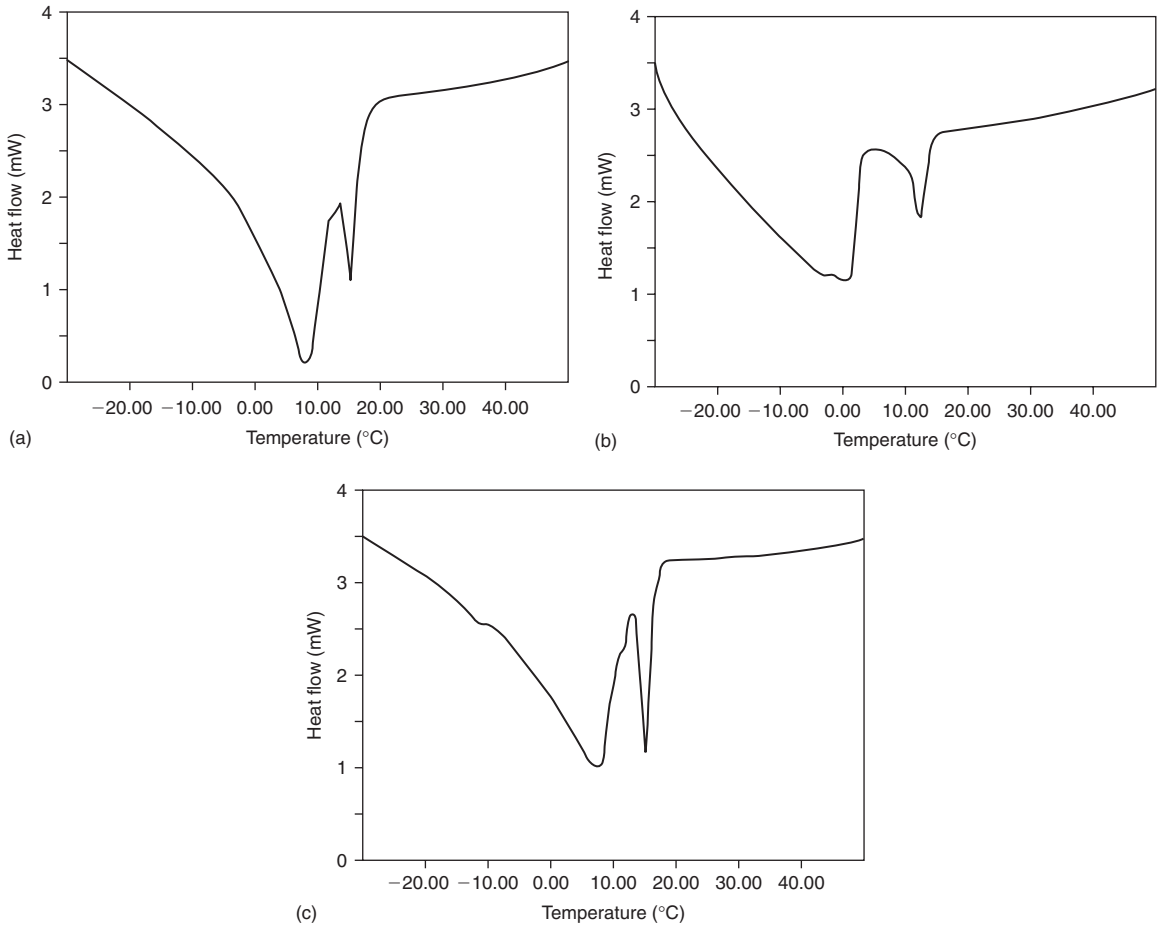

Figure 15.16 DSC cooling curves of (a) pure butterfat, (b) pure chicken fat and (c) butterfat blended with 20% chicken fat. Source: Coni *et al*. (1994).

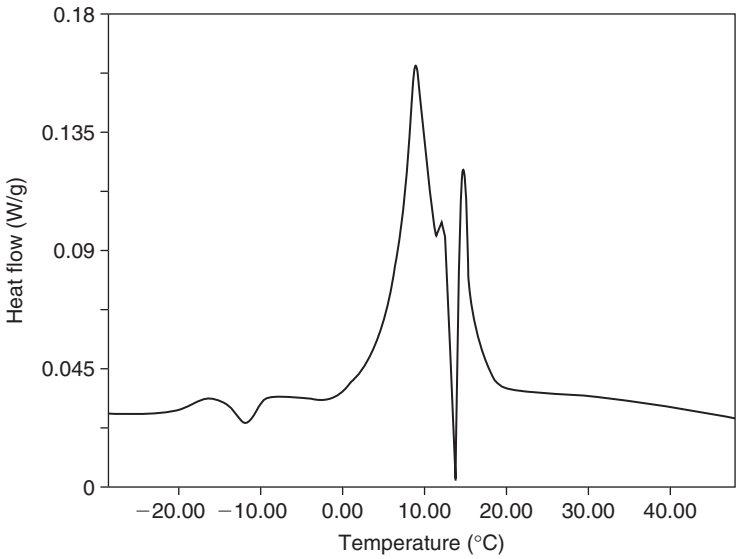

Figure 15.17 DSC subtracted curve of pure butterfat and butterfat blended with 20% chicken fat. Source: Coni *et al*. (1994).

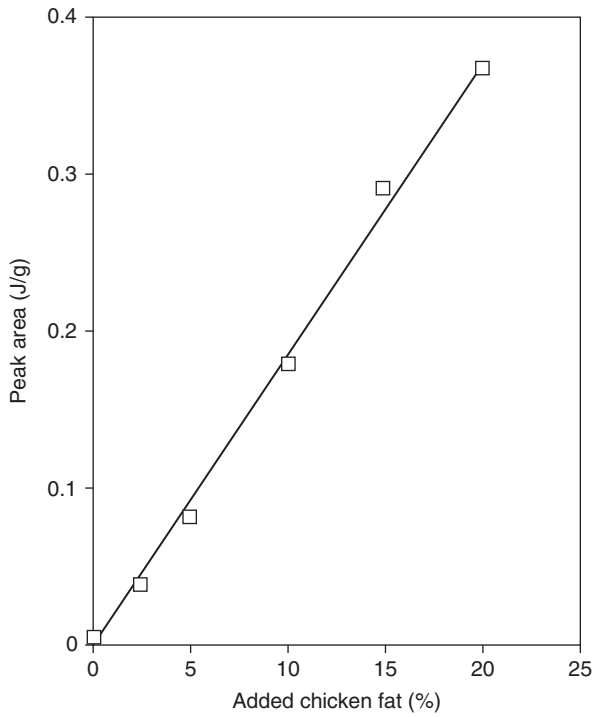

Figure 15.18 Correlation between mean values of peak area and concentration of chicken fat in butterfat. Source: Coni *et al*. (1994).

of 5, 10 and 20% beef tallow and margarine in butterfat on the DSC curves. The heating and cooling curves of pure butterfat, margarine and beef tallow are shown in Figure 15.19, while those of the mixtures are shown in Figure 15.20. From the results obtained, it is clear that the DSC curve of beef tallow is different from those of butterfat and margarine, while some differences between margarine and butterfat can be noted. The addition of 5, 10 and 20% of beef tallow or margarine to butterfat caused significant changes, especially between 10 and 20% concentrations, in the DSC heating and cooling curves of butterfat. In the cooling curves, changes in the peak areas of two peaks at temperatures of 6–7°C and 11–16°C were observed as the proportion of beef tallow or margarine increased. The major differences in the curve shape as a result of the presence of beef tallow or margarine content were manifested in the smaller peak. In general, the peak sharpness, broadness and area are increased as the adulterant concentration increases, and the effect was noted to be greater in the sample containing beef tallow. Similar to the observations by Coni *et al*. (1994),

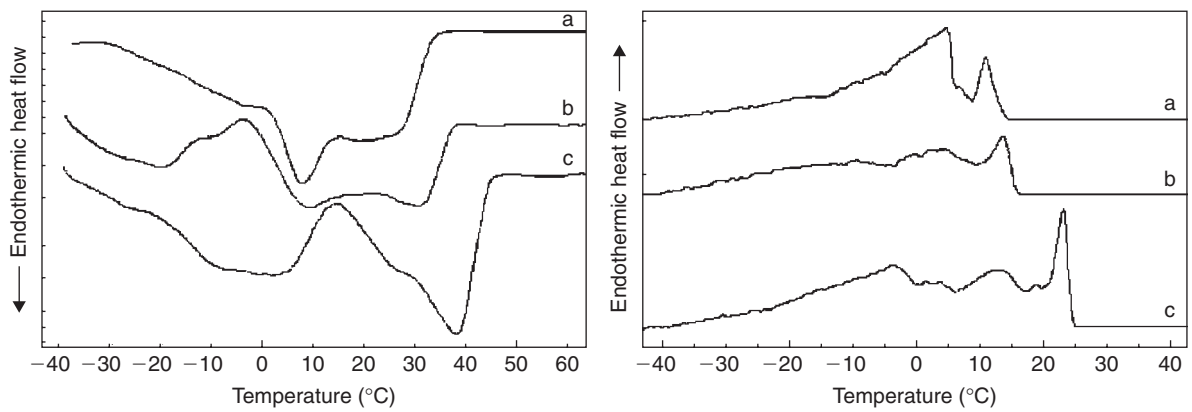

Figure 15.19 DSC heating and cooling curves of (a) butterfat, (b) margarine and (c) beef tallow. Source: Aktaş and Kaya (2001).

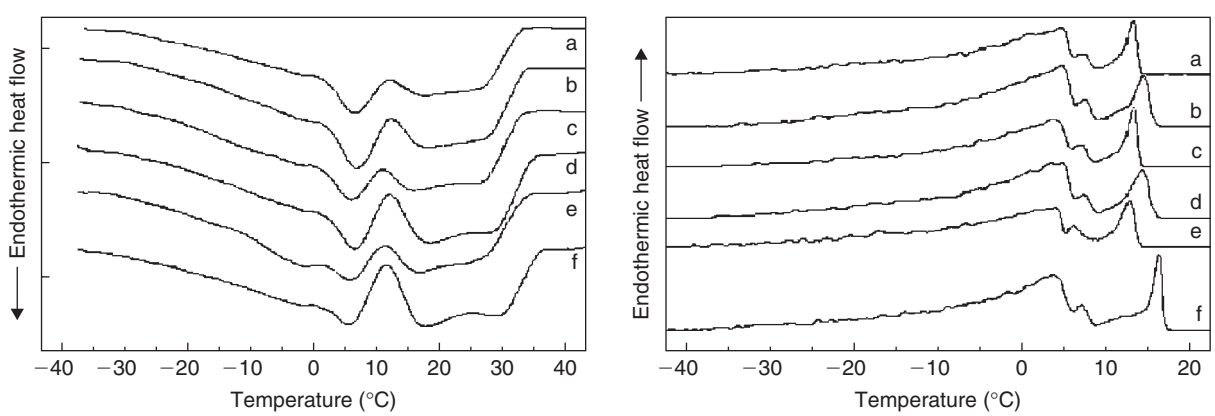

Figure 15.20 DSC heating and cooling curves of (a) butterfat + 5% margarine, (b) butterfat + 10% margarine, (c) butterfat + 20% margarines, (d) butterfat + 5% beef tallow, (e) butterfat + 10% beef tallow, and (f) butterfat + 20% beef tallow. Source: Aktaş and Kaya (2001).

linear correlation between the peak areas and the level of adulterants was found for the beef tallow adulterant. However, in the case of the margarine adulterant, a non-linear relationship was observed.

From these studies, it can be concluded that the use of DSC as a tool for the detection of adulterant fats of animal origin in butter is quite promising and straightforward, but this is not the case for margarines. The detection of margarines as an adulterant in butter using the DSC technique alone may not be sufficient to conclude its presence. Further analytical techniques are required and should be used in combination with the DSC data in order to allow valid conclusions regarding the authentication of butter.

Fried foods

Edible oils and fats are widely used for frying applications. Frying is an ancient but popular way of cooking, especially in Spain and the other Mediterranean countries. Fried foods can also be found in the menus of most fast-food outlets throughout the world. The frying process involves the transfer of heat, moisture and fat both within and around the food.

In the past, lard and other animal fats have been used as frying fats for a variety of foodstuffs (Weiss, 1983). It was only when reports were published on the adverse health effects of the high amounts of saturated fatty acids and cholesterol in these animal fats that there was a shift towards the use of vegetable fats as a frying medium (Love, 1996). Apart from health reasons, though, one of the main motivations leading to the development of methods for the authentication of fried foods has been the strict religious proscription regarding lard (Rashood *et al*., 1995). Marikkar *et al*. (2003b) investigated the detection of lard in fried foods. Peanuts, tempeh, chicken and beef slices were subjected to frying in lard at 180°C. Fats from the samples were then extracted and underwent further analysis using GC, HPLC and DSC. The DSC data (Figures 15.21–15.25) showed significant differences between the heating and

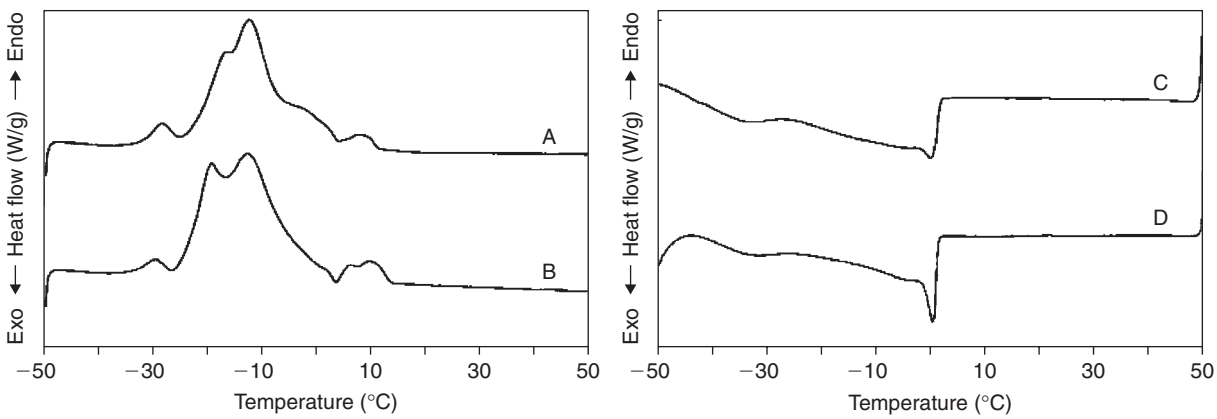

Figure 15.21 DSC heating curves of peanut fried in lard (A), peanut oil (B), and DSC cooling curves of peanut oil (C) and peanut fried in lard (D). Source: Marikkar *et al*. (2003b).

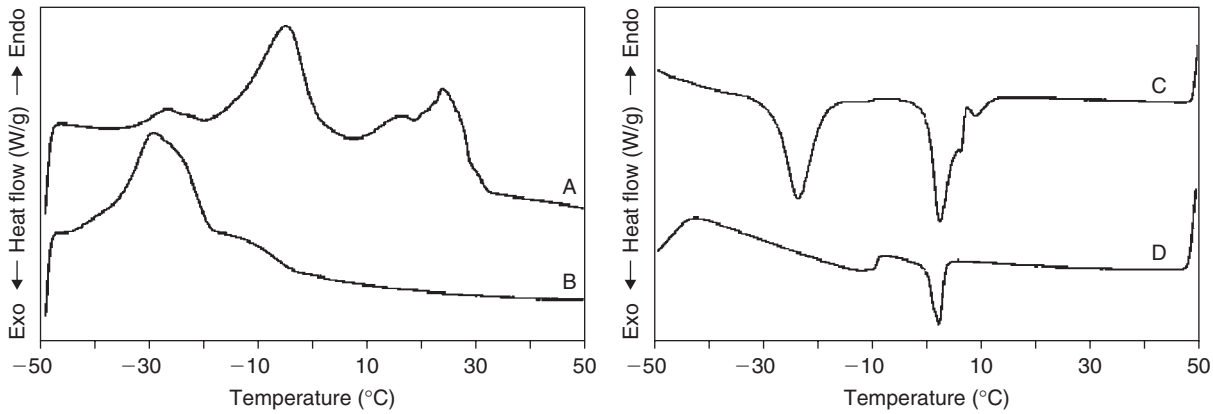

Figure 15.22 DSC heating curves of tempeh fried in lard (A), tempeh oil (B), and DSC cooling curves of tempeh fried in lard (C) and tempeh oil (D). Source: Marikkar *et al*. (2003b).

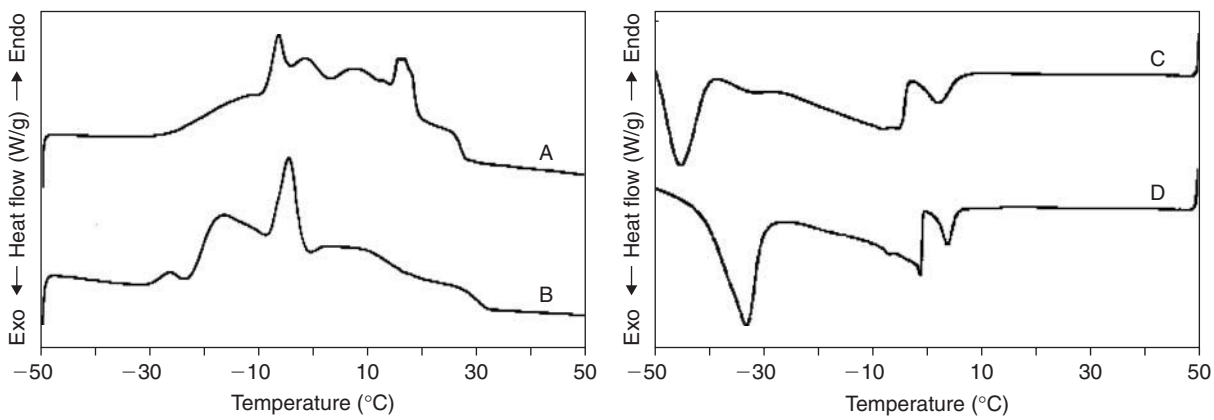

Figure 15.23 DSC heating curves of chicken fried in lard (A), chicken fat (B), and DSC cooling curves of chicken fat (C) and chicken fried in lard (D). Source: Marikkar *et al*. (2003b).

cooling profiles of the fat extracted from the fried foodstuff and the native oil present in the foodstuff itself. Lard adulteration when cooking tempeh and chicken resulted in a distinct endothermic peak at 22–23°C, while the adulterant in beef could only be detected in the subtracted curve (Figure 15.25). Marikkar *et al*. (2003b) also suggested that the use of cooling curves would be a better option for determining beef fried with lard, since a clear distinct adulteration peak emerged at lower temperatures. Detection of lard in the fried peanut sample was not possible by DSC alone.

Edible waxes and wax esters

Waxes have long been used in fruits and vegetables as a protective layer against water loss, for prevention of rot or mould infestation, and to provide a more appealing glazed or shiny appearance. The waxes that are commonly used in these foodstuffs are all derived from natural sources and have mandatory certification by the

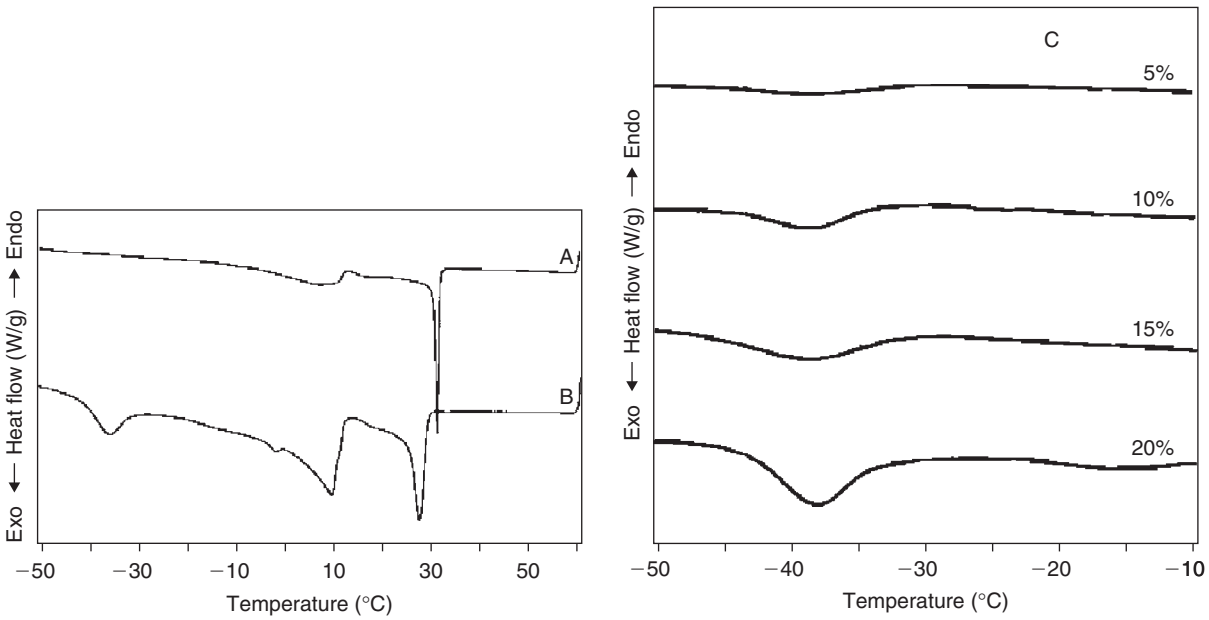

Figure 15.24 DSC cooling curves of beef tallow (A), beef fried in lard (B), and rescaled cooling curves of beef tallow adulterated with various proportions of lard (C). Source: Marikkar *et al*. (2003b).

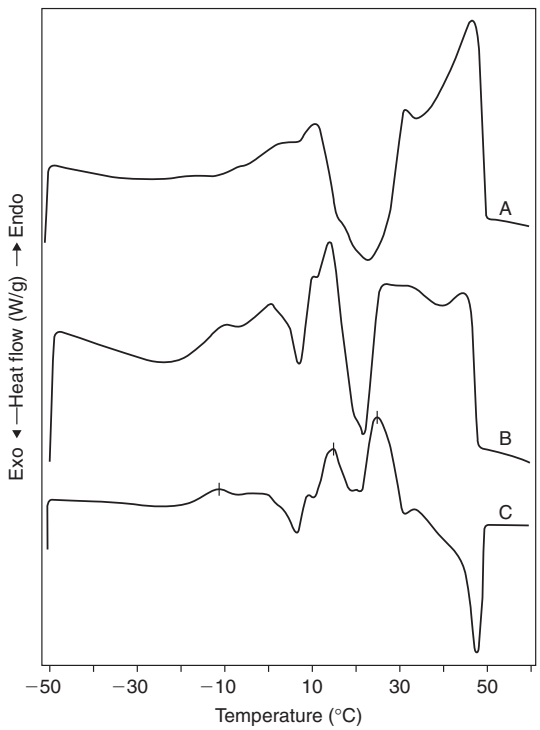

Figure 15.25 DSC heating curves of beef tallow (A), beef fried in lard (B), and subtracted DSC curve of beef fried in lard (C). Source: Marikkar *et al*. (2003b).

United States Food and Drug Administration (USFDA) to confirm their safety for human consumption. Some of the natural waxes approved by the USFDA for use as a food additive in the food industry include beeswax (E901), candelilla wax (E902) from the reed-like dessert plant of the genus *Euphorbia*, carnauba wax (E903) from the leaves of a Brazilian palm, shellac (E904), rice-bran wax (E908), and esters of colophonium (E915) from the resin of pine trees; some mineral waxes, such as paraffin wax (E905), microcrystalline wax (E905b) from the de-oiling of petrolatum, crystalline wax (E907) and oxidized polyethylene wax (E914) have also been approved.

In many apple-producing countries, these food-grade waxes are constantly used to coat the apples to protect them from dehydration and rot. In order to do this, the apples are submerged in or sprayed with a wax emulsion and then dried before packing. In compliance with the food additive laws and directives in most regions, the required amount ("*quantum satis*") of these glazing agents (such as E901, E902, E903 and E904, which are approved for the coating of apple surfaces) must be clearly defined. However, the detection of these coating agents on apples by conventional chromatographic methods is not easy, as the components of beeswax, candelilla wax and carnauba wax are very similar to those components found in the genuine surface wax of apples. These compounds consist of a wide range of lipid classes, such as hydrocarbons, wax esters, carbonyls, long-chain alcohols and triterpenecarbonic acids, in varying proportions (Ritter *et al.* 2001). Conventional chromatographic techniques could not provide a satisfactory quantitative analysis regarding the detection of these waxes on apples. Ritter *et al*. (2001) were successful in using the DSC technique for the detection of beeswax, candelilla wax, carnauba wax and shellac on the surfaces of various cultivars of apples, with clear and divergent curves (Figure 15.26) obtained. The temperature at the peak maximum and the phase transition enthalpy were used as the main parameters for the detection. The average peak maximum temperature and phase transition enthalpy of genuine surface wax of 10 apple cultivars were 64.4°C and $82\,J\,g^{-1}$, respectively. In samples of apples coated with beeswax, candelilla wax, carnauba wax and shellac, the average peak maximum temperatures and phase transition enthalpies were 68°C and $136–165\,J\,g^{-1}$, 77°C and $116–161\,J\,g^{-1}$, 89°C and $127–162\,J\,g^{-1}$, and 76–89°C and $141–208\,J\,g^{-1}$, respectively. This study also confirmed the suitability of DSC as a screening method for detecting mixtures of coating agents and apple wax, as well as the presence of illegal coating agents such as paraffins, montanic acid esters and oxidized polyethylene wax on apples.

Honey

Honey is a sweet and viscous liquid that is composed of fructose, glucose, water, trace enzymes, minerals, vitamins and amino acids. Historically, honey has been mixed with various ingredients such as flour, paraffin wax, glucose and sucrose. In the 1970s, the emergence of high-fructose corn syrup (HFCS) encouraged further adulteration of honey. HFCS is an isoglucose syrup obtained from the enzymatic processing of vegetable carbohydrates such as corn, wheat, beet and cane. Of the various types of HFCS, HFCS 55 (containing approximately 55% fructose and 45%

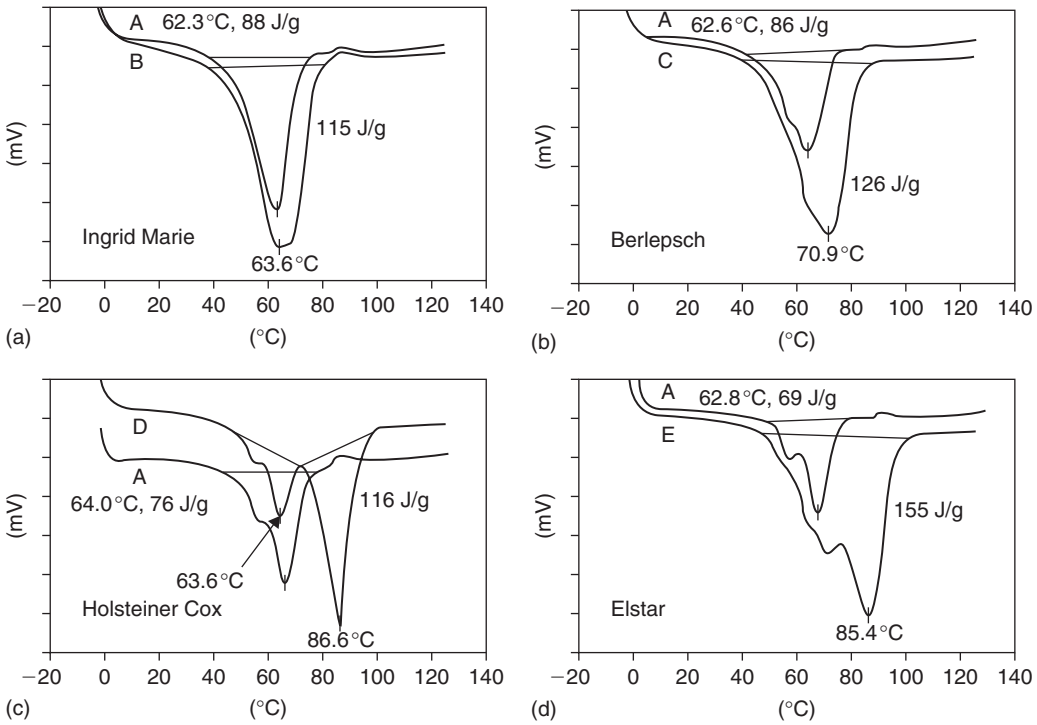

Figure 15.26 DSC cooling curves of apple wax samples and mixtures: cultivar apple wax (A); and mixtures with beeswax (B), with candelilla wax (C), with carnauba wax (D) and with shellac (E). Source: Ritter *et al*. (2001).

glucose) has been the choice for honey adulteration because its sugar composition is similar to that of honey. Later, in the 1980s, the wide availability of these complex isoglucose syrups resulted in its extensive use in the adulteration of honey. The addition of these syrups to honey leads to lower-quality honey products. Therefore, great efforts have been made to develop analytical methods for the detection of these adulterants. Of the methods developed to examine the authenticity of honey, none was dedicated to the overall characterization of these isoglucose syrups. Conventional chromatographic methods could not distinguish between the sugar profiles of honey and these syrups. Kerkvielt *et al*. (1995) and Kerkvielt and Meijer (2000) worked on an alternative technique for the detection of visible exogenous elements in honey by microscopic analysis. This method was adapted for the characterization of adulteration by cane sugar and cane-sugar products. However, it does have its drawbacks, as these vegetative key markers (such as sclerous rings or epidermic cells and others) may be removed by microfiltration (Antinelli *et al*., 2001). The application of stable carbon isotope ratio for the detection of adulterated honeys was also reported (White and Winters, 1989; White, 1992; White *et al*., 1998). This method applies only for the detection of C-4 plant sugar syrups. Cordella *et al*. (2002) reported on various limitations, in terms of pH, conductivity, humidity and acidity, of the methods defined both in the Codex Alimentarius and in European Directive 74/409 for the detection of the adulteration of honey. This led to them being the first to develop a method for the detection of adulterated honey by using DSC.

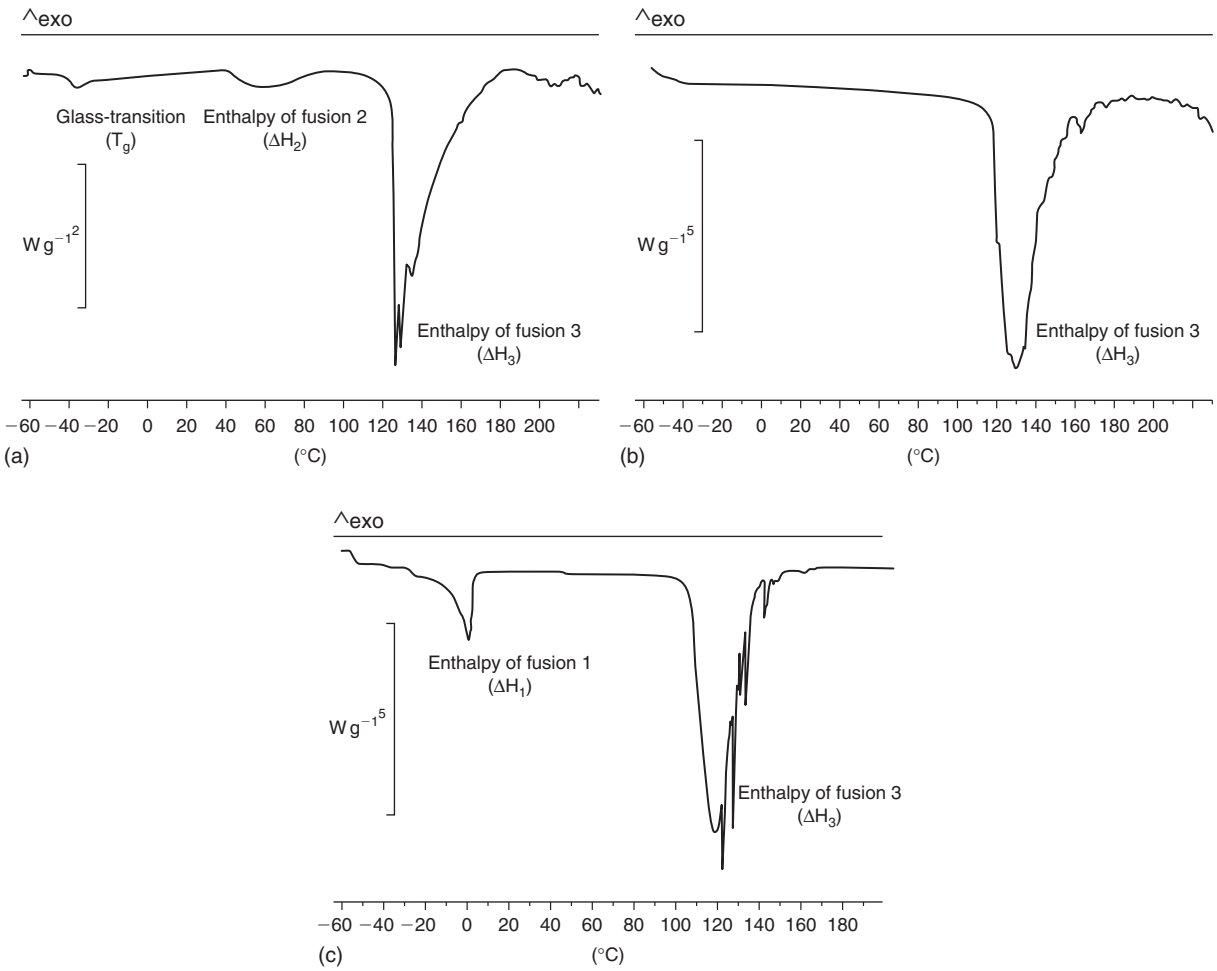

Figure 15.27 DSC cooling curves of (a) *Lavandula* honey, (b) isoglucose sugar syrup and (c) beet sugar syrup. Reprinted with permission from the *Journal of Agricultural and Food Chemistry* (2002), **50**, 203–208; ©2002, American Chemical Society.

Cordella *et al*. (2002) investigated the thermal behavior of authentic honeys derived from *Lavandula*, *Robinia* and *Fir*, as well as industrial sugar syrups. Data on thermal and thermochemical parameters, such as the glass transition temperature, enthalpies of fusion and heat capacity variation, revealed significant differences between the syrup and honey samples (Figure 15.27, Tables 15.1, 15.2). Adding different concentrations of syrup to the honey revealed a linear relationship in the glass transition temperature and the enthalpy of fusion of the sample mixture. Cordella *et al*. (2002) also reported that the method was able to detect the presence of industrial syrups in honeys at levels as low as 5%.

In a follow-up study, Cordella *et al*. (2003) further investigated the use of DSC to determine the differences between various varieties of honey (*Robinia*, *Lavender*, *Chestnut* and *Fir*). Cordella *et al*. (2003) observed significant differences in the glass transition temperature of the samples, indicating that this parameter was

Table 15.1 Transition temperature (T_{onset}, $T_{midpoint}$), ΔC_p, and enthalpy of honeys and syrups during heating

Sample		No. of replicates	Thermal phenomena					
			Glass transition					
			T_g			Fusion 1	Fusion 2	Fusion 3
			T_{onset}	$T_{midpoint}$	ΔC_p	$\Delta H_{1,fus}$	$\Delta H_{2,fus}$	$\Delta H_{3,fus}$
Syrups	Beet syrup	4	−34.3	−33.4	0.9	−67.7	A[a]	−849.9
	Can syrup	2	−32.0	−31.6	0.3	−95.9	A	−997.5
	Isoglucose 1	2	ND[b]	ND	ND	A	A	−560.8
	Isoglucose 2	2	ND	ND	ND	A	A	−508.6
	Isoglucose 3	2	ND	ND	ND	A	A	−466.3
	Isoglucose 4	2	ND	ND	ND	A	A	−505.4
Honeys	*Lavandula*	10	−41.1	−38.0	0.6	A	−23.7	−256.2
	Robinia	5	−42.5	−39.8	0.8	A	A	−213.1
Honeydew	*Fir*	8	−37.5	−33.5	0.6	A	<2	−228.9

[a]A, not measured due to absence; [b]ND, not determined due to lack of accessibility by cooling system.
Reprinted with permission from the *Journal of Agricultural and Food Chemistry* (2002), **50**, 203–208. ©American Chemical Society 2002.

Table 15.2 Experimental adulteration trials: Evolution of thermal parameters of *Lavandula* honey in terms of added syrup percentage (H in Jg^{-1}; T_{onset} in °C; ΔC_p in $Jg^{-1}K^{-1}$)

Sample	Fusion ($\Delta H_{2,fus}$)					Glass transition (T_{onset})			
	% Syrup	Syrup 1	Syrup 2	Syrup 3	Syrup 4	Syrup 1	Syrup 2	Syrup 3	Syrup 4
01	0	−23.7	−23.7	−23.7	−23.7	−41.12	−41.12	−41.12	−41.12
02	5	−19.1	−19.4	−17.9	−17.8	−42.89	−42.30	−42.14	−41.83
03	10	−14.3	−17.3	−14.1	−17.0	−43.95	−42.99	−43.45	−42.59
04	20	−14.7	−15.6	−15.9	−15.1	−44.93	−44.59	−45.24	−44.34
05	40	−8.9	−14.6	−11.0	−9.0	−48.43	−47.97	−47.50	−47.07
06	60	−0.6	−9.1	−3.3	−1.9	−50.16	−50.68	−50.41	−49.05
07	100	A[a]	A	A	A	ND[b]	ND	ND	ND

[a]A, not measured due to absence; [b]ND, not determined due to lack of accessibility by cooling system.
Reprinted with permission from the *Journal of Agricultural and Food Chemistry* (2002), **50**, 203–208. ©American Chemical Society 2002.

useful for characterizing and successfully distinguishing between the honey varieties. A TMDSC analysis was also performed by Cordella *et al*. (2003) on the samples, and the results revealed that a new thermal transition similar to that of a glass transition occurred between 40°C and 90°C (Figure 15.28). The deconvolution of the signal measured at that temperature range allows for the separation of the thermal effect related to the glass transition recorded in the reversing component of the signal from the endothermic effect recorded in the non-reversing signal. Based on the data, this endothermic peak can be attributed to the gelatinization of certain honey compounds such as starch, sugars and water, while other compounds undergo a simultaneous thermal transition (reversing signal). This work has shed some light on the use of certain parameters, such as glass transition temperature and enthalpy changes, to

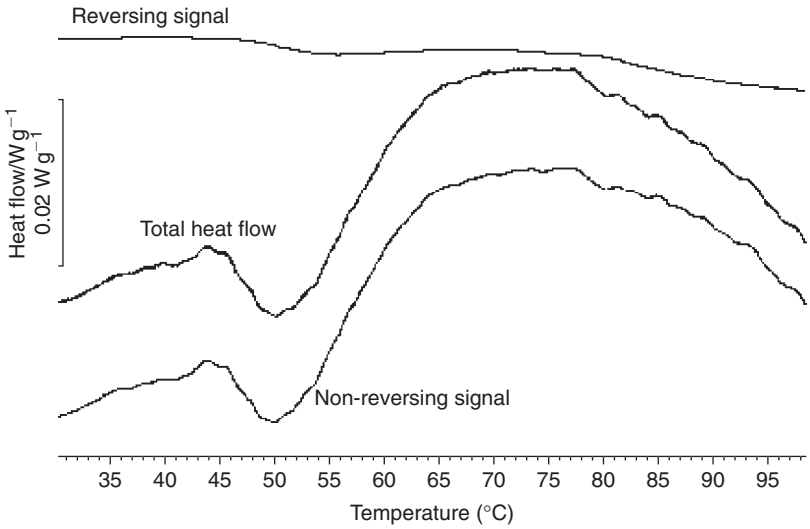

Figure 15.28 Total heat flow, reversing and non-reversing heat flow obtained from TMDSC curve of honey from *Lavender*. Source: Cordella *et al*. (2003).

detect the plasticizing effect of honey adulterants, as well as a better understanding of the relationship between chemical reactions and structural changes occurring during the heating of honey.

Shark

Sharks (superorder *Selachimorpha*) are often regarded as fish, although they are somewhat distantly related to the classical bony fish. Sharks have been a valuable resource of raw materials, including meat (fresh, frozen, salted and smoked), fins (one of the most expensive fish products in the world and commonly used in shark-fin soup in Chinese cuisine), shark-liver oil (used in the cosmetics and pharmaceutical industry), skin (used as leather and sandpaper), teeth (used as jewellery) and cartilage (beneficial in the treatment of diseases such as arthritis, psoriasis colitis, acne, enteritis, phlebitis, rheumatism, peptic ulcers, hemorrhoids, herpes simplex, melanoma and cancer) (Schubring, 2007). Shark meat has been consumed as food in many coastal regions for over 5000 years. Small sharks are preferred for meat in many markets. Shark fillets may be salted and diced or smoked. However, there are uncertainties during evaluation by the custom authorities worldwide regarding whether shark muscle has been heat-treated (smoked) or not. Different tariffs are charged for heated and untreated fish products, and this necessitates correct labeling of the products. The case becomes more problematic with hot and cold smoking of the fish product. Therefore, the Federal Research Centre for Nutrition and Food in Hamburg, Germany has taken on the task of carrying out investigations and establishing whether fish products are being declared truly by the manufacturers.

Schubring (2007) conducted tests to measure and compare the differences in thermal behavior between bony fish and various sharks (catsharks, smoothhounds and liveroil

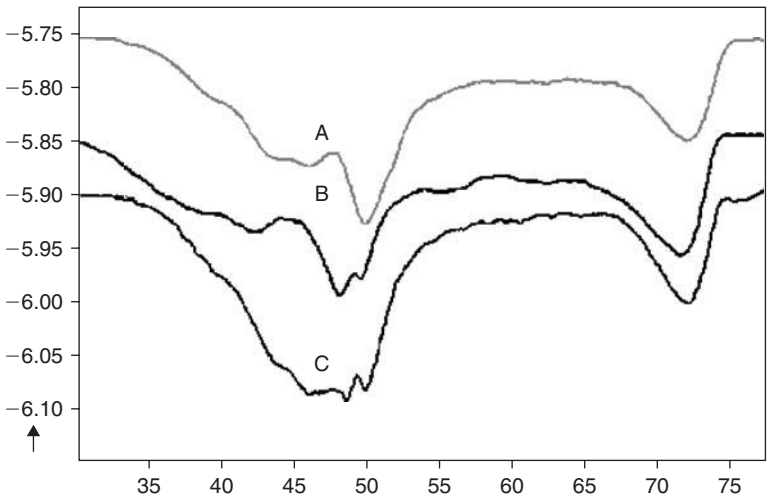

Figure 15.29 DSC cooling curves of smoothhound (A), catshark (B) and liveroil sharks (C). Source: Schubring (2007).

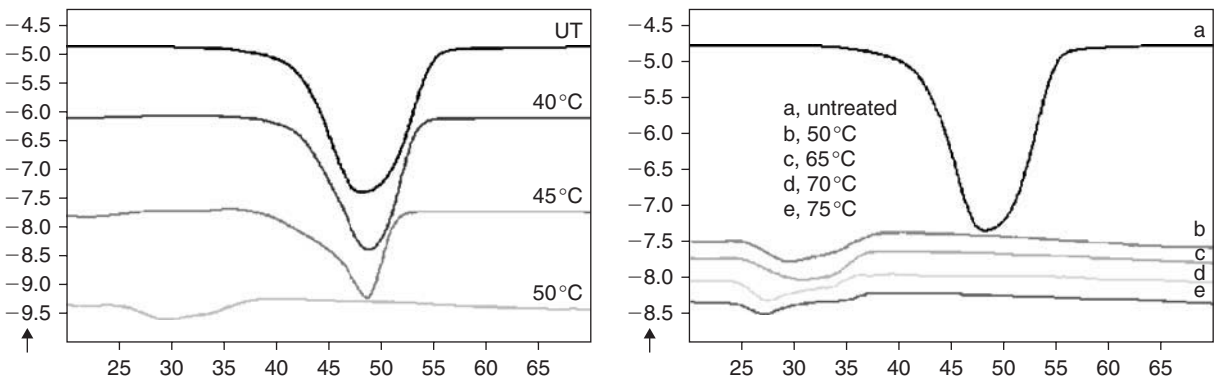

Figure 15.30 DSC curves taken on preheated samples of skin of smoothhounds dependent on heating temperature. Source: Schubring (2007).

sharks), using DSC. The influence of heating (designed to mimic smoking conditions) on shark muscle was also studied. Differences between shark species were obvious but not strong. DSC curves of shark meat showed two main endothermic peaks and a smaller one at a lower temperature (Figure 15.29). The changes in DSC curves caused by the effect of heating the meat are also shown (Figures 15.30 and 15.31). As the temperature increases, DSC peaks of the meat samples can be seen gradually to disappear. In the skin samples, the peak corresponding to collagen at 48°C disappeared completely after heating to 45–50°C, and a new small peak appeared at around 28°C. This finding may be due to the denaturation of collagen to gelatin. The influence of smoking on the DSC curve of the raw and smoked belly flaps of spiny dogfish (known as "*Schillerlocken*" in Germany) was also demonstrated (Figure 15.32). In the smoked sample, the lower temperature peak disappeared, leaving behind only the higher

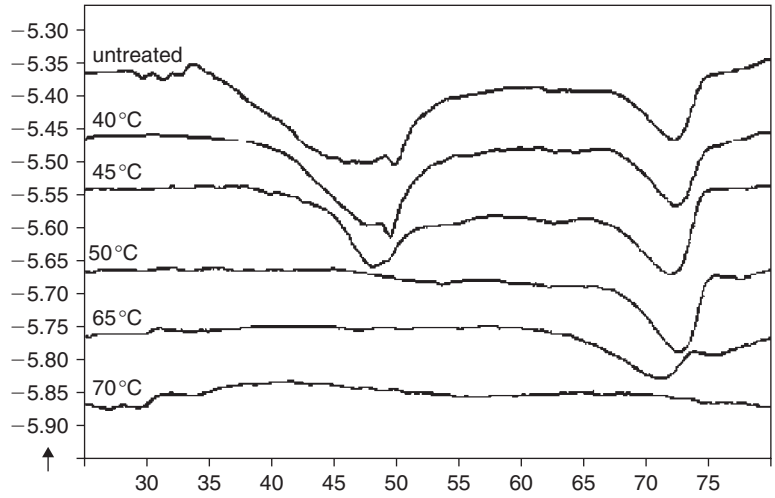

Figure 15.31 DSC curves taken on preheated meat samples of smoothhounds dependent on heating temperature. Source: Schubring (2007).

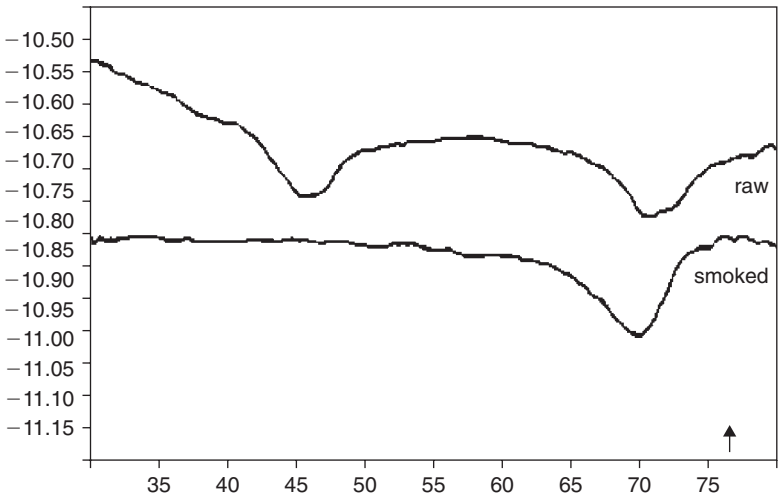

Figure 15.32 DSC curves of frozen-thawed belly flaps (above) and "*Schillerlocken*" (below). Source: Schubring (2007).

temperature peak. Unfortunately, from the DSC data that were found, Schubring (2007) noted that it was not possible to say that a core temperature of 60°C, as demanded by the guidelines of the German Food Code, had been applied to the product, since the lower temperature peak occurred below 50°C.

Conclusions

Rapid developments in DSC instrument technology have led to many new applications for DSC in fundamental research. Nevertheless, only a handful of researchers have

focused their attention on applying DSC for the detection of adulterants in food, especially the detection of certain animal fats in vegetable oils. Most of the studies reviewed in this chapter made use of the conventional DSC technique; we have yet to see any reports on the use of the latest HPDSC technology for the detection of food adulterants. Despite the advancement in food authentication techniques, those involved in the adulteration of food products are also developing new ways to overcome the current methods of food authentication. Therefore, an analytical technique such as HPDSC, which has a very short run time, is relatively easy to use, highly accurate and sensitive to subtle changes in chemical composition of the food product, while also providing the possibility of coupling with other analytical techniques such as microscopy, spectroscopy and chromatography, is potentially a very attractive option for use as a tool to detect fraudulent activities in food products. However, much work needs to be done to prove its worth in the detection of adulterants in food products other than those mentioned in this chapter.

Nomenclature

A	peak area
$C_{CR}(T)$	heat capacity of reference cell
$C_{CS}(T)$	heat capacity of sample cell
$C_R(T)$	heat capacity of reference
$C_S(T)$	heat capacity of sample
ϕ	density
dq_S/dt	heat transfer rate from furnace to sample
G	calibration factor
ΔH	heat of reaction or phase transition
k	thermal conductivity
l	sample length
m	sample mass
p	vapor pressure
r	sample radius
R	heat resistance between furnace and sample
t	time
ΔT	difference in temperature between sample and reference material
T_F	final peak temperature
T_I	initial deviation temperature
ΔT_{min}	change in minimum temperature
T_P	furnace temperature
T_R	reference temperature
T_S	sample temperature
V	volume of sample
ΔV	change in volume of the system due to the phase transition

References

Aktaş, N. and Kaya, M. (2001). Detection of beef body fat and margarine in butterfat by differential scanning calorimetry. *Journal of Thermal Analysis and Calorimetry*, **66**, 795–801.

Antinelli, J.F., Clément, M.C., Moussa, I. *et al*. (2001). Détection de canne à sucre dans les miels par analyses isotopique et microscopique: etude et comparaison. *Annales des Falsifications et de l'Expertise Chimique*, **93**, 13–22.

ASTM E 967 (1999). Standard practice for temperature calibration of differential scanning calorimeters and differential thermal analyzers. American Society for Testing and Materials (ASTM), Pennsylvania, USA.

Biliaderis, C.G. (1983). Differential scanning calorimetry in food research. *Food Chemistry*, **10**, 239–265.

Cebula, D.J. and Smith, K.W. (1992). Differential scanning calorimetry of confectionery fats: Part II – Effects of blends and minor components. *Journal of the American Oil Chemists' Society*, **69**, 992–998.

Coni, E., Pasquale, M.D., Coppolelli, P. and Bocca, A. (1994). Detection of animal fats in butter by differential scanning calorimetry: A pilot study. *Journal of the American Oil Chemists' Society*, **71**, 807–810.

Cordella, C., Antinelli, J.-F., Aurieres, C. *et al*. (2002). Use of differential scanning calorimetry (DSC) as a new technique for detection of adulteration in honeys. 1. Study of adulteration effect on honey thermal behaviour. *Journal of Agriculture and Food Chemistry*, **50**, 203–208.

Cordella, C., Faucon, J.-P., Cabrol-Bass, D. and Sbirrazzouli, N. (2003). Application of DSC as a tool for honey floral species characterization and adulteration detection. *Journal of Thermal Analysis and Calorimetry*, **71**, 279–290.

Ford, J.L. and Timmins, P. (1989). Instrumentation for thermal analysis. In: *Pharmaceutical Thermal Analysis: Techniques and Applications*. Chichester: Ellis Horwood Ltd, pp. 9–24.

Geeraert, E. and Sandra, P. (1985). Capillary gas chromatography of triglycerides in fats and oils using a high temperature phenylmethyl silicone stationary phase. Part 1. *Journal of High Resolution Chromatography and Chromatography Communications*, **8**, 415–422.

Gill, P.S., Sauerbrunn, S.R. and Reading, M. (1993). Modulated differential scanning calorimetry. *Journal of Thermal Analysis and Calorimetry*, **40**, 931–939.

Gray, I.K. (1973). Seasonal variations in the composition and thermal properties of New Zealand milkfat 1. Fatty acid composition. *Journal of Dairy Research*, **40**, 207–214.

Griffin, V.J. and Laye, P.G. (1992). Differential thermal analysis and differential scanning calorimetry. In: E.L. Charsley and S.B. Warrington (eds), *Thermal Analysis*. Cambridge: Royal Society of Chemistry, pp. 17–30.

Haines, P.J. and Wilburn, F.W. (1995). Differential thermal analysis and differential scanning calorimetry. In: P.J. Haines (ed.), *Thermal Method of Analysis: Principles, Applications and Problems*. Glasgow: Chapman & Hall, pp. 63–122.

International Dairy Federation (1965). Phytosteryl acetate test. International Standard IDF 32. Brussels: IDF.

International Dairy Federation (1966). TLC of steryl acetates. International Standard IDF 38. Brussels: IDF.

Kerkvielt, J.D., Shrestha, M., Tuladhar, K. and Manandhar, H. (1995). Microscopic detection of adulteration of honey with cane sugar and cane sugar products. *Apidologie*, **26**, 139–161.

Kerkvielt, J.D. and Meijer, H.A.J. (2000). Adulteration of honey: relation between microscopic analysis and $\delta^{13}C$ measurements. *Apidologie*, **31**, 717–726.

Lombardi, G. (1980). *For Better Thermal Analysis*, 2nd edn. Rome: ICTA.

Love, J.A. (1996). Animal fats. In: Y.H. Hui (ed.), *Bailey's Industrial Oil and Fat Products*, Vol. 1. New York, NY: John Wiley & Sons, Inc., pp. 1–16.

Mackenzie, R.C. (1980). Differential thermal analysis and differential scanning calorimetry: Similarities and differences. *Analytical Proceedings*, **17**, 217–220.

Marikkar, J.M.N., Lai, O.M., Ghazali, H.M. and Che Man, Y.B. (2001). Detection of lard and randomized lard as adulterants in refined-bleached-deodorized palm oil by differential scanning calorimetry. *Journal of the American Oil Chemists' Society*, **78**, 1113–1119.

Marikkar, J.M.N., Ghazali, H.M., Che Man, Y.B. and Lai, O.M. (2002a). The use of cooling and heating thermograms for monitoring of tallow, lard and chicken fat adulterations in canola oil. *Food Research International*, **35**, 1007–1014.

Marikkar, J.M.N., Lai, O.M., Ghazali, H.M. and Che Man, Y.B. (2002b). Compositional and thermal analysis of RBD palm oil adulterated with lipase-catalysed interesterified lard. *Food Chemistry*, **76**, 249–258.

Marikkar, J.M.N., Ghazali, H.M., Che Man, Y.B. and Lai, O.M. (2003a). Differential scanning calorimetric analysis for determination of some animal fats as adulterants in palm olein. *Journal of Food Lipids*, **10**, 63–79.

Marikkar, J.M.N., Ghazali, H.M., Long, K. and Lai, O.M. (2003b). Lard uptake and its detection in selected food products deep-fried in lard. *Food Research International*, **36**, 1047–1060.

McNaughton, J.L. and Mortimer, C.T. (1975). Differential scanning calorimetry. In: *IRS Physical Chemistry*, Series 2, Vol. 10. London: Butterworths.

Meisel, T. and Seyboldare, K. (1981). Modern methods of thermal analysis. *Critical Reviews in Anaytical Chemistry*, **12**, 267–343.

Muuse, B.G., Werdmuller, G.A., Geerts, J.P. and De Knegt, R.J. (1986). Fatty acid profile in Dutch butterfat. *Netherlands Milk and Dairy Journal*, **40**, 189–201.

Ozao, R. (2004). Differential thermal analysis (DTA) and differential scanning calorimetry (DSC). In: The Japan Society of Calorimetry and Thermal Analysis (ed.), *Comprehensive Handbook of Calorimetry & Thermal Analysis*. Chichester: John Wiley & Sons, pp. 128–134.

PerkinElmer (2003). Diamond DSC. *PerkinElmer Life and Analytical Sciences*, 006887_01.

Precht, D. (1990). Determination of milk fat in cocoa butter. *Fat Science Technology*, **92**, 153–161.

Rashood, K.A., Shaaban, R.R.A., Moety, E.M.A. and Rauf, A. (1995). Triacylglycerols profiling by high performance liquid chromatography: a tool for detection of pork fat in processed foods. *Journal of Liquid Chromatography and Related Technologies*, **18**, 2661.

Reading, M. (1993). Modulated DSC – a new way forward in materials characterization. *Trends in Polymer Science*, **8**, 248–253.

Reading, M., Elliott, D. and Hill, V.L. (1993). A new approach to the calorimetric investigations of physical and chemical transitions. *Journal of Thermal Analysis and Calorimetry*, **40**, 949–955.

Ritter, B., Schulte, J., Schulte, E. and Thier, H.-P. (2001). Detection of coating waxes on apples by differential scanning calorimetry. *European Food Research and Technology*, **212**, 603–607.

Sato, K.T., Arashima, Z.H., Wang, K. *et al*. (1989). Polymorphism of POP and SOS I. Occurrence and Polymorphic Transformation. *Journal of the American Oil Chemists' Society*, **66**, 664–674.

Schubring, R. (2007). DSC measurements on sharks. *Thermochimica Acta*, **458**, 124–131.

Simon, S.L. (2001). Temperature-modulated differential scanning calorimetry: theory and application. *Thermochimica Acta*, **374**, 55–71.

Sreenivasan, B. (1978). Interesterification of fats. *Journal of the American Oil Chemists' Society*, **55**, 796–805.

TA Instruments (undated). Thermal analysis review – Modulated DSC theory. In: *Thermal Analysis and Rheology*, TA-211B. New Castle, DE: TA Instruments Inc.

Takahashi, Y. (2004). Triple-cell DSC. In: The Japan Society of Calorimetry and Thermal Analysis (ed.), *Comprehensive Handbook of Calorimetry & Thermal Analysis*. Chichester: John Wiley & Sons, pp. 148–150.

Timms, R.E. (1980). Detection and quantification of non-milk fat in mixtures of milk and non-milk fats. *Journal of Dairy Research*, **47**, 295–303.

Timms, R.E. (2003). Production and characteristic properties. In: *Confectionery Fats Handbook: Properties, Production and Application*. Bridgewater: The Oily Press, pp. 191–254.

USDA (2007). Oilseeds: World Markets and Trade. Foreign Agricultural Service. United States Department of Agriculture. Circular Series. FOP 06–07.

Weiss, T.J. (1983). Bakery shortenings and frying shortenings. In: *Food Oils and Their Uses*. Westport, CT: The AVI Publishing Company Inc., pp. 153–165.

Wendlandt, W.W. (1986a). Thermal analysis nomenclature. In: W.W. Wendtland (ed.), *Thermal Analysis*, 3rd edn. New York, NY: John Wiley & Sons, Inc., pp. 799–810.

Wendlandt, W.W. (1986b). Applications of differential thermal analysis and differential scanning calorimetry. In: W.W. Wendtland (ed.) *Thermal Analysis*, 3rd edn. New York, NY: John Wiley & Sons, Inc., pp. 359–460.

Wendlandt, W.W. (1986c). Differential thermal analysis and differential scanning calorimetry. In: W.W. Wendtland (ed.), *Thermal Analysis*, 3rd edn. New York, NY: John Wiley & Sons, Inc., pp. 213–298.

Wendlandt, W.W. (1986d). Differential thermal analysis and differential scanning calorimetry instrumentation. In: W.W. Wendtland (ed.), *Thermal Analysis*, 3rd edn. New York, NY: John Wiley & Sons, Inc., pp. 299–357.

White, J.W. (1992). Internal standard stable carbon isotope ratio method for determination of C-4 plants sugars in honey: Collaborative study and evaluation of improved protein preparation procedure. *Journal of AOAC International*, **75**, 543–548.

White, J.W. and Winters, K. (1989). Honey protein as internal standard for stable carbon isotope ratio detection of adulteration of honey. *Journal of AOAC International*, **72**, 907–911.

White, J.W., Winters, K., Martin, P. and Rossmann, A. (1998). Stable carbon isotope ratio analysis of honey: Validation of internal standard procedure for worldwide application. *Journal of AOAC International*, **81**, 610–619.

Wunderlich, B. (1987). Development towards a single-run DSC for heat capacity measurements. *Journal of Thermal Analysis and Calorimetry*, **32**, 1949–1955.

Wunderlich, B., Androsch, R., Pyda, M. and Kwon, Y.K. (2000). Heat capacities by multi-frequencies saw-tooth modulation. *Thermochimica Acta*, **348**, 181–190.

This page intentionally left blank

16

Chemometric Methods in Food Authentication

Riccardo Leardi

Introduction

In this chapter the fundamentals of *chemometrics* will be presented by means of a quick overview of the most relevant techniques for *data display*, *classification*, *modeling*, *multivariate process monitoring*, *multivariate quality control* and *calibration*. The chapter is intended to make people aware of the great superiority of *multivariate analysis* over the commonly used univariate approach. Mathematical and algorithmical details will not be presented, since the chapter is mainly focused on the general problems to which chemometrics can be successfully applied in the field of food authentication.

As a matter of fact, many of the readers of this book may not be familiar with chemometrics, and a significant percentage of them may have never even heard of this "new" science (although it's quite strange that it is still considered a "new" science, when the Chemometrics Society was founded more than 30 years ago and the most basic algorithms date back to the beginning of the twentieth century). Furthermore, some may be quite put off by anything involving mathematical computations more advanced than a square root, or statistical tests more complex than a *t*-test.

Modern Techniques for Food Authentication
ISBN: 978-0-12-374085-4

Therefore, the goal of this chapter is simply that of being read and understood by the majority of the readers of this book. This goal will be completely achieved if some of them, after having read it, might say: "chemometrics is easy and powerful indeed, and from now on I will always think in a multivariate way".

Of course, to accomplish this goal in the limited space of a chapter, the attractive sides of chemometrics must be highlighted. Therefore, the intuitive aspects of each technique will be shown, without giving too much relevance to the algorithms.

First of all, what is chemometrics? According to the definition of the Chemometrics Society, it is "the chemical discipline that uses mathematical and statistical methods to design or select optimal procedures and experiments, and to provide maximum chemical information by analyzing chemical data".

One of the major mistakes that people make regarding chemometrics is thinking that, in order to use it, it is necessary to be a very good mathematician and to know the mathematical details of the algorithms being used. From the definition itself, it is clear instead that a chemometrician is a *chemist* who can *use* mathematical and statistical methods.

If we want to draw a parallel with everyday life, how many of us really know in detail how a TV set, a mobile phone, a car or a washing machine works? But everybody watches TV programs, makes phone calls, drives a car and starts a washing machine. Of course, what is important is that people know what each instrument is made for and that nobody tries to drive a TV set, or speak into a washing machine or do the laundry in a car.

Though chemometrics makes available a very wide range of techniques, some of them being very difficult to fully understand and use correctly, the great majority of the real problems can be solved by applying one of the basic techniques, the understanding of which, at least from an intuitive point of view, is relatively easy and does not require high-level mathematical skills.

Data collection

Chemometrics works on data matrices. This means that on each sample a certain number of variables have been measured (in the "chemometrical jargon", we say that each object is described by v variables). Although some techniques can work with a limited number of missing values, a chemometrical data set must be thought of as a spreadsheet in which all the cells are full.

Sometimes, instead, if data are gathered without having any specific project, it happens that the result is a "sparse" matrix containing some blank cells. In such cases, if the percentage of missing data is quite high, the whole data set is not suitable for a multivariate analysis; as a consequence, the variables and/or the objects with the lowest number of data must be removed, and therefore a huge amount of experimental effort can be lost.

All the chemometrical software allows the import of data from ASCII files or from spreadsheets. It is therefore suggested that the data be organized in matrix form from the start, as shown in Table 16.1, in such a way that the import can be performed

Table 16.1 The structure of a chemometrical data set

	Var. 1	Var. 2	Var. 3	Var. 4	Var. 5	Var. 6	Var. 7	...	Var. v
Obj. 1									
Obj. 2									
Obj. 3									
Obj. 4									
Obj. 5									
Obj. 6									
...									
Obj. n									

Table 16.2 Ten samples described by one variable

Sample	1	2	3	4	5	6	7	8	9	10
Value	25.3	22.1	25.5	25.6	19.4	25.7	20.2	21.3	25.9	21.8

in a single step. If, on the contrary, the data are spread over several files or sheets (e.g. one file for each sample or for each variable), then the import procedure will be much longer and more cumbersome.

Sometimes it also happens that people tend to "overcrowd" the data file with intermediate and therefore "useless" numbers (e.g. in the case of weighing, the gross weight and the tare). These values, being non-relevant for the data analysis, should anyway be removed before the chemometrical elaboration. It can be easily understood that a good data collection, resulting in a well-structured data sheet, is the first step towards successful data analysis.

This is especially true if the data have to be elaborated by an external consultant, who can therefore start his or her job with a simple and direct import of the data, without having to waste time (and possibly make mistakes) with boring tasks such as joining several files or removing redundant information.

Data display

The human mind can digest much more information when looking at plots rather than numbers. This is easily demonstrated by looking first at the sequence of numbers reported in Table 16.2, and then at the plot in Figure 16.1.

It is very clear that, even in a very simple data set like this (just 10 samples, and a single variable), the information obtained by looking at the plot is superior to and much more easily available than the information gained by analyzing the raw numbers. From the plot, it becomes evident that the samples are clustered into two groups of the same size, the one at higher values being much tighter than the one at low values. Much more time and effort are required when we want to get the same information from the table.

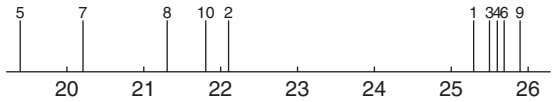

Figure 16.1 Scatter plot of the data in Table 16.2.

Table 16.3 Twenty samples described by two variables

Sample	Variable 1	Variable 2
1	21.2	32.5
2	16.2	21.0
3	13.1	21.7
4	11.6	21.3
5	20.8	29.9
6	10.4	20.6
7	19.5	26.8
8	9.8	25.2
9	15.2	31.2
10	12.0	26.0
11	17.6	28.5
12	24.0	30.0
13	17.8	33.1
14	15.0	24.0
15	11.0	24.2
16	24.8	25.3
17	12.8	23.3
18	26.5	30.6
19	22.9	27.5
20	9.7	22.8

Let us now take into account a more complex data set, i.e. the one reported in Table 16.3, where each object is described by two variables. The same data are plotted in Figure 16.2.

In this data set there are 20 samples, supposed to belong to the same population. When looking at one variable at a time (Figures 16.2a and 16.2b), it really seems that the samples constitute a single group. When looking at the bivariate plot shown in Figure 16.2c, we realize instead that we are in a situation very similar to that which we found with the univariate data set. The samples are split into two clusters of the same size, with the objects of the first one more tightly grouped than the objects of the second one. As previously shown, this conclusion cannot be reached when looking at one variable at a time, since neither of the two variables is able to discriminate between the two groups.

This bivariate data set, beyond showing once more that a plot is much more easily handled by the human brain than a data table, demonstrates that, when dealing with more than one variable, the analysis of just one variable at a time can lead to wrong results.

If we had a data set with three variables, it would still be possible to visualize the whole information by a three-dimensional scatter plot, in which the coordinates of each object were the values of the variables. However, what should we do if there were

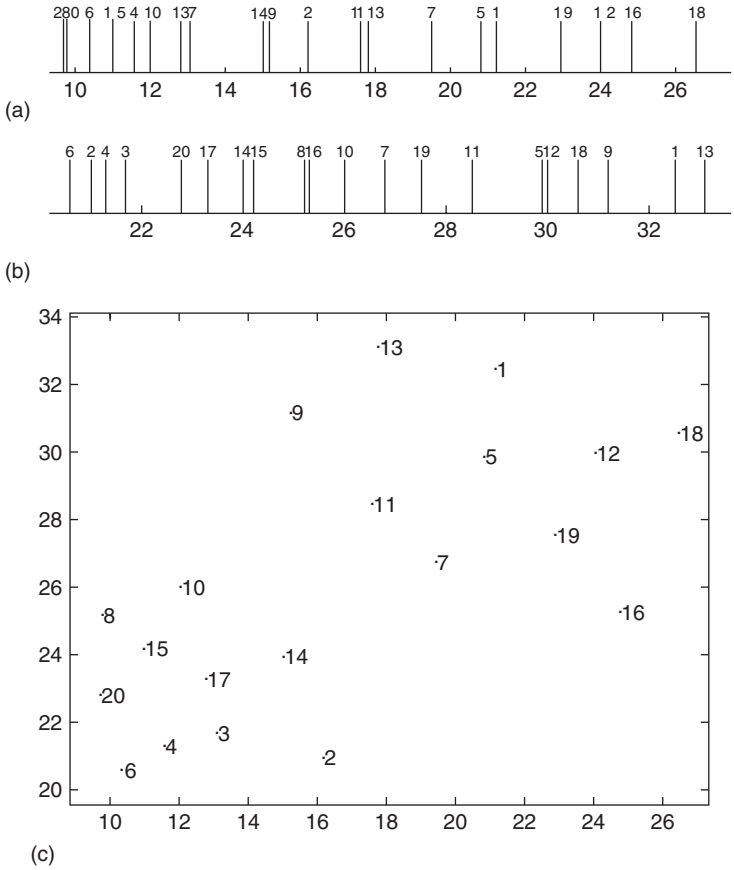

Figure 16.2 Scatter plots of the data in Table 16.3: (a) univariate scatter plot of variable 1; (b) univariate scatter plot of variable 2; (c) bivariate scatter plot.

more than three variables? What we need, therefore, is a technique permitting the visualization by simple bi- or tridimensional scatter plots of the majority of the information contained in a highly dimensional data set. This technique is *principal component analysis* (PCA), one of the simplest and most used methods of multivariate analysis. PCA is very important, especially in the preliminary steps of an elaboration, when performing an exploratory analysis in order to have an overview of the data.

It is quite common to have to deal with large data tables with, for instance, a series of samples described by a number (v) of chemico-physical parameters. Examples of such data sets could be samples of olive oils from different origins described by their content in fatty acids and sterols, or samples of wines described by Fourier-transformed infrared (FT-IR) spectra. It is easy to realize how, especially in spectral data sets, v can be very high (>1000). In such cases, it would be impossible to obtain valuable information without the help of multivariate techniques.

From a geometrical point of view, we can consider a v-dimensional space in which each dimension is associated to one of the variables. In this space, each sample (object) has coordinates corresponding to the values of the variables describing it.

Since it is impossible to visualize all the information at once, we can be content with the analysis of several bi- or tridimensional plots, each of them showing a different part of the global information.

It is also evident that not all possible combinations of two or three variables will give the same quality of information. For instance, if some variables are very highly correlated, then the information brought by each of them will be almost the same. If two variables are perfectly correlated, then one of them can be discarded, losing no information at all. In this way, the dimensionality of our space will be reduced from v to $v - 1$. If two variables are very highly correlated, then the elimination of one of them will produce only a slight loss of information, while the dimensionality of the space will be reduced to $v - 1$. So, we can deduce that the information contained in the "lost" v-th dimension was well below the average of the information contained in the other dimensions.

It is quite apparent now that not all the dimensions have the same importance, and that, owing to the correlations among the variables, the "real" dimensionality of our data matrix is somehow lower than v. Therefore, it would be very valuable to have a technique capable of concentrating in a few variables, and therefore in a few dimensions, the bulk of our information. This is exactly what is performed by PCA; it reduces the dimensionality of the data and extracts the most relevant part of the information, placing in the last dimensions the non-structured information – i.e. the noise. According to these two characteristics, the information contained in very complex data matrices can be visualized in just one or a few plots.

From the mathematical point of view, the goal of PCA is to obtain, from v variables (X_1, X_2, …, X_v), v linear combinations having two important features: to be uncorrelated, and to be ordered according to the explained variance (i.e. to the information they contain). The lack of correlation among the linear combinations is very important, since it means that each of them describes different "aspects" of the original data. As a consequence, the examination of a limited number of linear combinations (generally the first two or three) allows us to obtain a good representation of the studied data set.

From a geometrical point of view, what is performed by PCA corresponds to looking for the direction which, in the v-dimensional space of the original variables, brings the greatest possible amount of information (i.e. explains the greatest variance). Once the first direction is identified, the second one is looked for; it will be the direction explaining the greatest part of the residual variance, under the constraint of being orthogonal to the first one. This process goes on until the v-th direction has been found.

These new directions can be considered as the axes of a new orthogonal system, obtained after a simple rotation of the original axes. While in the original system each direction (i.e. each variable) brings with it, at least in theory, $1/v$ of total information, in the new system the information is concentrated in the first directions, and decreases progressively so that in the last ones no information can be found except noise.

The global dimensionality of the system is always that of the original data (v), but since the last dimensions explain only a very small part of the information, they can be neglected and we can take into account only the first dimensions (the "significant

components"). The projection of the objects in this space of reduced dimensionality retains almost all the information that can now also be analyzed in a visual way, by bi- or tridimensional plots. These new directions, linear combinations of the original ones, are the principal components (PC) or Eigenvectors.

With a mathematical notation, we can write:

$$\text{var}(Z_1) > \text{var}(Z_2) > \cdots > \text{var}(Z_v) \quad \textbf{(16.1)}$$

where $\text{var}(Z_i)$ is the variance explained by component *i*. Furthermore, since a simple rotation has been performed, the total variance is the same in the two systems of axes:

$$\sum \text{var}(X_i) = \sum \text{var}(Z_i) \quad \textbf{(16.2)}$$

The first PC is formed by the linear combination

$$Z_1 = a_{11}X_1 + a_{12}X_2 + \cdots + a_{1v}X_v \quad \textbf{(16.3)}$$

explaining the greatest variance, under the condition

$$\sum a_{1i}^2 = 1 \quad \textbf{(16.4)}$$

This last condition notwithstanding, the variance of Z_1 could be made greater simply by increasing one of the values of a.

The second PC

$$Z_2 = a_{21}X_1 + a_{22}X_2 + \cdots + a_{2v}X_v \quad \textbf{(16.5)}$$

is the one having $\text{var}(Z_2)$ as large as possible, under the conditions that

$$\sum a_{2i}^2 = 1 \quad \textbf{(16.6)}$$

and that

$$\sum a_{1i}a_{2i} = 0 \quad \textbf{(16.7)}$$

Equation (16.7) assures the orthogonality of components one and two.

The lower order components are computed in the same way, always under the two conditions previously reported.

From a mathematical point of view, PCA is solved by finding the eigenvalues of the variance–covariance matrix; they correspond to the variance explained by the corresponding principal component. Since the sum of the eigenvalues is equal to the sum of the diagonal elements (trace) of the variance–covariance matrix, and since the trace of the variance–covariance matrix corresponds to the total variance, we have confirmation that the variance explained by the principal components is the same as explained by the original data.

It is now interesting to locate each object in this new reference space. The coordinate on the first PC is computed simply by substituting into Equation (16.3), with X_i being the values of the corresponding original variables. The coordinates on the other principal components are then computed in the same way. These coordinates are named scores, while the constants a_{ij} are named loadings.

By taking into account the loadings of the variables on the different principal components, it is very easy to understand the importance of each single variable in constituting each PC. A high absolute value means that the variable under examination plays an important role for the component, while a low absolute value means that it has very limited importance.

If a loading has a positive sign, it means that the objects with a high value of the corresponding variable have high positive scores on that component. If the sign is negative, then the objects with high values of that variable will have high negative scores. As already mentioned, after a PCA, the information is mainly concentrated on the first components. As a consequence, a plot of the scores of the objects on the first components allows the direct visualization of the global information in a very efficient way. It is now very easy to detect similarity between objects (similar objects have a very similar position in the space) or the presence of outliers (they are very far from all other objects) or the existence of clusters. Taking into account at the same time the scores and loadings, it is also possible to interpret very easily the differences among objects or groups of objects, since it is immediately understandable which are the variables giving the greatest contribution to the phenomenon under study.

Mathematically speaking, we can say that the original data matrix $\mathbf{X}_{o,v}$ (having as many rows as objects and as many columns as variables) has been decomposed into a matrix of scores $\mathbf{S}_{o,c}$ (having as many rows as objects and as many columns as retained components, with c usually $<< v$) and a matrix of loadings $\mathbf{L}_{c,v}$ (having as many rows as retained components and as many columns as variables). If, as usual, $c < v$, a matrix of the residuals $\mathbf{E}_{o,v}$, having the same size as the original data set, contains the differences between the original data and the data reconstructed by the PCA model (the smaller the values of this matrix, the higher the variance explained by the model).

We can therefore write the following relationship:

$$\mathbf{X}_{o,v} = \mathbf{S}_{o,c} * \mathbf{L}_{c,v} + \mathbf{E}_{o,v}$$

Now, let us see the application of PCA to a real data set (K. MacNamara, personal communication, 2005). Twelve variables have been measured by gas chromatography on 43 samples of Irish whiskeys, of two different types; 19 samples were from type A and 24 samples were from type B, with the samples ordered according to the production time. The data are reported in Table 16.4.

Since a trained assessor can easily discriminate a whiskey of type A from a whiskey of type B, it is interesting to know whether this discrimination is possible also on a chemical basis, just taking into account the variables obtained by a routine analysis. When looking separately at each of the 12 variables, it can be seen that none of them completely separates the two types. Therefore, when thinking on a univariate basis, we could say that it is not possible to discriminate between the two types of whiskey. As a consequence, we could look for different (and possible more expensive to determine) variables.

After a PCA (Figure 16.3), it is instead evident that the information present in the 12 variables is sufficient to discriminate the two whiskeys clearly. Once more, it has

Table 16.4 Chemical composition of 43 whiskey samples

Sample	Type	(1) Acetaldehyde	(2) Ethyl acetate	(3) Acetal	(4) Propanol	(5) Isobutanol	(6) Isoamyl acetal	(7) Butanol-1	(8) 2-Me-1-butanol	(9) 3-Me-1-butanol	(10) Ethyl caproate	(11) Ethyl caprylate	(12) Ethyl caprate
1	A	80	408	37	583	466	24	15	388	988	3	13	45
2	A	76	327	40	507	483	25	18	396	1033	3	12	46
3	A	79	296	43	467	397	20	17	323	859	4	13	44
4	A	74	415	28	569	407	24	15	352	921	4	13	46
5	A	69	381	29	510	367	21	14	329	870	4	13	46
6	A	66	340	35	428	387	26	13	339	910	4	14	50
7	A	82	373	17	401	337	23	11	297	813	4	13	42
8	A	78	385	34	459	371	19	12	313	843	3	12	41
9	A	67	374	34	458	385	22	12	326	868	3	13	47
10	A	50	331	32	422	345	17	12	307	835	3	12	42
11	A	66	342	30	423	341	17	13	305	846	3	13	43
12	A	54	321	28	408	354	20	13	310	874	4	13	41
13	A	68	344	33	429	333	16	12	300	824	3	11	38
14	A	69	358	37	446	347	17	13	311	855	3	11	37
15	A	78	346	40	411	320	16	12	287	796	3	11	36
16	A	77	387	51	427	345	22	12	290	805	3	10	32
17	A	104	322	72	432	353	18	13	303	823	3	10	35
18	A	84	333	55	421	340	17	13	292	787	3	10	31
19	A	82	382	47	457	328	18	10	278	765	3	10	31
20	B	65	403	18	496	529	19	19	365	1014	3	11	35
21	B	58	352	18	434	457	17	17	312	907	3	8	26
22	B	71	394	25	555	560	18	20	391	1083	3	11	33
23	B	69	369	25	497	500	16	18	349	1005	3	10	29
24	B	83	344	28	489	479	15	17	352	957	3	10	29
25	B	93	344	31	500	481	15	18	352	990	3	10	29
26	B	65	453	18	503	529	21	17	390	1017	3	10	31
27	B	62	405	17	500	488	18	17	357	965	3	9	27
28	B	58	435	16	501	548	21	17	415	1056	3	10	31
29	B	63	459	17	544	575	21	19	426	1100	3	10	28
30	B	99	462	26	490	500	22	16	403	1057	3	10	30
31	B	81	357	21	402	396	16	14	310	814	2	7	17
32	B	80	380	23	497	483	18	17	395	1041	3	10	28
33	B	76	425	22	486	475	22	17	379	1007	4	10	25
34	B	79	446	24	446	418	18	14	319	803	3	9	25
35	B	78	461	24	478	458	19	16	352	908	3	9	23
36	B	108	477	29	493	430	16	14	329	811	3	11	28
37	B	111	481	28	494	429	16	15	330	833	3	9	22
38	B	82	408	22	473	431	18	12	317	774	3	10	27
39	B	73	428	20	493	445	18	13	327	804	3	8	20
40	B	102	469	25	490	457	20	11	327	776	3	10	27
41	B	90	463	22	491	452	20	12	324	774	3	9	21
42	B	50	410	14	440	419	19	12	300	704	3	11	28
43	B	61	425	17	445	432	20	12	318	758	3	10	23

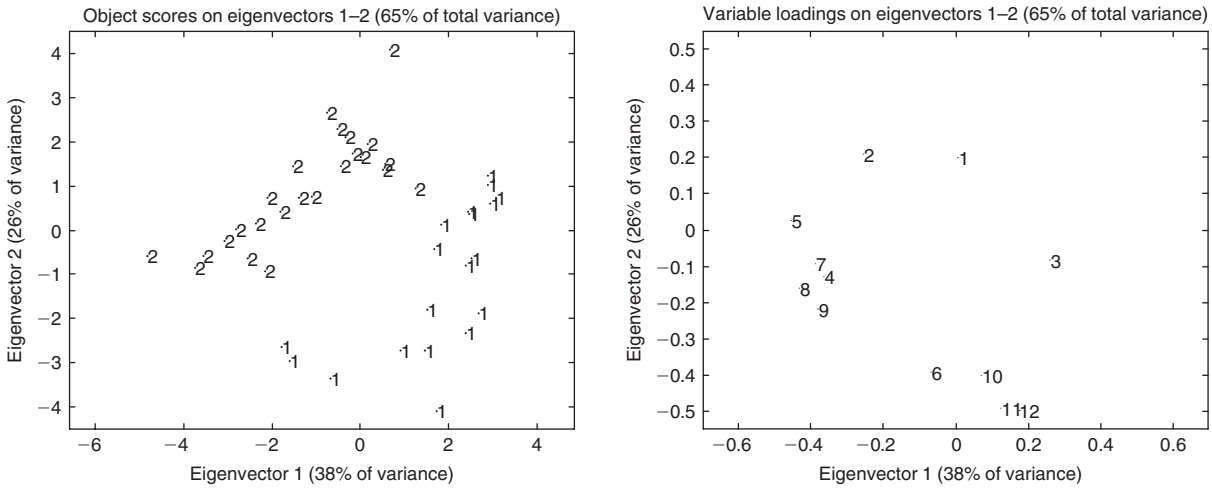

Figure 16.3 PCA of the data of Table 16.4. On the left is the score plot of the objects (coded according to the whiskey type), on the right is the loading plot of the variables (coded according to the order in Table 16.4).

to be pointed out that taking into account all the variables at the same time gives much more information than just looking at one variable at a time.

Now, let us go one step back and try to understand how this result has been obtained. First, since the variables have different magnitudes and variances, a normalization has to be performed, in such a way that each variable will have the same importance. Autoscaling is the most frequently used normalization, which is done by subtracting from each variable its mean value and then dividing the result by its standard deviation. After that, each normalized variable will have mean = 0 and variance = 1. Table 16.5 shows the data after autoscaling. The results of the PCA are such that PC1 explains 38.4% of the total variance and PC2 26.4%. This means that the PC1–PC2 plots shown in Figure 16.3 explain 64.8% of the total variance. Table 16.6 shows the loadings of the variables on PC1 and PC2. From it, the loading plot in Figure 16.3 is obtained.

From the score plot in Figure 16.3, it can be seen that the plane PC1–PC2 perfectly separates the two categories. By looking at the loading plot and at Table 16.6, it is possible to know which are the variables mainly contributing to each of the principal components. Variables 4, 5, 7, 8 and 9 (propanol, isobutanol, butanol-1, 2-Me-1-butanol and 3-Me-1-butanol – i.e. the alcohols) have the loadings with the highest absolute value on PC1, all of them being negative. This means that the alcohols are higher in those samples having the highest negative scores on PC1. Variables 6, 10, 11 and 12 (isoamyl acetal, ethyl caproate, ethyl caprylate and ethyl caprate – i.e. the esters) have the loadings with the highest absolute value on PC2, all of them being negative. This means that the esters are higher in those samples having the highest negative scores on PC2. Therefore, it can be said that the esters are the main responsible for the separation between the two types, while the alcohols are the main responsible for the variability within each type. The fact that all the alcohols have

Table 16.5 Autoscaled data

Sample	Type	(1) Acetaldehyde	(2) Ethyl acetate	(3) Acetal	(4) Propanol	(5) Isobutanol	(6) Isoamyl acetal	(7) Butanol-1	(8) 2-Me-1-butanol	(9) 3-Me-1-butanol	(10) Ethyl caproate	(11) Ethyl caprylate	(12) Ethyl caprate
1	A	0.288	0.340	0.672	2.507	0.553	1.743	0.187	1.348	0.936	−0.338	1.441	1.418
2	A	0.013	−1.285	0.927	0.791	0.796	2.105	1.335	1.559	1.366	−0.338	0.821	1.536
3	A	0.219	−1.907	1.183	−0.112	−0.435	0.295	0.952	−0.365	−0.297	2.084	1.441	1.301
4	A	−0.125	0.481	−0.095	2.190	−0.291	1.743	0.187	0.399	0.296	2.084	1.441	1.536
5	A	−0.469	−0.202	−0.010	0.858	−0.864	0.657	−0.196	−0.207	−0.192	2.084	1.441	1.536
6	A	−0.675	−1.024	0.501	−0.993	−0.578	2.467	−0.579	0.056	0.190	2.084	2.060	2.005
7	A	0.426	−0.362	−1.032	−1.602	−1.293	1.381	−1.344	−1.051	−0.737	2.084	1.441	1.066
8	A	0.150	−0.121	0.416	−0.293	−0.806	−0.067	−0.961	−0.629	−0.450	−0.338	0.821	0.949
9	A	−0.606	−0.342	0.416	−0.316	−0.606	1.019	−0.961	−0.286	−0.211	−0.338	1.441	1.653
10	A	−1.776	−1.205	0.246	−1.128	−1.178	−0.791	−0.961	−0.787	−0.526	−0.338	0.821	1.066
11	A	−0.675	−0.984	0.075	−1.106	−1.236	−0.791	−0.579	−0.840	−0.421	−0.338	1.441	1.184
12	A	−1.501	−1.406	−0.095	−1.444	−1.050	0.295	−0.579	−0.708	−0.154	2.084	1.441	0.949
13	A	−0.537	−0.944	0.331	−0.970	−1.350	−1.153	−0.961	−0.972	−0.631	−0.338	0.202	0.597
14	A	−0.469	−0.663	0.672	−0.586	−1.150	−0.791	−0.579	−0.682	−0.335	−0.338	0.202	0.480
15	A	0.150	−0.904	0.927	−1.377	−1.536	−1.153	−0.961	−1.314	−0.899	−0.338	0.202	0.363
16	A	0.082	−0.081	1.864	−1.015	−1.178	1.019	−0.961	−1.235	−0.813	−0.338	−0.418	−0.106
17	A	1.939	−1.386	3.654	−0.903	−1.064	−0.429	−0.579	−0.893	−0.641	−0.338	−0.418	0.245
18	A	0.563	−1.165	2.205	−1.151	−1.250	−0.791	−0.579	−1.183	−0.985	−0.338	−0.418	−0.224
19	A	0.426	−0.182	1.524	−0.338	−1.422	−0.429	−1.727	−1.552	−1.195	−0.338	−0.418	−0.224
20	B	−0.744	0.240	−0.947	0.542	1.454	−0.067	1.718	0.742	1.184	−0.338	0.202	0.245
21	B	−1.225	−0.784	−0.947	−0.857	0.424	−0.791	0.952	−0.655	0.162	−0.338	−1.657	−0.810
22	B	−0.331	0.059	−0.351	1.874	1.897	−0.429	2.100	1.427	1.844	−0.338	0.202	0.011
23	B	−0.469	−0.442	−0.351	0.565	1.039	−1.153	1.335	0.320	1.098	−0.338	−0.418	−0.458
24	B	0.494	−0.944	−0.095	0.384	0.739	−1.515	0.952	0.399	0.640	−0.338	−0.418	−0.458
25	B	1.182	−0.944	0.160	0.633	0.767	−1.515	1.335	0.399	0.955	−0.338	−0.418	−0.458
26	B	−0.744	1.243	−0.947	0.700	1.454	0.657	0.952	1.401	1.213	−0.338	−0.418	−0.224
27	B	−0.950	0.280	−1.032	0.633	0.867	−0.429	0.952	0.531	0.716	−0.338	−1.037	−0.693
28	B	−1.225	0.882	−1.117	0.655	1.726	0.657	0.952	2.060	1.586	−0.338	−0.418	−0.224
29	B	−0.881	1.364	−1.032	1.626	2.112	0.657	1.718	2.350	2.006	−0.338	−0.418	−0.575
30	B	1.595	1.424	−0.265	0.407	1.039	1.019	0.570	1.743	1.595	−0.338	−0.418	−0.341
31	B	0.357	−0.683	−0.691	−1.580	−0.449	−1.153	−0.196	−0.708	−0.727	−2.759	−2.276	−1.866
32	B	0.288	−0.222	−0.521	0.565	0.796	−0.429	0.952	1.533	1.442	−0.338	−0.418	−0.575
33	B	0.013	0.681	−0.606	0.317	0.681	1.019	0.952	1.111	1.117	2.084	−0.418	−0.927
34	B	0.219	1.103	−0.436	−0.586	−0.134	−0.429	−0.196	−0.471	−0.832	−0.338	−1.037	−0.927
35	B	0.150	1.404	−0.436	0.136	0.438	−0.067	0.570	0.399	0.171	−0.338	−1.037	−1.162
36	B	2.214	1.725	−0.010	0.475	0.038	−1.153	−0.196	−0.207	−0.756	−0.338	0.202	−0.575
37	B	2.420	1.805	−0.095	0.497	0.023	−1.153	0.187	−0.181	−0.545	−0.338	−1.037	−1.279
38	B	0.426	0.340	−0.606	0.023	0.052	−0.429	−0.961	−0.524	−1.109	−0.338	−0.418	−0.693
39	B	−0.194	0.742	−0.777	0.475	0.252	−0.429	−0.579	−0.260	−0.823	−0.338	−1.657	−1.514
40	B	1.801	1.564	−0.351	0.407	0.424	0.295	−1.344	−0.260	−1.090	−0.338	−0.418	−0.693
41	B	0.976	1.444	−0.606	0.429	0.352	0.295	−0.961	−0.339	−1.109	−0.338	−1.037	−1.396
42	B	−1.776	0.380	−1.288	−0.722	−0.120	−0.067	−0.961	−0.972	−1.778	−0.338	0.202	−0.575
43	B	−1.019	0.681	−1.032	−0.609	0.066	0.295	−0.961	−0.497	−1.262	−0.338	−0.418	−1.162

Table 16.6 Loadings of the variables on PC1 and PC2

	(1) Acetaldehyde	(2) Ethyl acetate	(3) Acetal	(4) Propanol	(5) Isobutanol	(6) Isoamyl acetal	(7) Butanol-1	(8) 2-Me-1-butanol	(9) 3-Me-1-butanol	(10) Ethyl caproate	(11) Ethyl caprylate	(12) Ethyl caprate
PC1	0.006	−0.253	0.261	−0.363	−0.452	−0.067	−0.385	−0.429	−0.378	0.071	0.146	0.159
PC2	0.196	0.206	−0.086	−0.129	0.023	−0.395	−0.096	−0.162	−0.221	−0.404	−0.493	−0.498

very similar loadings means that they are very much correlated, as is the case for the esters. This is a further demonstration of the superiority of multivariate analysis over univariate analysis. Indeed, it will be possible to adulterate a product in such a way that all the variables, singularly taken, fall inside their individual range of acceptance; much more difficult (not to say impossible) will be to have an adulterated product in which the correlations among the variables will also be preserved. Therefore, adulterated products that will be unnoticed by the "classical" univariate analysis will be easily detected by a multivariate analysis (see "Modeling", below).

Table 16.7 reports the scores of the objects on PC1 and PC2.

As previously shown, the scores of an object are computed by multiplying the loadings of each variable by the value of the variable. As an example, let us compute the score of sample 1 on PC1 (since the autoscaled data have been used, these are the values that must be taken into account):

$$0.288 * 0.006 + 0.340 * (-0.253) + 0.672 * 0.261 + 2.507 * (-0.363) + 0.553 * (-0.452) + 1.743 * (-0.067) + 0.187 * (-0.385) + 1.348 * (-0.429) + 0.936 * (-0.378) + (-0.338) * 0.071 + 1.441 * 0.146 + 1.418 * 0.159 = -1.778$$

So, we have demonstrated that the two types of whiskeys really are different, from the chemical point of view as well.

Now, let us look at Figure 16.4. In it, the samples are coded according to Table 16.4, i.e. following the production order. It can be seen that for both types there is a trend from the left-hand side of the plot (negative values of PC1) to the right-hand side of the plot (positive values of PC1), with this effect being much clearer for type 1. As has previously been said, PC1 is mainly related to the alcohols. Therefore, it can be concluded that throughout the production period taken into account there has been a progressive decrease of the alcohol content. While the previous finding was the answer to a question that was explicitly formulated by the producer ("are the two types of whiskey different?"), this result emerged totally unexpectedly. This demonstrates very well what Bro and colleagues have stated in a paper (Bro *et al.*, 2002):

> Usually, data analysis is performed as a confirmatory exercise, where a postulated hypothesis is claimed, data generated accordingly and the data analysed in order either to verify or reject this hypothesis.

Table 16.7 Scores of the objects on PC1 and PC2

Object	Category	Score on PC1	Score on PC2
1	A	−1.778	−2.654
2	A	−1.581	−2.974
3	A	1.477	−2.730
4	A	−0.679	−3.359
5	A	0.921	−2.744
6	A	1.737	−4.096
7	A	2.675	−1.889
8	A	1.673	−0.432
9	A	1.534	−1.811
10	A	2.526	−0.650
11	A	2.395	−0.793
12	A	2.395	−2.350
13	A	2.488	0.350
14	A	1.850	0.113
15	A	3.080	0.722
16	A	2.446	0.409
17	A	2.955	0.603
18	A	2.891	1.031
19	A	2.903	1.231
20	B	−2.546	−0.658
21	B	−0.426	1.448
22	B	−3.730	−0.862
23	B	−1.805	0.400
24	B	−1.093	0.748
25	B	−1.392	0.723
26	B	−3.069	−0.258
27	B	−2.090	0.724
28	B	−3.556	−0.589
29	B	−4.814	−0.585
30	B	−2.815	0.020
31	B	0.677	4.098
32	B	−2.361	0.140
33	B	−2.148	−0.925
34	B	0.180	1.939
35	B	−1.527	1.444
36	B	−0.173	1.729
37	B	−0.747	2.663
38	B	0.575	1.484
39	B	−0.510	2.283
40	B	0.012	1.648
41	B	−0.314	2.114
42	B	1.251	0.927
43	B	0.514	1.368

No new knowledge is obtained in confirmatory analysis except the possible verification of a prior postulated hypothesis. Using exploratory analysis the data are gathered in order to represent as broadly and as well as possible the problem under investigation.

The data are analysed and through the, often visual, inspection of the results, hypotheses are suggested on the basis of the empirical data. Consequently, exploratory data analysis is an extraordinary tool in displaying thus far unknown information from established and potential monitoring methods.

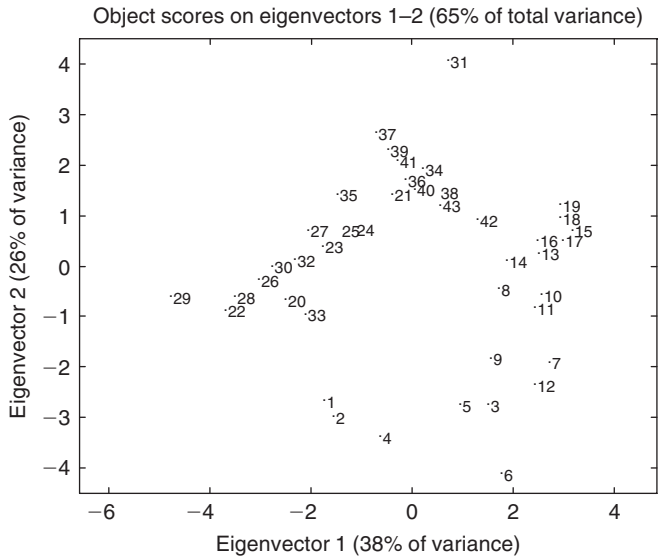

Figure 16.4 Score plot of the data in Table 16.4 (the samples are coded according to the order in Table 16.4).

Process monitoring and quality control

When running a process, it is very important to know whether it is under control (i.e. within its natural variability) or out of control (i.e. in a condition that is not typical and therefore can lead to an accident).

Analogously, when producing a product it is very important to know whether each single piece is within specifications (i.e. close to the "ideal" product, within its natural variability) or outside specification (i.e. significantly different from the "standard" product and therefore in a condition possibly leading to a complaint by the final client).

PCA is the basis for multivariate process monitoring and multivariate quality control, which are much more effective than the generally applied univariate approaches (Kourti and MacGregor, 1995).

Having collected a relevant number of observations describing the "normally operating" process (or the "within specification" products), encompassing all the sources of normal variability, it will then be possible to build a PCA model defining the limits within which the process (or the product) should stay.

Any new set of measurements (a vector $\mathbf{x}_{1,v}$) describing the process at a given moment (or a new product) will be projected onto the previously defined model by using the following equation: $\mathbf{s}_{1,c} = \mathbf{x}_{1,v} * \mathbf{L}_{c,v}'$. From the computed scores, it can be estimated how far from the barycenter of the model, i.e. from the "ideal" process (or product), it is.

Its residuals can also be easily computed: $\mathbf{e}_{1,v} = \mathbf{x}_{1,v} - \mathbf{s}_{1,c} * \mathbf{L}_{c,v}$ ($\mathbf{e}_{1,v}$ is the vector of the residuals, and each of its v elements corresponds to the difference between the

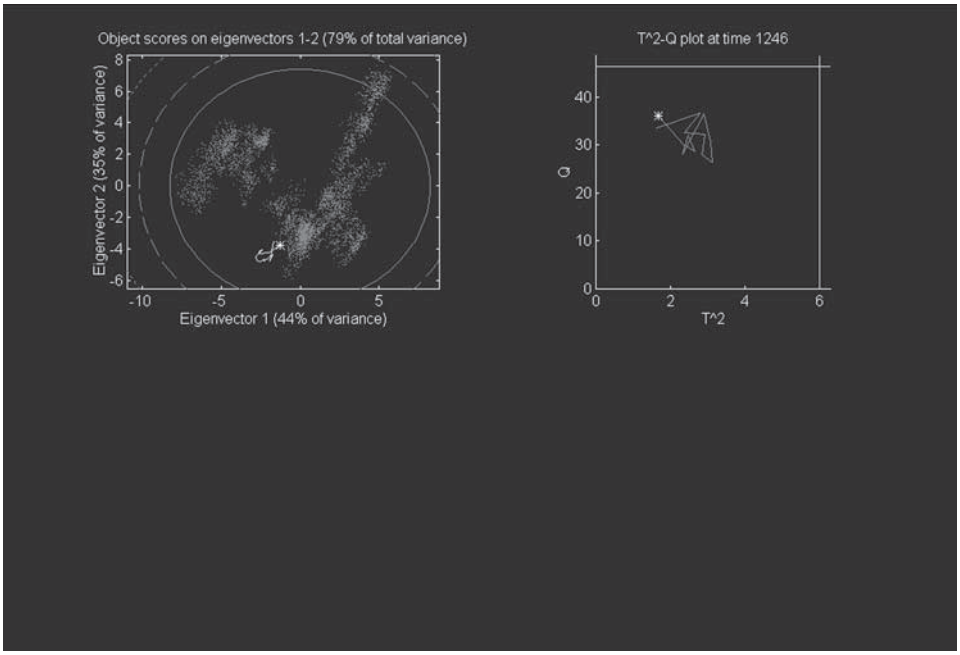

Figure 16.5 Output of process monitoring software when the process is under control.

measured and reconstructed values of each variable). From them, it can be understood how well the sample is reconstructed by the PCA model, i.e, how far from the model space (a plane, in the case c = 2) it lies.

Statistical tests make possible the automatic detection of an outlier in both cases (they are defined as T^2 outliers in the first case and Q outliers in the second case). With these simple tests it will be possible to detect a fault in a process or to reject a bad product by checking just two plots, instead of as many plots as variables, as in the case of the Sheward charts commonly used when the univariate approach is applied. Finally, the contribution plots will easily outline which variables are responsible for the sample being an outlier.

Figure 16.5 shows the output of process-monitoring software (Leardi *et al*., 2007) when the process (in this case, a continuous two-column whiskey distillation pilot plant, with 26 process variables being monitored) is in an ideal condition.

The actual situation of the plant (starred in Figure 16.5) is well within both the confidence ellipses of the PCA model (left-hand plot) and the critical limits of the T^2 and Q statistics (right-hand plot). Furthermore, the green trajectories in both plots also demonstrate that the variability of the plant in the last hour has been quite small.

From Figure 16.6, it is instead very easy to understand that the process is no longer under control. Looking at the PCA plot (left-hand plot), it can be seen that the star is at the border of the external ellipse, corresponding to p = 0.001; furthermore, the green trajectory shows the presence of a very clear trend which has taken place during the last hour. Looking at the T^2–Q plot, it is clear that, while the T^2 value is

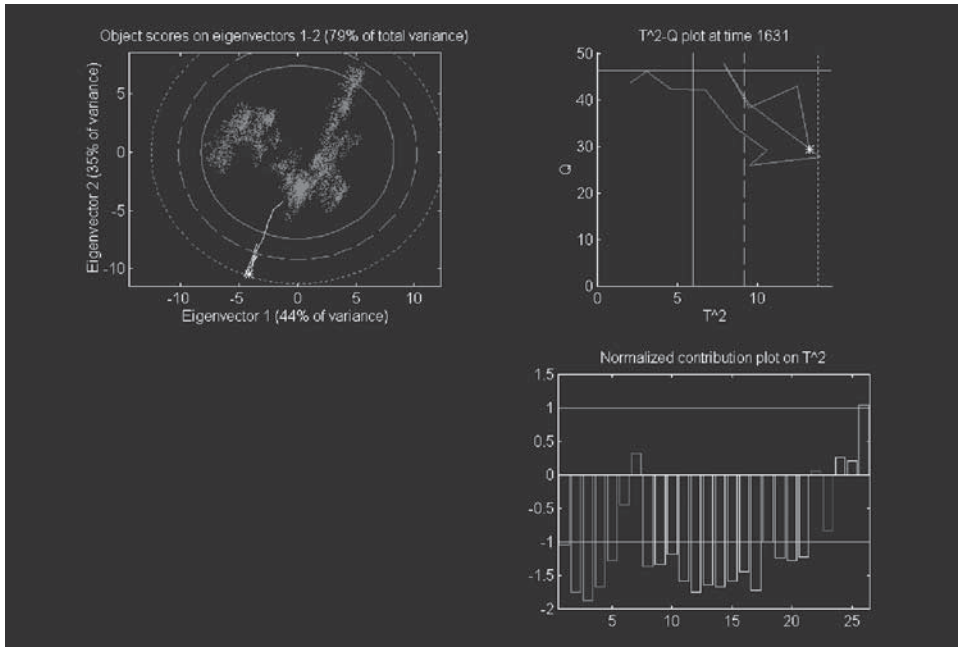

Figure 16.6 Output of process monitoring software when the process is out of control.

very close to the p = 0.001 critical limit, the Q value is well below any critical limit; this means that the correlations inside the plant are still preserved.

The T^2 normalized contribution plot shows that the anomalous situation depends on the fact that the temperatures in the two columns (variables 1–21 on the chart in Figure 16.6) are lower than the normal values.

Compared with the standard univariate approach, the multivariate approach is much more robust, since it will lead to a lower number of false-negatives and false-positives, and much more sensitive, since it allows the detection of faults at an earlier stage.

Furthermore, in many cases a process that is out of control produces a product which is also outside specification. Therefore, the multivariate process monitoring also gives an indirect estimation of the quality of the final product, without having to perform any direct analysis on the product itself, whose results would be known some time later.

Morris and Martin (2003) tried to quantify the advantage brought by multivariate process monitoring, and came to the following conclusions:

> Better process control not only increases yields and results in more consistent high-quality production, but has contributed to reducing specific energy costs by around 5% to 6%, coupled with production increases of up to 10%. It is conjectured that, if 10% of the 100 000 process manufacturing plants in Europe embrace these technologies, a net benefit of the order of €500 million per annum to the European process manufacturing industries could result (EU Project Prognosis).

Three-way PCA

It can happen that the structure of a data set is such that a standard two-way table (objects versus variables) is not enough to describe it. Let us suppose that some food samples have been analyzed by a panel of assessors, each of them giving scores to different attributes. A third way needs to be added to adequately represent the data set, which can be imagined as a parallelepiped of size $I \times J \times K$, where I is the number of food samples (objects), J is the number of attributes (variables) and K is the number of assessors (conditions) (Geladi, 1989; Smilde, 1992).

To apply standard PCA, these three-way data arrays $\underline{\mathbf{X}}$ have to be somehow transformed to obtain a two-way data table. This can be done in different ways, according to the focus of interest.

The usual and simplest transformation is to average the scores given by the different assessors. By doing that, a matrix with I rows and J columns is obtained. This is simply done, but the price to be paid is that, since we are now dealing with the scores given by a hypothetical "average" assessor, we have lost every kind of information related to the assessors, such as the variability with which each attribute is assessed and the systematic effect typical of each assessor.

A different transformation applied to study the food samples consists of matricizing the data array $\underline{\mathbf{X}}$ to $\mathbf{X}'_a$ (I rows, $J \times K$ columns). The interpretability of the score plot is usually very high, but since $J \times K$ is usually a rather large number, the interpretation of the loading plot is very difficult. The same considerations can be made when focusing on the assessors; in this case, $\mathbf{X}'_c$ is obtained (K rows, I $\times$ J columns).

Three-way PCA allows a much easier interpretation of the information contained in the data set, since it directly takes into account its three-way structure. If the Tucker3 model (Tucker, 1966) is applied, the final result is given by three sets of loadings together with a core array describing the relationship among them. If the number of components is the same for each way, the core array is a cube. Each of the three sets of loadings can be displayed and interpreted in the same way as a score plot of standard PCA.

In the case of a cubic core array, a series of orthogonal rotations can be performed on the three spaces of the objects, variables and conditions, looking for the common orientation for which the core array is as much body-diagonal as possible. If this condition is sufficiently achieved, then the rotated sets of loadings can also be interpreted jointly by overlapping them.

An example of application of three-way PCA is a data set from the field of sensory evaluation (Cordella and Leardi, 2008). In it, eight types of noodles, each corresponding to a different formulation, were produced in four independent replicates, with each replicate tested by the panel in two independent sessions. Each of the 12 panellists gave a score to 8 descriptors (1, yellow color; 2, translucency; 3, shininess; 4, surface smoothness; 5, firmness; 6, chewiness; 7, surface stickiness; 8, elasticity). The data set can therefore be seen as a $64 \times 8 \times 12$ data set.

By taking into account the loading plots of the objects (Figure 16.7), it can be seen that the regions occupied by the 8 samples of each noodle (4 replicates $\times$ 2 sessions)

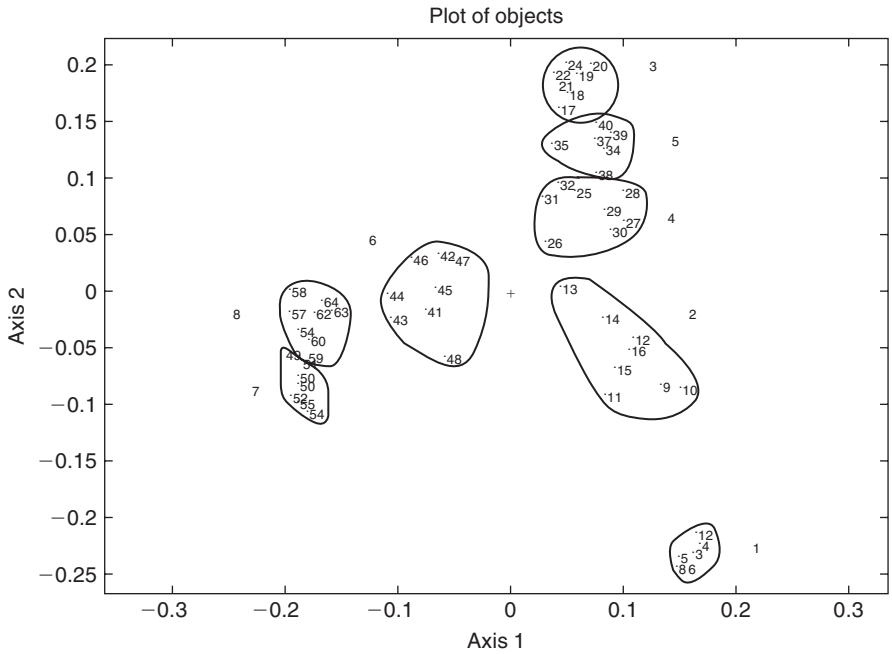

Figure 16.7 Scatter plot of the loadings of the objects. Objects 1–8, noodle 1; objects 9–16, noodle 2; objects 57–64, noodle 8.

never overlap. This means that the global variability (production + sensory evaluation) of each noodle is always smaller than the differences among the noodles. The fact that the region spanned by each noodle is approximately the same (with the exception of noodle 2) indicates that the global variability can be considered as independent of the type of noodle. It can also be seen that the variability between sessions is smaller than the variability among replicates; this means that the "instrumental error" of the judges is smaller than the variability of the production.

On the first axis, noodles 7 and 8 have the lowest loading, followed by noodle 6 and then by the remaining five types, all with very similar loading. This ranking ($7 = 8 > 6$) corresponds to the content of glyceryl monostearate (GMS, 2.8%, 2.8% and 1.4%, respectively, with the other noodles having no GMS). It can be concluded that the loadings of each noodle group on the first axis is directly related to the GMS content.

On the second axis, the five formulations having no GMS are discriminated, with noodle 3 having the highest loading and noodle 1 having by far the lowest loading. Noodle 3 is made only from durum wheat flour (DWF), while noodle 1 is the only one containing wheat starch (WS). On the same axis, noodles 5, 4 and 2 have decreasing loadings, and this corresponds to their amount of wheat gluten (WG, 6%, 3% and 0%, respectively).

Figure 16.8 shows the scatter plot of the loadings of the variables. Variables 5–8 (the texture-related descriptors) have the highest values on the first axis. This means that the first axis is mainly related to the texture of the product. Variables 1 and 4 (color and smoothness, both positive attributes) have positive loadings on axis 2, in

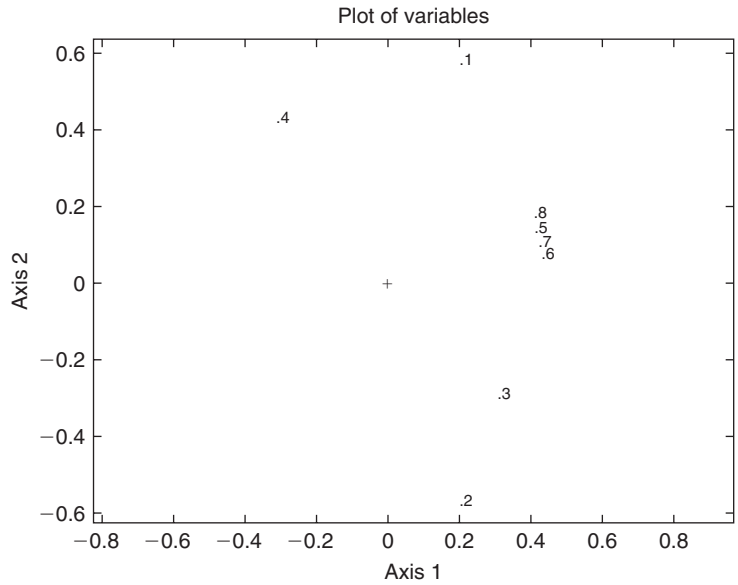

Figure 16.8 Scatter plot of the loadings of the variables.

Table 16.8 Data sets on which three-way PCA can be applied

Field of application	Objects	Variables	Conditions
Environmental analysis	Air or water samples	Chemico-physical analyses	Time
Environmental analysis	Water samples (different locations)	Chemico-physical analyses	Depth
Panel tests	Food products (oils, wines)	Attributes	Assessors
Food chemistry	Foods (cheeses, spirits, ...)	Chemical composition	Ageing
Food chemistry	Foods (oils, wines, ...)	Chemical composition	Crops
Sport medicine	Athletes	Blood analyses	Time after effort
Process monitoring	Batches	Chemical analyses	Time

contrast with variables 2 and 3 (translucency and shininess, both negative attributes). Therefore, the second axis is mainly related to the appearance attributes of the noodles.

It should also be noticed that variables 5–8 (the texture-related descriptors) have very similar loadings on both axes, and therefore are very highly correlated. As a result, it can be concluded that axis 1 is related to the amount of GMS and to the texture of the product; it can be seen that the addition of GMS gives a worse product.

Axis 2 is related to the aspect; it can be seen that noodle 3, obtained with DWF, is the product with the best appearance (it is the most yellow and the smoothest), while noodle 1, obtained with a large amount of WS, has the worst appearance (it is the most translucent and shiniest). The addition of WG also improves the appearance, since it results in an increase of the yellow color and of the smoothness. By taking into account both axes, it is easy to detect noodle 3 as being the best. Table 16.8 shows some types of data sets on which three-way PCA can be successfully applied.

Classification

Earlier in this chapter we verified that the two types of whiskey are indeed well separated in the multivariate space of the variables. Therefore, we can say that we have two really different classes. Let us suppose we now have some unknown samples and want to know what their class is. After having performed the chemical analyses, we can add these data to the previous data set, run a PCA and see where the new samples are placed. This will be fine if the new samples fall inside one of the clouds of points corresponding to a category, but what if they fall in an intermediate position? How can we say with "reasonable certainty" that the new samples are from type A or type B? We know that PCA is a very powerful technique for data display, but we realize that we need something different if we want to classify new samples. What we want is a technique producing some "decision rules" discriminating among the possible categories.

While PCA is an "unsupervised" technique, the classification methods are "supervised" techniques. In these techniques, the category of each of the objects on which the model is built must be specified in advance.

The most commonly used classification techniques *are linear discriminant analysis* (LDA) and *quadratic discriminant analysis* (QDA). They define a set of delimiters (according to the number of categories under study) in such a way that the multivariate space of the objects is divided into as many subspaces as the number of categories, and that each point of the space belongs to one, and only one, subspace. Rather than describing in detail the algorithms behind these techniques, special attention will be given to the critical points of a classification.

As previously stated, the classification techniques use objects belonging to the different categories to define boundaries delimiting regions of the space. The final goal is to apply these classification rules to new objects for their classification into one of the existing categories. The performance of the technique can be expressed as classification ability and prediction ability. The difference between "classification" and "prediction", though quite subtle at first glance, is actually very important, and its underestimation can lead to very bitter deceptions.

Classification ability is the capability of assigning to the correct category the same objects used to build the classification rules, while *prediction ability* is the capability of assigning to the correct category objects that have not been used to build the classification rules. Since the final goal is the classification of new samples, it has to be clear that the predictive ability is by far the most important figure of merit to be looked at.

The results of a classification method can be expressed in several ways. The most synthetic one is the percentage of correct classifications (or predictions). Note that in the following only the term "classification" will be used, but it has to be understood as "classification or prediction". This can be obtained as the number of correct classifications (independently of the category) divided by the total number of objects, or as the average of the performance of the model over all the categories. The two results are very similar when the size of all the categories is very similar, but can be very different if the size is quite different. Let us consider the case shown in Table 16.9.

Table 16.9 Example of the performance of a classification technique

Category No.	Objects	Correct classification	% Correct classification
1	112	105	93.8
2	87	86	98.9
3	21	10	47.6
Total	220	201	91.4/80.1

Table 16.10 Example of a classification matrix

Category	1	2	3
1	105	0	7
2	1	86	0
3	11	0	10

The very poor performance of category 3, by far the smallest one, hardly affects the classification rate computed on the global number of classifications, while it produces a much lower result if the classification rate is computed as the average of the three categories.

A more complete and detailed overview of the performance of the method can be obtained by using the classification matrix, which also allows to know the categories to which the wrongly classified objects are assigned (in many cases, the cost of an error can be quite different according to the category the sample is assigned to). In it, each row corresponds to the true category and each column to the category to which the sample has been assigned. Continuing with the previous example, a possible classification matrix is shown in Table 16.10.

From Table 16.10, it can be seen that the 112 objects of category 1 were classified in the following way: 105 correctly to category 1, none to category 2, and 7 to category 3. In the same way, it can be deduced that all the objects of category 3 which were not correctly classified have been assigned to category 1. Therefore, it is easy to conclude that category 2 is well defined and that the classification of its objects gives no problems at all, while categories 1 and 3 are overlapping. As a consequence, to achieve perfect classification more effort must be put into better separation of categories 1 and 3. All this information cannot be obtained from just the percentage of correct classifications.

If overfitting occurs, then the prediction ability will be much worse than the classification ability. To avoid it, it is very important that the sample size is adequate for the problem and the technique. A general rule is that the number of objects should be more than five times (at the very least no less than three times) the number of parameters to be estimated. LDA works on a pooled variance–covariance matrix; this means that the total number of objects should be at least five times the number of variables. QDA computes a variance–covariance matrix for each category, which makes it a more powerful method than LDA, but this also means that each category should have a number of objects at least three times higher than the number of variables.

This is a good example of how the more complex, and therefore "better" methods, sometimes cannot be used in a safe way because their requirements do not correspond to the characteristics of the data set.

Modeling

In classification, the space is divided into as many subspaces as categories, and each point belongs to one, and only one, category. This means that the samples that will be predicted by such methods must belong to one of the categories used to build the models; if not, they will anyway be assigned to one of them. To make this concept clearer, let us suppose the use of a classification technique to discriminate between water and wine. Of course, this discrimination is very easy. Each sample of water will be correctly assigned to the category "water" and each sample of wine will be correctly assigned to the category "wine". However, what will happen with classification of a sample of orange squash? The sample will be assigned either to the category "water" (if variables such as alcohol are taken into account) or to the category "wine" (if variables such as color are considered). The classification techniques are therefore not able to define a new sample as being "something different" from all the categories of the training set. This is instead the main feature of the modeling techniques.

Though several techniques are used for modeling purposes, UNEQ (one of the modeling versions of QDA) and SIMCA (soft independent model of class analogy) are the most used. While in classification every point of the space belongs to one and only one category, with these techniques the models (one for each category) can overlap and leave some regions of the space unassigned. This means that every point of the space can belong to one category (the sample has been recognized as a sample of that class), to more than one category (the sample has such characteristics that it could be a sample of more than one class) or to none of the categories (the sample has been considered as being different from all the classes).

Of course, the "ideal" performance of such a method would be not only to correctly classify all the samples in their category (as in the case of a classification technique), but also be such that the models of each category could be able to accept all the samples of that category and reject all the samples of the other categories. The results of a modeling technique are expressed the same way as in classification, plus two very important parameters: specificity and sensitivity. For category c, its specificity (how much the model rejects the objects of different categories) is the percentage of the objects of categories different from c rejected by the model, while its sensitivity (how much the model accepts the objects of the same category) is the percentage of the objects of category c accepted by the model.

While the classification techniques need at least two categories, the modeling techniques can also be applied when only one category is present. In this case, the technique detects whether the new sample can be considered as a typical sample of that category or not. This can be very useful in the case of Protected Denomination of Origin products, to verify whether a sample, declared as having been produced in a well-defined region, indeed has the characteristics typical of the samples produced in that region.

The application of a multivariate analysis will greatly reduce the possibility of fraud. While an "expert" can adulterate a product in such a way that all the variables, independently considered, still stay in the accepted range, it is almost impossible to adulterate a product in such a way that its multivariate "pattern" is still accepted by the model of the original product, unless the amount of the adulterant is so small that it becomes unprofitable from the economic point of view.

Calibration

Let us imagine we have a set of wine samples and that on each of them the FT-IR spectrum is measured, together with some variables such as alcohol content, pH or total acidity. Of course, chemical analyses will require much more time than a simple spectral measurement. It would therefore be very useful to find a relationship between each of the chemical variables and the spectrum. This relationship, after having been established and validated, will be used to predict the content of the chemical variables. It is easy to understand how much time (and money) this will save, since in a few minutes it will be possible to have the same results as previously obtained by a whole set of chemical analyses.

Generally speaking, we can say that *multivariate calibration* finds relationships between one or more response variables y and a vector of predictor variables $\mathbf{x}$. As the previous example has shown, the final goal of multivariate calibration is not just to "describe" the relationship between the $\mathbf{x}$ and the y variables in the set of samples on which the relationship has been computed, but to find a real practical application for samples that in a following time will have the $\mathbf{x}$ variables measured.

The model is a linear polynomial ($y = b_0 + b_1x_1 + b_2x_2 + \cdots + b_kx_k + f$), where b_0 is an offset, the b_k ($k = 1, \ldots, K$) are regression coefficients and f is a residual. The "traditional" method of calculating $\mathbf{b}$, the vector of regression coefficients, is *ordinary least squares* (OLS). However, this method has two major limitations that make it inapplicable to many data sets:

1. It cannot handle more variables than objects
2. It is sensitive to collinear variables.

It can easily be seen that both these limitations do not allow the application of OLS to spectral data sets, where the samples are described by a very high number of highly collinear variables. If we want to use OLS with such data anyway, the only way to do it is to reduce the number of variables and their collinearity through a suitable *variable selection* (see below).

When describing PCA, it can be seen that the components are orthogonal (i.e. uncorrelated) and that the dimensionality of the resulting space (i.e. the number of significant components) is much lower than the dimensionality of the original space. Therefore, it is clear that both the aforementioned limitations have been overcome. As a consequence, it is possible to apply OLS to the scores originated by PCA. This technique is *principal component regression* (PCR).

It has to be remembered that principal components are computed by taking into account only the **x** variables, without considering at all the *y* variable(s), and are ranked according to the explained variance of the "*x* space". This means that it can happen that the first PC has little or no relevance in explaining the response that we are interested in. This can be easily understood by considering that, even when we have several responses, the PCs to which the responses have to be regressed will be the same.

Nowadays, the most favored regression technique is *partial least squares regression* (PLS, or PLSR). As happens with PCR, PLS is based on components (or "latent variables"). The PLS components are computed by taking into account both the **x** and the **y** variables, and therefore they are slightly rotated versions of the principal components. As a consequence, their ranking order corresponds to the importance in the modeling of the response. A further difference of OLS and PCR is that, while the former must work on each response variable separately, PLS can be applied to multiple responses at the same time.

Because both PCR and PLS are based on latent variables, a critical point is the number of components to be retained. Though we know that information is "concentrated" in the first components and that the last components explain just noise, it is not always an easy task to detect the correct number of components (i.e. when information finishes and noise begins). Selecting a lower number of components would mean removing some useful information (underfitting), while selecting a higher number of components would mean incorporating some noise (overfitting).

Before applying the results of a calibration, it is very important to look for the presence of outliers. Three major types of outliers can be detected: outliers in the *x*-space (samples for which the *x*-variables are very different from that of the rest of the samples; they can be found by looking at a PCA of the *x*-variables), outliers in the *y*-space (samples with the *y*-variable very different from that of the rest of the samples; they can be found by looking at a histogram of the *y*-variable) and samples for which the calibration model is not valid (they can be found by looking at a histogram of the residuals).

The goodness of a calibration can be summarized by two values; the percentage of variance explained by the model, and the *root mean square error in calibration* (RMSEC). The former, being a "normalized" value, gives an initial idea about how much of the variance of the data set is "captured" by the model; the latter, being an absolute value to be interpreted in the same way as a standard deviation, gives information about the magnitude of the error.

As already described in the classification section and pointed out at the beginning of this section, the goal of a calibration is essentially not to describe the relationship between the response and the *x*-variables of the samples on which the calibration is computed (training, or calibration, set), but to apply it to future samples where only the cheaper *x*-variables will be measured. In this case too, the model must be validated by using a set of samples different from those used to compute the model (validation, or test, set). The responses of the objects of the test set will be computed by applying the model obtained by the training set, and then compared with their "true" response. From these values, the percentage of variance explained in prediction and the *root mean square error in prediction* (RMSEP) can be computed. Provided that

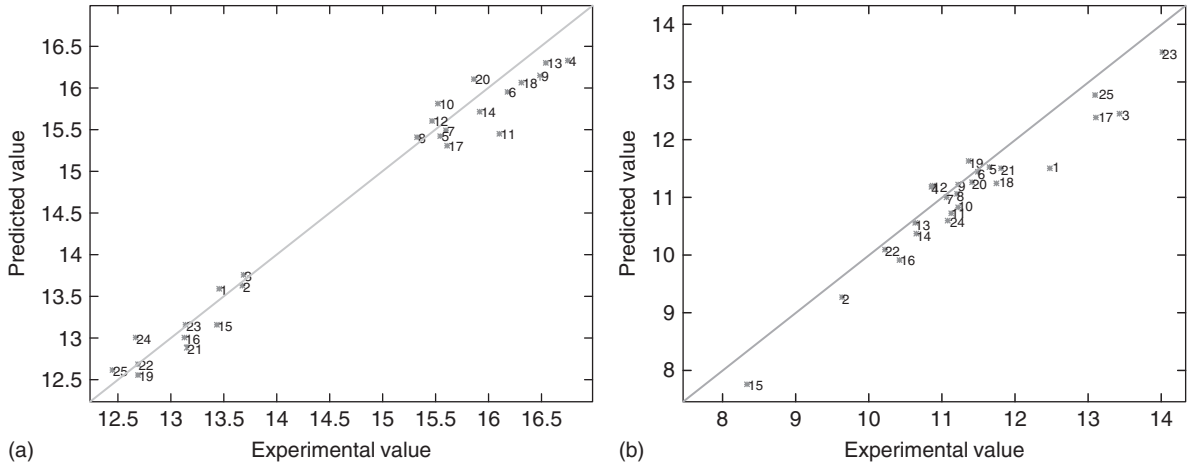

Figure 16.9 Experimental vs predicted values of the test set with PLS applied to the whole spectrum: (a) moisture, (b) protein.

the objects forming the two sets have been selected flawlessly, these values give the real performance of the model on new samples.

As an example, the results obtained on wheat samples (Kalivas, 1997) are reported. The NIR spectra of 100 samples were recorded from 1100 to 2500 nm in steps of 2 nm (701 wavelengths), and on the same samples two responses (moisture and protein) were measured. Of the samples, 75 were used as training set, while the remaining 25 constituted the test set. The ranges of the two responses were 12.45–17.36 and 7.75–14.28, and the RMSEP obtained by applying PLS to the whole spectrum were 0.28 and 0.43, respectively.

From Figure 16.9, showing the predictions on the test set, it can be seen that the accuracy of the estimation is quite good, though in the case of protein a systematic bias can be detected.

Variable selection

Usually, not all the variables of a data set bring useful and non redundant information. Therefore, a variable (or feature) selection can be highly beneficial because it will lead to the following results:

- Removal of noise and improvement of the performance
- Reduction of the number of variables to be measured and simplification of the model.

The removal of noisy variables should always be sought. Though some methods can give good results even with a moderate amount of noise disturbing the information, it is clear that their performance will increase when this noise is removed. Thus, feature selection is now widely applied also for those techniques (PLS and PCR) that in the beginning were considered to be almost insensitive to noise.

While noise reduction is a common goal for any data set, the relevance of the reduction of the number of variables in the final model depends very much on the kind of data constituting the data set, and a very wide range of situations are possible. Let us consider the extreme conditions:

- Each variable requires a separate analysis
- All the variables are obtained by the same analysis (e.g. chromatographic and spectroscopic data).

In the first case, each variable not selected means a reduction in terms of costs and/or analysis time. The variable selection should therefore always be made on a cost–benefit basis, looking for the subset of variables leading to the best compromise between performance of the model and cost of the analyses. This means that, in the presence of groups of useful but highly correlated (and therefore redundant) variables, only one variable per group should be retained. With such data sets, it is also possible that a subset of variables giving a slightly worse result may be preferred, if the reduction in performance is widely compensated for by a reduction in costs or time.

In the second case, the number of retained variables has no effect on the analysis cost, while the presence of useful and correlated variables improves the stability of the model. Therefore, the goal of variable selection will be to improve the predictive ability of the model by removing the variables giving no information, without being worried by the number of retained variables.

Intermediate cases can occur, in which "blocks" of variables are present. As an example, take the case of olive oil samples, on each of which the following analyses have been run: a titration for acidity, the analysis of peroxides, a UV spectroscopy for ΔK, a GC for sterols, and another GC for fatty acids. In such a situation, what counts is not the final number of variables, but the number of analyses that can be saved.

The only possible way to be sure that the "best" set of variables has been picked up is to use the "all-models" techniques to test all the possible combinations. Since with k variables the number of possible combinations is $2^k - 1$, it is easy to understand that this approach cannot be used unless the number of variables is really very low (for example, with 30 variables more than 10^9 combinations should be tested).

The simplest (but least effective) way of performing a feature selection is to operate on a "univariate" basis, by retaining those variables having the greatest discriminating power (in case of a classification) or the greatest correlation with the response (in case of a calibration). By doing that, each variable is taken into account by itself without considering how its information "integrates" with the information brought by the other (selected or unselected) variables. As a result, if several highly correlated variables are "good" they are all selected, without taking into account that, owing to their correlation, the information is highly redundant and therefore at least some of them can be removed without any decrease in performance. On the other hand, those variables that, although not themselves giving significant information, become very important when their information is integrated with that of other variables, are not taken into account.

An improvement is brought by the "sequential" approaches. They select the best variable first, then the best pair formed by the first and second, and so on in a forward

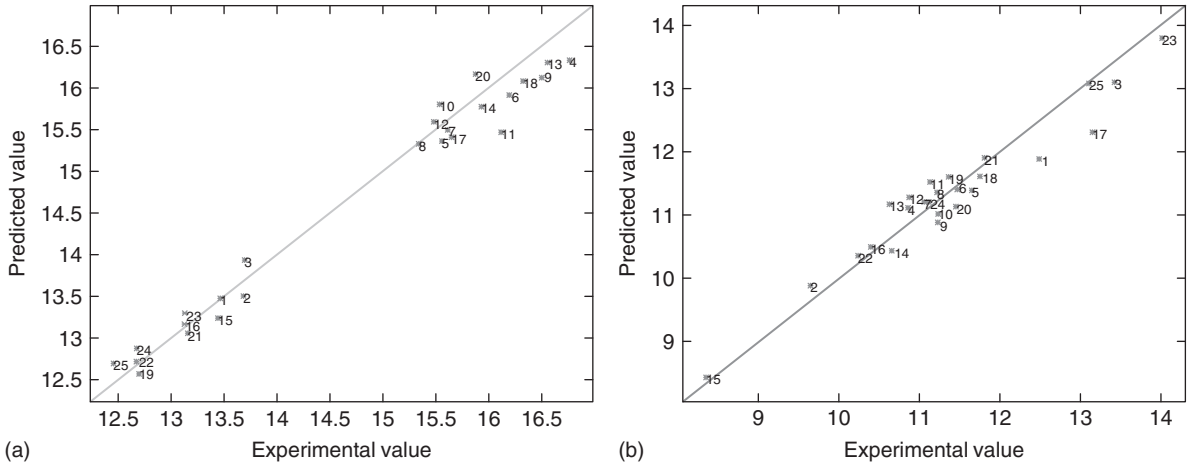

Figure 16.10 Experimental vs predicted values of the test set with PLS applied after variable selection: (a) moisture, (b) protein.

or backward progression. A more sophisticated approach applies a look back from the progression to reassess previous selections. The problem with these approaches is that only a very small part of the experimental domain is explored, and the number of models to be tested becomes very high in case of highly dimensional data sets (such as spectral data sets). For instance, with 1000 wavelengths, 1000 models are needed for the first cycle (selection or removal of the first variable), 999 for the second cycle, 998 for the third cycle, and so on.

More "multivariate" methods of variable selection, especially suited for PLS applied to spectral data, are currently available. Among them, we can *cite interactive variable selection* (Lindgren *et al*., 1994), *uninformative variable elimination* (Centner *et al*., 1996), *iterative predictor weighting PLS* (Forina *et al*., 1999) *and interval PLS* (Nørgaard *et al*., 2000). The improvements obtained by the application of a variable selection can be checked by looking at Figure 16.10.

In Figure 16.10, the predictions on the test set of the wheat data after variable selection by genetic algorithms (see below) are reported (Leardi, 2000). In Leardi's research, when the variables were reduced from the original 701 to 104 (for moisture) and 64 (for protein), the RMSEP decreased from 0.28 to 0.24 and from 0.43 to 0.30 respectively. In the case of protein, it can be seen that the bias present when the model was built on the whole spectrum totally disappeared.

Future trends

In future, multivariate analysis should be used more and more in everyday (scientific) life. Until a few decades ago, experimental work resulted in a very limited amount of data, the analysis of which was quite easy and straightforward. Nowadays, it is common to have instrumentation producing an almost continuous flow of data. One example is process monitoring, performed by measuring the values of several

process variables at a rate of one measurement every few minutes (or even seconds). Another example is quality control of a final product of a continuous process, on which an FT-IR spectrum is taken every few minutes (or seconds).

Earlier in this chapter the case of wine FT-IR spectra was cited, from which the main characteristics of the product can be directly predicted. It is therefore clear that the main problem has shifted from obtaining a few data to the treatment of a huge amount of data. It is also clear that standard statistical treatment is not enough to extract the whole information buried in them.

Many instruments already have some chemometrics routines built into their software in such a way that their use is totally transparent to the final user (and sometimes the word "chemometrics" is not even mentioned, to avoid possible aversion). Of course, they are "closed" routines, and therefore users cannot modify them. It is quite obvious that it would be much better if chemometric knowledge were much more widespread, in order that users could better understand what kind of treatment the data have undergone and eventually modify the routines in order to make them more suitable to their requirements.

As computers become faster and faster, it is nowadays possible to routinely apply some approaches that require very high computing power. Two of them are genetic algorithms (GA) and artificial neural networks (ANN).

Genetic algorithms are a general optimization technique with good applicability in many fields, especially when the problem is so complex that it cannot be tackled with "standard" techniques. In chemometrics, it has been applied particularly in feature selection (Leardi, 2000). GA try to simulate the evolution of a species according to the Darwinian theory. Each experimental condition (in this case, each model) is treated as an individual, whose "performance" (in the case of a feature selection for a calibration problem, it can be the explained variance) is treated as its "fitness". Through operators simulating fights among individuals (the best ones have the greatest probability of mating and thus spreading their genome), the mating among individuals (with the consequent "birth" of "offspring" having a genome that is derived by both the parents) and the occurrence of mutations, the GA result in a pattern of search that, by mixing "logical" and "random" features, allows a much more complete search of complex experimental domains.

Artificial neural networks try to mimic the behavior of the nervous system to solve practical computational problems. As in life, the structural unit of ANN is the neuron. The input signals are passed to the neuron body, where they are weighted and summed, then they are transformed, by passing through the transfer function into the output of the neuron. The propagation of the signal is determined by the connections between the neurons and by their associated weights. The appropriate setting of the weights is essential for the proper functioning of the network. Finding the proper weight setting is achieved in the training phase. The neurons are usually organized into three different layers: the input layer contains as many neurons as input variables, the hidden layer contains a variable number of neurons, and the output layer contains as many neurons as output variables. All units from one layer are connected to all units of the following layer. The network receives the input signals through the

input layer. Information is passed to the hidden layer and finally to the output layer that produces the response.

These techniques are very powerful, but frequently they are not applied in the correct way. In such cases, despite a very good performance on the training set (due to overfitting), they will show very poor results when applied to external data sets.

Advantages and disadvantages of chemometrics

In an issue of the *North American International Chemometrics Society Newsletter*, Schönkopf (1998) lists some of the results obtained by applying chemometrics:

- A petroleum producer used chemometrics and increased productivity by 30% in one oil refinery, earning US$14 million extra per year.
- A dairy saved $130 000 by not investing in new cooling equipment – a conclusion they came to from smart experiments
- A petroleum company saved US$1 million per year using chemometrics-based measurements
- An agricultural researcher got the same results in 10 minutes with chemometrics as he achieved by analyzing his data over 3 months with classical statistics
- A meat manufacturer saved US$150 000 per year by reducing waste in a process they optimized
- A food producer's first chemometric project saved US$115 000
- A dispersant developer carried out 20 experiments and simulated 380, thus reducing their experimental efforts by 95%
- An oil manufacturer solved a quality problem in 2 weeks with chemometrics after 2 years of failure using traditional methods.

The results are really impressive in terms of money and time (which is same…) saved. It has also to be noticed that four out of the eight examples mentioned are related with the food industry.

In one of his papers, Workman (2002) very efficiently depicts the advantages and disadvantages of multivariate thinking for scientists in industry. Of the eight advantages of chemometrics that he clearly outlines, special relevance should be given to the following:

1. Chemometrics provides speed in obtaining real-time information from data.
2. Chemometrics allows high quality information to be extracted from less resolved data.
3. Chemometrics promises to improve measurements.
4. Chemometrics improves knowledge of existing processes.
5. Chemometrics has very low capital requirements – it is cheap.

The last point especially should convince people to give chemometrics a try. No extra equipment is required – just an ordinary computer and some chemometrical knowledge (or a chemometrical consultancy). It is certain that in the very worst cases the

same information as is found from a classical analysis will be obtained in a much shorter time and with much more evidence. In the great majority of cases, however, a simple PCA can provide much more information than that which was previously collected. So why are people so shy of applying chemometrics? In the same paper previously cited, Workman gives some very common reasons:

1. The perceived disadvantage of chemometrics is that there is widespread ignorance about what it is and what it can realistically accomplish.
2. This science is considered too complex for the average technician and analyst.
3. Chemometrics requires a change in one's approach to problem solving, from univariate to multivariate thinking.

Thus, while chemometrics leads to several real advantages, its "disadvantage" lies only in the general reluctance to use it, and acceptance that the approach that has been followed for many years can turn out not to be the best one.

Conclusions

This chapter clearly shows that standard univariate methods are not sufficient to extract the maximum possible information from a data set. To do that, multivariate techniques must be applied. By using them, data display, classification, modeling, process monitoring and multivariate calibration can be performed much more efficiently, and the results can be interpreted much more easily.

Unfortunately, quite often people devote almost all their efforts to collecting the data, while paying almost no attention to the crucial step of transforming them into information.

References and further reading

References

Bro, R., van den Berg, F., Thybo, A. *et al*. (2002). Multivariate data analysis as a tool in advanced quality monitoring in the food production chain. *Trends in Food Science & Technology*, **13**, 235–244.

Centner, V., Massart, D.L., de Noord, O.E. *et al*. (1996). Elimination of uninformative variables for multivariate calibration. *Analytical Chemistry*, **68**, 3851–3858.

Cordella, C. and Leardi, R. (2008). Three-way Principal Component Analysis applied to noodles sensory data analysis (in preparation).

Forina, M., Casolino, C. and Pizarro Millán, C. (1999). Iterative predictor weighting (IPW) PLS: a technique for the elimination of useless predictors in regression problems. *Journal of Chemometrics*, **13**, 165–184.

Geladi, P. (1989). Analysis of multi-way (multi-mode) data. *Chemometrics and Intelligent Laboratory Systems*, **7**, 11–30.

Kalivas, J.H. (1997). Two data sets of near infrared spectra. *Chemometrics and Intelligent Laboratory Systems*, **37**, 255–259.

Kourti, T. and MacGregor, J.F. (1995). Process analysis, monitoring and diagnosis, using multivariate projection methods. *Chemometrics and Intelligent Laboratory Systems*, **28**, 3–21.

Leardi, R. (2000). Application of genetic algorithm-PLS for feature selection in spectral data sets. *Journal of Chemometrics*, **14**, 643–655.

Leardi, R., MacNamara, C. and MacNamara, K. (2007). Multivariate on-line process monitoring applied to a continuous two-column distillation pilot plant. *VI Colloquium Chemiometricum Mediterraneum, Saint-Maximin-la-Sainte-Baume, September 5–7*. Book of Abstracts, pp. 15–16.

Lindgren, F., Geladi, P., Rännar, S. and Wold, S. (1994). Interactive Variable Selection (IVS) for PLS. 1. Theory and algorithms. *Journal of Chemometrics*, **8**, 349–363.

Morris, J. and Martin, E. (2003). Business Briefing: CPI Technology. Pennsylvania, PA: CPI Technology.

Nørgaard, L., Saudland, A., Wagner, J. *et al*. (2000). Interval partial least-squares regression (iPLS): a comparative chemometric study with an example from near-infrared spectroscopy. *Applied Spectroscopy*, **54**, 413–419.

Schönkopf, S. (1998). Chemometrics saves Time & Money. *NAmICS Newsletter*, **No. 17** (http://namics.nysaes.cornell.edu/news17/money.html).

Smilde, A.K. (1992). Three-way analyses. Problems and prospects. *Chemometrics and Intelligent Laboratory Systems*, **15**, 143–157.

Tucker, L.R. (1966). Some mathematical notes on three mode factor analysis. *Psychometrika*, **31**, 279–311.

Workman, J. Jr. (2002). The state of multivariate thinking for science in industry: 1980–2000. *Chemometrics and Intelligent Laboratory Systems*, **60**, 13–23.

Further reading

Books

Beebe, K.R., Pell, R.J. and Seasholtz, M.B. (1998). *Chemometrics: A Practical Guide*. New York, NY: Wiley & Sons.

Brereton, R.G. (2003). *Chemometrics – Data Analysis for the Laboratory and Chemical Plant*. Chichester: Wiley.

Leardi, R. (ed.) (2003). *Nature-Inspired Methods in Chemometrics: Genetic Algorithms and Artificial Neural Networks*. The Data Handling in Science and Technology Series, Vol. 23. Amsterdam: Elsevier.

Manly, B.F.J. (1986). *Multivariate Statistical Methods. A Primer*. London: Chapman & Hall.

Martens, H. and Naes, T. (1991). *Multivariate Calibration*. New York, NY: Wiley & Sons.

Massart, D.L., Vandeginste, B.G.M., Deming, S.N. *et al*. (1990). *Chemometrics: A Textbook*. The Data Handling in Science and Technology Series, Vol. 2. Amsterdam: Elsevier.

Massart, D.L., Vandeginste, B.G.M., Buydens, L.M.C. *et al*. (1997). *Handbook of Chemometrics and Qualimetrics, Part A*. The Data Handling in Science and Technology Series, Vol. 20A. Amsterdam: Elsevier.

Massart, D.L., Vandeginste, B.G.M., Buydens, L.M.C. *et al. Handbook of Chemometrics and Qualimetrics*, *Part B*. The Data Handling in Science and Technology Series, Vol. 20B. Amsterdam: Elsevier.

Meloun, M., Militky, J. and Forina, M. (1992). *Chemometrics for Analytical Chemistry,* Vol. 1: *PC-Aided Statistical Data Analysis*. Chichester: Ellis Horwood.

Meloun, M., Militky, J. and Forina, M. (1994). *Chemometrics for Analytical Chemistry,* Vol. 2: *PC-Aided Regression and Related Methods*. Hemel Hempstead: Ellis Horwood.

Sharaf, M.A., Illman, D.L. and Kowalski, B.R. (1986). Chemometrics. In: P.J. Elving and J.D. Winefordner (eds), *Chemical Analysis, a Series of Monographs on Analytical Chemistry and its Applications Series*, Vol. 82. New York, NY: Wiley & Sons.

Websites

http://ull.chemistry.uakron.edu/chemometrics/
http://www.chemometrics.se/
http://www.models.kvl.dk/
http://www.namics.nysaes.cornell.edu/
http://www.statsoft.com/textbook/stathome.html

17

Trends in Food Authentication

Ioannis S. Arvanitoyannis

Introduction

Food authenticity has been an issue since the early 1800s, mainly related to improper labeling and *economic adulteration* (EA) – i.e. the substitution, in part or whole, of cheaper and inferior food products for high-cost foods in order to defraud the consumer. An authentic food, defined as a food that "conforms to the description provided by the producer or processor", includes the process history of a product or ingredient, its geographic region of origin, or the species or variety of the ingredient. Although rarely a health hazard, economic adulteration is driven by the demand for higher-value goods, by global trading and price fluctuations – factors that provide an opportunity for illegal profits. For these reasons, food-processing industries and regulatory agencies have pushed for analytical methods to confirm food product authenticity (Gayo and Hale, 2007).

The development of new and increasingly sophisticated techniques for the authentication of food products continues apace with increasing consumer awareness of food safety and authenticity issues. Food authentication is also of concern to food processors who do not wish to be subjected to unfair competition from unscrupulous processors who would gain an economic advantage from the misrepresentation of the food that they are selling (Reid *et al*., 2006).

Taking the fishing industry as an example, the development of worldwide high-seas fishing vessels, the improvement in food processing and storage, and the establishment of fishing industries in developing countries have increased the variety of seafood species, both fresh and processed, currently available in markets. These factors have contributed to an increase in total catches from fisheries and, thus, seafood consumption worldwide. The demand for a year-round seafood supply, however, has negatively

Modern Techniques for Food Authentication
ISBN: 978-0-12-374085-4

impacted the number of some valued and appreciated species due to exploitation. Therefore, some have turned to illegal practices in order to meet the high demand for these valued and appreciated seafood products (Downey, 1998). Because most consumers are not very familiar with the taxonomical and morphological characteristics of seafood species, such as skin pattern, body appearance and size, eyes, shape and number of fins, they are subject to being defrauded by buying a seafood product that is not what it claims to be. In addition, the processing of seafood products, which often requires the removal of significant morphological characteristics, hinders species recognition. For these reasons, species substitution has become the main form of adulteration in the seafood-processing industry (Sotelo and Perez-Martin, 2003).

Food authenticity is a major issue for producers, processors, distributors, consumers and regulators. Many consumers are prepared to pay a premium for products that they consider to be of superior quality, whether that is because of the manner of production (as in organic food) or for other reasons, such as the geographical origin of a product. For the industry, the presence of "fake" foodstuffs obviously damages profits as well as consumer confidence. Food manufacturers need to ensure that tested and valid methods are available to meet the needs of industry and to protect the public from misleading or fraudulent labeling (Kvasnicka, 2005).

Spectroscopy, protein-based methods and DNA-based methods are the main techniques for the detection of food authenticity. Some PCR-based techniques that address the problem of establishing a relationship between the concentration of target DNA and the amount of PCR product generated by the amplification have been recently developed. The two principal techniques of quantitative PCR in use at the moment are QC-PCR (quantitative-competitive PCR) and real-time PCR (Marmiroli, 2003). The authenticity testing of variety and geographical origin and traceability testing, examples of food authenticity issues, and the most commonly employed methods for testing the presence of GMOs in foods are given in Tables 17.1, 17.2 and 17.3, respectively.

Emerging authentication methods

Physicochemical/chemical fingerprinting methods

Nuclear magnetic resonance (NMR)/SNIF-NMR

NMR spectroscopy is nowadays being used more and more to analyze foods. Advantages such as the simplicity of the sample preparation and measurement procedures, the instrumental stability and the ease with which spectra can be interpreted have contributed to the growing popularity of the technique. NMR spectra of food products can act as "fingerprints" that can be used to compare, discriminate or classify samples. Selected variables that characterize the samples in some specific way are also used, instead of the whole spectra (Le Gall and Colquhoun, 2003).

Chemometric techniques are often employed to analyze the data, as the information contained in the spectra is of a high degree of complexity. These statistical techniques serve several purposes in comparing and classifying samples or in quantifying

Table 17.1 Authenticity testing of variety and geographical origin, and traceability testing

Test method	Item of interest	Authenticity factor	Reference
DNA technology	Potato	Commercial variety	Ashkenazi *et al*., 2001
PCR	Tomato, maize, soybean	Transgenecity	Popping, 2002
	Cow, ewe, goat, buffalo	Breed identification	Plath *et al*., 1997
	Fish	Detection of white fish species	Dooley *et al*., 2005
SNIF-NMR	Olive oil, wine	Geographic location	Gonzales *et al*., 1999
	Basmati rice	Geographic location	Verma *et al*., 1999
Real-time PCR	Pasta	Commercial variety	Bryan *et al*., 1998
AFLP	Salmon	Distinguishing 10 different salmon-like species	Russell *et al*., 2000
	Fish and seafood	Identification of the species of origin	Maldini *et al*., 2006
Qualitative PCR	Meat	Presence or absence of pork	Popping, 2002
Quantitative real-time PCR	Meat	Beef meat quantification	Popping, 2002
	Meat	Meat quantification	Lopez-Andreo *et al*., 2006
DNA test (protein-based BSE test)	Cattle traceability	Geographical origin BSE tested	Popping, 2002
HPLC	Cow, ewe, goat, buffalo	Identification of the species of origin	De La Fuente and Juarez, 2005
	Cheese	Detection of rennet whey	De La Fuente and Juarez, 2005
	Seafood	Detection of species	Arvanitoyannis *et al*., 2005
	Chili powder	Classification of chili powders	Forgacs and Cserhati, 2006
ELISA	Cow, ewe, goat, buffalo	Identification of the species of origin	De La Fuente and Juarez, 2005
	Vegetable	Addition of vegetable proteins	Sanchez *et al*., 2002
DNA analysis	Rice-based food products	Identification of GMOs	Ren *et al*., 2005

Table 17.2 Most commonly employed methods for testing the presence of GMOs in foods (adapted from Arvanitoyannis, 2003a)

Method	Ease of use	Equipment cost	Sensitivity	Duration	Qualification
SNIF-NMR	Difficult	High	High	Depends on isotope measured	Yes
LC-NMR	Difficult	High	High	Depends on isotope measured	Yes
NIR	Easy	Low	Medium	Short	No
Affinity gel electrophoresis	Moderate	Low	High	Short	No
Western blot	Difficult	High	Medium	Medium	No
ELISA	Moderate	Medium	High	Short	Yes
Lateral flow strip	Easy	Low	High	Short	No
Microarrays	Moderate	High	High	Short	Yes
Southern blot	Difficult	High	Medium	Medium	No
Qualitative PCR	Difficult	Medium	High	Long	No
QC-PCR	Difficult	Medium	High	Medium	Yes
Real-time PCR	Difficult	Medium	High	Medium	Yes
RAP-DNA	Difficult	Medium	High	Medium	Yes

Table 17.3 Examples of food authenticity issues (adapted from Kvasnicka, 2005)

Commodity	Issue
Herbs and spices	Adulteration with water to increase weights
	Incorrect botanical declaration
	Intentional addition of low-value materials
Fruit and vegetable	Undeclared water, sugar and acid addition to fruit juice
	Undeclared pulpwash or peel extract addition into fruit juice
	Incorrect declaration of fruit type
Cereals	Basmati rice replaced with non-Basmati rice
	Undeclared replacement of durum wheat with common wheat
	Incorrect declaration of geographical and cultivar origin of premium long grain rice
Oils and fats	Undeclared addition of other vegetable oils to single-seed oils
	Undeclared addition of poorer-quality oils to extra-virgin olive oil
	Butter adulterated with hydrogenated oil and animal fat
Milk and dairy	Undeclared addition of water to milk
	Cows' milk in sheep's, goats' or buffalo milk yoghurt or cheese
	Distinction between cheese made from raw or heat treated milk
Meat and fish	Incorrect declaration of species
	Labeling previously frozen meat as fresh
	Undeclared water addition to bacon and ham in excess of legally permitted amounts
Beverages	Single malt whisky replaced by blended whisky
	Inappropriate sugar addition to increase alcohol content in wine
	Incorrect declaration of vintage or geographical origin of wine
Miscellaneous	Incorrect declaration of floral or geographical origin of honey
	Undeclared sugar addition to honey
	Undeclared use of genetically modified food

adulterants using calibration sets. Several reviews have already been published on the subject of NMR and food, and on NMR and chemometrics (Colquhoun and Goodfellow, 1994; Colquhoun, 1998; Colquhoun and Lees, 1998; Lindon *et al*., 2001).

NMR spectroscopy involves the analysis of the energy absorption by atomic nuclei with non-zero spins in the presence of a magnetic field. The energy absorptions of the atomic nuclei are affected by the nuclei of surrounding molecules, which cause small local modifications to the external magnetic field. NMR spectroscopy can therefore provide detailed information about the molecular structure of a food sample, given that the observed interactions of an individual atomic nucleus are dependent on the atoms surrounding it (Reid *et al*., 2006).

There are several ways of preparing the food sample itself (solid, liquid) and deciding which type of analysis is to be carried out. Some targeted analyses tend to include an extraction of fractionation step, while other samples are used as they are for non-targeted analyses (Andreotti *et al*., 2002). Solid samples (fruits, vegetables, green tea) are freeze-dried and/or ground and then extracted into a deuterated solvent. High-protein samples (fish muscle, meat, cheese) may be homogenized in hydrochloric acid. In both cases, the samples are centrifuged, and then the supernatant is collected for analysis (Le Gall and Colquhoun, 2003). Data sets for NMR/authenticity studies are commonly acquired under automation using a sample changer to acquire spectra for 20–60 samples in a batch. Prior to any data acquisition, it is recommended that

the NMR spectrometer be tuned on the first sample of a series, to check the 90° pulse length of the instrument and to optimize the field homogeneity.

There are several independent approaches for the conversion of the raw NMR spectra into data suitable for chemometric analysis. One procedure is to transfer the transformed spectra to a PC and use them as they are (Duarte *et al*., 2002). Another option is to divide the spectra into segments, and sum the intensities of the data points in each segment (Spraul *et al*., 1994). There is also the popular alternative of selecting a series of signals from the NMR spectra using the spectrometer's own "peak-picking" routine, which gives peak positions and heights (Mannina *et al*., 2001).

In chemistry, it is possible to record many pieces of information, such as spectroscopic and chromatographic intensities for each sample. Therefore, most chemical experiments are multivariate. The way to deal with such a wealth of information is to use *multivariate analysis*, which includes applied statistics. One definition of chemometrics is as follows: the chemical discipline that uses mathematical and statistical methods for handling, analyzing, interpreting and predicting chemical data (Malinowski, 1991). Chemometrics represents a wide range of statistical methods aimed at tackling three different main objectives: simplifying complex and massive data sets, classifying objects or predicting analytical parameters.

The first limitation in using NMR for food authentication is the cost of equipment. Food authentication research is constantly looking for techniques that can identify marker compounds to permit the detection of adulteration or testify to the quality of a high-price food product. An advantage is that NMR is probably the best non-targeted technique to use for the screening of food extracts; all the main metabolites can be detected in a single spectrum with minimal and non-destructive sample preparation (Zamora *et al*., 2002). For the detection of minor components, larger amounts of the starting material can be extracted initially and then fractionation steps can be added to the sample preparation in order to concentrate certain types of compound (Lommen *et al*., 1998). Also, high field NMR instruments allow more compounds to be detected, since they provide improved sensitivity and signal dispersion, and the introduction of cryo-probes will give significantly increased sensitivity on existing instruments. Another advantage of using NMR is the fact that it is quantitative (Holland *et al*., 1995).

The measurements are easily repeatable and reproducible over the long term. The instrumental parameters that need careful attention from the analyst and that may vary from one data recording session to another are the tuning and the resolution. A difference in tuning will affect the intensity of all peaks in the spectra. In order to compare quantitatively sets of spectra recorded at different times, all the spectra can be normalized to the reference peak, provided that a fixed amount of internal standard is added to all the samples. The problems of repeatability and reproducibility of chromatographic techniques that are caused by the ageing of columns and to temperature fluctuations are not applicable to NMR (Le Gall *et al*., 2003).

The authenticity of a food product is essentially defined by a legally recognized description that concerns its characteristics (quality, origin, process). An authentic food product has to be properly labeled according to the appropriate national and international regulations when presented for sale in the marketplace. Mislabeling may arise, for example, when the legal definition of a given product traded on the

global market differs from one country to another. The list of mislabeling problems is potentially endless, and can relate to the truthfulness of the claimed geographical origin (wine and olive oil), the species of plant or animal (beef or pork in sausage), the processing used (whether food has been irradiated or not) and the quality claimed (farmed versus wild, natural versus artificial, organic versus conventional). In response, the investigation of NMR methods for authenticating food has blossomed during recent years (Le Gall and Colquhoun, 2003).

High resolution ^{13}C NMR has been proposed to discriminate virgin olive oils originating from several countries from other oleic oils and high linoleic oils (Zamora *et al*., 2001). Mavromoustakos *et al*. (2000) have used the olefinic signals obtained by ^{13}C NMR to differentiate virgin olive oils from oils adulterated with soybean, cottonseed, corn and sunflower-seed oils. Belton *et al*. (1996) highlighted the potential of high-resolution ^{1}H NMR to authenticate fruit juices. The sample preparation and acquisition were straightforward, and the clear differences in the chemical composition of juices like grape, apple, pineapple, orange and grapefruit suggest that authenticity problems could be tackled in this way.

Both ^{13}C and ^{1}H NMR have been applied to freeze-dried wine extracts dissolved in D_2O to successfully classify white wines from three German regions (Vogels *et al*., 1996) and red wines from three areas of the Apulia region in Italy (Brescia *et al*., 2002). Beer has also been analyzed by ^{1}H NMR. Duarte *et al*. (2002) have identified around 30 compounds in degassed beer samples, and identified as many unassigned spin systems. Ale and lager were compared and, although the high and mid-field regions (amino, fatty and organic acids plus fermented sugars and dextrins) allowed some separation, it was the low field region (aromatic compounds) that gave the best discrimination.

^{1}H NMR has been used to evaluate the freshness of halibut on the basis of the level of metabolites such as adenosine triphosphate (ATP), adenosinediphosphate (ADP), adenosine monophosphate (AMP), inosine monophosphate (IMP), inosine and hypoxanthine. Amounts of ATP, ADP and AMP decreased with time, while IMP, inosine and hypoxanthine increased (Sitter *et al*., 1999).

The specific proportions of the particular isotopes of hydrogen and oxygen present in molecules are dependent mainly on climatic and geographical conditions and, to a lesser extent, on the photosynthetic metabolism of plants. The effect of these conditions on the final isotopic composition of a molecule is known as *isotopic fractionation*. This natural phenomenon is exploited by two particular analytical techniques – SNIF-NMR and IRMS – which are perhaps the most sophisticated and specific techniques for determining food authenticity. Both techniques are capable of determining the exact proportion and location of specific isotopes within a food sample. However, the financial cost of purchasing and operating such high-specification NMR and MS instruments is quite high and time-consuming sample preparation is required before analysis can take place (Reid *et al*., 2006).

Fourier transform infrared spectroscopy (FT-IR)

The FT-IR analyzer measures the absorbed radiation at different frequencies and obtains spectra which, similar to fingerprinting, reveal the identity of the specific molecule. FT-IR provides detailed information about the chemical structure and

composition of a sample. FT-IR analysis can also be associated with GC; for example, GC-FT-IR was used to determine the presence of mercury in seafood. Acid leaching with toluene extraction was first performed, with subsequent GC-FT-IR detection (Quevauviller *et al*., 2000). FT-IR together with near-infrared (NIR), mid-infrared (MIR) and Raman spectroscopic techniques fall among the fingerprinting techniques; the latter are the ones which provide a means for rapid and high throughput monitoring and would be ideally suited for rapid characterizations if prominent changes could be captured in a reproducible manner (Vaidyanathan and Goodacre, 2003).

There is an evolving trend towards the use of profiling methods combined with chemometrics for the determination of authenticity. The advantage of the profiling methods would be the evaluation of the overall components in a sample rather than looking for a single marker compound. Contemporary Fourier transform infrared (FT-IR) spectroscopy has the capability of rapidly obtaining reproducible biochemical patterns that would allow for the composition-based statistical classification.

Infrared (IR) spectroscopy is ideal for rapid screening and characterization of chemical composition variation. Distinct and reproducible components exist in different fruit commodities (Taruscio *et al*., 2004); thus, biochemical fingerprints may be produced by FT-IR to allow for the differentiation of subtle differences. Variation in the chemical composition attributed to variety, geographical origin or alien ingredients might be elucidated through chemometric analysis of spectral-based grouping (Kemsley *et al*., 1996). Advances in instrument design and auxiliary optics as well as the development of powerful supervised chemometric software have made FT-IR spectroscopy a suitable tool for the assessment of quality and authenticity in various foods (Edelmann *et al*., 2001). This technique requires low sample volume and is environmental friendly. It does not require a large amount of hazardous organic solvents, as is necessary for liquid chromatography. Minimal or no sample preparation is required, which greatly speeds up sample analysis. Nearly real-time measurement has been made possible by immediate software prediction, and once the instrument has been purchased there is minimal operational cost involved in performing the technique (He *et al*., 2007).

Such FT-IR fingerprints can be useful for assessing bacterial contamination of meat (Goodacre, 2002) and for confirming food authenticity in general (Downey, 1998). Metabolite information obtained from FT-IR fingerprints of mutant strains may also be useful in evaluating and assessing gene function (Oliver *et al*., 1998) or changes in physiology (Goodacre *et al*., 2000). The major advantage of this technique is its rapidity and ease of spectral acquisition, enabling non-invasive measurements to be made with little or no sample preparation. However, sufficient signal resolution must be ascertained for the desired effect to be monitored, in order to use spectral information as protein or metabolic fingerprints.

Gallignani *et al*. (1994) applied FT-IR for the direct determination of ethanol in alcoholic beverages. This provided accurate results, without requiring any previous chemical treatment of the sample. Implementation of FT-IR spectroscopy on the extracted polymeric materials of Portuguese white wines revealed that this technique can be used effectively to characterize white wine polysaccharide composition (Arvanitoyannis, 2003b). It was possible to identify the wine-making process

involved, and its influence on the amount and type of wine polysaccharides. Finally, the results showed that it is possible to use FT-IR combined with multivariate techniques for an in-depth characterization of white wine polymeric fractions (Coimbra *et al*., 2002).

Near infra-red (NIR)

NIR measurement technology offers an amazingly diverse capability for the analysis of many different constituents or properties of food products. Moisture, fat, protein and sugar content are perhaps the most well-known applications in products such as grain, flour, cereals, dairy products, snacks and coffee, but NIR has also found applications in the measurement of chocolate thickness on refiner rollers, the thickness of sausage casings, the alcohol content of beverages, the maturity of peas and even the quality of fruit juices (Cowe and McNicol, 1985).

NIR measurement is a well-established analytical technique, and many examples of its applications can be found in the literature going back as far as the 1950s and even earlier. Specifically, early laboratory applications of NIR concentrated upon quantitative and qualitative studies of liquids and solvent mixtures (Kaye, 1954). NIR measurement has broadly evolved on two fronts; laboratory applications, and on-line application of the technique. This division has resulted from the very different demands that the two approaches place upon the instrument design and specification. Laboratory measurement has the benefit of offering very controlled measurement conditions. The product can be appropriately prepared – for example, it can be ground to a specific particle size and consistently presented to the instrument, usually in some form of windowed cell. Also, an acceptable time for each measurement may be 30 seconds or more, which is obviously faster than the laboratory wet chemical equivalent, but slow in terms of continuous on-line analysis. Infrared light is part of the broad spectrum of energy known as electromagnetic radiation (Bruton, 1970).

The measurement range of the NIR is well suited to the needs of food processing since a wide range of different constituents may need to be measured, such as moisture, fat, sugar, caffeine, oil and protein. In NIR, the most important and prominent absorptions are due to the –OH, –NH and –CH groups. These absorption features are very specific to the constituent in question, as discussed above, and so the technique readily lends itself to quite detailed discrimination of constituent parts of a foodstuff. In addition, the technique has one further important strength – a choice of absorption sensitivities for a given constituent. Each of the absorbing groups characteristically exhibits three main absorption bands in the NIR (Benson, 2003).

When considering the possibility of using the NIR technique to solve a particular measurement problem, it is necessary to appreciate both its scope and its limitations. The non-contact characteristic is very attractive, since the measurement will not normally interfere with product flow. Also, for food processing, non-contact measurements are favored for hygiene reasons. NIR measurement is unaffected by changes in the electrical properties of foodstuffs, such as electrical conductivity or dielectric behavior; such parameters can easily change if the salt or other ionic material content varies (McCallum, 1961). This provides a distinct advantage over alternative methods of on-line moisture measurement based upon monitoring the electrical properties

of the product, such as capacitance or conductance, which can be related to moisture content.

It seems ironic that an NIR gauze can measure moisture precisely, but when compared with a technique that essentially measures volatiles it will appear to have product-type/variation sensitivity. The effect that is being observed is that the non-moisture volatile materials present in the product are also removed to a lesser or greater extent during oven testing. These losses contribute to the apparent moisture content. In the application of NIR to moisture determination, the response to free or associated moisture and bound water should be appreciated. In most materials, the difference in wavelength between the absorption bands for these two forms of moisture is very small, and therefore they cannot usually be treated separately. Whether this is an advantage or a drawback depends on the requirements of the individual application (Bruton, 1970).

The concern for materials with large particle size, especially those that have recently been dried or steam conditioned, is whether the surface moisture represents the internal condition. Indeed, it is frequently the case in drying processes that the surface and internal moisture levels of bulky materials differ. In many situations this potential difficulty is not a problem, because there is some form of relationship between the surface and total moisture content which can be exploited to provide a measurement. The classic example of this is the on-line measurement of biscuit moisture. Microwave measurement can be a useful alternative technique when the limited penetration of NIR measurement is a problem (Osbourne and Fearn, 1986).

There are instances where NIR measurement may not be successful. Backscatter gauzes work on the absorption characteristics, and if they are subject to specular energy from shiny surfaces then the measurements can become noisy and ultimately worthless. The light directly reflected has no absorption information; products such as caramels, syrups and fondants fall into this category. In these instances it is possible to consider a special optical arrangement for the gauze to ignore specular light, or even to use a transmission configuration (Benson, 2003).

The future for the application of on-line NIR technology looks very promising, with increasing opportunity for its application as the food industry becomes ever more concerned with accurate process control. Moisture assessment is likely to remain the principal application for an on-line gauze because it has such obvious possibilities for control and has a far-reaching impact on product quality, keeping characteristics, yield optimization and process energy usage. However, other parameters, such as oil or fat, where their control can be affected, are becoming and will continue to become more important.

High-pressure liquid chromatography (HPLC)

The HPLC technique is highly sensitive and very fast in response. The efficiencies of separation are very high. A wide range of compounds may be separated by HPLC because the technique has a wide range of selectivity through the availability of many solvent combinations and packings. New substances to be used as stationary phases are continually being developed. No restriction has to be made to sample volatility and derivatization. In most cases, samples are small and preparation takes little time.

Detectors can work continuously and detect very small amounts. The combination of HPLC and mass detectors opens new and wide horizons. A further trend is the miniaturization of apparatus, resulting in less solvent use. For the detection of phenolic compounds, anthocyanins and organic acids, HPLC is the ideal technique. For other compounds, it is *a* technique rather than *the* technique (Nollet, 2003).

Chromatography is a method for the separation of components between two phases. One phase is a stationary bed (the *stationary phase*) and the other phase is a fluid moving through the stationary phase (the *mobile phase*). In high-performance liquid chromatography (HPLC), the mobile phase is pumped through the column. The LC instrument includes: (i) solvent reservoirs, (ii) a solvent delivery system, (iii) an injection device, (iv) the column, (v) a detector and (vi) a data-acquisition system. The mass spectrometry (MS) detector currently has many applications with LC. Different techniques to interface or couple liquid chromatography and mass spectrometry are available. A widely used interface is atmospheric pressure ionization (API) (Scot, 1995).

Electrospray MS has three steps: nebulization of the solution into electrically charged droplets, liberation of ions from the droplets, and transportation of ions into the vacuum of the analyzer. Evidently, the cited MS techniques are not exhaustive (Meyer, 1994). Sample preparation and clean-up are very important steps of analyses. The components of interest have to be isolated from the sample matrix, and interfering substances have to be removed. Accuracy, detectability and selectivity are highly improved. Frequently employed procedures include lyophilization, ultrafiltration and liquid–liquid extraction.

In fruit and fruit products, different compounds can be monitored for authenticity purposes: phenolic compounds, organic acids, carotenoids, amino acids, anthocyanins and sugars. Phenolic compounds, a diverse class of compounds containing a hydroxyl group on a benzene ring, include (among others) flavones, flavonols, flavonoids, polyphenols and chalcones. Silva *et al*. (2000) analyzed the phenolic compounds and procyanidin polymers by reversed-phase HPLC.

The use of soybean proteins in bovine milk is forbidden in many countries, and other countries have regulations regarding maximum allowance levels. Soy proteins in unheated milk were analyzed by Ashoor and Stiles (1987). De Frutos *et al*. (1992) used HPLC to separate whey proteins from bovine, ovine and caprine species. Identification of the presence of soy protein, caseinate and whey protein in unheated beef, pork, chicken and turkey was possible, as was that of added non-meat protein. Added soy protein could also be detected at levels of $6\,g\,kg^{-1}$ in cheese samples. Identification of the presence of animal whey proteins in vegetable milks or of soybean in animal milk was possible using the HPLC method (Garcia *et al*., 1997).

Downscaling or miniaturization of columns and sample treatment are challenges for the future. Miniaturization involves less sample volume, fewer solvents and less time. Regulations and government commitments require more separation efficiency; the hyphenation of HPLC and MS, allowing the development of new methodologies, is a move in the right direction. Automation of separation and detection and lower costs of apparatus will be helpful (Nollet, 2003).

Protein-based methods

ELISA

Microarray-based approaches involve miniaturization of standard assay procedures in multiple arrays to allow simultaneous analysis of multiple determinants/analytes. Such assays are very popular in transcriptomics, but have also been extended to proteome analyses. Microspots of "bait" molecules are immobilized in rows and columns onto a solid support, and exposed to samples containing the corresponding binding molecules. The complex formation within each microspot can be detected using readout systems based on fluorescence, chemiluminescence, electrochemistry, mass spectrometry or radioactivity. Large-scale assessment of protein profiles can be carried out by the use of immunoassays on microarrays (Schweitzer and Kingsmore, 2002).

The analysis involves a scale-up of enzyme-linked immunoassays (ELISA) that have been in use for protein analysis. Antibodies immobilized in an array format onto specifically treated surfaces act as "baits" to probe the sample of interest to detect proteins that bind to the relevant antibodies, using, say, fluorescence detection (Vaidyanathan and Goodacre, 2003).

The majority of reported studies on immunological techniques for food authentication concern the use of ELISA. This technique involves the cultivation of antibodies or antisera that are capable of binding to a protein of interest, thereby enabling the detection of that protein, both qualitatively and quantitatively. The major advantage of this approach is that antibodies or antisera can be manufactured to respond specifically to the protein of interest, thereby enabling recognition and quantitation of that protein exclusively. The disadvantages of the ELISA approach include the initial difficulty in producing an antibody specific to a particular protein. However, this is a relatively minor difficulty to overcome when the selectivity of the technique is taken into account (Reid *et al*., 2006).

Recent research using ELISA-based techniques includes detecting the presence of meat from different species in food products (Jha *et al*., 2003) and the presence of vegetable proteins in milk powder (Sanchez *et al*., 2002). There have been promising results for the use of ELISA to differentiate milk from different species (Moatsou and Anifantakis, 2003), as well as to detect the adulteration of sheep's and goat's milk with cow's milk at levels as low as 0.1% (Hurley *et al*., 2004). This technique holds much potential for the authentication of food products, but, to date, limited advances have been made in extending its authentication capabilities.

Protein microarrays can also be developed for assessing protein–protein, enzyme–substrate and other protein–metabolite interactions (MacBeath and Schreiber, 2000). In one study, 119 yeast protein kinases were arrayed in microwells and examined for kinase activity with 17 substrates, demonstrating the value of microarrays in multiplexed protein functional assessments (Zhu *et al*., 2000). Carbohydrate-based microarrays have also been devised (Wang *et al*., 2002). Microarray technology for the examination of proteins on a large scale is still in the developmental stage (Ringeisen *et al*., 2002), and there are several challenges to be considered, particularly with

respect to reproducibility and quantification, compared with the technology used for nucleic acids (Templin *et al*., 2002).

Western blot

An assay based on Western blotting and detection of central nervous system (CNS)-specific antigens was developed to detect brain tissue in processed (heated) meat products. Bands of antigen-bound primary antibodies were visualized through secondary anti-antibodies labeled with peroxidase, which generated chemiluminescence that was documented by a photographic film. Ponceau-S staining before antibody incubation and molecular-mass information regarding detected antigens after immunoreactions added information that supported correct identification of brain tissue in the meat products. In this approach B_{50}/growth-associated protein (B_{50}), glial fibrillary acidic protein (GFAP), myelin basic protein (MBP), neurofilament (NF), neuron-specific enolase (NSE) and synaptophysin (Syn) proteins were detected in raw luncheon meat and a liver product enriched with brain tissue at a level of 5% (m/m). Only MBP and NSE were considered suitable biomarkers for detection of 1% (m/m) brain tissue in meat products pasteurized at 70°C or sterilized at 115°C. The use of an anti-monkey MBP instead of anti-human MBP enabled speciation of the CNS material, whether from bovine and ovine brains or from porcine brain tissue. This immunoblot assay potentiates the analysis of approximately 70 samples within 8 hours, including sample preparation and the simultaneous probing of NSE and MBP target antigens (Sultan *et al*., 2004).

However, a Western blot based on this antigen demonstrated difficulty in the interpretation of results from heat-treated retail meat products (Lucker *et al*., 2000). Incidentally, a reverse transcription PCR coupled with restriction fragment length polymorphism was described as detecting successfully GFAP mRNA in (stored) ground meat and pasteurized meat products fortified with brain tissue at levels above 0.5% (Seyboldt *et al*., 2003). Like GFAP, NF is a marker for intermediate filament, but is present in equal amounts in spinal cord and in peripheral nerves (Kelley *et al*., 2000). Immunohistochemical detection of brain tissue was obtained with anti-NF in processed and heat-treated bovine and porcine brains, but diminished rapidly in raw as well as in heated luncheon meat (Tersteeg *et al*., 2002). Western blot assays were performed to determine the utility of the antiserum in recognizing specific proteins that contained nitrated tyrosine residues (Hinson *et al*., 2000).

Lateral flow strip

A typical lateral flow strip comprises a microporous material, such as nitrocellulose, cellulose acetate or a glass fiber membrane. Nitrocellulose (NC) is typically brittle and fragile as a pure sheet, so it is laminated onto a semi-rigid plastic substrate, such as polyester, styrene or polyvinyl chloride (PVC), often using a pressure-sensitive or heat-sensitive adhesive (Green and Rathe, 2006).

For protein-based detection, specific monoclonal and polyclonal antibodies have been mainly developed for immunochemical detection, Western blot analysis and enzyme-linked immunosorbent assays (ELISA). The immunochromatographic assays

(also known as lateral flow strip tests, Reveal CP4 and Reveal Cry9C) detect 5-enol-pyruvyl-shikimate-3-phosphate synthase (EPSPS), derived from *Agrobacterium* sp. strain CP4 which confers resistance to the herbicide glyphosate in soybeans and corn, and *Bacillus thuringiensis* Cry proteins which confer protection against insects in corn plants, seeds and grains, respectively. Both kits, which are commercialized by Neogen (http://www.neogen.com), detect GMO presence in 5–20 min at a low price, with high sensitivity (<0.125% mass fraction of GMO); both are reliable field tests for controlling the distribution of biotechnology-derived products (Ahmed, 2002).

DNA-based methods

Microarrays

Microscopic arrays of oligonucleotides or cDNA containing up to several hundred thousand different sequences are starting to influence methodologies and paths to discovery in genomics (Graves, 1999). Microarrays of DNA and oligonucleotides are beginning to have a similar impact on the biological sciences to that which integrated circuits have already produced on the physical sciences, and for similar reasons they can do many things in parallel, with very little material and a modest investment of labor. They can be used, for example, in expression analysis, polymorphism detection, DNA resequencing and genotyping on a genomic scale (Marmiroli, 2003).

These arrays consist of many microscopic spots, each of which contains identical single-stranded polymeric molecules of deoxyribonucleotide attached to a solid support such as glass or a polymer. Each spot contains many copies of a particular sequence, which can range in length from 10 or 20 bases up to 1000 to 2000. The utility of these spots arises from the tendency of their component bases to pair up or hybridize with a second strand containing a complementary sequence. It is easy to see how an array of different sequences can be used to identify one or more pieces of DNA or RNA in a solution. These unknown sequences are all tagged by attaching a fluorescent dye to them, and then exposed to an array containing hundreds or thousands of different sequences, each in a known location. When the array is examined, it is possible to identify which molecules are present in the solution by determining which spots fluoresce. Peptide nucleic acid (PNA) arrays could also form powerful tools for hybridization-based DNA screening assays, due to some favorable features of the PNA molecules (Weiler *et al*., 1997).

DNA chips can also find great applicability in agricultural biotechnology. Microarrays will assist plant biotechnology companies by allowing rapid analysis of transgenic plants (Lemieux *et al*., 1998). The link existing between microarrays and PCR is great; in fact the PCR product could be tested directly on a DNA chip, rendering an easy and very fast phase of screening even for different target sequences in the same reaction; this technique will find a great field of applicability in GMO traceability.

Southern blot

The need to monitor and verify the presence and the amount of GMOs in agricultural products has generated a demand for analytical methods. Luthy (1999) reported that the analytical technique divides into the detection of the introduced DNA, and detection

of the expressed protein in transgenic plants. The method of detecting expressed protein (such as enzyme-linked immunoabsorbent assays (ELISA)) was simple, highly specific and easy to quantitate, although the sensitivity was low and it was found frequently to fail to detect fully processed products (Anklam *et al*., 2002). The method of detecting target DNAs with polymerase chain reaction (PCR) was reliable and highly sensitive, although it was difficult to use the routing agarose gel analysis and Southern blot confirmation of the PCR products for massive samples (Meyer, 1999). Here, we describe an improved liquid-phase hybridization (LPH) PCR-ELISA technique for the specific detection of PCR products. In this method, the biotinylated PCR products were hybridized *in situ* with the digoxigenin-labeled probe in the PCR reaction mixtures, and then captured with Streptavidin-coated tubes. The PCR products were analyzed with agarose electrophoresis and then verified with Southern blotting (Liu *et al*., 2004). In PCR-based assays, the results are usually analyzed by electrophoresis and Southern blotting. The gel electrophoresis method is rapid but hazardous, and the Southern blotting method makes the testing of multiple samples tedious and time-consuming (Li *et al*., 2001).

Chickpea (*Cicer arietinum* L.) is an important food legume, cultivated in over 40 countries, with a high nutritional value. Lack of appropriate DNA isolation protocol is a limiting factor for any molecular studies of this crop. The present report describes a rapid and efficient protocol for small- and large-scale preparation of a superior quality and quantity of DNA from four cultivars (JG62, WR315, C235 and ICCV89314) compared with that of earlier reports. The yield of DNA through both the methods was estimated to be approximately 80 $\mu g\ g^{-1}$ of plant tissue. Both small- and large-scale preparations were essentially suitable for PCR and Southern blot hybridization analyses, which are the key steps in crop improvement programs through marker development and genetic engineering techniques (Chakraborti *et al*., 2006). The emergence of plant transformation and molecular marker analyses in genome studies has greatly enhanced the speed and efficacy of crop improvement and breeding programs. A prerequisite for taking advantage of these methods is the ability to isolate genomic DNA of superior quality and quantity for analyzing through PCR, restriction enzyme digestion and subsequent Southern blot hybridization. To fulfil this criterion, a rapid, simple and reliable DNA isolation method is highly sought. Since the size, content and organization of genome and contents of metabolites of different plant systems vary from each other to a great extent, a single DNA isolation protocol is not likely to be applicable for all plant systems (Loomis, 1974).

Qualitative polymerase chain reaction (PCR)

PCR has been used in many different applications because it has very great flexibility in the field of molecular biology. Its principal use is to generate a large amount of a desired DNA product starting from a given template, but it can also be used to amplify very long fragments of DNA and in such a way to synthesize whole genes, amplify and quantify specific RNA species, produce RNA fingerprinting or PCR mediated cloning, screen DNA libraries and produce DNA sequences (Marmiroli, 2003).

Long-distance PCR amplifies and detects routinely and specifically PCR products ranging in size from less than 1 kb to more than 50 kb (Foord and Rose, 1995),

regardless of target template sequence or structure. Long-distance PCR facilitates the amplification of eukaryotic genomic DNA segments containing introns of varying number and lengths, thus permitting the definition of intron/exons boundaries. About 10 years ago, direct cellular localization of a DNA or RNA target was routinely achieved by *in situ* hybridization. This method has been dramatically improved in its sensitivity. However, despite these improvements the relatively high detection threshold of *in situ* hybridization of about 10 copies per cell limits its usefulness (Nuovo, 1994).The advent of PCR made possible the detection of the low copy events as well.

PCR starting from RNA detects or measures a defined RNA species, ranging from mRNAs for gene products to the level of viral RNA in plasma. RNA-PCR is a good method for screening cells and tissues for the expression of an mRNA (Rashtchian, 1994). The extension of arbitrarily primed PCR (AP-PCR) fingerprinting to RNA has resulted in a tool with exciting potential for detecting differential gene expression. It is now possible to obtain a partially abundance-normalized sample of cDNA produced in a single tube in a few hours (Liang and Pardee, 1992). Under standard PCR conditions, sufficient sequence information from a template is required to design two primers that hybridize to each strand of the DNA (Dieffenbach and Dveksler, 1995).

Screening DNA libraries of high complexity for rare sequences is one of the fundamental techniques of molecular biology. When applied to the screening of highly complex DNA libraries contained within either bacteriophage or plasmid vectors, PCR offers the opportunity to identify rare DNA sequences in complex mixtures of molecular clones by increasing the abundance of a particular sequence (Israel, 1993). The technique employs a thermostable DNA polymerase in a temperature cycling format to perform multiple rounds of dideoxynucleotide sequencing on the template (Murray, 1989).

Quantitative-competitive PCR (QC-PCR)

QC-PCR is the co-amplification of a target analyte with an internal standard. In particular, it involves the co-amplification of unknown amounts of an internal control template in the same reaction tube by the identical primer pair (Studer *et al*., 1998). The reaction conditions can be maintained to generate amplification products that should differ by more than 40 bp. Multiple PCR reactions are needed as each sample is amplified with increasing amounts of competitor, while maintaining constant the sample volume/concentration. Qualification is achieved by comparing the equivalence point at which the amplicon from the competitor gives the same signal intensity as that of the target DNA on stained agarose gels (Hardegger *et al*., 1999).

A quantitative competitive PCR (QC-PCR) assay was developed to detect and quantify *Escherichia coli* O157:H7 cells. From 10^3 to 10^8 CFU of *E. coli* O157:H7 cells ml^{-1} was quantified in broth or skim milk, and cell densities predicted by QC-PCR were highly related to viable cell counts. QC-PCR has the potential for quantitative detection of pathogenic bacteria in foods (Li and Drake, 2001). For QC-PCR, a dilution series of three to five PCR reaction mixtures are made, each with a constant (unknown) amount of added target DNA and a known dilution series of competitor DNA. The target and competitor DNA compete for the same primers; when the concentration of each is equivalent, band intensities will be equivalent. The point

of equivalence is determined by visual assessment of band intensities or by digital analysis of the gel image and generation of a regression line. Quantitation of the gene copy number can be converted to chromosomal equivalents and cell numbers. The objectives of this study were to determine whether QC-PCR could be applied to foods, and to develop a quantitative PCR assay for detection and enumeration of *E. coli* O157:H7 cells in broth and skim milk (Raeymaekers, 1993).

To confirm that the developed QC-PCR assay could be applied quantitatively, DNA was extracted from an overnight culture and diluted 100- and 200-fold, resulting in DNA samples I and II, respectively. Constant amounts of DNA from each sample were co-amplified with corresponding sets of serially diluted competitor DNA in QC-PCR. The DNA concentration in each sample was determined and compared to confirm whether the results predicted by QC-PCR were equivalent to the actual two-fold difference in DNA concentration (Li and Drake, 2001).

Real-time PCR

Real-time PCR was originally developed in 1992 by Higuchi *et al*. (1992), and has rapidly gained popularity due to the introduction of several real-time complete instruments and easy-to-use PCR assays. With this technique, the amplification of the target DNA sequence can be followed throughout the whole reaction by the indirect monitoring of the product formation. Real-time detection strategies rely on continuous measurements of the increment in fluorescence generated during the PCR reaction. The number of PCR cycles necessary to generate a signal that is significantly and statistically above noise level is taken as a quantitative measure, and is called the cycle threshold (Ct). As long as the Ct value is measured at the stage of PCR where the efficiency is still constant, the Ct value is inversely proportional to the log of the initial amount of target molecules. The reaction does not proceed linearly, but plateaus in later cycles. The reasons for this are: (i) the reannealing of PCR products competing more efficiently with hybridization of primers, (ii) the inhibition of reactions by reaction by-products, and (iii) the limiting of the polymerizing compounds (Grove, 1999).

Real-time PCR has replaced double competitive PCR as the preferred quantitative PCR-based technology for several reasons: it is faster; the quantitative results are produced without the need for error-prone pipetting and image analysis; the risk of carry-over contamination is minimized by the lack of post-PCR pipetting; and the production and calibration of competitors is not required (Holst-Jensen, 2003).

Molecular beacons have been successfully employed in real-time PCR and for the generation of melting curves, including the multiplex PCR format, and they are widely used for discriminating single base-pair differences (SNP). They may be tailored for the detection and quantification of new GM crops that feature single nucleotide genetic modifications (Seitz, 2000). The growing number of commercially available real-time thermocyclers is an indication of the success of this technology. Presently, real-time quantifications can be considered as the more powerful tool for the detection and quantification of GMOs in a wide variety of agricultural and food products (Hubner *et al*., 2001).

Random amplified polymorphic DNA (RAPD)

RAPDs are in fact just one example of a whole set of PCR-based molecular markers, which have been collectively termed as MAAP (multiple arbitrary amplicon profiling) (Caetano-Anolles, 1993). These approaches have in common the use of one (usually) or two primers of random sequence to amplify multibanded fingerprints from a complex genome. The techniques differ in the length and sequence of the primers, number of amplification cycles, temperature of the annealing stage and methods for evidencing polymorphisms (Caetano-Anolles, 1994).

The classic RAPD technique (Williams *et al*., 1990) uses one single primer, 10-nt long, with a GC percentage between 50 and 70%, to amplify sequences encompassed by imperfect inverted repeats of the primer in a low-stringency reaction (annealing at 34–36°C). This technique has been applied to all types of organisms for different purposes. Its main advantages are that it is fast, easy to perform and requires small amounts of DNA. The disadvantages are the dominance of RAPD patterns in different laboratories. The AP-PCR (amplified molymorphic-PCR) technique uses a longer primer of arbitrary sequence in a reaction that includes some cycles at a lower annealing temperature (Welsh and McClelland, 1990). A particular modification could involve the use of two different random primers, thereby increasing the number of bands in the fingerprint (Diaz and Ferrer, 2003).

A different example can be derived from the identification of marine mammals (seal, whale) in processed seafood products, performed with species-diagnostic molecular markers, including RAPDs (Martinez and Danielsdottir, 2000). Similarly, a polymorphism in a specific gene affecting coat color allowed detection in cheese of milk coming from a particular breed not permitted in the production of Registered Designation of Origin cheeses (Maudet and Taberlet, 2002).

Enzyme immunoassays

Besides biomedical research and clinical chemistry, enzyme immunoassays have been used in a broad range of applications in food analysis, including analytes of low molecular weight such as mycotoxins, anabolics, antimicrobial drugs, pesticides and vitamins, as well as macromolecules such as bacterial toxins, enzymes, hormones, food proteins and even living organisms, including bacteria and moulds (Fukal and Kas, 1989).

Immunochemical methods are based on the ability of antibodies to recognize three-dimensional structures and play a major role in biochemical research. Being primarily a part of the immune system in most classes of vertebrates (Stanworth and Turner, 1979), immunoglobulins have been utilized as the key substances in any immunoassay for more than 40 years. Antibodies represent a group of glycoproteins possessing two distinct types of polypeptide chains linked by both covalent and non-covalent bonds. Both the light chain and the heavy chain show a variable region at their amino terminal end of about 110 amino acids residues, whereas the remaining part of the polypeptide chain is referred to as the constant region (Kohler and Milstein, 1975).

The most prevalent test format of enzyme immunoassays is still the microtiter plate assay, which is usually performed by employing automated absorbance measurement

and calculation of the results. Depending on the individual test specificity, these assays are either quantitative or qualitative methods which can easily be performed in routine laboratories. Dipstick tests use either membranes or plastic materials as the solid phase. Depending on the pre-treatment of the solid support, antigens or antibodies are bound covalently or just adsorbed by multiple non-covalent bonds on the surface of the membrane as dots or lines (Martlbauer, 2003).

The potential sensitivity of any immunoassay is directly related to the affinity of the antibody, and may be calculated if the equilibrium constant is known. Since the antigen–antibody reaction may be described using reaction kinetics as well as thermodynamic equations, reaction time and temperature also influence assay sensitivity. Relying on antibody affinity, there is a significant difference between competitive and non-competitive methods (Jackson and Ekins, 1986).

One main area for the application of antibody techniques is the authenticity of food of animal origin. Most applications in this field have focused on identification of meat and milk of numerous animal species, either directly in the raw material or in processed food. The target antigens used in most studies on meat and meat products are blood or serum proteins, such as albumin. The proteins used for the immunization procedure cover a wide range of animal species, such as horse, cattle, pig, sheep, and exotic species such as impala and topi. Usually, the reliability and sensitivity of these assays decreases with increased heating of the samples, even with relatively stable proteins such as myoglobulin, adrenal preparations or troponin (Schweiger *et al*., 1983). Enzyme immunoassays utilizing blood or serum proteins (such as albumin) as the target antigen show limited suitability in testing heat-treated sample materials. A progressive loss in activity is observed with increased heat treatment due to denaturation of the antigen (Goodwin, 1992).

As well as the identification of the meat and milk of different mammalian species, only a few other applications, such as an enzyme immunoassay for distinguishing between crustacean tail-meat and white fish (Taylor and Jones, 1992), have been described. Substitution of canned sardine with other species and adulteration of canned tuna with bonito are two other specific authentication issues that have been addressed (Taylor *et al*., 1994). Also, a relatively low number of applications have focused on the detection of plant proteins (soy in meat products, or soy, wheat and pea proteins in milk powder) (Haasnoot *et al*., 2001).

The main advantages of enzyme immunoassay over immunodiffusion or immunoelectrophoresis procedures are reduced assay time, the requirement for only small amounts of antisera, and the possibility of obtaining quantitative results. In addition, the enzyme immunoassay microtiter plate assay may be automated, thus allowing a large number of samples to be processed, whereas rapid tests like dipsticks may be used as field tests to screen suspicious samples. Compared with physicochemical methods of analysis, microtiter tests have advantages regarding aspects of the sample treatment necessary prior to analysis. The sample extract clean-up in particular can be simplified or even totally omitted (Martlbauer, 2003). A general disadvantage of antibody techniques in this particular area is the limited availability of commercial test kits. The main reason for this limitation is the particular structure of the market for immunochemical methods in food analysis, which is characterized by a broad range

of potential products requiring a high degree of innovation but having relatively low sales per product.

Conclusions

Food authentication is the process by which a food is verified as complying with its label description. Labeling and compositional regulations, which may differ from country to country, have a fundamental place in determining which scientific tests are appropriate for a particular issue. Of course, claims concerning the species of origin concern mainly the genetic make-up of the organism, and the definition of a species may make this a rather arbitrary classification. Some claims may go beyond the species barrier to the variety of the organism. Another authenticity issue which may commonly arise is the need to determine whether food products from one species have been mixed with similar material from a cheaper species. Enzyme-linked immunosorbent assay (ELISA) and agar-gel immunodiffusion have been employed for analysis. The development of DNA methods continues to have a major place in meat authentication. Hunt *et al*. (1997) used oligonucleotide probes to identify the species of origin of raw and cooked meat. The benefit of this procedure is that the polymerase chain reaction (PCR) approach is not required. This is advantageous, because this equipment is not available in all laboratories, and it may also give rise to undesirable assay variability. It is considered superior to immunological techniques because the latter detect soluble plasma proteins.

Nuclear magnetic resonance (NMR) is the third spectroscopic technique which is being increasingly applied to food authentication. It can be used in a number of different ways. The entire spectrum can be used to generate a database, which is subsequently interpreted by statistical techniques. In this, it is analogous to using FT-IR or FT-Raman spectroscopy. Alternatively, it can be used to measure small amounts of specific compounds in the sample, which are then used as markers of authenticity.

References

Ahmed, F.E. (2002). Detection of genetically modified organisms in foods. *Trends in Biotechnolology*, **20**, 215–223.

Andreotti, G., Lamanna, R., Trivellone, E. and Motta, A. (2002). C-13 NMR spectra of TAG: An easy way to distinguish milks from different animal species. *Journal of American Oil Chemists' Society*, **79**, 123–127.

Anklam, E., Gadani, F., Heinze, P. *et al*. (2002). Analytical methods for detection and determination of genetically modified organisms in agricultural crops and plant-derived food products. *European Food Research and Technology*, **214**, 3–26.

Arvanitoyannis, I.S. (2003a). Genetically engineered/modified organisms in foods. *Applied Biotechnology, Food Science and Policy*, **1**(1), 3–12.

Arvanitoyannis, I.S. (2003b). Wine authenticity. In: M. Lees (ed.), *Food Authenticity and Traceability*. New York, NY: Woodhead Publishing Ltd, pp. 426–450.

Arvanitoyannis, I.S., Tsitsika, E.V. and Panagiotaki, P. (2005). Implementation of quality control methods (physicochemical, microbiological and sensory) in conjunction with multivariate analysis towards fish authenticity. *International Journal of Food Science and Technology*, **40**, 237–263.

Ashkenazi, V., Chani, E., Lavi, U. *et al*. (2001). Development of microsatellite markers in potato and their use in phylogenetic and fingerprinting analyses. *Genome*, **44**, 50–62.

Ashoor, S.H. and Stiles, P.G. (1987). Determination of soy protein, whey protein and casein in unheated meats by high-performance liquid chromatography. *Journal of Chromatography*, **393**, 321–328.

Belton, P.S., Delgadillo, I., Holmes, E. *et al*. (1996). Use of high field H-1 NMR spectroscopy for the analysis of liquid foods. *Journal of Agricultural and Food Chemistry*, **44**, 1483–1487.

Benson, I.B. (2003). Near infra-red absorption technology for analyzing food composition. In: M. Lees (ed.), *Food Authenticity and Traceability*. New York, NY: Woodhead Publishing Ltd, pp. 101–128.

Brescia, M.A., Caldarola, V., De Giglio, A., Benedetti, D., Fanizzi, F.P. and Sacco, A. (2002). Characterization of geographical origin of Italian red wines based on traditional and nuclear magnetic resonance spectrometric determinations. *Analytica Chimica Acta*, **458**(1), 177–186.

Bruton, D.C. (1970). Measurement of moisture and substance by infra-red radiation. *Measurement and Control*, **3**, T89–T92.

Bryan, G.J., Dixon, A., Gale, M.D. and Wiseman, G. (1998). A PCR-based method for the detection of exaploid bread wheat adulteration of durum and pasta. *Journal of Cereal Science*, **28**, 135–146.

Caetano-Anolles, G. (1993). Amplifying DNA with arbitrary oligonucleotides primers. *PCR Methods and Applications*, **3**, 85–94.

Caetano-Anolles, G. (1994). MAAP: a versatile and universal tool for genome analysis. *Plant Molecular Biology*, **25**, 1011–1026.

Chakraborti, D., Sarkar, A., Gupta, S. and Das, S. (2006). Small and large scale genomic DNA isolation protocol for chickpea (*Cicer arietinum* L.) suitable for molecular marker and transgenetic analyses. *African Journal of Biotechnology*, **5**(8), 585–589.

Coimbra, M.A., Gonsalves, F., Barros, A.S. and Delgadillo, I. (2002). Fourier transform infrared spectroscopy of white wine polysaccharide extracts. *Journal of Agricultural and Food Chemistry*, **50**, 3405–3411.

Colquhoun, I.J. and Goodfellow, B.J. (1994). NMR spectroscopy. In: R.H. Wilson (ed.), *Spectroscopic Techniques in Food Analysis*. New York, NY: VCH Publishing, pp. 87–145.

Colquhoun, I.J. (1998). High resolution NMR spectroscopy in food analysis and authentication. *Spectroscopy Europe*, **10**, 8–18.

Colquhoun, I.J. and Lees, M. (1998). Nuclear magnetic resonance spectroscopy. In: P.R. Ashurst and M.J. Dennis (eds), *Analytical Methods of Food Authentication*. London: Blackie Academic and Professional, pp. 36–75.

Cowe, I.A. and McNicol, W.H. (1985). Principal component analysis. *Applied Spectroscopy*, **39**, 257.

De Frutos, M., Cifuentes, A., Diez-Masa, J.C. *et al*. (1992). Application of HPLC for the detection of proteins in whey mixtures from different animal species. *Journal of High Resolution Chromatography*, **14**, 289–291.

De La Fuente, M.A. and Juarez, M. (2005). Authenticity assessment of dairy products. *Critical Reviews in Food Science and Nutrition*, **45**, 563–585.

Diaz, V., and Ferrer, E. (2003). Genetic variation of populations of Pinus oocarpa revealed by resistance gene analog polymorphism RGAP. *Genome*, **46**(3), 404–410.

Dieffenbach, C.W. and Dveksler, G.S. (1995). *PCR Primer: A Laboratory Manual*. Cold Spring Harbor, NY: Cold Spring Harbor Laboratory Press.

Dooley, J.J., Sage, H.D., Clarke, M.A.L. *et al*. (2005). Fish species identification using PCR-RFLP analysis and lab-on-a-chip capillary electrophoresis: application to detect white fish species in food products and an interlaboratory study. *Journal of Agricultural and Food Chemistry*, **53**, 3348–3357.

Downey, G. (1998). Food and food ingredient authentication by mid-infrared spectroscopy and chemometrics. *Trends in Analytical Chemistry*, **17**(7), 418–424.

Duarte, I., Barros, A., Belton, P.S. *et al*. (2002). High resolution nuclear magnetic resonance spectroscopy and multivariate analysis for the characterization of beer. *Journal of Agricultural and Food Chemistry*, **49**, 580–588.

Edelmann, A., Diewok, J., Schuster, K.C. and Lendl, B. (2001). Rapid method for the discrimination of red wine cultivars based on mid-infrared spectroscopy of phenolic wine extracts. *Journal of Agricultural and Food Chemistry*, **49**, 1139–1145.

Foord, O.S. and Rose, E.A. (1995). Long-distance PCR. In: C.W. Dieffenbach and G.S. Dveksler (eds), *PCR Primer: A Laboratory Manual*. Cold Spring Harbor, NY: Cold Spring Harbor Laboratory Press, pp. 63–77.

Forgacs, E. and Cserhati, T. (2006). Classification of chilli powders by high performance liquid chromatography-diode array detection. *Analytical Letters*, **39**, 2775–2785.

Fukal, L. and Kas, J. (1989). The advantages of immunoassay in food analysis. *Trends in Analytical Chemistry*, **8**, 112–116.

Gallignani, M., Garrigues, S. and De La Guardia, M. (1994). Derivative Fourier transform infrared spectrometric determination of ethanol in alcohol beverages. *Analytical Chimica Acta*, **287**(3), 275–283.

Garcia, M.C., Marina, M.L. and Torre, M. (1997). Simultaneous separation of soya bean and animal whey proteins by reversed-phase high-performance liquid chromatography. Quantitative analysis in edible samples. *Analytical Chemistry*, **69**, 2217–2220.

Gayo, J. and Hale, S.A. (2007). Detection and quantification of species authenticity and adulteration in crabmeat using visible and near-infrared spectroscopy. *Journal of Agricultural and Food Chemistry*, **55**, 585–592.

Gonzales, J., Remaud, G., Jamin, E. *et al*. (1999). Specific natural isotope profile studied by isotope ratio mass spectrometry (SNIP-IRMS): 13C/12C ratios of fructose, glucose, and sucrose for improved detection of sugar addition to pineapple juices and concentrates. *Journal of Agricultural and Food Chemistry*, **47**, 2316–2321.

Goodacre, R. (2002). *Trac-trends in Analytical Chemistry*, **21**, III–III.

Goodacre, R., Shann, B., Gilbert, R.J. *et al*. (2000). *Analytical Chemistry*, **72**, 119–127.

Goodwin, P. (1992). Immunoassay methods for animal speciation. In: M.R.A. Morgan, C.J. Smith and O.A. Williams (eds), *Food Safety Assurance: Applications of Immunoassay Systems*. London: Elsevier Science Publishers, pp. 33–40.

Graves, D.J. (1999). Powerful tools for genetic analysis come of age. *Trends in Biotechnology*, **17**, 127–134.

Green, L.R. and Rathe, C.V. (2006). Methods for detection of counterfeit liquids and foods. Available at http://www.freepatentsonline.com/20060035288.html.

Grove, D.S. (1999). Quantitative real-time polymerase chain reaction for the core facility using TaqMan and the Perkin-Elmer/Applied Biosystems Division 7700 sequence detector. *Journal of Biomolecular Techniques*, **10**, 11–16.

Haasnoot, W., Olieman, K., Cazemier, G. *et al*. (2001). Direct biosensor immunoassays for the detection of non-milk proteins in milk powder. *Journal of Agricultural and Food Chemistry*, **49**, 5201–5206.

Hardegger, M., Brodmann, P. and Herrmann, A. (1999). Quantitative detection of the 35S promoter and the NOS terminator using quantitative competitive PCR. *European Food Research and Technology*, **209**, 83–87.

He, J., Rodriguez-Saona, L.E. and Guisti, M.M. (2007). Mid-infrared spectroscopy for juice authentication – rapid differentiation of commercial juices. *Journal of Agricultural and Food Chemistry*, **55**, 4443–4452.

Higuchi, R., Dollinger, G., Walsh, P. and Griffith, R. (1992). Simultaneous amplification and detection of specific DNA sequences. *Bio/Technology*, **10**, 413–417.

Hinson, J.A., Michael, S.L., Ault, S.G. and Pumford, N.R. (2000). Western blot analysis for nitrotyrosine protein adducts in livers of saline-treated and acetaminophen-treated mice. *Toxicological Sciences*, **53**, 467–473.

Holland, M.V., Bernreuther, A. and Reniero, F. (1995). The use of amino acids as a fingerprint for the monitoring of European wines. In: P.S. Belton, I. Delgadillo, A.M. Gil and G.A. Webb (eds), *Magnetic Resonance in Food Science*. Cambridge: Royal Society of Chemistry, pp. 136–145.

Holst-Jensen, A. (2003). Advanced DNA-based detection techniques for genetically modified food. In: M. Lees (ed.), *Food Authenticity and Traceability*. New York, NY: Woodhead Publishing Ltd, pp. 575–592.

Hubner, P., Waiblinger, H.U., Pietsch, K. and Brodmann, P. (2001). Validation of PCR methods for quantitation of genetically modified plants in food. *Journal of AOAC International*, **84**, 1855–1864.

Hunt, D.J., Parkes, H.C. and Lumley, I.D. (1997). Identification of the species of origin of raw and cooked meat products using oligonucleotide probes. *Food Chemistry*, **60**(3), 437.

Hurley, I.P., Coleman, R.C., Ireland, H.E. and Williams, J.H.H. (2004). Measurement of bovine IgG by indirect competitive ELISA as a means of detecting milk adulteration. *Journal of Dairy Science*, **87**, 543–549.

Israel, D.I. (1993). A PCR-based method for high stringency screening of DNA libraries. *Nucleic Acids Research*, **21**, 2627–2631.

Jackson, T.M. and Ekins, R.P. (1986). Theoretical limitations on immunoassays sensitivity. Current practice and potential advantages of fluorescent Eu^{+3} chelates as non-radioisotopic tracers. *Journal of Immunological Methods*, **87**, 13.

Jha, V.K., Kumar, A. and Mandokhot, U.V. (2003). Indirect enzyme-linked immunosorbent assay in detection and differentiation of cooked and raw pork from meats of other species. *Journal of Food Science and Technology-Mysore*, **40**, 254–256.

Kaye, W. (1954). Spectral identification and analytical applications. *Spectrochimica Acta*, **6**, 257.

Kelley, L.C., Hafner, S., McCaskey, P.C. *et al*. (2000). Identification of the species of origin of raw and cooked meat products using oligonucleotide probes. *Journal of Food Protection*, **63**, 1107–1112.

Kemsley, E.K., Holland, J.K., Defernez, M. and Wilson, R.H. (1996). Detection of adulteration of raspberry purees using infrared spectroscopy and chemometrics. *Journal of Agricultural and Food Chemistry*, **44**, 3864–3870.

Kohler, G. and Milstein, C. (1975). Continuous cultures of fused cells secreting antibody of predefined specificity. *Nature*, **256**, 495–497.

Kvasnicka, F. (2005). Capillary electrophoresis in food authenticity. *Journal of Separation Science*, **28**, 813–825.

Le Gall, G. and Colquhoun, I.J. (2003). NMR spectroscopy in food authentication. In: M. Lees (ed.), *Food Authenticity and Traceability*. New York, NY: Woodhead Publishing Ltd, pp. 131–148.

Le Gall, G., Colquhoun, I.J., Davis, A.L. *et al*. (2003). Metabolite profiling of tomato using ^{1}H NMR spectroscopy as a tool to detect potential unintended effects following a genetic modification. *Journal of Agricultural and Food Chemistry*, **51**, 2447–2456.

Lemieux, B., Aharoni, A. and Schena, M. (1998). Overview of DNA chip technology. *Molecular Breeding*, **4**, 277–289.

Liang, P. and Pardee, A. (1992). Differential display of eukaryotic messenger RNA by means of the polymerase chain reaction. *Science*, **257**, 967–971.

Li, D., Cheng, J., Luo, W. *et al*. (2001). Liquid-phase hybridization in PCR-enzyme linked immunosorbent assay. *Chinese Journal of Laboratory Medicine*, **1**, 34–36.

Li, W. and Drake, M.A. (2001). Development of a QC-PCR assay for detection and quantification of *Escherichia coli* O157:H7 cells. *Applied and Environmental Microbiology*, **67**(7), 3291–3294.

Lindon, J.C., Holmes, E. and Nicholson, J.K. (2001). Pattern recognition methods and applications in biomedical magnetic resonance. *Progress in Nuclear Magnetic Resonance Spectroscopy*, **39**, 1–40.

Liu, G., Su, W., Xu, Q. *et al*. (2004). Liquid-phase hybridization based PCR-ELISA for detection of genetically modified organisms in food. *Food Control*, **15**(4), 303–306.

Lommen, A., Weseman, J.M., Smith, G.O. and Notborn, H.P.J.M. (1998). On the detection of environmental effects on complex matrices combining off-line liquid chromatography and H-1 NMR. *Biodegradation*, **9**, 513–525.

Loomis, M.D. (1974). Overcoming problems of phenolics and quinones in the isolation of plant enzymes and organelles. *Methods in Enzymology*, **31**, 528–544.

Lopez-Andreo, M., Garrido-Pertierra, A. and Puyet, A. (2006). Evaluation of post-polymerase chain reaction melting temperature analysis for meat species identification in mixed DNA samples. *Journal of Agricultural and Food Chemistry*, **54**, 7973–7978.

Lücker, E.H., Eigenbrodt, E., Wenisch, S. *et al*. (2000). *Journal of Food Protection*, **63**, 258–263.

Luthy, J. (1999). Detection strategies for food authenticity and genetically modified foods. *Food Control*, **10**, 359–361.

MacBeath, G. and Schreiber, S.L. (2000). Printing proteins as microarrays for high-throughput function determination. *Science*, **289**, 1760–1763.

Maldini, M., Marzano, F.N., González-Fortes, G. *et al*. (2006). Fish and seafood traceability based on AFLP markers: elaboration of a species database. *Aquaculture*, **261**, 487–494.

Malikowski, R. (1991). *Factor Analysis in Chemistry*, 2nd edn. New York, NY: Wiley.

Mannina, L., Patumi, M., Proietti, N. *et al*. (2001). Geographical characterization of Italian extra virgin olive oils using high field H-1 NMR spectroscopy. *Journal of Agricultural and Food Chemistry*, **49**, 2687–2696.

Marmiroli, N. (2003). Advanced PCR techniques in identifying food components. In: M. Lees (ed.), *Food Authenticity and Traceability*. New York, NY: Woodhead Publishing Ltd, pp. 3–29.

Martinez, I. and Danielsdottir, A.K. (2000). Identification of marine mammal species in food products. *Journal of the Science of Food and Agriculture*, **80**, 527–533.

Martlbauer, E. (2003). Enzyme immunoassays for identifying animal species in food. In: M. Lees (ed.), *Food Authenticity and Traceability*. New York, NY: Woodhead Publishing Ltd, pp. 54–66.

Maudet, C. and Taberlet, P. (2002). Holstein's milk detection in cheeses inferred from melanocortin receptor 1 (MC1R) gene polymorphism. *Journal of Dairy Science*, **85**, 707–715.

Mavromoustakos, T., Zervou, M., Bonas, G. *et al*. (2000). A novel analytical method to detect adulteration of virgin olive oil by other oils. *Journal of the American Oil Chemists' Society*, **77**, 405–411.

McCallum, J.D. (1961). Limitations and design philosophy in ultraviolet, visible and near-infra-red spectrophotometers. *Transactions of the New York Academy of Sciences*, **24**, 140–157.

Meyer, R.W. (1994). *Practical High-performance Liquid Chromatography*. New York, NY: Wiley.

Meyer, R.W. (1999). Development and application of DNA analytical methods for the detection of GMOs in food. *Food Control*, **10**, 395–397.

Moatsou, G. and Anifantakis, E. (2003). Recent developments in antibody-based analytical methods for the differentiation of milk from different species. *International Journal of Dairy Technology*, **56**, 133–138.

Murray, V. (1989). Improved double-stranded DNA sequencing using the linear polymerase chain reaction. *Nucleic Acids Research*, **17**, 8889.

Nollet, L.M.L. (2003). High pressure liquid chromatography (HPLC) in food authentication. In: M. Lees (ed.), *Food Authenticity and Traceability*. New York, NY: Woodhead Publishing Ltd, pp. 218–233.

Nuovo, G.J. (1994). *PCR In Situ Hybridizations: Protocols and Applications*. New York, NY: Raven Press.

Oliver, S.G., Winson, M.K., Kell, D.B. and Baganz, F. (1998). *Trends in Biotechnology*, **16**, 373–378.

Osbourne, B.G. and Fearn, T. (1986). *Near Infrared Spectroscopy in Food Analysis*. Harlow: Longman Scientific and Technical.

Plath, A., Krause, I. and Einspanier, R. (1997). Species identification in dairy products by three different DNA-based techniques. *Zeitschrift für Lebensmittel-Untersuchung und -Forschung*, **205**, 437–441.

Popping, B. (2002). The application of biotechnological methods in authenticity testing. *Journal of Biotechnology*, **98**, 107–112.

Quevauviller, P., Filippelli, M. and Horvat, M. (2000). Method performance evaluation for methyl mercury determination in fish and sediment. *Trends in Analytical Chemistry*, **19**, 34–41.

Raeymaekers, L. (1993). Quantitative PCR: theoretical considerations with practical implications. *Analytical Biochemistry*, **214**, 582–585.

Rashtchian, A. (1994). Amplification of RNA. *PCR Methods and Applications*, **4**, S83–S91.

Reid, L.M., O'Donnell, C.P. and Downey, G. (2006). Recent technological advances for the determination of food authenticity. *Trends in Food Science and Technology*, **17**, 344–353.

Ren, X., Zhu, X., Warndorff, M. *et al*. (2006). DNA extraction and fingerprinting of commercial rice cereal products. *Food Research International*, **39**, 433–439.

Ringeisen, B.R., Wu, P.K., Kim, H. *et al*. (2002). Picoliter-scale protein microarrays by laser direct white. *Biotechnology Progress*, **18**, 1126–1129.

Russell, V.J., Hold, G.L., Pryde, S.E. *et al*. (2000). Use of restriction fragment length polymorphism to distinguish between salmon species. *Journal of Agricultural and Food Chemistry*, **48**, 2184–2188.

Sanchez, L., Perez, M.D., Puyol, P. *et al*. (2002). Determination of vegetal proteins in milk powder by enzyme-linked immunosorbent assay: Interlaboratory study. *Journal of AOAC International*, **85**, 1390–1397.

Schweiger, A., Baudner, S. and Gunther, H.O. (1983). Isolation by free-flow electrophoresis and immunological detection of troponin T from turkey muscle: an application in food chemistry. *Electrophoresis*, **4**, 158–163.

Schweitzer, B. and Kingsmore, S.F. (2002). Measuring protein on microarrays. *Current Opinion in Biotechnology*, **13**, 14–19.

Scot, R.P.W. (1995). *Techniques and Practices of Chromatography*. New York, NY: Marcel Dekker.

Seitz, O. (2000). Solid-phase synthesis of doubly labeled peptide nucleic acids as probes for the real-time detection of hybridization. *Angewandte Chemistry International Edition*, **39**, 3249–3252.

Seyboldt, C., John, A., von Mueffling, T. *et al*. (2003). Reverse transcription-polymerase chain reaction assay for species-specific detection of bovine central nervous system tissue in meat and meat products. *Journal of Food Protection*, **66**, 644–651.

Silva, B.M., Andrade, P.B., Mendes, G.C. *et al*. (2000). Analysis of phenolic compounds in the evaluation of commercial quince jam authenticity. *Journal of Agricultural and Food Chemistry*, **48**(7), 2583–2587.

Sitter, B., Krane, J., Gribbestad, I.S., Jorgensen, L. and Aursand, M. (1999). Quality evaluation of Atlantic Halibut (Hippoglossus hippoglossus L) during ice storage using

^{1}H NMR spectroscopy. In: G.A. Webb, P.S. Belton and B.P. Hills (eds), *Magnetic Resonance in Food Science*. Cambridge, London: Royal Society of Chemistry, pp. 226–237.

Sotelo, C.G. and Perez-Martin, R.I. (2003). Species identification in processed seafoods. In: M. Lees (ed.), *Food Authenticity and Traceability*. New York, NY: Woodhead Publishing Ltd, pp. 323–340.

Spraul, M., Neidig, P., Klauck, U. *et al*. (1994). Automatic reduction of NMR spectroscopic data for statistical and pattern-recognition classification of samples. *Journal of Pharmaceutical and Biomedical Analysis*, **12**, 1215–1225.

Stanworth, D.R. and Turner, M.W. (1979). Immunochemical analysis of immunoglobulins and their sub-units. In: D.M. Weir (ed.), *Handbook experimental immunology*. Oxford: Blackwell Scientific Publishing, pp.6.1–6.13.

Studer, E., Rhyner, C., Luthy, J. and Hubner, P. (1998). Quantitative competitive PCR for the detection of genetically modified soybean and maize. *Zeitschrift für Lebensmittel-Untersuchung und -Forsuchung A*, **207**, 207–213.

Sultan, K.R., Tersteeg, M.H.G., Koolmees, P.A. *et al*. (2004). Western blot detection of brain material in heated meat products using myelin basic protein and neuron-specific enolase as biomarkers. *Analytical Chimica Acta*, **520**(1–2), 183–192.

Taruscio, T.G., Barney, D.L. and Exon, J. (2004). Content and profile of flavanoid and phenolic acid compounds in conjunction with the antioxidant capacity for a variety of northwest Vaccinium berries. *Journal of Agricultural and Food Chemistry*, **52**, 3169–3176.

Taylor, W.J. and Jones, J.L. (1992). An immunoassay for distinguishing between crustacean tail meat and white fish. *Food and Agricultural Immunology*, **4**, 177–180.

Taylor, W.J., Patel, N.P. and Jones, J.L. (1994). Antibody-based methods for assessing seafood authenticity. *Food and Agricultural Immunology*, **6**, 305–314.

Templin, M.F., Stoll, D., Schrenk, M. *et al*. (2002). Protein microarray technology. *Trends in Biotechnology*, **20**, 160–166.

Tersteeg, M.H.G., Koolmees, P.A. and van Knapen, F. (2002). Immunohistochemical detection of brain tissue in heated meat products. *Meat Science*, **61**, 67–72.

Vaidyanathan, S. and Goodacre, R. (2003). Proteome and metabolome analyses for food authentication. In: M. Lees (ed.), *Food Authenticity and Traceability*. New York, NY: Woodhead Publishing Ltd, pp. 71–100.

Verma, S.K., Khanna, V. and Singh, N. (1999). Random amplified polymorphic DNA analysis of Indian scented basmati rice (*Oryza sativa* L.) germplasm for identification of variability and duplicate accessions, if any. *Electrophoresis*, **20**, 1786–1789.

Vogels, J.T.W.E., Terwel, L., Tas, A.C. *et al*. (1996). Detection of adulteration in orange juices by a new screening method using proton NMR spectroscopy in combination with pattern recognition techniques. *Journal of Agricultural Food Chemistry*, **44**, 175–180.

Wang, D.N., Liu, S.Y., Trummer, B.J. *et al*. (2002). Structure–function of carbohydrates by neoglycolipid. *Nature Biotechnology*, **20**, 275–281.

Weiler, J., Gausepohl, H., Hauser, N. *et al*. (1997). Hybridisation based DNA screening on peptide nucleic acid (PNA) oligomer arrays. *Nucleic Acids Research*, **25**, 2792–2799.

Welsh, J. and McClelland, M. (1990). Fingerprinting genomes using PCR with arbitrary primers. *Nucleic Acids Research*, **19**, 861–866.

Williams, J.G.K., Kubelik, A.R., Livak, K.J. *et al*. (1990). DNA polymorphisms applied by arbitrary primers are useful as genetic markers. *Nucleic Acids Research*, **18**, 6531–6535.

Zamora, R., Alba, V. and Hidalgo, F.J. (2001). Use of high resolution C-13 nuclear magnetic resonance spectroscopy for the screening of virgin olive oils. *Journal of the American Oil Chemists' Society*, **78**, 89–94.

Zamora, R., Gomez, G. and Hidalgo, F.J. (2002). Classification of vegetable oils by high resolution C-13 NMR spectroscopy using chromatographically obtained oil fractions. *Journal of the American Oil Chemists' Society*, **79**, 267–272.

Zhu, H., Klemic, J.F., Chang, S. *et al*. (2000). Analysis of yeast protein kinases using protein chips. *Nature Genetics*, **26**, 283–289.

This page intentionally left blank

Index

Modern Techniques for Food Authentication
ISBN: 978-0-12-374085-4